



UNIVERSITY
OF WARSAW



THE JOINT EUROPEAN MAGNETIC SYMPOSIA

HYBRID CONFERENCE

JULY 24–29, 2022

WARSAW, POLAND

BOOK OF ABSTRACTS



ORGANIZERS



Conference under the patronage of the Rector of the University of Warsaw

CONFERENCE PARTNERS



We would like to acknowledge the support provided by the US Army Research Office to help make this event possible.



Outline

| | |
|--|-----|
| Plenary sessions | 4 |
| Semi-plenary sessions | 10 |
| EMA Awards Special Session | 21 |
| Gender Equality in Science | 24 |
| Symposium 1. Biomagnetism and medical applications | 26 |
| Symposium 2. Electronic structure and strongly correlated electron systems including superconductivity and superconducting spintronics | 45 |
| Symposium 3. Frustrated and disordered magnetism, including artificial spin ice | 60 |
| Symposium 4. Antiferromagnetism and antiferromagnetic spintronics | 86 |
| Symposium 5. Artificial intelligence in magnetism | 133 |
| Symposium 6. Novel 2D magnetic systems and heterostructures, including bi-layer graphene | 143 |
| Symposium 7. Magnetism and spintronics in molecular materials and inorganic materials | 165 |
| Symposium 8. Magnetic materials for energy applications, including magnetocalorics | 187 |
| Symposium 9. Micromagnetic modelling and magnetization processes | 235 |
| Symposium 10. Novel magnetic techniques and instrumentation, including metrology | 265 |
| Symposium 11. Magnetic materials: alloys, thin-films, interfaces, multilayers and nanomaterials | 290 |
| Symposium 12. Magnetorecording media, magnetic memories and magnetic sensors | 402 |
| Symposium 13. Domain walls, Skyrmions and spin-orbit related phenomena | 432 |
| Symposium 14. Spin waves, magnonics, magnetoplasmonics, ultrafast magnetization dynamics, terahertz spintronics and optically driven spin excitations | 499 |
| Symposium 15. Magnetotransport, spin transport, spintronics, spin orbitronics and spin caloritronics, including devices | 578 |
| Symposium 16. Magnetism and spin transport in topological materials and Weyl semimetals | 642 |
| Symposium 17. Multifunctional and magnetoelastic magnetic materials, complex oxides, multiferroics and composite multiferroics | 662 |
| Symposium 18. Spins for quantum technologies | 694 |

Plenary sessions

| | | |
|----------------------|---|---|
| Laurens W. Molenkamp | <i>Making Sense of the Quantum Anomalous Hall Effect</i> | 5 |
| Felix Casanova | <i>Spin-orbit proximity in van der Waals heterostructures for logic devices</i> | 6 |
| Nora Dempsey | <i>Hard magnetic films: from material studies to micro-system applications</i> | 7 |
| Mathias Kläui | <i>From Spin-Orbitronics to Orbitronics – novel science and applications in memory & non-conventional computing</i> | 8 |
| Geoffrey S. D. Beach | <i>Domain Walls and Skyrmions: From Ferromagnets to Ferrimagnets</i> | 9 |

Making Sense of the Quantum Anomalous Hall Effect

Laurens W. Molenkamp

¹ *Physikalisches Institut (EP3) and Institute for Topological Insulators, Würzburg University, Am Hubland, 97074 Würzburg, Germany*

The anomalous Hall effect, despite being over a century old, remains of great interest for fundamental research purposes, especially in the context of novel magnetic materials such as magnetic topological insulators. The rich phenomenology of this effect has however often been the victim of misinterpretations based on too hasty conclusions often based on misconceptions. Here, I review our careful and comprehensive studies in this area, and aim to clarify the true nature of the effect.

Anomalous Hall transport in the magnetic topological insulator, V-doped (Bi,Sb)₂Te₃, indicates the presence of two contributions of opposite sign. Their response to a variety of experimental parameters suggests that one contribution originates on the surface, and the other in the bulk of the magnetic topological insulator layer [1].

When the structural parameters of V (or Cr)-doped (Bi,Sb)₂Te₃ material are carefully optimized, at sufficiently low temperatures this ferromagnetic material is known to exhibit the quantum anomalous Hall effect [2], characterized by conduction through a single dissipationless chiral edge channel, even at zero external magnetic field. This perfect electronic transport quantization was quickly recognized as a promising platform for quantum metrology, as a zero-field quantum resistance standard. Metrologically comprehensive experiments reveal a great precision of the anomalous Hall resistance quantization in our films [3].

Temperature stability of the edge state transport is carefully investigated. By implementation of a novel multiterminal Corbino geometry we demonstrate that the quantum anomalous Hall edge channels survive up to the bulk Curie temperature. The transport quantization breakdown observed above 100 mK is solely a consequence of thermally activated bulk carriers electrically shorting the edge channels [4].

Proper analysis of the underlying fundamental physics reveals the existence of two distinct types of quantum anomalous Hall states, related to the systems' dimensionality. Both regimes are experimentally accessible by changing the layer thickness. Thinner films exhibit a conductivity tensor flow diagram equivalent to that of a two-dimensional electron gas, implying a fundamentally two-dimensional origin of the effect. When the film thickness is increased, a transition to the three-dimensional regime is observed. In the three-dimensional limit, the conductivity scaling changes to the one expected for electronic transport on two parallel topological interfaces, encapsulating a volume of distinct topology. This in turn provides a manifestation of what has been dubbed an "axion insulator" state [5,6].

Finally magneto-transport investigations of (V,Bi,Sb)₂Te₃ nanostructures in the quantum anomalous Hall regime exhibit intriguing large scale quantum fluctuations [7].

[1] K. M. Fijalkowski *et al.*, *Phys. Rev. X* **10**, 011012 (2020)

[2] C.-Z. Chang *et al.*, *Science* **340**, 6129 (2013)

[3] M. Götz *et al.*, *Appl. Phys. Lett.* **112**, 072102 (2018)

[4] K. M. Fijalkowski *et al.*, *Nat. Comm.* **12**, 5599 (2021)

[5] S. Grauer *et al.*, *Phys. Rev. Lett.* **118**, 246801 (2017)

[6] K. M. Fijalkowski *et al.*, *Phys. Rev. B* **103**, 235111 (2021)

[7] K. M. Fijalkowski *et al.*, *In Preparation* (2022)

Spin-orbit proximity in van der Waals heterostructures for logic devices

Fèlix Casanova^{1,2}

¹ CIC nanoGUNE, 20018 Donostia-San Sebastián, Basque Country, Spain.

² IKERBASQUE, Basque Foundation for Science, 48009 Bilbao, Basque Country, Spain.

The integration of logic and memory in spin-based devices, such as the recent MESO proposal by Intel [1], could represent a post-CMOS paradigm. A key player is the spin Hall effect (SHE), which allows to electrically create or detect pure spin currents without using ferromagnets (FM). Understanding the different mechanisms giving rise to SHE allows to optimize spin-to-charge conversion (SCC) in heavy metals. With this knowledge, we developed a novel and simple FM/Pt nanodevice to readout the in-plane magnetic state of the FM electrode using SHE [2]. The spin-orbit based detection allows us to independently enhance the output voltage (needed to read the in-plane magnetization) and the output current (needed for cascading circuit elements) with downscaling of different device dimensions, which are necessary conditions for implementing the MESO logic [1].

Next, I will present a radically different approach to further enhance SCC. By engineering a van der Waals heterostructure which combines graphene with a transition metal dichalcogenide (TMD), we first demonstrated SHE in graphene due to spin-orbit proximity [3], which survives to room temperature and can be tuned by electric field [4]. The combination of long-distance spin transport and SHE in the same material gives rise to an unprecedented SCC efficiency, making graphene-based systems excellent candidates for MESO logic [1,2].

Beyond the SHE, the spin-orbit proximity effect in van der Waals heterostructures opens the way to new spin transport phenomena. I will show how we exploit the Valley-Zeeman coupling in optimized bilayer graphene/TMD heterostructures to achieve magnetic-field-free spin precession. Remarkably, we observe that the sign of the precessing spin polarization can

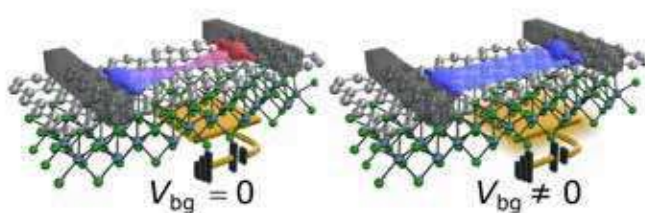


Figure 1: Sketch of a spin field-effect transistor operating at the strong spin-orbit coupling regime, where the valley-Zeeman induced spin precession is tuned by a back gate voltage to control the sign reversal.

be tuned electrically by a back gate voltage and by a drift current [5]. Our result is the first realization of a spin field-effect transistor at room temperature in a diffusive system, a long-awaited goal of spintronics that could be a cornerstone for the implementation of energy efficient spin-based logic.

- [1] S. Manipatruni et al., *Nature* **565**, 35 (2019)
- [2] V.T. Pham et al., *Nature Electron.* **3**, 309 (2020)
- [3] C.K. Safeer et al., *Nano Lett.* **19**, 1074 (2019)
- [4] F. Herling et al., *APL Mater.* **8**, 071103 (2020)
- [5] J. Ingla-Aynés et al., *Phys. Rev. Lett.* **127** (2021)

Hard magnetic films: from material studies to micro-system applications

Nora Dempsey¹

¹ *Institut NEEL, CNRS/UGA, 25 Rue de Martyrs, 38042, Grenoble, France*

High-performance rare earth transition metal (RE-TM) magnets are used in a wide range of applications and are key components for the transition towards green energy (hybrid-electric vehicles, wind mills). Reducing the size of such magnets to the microscale holds enormous potential for the development of micro-systems (μ -motors, μ -generators, μ -actuators, μ -sensors...) with applications in domains as diverse as tele-communications, consumer electronics, energy management and biotechnology. While the demand for RE-TM magnets is projected to grow significantly, raw material supply risks threaten their future production.

In this talk I will show how excellent extrinsic magnetic properties, namely coercivity and remanence, can be achieved in rare earth transition metal films. I will go on to describe techniques used to pattern such films at the micro-scale, so as to produce micro-magnets with field gradients of the order of a million T/m. I will give examples of the use of such high performance micro-magnets in various prototype applications. I will finish up by presenting the high throughput fabrication and characterization of compositionally graded films, which can be used to guide the future development of bulk magnets which are less dependent on critical elements.

From Spin-Orbitronics to Orbitronics – novel science and applications in memory & non-conventional computing

Mathias Kläui^{1,2}

¹ *Institute of Physics, Johannes Gutenberg University Mainz, 55099 Mainz, Germany*

² *Centre for Quantum Spintronics, Department of Physics, Norwegian University of Science and Technology, 7034 Trondheim, Norway.*

Novel spintronic devices can play a role in the quest for GreenIT if they are stable and can transport and manipulate spin with low power. Devices have been proposed, where switching by energy-efficient approaches, such as spin-polarized currents is used to manipulate topological spin structures [1,2].

Firstly, to obtain ultimate stability of states, topological spin structures that emerge due to the Dzyaloshinskii-Moriya interaction (DMI) at structurally asymmetric interfaces, such as chiral domain walls and skyrmions with enhanced topological protection can be used [3-5]. Here we will introduce these spin structures and we have investigated in detail their dynamics and find that it is governed by the topology of the spin structure [3]. By designing the materials, we can even obtain a skyrmion lattice phase as the ground state [4]. Beyond 2D structures, we recently developed also systems with chiral interlayer exchange interactions that lend themselves to the formation of chiral 3D structures [6].

Secondly, for ultimately efficient spin manipulation, we use spin-orbit torques, that can transfer more than $1\hbar$ per electron by transferring not only spin but also orbital angular momentum. We combine ultimately stable skyrmions with spin orbit torques into a skyrmion racetrack memory device [4], where the real time imaging of the trajectories allows us to quantify the skyrmion Hall effect [5]. Recently, we determined the possible mechanisms that lead to a dependence of the skyrmion Hall effect on skyrmion velocity [7]. We furthermore use spin-orbit torque induced skyrmion dynamics for non-conventional stochastic computing applications, where we have developed a skyrmion reshuffler device [8] based on skyrmion diffusion, which also reveals the origin of skyrmion pinning [8]. Such diffusion can furthermore be used for Token-based Brownian Computing and Reservoir Computing [9].

Beyond dynamics excited by spin-orbit torques the next step is to use orbital currents that generate orbital torques [10]. We have demonstrated that by adding to a conventional spin – orbitronic layer an additional Cu/CuOx layer, the acting torques can be increased by more than a factor 10 [10]. This effect has been interpreted as resulting from an orbital Hall current that is converted to a spin current. Finally, also an interfacial Orbital Rashba Edelstein Effect has been found, highlighting that the orbital analogues of both the spin Hall effect and the spin-based Rashba Edelstein or Inverse Spin Galvanic effect exist [11].

[1] G. Finocchio et al., J. Phys. D: Appl. Phys., vol. 49, no. 42, 423001, 2016.

[2] K. Everschor-Sitte et al., J. Appl. Phys., vol. 124, no. 24, 240901, 2018.

[3] F. Büttner et al., Nature Phys., vol. 11, no. 3, pp. 225–228, 2015.

[4] S. Woo et al., Nature Mater., vol. 15, no. 5, pp. 501–506, 2016.

[5] K. Litzius et al., Nature Phys., vol. 13, no. 2, pp. 170–175, 2017.

[6] D. Han et al., Nature Mater., vol. 18, no. 7, pp. 703–708, 2019.

[7] K. Litzius et al., Nature Electron., vol. 3, no. 1, pp. 30–36, 2020.

[8] J. Zázvorka et al., Nature Nanotechnol., vol. 14, no. 7, pp. 658–661, 2019;

R. Gruber et al., arxiv:2201.01618 (Nature Commun. in press (2022)).

[9] K. Raab et al., arxiv: 2203.14720; M. Brems et al., Appl. Phys. Lett. 119, 132405, 2021.

[10] S. Ding et al. Phys. Rev. Lett. 125, 177201, 2020; Phys. Rev. Lett. 128, 067201, 2022.

[11] D. Go et al., EPL 135, 037002 (2021)

Domain Walls and Skyrmions: From Ferromagnets to Ferrimagnets

Geoffrey S. D. Beach¹

¹ *Massachusetts Institute of Technology, 77 Massachusetts Ave., Cambridge, MA, USA*

Tremendous progress has been made in engineering highly mobile domain walls and skyrmions in room temperature materials for racetrack-based applications. Most recent efforts have focused on heavy-metal/ferromagnet heterostructures with Dzyaloshinskii-Moriya interactions and spin-orbit torques, in which chiral domain walls and skyrmions can be stabilized at room temperature and readily manipulated [1,2]. However, ferromagnets possess fundamental limitations on spin texture speed and size owing to stray fields and precessional dynamics [3]. Antiferromagnets, on the other hand, possess no stray fields, and are angular-momentum-compensated, yielding extremely fast dynamics. Ferrimagnets exhibit similar behaviors at compensation, but are more readily probed since the individually sublattices are detectible and addressable owing to the fact that the electronic and optical properties of the elements on these sites are typically different. Here, I describe ferrimagnetic spin textures and dynamics in metallic and insulating ferrimagnets. Using Pt/GdCo/TaOx films with sizable Dzyaloshinskii-Moriya interaction, we realize current-driven domain wall motion with a speed of 1.3 km/s near the angular momentum compensation temperature (T_A) and room-temperature stable skyrmions with minimum diameters close to 10 nm near magnetic compensation (T_M) [4]. By using temperature as a knob, the roles of compensation on the dynamics can be clearly extracted. I then describe recent work on insulating magnetic garnets with perpendicular anisotropy, in which we have discovered an interfacial Dzyaloshinskii-Moriya interaction [5,6] which, combined with low damping and pure spin current injection mediated by a Pt overlayer [7], leads to exceptionally fast motion at extremely low current densities [8]. Finally, I will discuss all-optical manipulation of skyrmions using ultrafast laser excitations, including picosecond generation of topological charge [9] tracked in real time via single-shot soft x-ray scattering, and all-optical writing, deleting, and two-dimensional steering of skyrmions by light alone [10]. Recent progress and future directions in these areas will be discussed.

- [1] S. Emori, *et al.*, *Nature Mater.* 12, 611 (2013)
- [2] S. Woo, *et al.*, *Nature Mater.* 15, 501 (2016)
- [3] F. Büttner, *et al.*, *Sci. Rep.* 8, 4464 (2018)
- [4] L. Caretta, *et al.*, *Nature Nano.* 13, 1154 (2018)
- [5] C. O. Avci, *et al.*, *Nat. Mater.* 14, 561 (2019)
- [6] L. Caretta, *et al.*, *Nat. Comm.* 11, 1090 (2020)
- [7] C.O. Avci, *et al.*, *Nature Mater.* 16, 309 (2017)
- [8] L. Caretta, *et al.*, *Science* 18, 1438 (2020)
- [9] F. Büttner, *et al.*, *Nat. Mater.* 20, 30 (2021)
- [10] L. Caretta, *et al.*, to be submitted (2022)

Semi-plenary sessions

| | | |
|--------------------------|---|----|
| Katharina J. Franke | <i>Artificially-constructed chains of magnetic adatoms on superconducting 2H-NbSe₂</i> | 11 |
| Bert Koopmans | <i>Femtomagnetism meets Spintronics</i> | 12 |
| Oksana Chubykalo-Fesenko | <i>Modeling of spin-Seebeck and spin-Peltier effects for magnetic textures</i> | 13 |
| Tomas Jungwirth | <i>Emerging research landscape of altermagnetism</i> | 14 |
| Hideo Ohno | <i>Spintronics for Green Society</i> | 15 |
| Dawid Pinkowicz | <i>Can photons generate magnetization in non-magnetic materials? - design of molecular photomagnets via the photochemical route</i> | 16 |
| Claire Donnelly | <i>Revealing three-dimensional spin textures, and their dynamics, with X-rays</i> | 17 |
| Jason Robinson | <i>Absolute spin-valve effect in magnetic superconducting switches with spin-orbit coupling</i> | 18 |
| Myriam Pannetier Lecoeur | <i>Magnetic field detection with spintronics: state of the art and innovations</i> | 19 |
| Andrzej Stupakiewicz | <i>Ultrafast nonthermal all-optical switching of magnetization in dielectrics</i> | 20 |

Artificially-constructed chains of magnetic adatoms on superconducting 2H-NbSe₂

Eva Liebhaber¹, Lisa Rütten¹, Gaël Reecht¹, Jacob F. Steiner², Sebastian Rohlf³, Kai Rossnagel³, Felix von Oppen², Katharina J. Franke³

¹ *Fachbereich Physik, Freie Universität Berlin, 14195 Berlin, Germany*

² *Dahlem Center for Complex Quantum Systems and Fachbereich Physik, Freie Universität Berlin, 14195 Berlin, Germany*

³ *Institut für Experimentelle und Angewandte Physik, Christian-Albrechts-Universität zu Kiel, 24118 Kiel, Germany*

Magnetic adatom chains on superconducting substrates are promising platforms for topological superconductivity and Majorana zero modes. Signatures of these have been found in densely packed chains with direct exchange interaction among the adatoms. In contrast, the dilute limit of chains, where the atoms are sufficiently far spaced that direct hybridization of their d orbitals is negligible, but close enough for substrate-mediated interactions, has not been investigated previously.

Here, we explore the quasi-two-dimensional superconductor 2H-NbSe₂ as a substrate for magnetic adatom structures. Individual Fe atoms induce Yu-Shiba-Rusinov (YSR) states, which spatially extend over several nanometers with their energy and symmetry influenced by the crystal field and by the co-existing charge-density wave (CDW) [1]. We detect signatures of quantum spins coupled via RKKY interaction in dimers of Fe atoms by the energy shift and split of the YSR states [2].

We deliberately increase the chain length by adding individual Fe atoms with the STM tip, up to a length of 51 atoms. In each step we track the evolution of the YSR states. We find signatures of YSR band formation consistent with ferromagnetic coupling of quantum spins [2,3].

[1] E. Liebhaber et al., Nano Lett. **20**, 339 (2020).

[2] E. Liebhaber, et al., Nature Commun. **13**, 2160 (2022).

[3] J. F. Steiner, et al., Phys. Rev. Lett. **128**, 036801 (2022).

Femtomagnetism meets Spintronics

Bert Koopmans

¹*Department of Applied Physics, Eindhoven Hendrik Casimir Institute,
Eindhoven University of Technology, P.O. Box 513, 5600 MB Eindhoven, The Netherlands
b.koopmans@tue.nl*

Novel schemes for controlling the ferromagnetic state at femtosecond time scales by pulsed laser excitation have received great interest. By driving systems into the strongly non-equilibrium regime, it has been shown possible not only to quench magnetic order, but also to switch the magnetization by single laser pulses – so-called all-optical switching (AOS). In parallel, it has been found that pulsed laser excitation can also induce spin currents over several to tens of nanometers, which can act as an additional source of sub-picosecond magnetization dynamics. Thereby, a scientifically exciting link between the fields of ‘femtomagnetism’ and spintronic transport physics has emerged. Moreover, it is being envisioned that combining the two fields could pave the way to a new class of hybrid spintronic-photonic devices (Fig. 1), in which data is copied between photonic and magnetic (spintronic) domain without any intermediate electronic steps, leading to ultrafast and highly energy-efficient IT solutions.

In this presentation, some of the underlying phenomena will be addressed, new theoretical insights will be shared [1], and a selection of recent experimental results combining AOS and spin transport will be presented. In particular, focus will be on highly efficient AOS and current-induced domain wall motion in the very same system: Pt/Co/Gd trilayers, displaying strong spin-orbit torques and Dzyaloshinskii-Moriya interaction. It will be shown that the magnetization of this synthetic ferrimagnetic thin film system can be reversed fully deterministically using single fs pulses [2]. Although the switching displays toggle characteristics, transfer of angular momentum by laser-induced spin currents from a reference layer can be used to deterministically set the magnetization to the up and down state [3]. More recently, we explored spin currents generated in the Co/Gd bi-layer upon pulsed laser irradiation [4]. Currents due to Co and Gd could be distinguished by carefully analyzing the GHz and THz spin waves in a neighboring non-collinearly aligned ferromagnetic layer experiencing a torque by the absorbed spin current [5]. Finally, some examples of recent progress towards integrated spintronic-photonic devices will be presented, including current-induced domain wall motion in Pt/Co/Gd-based conduits that display efficient AOS [6], with domain-wall velocities over 2000 m/s [7].

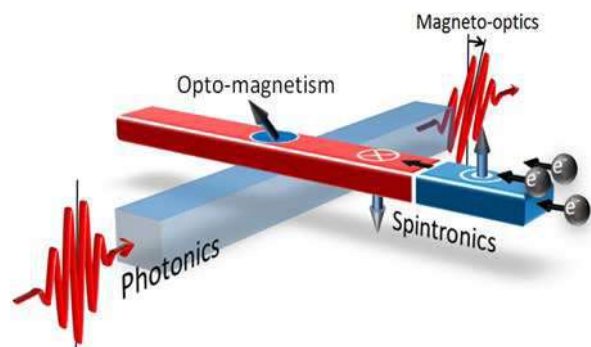


Figure 1: Artist's impression of integrated spintronic-photonic devices

- [1] M. Beens *et al.*, *Phys. Rev. B*, 220409 (R), (2019); *Phys. Rev. B* 102, 05442 (2020).
- [2] M.L.M. Laliu, *et al.*, *Phys. Rev. B* 96, 220411(R) (2017).
- [3] Y.L.W. van Hees *et al.*, *Nat. Commun.* 11, 3835 (2020).
- [4] G.-M. Choi *et al.*, *Phys. Rev. B* 97, 014410, (2018).
- [5] T. Lichtenberg, Y.L.W. van Hees *et al.*, in preparation.
- [6] M.L.M. Laliu *et al.*, *Nat. Commun.* 10, 110 (2019).
- [7] P. Li, T. Kools, *et al.*, *arXiv:2204.11595*.

Modeling of spin-Seebeck and spin-Peltier effects for magnetic textures.

Oksana Chubykalo-Fesenko, Elias Saugar

Instituto de Ciencia de Materiales de Madrid, CSIC, c/Sor Juana Inés de la Cruz, 3, Madrid, Spain

The possibility to move magnetic textures by thermal gradient is known as a spin-Seebeck effect for domain walls. Less known is the opposite effect- i.e. domain wall motion produces heat in the system. In the present talk I will discuss our multi-scale framework to model both situations. Typically, domain walls or skyrmion are moving to the hot region, albeit for skyrmions with a skyrmion Hall angle [1]. Several torques in this motion can be distinguished: (i) the entropy contribution which among other effects is included in the temperature-dependent parameters (ii) the spinwave generation which transfers angular momentum to the domain wall. The first contribution leads to rotational motion of domain walls in the perpendicular materials, and the oscillation of their position for large gradients which finally produce an effect similar to the Walker breakdown. In the presence of hot spots, we also observed domain wall oscillations as a function of time, particularly in the presence of pinning centers (Fig.1). For skyrmions, we also report a motion to the cold region in multilayered systems contrary to what happens in the ultrathin single layer case [1].

Similarly, since the domain wall can be moved under thermal gradient, one can expect the reciprocal effect - the domain wall motion could be accompanied by a temperature release (the spin-Peltier effect for domain wall [2]). In this case the released temperature is proportional to the ratio of domain wall velocity/width. Here we consider the antiferromagnetic MnAu material, where ultra-high velocities are predicted when the domain wall is moved under current by spin-orbit torque. Importantly, when the domain wall velocities are high, its width decreases due to relativistic effects. We estimate that the domain wall motion in this material can be accompanied by a localized ultrafast heat pulse as strong as 0.1K, much higher than for coherent magnetization switching. The energy release is especially efficient under elastic collision of domain walls with the same topological charge (Fig.1 right) [3].

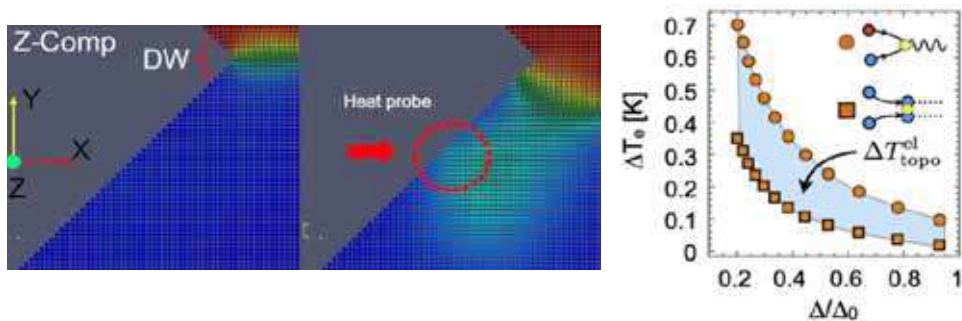


Figure 1: (a) Micromagnetic modelling showing the depinning of domain wall from the notch due to thermal gradients created by a localized heat probe (b) Energy release (electron temperature) during elastic (the same topological charges) and inelastic (opposite charges) domain wall collisions

[1] E. Raimondo et al <https://arxiv.org/abs/2205.04385>

[2] R.M. Otxoa et al Comm. Phys 3, 31 (2020)

[3] R.M. Otxoa et al Phys.Rev.Res. 3, 043069 (2021)

Emerging research landscape of altermagnetism

Tomas Jungwirth

Institute of Physics, Czech Academy of Sciences, Cukrovarnická 10, 162 00 Praha 6 Czech Republic

School of Physics and Astronomy, University of Nottingham, Nottingham NG7 2RD, United Kingdom

Magnetically ordered crystals are traditionally divided into two basic phases – ferromagnetism and antiferromagnetism. The ferromagnetic order offers a range of phenomena and device applications. The vanishing net magnetization in antiferromagnets is potentially favorable for spatial and temporal scalability of devices. Recently, our team and others have predicted instances of strong time-reversal symmetry breaking and spin splitting in electronic bands, typical of ferromagnetism, in crystals with antiparallel compensated magnetic order, typical of antiferromagnetism [1-3]. The central idea of the talk, resolving this apparent fundamental conflict in magnetism, is that symmetry classifies a third basic magnetic phase [4]. Its alternating spin polarizations in both crystal-structure real space and electronic-structure momentum space suggest a term altermagnetism. We will demonstrate that altermagnets combine merits of ferromagnets and antiferromagnets, that were regarded as principally incompatible, and have merits unparalleled in either of the two traditional basic magnetic phases. We will introduce materials landscape of altermagnetism and show how its anisotropic (d -wave) nature enriches fundamental physics concepts of lifted Kramers spin-degeneracy, Fermi-liquid instabilities and electron quasiparticles [3,4]. We will show that this underpins a development of a new avenue in spintronics, elusive within the two traditional magnetic phases, based on strong non-relativistic spin-conserving phenomena, without magnetization imposed scalability limitations, and with complex functionalities [1-6].

- [1] L. Smejkal, R. Gonzalez-Hernandez, J. Sinova, T. Jungwirth, *Science Adv.* 6, eaaz8809 (2020).
- [2] L. Smejkal, A. H. MacDonald, J. Sinova, S. Nakatsuji, and T. Jungwirth, *Nature Rev. Mater.* published on-line 30 March (2022)
- [3] L. Smejkal, J. Sinova, T. Jungwirth, *arXiv:2204.10844*.
- [4] L. Smejkal, J. Sinova, T. Jungwirth, *arXiv:2105.05820*.
- [5] R. Gonzalez-Hernandez, L. Smejkal, K. Vyborny, Y. Yahagi, J. Sinova, T. Jungwirth, and J. Zelezny, *Phys. Rev. Lett.* 126, 127701 (2021).
- [6] L. Smejkal, A. B. Hellenes, R. Gonzalez-Hernandez, J. Sinova, and T. Jungwirth, *Phys. Rev. X* 12, 011028 (2022).

Spintronics for Green Society

Hideo Ohno¹⁻⁵¹ *Laboratory for Nanoelectronics and Spintronics, Research Institute of Electrical Communication, Tohoku University, 2-1-1 Katahira, Aoba-ku, Sendai, 980-8577 Japan*² *Center for Innovative Integrated Electronic Systems, Tohoku University*³ *Center for Spintronics Research Network, Tohoku University*⁴ *Center for Science and Innovation in Spintronics, Tohoku University*⁵ *WPI-Advanced Institute for Materials Research, Tohoku University**Email: ohno@riec.tohoku.ac.jp*

The pathway to the carbon-neutral Green Society requires low power consumption integrated system. Big data generated by Internet-of-Things (IoT) sensors and devices and AI for processing data allow us to better understand the society we live in and manage society to minimize our carbon footprint. Both IoT and AI have to be low energy: For example, the trillion IoT devices can be embedded in our society only when they require much less energy or operate without a battery (i.e. energized by energy harvesting). AI is known to be extremely power-hungry, calling for a way to reduce its power use drastically. Spintronics nonvolatile device, magnetic tunnel junction (MTJ), has been shown to reduce the power of CMOS-based microprocessor orders of magnitude, suitable for IoT [1], AI, and other applications. MTJs are scalable down to 2.3 nm without resorting to new materials [2-4], a significant advantage along with high thermal stability, high endurance, and low voltage operation. In addition, new computing schemes based on spintronics technology potentially having higher performance than silicon-based digital processing are emerging. One is neuromorphic computing; we have made proof-of-concept spintronics devices for artificial synapses and neurons for neuromorphic applications [5, 6]. Another is to utilize less stable MTJs for a novel form of computing, probabilistic computing, to address optimization problems [7]. The time scale involved in these probabilistic MTJs is also discussed [8, 9]. If time allows, I will touch upon synthetic antiferromagnetic skyrmions for information carriers [10].

Work done in collaboration with S. Fukami, B. Jinnai, S. Kanai, and the CSIS team and supported in part by, JST-OPERA JPMJOP1611, JST-CREST JPMJCR19K3, Grant-in-Aid for Specially Promoted Research (17H06093) and for Scientific Research (16H05622). A portion of the work described here is a result of collaboration with A. Z. Pervaiz, K. Y. Camsari, and S. Datta of Purdue University.

[1] M. Natsui, et al. IEEE Int. Solid-State Circuits Conf. (ISSCC) 12.1 (2019).

[2] B. Jinnai, et al. IEDM 24.6. (2020).

[3] B. Jinnai, et al. Appl. Phys. Lett. (review) 116, 160501 (2020).

[4] K. Watanabe, et al. Nature Commun. 9, 663 (2018).

[5] W. A. Borders et al., Appl. Phys. Express 10, 013007 (2017).

[6] A. Kurenkov, et al., Advanced Materials 31, 1900636 (2019).

[7] W. A. Borders, et al. Nature 573, 390-393 (2019).

[8] K. Hayakawa, et al. Phys. Rev. Lett. 126, 117202 (2021).

[9] S. Kanai, et al. Phys. Rev. B 103, 094423 (2021).

[10] T. Dohi, et al. Nature Comm. 10, 5153 (2019).

Can photons generate magnetization in non-magnetic materials? - design of molecular photomagnets via the photochemical route

Dawid Pinkowicz

Jagiellonian University, Faculty of Chemistry, Gronostajowa 2, 30-387 Kraków, Poland

The efficient use of the visible spectrum of the Sun takes many forms leading to the production of biofuels or the generation of electricity. Interestingly, photoexcitation can also result in a dramatic change of the magnetization[1] or can generate magnetic moments in non-magnetic compounds[2] (Fig. 1) – this is the so-called photomagnetic effect. In other words, photons can write, read and erase magnetic states of photomagnets.

Molecular photomagnets can be designed and prepared via a bottom-up modular approach using low-energy preparation methods developed by coordination, organometallic or supramolecular chemistry, and crystal engineering with the support from physical and computational sciences. They belong to the class of smart multifunctional molecular materials that become paramagnetic, ferromagnetic or simply change their magnetic properties upon illumination - a feature that is hardly accessible in conventional solids - metal alloys and oxides.

Currently known photomagnetic compounds are merely laboratory curiosities due to the low operation temperatures below the boiling point of nitrogen in most cases[3,4]. Hence, the major goal of this field of research is the discovery of new strategies for room temperature (RT) photomagnets that would show light-induced ON/OFF ferromagnetic switching under normal conditions. The rational design and use of photomagnetic chromophores – the molecular components responsible for the photomagnetic effect in photomagnets – play the key role here. The talk will focus on (i) the design and synthesis of novel photomagnetic chromophores based on the ligand photodissociation reactions, (ii) explanation of the mechanism of the photochemical switching, and (iii) the rationale for achieving the RT photomagnets by the rational incorporation of suitable photomagnetic chromophores in the structure of coordination polymers and metal-organic frameworks.

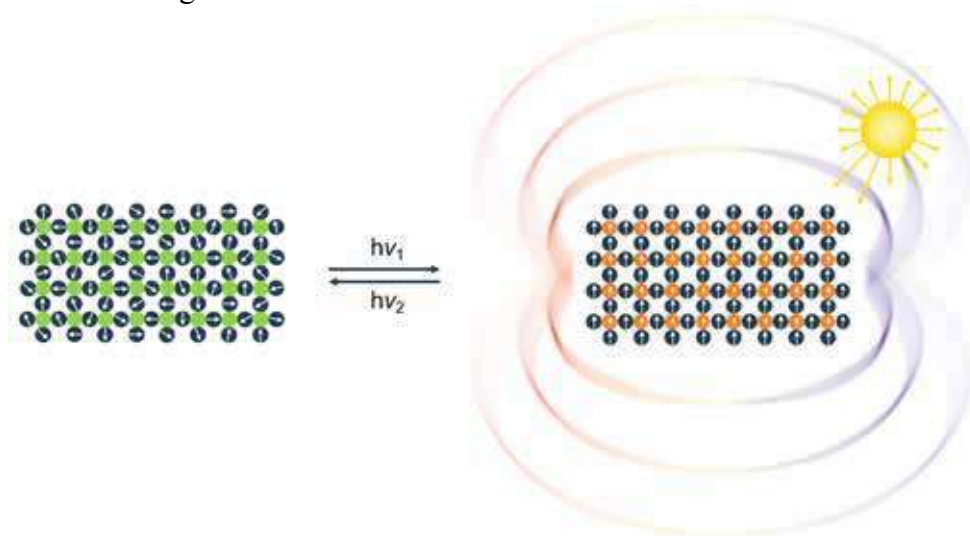


Figure 1: The concept of a molecular photomagnet – the photomagnetic chromophores (green balls) bridged to paramagnetic species (black balls) become magnetic after photoexcitation (orange balls) resulting in long-range magnetic ordering.

- [1] A. Stupakiewicz, et al., *Nature* **542**, 71 (2017)
- [2] X. Qi, et al., *Angew. Chem. Int. Ed.* **59**, 3117 (2021)
- [3] M. Magott, et al., *J. Am. Chem. Soc.* **140**, 15876 (2018)

Revealing three-dimensional spin textures, and their dynamics, with X-rays

Claire Donnelly¹

¹Max Planck Institute for Chemical Physics of Solids, Noethnitzer Str 40, 01187 Dresden, Germany

Three dimensional magnetic systems promise significant opportunities for applications, for example providing higher density devices and new functionalities associated with complex topology and greater degrees of freedom [1,2]. With recent advances in both characterization and nanofabrication techniques, the experimental investigation of these complex systems is now possible, opening the door to the elucidation of new physical properties, and representing the first steps towards higher dimensional magnetic devices.

For the characterization of 3D nanomagnetic systems, the development of magnetic tomographic techniques have opened up the possibility to map both the three-dimensional magnetic structure [3,4,5,6], and its dynamical response to external excitations [4,7]. In this way, both the static configuration, and dynamical behaviour, of topological structures within the bulk of a system [3,4,8], as well as in nanoscale structures [6,7,11] have been revealed. Within these complex configurations, recent advances in analytical techniques [5,8] have provided new capabilities to locate and identify 3D magnetic solitons, leading to the first observation of nanoscale magnetic vortex rings [8,9] (Figure 1a).

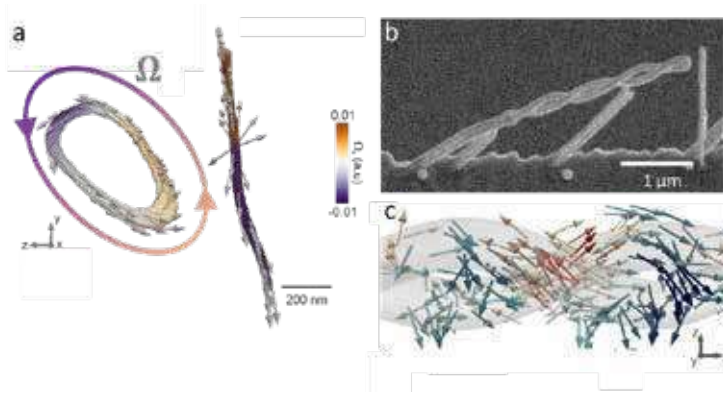


Figure 1: X-ray magnetic imaging has led to the observation of new textures, a) magnetic vortex rings within the bulk [8] and b,c) coupled domain wall states in three-dimensional magnetic double helices [11].

As well as existing within bulk and thin film systems, 3D spin textures can be introduced via the patterning of complex 3D magnetic nanostructures [10], leading to the realisation of highly coupled curvilinear systems [11]. These new experimental capabilities for 3D magnetic systems open the door to complex three-dimensional magnetic structures, and their dynamic behaviour.

- [1] Fernández-Pacheco et al., Nature Communications **8**, 15756 (2017).
- [2] C. Donnelly and V. Scagnoli, J. Phys. D: Cond. Matt. **32**, 213001 (2020).
- [3] C. Donnelly et al., Nature **547**, 328 (2017).
- [4] C. Donnelly et al., Nature Nanotechnology **15**, 356 (2020).
- [5] A. Hierro Rodriguez et al., Nature Communications **11**, 1 (2020).
- [6] K. Witte, et al., Nano Letters **20**, 1305 (2020).
- [7] S. Finizio et al., Nano Letters (2022)
- [8] C. Donnelly et al., Nat. Phys. **17**, 316 (2020)
- [9] N. Cooper, PRL. **82**, 1554 (1999).
- [10] L. Skoric et al., Nano Letters **20**, 184 (2020).
- [11] C. Donnelly et al., Nature Nanotechnology **17**, 136 (2022)

Absolute spin-valve effect in magnetic superconducting switches with spin-orbit coupling

Hisakazu Matsuki¹, Jason Robinson¹

¹ *Department of Materials Science & Metallurgy, University of Cambridge, 27 Charles Babbage Road, Cambridge, CB3 0FS, United Kingdom*

At a thin-film superconductor (S) interface with a ferromagnetic insulator (FI), the magnetic exchange field of the FI can spin-split the superconducting density of states in the S layer within a coherence length,^{1–3} causing a suppression of the superconducting critical temperature (T_c).⁴ In a FI/S/FI superconducting switch, the suppression of T_c is reduced for an antiparallel (AP) configuration between the two FI layer magnetisations due to a net cancellation effect of the magnetic exchange fields acting on S. Conversely, for parallel (P) magnetisations between the FI layers the exchange fields add, enhancing the suppression of T_c i.e., $\Delta T_c = T_c(\text{AP}) - T_c(\text{P}) > 0$. For S materials with weak spin-orbit coupling (SOC) such as Al the spin splitting in S can exceed several Tesla^{2,3} and ΔT_c can reach tens of mK.⁴ It has also been shown that a sub-nm-thick layer of Au or Pt near a Au/EuS interface quenches the spin splitting in Al due to SOC^{5,6}. Here we report EuS/Nb/EuS superconducting switches in which the superconducting layer of Nb layer has strong SOC and a sharp superconducting transition down to a thickness of only 2 nm. By optimising the EuS/Nb interface we obtain record-breaking values of ΔT_c that exceed 1.5 K with a $\Delta T_c/T_c(\text{P})$ ratio of nearly 100%. The results indicate physics that goes beyond the standard quasiclassical picture of S/FI proximity effects in which superconducting spin-switch performance is boosted by the large values of T_c in the nearly nm-thick layer of Nb in conjunction with strong SOC. The results are key to the development of superconducting spintronics.

- [1] P. Fulde, Adv. in Phys. 22, 667–719 (1973).
- [2] X. Hao, J. S. Moodera, R. Meservey, Phys. Rev. Lett. 67, 1342–1345 (1991).
- [3] E. Strambini, et al., Phys. Rev. Mat. 1, 054402 (2017).
- [4] B. Li, et al. Phys. Rev. Lett. 110, 097001 (2013).
- [5] P. Wei, et al., Phys. Rev. Lett. 122, 247002 (2019).
- [6] P. M. Tedrow & R. Meservey, Phys. Rev. B 25, 171–178 (1982).
- [7] J. Linder, J. W. A. Robinson, Nat. Phys. 11, 307–315 (2015).
- [8] G. Yang, C. Ciccarelli, J. W. A Robinson, APL Materials 9, 050703 (2021).

Magnetic field detection with spintronics: state of the art and innovations

Myriam Pannetier Lecoeur

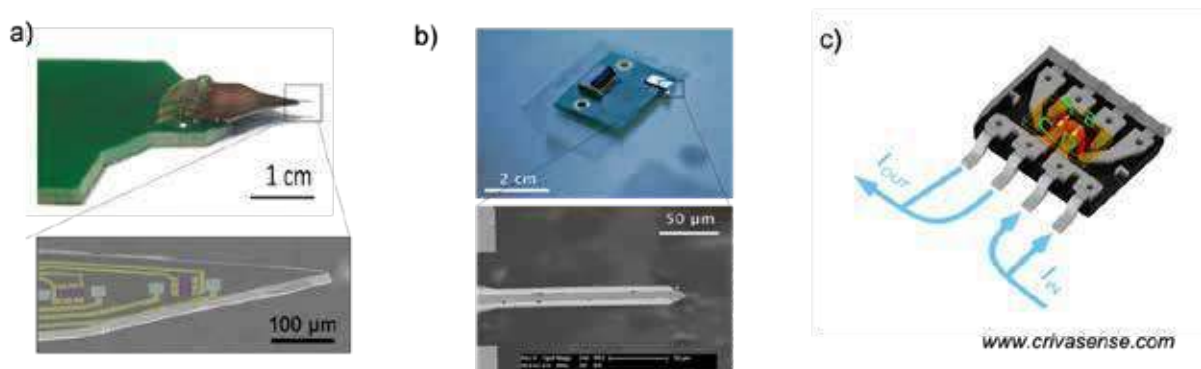
SPEC - CEA Saclay – CNRS UMR3680, 91191 Gif-sur-Yvette, France

Spin electronics offers rich physics associated with nano-scale magnetism from which many applications have emerged [1], including information reading (Hard Disk Drive read heads) and storage (MRAM) [2].

Spin electronics has also opened up a new approach for magnetic field measurement, offering a high sensitivity and integration on CMOS electronics. The market for magnetic sensors is growing rapidly (8% annually) [3] and the share of spintronic sensors is increasing (>10%).

In this presentation, we will first discuss magnetic measurement and its diversity, we will see what are the main technologies for magnetic sensing focusing on the strengths and particularities of spin electronics in this field.

The main characteristics, signal, noise, integration and stability, will be discussed as well as recent and innovative approaches. We will illustrate our talk with applications in the field of biological signal measurements, magnetic imaging and automotive.



Examples of spintronics sensors: a) magnetorode for in vivo neuronal signal recordings b) magnetic imaging tip c) integrated current sensor.

[1] *Nanomagnetism: Applications and Perspectives: Applications and Perspectives*, Editor(s): M. Van de Voorde, C. Fermon, 2017 Wiley-VCH Verlag GmbH & Co. KGaA, DOI:10.1002/9783527698509.

[2] *Introduction to Magnetic Random-Access Memory* B. Dieny, R.B. Goldfarb and K. Lee (eds). John Wiley Sons, Hoboken, NJ 101–164, 2016, pp. 101–165. isbn: 9781119079415.

[3] <https://www.gminsights.com/industry-analysis/magnetic-sensor-market>

Ultrafast nonthermal all-optical switching of magnetization in dielectrics

Andrzej Stupakiewicz

Faculty of Physics, University of Białystok, 15-245 Białystok, Poland

Rapid progress toward deployment of fiber-optic networks has led to the application of laser pulses to implement the fastest digital data transfer. At the same time, magnetism provides the cheapest and most reliable data recording. The integration of these areas has triggered an intense search for fundamental capabilities allowing for magnetic recording using only light.

The discovery of the magnetization switching only by a femtosecond laser pulse [1] triggered intense discussions about mechanisms responsible for laser-induced changes. All-optical magnetization switching, investigated so far predominantly in metallic systems [2,3], was recently also discovered in transparent dielectrics [4].

We demonstrated the all-optical photo-magnetic switching in Co-ions doped garnet films using a time-resolved magneto-optical spectroscopy and single-shot ultrafast imaging of magnetic domains. The photo-magnetic effect is a general phenomenon in numerous dielectrics. However, by using ultrashort laser pulses and precisely tuning to optical resonances we vastly enhance the effective light-induced field amplitude [5]. The switching properties at the observed resonances are vastly different, related to the crystal site hosting the excited Co-ions. As these ions are the source of the strong magnetic anisotropy in a garnet, their excitation between the crystal field split states results in a coherent and ultrafast manipulation of spin-orbital interaction. Moreover, another nonthermal mechanism of ultrafast magnetization switching was found in these unique magnetic garnets by resonant pumping of phonon modes [6]. This novel understanding highlights the principles for the engineering of materials for the cold all-optical recording.

- [1] Kirilyuk, A, Kimel, A.V, and Rasing, Th., *Rev. Mod. Phys.* **82**, 2731 (2010).
- [2] Stanciu, C.D. *et al. Phys. Rev. Lett.* **99**, 047601 (2007).
- [3] Lambert, C-H. *et al. Science* **345**, 1337 (2014).
- [4] Stupakiewicz, A. *et al. Nature* **542**, 71 (2017).
- [5] Stupakiewicz, A. *et al. Nat. Commun.* **10**, (2019).
- [6] Stupakiewicz, A. *et al. Nat. Phys.* **17**, 489 (2021).

EMA Awards Special Session

| | | |
|---------------|---|----|
| Jan Masell | <i>Large antiskyrmions and small scalar spin chirality fluctuations</i> | 22 |
| Libor Šmejkal | <i>Anomalous Hall responses in unconventional d-wave magnets</i> | 23 |

Large antiskyrmions and small scalar spin chirality fluctuations

Jan Masell^{1,2}

¹*Institute of Theoretical Solid State Physics, Karlsruhe Institute of Technology (KIT), Karlsruhe, 76049, Germany*

²*RIKEN Center for Emergent Matter Science (CEMS), Wako, 351-0198, Japan*

The physics of magnetic textures are rich of fascinating phenomena, on length scales from individual spins in the atomic limit to macroscopically large textures. In my talk, I will give an overview of our recent studies, discussing large topologically non-trivial textures such as antiskyrmions on the micrometer scale and non-coplanar fluctuations of spins on the atomic level.

Magnetic skyrmions are vortex-like, rotationally symmetric whirls whereas their anti-vortex-like partners, consequently dubbed anti-skyrmions, break this rotational symmetry. Unlike for skyrmions, only a limited number of antiskyrmion-hosting materials are known and, until recently, they all belonged to the D_{2d} symmetry class despite early predictions.[1] Combining experiments and theory, we studied antiskyrmions, skyrmions, and other textures in the S_4 -symmetric family of schreibersites $(Fe,Ni)_3P$. [2,3,4,5] The competition between the dominant demagnetization energy and small Dzyaloshinskii-Moriya interaction stabilizes both antiskyrmions and skyrmions in the transition region from the stripe phase to the field-aligned ferromagnet and, moreover, renders antiskyrmions square-shaped and skyrmions elliptical.[2] In general, antiskyrmions form in thicker samples and samples with larger uniaxial anisotropy where the bulk DMI can compete with dipolar interactions. Vice versa, skyrmions form in thinner samples where they profit from the strong dipolar interaction.[3]

The topological winding number of skyrmions also manifests in the Hall effect as it directly relates to the geometrical Berry phase. However, also topologically trivial textures can have finite geometrical Hall effect if the crystal lattice is non-trivial. As a result, even thermal fluctuations around an otherwise trivial state can give a large geometrical Hall effect on a Kagomé lattice with its two minimal plaquettes whereas such fluctuations precisely cancel on the trivial triangular lattice where all plaquettes are equivalent.[6,7]

[1] A. N. Bogdanov and D. A. Yablonskii, *Sov. Phys. JETP* **68**, 101-103 (1989).

[2] K. Karube, L. C. Peng, J. Masell, *et al.*, *Nat. Mater.* **20**, 335-340 (2021).

[3] K. Karube, L. C. Peng, J. Masell, *et al.*, *Adv. Mater.* 202108770 (2022).

[4] S. Schneider, J. Masell, F. S. Yasin, *et al.* (in preparation).

[5] F. S. Yasin, J. Masell, *et al.* (in preparation).

[6] K. K. Kolincio, M. Hirschberger, J. Masell, *et al.*, *PNAS* **118**, e2023588118 (2021).

[7] K. K. Kolincio, M. Hirschberger, J. Masell, *et al.* (in preparation).

Anomalous Hall responses in unconventional d-wave magnets

Libor Šmejkal

¹Institut für Physik, Johannes Gutenberg Universität Mainz, Germany

²Institute of Physics, Czech Academy of Sciences

Electronic structures of magnets are intensively researched for possibilities of anomalous band topologies and applications in nanoelectronics and spintronics [1,2,3]. Therefore, it is highly desirable to understand the relationship of the electronic structure to different types of magnetic ordering, or more generally microscopic magnetization densities [3], in crystals. Magnets are commonly divided into ferromagnets and antiferromagnets according to whether their magnetic symmetry allows for a net macroscopic magnetization. However, the conventional relativistic magnetic symmetries cannot disentangle non-relativistic magnetic and relativistic spin-orbit interactions because the symmetry transformations act simultaneously in crystallographic and spin space.

In this talk, we will classify all possible collinear magnetic orderings via non-relativistic spin symmetry transformations which act separately in crystallographic and spin space [4,5]. Our spin symmetry group classification reveals three basic types of magnetic orderings: Conventional ferromagnets and antiferromagnets, and a third unconventional phase. Ferromagnets are characterized by one spin lattice or opposite-spin sublattices not connected by any symmetry transformation.

Conventional antiferromagnets exhibit opposite-spin sublattices connected by translation or inversion (see Figure 1) [6]. In the third, unconventional phase, the opposite spin sublattices are connected via rotational symmetry (indicated by the curved arrow in Figure 1). These unconventional magnets exhibit characteristic spontaneous breaking of time-reversal symmetry in the form of alternating spin polarisation in the momentum space (see Figure) [2-5,7], and are therefore also called altermagnets [2,4]. We identify altermagnets with d-wave, as well as g or i-wave, form of spin-momentum locking [4]. In the second part of the talk we will show that altermagnetism provides a unifying explanation of recent surprising predictions of effects that are incompatible with conventional ferromagnetism or antiferromagnetism (see Refs. 2-4 and references therein). We will focus on predictions and observations of anomalous Hall effects, i.e. dissipationless transverse responses, in RuO₂, MnTe and Mn₅Si₃ crystals with vanishing net magnetization [3,8]. We will show that large contributions to the intrinsic anomalous Hall vector $\mathbf{h}=(\sigma_{zy}, \sigma_{xz}, \sigma_{yx})$ (σ_{ij} are Hall conductivity components) are generated along pseudo-nodal surfaces in momentum space protected by the spin symmetries [3,7].

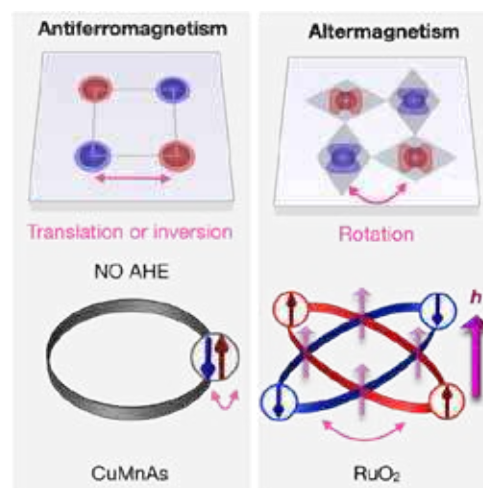


Figure. Comparison of antiferromagnets and altermagnets in real and momentum space. The light magenta arrows indicate hotspots of intrinsic anomalous Hall vector \mathbf{h} .

- [1] L.Šmejkal, Y. Mokrousov, B. Yan, and A. H. MacDonald, *Nat. Phys.* **14**, 242 (2018)
- [2] L.Šmejkal, A. H. MacDonald, J. Sinova, S. Nakatsuji, and T. Jungwirth, *Nat. Rev. Mat.* **7**, 482 (2022)
- [3] L.Šmejkal et al., *Science Advances* **6**, eaaz8809 (2020)
- [4] L.Šmejkal, J. Sinova, and T. Jungwirth, [arXiv:2105.05820v2](https://arxiv.org/abs/2105.05820v2), [arXiv:2204.10844](https://arxiv.org/abs/2204.10844)
- [5] L.Šmejkal et al., *PRX*, **12**, 011028 (2022), R. González-Hernández et al., *PRL* **126**, 127701 (2021)
- [6] L.Šmejkal et al., *PRL* **118**, 106402 (2017)
- [7] I. I. Mazin, et al., *PNAS* **118** (42) e2108924118 (2021)
- [8] Feng et al., [arxiv:2020.08712](https://arxiv.org/abs/2020.08712), Reichlova et al., [arXiv:2012.15651](https://arxiv.org/abs/2012.15651), Gonzales-Betancourt et al. [arXiv:2112.06805](https://arxiv.org/abs/2112.06805)

Gender Equality in Science

Angela Wroblewski

Reaching the goal with gender equality plans? How GEPs contribute to a reflexive gender equality policy

25

Reaching the goal with gender equality plans? How GEPs contribute to a reflexive gender equality policy

Angela Wroblewski¹

¹ *Institute for Advanced Studies (IHS)*

Gender Equality Plans (GEPs) are the main instrument to support gender equality and structural change in the new European Research Area (ERA). In the main European research funding scheme, Horizon Europe, GEPs became an eligibility criterion for applying institutions.

The presentation will discuss the requirements for GEPs formulated by Horizon Europe and how GEPs may contribute to a reflexive gender equality policy and thus to structural change. Structural change requires a reflection of gendered practices and structures in R&I and the development of non-biased alternatives. GEPs developed in an evidence based and cyclical process provide a basis to identify gender bias, to tackle it with specific measures and to initiate a gender equality discourse within research organisations.

References

- [1] Council of the European Union (2021). Future governance of the European Research Area (ERA) -Council conclusions (14308/21). Brussels.
<https://data.consilium.europa.eu/doc/document/ST-14308-2021-INIT/en/pdf>
- [2] European Commission (2021). Horizon Europe Guidance on Gender Equality Plans. Luxembourg: Publications Office of the European Union. doi:10.2777/876509
- [3] Wroblewski, Angela; Palmén, Rachel (eds.) (2022, in print). Overcoming the challenge of structural change in research organisations. A reflexive approach to gender equality, Bingley: Emerald.

Symposium 1. Biomagnetism and medical applications

| | | |
|----------------------|---|----|
| Helene Joisten | <i>Magnetomechanical actuation of microdisks and magnetoelastic membranes used as bioreactor for pancreatic cells stimulation</i> | 28 |
| Denys Makarov | <i>Flexible and printed electronics: from interactive on-skin devices to bio/medical applications</i> | 29 |
| Claire Wilhelm | <i>Magnetic Nanoparticles – Mediated Cancer Therapies and Magnetic Tissue Engineering</i> | 30 |
| Soudabeh Aarsalani | <i>Influence of temperature on the relaxation signal of magnetic nanoparticles by magnetorelaxometry</i> | 32 |
| Findan Block | <i>Magnetic bucket brigade networks as rails for single cell transportation</i> | 33 |
| Zoe Boekelheide | <i>Theoretical calibration factors of AC magnetometers for measuring magnetic fluid magnetization</i> | 34 |
| Maïkane Deroo | <i>Innovative dynamic detection for early diagnosis with a lab-on-a-chip based on "two-stage" giant magnetoresistance sensors</i> | 35 |
| Mariia Efremova | <i>Room-temperature synthesis of AuFe solid solution nanoparticles and their transformation to Au/Fe Janus nanostructures</i> | 36 |
| Santiago Helbig | <i>Single-domain particle heating in a viscous fluid</i> | 37 |
| Celia Sousa | <i>Magnetic properties of Fe vortex nanodiscs and nanowires for emerging biomedical applications.</i> | 38 |
| Paola Tiberto | <i>Factors affecting Magnetic Particle Imaging: Challenges and Solutions</i> | 39 |
| Jim Webb | <i>Recording activity from mammalian tissue via induced biomagnetic field using colour centers in diamond</i> | 40 |
| Yuko Ichiyanagi | <i>Magnetic susceptibilities at low magnetic fields and 3rd harmonic response of Cu-Zn ferrite nanoparticles for MPI applications</i> | 42 |
| Anca Emanuela Minuti | <i>A ferrofluid based on Fe-Cr-Nb-B magnetic particles for biomedical application</i> | 43 |
| Hidenori Nakagawa | <i>An ELF magnetic Control Study for Metamorphic Qualities in Thyroxine-Administrated Axolotls (<i>Ambystoma mexicanum</i>)</i> | 44 |

Invited Oral Presentations

| | | |
|----------------|---|----|
| Helene Joisten | <i>Magnetomechanical actuation of microdisks and magnetoelastic membranes used as bioreactor for pancreatic cells stimulation</i> | 28 |
| Denys Makarov | <i>Flexible and printed electronics: from interactive on-skin devices to bio/medical applications</i> | 29 |
| Claire Wilhelm | <i>Magnetic Nanoparticles – Mediated Cancer Therapies and Magnetic Tissue Engineering</i> | 30 |

Magnetomechanical actuation of microdisks and magnetoelastic membranes used as bioreactor for pancreatic cells stimulation

Svetlana Ponomareva ¹, Helene Joisten ^{1,3}, Cecile Naud ¹, Robert Morel ¹, Yanxia Hou ², Bernard Dieny ¹ and Marie Carriere ²

¹ Univ. Grenoble Alpes, CEA, CNRS, Spintec, 38000 Grenoble, France.

² Univ. Grenoble Alpes, CEA, CNRS, IRIG-SyMMES, 38000 Grenoble, France

³ CEA-Leti, Univ. Grenoble Alpes, F-38000 Grenoble, France

In the growing field of mechanobiology, purely mechanical effects on living cells – without heat production or specific molecular targeting – have received a great deal of attention over the past two decades. In particular, the magnetomechanical actuation of magnetic particles provides an efficient way to exert forces and torques at micro/nano-scale on biological cells. Our disk $\text{Ni}_{80}\text{Fe}_{20}$ particles, with in-plane magnetization in vortex configuration, have been studied either dispersed in fluidic solutions, or more recently embedded as a regular array in flexible polydimethylsiloxane (PDMS) membranes. The membrane deformation under magnetic field can be characterized optically by their diffraction pattern (Fig.1) [1]. Widely explored for potential cancer therapy, the magnetomechanical actuation of magnetic particles has proven its ability to destroy cancer cells [2-3].

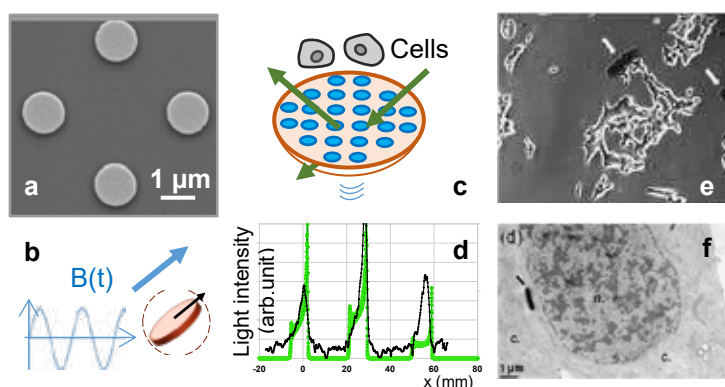


Figure 1: a) NiFe disks 60nm thick, dispersed or embedded in a 5μm thick PDMS membrane, for pancreatic cells stimulation. b-c) Sketch of particles and membrane actuation in magnetic field $B(t)$. d) Deformations controlled through diffraction patterns. e) Optical microscopy image of INS-1E cells exposed to 50 μg/mL of magnetic particles [4]. f) Transmission electron microscopy image of INS-1E cells exposed to magnetic particles (50 μg/mL) and 20 Hz $B(t)$. (n = nucleus, c = cytoplasm) [4].

Moreover, in a recent study, we demonstrate that magnetic particles or flexible membranes can be used to mechanically stimulate pancreatic cells. Our experiments revealed that this stimulation enhances insulin granule secretion [4]. Such observation can be of very high interest for innovative diabetes treatment. Overall, actuated magnetic membranes are promising for biotechnological applications involving mechanical actions on cells.

Support by EU's H2020 Fet Open Abiomater No 665440, and H2020 ERA-Net Euronanomed II Nanoviber are acknowledged.

[1] H. Joisten et al., *Nanoscale* **11**, 10667-10683 (2019).

[2] S. Leulmi et al., *Nanoscale* **7**, 15904-15914 (2015).

[3] C. Naud et al, *Nanoscale Adv.* **2**, 3632-3655 (2020).

[4] S. Ponomareva, H. Joisten, T. François, C. Naud, R. Morel, Y. Hou, T. Myers, I. Joumard, B. Dieny, M. Carriere, submitted, in peer review (2022).

Flexible and printed electronics: from interactive on-skin devices to bio/medical applications

Denys Makarov ¹

¹ Helmholtz-Zentrum Dresden-Rossendorf e.V., Institute of Ion Beam Physics and Materials Research, Bautzner Landstrasse 400, 01328 Dresden, Germany

Extending 2D structures into 3D space has become a general trend in multiple disciplines, including electronics, photonics, plasmonics and magnetics. This approach provides means to modify conventional or to launch novel functionalities by tailoring curvature and 3D shape. We study fundamentals of 3D curved magnetic thin films [1] and explore their application potential for flexible electronics, eMobility and health. We put forth the concept of shapeable magnetoelectronics [2] for various applications ranging from automotive through consumer electronics to virtual and augmented reality applications [3]. These skin-conformal flexible and printable magnetosensitive elements enable touchless interactivity with our surroundings based on the interaction with magnetic fields, which is relevant for smart skins for human-machine interfaces [4-9] and soft robotics [10].

Highly flexible functional elements are demanded for bio/medical applications. We will introduce an implantable, multifunctional device on ultrathin polymeric foils for targeted thermal treatment of cancer [11] as well as a flexible light weight diagnostic platform based on highly sensitive Si nanowire field effect transistors revealing remarkable limit of detection at 40 pM for Avian Influenza Virus (AIV) subtype H1N1 DNA sequences [12].

For the emerging field of biosensing technologies, we developed droplet-based magnetofluidic platforms encompassing integrated novel functionalities [13] including analytics in a flow cytometry format [14], magnetic detection, barcoding and sorting of magnetically encoded emulsion droplets using rigid [15,16] and flexible [17] microfluidic devices. These features are crucial to address the needs of modern medical research, e.g. drug discovery.

- [1] D. Makarov et al., *Adv. Mater. (Review)* **34**, 2101758 (2022).
- [2] D. Makarov et al., *Appl. Phys. Rev. (Review)* **3**, 011101 (2016).
- [3] G. S. Cañón Bermúdez et al., *Adv. Funct. Mater. (Review)* **31**, 2007788 (2021).
- [4] G. S. Cañón Bermúdez et al., *Science Advances* **4**, eaao2623 (2018).
- [5] G. S. Cañón Bermúdez et al., *Nature Electronics* **1**, 589 (2018).
- [6] J. Ge et al., *Nature Communications* **10**, 4405 (2019).
- [7] M. Ha et al., *Adv. Mater.* **33**, 2005521 (2021).
- [8] P. Makushko et al., *Adv. Funct. Mater.* **31**, 2101089 (2021).
- [9] S. Li et al., *Nano Energy* **92**, 106754 (2022).
- [10] M. Ha et al., *Adv. Mater.* **33**, 2008751 (2021).
- [11] G. S. Cañón Bermúdez et al., *Adv. Eng. Mater.* **21**, 1900407 (2019).
- [12] D. Karnaushenko et al., *Adv. Healthcare Mater.* **4**, 1517 (2015).
- [13] G. Lin et al., *Lab Chip (Review)* **17**, 1884 (2017).
- [14] G. Lin et al., *Small* **12**, 4553 (2016).
- [15] J. Schütt et al., *ACS Omega* **5**, 20609 (2020).
- [16] W. Song et al., *ACS Sensors* **2**, 1839 (2017).
- [17] G. Lin et al., *Lab Chip* **14**, 4050 (2014).

Magnetic Nanoparticles – Mediated Cancer Therapies and Magnetic Tissue Engineering

C. Wilhelm¹

¹ PCC laboratory, Curie Institute, CNRS UMR168, IPGG, 6 rue Jean Calvin, 75005 PARIS

The emergence of multifunctional inorganic nanohybrids providing multiples functions recently paved the way to tailor-made therapeutic prescriptions and theranostic functionalities. In cancer therapy, they have raised the prospect of thermal treatments that have few if any adverse effects, which we extensively explored this last decade [1-8].

However, the magnetism of iron oxide - based nanoparticles also provide cells with sufficient magnetization to manipulate them. Magnetic nanoparticles thus appear as a promising tool for tissue engineering opening up challenging perspectives. We developed magnetic-based methods to manipulate cells, towards the goal to provide magnetic artificial tissue replacements [9,10,11,12], that can be stimulated on demand. For instance, it could induce mechanically stem cells differentiation [13,14]. Similarly, it allows to magnetically compress cancer spheroids alongside their genesis or drug testing and even nanoparticles-mediated therapy, then in an all-in-one actor/probe action of the magnetic nanoparticles [15].

The therapeutic use of nanoparticles in cancer therapy or regenerative medicine application still raises the more general issue of intracellular nanoparticle long-term fate [16]. Cell spheroids models and magneto-thermal tools will be introduced, as tools to monitor long-term nanomaterials intracellular integrity. It evidenced a massive intracellular degradation [17], which could be prevented by a polymeric coating [18] or an inert gold shell [19,20]. Remarkably, human cells could also biosynthesize their own magnetic nanoparticles [21-23], with longer persistence, and limited toxicity.

- [1] Adv Funct Mat, **28**, 1803660 (2018);
- [2] J Controlled Release, **279**, 271-281 (2018);
- [3] Adv HealthCare Mat, **5**, 1040- 48 (2016);
- [4] ACS Nano, **9**, 2904-2916 (2015);
- [5] ACS nano, **10**, 2436-2446 (2016);
- [6] Nanoscale, **7**, 18872-18877 (2015);
- [7] Theranostics, **9**, 1288 (2019);
- [8] Theranostics, **9**, 5924 (2019);
- [9] Advanced Materials. **25**, 2611-2616 (2013);
- [10] Acta Biomaterialia, **37**, 101-110 (2016);
- [11] Phys Rev Lett, **114**, 098105 (2015);
- [12] Biofabrication **13**, 015018 (2020);
- [13] Nature Communications, **8**, 400 (2017);
- [14] Adv Funct Mat, **30**, 2002541 (2020);
- [15] Cancers, **14**, 366 (2022);
- [16] Accounts Chem Res **53**, 2212-24 (2020);
- [17] ACS nano, **10**, 7627-7638 (2016);
- [18] Nanoscale, **11**, 16488 (2019);
- [19] Adv Funct Mat, **27**, 1605997 (2017);
- [20] ACS nano, **12**, 6523-6535 (2018);
- [21] PNAS **116**, 4044-4053 (2019);
- [22] ACS nano, **14**, 1406-17 (2020);
- [23] ACS nano, **15**, 9783-9795 (2021).

Oral Presentations

| | | |
|-------------------|---|----|
| Soudabeh Arsalani | <i>Influence of temperature on the relaxation signal of magnetic nanoparticles by magnetorelaxometry</i> | 32 |
| Findan Block | <i>Magnetic bucket brigade networks as rails for single cell transportation</i> | 33 |
| Zoe Boekelheide | <i>Theoretical calibration factors of AC magnetometers for measuring magnetic fluid magnetization</i> | 34 |
| Maïkane Deroo | <i>Innovative dynamic detection for early diagnosis with a lab-on-a-chip based on "two-stage" giant magnetoresistance sensors</i> | 35 |
| Mariia Efremova | <i>Room-temperature synthesis of AuFe solid solution nanoparticles and their transformation to Au/Fe Janus nanostructures</i> | 36 |
| Santiago Helbig | <i>Single-domain particle heating in a viscous fluid</i> | 37 |
| Celia Sousa | <i>Magnetic properties of Fe vortex nanodiscs and nanowires for emerging biomedical applications.</i> | 38 |
| Paola Tiberto | <i>Factors affecting Magnetic Particle Imaging: Challenges and Solutions</i> | 39 |
| Jim Webb | <i>Recording activity from mammalian tissue via induced biomagnetic field using colour centers in diamond</i> | 40 |

Influence of temperature on the relaxation signal of magnetic nanoparticles by magnetorelaxometry

Soudabeh Aarsalani, Patricia Radon, Maik Liebl, Uwe Steinhoff, Frank Wiekhorst

Physikalisch-Technische Bundesanstalt, Abbestrasse 2-12, D-10587 Berlin, Germany

Magnetic nanoparticles (MNPs) are a promising tool for biomedical applications such as hyperthermia and drug delivery. It is necessary for these applications to quantify and localize the therapeutic agents in the body before treatment. Magnetorelaxometry (MRX) is one of the methods that can provide this information [1]. MRX is based on the measurement of the decaying net magnetic moment from an MNP ensemble, and the signal is dependent on several parameters such as the magnetic properties and amount of MNPs, temperature of the MNP environment and applied magnetic field.

Since temperature is one of the most essential factors influencing the biological processes and reflecting the physiological activities of the body, we need to investigate the effect of temperature on the MNP relaxation more than room temperature such as body temperature or even higher in magnetic hyperthermia. In this work, the relaxation behavior at elevated temperatures from 27 °C to 75 °C for 2 sample types BNF and Perimag® (from Micromod Partikeltechnologie, Germany) with different magnetic properties in fluid and immobilized form has been investigated using our 6 channel MRX device applying a 4 mT magnetizing field. Figure 1 (a,b) shows the MRX signal for BNF and Perimag sample in fluid form at different temperatures. Both these systems show a significant decrease of their relaxation amplitude with increasing the temperature, where the thermal fluctuations are speeding up the MNP relaxation. However, for immobilized BNF sample we observed a different behavior, i.e. the relaxation amplitude increased with increasing temperature, which may be due to its higher blocking temperature compared to Perimag MNPs.

Hence, temperature has a very significant influence on the MRX signal for both fluid and immobilized samples. These results could be useful for estimating relative temperature changes of tumor region right after magnetic heating treatments by calibrating a sample at room temperature. In addition, with this technique we can select a sample with the strongest temperature dependency to apply in MRX imaging, that we are developing for human application, for disease detection such as inflammation in all human body.

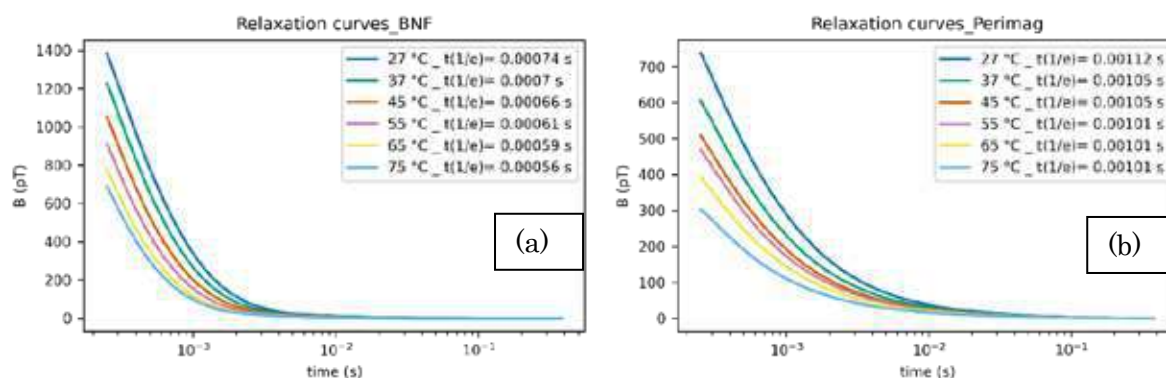


Figure 1. (a) Relaxation curves of fluid BNF and (b) Perimag system in different temperatures.

[1] M. Liebl, F. Wiekhorst, et al. Biomed. Eng.-Biomed. Tech. 2015; 60(5): 427–443.

Magnetic bucket brigade networks as rails for single cell transportation

F. Block¹, F. Klingbeil¹, U. Sajjad¹, C. Arndt², S. Sindt², D. Seidler¹,
C. Selhuber-Unkel² and J. McCord¹

¹ Institute for Materials Science, Kiel University, Kaiserstraße 2, 24143 Kiel, Germany

² Institute for Molecular Systems Engineering (IMSE), Heidelberg University,
Im Neuenheimer Feld 253, 69120 Heidelberg, Germany

A key feature for all kind of transport mechanisms is a comprehensive and flexible infrastructure. In that context, bucket brigades represent an efficient concept for the handling of water buckets or for analog delay lines. Transferring these concepts to a microscopic structure level allows a flexible and efficient transfer of biological cells to different destinations on a microchip. Single cell control is an important feature in modern biomedicine as for example in fields as immunology, gene sequencing, cell force analysis, or tissue engineering. Magnetic microbeads (MBs) turned out to be versatile carriers for biological cells in fluidic environments. Using these in combination with structured ferromagnetic thin films and in-plane magnetic fields provide controllable and computable motion patterns [1, 2]. Lined up magnetic

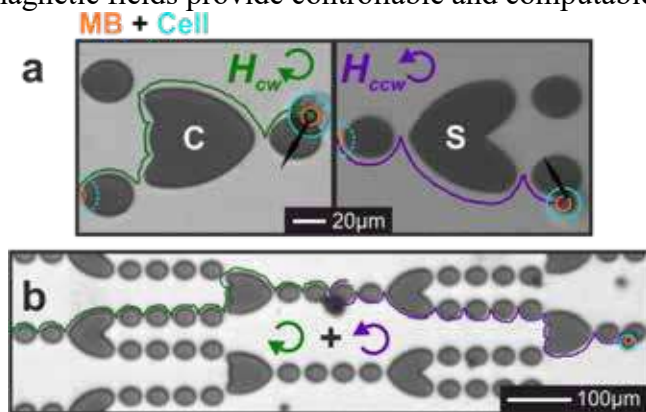


Figure 1: Transport of REF cells labelled with magnetic beads along ferromagnetic elements. (a) Cell trajectories around collecting (C) and switching (S) elements for clockwise (cw) and counter-clockwise (ccw) rotating magnetic fields. (b) Long distance transport of a REF cell along a network of multiple elements with combined cw and ccw magnetic field rotation.

oval elements exhibit a unidirectional flow less transport mechanism using different radii of curvature [3]. Here, a network of different magnetic elements featuring in situ steering of rat embryonic fibroblast (REF) cells is presented. Simple oval structures form the basic transport elements, exhibiting a rectifying motion scheme. Modifying the base oval structures various functionalities can be included in the transportation scheme dependent on the rotation sense of an external magnetic field. Caved oval elements enable transportation breakpoints, blocking the particle motion for one sense of field rotation, and releasing

them for the opposite one. Bifurcation elements are realized that guide MBs and cells along different paths, again with the field rotation direction as the decisive parameter, while nearly reversely built unification elements collect carriers back on a single track. By these building blocks, flexible magnetic transport networks are constructed to program the movement of microspheres and fibroblasts over long distances. The platform constitutes an integrable multifunctional system featuring a backflow free transport scheme with great capabilities for future lab-on-a-chip technologies. All data is backed up by numerical simulations. The flexibility of cell steering of the system will be demonstrated on various examples.

J.M. and F.B. acknowledge funding by the Deutsche Forschungsgemeinschaft through DFG MC 9/13-2.

[1] U. Sajjad, R. B. Holländer, F. Klingbeil and J. McCord, *J. Phys. D. Appl. Phys.* **50**, (2017).

[2] U. Sajjad, E. Lage, J. McCord, *Adv Mater. Interfaces* **5**, (2018)

[3] F. Block, F. Klingbeil, S. Deshpande, U. Sajjad, D. Seidler, C. Arndt, S. Sindt, C. Selhuber-Unkel and J. McCord, *Appl. Phys. Lett.* **118**, (2021).

Theoretical calibration factors of AC magnetometers for measuring magnetic fluid magnetization

Henry Steintal¹, Zoe Boekelheide¹

¹Lafayette College, Easton, Pennsylvania, USA

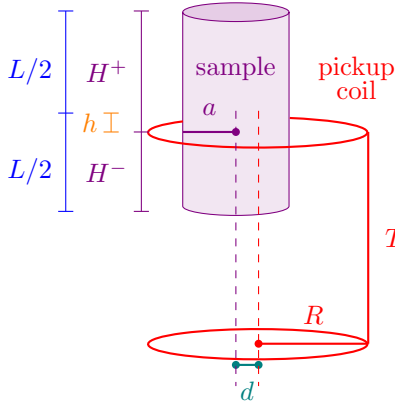


Figure 1: Model geometry.

AC magnetometers for magnetic nanoparticles in fluid are gaining popularity as the applications of magnetic nanoparticle fluids at AC frequencies, such as magnetic hyperthermia and magnetic particle imaging, increase[1]. A typical geometry is two counterwound pickup coils, with a cylindrical vial sample inserted in one of the coils, in a first-order gradiometer style (Fig. 1). Constraints on the size and shape of the pickup coils, the sample vial, and the near-uniform magnetic field region lead to a geometry in which the sample is too small to approximate as a long rod but too large for a point-dipole approximation, which makes a theoretical relationship between the pickup coil signal and sample magnetization unstraightforward.

We modelled the sample as a uniformly magnetized cylinder[2] with radius a and magnetization M . We calculated the flux Φ_B through both pickup coils, normalized by $\mu_0 M \pi a^2$. We called $\Phi_B / \mu_0 M \pi a^2 = X$, the calibration factor, which depends only on the dimensions (L , T , R , h , and d shown in Fig. 1). Thus, as long as the dimensions are known, X can be found from the model, and the relationship between the pickup coil signal $\int \varepsilon dt$ and magnetization of the sample M can be found from Faraday's Law.

Fig. 2 shows the calculated calibration factor X for a range of dimensions R/a and L/a . Note that in the limit $R/a \rightarrow 1$ and $T/a \rightarrow \infty$, the situation is described by the fluxmetric demagnetization factor N_f , with $X = 1 - N_f$ [3]. Calibration factors for miscentered samples (d/a or $h/a \neq 0$) will also be shown.

Theoretical calibration factors are valuable because they can show how the measured signal changes with deviations in geometry, e.g. due to meniscus, evaporation, or sedimentation.

[1] I. Rodrigo et al, *Int. J. Hypertherm.* **37**, 976 (2020).

[2] A. Caciagli et al, *JMMM* **456**, 423 (2018).

[3] D. X. Chen et al, *IEEE Trans. Mag.* **27**, 3601 (1991).

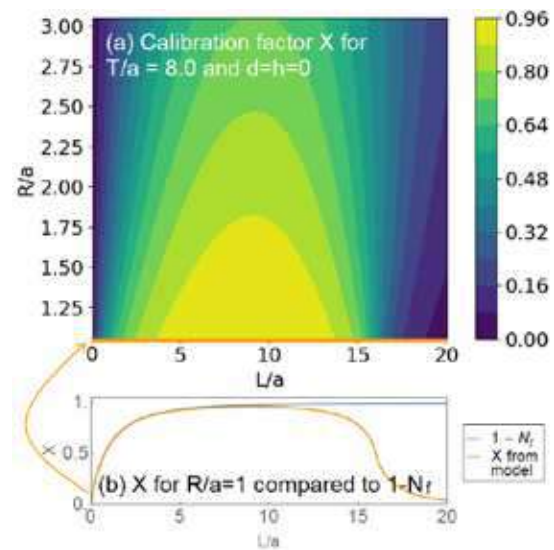


Figure 2: (a) X for a range of R/a and L/a , for $T/a = 8.0$ and $d = h = 0$. (b) Comparison of $1 - N_f$ and X for $R/a = 1$.

Innovative dynamic detection for early diagnosis with a lab-on-a-chip based on “two-stage” giant magnetoresistance sensors

M. Deroo¹, M. Giraud¹, F.D. Delapierre¹, M. Jeckelmann¹, P. Bonville¹, A. Solignac¹, M. Thévenin¹, F. Coneggo¹, E. Paul¹, C. Fermon¹, S. Simon², C. Féraudet-Tarisse² and G. Jasmin-Lebras¹

¹CEA/DRF/IRAMIS/SPEC/LNO: Orme des merisiers bat 772 CP 135 - 91191 Gif-sur-Yvette France

²CEA/DRF/DMTS/JOLIOT/SPI/LERI: SPI Bât. 136 - 91191 Gif-sur-Yvette France

The development of early diagnosis techniques, that are fast, sensitive, inexpensive and point of care, is a challenge in the field of health but also in the field of defense or the environment. Currently, among the easy-to-use early diagnostic devices, there are strip tests in which the targets migrate in the cellulose. Other methods used routinely in biology laboratories, such as ELISA or PCR tests, have better sensitivities but require a qualified staff. Optical detection is still not suitable for some opaque matrices and electrochemical or static magnetic detection have too many non-specific interactions. In this context, we propose a patented biochip, based on Giant MagnetoResistance (GMR), to detect biological objects in very small quantities, in complex matrices without a prior washing step. This approach is based on the use of magnetic nanoparticles functionalized by monoclonal antibodies, directed against target biological objects. Their dynamic detection, after interaction with the magnetic nanoparticles, is carried out using GMR sensors which allow to count the magnetically targeted biological objects one by one.

Very promising results were obtained with a first GMR biochip [1] based on GMR sensors placed under the microfluidic channel, developed on a eukaryotic cell model, allowing reaching sensitivities and specificities equivalent to those obtained on the same biological model in ELISA tests, with a greater ease of use and a slight time gain. Until now, the main limitation has been the bead aggregates that lead to false positives.

The new patented biochip [2] has sensors arranged face to face on either side of the microfluidic channel, which allow each magnetic object to be detected simultaneously. For the first time, thanks to this technique, it is possible to determine the magnetic moment of the objects flowing in the channel and thus to discriminate the aggregates of beads from the targeted biological objects. This detection technique allows to obtain a sensitivity 30 times higher than that obtained with the Elisa test or with the first prototype. Moreover, this device is inexpensive, transportable and it is possible to easily adapt the height of the channel to the size of the biological objects studied. It therefore has the potential to become a very competitive early field diagnostic tool.

[1] Giraud, M.; Delapierre, F.D.; Wijkhuisen, A.; Bonville, P.; Thévenin, M.; Cannies, G.; Plaisance, M.; Paul, E.; Ezan, E.; Simon, S.; Fermon, C.; Féraudet-Tarisse, C.; and Jasmin-Lebras, G. Evaluation of In-Flow Magnetoresistive Chip Cell-Counter as a Diagnostic Tool. In: Biosensors. Vol. 9, n° 3, pp. 105. 31st August 2019.

[2] French Patent n° 1855217 (extended by international agreement), C. Fermon, M. Giraud, F.D. Delapierre, G. Jasmin.

Room-temperature synthesis of AuFe solid solution nanoparticles and their transformation to Au/Fe Janus nanostructures

Mariia Efremova³, Marina Spasova², Markus Heidelmann³, Ivan S. Grebennikov³, Zi-An Li², Anastasiia S. Garanina⁴, Iana O. Tcareva⁴, Alexander G. Savchenko⁴, Michael Farle², Natalia L. Klyachko⁵, Alexander G. Majouga^{4,6}, Ulf Wiedwald²

¹ *Department of Applied Physics, Eindhoven University of Technology, Cascade, P.O. Box 513, 5600 MB Eindhoven, Netherlands*

² *Faculty of Physics and Center for Nanointegration Duisburg-Essen, University of Duisburg-Essen, Lotharstr. 1, 47057 Duisburg, Germany*

³ *ICAN - Interdisciplinary Center for Analytics on the Nanoscale and Center for Nanointegration Duisburg-Essen, University of Duisburg-Essen, Carl-Benz-Str. 199, 47057 Duisburg, Germany*

⁴ *National University of Science and Technology «MISIS», Leninsky Pr. 4, 11999 Moscow, Russia*

⁵ *Department of Chemistry, Lomonosov Moscow State University, Leninskie gory 1, 119991 Moscow, Russia*

⁶ *D.Mendeleev University of Chemical Technology of Russia, Miusskaya Pl. 9, 125047 Moscow, Russia*

In the present work, we show the synthesis of AuFe solid solution nanoparticles (NPs), for the first time in ambient conditions, by the methods of colloidal chemistry previously established for a Fe₃O₄-Au core-shell morphology [1]. These AuFe NPs preserve the fcc structure of Au with paramagnetic Fe ions incorporated. Interestingly, the solid solution is metastable at room temperature forming Fe-rich regions in the Au matrix during storage. By *in situ* annealing experiments up to 700°C in a transmission electron microscopy and vibrating sample magnetometry, we prove the segregation of metallic Fe from the AuFe solid solution finally forming Au/Fe Janus NPs. The ferromagnetic bcc Fe (estimated T_C = 1006 K) grows epitaxially on low index fcc Au planes. Therefore, this study provides new insights into the established synthesis of core-shell NPs suggesting completely different underlying mechanisms and final structures. It facilitates the reassessment of possible applications of such NPs leading to a new material for magnetoplasmonics.

We obtained preliminary data on the optical properties of AuFe NPs, which proves the presence of the expected plasmon resonance peak at 533 nm. Remarkably, the Fe dissolved in the Au matrix does not alter the Au plasmon peak significantly at similar sizes. We also tested the viability of human cancer cell lines LNCaP and PC-3 in the presence of AuFe NPs coated with the sulfur-containing derivative of polyethylenglycol (2000 Da). The results indicate that the NPs are non-toxic for these cells for the entire tested concentration range up to 150 µg/mL Au after 48 hours of co-incubation. While large-scale production of Janus Au/Fe NPs with segregated iron and gold phases still has to be optimized, we believe that this new preparation route will allow for a variety of theranostic applications such as magnetic hyperthermia combined with photothermal therapy as well as dual-mode contrast agents for magnetic resonance imaging and computer tomography.

M.E. gratefully acknowledges the support of the Humboldt Research Fellowship for Postdoctoral Researchers provided by the Alexander von Humboldt Foundation and the support of the Add-on Fellowship for Interdisciplinary Life Science provided by the Joachim Herz Foundation.

[1] M.V. Efremova, M. Spasova, M. Heidelmann, et al., *Nanoscale* **13** (2021), 10402-10413

Single-domain particle heating in a viscous fluid

S. Helbig¹, C. Abert¹, P. A. Sánchez¹, S. Kantorovich¹, and D. Suess¹

¹University of Vienna, Kolingasse 14-16, Vienna, Austria

Magnetic fluids are suspensions of magnetic nano-particles in an viscous fluid and are nowadays widely used in various technologies. Of particular interest is the application in magnetic hyperthermia for cancer therapy [1]. Here, an alternating magnetic field can be used to invoke heating processes in the magnetic fluid which lead to ablation of the cancer cells. The occurring heating mechanisms are of mechanical and magnetic nature and referred to as Brownian and Néel relaxation respectively.

Simulating the behavior of a single-domain nano-particle with uniaxial anisotropy is the first step to understanding the heating processes of magnetic fluids. In this work we want to introduce a new method that aims to combine aspects of micro-magnetism and mechanical motion. Utilizing a coupled system of torques and the Landau-Lifshitz-Gilbert equation, a fully-coupled hybrid model has been developed and used to quantify both heating processes and their individual contribution to the total heating rate. Their dependency on the field parameter becomes obvious in parameter-space plots and show clear regions of different steady-state behavior, see Fig. 1. By varying the material parameters and the viscosity of the fluid as well as including thermal fluctuations, these regions shift their position in the parameter-space of the field. The initial orientation of the anisotropy axis of the particle relative to the field axis can also lead to different steady-states for certain configurations (see "transient"-region in Fig. 1.).

Our model allows to investigate the time evolution of both the magnetization dynamics as well as mechanical motion. Moreover, the hysteresis loops that are generated by the coupled motion are used in order to derive the energy losses connected to the different heating processes. While the particle is submitted to the alternating field, the system tends to a state of least energy dissipation and periodic behavior of magnetization and anisotropy axis. During an initial transient phase the particles behavior might change from one relaxation mechanism to the other before finally settling in its steady-state. In the conference talk the occurring processes will be discussed in more detail and visualized with the help of animations.

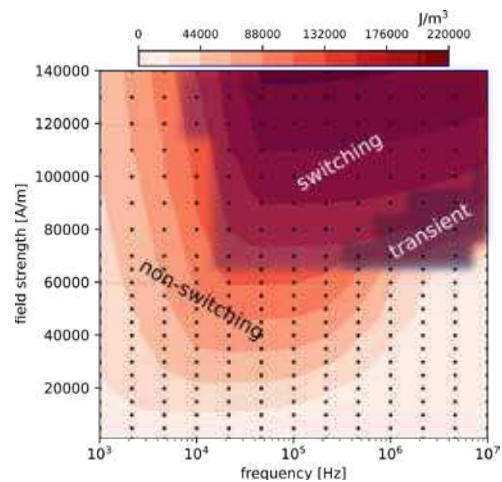


Figure 1: The energy dissipation (red contours) and different steady-state regions (dark overlays) for a magnetic nano-particle depending on frequency and field strength.

[1] E. A. Périgo *et al.*, *Appl. Phys. Rev.* **2**, 041302 (2015).

Magnetic properties of Fe vortex nanodiscs and nanowires for emerging biomedical applications.

C.T. Sousa^{*1,2}, R. Magalhães¹, S. Caspani¹, D. Navas³, C. Redondo⁴, R. Morales^{4,5,6}, S. Lima⁷, C. Nunes⁷, S. Reis⁷ and J.P. Araújo¹

¹ IFIMUP and DFA, FCUP, 4169 Porto, Rua do Campo Alegre 1021/1055, Portugal

² Departamento de Física Aplicada, UAM, Campus de Cantoblanco, Madrid, Spain

³ ICMN-CSIC, Sor Juana Ines de la Cruz 3, 28049 Madrid, Spain

⁴ Dpto. de Química-Física, Universidad del País Vasco UPV/EHU, 48940 Leioa, Spain.

⁵ Dpto. de Química-Física & BCMaterials, UPV/EHU, 48940 Leioa, Spain

⁶ IKERBASQUE, Basque Foundation for Science, 48011 Bilbao, Spain

⁷ LAQV, REQUIMTE, Faculty of Pharmacy of Porto University, Portugal.

* celiasousa@fc.up.pt

Some magnetic nanostructures (MNS) present a unique spin arrangement in the magnetic ground state, namely spin-vortex or synthetic antiferromagnetic state. MNS showed promising results in cell separation, as a contrast enhancing agents in MRI and in magneto-mechanically induced cell annihilation [1]. Magneto-mechanically induced cell annihilation is a competitive technique with MFH for cancer therapy, where instead of superparamagnetic particles, micro/nano-discs in the spin-vortex state or synthetic antiferromagnetic nanostructures are employed. The main advantages of this novel approach are the usage of weaker magnetic fields with lower frequencies, as well as the need for a lower concentration of particles. In this work, we developed one subset of biocompatible magnetic nanostructures that exhibit a spin-vortex state with interest in analysing their application in magneto-mechanically induced cell death. First, micromagnetic simulations, using mumax3 of sub-micron iron discs and nanowires, were performed for different interdot distance and aspect-ratio (thickness/diameter), to better understand the magnetic behaviour of these nanostructures. By analysing the nucleation and annihilation fields, as well as the magnetic susceptibility, it was found that the (ideal) discs could be considered as isolated for interdot distances greater than twice the radius of the disc ($2R$) [2]. We also found that discs with an aspect ratio between 5 and 15 should sustain the vortex state in remanence. Iron nano-discs, with a diameter of about 500 nm, were fabricated by electron beam evaporation on a Si substrate pre-patterned by interference lithography [3], whereas Fe nanowires with 50 nm in diameter and length ranging from 10 to 300 nm were fabricated by a template assisted method [4]. The synthesized nanostructures showed the desired vortex state configuration. The obtained magnetic measurements are in good agreement with the micromagnetic simulations. Then, the magnetic vortex nanostructures were released from the substrate by chemical etching of a sacrificial layer. Subsequently, cell viability and uptake assays were performed in a human leukaemia monocyte cell line (THP-1). Several concentrations of nanostructures were studied by flow cytometry. As a result, the discs were internalized by the cells and found to be innocuous to them, in the absence of an external magnetic field.

References

- [1] L. Peixoto, R. Magalhães, D. Navas, S. Moraes, C. Redondo, R. Morales, J. P. Araújo, C.T. Sousa, Appl. Phys. Rev., 7 (2020) 011310.,
- [2] L. Peixoto, C. Sousa, D. Navas, and J. P. Araújo, EPJ Web of Conferences 233 (2020) 05002.
- [3] B. Mora, A. Perez-Valle, C. Redondo, M.D. Boyano, R. Morales, ACS Appl. Mater. Interfaces 10 (2018) 8165.
- [4] S. Caspani, S. Moraes, D. Navas, M.P. Proenca, R. Magalhães, C. Nunes, J.P. Araújo, C.T. Sousa, Nanomaterials 11, 2729 (2021).

Factors affecting Magnetic Particle Imaging: Challenges and Solutions

Gabriele Barrera¹, Paolo Allia¹, and Paola Tiberto¹

¹ I. INRIM, Advanced materials metrology and life sciences, Strada delle Cacce 91, I-10135 Torino, Italy.

Magnetic Particle Imaging (MPI) has emerged as a novel tomographic technique [1] with widespread prospective applications in bio-medicine as a standalone method of diagnostic imaging and as a diagnostic tool in therapies for precision nanomedicine.

In this work we study the factors affecting the magnetic response of realistic systems of nanoparticles of magnetite submitted to a sinusoidal driving field $H(t)$ of magnitude and frequency appropriate to typical MPI operations. The model makes use of a set of magnetic rate equations which give the time-dependent magnetization $M(t)$ over a wide interval of driving-field frequencies [2]. The magnetic behaviour of arrays of magnetite particles (including effects of magnetic hysteresis and dipolar interaction) pose some challenges to the existing methods of analysis exploited to produce a MPI map.

In fact, the present-day working principle of MPI is based on detection and analysis of the magnitude of the third harmonic of the $M(t)$ waveform under the assumptions that the magnetic response of nanoparticles is not characterized by magnetic hysteresis at the operating frequency and that particles are ideally noninteracting. We show that both assumptions are not correct for the magnetite nanoparticles currently used in MPI.

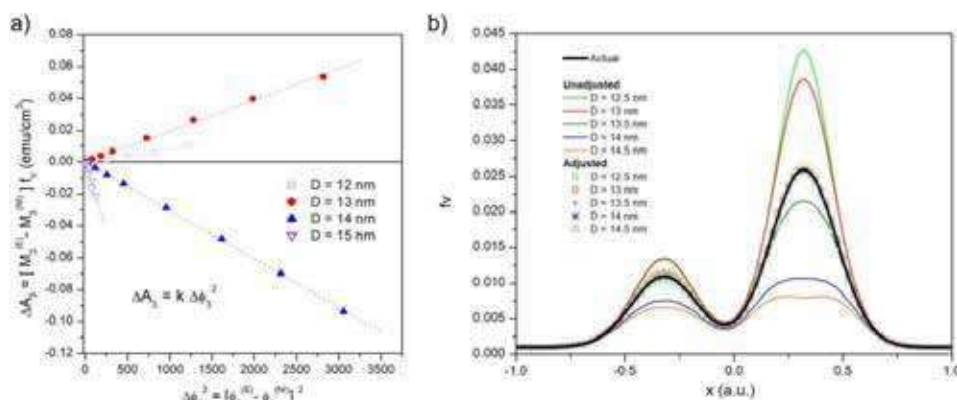


Fig. 1 a) Linear relationship between variation of the magnitude of the third harmonic of the signal with respect to the noninteracting case (ΔA_3) and the square of the variation of the corresponding phase shift ($\Delta \phi_3^2$); b): check of the validity of the adjustment procedure in one dimension.

In the presence of dipolar interaction the particle concentration estimated through the standard procedure can be significantly different (either by excess or by defect) from the real value. We show that making a more complete use of the information contained in the third harmonic of $M(t)$ (basically, measuring not only its magnitude but also its phase shift with respect to the driving field) it is possible to overcome this difficulty by an appropriate technique of signal adjustment making use of the same type of settings as found in present-day MPI operating devices (Figure 1a). The validity of the proposed adjustment procedure has been checked by means of a proof of concept using a nanoparticle concentration which is non uniform in space (Figure 1b).

[1] B. Gleich, Principles and Applications of Magnetic Particle Imaging, 2013, Springer Vieweg, Wiesbaden 2012

[2] G. Barrera, P. Allia, P. Tiberto Nanoscale, 2021, 13, 4103

Recording activity from mammalian tissue via induced biomagnetic field using colour centers in diamond

James Webb¹, Luca Troise¹, Nikolaj Winther Hansen², Christoffer Olsson³, Leo Tomasevic⁴, Ovidiu Brinza⁵, Jocelyn Achard⁵, Robert Staacke⁶, Michael Kieschnick⁶, Jan Meijer⁶, Axel Thielscher³, Hartwig Roman Siebner^{4,7}, Jean-Francois Perrier², Kirstine Berg-Sørensen², Alexander Huck¹, Ulrik Lund Andersen¹

¹ Department of Physics, Technical University of Denmark, Kongens Lyngby, Denmark

² Department of Neuroscience, University of Copenhagen, Copenhagen, Denmark

³ Department of Healthcare Technology, Technical University of Denmark, Kongens Lyngby, Denmark

⁴ Danish Research Center for Magnetic Resonance, Center for Functional and Diagnostic Imaging and Research, Copenhagen University Hospital, Hvidovre, Denmark

⁵ LSPM, Université Sorbonne Paris Nord, Villetaneuse, France

⁶ Felix Bloch Institute for Solid State Physics, Leipzig University, Leipzig, Germany

⁷ Department of Clinical Medicine, Faculty of Health and Medical Sciences, University of Copenhagen, Copenhagen, Denmark

The sensing and recording of electrical activity in living organisms is essential for both developing physiological understanding and for medical diagnosis of disease. Such activity can be monitored by invasive electrical probes, but this risks potentially fatal damage to healthy tissue. A noninvasive alternative is to monitor the biomagnetic field induced by the movement of ionic charge. Such fields are extremely small (femto- to pico-tesla), making signal recovery challenging.

In recent years, a new biocompatible technique has emerged with the capability to record such biomagnetic signals using colour centers in solid state materials. Such point defects can have optical properties highly sensitive to magnetic field, as well as strain and temperature. In particular, nitrogen-vacancy (NV) centers in diamond [1] have proven highly suitable, capable of high sensitivity recording of magnetic field under ambient conditions.

Here, we report on our experiments using NV centers to recover biomagnetic signals from living tissue *in vitro*. Using electrical and optogenetic stimulation, we are able to trigger and record compound action potentials and excitatory postsynaptic potentials from muscle tissue [2] and from the brain (corpus callosum) of mice, with high stability over the course of many hours. We show that by using signal filtering techniques, we can recover these signals in an ordinary laboratory environment, without the need for extensive shielding against background magnetic noise. Finally, we discuss prospects of biosignal propagation imaging via the induced biomagnetic field using an NV center widefield microscope.

[1] Taylor et al., Nature Physics, vol. 4, pp 810–816 (2008), doi: 10.1038/nphys1075

[2] Webb et al., Scientific Reports 11, 2412 (2021), doi: 10.1038/s41598-021-81828-x

Posters

| | | |
|----------------------|---|----|
| Yuko Ichiyanagi | <i>Magnetic susceptibilities at low magnetic fields and 3rd harmonic response of Cu-Zn ferrite nanoparticles for MPI applications</i> | 42 |
| Anca Emanuela Minuti | <i>A ferrofluid based on Fe-Cr-Nb-B magnetic particles for biomedical application</i> | 43 |
| Hidegori Nakagawa | <i>An ELF magnetic Control Study for Metamorphic Qualities in Thyroxine-Administrated Axolotls (<i>Ambystoma mexicanum</i>)</i> | 44 |

Magnetic susceptibilities at low magnetic fields and 3rd harmonic response of Cu-Zn ferrite nanoparticles for MPI applications

Kentaro Nashimoto¹, Takeshi Sakamoto¹, and Yuko Ichiyanagi^{1,2}

¹ Dept. of Phys., Grad Sch. of Eng., Yokohama National Univ., 79-5 Tokiwadai, Hodogaya, Yokohama, Kanagawa 240-8501 Japan

² Graduate School of Science, Research Center for Thermal and Entropic Science Osaka University, 1-1 Machikaneyama-cho, Toyonaka, Osaka 560-0043 Japan

Magnetic nanoparticles have attracted attention for their applications in various fields, including magnetic recording, electronic devices, and biomedical materials. Cu-Zn ferrite nanoparticles encapsulated in amorphous SiO₂ with particle sizes of approximately 17 nm were prepared for the estimation for magnetic particle imaging (MPI). The composition of Cu and Zn ions were varied and DC magnetization, AC magnetic susceptibility, and 3rd harmonic response were observed. The composition of Cu_{0.5}Zn_{0.5}Fe₂O₄ showed the largest magnetization value with superparamagnetic behavior. Interaction between particles were also considered by varying the amount of SiO₂ covering the particles.

Measurement system to observe the harmonic components was constructed (Fig.1). The 3rd harmonic response of Cu_{0.5}Zn_{0.5}Fe₂O₄ with various amount of SiO₂ was measured at AC magnetic field of $f = 500$ Hz, $h = 50$ Oe. The fundamental and harmonics were measured simultaneously using a lock-in amplifier. The interparticle distance was varied with SiO₂ content. As a result, the optimal distance between the particles for harmonic response was found depending on the SiO₂ amount. The highest harmonic components were found when the metals to silicon ratio was 3:2 (Fig.2). The imaginary part of AC magnetic susceptibility χ'' suggested that the sample with higher amount of SiO₂ consumed more energy for heat dissipation.

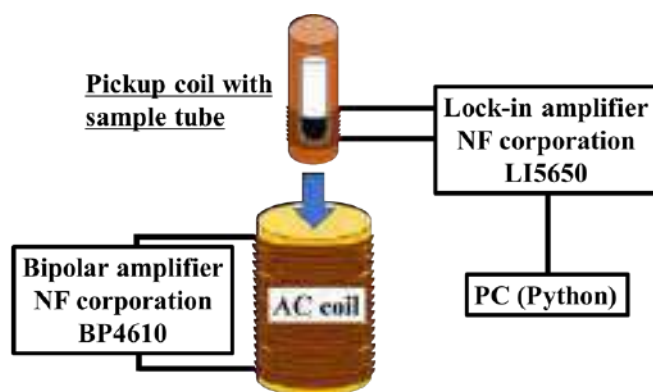


Figure 1: Measurement system of harmonic components at AC magnetic field.

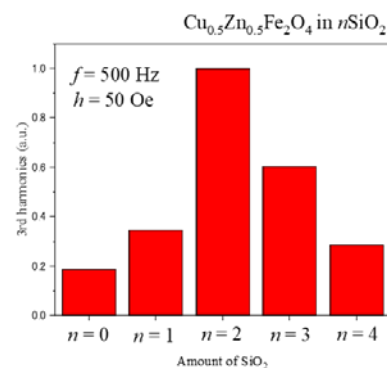


Figure 2: The 3rd harmonic response strength depending on SiO₂ amount for Cu_{0.5}Zn_{0.5}Fe₂O₄ nanoparticles.

[1] B. Gleich, J. Weizenecker, *Nature*. **435**, 1214 (2005).

[2] S. Fujiwara, S. Kimura, S. Miyano, T. Ide and Y. Ichiyanagi, *J. Magn. Soc. Jpn.* **43** 59(2019)

A ferrofluid based on Fe-Cr-Nb-B magnetic particles for biomedical application

Anca Emanuela Minuti^{1,2}, George Stoian¹, Dumitru-Daniel Herea¹, Ecaterina Radu^{1,2}, Nicoleta Lupu¹, Horia Chiriac¹

¹ National Institute of Research and Development for Technical Physics, 47 Mangeron Boulevard, Iasi, Romania

² Faculty of Physics University Alexandru Ioan Cuza, 11 Carol I Boulevard, Iasi, Romania

Ferrofluids are currently studied for the possibility of using them to treat cancer through magnetic hyperthermia and magneto-mechanical actuation [1]. In our previous work, we have shown that Fe-Cr-Nb-B particles (MPs), with low Curie temperature, might be applied for cancer therapy. In this work, we prepared a stable biocompatible ferrofluid based on this new type of particles. Starting from a superferromagnetic Fe-Cr-Nb-B glassy ribbon as precursor, we were able to obtain magnetic particles in nanometric range, following a wet milling of the ribbon. The obtained particles were dispersed in a calcium gluconate solution and a stable ferrofluid was obtained. Calcium gluconate is widely used for hypocalcemia treatment and has a wide range of biomedical applications. The ferrofluid has a magnetization

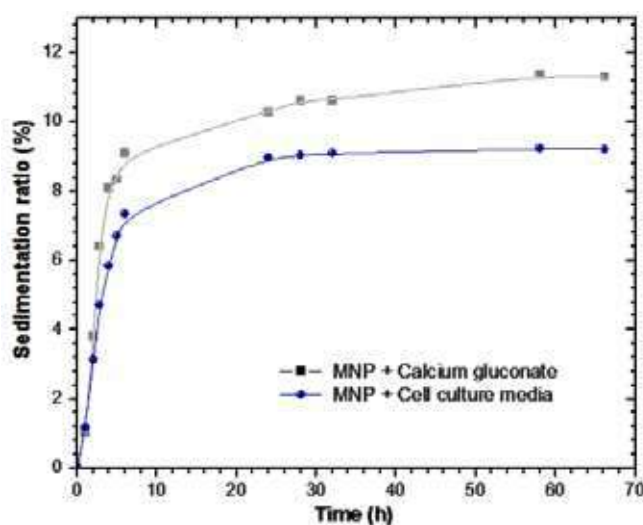


Figure 1: Sedimentation ratio of the Fe-Cr-Nb-B MPs-based ferrofluid in calcium gluconate and cell culture media

of 0.02 to 0.08 emu/cm³, depending on the particle concentration, whereas an undetectable variation of the viscosity with the magnetic field was noted. Furthermore, the sedimentation ratio of the ferrofluid appears to be under 12% after more than 60h of evaluation (Figure 1).

The ferrofluid appears to be biocompatible, as the tests on normal and tumor cell lines demonstrated, even if high ferrofluid concentration are used. In conclusion, this new type of ferrofluid showed a fine potential to be used successfully at least on in vitro

biomedical applications.

[1] H. Chiriac, E. Radu, M. Tibu, G. Stoian, G. Ababei, L. Labusca, D. D. Herea, N. Lupu, Fe-Cr-Nb-B ferromagnetic particles with shape anisotropy for cancer cell destruction by magneto-mechanical actuation. *Sci Rep.* **8**, 11538 (2018).

An ELF magnetic Control Study for Metamorphic Qualities in Thyroxine-Administrated Axolotls (*Ambystoma mexicanum*)

H. Nakagawa¹, M. Fujimoto², S. Fujiwara³ and T. Tadokoro¹

¹ Department of Electrical and Electronic Engineering, Tokyo Denki University, Tokyo, Japan

² Department of Health and Nutrition, University of Human Arts and Sciences, Saitama, Japan

³ Division of Clinical Research, CPCC, Tokyo, Japan



Figure 1:
Mexican axolotl.
(A) Leucistic.
(B) Marble.
(C) Golden.
(D) Black.
(E) Albino.
The albino and golden species have congenitally poor eyesight.

Recently, it has been shown that exposures to magnetic fields were able to affect magnetic compass orientation [1], [2], amphibian metamorphosis [3], [4], developing egg/larvae [5], [6], background adaptation [7], etc. In [8], we already showed the possibility that extremely low frequency (ELF)-field exposures might modify axolotl metamorphosis minutely, depending on the frequency, the field strength, the exposure timing, and so on. As a proof-of-concept proposal, we performed further research into the metamorphic qualities of thyroxine (T₄)-administrated axolotls.

Mexican axolotls (88 individuals, 5–12 months old, 80–160 mm) (Fig. 1) were individually kept in appropriate square boxes containing a de-chlorinated water with and without aeration. Following a soak with a thyroid hormone for 60 h, the T₄ solution was displaced by a dechlorinated water, employing an original water-renewing system (Fig. 2). Exposures of T₄-administrated axolotls to ELF fields (10 mT at 10–50 Hz) were performed using an air-cored coil system [8]. The water temperature was strictly controlled at 24°C.

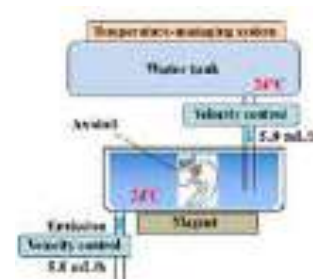


Figure 2:
Schematic illustration of water-renewing system.

To detect the differences in the metamorphic rapidity for some of the axolotl groups, we first observed the morphological changes of the axolotls inspired by the presence of T₄. As a consequence, we discovered that the initiation timings of ELF field exposure influence the rapidity, as well as the survival rates of the T₄-administrated axolotls. There was a close connection between T₄-inducing forced metamorphoses and axolotl subjects' ages. Next, we attempted the comparison between three waveform signals (sinusoidal, rectangular and sawtooth) in the metamorphic rapidity; nevertheless, the differences in the rapidity for the three kinds of waveforms were not observed. But as a noteworthy point, there were a few distinct patterns that revealed a serious indigestion in each of the salamandered bodies. Further minute analyses on the metamorphic qualities in T₄-administrated axolotls are now under investigation.

- [1] F. J. D. Rasilla *et al.*, *Behav. Processes* **118**, 1 (2015).
- [2] F. J. D. Rasilla *et al.*, *Naturwissenschaften* **97**, 1077 (2010).
- [3] M. Severini *et al.*, *Int. J. Radiat. Biol.* **86**, 37 (2010).
- [4] S. Grimaldi *et al.*, *Sci. World J.* **4** Suppl.2, 41 (2004).
- [5] M. Severini *et al.*, *Int. J. Biometeorol.* **48**, 91 (2003).
- [6] M. Asashima *et al.*, *Bioelectromagnetics* **12**, 215 (1991).
- [7] T. Leucht, *Naturwissenschaften* **74**, 192 (1987).
- [8] H. Nakagawa and M. Ohuchi, *IEEE Trans. Magn.* **54**, 5000405 (2018).

Symposium 2. Electronic structure and strongly correlated electron systems including superconductivity and superconducting spintronics

| | | |
|---------------------------|--|----|
| Giovanni Vinai | <i>Evidence of Robust Half-Metallicity in Strained Manganite Films</i> | 47 |
| Uriel A. Aceves Rodriguez | <i>Effect of superconductivity on magnetic exchange interactions</i> | 49 |
| Tadeusz Domański | <i>Dynamical effects of correlated superconducting nanostructures</i> | 50 |
| Tania Paul | <i>Interplay of excitonic correlations, quantum spin Hall effect and superconductivity in electron-hole bilayers</i> | 51 |
| Paweł Sidorczak | <i>Point Contact Spectroscopy of Interfacial Superconductivity of PbTe/SnTe Layered System with Dislocation Grid</i> | 52 |
| Vrishali Sonar | <i>Spin-dependent thermoelectric response of multi-terminal hybrid quantum dot-based device</i> | 53 |
| Irina Zajcewa | <i>Coulomb blockade in compressed $\text{La}_{1.952}\text{Sr}_{0.048}\text{CuO}_4$ thin films</i> | 54 |
| Samuel Nalevanko | <i>Increasing superconducting transition temperature of Heusler ferromagnetic superconductor Ni_2NbSn</i> | 56 |
| Liudmyla Omelchenko | <i>Pseudogap and excess conductivity in $\text{YBa}_2\text{Cu}_3\text{O}_{7-\delta}$ single crystals under electron irradiation</i> | 57 |
| Eugene Petrenko | <i>Coherence lengths determination for optimally-doped $\text{YBa}_2\text{Cu}_3\text{O}_{7-\delta}$ thin films</i> | 58 |
| Taiki Shiotani | <i>Strong Magnetism in Site-ordered C15b-type Laves-Phase Compound YMgCo_4</i> | 59 |

Invited Oral Presentation

Giovanni Vinai

Evidence of Robust Half-Metallicity in Strained Manganite Films

47

Evidence of Robust Half-Metallicity in Strained Manganite Films

G. M. Pierantozzi¹, G. Vinai¹, A. Yu. Petrov¹, A. De Vita^{1,2}, F. Motti^{1,2}, V. Polewczyk¹, D. Mondal¹, T. Pincelli^{1,2}, R. Cucini¹, C. Bigi^{1,2}, I. Vobornik¹, J. Fujii¹, P. Torelli¹, F. Offi³, G. Rossi^{1,2}, G. Panaccione¹, and F. Borgatti⁴

¹ Laboratorio TASC, IOM-CNR, Trieste I-34149, Italy

² Dipartimento di Fisica, Università degli Studi di Milano, Milano I-20133, Italy

³ Dipartimento di Scienze, Università degli Studi Roma Tre, Roma I-00146, Italy

⁴ Istituto per lo Studio dei Materiali Nanostrutturati, Consiglio Nazionale delle Ricerche (CNR-ISMN), Bologna, Italy

The electronic, magnetic, and transport properties of the mixed-valence manganite oxides with the $R_{1-x}A_x\text{MnO}_3$ perovskite structure (R = rare earth ion; A = alkaline ion) are mainly governed by the electron states of the Mn and O ions that are involved in the double-exchange (DE) mechanism, with hopping of e_g electrons favoured when the spins of the Mn ions are parallel, hence leading to a metallic ferromagnetic behavior.[1] If the exchange splitting energy between spin up and spin down states is larger than the bandwidth, half-metallicity is expected, with a 100% spin polarization at the Fermi level.

Direct evidence of half metallicity through spin-polarized photoemission spectroscopy has been achieved only in the case of optimally doped $\text{La}_{0.67}\text{Sr}_{0.33}\text{MnO}_3$,[2] while in the case of phase-coexistent films, i.e. when both metallic ferromagnetic and insulating paramagnetic domains are present, it has been indirectly proved via tunnel magnetoresistance measurements.[3]

In this presentation, we show a direct proof of half-metallic behavior in strained $\text{La}_{0.67}\text{Ca}_{0.33}\text{MnO}_3$ films by combining spectroscopic characterizations sensitive to the

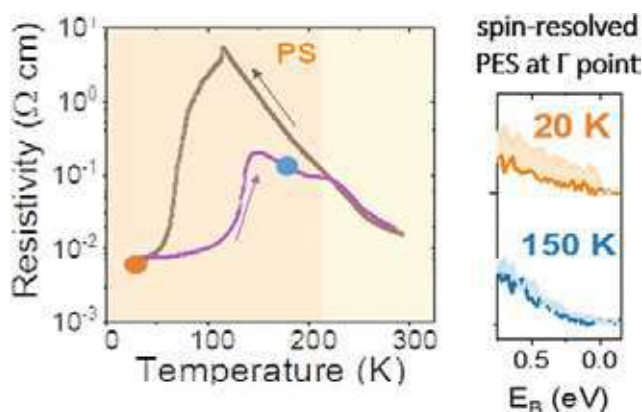


Figure 1: on the left, charge transport measurement on both heating and cooling branches; on the right, spin resolved Fermi edge at the metallic phase (orange) and in the phase separation regime (blue).

ferromagnetic order, such as spin-resolved ARPES, XAS/XMCD and MOKE, charge transport measurements. In particular, we have evidenced: a) the half-metallic character of the metallic ferromagnetic phase, with almost 100% spin polarization in the fundamental state; b) a direct link between ferromagnetism and metallicity all along the temperature dependence, from both a surface and a bulk point of view, even in the phase separation regime. Finally, combining zero field and low field (40 mT) dichroic measurements allowed us to confirm the percolative model for

phase separated manganites. This work has been recently published in *J. Phys. Chem. C*. [4]

[1] C. Zener *et al.*, Phys. Rev. **82**, 403 (1951)

[2] J. -H. Park, E. Vescovo *et al.*, *Nature* **392**, 794 (1998)

[3] W. Yang, Q. Shi *et al.*, *Nat. Commun.* **10**, 3877 (2019)

[4] G. M. Pierantozzi, G. Vinai *et al.*, *J. Phys. Chem. C* **125**, 14430 (2021).

Oral Presentations

| | | |
|---------------------------|--|----|
| Uriel A. Aceves Ridriguez | <i>Effect of superconductivity on magnetic exchange interactions</i> | 49 |
| Tadeusz Domański | <i>Dynamical effects of correlated superconducting nanostructures</i> | 50 |
| Tania Paul | <i>Interplay of excitonic correlations with quantum spin Hall effect and superconductivity</i> | 51 |
| Paweł Sidorczak | <i>Point Contact Spectroscopy of Interfacial Superconductivity of PbTe/SnTe Layered System with Dislocation Grid</i> | 52 |
| Vrishali Sonar | <i>Spin-dependent thermoelectric response of multi-terminal hybrid quantum dot-based device</i> | 53 |
| Irina Zajcewa | <i>Coulomb blockade in compressed $\text{La}_{1.952}\text{Sr}_{0.048}\text{CuO}_4$ thin films</i> | 54 |

Effect of superconductivity on magnetic exchange interactions

Uriel A. Aceves Rodriguez^{1,2}, Sascha Brinker¹, Filipe Souza Mendes Guimaraes³, and Samir Lounis^{1,2}

¹*Peter Grünberg Institut and Institute for Advanced Simulation, Forschungszentrum Jülich & JARA, 52425, Jülich, Germany*

²*Faculty of Physics & CENIDE, University of Duisburg-Essen, 47057, Duisburg, Germany*

³ Jülich Supercomputing Centre, Forschungszentrum Jülich & JARA, 52425 Jülich, Germany

Exciting phenomena occur when magnetic impurities and nanostructures couple with superconductors, giving rise to sub-gap states like Yu-Shiba-Rusinov states and Majorana zero modes; both fundamental items for the development of topological quantum computers. The interplay of spin-orbit coupling and (non-collinear) magnetism enriches the complexity and topological nature of the in-gap states hosted in proximity-induced superconductors. Nevertheless, little is known about the impact of superconductivity on the different contributions to the magnetic exchange interactions, like the bilinear isotropic exchange and the Dzyaloshinskii-Moriya interaction — and in turn the impact magnetic textures. It is necessary to have realistic methods to explore and extract information about the magnetic state and interactions in such impurity-superconductor systems. The results of explorations on these structures would have an impact not only in topological quantum computing but also nanoelectronics.

In this work, we propose a method to extract the tensor of exchange interactions in the superconducting regime as described by the Bogoliubov-de Gennes equations. Finally, with our multi-orbital tight-binding code TITAN, we investigate a Mn (110) monolayer deposited on the Nb (110) surface and analyze the magnetic interactions of the superconducting and metallic phases.

—Work funded by Horizon 2020–ERC (CoG 681405–DYNASORE).

Dynamical effects of correlated superconducting nanostructures

T. Domański¹, I. Weymann², B. Baran¹, and K. Wrzeńniewski²

¹*Institute of Physics, M. Curie-Skłodowska University, 20-031 Lublin, Poland*

²*Institute of Spintronics and Quantum Information, Faculty of Physics,
A. Mickiewicz University, 61-614 Poznań, Poland*

We study nonequilibrium phenomena driven by abrupt changes of the superconducting hybrid structures. Specifically, we consider the double quantum dot embedded between one metallic and another superconducting lead (Fig. 1) whose in-gap bound states can be used to construct, so called, Andreev qubit [1]. Practical use of this qubit would require either charge or spin operations, it is hence of essential importance to establish how such in-gap bound states react upon applying external fields.

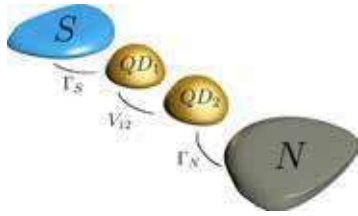


Figure 1: Schematic view of superconducting hybrid structure

In particular, we investigate the unique type of blockade evidenced recently by the Josephson [2] and the Andreev [3] spectroscopies. Its mechanism relies on prohibiting the Cooper-pairs to leak on both quantum dots whenever they are singly occupied by the identical spin electrons. This triplet-blockade regime can be tuned either by gate potentials [3] or by magnetic field [2]. We analyze how to get rid of such problematic configuration, enabling the superconducting proximity effect to develop the in-gap bound states. For this purpose we study analytically the uncorrelated heterostructure and address the correlations effects

using the time-dependent numerical renormalization group approach [4].

Furthermore, we inspect possible scenarios of the dynamical phase transitions originating from a competition of the induced on-dot pairing with the Coulomb repulsion. Quenches imposed on the quantum dot levels or their couplings to external leads can qualitatively affect the ground state configuration. We study its evolution, revealing non-analytic features in the Loschmidt amplitude in analogy to the dynamical singlet-doublet transition of the similar superconducting junction with the single quantum dot [5].

[1] M. Hays et al, *Science* **373**, 430 (2021).

[2] D. Bouman et al, *Phys. Rev. B* **102**, 220505(R) (2020);

J. C. Estrada Saldana et al, *Phys. Rev. B* **102**, 195103 (2020).

[3] P. Zhang et al, *Phys. Rev. Lett.* **128**, 046801 (2022);

D. Pekker, P. Zhang, S.M. Frolov, *SciPost Phys.* **11**, 081 (2021).

[4] K. Wrzeńniewski, B. Baran, R. Taranko, T. Domański, and I. Weymann, *Phys. Rev. B* **103**, 155420 (2021); R. Taranko, K. Wrzeńniewski, B. Baran, I. Weymann, and T. Domański, *Phys. Rev. B* **103**, 165430 (2021).

[5] K. Wrzeńniewski, I. Weymann, N. Sedlmayr, T. Domański, arXiv:2112.10126 (2021).

Interplay of excitonic correlations, quantum spin Hall effect and superconductivity in electron-hole bilayers

T. Paul¹, V.F.Becerra¹, D.I. Pikulin^{2,3}, T.Hyart⁴

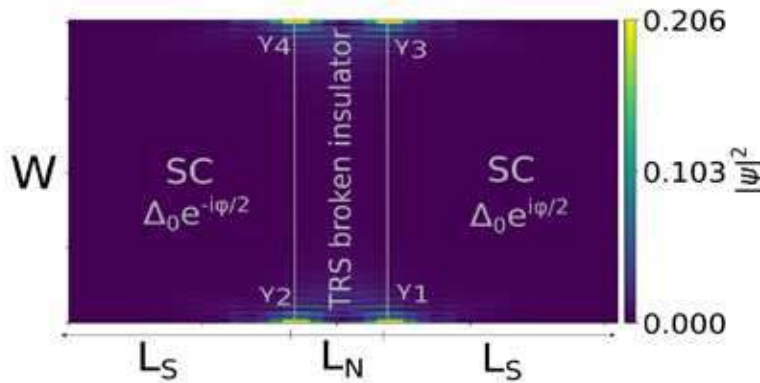
¹ International Research Center MagTop, IFPAN, Aleja Lotnikow 32/46, Warsaw, Poland

² Microsoft Quantum, Redmond, Washington 98052, USA

³ Microsoft Quantum, Station Q, Santa Barbara, California 93106-6105, USA

⁴ Department of Applied Physics, Aalto University 00076 Aalto, Espoo, Finland

It has been proposed that band-inverted electron-hole bilayers support a phase transition from an insulating phase with spontaneously broken time-reversal symmetry to a quantum spin Hall insulator phase as a function of increasing electron and hole densities. Here, we show that in the presence of proximity-induced superconductivity it is possible to realize Majorana zero modes in the time-reversal symmetry broken phase in the absence of magnetic field. We develop an effective low-energy theory for the system in the presence of time-reversal symmetry breaking order parameter to obtain analytically the Majorana zero modes and we find a good agreement between the numerical and analytical results in the limit of weakly broken time-reversal symmetry. We show that the Majorana zero modes can be detected in superconductor/time-reversal symmetry broken insulator/superconductor Josephson junctions through the measurement of a 4π Josephson current.



Superconductor/TRS broken insulator/ superconductor Josephson junction for detection of the MZMs via the 4π Josephson effect. The system supports two MZMs γ_1 and γ_2 (γ_3 and γ_4) on the bottom (top) edge with the corresponding low-energy local density of states indicated with the colors. The hybridization of the MZMs across a TRS broken regime of length L_N gives rise to a 4π -periodic component in the Josephson current-phase characteristic $I(\phi)$.

[1] D.I. Pikulin, T.Hyart, Interplay of exciton condensation and quantum spin Hall effect, Phys. Rev. Lett. 112, 176403(2014).

[2] L.Fu and C.L. Kane, Superconducting Proximity effect and Majorana Fermions at the surface of a Topological Insulator, Phys. Rev. Lett. 100, 096407(2009).

Point Contact Spectroscopy of Interfacial Superconductivity of PbTe/SnTe Layered System with Dislocation Grid

P. Sidorczak^{1,2}, W. Wołkanowicz³, R. Minikayev³, A. Kaleta³, S. Kret³,
Z. Ogorzałek¹, T. Wojtowicz², D. Wasik¹, M. Gryglas-Borysiewicz¹, K. Dybko^{2,3}

¹*Faculty of Physics, University of Warsaw, Warsaw, Poland,*

²*International Research Centre MagTop, Institute of Physics,
Polish Academy of Sciences, Warsaw, Poland,*

³*Institute of Physics, Polish Academy of Sciences, Warsaw, Poland*

The superconductivity of IV-VI semiconductor heterostructures has been a puzzling phenomenon for many years [1,2]. The underlying mechanism seems to be based on the inversion of the band structure induced by compression due to periodic dislocation grids on the interface, giving rise to topological crystalline insulator surface states. At the same time, the resulting periodically varying strain acting on these states creates topological flat bands, strongly increasing the density of states leading to superconducting phase transition [3]. However, the pairing mechanism behind this superconductivity has not yet been demonstrated to the best of our knowledge.

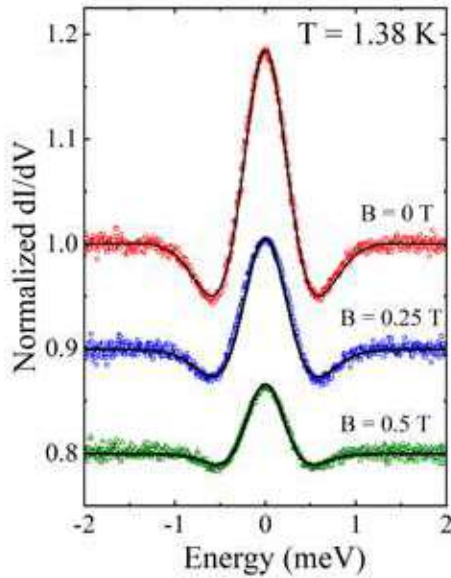


Figure 1: Measured conductance spectra (points) normalized to the value in normal state, fitted with ABM model (line).

We present yet unpublished results of soft point contact spectroscopy of PbTe/SnTe heterostructures, in which the presence of dislocations was revealed with the TEM method. The spectra show a distinct zero-bias conductance peak, which perfectly fits with the Anderson-Brinkman-Morel model for p-wave superconductors [4] in Fig. 1. At ultra-low temperatures we resolved admixture of s-type superconductivity in the spectra, most probably of the SnTe superconductivity itself ($T_c < 220$ mK [5]). We will present a discussion that sheds light on the mechanism of the unconventional superconductivity observed in this class of narrow-gap semiconductor heterostructures.

The research was partially supported by the Foundation for Polish Science through the IRA Programme co-financed by EU within SGOP and the National Science Centre (Poland) through OPUS (UMO-2017/27/B/ST3/02470) project.

- [1] K. Murase et al., *Surf. Sci.* **170**, 486 (1986)
- [2] N. Ya. Fogel et al., *Phys. Rev. Lett* **86**, 512 (2001)
- [3] E. Tang, L. Fu, *Nat. Phys.* **10**, 964 (2014)
- [4] J. C. He, Y. Chen, arXiv:2109.05202 (2021)
- [5] R. A. Hein, P. H. E. Meijer, *Phys. Rev.* **179**, 497 (1969)

Spin-dependent thermoelectric response of multi-terminal hybrid quantum dot-based device

Vrishali Sonar¹ and Piotr Trocha¹

¹*Institute of Spintronics and Quantum Information, Faculty of Physics, Adam Mickiewicz University, 61-614 Poznan, Poland*

Superconductors perfectly conduct electric current but are poor thermal conductors exhibiting small thermoelectric response. It is also known that at low temperature in a normal metal - superconductor bilayer the main contribution to the transport is due to Andreev states. However, these states reveal particle-hole symmetry and thus Andreev processes cannot alone generate any voltage when temperature gradient is applied to such a hybrid. Fortunately, this problem can be overcome by inserting quantum dot (QD) between normal metal and superconductor and making use of quasiparticle states [1]. As a result, the sign and magnitude of thermovoltage can be tuned by gate voltage applied to the dot.

Here, we consider a multi-terminal hybrid quantum dot-based system. Particularly, we investigate spin-dependent thermoelectric properties of a quantum dot coupled to one superconducting lead and two ferromagnetic metal electrodes. Such a configuration allows us to study both local and non-local spin-resolved thermoelectric response in a Cooper beam splitter device. To describe thermal properties of multi-terminal system we provide local and non-local transport coefficients like electrical and thermal conductances, thermoelectric powers and its spin counterparts. These quantities have been calculated with the help of non-equilibrium Green's function method within the Hubbard I approximation in respect to on-site dot's Coulomb repulsion. Moreover, we present the efficiency at maximum power written in terms of generalized figures of merit [2]. The main goal of the work is to show how an additional terminal changes/improves the hybrid QD-based device's performance and under which conditions non-local thermoelectric effects can be observed.

[1] P. Trocha and J. Barnaś, Phys. Rev. B **95**, 165439 (2017).

[2] F. Mazza *et al.*, New J. Phys. **16**, 085001 (2014).

Coulomb blockade in compressed $\text{La}_{1.952}\text{Sr}_{0.048}\text{CuO}_4$ thin films

I. Zajcewa¹, M. Chrobak^{2,3}, and M. Z. Cieplak¹

¹*Institute of Physics, Polish Academy of Sciences, 02 668 Warsaw, Poland*

²*AGH University of Science and Technology, Faculty of Physics and Applied Computer Science, Solid State Physics Department, al. A. Mickiewicza 30, 30-059, Krakow, Poland*

³*AGH University of Science and Technology, Academic Center for Materials and Nanotechnology, al. A. Mickiewicza 30, 30-059 Krakow, Poland*

In thin epitaxial films superconductivity may be enhanced by the strain resulting from the lattice mismatch between the film and the substrate, while perpendicular magnetic field can induce the superconductor-insulator transition (SIT). Many recent studies reveal unusual, not yet well understood effects in thin films in the vicinity of the SIT, such as, for example, the existence of metallic intermediate phase, or the development of electronic granularity on the approach to transition. This last effect is well documented by scanning tunneling experiments in case of strongly underdoped high temperature superconductors.

In this work we study: 1) the evolution of the structural and transport properties of underdoped $\text{La}_{1.952}\text{Sr}_{0.048}\text{CuO}_4$ thin films under compressive epitaxial strain; 2) current-voltage characteristics $I - V$ for two films with different thickness and different degree of built-in compressive strain.

The films are deposited from non-superconducting target with $x = 0.048$, but in thin films the superconductivity becomes apparent as a result of large, compressive, substrate-induced strain [1]. We observe that the SIT in the LSCO films is strongly dependent both on the film thickness, and on the strain. In particular, the zero-resistive superconducting state is absent in the thinner and more strained films while the temperature dependence of the magnetoresistance and $I-V$ characteristics resemble the behaviors for arrays of superconducting islands coupled by proximity effect. The Coulomb blockade effect is evidenced in one of the thin films in the mK temperature range [2]. The resistance starts to decrease with cooling and reaches the minimum. With further cooling a reentrant increase of resistance appears, reaching several orders of magnitude and saturating at lowest temperatures. The saturation is accompanied by Coulomb blockade, which resembles blockade reported for Josephson junction (JJ) arrays. However, increasing magnetic field quickly diminishes the influence of Coulomb blockade on transport, what is distinct from the behavior observed for JJ arrays. The observation of Coulomb blockade indicates that Cooper pairs survive in the insulating state, suggesting the local character of pairing.

[1] I. Zaytseva, R. Minikayev, E. Dobročka, M. Špankova, N. Bruyant, and M. Z. Cieplak, *J. Appl. Phys.* **127**, 073901 (2020).

[2] I. Zajcewa, M. Chrobak, K. Maćkosz, M. Jurczyszyn, R. Minikayev, A. Abaloszew, and M. Z. Cieplak, *Supercond. Sci. Technol.* **35** 015009 (2022).

Posters

| | | |
|---------------------|--|----|
| Samuel Nalevanko | <i>Increasing superconducting transition temperature of Heusler ferromagnetic superconductor Ni_2NbSn</i> | 56 |
| Liudmyla Omelchenko | <i>Pseudogap and excess conductivity in $\text{YBa}_2\text{Cu}_3\text{O}_{7-\delta}$ single crystals under electron irradiation</i> | 57 |
| Eugene Petrenko | <i>Coherence lengths determination for optimally-doped $\text{YBa}_2\text{Cu}_3\text{O}_{7-\delta}$ thin films</i> | 58 |
| Taiki Shiotani | <i>Strong Magnetism in Site-ordered C15b-type Laves-Phase Compound YMgCo_4</i> | 59 |

Increasing superconducting transition temperature of Heusler ferromagnetic superconductor Ni_2NbSn

S. Nalevanko^{1,2}, L. Galdun², J. Kačmarčík³, R. Varga²

¹*Institute of Physics, Faculty of Science UPJS, Park Angelinum 9, Kosice, Slovakia*

²*Centre of Progressive Materials, TIP-UPJS, Trieda SNP 1, Kosice, Slovakia*

³*UEF SAV, Watsonova 47, Kosice, Slovakia*

Increasing a superconducting transition temperature, mainly to the room temperatures, represents a hot topic nowadays. Heusler-based ferromagnetic superconductor Ni_2NbSn has a T_C of 3.4 K [1], which is relatively low for practical applications. Heusler alloys are well-known for their peculiar properties, such as ferromagnetic superconductors. [2] Since this feature was observed only at low temperatures, we have searched for new possibilities to increase the critical temperature.

The first approach of increasing the critical temperature represents the 1 % doping by elements with different atomic radii (*Ga*, *Ge*, *Sb*). The doping increases the chemical pressure in the lattice, which creates a similar effect as increasing the critical temperature by external pressure. [3] This method allows increasing the transition temperature up to 6 K.

Another approach represents changing the number of valence electrons by increasing the *Nb* and *Sn* values by 10, 15, and 20 % at the expense of *Ni*. The idea behind this method was to find a model that would describe the behavior of the critical temperature depending on the valence electron concentration. As a result, increasing the concentration of *Nb* and *Sn* was more favorable for the origin of a new high-temperature superconducting phase with the T_C of around 17 K.

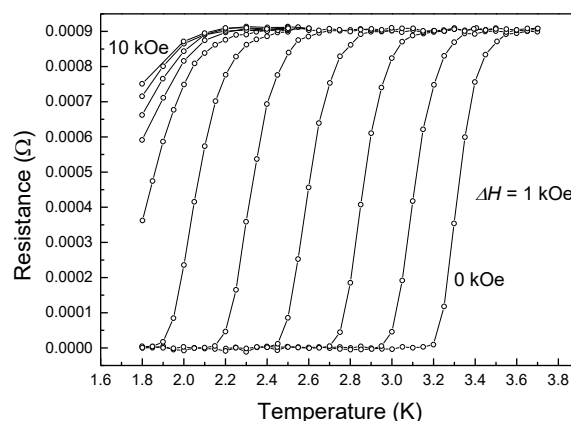


Figure 1: Temperature dependent resistance of the low-temperature phase of Ni_2NbSn

This work was supported by Slovak Grant Agency grant number APVV-16-0079 and VEGA 2/0058/20.

[1] J. H. Wernick, G. W. Hull, T. H. Geballe, et al., *Materials Letters* **2**, 90 – 90 (1983)

[2] T. Graf, C. Felser, S. S. P. Parkin, *Progress in Solid State Chemistry* **39**, 1 – 50 (2011)

[3] A. Yamato, N. Takeshita, C. Terakura, et al., *Nat Commun* **6**, 8990 (2015)

Pseudogap and excess conductivity in $\text{YBa}_2\text{Cu}_3\text{O}_{7-\delta}$ single crystals under electron irradiation

L. V. Omelchenko¹, E. V. Petrenko¹, A. L. Solovjov^{1,2}, R. V. Vovk², G. Ya. Khadzhai²

¹ *B. Verkin Institute for Low Temperature Physics and Engineering of NAS of Ukraine,
Nauky Ave., 47, Kharkiv 61103, Ukraine*

² *V. N. Karazin National University, Physics Department,
4 Svoboda Sq., 61077 Kharkiv, Ukraine
omelchenko@ilt.kharkov.ua*

Elucidation of the conditions for the occurrence of high-temperature superconductivity and the study of the physical properties of high-temperature superconductors (HTSCs) continues to be one of the most important areas of solid-state physics. Despite the fact that more than 30 years have passed since the discovery of HTSCs, its microscopic mechanism is still controversial. According to modern concepts, the key to understanding the nature of the superconducting state and various physical properties of HTSCs materials is the study of unusual phenomena that manifest themselves in these compounds in the normal state. A key issue of HTSCs physics is the study of the anomalies of the pseudogap state [1], which is observed below the pseudogap (PG) opening temperature, $T^* \gg T_c$.

The effect of electron irradiation with energy of 2.5 MeV on the temperature dependences of the resistivity $\rho(T)$ of an optimally doped $\text{YBa}_2\text{Cu}_3\text{O}_{7-\delta}$ single crystal has been studied. The temperature dependences of both fluctuation conductivity, $\sigma'(T)$, and the PG, $\Delta^*(T)$, on irradiation dose ϕ have been calculated within the local pair model. The analysis shows that with an increase in ϕ , the value of $\rho(300\text{K})$ increases linearly, while T_c decreases linearly. Concurrently, the value of $\rho(100\text{K})$ increases nonlinearly, demonstrating a feature for $\phi_3 = 4.3 \times 10^{18} \text{ e/cm}^2$, which is also observed on the number of other dose dependent parameters [2]. Regardless of the irradiation dose, in the temperature range from T_c up to T_{01} , $\sigma'(T)$ obeys the classical fluctuation theories of Aslamazov - Larkin (3D-AL) and Maki-Thompson (2D-MT), demonstrating 3D-2D crossover with increasing temperature. The crossover temperature T_0 makes it possible to determine the coherence length along the c-axis, $\xi_c(0)$, which increases by ~ 3 times under irradiation. Furthermore, the range of superconducting fluctuations above T_c also noticeably increases. At $\phi_1 = 0$, a "classical" $\Delta^*(T)$ dependence is observed with a maximum at $T_{\text{pair}} \sim 120 \text{ K}$ and a clear minimum at $T = T_{01}$. For the first time, it was determined that at $\phi_3 = 4.3 \times 10^{18} \text{ e/cm}^2$, the shape of $\Delta^*(T)$ changes significantly and becomes the same as in optimally doped $\text{YBa}_2\text{Cu}_3\text{O}_{7-\delta}$ single crystals, with a very low pseudogap opening temperature T^* and noticeably reduced T_{pair} , while at $T_c(\phi)$, there are no singularities. With an increase in the irradiation dose up to $\phi_4 = 8.8 \times 10^{18} \text{ e/cm}^2$, the shape of $\Delta^*(T)$ is restored and becomes the same as in well-structured $\text{YBa}_2\text{Cu}_3\text{O}_{7-\delta}$ films and untwined single crystals. Moreover, in this case, T_{pair} and T^* increase noticeably.

[1] R. V. Vovk, & A. L. Solovjov, *Low Temp. Phys.* **44**, 111-153 (2018).

[2] R. V. Vovk, G. Ya. Khadzhai, & O. V. Dobrovolskiy, *Solid State Commun.*, **282**, 5-8 (2018).

Coherence lengths determination for optimally-doped $\text{YBa}_2\text{Cu}_3\text{O}_{7-\delta}$ thin films

**E. V. Petrenko¹, L. V. Omelchenko¹, A. V. Terekhov¹, Yu. A. Kolesnichenko¹,
K. Rogacki², D. M. Sergeyev³ and A. L. Solovjov^{1,4}**

¹ *B.Verkin Institute for Low Temperature Physics and Engineering of NAS of Ukraine,
47 Nauky Ave., Kharkiv, 61103, Ukraine*

² *Institute for Low Temperatures and Structure Research, Polish Academy of Sciences,
P.O. Box 1410, 50-950 Wroclaw, Poland*

³ *K.Zhubanov Aktobe Regional State University,*

34 A. Moldagulova Prospect, 030000, Aktobe, Kazakhstan

⁴ *The faculty of physics, V.N. Karazin Kharkiv National University,
Svobody Sq. 4, 61022 Kharkiv, Ukraine*

Currently, there is still no comprehensive theory that could fully describe high-temperature superconductors (HTSCs). One may agree that is the most actual challenge in modern solid-state physics. Among HTSCs with a superconducting (SC) transition temperature T_c exceeding the boiling point of liquid nitrogen, scientists distinguish a class of metal oxides with an active plane CuO_2 such as $\text{YBa}_2\text{Cu}_3\text{O}_{7-\delta}$ (or YBCO), called cuprates. These type-II superconductors are known to have a strong d -wave anisotropy expressed in a low density of charge carriers, strong electronic correlations and quasi-two-dimensionality, according to a great number of studies [1, 2, 3, 4].

The high value of T_c results in short size of Cooper pairs determined by the coherence length. Depending on the given direction in a crystal lattice, the corresponding sizes of Cooper pairs in ab -plane ξ_{ab} are of an order of magnitude greater than ones along c -axis ξ_c . To determine $\xi_{ab}(T)$ and $\xi_c(T)$ coherence lengths, one needs to obtain preferably wide temperature dependences of the upper critical field $H_{c2}(T)$ in orientations of applied magnetic field both parallel to the ab -plane and c -axis.

We report in detail the comparison of the upper critical fields $H_{c2}(T)$ obtained within Ginzburg-Landau (GL) and Werthamer – Helfand – Hohenberg (WHH) theories for optimally-doped $\text{YBa}_2\text{Cu}_3\text{O}_{7-\delta}$ thin films. For different orientations of the magnetic field, the calculations give 638 and 153 T for $\mu_0 H_{c2}(0) \parallel ab$ and $\mu_0 H_{c2}(0) \parallel c$, respectively, using WHH theory. The GL theory is able to describe experiment giving much higher values of $\mu_0 H_{c2}(0)$. For the first time, we obtained the temperature dependences of coherence lengths $\xi_{ab}(T)$ and $\xi_c(T)$ within proposed theories as well as using 50% and 90% criteria of the normal state resistivity value. The WHH(0.9 ρ_N) approach gives $\xi_{ab}(0) = 14.7 \text{ \AA}$ and $\xi_c(0) = 3.5 \text{ \AA}$ which correlates with literature data.

[1] R. Haussmann, *Phys. Rev. B* **49**, 12975 (1994).

[2] V. M. Loktev, R. M. Quick, and S. G. Sharapov, *Phys. Rep.* **349**, 1 (2001).

[3] O. Tchernyshyov, *Phys. Rev. B* **56**, 3372 (1997).

[4] J. R. Engelbrecht, A. Nazarenko, M. Randeria, and E. Dagotto, *Phys. Rev. B* **57**, 13406 (1998).

Strong Magnetism in Site-ordered C15b-type Laves-Phase Compound YMgCo₄

T. Shiotani, T. Waki, Y. Tabata and H. Nakamura

Department of Materials Science and Engineering, Kyoto University, 606-8501, Kyoto, Japan

The Y-Co binary system contains several intermetallic compounds, and their magnetic properties vary significantly by the Y/Co ratio. For example, the Laves-phase compound, YCo₂, exhibits enhanced Pauli paramagnetism [1], whereas YCo₅ and Y₂Co₁₇ with the same structures as Sm-based permanent magnets are strong ferromagnets with large magnetic anisotropy as well as high Curie temperatures (T_C) and large saturation magnetization (M_s) [2,3]. In the Laves-phase compounds, RCo₂ (R : rare-earth element), generally, the Co sublattice does not show spontaneous magnetic ordering, whereas Co 3d bands are magnetically polarized by the molecular field from the R sublattice [4]. On the other hand, cobalt Laves-phase compounds consisting of a divalent alkaline metal, MgCo₂ and CaCo₂, exhibit strong ferromagnetism with relatively high T_C [5].

A recent study reported the presence of a cubic Laves phase compound, YMgCo₄, which forms a A -site ordered structure (C15b) of the cubic laves phase (C15) [6]. YMgCo₄, locating just between nearly ferromagnetic YCo₂ and strongly ferromagnetic MgCo₂, is attractive and promising for novel magnetism. If cobalt has both strong ferromagnetic correlation and local magnetic anisotropy, spin-ice-like behavior is expected in the Co sublattice forming the pyrochlore lattice. However, no physical properties have been reported because a single phase has not been extracted due to the high vapor pressure of Mg.

We have succeeded in synthesizing a single phase of YMgCo₄ by a solid-state reaction in a sealed stainless tube and confirmed by the powder X-ray diffraction measurements the presence of superstructure peak characteristic of the A -site ordered C15b structure. The magnetization of YMgCo₄ shows a typical temperature dependence of a strong ferromagnet with $T_C \approx 425$ K, which is higher than that of MgCo₂, and $M_s = 1.2 \mu_B/\text{Co}$. Zero-field NMR measurement at 4.2 K revealed the presence of ⁵⁹Co signal at around 70–110 MHz, which is roughly consistent with the above macroscopic observation.

- [1] R. Lemaire, *Cobalt* **33**, 201 (1966).
- [2] K. Nassau, L. V. Cherry, and W. E. Wallace, *J. Phys. Chem. Solids* **16**, 131 (1960).
- [3] K. Strnat, G. Hoffer, W. Ostertag, and J. C. Olson, *J. Appl. Phys.* **37**, 1252 (1966).
- [4] for example, E. Gratz and A. S. Markosyan, *J. Phys.: Condens. Matter* **13**, R385 (2001).
- [5] K. H. J. Buschow, *Solid. State. Commun.* **17**, 891 (1975).
- [6] Q. Q. Jin, and S. B. Mi, *J. Alloys Compd.* **582**, 130 (2014).

Symposium 3. Frustrated and disordered magnetism, including artificial spin ice

| | | |
|---------------------------|---|----|
| Konstantinos Papadopoulos | <i>Spin arrangements in the double perovskite $\text{LaSr}_{1-x}\text{Ca}_x\text{NiReO}_6$</i> | 62 |
| Ana Parente | <i>Topological effects in different magnetic spin ice geometries</i> | 63 |
| Benjamin Verlhac | <i>Thermally-induced magnetic order from glassiness in elemental neodymium</i> | 64 |
| Teresa Weißels | <i>Quantitative analysis of the magnetic field distribution in an artificial spin ice by off-axis electron holography</i> | 65 |
| Denis Arčon | <i>π-orbital order coupled to the spin-$\frac{1}{2}$ pyrochlore lattice in alkali-sesquioxides</i> | 67 |
| Raymond Bishop | <i>Frustrated spin-$\frac{1}{2}$ J_1-J_2-JJ_1^\perp Heisenberg magnet on a honeycomb bilayer: High-order coupled cluster study of its phase diagram</i> | 68 |
| Matjaž Gomilšek | <i>Randomness-driven Spin Liquid in a Frustrated Antiferromagnet</i> | 69 |
| Mateusz Goryca | <i>Magnetic-Field-Dependent Thermodynamic Properties of Square and Quadrupolar Artificial Spin Ice</i> | 70 |
| Zexiang Hu | <i>Multi-ring patterns in the single pulse all-optical toggle switching and partial demagnetization of amorphous DyCo_x and TbCo_x</i> | 71 |
| Sergio Magalhães | <i>Role of Geometric Frustration in a Weakly Disordered Checkerboard Lattice</i> | 72 |
| Adrian Merritt | <i>Fractional Excitation-induced Phonon Renormalization in $\alpha\text{-RuCl}_3$</i> | 73 |
| Robert Puttock | <i>Magnetic defect-driven dynamics in artificial spin ice</i> | 74 |
| Nicolas Rougemaille | <i>Ice regime and approximate of the low-energy physics of the F-model in a two-dimensional artificial vertex system</i> | 75 |
| Joao Salgado Cabaco | <i>Properties of systematically disordered Cr_2AlC thin films</i> | 76 |
| Markos Skoulatos | <i>Putative spin-nematic phase in $\text{BaCdVO}(\text{PO}_4)_2$</i> | 77 |
| Sawssen Slimani | <i>Magnetic anisotropy in CoFe_2O_4 based nanocomposite</i> | 78 |
| Takeshi Waki | <i>Pulse High-Field Magnetization of frustrated FCC magnet RInCu_4</i> | 79 |
| Pavlo Baloh | <i>Correlation between As-S nanocluster structures and low-temperature anomalies in amorphous solids</i> | 81 |
| Shruti Chakravarty | <i>Disorder driven cluster glass state in a geometrically frustrated hexagonal perovskite</i> | 82 |
| Uladzislau Makartsou | <i>Control of the magnetization in ferromagnetic rings using ferromagnetic nanoelement</i> | 83 |
| Konrad Puzniak | <i>Spin-$\frac{1}{2}$ antiferromagnetic XXZ chain $\text{BaCo}_2\text{V}_2\text{O}_8$ in a transverse external magnetic field - dispersion of E8 particles</i> | 84 |
| Konrad Puzniak | <i>Study of the spin-$\frac{1}{2}$ antiferromagnetic XXZ chain $\text{SrCo}_2\text{V}_2\text{O}_8$ in a transverse external magnetic field</i> | 85 |

Invited Oral Presentations

| | | |
|---------------------------|---|----|
| Konstantinos Papadopoulos | <i>Spin arrangements in the double perovskite $\text{LaSr}_{1-x}\text{Ca}_x\text{NiReO}_6$</i> | 62 |
| Ana Parente | <i>Topological effects in different magnetic spin ice geometries</i> | 63 |
| Benjamin Verlhac | <i>Thermally-induced magnetic order from glassiness in elemental neodymium</i> | 64 |
| Teresa Weißels | <i>Quantitative analysis of the magnetic field distribution in an artificial spin ice by off-axis electron holography</i> | 65 |

Spin arrangements in the double perovskite $\text{LaSr}_{1-x}\text{Ca}_x\text{NiReO}_6$

Konstantinos Papadopoulos¹, Ola Kenji Forslund^{1,2}, Elisabetta Nocerino²,
 Fredrik O.L. Johansson^{3,4,5}, Gediminas Simutis^{6,1}, Nami Matsubara²,
 Gerald Morris⁷, Bassam Hitti⁷, Donald Arseneau⁷, Peter Svedlindh⁸,
 Marisa Medarde⁹, Daniel Andreica¹⁰, Jean-Christophe Orain¹¹,
 Vladimir Pomjakushin¹², Lars Börjesson¹, Jun Sugiyama¹³, Martin Månsson²,
 Yasmine Sassa¹

¹Department of Physics, Chalmers University of Technology, SE-41296 Göteborg, Sweden

²Department of Applied Physics, KTH Royal Institute of Technology, SE-106 91 Stockholm, Sweden

³Division of Molecular and Condensed Matter Physics, Uppsala University, SE-752 37 Uppsala, Sweden

⁴Division of Applied Physical Chemistry, KTH Royal Institute of Technology, SE-100 44 Stockholm, Sweden

⁵Sorbonne Université, UMR CNRS 7588, Institut des Nanosciences de Paris, F-75005 Paris, France

⁶Laboratory for Neutron and Muon Instrumentation, Paul Scherrer Institut, CH-5232 Villigen PSI, Switzerland

⁷TRIUMF, 4004 Wesbrook Mall, Vancouver, BC, V6T 2A3, Canada

⁸Uppsala University, Department of Materials Science and Engineering, Uppsala University, 751 03, Uppsala, Sweden

⁹Laboratory for Multiscale materials eXperiments, Paul Scherrer Institut, CH-5232 Villigen PSI, Switzerland

¹⁰Faculty of Physics, Babes-Bolyai University, 400084 Cluj-Napoca, Romania

¹¹Laboratory for Muon Spin Spectroscopy, Paul Scherrer Institute, CH-5232 Villigen PSI, Switzerland

¹²Laboratory for Neutron Scattering and Imaging, Paul Scherrer Institute, CH-5232, Villigen, PSI, Switzerland

¹³Neutron Science and Technology Center, Comprehensive Research Organization for Science and Society (CROSS), Tokai, Ibaraki 319-1106, Japan

Double perovskite oxides are a class of multifunctional materials exhibiting various magnetic orders and electronic states. Their general composition is $\text{A}_2\text{BB}'\text{O}_6$ and can accommodate almost any of A_2 : alkaline earth or lanthanide cations and $\text{BB}'\text{O}_6$: transition metals in various oxidation states. Consequently, the structure is flexible to expand, contract and distort with cation exchanges. We use the muon spin rotation, relaxation and resonance ($\mu^+\text{SR}$) technique to study the magnetic properties of $\text{LaSr}_{1-x}\text{Ca}_x\text{NiReO}_6$ which are determined by geometry and cation exchange. With its unique length and time scales, the implantation of muons in specific crystallographic sites acts as a local magnetic probe of the static and dynamic spin arrangements. In our study we elucidate the type of ordering of the magnetic ground states for the $x=0,1$ compounds, resulting from two interacting Ni and Re magnetic sub-lattices. For $x=0$, a glassy state between $75\text{ K} > T > 23\text{ K}$ transforms into an incommensurate long-range order below $T_c=23\text{ K}$. For $x=1$, a commensurate long-range order is achieved from a metastable ferrimagnetic ordering at $T_c=103\text{ K}$ to a stable one at $T_{xy}=50\text{ K}$. A dilute moment state which was identified in both compounds with increasing temperature is eventually dissolved ($T > 250\text{ K}$) into a paramagnetic state.

Topological effects in different magnetic spin ice geometries

**A. Parente¹, M. Abuin², A. Rivelles², V. Rollano¹, I. Figueruelo³, A. Gómez⁴,
M. Menghini³, A. Muñoz-Noval^{1,3} and E. M. González^{1,3}**

¹ *Facultad CC. Físicas, Plaza Ciencias 1, Universidad Complutense, 28040 Madrid, Spain*

² *Instituto de Sistemas Optoelectrónicos y Microelectrónica (ISOM), Universidad Politécnica de Madrid, Avda. Complutense 30, 28040 Madrid, Spain*

³ *IMDEA Nanociencia, Calle Faraday 9, Campus de Cantoblanco, 28049 Madrid, Spain*

⁴ *Centro de Astrobiología INTA-CSIC, 28850 Torrejón de Ardoz, Spain*

New emergent phenomena arising from topological effects have become a very active research frontier in condensed matter physics. Artificial spin ices (ASI) are examples of magnetic interacting nanostructures which have opened a way to study topological phenomena such as frustration, emergent magnetic monopoles and phase transitions. Geometric properties of the ASI are key to determine the dynamics of the magnetic charges and the possible energetic configurations, which can also have an influence on the magnetic textures present in these systems. Furthermore, interplay between magnetism and superconductivity can lead to new effects that allow us to develop hybrid devices that synergize properties of both magnetic and superconducting (SC) materials. For example, the study of vortex dynamics in a type-II superconductor in proximity to an ASI structure can be used to analyze the magnetic textures that originate in the areas of accumulation of magnetic charges.

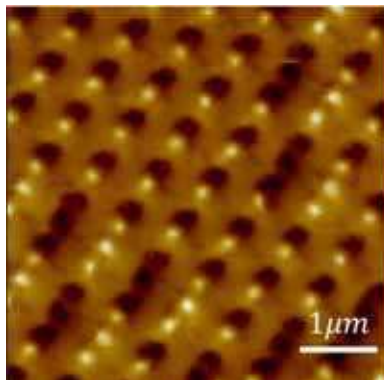


Figure 1: MFM image of a type I artificial spin ice

The main goal of this work is to characterize the magnetic properties, spin textures and frustration in ASIs with different geometries and its influence in the formation and ordering of magnetic features. ASIs with different geometries and types of topological protection will be presented. Furthermore, we study their interplay with type II superconductors through the interaction of the magnetic topological textures with superconducting vortices.

Different geometries of ASI systems had been fabricated by combining nanolithography techniques (optical and electronic lithography) and DC magnetron sputtering. Nanostructures were characterized using different microscopy techniques (AFM and SEM), magnetic force microscopy (MFM) (Fig.1), magneto-optical Kerr effect (MOKE), vibrating sample magnetometry (VSM), micromagnetic simulations, and complemented with transport measurements to study the superconductor/magnetic interaction.

Thermally-induced magnetic order from glassiness in elemental neodymium

Benjamin Verlhac¹, Lorena Niggli¹, Anders Bergman², Umut Kamber¹, Andrey Bagrov^{1,2}, Diana Iușan², Lars Nordström², Mikhail I. Katsnelson¹, Daniel Wegner¹, Olle Eriksson^{2,3}, and Alexander A. Khajetoorians¹

¹*Institute for Molecules and Materials, Radboud University, Nijmegen, The Netherlands*

²*Department of Physics and Astronomy, Uppsala University, Uppsala, Sweden — ³School of Science and Technology, Örebro University, SE-701 82 Örebro, Sweden*

In thermodynamic systems, temperature is synonymous with disorder as phase transitions between order to disorder occur when temperature is increased. Recently, the first example of a spin-Q glass was found in elemental neodymium between 30mK and 4K[1]. This phase originated from magnetic frustration within the dhcp lattice of neodymium. In this study, we show by means of spin-polarized scanning tunneling microscopy that neodymium undergoes an unusual magnetic transition, where long range multi-Q order emerges from the spin-Q glass phase as temperature is increased from 5 K to 15 K[2] (See figure). We also developed a new analysis method, which analyzes the experimental data and extracts the phase transition temperature. These findings are supported by atomistic spin dynamics simulations, in which the phase transition is qualitatively explained by destroying spin frustration due to various exchange contributions of the different sublattices.

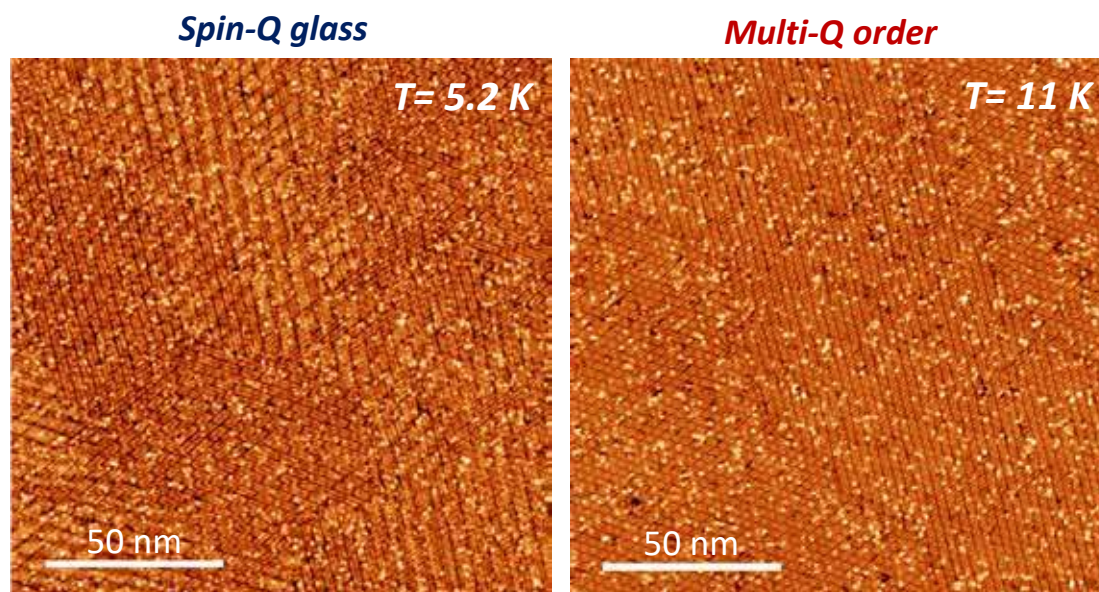


Figure: Magnetization images based on SP-STM of Nd(0001) at $T = 5.2$ K and 11 K. ($I_t = 100$ pA)

[1] Kamber, U. et al. Self-induced spin glass state in elemental and crystalline neodymium. *Science* **368**, eaay6757, (2020)

[2] Verlhac, B. et al. Thermally-induced magnetic order from glassiness in elemental neodymium. arXiv:2109.04815 [cond-mat], (2021)

Quantitative analysis of the magnetic field distribution in an artificial spin ice by off-axis electron holography

T. Weßels^{1,2}, S. Gliga³, S. Finizio³, A. Kovács², and R.E. Dunin-Borkowski²

¹ Faculty of Physics and Center for Nanointegration Duisburg-Essen (CENIDE),
University of Duisburg-Essen, Lotharstr.1, 47057 Duisburg, Germany

² Ernst Ruska-Centre for Microscopy and Spectroscopy with Electrons and
Peter Grünberg Institute, Forschungszentrum Jülich, 52425 Jülich, Germany

³ Swiss Light Source, Paul Scherrer Institut, Forschungsstrasse 111, 5232 Villigen PSI,
Switzerland

Through their collective behaviour, artificial spin ices allow desired magnetic states, dynamics and functionalities to be defined. Their emergent properties are driven by the magnetostatic coupling between elongated single-domain patterned nanomagnets, giving rise *e.g.*, to chiral dynamics [1]. In this work, we study a ‘chiral ice’ (Fig. 1(a)) by directly measuring its magnetic field distribution and reconstructing the magnetization within the nanomagnets [2].

We used off-axis electron holography in a transmission electron microscope equipped with an electron biprism to quantitatively measure the magnetic contribution to the electron optical phase shift induced by the sample. The microscope was operated in magnetic-field-free conditions in Lorentz mode. The conventional microscope objective lens was used to apply vertical magnetic fields to the sample. The projected in-plane magnetisation was retrieved from the recorded magnetic contribution to the phase shift using a model-based iterative reconstruction algorithm and compared with micromagnetic simulations.

The sample comprised permalloy nanomagnets that had been patterned onto a SiN membrane using lift-off lithography. Their magnetic interactions were studied by applying in-plane magnetic fields to the sample and subsequently recording off-axis electron holograms with the sample at remanence. The measurements revealed a zigzag magnetization distribution within the array, with stray fields that were more complex at the edges (Fig. 1(b)). The reconstructed magnetization (Fig. 1(c)) shows that the nanomagnets are in single-domain states with an average magnetic polarization of 0.73 T. The low magnetic polarization may result from an interplay between the microstructure of the sample, its composition and oxidation.

This study is supported by the DFG through CRC/TRR 270 and the European Research Council through ERC-2019-SyG project 856538.

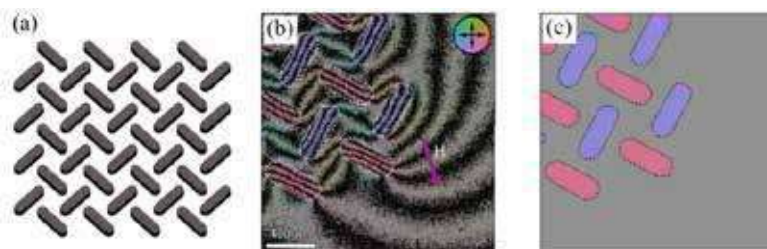


Figure 1: Magnetic state of chiral ice. (a) Sketch of sample geometry. (b) Map of projected in-plane magnetic induction. The arrow indicates the direction of the magnetic field \mathbf{H} used to saturate the sample. (c) Reconstructed projected in-plane magnetisation.

[1] S. Gliga et al., *Nature Mater.* **16**, 1106-1111 (2017)

[2] T. Weßels et al., *J. Magn. Magn. Mater.* **543**, 168535 (2022)

Oral Presentations

| | | |
|---------------------|--|----|
| Denis Arčon | <i>π-orbital order coupled to the spin-$\frac{1}{2}$ pyrochlore lattice in alkali-sesquioxides</i> | 67 |
| Raymond Bishop | <i>Frustrated spin-$\frac{1}{2}$ J_1-J_2-J_1^\perp Heisenberg magnet on a honeycomb bilayer: High-order coupled cluster study of its phase diagram</i> | 68 |
| Matjaž Gomilšek | <i>Randomness-driven Spin Liquid in a Frustrated Antiferromagnet</i> | 69 |
| Mateusz Goryca | <i>Magnetic-Field-Dependent Thermodynamic Properties of Square and Quadrupolar Artificial Spin Ice</i> | 70 |
| Zexiang Hu | <i>Multi-ring patterns in the single pulse all-optical toggle switching and partial demagnetization of amorphous DyCo_x and TbCo_x</i> | 71 |
| Sergio Magalhaes | <i>Role of Geometric Frustration in a Weakly Disordered Checkerboard Lattice</i> | 72 |
| Adrian Merritt | <i>Fractional Excitation-induced Phonon Renormalization in $\alpha\text{-RuCl}_3$</i> | 73 |
| Robert Puttock | <i>Magnetic defect-driven dynamics in artificial spin ice</i> | 74 |
| Nicolas Rougemaille | <i>Ice regime and approximate of the low-energy physics of the F-model in a two-dimensional artificial vertex system</i> | 75 |
| Joao Salgado Cabaco | <i>Properties of systematically disordered Cr_2AlC thin films</i> | 76 |
| Markos Skoulatos | <i>Putative spin-nematic phase in $\text{BaCdVO}(\text{PO}_4)_2$</i> | 77 |
| Sawssen Slimani | <i>Magnetic anisotropy in CoFe_2O_4 based nanocomposite</i> | 78 |
| Takeshi Waki | <i>Pulse High-Field Magnetization of frustrated FCC magnet RInCu_4</i> | 79 |

π -orbital order coupled to the spin-1/2 pyrochlore lattice in alkali-sesquioxides

D. Arčon^{1,2}, Ž. Gosar¹, P. Adler³, C. Felser³, H. Nojiri⁴

¹ Institute Jožef Stefan, Ljubljana, Slovenia

² Faculty of mathematics and physics, University of Ljubljana, Ljubljana, Slovenia

³ Max Planck Institute for Chemical Physics of Solids, Dresden, Germany

⁴ Institute for Materials Research, Tohoku University, Sendai, Japan

For the antiferromagnets with spins on a geometrically frustrated lattices, the conventional long range Néel magnetic order may be completely suppressed and replaced by a quantum spin liquid. The latter does not undergo any spontaneous symmetry breaking, despite strong entanglement of spins even at large spacial distances, and generally possesses high spin degeneracy, strong quantum fluctuations and unconventional fractional excitations [1]. When orbital degeneracy is superimposed on top of the geometrical spin frustration, orbital degrees of freedom can remove infinite spin degeneracy. However, as the orbital degrees of freedom have a directional character, the degeneracy of emerging states remains high. In general, the interplay of geometric frustration and orbital degeneracy can reduce magnetic dimensionality [2], lead to intricate spin-orbital quantum liquids or establish a state with a residual extensively degenerate manifold of spontaneously dimerized spins [3].

Here we report that mixed-valence alkali sesquioxides A_4O_6 (A = alkali metal) represent a distinct class of compounds showing orbital degeneracy coupled to the spin-1/2 pyrochlore lattice frustration. These anionic mixed-valence compounds with a simple cubic structure at

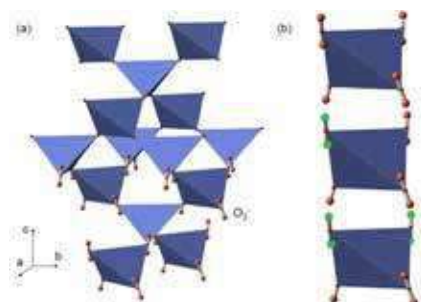


Figure 1: (a) The pyrochlore lattice of O_2^- tetrahedra in the low-temperature tetragonal phase of Rb_4O_6 . (b) Three possible $O_2^- \pi^*$ orbital orders for each individual tetrahedron.

high temperatures first undergo a structural transition to the tetragonal phase just below the room temperature that is accompanied by a charge ordering reminiscent of the Verwey transition [4,5]. The low-temperature charge-ordered phase comprises non-magnetic O_2^{2-} and magnetic O_2^- ($S = 1/2$) anions, where the latter form a geometrically frustrated pyrochlore lattice (Fig. 1a). Extensive muon spin relaxation, electron paramagnetic resonance (EPR) and nuclear magnetic resonance (NMR) over broad temperature and magnetic field range show that the coupling between spin and orbital degrees of freedom dimerizes the lattice of Rb_4O_6 , triggers the long-range orbital ordering (Fig. 1b) and opens up a spin-gap in the excitation spectrum. The spin-gap initially decreases with increasing magnetic field but the quantum phase transition to the condensed triplet phase at the critical field of 14.2 T is absent due to the Dzyaloshinskii-Moriya interaction. Nevertheless, the quantum critical phenomena of the spin-dimer state is clearly revealed from the nuclear spin-lattice relaxation rates in this field range [6]. The A_4O_6 family thus emerges as one of the very few π -electron systems showing coupling of the orbital order to a geometrically frustrated spin lattice.

[1] M. Klanjšek, D. Arčon, et al., *Nat. Phys.* **13**, 1130 (2017).

[2] M. Klanjšek, D. Arčon, et al., *Phys. Rev. Lett.* **115**, 057205 (2015).

[3] S. Di Matteo, G. Jackeli, C. Lacroix, and N.B. Perkins, *Phys. Rev. Lett.* **93**, 077208 (2004).

[4] P. Adler, P. Jeglič, D. Arčon, et al., *Sci. Adv.* **4**, eaap7581 (2018).

[5] T. Knaflič, D. Arčon et al., *Phys. Rev. B* **101**, 024419 (2020).

[6] Ž. Gosar, D. Arčon et al., submitted (2022).

Frustrated spin- $\frac{1}{2}$ J_1 - J_2 - J_1^\perp Heisenberg magnet on a honeycomb bilayer: High-order coupled cluster study of its phase diagram

Raymond F. Bishop^{1,2} and Peggy H.Y. Li^{1,2}

¹*Department of Physics and Astronomy, The University of Manchester, UK*

²*School of Physics and Astronomy, University of Minnesota, USA*

The frustrated spin- $\frac{1}{2}$ J_1 - J_2 model on the honeycomb lattice has become a prototypical model in quantum magnetism. After over 30 years of study, and several hundreds of papers devoted to it, there is no overall consensus on the details of its quantum phase diagram, particularly in the region without magnetic long-range order. By contrast, there are far fewer papers devoted to the even more challenging, analogous bilayer models. Indeed, for the particular frustrated model presented here we know of *no* other theoretical investigation using accurate modern techniques. Here we use the coupled cluster method (CCM) [1], which has become one of the most pervasive and most successful of all *ab initio* formulations of quantum many-body theory. It has been applied to more systems in quantum chemistry (where it has become the “gold standard”), quantum field theory, atomic, nuclear, subnuclear, condensed matter, and other areas of physics than any other competing method. By now it has also very successfully been applied to a wide variety of highly frustrated and strongly entangled spin-lattice systems in quantum magnetism [2].

We present results for the (zero-temperature) quantum phase diagram of the spin- $\frac{1}{2}$ J_1 - J_2 - J_1^\perp Heisenberg magnet on an AA-stacked honeycomb bilayer lattice, using the CCM implemented to very high orders [3]. On each monolayer the spins interact via nearest-neighbour (NN) and frustrating next-nearest-neighbour isotropic antiferromagnetic Heisenberg interactions with respective strength parameters $J_1 > 0$ and $J_2 \equiv \kappa J_1 > 0$. The two layers are coupled such that NN interlayer pairs of spins interact via a similar isotropic Heisenberg interaction of strength $J_1^\perp \equiv \delta J_1$, which may be of either sign. We locate with high accuracy the complete phase boundaries in the κ - δ half-plane with $\kappa > 0$ of the two quasiclassical collinear antiferromagnetic phases with Néel and Néel-II magnetic order in each monolayer, and the interlayer NN pairs of spins either aligned (for $\delta < 0$) or anti-aligned (for $\delta > 0$) to one another. Compared to the two-sublattice Néel order, in which all NN intralayer pairs of spins are antiparallel to one another, the four-sublattice Néel-II order is characterized by NN intralayer pairs of spins on the honeycomb lattice being antiparallel to one another along zigzag (or sawtooth) chains in a specified direction from among the three equivalent honeycomb-lattice directions, and parallel to one another for the corresponding NN interchain pairs.

RFB gratefully acknowledges the Leverhulme Trust (United Kingdom) for the award of an Emeritus Fellowship (EM-2020-013).

[1] R.F. Bishop, *Theor. Chim. Acta* **80**, 95 (1991).

[2] D.J.J. Farnell and R.F. Bishop, *Quantum Magnetism* (eds. U. Schollwöck, J. Richter, D.J.J. Farnell and R.F. Bishop), Lecture Notes in Physics Vol. **645**, Springer, Berlin (2004), 307.

[3] P.H.Y. Li and R.F. Bishop, eprint arXiv:2109.14390 (2021).

Randomness-driven Spin Liquid in a Frustrated Antiferromagnet

J. Khatua¹, M. Gomilšek^{2,3}, J. C. Orain⁴, A. M. Strydom^{5,6}, Z. Jagličić^{3,7}, C. V. Colin⁸, S. Petit⁹, A. Ozarowski¹⁰, L. Mangin-Thro¹¹, K. Sethupathi¹, M.S. Ramachandra Rao¹, A. Zorko^{2,3} and P. Khuntia¹

¹ Indian Institute of Technology Madras, Chennai 600036, India

² Jožef Stefan Institute, Jamova c. 39, 1000 Ljubljana, Slovenia

³ University of Ljubljana, 1000 Ljubljana, Slovenia

⁴ Paul Scherrer Institute, LMU 5232 Villigen PSI, Switzerland

⁵ University of Johannesburg, PO Box 524, Auckland Park 2006, South Africa

⁶ Max Planck Institute for Chemical Physics of Solids, 40 Nöthnitzerstr., Dresden D-01187, Germany

⁷ Institute of Mathematics, Physics and Mechanics, 1000 Ljubljana, Slovenia

⁸ Institut Néel, Université Grenoble Alpes, CNRS, Grenoble, 38042, France

⁹ LLB, CEA, CNRS, Université Paris-Saclay, CEA Saclay, 91191 Gif-sur-Yvette, France

¹⁰ National High Magnetic Field Laboratory, Florida State University, Tallahassee, FL 32310, USA

¹¹ Institut Laue-Langevin, 38042 Grenoble, France

The impact of quenched disorder on the ground state of frustrated magnets is a pressing topic both from a fundamental point of view, but also as a practical matter, since disorder in many of the most studied quantum magnets, like the kagome antiferromagnet herbertsmithite, is often unavoidable [1]. Particularly interesting are cases where strong disorder stabilizes a randomness-induced spin-liquid state (a disordered, dynamical, and highly-entangled ground state of spins); for example a random-singlet state where a distribution of antiferromagnetic exchange interaction strengths between spins leads to characteristic, unconventional scaling laws for observables like magnetic susceptibility and specific heat at low temperatures [2].

The recently synthesized frustrated antiferromagnet $\text{Li}_4\text{CuTeO}_6$ (LCTO) [3] consists of spin-1/2 Cu^{2+} ions forming parallel random spin chain fragments with random 3D inter-chain couplings (Fig. 1) [4]. Using thermodynamic, muon spin relaxation, electron spin resonance, and scattering measurements, complemented by *ab initio* (DFT) and exact diagonalization calculations, we find that disorder in LCTO stabilizes a novel, dynamical random-singlet state with peculiar scaling behavior but no spin freezing down to 45 mK. LCTO thus represents a rare, and particularly clear, realization of a 3D randomness-driven spin-liquid state.

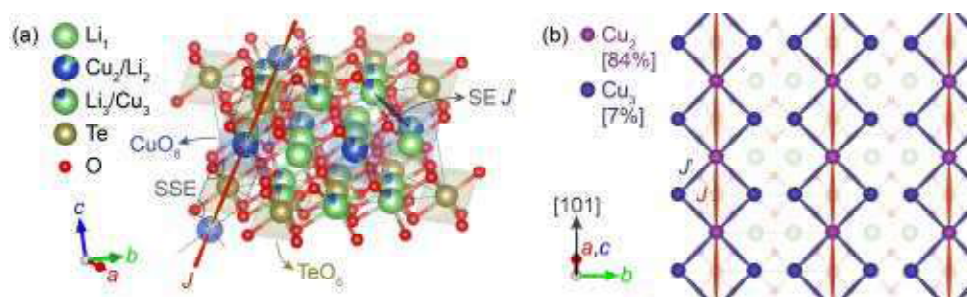


Figure 1: (a) Crystal structure and (b) high temperature random spin model of $\text{Li}_4\text{CuTeO}_6$ from density functional theory, consisting of random 1D spin chain and ladder fragments that couple in a random 3D lattice.

[1] M. R. Norman, Rev. Mod. Phys. **88**, 041002 (2016).

[2] I. Kimchi, A. Nahum, and T. Senthil, Phys. Rev. X **8**, 031028 (2018).

[3] V. Kumar *et al.*, Inorg. Chem. **51**, 10471 (2012).

[4] J. Khatua, M. Gomilšek *et al.*, Commun. Phys. **5**, 1 (2022).

Magnetic-Field-Dependent Thermodynamic Properties of Square and Quadrupolar Artificial Spin Ice

M. Goryca¹, X. Zhang², J. D. Watts³, C. Nisoli⁴, C. Leighton³, P. E. Schiffer², and S. A. Crooker⁴

¹ Institute of Experimental Physics, Faculty of Physics, University of Warsaw, Warsaw, Poland

² Department of Applied Physics, Yale University, New Haven, USA

³ Department of Chemical Engineering and Materials Science, University of Minnesota, Minneapolis, USA

⁴ National High Magnetic Field Lab, Los Alamos National Laboratory, Los Alamos, USA

Arrays of interacting nanomagnets known as Artificial Spin Ice (ASI) have allowed the design of geometrically frustrated exotic collective states not found in natural magnets. A key emergent description of fundamental excitations in ASIs is that of magnetic monopoles – mobile quasiparticles that carry an effective magnetic charge. While the presence of monopoles in ASI has been observed in pioneering imaging measurements, studies of their properties in applied static magnetic fields remain at an early stage. This is despite the fact that magnetic fields are an important tuning parameter for ASI systems, as they can drive phase transitions between different magnetic ground states, or tune through regimes with high populations of magnetic monopoles [1].

In this work, using both simulations and experiments, we thoroughly investigate the thermodynamic properties and magnetic phases of square and quadrupolar ASI as a function of applied in-plane magnetic fields. Monte Carlo (MC) simulations are used to generate field-dependent maps of the magnetization, the magnetic specific heat, and the thermodynamic magnetization fluctuations (Fig. 1), all under equilibrium conditions. These maps reveal the diversity of magnetic orderings and the phase transitions that occur in different regions of the phase diagrams of these ASIs [2]. Furthermore, the MC calculations allow us to probe the stability of different phases as a function of applied field and temperature. Those calculations are experimentally supported by magneto-optical measurements of the equilibrium "magnetization noise" in thermally-active ASIs. The experiment is performed with the use of a high-bandwidth magneto-optical noise spectrometer which passively "listens" to spontaneous magnetization fluctuations. Our results provide a window into a rich landscape of collective magnetic behavior associated with the application of magnetic field to ASI systems and provides a new paradigm for studies of magnetism in artificial magnetic materials.

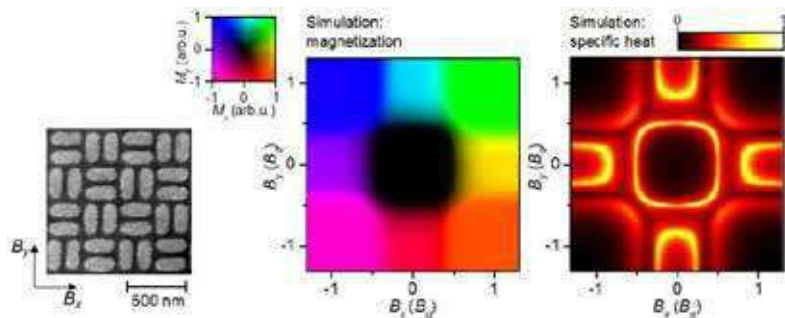


Figure 1: An SEM image of a quadrupolar ASI (left), together with magnetic field-dependent maps of magnetization (center) and specific heat (right) of such system.

[1] M. Goryca, X. Zhang, J. Li, A. L. Balk, J. D. Watts, C. Leighton, C. Nisoli, P. Schiffer, and S. A. Crooker, *Phys. Rev. X* **11**, 011042 (2021).

[2] M. Goryca, X. Zhang, J. D. Watts, C. Nisoli, C. Leighton, P. Schiffer, and S. A. Crooker, *Phys. Rev. B* **105**, 094406 (2022).

Multi-ring patterns in the single pulse all-optical toggle switching and partial demagnetization of amorphous DyCo_x and TbCo_x

Zexiang Hu*, J. Besbas, K. Rode, J. M. D. Coey and P. Stamenov

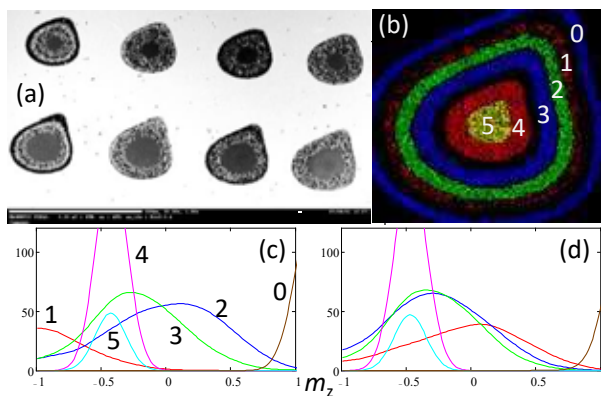
CRANN, AMBER and School of Physics, Trinity College Dublin, Dublin 2, Ireland.

*zehu@tcd.ie

The manipulation of magnetic states by ultrafast laser pulses has become a hot topic of research, due to its high potential impact in the area integrated magneto-photonics [1]. Single pulse all-optical switching (SP-AOS) of the magnetization on picosecond time scales was established by Ostler *et al.* in ferrimagnetic amorphous GdFeCo [2]. In the intervening decade, the search for systems with a different rare earth (RE) elements has met little success.

We have recently reported single-pulse all-optical switching in amorphous DyCo_x and TbCo_x [3]. Gd is spherically symmetric ion and amorphous GdFeCo is ferrimagnetic, with a net perpendicular anisotropy, when sufficiently thin. However, in amorphous DyCo_x and TbCo_x, the random local electrostatic fields acting on the non-spherical 4f charge distribution creates random local anisotropy in the magnetically ordered state [4].

Here, we look to understand in detail the unusual switching patterns observed in the outer perimeter of the irradiated spots in amorphous DyCo₃ and TbCo₃ films, deposited on Si/SiO₂ (500 nm thermal oxide) wafers and on single crystal quartz. Films are deposited by DC magnetron sputtering at room temperature. The coercivity is 30-45 mT, at RT, and the compensation temperature T_{comp} is well below 300 K. The behavior is surprising. A single 200 fs pulse creates a multi-ring switching pattern, ~85 μm dark spot on an otherwise uniformly-magnetized (in remanence) film. The image in fig1.(a) shows the aftermath of two sequences of one to four 200 fs pulses of two different fluences (12 (top row) and 20 mJ/cm², resp., 1 s delay). In fig.1(b), number 0 represents the unirradiated region with magnetization pointing up, while the following rings 1 to 5 are labelled from the outside in. Each ring shows a switching process, with the contrast alternating with each pulse. The process involves both toggling and demagnetization of the corresponding regions as illustrated on fig1(c and d) for 1 and two pulses. The fidelity of the toggling is lost after about 10 pulses, but for the central spot where the anisotropy is changed to in-plane, with the majority of the spot area being demagnetized. We attribute the observed pattern to the propagation of heat waves in the substrate. The reproducible partial toggling of the central region may pave ways for the optical writing and control of magnetic logic devices, realized in sperimagnetic active layers.



[1] M. Lalieu, *et al.* Phys. Rev. B 96, 220411 (2017).

[2] T.A. Ostler, *et al.* Nat. Commun. 3, 666 (2012).

[3] Zexiang Hu, *et al.* Appl. Phys. Lett. 120, 112401 (2022)

[4] J. M. D. Coey, Magnetism and Magnetic Materials (Cambridge University Press, 2010).

Role of Geometric Frustration in a Weakly Disordered Checkerboard Lattice

F. M. Zimmer¹, M. Schmidt², W. C. Silva¹, and S. G. Magalhaes³

¹ Universidade Federal de Mato Grosso do Sul, Instituto de Física, Campo Grande, Brazil

² Universidade Federal de Santa Maria, Departamento de Física, Santa Maria, Brazil

³ Universidade Federal do Rio Grande do Sul, Instituto de Física, Porto Alegre, Brazil

Quenched disorder effects on frustrated systems are explored by considering random fluctuations on the antiferromagnetic (AF) interactions between spins on the checkerboard lattice. In this model, first (J_1) and second-neighbor (J_2) AF interactions lead to a frustrated situation that can also be affected by random deviations coming from disorder J . In this way, we can assess the interplay between frustration coming from different sources (the AF competing interactions and the quenched disorder) on the glassy behavior. The problem is dealt with a replica-cluster mean-field formalism within a one-step replica symmetry breaking (RSB) approach, leading to an effective single-cluster model which is solved with exact evaluations for all intracluster interactions. Competing interactions are introduced by tuning the ratio J_2/J_1 , which can lead to a highly frustrated scenario when $J_2/J_1 > 1$, where a phase transition between AF orders takes place in the absence of disorder. In particular, the AF order appears at lower values of J_2/J_1 , with the Néel temperature decreasing as the frustration increases. However, quenched disorder changes this description, introducing a RSB spin glass phase for strong enough disorder intensity J . Interestingly, for low levels of disorder, a RSB solution with staggered magnetization (mixed phase) emerges from the maximum frustration region (see Fig. 1). It suggests that, in the presence of weak quenched disorder, systems with competing interactions are prone to present a glassy behavior instead of conventional long-range orders [1]. It also suggests that even when frustration is not strong enough to avoid an ordered phase, it can still favor the onset of a RSB phase at low levels of disorder. This phase can occur as a reentrant mixed spin-glass phase or a canonical spin-glass, depending on the subtle balance of disorder and frustration of the system.

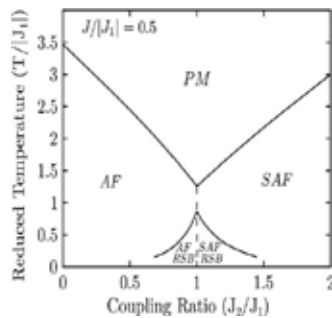


Figure 1: Phase diagram of temperature versus antiferromagnetic competing interactions for a weak intensity of disorder ($J/|J_1| = 0.5$). PM represents the paramagnetic phase and SAF stands for an AF stripe order favored by the second-neighbor couplings.

[1] F. M. Zimmer, W. C. Silva, M. Schmidt, and S. G. Magalhaes, ArXiv 2111.06176.

Fractional Excitation-induced Phonon Renormalization in α -RuCl₃

Adrian M. Merritt¹, Xiao Wang¹, Alexei Bosak³, Luigi Paolasini³, Alexandre Ivanov⁴, Rolf Heid², Yixi Su¹

¹ Jülich Centre for Neutron Science JCNS-FRM II, Forschungszentrum Jülich GmbH, Outstation at FRM II, Lichtenbergstrasse 1, D-85747 Garching, Germany

² European Synchrotron Radiation Facility (ESRF), BP 220, F-38043 Grenoble Cedex, France.

³ Institute for Quantum Materials and Technologies, Karlsruhe Institute of Technology, 76021, Karlsruhe, Germany

⁴ Institut Laue-Langevin, 71 Avenue des Martyrs CS 20156, 38042 Grenoble Cedex 9, France.

The quantum spin liquid (QSL) phase is of immense interest to condensed matter physicists, and have been studied for decades. With a Kitaev model that is exactly solvable and gives a QSL ground state, more recent work has focused on the $J_{\text{eff}}=1/2$ materials; in particular, α -RuCl₃ is a promising Kitaev QSL candidate. Above the critical magnetic field $B_c \sim 7\text{T}$ and below $T \sim 6\text{K}$ there is evidence for the half-integer quantized plateau where large thermal Hall effect measurement signal and an anomalous T dependence possibly arise from the fractional excitations in the QSL phase.

Although previous inelastic neutron scattering measurements have focused on magnetic excitations, the phonon dispersions have not been well-studied. However, recent theoretical work has shown that the fractional excitations can induce phonon renormalization via the spin-lattice coupling, and would in particular affect the acoustic phonons, where

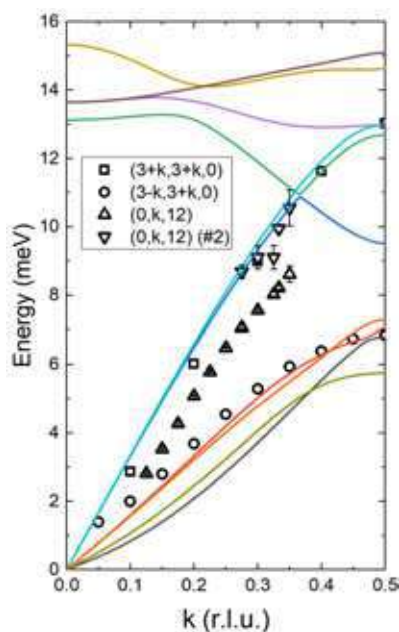


Figure 1. Measured phonon dispersion (symbols) versus predicted phonon dispersion (solid lines). Measurements shown taken at 300K and zero magnetic field.

longitudinal/transverse phonons harden/soften, respectively, as they approach the zone boundary [1,2]. Our measurements have focused on the phonon dispersion in α -RuCl₃ to observe this phonon renormalization effect in the putative QSL phase. We have used high-quality in-house grown α -RuCl₃ single crystals for inelastic neutron and x-ray scattering measurements, combined with phonon dynamics calculations, to survey the acoustic phonons in the relevant scattering directions, in particular under magnetic fields. We will discuss our results with a focus on examining the low-energy acoustic phonon branches we measured in comparison to published work as well as the observed phonon renormalization effect. Notably, our inelastic neutron scattering measurements under magnetic field will be compared with inelastic x-ray scattering measurements without a magnetic field and with DFT calculations of the phonon branches to clarify the behavior of these phonon branches in this phase of interest.

[1] Alexandros Metavitsiadis and Wolfram Brenig. *Phys. Rev. B* **101**, 035103 (2020).

[2] Mengxing Ye, Rafael M. Fernandes, and Natalia B. Perkins. *Phys. Rev. Research* **2**, 033180 (2020).

Magnetic defect-driven dynamics in artificial spin ice

R. Puttock^{1*}, I. M. Andersen², C. Gatel², B. Park², M. Rosamond³, E. Snoeck², and O. Kazakova¹

¹*Quantum Materials and Sensors, National Physical Laboratory, Hampton Road, Teddington, TW11 0LW, UK.*

²*Centre d'Elaboration de Matériaux et d'Etudes Structurales–CNRS, 29 Jeanne Marvig, Toulouse, 31055, France.*

³*School of Electronic and Electrical Engineering, University of Leeds, Leeds, LS2 7EZ, UK.*

Despite attempts to design correlated systems to influence the properties of a physical system, it is often those inspired by nature that yield the best results. Artificial spin ice (ASI) are 2D projections of geometrically frustrated materials that are often used to experimentally model more complex atomistic systems. In addition, ASI exhibit collective dynamic behaviour and emergent monopole stabilisation that can be applied to probabilistic computing, signal propagation, and logic devices. The capacity to design an almost infinite number of topologies to induce novel effects, and the ability to probe these characteristics optically, electrically and by scanning probe techniques have made ASI an exciting candidate for probabilistic computing.

Defects in crystal systems can have bountiful effects on the local physical properties. Here, we present a study on the influence of a magnetic defect with shape anisotropy on the local dynamics of a Kagome ASI system (Fig. 1(a)). The defect acts as a source of emergent monopoles at lower energy-barriers than in the pristine lattice. Recent results of the delicate interplay between defect and lattice states are studied in the context of signal propagation applications by magnetic imaging techniques, by Lorentz TEM; electron holography (Fig. 1(b)) and micromagnetic modelling. We show it is possible to manipulate the defect-induced monopoles in the lattice whilst minimizing parasitic nucleation events in the lattice bulk (Fig. 1(c)). We reveal how the magnetic defect affects the surrounding structure compared to those formed independently from the defect, e.g., from discontinuous lattice-edges.

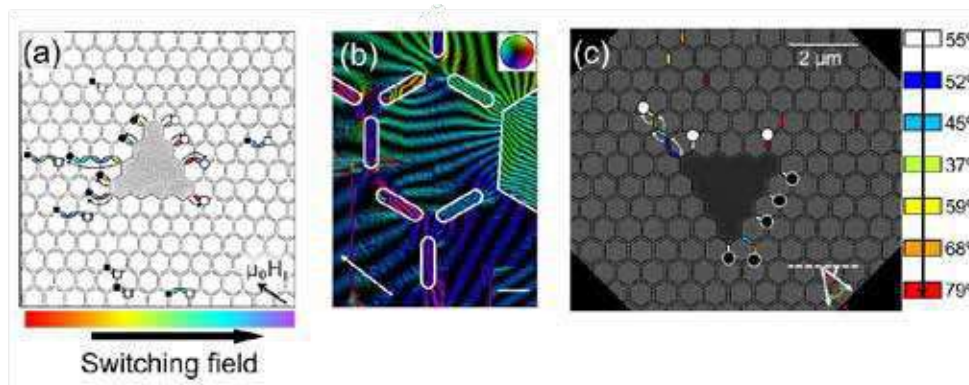


Figure 1. **(a)** Labelled LTEM, where colours represent individual island switching fields of the Defect ASI lattice undergoing field reversal; positive and negative monopoles are represented by black and white symbols, respectively). **(b)** Electron holograph reconstructed phase contour image in Defect ASI whilst undergoing field reversal; colours and contour density represent the direction and magnitude of the magnetic flux, respectively. **(c)** Labelled LTEM of scheme demonstrating defect-bound monopole propagation by teetering the field angle at fixed field magnitude.

Ice regime and approximate of the low-energy physics of the F-model in a two-dimensional artificial vertex system

V. Schánilec,^{1,2} O. Brunn,^{1,3,4} M. Horáček,³ S. Krátký,³ P. Meluzín,³ T. Šíkola,^{2,4} B. Canals,¹ and N. Rougemaille¹

¹Univ. Grenoble Alpes, CNRS, Grenoble INP, Institut NEEL, Grenoble, France

²Central European Institute of Technology, Brno Univ. of Technology, Brno, Czech Republic

³Institute of Scientific Instruments of the Czech Academy of Sciences, Brno, Czech Republic

⁴Institute of Physical Engineering, Brno Univ. of Technology, Brno, Czech Republic

We demonstrate experimentally that the physics of the F-model [1,2] can be approached very closely in a purely two-dimensional artificial system. Faraday lines spanning across the lattice and carrying a net polarization, together with chiral Faraday loops characterized by a zero magnetic susceptibility are imaged in real space for several fictional temperatures (Fig.1). Our measurements reveal the proliferation of Faraday lines and Faraday loops as the system is warmed up from low-energy configurations. They also reveal a link between the Faraday loop density and ice-like spin-spin correlations in the magnetic structure factor. Key for this work, the density of topological defects remains small for all probed fictional temperatures, and negligible compared to the density of Faraday loops. This is made possible by replacing the spin degree of freedom used in conventional artificial spin ice systems by a micromagnetic knob, which can be finely tuned to adjust the vertex energy directly, rather than modifying the two-body interactions [3].

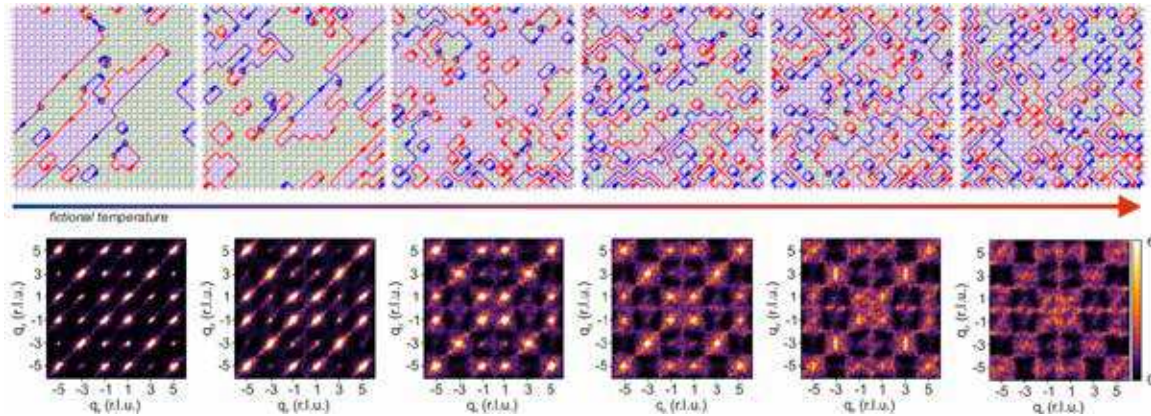


Figure 1: Real space and reciprocal space analyses of the magnetic configurations obtained after demagnetizing six different lattices. The two degenerate antiferromagnetic domains of the F-model ground state are shaded in blue and green. These domains are separated by Faraday loops represented by directed lines colored in blue and red depending on their parity. Faraday lines having different parities never intersect, except in the presence of an ice-rule defect (shown by a colored open circle). The associated magnetic structure factors are averaged over four real space configurations (i.e., 3600 vertices / 7440 spins) to improve statistics.

[1] C. Nisoli, *Eur. Phys. Lett.* **132**, 47005 (2020).

[2] D. M. Arroo and S. T. Bramwell, *Phys. Rev. B* **102**, 214427 (2020).

[3] V. Schánilec *et al.*, under review at *Phys. Rev. Lett.*

Properties of systematically disordered Cr₂AlC thin films

J. S. Cabaco¹, U. Kentsch¹, J. Lindner¹, J. Fassbender¹, C. Leyens^{2,3}, R. Bali¹ and R. Boucher²

¹*Institute of Ion Beam Physics and Materials Research, HZDR, Dresden, Germany*

²*Institute for Materials Science, TU Dresden, Germany*

³*Fraunhofer Institute for Material and Beam Technology IWS, Dresden, Germany*

MAX phases are nano-lamellar composite materials of the form M_{n+1}AX_n, where n is 1, 2 or 3; M an early transition metal; A is an A-group element and X is carbon or nitrogen [1,2]. An interesting combination of metallic and ceramic properties as well as potential applications in spintronics [1,3] led to significant research interest in MAX phases. Literature on the effect of systematic disordering of the nano-laminar structure on the magnetic and transport properties is still limited. In particular, MAX phase systems doped with magnetic ions via ion-irradiation may result in large variations of the magneto-transport properties.

Here we observe the magneto-transport properties and attempt to separate the contributions of structural changes due to the irradiation and magnetic effects due to the doping on the magneto-transport. A prototype material is Cr₂AlC, formed from a unit cell of Cr₂C sandwiched between atomic planes of Al. In this work, we study 50 nm and 500 nm thick thin films of Cr₂AlC grown on Si (111) by sputtering and subsequent annealing.

Structural characterization using X-ray Diffraction in Bragg-Brentano geometry shows a pronounced MAX phase, confirmed by the occurrence of the 002 superstructure reflection. The films were irradiated with Co⁺ at 450 (50) keV for the 500 (50) nm thick films. The Co⁺-fluence varied between 1×10¹² - 1×10¹⁵ ions.cm⁻², in full order steps. The Co⁺-irradiation led to a gradual suppression of the 002 superstructure reflection, while preserving the fundamental peaks, implying the intermixing of the nano-laminar MAX phase structure. The magnetic properties are characterized using vibrating sample magnetometry at low temperatures (Fig.1a), showing an increasing paramagnetic behavior as the Co⁺-fluence increases. In comparison, magneto-resistance measurements (Fig.1b-c) show that for the 500 nm film thickness, the magnetoresistance reaches up to 3 % (10 T) for 100 K, at an optimized Co⁺-fluence of 5×10¹³ ions.cm⁻². The above results suggest that in the low-fluence regime, the irradiation induced disorder remains sufficiently low to obtain pronounced magneto-resistance values. Understanding the defect state in the optimized MAX phase films will shed light on the magneto-transport mechanisms in these nano-laminated materials.

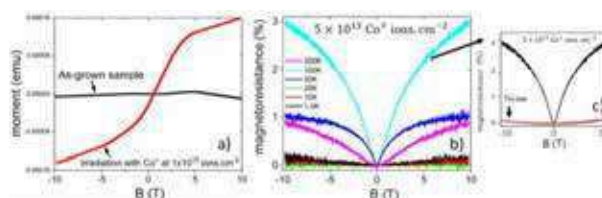


Figure 1. a) Magnetic moment as a function of applied field for Cr₂AlC 500 nm film irradiated with cobalt at 1×10¹⁵ ions.cm⁻² and no-ion case (at 1.7 K). b) Magnetoresistance for cobalt irradiation at 5×10¹³ ions.cm⁻² with different temperatures, and c) comparison with no-ion irradiation case.

[1] M. W. Barsoum, Prog. Solid State Ch. 28 (2000) 201-281.

[2] P. Eklund, M. Beckers, U. Jansson et al, Thin solid Films 2010, 518, 1851-1878.

[3] O. Berger, C. Leyens, S. Heize et al., Thin solid films 2015, 580, 6-11.

Acknowledgements: Funding by the Deutsche Forschungsgemeinschaft (DFG) - Project number 456078299.

Putative spin-nematic phase in $\text{BaCdVO}(\text{PO}_4)_2$

M. Skoulatos¹, H. Gabold¹, G. Brandl², F. Rucker³, G.J. Nilsen⁴, A. Bertin⁵, E. Pomjakushina⁶, J. Ollivier⁷, A. Schneidewind², R. Georgii¹, O. Zaharko⁸, L. Keller⁸, Ch. Rüegg⁹, C. Pfleiderer³, B. Schmidt¹⁰, N. Shannon¹¹, A. Kriele¹², A. Senyshyn¹, A. Smerald¹³

¹Heinz Maier-Leibnitz Zentrum (MLZ) and Physics Department, Technical University Munich, D-85748 Garching, Germany

²Jülich Centre for Neutron Science JCNS at Heinz Maier-Leibnitz Zentrum (MLZ), D-85748 Garching, Germany

³Physics Department E51, Technische Universität München, D-85748 Garching, Germany

⁴ISIS Neutron and Muon Facility, Rutherford Appleton Laboratory, Didcot OX11 0QX, United Kingdom

⁵Institut für Festkörperphysik, TU Dresden, D-01062, Dresden, Germany

⁶Laboratory for Multiscale Materials Experiments, Paul Scherrer Institute, CH-5232 Villigen, Switzerland

⁷Institut Laue-Langevin, 6 rue Jules Horowitz, 38042 Grenoble, France

⁸Laboratory for Neutron Scattering and Imaging, Paul Scherrer Institute, CH-5232 Villigen, Switzerland

⁹Quantum Criticality and Dynamics Group, Paul Scherrer Institute, CH-5232 Villigen-PSI, Switzerland

¹⁰Max Planck Institute for the Chemical Physics of Solids, 01187 Dresden, Germany

¹¹Okinawa Institute of Science and Technology Graduate University, Onna-son, Okinawa 904-0495, Japan

¹²German Engineering Materials Science Centre at MLZ, Helmholtz-Zentrum Hereon, Lichtenbergstr. 1, D-85748, Garching, Germany

¹³Max Planck Institut für Festkörperforschung, Quantum Materials Unit, D-70569, Stuttgart, Germany

We report neutron scattering and AC magnetic susceptibility measurements of the 2D spin-1/2 frustrated magnet $\text{BaCdVO}(\text{PO}_4)_2$ [1]. At temperatures well below $T_N \approx 1\text{K}$, we show that only 34% of the spin moment orders in an up-up-down-down strip structure. Dominant magnetic diffuse scattering and comparison to published μSR measurements indicates that the remaining 66% is fluctuating. This demonstrates the presence of strong frustration, associated with competing ferromagnetic and antiferromagnetic interactions, and points to a subtle ordering mechanism driven by magnon interactions. On applying magnetic field, we find that at $T = 0.1\text{K}$ the magnetic order vanishes at 3.78T, whereas magnetic saturation is reached only above 4.5T. We argue that the putative high-field phase is a realisation of the long-sought bond-spin-nematic state.

[1] Phys. Rev. B **100**, 014405

Magnetic anisotropy in CoFe₂O₄ based nanocomposite

S. Slimani^{1,3,4}, G. Concas², F. Congiu², G. Barucca⁵, N. Yaacoub⁶, A. Talone^{4,7}, M. Smari³, E. Dhahri³, D. Peddis^{1,4}, G. Muscas².

¹*Università di Genova, Dipartimento di Chimica e Chimica Industriale, nM2-Lab, Via Dodecaneso 31, I-16146, Genova, Italy.*

²*Department of Physics, University of Cagliari, Cittadella Universitaria di Monserrato, S.P. 8 Km 0.700, I-09042 Monserrato (CA), Italy.*

³*Laboratoire de Physique Appliquée, Faculté des Sciences, Université de Sfax, B.P. 1171, 3000 Sfax, Tunisie.*

⁴*CNR, Istituto di Strutturistica della Materia, nM2-Lab, Monterotondo Scalo (Roma), 00015, Italy.*

⁵*Università Politecnica delle Marche, Dipartimento di Scienze e Ingegneria della Materia, dell'Ambiente ed Urbanistica, Via Brecce Bianche 12, 60131 Ancona, Italy.*

⁶*IMMM, Université du Maine, CNRS UMR-6283, Avenue Olivier Messiaen, Le Mans 72085, France.*

⁷*Università degli Studi 'Roma Tre', Dipartimento di Scienze, Roma, Italy.*

The presence of an amorphous component is often considered a weakness of the synthesis method of the nanostructured magnetic materials. This stems from the fact that any amorphous fraction is often considered as a “dead” magnetic component, showing little to no contribution to the magnetic properties such as saturation magnetization. Here we investigated a hybrid-structured nanoarchitecture combining crystalline CoFe₂O₄ and the amorphous parent material. The nanocomposite was prepared by a single-step coprecipitation method. Transmission electron microscopy (TEM) analysis evidenced small crystalline particles (≈ 3 nm) embedded in an amorphous matrix. Applying the Debye-Scherrer formula to the most intense reflection of the X-Ray Diffraction pattern confirmed an average size of the crystalline structure of about 3 nm. The investigation of the magnetic properties by SQUID magnetometer and the magnetic structure by means of Mössbauer spectrometry pointed out that the amorphous phase contributes partially to the total magnetic moment accompanied by a strong variation in the anisotropy (i.e., coercive field ≈ 1.3 T, at 5K) and the presence of a significant interparticle interacting regime (i.e., blocking temperature ≈ 95 K). Cross-checking the obtained information from structural and magnetic characterization, we have proposed a micromagnetic model using the software Mumax3, which sheds light on the contribution of each component elucidating the active role of the amorphous phase as a “non-dead magnetic phase”, but a magnetically canted structure, with low effective magnetization and very large magnetic anisotropy coupled with the regular core structure [1].

[1] Slimani, S., Concas, G., Congiu, F., Barucca, G., Yaacoub, N., Talone, A., Smari, M., Dhahri, E., Peddis, D., and Muscas, G., The Journal of Physical Chemistry C, **2021**.

Pulse High-Field Magnetization of frustrated FCC magnet RInCu_4

T. Waki¹, F. Kihara¹, Y. Tabata¹, Y. Narumi², M. Hagiwara²,
and H. Nakamura¹

¹*Dept. Mater. Sci. and Eng., Kyoto Univ., Kyoto, Japan*

²*AHMF, Grad. Sch. Sci., Osaka Univ., Toyonaka, Osaka, Japan*

RInCu_4 forms the C15b structure and is a frustrated magnet in which the heavy rare earth R form the FCC lattice. It has been reported that GdInCu_4 undergoes antiferromagnetic ordering at a low temperature, where some components remain in a partially disordered state^[1]. Recently, we succeeded in synthesizing single crystals of GdInCu_4 and observed two anomalies in the magnetic susceptibility at 2.5 K ($= T_M$) and 5 K ($= T_N$). We also confirmed the magnetic structure is such that $\langle 100 \rangle$ is the easy axis below T_N . Non-trivial magnetic ordered states such as partially disordered states are manifestations of frustration effects, and since such states are susceptible to perturbations, phase transitions in magnetic fields are expected. In this study, we measured the magnetization using a pulse high magnetic field to obtain knowledge about high-field phases. Figure 1 (a) shows magnetization curves at $T = 1.3$ K ($< T_M$) and $T = 4.2$ K ($> T_M, < T_N$). At $T = 1.3$ K, the magnetization shows a hysteresis, although it saturated to $7 \mu_B$ at around 35 T. A hysteresis was also observed at $T = 4.2$ K at high field. The value of dM/dH is not constant but decreases with increasing field. A clear hysteresis was observed in the vicinity of the saturation field. These behaviors suggest the existence of fluctuating spins consistent with the partially disordered model. At $T = 1.3$ K, dM/dH changes the slope at around $H = 10$ T suggesting the presence of a field induced magnetic phase transition. This also suggests that the anomaly of susceptibility at T_M represents the occurrence of a magnetic phase transition.

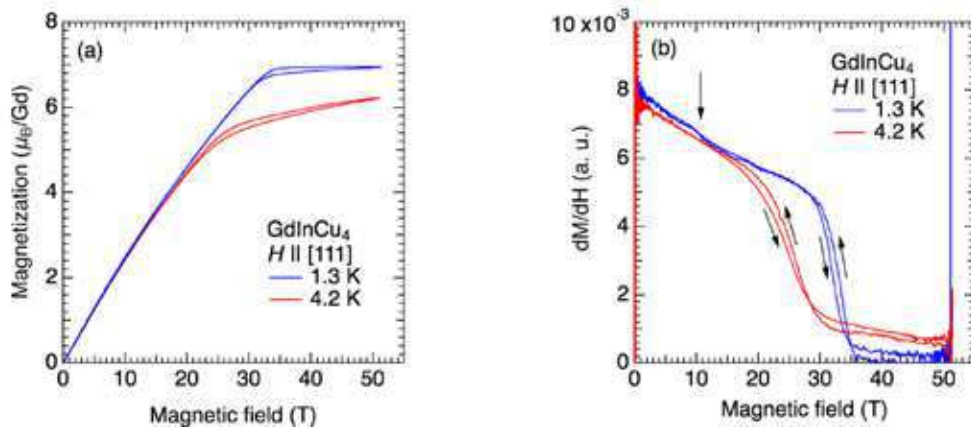


Figure 1: Pulse high-field magnetization (a) and dM/dH (b).

[1] H. Nakamura et al., *J. Phys.: Condens. Matter* **11** (1999) 1095.

Posters

| | | |
|----------------------|--|----|
| Pavlo Baloh | <i>Correlation between As-S nanocluster structures and low-temperature anomalies in amorphous solids</i> | 81 |
| Shruti Chakravarty | <i>Disorder driven cluster glass state in a geometrically frustrated hexagonal perovskite</i> | 82 |
| Uladzislau Makartsou | <i>Control of the magnetization in ferromagnetic rings using ferromagnetic nanoelement</i> | 83 |
| Konrad Puzniak | <i>Spin-$\frac{1}{2}$ antiferromagnetic XXZ chain $\text{BaCo}_2\text{V}_2\text{O}_8$ in a transverse external magnetic field - dispersion of E8 particles</i> | 84 |
| Konrad Puzniak | <i>Study of the spin-$\frac{1}{2}$ antiferromagnetic XXZ chain $\text{SrCo}_2\text{V}_2\text{O}_8$ in a transverse external magnetic field</i> | 85 |

Correlation between As-S nanocluster structures and low-temperature anomalies in amorphous solids

P. Baloh¹, V. Tkáč¹, R. Tarasenko¹, M. Orendáč¹, A. Orendáčová¹, E. Gažo², V. Mitsa³, R. Holomb^{3,4}, and A. Feher¹

¹ P. J. Šafárik University in Košice, Park Angelinum 9, Košice 040 01, Slovakia

² Institute of Experimental Physics, SAS, Watsonova Str. 47, Košice 040 01, Slovakia

³ Uzhhorod National University, Voloshin str. 59, Uzhhorod 88 000, Ukraine

⁴ Wigner Research Centre for Physics, Konkoly-Thege Miklós str. 29-33, Budapest 1123, Hungary

The low-temperature specific heat (2–20 K) of many glasses reveals a broad maximum in Debye reduced form (C_p/T^3) which is commonly named a Boson Peak (Fig. 1a). At the same time, the thermal conductivity $k(T)$ is characterized by a plateau at temperatures above 1 K and followed by $k(T) \sim T^2$ dependence below 1 K (Fig. 1b). It is believed over 50 years that those features are a universal “anomalous” property of glasses [1]. Combined analysis using two approaches, the Soft-Potential Model (SPM) [2] and nanocluster approximation [3] allowed us to identify the exact structure of nanoclusters in a rigid glass matrix responsible for the mentioned universality.

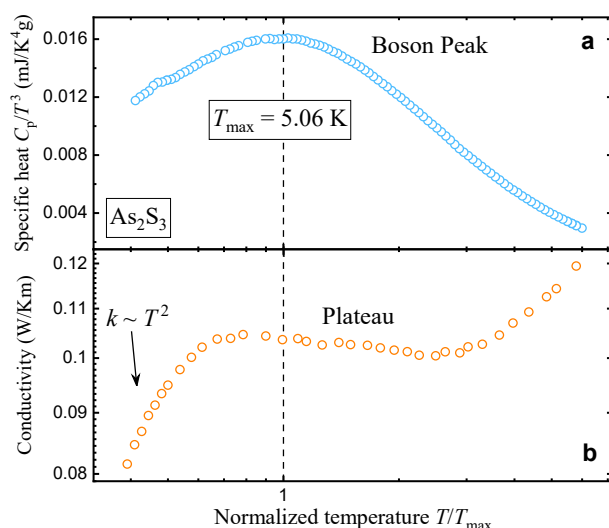


Figure 1: Temperature dependence of specific heat (a) and thermal conductivity (b) of As_2S_3 between 2–30 K.

The nanocluster approach is based on a low-frequency Raman spectra analysis, which identifies various types of nanoclusters. Two types of nanoclusters, namely, a ring- and branchy-like nanoclusters, are shown to have the most pronounced effect. Using the SPM approach, it has been established that the lower temperature region ($k(T) \sim T^2$) is mostly influenced by a branchy- $\text{As}_{2+4/3}\text{S}_5$ nanocluster and a higher (plateau) region is supposedly governed by the concentration of S_8 rings.

In this work we clarified the effect of the nanocluster concentration on low-temperature thermal properties of As-S glassy systems. Understanding of lattice dynamics is necessary for the future analysis of magnetic ion doped glasses.

Acknowledgements

This work was supported by the Slovak Research and Development Agency Projects numbers APVV-18-0197, APVV-14-0073, and APVV-SK-BY-RD-19-0008.

[1] R. C. Zeller, and R. O. Pohl, Phys. Rev. B **4**, 2029 (1971);

[2] M. A. Ramos, and U. Buchenau, Phys. Rev. B **55**, 5749 (1997);

[3] R. Holomb, P. Ihnatolia, O. Mitsa, V. Mitsa, L. Himics, and M. Veres, Appl. Nanosci. **9**, 975–986 (2019).

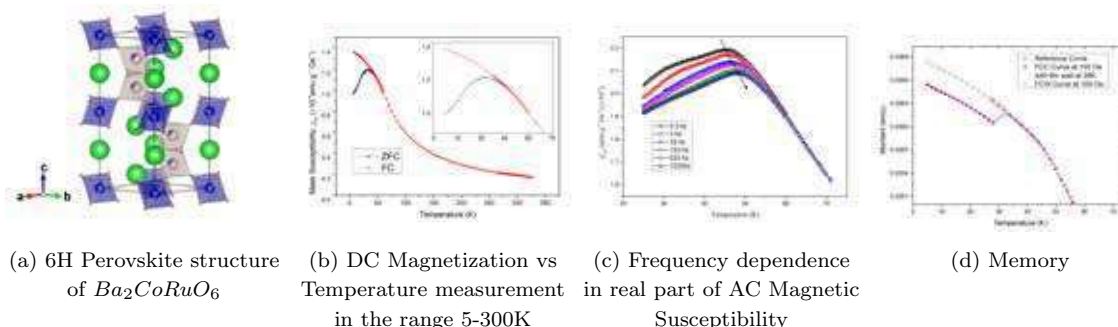
Disorder driven cluster glass state in a geometrically frustrated hexagonal perovskite

Shruti Chakravarty¹, Sunil Nair^{1,2}

¹*Department of Physics, Indian Institute of Science Education and Research, Pune, India*

²*Centre for Energy Sciences, Indian Institute of Science Education and Research, Pune, India*

We report the observation of cluster glass-like properties in a 6H double perovskite Ba_2CoRuO_6 through structural, magnetic and transport measurements. Magnetization data shows that the system undergoes a freezing transition around 43K ($H = 5T$) evident from the bifurcation of the ZFC and FC curves [1]. This bifurcation point shows a strong dependence on applied field, but the T-H phase diagram does not follow the AT line. Short-range correlations persist well-above room temperature and no paramagnetic region is found upto 330 K. The system exhibits classic glassy characteristics like a frequency dependence in AC Magnetization, aging and memory effects [1]. Neutron Diffraction at 2K shows two extremely weak peaks possibly reflecting existence of antiferromagnetically ordered clusters. Hysteresis measurements show loop opening at low temperature likely reflecting a small contribution from weak ferromagnetism often seen in cluster glasses. Specific Heat data is featureless as expected [1] for spin glasses. The magnetic specific heat and the corresponding entropy change is calculated to be negligible. Deviation from the Debye behaviour in low temperature specific heat strongly points to a frustrated glassy state [2]. The sample is insulating and the 3D Mott Variable Range Hopping mechanism governs the conduction mechanism [3]. A subtle feature is observed around T_f in both resistivity and dielectric measurements implying that the spin and charge/polar degrees of freedom might not be greatly correlated. The significant ($\sim 30\%$) anti-site disorder on the dimer sites which when coupled with the geometrical and exchange frustration in this system paves way for the cluster glass behaviour.



- [1] J. A. Mydosh, Spin glasses : An Experimental Introduction (Taylor and Francis, 1993) p. 256
- [2] A. Banerjee, R. Rawat, K. Mukherjee, and P. Chaddah, *Physical Review B* **79**, 212403 (2009)
- [3] N. F. Mott, *Philosophical Magazine* **19**, 835 (1969)

Control of the magnetization in ferromagnetic rings using ferromagnetic nanoelement

Uladzislau Makartsou¹, Mathieu Moalic¹, Mateusz Zelent¹, Maciej Krawczyk¹

¹Institute of Spintronics and Quantum Information, Faculty of Physics, Adam Mickiewicz University, Uniwersytetu Poznańskiego 2, 61-614 Poznań, Poland

Controlling the direction of vortex chirality in ferromagnetic nanodots and nanorings is a topic of investigations from 20 years [1]. Many approaches were proposed and it was found that this control is strongly related to the breaking of the circular symmetry [2]. We present a theoretical study demonstrating control of the chirality in ferromagnetic rings without directly breaking the symmetry of the rings but instead by placing near the ring a singly ferromagnetic nanoelement (FEN) with strong shape anisotropy, located asymmetrically with respect of the nanoring (Fig. 1). Interestingly, the effect of chirality control is observed only if the FEN magnetization is parallel to the nearest part of the ring, and this element is located along the inner wall of the nanoring. The chirality control depends on few factors: the direction of magnetization in FEN, magnetostatic interaction between MFE and ring, a correct value of the coercive field, and the remagnetization direction. With micromagnetic simulations we explain the effect and demonstrate the chirality control in Fe nanorings with outer and inner diameters $d_{out}/d_{in} = 800 \text{ nm} / 500 \text{ nm}$, and the thickness $t = 80 \text{ nm}$ [3]. The proposed shape of the FEN offers sufficient shape anisotropy and is suitable for the state-of-the-art of the lithographic manufacturing methods, promising future practical realizations. Offered approach can be further explored for reprogrammable control of the magnetization chirality in the arrays of nanoring for magnonic and spintronic applications.

We acknowledge the funding from the Polish National Science Centre, project No. UMO-2020/37/B/ST3/03936.

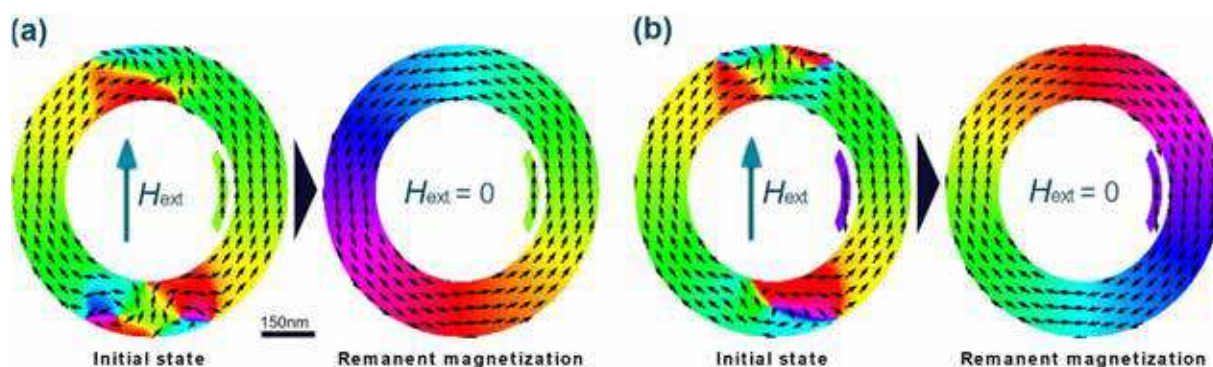


Fig. 1: The simulations of the ring and the FEN with shape magnetic anisotropy. (Left) The initial state of magnetization and (right) the state after the removing of the external magnetic field, the counter-clockwise chirality (a) and the clockwise chirality state (b).

References:

- [1] Y. Zheng, et al., Rep. Prog. Phys. 80, 086501 (2017).
- [2] E. Saitoh, M. Kawabata, K. Harii, and H. Miyajima, Journal of Applied Physics 95, 1986 (2004);
- [2] T. Miyawaki, K. Toyoda, M. Kohda, and A. Fujita, Appl. Phys. Lett. 89, 122508 (2006)

Spin-1/2 antiferromagnetic XXZ chain $\text{BaCo}_2\text{V}_2\text{O}_8$ in a transverse external magnetic field - dispersion of E_8 particles

K. Puzniak^{1,2}, B. Lake^{1,2}, X. Wang³, J. Wu³, J. Ma⁴, M. Hagiwara⁵, K. Schmalzl⁶

¹ *Helmholtz-Zentrum Berlin für Materialien und Energie GmbH, Hahn-Meitner Platz 1, D-14109 Berlin, Germany*

² *Institut für Festkörperphysik, Technische Universität Berlin, Hardenbergstraße 36, D-10623 Berlin, Germany*

³ *Key Lab. of Artificial Structures and Quantum Control, Shenyang National Lab. for Materials Science, Shanghai, China*

⁴ *Tsung-Dao Lee Institute School of Physics and Astronomy, Shanghai Jiao Tong University, Shanghai, China*

⁵ *Center for Advanced High Magnetic Field Science, Graduate School of Science, Osaka University, Osaka 560-0043, Japan*

⁶ *Institut Laue Langevin, 6 rue Jules Horowitz, BP 156, F-38042 Grenoble, France*

The one-dimensional (1D) spin-1/2 antiferromagnet (AFM) with Heisenberg-Ising (XXZ) anisotropy is an ideal model system to explore fundamental physics concepts. In zero applied magnetic field, this system hosts spinon excitations - quite different from the magnons of conventional three-dimensional (3D) magnets which have integer spin. A very interesting spin-1/2 quasi-1D antiferromagnetic XXZ material is $\text{BaCo}_2\text{V}_2\text{O}_8$. This compound crystallizes in the tetragonal space group $I4_1/acd$ (No. 142). The Co^{2+} ions have effective $S=1/2$ moments that are arranged in screw chains along the c-axis. The Co^{2+} ions are coupled by strong antiferromagnetic interactions within the screw chains which have partial Ising (XXZ) anisotropy where the interaction strength is $J=5.6$ meV and the anisotropy parameter is $\epsilon=0.46$ with the c-axis being the easy-axis. Weak inter-chain coupling gives rise to long-range magnetic order below $T_N=5.5$ K [1]. The spins are aligned antiferromagnetically along the screw chains. The behavior of $\text{BaCo}_2\text{V}_2\text{O}_8$ in a transverse magnetic field applied perpendicular to the easy-axis is equally fascinating [2]. The transverse field suppresses long-range magnetic order and results in a 1D Quantum Critical Point (QCP) at $B_c^{1D}=4.7$ T and a 3D QCP at $B_c^{3D}=10.3$ T. The 1D QCP has a class of universality described in terms of the E_8 Lie algebra which is characterized by 8 gapped excitations whose gaps are theoretically predicted to have precise values and have been observed by inelastic neutron scattering [3] and terahertz spectroscopy [4]. We report on the observations of the E_8 excitations, which have been found during the inelastic neutron scattering measurements of this compound and we follow their dispersion as a function of wavevector along the chain. We find excellent agreement with the results of the quantum integrable field theory and ITEBD numerical calculations.

[1] B. Grenier et al, *Phys. Rev. Lett.* **114**, 017201 (2015).

[2] Q. Faure et al, *Nat. Phys.* **14**, 716 (2018).

[3] H. Zou et al, *Phys. Rev. Lett.* **127**, 077201 (2021).

[4] Z. Zhang et al, *Phys. Rev. B* **101**, 220411(R) (2020).

Study of the spin-1/2 antiferromagnetic XXZ chain $\text{SrCo}_2\text{V}_2\text{O}_8$ in a transverse external magnetic field

K. Puzniak^{1,2}, B. Lake^{1,2}, N. Islam¹, R. Feyerherm¹, M. Reehuis¹, W. Schmidt³, M. Boehm³, P. Steffens³, A. Schneidewind⁴, I. Radelytskyi⁴, C. Balz⁵, R. Stewart⁵

¹ *Helmholtz-Zentrum Berlin für Materialien und Energie GmbH, Hahn-Meitner Platz 1, D-14109 Berlin, Germany*

² *Institut für Festkörperphysik, Technische Universität Berlin, Hardenbergstraße 36, D-10623 Berlin, Germany*

³ *Institut Laue Langevin, 6 rue Jules Horowitz, BP 156, F-38042 Grenoble, France*

⁴ *Jülich Centre for Neutron Science at Heinz Maier-Leibnitz Zentrum, 85747 Garching, Germany*

⁵ *Neutron and Muon Source, STFC Rutherford Appleton Laboratory, Didcot OX11 0QX, United Kingdom*

The one-dimensional (1D) spin-1/2 antiferromagnet (AFM) with Heisenberg-Ising (XXZ) anisotropy is an ideal model system to explore fundamental physics concepts. In zero applied magnetic field, this system hosts spinon excitations which are particles with fractional spin quantum number - quite different from the magnons of conventional three-dimensional (3D) magnets which have integer spin. A very interesting spin-1/2 quasi-1D antiferromagnetic XXZ material is $\text{SrCo}_2\text{V}_2\text{O}_8$. This compound crystallizes in the tetragonal space group $I4_1cd$ (No. 110). The Co^{2+} ions have effective $S=1/2$ moments that are arranged in screw chains along the c -axis. The Co^{2+} ions are coupled by strong antiferromagnetic interactions within the screw chains which have partial Ising (XXZ) anisotropy where the interaction strength is $J=7.0$ meV and the anisotropy parameter is $\epsilon=0.56$ where the c -axis is the easy-axis. Weak interchain coupling gives rise to long-range magnetic order below $T_N=5.2$ K [1]. The spins are aligned antiferromagnetically along the screw chains and ferromagnetically (antiferromagnetically) along the a (b) direction respectively. In a transverse magnetic field applied along the $[1,0,0]$ direction, $\text{SrCo}_2\text{V}_2\text{O}_8$ undergoes a transition at the field of $B_c^{3D}=6.96$ T, which is the 3D Quantum Critical Point (QCP) [2].

The effects of a $[1,0,0]$ transverse magnetic field have been also explored in the related compound $\text{BaCo}_2\text{V}_2\text{O}_8$ [3], which has a very similar structure to $\text{SrCo}_2\text{V}_2\text{O}_8$. In $\text{BaCo}_2\text{V}_2\text{O}_8$ a 1D QCP was also found, however in case of $\text{SrCo}_2\text{V}_2\text{O}_8$ no experimental indications of this second QCP were observed. In this work we report on: the heat capacity, inelastic neutron scattering and neutron diffraction measurements of $\text{SrCo}_2\text{V}_2\text{O}_8$ (under transverse fields along the tetragonal b direction) in order to explore the nature of its magnetic excitations and magnetic order for fields below and above the 3D QCP.

[1] A. K. Bera, B. Lake. et al, *Phys. Rev.B* **96**, 054423 (2017).

[2] X. Zhang, Z. He. et al, *Phys. Rev.B* **103**, 144405 (2021).

[3] Q. Faure, S. Takayoshi et al, *Nat. Phys.* **14**, 716 (2018).

Symposium 4. Antiferromagnetism and antiferromagnetic spintronics

| | | |
|------------------------------|---|-----|
| Nikolaos Biniskos | <i>Complex ground state, spin waves and field induced transitions of the noncollinear antiferromagnet Mn_5Si_3</i> | 89 |
| Akashdeep Kamra | <i>Antiferromagnetic magnon pseudospin and Hanle effect</i> | 90 |
| Tim Ludwig | <i>Antiferromagnetic dynamics: dissipative and non-dissipative baths</i> | 91 |
| Hendrik Meer | <i>Shape Anisotropy in Antiferromagnetic structures</i> | 92 |
| Matthias Opel | <i>Magnonic Hanle Effect in Easy-Plane Antiferromagnets</i> | 93 |
| Vincent Polewczyk | <i>Epitaxial strain tailoring of the antiferromagnetic properties in $LaFeO_3$ thin films</i> | 94 |
| Antonin Badura | <i>Anomalous Nernst effect of the spin-split antiferromagnet Mn_5Si_3</i> | 97 |
| Ilaria Bergenti | <i>Exchange bias effects in Co/CoO coupled with molecular layers</i> | 98 |
| Xin Chen | <i>Enhanced anomalous Hall effect in Cr modulation-doped Mn_3Sn thin films</i> | 99 |
| Tobias Dannegger | <i>An ab initio parameterised spin model of hematite</i> | 100 |
| Edgar Felipe Galindez-Ruales | <i>Long-distance magnon spin transport in antiferromagnetic insulators</i> | 101 |
| Olena Gomonay | <i>Gradient magnetoelasticity: tailoring of antiferromagnetic textures</i> | 102 |
| Krzysztof Grochot | <i>Current induced magnetization field free switching in exchange biased $Pt(W)/Co/NiO$ heterostructures</i> | 103 |
| Michał Grzybowski | <i>Antiferromagnetic Hysteresis above the Spin Flop Field</i> | 104 |
| Mohammad Hamdi | <i>Towards antiferromagnetic dynamic solitons: terahertz Slonczewskii spin waves in antiferromagnetic spin-Hall nano-oscillators</i> | 105 |
| Zdenek Kaspar | <i>Quenching of an antiferromagnet into high resistivity states using electrical or ultrashort optical pulses</i> | 106 |
| Muhammad Waqas Khaliq | <i>XPEEM Imaging of Magneto-acoustic Waves at GHz Frequency</i> | 107 |
| Roman Khymyn | <i>Antiferromagnetic domain wall as a reconfigurable long Josephson junction</i> | 108 |
| Johannes Kleinlein | <i>Molecular beam epitaxy of the half-Heusler antiferromagnet $CuMnSb$</i> | 109 |
| Kacper Kluczyk | <i>Bulk Hexagonal $MnTe$ - a Room Temperature Antiferromagnet</i> | 110 |
| Dominik Kriegner | <i>Spontaneous anomalous Hall effect arising from antiparallel magnetic order in a semiconductor</i> | 111 |
| Miina Leiviskä | <i>Anisotropic spontaneous Hall effect in unconventional antiferromagnet Mn_5Si_3</i> | 112 |
| Priyanka Nehla | <i>Unveiling Oxidation and Spin State of Fe in $Li_{1-x}Zn_xFeO_2$</i> | 113 |
| Panagiota Ntetsika | <i>Ferromagnetic resonance study of acoustic, optic and mixed excitations in $Ru/Cr/Co$ and Ru/Co multilayers</i> | 114 |

| | | |
|-----------------------|---|-----|
| Sonka Reimers | <i>Impact of magnetoelastic coupling on antiferromagnetic spintronics</i> | 115 |
| Yuliya Savina | <i>Magnetic properties of biphasic $\text{LaCr}_3(\text{BO}_3)_4$ crystal</i> | 116 |
| Casper Schippers | <i>Suppressing electrical switching of antiferromagnets with high magnetic fields</i> | 117 |
| Paweł Sobieszczyk | <i>Compensation point in the ferrimagnetic nanoparticles</i> | 118 |
| Ilja Turek | <i>Altermagnetism and magnetic groups with pseudoscalar electron spin</i> | 119 |
| Jiří Volný | <i>Single crystal studies of NaMnAs, a rediscovered room temperature antiferromagnetic semiconductor</i> | 120 |
| Angela Wittmann | <i>Role of substrate clamping on anisotropy and domain structure in the canted antiferromagnet $\alpha\text{-Fe}_2\text{O}_3$</i> | 121 |
| Marcin Wysokiński | <i>False antiferromagnetic component in ferromagnetic $\text{La}_5\text{Co}_2\text{Ge}_3$ under pressure</i> | 122 |
| Jakub Železný | <i>Spin-transfer torque in non-collinear antiferromagnetic junctions</i> | 123 |
| Jan Zubáč | <i>Hysteretic effects and magnetotransport of electrically switched CuMnAs</i> | 124 |
| Aleksei Bludov | <i>Magnetic properties of $\text{RCr}_3(\text{BO}_3)_4$ crystals with Tb^{3+} and Dy^{3+} ions</i> | 126 |
| Irina Dolgikh | <i>Ultrafast Emergence of Ferromagnetism in Antiferromagnetic FeRh in High Magnetic Fields</i> | 127 |
| Anna Hellenes | <i>Giant and tunneling magnetoresistance in unconventional collinear antiferromagnets with nonrelativistic spin-momentum coupling</i> | 128 |
| Arturo Rodríguez Sota | <i>Magnetism and growth of a Mn monolayer on Ir (111) investigated by SP STM</i> | 129 |
| Vishesh Saxena | <i>Exploring the antiferromagnetic ground states and domain walls of Mn bi- and trilayers on Ir (111) by SP-STM</i> | 130 |
| Maria Stamenova | <i>Resistance of atomically sharp domain walls in CuMnAs from first principles</i> | 131 |
| Oleksii Zadorozhnyi | <i>In-situ electrically and thermally controlled magnetic imaging of metamagnetic FeRh in transmission electron microscope</i> | 132 |

Invited Oral Presentations

| | | |
|-------------------|---|----|
| Nikolaos Biniskos | <i>Complex ground state, spin waves and field induced transitions of the noncollinear antiferromagnet Mn_5Si_3</i> | 89 |
| Akashdeep Kamra | <i>Antiferromagnetic magnon pseudospin and Hanle effect</i> | 90 |
| Tim Ludwig | <i>Antiferromagnetic dynamics: dissipative and non-dissipative baths</i> | 91 |
| Hendrik Meer | <i>Shape Anisotropy in Antiferromagnetic structures</i> | 92 |
| Matthias Opel | <i>Magnonic Hanle Effect in Easy-Plane Antiferromagnets</i> | 93 |
| Vincent Polewczyk | <i>Epitaxial strain tailoring of the antiferromagnetic properties in $LaFeO_3$ thin films</i> | 94 |

Complex ground state, spin waves and field induced transitions of the noncollinear antiferromagnet Mn_5Si_3

N. Biniskos¹, F. J. dos Santos², K. Schmalzl³, S. Raymond⁴, M. dos Santos Dias⁵, S. Blügel⁵, S. Lounis⁵ and T. Brückel⁶

¹ Forschungszentrum Jülich GmbH, JCNS at MLZ, Lichtenbergstrasse 1, 85748 Garching, Germany

² École Polytechnique Fédérale de Lausanne, THEOS and MARVEL, 1015 Lausanne, Switzerland

³ Forschungszentrum Jülich GmbH, JCNS at ILL, 38000 Grenoble, France

⁴ Université Grenoble Alpes, CEA, IRIG, MEM, MDN, 38000 Grenoble, France

⁵ Forschungszentrum Jülich GmbH, PGI and IAS, 52425 Jülich, Germany

⁶ Forschungszentrum Jülich GmbH, JCNS-2 and PGI-4, JARA-FIT, 52425 Jülich, Germany

Noncollinear spin configurations in magnetic materials gives rise to important macroscopic phenomena that can be exploited for developing future information and communication technologies. In this context the metallic compound Mn_5Si_3 is a promising material for applications due to its interesting transport and thermodynamic properties, such as the anomalous Hall conductivity [1] and the inverse magnetocaloric effect [2]. In the paramagnetic state, Mn_5Si_3 crystallizes in hexagonal space group $P6_3/mcm$ with two distinct crystallographic positions for the Mn atoms (sites Mn1 and Mn2) and it undergoes two phase transitions towards a collinear and non collinear antiferromagnetic (AFM) phase at $T_{N2}=100\text{K}$ (AFM2) and $T_{N1}=66\text{K}$ (AFM1), respectively. The crystal structure of the AFM2 phase can be described by a centrosymmetric orthorhombic cell with space group $Ccmm$, where Mn2 divides into two sets of nonequivalent positions. In this cell, magnetic reflections follow the condition $h + k$ odd, the magnetic propagation vector is $\kappa = (0, 1, 0)$, and only two-thirds of the Mn2 atoms acquire magnetic moments aligned parallel and antiparallel to the b axis of the orthorhombic unit cell [3]. While neutron diffraction studies and density functional theory calculations are in agreement regarding the collinear spin arrangement in the AFM2 phase, in past years several contradicting spin structures have been proposed for the noncollinear AFM1 phase. The noncollinear spin configuration of this system (AFM1 phase), is believed to be the origin of its important properties. In this work [4], we determine the magnetic exchange couplings of the AFM1 phase of Mn_5Si_3 using inelastic neutron scattering measurements and density functional theory calculations. We obtain the ground-state spin configuration and compute its magnon dispersion relations which are in good agreement with the ones obtained experimentally. Furthermore, we investigate the evolution of the spin structure under the application of an external magnetic field to demonstrate theoretically the multiple field-induced phase transitions which the system undergoes. Finally, we model the instability of some Mn magnetic moments in a frustrated environment to unveil their behavior under an external magnetic field.

[1] C. Sürgers, G. Fischer, P. Winkel, and H. v. Löhneysen, *Nat. Commun.* **5**, 3400 (2014).

[2] N. Biniskos, K. Schmalzl, S. Raymond, S. Petit, P. Steffens, J. Persson, and T. Brückel, *Phys. Rev. Lett.* **120**, 257205 (2018).

[3] F. J. dos Santos, N. Biniskos, S. Raymond, K. Schmalzl, M. dos Santos Dias, P. Steffens, J. Persson, S. Blügel, S. Lounis, and T. Brückel, *Phys. Rev. B* **103**, 024407 (2021).

[4] N. Biniskos, F. J. dos Santos, K. Schmalzl, S. Raymond, M. dos Santos Dias, J. Persson, N. Marzari, S. Blügel, S. Lounis, and T. Brückel, *Phys. Rev. B* **105**, 104404 (2022).

Antiferromagnetic magnon pseudospin and Hanle effect

Akashdeep Kamra

Condensed Matter Physics Center (IFIMAC) and Departamento de Física Teórica de la Materia Condensada, Universidad Autónoma de Madrid, Spain

Exploiting the spin of electrons for information transport and processing led to the field of *spintronics*, that has played a crucial role in achieving the contemporary data-heavy information technology. In electrically insulating magnets, spin can be carried by fundamentally different bosonic excitations called magnons. These offer several advantages over electrons as information carriers.

In contrast with ferromagnets, magnons occur in pairs of spin-up and -down modes in antiferromagnets. I will discuss how antiferromagnetic magnons admit a magnon pseudospin degree of freedom, mathematically analogous to the spin of an electron [1,2,3]. This potentially enables combining the advantages of electrons and magnons into one fertile platform for science and technology.

The crucial ingredient in exploiting magnon pseudospin is the ability to manipulate this degree of freedom. This has been realized recently and observation of the magnon Hanle effect has been reported [2,4].

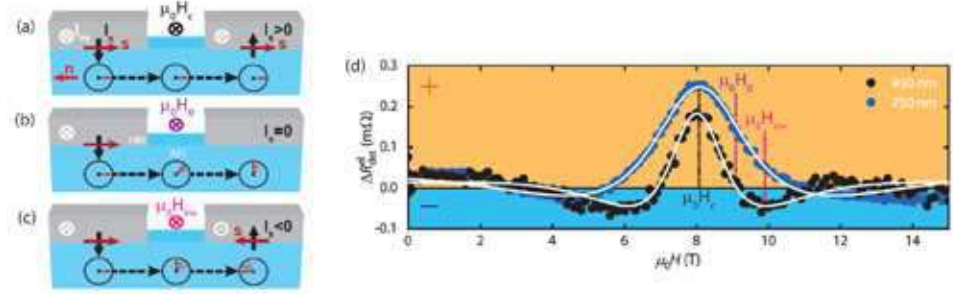


Figure 1: Figure adapted from [2].

The corresponding experiments accomplished a spin injection from a platinum electrode into an antiferromagnetic insulator and detection of the magnon spin at a distant electrode. The detected spin exhibits the sign-reversal behavior previously known in electronic spin transport and Hanle effect. In this manner, it provides a proof-of-concept for a high-potential direction of scientific inquiry - *magnon pseudospintronics*. We will close the discussion with an outlook on challenges and opportunities ahead in accomplishing a better control over the magnon pseudospin.

- [1] A. Kamra et al. *Phys. Rev. B* **102**, 174445 (2020).
- [2] T. Wimmer et al. *Phys. Rev. Lett.* **125**, 247204 (2020).
- [3] L. Liensberger et al. *Phys. Rev. Lett.* **123**, 117204 (2019).
- [4] A. Ross et al. *Appl. Phys. Lett.* **117**, 242405 (2020).

Antiferromagnetic dynamics: dissipative and non-dissipative baths

Daan van Seters¹, Tim Ludwig¹, Huaiyang Yuan¹, and Rembert A. Duine^{1,2}

¹*Institute for Theoretical Physics, Utrecht University,
Princetonplein 5, 3584 CC Utrecht, The Netherlands*

²*Department of Applied Physics, Eindhoven University of Technology,
P.O. Box 513, 5600 MB Eindhoven, The Netherlands*

The low dissipation of the Néel vector makes antiferromagnets particularly interesting for low-power spintronic applications. In microscopic models, dissipation typically arises when the subsystem of interest (e.g. sublattice magnetizations) is coupled to some bath that can absorb energy, angular momentum, or other conserved quantities. However, we argue that this is not necessarily true for antiferromagnetic dynamics; namely, the Néel vector can remain non-dissipative even when the sublattice magnetizations are coupled to a bath.

As a simple model for a typical two-sublattice antiferromagnet, we consider two macrospins that are coupled antiferromagnetically to each other and linearly to a bath of harmonic oscillators (Caldeira-Leggett model). For the standard case of an Ohmic bath, a Gilbert-damping term arises for each macrospin. However, we show that, when the bath is shared between the two macrospins, it does not contribute to the dissipation of the Néel vector. Generalizing back to two-sublattice antiferromagnets, we argue that—from the perspective of the Néel vector—baths are non-dissipative when shared between the sublattice magnetizations, whereas baths are dissipative when exclusive for one sublattice magnetization.

We expect our results to give new insights into dissipation in antiferromagnetic dynamics. Building on those insights, our results might help to create or identify new materials with particularly low dissipation of the Néel vector.

Shape Anisotropy in Antiferromagnetic structures

H. Meer¹, O. Gomonay¹, C. Schmitt¹, R. Ramos^{2,3}, L. Schnitzspan¹,
M. A. Mawass⁴, F. Kronast⁴, S. Valencia⁴, E. Saitoh^{2,5,6,7}, J. Sinova¹, L. Baldrati¹
and M. Kläui¹

¹ Institute of Physics, Johannes Gutenberg-University Mainz, 55099 Mainz, Germany

² WPI-Advanced Institute for Materials Research, Tohoku University, Sendai 980-8577, Japan

³ Centro de Investigación en Química Biológica e Materiais Moleculares (CIQUS), Departamento de Química-Física, Universidade de Santiago de Compostela, Santiago de Compostela 15782, Spain

⁴ Helmholtz-Zentrum Berlin für Materialien und Energie, D-12489 Berlin, Germany

⁵ Department of Applied Physics, The University of Tokyo, Tokyo 113-8656, Japan

⁶ Center for Spintronics Research Network, Tohoku University, Sendai 980-8577, Japan

⁷ Advanced Science Research Center, Japan Atomic Energy Agency, Tokai 319-1195, Japan

Conventional shape anisotropy in ferromagnets leads to geometrically-induced domain structures due to dipolar interactions. In antiferromagnets without net moments, we demonstrate how shape-induced strain can be used analogously to control antiferromagnetic (AFM) ordering in epitaxial NiO/Pt thin films [1]. Previous investigations of patterning-induced modification of the AFM order near the patterning edge have focused on the passive application of AFMs in AFM/FM bilayers [2]. However, considering the potential of antiferromagnets as active elements in spintronic devices [3], it is important to investigate shape-induced effects in AFMs without an adjacent FM layer. To this end, we investigate the domain structures of patterned elements of antiferromagnetic NiO. We observe different domain structures for rectangular elements of NiO patterned along the easy and hard magnetocrystalline anisotropy axes of the film and we can identify magnetoelastic interactions resulting in the different domain configurations. We reproduce the experimental observations by modeling magnetoelastic interactions, considering spontaneous strains induced by the domain configuration, as well as

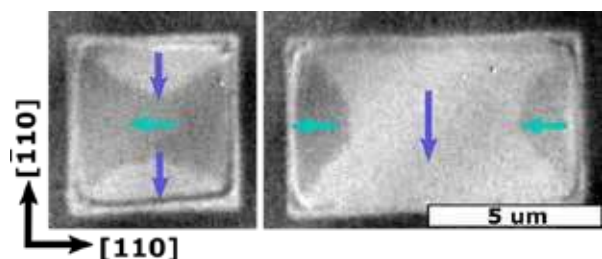


Figure 1: XMLD-PEEM image of shape-induced NiO domains inside rectangular shaped elements, with edges oriented along the in-plane projection of the easy axes in MgO//NiO(10nm)/Pt(2nm) thin films. The in-plane component of the Néel vector in the domains is indicated by the arrows.

elastic strains due to the substrate and the geometry of the patterns. By varying the aspect ratio of rectangular elements, we demonstrate control of the antiferromagnetic ground-state domain configuration, see Fig. 1. Thus, shape-induced strain does not only need to be considered in the design of antiferromagnetic devices, but can potentially be used to tailor their properties, providing an additional handle to control AFM domain structures.

- [1] H. Meer, F. Schreiber, C. Schmitt, R. Ramos, E. Saitoh, O. Gomonay, J. Sinova, L. Baldrati, and M. Kläui, *Nano Lett.* **21**, 114-119 (2021).
- [2] E. Folven, T. Tybell, A. Scholl, A. Young, S. T. Retterer, Y. Takamura, and J. K. Grepstad, *Nano Lett.* **10**, 4578 (2010).
- [3] V. Baltz, A. Manchon, M. Tsoi, T. Moriyama, T. Ono, and Y. Tserkovnyak, *Rev. Mod. Phys.* **90**, 015005 (2018).

Magnonic Hanle Effect in Easy-Plane Antiferromagnets

Janine Gückelhorn^{1,2}, Akashdeep Kamra³, Tobias Wimmer^{1,2}, Matthias Opel¹,
Stephan Geprägs¹, Rudolf Gross^{1,2,4}, Hans Huebl^{1,2,4}, and Matthias Althammer^{1,2}

¹ Walther-Meißner-Institut, Bayerische Akademie der Wissenschaften, Garching, Germany

² Physik-Department, Technische Universität München, Garching, Germany

³ Condensed Matter Physics Center (IFIMAC) and Departamento de Física Teórica de la Materia Condensada, Universidad Autónoma de Madrid, Madrid, Spain

⁴ Munich Center for Quantum Science and Technology (MCQST), München, Germany

Antiferromagnetic materials host pairs of spin-up and spin-down magnons, which we describe in terms of a magnonic pseudospin [1]. Its close analogy to the spin of electronic charge carriers leads to the prediction and observation of fascinating spin transport phenomena [2,3]. In its antiferromagnetic phase below 953 K, the oxide insulator α -Fe₂O₃ (hematite) shows a finite anisotropic spin-spin (“Dzyaloshinskii-Moriya”) interaction with a slight canting of the antiferromagnetic sublattice magnetizations in the magnetic easy (0001) plane at room temperature, giving rise to a residual net magnetization [4,5]. Bilayers of α -Fe₂O₃ and the heavy metal Pt exhibiting a large spin-orbit coupling represent a prototypical system to investigate electrical magnon injection and detection, spin-Hall magnetoresistance [6], as well as antiferromagnetic magnon propagation [1,2,3].

In two-terminal devices, each consisting of two Pt electrodes on both a 15 nm and a 100 nm thin α -Fe₂O₃ film, we study the diffusive spin transport in a non-local geometry via pairs of spin-up and spin-down magnons as the quantized spin excitations. Using a current reversal method enables us to discriminate between electrical and thermal effects. We demonstrate the electrical magnon injection, diffusive magnon transport, and magnon detection [2,3]. We observe the coherent precession of the magnonic pseudospin caused by the easy-plane anisotropy and the Dzyaloshinskii-Moriya interaction [2,3]. By applying an external magnetic field, we further control this precession and interpret our observation as the magnonic analogue of the electronic Hanle effect [2,3]. In the thicker film, we additionally observe an oscillating behavior of the magnon spin signal in the high magnetic field range as well as an offset signal in the low magnetic field regime [3]. We attribute this offset signal to the presence of finite-spin low-energy magnons [3]. Our findings unlock the high potential of antiferromagnetic magnonics towards the realization of electronics-inspired phenomena.

We gratefully acknowledge financial support from the German Research Foundation under Germany's Excellence Strategy – EXC-2111 – 390814868 and project AL2110/2-1 and the Spanish Ministry for Science and Innovation – AEI Grant CEX2018-000805-M.

[1] A. Kamra *et al.*, *Physical Review B* **102**, 174445 (2020).

[2] T. Wimmer *et al.*, *Physical Review Letters* **125**, 247204 (2020).

[3] J. Gückelhorn *et al.*, *submitted to Physical Review B*, *arXiv:2112.03820* (2021).

[4] I. Dzyaloshinsky, *Journal of the Physics and Chemistry of Solids* **4**, 241 (1958).

[5] T. Moriya, *Physical Review* **120**, 91 (1960).

[6] J. Fischer *et al.*, *Physical Review Applied* **13**, 014019 (2020).

Epitaxial strain tailoring of the antiferromagnetic properties in LaFeO_3 thin films

V. Polewczyk¹, A. Y. Petrov¹, B. Sarpi², D. Backes², G. Vinai¹, P. Torelli¹, F. Maccherozzi², B. A. Davidson^{1,3}

¹ *Istituto Officina dei Materiali, Area Science Park, S.S.14, km 163.5, I-34149 Trieste, Italy*

² *Diamond Light Source, Harwell Science and Innovation Campus, Didcot OX110DE, UK*

³ *Stewart Blusson Quantum Matter Institute, British Columbia, Vancouver BCV6T1Z4, Canada*

The behavior of antiferromagnetic (AF) materials has been the focus of intense investigation in the last decade, due to the potential control of exchange coupling phenomena at interfaces with ferromagnetic materials [1] and more recently in their own right as the basis of new approaches to spintronic devices [2]. Among the various candidates, a prototypical case is the LaFeO_3 (LFO) compound. Bulk LFO has an orthorhombic structure that can be described as pseudocubic (3.93\AA), with the AF axis along the pseudocubic $\langle 110 \rangle$ axis and a high Néel temperature of 740K [3].

In this work, we study the AF properties of stoichiometric LFO films coherently grown on a different substrates that span across a wide range of compressive and tensile strains (from -1.831% for NGO (110) up to 1.5% for BTO (001)), including tetragonal, cubic and orthorhombic substrates with different crystallographic orientations. The films are grown by oxide molecular beam epitaxy using the shutter method that provides precise control of stoichiometry, yielding high-quality films whose thicknesses are kept below the critical thickness for strain relaxation, typically ≤ 100 uc, on all substrates. We then element-selective

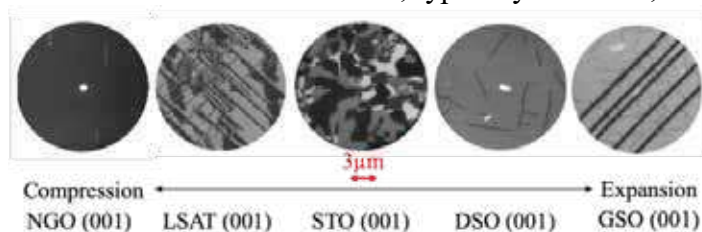


FIGURE 1: XMLD-PEEM images of LFO domains on various substrates recorded at the $\text{Fe } L_2$ chemical threshold for a random light direction and polarization recorded.

soft x-ray magnetic linear dichroism photoemission electron microscopy (XMLD-PEEM) at the I06 beamline of the Diamond light source to probe the AF properties of the films. Fig. 1 shows some selected XMLD-PEEM images recorded at 170K on different LFO/substrates. A wide variation of AF domains is observed according to the substrate-induced strain. LFO

films grown on cubic substrates such as STO show an undesirable fourfold distribution of AF domains, in agreement with similar studies [3], [4] distributed mostly in-plane with an out of the plane contribution varying between 20° up to 45° . For the first time, we report nearly monodomain properties when deposited onto orthorhombic substrates such as NGO (001), DSO (001) and GSO (001), where a single AF axis direction is recorded over more than 90% of the probed area. These tendencies follow the strain state imposed by the substrates with compressive and tensile strains, which lead to in-plane and out of the plane orientations of the AF axis respectively. However, when the strain is too large and the thin film layer starts relaxing, as in the case of NGO (110), an AF multidomain state with small lateral extension appear. These findings constitute a crucial step towards the understanding of strain control of the AF axis and paths the way towards AF spintronics of heterostructure oxide layers.

[1] J. Nogués *et al.*, *Physics Reports*, 422:65-117 (2005).

[2] A. Brataas *et al.*, *Physics Reports*, 885:1–27 (2020).

[3] J. Luning *et al.*, *Physical Review B*, 67:214433 (2003).

[4] S. Czekaj *et al.*, *Physical Review B*, 73:02040 (2006).

Oral Presentations

| | | |
|------------------------------|--|-----|
| Antonin Badura | <i>Anomalous Nernst effect of the spin-split antiferromagnet Mn_5Si_3</i> | 97 |
| Ilaria Bergenti | <i>Exchange bias effects in Co/CoO coupled with molecular layers</i> | 98 |
| Xin Chen | <i>Enhanced anomalous Hall effect in Cr modulation-doped Mn_3Sn thin films</i> | 99 |
| Tobias Danneegger | <i>An ab initio parameterised spin model of hematite</i> | 100 |
| Edgar Felipe Galindez-Ruales | <i>Long-distance magnon spin transport in antiferromagnetic insulators</i> | 101 |
| Olena Gomonay | <i>Gradient magnetoelasticity: tailoring of antiferromagnetic textures</i> | 102 |
| Krzysztof Grochot | <i>Current induced magnetization field free switching in exchange biased Pt(W)/Co/NiO heterostructures</i> | 103 |
| Michał Grzybowski | <i>Antiferromagnetic Hysteresis above the Spin Flop Field</i> | 104 |
| Mohammad Hamdi | <i>Towards antiferromagnetic dynamic solitons: terahertz Slonczewskii spin waves in antiferromagnetic spin-Hall nano-oscillators</i> | 105 |
| Zdenek Kaspar | <i>Quenching of an antiferromagnet into high resistivity states using electrical or ultrashort optical pulses</i> | 106 |
| Muhammad Waqas Khaliq | <i>XPEEM Imaging of Magneto-acoustic Waves at GHz Frequency</i> | 107 |
| Roman Khymyn | <i>Antiferromagnetic domain wall as a reconfigurable long Josephson junction</i> | 108 |
| Johannes Kleinlein | <i>Molecular beam epitaxy of the half-Heusler antiferromagnet CuMnSb</i> | 109 |
| Kacper Kluczyk | <i>Bulk Hexagonal MnTe - a Room Temperature Antiferromagnet</i> | 110 |
| Dominik Kriegner | <i>Spontaneous anomalous Hall effect arising from antiparallel magnetic order in a semiconductor</i> | 111 |
| Miina Leiviskä | <i>Anisotropic spontaneous Hall effect in unconventional antiferromagnet Mn_5Si_3</i> | 112 |
| Priyanka Nehla | <i>Unveiling Oxidation and Spin State of Fe in $\text{Li}_{1-x}\text{Zn}_x\text{FeO}_2$</i> | 113 |
| Panagiota Ntetsika | <i>Ferromagnetic resonance study of acoustic, optic and mixed excitations in Ru/Cr/Co and Ru/Co multilayers</i> | 114 |
| Sonka Reimers | <i>Impact of magnetoelastic coupling on antiferromagnetic spintronics</i> | 115 |
| Yuliya Savina | <i>Magnetic properties of biphasic $\text{LaCr}_3(\text{BO}_3)_4$ crystal</i> | 116 |
| Casper Schippers | <i>Suppressing electrical switching of antiferromagnets with high magnetic fields</i> | 117 |
| Paweł Sobieszczyk | <i>Compensation point in the ferrimagnetic nanoparticles</i> | 118 |
| Ilja Turek | <i>Altermagnetism and magnetic groups with pseudoscalar electron spin</i> | 119 |
| Jiří Volný | <i>Single crystal studies of NaMnAs, a rediscovered room temperature antiferromagnetic semiconductor</i> | 120 |
| Angela Wittmann | <i>Role of substrate clamping on anisotropy and domain structure in the canted antiferromagnet $\alpha\text{-Fe}_2\text{O}_3$</i> | 121 |

| | | |
|-------------------|---|-----|
| Marcin Wysokiński | <i>False antiferromagnetic component in ferromagnetic $\text{La}_5\text{Co}_2\text{Ge}_3$ under pressure</i> | 122 |
| Jakub Železný | <i>Spin-transfer torque in non-collinear antiferromagnetic junctions</i> | 123 |
| Jan Zubáč | <i>Hysteretic effects and magnetotransport of electrically switched CuMnAs</i> | 124 |

Anomalous Nernst effect of the spin-split antiferromagnet Mn_5Si_3

A. Badura^{1,4}, S. Beckert², H. Reichlova^{2,3}, M. Villanueva⁴, E. Schmoranzero¹, R. Lopes Seeger⁵, M. Leiviskä⁵, I. Kounta⁶, L. Michez⁶, D. Kriegner^{2,3}, V. Baltz⁵, L. Šmejkal^{7,3}, J. Sinova^{7,3}, T. Jungwirth³, and S. T. B. Goennenwein⁴

¹Department of Chemical Physics and Optics, Faculty of Mathematics and Physics, Charles University, Prague, Czechia

² Institute of Solid State and Materials Physics, TU Dresden, Dresden, Germany

³Institute of Physics, Czech Academy of Sciences, Prague, Czechia

⁴ AG Modern Materials Science, University of Konstanz, Konstanz, Germany

⁵ University Grenoble Alpes, CNRS, CEA, Grenoble INP, Spintec, Grenoble, France

⁶ Aix-Marseille University, CNRS, CINaM, Marseille, France

⁷ Institute for Physics, Johannes Gutenberg University Mainz, Mainz, Germany

Traditional collinear antiferromagnets with time-reversal and space-inversion symmetries do not exhibit the anomalous Hall and Nernst effects. Recent theory development predicts that collinear antiferromagnets with particular crystal and spin symmetry can macroscopically break the time-reversal symmetry. Our current results show that Mn_5Si_3 thin films exhibit a robust spontaneous Hall effect in collinear and non-collinear antiferromagnetic phases despite negligible net magnetization [1].

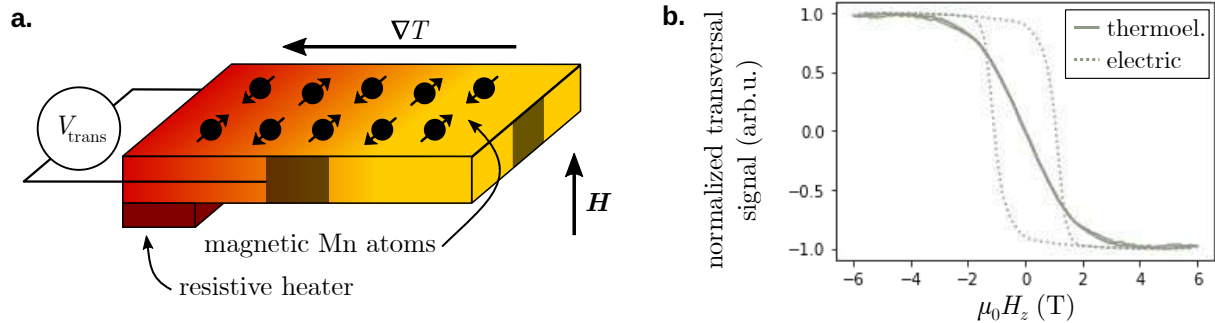


Figure 1: **a.** Schematics of the Nernst effect measurement in a spin-split collinear antiferromagnet (note that for the spin-splitting also non-magnetic atoms are crucial). **b.** Magnetic field dependence of transversal signal in a Mn_5Si_3 thin-film for electric and thermo-electric transport measured at 170 K (the signals are normalized for comparison).

In this contribution, we would like to show the breaking of the time-reversal symmetry in Mn_5Si_3 thin-films by measuring their thermo-electric response, i.e. the anomalous Nernst effect. Our Mn_5Si_3 samples consisted of 17-nm epitaxial Mn_5Si_3 layers grown using molecular-beam epitaxy on a Si(111) substrate. The thermal gradient was generated by macroscopic heaters in the film plane and the magnetic field was swept in the direction out of the sample plane, as shown in Fig. 1a. We observe both robust anomalous Hall and Nernst signals, as shown in Fig. 1b. Interestingly, the field dependence of these two signals is different. A systematic set of magneto-thermal transport data will be presented and differences compared to magneto-transport data discussed.

[1] H. Reichlova et al. *arXiv preprint arXiv:2012.15651*, 2020.

Exchange bias effects in Co/CoO coupled with molecular layers

Ilaria Bergenti¹, Luca Gnoli¹, Mattia Benini¹, Alberto Riminucci¹, Valentin Dediu¹

¹ *Institute of Nanostructured Materials ISMN-CNR Via Gobetti 101 40129 Bologna, Italy*

The distinctive features of Exchange bias (EB) at FM/AFM interface are a shift of the FM hysteresis loop and the modification of its coercivity. The ratio between the interface coupling energy and the anisotropy energy of the AFM determines the coupling regime and the magnetization reversal mechanism. In this work we were able to tune the EB effect acting on the spin configuration of the AFM layer by the insertion of a molecular layer on top of the FM/AFM interface.

We deposited polycrystalline thin films of Co (ranging from 5 to 10 nm thick) and we formed a bilayer with a single interface between Co and CoO by exposing the sample to a controlled oxygen atmosphere (10^2 - 10^4 L), generating an oxide thickness of 2 nm. On the top of CoO a thick molecular layer (25nm) was deposited. We focus on Gaq3(Gallium-quinoline) and C60 (buckminsterfullerene) as molecular layers because they have been proved to hybridize with magnetic layers modifying their magnetic properties [1,2] The magnetic properties of the Co/CoO/MOL stacks were determined with a MOKE apparatus. Temperature dependent of Co hysteresis loops of the samples were acquired after cooling down to 50 K after appropriate training. The presence of the molecular layer determines an hardening of the Co layer: C60 shows the largest increase of coercive field of Co for CoO generated by 10^2 L Oxygen, while samples with thicker oxide layer (10^4 L) do not shows any appreciable change as a function of the organic overlayer.

We interpret our data considering the hybridization with molecular layer as source of AFM magnetic defects[3]. These defects decrease the anisotropy locally and lead to an overall reduction of the AF energy. This reduction of the AF energy gives rise to a local energy minimum for certain defect positions relative to the interface. The domain walls can be pinned at such positions and contribute to the increase of coercivity

[1] I. Bergenti and V. Dediu, V, *Nanomaterials science* 2019 1, 149.

[2] M. Cinchetti, V. Dediu, L.E. Hueso, *Nat. Mater.*, 2017, 16, 507

[3] R.E. Camley et al., *J. Vac Sci. & Tec. A* 1999, 17, 1335;

Enhanced anomalous Hall effect in Cr modulation-doped Mn₃Sn thin films

Xin Chen¹, Hang Xie¹, Ziyang Luo², Lei Shen^{3,4}, and Yihong Wu^{1,5}

¹Department of Electrical and Computer Engineering, National University of Singapore, Singapore 117583

²School of Physics and Electronics, Central South University, Changsha 410083, China

³Department of Mechanical Engineering, National University of Singapore, Singapore 117575

⁴Engineering Science Programme, National University of Singapore, Singapore 117575

⁵National University of Singapore (Chong Qing) Research Institute, Chongqing Liang Jiang New Area, Chongqing 401123, China

Non-collinear antiferromagnet has recently attracted attention due to its peculiar magnetotransport properties [1]. Here, we report on Cr doping effect in polycrystalline Mn₃Sn films with both uniform and modulation doping [2]. The uniform doping is achieved through co-sputtering of Mn₃Sn and Cr, whereas modulation doping is realized through the formation of Mn₃Sn/Cr multilayers with ultrathin Cr layer. Figures 1(a)-(d) show the AHE loops at different temperatures (T) for four samples: 72 nm Mn₃Sn, [Mn₃Sn(2.4)/Cr(t)]₃₀ with $t = 0.15$ and 0.6, and a co-sputtered sample (MS50Cr10) deposited with Mn₃Sn and Cr sputtering power of 50 W and 10 W, respectively (number inside parentheses indicate thickness in nm). The zero-field Hall resistivity (ρ_{xy}) for Mn₃Sn is 2.3 $\mu\Omega$ cm at 300 K and it decreases with decreasing T , which is consistent with previous reports [3,4]. In contrast, a significant enhancement in ρ_{xy} is observed in both types of Cr-doped samples, in particular ρ_{xy} of [Mn₃Sn(2.4)/Cr(t)]₃₀ keeps increasing down to 50 K (limited by the equipment). Figure 1(e) summarizes the temperature dependent Hall conductivity. As can be seen, the Hall conductivity increases with decreasing T for the three doped samples, and a Hall conductivity as high as 184.8 Ω^{-1} cm⁻¹ is obtained for [Mn₃Sn(2.4)/Cr(0.15)]₃₀ at 50 K, which is significantly larger than that of Mn₃Sn. The large enhancement is presumably caused by doping induced Fermi level shift in Mn₃Sn.

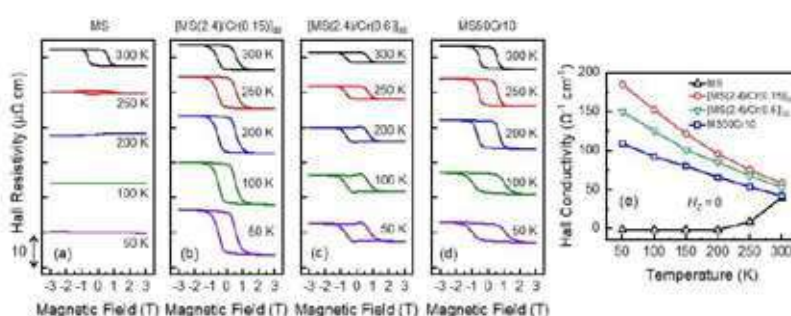


Figure 1: (a)-(b) Magnetic field-dependent anomalous Hall resistivity loops at different temperatures for different samples. (e) Temperature-dependent Hall conductivity curves.

References

- [1] S. Nakatsuji et al., *Nature* **527**, 212 (2015).
- [2] X. Chen et al., arXiv preprint arXiv:2107.00959.
- [3] T. Higo et al., *Appl. Phys. Lett.* **113**, 202402 (2018).
- [4] T. Ikeda et al., *Appl. Phys. Lett.* **113**, 222405 (2018).

An ab initio parameterised spin model of hematite

Tobias Dannegger¹, András Deák², Shubhankar Das³, E. F. Galindez Ruales³, Eunchong Baek³, Mathias Kläui³, László Szunyogh^{2,4}, and Ulrich Nowak¹

¹*Fachbereich Physik, Universität Konstanz, DE-78457 Konstanz, Germany*

²*Department of Theoretical Physics, Institute of Physics, Budapest University of Technology and Economics, Műegyetem rkp. 3., HU-1111 Budapest, Hungary*

³*Institute of Physics, Johannes Gutenberg University Mainz, Staudingerweg 7, 55128 Mainz, Germany*

⁴*MTA-BME Condensed Matter Research Group, Budapest University of Technology and Economics, Budafoki út 8, HU-1111 Budapest, Hungary*

The canted antiferromagnetic insulator hematite (α -Fe₂O₃) is well-known as the material in which the Morin transition was first observed [1], a phase transition where the magnetic moments flip from a perfectly antiferromagnetic configuration into a canted configuration with finite net magnetisation. It was also the observation of this “weak ferromagnetism” that later led to the theory of the Dzyaloshinskii–Moriya interaction (DMI) [2, 3]. Today, hematite continues to play an important role in antiferromagnetic spintronics research because of its long-distance transport of magnonic spin currents [4].

Here, we present an atomistic spin model of hematite, parameterised with ab initio calculations based on the screened Korringa–Kohn–Rostoker (SKKR) method. The ab initio results were mapped onto an extended classical Heisenberg model with tensorial exchange interactions and additional terms for first and second order on-site anisotropies. Dipole-dipole interactions were also taken into account, which lead to effective two-site anisotropy terms. Despite the material’s antiferromagnetic order, we found that these dipolar terms are the largest contribution to the anisotropy and can therefore not be neglected. The simulation results show that this spin model accurately reproduces the experimentally measured equilibrium properties and phase transitions of hematite, in particular the Morin transition can be observed.

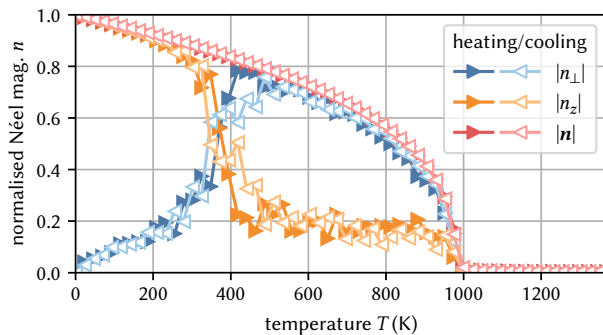


Figure 2: Simulated Morin transition (between 300 and 400 K) and Néel transition (below 1000 K).

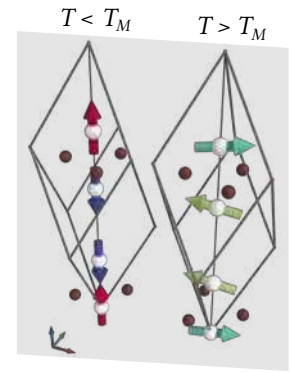


Figure 1: Antiferromagnetic and weak ferromagnetic phase of hematite.

- [1] F. J. Morin, *Phys. Rev.* **78**, 819 (1950).
- [2] I. Dzyaloshinskii, *J. Phys. Chem. Solids* **50**, 241 (1958).
- [3] T. Moriya, *Phys. Rev.* **120**, 91 (1960).
- [4] R. Lebrun, A. Ross, S. A. Bender, A. Qaiumzadeh, L. Baldrati, J. Cramer, A. Brataas, R. A. Duine, and M. Kläui, *Nature* **561**, 222-225 (2018).

The authors acknowledge support from the DFG Project No. 423441604.

Long-distance magnon spin transport in antiferromagnetic insulators

Shubhankar Das¹, E. F. Galindez-Ruales¹, A. Ross², X. X. Ma³, C. Schmitt¹, F. Fuhrmann¹, M.-A. Syskaki¹, H. Y. Chen³, J. Sinova¹, G. Jakob¹, S. X. Cao³, O. Gomony¹, R. Lebrun² and Mathias Kläui¹

¹Institute of Physics, Johannes Gutenberg University Mainz, Staudingerweg 7, 55128 Mainz, Germany

²Unité Mixte de Physique CNRS, Thales, Université Paris-Saclay, Palaiseau 91176, France

³Department of Physics, Materials Genome Institute, International Center for Quantum and Molecular Structures, Shanghai University, Shanghai, 200444, China

Antiferromagnetic (AFM) materials have become the center of attraction in spintronics research due to the advantages over ferromagnets such as absence of stray fields, terahertz-range magnetization dynamics and stability against external magnetic fields. In particular, AFM insulators are potentially power-efficient materials for devices due to the absence of Joule heating. Apart from reading and writing the magnetic order in antiferromagnets, a relatively new area that is rapidly expanding is the spin transport in AFM insulators, where the spin information is carried by the quanta of spin waves i.e., the magnon. In 2018 Lebrun et al. reported the first AFM insulators which can accommodate long-distance spin transport, that is α -phase of iron oxide (hematite) [1]. At the low temperature easy-axis phase of hematite, the spin information is carried by circularly polarized magnons [1], whereas at high temperature easy-plane phase, it is carried by superposition of two linearly polarized magnons which dephase [2]. Although hematite shows spin transport over tens of microns, the identified transport modes are not unique and not necessarily applicable to other AFMs. Hence, the quest for other materials that exhibit long distance spin transport has intensified.

We have recently reported a second antiferromagnet that accommodates long-distance spin transport (Figure 1) is the canted AFM orthoferrite YFeO₃ [3]. Although the magnetic damping in YFeO₃ is of the same order of hematite, the spin transport mode is significantly different. Unlike in hematite, where both the Néel vector and the weak canted moment can contribute, we find here that the transport mediated by the Néel vector dominates in all cases. At zero field, the magnon modes in YFeO₃ are non-degenerate due to orthorhombic structural symmetry and also the magnon modes are linearly polarized, which cannot transport the spin angular momentum. However, due to the presence of Dzyaloshinskii-Moriya interaction, the external magnetic field induces a smooth rotation of Néel vector instead of spin flop and when the field makes an angle with Néel vector, elliptically polarized modes are enabled, which carry spin information in YFeO₃. We also observed anisotropy in the spin diffusion length scale with respect to crystallographic axes, which highlights the role of magnon group velocity in magnon spin transport. We believe that the spin transport mode in YFeO₃ will open up an essential and technologically relevant class of low-damping materials, i.e., canted AFMs, to long-distance spin transport.

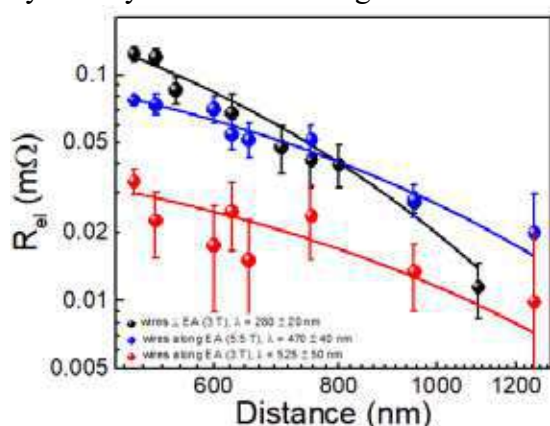


Figure 1: The electrical spin transport signal as a function of distance between the center of the wires in the non-local devices. The exponential fitting yields spin diffusion length of 525 ± 50 nm and 470 ± 40 nm at 3 T and 5 T field, respectively, for devices where wire are along easy axis and 280 ± 20 nm for device where wires are perpendicular to easy axis.

However, due to the presence of Dzyaloshinskii-Moriya interaction, the external magnetic field induces a smooth rotation of Néel vector instead of spin flop and when the field makes an angle with Néel vector, elliptically polarized modes are enabled, which carry spin information in YFeO₃. We also observed anisotropy in the spin diffusion length scale with respect to crystallographic axes, which highlights the role of magnon group velocity in magnon spin transport. We believe that the spin transport mode in YFeO₃ will open up an essential and technologically relevant class of low-damping materials, i.e., canted AFMs, to long-distance spin transport.

[1] R. Lebrun et al., Nature **561**, 223-225 (2018).

[2] R. Lebrun et al., Nat. Commun. **11**, 6332 (2020).

[3] S. Das. et al., arXiv:2112.05947.

Gradient magnetoelasticity: tailoring of antiferromagnetic textures

Olena Gomonay¹

¹ Johannes Gutenberg University, Mainz, Germany

Nowadays antiferromagnets are considered as important constituents of the spintronic devices. They show fast magnetic dynamics and can be effectively manipulated by the electric current or laser pulses. Many of technologically attractable antiferromagnets also show strong magnetoelastic effects, which can prevail over the direct spin-torque mechanism [1] and can be used for control and manipulation of the devices. However, an important prerequisite of such thermomagnetoelastic effects is inhomogeneous distribution of strains. In this presentation we discuss the effects associated with the strain gradients that appear in antiferromagnetic devices due to the clamping by nonmagnetic substrate, patterning, or current/temperature gradients. Following the ideas of Kléman [2] we treat magnetic inhomogeneities as a potential source of magnetoelastic defects associated with incompatibility (break of continuity) of the spontaneous

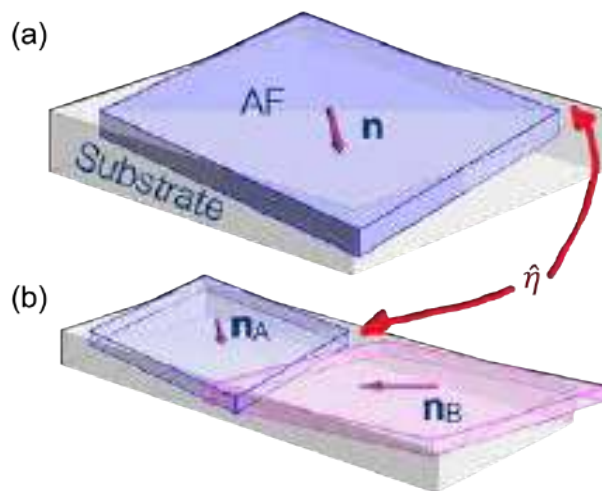


Figure 1: Incompatibility η induced by the magnetic inhomogeneities between (a) antiferromagnetic layer and substrate; (b) between two domains

strains (see Fig. 1). Incompatibility, treated further as a magnetoelastic charge, -- is a source of a long-range strain field that controls distribution of antiferromagnetic domains and orientation of the domain walls, and modifies local magnetic anisotropy. Inspired by the gradient elasticity approach [3] we generalize it to include magnetoelastic effects and apply it to interpretation of the observed magnetic textures in different antiferromagnets relevant for spintronic applications. Our findings open new ways to manipulate antiferromagnetic textures by proper tailoring of the magnetic and

magnetoelastic gradients.

[1] H. Meer, H., F. Schreiber, C. Schmitt, et al, *Nano Letters*. **21**, 114 (2021).

[2] M. Kléman, and M. Schlenker, *J. Appl. Phys.*, **43**, (1972).

[3] H. Askas, and E. C. Aifantis, *Int. J. Solids Struct.* **48**, 1962 (2011).

Current induced magnetization field free switching in exchange biased Pt(W)/Co/NiO heterostructures

K. Grochot^{1,2}, Ł. Karwacki^{3,4}, S. Łazarski¹, W. Skowroński¹, J. Kanak¹, W. Powroźnik¹, P. Kuświk⁴, M. Kowacz⁴, F. Stobiecki⁴, T. Stobiecki^{1,2}

¹*Institute of Electronics, AGH University of Science and Technology, Cracow, Poland.*

²*Faculty of Physics and Applied Computer Science, AGH University of Science and Technology, Cracow, Poland*

³*Institute for Theoretical Physics, Utrecht University, Utrecht, Netherlands*

⁴*Institute of Molecular Physics, Polish Academy of Sciences, Poznan, Poland*

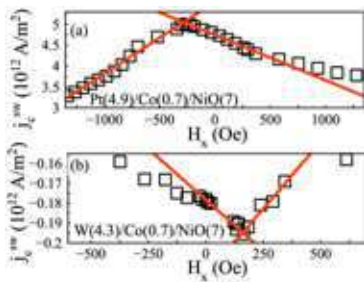


Figure 1: Critical switching-current densities as a function of applied external magnetic field H_x for Pt(4.9)/Co(0.7)/NiO(7) (a) and W(4.3)/Co(0.7)/NiO(7) (b) (thicknesses in nanometers). The red line represents the model fitted to the data with $H_{\text{exb}}^{(x)} = 522 \pm 14$ Oe, $\theta_{\text{SH}} = 5.8 \pm 1.3\%$ and $H_{\text{exb}}^{(x)} = -158 \pm 29$ Oe, $\theta_{\text{SH}} = -44 \pm 5\%$, respectively.

Current induced spin-orbit torque (SOT)-switching of perpendicular magnetization is observed in an external magnetic field collinear with the current (but non-collinear with the magnetization), which, however, is impractical in device applications.

In this work, we study magnetization switching induced by SOT in Pt(W)/Co/NiO heterostructures with variable thickness of W and Pt heavy-metal layers, a perpendicularly magnetized Co layer, and an antiferromagnetic NiO layer [1]. Using current-driven switching, magnetoresistance, and anomalous-Hall-effect (AHE) measurements, we determine the perpendicular and in-plane exchange-bias field ($H_{\text{exb}}^{(x)}$). Several Hall-bar devices possessing $H_{\text{exb}}^{(x)}$ from both systems are selected and analyzed in relation to our analytical switching model of the critical current density as a function of Pt and W thickness. As a result, the effective spin Hall angle (θ_{SH}) and perpendicular effective magnetic anisotropy were estimated. The expression of the critical current j_c^{sw} , is given as follows:

$$j_c^{\text{sw}} = \frac{2e\mu_0 M_s t_{\text{FM}}}{\hbar \theta_{\text{SH}}} \left(\frac{H_{\text{K,eff}}}{2} - \frac{H_x - H_{\text{exb}}^{(x)}}{\sqrt{2}} \right) \quad (1)$$

We demonstrate in both the Pt(W)/Co/NiO systems deterministic Co magnetization switching without an external magnetic field, which is replaced by $H_{\text{exb}}^{(x)}$ (Fig. 1). Moreover, we show that due to a higher θ_{SH} in the W-based system than in Pt, the critical switching current density in W-based devices is one order lower than in Pt. The current switching stability and the training process are discussed in detail. In conclusion, we consider our results interesting for SOT memory applications.

This work is funded by National Science Centre, Poland, Grant no. 2016/23/B/ST3/01430 SpinOrbitronics. KG acknowledges support for conference participation by the EU Project POWR.03.02.00-00-I004/16.

[1] Grochot et al., Phys. Rev. Appl. 215, 014017 (2021)

Antiferromagnetic Hysteresis above the Spin Flop Field

M. J. Grzybowski^{1,2}, C. F. Schippers¹, O. Gomonay³, K. Rubi⁴, M. E. Bal⁴,
U. Zeitler⁴, B. Koopmans¹, H. J. M. Swagten¹

¹Department of Applied Physics, Eindhoven University of Technology,
PO Box 513, 5600 MB Eindhoven, The Netherlands

²Institute of Experimental Physics, Faculty of Physics, University of Warsaw,
ul. Pasteura 5, PL-02-093 Warsaw, Poland

³Institute of Physics, Johannes Gutenberg-University Mainz, 55128 Mainz, Germany

⁴High Field Magnet Laboratory (HFML -EMFL), Radboud University,
6525 ED Nijmegen, The Netherlands

Magnetocrystalline anisotropy is essential in the physics of antiferromagnets and commonly treated as a constant, not depending on an external magnetic field. However, we demonstrate that in a thin-film antiferromagnetic CoO / Pt device the anisotropy should necessarily depend on the magnetic field, which is shown by the spin Hall magnetoresistance. Below the Néel temperature CoO reveals a spin-flop transition at 240 K at 7.0 T, above which a hysteresis in the angular dependence of magnetoresistance (Fig. 1) unexpectedly persists up to 30 T (Fig. 2). We present the phenomenological model that describes well the experimental observations. We explore possible reasons of this surprising behavior such as the magnetic domain structure or the presence of the unquenched orbital momentum [1], which can play an important role in antiferromagnetic spintronics.

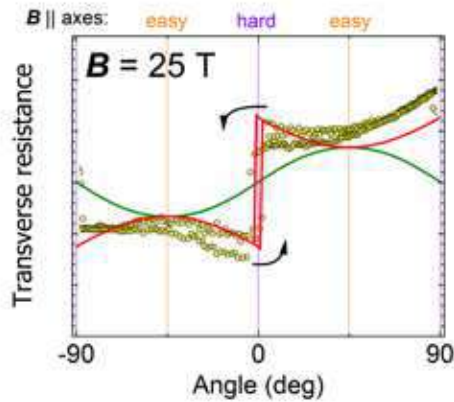


Figure 1: Relative changes of transverse resistance of CoO / Pt device as a function of orientation of the magnetic field.

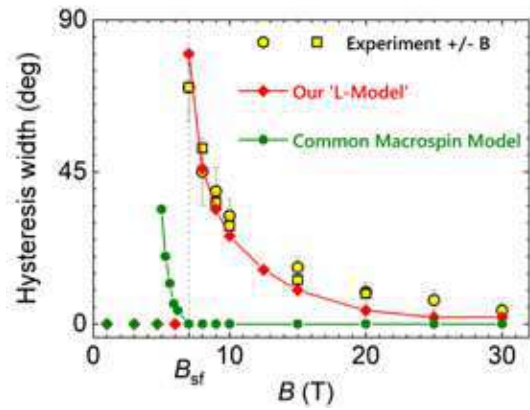


Figure 2: Hysteresis width in the transverse resistivity as a function of the magnetic field.

[1] M. J. Grzybowski et al., arXiv:2109.00093 (2021).

Towards antiferromagnetic dynamic solitons: terahertz Slonczewskii spin waves in antiferromagnetic spin-Hall nano-oscillators

Mohammad Hamdi¹, and Dirk Grundler^{1,2}

¹ *École Polytechnique Fédérale de Lausanne (EPFL), Institute of Materials, Laboratory of Nanoscale Magnetic Materials and Magnonics, CH-1015 Lausanne, Switzerland*

² *École Polytechnique Fédérale de Lausanne (EPFL), Institute of Electrical and Micro Engineering, Laboratory of Nanoscale Magnetic Materials and Magnonics, CH-1015 Lausanne, Switzerland*

Data traffic in wireless communication networks reflects explosive growth and has accounted for more than 60 % of the overall Internet traffic by the end of 2021 [1,2]. To overcome the associated capacity challenges, future wireless communication networks might exploit frequencies up to the terahertz (THz) frequency. However, currently scalable and efficient THz sources and detectors are missing giving rise to the so-called THz gap [3]. Therefore, there is an urgent need to develop small-sized solid-state THz components. Spin wave (SW) excitations in antiferromagnetic materials (AFMs) offer frequencies in the range of 0.1-10 THz which cover perfectly the THz gap. These materials can be utilized to close the THz gap in terms of antiferromagnetic spintronic and magnonic devices [4–6].

We study theoretically and by means of micromagnetic simulations antiferromagnet-based spin-Hall nano-oscillators (AFM-SHNOs). We derive the SW equation for a thin AFM film subjected to a local spin current in a nanometer-sized area called nano-constriction (NC). By solving the SW equation we demonstrate that the excited SWs are terahertz antiferromagnetic Slonczewskii SWs (THz-ASSW) and obtain, both, the threshold frequency and current for these excitations. Employing micromagnetic simulations we validate the analytical equations and use them to investigate the effect of material parameters on the excited SWs. The threshold current for THz-ASSWs exhibits a minimum with respect to the NC radius. The optimized radius is in the range of a few tens to few hundreds of nanometers accessible by state-of-the-art nanofabrication technology. Our findings provide a framework for optimizing the design of practical AFM-SHNO devices. Our results not only contribute to the fundamental understanding of the current-driven SWs in AFM-SHNOs, but considering the existence of THz-ASSWs, we predict also large amplitude antiferromagnetic dynamic solitons which can pave the way for high power THz generation. Our work is supported by SNSF via grant 177550 in ERA-NET RUS Plus.

- [1] T. Nagatsuma et al., Nat. Photonics 10, 371 (2016).
- [2] S. Ummethala et al., Nat. Photonics 13, 519 (2019).
- [3] C. Sirtori, Nature 417, 132 (2002).
- [4] T. Jungwirth et al., Nat. Nanotechnol. 11, 231 (2016).
- [5] V. Baltz et al., Rev. Mod. Phys. 90, 015005 (2018).
- [6] R. Cheng et al., Phys. Rev. Lett. 116, 207603 (2016).

Quenching of an antiferromagnet into high resistivity states using electrical or ultrashort optical pulses

Zdenek Kaspar^{1,2}, **Miroslav Surýnek**³, **Jan Zubáč**^{2,3}, **Filip Krizek**², **Vít Novák**²
Petr Němec³, **Tomáš Jungwirth**^{2,4} and **Kamil Olejník**²

¹ *Freie Universität Berlin, Arnimallee 14, 14195 Berlin, Germany*

² *Institute of Physics, Czech Academy of Sciences, Cukrovarnická 10, 162 00 Prague 6, Czech Republic*

³ *Charles University, Faculty of Mathematics and Physics, Ke Karlovu 3, 121 16 Prague 2, Czech Republic*

⁴ *School of Physics and Astronomy, University of Nottingham, Nottingham NG7 2RD, United Kingdom*

Antiferromagnetic materials have numerous advantages over their ferromagnetic counterparts in spintronic applications. The magnetization dynamics exceed the GHz range due to large exchange interaction, and the zero stray field allows for a further shrinking of memory bits.

On the other hand, challenging manipulation of the antiferromagnetic moments limits their potential applications. The discovery of Neel-order spin-orbit torque in antiferromagnets allows electrical manipulation [1]. Two materials, Mn₂Au and CuMnAs, became the workhorses of antiferromagnetic spintronic, where allowing for multiple breakthrough experiments. For example, the electrical reorientation switching of Neel vector [1][2][3] and its manipulation by ultrafast THz pulses [5][6].

We will present a new mechanism of reversible resistive quenching into a high resistive state in a single layer antiferromagnetic thin film [7]. In CuMnAs, this effect reaches up to 20% of the sheet resistance at room temperature, exhibiting superior reproducibility. Room temperature relaxation on a time scale of seconds, which follows a stretched exponential decay, and our recent observation of magnetic order with atomistic resolution [8] indicates the magnetic origin of this effect.

[1] J. Železný et al., *Physical Review Letters* **113**, 157201 (2014).

[2] P. Wadley et al., *Science* **351**, 587 (2016).

[3] J. Godinho et al., *Nat Commun* **9**, 4686 (2018).

[4] S. Y. Bodnar et al., *Nat Commun* **9**, 348 (2018).

[5] K. Olejník et al., *Sci. Adv.* **4** (3), eaar3566 (2018).

[6] J. J. F. Heitz et al., *Phys. Rev. Applied* **16**, 064047 (2021).

[7] Z. Kaspar et al., *Nat Electronics* **4**, 30–37 (2021).

[8] F. Krizek et al., *Sci. Adv.* **8**, eabn3535 (2022).

XPEEM Imaging of Magneto-acoustic Waves at GHz Frequency

M. W. Khaliq^{1,2}, O. Amin³, A. Hernández-Mínguez⁴, M. Rovirola², B. Casals⁵, K. Omari⁶, S. Ruiz-Gómez⁷, S. Finizio⁸, K. Edmonds³, L. Aballe¹, M. A. Niño¹, J. M. Hernández², F. Macià², P. Wadley³ and M. Foerster¹

¹ ALBA Synchrotron Light Facility, Cerdanyola del Valles-08290, Barcelona, Spain

² Dept. of Condensed Matter Physics, University of Barcelona, Barcelona-08028, Spain

³ School of Physics and Astronomy, University of Nottingham, NG7 2RD, UK

⁴ Paul Drude Institute for Solid State Electronics, Berlin-510117, Germany

⁵ Institut Català de Nanociència i Nanotecnologia (ICN2), Bellaterra-08193, Barcelona

⁶ Dept. of Electronic Engineering, Royal Holloway, University of London, Egham-TW20 0EX, UK

⁷ Max Planck Institute for Chemical Physics of Solids, Dresden-01069, Germany

⁸ Swiss Light Source, Paul Scherrer Institute, Villigen PSI-5232, Switzerland

Magnetization oscillations in thin films with spatial variations at the nano- and microscale are interesting in the development devices for high-speed and low-power signal processing compatible with existing technology. Surface acoustic waves (SAWs) are an alternative to magnetic fields in the excitation and control of magnetization dynamics, which use electric fields in order to induce magnetoelectric and magneto-elastic effects [1]. Casals *et al.* employed 500 MHz SAWs to create long range magnetization waves in Ni thin films [2]. More recently we have extended this method to include antiferromagnetic CuMnAs. For the observations we used PhotoEmission Electron Microscopy (PEEM) with magnetic contrast based on x-ray magnetic linear dichroism (XMLD), and the SAW excitation synchronized with the x-ray illumination.

Wadley *et al.* demonstrated the control of antiferromagnetic (AFM) domains in CuMnAs by electrical currents [3]. In principle, alternative switching methods such as the magnetoelastic effect should be equally possible but are so far relatively unexplored in AFM materials. We have for the first time detected antiferromagnetic magneto-acoustic waves in epitaxial CuMnAs films excited by SAW in the GaAs substrate (Fig. 1a). On the other hand, exciting magneto-acoustic waves at higher frequencies, approaching the intrinsic ferromagnetic resonance frequencies, can lead to higher amplitudes, larger propagating distance of magnons and increased phonon-magnon interaction. For ferromagnetic Ni thin films on LiNbO₃ we have already increased the frequency into the GHz range, see Fig. 1(b) for magneto-acoustic waves at 1 GHz.

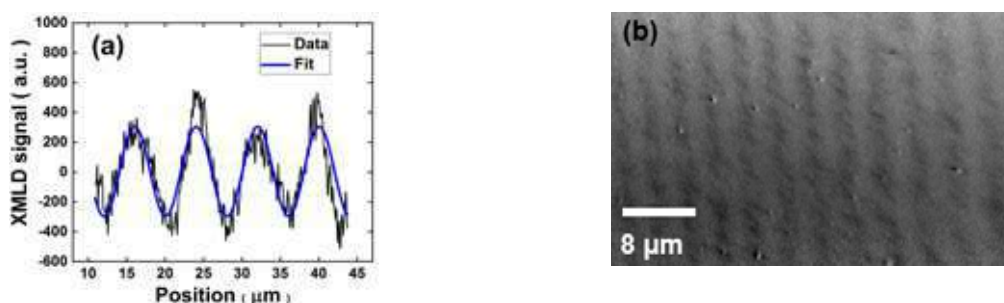


Figure 1: (a) Magneto-acoustic wave signal in AFM CuMnAs. (b) Magneto-acoustic waves in Ni at 1 GHz.

[1] M. Foerster *et al.*, *Nature Comm.* **8**, 407 (2017).

[2] B. Casals *et al.*, *Phys. Rev. Lett.* **124**, 137202 (2020).

[3] P. Wadley *et al.*, *Science* **351**, 587 (2016).

Antiferromagnetic domain wall as a reconfigurable long Josephson junction

Roman Ovcharov¹, Roman Khymyn¹, Boris Ivanov², and Johan Åkerman¹

¹*Department of Physics, University of Gothenburg, Gothenburg 41296, Sweden*

²*Institute of Magnetism of the National Academy of Sciences of Ukraine and the Ministry of Education and Science of Ukraine, Kyiv 03142, Ukraine*

Self-localized spin structures can substantially enrich the scope of the field-free antiferromagnetic spintronics [1]. One of them - the domain wall (DW) is a topological soliton that bridges a connection between two ground states, similar to a link in a Josephson junction (JJ) between two superconductors. JJs have been intensively investigated for decades as they promise important advantages for electronics. In particular, JJ-based qubits are already successfully realized and commercialized.

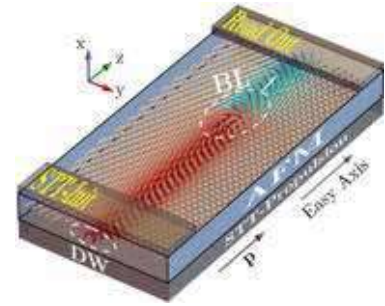


Figure 1: Generation of the Bloch line, - an analog of the Josephson vortex.

We demonstrate that the DW in bi-axial AFM with the easy-axis type of primary anisotropy driven by a spin current is a close analogy of a long Josephson junction (LJJ). Thus, the dynamics of the Neel vector angle inside the DW (Josephson phase Φ) is described by a sine-Gordon type of equation, where applied spin-transfer torque (STT) represents a bias current through the junction, anisotropy in a basal plane defines a plasma frequency, and characteristic speed of magnons, defined by nonhomogeneous exchange energy, corresponds to Swihart velocity.

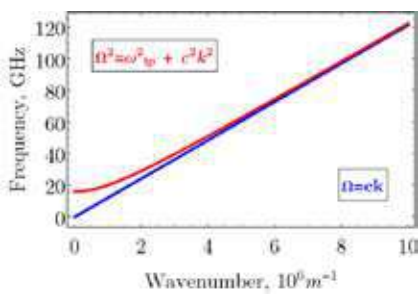


Figure 2: Dispersion law for Φ (red) and Y (blue) intrawall modes in easy-axis Cr2O3 antiferromagnet with the presence of in-plane anisotropy.

In contrast with a conventional LJJ, a DW has additional degrees of freedom, namely the position of its center Y and distribution of the current along with a DW. We show by micromagnetic simulations that when the polarization of the STT is parallel to the easy axis of an AFM, the above allows to nucleate and propel a single kink-type Φ soliton [2], which is Bloch line (Fig.1) that corresponds to the Josephson vortex in LJJ. Withal, a weak alternate current excites Φ -type intrawall spin waves, an analog of plasma waves in LJJ, which spectrum has a bandgap, defined by the anisotropy (Fig.2). STT with a perpendicular polarization allows manipulating the Y position, particularly to excite the flexural vibrations of the DW with a gapless spectrum [3] (Fig.2).

- [1] O. Gomonay, V. Baltz, A. Brataas, and Y. Tserkovnyak, *Nature Physics* **14**, 3 (2018).
- [2] S.K. Kim and Y. Tserkovnyak, *Physical review letters* **119**, 4 (2017).
- [3] H.-K. Park and S.-K. Kim, *Physical Review B* **103**, 214420 (2021).

Molecular beam epitaxy of the half-Heusler antiferromagnet CuMnSb

L. Scheffler^{1,2}, K. Gas³, M. Kamp⁴, C. Schumacher^{1,2}, C. Gould^{1,2}, M. Sawicki³,
J. Kleinlein^{1,2} and L. W. Molenkamp^{1,2}

¹Physikalisches Institut (EP3), Universität Würzburg, 97074 Würzburg, Germany

²Institute for Topological Insulators, Universität Würzburg, 97074 Würzburg, Germany

³Institute of Physics, Polish Academy of Sciences, Aleja Lotnikow 32/46, PL-02668 Warsaw, Poland

⁴Physikalisches Institut and Röntgen Center for Complex Material Systems, Universität Würzburg, 97074 Würzburg, Germany

Current trends in antiferromagnetic spintronics [1] are driving a demand for high-quality materials to reliably study the phenomenology in this material class. A promising antiferromagnetic model system is the half-Heusler compound CuMnSb. We grow CuMnSb by molecular beam epitaxy to address the requirements for detailed transport experiments and device applications: thin film specimens with a high degree of crystalline order and a low defect density, and sharp and well-defined interfaces to other materials. This approach additionally offers the possibility of combining CuMnSb with its ferromagnetic counterpart, the half-metallic NiMnSb, in epitaxial heterostructures. Moreover, CuMnSb is a noncentrosymmetric antiferromagnet for which antidamping spin-orbit torques are envisioned for Néel vector switching [2].

We recently demonstrated molecular beam epitaxy of strained antiferromagnetic CuMnSb thin films on InAs (001) substrates [3]. For these layers, magnetic studies revealed two major deviations in magnetic properties as compared to bulk material. An increase in Curie-Weiss temperature attributed to a reduction in geometric frustration due to reduced symmetry caused by epitaxial strain, and near the Néel temperature, an additional linear region in the temperature dependent inverse susceptibility.

Additionally, we will present a study of the influence of molecular beam epitaxial growth conditions on the structural and magnetic characteristics of CuMnSb films on lattice matched GaSb. In a first step we analyze a series of samples which have been grown with various Mn to Sb flux ratios and establish the optimum growth conditions for the stoichiometric composition of CuMnSb epilayers. We use these growth conditions to prepare a second set of stoichiometric samples where we vary the CuMnSb layer thickness from 5 to 510 nm. We will present and discuss the temperature dependence of the magnetization of a CuMnSb layer at selected external magnetic fields as well as our observation regarding the effect of the layer thickness on the Néel temperature. All findings are of particular relevance for studies aiming at the demonstration of Néel vector switching and detection in this noncentrosymmetric antiferromagnet.

[1] T. Jungwirth, J. Sinova, A. Manchon, X. Marti, J. Wunderlich, and C. Felser, *Nat. Phys.* **14**, 200 (2018).

[2] J. Železný, H. Gao, A. Manchon, F. Freimuth, Y. Mokrousov, J. Zemen, J. Mašek, J. Sinova, and T. Jungwirth, *Phys. Rev. B* **95**, 014403 (2017).

[3] L. Scheffler, K. Gas, S. Banik, M. Kamp, J. Knobel, H. Lin, C. Schumacher, C. Gould, M. Sawicki, J. Kleinlein, and L. W. Molenkamp, *Physical Review Materials* **4**, 114402 (2020).

Bulk Hexagonal MnTe – a Room Temperature Antiferromagnet

K. P. Kluczyk¹, M. Grzybowski¹, M. A. Borysiewicz², T. Fąs², J. Suffczyński²,
P. Skupiński³, K. Graszka³, A. Mycielski³, K. Gas³,
M. Sawicki³ and M. Gryglas-Borysiewicz¹

¹ Faculty of Physics, University of Warsaw, Pasteura 5, Warsaw, Poland

² Łukasiewicz Research Network - Institute of Microelectronics and Photonics,
Al. Lotników 32/46, 02-668 Warsaw, Poland

³ Institute of Physics, Polish Academy of Sciences, Al. Lotników 32/46, 02-668 Warsaw, Poland

Antiferromagnets have gained considerable attention recently. In contrast to ferromagnets, the magnetic state of an antiferromagnet (AFM) is far more robust, opening perspectives for long-lasting data storage. For that aim the knowledge of the electric properties of AFM materials is crucial to both facilitate the readout of magnetization state and also to manipulate it, e.g. by an electric current. Thus conductive AMF materials are of a great importance. A canonical example of such material is hexagonal MnTe, which is a semiconductor with a moderate bandgap (EG ~1.3 eV) and the Néel temperature T_N just above 300 K.

In this paper we explore the structural, electric, optical and magnetic properties of bulk hexagonal MnTe polycrystals. They have been grown by two methods: from the liquid phase where a mixture of Mn and Te powders was sealed and heated in a quartz ampule, and from the vapour phase via the reaction of tellurium vapors with manganese powder at a reduced temperature, which should prohibit the formation of unwanted crystal phases. Indeed, our XRD measurements revealed the presence of MnTe₂ and tellurium precipitates for the samples from the first method and the single MnTe phase for the latter one.

For both kinds of samples a clear phase transition between the antiferromagnetic and paramagnetic states was observed at about 310 K, in agreement with the previous studies [1]. It was resolved as a peak of the derivative of the magnetic susceptibility $d\chi(T)/dT$, as a kink in the resistance dependence on temperature $R(T)$ and by an increase of E_{2g} phonon line intensity in the Raman scattering measurement. Both $\chi(T)$ and $R(T)$ dependences revealed also traces of antiferromagnetic MnTe₂ with its T_N close to 90 K. A significant rise of resistivity was observed below 20 K for both samples. It indicates an activated character of the charge carriers, with two activation energies of about 6 meV and 0.3 meV. Magnetization dependence on the magnetic field shows numerous mechanisms of spin rotation: from the presence of the spin-flip processes transition at around 0.4 T, followed by the spin canting till about 2 T. The first value is about 5 times smaller than observed in epitaxial MnTe [2]. We attempt to model such behavior by a macro-spin model. Moreover, we want to extend our investigations to single crystalline hexagonal bulk MnTe samples.

[1] K. Ozawa et al., *Phys. Lett.* **20**, 132 (1966).

[2] D. Kriegner et al., *Nat. Commun.* **7**, 1162 (2016).

This work was partially supported by the Polish National Centre for Research and Development through grant No. TECHMATSTRATEG1/346720/8/NCBR/2017 and by the National Science Centre, Poland under Grant 2021/40/C/ST3/00168.

Spontaneous anomalous Hall effect arising from antiparallel magnetic order in a semiconductor

Ruben D. Gonzalez Betancourt^{1,2,3}, Jan Zubáč^{3,4}, Rafael J. Gonzalez Hernandez⁵, Kevin Geishendorf³, Zbynek Šobán³, Gunther Springholz⁶, Kamil Olejník³, Libor Šmejkal³, Tomas Jungwirth^{3,7}, Sebastian T. B. Goennenwein^{1,8}, Andy Thomas^{1,2}, Helena Reichlová¹, Jakub Železný³, and Dominik Kriegner^{1,3}

¹IFMP, Technical University Dresden, Dresden, Germany

²IFW, Dresden, Germany

³Institute of Physics, Academy of Science of the Czech Republic, Prague, Czech Republic

⁴Charles University, Faculty of Mathematics and Physics, Prague, Czech Republic

⁵Departamento de Física y Geociencias, Universidad del Norte, Barranquilla, Colombia

⁶Semiconductor Physics, Johannes Kepler University Linz, Linz, Austria

⁷School of Physics and Astronomy, University of Nottingham, United Kingdom

⁸Department of Physics, University of Konstanz, Konstanz, Germany

It is known that collinear antiferromagnets cannot host a spin split band structure and therefore not show any anomalous Hall effect. Following the recent theory development [1], we experimentally show that this paradigm needs to be revised. We theoretically identify and experimentally confirm the symmetry components of the longitudinal and transversal anisotropic magnetoresistance in thin films of the compensated collinear antiferromagnet MnTe (Fig.1-a).

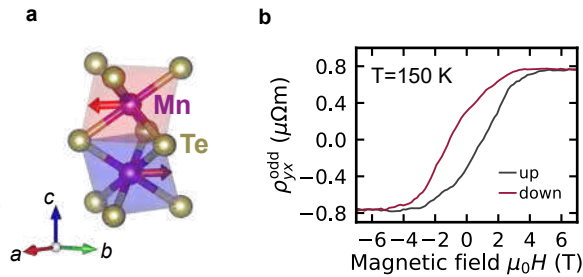


Figure 1: (a) Atomic and magnetic configuration of MnTe with hexagonal NiAs structure.(b) Transversal magnetoresistance recorded at an applied magnetic field tilted 30° from the current (along $[11\bar{2}0]$) towards the out of plane c direction.

In a Hall bar fabricated in c plane oriented thin films, we experimentally find a hysteretic signal odd in magnetic field in the transversal magnetoresistance, i.e. spontaneous anomalous Hall effect(Fig.1-b)[2].

This effect can be rationalized considering nonmagnetic atoms at non-centrosymmetric lattice sites which break additional symmetries and cause a spin splitting in certain parts of the Brillouin zone.

[1] L. Šmejkal et al., *Sci. Adv.* **6**, aaz8809(2020)

[2] R. D. Gonzalez Betancourt et al., (2021) *arXiv:2112.06805*, [cond-mat.mtrl-sci]

Anisotropic spontaneous Hall effect in unconventional antiferromagnet Mn_5Si_3

M. Leiviskä ¹, R. Lopes Seeger ¹, H. Reichlova ^{2,3}, I. Kounta ⁴, L. Smejkal ^{5,3},
S. Beckert ², M. Villanueva ⁷, A. Badura ^{6,7}, D. Kriegner ^{2,3}, I. Joumard ¹, E.
Schmoranzero ⁶, T. Jungwirth ³, J. Sinova ⁵, L. Michez ⁴, S.T.B
Goennenwein ⁷, and V. Baltz ¹

¹ *Univ. Grenoble Alpes, CNRS, CEA, Grenoble INP, IRIG-SPINTEC, F-38000 Grenoble*

² *Institute of Solid State and Materials Physics, TU Dresden, Dresden, Germany*

³ *Institute of Physics, Czech Academy of Sciences, Prague, Czechia*

⁴ *Aix-Marseille University, CNRS, CINaM, Marseille, France*

⁵ *Institute for Physics, Johannes Gutenberg University Mainz, Mainz, Germany*

⁶ *Department of Chemical Physics and Optics, Faculty of Mathematics and Physics, Charles University, Prague, Czechia*

⁷ *Department of Physics, University of Konstanz, Konstanz, Germany*

Epitaxial films of Mn_5Si_3 , an unconventional antiferromagnet, exhibit a spontaneous Hall effect despite the vanishing net magnetization and small spin-orbit coupling [1]. The spontaneous Hall effect can be explained by unconventional, non-relativistic time-reversal symmetry breaking, which allows a momentum-locked alternating spin-splitting of the bands [1,2,3]. This is in contrast with conventional ferromagnets, where the spin splitting and hence the spontaneous Hall effect originates from magnetization. For this reason, the spontaneous Hall effect in antiferromagnets can be anisotropic while in common ferromagnets it is isotropic.

In this work, we investigate the extent of anisotropy of the spontaneous Hall effect in epitaxial thin films of Mn_5Si_3 through static and dynamic magnetotransport measurements. We have measured the field orientation dependence of the spontaneous Hall effect and observed unconventional behaviour that strongly deviates from the cosine dependence typical for ferromagnets. Moreover, the exact behavior depends on the crystallographic plane in which the field is rotated. We have also further explored this anisotropy by studying the dynamic coercivity of the spontaneous Hall effect. Our results highlight the anisotropic nature of the antiferromagnetic spontaneous Hall effect.

[1] H. Reichlova et al. arXiv:2012.15651, 2020

[2] L. Smejkal et al. arXiv:2107.03321, 2021

[3] L. Smejkal et al. arXiv:2105.05820, 2021

Unveiling Oxidation and Spin State of Fe in $\text{Li}_{1-x}\text{Zn}_x\text{FeO}_2$

Priyanka Nehla^{1,2}, Hyeyun Kim¹, Seda Ulusoy^{1,2}, Mikhail Feygenson³, Peter Svedlindh¹, Germán Salazar-Alvarez^{1,2}

¹ Dept. of Materials Science and Engineering, Ångström Laboratory, Uppsala University

² Center for Neutron Scattering, Ångström Laboratory, Uppsala University

³ European Spallation Source, ESS

Lithium iron oxides have been studied for decades for Li-ion battery applications [1,2]. Herein, the oxidation and spin state of Fe is crucial to the magnetic properties and also to the crystal structure, as it also influences the presence of other polymorphic phases arising during the synthesis procedures. In this work, we investigate the structural and magnetic properties of $\text{Li}_{1-x}\text{Zn}_x\text{FeO}_2$ ($x=0, 0.05, 0.10, 0.15, 0.20$) and their use for battery applications. The neutron diffraction and x-ray diffraction (XRD) patterns of the of parent compound have been refined using Rietveld refinement with cubic structure using the ***Fm-3m*** space group. As x increases, the integrated intensity ratio of the 220/111 Bragg reflections changes and the lattice parameter increases due to the substitution of Li for Zn and the change of oxidation state of Fe. The elemental composition has been confirmed by time-of-flight elastic recoil detection analysis (ToF-ERDA). Intriguingly, the magnetic ordering/transition temperature decreases with an increase in x , i.e., it shifts from 90 K for the parent compound to 42 K for $x=0.20$. A magnetic irreversibility/bifurcation in zero field cooled (ZFC)- field cooled (FC) magnetization has also been found below the transition temperature for all the samples. The suppression of the ZFC-FC bifurcation and transition temperature at around 20 K under a 10 kOe dc magnetic field indicate a deviation from purely AFM interactions, which is further supported by a small hysteresis in the isothermal magnetization at 5 K. The onset of a weakly frequency dependent in-phase component close the bifurcation temperature clearly indicates the presence of slow magnetic relaxation, tentatively explained by the presence of both AFM and FM interactions even though the AFM interactions are dominating. Furthermore, the presence of different Fe spin states is discussed to understand the magnetic interactions in the system, which motivates the detailed investigation by thermoremanent magnetization and high frequency ac susceptibility measurements.

Acknowledgments: We thank the Swedish Research council, VR, (Grant no. 2016-06959) for financial support. PN acknowledges the financial support from Swedish Agency for Economic and Regional Growth under the project SSRE.

References

- [1] J. Luo, J. Liu, Z. Zeng, C.F. Ng, L. Ma, H. Zhang, J. Lin, Z. Shen, and H. J. Fan, *Nano Lett.* **13**, 6136 (2013).
- [2] W. Zhang, D. C. Bock, C. J. Pelliccione, Y. Li, L. Wu, Y. Zhu, A. C. Marschilok, E. S. Takeuchi, K. J. Takeuchi, and F. Wang, *Adv. Energy Mater.* **6**, 1502471 (2016).

Ferromagnetic resonance study of acoustic, optic and mixed excitations in Ru/Cr/Co and Ru/Co multilayers

P. Ntetsika¹, G. Mitrikas², G. Litsardakis³, I. Panagiotopoulos¹

¹ Department of Materials Science and Engineering, University of Ioannina, Ioannina 45110, Greece

² Institute of Nanoscience and Nanotechnology, National Centre for Scientific Research-Demokritos, Athens, Greece

³ Laboratory of Materials for Electrotechnics, Department of Electrical and Computer Engineering, Aristotle University of Thessaloniki, Thessaloniki, Greece.

Synthetic antiferromagnets (SAFs) are based on the oscillatory interlayer exchange coupling of thin magnetic layers with the Ruderman–Kittel–Kasuya–Yosida (RKKY) mechanism. The antiferromagnetic interlayer exchange coupling in SAFs gives rise to two distinct modes (acoustic / optical). For the acoustic modes the resonances approach zero at zero field, while the optical modes possess useful high frequencies at zero-applied field [1,2]. The frequencies of these modes depend on the magnetic state and therefore on uniaxial magnetic anisotropy (H_K) and antiferromagnetic interlayer exchange coupling (H_{ex}), which provide control parameters of the dynamic properties. As the frequencies of the optical and acoustic modes also depend on the applied field, there is a point where they tend to coincide. The optical and acoustic spin-wave modes get hybridized at these degeneracy points. Here we

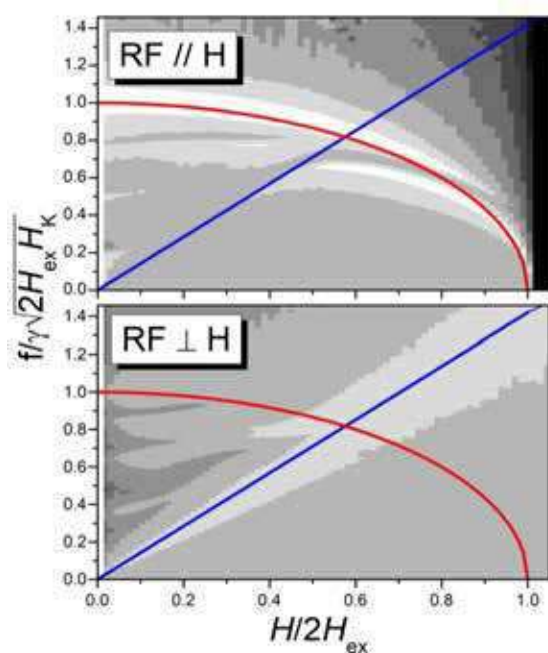


Figure 1: FFT transform amplitude as a function of frequency and applied field. The frequency is normalized to the value of the zero-field optical mode. The frequencies predicted by the macrospin model are superimposed.

present a Ferromagnetic Resonance (FMR) study of two series of $[\text{Ru}_{10}/\text{Co}_x]_{12}$ and $[\text{Ru}_6/\text{Cr}_3/\text{Co}_x]_{12}$ $x=16\text{--}60\text{\AA}$, prepared by sputter deposition having easy-plane anisotropy and zero anisotropy within the plane. The acoustic/optical modes are studied by cavity FMR by setting the RF field perpendicular/parallel to the saturating in-plane field. The resonance fields are in good agreement with the values predicted for acoustic modes by a macrospin model. The resonance fields of the modes excited by setting the RF field parallel to the saturating field, are lower than those expected for optical modes. This is attributed to the existence of hybridized mixed modes, in accordance to results of micromagnetic simulations which also show that the mode mixing is related to the inhomogeneous magnetization profile along the multilayer thickness.

[1] H. J. Waring, et al. “Zero-field Optic Mode Beyond 20 GHz in a Synthetic Antiferromagnet”, Phys. Rev. Applied 13, 034035 (2020), 10.1103/PhysRevApplied.13.034035.

[2] A. Sud, et al. “Tunable magnon-magnon coupling in synthetic antiferromagnets”, Phys. Rev. B 102, 100403(R) (2020). 10.1103/PhysRevB.102.100403.

Impact of magnetoelastic coupling on antiferromagnetic spintronics

S. Reimers^{1,2,3}, Y. Lytvynenko¹, A. Kleibert⁴, F. Maccherozzi⁴, P. Wadley², S.S. Dhesi³, M. Kläui^{1,5}, K.W. Edmonds² and M. Jourdan¹

¹*Johannes Gutenberg University Mainz IPH, Staudingerweg 7, 55128 Mainz, Germany*

²*University of Nottingham, University Park, Nottingham NG7 N2RD, United Kingdom*

³*Diamond Light Source, Didcot OX11 0DE, United Kingdom*

⁴*SLS Paul Scherrer Institut, Villigen PSI, 5232 Villigen PSI, Switzerland*

⁵*Center for Quantum Spintronics, Norwegian University of Science and Technology, NO - 7491 Trondheim, Norway*

Antiferromagnetic (AF) spintronics research promises to overcome fundamental limits of conventional spintronic technology in terms of speed and density. However, specific functionalities and the efficiency of spintronic devices rely sensitively on the magnetic anisotropy and domain structure of the material. Antiferromagnets are known to be sensitive to strain. Hence, for AF films grown on substrates, the most relevant geometry for applications, externally applied strain, the coupling to the substrate and crystallographic defects can be relevant. To date, the relative contributions of the different effects and the complex interactions between them are largely unknown. Here, we investigate the effect of strain on the AF domain structure of epitaxially grown Mn_2Au and CuMnAs films. CuMnAs and Mn_2Au are two of the most promising metallic AF materials for spintronic applications, since their AF order can be manipulated by electrical currents [1,2]. We explore, how magnetostriction can be used to engineer the AF domain structure and anisotropy of the materials. We reveal how the effect of externally applied strain on the AF domains depends on the magnetocrystalline anisotropy and on the way the crystallographic structure responds to strain, by comparing the two materials and samples of the same material grown on different substrates.

CuMnAs films grown on GaP can relax strain by forming twin defects. The twin defects dominate the AF domain structure, as shown in Fig. 1. The coupling between the defects and domains stems from a local change of the magnetocrystalline anisotropy and the strain fields generated by the defects [3]. The twin defects are absent in CuMnAs film grown on GaAs, where external applied strain induces a small rotation of the spin axis towards a strain-imposed easy axis. In contrast, in Mn_2Au , a material with a much larger magnetocrystalline anisotropy, uniaxial strain applied along a magnetic easy axis shifts the relative domain populations.

[1] P.Wadley, B. Howells, J. Zelezny et al., *Science* **351**, 6273 (2016).

[2] S.Y. Bodnar, L. Smejkal., I. Turek et al., *Nat Commun* **9**, 348 (2018).

[3] S. Reimers, D. Kriegner, O. Gomonay et al., *Nat Commun* **13**, 724 (2022).

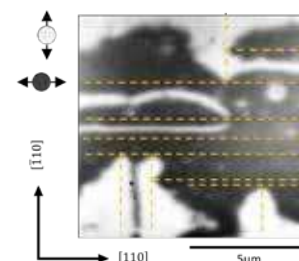


Figure 1: X-PEEM image of the AF domain structure superimposed with the twin defect structure (yellow-dashed lines) in a $\text{CuMnAs}/\text{GaP}(001)$ film. The twins pin domains and domain walls.

Magnetic properties of biphasic $\text{LaCr}_3(\text{BO}_3)_4$ crystal

Yu. Savina ¹, A. Bludov ¹, V. Pashchenko ¹, A. Lynnyk ², T. Zajarniuk ²,
M.U. Gutowska ², A. Szewczyk ², I. Kolodiy ³

¹ *B. Verkin Institute for Low Temperature Physics and Engineering of the NAS of Ukraine,
47 Nauky Ave., 61103 Kharkiv, Ukraine*

² *Institute of Physics, Polish Academy of Sciences, al. Lotników 32/46, 02-668 Warsaw, Poland*

³ *National Science Center «Kharkov Institute of Physics and Technology», 1 Akademichna St., 61000
Kharkiv, Ukraine*

Compounds with the general formula $RM_3(\text{BO}_3)_4$ ($R = \text{Y}$ or rare-earth elements; $M = \text{Al}$, Ga , Fe , Cr , and Sc) attract considerable attention of scientists due to their optical, magnetic and ferroic properties. Majority of the $RM_3(\text{BO}_3)_4$ compounds crystallize in huntite-like rhombohedral structure with space group $R\bar{3}2$. However, two monoclinic structural modifications with space groups $C2/c$ and $C2$ have been found too. Coexistence of the rhombohedral ($R\bar{3}2$) and the monoclinic ($C2/c$) structures in one sample is an unwanted feature of the rare-earth chromium borate $\text{RCr}_3(\text{BO}_3)_4$. Both structural modifications can be represented as spiral chains of CrO_6 octahedra with common edges that are interconnected into a three-dimensional structure using BO_3 planar triangular groups and RO_6 trigonal prisms. The main differences between these modifications consists in slightly different topology of the chains and some variation of the $\text{Cr}-\text{Cr}$ distances into the chains.

Present research has been aimed at experimentally determining the nature and temperature of magnetic ordering, which takes place in $\text{LaCr}_3(\text{BO}_3)_4$, as well as at estimation of the exchange interactions (intrachain and interchain) between chromium ions.

The presence of two structural phases into powder sample ($R\bar{3}2$ – wt. 40% and $C2/c$ – wt. 60%) have been detected by the X-ray studies. Magnetic and heat capacity investigations of the $\text{LaCr}_3(\text{BO}_3)_4$ have been carried out by using a SQUID magnetometer MPMS-XL7 and PPMS Heat Capacity option, respectively. The magnetization has been measured for two external magnetic field orientations: for $H \parallel c^*$ and $H \perp c^*$, where c^* -axis coincides with the crystallographic c -axis of the rhombohedral modification of the $\text{LaCr}_3(\text{BO}_3)_4$.

It has been found that both structural modifications of lanthanum chromium borate undergo into antiferromagnetically ordered state at 6.5 K and 8.5 K for $C2/c$ and $R\bar{3}2$ phases, respectively. It has been shown that the magnetic susceptibility obeys the Curie–Weiss law with effective magnetic moment $\mu_{\text{eff}} = 3.86 \mu_B/\text{Cr}^{3+}$ and Curie–Weiss temperature $\theta = -23$ K. The best approximation of the experimental data within the model of interacting Heisenberg spin chains in the classical limit has been obtained at $T > 15$ K for the following exchange interaction constants: the antiferromagnetic intrachain exchange $J/k = 4.8$ K, and the ferromagnetic interchain exchange $J'/k = -0.28$ K. From the analysis of the magnetic part of crystal heat capacity the value and sign of the intrachain exchange have been proved. Two spin-reorientation phase transitions for $H \perp c^*$ at 2.4 T ($C2/c$) and near 5.6 T ($R\bar{3}2$) for $T = 2$ K have been found.

This work was supported partially by the National Science Centre, Poland, under project No. 2018/31/B/ST3/03289.

Suppressing electrical switching of antiferromagnets with high magnetic fields

C.F. Schippers¹, M.J. Grzybowski¹, M.E. Bal², K. Rubi², U. Zeitler², H.J.M. Swagten¹

¹Eindhoven University of Technology, P.O. Box 513, 5600 MB, Eindhoven, the Netherlands

²Radboud University, Toernooiveld 5, 6525 ED Nijmegen, The Netherlands

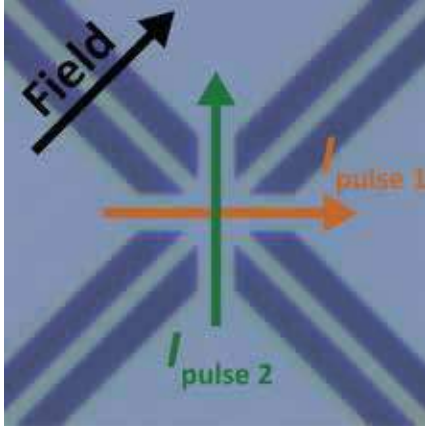


Figure 1: Micrograph of the device used for the experiments.

Antiferromagnetic (AF) spintronics received an enormous impulse after the first demonstrations of electrical switching of the AF order [1]. However, a lot of these observations can equally well be explained by non-magnetic, parasitic effects caused by the same electrical current pulses that are intended to manipulate the magnetic state of the AF [2].

While it is possible to distinguish between magnetic and non-magnetic effects using imaging techniques that can resolve the AF order [3], these techniques are usually very complex. Moreover, since they require access to the AF layer, they are not suitable for systems where the AF is buried beneath other layers.

Our approach is to distinguish between the magnetic and non-magnetic effects by suppressing the magnetic effects using high magnetic fields.

In this contribution, we study the high magnetic field behavior of the electrical switching of thin-film AFs NiO and CoO, using the devices shown in Fig. 1. We perform switching experiments in magnetic fields up to 16 Tesla (Fig. 2). The measurements show that these high magnetic fields indeed suppress the current-induced switching of the AF order, whereas the thermal effects remain unaffected. Hence, this technique allows to irrefutably separate the magnetic and non-magnetic effects. These results are corroborated by a model accounting for the multi-domain character of the AF.

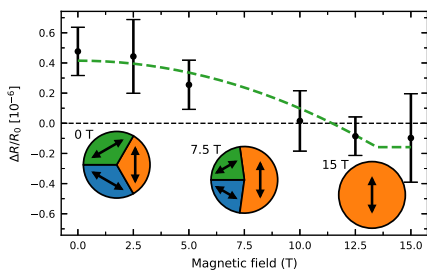


Figure 2: Switching amplitude as a function of magnetic field. The dashed line is calculated with the model; the pie charts represent the modelled domain distribution.

These results both demonstrate that combining electrical methods with strong magnetic fields can be a valuable tool for AF spintronics, and give invaluable insight into the interplay of spin-Hall magnetoresistance and thermal effects as well as the domain structure and complex anisotropy of thin-film antiferromagnets.

[1] X. Z. Chen, et al., *Phys. Rev. Lett.* **120**, 207204 (2018)

[2] A. Churikova, et al., *Appl. Phys. Lett.* **116**, 022410 (2020)

[3] H. Meer, et al., *Nano Lett.* **21**, 1, 114–119 (2021)

Compensation point in the ferrimagnetic nanoparticles

Paweł Sobieszczyk, Michał Krupiński

Institute of Nuclear Physics Polish Academy of Sciences, Radzikowskiego 152, 31342 Kraków, Poland

The great interest of the 3d-transition metal - rare earth ferrimagnetic alloys has been emerged due to their possible applications in magneto-optical recording and ultrafast laser switching [1]. The most interesting properties for the magnetic reorientation process occurs at the compensation temperature (T_n) where no magnetisation appears below Curie temperature. The value of the compensation point can be controlled through the composition and structure of the alloy as well as by ion irradiation and annealing [2, 3]. With the help of Vampire atomistic simulation software [4] we explore other possibilities of tuning the compensation point by changing the bulk to surface ratio. We studied the Tb_xFe_{1-x} nanospheres with diameters (D) ranging from 3 nm to 12 nm and it has been observed that T_n depends on the diameter as $1/D$, which may be attributed to changes in the spin direction on the nanoparticle surface. The distribution of spin direction in the bulk and at the surface for various temperatures will be also presented. The results performed in the atomistic approach are also confirmed with the mean-field approximation.

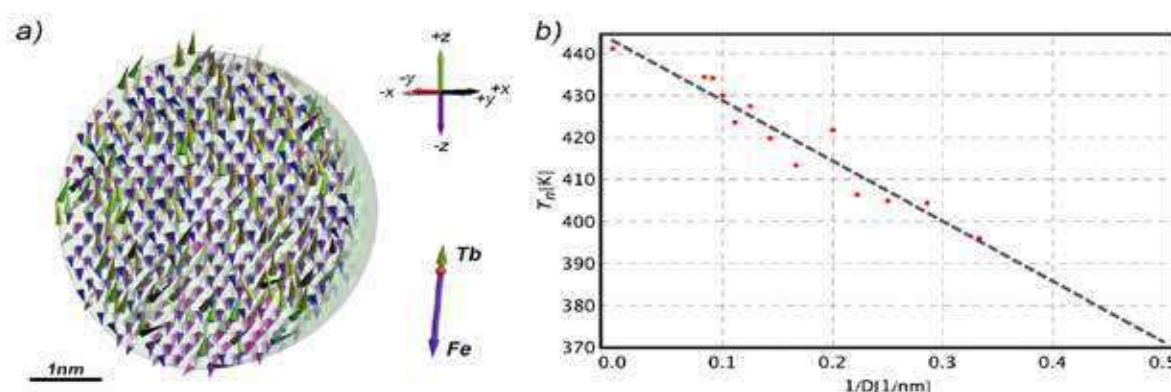


Figure 1: a) Distribution of spins in the ferrimagnetic $Tb_{24}Fe_{76}$ nanoparticle at $T=100K$. b) Compensation point as a function of nanosphere diameter (D).

[1] S. Mangin, M. Gottwald, C.-H. Lambert, D. Steil, V. Uhler, L. Pang, M. Hehn, S. Alebrand, M. Cinchetti, G. Malinowski, Y. Fainman, M. Aeschlimann, and E. E. Fullerton, *Nat. Mater.* **13**, 286 (2014).

[2] M. Heigl, C. Mangkornkarn, A. Ullrich, M. Krupinski, M. Albrecht, *AIP Advances* **11**, 085112 (2021).

[3] M. Krupiński, J. Hintermayr, P. Sobieszczyk, and M. Albrecht, *Phys. Rev. Materials* **5**, 024405 (2021)

[4] R. F. L. Evans, W. J. Fan, P. Chureemart, T. A. Ostler, M. O. A. Ellis and R. W. Chantrell *J. Phys.: Condens. Matter* **26**, 103202 (2014)

Altermagnetism and magnetic groups with pseudoscalar electron spin

Ilja Turek¹

¹*Institute of Physics of Materials, Czech Academy of Sciences, Brno, Czech Republic*

In order to understand various aspects of the space-time symmetry of magnetic crystals, several extensions of ordinary crystallographic groups were introduced, see Fig. 1.

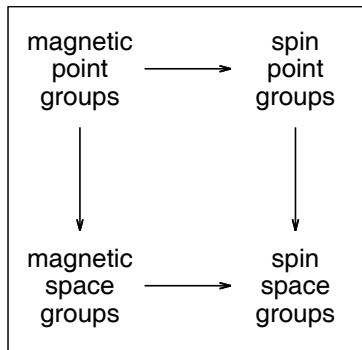


Figure 1: Extensions of crystallographic groups; the arrows mark increasing level of sophistication.

For systems with nonzero spin-orbit interaction (SOI), the magnetic point groups are indispensable for an analysis of symmetry-imposed shapes of the charge and spin conductivity tensors [1], while the magnetic space groups are needed for labelling electron eigenvalues [2]. For systems without SOI, the spin groups are considered, featured by independent rotations in the spin and configuration spaces [3,4]. These extensions proved useful in recent theoretical studies of antiferromagnetism-induced spin splitting of electron states in collinear magnets [2,3].

In this contribution, we report about a unified group-theoretical approach to the spin splitting and the transport properties of collinear antiferromagnets without SOI (altermagnets) based on modified magnetic point groups [5]. The developed scheme reflects modified transformation properties of electron spin, which in the considered systems becomes effectively a pseudoscalar quantity remaining unchanged upon spatial operations but changing its sign upon time reversal. We introduce a unitary representation of the relevant magnetic point groups and use it for a classification of collinear magnets from the viewpoint of spin splitting of electron bands near the center of Brillouin zone. We prove that the recently revealed different altermagnetic classes [3] correspond in a unique way to all nontrivial magnetic Laue classes, i.e., to the Laue groups containing time reversal only in combination with a spatial rotation. Four of these Laue classes are found compatible with a nonzero spin conductivity. Subsequent inspection of a simple model allows us to address briefly the physical mechanisms responsible for the spin splitting in real systems.

[1] M. Seemann et al., *Phys. Rev. B* **92**, 155138 (2015).

[2] L.-D. Yuan et al., *Phys. Rev. B* **102**, 014422 (2020).

[3] L. Šmejkal et al., *arXiv*: 2105.05820 (2021).

[4] P. Liu et al., *arXiv*: 2103.15723 (2021).

[5] I. Turek, *arXiv*: 2201.11452 (2022).

Single crystal studies of NaMnAs, a rediscovered room temperature antiferromagnetic semiconductor

Jiří Volný¹, Karel Výborný², Alberto Marmodoro², Martin Veis³, Klára Uhlířová¹

¹ *Department of Condensed Matter Physics, Faculty of Mathematics and Physics, Charles University, Ke Karlovu 5, Praha 2, CZ-12116*

² *Institute of Physics, Academy of Science of the Czech Republic, Cukrovarnická 10, Praha 6, CZ-16253*

³ *Institute of Physics of Charles University, Faculty of Mathematics and Physics, Ke Karlovu 5, Prague, Cz-121 16*

NaMnAs belongs to a rich group of I-Mn-V layered tetragonal compounds with the non-symmorphic space group P4/nmm such as NaMnSb, NaMnBi, LiMnAs, KMnAs or CuMnAs [1], which are all magnetically ordered at room temperature. Currently, the most prominent compound from this group is CuMnAs (a room-temperature antiferromagnetic semi-metal) which has been intensively studied for the Néel spin-orbit torque [2]. However, other materials have recently also attracted attention in the context of spintronic applications where the presence of a band gap is of advantage. An example of such material is NaMnAs.

We show[3] the synthesis of single-crystalline NaMnAs using the flux method with crystals being few mm large and around hundred μm thick. The X-ray diffraction confirmed the previously reported tetragonal structure with a lattice parameters $a = b = 4.213 \pm 0.002 \text{ \AA}$ and $c = 7.0955 \pm 0.0005 \text{ \AA}$. From the temperature dependence of magnetization we determined the Néel temperature to be at 350 K, which is in a good agreement with our Monte Carlo simulations. Room temperature spectral dependence of optical transmission shows an absorption edge at around 0.9-1.16 eV confirming the predicted [4] semiconducting behavior. Our LDA+U and Monte Carlo calculations reproduce available experiments, and suggest in particular that the Heisenberg exchange coupling between Mn atoms is mainly 2D-like, with a smaller critical temperature than suggested in earlier estimates due to dominant nearest-neighbors ferromagnetic interactions within the flat sheets of the transition metal, and much weaker antiferromagnetic coupling between individual layers.

- [1] W. Bronger, *et al*, “The magnetic properties of NaMnP, NaMnAs, NaMnSb, NaMnBi, LiMnAs, and KMnAs, characterized by neutron diffraction experiments,” *Zeitschrift fuer Anorg. und Allg. Chemie*, pp. 175–182, 1986.
- [2] P. Wadley *et al.*, “Electrical switching of an antiferromagnet,” vol. 1031, no. January, pp. 1–10, 2015.
- [3] J. Volný *et al.*, “Single-crystal studies and electronic structure investigation of the room-temperature semiconductor NaMnAs,” *Phys. Rev. B*. (Accepted 31.1.2022).
- [4] W. Zhou, *et al*, “First-principles study of the magnetic and electronic properties of AMnAs (A=Li, Na, K, Rb, Cs),” *J. Magn. Magn. Mater.*, vol. 420, pp. 19–22, 2016.

Role of substrate clamping on anisotropy and domain structure in the canted antiferromagnet α -Fe₂O₃

A. Wittmann^{1,2}, O. Gomonay¹, K. Litzius^{2,3}, A. Churikova², N. O. Birge^{2,4}, F. Büttner⁵, S. Wintz³, M. Mawass⁵, M. Weigand⁵, F. Kronast⁵, L. Scipioni⁶, A. Shepard⁶, T. Newhouse-Illige⁶, J. A. Greer⁶, J. Sinova¹, G. Schütz³, G. S. D. Beach²

¹ Johannes Gutenberg University, 55128 Mainz, Germany

² Massachusetts Institute of Technology, Cambridge, Massachusetts 02139, USA

³ Max Planck Institute for Intelligent Systems, 70569 Stuttgart, Germany

⁴ Michigan State University, East Lansing, Michigan 48912, USA

⁵ Helmholtz-Zentrum für Materialien und Energie GmbH, 14109 Berlin, Germany

⁶ PVD Products, Wilmington, Massachusetts 01887, USA

Antiferromagnets are at the forefront of research in spintronics and demonstrate high potential for revolutionizing memory technologies. However, many of the underlying phenomena remain to be explored. In this work, we investigate the domain structure in a thin-film canted antiferromagnet α -Fe₂O₃ with magnetic field.

We observe a strongly field-dependent domain structure of α -Fe₂O₃ using x-ray magnetic linear dichroism (XMLD) (see Fig. 1a) and spin Hall magnetoresistance (SMR) measurements. Fig. 1b shows that the remanent resistance R_{rem} (dark) and the saturated resistance R_{sat} (light) follow the same symmetry. We find that the internal destressing fields driving the formation of domains do not follow the crystal symmetry of α -Fe₂O₃ but fluctuate due to substrate clamping. This leads to locally varying effective anisotropy in thin films.

Moreover, we show that the weak ferromagnetic nature of α -Fe₂O₃ leads to a qualitatively different dependence on the external magnetic field compared to collinear antiferromagnets such as NiO.

The insights gained from our work serve as a foundation for further studies of electrical and optical manipulation of the domain structure of antiferromagnetic thin films.

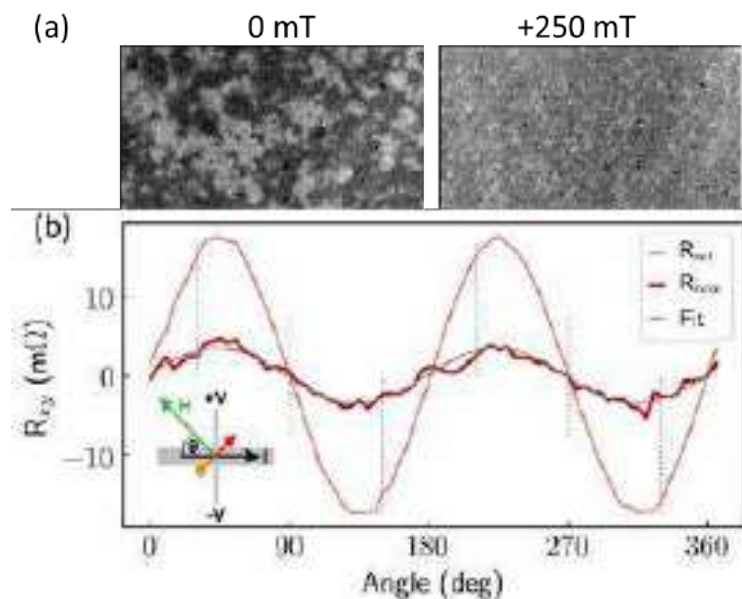


Figure 1: (a) XMLD image of the domain structure of α -Fe₂O₃ at 0 mT (left) and in 250 mT in-plane magnetic field (right). (b) Transverse remanent SMR signal R_{rem} (dark red) of α -Fe₂O₃/Pt Hall cross after H has been reduced from a saturated state R_{sat} (light red) to zero field as a function of angle of the applied magnetic field.

False antiferromagnetic component in ferromagnetic $\text{La}_5\text{Co}_2\text{Ge}_3$ under pressure

Giuseppe Cuono¹, Carmine Autieri¹ and Marcin M. Wysokiński¹

¹*International Research Centre MagTop, Institute of Physics, Polish Academy of Sciences, al. Lotników 32/46, 02-668 Warszawa, Poland*

Transport measurements for the low- T_c metallic ferromagnet $\text{La}_5\text{Co}_2\text{Ge}_3$ indicate the appearance of an antiferromagnetic component under pressure [1]. With density functional theory calculations for this material at ambient and applied pressures [2] we have proposed a possible interpretation to transport properties, alternative to suggested ferromagnetic quantum critical point avoidance. Namely, we have shown that observed transport anomaly is indeed related to spatial modulation of magnetization under pressure, which however has structural rather than electronic origin. Particularly, we reveal that the system is a quasi-one-dimensional ferromagnet with a peculiar coexistence of two different orbital-selective magnetic moments at two crystallographically inequivalent cobalt atoms, Co1 and Co2. We have supported our interpretation with transport calculations for a toy model mimicking found orbital-selective ferromagnetic order.

Acknowledgments We are supported by the International Centre for Interfacing Magnetism and Superconductivity with Topological Matter project, carried out within the International Research Agendas program of the Foundation for Polish Science co-financed by the European Union under the European Regional Development Fund.

- [1] L. Xiang, E. Gati, S. L. Bud'ko, S. M. Saunders, and P. C. Canfield, Phys. Rev. B **103**, 054419 (2021).
- [2] G. Cuono, C. Autieri, M.M. Wysokiński, Phys. Rev B **104**, 024428 (2021)

Spin-transfer torque in non-collinear antiferromagnetic junctions

J. Železný¹, S. Ghosh¹, and A. Manchon²

¹*Institute of Physics, Czech Academy of Sciences, Prague, Czech Republic*

²*CINaM, Aix-Marseille Univ, CNRS, Marseille, France*

Ferromagnetic spin-valves and tunneling junctions are one of the most fundamental and important spintronics devices. Their functionality is based on two effects: the giant or tunneling magnetoresistance for electrical readout and the spin-transfer torque allowing for electrical switching. It has been predicted previously that the same functionality could be achieved with antiferromagnetic junctions, which would provide various advantages over ferromagnets, such as a much faster switching speed. However, these devices are very sensitive to disorder and have never been experimentally demonstrated [1].

Here we show that the key to obtaining robust spin-transfer torque and magnetoresistance in antiferromagnets is utilizing lower symmetry antiferromagnets, in which electrical current is spin-polarized [2,3]. We consider junctions composed of non-collinear antiferromagnets and find a spin-transfer torque and magnetoresistance with a magnitude and robustness against disorder comparable to ferromagnetic junctions [3]. Furthermore, our calculations reveal novel aspects of the torque in non-collinear junctions. In particular, we find that apart from the conventional spin-transfer torque, a novel self-generated torque appears. This torque is similar to a spin-orbit torque but has a non-relativistic origin. We also find that a torque appears for any configuration of the junction, in contrast to ferromagnetic junctions where the torque vanishes in the parallel or antiparallel configurations.

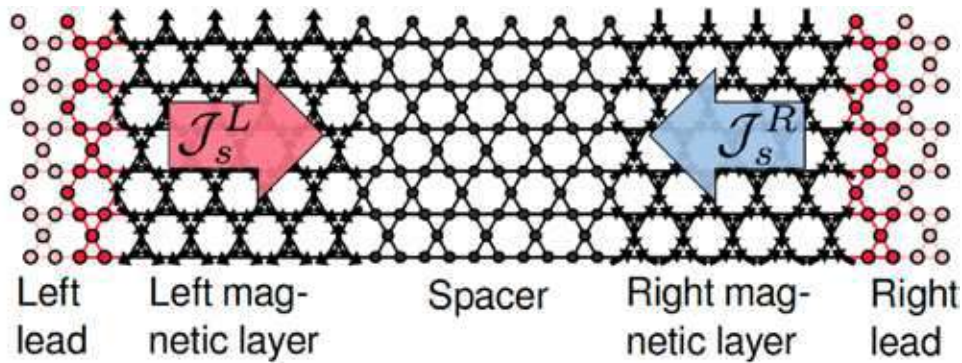


Figure 1: Illustration of the non-collinear junction. $\mathcal{J}_s^L, \mathcal{J}_s^R$ denote the spin-polarized current in the left and right magnetic layers respectively.

- [1] J. Železný et al., *Nature Physics* **14**, 220–228 (2018)
- [2] J. Železný et al., *PRL* **119**, 187204 (2017)
- [3] S. Ghosh et al., *PRL* to appear, arXiv:2109.01399 (2021)

Hysteretic effects and magnetotransport of electrically switched CuMnAs

Jan Zubáč^{1,2}, Zdeněk Kašpar^{3,1}, Filip Krizek¹, Tobias Förster⁴,
Richard P. Campion⁵, Vít Novák¹, Tomáš Jungwirth^{1,5}, and Kamil Olejník¹

¹*Institute of Physics, Czech Academy of Sciences, Cukrovarnická 10, 162 00, Prague 6, Czech Republic*

²*Charles University, Faculty of Mathematics and Physics, Ke Karlovu 3, 121 16 Prague 2, Czech Republic*

³*Department of Physics, Freie Universität Berlin, 14195 Berlin, Germany*

⁴*Hochfeld-Magnetlabor Dresden (HLD-EMFL) and Würzburg-Dresden Cluster of Excellence ct.qmat, Helmholtz-Zentrum Dresden-Rossendorf, 01328 Dresden, Germany*

⁵*School of Physics and Astronomy, University of Nottingham, Nottingham NG7 2RD, United Kingdom*

Antiferromagnetic spintronics allows us to explore storing and processing information in magnetic crystals with vanishing magnetization. In this contribution, we report on magnetoresistance effects in antiferromagnetic CuMnAs upon switching into high-resistive states using electrical pulses. By employing magnetic field sweeps up to 14 T and magnetic field pulses up to ~ 60 T, we reveal hysteretic phenomena and changes in the magnetoresistance (Fig. 1), as well as the robustness of the switching signal in CuMnAs against the high magnetic field [1]. These properties of the switched state are put in the context of studies of antiferromagnetic textures in CuMnAs [2].

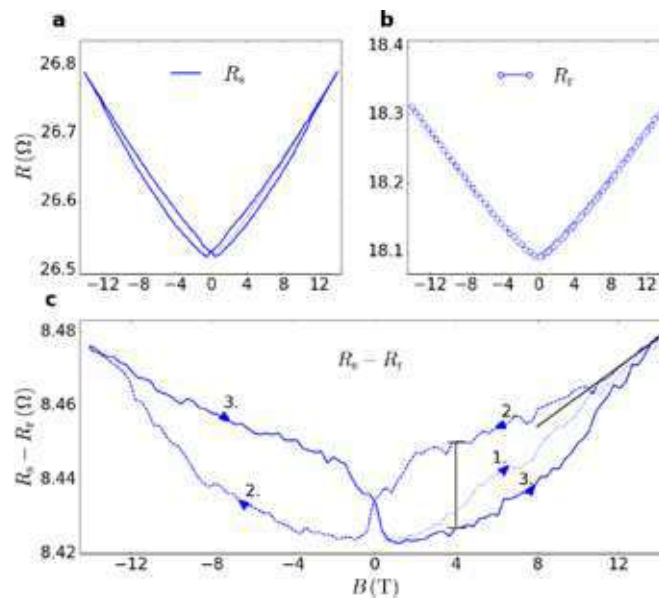


Figure 1: Magnetoresistance of CuMnAs at 2 K (a) in the high-resistance switched state (R_s) and (b) in the low-resistance relaxed state (R_r). (c) Difference $R_s - R_r$ between the switched-state and the relaxed state magnetoresistance showing hysteretic effects induced by the quench switching.

[1] J. Zubáč et al., *Phys. Rev. B* **104.18**, 184424, (2021).

[2] F. Krizek et al., *in press, Sci. Adv.*, (2022).

Posters

| | | |
|-----------------------|---|-----|
| Aleksei Bludov | <i>Magnetic properties of $RCr_3(BO_3)_4$ crystals with Tb^{3+} and Dy^{3+} ions</i> | 126 |
| Irina Dolgikh | <i>Ultrafast Emergence of Ferromagnetism in Antiferromagnetic FeRh in High Magnetic Fields</i> | 127 |
| Anna Hellenes | <i>Giant and tunneling magnetoresistance in unconventional collinear antiferromagnets with nonrelativistic spin-momentum coupling</i> | 128 |
| Arturo Rodríguez Sota | <i>Magnetism and growth of a Mn monolayer on Ir (111) investigated by SP STM</i> | 129 |
| Vishesh Saxena | <i>Exploring the antiferromagnetic ground states and domain walls of Mn bi- and trilayers on Ir (111) by SP-STM</i> | 130 |
| Maria Stamenova | <i>Resistance of atomically sharp domain walls in CuMnAs from first principles</i> | 131 |
| Oleksii Zadorozhnyi | <i>In-situ electrically and thermally controlled magnetic imaging of metamagnetic FeRh in transmission electron microscope</i> | 132 |

Magnetic properties of $\text{RCr}_3(\text{BO}_3)_4$ crystals with Tb^{3+} and Dy^{3+} ions

Yu. Savina ¹, A. Bludov ¹, V. Pashchenko ¹, A. Lynnyk ², T. Zajarniuk ²,
M.U. Gutowska ², A. Szewczyk ², I. Kolodiy ³

¹ *B. Verkin Institute for Low Temperature Physics and Engineering of the NAS of Ukraine,
47 Nauky Ave., 61103 Kharkiv, Ukraine*

² *Institute of Physics, Polish Academy of Sciences, al. Lotników 32/46, 02-668 Warsaw, Poland*

³ *National Science Center «Kharkov Institute of Physics and Technology», 1 Akademichna St., 61000
Kharkiv, Ukraine*

Complex oxides with ions of 3d transition and rare-earth (4f) metals attract considerable attention of scientists. In such compounds 3d ions can provide comparative high temperature of magnetic ordering, while features of electronic properties of rare-earth ions can form electric polarization and elastic deformation. Magnetoelectric and magnetoelastic effects, giant magnetocaloric effect and exotic magnetic phases can be found in the mixed 3d-4f compounds due to interaction between 3d and 4f subsystems.

The rare-earth chromium borates $\text{TbCr}_3(\text{BO}_3)_4$ and $\text{DyCr}_3(\text{BO}_3)_4$ belong to the large family of compounds with a general chemical formula $\text{RM}_3(\text{BO}_3)_4$ (R = lanthanides or Y; M = Al, Ga, Sc, Fe or Cr). The majority of crystals of this family have the structure of huntite mineral, which crystallizes in the trigonal crystal system with space group $R32$. The crystal structure consists of spiral chains of sharing edges MO_6 octahedra along the c axis. The RO_6 prisms and the planar triangular BO_3 groups combine the chains into 3D framework. Several other structural polytypes with similar motif (chains of MO_6 octahedra) are known for the family.

Crystal structure characterization carried out by using X-ray powder diffraction technique show that $\text{TbCr}_3(\text{BO}_3)_4$ crystals are single phase with $R32$ space group, while $\text{DyCr}_3(\text{BO}_3)_4$ samples turned out to be biphasic ($R32$ – 49wt.% and $C2/c$ – 51wt.%). Magnetic and heat capacity measurements of the studied samples have been performed by the SQUID magnetometer MPMS-XL7 and the PPMS system, respectively.

The phase transition into antiferromagnetically ordered state in $\text{TbCr}_3(\text{BO}_3)_4$ crystal occurs at $T_N = 8.8$ K. Spontaneous spin-reorientation phase transition from the easy-plane (EP) antiferromagnetic state to the easy-axis (EA) one takes place in the vicinity of 5 K. The EA state exists in a limited range of temperatures (below 5 K) and magnetic fields (below 0.5 T for $H||c$). Values of the intrachain ($J/k = 3.2$ K) and interchain ($J'/k = -0.7$ K) Cr-Cr exchange interaction have been evaluated. The H - T phase diagram of $\text{TbCr}_3(\text{BO}_3)_4$ for $H||c$ has been constructed.

It was found that both structural modifications of $\text{DyCr}_3(\text{BO}_3)_4$ are ordered antiferromagnetically ($R32$ - $T_{N1} = 9.1$ K, $C2/c$ - $T_{N2} = 7.5$ K) and the spontaneous magnetic phase transitions, which are similar to the found one in $\text{TbCr}_3(\text{BO}_3)_4$, are observed at temperatures 3.6 K and 4.6 K.

Ultrafast Emergence of Ferromagnetism in Antiferromagnetic FeRh in High Magnetic Fields

I. A. Dolgikh^{1,2}, T. G. H. Blank¹, G. Li¹, K. H. Prabhakara¹, S. K. K. Patel³, A. G. Buzdakov^{4,6}, R. Medapalli^{3,7}, E. E. Fullerton³, O. V. Koplak⁸, J. H. Mentink¹, K. A. Zvezdin^{6,9}, A. K. Zvezdin^{4,9}, P. C. M. Christianen^{1,2} and A. Kimel¹

¹*Institute for Molecules and Materials, Radboud University, 6525 AJ Nijmegen, The Netherlands.*

²*High Field Magnet Laboratory (HFML—EMFL), Radboud University, 6525 ED Nijmegen, The Netherlands.*

³*Center for Memory and Recording Research, University of California, San Diego, La Jolla, California 92093-0401, USA.*

⁴*Moscow Institute of Physics and Technology (State University), 141700 Dolgoprudny, Russia.
5I-FEVS, Via Carignano, 50/1, 10040 La Loggia TO, Italy.*

⁶*New Spintronic Technologies, Russian Quantum Center, Bolshoy Bulvar 30, bld. 1, Moscow 121205, Russia.*

⁷*Department of Physics, Lancaster University, Bailrigg, Lancaster LA1 4YW, United Kingdom.*

⁸*Institute of Problems of Chemical Physics, Russian Academy of Sciences, Chernogolovka, Moscow region, 142432 Russia.*

⁹*Prokhorov General Physics Institute of the Russian Academy of Sciences, 119991 Moscow, Russia.*

The future of magnetic data storage crucially depends on our understanding of the mechanisms and fundamental limits on the speed of angular momentum transfer between lattice and spins. In the case of antiferromagnetic FeRh, this is a particularly interesting problem. Upon a temperature increase, the spins of Fe in FeRh suck angular momentum from the lattice - the medium becomes ferromagnetic, while the lattice expands [1]. Aiming to reveal the mechanism and the fastest possible time-scale of the magneto-structural phase transition resulted in a spin-and-lattice causality dilemma also known as a chicken-and-egg problem we carried out a time-resolved optical measurement in extreme conditions [2]. Here we resolve the problem by accelerating the spin dynamics in high (25 T) fields and observing both structural and spin dynamics with the help of time-resolved optical and magneto-optical measurements, respectively (see Fig.1). We observe that the fastest possible induction of ferromagnetism occurs on a time scale of the lattice expansion (3 ps). The regime implies that the laser excitation first modifies the exchange interaction on a sub-ps time-scale launching coupled magneto-structural spin dynamics such that the total spin-lattice angular momentum can be conserved.

[1] L. H. Lewis, C. H. Marrows, & S. Langridge. *J. of Phys. D: Appl. Phys.* **49**, 323002 (2016).

[2] I. A. Dolgikh, T. G. H. Blank, G. Li, et al. *Prepr. arXiv:2202.03931* (2022).

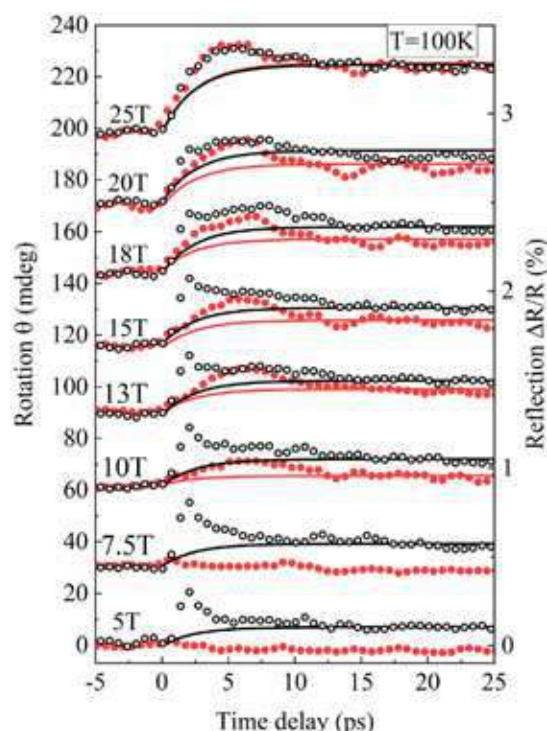


Figure 1: The polarization rotation induced by the magneto-optical Kerr effect (red) and reflectivity change (black) at 100 K and various magnetic fields. The open circles represent the experimental data and the solid lines are their respective fits. The curves are plotted with an offset.

Giant and tunneling magnetoresistance in unconventional collinear antiferromagnets with nonrelativistic spin-momentum coupling

Libor Šmejkal^{1,2}, Anna Birk Hellenes¹, Rafael González-Hernández³, Jairo Sinova^{1,2}, and Tomáš Jungwirth^{2,4}

¹Johannes Gutenberg Universität Mainz, D-55099 Mainz, Germany

²Czech Academy of Sciences, Cukrovarnická 10, 162 00 Praha 6 Czech Republic

³Universidad del Norte, Barranquilla, Colombia

⁴University of Nottingham, Nottingham NG7 2RD, United Kingdom

Magnetoresistance effects of multilayer structures with ferromagnetic electrodes are used in commercial spintronics devices. The effects rely on spin current generated by the time-reversal broken band structure of the ferromagnets. Realizing the counterpart effects in structures with all-antiferromagnetic electrodes remained hitherto experimentally elusive, as the conventional antiferromagnets exhibit symmetries that combine time-reversal with translation or inversion and thus prohibit nonrelativistic spin polarized bands and spin currents. Recently, we have predicted large magnetoresistance effects[1,2] in multilayers with unconventional antiferromagnets (see Figure) which break these combined

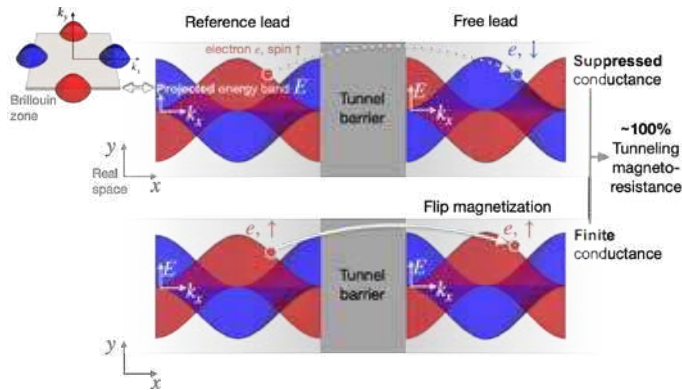


Figure 1: Large tunneling magnetoresistance $\sim 100\%$ is found for a band structure with spin-polarized valleys where the opposite spin channels are separated in momentum space by large wave vectors.

time-reversal symmetries[3,4,5]. The opposite spin sublattices in the unconventional antiferromagnets are connected by nonrelativistic rotational symmetries, resulting in nonrelativistic spin-momentum coupling which alternates in the Brillouin zone but integrates to zero net magnetization (see Figure inset)[1,5]. In the present contribution, we will describe in detail mechanisms for the giant and tunneling magnetoresistance effects in unconventional antiferromagnets[1]. We will explain, based on our minimal models, that a large signal

can be attributed to archetype features in the band structures, such as spin-polarised valleys[1]. Finally, we will list possible material candidates[1,6].

[1] L. Šmejkal, A. B. Hellenes et al., Physical Review X 12, 011028 (2022)

[2] H. Reichlova et al., arxiv:2012.15651v2 (2020)

[3] L. Šmejkal et al., Science Advances, 6, 23, 6 (2020)

[4] I. Mazin et al., Proceedings of the National Academy of Sciences, 118, 42, 20 (2021)

[5] L. Šmejkal et al., arXiv:2105.05820 (2021)

[6] D-F. Shao et al., Nature Communications, 12, 1, 12 (2021)

Magnetism and growth of a Mn monolayer on Ir (111) investigated by SP STM

Arturo Rodríguez Sota¹, Vishesh Saxena¹, André Kubetzka¹,
Roland Wiesendanger¹, Kirsten von Bergmann¹

¹*Institute for Nanostructure and Solid-State Physics, Department of Physics,
University of Hamburg, Hamburg, Germany*

Antiferromagnetic materials have moved into the focus of current research due to their potential for spintronics applications. In a hexagonal monolayer a nearest-neighbour antiferromagnetic interaction leads to geometric frustration and the ground state is the Néel state [1] with 120° between adjacent magnetic moments. However, also other magnetic states like a row-wise antiferromagnetic state or a hexagonal triple-Q state have been reported [2]. A powerful tool to investigate atomic-scale magnetic order is spin-polarized scanning tunnelling microscopy (SP-STM).

Here, we study Mn, one of the elements that typically show antiferromagnetic coupling, and grow it on a hexagonal Ir(111) surface. When the Mn coverage exceeds one atomic layer we observe the Néel state in the pseudomorphic monolayer. However, when submonolayer amounts of Mn are deposited, we find a coexistence of islands and clusters; such a peculiar growth has barely been documented before [3].

In contrast to the fully closed pseudomorphic Mn film, the submonolayer Mn islands present a Moiré-like reconstruction, as seen in Fig. 1 (left), in which the Mn atoms periodically change their adsorption sites. We have studied the impact of these structural feature on the magnetic properties of the Mn film.

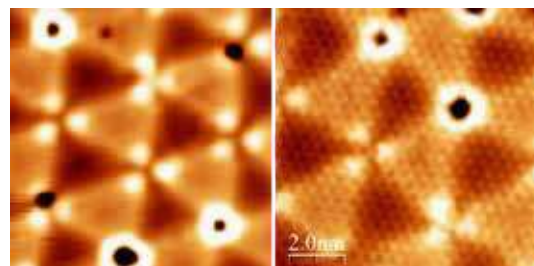


Figure 1- Constant-current topographic measurements of the reconstructed Mn monolayer on Ir(111) at 10K. Comparison of a spin-averaging (left) and a spin-polarized (right) measurement.

- [1] C. L. Gao, W. Wulfhekkel, and J. Kirschner, *Revealing the 120° Antiferromagnetic Néel Structure in Real Space: One Monolayer Mn on Ag(111)*, Physical Review Letters **101**, (2008).
- [2] J. Spethmann, S. Meyer, K. von Bergmann, R. Wiesendanger, S. Heinze, and A. Kubetzka, *Discovery of Magnetic Single- And Triple- q States in Mn/Re (0001)*, Physical Review Letters **124**, (2020).
- [3] D. F. Förster, T. O. Wehling, S. Schumacher, A. Rosch, and T. Michely, *Phase Coexistence of Clusters and Islands: Europium on Graphene*, New Journal of Physics **14**, (2012).



This project has received funding from the European Union's Horizon 2020 research and innovation program under the Marie Skłodowska-Curie grant agreement No 955671.

Exploring the antiferromagnetic ground states and domain walls of Mn bi- and trilayers on Ir (111) by SP-STM

Vishesh Saxena¹, Arturo Rodríguez Sota¹, André Kubetzka¹,
Roland Wiesendanger¹, Kirsten von Bergmann¹

¹*Institute for Nanostructure and Solid-State Physics, Department of Physics,
University of Hamburg, Hamburg, Germany*

Conventional magnetic skyrmions are susceptible to unwanted phenomena such as the skyrmion Hall effect, hindering their applications in spintronic devices. An alternative are antiferromagnetic (AFM) skyrmions which do not show a skyrmion Hall effect.

In the quest to explore systems that can host AFM skyrmions, we have studied the

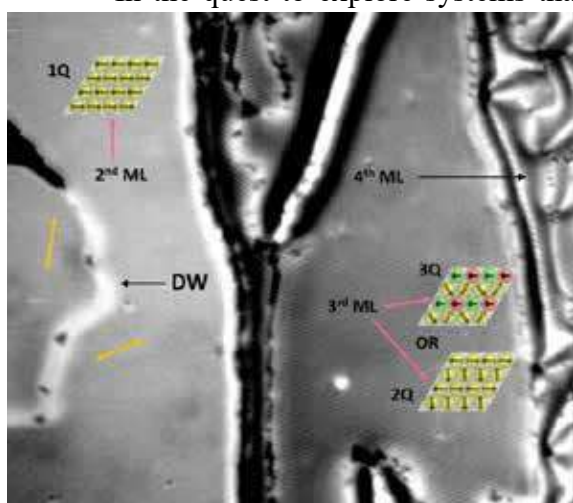


Figure 1: Constant-current STM image, showing the 2nd, 3rd, and 4th Mn layers on Ir(111) exhibiting different magnetic ground states. The yellow arrows on the 2nd ML show the different orientations of the 1Q row-wise AFM states separated by a domain wall (DW)

magnetism of Mn on Ir (111) using spin-polarized scanning tunneling microscopy (SP-STM). Having an AFM spin coupling on a hexagonal periodic lattice induces geometric frustration leading to a Néel state. However, also other magnetic states have been observed, such as the row-wise AFM state (1Q) or a superposition of the 1Q states resulting in a 3Q state (hexagonal magnetic superstructure), depending on the stacking of Mn as observed for Mn on Re(0001) [1].

In the present work, the magnetic properties of the monolayer, bi-layer, and the tri-layer of Mn on Ir(111) are studied. The first monolayer of Mn exhibits the Néel state as the magnetic ground state. The bi-layer is shown to exhibit a row-wise AFM magnetic ground state.

Several different types of structural defects on the bilayer induce a certain type of orientation of the 1Q states thus leading to many domains and domain walls. Within the domain walls (DW), a hexagonal pattern is observed, similar to the superposition state observed previously [2]. We find that the details of such domain walls depend on their direction relative to the adjacent magnetic states. A good understanding of AFM domain walls is desirable with regard to applications for domain wall transport-based memory devices [3]. The third layer exhibits a hexagonal magnetic superstructure, indicative of a 2Q or 3Q superposition of 1Q states.

[1] J. Spethmann, S. Meyer, K. von Bergmann, R. Wiesendanger, S. Heinze, and A. Kubetzka, *Discovery of magnetic single- and triple-q states in Mn/Re (0001)*, Phys. Rev. Lett. **124**, 227203 (2020).

[2] J. Spethmann, M. Grünebohm, R. Wiesendanger, K. von Bergmann, and A. Kubetzka, *Discovery and Characterization of a New Type of Domain Wall in a Row-Wise Antiferromagnet*, Nature Commun. **12**, (2021). This project has received funding from the European Union's Horizon 2020 research and innovation program under the Marie Skłodowska-Curie grant agreement No 955671

Resistance of atomically sharp domain walls in CuMnAs from first principles

Maria Stamenova¹, Plamen Stamenov¹ and Stefano Sanvito¹

¹ School of Physics and CRANN, Trinity College Dublin, Dublin 2, Ireland

Low-moment ferrimagnets and anti-ferromagnets hold promise for realizing spintronic devices with extreme properties: ultra-low power dissipation, high writing speeds (oscillation frequencies) and immunity to stray magnetic fields. Recently, the tetragonal non-inversion-symmetric antiferromagnet CuMnAs has been promoted as the active layer for devices relying on electrical Néel vector switching [1] or electrical/optical heat-assisted toggling into a nan-fragmented domain state with a GMR-like level of resistance change [2]. The already demonstrated atomically-sharp domain walls [3] can contribute to the magneto-galvanic effects in the thin CuMnAs films. Here we investigate from first principles (NEGF+DFT) the spin-polarised ballistic transport through domain walls (DW) of different thickness in a transverse-periodic scattering geometry of bulk-like tetragonal CuMnAs. We find that the DW magneto-resistance (MR) scales inversely with the DW width for atomic thicknesses – it reaches a maximum of around 60% for an atomically-abrupt 0-180° DW, which decreases to 40% if a additional 90°-spin layer is introduced, and saturates to around 20% in the adiabatic limit. The energy dependence of the transmission coefficient attains little additional structure even for the thinnest of DWs. The short carrier scattering times (~ 2 fs), degenerately-high hole densities and relatively high effective mass ($\sim 0.8 m_e$), experimentally demonstrated at RT [4], would dilute down the useful DW MR substantially, even for large-volume devices, containing multiple walls. Alternative material classes, i.e. ferrimagnets supporting ultra-thin DWs, may offer a different balance between addressability and magneto-galvanic readout functionality and warrant the deployment of the computational methods illustrated here.

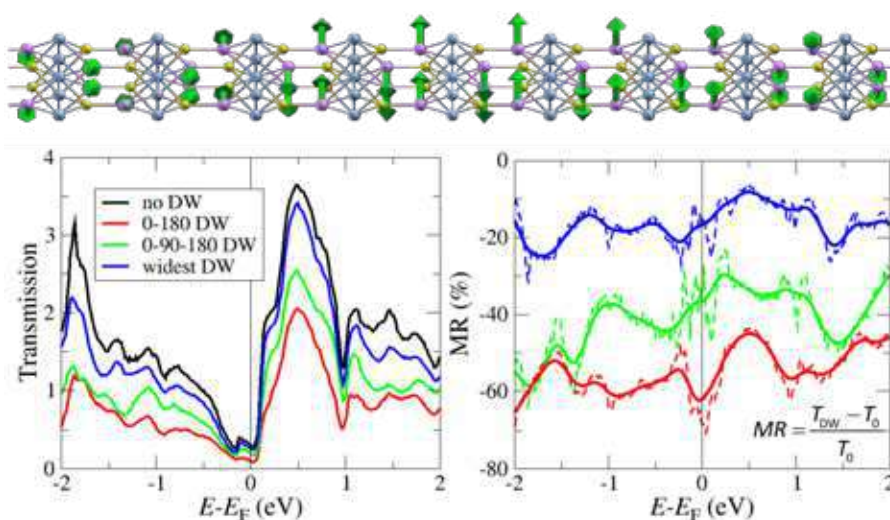


Figure 1: A schematic of the CuMnAs structure with the widest DW simulated and the energy-resolved transmission coefficient and MR (as defined in the inset through the corresponding transmission coefficients) for three DWs of different widths (as per the color legend).

[1] P. Wadley, et al. (2016), *Science* **351**, 587.

[2] Z. Kaspar, et al. (2022), *Nature Electronics* **4**, 30.

[3] S. Reimers, et al. (2022), *Nature Comm.* **13**, 724.

[4] V. Hills, et al. (2015), *Journ. Appl. Phys.* **117**, 172608.

In-situ electrically and thermally controlled magnetic imaging of metamagnetic FeRh in transmission electron microscope

Jan Hajduček¹, Oleksii Zadorozhnii¹ and Vojtěch Uhlíř¹

¹ CEITEC BUT, Brno University of Technology, Purkyňova 123, Brno, Czech Republic

Antiferromagnets (AFs) are a promising material class for spintronic technology, due to their robustness in external magnetic fields, fast dynamics, and possibility of low-power switching [1]. Metamagnetic materials featuring the phase transition from AF to ferromagnetic (FM) order are a class of AFs that can be thermally activated to alter their AF configuration using field cooling [2]. Visualization of the AF and FM phase coexistence has been recently demonstrated by imaging the distribution of FM domains by Electron Holography [3] and Differential Phase Contrast (DPC) in Scanning Transmission Electron Microscopy (STEM) [4].

Here, we focus on in-situ analysis of magnetic order in metamagnetic FeRh using the DPC-STEM technique upon simultaneous application of external magnetic field, temperature, and electrical bias. By combining imaging of the phase coexistence with measuring the integrated resistance of the FeRh TEM lamella we describe the memory of the AF and FM configurations to thermal cycling in different applied magnetic fields.

- [1] V. Baltz, A. Manchon, M. Tsoi, T. Moriyama, T. Ono, and Y. Tserkovnyak. *Rev. Mod. Phys.* **90**, 015005 (2018).
- [2] X. Marti, I. Fina, C. Frontera, Jian Liu, P. Wadley, Q. He, R. J. Paull, J. D. Clarkson, J. Kudrnovský, I. Turek, J. Kuneš, D. Yi, J-H. Chu, C. T. Nelson, L. You, E. Arenholz, S. Salahuddin, J. Fontcuberta, T. Jungwirth and R. Ramesh. *Nat. Mater.* **13**, 367–374 (2014).
- [3] C. Gatel, B. Warot-Fonrose, N. Biziere, L.A. Rodríguez, D. Reyes, R. Cours, M. Castiella and M.J. Casanove. *Nat. Commun.* **8**, 15703 (2017).
- [4] T. P. Almeida, D. McGrouther, R. Temple, J. Massey, Y. Li, T. Moore, C. H. Marrows and S. McVitie. *Phys. Rev. Mater.* **4**, 034410 (2020).

Symposium 5. Artificial intelligence in magnetism

| | | |
|----------------------|--|-----|
| Jack Carter-Gartside | <i>Neuromorphic Spin-Wave Computing in Hybrid Multi-Array Nanomagnetic Architectures</i> | 135 |
| Ian Vidamour | <i>Experimental Demonstration of Reservoir Computation using Emergent Domain Wall Dynamics in a Patterned Magnetic Substrate</i> | 136 |
| Vanessa Nehruji | <i>Machine learning informing computational modelling of complex magnetic spin textures</i> | 138 |
| Piotr Rzeszut | <i>Serial and Parallel Magnetic Tunnel Junction Configuration for RF applications and neuromorphic computing.</i> | 139 |
| Alexander Welbourne | <i>Stochastic Computing and Machine Learning with Magnetic Domain Walls</i> | 140 |
| Alexander Welbourne | <i>Voltage Controlled Superparamagnetic Ensembles for Low Power Reservoir Computing</i> | 142 |

Invited Oral Presentations

| | | |
|----------------------|--|-----|
| Jack Carter-Gartside | <i>Neuromorphic Spin-Wave Computing in Hybrid Multi-Array Nanomagnetic Architectures</i> | 135 |
| Ian Vidamour | <i>Experimental Demonstration of Reservoir Computation using Emergent Domain Wall Dynamics in a Patterned Magnetic Substrate</i> | 136 |

Neuromorphic Spin-Wave Computing in Hybrid Multi-Array Nanomagnetic Architectures

**Jack C. Gartside¹, Kilian D. Stenning¹, Alex Vanstone¹, Holly H. Holder¹, Troy Dion², Francesco Caravelli³, Christopher Chueng¹, Tony Chen¹, Daan M. Arroo¹,
Hidekazu Kurebayashi⁴, Will R. Branford⁵**

¹ *Imperial College London, London, United Kingdom*

² *Kyushu University, Fukuoka, Japan*

³ *Los Alamos National Lab, Los Alamos, USA*

⁴ *University College London, London, United Kingdom*

The vast microstate space of artificial spin ice (ASI) & related nanomagnetic arrays is both hugely powerful for data processing^{1,2}, and highly challenging to experimentally reconfigure into more than a handful of states.

Subtle changes in array geometry, nanoisland fabrication & inter-island coupling have large impact on neuromorphic processing & memory capabilities. Similarly, the energy landscape of the microstate space is vast, highly-sensitive to array design choices and of critical importance to neuromorphic computing performance. Any single physical array must be nanofabricated with one set of parameters – and a corresponding compromise of computational performance, an array excelling at nonlinear transformation capability will inherently struggle with future prediction tasks and vice-versa.

We explore the array parameter space & map specific computation-performance metrics onto physical array parameters. We use this approach to fabricate a diverse suite of nanomagnetic arrays with specialised functionalities, then integrate them into hybrid multi-array networked computing architectures³ to overcome & outperform the limitations of single network physical computing systems. Benchmark tasks are evaluated for a variety of single & multi-network computing architectures, with flexible, task-adaptable performance demonstrated for hybrid network systems.

[1] Gartside, Jack C., et al. "Reconfigurable training and reservoir computing in an artificial spin-vortex ice via spin-wave fingerprinting." *Nature Nanotechnology* 17.5 (2022): 460-469.

[2] Gartside, Jack C., et al. "Reconfigurable magnonic mode-hybridisation and spectral control in a bicomponent artificial spin ice." *Nature Communications* 12.1 (2021): 1-9.

[3] Manneschi, Luca, et al. "Exploiting multiple timescales in hierarchical echo state networks." *Frontiers in Applied Mathematics and Statistics* 6 (2021): 76.

Experimental Demonstration of Reservoir Computation using Emergent Domain Wall Dynamics in a Patterned Magnetic Substrate

Vidamour, I¹; Swindells, C¹; Venkat, G¹; Vasilaki, E²; Allwood, D.A.¹; Hayward, T.J.¹

¹Department of Materials Science and Engineering, University of Sheffield

²Department of Computer Science, University of Sheffield

Reservoir computing (RC) is a machine learning paradigm where computation is performed using the intrinsic memory and nonlinearity of a dynamical system. Traditionally, the dynamic system is provided algorithmically by a recurrent neural network, though recent studies show this network can be substituted with a physical dynamic system to realise the paradigm in hardware. Many nano-scale magnetic systems have been proposed as potential candidates for RC, including spin torque oscillators (STOs) [1], superparamagnetic arrays [2], and individual domain walls [3]. However, aside from STOs, few proposed systems have been experimentally realised. Here, we experimentally demonstrate RC using a single-layer array of permalloy nanorings, which exhibit emergent domain wall dynamics [4].

First, we show how data can be encoded to the array by modulating the amplitude of an applied rotating magnetic field, and how we can extract information on the magnetic state of the array through anisotropic magnetoresistance (AMR) measurements. We show that the measured AMR had a highly non-linear response to the applied field amplitude, and exhibited a fading memory of past inputs, thus meeting the two critical criteria for performing RC. Next, we show how the arrays can be exploited to perform spoken and written digit recognition tasks with a high level of accuracy. We believe that the ease of measurement, relative simplicity of manufacture, as well as the wide range of available parameter space to explore makes the arrays an exciting platform for neuromorphic computation.

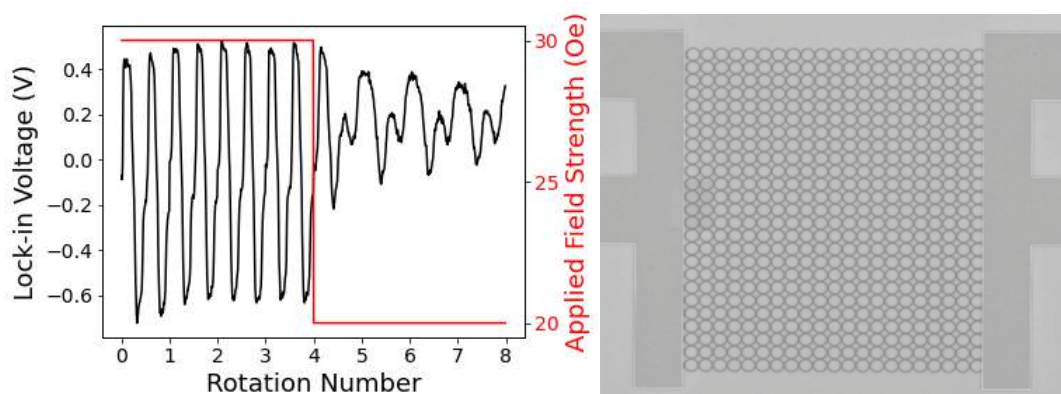


Figure 1- Measured AMR response for 4 rotations of 30 Oe applied field, followed by 4 rotations of 20 Oe applied field, showing both a nonlinear response and fading memory.

Figure 2- Micrograph of patterned nanoring array and electric contacts taken from RAITH Voyager electron beam lithography system.

[1]-J. Torrejon et al., “Neuromorphic computing with nanoscale spintronic oscillators,” *Nature*, vol. 547, no. 7664, pp. 428–431, Jul. 2017, [2]-A. Welbourne *et al.*, “Voltage-controlled superparamagnetic ensembles for low-power reservoir computing,” *Appl. Phys. Lett.*, vol. 118, [3]- R. V Ababei *et al.*, “Neuromorphic computation with a single magnetic domain wall,” *Sci. Rep.* 11, [4]- R. W. Dawidek *et al.*, “Dynamically-Driven Emergence in a Nanomagnetic System,” *Adv. Funct. Mater.*, vol. 31

Oral Presentations

| | | |
|---------------------|---|-----|
| Vanessa Nehruji | <i>Machine learning informing computational modelling of complex magnetic spin textures</i> | 138 |
| Piotr Rzeszut | <i>Serial and Parallel Magnetic Tunnel Junction Configuration for RF applications and neuromorphic computing.</i> | 139 |
| Alexander Welbourne | <i>Stochastic Computing and Machine Learning with Magnetic Domain Walls</i> | 140 |

Machine learning informing computational modelling of complex magnetic spin textures

V. Nehruji¹, H. Fangohr^{1,2}, and O. Hovorka¹

¹*Faculty of Engineering and Physical Sciences, University of Southampton, UK*

²*Max-Planck Institute for Structure and Dynamics of Matter, Luruper Chaussee 149, 22761 Hamburg, Germany*

Quite recently, there have been numerous studies focusing on the application of deep learning (DL) algorithms to classify states found in classic magnetic models, such as the Ising and XY systems. Unsupervised classification models, such as the variational autoencoders, can encode the information contained in large lattice structures down to fewer variables, which have been shown to correlate with the order parameter of the system [1,2]. This discovery is especially useful for identifying order parameters in more complex magnetic systems and can allow for the large-scale data processing required to analyse systems with disorder.

In this presentation, we discuss the utilisation of convolutional variational autoencoders (CVAEs) of varying architectures for classification of complex magnetic domains. The computational data used to train the CVAEs were based on the mean-field model of a classical spin Hamiltonian, which in addition to the Heisenberg exchange and Dzyaloshinskii-Moriya interactions included also uniaxial anisotropy and dipolar interaction. The model allows performing finite-temperature simulations and recovers the micromagnetic framework in the coarse-grained zero-temperature limit. We ran temperature-dependent hysteresis loops of systems with and without defects and produced a large-scale database of the observed spin textures, such as magnetic stripe domains, skyrmions, and labyrinth structures, for example, and used the database for training the CVAEs.

We discuss (i) the accuracy of the approach to predict the phase assuming representative magnetic textures, (ii) the feasibility of generalising the approach to more complex models and (iii) address the prospects for predicting the order parameter of complex magnetic systems. Since the data generation is based on physically realistic field and temperature dependent experimental protocols, the hope is that the spin textures naturally stabilised in this study can be practically realisable by equivalent experimental protocols.

[1] N. Walker, K. M. Tam, and M. Jarrell, *Sci Rep* **10**, 13047 (2020).

[2] S. Wetzel, *Phys. Rev. E* **96**, 022140 (2017).

Serial and Parallel Magnetic Tunnel Junction Configuration for RF applications and neuromorphic computing

Rzeszut P.¹, Zietek S.¹, Mojsiejuk J.¹, Skowroński W.¹, and Yakushiji K.²

¹AGH University of Science and Technology, Institute of Electronics,

Al. Mickiewicza 30, 30-059 Kraków, Poland

²National Institute of Advanced Industrial Science and Technology (AIST),

Spintronics Research Center, Tsukuba, Ibaraki, 305-8568, Japan

Magnetic Tunnel Junctions (MTJ) have been used in various technological applications, such as magnetic field sensors or information storage medium. Nowadays new applications are proposed, such as neuromorphic computing [1], high-frequency detectors and generator or energy-harvesting devices[2].

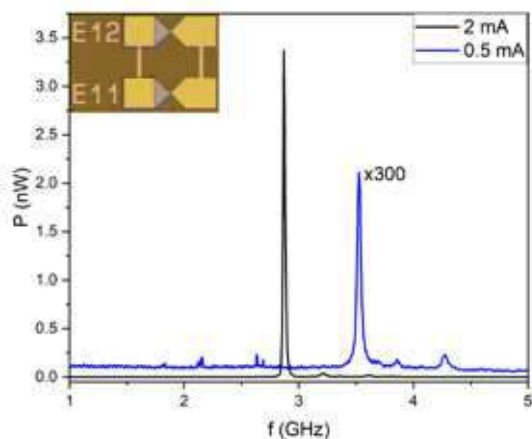


Figure 1: Representative power density vs. frequency generated by two oscillators connected in parallel for 2 mA (black) and 0.5 mA (blue, signal magnified 300 times) DC supply. Blue shift is characteristic for PMA present in the MTJ. Inset: parallel connection of STNO as manufactured.

Recently we have proposed a hardware neural network circuit for handwritten digits recognition based on serially connected MTJs [3] acting as programmable memristors used to define network parameters [4]. In different approaches MTJs are also used as spin torque nano oscillator (STNO) in neuromorphic computing systems, such as spoken digit recognition [1].

In the present work we investigate the behaviour of on-chip serial and parallel connections of MTJs in terms of synchronization of their oscillations. For serially connected STNO we expect anti-synchronization [5], while for parallel connection - electrical synchronization [2] which leads to an increased output power, as well as better Q-factor. The multilayer consist

of SAF/CoFeB(2.5)/MgO(1)/CoFeB(1.8)/MgO(1)/cap (thickness in nm), with a bottom CoFeB coupled to synthetic antiferromagnet (SAF). The top CoFeB is characterized by perpendicular magnetic anisotropy (PMA), leading to high oscillations power upon bias current application. Two STNO connected in series show sign of anti-synchronization, whereas parallel connection leads to an increased power - Fig. 1. Research project partly supported by program Excellence initiative – research university” for the AGH University of Science and Technology

- [1] Torrejon, J. et al., *Nature* **547**, 428-431 (2017).
- [2] Sharma, R. et al., *Nature Comm.*, **12**, 1-10, (2021).
- [3] Rzeszut, P. *J. Appl. Phys.*, **125**, 223907 (2019)
- [4] Rzeszut, P. et al., *arXiv preprint* arXiv:2102.03415 (2021).
- [5] Taniguchi, T. *AIP Advances*, **9**, 035310 (2019).
- [6] Skowronski, W. et al., *Sci. Rep.* **9**, 19091 (2019).

Stochastic Computing and Machine Learning with Magnetic Domain Walls

**A. Welbourne¹, M. O. A. Ellis², M. Chambard¹, S.J. Kyle¹, M. Drouhin¹, L.T. Haigh¹,
A.M. Keogh¹, A. Mullen¹, P.W. Fry³, F. Maccherozzi⁴, T. Forest⁴, E. Vasilaki², D.A.
Allwood¹ and T.J. Hayward¹**

¹Materials Science and Engineering, ³Electronic and Electrical Engineering, ²Computer Science,
University of Sheffield, UK. ⁴Light Source, Harwell Science and Innovation Campus, UK.

Non-volatile logic and memory devices based on domain wall (DW) motion have technological promise [1,2], but stochastic behaviour, which typically has to be overcome for proper device functionality, has impeded development [3]. Here, we propose that the intrinsic stochastic behaviours of these devices can be harnessed to perform computation.

Fig. 1a shows that a notch defect in a nanowire (NW) provides a tunable stochastic element: varying the propagation field tunes the pinning probability of a DW continuously from 100%–0%. We explore the use of this element in two paradigms: Firstly, we demonstrate hardware-based “stochastic computing”. Floating-point numbers are encoded as the average value of random bit streams, and individual logic gates perform complex operations that would conventionally require many gates. The uncorrelated, random bitstreams naturally produced by the notch (i.e. presence or absence of DWs at device output) are challenging to generate in conventional CMOS devices [4]. We demonstrate DW AND gates based on this NW architecture that allow multiplication of the encoded values (Fig. 1b).

Secondly, we make use of the stochastic element as a binary stochastic synapse in a neural network (NN). Despite the success of artificial NNs, they are significantly limited by their energy cost [5]. A potential solution is the use of physical devices, such as this tunable element, that can mimic brain-like behaviour. Repeated sampling of the stochastic NN leads to performance converging towards an analogue network in recognizing handwritten digits. This is verified experimentally by repeated sampling of a single hardware synapse (Fig. 1c).

In summary, our work demonstrates how intrinsically stochastic DW pinning allows realisation of two stochastic computing paradigms using devices where random processes occur naturally, providing a potential alternative to implementation with CMOS architectures.

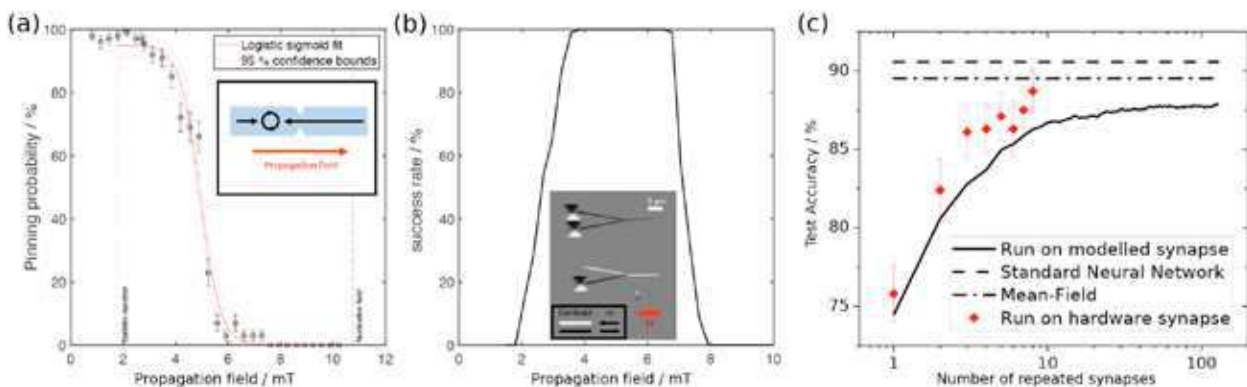


Fig. 1: (a) Notch defects in 400 nm wide (20 nm thick) permalloy nanowires provide sites with tunable pinning probability. DWs driven under increasing propagation fields pin with a probability following a logistic sigmoid-like decrease. (b) Operational range of a DW-based AND gate. Within the range ~4–7 mT, the gate behaves deterministically as an AND gate. PEEM images (inset) illustrate this functionality. (c) The test accuracy of classifying handwritten digits using an increasing number of repeats of a stochastic single-layer network.

[1] D. A. Allwood, et al., Science, Vol. 309, p.1688-1692 (2005). [2] S. S. P. Parkin, et al., Science, Vol. 320, p.190-194 (2008). [3] T. J. Hayward and K. A. Omari, J. Phys. D: Appl. Phys., Vol.50, p.084006 (2017). [4] A. Alaghi and J. P. Hayes, IEEE Trans. Comput. Des. Integr. Circuits Syst., Vol.37, p.139-46 (2013). [5] Aly et al. Proc. IEEE 107 (2019)

Posters

Alexander Welbourne

Voltage Controlled Superparamagnetic Ensembles for Low Power Reservoir Computing

140

Voltage Controlled Superparamagnetic Ensembles for Low Power Reservoir Computing

A. Welbourne¹, A. L. R. Levy³, M. O. A. Ellis², H. Chen¹, M. J. Thompson¹, E. Vasilaki², D.A. Allwood¹ and T.J. Hayward¹

Department of: ¹Materials Science and Engineering, ²Computer Science, University of Sheffield, UK.

³Department of Physics, École Polytechnique, Paris, France

Physical reservoir computing is gaining traction as a bio-inspired, machine-learning approach to solving the computational problems, such as speech recognition and prediction of chaotic time series, that are fundamental to modern technology [1]. Many magnetic systems fulfill the requirements of hardware-based reservoirs (non-linearity, memory, and a reproducible response) and single devices, subject to a temporal input sequence, can replace complex algorithms [2]. This offers potential for compact devices, with reduced energy costs.

Here, we propose voltage-controlled superparamagnetic ensembles as ultra-low-energy reservoirs. In these devices, thermal noise is utilised to drive dynamics and data input is provided by strain-mediated voltages [3]. Using an analytical model (confirmed by micromagnetics) of the response of the system [4], we simulate (Fig. 1a) the physical reservoir. By inputting a temporal sequence and training a single layer of output weights, we have performed standard machine learning benchmarks with competitive performance: spoken digit recognition (TI-46) with 95 % accuracy, and chaotic time series prediction (NARMA10) with error (NRMSE = 0.42) comparable to current reservoir approaches [1,2].

We also explore how the use of a non-standard delayed feedback (where the delay time differs from the intrinsic timescale of the input) can provide substantial error reductions in chaotic time series prediction tasks. Fig. 1b illustrates how high performance (NRMSE \approx 0.2) on the NARMA10 task can be maintained on timescales from $\tau = 1.4 \mu\text{s}$ ($KV/K_B T = 20$) to $\tau = 66 \text{ ms}$ ($KV/K_B T = 50$) by tuning the strength of the delayed feedback. Further exploration examines the effect of temperature fluctuations on the system.

We suggest that the low energy consumption expected for these voltage-controlled and thermally-driven devices makes them ideal candidates for edge computing applications, where high performance is needed at very low latency and power.

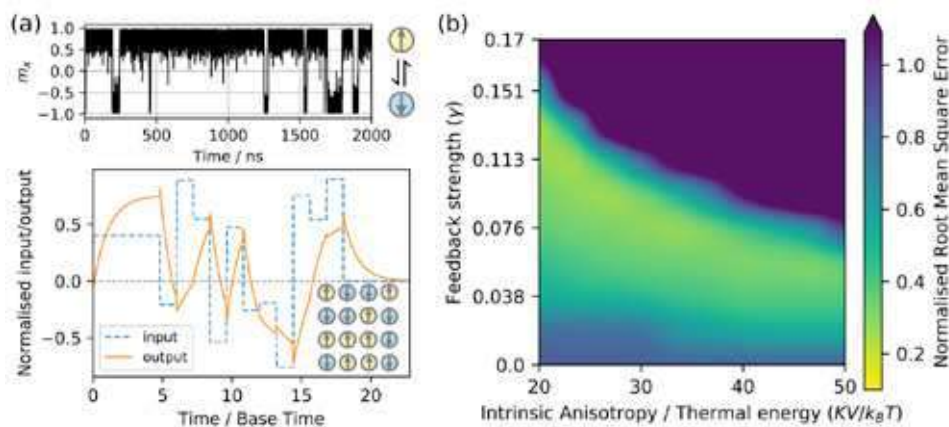


Fig. 1: (a) Superparamagnetic ensemble. Applied strain biases dwell times of individual dots in up versus down states. A reproducible non-linear response with fading memory emerges from the ensemble average of many stochastic nanodots subject to the same temporal input.

(b) Performance in chaotic time series prediction (NARMA10) as a function of uniaxial anisotropy strength (normalized by thermal energy). Performance is maintained across a range of timescales by tuning the strength of delayed feedback into the reservoir.

[1] L. Appeltant, et al., Nature Communications, Vol. 2, p.468 (2011). [2] J. Grollier, et al., Nature Electronics, Vol. 3, p.360-370 (2020). [3] A. Welbourne, et al., Applied Physics Letters, Vol. 118, p.202402 (2021). [4] O. Hovorka, et al., Applied Physics Letters, Vol.97, p.062504 (2010)

Symposium 6. Novel 2D magnetic systems and heterostructures, including bi-layer graphene ...

| | | |
|----------------------|--|-----|
| Karel Carva | <i>Magnetic Ordering in van der Waals Halides with Weak Interlayer Coupling</i> | 145 |
| Saroj Dash | <i>van der Waals Ferromagnet Fe_5GeTe_2 -Graphene Heterostructure Spin-Valve Devices at Room Temperature</i> | 146 |
| Talieh S. Ghiasi | <i>Electrical and thermal generation of spin currents by magnetic graphene</i> | 147 |
| Namrata Bansal | <i>Detection of magnetic domains in two dimensional Fe_3GeTe_2 using spin-polarized scanning tunneling microscopy</i> | 149 |
| Magdalena Birowska | <i>Scarce ferromagnetic interactions in monolayers of MPS_3</i> | 150 |
| Quentin Guillet | <i>Proximity effects between Cr_2Te_3 vdW ferromagnet and 2D materials</i> | 151 |
| Junhyeon Jo | <i>Exchange bias in molecule/Fe_3GeTe_2 van der Waals heterostructures via spinterface effects</i> | 152 |
| Łucja Kipczak | <i>Brightening of the dark excitons due to the proximity effect</i> | 153 |
| Kinga Lasek | <i>Van der Waals epitaxy of 2D ferromagnetic $\text{Cr}_{(1+\delta)}\text{Te}_2$ nanolayers</i> | 154 |
| Zuzanna Ogorzałek | <i>Magnetotransport properties of TaAs layers grown by MBE on GaAs (001) substrates</i> | 155 |
| Patrick Reiser | <i>Quantitative Magnetometry on Nanostructured MBE Grown 2D In-Plane Ferromagnet</i> | 156 |
| Gregor Zinke | <i>Spin and charge carrier dynamics at a CuPc/WSe_2 heterostructure</i> | 157 |
| Nihad AbuAwwad | <i>Magnetism in two-dimensional CrTe_2</i> | 159 |
| Pankhuri Gupta | <i>Ferromagnetic resonance study of 2D-$\text{SnS}/\text{Ni}_{80}\text{Fe}_{20}$ heterostructures</i> | 160 |
| Ralf Hemm | <i>Spin-dependent interfacial band structure and charge transfer phenomena at the $\text{C60}/\text{graphene}$ interface on Ni(111)</i> | 161 |
| Mirali Jafari | <i>DFT study of the electronic and magnetic properties of monolayer and bilayer of VS_2</i> | 162 |
| Tae Hee Kim | <i>Magnetotransport Properties of Graphene with Magnetic Defects</i> | 163 |
| Stefan Stagraczyński | <i>Magnetism in van der Waals materials</i> | 164 |

Invited Oral Presentations

| | | |
|------------------|---|-----|
| Karel Carva | <i>Magnetic Ordering in van der Waals Halides with Weak Interlayer Coupling</i> | 145 |
| Saroj Dash | <i>van der Waals Ferromagnet Fe_5GeTe_2 -Graphene Heterostructure Spin-Valve Devices at Room Temperature</i> | 146 |
| Talieh S. Ghiasi | <i>Electrical and thermal generation of spin currents by magnetic graphene</i> | 147 |

Magnetic Ordering in van der Waals Halides with Weak Interlayer Coupling

K. Carva¹, J. Šebesta², K. Pokhrel¹, A. Marmodoro³, and J. Pospíšil¹

¹Charles University Prague, DCMP, Ke Karlovu 5, 121 16 Prague, Czech Republic

²Uppsala University, Department of Physics and Astronomy, 75120 Uppsala, Sweden

³Institute of Physics ASCR, Na Slovance 2, CZ-18221 Prague, Czech Republic

Systems with magnetically ordered two-dimensional (2D) layers bound by van der Waals (vdW) interaction are getting increasingly interesting for high-tech magneto-electric and magneto-optic applications in nanostructures. Due to their intrinsic magnetocrystalline anisotropy, several vdW magnets could be thinned down to nanoscale thickness, while still maintaining magnetic order. A prominent example of such materials are transition metal trihalides, in particular CrI₃, a first atomically thin ferromagnet [1].

In van der Waals magnetic materials the exchange coupling between layers is rather weak and can be relatively easily modified. Regime of weak interlayer coupling represents transition between the more explored cases of isotropic bulk-like exchange and the ideal 2D limit (monolayer). Here we examine general features of finite temperature magnetic order in this regime by atomistic spin dynamics methods. The method is applied to several particularly interesting systems from this class, in particular trihalides VI₃ and VBr₃. These are ferromagnets and antiferromagnets, respectively. VI₃ exhibits a rather unusual magnetic anisotropy [2]. The anisotropy was reproduced by first-principles calculations only if lattice distortions present at its low temperature phases were taken into account [3]. The calculations also revealed an exceptionally large orbital momentum on V atoms, showing that the effect of spin-orbit interaction is more important than the crystal field in this case.

Employing calculated exchange interactions we study how is the Curie temperature affected by interlayer coupling in these systems and how much this solution differs from the mean-field model results. We also predict a possibility of magnetic order with parallel aligned spins inside layers that are magnetically decoupled from each other. This phase may occur at some temperatures above T_C in case that magnetic anisotropy and specific exchange interactions fall within a certain range of values.

[1] B. Huang, et al., *Nature* **546**, 270 (2017).

[2] A. Koriki et al., *Phys. Rev. B* **103**, 174401 (2021).

[3] L. M. Sandratskii, K. Carva, *Phys. Rev. B* **103**, 214451 (2021).

van der Waals Ferromagnet Fe₅GeTe₂-Graphene Heterostructure Spin-Valve Devices at Room Temperature

Saroj Dash¹

¹ Department of Microtechnology and Nanoscience, Chalmers University of Technology, SE-41296, Göteborg, Sweden

The discovery of van der Waals (vdW) magnets opened a new paradigm for condensed matter physics and spintronic technologies. However, the operations of active spintronic devices with vdW ferromagnets (vFM) are limited to cryogenic temperatures, inhibiting its broader practical applications. Here, we demonstrate robust room-temperature operation of spin-valve devices using vdW itinerant ferromagnet Fe₅GeTe₂ (FGT) in heterostructures with graphene [1]. The magnetic properties of the Fe₅GeTe₂ is found to be enhanced at the interface with graphene with a large and negative spin polarization at room temperature, which are different from their bulk properties. Lateral spin-valve and spin precession measurements provide unique insights by probing interface spintronic properties via spin dynamics in Fe₅GeTe₂/graphene heterostructure devices, revealing a perpendicular magnetic anisotropy of Fe₅GeTe₂ (see Fig 1). These findings open opportunities for tuning magnetic properties by vdW interface design and applications of vdW magnet-based spintronic devices at ambient temperatures.

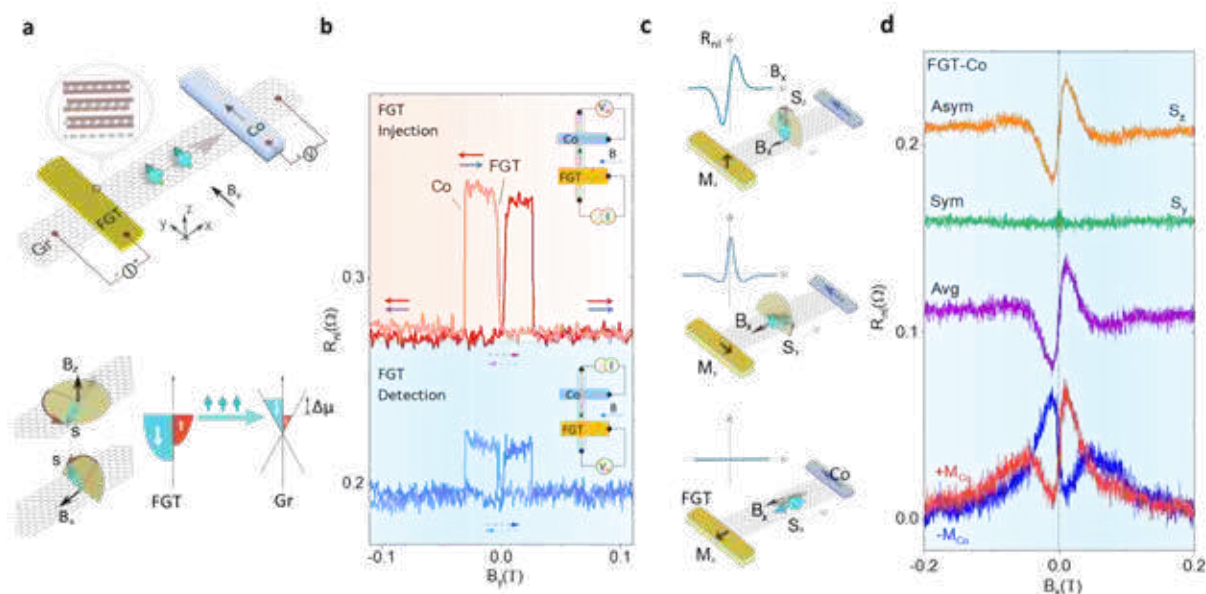


Figure 1. **a.** Schematics of spin-valve device with van der Waals ferromagnet Fe₅GeTe₂ (FGT) and graphene heterostructure. **b.** The measured nonlocal (NL) spin-valve signal $R_{nl}=V_{nl}/I$ for parallel and antiparallel alignment of FGT and Co magnetic moments. **c.** Schematics of xHanle measurement geometry and expected lineshape of the spin precession signal for all the possible FGT magnetization scenarios (M_x , M_y , and M_z). **d.** Raw xHanle signals were measured in the FGT-Co spin valve with different magnetic configurations $\pm M_{Co}$ of detector Co electrode. The averaged (Avg) Hanle signal and extracted symmetric (Sym) and anti-symmetric (Asym) components are presented. The strong Asym component indicate out-of-plane component of spin polarization in FGT in remanence.

[1] Van der Waals Magnet based Spin-Valve Devices at Room Temperature

B Zhao, R Ngalyo, AM Hoque, B Karpiak, D Khokhriakov, **SP Dash**; arXiv:2107.00310 (2022).

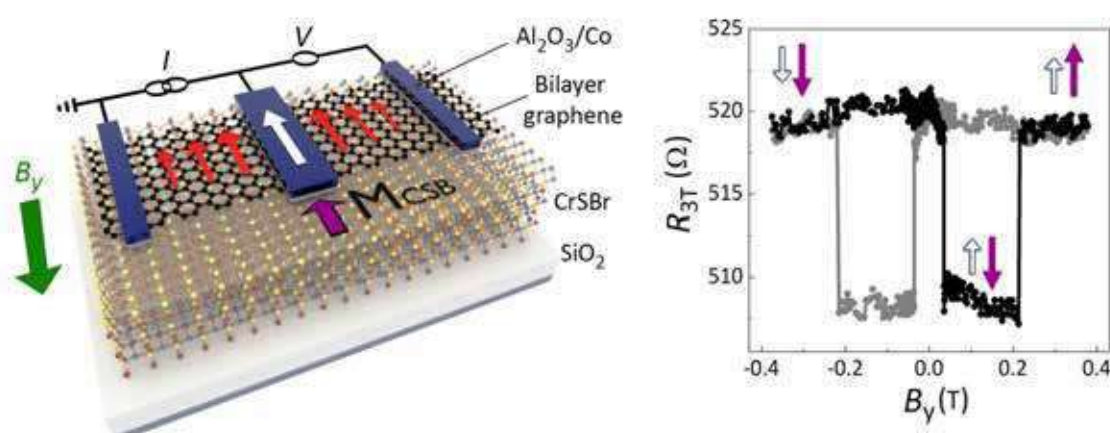
Electrical and thermal generation of spin currents by magnetic graphene

Talieh S. Ghiasi^{1,2}

¹ Zernike Institute for Advanced Materials, University of Groningen, The Netherlands

² Kavli Institute of Nanoscience, Delft University of Technology, The Netherlands

Van der Waals heterostructures provide a platform for designing new materials with superior properties that allow for the emergence of unprecedented functionalities in two-dimensional (2D) spintronic devices. This has been experimentally shown in graphene-based spintronic devices, where the spin and charge transport properties of graphene are enriched by the proximity of the other 2D materials [1]. Here we show that, by the proximity of a 2D antiferromagnet (CrSBr), we can induce spin-orbit and magnetic exchange interactions in graphene, resulting in a strong coupling between charge and spin currents. This is directly measured as a large spin polarization of the conductivity of graphene (about 14%) which also leads to the observation of spin-dependent Seebeck and anomalous Hall effects. These results address the most technologically relevant aspects of the induced magnetism in graphene. They show the active role of the magnetized graphene in the electrical and thermal generation of spin currents, allowing for ultra-compact 2D spintronic and spin caloritronic devices [2,3].



Schematic picture of the studied device with a bilayer graphene/CrSBr van der Waals heterostructure. The resistance measured in the three-terminal geometry ($R_{3T}=V/I$) with Al₂O₃/Co electrodes versus the external magnetic field (B_y) shows a considerable change, depending on the relative orientation of the Co magnetization (white arrow) and that of CrSBr (M_{CSB} , purple arrow). The induced magnetization in graphene by M_{CSB} , allows for higher conductivity of the spin up electrons (red arrows) in the graphene channel.

- [1] JF Sierra, et al. *Nature Nanotechnology* 16, 856–868 (2021).
- [2] TS Ghiasi, et al. *Nature Nanotechnology* 16, 788–794 (2021).
- [3] AA Kaverzin, TS Ghiasi, et al., preprint arXiv:2202.09972 (2022).

Oral Presentations

| | | |
|--------------------|--|-----|
| Namrata Bansal | <i>Detection of magnetic domains in two dimensional Fe_3GeTe_2 using spin-polarized scanning tunneling microscopy</i> | 149 |
| Magdalena Birowska | <i>Scarce ferromagnetic interactions in monolayers of MPS_3</i> | 150 |
| Quentin Guillet | <i>Proximity effects between Cr_2Te_3 vdW ferromagnet and 2D materials</i> | 151 |
| Junhyeon Jo | <i>Exchange bias in molecule/Fe_3GeTe_2 van der Waals heterostructures via spinterface effects</i> | 152 |
| Łucja Kipczak | <i>Brightening of the dark excitons due to the proximity effect</i> | 153 |
| Kinga Lasek | <i>Van der Waals epitaxy of 2D ferromagnetic $\text{Cr}_{(1+\delta)}\text{Te}_2$ nanolayers</i> | 154 |
| Zuzanna Ogorzałek | <i>Magnetotransport properties of TaAs layers grown by MBE on GaAs (001) substrates</i> | 155 |
| Patrick Reiser | <i>Quantitative Magnetometry on Nanostructured MBE Grown 2D In-Plane Ferromagnet</i> | 156 |
| Gregor Zinke | <i>Spin and charge carrier dynamics at a CuPc/WSe_2 heterostructure</i> | 157 |

Detection of magnetic domains in two dimensional Fe₃GeTe₂ using spin-polarized scanning tunneling microscopy

Namrata Bansal^{1*}, Hung-Hsiang Yang¹, Philipp Rueßmann², Markus Hoffmann², Lichuan Zhang², Dongwook Go², Amir-Abbas Haghighirad³, Kaushik Sen³, Matthieu Le Tacon³, Yuriy Mokrousov², and Wulf Wulfhekel^{1,3}

¹*Physikalisches Institut (PHI), Karlsruhe Institute of Technology, 76131 Karlsruhe, Germany

²Peter Gruenberg Institut (PGI-1) and Institute for Advanced Simulation (IAS-1) Forschungszentrum Juelich GmbH, D-52425 Juelich, Germany

³Institute for Quantum Materials and Technologies, Karlsruhe Institute of Technology, 76131 Karlsruhe, Germany

*Email: bansal.namrata08@gmail.com

Two-dimensional (2D) magnets play an essential part in the field of spintronics. In this work, we investigate the magnetic structure of the 2D van der Waals material Fe₃GeTe₂ (FGT) [1, 2] using low temperature (0.7 K) spin-polarized scanning tunneling microscopy (SP-STM). Using chromium-coated tungsten tips [3], we execute the out-of-plane magnetic imaging on FGT. We recorded differential tunneling conductance (dI/dU) maps to investigate the magnetic contrasts as a function of the magnetic field (B_z). We observed a shape transition of magnetic domain bubbles from elliptical to circular shape and finally collapsing of the topologically protected bubble at an out-of-plane magnetic field of 0.32 T [Fig. 1(a)]. An inverse relation between the size of the magnetic bubbles and magnetic field was observed [Fig. 1 (b)]. We resolve the domain wall profile and width as a function of magnetic field and determined the corresponding domain wall width using the spatial resolution of the SP-STM, which is in good agreement with micromagnetic calculations based on the exchange stiffness and the anisotropy constant of FGT. Moreover, we observe a weak magneto-electric coupling in voltage-dependent measurements of the wall thickness.

References

- [1] Y. Deng, *et al.*, Nature 563, 94 (2018).
- [2] H. J. Deiseroth, *et al.*, European Journal of Inorganic Chemistry, 1561 (2006).
- [3] A. Wachowiak, *et al.*, Science (New York, N.Y.) 298, 577 (2002).

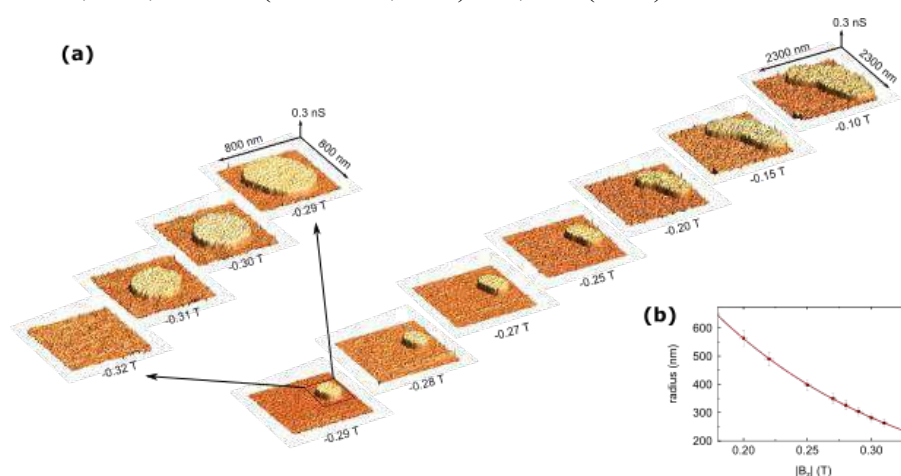


Fig 1. (a) Pseudo three-dimensional representation of the differential tunnelling conductance dI/dU maps under various of magnetic fields (B_z). (b) Graph represents the radius of the skyrmionic bubble as a function of magnetic fields. Measuring conditions: Bias voltage (U) = -500 mV, Tunneling current (I) = 50 pA, and Bias modulation (U^{rms}) = 80 mV.

Scarce ferromagnetic interactions in monolayers of MPS₃

**C. Autieri^{1,2}, G. Cuono¹, C. Noce^{2,3}, M. Rybak⁴, K. M. Kotur⁵, C. E. Agrapidis⁵,
K. Wohlfeld⁵, M. Birowska⁵**

¹ *International Research Centre Magtop, Institute of Physics, Polish Academy of Sciences, Aleja Lotników 32/46, PL-02668 Warsaw, Poland*

² *Consiglio Nazionale delle Ricerche CNR-SPIN, UOS Salerno, I-84084 Fisciano (SA), Italy*

³ *Dipartimento di Fisica, Università degli Studi di Salerno, I-84084 Fisciano (SA), Italy*

⁴ *Faculty of Fundamental Problems of Technology, Wrocław University of Science and Technology, Wybrzeże Wyspiańskiego 27, PL-50370 Wrocław, Poland*

⁵ *Faculty of Physics, University of Warsaw, Pasteura 5, PL-02093 Warsaw, Poland*

The family of 2D materials has grown considerable, with new additions exhibiting intrinsic magnetism, such as the family of transition metal phosphorus trisulfides (MPS₃) [1]. The MnPS₃ and NiPS₃ materials are the representatives of this family of compounds. Recent theoretical predictions point to the existence of a large binding energy of excitons in MnPS₃ [2], whereas the experimental reports have observed excitons in few layers of NiPS₃ strongly related to magnetic order [3]. Thus, these systems can be considered as a platform to study magnetism, optics and correlation effects in one single stable material. There is no precedence of such a platform in the realm of conventional materials.

Our findings are based on DFT+U and model Hamiltonian calculations and provide a successful quantitative explanation of the origin of the magnetic (exchange) couplings strengths for MnPS₃ and NiPS₃ [4]. We discuss in detail the competition between the direct exchange and the superexchange mechanisms in these systems. We demonstrate that all antiferromagnetic exchange couplings can successfully be explained using an effective direct exchange model. We point out the processes that lead to the moderate ferromagnetic exchange couplings in NiPS₃, are quite specific and can only be explained within a more complex superexchange model.

In addition, in the case of the doped systems, we performed extensive and systematic DFT+U calculations which reveal that magnetic impurities do not affect the magnetic order observed in the pure phases. Thus, in general, in these systems ferromagnetism may not be easily induced by elemental doping. Nevertheless, for particular concentrations and types of magnetic dopants, a non-zero net magnetization can appear, leading to the ferrimagnetic phase transition, while preserving the semiconducting nature of these compounds. Interestingly, by considering the exchange couplings of ordered alloys, our study confirms the experimental observation of lowering the magnetic ordering temperature of these doped systems which we attribute to impurity-induced frustration of magnetic interactions.

[1] B. L. Chittari, Y. Park, D. Lee, M. Han, A. H. MacDonald, E. Hwang, J. Jung, *Phys. Rev. B* **94**, 184428 (2016).

[2] M. Birowska, P.E.F. Junior, J. Fabian, J. Kuntsmann, *Phys. Rev. B* **103**, L121108 (2021).

[3] S. Y. Kim, T. Y. Kim, L. J. Sandilands, S. Sinn, M.-C. Lee, J. Son, S. Lee, K.-Y. Choi, W. Kim, B.-G. Park, C. Jeon, H.-D. Kim, C.-H. Park, J.-G. Park, S. J. Moon, and T. W. Noh, *Phys. Rev. Lett.* **120**, 136402 (2018).

[4] C. Autieri, G. Cuono, C. Noce, M. Rybak, K. Kotur, C. E. Agrapidis, K. Wohlfeld, M. Birowska, <https://arxiv.org/abs/2111.15004>.

Proximity effects between Cr₂Te₃ vdW ferromagnet and 2D materials

Quentin Guillet¹, Hervé Boukari², Libor Vojacek¹, Céline Vergnaud¹, Alain Marty¹,
Frédéric Bonell¹, Mair Chshiev¹ and Matthieu Jamet¹

¹ Univ. Grenoble Alpes, CEA, CNRS, IRIG-SPINTEC 38000 Grenoble, France

² Univ. Grenoble Alpes, CNRS, Institut Neel, 38000 Grenoble, France

Achieving the large-scale growth of 2D ferromagnetic materials with high Curie temperature and perpendicular magnetic anisotropy is highly desirable for the development of future ultra-compact magnetic sensors or magnetic memories. In this context, van der Waals (vdW) Cr₂Te₃ appears as a promising candidate. It exhibits strong perpendicular magnetic anisotropy and a Curie temperature in bulk of 180 K. In this work, we will demonstrate that few layers of Cr₂Te₃ can exhibit strong variation in terms of magnetic anisotropy and Curie temperature as a function of strain (in-plane as well as out-of-plane) [1] and due to proximity effects with 2D materials.

Successful epitaxial growth of vdW Cr₂Te₃ layers was achieved by molecular beam epitaxy (MBE) on various substrates such as monolayer (ML) graphene/SiC(001), monolayer WSe₂/GaAs(111) and few layers of Bi₂Te₃/Al₂O₃. We obtained single crystalline growth on a

centimeter scale surface, verified by reflection high-energy electron diffraction and x-ray diffraction and well-defined magnetic properties (Figure 1).

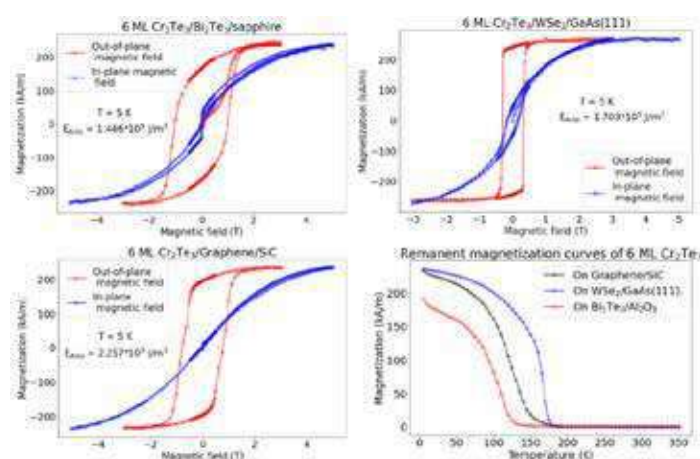


Figure 1: Magnetic properties of Cr₂Te₃ measured by SQUID magnetometry at 5K on graphene/SiC, WSe₂/GaAs and on Bi₂Te₃/Al₂O₃. Remanent magnetization obtained by heating the samples without any applied magnetic field starting from a saturated state.

We observed - by SQUID magnetometry - perpendicular magnetic anisotropy and long range ferromagnetic order for all vdW heterostructures. We also found strong variation in terms of coercivity, magnetic anisotropy and Curie temperature of the various layers (Figure 1), that we attribute to both structural variation and proximity effects with the different substrates. Complementary *ab initio* calculations are performed to support the experimental observations. We obtained a strong correlation between magnetic anisotropy and the out-of-plane lattice parameter of the Cr₂Te₃.

Finally, magnetotransport measurements in Cr₂Te₃ epitaxially grown on the three 2D materials as well as in reference samples grown on sapphire will be discussed with the demonstration of proximity effects like topological Hall effect [2] and spin-orbit torques.

Support by ANR projects MAGICVALLEY (ANR-18-CE24-0007) and ELMAX (ANR-20-CE24-0015) is gratefully acknowledged.

[1] Y. Wen et al. Nano Lett, 20, 3130–3139 (2020)

[2] J. Chen et al. Nano Lett, 19, 6144–6151. (2019)

Exchange bias in molecule/ Fe_3GeTe_2 van der Waals heterostructures via spinterface effects

Junhyeon Jo¹, Francesco Calavalle¹, Beatriz Martín-García¹, Fèlix Casanova^{1,2},
Andrey Chuvilin^{1,2}, Luis E. Hueso^{1,2}, and Marco Gobbi^{1,2,3}

¹ CIC nanoGUNE, 20018 Donostia-San Sebastian, Basque Country, Spain

² IKERBASQUE, Basque Foundation for Science, 48013 Bilbao, Basque Country, Spain

³ Centro de Física de Materiales (CFM-MPC) Centro Mixto CSIC-UPV/EHU, San Sebastián/Donostia 20018, Spain

Exfoliated two-dimensional layered magnetic materials generate atomically thin films having an ultrahigh surface sensitivity, which makes their magnetic properties tunable via external stimuli, such as electrostatic gating and proximity effects. Another powerful approach to engineer magnetic materials is molecular functionalization, which generates a hybrid interface with tailored magnetic interaction, called spinterface [1,2].

Here, we demonstrate the emergence of a spinterface effect at the interface between flakes of the prototypical layered magnetic Fe_3GeTe_2 and Co-phthalocyanine films. Magnetotransport measurements show that the molecular layer induces a magnetic exchange bias in Fe_3GeTe_2 , indicating that the unpaired spins in Co-phthalocyanine layers develop antiferromagnetic ordering and pin the magnetization switching of Fe_3GeTe_2 via magnetic proximity. The effect is strongest for a Fe_3GeTe_2 thickness of 20 nm, for which the exchange bias field reaches -840 Oe at 10 K and is measurable up to approximately 110 K. This value compares very favorably with the previous exchange bias fields reported for Fe_3GeTe_2 in all-inorganic van der Waals heterostructures, demonstrating the potential of molecular functionalization to tailor the magnetic property of van der Waals layered materials.

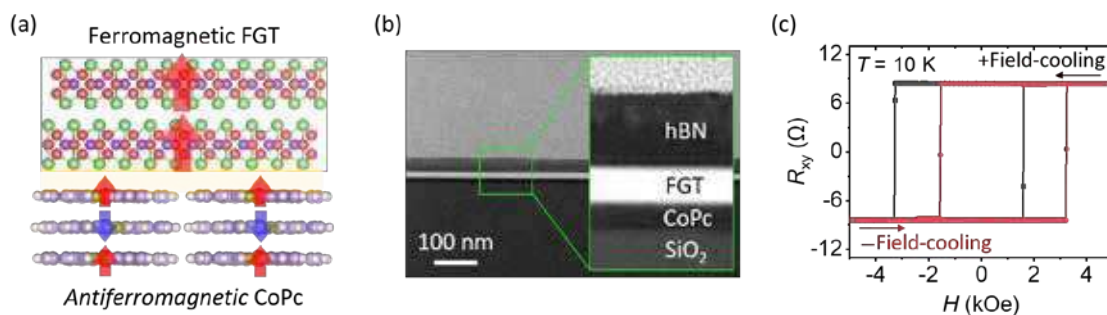


Figure 1: Exchange bias in a Co-phthalocyanine/ Fe_3GeTe_2 (CoPc/FGT) heterostructure. (a) Schematic illustration and (b) cross-sectional scanning transmission electron microscopy images of a hybrid van der Waals heterostructure of CoPc/FGT. (c) Demonstration of exchange bias in the CoPc/FGT via magnetotransport measurement after positive and negative magnetic-field-cooling.

[1] S. Sanvito et al., *Nat. Phys.* **6**, 562 (2010).

[2] M. Cinchetti et al. *Nat. Mater.* **16**, 507 (2017).

Brightening of the dark excitons due to the proximity effect

L. Kipczak¹, J. Szpakowski¹, Z. Chen², K. Vaklinova², T. Taniguchi³,
K. Watanabe³, A. Babiński¹, M. Koperski², M. R. Molas¹

¹University of Warsaw, Warsaw, Poland

²National University of Singapore, Singapore, Singapore

³National Institute for Materials Science, Tsukuba, Japan

Monolayers (MLs) of WSe₂ are darkish materials with ground dark (optically inactive) exciton state. The neutral dark excitons exhibit a double (fine) structure comprising so-called grey (X^G) and dark (X^D) complexes, characterized by the out-of-plane and zero excitonic dipole momenta, respectively. The X^D emission can be observed only due to the applied in-plane and out-of-plane applied magnetic field [1]. Magnetic layered materials with intrinsic magnetic order [2] are perfect candidates to be used to brighten the dark exciton due to the proximity effect.

We employ the polarization-resolved photoluminescence (PL) at low temperature ($T=5$ K) to investigate the proximity effect in heterostructures comprising the WSe₂ ML, capped with the CrCl₃ layer and encapsulated in hexagonal BN.

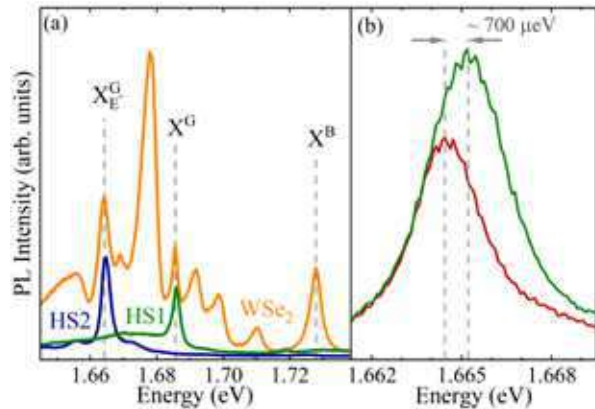


Figure 1: (a) PL spectra of ML of WSe₂ and of CrCl₃-WSe₂ HSs. (b) The X_E^G line seen on HS2 sample recorded for two orthogonal linear polarizations.

The reference spectrum of the WSe₂ ML is shown in Fig. 1 (a). The spectrum is analogous to those previously reported and comprises in particular emission lines related to the bright neutral exciton (X^B), bright grey exciton (X^G), and its phonon replica (X_E^G). The PL spectra, measured at the edges of two WSe₂-CrCl₃ heterostructures (HSs), labelled HS1 (20 nm thick CrCl₃ layer) and HS2 (10 nm thick CrCl₃ layer) are also shown in the Figure (no appreciable emission was observed from the centre of HSs). The PL spectra of the HS1 and HS2 structures are dominated by single narrow lines, with energies close to the X^G and X_E^G , respectively. Moreover, it has been found that the X_E^G line comprises two components linearly polarized along two perpendicular directions with the energy separation of about 700 μ eV (see Fig.1 (b)). The splitting is similar to the splitting of the grey-dark fine structure in WSe₂ ML (~ 660 μ eV) [1].

We conclude that emission lines in the HSs are related to the grey/dark excitons brightened by the in-plane magnetic field due to the non-zero net in-plane magnetization of the CrCl₃ layer. We extend our studies using external in-plane and out-of-plane magnetic fields in order to further investigate the proximity effect of the CrCl₃ in-plane magnetization.

[1] M. R. Molas, et al., *Phys. Rev. Lett.* **123**, 096803 (2019).

[2] M. Gilbertini, M. Koperski, et al. *Nat. Nanotechnol.* **14**, 408-419 (2019).

Van der Waals epitaxy of 2D ferromagnetic $\text{Cr}_{(1+\delta)}\text{Te}_2$ nanolayers

Kinga Lasek,¹ Paula M. Coelho,¹ Pierluigi Gargiani,² Manuel Valvidares,² Katayoon Mohseni,³ Holger L. Meyerheim,³ Ilya Kostanovskiy,³ Krzysztof Zborecki,⁴ Matthias Batzill¹

¹ Department of Physics, University of South Florida, Tampa, FL 33620, USA

² ALBA Synchrotron Light Source, E-08290 Cerdanyola del Vallès, Barcelona, Spain

³ Max-Planck-Institut f. Mikrostrukturphysik, Weinberg 2, D-06120 Halle, Germany

⁴ Faculty of Physics, Warsaw University of Technology, ul. Koszykowa 75, Warsaw, 00-662 Poland

$\text{Cr}_{(1+\delta)}\text{Te}_2$, with $0 < \delta < 1$, are described as transition metal dichalcogenides (TMDs) with additional (δ) self-intercalated Cr atoms in between the TMD layers. These (self) intercalation compounds exist in different compositional phases that vary by the amount of Cr intercalated between CrTe_2 layers.^[1] The variation of the amount of intercalated Cr is represented by δ , which indicates the fraction of intercalated Cr compared to the amount of Cr in a CrTe_2 -TMD layer. The model of these structures is schematically illustrated in Fig. 1(a).

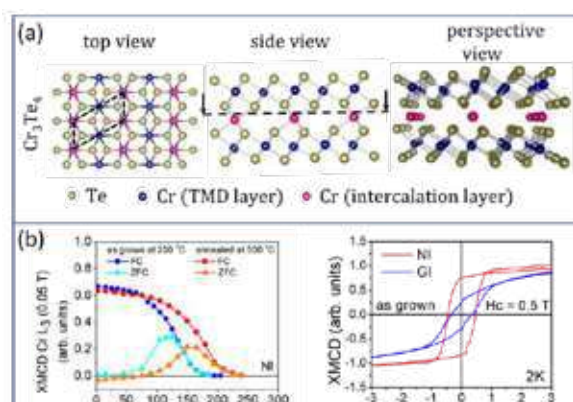


Figure 1. Structure models and magnetic properties of $\text{Cr}_{(1+\delta)}\text{Te}_2$ films with $\delta = \frac{1}{2}$ stoichiometry.

This class of materials exhibits well-known ferromagnetic ordering.^[2,3] The recent search for ferromagnetic 2D materials and the similarities of these self-intercalation compounds with 2D-TMDs revived the interest in chromium tellurides as potential materials for van der Waals (vdW) heterostructures. We will show that self-intercalated $\text{Cr}_{(1+\delta)}\text{Te}_2$ can be grown by van der Waals epitaxy with TMD-like terminations on MoS_2 (0001). Specifically, we will present the detailed compositional and structural characterization, by scanning tunneling microscopy (STM), and high-resolution Rutherford backscattering

(HR-RBS). We will show that the amount of self-intercalated Cr can be controlled by post-growth annealing. Such modified films are characterized by an increased T_c , a coercive field being reduced from 0.5 T to 0.3 T, and an isotropization of the magnetic anisotropy confirmed by XMCD measurements presented in Fig. 1(b).

Finally, we will demonstrate that ultrathin vdW films can be prepared with the ultimate limit of a single self-intercalated layer by vdW epitaxy. These vdW materials maintain their ferromagnetic properties with desirable out-of-plane anisotropy and thus are potential ferromagnetic (pseudo) 2D materials that can be combined in vdW heterostructures by a bottom-up growth process.

- [1] Chattopadhyay, G. The Cr-Te (Chromium-Tellurium) System. *J. Phase Equil.* **19**, 431 (1994).
- [2] Fujisawa, Y.; Pardo-Almanza, M.; Garland, J.; Yamagami, K.; Zhu, X.; Chen, X.; Araki, K.; Takeda, T.; Kobayashi, M.; Takeda, Y., *Phys. Rev. Materials* **4**, 114001 (2020).
- [3] Burn, D. M., Duffy, L. B., Fujita, R., Zhang, S.L., Figueroa, A.I., Herrero-Martin, J., van der Laan, G., Hesjedal, T., *Sci Rep.* **9**, 10793 (2019).

Magnetotransport properties of TaAs layers grown by MBE

Z. Ogorzalek¹, R. Bożek¹, M. Baj¹, D. Wasik¹, J. Z. Domagala², W. Zajkowska², S. Kret², B. Seredyński¹, W. Pacuski¹, J. Sadowski^{1,2,3} and M. Gryglas-Borysiewicz¹

¹ Faculty of Physics, University of Warsaw, ul. Pasteura 5, 02-093 Warsaw, Poland

² Institute of Physics PAS, al. Lotników 32/46, 02-668 Warsaw, Poland

³ Department of Physics and Electrical Engineering, Linnaeus University, 391 82 Kalmar, Sweden

Weyl materials are at the forefront of condensed matter physics research due to their topological properties. The presence of Weyl nodes leads to the existence of unusual Fermi arc surface states [1,2]. Tantalum arsenide is the first experimentally identified Weyl material. Its growth is however a challenge, due to its decomposition prior to reaching its melting point [1,3]. Here, the molecular beam epitaxy (MBE) comes into play [1,4] as it enables a non-equilibrium growth, and also gives the perspective for creating heterostructures.

In this paper we present magnetotransport studies of thin TaAs films. The samples were grown by MBE on semi-insulating GaAs (001) substrates. Structural characterisation (XRD, AFM, TEM) revealed that samples are composed of nanocolumn crystalites, aligned along [110] directions. They are 10-20 nm wide and 100-200 nm in length, depending on the details of the sample growth process. For transport studies, the hall bar geometry was used, and two sets of macroscopic (current path 600 μm in length and 200 μm in width) specimens, along and across the nanocolumns were prepared. Resistivity tensor measurements were performed in magnetic fields up to 12 T and in the temperature range 1.4 - 300 K. The samples showed an anisotropy of resistivity, with 5 times lower resistivity with the current path along the nanocolumns. Hall effect measurements reveal that the hole concentrations are equal for both sample configurations, thus the difference in resistivity may be ascribed to the difference in mobilities. For the samples with lower resistivities a decrease of resistivity was observed at low temperatures, in contrast to an increase for the samples with the current path perpendicular to nanocolumns. Negative magnetoconductance is observed up to 50 K. Weak antilocalization Hikami-Larkin-Nagaoka model is applied to the data giving reasonable phase coherence lengths of a few tens of nm and relatively large values of conductivity amplitudes α staying in the range 1.5 - 13. A discussion will be provided on the possible topological origin of the observed negative magnetoconductance.

This work has been supported by the National Science Centre (Poland), through the project No. 2017/27/B/ST5/02284.

- [1] Weng, H., Fang, C., Fang, Z., Bernevig, B. A., Dai, X. Phys. Rev. X, 5, 011029, (2015)
- [2] Huang, X., Zhao, L., Long, Y., Wang, P., Chen, D., Yang, Z., Liang, H., Xue, M., Weng, H., Fang, Z., Dai, X., Chen, G. Phys. Rev. X, 5, 031023, (2015)
- [3] Huang, S. M., Xu, S. Y., Belopolski, I., Lee, C. C., Chang, G., Wang, B., Alidoust, N., Bian, G., Neupane, M., Zhang, C., Jia, S., Bansil, A., Lin, H. Hasan, M. Z. Nat. Commun, 6, 7373, (2015)
- [4] Yanez W., Ou Y., Xiao R., Ghosh S., Dwivedi J., Steinebronn, E., Richardella A., Mkhoyan K. A., Samarth N., arXiv:2202.10656

Quantitative Magnetometry on Nanostructured MBE Grown 2D In-Plane Ferromagnet

P. Reiser¹, M. Tschudin¹, D. A. Broadway¹, and P. Maletinsky¹

¹University of Basel, Klingelbergstrasse 82, 4055 Basel, Switzerland

The discovery of ferromagnetic 2D van der Waals (vdW) crystals allows the study of novel magnetic phenomena at a reduced dimensionality and opens new possibilities for spintronic device concepts [1,2]. Though different physical phenomena can be well studied in exfoliated 2D vdW crystals, these material systems only offer limited control of their exact geometry. Contrary, 2D magnets grown by molecular beam epitaxy (MBE) allow to overcome this limitation [3,4]. Here, we investigate MBE grown EuGe₂ on a micron-sized structured substrate to reveal the influence of the geometry on its magnetic state.

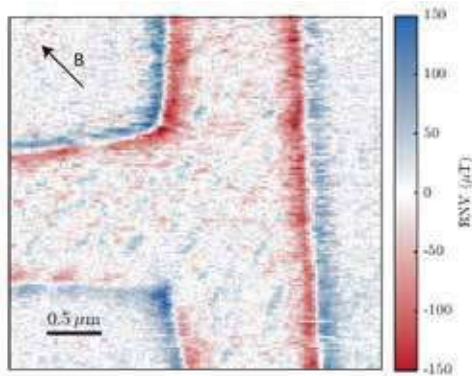


Figure 1: Stray magnetic field map of bilayer EuGe₂ grown on a T-shape structure measured at a bias field of 2000 G applied along the direction indicated by the arrow.

EuGe₂ belongs to the lanthanide metalloxenes and exhibits an in-plane ferromagnetic intralayer coupling. While the interlayer coupling in bulk is antiferromagnetic, a net magnetic moment remains in the few layer limit [3]. We use the single spin of a nitrogen-vacancy in diamond embedded into an all-diamond atomic force microscope tip to directly measure the stray field of these structures quantitatively with a spatial resolution of around 50 nm. We are able to directly compare the net magnetic moment of mono- and bilayer EuGe₂ at various temperatures and bias magnetic fields. Moreover, we observe how the net magnetic moment of the micron-sized structures evolves from a nano-sized magnetic substructure as a function of applied magnetic field and how this substructure is influenced by

the micron-sized geometry (Fig. 1).

We offer new insights into the transition from bulk properties to the 2D limit in this class of material. Additionally, we provide the basis for targeted engineering of geometries to nucleate novel spin-textures and domain structures at a reduced dimensionality.

- [1] B. Huang *et al.*, *Nature* **546**, 7657 (2017).
- [2] C. Gong *et al.*, *Nature* **546**, 7657 (2017).
- [3] A. Tokmachev *et al.*, *Mater. Horiz.* **6**, 7 (2019).
- [4] A. Bedoya-Pinto *et al.*, *Science* **374**, 6567 (2022).

Spin and charge carrier dynamics at a CuPc/WSe₂ heterostructure

Sebastian Hedwig¹, Gregor Zinke¹, Benito Arnoldi¹, Martin Aeschlimann¹ and Benjamin Stadtmüller^{1,2}

¹Department of Physics and Research Center OPTIMAS, TU Kaiserslautern, Erwin-Schroedinger-Str. 46, 67663 Kaiserslautern, Germany

²Institute of Physics, Johannes Gutenberg University Mainz, Staudingerweg 7, 55128 Mainz, Germany

2D-Van-der-Waals systems are a highly intriguing class of low dimensional materials with promising spin functionalities for future nanoscale spintronic applications. Tuning the electronic properties of such materials is still a great challenge and is often achieved by forming heterostructures with other 2D systems.

Here, we present our approach to control the spin and charge carrier dynamics of the Van-der-Waals material WSe₂ by the formation of a 2D heterostructure with the aromatic molecule CuPc. Using a NIR-pump (1.57 eV) XUV-probe (22.0 eV) setup based on high harmonic generation, we conduct time-, angle- and spin-resolved photoemission experiments

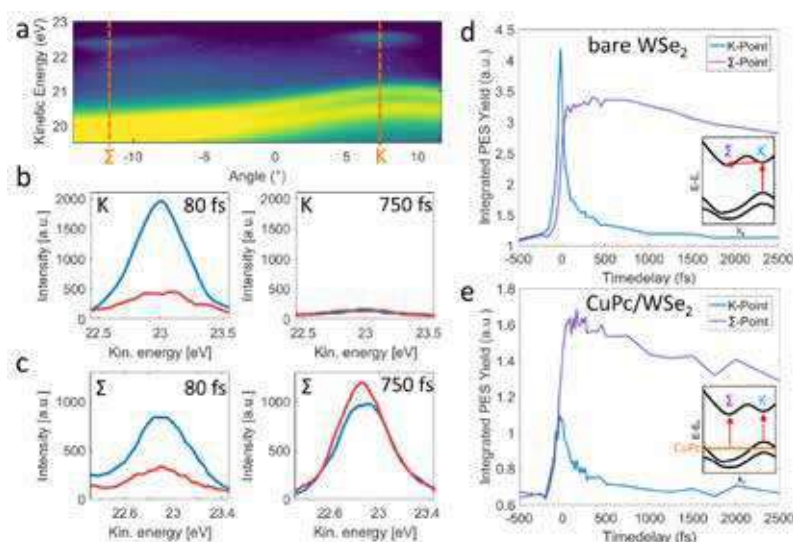


Figure 1: (a) Bandstructure of WSe₂ as obtained in a timeresolved ARPES measurement. The orange lines mark the K- and Σ-point. (b,c) Spinresolved photoemission spectra of the transient population in the conductionband of WSe₂ at the K- (b) and Σ-point (c) 80 fs and 750 fs after an optical excitation. Lines of blue (red) color refer to spin up (down). (d,e) Dynamics of the excitation at the K- and Σ-point for bare WSe₂ (d) and CuPc/WSe₂ (e). The insets show a sketch of the proposed excitation geometry.

actively modified by the adsorption of CuPc. In particular, the dominant optical excitation at the K-point of WSe₂ is replaced by a direct interlayer excitation from the CuPc into the WSe₂ layer (Fig. 1 d and e). We will show that the strength of the interlayer excitation can be tuned and controlled by the polarization of the exciting light field.

to investigate the optically excited carrier dynamics at the K- and Σ-points of WSe₂. We find a characteristic spin-polarization of the excited carriers at the K-point that depends on the pump light polarization as recently suggested by Bertoni et al. [1]. The subsequent intraband scattering from the K- to the Σ-point of the bare WSe₂ conduction band (Fig. 1 b and c) coincides with a change of the carriers spin polarisation. This change is discussed in the light of interband and spin flip scattering.

Most importantly, the optical excitation and the subsequent relaxation process of the hot carriers can be

[1] Bertoni *et al.*; *Phys. Rev. Lett.* **117**, 277201 (2016)

Posters

| | | |
|----------------------|---|-----|
| Nihad AbuAwwad | <i>Magnetism in two-dimensional CrTe₂</i> | 159 |
| Pankhuri Gupta | <i>Ferromagnetic resonance study of 2D-SnS/Ni₈₀Fe₂₀ heterostructures</i> | 160 |
| Ralf Hemm | <i>Spin-dependent interfacial band structure and charge transfer phenomena at the C60/graphene interface on Ni(111)</i> | 161 |
| Mirali Jafari | <i>DFT study of the electronic and magnetic properties of monolayer and bilayer of VS₂</i> | 162 |
| Tae Hee Kim | <i>Magnetotransport Properties of Graphene with Magnetic Defects</i> | 163 |
| Stefan Stagraczyński | <i>Magnetism in van der Waals materials</i> | 164 |

Magnetism in two-dimensional CrTe₂

Nihad AbuAwwad^{1,2,3}, Manuel dos Santos Dias^{2,1}, Hazem Abusara³, and Samir Lounis^{1,2}

¹*Peter Grünberg Institut and Institute for Advanced Simulation, Forschungszentrum Jülich & JARA, 52425 Jülich, Germany*

²*Faculty of Physics, University of Duisburg-Essen, 47053 Duisburg, Germany*

³*Department of Physics, Birzeit University, Ramallah, Palestine*

The discovery of two-dimensional (2D) van der Waals magnets opened unprecedented opportunities for the fundamental exploration of magnetism in quantum materials and the realization of next generation spintronic devices. Recently, thin CrTe₂ films were demonstrated to be ferromagnetic up to room temperature, with an intriguing dependence of the easy axis on the thickness of the material[1,2]. On the other hand, a zig-zag antiferromagnetic state has been observed by spin-polarized scanning tunneling microscopy in a monolayer[3]. Here, we demonstrate using first principles a strong coupling between magnetism and structure in a single layer of CrTe₂ through calculating the magnetic interactions. Also, utilizing atomistic spin dynamics, we perform a detailed investigation of the complex magnetic properties pertaining to this 2D material.

–Work funded by the Palestinian German Science Bridge (BMBF–01DH16027) and Priority Programme SPP 2244 2D Materials Physics of van der Waals Heterostructures of the DFG (project LO 1659/7-1).

[1] Zhang, et al, *Nat. Commun.* **12**, 2492 (2021).

[2] Meng, et al, *Nat. Commun.* **12**, 2492 (2021).

[3] Jing-Jing Xian, et al, *Nat. Commun.* **13**, 2492 (2022).

Ferromagnetic resonance study of 2D-SnS/Ni₈₀Fe₂₀ heterostructures

Himanshu Bangar^{1*}, Pankhuri Gupta¹, Sheetal Dewan³, Richa Mudgal¹, Samaresh Das², and P.K. Muduli¹

¹Department of Physics, Indian Institute of Technology Delhi, Hauz Khas, New Delhi-110016, India

²Center for Applied Research in Electronics, Indian Institute of Technology Delhi, Hauz Khas, New Delhi-110016, India

³School of Interdisciplinary Research, Indian Institute of Technology Delhi, Hauz Khas, New Delhi-110016, India

*Email: bangarhimanshu9@gmail.com

Recently, two-dimensional (2D) materials have emerged as a replacement for heavy metals (HM) because of their large spin-charge interconversion efficiency [1]. In this work, we perform FMR measurements in a promising and relatively less explored 2D material SnS. Through symmetry arguments, it is proposed that SnS may exhibit unconventional spin-orbit torques (SOTs), which is very important for energy-efficient switching of magnets with perpendicular magnetic anisotropy (PMA) [1]. SnS thin films up to monolayer (ML) thickness have been grown on Si/SiO₂ substrates using pulsed laser deposition (PLD) technique. Two typical Raman active modes (A_g and B_{3g}) [2] can be distinguished in the acquired Raman spectra (Fig. 1). Subsequently, we deposited Py (8 nm)/ AlO_x (2 nm) on top of SnS through the magnetron sputtering technique. We performed ferromagnetic resonance (FMR) measurements to determine the Gilbert damping parameter (α_{eff}). We observed a giant increase in α_{eff} with the thickness of SnS (Fig. 2) together with a decrease of effective saturation magnetization (M_{eff}). The results indicate that behaviour may be related to proximity effect induced enhancement of damping constant due to antiferromagnetic ordering at the interface.

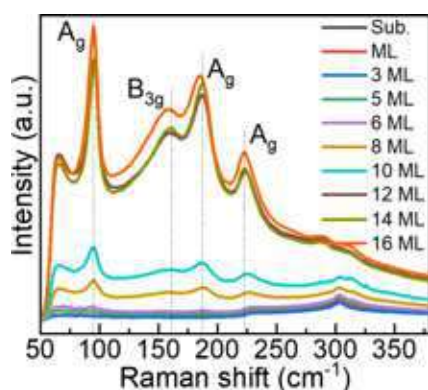


Figure 1. Acquired Raman spectra.

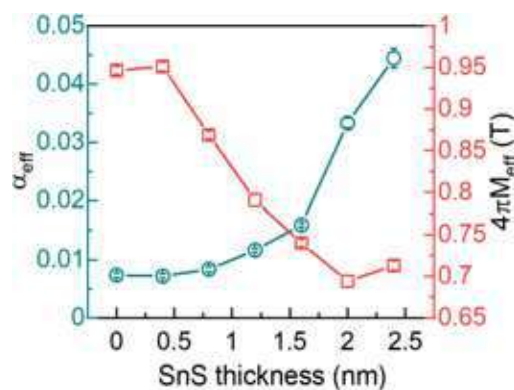


Figure 2. The trend of α_{eff} and M_{eff} with SnS thickness.

References

- [1] Y. Liu and Q. Shao, *ACS Nano* **14**, 9389 (2020).
- [2] A.N. Mehta, H. Zhang, A. Dabral, O. Richard, P. Favia, H. Bender, A. Delabie, M. Caymax, M. Houssa, G. Pourtois and W. Vandervorst, *J. Microsc.* **268**, 276 (2017).

Intermolecular band dispersion, charge transfer and spin-polarization at the C60/graphene interface on Ni(111)

Ralf Hemm¹, Aaron Gebert¹, Fabian Pham¹, Ka Man Yu¹, Martin Mitkov¹, Christina Schott¹, Martin Aeschlimann¹, Stefan Lach¹, Christiane Ziegler¹ and Benjamin Stadtmüller^{1,2}

¹ University of Kaiserslautern (TUK) and research center OPTIMAS, Erwin-Schroedinger-Str. 46, 67663 Kaiserslautern, Germany

² Institute of Physics, Johannes Gutenberg-University Mainz, 55128 Mainz, Germany

The strong chemical interaction at ferromagnetic molecule-metal interfaces can drastically change the molecular energy level alignment and the corresponding functionalities that are desired for applications. Such adsorption-induced modifications of molecular adsorbates are normally avoided by passivating the metallic surface using a 2D buffer layer like graphene [1].

Here, we focus on the interfacial band structure of a monolayer film of the prototypical organic semiconductor C60 on top of a graphene/Ni(111) hybrid interface (see Fig. 1) using momentum microscopy. As observed for the C60 multilayer the valence states of the monolayer also exhibit a strong intermolecular dispersion that can be attributed to an intermolecular interaction [2]. An energetical splitting of the HOMO level indicates a separation of spin carriers due to a possible hybridization between the C60 HOMO and orbitals of the graphene layer. Interestingly we can identify a charge transfer state of the C60 monolayer in the vicinity of the Fermi edge that can be attributed to an adsorption induced population of the lowest unoccupied molecular orbital (LUMO) of C60. Our findings point to a non-vanishing interaction between C60 and the Ni surface despite the passivating graphene layer and to a potentially spin-polarized charge transfer into the C60 LUMO level.



Fig. 1: Schematic composition of the investigated sample system

[1] M. Scardamaglia et al., J. Phys. Chem. C 117, 6, 3019-3027 (2013)

[2] N. Haag et al., Phys. Rev. B 101, 165422 (2020)

DFT study of the electronic and magnetic properties of monolayer and bilayer of VS_2

M.A. Jafari¹ and A. Dyrdał¹

¹*Department of Mesoscopic Physics, ISQI, Faculty of Physics, Adam Mickiewicz University,
ul. Uniwersytetu Poznańskiego 2, 61-614 Poznań, Poland*

We have performed first-principles calculations to study the electronic and magnetic properties of the VS_2 two-dimensional materials, in which magnetic Vanadium atoms are arranged in a hexagonal lattice. Numerical results have been obtained for the monolayer VS_2 in hexagonal (H) and trigonal (T) phases that reveal semiconducting behaviour with a narrow bandgap of 0.048 eV and magnetic metallic behaviour, respectively. Based on the mean-field approximation, we have evaluated the Curie-temperature of 205.1 K for the H phase and of 136.3 K for the T phase. We have also calculated the magnetic anisotropy energy (MAE) for both phases. The obtained results are in agreement with other calculations [1,2]. Similarly, we have also considered a bilayer of Vanadium Disulfide, which shows a ferromagnetic and antiferromagnetic interlayer exchange coupling for $2H$ and $2T$ phases, respectively. For these two phases ($2H$ and $2T$), we have also calculated the corresponding MAE and Curie temperature. In addition, we have also determined thermoelectric characteristics for monolayers and bilayers of VS_2 .

- [1] Y. Yunliang, *Journal of Superconductivity and Novel Magnetism* **30.5**, 1201-1206 (2017).
- [2] H. Fuh, C.Chang, Y. Wang, R. Chantrell, and H. Jeng *Journal of Scientific reports* **6**, 1-11 (2016).

This work has been supported by the Norwegian Financial Mechanism 2014- 2021 under the Polish-Norwegian Research Project NCN GRIEG “2Dtronics” no. 2019/34/H/ST3/00515.

Magnetotransport Properties of Graphene with Magnetic Defects

Nga T. Do¹, Youngrok Jang², Sijin Park³, Chanyong Hwang³ & Tae Hee Kim¹

¹*Department of Physics, Ewha Womans University, 03760, Seoul, Korea*

²*Department of Physics, Incheon National University, 22012, Incheon, Korea*

³*Korea Research Institute of Standards and Science, 34113, Daejeon, Korea*

In this work, we focused on the interplay between Gr and Pt layer by introducing an ultrathin Co (or Mn) defects. As the Co (or Mn) thickness increases from 0.5 to 25 Å in Pt/Gr/SiO₂/Si perpendicular stacks, different magnetoresistance behaviors have been observed in the intermediate temperature range (77-300K). The Co (or Mn) films were prepared on the wafer-scale CVD-grown multilayer, and covered with a 3-nm-thick of Pt using the UHV-Molecular Beam Epitaxy (MBE) film deposition technique. For the transport measurement, Pt-Hall bar devices were also prepared using the *in-situ* shadow mask system in the same UHV-MBE chamber. Our results showed that the quantum interference effect could be observed even at 77 K for the samples with the magnetic defect thickness less than 2 Å. Particularly, for the sample with 0.5-Å-thick Co, the WL-WAL crossover was clearly shown in the perpendicular MR measured at 77 K. The larger perpendicular MR effect was observed for the sample with 0.5-Å-thick Mn than that of the sample with 0.5-Å-thick Co. To understand more physical insights of the magnetic defect effects at the Pt/Gr interfaces, a theoretical analysis was performed using modified the Hikami-Larkin-Nagaoka (HLN) equation.¹ For microstructural characterization of the heterostructures, the careful analysis of interface properties was also carried out using AFM and HR-TEM.

Our results provide further insights into the transport phenomena and highlight the defect engineering of 2D-material with other ferromagnetic materials to manipulate and develop highly effective spintronic devices with new functionalities.

[Reference]

- ¹. Shinobu Hikami, Anatoly I. Larkin and Yosuke Nagaoka, *Prog Theor Phys* **63**, 707-710 (1980).

Magnetism in van der Waals materials

S. Stagraczyński¹, A. Dyrdał¹, J. Barnaś^{1,2}

¹*Department of Mesoscopic Physics, ISQI, Faculty of Physics, Adam Mickiewicz University,
ul. Uniwersytetu Poznańskiego 2, 61-614 Poznań, Poland*

²*Institute of Molecular Physics, Polish Academy of Sciences, M. Smoluchowskiego 17, 60-179
Poznań, Poland*

Magnetism in two-dimensional materials received a lot of attention in the last decade. It comes out that this kind of system has many phase transitions and is suitable for studying skyrmions, magnetic patterns, and become a fundamental tool for magnonics applications. Thanks to the advanced numerical modeling, such as atomistic spin dynamic(ASD) method, it is possible to study the magnetic properties and spin dynamics of single and two-layered van der Waals(vdW) materials.

Our consideration is based on the ASD which opened a new bridge between quantum and microscopic simulation methods [1, 2]. It consists of two main parts. Firstly, the spin model Eq.(1) describes the energetic properties of the system,

$$\mathcal{H} = - \sum_{i<j} J_{ij} \mathbf{S}_i \cdot \mathbf{S}_j - k_2 \sum_i S_z^2 - \mu_S \sum_i \mathbf{B}_{app} \cdot \mathbf{S}_i, \quad (1)$$

where \mathbf{S} is a unit vector for the local spin moment, μ_S is the atomic spin moment, k_2 correspond to the anisotropy constant and J_{ij} are the Heisenberg exchange parameters. Secondly, Eq.(2) describe the spin dynamics of atomic spins

$$\frac{\partial \mathbf{S}_i}{\partial t} = - \frac{\gamma}{(1 + \lambda^2)} [\mathbf{S}_i \times \mathbf{B}_{eff}^i + \lambda \mathbf{S}_i \times (\mathbf{S}_i \times \mathbf{B}_{eff}^i)], \quad (2)$$

where γ is a gyromagnetic ratio, $\mathbf{B}_{eff}^i = - \frac{\partial \mathcal{H}}{\partial \mathbf{S}_i}$ is the effective magnetic field which the atomic spin S_i experiences.

In detail, we have focused on mono- and bi-layers of vdW structures with ferro-/and anti-ferromagnetic ordering, DMI, in- and out-of-plane anisotropies, external fields, temperature, and different lattice types like cubic, Kagome and hexagonal structures with AA and AB stacking. By moderating the effective parameters it is possible to find variety of phase transitions. In the case of mono/bi-layer models, it could be perceived by change from ordinary to double-like hysteresis loops. The possibility to introduce DMI via an external electric field allows controlling of the transition effectively.

[1] R. F. L. Evans, W. J. Fan, P. Chureemart, T. A. Ostler, M. O. A. Ellis and R. W. Chantrell, J. Phys.: Condens. Matter 26, 103202 (2014).

[2] B. Skubic, J. Hellsvik, L. Nordström, O. Eriksson, J. Phys.: Condens. Matter 20, 315203 (2008).

This work has been supported by the Norwegian Financial Mechanism 2014- 2021 under the Polish-Norwegian Research Project NCN GRIEG "2Dtronics" no. 2019/34/H/ST3/00515.

Symposium 7. Magnetism and spintronics in molecular materials and inorganic materials

| | | |
|-----------------------|--|-----|
| Szymon Chorazy | <i>Lanthanide single-molecule magnets functionalized by cyano transition metal complexes</i> | 167 |
| Alicia Forment-Aliaga | <i>Magnetic molecular systems to tune 2D materials properties</i> | 168 |
| Alejandro Gaita-Ariño | <i>Data-powered insights into single-ion magnetism: the hidden role of vibronic coupling in the effective barrier</i> | 169 |
| Fernando Bartolomé | <i>Nanostructuring magnetic systems by means of a 2D Metalorganic Network</i> | 171 |
| Sumanta Bhandary | <i>Dynamical screening at the metal-molecule interfaces: a hindrance to molecular spintronic device development?</i> | 172 |
| Dominik Czernia | <i>Effect of proton irradiation on magnetic properties of two-dimensional Ni(II) molecular magnet</i> | 173 |
| Magdalena Fitta | <i>Construction of thin film systems using solvatomagnetic coordination polymers</i> | 174 |
| Magdalena Foltyn | <i>[Co(NCS)₂(L)₂]_n spin chains: a new relaxation pathway observed for single crystal samples</i> | 175 |
| Jerzy Goraus | <i>Spectroscopic and elastic properties of some Heusler alloys which were predicted to be Spin-Gapless-Semiconductors or Half-Metallic Ferromagnets</i> | 176 |
| Gabriela Handzlik | <i>Slow spin dynamics in Gd^{III}-based propeller-like qubit candidate and its structural analogues with other lanthanide ions</i> | 177 |
| Piotr Kozłowski | <i>Magnetism of vanadium and tungsten based polyoxometalates functionalized with phthalocyaninato lanthanide (Y,Yb,Dy) moieties</i> | 178 |
| Michał Magott | <i>Magnetic superexchange controlled by light in the family of molecular photomagnets</i> | 179 |
| Manoj Talluri | <i>Giant Spin Pumping at Ferromagnet (Permalloy) – Organic Semiconductor (Perylene diimide) Interface</i> | 180 |
| Anastasiia Doroshenko | <i>Anomalous slow spin relaxation in [Gd₂(H₂O)₆(C₂O₄)₃].2.5H₂O complex induced by magnetic field.</i> | 182 |
| Liliia Kotvytska | <i>Realization of low-dimensional magnetism in zeolitic imidazolate frameworks</i> | 183 |
| Robert Ranecki | <i>Spin properties of high-spin ground state, 12-metallacrown-4 complexes on Au(III) investigated by inelastic tunneling spectroscopy</i> | 184 |
| Sawssen Slimani | <i>Colossal magnetoresistance (CMR) and Density functional theory in La_{0.4}Ag_{0.2}Ca_{0.4}MnO₃ polycrystal</i> | 185 |
| Olha Vinnik | <i>Effect of en – H₂O substitution on the ground-state properties of Cu(en)SO₄X (X = en, (H₂O)₂) compounds</i> | 186 |

Invited Oral Presentations

| | | |
|-----------------------|---|-----|
| Szymon Chorazy | <i>Lanthanide single-molecule magnets functionalized by cyanido transition metal complexes</i> | 167 |
| Alicia Forment-Aliaga | <i>Magnetic molecular systems to tune 2D materials properties</i> | 168 |
| Alejandro Gaita-Ariño | <i>Data-powered insights into single-ion magnetism: the hidden role of vibronic coupling in the effective barrier</i> | 169 |

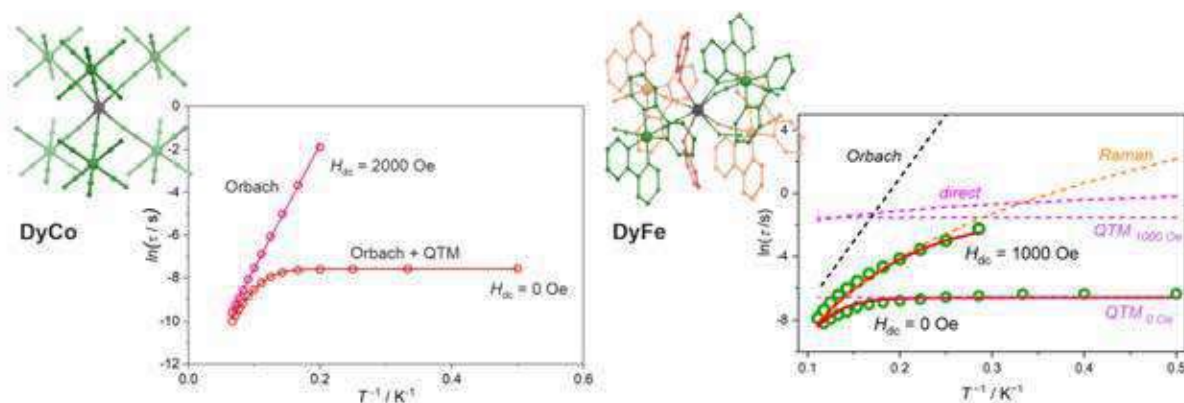
Lanthanide single-molecule magnets functionalized by cyanido transition metal complexes

Szymon Chorazy¹, Jakub J. Zakrzewski², Michal Liberka², Mikolaj Zychowicz², Pawel Bonarek², Junhao Wang², Yue Xin², and Shin-ichi Ohkoshi²

¹ Faculty of Chemistry, Jagiellonian University, Gronostajowa 2, 30-387 Krakow, Poland

² Department of Chemistry, School of Science, The University of Tokyo, 7-3-1 Hongo, Bunkyo-ku, 113-0033 Tokyo, Japan

Lanthanide single-molecule magnets (Ln-SMMs) can reveal strong magnetic anisotropy due to the combined contributions from spin-orbit coupling and crystal-field effects. As the result, they exhibit very slow relaxation of magnetization that leads to the magnetic hysteresis loop below the blocking temperature. Recently, they arouse also the increasing research interest as promising opto-magnetic systems linking designable luminescent and magnetic properties, and their correlations.[1] There are several synthetic approaches toward the rational design and functionalization of Ln-SMMs. In our work, we take advantage of cyanido transition metal complexes that can be used as advanced metalloligands for other d- or f-block metal ions inducing their magnetic, optical, electrical, or mechanical properties, and their fruitful combinations.[2] Here, we present a few recent examples of the generation and further functionalization of Ln-SMMs using the anionic polycyanidometallates, including (i) classical hexacyanidometallates,[3–5] well-known in the chemistry and physics as the components of magnetic Prussian Blue analogs, and (ii) much less common polycyanidometallates with the lower number of cyanido ligands,[5–7] such as dicyanidoferrate(II) or dicyanidoplatinate(II) complexes bearing additional organic ligands (see figure below).



- [1] R. Marin, G. Brunet, and M. Murugesu, *Angew. Chem. Int. Ed.* **60**, 1728 (2021).
- [2] S. Chorazy, J. J. Zakrzewski, M. Magott, T. Korzeniak, B. Nowicka, D. Pinkowicz, R. Podgajny, and B. Sieklucka, *Chem. Soc. Rev.* **49**, 5945 (2020).
- [3] Y. Xin, J. Wang, M. Zychowicz, J. J. Zakrzewski, K. Nakabayashi, B. Sieklucka, S. Chorazy, and S. Ohkoshi, *J. Am. Chem. Soc.* **141**, 18211 (2019).
- [4] J. Wang, J. J. Zakrzewski, M. Zychowicz, V. Vieru, L. F. Chibotaru, K. Nakabayashi, S. Chorazy, and S. Ohkoshi, *Chem. Sci.* **12**, 730 (2021).
- [5] J. J. Zakrzewski, K. Kumar, M. Zychowicz, R. Jankowski, M. Wyczescany, B. Sieklucka, S. Ohkoshi, and S. Chorazy, *J. Phys. Chem. Lett.* **12**, 10558 (2021).
- [6] M. Liberka, K. Boidachenko, J. J. Zakrzewski, M. Zychowicz, J. Wang, S. Ohkoshi, and S. Chorazy, *Magnetochemistry* **7**, 79 (2021).
- [7] M. Liberka, M. Zychowicz, W. Zychowicz, and S. Chorazy, *Chem. Commun.* doi: 10.1039/D2CC02238A (2022).

Magnetic molecular systems to tune 2D materials properties.

A. Forment-Aliaga, R. Torres-Cavanillas, M. Morant-Giner, M. Galbiati, and E. Coronado

¹ Instituto de Ciencia Molecular-Universitat de València, C/ Catedrático José Beltrán, 2, Paterna, Spain

Since the isolation of graphene in 2004, there has been an explosion in the search for other two-dimensional (2D) materials. Among them, special attention has been paid to transition metal dichalcogenides (TMDCs) of general formula of MX_2 (M: transition metal, and X: chalcogen S, Se, or Te) due to their broad spectrum of electronic properties coming from a large variety of compositions and polytypes.

One step forward, to improve the properties and processability of bare 2D materials, the preparation of hybrid multifunctional heterostructures based on molecular materials and 2D layers has become a hot topic.[1]

In this presentation we will show some examples regarding the use of magnetic molecular based materials to functionalize MoS_2 , the archetypical TMDC. In particular, we will show how MoS_2 decorated with Prussian blue coordination compounds boost the potential of both components as efficient cathode materials for Na^+ and K^+ ion batteries. [2] Moreover, we will demonstrate how the covalent functionalization of MoS_2 with spin crossover (SCO) nanoparticles gives rise to a smart 2D heterostructure where the volume change that takes place when spin transition is externally induced by light or temperature, produces a reversible strain on the 2D layer modulating its electronic structure and consequently its electrical and optical properties. [3]

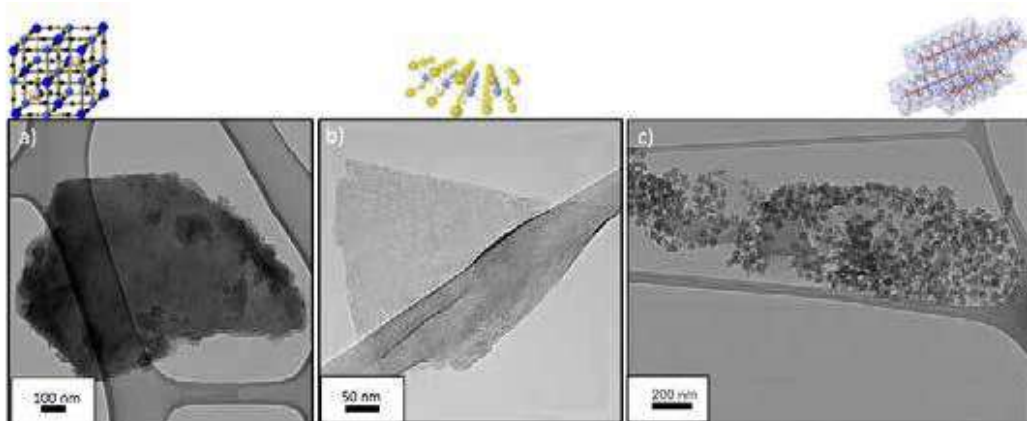


Figure 1: Transmission electron microscopy images of MoS_2 (b), functionalized MoS_2 with Prussian blue (a) and functionalized MoS_2 with SCO nanoparticles.

[1] S. Bertolazzi, M. Gobbi, Y. Zhao, C. Backes and P. Samorì, *Chem. Soc. Rev.* **47**, 6845 (2018).

[2] M. Morant-Giner, R. Sanchis-Gual, J. Romero, A. Alberola, L. García-Cruz, S. Agouram, M. Galbiati, N. M. Padial, J. C. Waerenborgh, C. Martí-Gastaldo, S. Tatay, A. Forment-Aliaga, and E. Coronado *Adv. Funct. Mater.* **28**, 1706125 (2018)

[3] R. Torres-Cavanillas, M. Morant-Giner, G. Escorcía-Ariza, J. Dugay, J. Canet-Ferrer, S. Tatay, S. Cardona-Serra, M. Giménez-Marqués, M. Galbiati, A. Forment-Aliaga and E. Coronado *Nat. Chem.* **13**, 1101 (2021)

Data-powered insights into single-ion magnetism: the hidden role of vibronic coupling in the effective barrier

Alejandro Gaita-Ariño¹, Silvia Giménez-Santamarina¹, Salvador Cardona-Serra¹ and Lorena E. Rosaleny¹

¹ICMol, Universitat de València, c/ cat José Beltrán, 2, Paterna, Spain

Decades of research in molecular nanomagnets have brought the magnetic memory in molecules up to 80K.[1] Besides a wise choice of the magnetic ion and the coordination environment, one has to admit that serendipity, oversimplified theories and chemical intuition have played a leading role. In order to establish a powerful framework for statistically driven chemical design, we collected chemical and physical data for lanthanide-based nanomagnets to create a catalogue of over 1400 published experiments, developed an interactive dashboard (SIMDAVIS)[2] to visualise the dataset, and applied inferential statistical analysis to it. We found that the effective energy barrier U_{eff} derived from the Arrhenius equation displays an excellent correlation with the magnetic memory, and that among all chemical families studied, only terbium bis-phthalocyaninato sandwiches and dysprosium metallocenes consistently present magnetic memory up to high temperature, but that there are some promising strategies for improvement.[3]

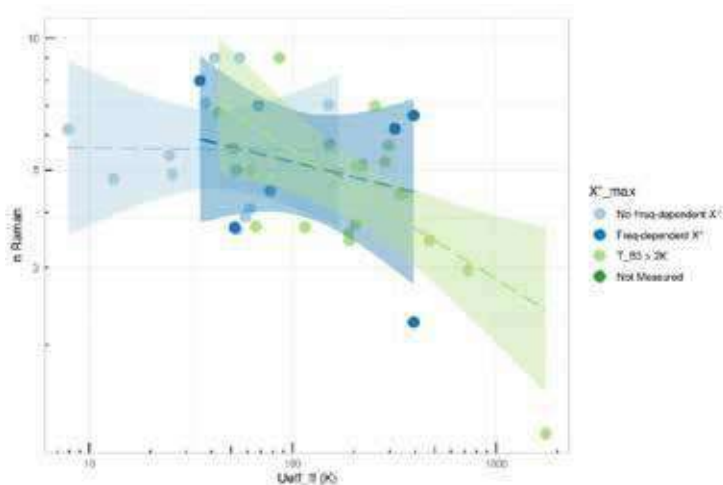


Figure 1: Raman exponent and U_{eff} are independent for samples with no magnetic memory but correlated for good SIMs.

The unreasonably good predicting power of the effective energy barrier prompted a second phase in the study, where we analyzed the reported parameters for the Raman mechanism. We found a puzzling correlation between Orbach and Raman relaxation mechanisms. Based on recent theoretical studies,[4] we postulate that slow relaxation in either case (Raman and Orbach) arises from an effectively low vibronic coupling, so that looking at the two mechanisms as independent is a flawed approach. Furthermore, we postulate that precisely this common origin of slow Raman and slow Orbach in low vibrational coupling is a major reason why the only successful families are based on aromatic ligands providing a rigid coordination environment.

[1] F.-S. Guo et al, *Science* **362**, 1400 (2018).

[2] <https://rosaleny.shinyapps.io/simdavis-dashboard/>

[3] Y. Duan et al, arXiv:2103.03199 (2021).

[4] L. Gu and R. Wu, *Phys. Rev. B* **103**, 014401 (2021).

Oral Presentations

| | | |
|--------------------|---|-----|
| Fernando Bartolomé | <i>Nanostructuring magnetic systems by means of a 2D Metalorganic Network</i> | 171 |
| Sumanta Bhandary | <i>Dynamical screening at the metal-molecule interfaces: a hindrance to molecular spintronic device development?</i> | 172 |
| Dominik Czernia | <i>Effect of proton irradiation on magnetic properties of two-dimensional Ni(II) molecular magnet</i> | 173 |
| Magdalena Fitta | <i>Construction of thin film systems using solvatomagnetic coordination polymers</i> | 174 |
| Magdalena Foltyn | <i>[Co(NCS)₂(L)₂]_n spin chains: a new relaxation pathway observed for single crystal samples</i> | 175 |
| Jerzy Goraus | <i>Spectroscopic and elastic properties of some Heusler alloys which were predicted to be Spin-Gapless-Semiconductors or Half-Metallic Ferromagnets</i> | 176 |
| Gabriela Handzlik | <i>Slow spin dynamics in Gd^{III}-based propeller-like qubit candidate and its structural analogues with other lanthanide ions</i> | 177 |
| Piotr Kozłowski | <i>Magnetism of vanadium and tungsten based polyoxometalates functionalized with phthalocyaninato lanthanide (Y,Yb,Dy) moieties</i> | 178 |
| Michał Magott | <i>Magnetic superexchange controlled by light in the family of molecular photomagnets</i> | 179 |
| Manoj Talluri | <i>Giant Spin Pumping at Ferromagnet (Permalloy) – Organic Semiconductor (Perylene diimide) Interface</i> | 180 |

Nanostructuring magnetic systems by means of a 2D Metalorganic Network

**L. Hernández-López^{1,2}, I. Piquero-Zulaica^{3,4}, D. Serrate^{1,2}, J. Lobo-Checa^{1,2},
Fernando Bartolomé^{1,2}**

¹ *Instituto de Nanociencia y Materiales de Aragón, CSIC-Universidad de Zaragoza
50009 Zaragoza (Spain)*

² *Departamento de Física de la Materia Condensada, Universidad de Zaragoza
50009 Zaragoza (Spain)*

³ *Centro de Física de Materiales CSIC/UPV-EHU - Materials Physics Center
20018 San Sebastián, Spain*

⁴ *Physics Department E20, Technical University of Munich, 85748 Garching, Germany*

Individual atoms and small atomic clusters are model systems that are widely studied due to their potential use in the field of electronic and spintronic devices. These units can exhibit magnetocrystalline anisotropies considerably larger than thin films or their bulk counterparts. However, the experimental characterization of such low-dimensional is challenging since the structures of interest are generally diluted and must be supported onto metallic substrates.

Supramolecular assembly of organic molecules in the form of 2D Metal Organic Coordinated Networks (MOCN) is a vantage tool for on-surface self-assembled templating. The adatoms that laterally coordinate the molecular ligands can yield unsaturated (yet stable) coordination bonds that result in chemical modifications that influence their electronic and magnetic properties, and considerably differ from single molecule magnets. Several works report on the magnetic character of MOCN adatoms [1-3], but the major constraint is that they often present many coexisting geometries, each showing different registry with the substrate and usually incorporating considerable amount of defects.

We have prepared a series of six periodic and extended MOCN of extremely high structural quality by depositing up to a monolayer of 9,10 dicyanoanthracene (DCA) both on Au(111) and Ag(111), and adding the corresponding stoichiometric amount of coordination atoms, which in our case are Cu, Co and Fe. The high molecular mobility that our anthracene derivatives exhibit at room temperature facilitates the bonding to the coordinating adatoms that are slowly evaporated onto the surface. Moreover, we have achieved a hexagonal array of Sm single atoms by adding minute atomic amounts of Sm on the Cu+DCA MOCN on Cu. Finally, we have also prepared metallic nanoclusters (Fe and Er among others) on top of the formed MOCN, achieving nanoplatelet sets with enhanced properties.

[1] P. Gambardella et al., Nature Materials 8, 189 (2009);

[2] T. Umbach et al., PRL 109, 267207 (2012);

[3] S.O.Parreiras et al., Small 17 2102753 (2021);

Dynamical screening at the metal-molecule interfaces: a hindrance to molecular spintronic device development?

Sumanta Bhandary¹, Emiliano Poli², Gilberto Teobaldi² and David D. O'Regan¹

¹*School of Physics and CRANN Institute, Trinity College Dublin, The University of Dublin, Dublin 2, Ireland*

²*Scientific Computing Department, STFC UKRI, Rutherford Appleton Laboratory, Didcot OX11 0QX, United Kingdom*

Advancement towards device development in the field of molecular spintronics has its particular challenges. In spite of having an unmatched inherent size advantage and multiple exploitable intrinsic and extrinsic molecular features, such as switchable structural, charge-state, and magnetic conformations, robust device integration has remained

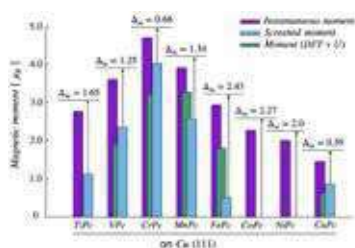


Figure 1: Dynamical screening effects on the local magnetic moment in TMPc molecules on Cu(111). The purple, cyan bars represent the instantaneous and screened moments, respectively, while the green bars compare the same obtained within DFT+U. Δ_m represents the amount of moment reduction due to screening.

a key bottleneck. In this context, transition-metal phthalocyanine molecules have attracted considerable interest in the context of spintronics device development, due to their amenability to diverse bonding regimes and their intrinsic magnetism. While maximizing local magnetic moments is an important and critical step towards hybrid spintronics applications, the quantum fluctuations that arise at the inevitable metal-molecule interface in a device architecture highly influence them. In this work, we have systematically studied the dynamical screening effects in phthalocyanine molecules hosting a series of transition-metal ions (Ti, V, Cr, Mn, Fe, Co, Ni, and Cu) in contact with the Cu(111) surface. Using comprehensive density functional theory (DFT) plus Anderson's Impurity model calculations (AIM), namely DFT++, we show that the orbital-dependent hybridization and electron correlation together result in strong valence, charge, and spin fluctuations. While the instantaneous spin moments of the transition-metal ions are near atomic-like, we find that screening gives rise to considerable lowering or even quenching of these.

Our results highlight the importance of quantum fluctuations in metal-contacted molecular devices, at the same time, highlight the possible discrepancies that may appear due to the difference in the material-specific characteristic time-scale of the fluctuating moment in molecular systems and intrinsic time-scale of specific experimental probe.

We acknowledge financial support from the Science Foundation Ireland [19/EPSC/3605], the Engineering and Physical Sciences Research Council [EP/S030263/1, EP/S031081/1] and Irish Centre for High-End Computing (ICHEC) for computational support.

[1] S. Bhandary, E. Poli, G. Teobaldi and D. D. O'Regan, *Manuscript*, (2022).

Effect of proton irradiation on magnetic properties of two-dimensional Ni(II) molecular magnet

D. Czernia¹, P. Konieczny¹, E. Juszyńska-Gałązka¹, J. Lekki¹, A. B. González Guillén²

¹*Institute of Nuclear Physics PAN, ul. Radzikowskiego 152, 31-342 Kraków, Poland*

²*Faculty of Chemistry, Jagiellonian University, ul. Gronostajowa 2, 30-387 Kraków, Poland*

The broad capability of the molecular magnetic materials emerges from the variety of available systems with unique properties that can be altered by external stimuli such as temperature, pressure, light irradiation, or sorption of guest molecules. Although not popular in the field of molecular magnetism, ion irradiation is the other approach for tailoring the material's parameters. Energetic particles expose solids to the high-density local energy deposition, leading to non-linear and threshold effects that may create new materials with novel properties.

In particular, the irradiation-induced defects may give rise to the magnetism in initially non-magnetic materials and modify the magnetic properties of a system with a non-zero magnetic moment, especially when strong magneto-structural correlations are present. The studies of the response of thin films and bulk samples to ion irradiation show there is a possibility to alternate such parameters as the critical temperature, g-factor, or coercivity by energetic particles deposition. However, no systematic studies can be found regarding the effects of ion irradiation on molecular magnetic materials.

Here we examine the magnetic properties of 2D coordination polymer based on nickel sulfate and a 1,3-phenylenediamine ligand that was irradiated with 1.9 MeV protons using fluences ranging from $5 \cdot 10^{13} \text{ p} \cdot \text{cm}^{-2}$ to $2 \cdot 10^{15} \text{ p} \cdot \text{cm}^{-2}$. The samples irradiated with the high fluence showed an increase in magnetization saturation up to 200 percent and the reduced coercive field to even 10 percent of the reference level. Simultaneously, the critical temperature remained the same ($T_c = 24.5 \text{ K}$) regardless of the received radiation dose. The IR spectroscopy showed that the overall structure of the studied compound was preserved after proton irradiation, and only minor changes are present in the local structure.

Construction of thin film systems using solvatomagnetic coordination polymers

Magdalena Fitta¹, Aleksandra Pacanowska¹ and Beata Nowicka²

¹ Institute of Nuclear Physics Polish Academy of Sciences, Radzikowskiego 152, 31-342 Kraków, Poland

² Faculty of Chemistry, Jagiellonian University, Gronostajowa 2, 30-387 Kraków, Poland

Strong motivation for the synthesis of molecular materials is the merging of multifunctionality into these systems. Among molecular magnets, one can find solvatomagnetic compounds showing the reversible changes in structure and magnetic properties upon dehydration or sorption of small molecules [1,2]. On the other hand, many potential applications of molecular magnets require the deposition of these materials on surfaces.

In this report, we present two types of thin films of microporous CN-bridged hybrid organic-inorganic $\{[\text{Ni}^{\text{II}}(\text{cyclam})]_3[\text{M}^{\text{III}}(\text{CN})_6]_2 \cdot n\text{H}_2\text{O}\}_n$ ($\text{M} = \text{Cr}$ or Fe , cyclam = 1,4,7,11-tetraazacyclotetradecane) coordination networks. The films were obtained by using physical and chemical deposition techniques. By adsorption on the PET/ITO substrate of the pre-formed nano-sized crystallites from water suspension, films of 1-2 μm thickness composed of 40-200 nm size particles were obtained. In the second approach, the chemical sequential growth method was implemented, in which the coordination framework is anchored to the gold surface and built directly on the substrate from cationic and anionic building blocks. As the result, we obtained films of reduced thickness (ca. 100 nm) and drastically improved morphology. Both types of thin films show solvatomagnetic behavior characteristic for bulk compounds and change magnetic characteristics, including the shape of the magnetic hysteresis, under different humidity conditions.

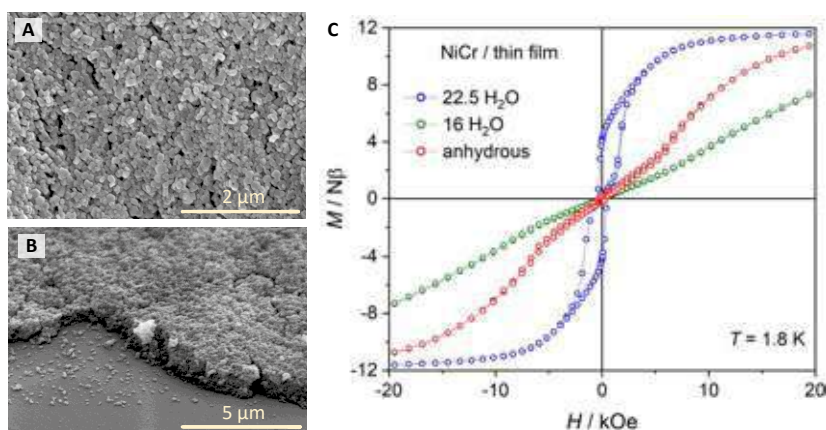


Figure 1: SEM images of the $[\text{Ni}(\text{cyclam})]_3[\text{Cr}(\text{CN})_6]_2$ film surface (A, B) and the shape of magnetic hysteresis depending on the degree of hydration (C).

[1] B. Nowicka, M. Reczyński, M. Rams, W. Nitek, J. Żukrowski, C. Kapusta, B. Sieklucka, *Chem. Commun.*, **51**, 11485 (2015).

[2] B. Nowicka, M. Reczyński, M. Bałanda, M. Fitta, B. Gaweł, B. Sieklucka, *Cryst. Growth Des.*, **16**, 4736 (2016).

[Co(NCS)₂(L)₂]_n spin chains: a new relaxation pathway observed for single crystal samples

Magdalena Foltyn¹, Dawid Pinkowicz², Christian Näther³, and Michał Rams¹

¹ Institute of Physics, Jagiellonian University, Kraków, Poland.

² Faculty of Chemistry, Jagiellonian University, Kraków, Poland.

³ Institut für Anorganische Chemie, Christian-Albrechts-Universität, Kiel, Germany.

The slow relaxation of magnetization in spin chains based on Co(II) ion is a very complex issue, as its mechanism usually cannot be explained using the standard approach [1]. Some progress to understand this behavior was made using the first single crystal sample from the family [Co(NCS)₂(ligand)₂]_n [2]. Realizing how much more information can be gained from the single crystal investigations, we decided to synthesize other single crystals from the same family. We will present investigations of a single crystal of [Co(NCS)₂(4-methoxypyridine)₂]_n. This compound orders antiferromagnetically at 3.95 K. The magnetic measurements were performed along three perpendicular crystallographic directions. The inter- and intrachain interactions do not differ between single crystal and powder, however, surprisingly, the energy barriers of the single chain relaxation process differ noticeably, indicating a change of a single spin relaxation mechanism. For the single crystal sample, we also observe a second process, however, only close to the critical temperature (Figure). The relaxation time of this process is temperature independent, which means that the energy barrier is negligible. Such phenomenon was previously not observed for any of the powder samples of compounds from the investigated family, therefore, we associate its origin with the much lower number of defects in the single crystal samples than in polycrystals [3]. *This project is supported by National Science Centre, Poland (Project Preludium 19 no. 2020/37/N/ST3/02526).*

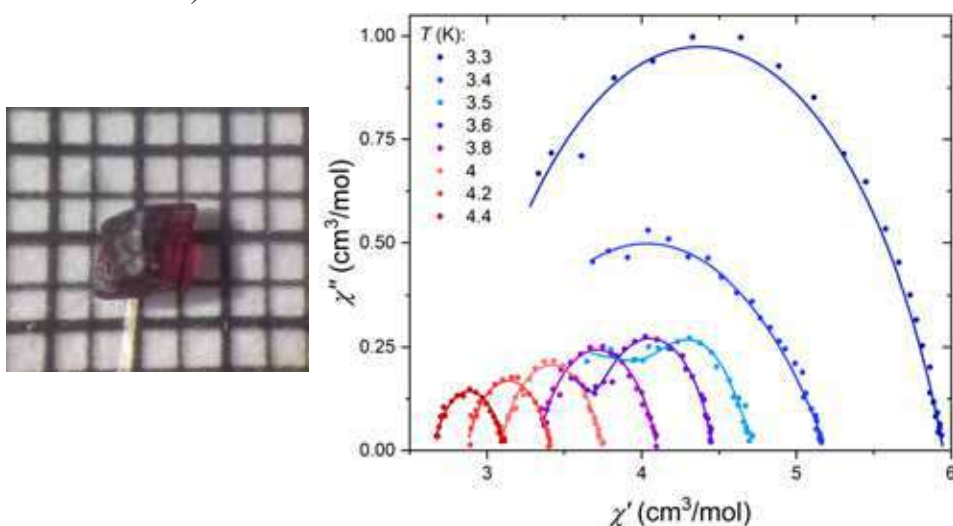


Figure: Left: A photo of a single crystal sample. Right: Ac magnetic susceptibility measured for a single crystal sample. At 3.5 and 3.6 K, there are visible both processes simultaneously.

[1] C. Coulon, H. Miyasaka and R. Clérac, *Struct. Bonding*, **122**, 163 (2006).

[2] M. Ceglarska *et al.*, *Phys. Chem. Chem. Phys.* **23**, 10281 (2021).

[3] M. Ceglarska *et al.*, to be published.

Spectroscopic and elastic properties of some Heusler alloys which were predicted to be Spin-Gapless-Semiconductors or Half-Metallic Ferromagnets

Jerzy Goraus¹, Marcin Zajac², Adrian Barylski³

¹*Institute of Physics, University of Silesia, ul. 75 Pułku Piechoty 1a, Chorzów, Poland*

²*Solaris National Synchrotron Radiation Centre, Jagiellonian University, ul. Czerwone Maki
98, Cracow, Poland*

³*Institute of Materials Engineering, University of Silesia, ul. 75 Pułku Piechoty 1a, Chorzów,
Poland*

Here, we present the recent results of XAS measurements of some Heusler alloys, most notably Ti_2CrAl [1], where by comparison with DFT (Density Functional Theory) simulations for simple and inverted Heusler structure, we judge that these compounds crystallize in simple Heusler structure. Basing upon DFT simulations, these two structures, have different shape of XAS (X-ray Absorption Spectroscopy) spectra, and experimental shape of XAS Cr L_3 line fits better the model with simple Heusler structure. These results are important because earlier theoretical reports have shown that these Ti-based Heuslers (e. g. Ti_2MnAl) may exhibit Spin Gapless Semiconductor state (SGS) [2], if they would crystallized in inverted Heusler structure. Very few SGS compounds are known, and in Heusler family perhaps only one – Mn_2CoAl [3]. In addition, we show the elastic properties (hardness and elastic modulus) of these materials measured by indentation probe, and we try to compare them with our DFT simulations.

[1] J. Goraus, J. Czerniewski, K. Prusik, M. Fijałkowski, *Journal of Alloys and Compounds* 867 (2021) 159078

[2] X. L. Wang, *Phys. Rev. Lett.* 100, (2008) 156404.

[3] S. Ouardi, G. H. Fecher, C. Felser, J. Kübler, *Phys. Rev. Lett.* 110, (2013) 100401;
S. Ouardi, G. H. Fecher, C. Felser, J. Kübler, *Phys. Rev. Lett.* 122, (2019) 059901(E).

Slow spin dynamics in Gd^{III}-based propeller-like qubit candidate and its structural analogues with other lanthanide ions

Gabriela Handzlik¹, Michał Magott¹, Mirosław Arczyński¹, Katarzyna Rzepka¹ and Dawid Pinkowicz¹

¹ Faculty of Chemistry, Jagiellonian University, Gronostajowa 2, 30-387 Kraków, Poland

The family of isostructural complexes [Ln(*phendo*)₄](NO₃)₃·xMeOH (Ln = Y, Gd, Er, Yb) with a helicene-type 1,10-phenanthroline-N,N'-dioxide (*phendo*) ligand was obtained and characterized. AC magnetic measurements revealed that Er^{III}- and Yb^{III}-based compounds exhibit slow relaxation of the magnetization typical for Ln^{III} Single Ion Magnets (SIMs) [1]. Surprisingly, the complex with magnetically isotropic Gd^{III} also shows similar behavior [2].

We have prepared solid state diamagnetic dilutions with the Y^{III} analogue (Gd_xY_{1-x}, x = 0.0017, 0.0047 and 0.0273) in order to eliminate dipole-dipole interactions between paramagnetic ions and the relaxation process related to it. The diamagnetic dilution leads also to a significant shift of the out-of-phase AC magnetic susceptibility maxima towards lower frequencies, therefore we were able to better analyze the processes of slow magnetic relaxation in this complex. Such a slow magnetization dynamics was previously observed only for a handful of Gd^{III} complexes.

Gd_xY_{1-x} compounds were also studied by means of pulse EPR spectroscopy, which revealed that it is a good molecular qubit candidate. The ability to generate arbitrary coherent superposition of states was probed by transient nutation experiments. The resulting Rabi oscillations at different microwave power settings were observed at 20 K (Fig. 1).

Recently, we have been able to separate enantiomers of Δ/Λ-[Ln(*phendo*)₄]³⁺ cations by using enantiomerically pure tris(catechol)arsenate(V) Δ/Λ-[As(cat)₃] counterions. The obtained optically pure complexes {Δ-[Ln(*phendo*)₄]} {Δ-[As(cat)₃]}₂(NO₃)·5MeCN (as well as the opposite Λ enantiomer) open up the possibilities for taking advantage of the chirality of the *phendo* in properties like circular dichroism (Fig. 2) and magneto-chiral dichroism [3].

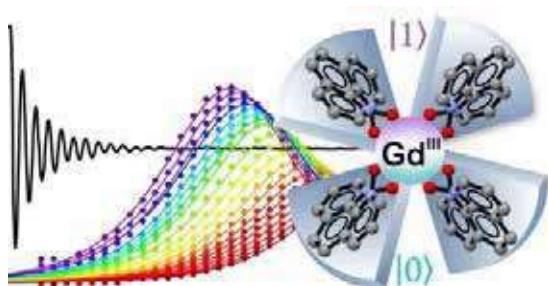


Figure 1: Gd^{III}-based complex as qubit candidate.

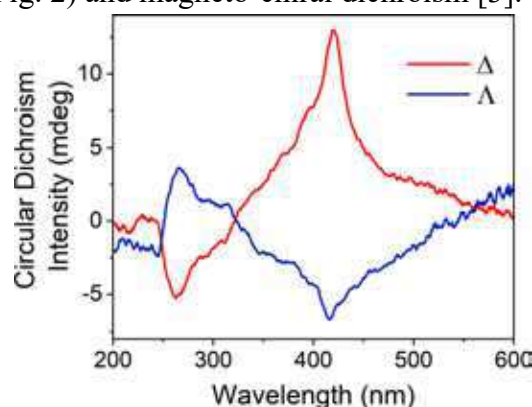


Figure 2: CD spectra of Δ and Λ enantiomers of [Ln(*phendo*)₄][As(cat)₃]₂(NO₃)·5MeCN.

[1] G. Handzlik, M. Magott, M. Arczyński, A. M. Sheveleva, F. Tuna, S. Baran and D. Pinkowicz, *Dalton Trans.* **49** (2020).

[2] G. Handzlik, M. Magott, M. Arczyński, A. M. Sheveleva, F. Tuna, M. Sarewicz, A. Osyczka, M. Rams, V. Vieru, L. F. Chibotaru and D. Pinkowicz, *J. Phys. Chem. Lett.* **11**, 4 (2020).

[3] G. Handzlik, K. Rzepka and D. Pinkowicz, *Magnetochemistry* **7**, 10 (2021).

Magnetism of vanadium and tungsten based polyoxometalates functionalized with phtalocyaniato lanthanide (Y,Yb,Dy) moieties

P. Kozłowski¹, K. Załęski², I. Werner³, R. Pütt⁴ and K.Yu. Monakhov³

¹*Institute of Spintronics and Quantum Information, Faculty of Physics, Adam Mickiewicz University in Poznań, 61-614 Poznań, Poland*

²*NanoBioMedical Centre, Adam Mickiewicz University in Poznań, 61-614 Poznań, Poland*

³*Leibniz Institute of Surface Engineering (IOM), 04318 Leipzig, Germany*

⁴*Institute of Inorganic Chemistry, RWTH Aachen University, 52074 Aachen, Germany*

Lanthanides based single ion magnets have been long considered as candidates for application in spintronics and quantum computing due to their high magnetic moment and high anisotropy resulting in long relaxation time. Polyoxometalates (POM) in turn have usually small anisotropy and a rather small magnetic moment ascribed to a single magnetic ion. However, they are very susceptible to redox processes and as a result often exhibit mixed valence and delocalized magnetism. In this contribution we present hybrid molecules containing a POM core functionalized with a phtalocyaniato lanthanide moiety (LnPc). The main idea behind this concept is to build up systems with a large magnetic moment and a long relaxation time that can be manipulated by a redox prone POM.

It is demonstrated by modeling the DC susceptibility and magnetization that the hybrid based on $P_2V_3W_{15}O_{59}$ Wells-Dawson polyoxometalate reveals localized spin and orbital magnetism for $Ln=Yb^{3+}$. However for a nonmagnetic $Ln=Y^{3+}$ the entire hybrid has a radical character which is due to itinerant unpaired electrons resulting from inter or/and intramolecular charge transfer. None of these hybrids have measurable AC out-of-phase signal. [1]

Hybrid molecules based on $V_{12}O_{32}$ POM and containing $Ln=Dy^{3+}$ exhibit measurable relaxation time, as revealed by AC susceptibility measurements, but only in the magnetic field. The theoretical modeling shows that magnetism in these molecules has two sources: a localized spin and orbital magnetic moment of Dy^{3+} and a magnetic moment coming from an unpaired electron delocalized over POM. The later is due to intermolecular charge transfer. Moreover, it can be demonstrated that there is a weak interaction between Dy^{3+} and a radical electron at POM. The relaxation mechanism is mostly due to quantum tunneling and thermally assisted quantum tunneling which is probably triggered by dipolar magnetic interactions between Dy^{3+} ions and between Dy^{3+} and itinerant electrons. In higher magnetic field also direct processes play a role. [2,3]

[1] R. Pütt, P. Kozłowski, I. Werner, J. Griebel, S. Schmitz, J. Warneke, and K. Yu. Monakhov, *Inorg. Chem.* **60**, 803 (2021).

[2] R. Pütt, X. Qiu, P. Kozłowski, H. Gildenast, O. Linnenberg, S. Zahn, R. C. Chiechi and K. Yu. Monakhov, *Chem. Commun.* **55**, 13554 (2019)

[3] I. Werner, *et al*, *Chemical Science* - in preparation

Magnetic superexchange controlled by light in the family of molecular photomagnets

M. Magott¹, M. Ceglarska², M. Rams², B. Sieklucka¹, D. Pinkowicz¹

¹ Faculty of Chemistry, Jagiellonian University, Gronostajowa 2, 30-387 Kraków, Poland

² Jagiellonian University, Institute of Physics, Łojasiewicza 11, 30-348 Kraków, Poland

Spins can be reversibly generated within a molecular framework as a result of electron transfer triggered by visible light irradiation.^[1] Recently, we have demonstrated that transition from the paramagnetic to the ferrimagnetic state may be also caused by the photochemical process of cyanide dissociation,^[2,3] giving rise to the high-temperature molecular photomagnets.^[4] This is enabled by the effective magnetic interaction between permanently paramagnetic transition metal ions and photogenerated high-spin species. Herein, we show a family of hybrid organic-inorganic frameworks incorporating iron(II) and molybdenum(IV), tungsten(IV), or niobium(IV) ions.^[5] The niobium-analog shows a two-step transition to the antiferromagnetic state, which results from cooperating intra- and inter-chain antiferromagnetic interactions transmitted through cyanides and organic ligands. On the other hand molybdenum- and tungsten-based congeners behave as paramagnets down to 1.2 or 1.3 K, respectively, but due to the 450 nm light irradiation at cryogenic regime ferromagnetic intrachain interactions are activated. This photo-induced switching of the superexchange pathways is reversed upon heating the compounds up to 240 K.

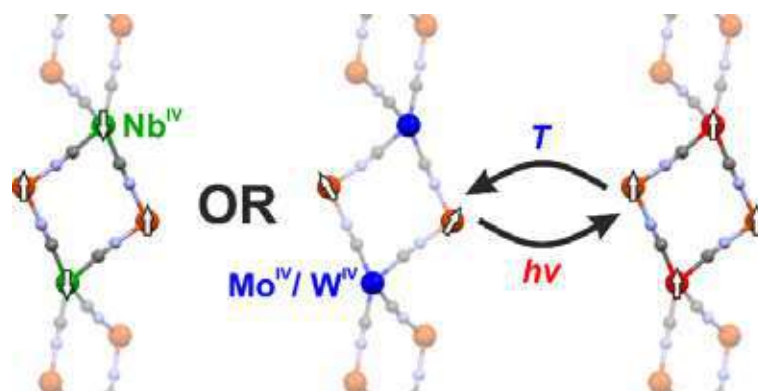


Figure 1: Antiferromagnetic, paramagnetic or ferromagnetically-coupled materials may be achieved in the isostructural family of molecular magnets by combination of chemical design and physical stimuli (light and temperature).

[1] O. Sato, T. Iyoda, A. Fujishima, K. Hashimoto, *Science*, **272**, 704 (1996).

[2] M. Magott, O. Stefańczyk, B. Sieklucka, D. Pinkowicz, *Angew. Chem. Int. Ed.*, **56**, 13283 (2017).

[3] X. Qi, S. Pillet, C. de Graaf, M. Magott, E. Bendeif, P. Guionneau, M. Rouzières, V. Marvaud, O. Stefańczyk, D. Pinkowicz, C. Mathonière, *Angew. Chem. Int. Ed.*, **59**, 3117 (2020).

[4] M. Magott, M. Reczyński, B. Gawęł, B. Sieklucka, D. Pinkowicz, *J. Am. Chem. Soc.*, **140**, 15876 (2018).

[5] M. Magott, M. Ceglarska, M. Rams, B. Sieklucka, D. Pinkowicz, *manuscript under review*

Giant Spin Pumping at Ferromagnet (Permalloy) - Organic Semiconductor (Perylene diimide) Interface

Talluri Manoj,¹ Srinu Kotha,² Bibekananda Paikaray,¹ Dasari Srideep,² Arabinda Haldar,³ Kotagiri Venkata Rao² and Chandrasekhar Murapaka¹

¹ Department of Materials Science and Metallurgical Engineering, Indian Institute of Technology Hyderabad, Kandi-502285, Telangana, India

² Department of Chemistry, Indian Institute of Technology Hyderabad, Kandi-502285, Telangana, India,

³ Department of Physics, Indian Institute of Technology Hyderabad, Kandi-502285, Telangana, India

Spin current injection into non-magnetic materials is essential for the design and development of spintronic devices. So far heavy metals (HM) are used in most of the spintronic devices as non-magnetic layers because of the high spin-orbit coupling (SOC). However, for the very same reason, HM doesn't possess good spin diffusion length and long spin-relaxation time. On the other hand, organic semiconductors (OSC) can host spin current with a large spin diffusion length and long spin-relaxation time due to relatively low SOC. In addition to that, tunability of SOC in OSCs make them a potential contender for HM. In this work, we have employed a robust perylene diimide (PDI) shown in Fig.1(a) which is an n-type organic semiconductor as a non-magnetic material to host spin current. We have deposited various thickness of permalloy (Py or Ni₈₀Fe₂₀) on spin coated PDI (Si/PDI) using magnetron sputtering. Through spin-pumping technique using ferromagnetic resonance (FMR), we have successfully injected spin currents from permalloy (FM) into adjacent PDI(OSC) layer as shown in Fig.1(a). We have confirmed the spin injection through linewidth broadening associated with FMR, which is widely accepted as a direct method to validate spin injection.[1]

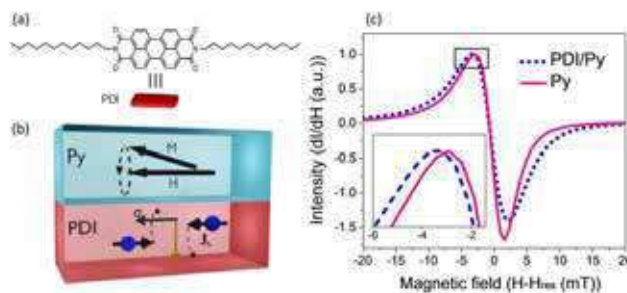


Fig. 1. (a) Molecular structure and schematic representation of PDI, (b) Schematic illustration of device architecture used for spin pumping experiments under FMR conditions. (c) FMR spectra showing change in linewidth.

$$\alpha_{eff} = \alpha_o + \frac{\gamma \hbar g_{TL}}{4\pi M_s t_{FM}} \quad (1)$$

The linewidth broadening is consistently observed in all the samples of PDI/Py(t) where the thickness of Py is 4, 8, 12 and 16 nm. The observed FMR associated linewidth broadening is found to be one order higher (0.53-2.18 mT) than what is reported (0.05 mT) earlier in FM/OSC bilayers [2]. We have quantified the amount of the spin current injected via spin mixing conductance ($g_{\uparrow\downarrow}$) by fitting α_{eff} vs $1/t_{FM}$ to equation (1) and it is found to be $1.54 \times 10^{18} \text{ m}^{-2}$ which is in the similar order of FM/Heavy metal bilayer structures.

[1] Talluri Manoj et.al, RSC Adv., 2021,**11**, 35567-35574

[2] A. Wittmann, G. Schweicher, K. Broch et.al, *Phys. Rev. Lett.*, 2020, **124**, 027204.

Posters

| | | |
|-----------------------|---|-----|
| Anastasiia Doroshenko | <i>Anomalous slow spin relaxation in $[\text{Gd}_2(\text{H}_2\text{O})_6(\text{C}_2\text{O}_4)_3] \cdot 2.5\text{H}_2\text{O}$ complex induced by magnetic field.</i> | 182 |
| Liliia Kotvytska | <i>Realization of low-dimensional magnetism in zeolitic imidazolate frameworks</i> | 183 |
| Robert Ranecki | <i>Spin properties of high-spin ground state, 12-metallacrown-4 complexes on Au(III) investigated by inelastic tunneling spectroscopy</i> | 184 |
| Sawssen Slimani | <i>Colossal magnetoresistance (CMR) and Density functional theory in $\text{La}_{0.4}\text{Ag}_{0.2}\text{Ca}_{0.4}\text{MnO}_3$ polycrystal</i> | 185 |
| Olha Vinnik | <i>Effect of en – H_2O substitution on the ground-state properties of $\text{Cu}(\text{en})\text{SO}_4\text{X}$ ($\text{X} = \text{en}, (\text{H}_2\text{O})_2$) compounds</i> | 186 |

Anomalous slow spin relaxation in $[\text{Gd}_2(\text{H}_2\text{O})_6(\text{C}_2\text{O}_4)_3] \cdot 2.5\text{H}_2\text{O}$ complex induced by magnetic field.

A. Doroshenko¹, R. Tarasenko¹, V. Tkáč¹, V. Kavečanský², E. Čižmár¹, A. Orendáčová¹, R. Smolko³, J. Černák³, M. Orendáč¹

¹*Institute of Physics, Faculty of Science, P.J. Šafárik University in Košice, Park Angelinum 9, 04154 Košice, Slovakia*

anastasiia.doroshenko@student.upjs.sk

²*Slovak Academy of Sciences, Institute of Experimental Physics, Watsonova 47, 04001 Košice, Slovakia*

³*Institute of Chemistry, Faculty of Science, P.J. Šafárik University, Moyzesova 11, 04154 Košice, Slovakia*

Abstract:

Static and alternating magnetic susceptibility, magnetization and electron-spin resonance studies of Gd(III) complex $[\text{Gd}_2(\text{H}_2\text{O})_6(\text{C}_2\text{O}_4)_3] \cdot 2.5\text{H}_2\text{O}$ (GdCO) are reported. The crystal structure of GdCO is built of (6,3) honeycomb layers packed in the ABAB fashion. Magnetic Gd(III) ions occupy the apexes of the slightly deformed hexagons within the layers, while the edges of the hexagons are formed by μ_4 -bis(bidentate) oxalato ligands. The coordination environment of Gd (III) atoms is completed by three aqua ligands and solvate water molecules are enclosed between the layers.

The investigation of static susceptibility in zero-field and field-cooled regimes down to 2 K excluded the formation of magnetically ordered or spin-glass state. The obtained value of the effective magnetic moment at room temperature 8.06 emu.K/mol agrees reasonably with 7.88 emu.K/mol representing the theoretical value expected for isotropic Gd(III) ion with ground multiplet $^8S_{7/2}$, and g-factor $g = 2.0$. Single-ion anisotropy was studied using electron-spin resonance, the analysis of the resonant spectrum at 2 K and in X-band suggested easy-axis anisotropy $D/k_B = -91.2$ mK. with neglected rhombic anisotropy and hyperfine interaction neglected. The magnitude of dipolar interaction $|J/k_B| \approx 12$ mK was estimated considering the distances among Gd(III) ions in the structure.

Dynamic properties were investigated by alternating susceptibility measurements performed in a wide range of frequencies (100 Hz – 10 kHz), temperatures (2 – 30 K) and magnetic fields (0 – 1 T). The width of the distribution of the relaxation times was deduced from the analysis of Cole-Cole diagrams, the resultant values of $\alpha < 0.15$ strongly suggest Debye-type relaxation. Magnetic field significantly slows down spin dynamics and introduces two regimes. At high temperatures, the data can be analyzed assuming standard direct process with pronounced effect of phonon bottleneck. The conditions for the onset of resonant phonon trapping as a potential origin of the phonon bottleneck was verified. The low-temperature regime in which dynamic response accelerates upon cooling is characterized by $\tau \sim T^\beta$ dependence of the relaxation time with $\beta = 1.7 - 3.9$ for magnetic fields in the range 0.1 T – 1 T. The obtained values are consistent with reciprocating thermal behavior proposed for several transition metal and rare-earth-based complexes. However, the difference persists between these experimental results and $\tau \sim T$ dependence representing an alternative prediction for phonon bottleneck effect.

This work was supported by projects **APVV-18-0197** and **GACR 20-01768S**.

Realization of low-dimensional magnetism in zeolitic imidazolate frameworks

L. A. Kotvytska¹, R. Tarasenko¹, R. Feyerherm², S. Gabáni³, O. Lyutakov⁴, M. Orendáč¹, A. Orendáčová¹

¹*Institute of Physics, P. J. Šafárik University, Park Angelinum 9, 04001 Košice, Slovakia*

²*Institut für Quantenphänomene in neuen Materialien Helmholtz-Zentrum Berlin GmbH Hahn-Meitner-Platz 1, 14109 Berlin, Germany*

³*Institute of Experimental Physics of SAS, Watsonova 47, 04001 Košice, Slovakia*

⁴*University Chem & Technol., Dept. Solid State Engn, Technická 5, Prague 16628, Czech Republic*

Zeolitic imidazolate frameworks (ZIFs) are a class of porous metal-organic frameworks that are topologically isomorphic with zeolites. ZIFs are composed of tetrahedrally-coordinated transition metal ions connected via imidazolate linkers.

This work is devoted to the study of the thermodynamic and magnetic properties of two compounds $[\{Zn(mIm)_2 \cdot 2H_2O\}_\infty]$ known as ZIF-8 and $[\{Cu(mIm)_2 \cdot 2H_2O\}_\infty]$, abbreviated as Cu-ZIF-8 where $mIm = 2\text{-methylimidazole} = C_4H_6N_2$. The sample Cu-ZIF-8 can be considered as a structural analog of ZIF-8, since it was found that partial replacement of the Zn(II) ion for Cu(II) did not lead to the significant change in the crystal structure [1].

The heat capacity of powdered samples was measured at temperatures from 0.4 K to 300 K in magnetic fields up to 9 T. Within experimental accuracy, both ZIF-8 and Cu-ZIF-8 data sets are nearly identical, suggesting that the lattice dynamics is not sensitive to the Cu-Zn substitution. At low temperatures, it was found that in a zero magnetic field, the heat capacity of the nonmagnetic ZIF-8 drops to zero, while the Cu-ZIF-8 data begin to grow and form a round maximum at a temperature ~ 0.4 K. The character of the low-temperature data is preserved in the magnetic fields up to 5 T whereas the application of higher fields leads to the significant reduction of the maximum and its shift towards higher temperatures.

The temperature dependence of the magnetic susceptibility of polycrystalline samples was measured in constant magnetic fields of 10 mT and 1 T in the temperature range from 2 to 300 K in field cooling (FC) and zero field cooling (ZFC) regimes. The ZFC susceptibilities of Cu-ZIF-8 and ZIF-8 are characterized by a sharp maximum at about 50 K which shifts towards lower temperatures in the FC data. The origin of the sharp maximum is most likely related to the atmospheric oxygen, which should be to some extent present in the pores of our compounds. At higher temperatures, FC and ZFC data of Cu-ZIF-8 are identical and are characterized by a broad maximum at about 130 K, typical for low-dimensional magnets. The best agreement with the data was obtained for the Heisenberg antiferromagnetic chain model with spin $\frac{1}{2}$ and intrachain interaction $J/k_B \sim 217$ K and $g = 2$. Such a high value of the exchange interaction also explains why it was impossible to observe the corresponding magnetic contribution with the maximal value $C_{\max} \sim 3\text{ J/Kmol}$ at about 100 K in the experimental specific heat which is dominated by lattice contribution. The origin of the aforementioned low-temperature specific heat maximum as well as extremely low values of isothermal magnetizations at helium temperatures are discussed.

[1] K.S. Park et al., Proc. Nat. Acad. Sci. U.S.A. 103 (2006) 10186.

Acknowledgement: The work was supported by the project APVV-18-0197 and GAČR 20-01768S.

Spin properties of high-spin ground state , 12-metallacrown-4 complexes on Au(111) investigated by inelastic tunneling spectroscopy

R. Ranecki¹, S. Lach¹, A. Lüpke², A. Athanasopoulou²,
E. Rentschler², and Ch. Ziegler¹

¹*University of Kaiserslautern (TUK) and Research Center OPTIMAS, Erwin-Schrödinger-Str. 56,
67663 Kaiserslautern, Germany*

²*Inst. of Inorganic and Analytical Chemistry, Johannes Gutenberg, University Mainz, Germany*

High-spin metal-organic complexes are very attractive for the development of memory devices in spintronic applications. However, adsorption of such molecules on a substrate can alter the intermolecular correlation of the spins, resulting in the loss of desired electronic and especially magnetic properties. To investigate such impacts on the magnetic properties, we adsorbed homo-metallic (penta copper(II) core) and hetero-metallic (tetra iron(III)copper(II) core) 12-MC-4 metallacrown molecules [1] on an Au(111) surface by means of new solvent-based in-situ preparation methods. To understand the spin correlation of these adsorbed molecules in more depth, we used Spin-Flip Inelastic Tunneling Spectroscopy (SF-IETS) measurements on single adsorbed molecules. For both metallacrowns, we observe features on the differential conductance spectra, which are symmetric around zero bias and can be attributed to spin-flip excitations. To analyze these data, we use an up to third-order electron transport model [2]. The obtained results of the SF-ITES measurements provide information on the exchange coupling constants and, therefore, the spin multiplicity of the 12-MC-4 metallacrown molecules on the Au(111) surface.

[1] P. Happ et al. Phys. Rev. B 93, 174404 (2016)

[2] M. Ternes, et al. J. Phys. Condens. Matter 21 053001 (2009).

Colossal magnetoresistance (CMR) and Density functional theory in $\text{La}_{0.4}\text{Ag}_{0.2}\text{Ca}_{0.4}\text{MnO}_3$ polycrystal.

S.Slimani ^{*1,2,3}, M.Smari³, R.Hamdi^{3,4}, A.Bajorek⁵, D.Peddis^{1,2}, A.Mabrouki³, I. Walha³, U. Koneva⁶, E. Dhahri³, and Y. Haik⁷.

¹*Istituto di Struttura della Materia, Consiglio Nazionale delle Ricerche, 00010 Rome, Italy.*

²*Dipartimento di Chimica e Chimica Industriale, Università di Genova, 16126 Genova, Italy.*

³*Laboratory of Applied Physics, Faculty of Sciences of Sfax, University of Sfax, 3029 Sfax, Tunisia.*

⁴*College of Health and Life Sciences, Hamad Bin Khalifa University, Qatar Foundation, Doha 34110, Qatar.*

⁵*A.Chelkowski Institute of Physics, University of Silesia, 40-007 Katowice, Poland.*

⁶*REC "Functional Nanomaterials", Immanuel Kant Baltic Federal University, 236001 Kaliningrad, Russia.*

⁷*Department of Mechanical and Industrial Engineering, Texas A & M University, Kingsville, Texas 78363, United States.*

$\text{R}_{1-x}\text{A}_x\text{MnO}_3$ are a class of materials display a broad range of interesting phenomena, due to the interplay of charge, spin, orbital ordering, competing states, and lattice degrees of freedom. Among the exotic phenomena arising from such an interplay, colossal magnetoresistance (CMR), where huge variations in resistance are produced by small magnetic field changes. Here we investigated, morpho-structural, magnetoelectrical, and theoretical studies on $\text{La}_{0.4}\text{Ag}_{0.2}\text{Ca}_{0.4}\text{MnO}_3$ (LACMO) sample. LACMO sample with size distribution $D_{\text{SEM}} = 2.5 \mu\text{m}$ was synthesized using a conventional sol-gel chemical method. The mixed valence states of different chemical elements were revealed by X-ray photoemission spectroscopy. Magnetic characterizations (i.e., magnetic susceptibility, ZFC/FC and magnetic entropy) were carried out using a superconducting quantum interference device magnetometer. Phase separation (PS) phenomenon [1] was observed due of the competition between the super-exchange and the double-exchange (DE) mechanisms [2] within the same material. The MR value was found to be 99% under an applied field of 2 T and the metal-insulator phase transition was found at $T_p \cong 64$ K. Cross-checking the obtained information from structural and magnetic characterization, we have applied the Density functional theory (DFT) and mean-field theory to study the complex behavior of the sample [3].

[1] A.I. Kurbakov, V.A. Ryzhov, V. V. Runov, E.O. Bykov, I.I. Larionov, V. V. Deriglazov, et al., Phys. Rev. B. 100, 1, **2019**.

[2] J.M.D. Coey, M. Viret, S. Von Molnár, Adv. Phys. 48, 167, **1999**.

[3] M. Smari, R. Hamdi, S. Slimani, A. Bajorek, D. Peddis, I. Walha, et al., J. Phys. Chem. C. 124, 23324, **2020**.

Effect of *en* - H₂O substitution on the ground-state properties of Cu(*en*)SO₄X (X = *en*, (H₂O)₂) compounds

O. Vinnik¹, R. Tarasenko¹, M. Orendáč¹, A. Orendáčová¹

¹ Institute of Physics, P. J. Šafárik University, Park Angelinum 9, 04001 Košice, Slovakia

This work is devoted to the comparative study of the magnetic susceptibility and magnetization in quasi-one-dimensional polymer structures Cu(*en*)SO₄X where X = (H₂O)₂ and *en* = ethylenediamine = C₂H₈N₂. The compounds represent the realization of the $S = 1/2$ Heisenberg antiferromagnet on a spatially anisotropic zig-zag square lattice. Previous studies [1] of the organometallic compound Cu(*en*)SO₄(H₂O)₂ showed that the zig-zag square lattice is formed by zig-zag chains with intrachain interaction $J/k_B = 3.5$ K coupled via zig-zag chains with intrachain interaction $J' = 0.35 J$. The magnetic layers organize to 3d long range magnetic order at $T_c = 0.93$ K. The replacement of the water molecule by *en* component preserved the chain-like crystal structure, but the spatial packing introduced changes into the exchange pathways between Cu(II) spins resulting in the more complicated spatial anisotropy of the zig-zag square lattice. The resulting structure consists of zig-zag chains with alternating intrachain interactions J and J' . The intrachain spatial anisotropy is so strong that it precludes the formation of 3d long range order at finite temperatures, suggesting nonmagnetic ground state [2].

To study the influence of the substitution on the properties of Cu(*en*)₂SO₄, the magnetic susceptibility and magnetization of a single crystal were investigated in the magnetic field applied along the *c*-axis. The analysis of the susceptibility measured in the field $B = 1$ T in the temperature range from 2 to 300 K was performed within the Curie-Weiss law and indicates the antiferromagnetic nature of the exchange coupling $zJ/k_B \approx -8.7$ K. In further step the susceptibility data were analyzed within the coupled dimer model in the mean-field approximation. The best results were achieved for the intradimer interaction $J/k_B = -5.5$ K, the effective interdimer coupling $J'/k_B \approx -0.3$ K, and $g = 2.31 \pm 0.1$. The scaling of susceptibility and magnetization data sets measured in $B \parallel c$ and $B \parallel b$ (the latter was taken from ref. 2) revealed good isotropy of exchange couplings. The anisotropy of *g*-factor is the only source of the observed anisotropic behavior in different orientations of magnetic field. Slight differences appear below 4 K as possible manifestation of spin anisotropy. The possibility of field-induced phase transitions to the magnetic ordered state and the impact of the spin anisotropy on their character is discussed for fields higher than the critical field of 7 T at sufficiently low temperatures. The financial support of APVV-18-0197 is acknowledged.

[1] L. Lederová et al., *Phys. Rev. B* **95** (2017) 054436.

[2] O. Vinnik et al., *J. Magn. Mater.* **547** (2022) 168789.

Symposium 8. Magnetic materials for energy applications, including magnetocalorics

| | | |
|-------------------------|---|-----|
| Jader Barbosa Jr. | <i>Developing Near Room-Temperature Magnetic Refrigerators: Lessons Learned and Future Challenges</i> | 190 |
| Daniel José Da Silva | <i>Fully solid state magnetocaloric cooling: an efficient alternative solution for refrigeration</i> | 191 |
| Fengxia Hu | <i>Magnetocaloric materials and multifunctional properties</i> | 192 |
| Francis Johnson | <i>Iron Nitride: a Non-Rare-Earth Containing Permanent Magnet</i> | 193 |
| Jia Yan Law | <i>Designing Competitive High Entropy Alloys for Magnetocalorics</i> | 194 |
| Yaroslav Mudryk | <i>Designing rare earth materials for basic science and magnetic refrigeration</i> | 195 |
| Vivian Andrade | <i>Magnetically Actuated Thermal Switch System: A Performance Evaluation</i> | 198 |
| Siegfried Arneitz | <i>Investigation of the influence of printing parameters and post-processing conditions on the magnetic properties of an additive manufactured Fe-Cr-Co alloy</i> | 199 |
| Agustina Asenjo | <i>Anomalous Nernst effect on magnetic multilayers with perpendicular magnetic anisotropy</i> | 200 |
| Benedikt Beckmann | <i>Arrested martensitic transformations in multicaloric all-d-metal Ni-Co-Mn-Ti Heusler alloys</i> | 201 |
| Alberto Bollero | <i>Sustainability through industrial recycling and advanced manufacturing of nanocrystalline ferrite permanent magnet material</i> | 202 |
| Imants Dirba | <i>High Pressure Reactive Milling of Nd₂Fe₁₄B-based alloys</i> | 203 |
| Andrea Dzubinska | <i>Evolution of magnetic properties of Mn-Fe-P-Si-B alloy: from bulk to microwire</i> | 204 |
| Benedikt Eggert | <i>Modifying magnetic interactions and hysteresis by introducing Mn in La(Fe,Si)₁₃</i> | 205 |
| Cathrine Frandsen | <i>Induction-heated magnetic nanoparticles for catalytic hydrogen production</i> | 206 |
| Andrés García Franco | <i>Fabrication and characterization of Sm-based ThMn₁₂-type compounds for applications as permanent magnets</i> | 207 |
| Sagar Ghorai | <i>Magnetoelastic tuning with site-specific substitution in giant magnetocaloric Fe₂P-type system</i> | 208 |
| Joao H. Belo | <i>Magnetocaloric Effect direct measurement through Time-Dependent Magnetometry</i> | 209 |
| Aritz Herrero Hernandez | <i>High magnetic anisotropy and rotating magnetocaloric effect in Tb₃Ni single crystal</i> | 210 |
| Mieszko Kołodziej | <i>Formation of ThMn12-type phase in (Zr, Nd)_{0.4}Ce_{0.6}Fe₁₀Si₂ alloys and the role of Nd substitution</i> | 211 |
| Piotr Konieczny | <i>Rotating magnetocaloric effect in 2D molecular magnets</i> | 212 |
| Primož Koželj | <i>The FeCoNiPdCu high-entropy alloy: Excellent magnetic softness arising from a nanocomposite structure</i> | 213 |
| Dominik Legut | <i>In search for new rare earth free permanent magnets in CoFeTa system</i> | 214 |
| Johanna Lill | <i>Tuning the magnetic properties of magnetocaloric La(Fe,Si)₁₃ using rare earth doping</i> | 215 |

| | | |
|------------------------|---|-----|
| Ester M. Palmero | <i>Effect of Particle Size in Extruding Flexible Permanent Magnet Filaments from Tuned Composites for Additive Manufacturing</i> | 216 |
| Bosco Rodriguez-Crespo | <i>Additive manufacturing of magnetocaloric 3D structures: A cost-effective way for printing cellulose-based metallic structures</i> | 217 |
| Lukas Schäfer | <i>Novel Processing of Nano-Composite Magnets for Improved Remanence and Coercivity</i> | 218 |
| Ryan Sedek | <i>Nitrogenation study of $\text{Nd}(\text{Fe},\text{Mo})_{12}$ compounds produced by Strip Cast methods</i> | 219 |
| Emil Siuda | <i>Two terminal quantum dot hybrid system as a heat engine</i> | 220 |
| Alessandro Sola | <i>Anomalous Nernst Effect in Polycrystalline MnBi</i> | 221 |
| Milad Takhsha | <i>Influence of Martensitic Configuration on Hysteretic Properties of Heusler Films Studied by Advanced Imaging in Temperature and Magnetic Field</i> | 222 |
| Przemyslaw Zackiewicz | <i>Magnetic properties of high induction metallic ribbons $\text{Fe}_{67}\text{Co}_{20}\text{B}_{13}$ prepared by continuous ultra-rapid annealing method.</i> | 223 |
| Fengqi Zhang | <i>Impact of F and S doping on $(\text{Mn},\text{Fe})_2(\text{P},\text{Si})$ giant magnetocaloric materials</i> | 224 |
| Ivan Batashev | <i>A computer assisted search for the novel magnetocaloric materials</i> | 226 |
| Petro Danylchenko | <i>Experimental Study of Large Rotational Magnetocaloric Effect in $\text{Ni}(\text{en})(\text{H}_2\text{O})_4 \cdot 2\text{H}_2\text{O}$</i> | 227 |
| H Hanggai | <i>Optimization in Room Temperature Magnetocaloric Materials $(\text{MnFe})_{1.9}(\text{PSi})$ Fe-Rich Compounds</i> | 228 |
| Miroslav Hennel | <i>Direct magnetocaloric measurements of Heusler Ni_2MnGa microwires</i> | 229 |
| Anika Kiecana | <i>Magnetism, structure and magnetocaloric properties of $\text{Mn}_3\text{Sn}_{1-x}\text{Zn}_x\text{C}$ antiperovskite carbide</i> | 230 |
| Karolina Kowalska | <i>Rear-earth-based magnetocaloric composites for magnetic refrigerators systems</i> | 231 |
| Ivan Petryshynets | <i>Effect of the shear cutting parameters on the magnetic behavior of Fe-Si electrical steel.</i> | 232 |
| Nakai Shinji | <i>Thermal Equilibrium Compositions of Divalent Cation Substituted W-type Ferrites</i> | 233 |
| Sviatoslav Vovk | <i>Influence of the temperature on electro-magnetic properties of hybrid SMC material</i> | 234 |

Invited Oral Presentations

| | | |
|----------------------|---|-----|
| Jader Barbosa Jr. | <i>Developing Near Room-Temperature Magnetic Refrigerators: Lessons Learned and Future Challenges</i> | 190 |
| Daniel José Da Silva | <i>Fully solid state magnetocaloric cooling: an efficient alternative solution for refrigeration</i> | 191 |
| Fengxia Hu | <i>Magnetocaloric materials and multifunctional properties</i> | 192 |
| Francis Johnson | <i>Iron Nitride: a Non-Rare-Earth Containing Permanent Magnet</i> | 193 |
| Jia Yan Law | <i>Designing Competitive High Entropy Alloys for Magnetocalorics</i> | 194 |
| Yaroslav Mudryk | <i>Designing rare earth materials for basic science and magnetic refrigeration</i> | 195 |

Developing Near Room-Temperature Magnetic Refrigerators: Lessons Learned and Future Challenges

Jader R. Barbosa Jr.

*POLO – Research Laboratories for Emerging Technologies in Cooling and Thermophysics
Department of Mechanical Engineering, Federal University of Santa Catarina, Brazil*

The magnetocaloric effect (MCE) is the thermal response of a magnetic material subjected to a changing magnetic field. Magnetic refrigeration (MR) harvests the MCE in a regenerative thermodynamic cycle to transfer heat from a low-temperature heat source to a high-temperature heat sink by means of magnetic work. Some advantages of MR in comparison with other cooling technologies are (i) the reversibility of the MCE in some materials, (ii) the recovery of magnetization work with the use of permanent magnets and (iii) the absence of harmful substances (e.g., ozone depleting and flammable gases).

Recent results on the design, commissioning and testing of two magnetic cooling prototypes are presented and discussed. The first prototype is a 31-bottle compact magnetic wine cooler; the second prototype is a TRL-6 9000-BTU/h magnetic air conditioner. The presentation focuses on:

1. Developing high-fidelity, artificial intelligence-based methods to design and optimize magnetic circuit-AMR assemblies;
2. Designing, optimizing and integrating ancillary sub-systems, such as heat exchangers, insulated cabinet and hydraulic management systems (flow-magnetic field synchronization and control); and
3. Establishing thermodynamic performance evaluation criteria and test procedures for magnetic refrigerators based on standards and test methods for conventional systems.

Fully solid state magnetocaloric cooling: an efficient alternative solution for refrigeration

D. J. Silva¹

¹ IFIMUP - Institute of Physics for Advanced Materials, Nanotechnology and Photonics, Faculty of Science of the Porto University, Porto, Portugal

The efficient use of energy has become a mainstay in the current world economic growth. The fact that approximately 30% of all energy consumed in the world is used in cooling and heating engines places refrigeration on the top of the priority lists of any modern economy [1]. Vapour compression is still the most used refrigeration technology. However, it requires bulky and noisy compressors. Alternative thermoelectric refrigerators are more compact and environmentally friendly, but at the cost of a much lower efficiency. In a different rank, mainly due to its higher efficiency, is magnetic refrigeration. However, there are still obstacles to overcome. One of the drawbacks is the required complex hydraulic system for the heat transfer phenomena between the magnetocaloric material and the heat exchangers [2].

Fully solid state magnetocaloric refrigerators do not use hydraulic systems. Instead, they rely on thermal management elements (TMEs) to direct the heat flow [3]. Thermal switches and thermal diodes are the most known examples of TMEs. So far, most of the investigation has been devoted to the numerical assessment of the concept applicability [4]. However, efforts in developing proof of concept devices relying in the fully solid state mechanism are now showing some progress. In this talk, an overview of the mechanisms underlying fully solid state magnetocaloric cooling will be given. The status of the ongoing effort in developing an experimental setup will also be covered.

- [1] U. N. E. Programme, The importance of energy efficiency in the refrigeration, air-conditioning and heat pump sectors, Briefing note, 2018.
- [2] A. Kitanovski, *Adv. Energy Mater.* 10 (2020) 1903741.
- [3] D. J. Silva et al., *Applied Energy* 93 (2012) 570.
- [4] D. J. Silva et al., *Int. J. Energy Res.* 45 (2021) 18498.

Magnetocaloric materials and multifunctional properties

Fengxia Hu^{1,2,3}, Jing Wang¹, Baogen Shen^{1,2,3,4}

¹ State Key Laboratory of Magnetism, Institute of Physics, Chinese Academy of Sciences, Beijing 100190, P. R. China

² School of Physical Sciences, University of Chinese Academy of Sciences, Beijing 100049, PR China

³ Songshan Lake Materials Laboratory, Dongguan, Guangdong 523808, PR China

⁴ Ningbo Institute of Materials Technology & Engineering, Chinese Academy of Sciences, Ningbo, 315201, Zhejiang, China

Solid state refrigeration based on magnetocaloric effect has important potential applications and is one of the research hotspots of material science and condensed matter physics. Recently, we have carried out a series of studies on magnetocaloric materials and multifunctional properties [1-5]. Stress regulated phase transition, spin structure and magnetocaloric effect have been investigated. In FeRh/PMN-PT film, nonvolatile reduction of hysteresis loss and dynamic regulation of refrigeration temperature span were realized by introducing strain via electric field [2,3]. Enhanced magnetocaloric effect (MCE) and barocaloric effect (BCE) by hydrostatic pressure have been demonstrated in La(Fe,Co,Si)₁₃ materials, and relevant mechanism was clarified by in-situ neutron powder diffraction (NPD) and first principles calculations. Compared to chemical pressure, the distinct change of atomic environments by physical pressure and the evolution of phase transition nature are responsible for the enhanced MCE and BCE [4]. Moreover, a new cycloidal spiral antiferromagnetic (AFM) structure (CyS-AFM^b), distinct from the AFM configuration of undoped MnNiGe, was found in magnetocaloric material Mn_{0.87}Fe_{0.13}NiGe with Fe doping. In-situ NPD under hydrostatic pressure and magnetic field combined with first principles calculations were conducted to reveal the spin configuration, instabilities and relevant mechanism, and giant baromagnetic effect was demonstrated [1]. By utilizing cone-spiral magnetic structure dominated lattice distortion, giant negative thermal expansion (NTE) was observed in Fe-doped MnNiGe compounds, which provides a new strategy for exploring novel NTE materials [5].

[1] F. R. Shen, F. X. Hu*, B. G. Shen*, et al, *J. Am. Chem. Soc.* **143**, 6798 (2021).

[2] K. M. Qiao, F. X. Hu*, B. G. Shen*, et al, *Nano energy* **59**, 285 (2019).

[3] K. M. Qiao, F. X. Hu*, V. Franco, B. G. Shen*, et al, *Acta Mater.* **191**, 51 (2020).

[4] J. Z. Hao, F. X. Hu*, B. G. Shen*, et al, *Chem. Mater.* **32**, 1807 (2020).

[5] F. R. Shen, F. X. Hu*, B. G. Shen*, et al, *Mater. Horiz.* **7**, 804 (2020).

Iron Nitride: a Non-Rare-Earth Containing Permanent Magnet

Francis Johnson ¹

¹ *Niron Magnetics, Inc., 650 Taft St Suite 400, Minneapolis, MN 55413 USA*

Niron Magnetics, Inc. is commercializing Iron Nitride, a high performance, completely rare earth free permanent magnet technology. Iron Nitride will act as an economical substitute for several grades of both sintered and bonded NdFeB magnets. Niron's Iron Nitride technology is based on progress achieved by the University of Minnesota under work supported by the Department of Energy's Rare Earth Alternatives in Critical Technologies ARPA-E REACT program [1].

These magnets are based on α "-Fe₁₆N₂ compound which has high saturation magnetization and a moderate magnetocrystalline anisotropy due to a tetragonal crystal structure. Iron Nitride is manufactured from low-cost, non-critical elemental components. The unique characteristics of Iron Nitride include a magnetic strength higher than most grades of NdFeB permanent magnets. Test data also indicates that iron nitride exhibits superior temperature stability when compared to NdFeB. Niron's magnets are positioned to substitute for NdFeB in applications such as motors with high torque output.

[1] Jian-Ping Wang, "Environment-friendly bulk Fe₁₆N₂ permanent magnet: Review and Prospective," *J. Mag. Mag. Mat'l*, **497**, 165962 (2020).

Designing Competitive High-Entropy Alloys for Magnetocalorics

Jia Yan Law¹, Álvaro Díaz-García¹, Luis M. Moreno-Ramírez¹ and Victorino Franco¹

¹ Dept. Condensed Matter Physics, ICMS-CSIC, University of Seville, PO Box 1065. 41080-Seville, Spain

High-entropy alloys (HEAs), unlike traditional alloy development, adopt a different design concept: classic alloy design approach uses one or two main constituents while HEAs comprise of several principal elements in large concentrations forming baseless alloys. This design concept enable them with large configurational entropy of mixing values and a huge compositional space which offers a sizeable window of exploration opportunities.

For HEAs in magnetocalorics, they were limited to low-temperature range or showing sub-par performance until recently extensions to the first-generation equiatomic HEA design approach have been devised [1, 2]. Without the reliance on the intrinsic large magnetic moments of rare-earth (RE) elements, a directed search strategy in the non-equiatomic HEA compositional space for RE-free HEAs greatly boosts their performance by orders of magnitude. As shown in Figure 1, this enhancement further closes the pre-existing gap between HEAs versus high-performance conventional magnetocaloric materials [3,4]. In this talk, we will show the strategies to tackle the vast HEA space to tune for the desired magnetocaloric properties (based on isothermal entropy change), surpassing the previous limits of each group of magnetocaloric HEAs.

Work supported by Grant PID2019-105720RB-I00 funded by MCIN/AEI/10.13039/501100011033. Additional support from US/JUNTA/FEDER-UE (grant US-1260179), Consejería de Economía, Conocimiento, Empresas y Universidad de la Junta de Andalucía (grant P18-RT-746), US Air Force Office of Scientific Research (FA8655-21-1-7044) and Sevilla University under VI PPIT-US program.

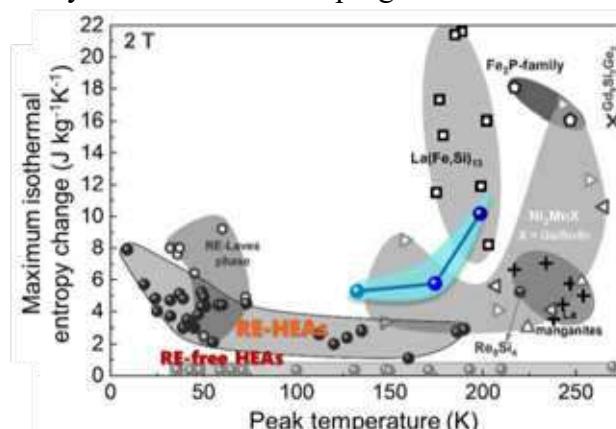


Figure 1. Recently found HEAs through directed search strategy (highlighted blue region) closes the pre-existing gap between HEAs versus high-performance conventional La(Fe,Si)_{13} and Fe_2P materials

- [1] J.Y. Law, V. Franco, Review paper submitted to Journal of Materials Research (2022).
- [2] J.Y. Law, V. Franco, APL Mater. **9**, 080702 (2021).
- [3] J.Y. Law, Á. Díaz-García, L. M. Moreno-Ramírez, and V. Franco, Acta Mater. **212**, 116931 (2021)
- [4] J.Y. Law, L. M. Moreno-Ramírez, Á. Díaz-García, A. Martín-Cid, S. Kobayashi, S. Kawaguchi, T. Nakamura, and V. Franco, J. Alloys Compd. **855**, 157424 (2021).

Designing rare earth materials for basic science and magnetic refrigeration

Y. Mudryk¹, A. Biswas¹, A. K. Pathak,² D. L. Schlagel,¹ and V. K. Pecharsky^{1,3}

¹Ames Laboratory of US Department of Energy, Iowa State University, Ames, IA, USA

²Department of Physics, SUNY Buffalo State, Buffalo, New York 14222, USA

³Department of Materials Science and Engineering, Iowa State University, Ames, IA, USA

Magnetically responsive rare earth (R) compounds find use in a variety of magneto-functional applications due to their unconventional physics and rich chemistry that allows control of their chemical behaviors by chemical substitution. Many important advances in magnetic refrigeration, starting from the first successful demonstration of cooling by adiabatic demagnetization of gadolinium sulfate to the discovery of giant magnetocaloric effect (MCE) near room temperature in $\text{Gd}_5\text{Si}_2\text{Ge}_2$ [1], involve rare earths.

Cryogenic magnetic cooling is a well-established technology of rapidly emerging technological importance. As the practical need to liquefy industrial gases, such as hydrogen and natural gas, for storage and transportation increases, an efficient and environmentally friendly cryogenic refrigeration offers a solution. The successful advance of this technology, however, requires discovery and design of novel magnetic materials that exhibit strong responses to external stimuli, enabling, among other phenomena, large MCE. Rare earth alloys and compounds are best suited for such purpose, and the search for ideal material among them is a prudent and promising approach.

Here, we report our recent fundamental research on two families of rare earth based intermetallic compounds that exhibit some of the largest MCEs, but also present interesting basic science questions about the nature of their magnetic phase transitions. First, we will present how replacing the most magnetic rare earth element, Gd, with non-magnetic Sc, results in the rise of ferromagnetism [2] and report our recent observation of unconventional electrical transport phenomena in Gd_4ScGe_4 single crystal [3]. The second part of the presentation will focus on R_2In compounds, which undergo discontinuous magnetoelastic transitions at T_C when $\text{R} = \text{Pr}, \text{Nd}, \text{Eu}$ [4]. Recently, we found that the thermodynamic nature of the magnetic ordering transition in Nd_2In is difficult to classify unambiguously, making it a true borderline 1st-to-2nd order material with optimal properties for magnetic refrigeration.

This work was performed at Ames Laboratory and was supported by the Division of Materials Science and Engineering of the Office of Basic Energy Sciences of the U.S. Department of Energy (DOE). Ames Laboratory is operated for the U.S DOE by Iowa State University under Contract No. DE-AC02-07CH11358.

[1] V. K. Pecharsky, K. A. Gschneidner, Jr., *Phys. Rev. Lett.* **78**, 4494 (1997).

[2] Y. Mudryk, D. Paudyal, J. Liu, and V. K. Pecharsky, *Chem. Mater.* **29**, 3962 (2017).

[3] Y. Mudryk, A.K. Pathak, D.L. Schlagel, T.A. Lograsso, and V.K. Pecharsky, *Phys. Rev. B* (submitted).

[4] F. Guillou et al., *Nat. Comm.* **9**, 2925 (2018); A. Biswas, et al., *Phys. Rev. B* **101**, 224402 (2020); W. Liu et al., *Appl. Phys. Lett.* **119**, 022408 (2021).

Oral Presentations

| | | |
|-------------------------|---|-----|
| Vivian Andrade | <i>Magnetically Actuated Thermal Switch System: A Performance Evaluation</i> | 198 |
| Siegfried Arneitz | <i>Investigation of the influence of printing parameters and post-processing conditions on the magnetic properties of an additive manufactured Fe-Cr-Co alloy</i> | 199 |
| Agustina Asenjo | <i>Anomalous Nernst effect on magnetic multilayers with perpendicular magnetic anisotropy</i> | 200 |
| Benedikt Beckmann | <i>Arrested martensitic transformations in multicaloric all-d-metal Ni-Co-Mn-Ti Heusler alloys</i> | 201 |
| Alberto Bollero | <i>Sustainability through industrial recycling and advanced manufacturing of nanocrystalline ferrite permanent magnet material</i> | 202 |
| Imants Dirba | <i>High Pressure Reactive Milling of Nd₂Fe₁₄B-based alloys</i> | 203 |
| Andrea Dzubinska | <i>Evolution of magnetic properties of Mn-Fe-P-Si-B alloy: from bulk to microwire</i> | 204 |
| Benedikt Eggert | <i>Modifying magnetic interactions and hysteresis by introducing Mn in La(Fe,Si)₁₃</i> | 205 |
| Cathrine Frandsen | <i>Induction-heated magnetic nanoparticles for catalytic hydrogen production</i> | 206 |
| Andrés García Franco | <i>Fabrication and characterization of Sm-based ThMn₁₂-type compounds for applications as permanent magnets</i> | 207 |
| Sagar Ghorai | <i>Magnetoelastic tuning with site-specific substitution in giant magnetocaloric Fe₂P-type system</i> | 208 |
| Joao H. Belo | <i>Magnetocaloric Effect direct measurement through Time-Dependent Magnetometry</i> | 209 |
| Aritz Herrero Hernandez | <i>High magnetic anisotropy and rotating magnetocaloric effect in Tb₃Ni single crystal</i> | 210 |
| Mieszko Kołodziej | <i>Formation of ThMn₁₂-type phase in (Zr, Nd)_{0.4}Ce_{0.6}Fe₁₀Si₂ alloys and the role of Nd substitution</i> | 211 |
| Piotr Konieczny | <i>Rotating magnetocaloric effect in 2D molecular magnets</i> | 212 |
| Primož Koželj | <i>The FeCoNiPdCu high-entropy alloy: Excellent magnetic softness arising from a nanocomposite structure</i> | 213 |
| Dominik Legut | <i>In search for new rare earth free permanent magnets in CoFeTa system</i> | 214 |
| Johanna Lill | <i>Tuning the magnetic properties of magnetocaloric La(Fe,Si)₁₃ using rare earth doping</i> | 215 |
| Ester M. Palmero | <i>Effect of Particle Size in Extruding Flexible Permanent Magnet Filaments from Tuned Composites for Additive Manufacturing</i> | 216 |
| Bosco Rodriguez-Crespo | <i>Additive manufacturing of magnetocaloric 3D structures: A cost-effective way for printing cellulose-based metallic structures</i> | 217 |
| Lukas Schäfer | <i>Novel Processing of Nano-Composite Magnets for Improved Remanence and Coercivity</i> | 218 |
| Ryan Sedek | <i>Nitrogenation study of Nd(Fe,Mo)₁₂ compounds produced by Strip Cast methods</i> | 219 |
| Emil Siuda | <i>Two terminal quantum dot hybrid system as a heat engine</i> | 220 |
| Alessandro Sola | <i>Anomalous Nernst Effect in Polycrystalline MnBi</i> | 221 |

| | | |
|-----------------------|---|-----|
| Milad Takhsha | <i>Influence of Martensitic Configuration on Hysteretic Properties of Heusler Films Studied by Advanced Imaging in Temperature and Magnetic Field</i> | 222 |
| Przemyslaw Zackiewicz | <i>Magnetic properties of high induction metallic ribbons $\text{Fe}_{67}\text{Co}_{20}\text{B}_{13}$ prepared by continuous ultra-rapid annealing method.</i> | 223 |
| Fengqi Zhang | <i>Impact of F and S doping on $(\text{Mn},\text{Fe})_2(\text{P},\text{Si})$ giant magnetocaloric materials</i> | 224 |

Magnetically Actuated Thermal Switch System: A Performance Evaluation

Vivian M. Andrade^{1,2}, Ana L. Pires², Daniel Silva², Joana S. Teixeira^{2,3}, Cláudia R. Fernandes², Clara Pereira³, João Ventura² and Joana Oliveira^{1,4}

¹ Department of Engineering Physics, Faculty, of Engineering of University of Porto, R. Roberto Frias, s/n 4200-465 Porto, Portugal

² Institute of Physics for Advanced Materials, Nanotechnology and Photonics of University of Porto, R. do Campo Alegre s/n, 4169-007, Porto - Portugal.

³ REQUIMTE/LAQV, Department of Chemistry and Biochemistry, Faculty of Science of University of Porto, R. do Campos Alegre s/n, 4169-007 Porto, Portugal

⁴ LAETA - INEGI, R. Roberto Frias, s/n 4200-465 Porto, Portugal

Magnetic refrigeration (MR) is among the main candidates to substitute and improve the current conventional systems since it is an environmentally friendly technology; however, the associated high cost still reduces its commercial viability [1]. The use of magnetic nanofluids (MN) has already shown its potential for thermal switches, by reducing the cost and improving the operation efficiency of MR prototypes [2]. A strong sensitiveness of the MN thermal conductivity turns them suitable for high-flux exchange heat systems such as micro-cooling devices, heat pipes and nuclear reactors [3]. For instance, J. Puga et al. have already demonstrated that the heat rejected by a magnetically activated thermal switch (MATS) allows an LED temperature control [4], achieving a 60% temperature span for 10 Hz of operating frequency. The observed temperature span reduction for higher frequencies should be related to the fluid's high viscosity that limits the motion velocity from the heat source to the sink. In this regard, understanding the role of the viscosity and turbulence on the MATS system is required to improve heat exchange rates and, consequently, device operation. Additionally, aiming large-scale purposes, a low-cost and simple MN preparation should be approached using hydrothermal and coprecipitation processes.

Herein, we report the results of a MATS system to evaluate the efficiency of a colloidal dispersion composed of superparamagnetic MnFe_2O_4 nanoparticles ($D=12$ nm,) in 60:40 (V:V) ethylene glycol (EG): H_2O [5] and compare its performance with that of a commercial Fe_3O_4 oil-based system. As given in Figure 1, for 80 vol.% of the filled recipient, the temperature span and heat transfer velocity were found to double for the EG: H_2O -based dispersion which presented lower viscosity. This observation is linked to the higher effective conductivity of the EG: H_2O mixture ($0.63 \text{ Wm}^{-1}\text{K}^{-1}$) over the oil ($0.42 \text{ Wm}^{-1}\text{K}^{-1}$) and to the lower viscosity that allows a faster fluid motion between the cold and hot extremities. To understand this behaviour, the MATS recipient (with 3 cm height) was filled with MnFe_2O_4 fluid from 70 to 100 vol.% under the same heating supply ($Q = 238 \text{ W/m}^2$). We found that the 95 vol.% fraction of the MnFe_2O_4 colloidal solution is the best suitable to improve the heat transfer, presenting temperature spans above 60%. For all the measured nanofluid volumes, a three-step temperature change is seen when the magnetic field is applied, expanding the heat exchange time during the operation. In addition, a polynomial trend is observed for the temperature difference between the cold and hot walls, with a maximum efficiency occurring for an operation frequency of 0.3 Hz. These observations reveal that surface tensions and viscosity play an important role in the operation optimization of the MATS system [3,4].

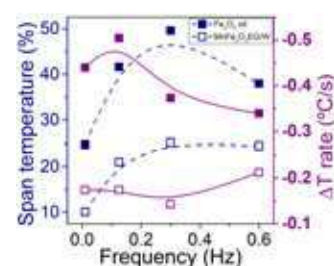


Figure 1: Frequency dependence of (right) Span temperature and (left) temperature change rate for Fe_3O_4 (open) and MnFe_2O_4 (closed) fluids.

- [1] A. Kitanovsky, *Advanced Energy Materials* 10, 1903741 (2020).
- [2] D. Silva et al., *J. of Magnetism and Magnetic Materials* 533, 167979 (2022)
- [3] R. B. Ganvir et al., *Renewable and Sustainable Energy Reviews* 75, 451 (2017).
- [4] J. Puga et al., *Nano Energy* 31, 278 (2017).
- [5] C. Pereira et al., *Chemistry of Materials*, 24, 1496 (2012).

Investigation of the influence of printing parameters and post-processing conditions on the magnetic properties of an additive manufactured Fe-Cr-Co alloy

S. Arneitz¹, R. Buzolin¹, S. Rivoirard² and C. Sommitsch¹

¹ Institute of Materials Science, Joining and Forming, Graz University of Technology, Kopernikusgasse 24/I, 8010 Graz (Austria)

² Institute Néel, CNRS, 25 rue the Martyrs BP 166, 38042 Grenoble Cedex 9 (France)

1. Incentive of the study

In recent years, additive manufacturing has become more and more relevant for producing magnetic materials due to higher demands for miniaturisation and complex-shaped magnet parts. [1] With laser powder bed fusion (LPBF), magnet parts of the Fe-Cr-Co system can be produced with notable shape accuracy. The chemical composition can be modified directly in the printing chamber with the in-situ alloying technique. With this novel method, complex alloys can be produced with a chemical composition accustomed to each specific application case. This study aimed to determine the influence of the process conditions on the magnetic properties of selected 3D printed magnet parts.

2. Description of the work

Fe-Cr-Co is an Fe-Co based magnetic alloy, which obtains its hard magnetic properties due to a spinodal decomposition of a solid- solution alpha phase with bcc crystal structure into a ferromagnetic Fe-Co phase and a paramagnetic Cr-Fe matrix. The phase transformation occurs during heat treatment at a given temperature in the presence of a high magnetic field. The LPBF process in combination with in-situ alloying can have a considerable influence on microstructure (e.g. homogeneity, grain size, amount of misorientation). The effect of this influence on magnetic properties has been investigated by treating samples, printed with a defined set of printing parameter which are known to produce sound parts in this material, inside a high magnetic field. Additionally, the influence of different post- processing steps has been investigated by subjecting samples printed with identical parameter to different treatments before magnetic measurement. The magnetic properties (i.e. coercivity, remanence and maximum energy product) have been measured and different materials characterisation methods (i.e. EBSD, TEM) have been applied to obtain a complete picture of the influence of process conditions on magnetic properties.

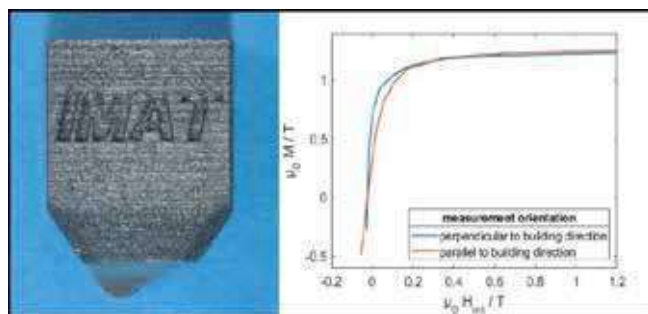


Figure 1: One of the Fe- Cr- Co samples printed with LPBF and its corresponding measured coercivity. A slight anisotropy in magnetic properties with respect to the build-up direction of the process can be observed

[1] E. A. Périgo, J. Jacimovic, F. García Ferré, und L. M. Scherf, *Addit. Manuf.* **30**, 100870 (2019)

Anomalous Nernst effect on magnetic multilayers with perpendicular magnetic anisotropy

Guillermo Lopez-Polin¹, Hugo Aramberri², Jorge Marques-Marchan¹, Ben Weintrub³, Kirill I. Bolotin³, Jorge Iribas Cerda¹, Agustina Asenjo¹

¹Instituto de Ciencia de Materiales de Madrid (ICMM-CSIC), 28049, Madrid, Spain

²Luxembourg Institute of Science and Technology, 4362 Esch-sur-Alzette, Luxembourg

³Freie Universitat Berlin, 14195, Berlin, Germany

Anomalous Nernst Effect (ANE) is a thermomagnetic effect, which has attracted interest during the last decade due to its potential to produce electric harvesting devices. Nernst effect arises in presence of a thermal gradient perpendicular to a magnetic field, resulting in an electric field perpendicular to both [1]. The effect is anomalous when it is produced by the intrinsic magnetization instead of an external magnetic field. During the last decade, materials with increasing ANE coefficients and lower costs has been found [2,3].

In comparison with Seebeck effect, the transversal nature of ANE have some advantages, namely it allows lateral configurations with simpler design, higher performance and much lower production cost. Moreover, to optimize the ANE a high remanent magnetization is needed, as occurs in materials with high Perpendicular Magnetic Anisotropy as the Co/Pt multilayers [4]. Microscale devices of CoPt (Fig 1a) are used to study the dependence of the Nernst effect with the temperature (Fig 1c) and the magnetic configuration. Magnetic Force Microscope (MFM) images of the CoPt stripe were obtained during the measurements of the Nernst voltage (Fig 1b). A maximum ANE coefficient of $\sim 1\mu\text{V/K}$ for [CoPt] $\times 10$, which is much higher than that of Co and in the same order of magnitude of the higher values measured so far [5,3]. Record power densities of around 11W/cm^3 were also obtained in this CoPt based microdevices.

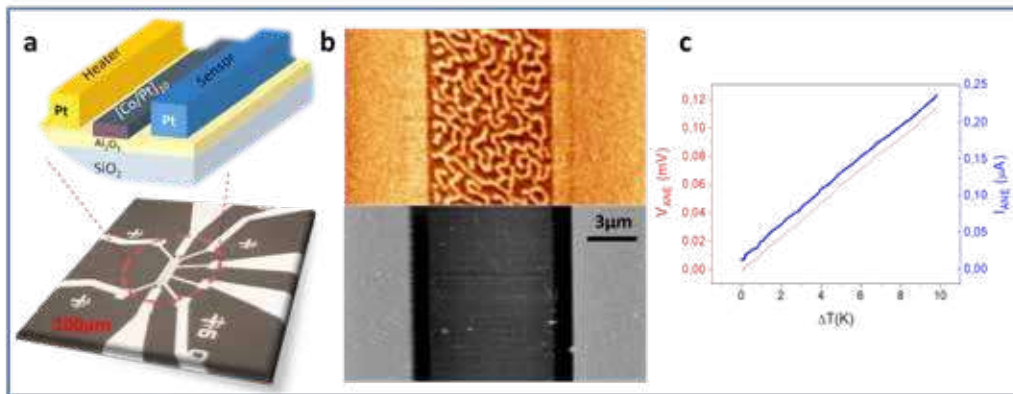


Figure 1: a) Scheme and optical microscope image of the microdevice. b) AFM and MFM images of the microdevice at remanent state. c) Voltage and current obtained as a function of the thermal gradient

- [1] G. E. Bauer, E. Saitoh, B. J. Van Wees, *Nature Materials* **11** (5), 391-399 (2012),
- [2] A. Sakai et al., *Nature Physics* **14** (11), 1119-1124 (2018).
- [3] B. He et al., *Joule* **5** (11), 3057-3067 (2021).
- [4] S. Hashimoto et al. *Journal of Applied Physics* **66**, 4909 (1989)
- [5] A. Sakai et al. *Nature*, 581(7806), 53-57 (2020).

Arrested martensitic transformations in multicaloric all-d-metal Ni-Co-Mn-Ti Heusler alloys

B. Beckmann¹, A. Taubel¹, L. Pfeuffer¹, T. Gottschall², D. Koch¹,
F. Scheibel¹, K. Skokov¹ and O. Gutfleisch¹

¹Institute of Materials Science, Technical University of Darmstadt, Darmstadt 64287, Germany

²Dresden High Magnetic Field Laboratory (HLD-EMFL), Helmholtz-Zentrum
Dresden-Rossendorf, Dresden 01328, Germany

Ni-Mn-based Heusler alloys display precisely tunable first-order martensitic transformations and are promising candidates for multicaloric cooling cycle applications [1]. In this work, novel all-d-metal $\text{Ni}_{50-x}\text{Co}_x\text{Mn}_{50-y}\text{Ti}_y$ Heusler alloys (Fig. 1 (a)), showing an enhanced mechanical stability, are analyzed with respect to their magnetic, structural, microstructural and caloric properties [2]. A systematic heat treatment optimization results in a tailored microstructure and leads to large isothermal entropy changes up to $38 \text{ Jkg}^{-1}\text{K}^{-1}$ and adiabatic temperature changes up to -3.8 K for the first field application in moderate magnetic field changes of 2 T . In addition, the contradictory role of the magnetic entropy contribution [3,4], which leads to arrested martensitic transformations in the $\text{Ni}_{50-x}\text{Co}_x\text{Mn}_{50-y}\text{Ti}_y$ inverse magnetocaloric Heusler alloys (Fig. 1 (b)), is discussed.

We acknowledge financial support from DFG (CRC/TRR 270) and ERC (Adv. Grant No. 743116).

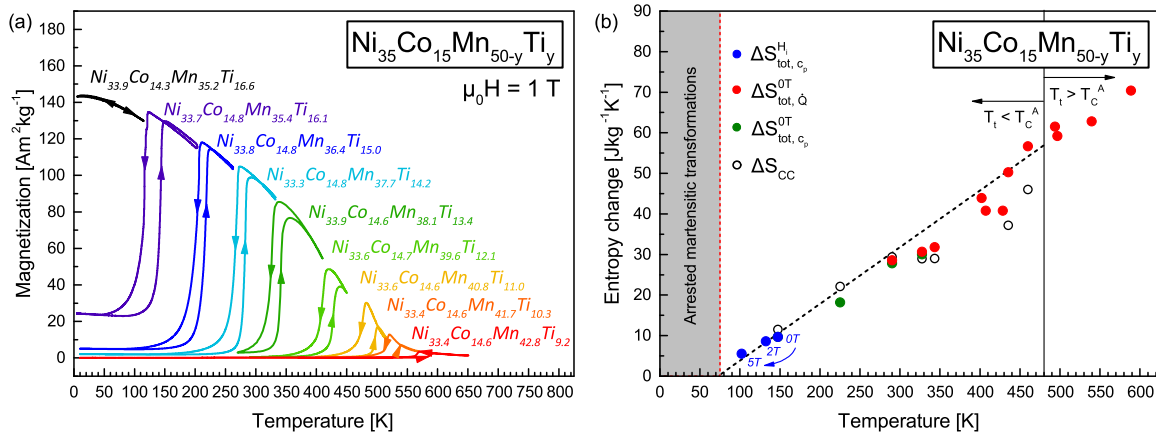


Figure 1: Temperature-dependent magnetization in a magnetic field of 1 T (a) and total entropy change (b) of the martensitic transformations of $\text{Ni}_{35}\text{Co}_{15}\text{Mn}_{50-y}\text{Ti}_y$ Heusler alloys.

- [1] T. Gottschall et al., *Nat. Mater.* **17**, 929-934 (2018).
- [2] A. Taubel et al., *Acta Mater.* **201**, 425-434 (2021).
- [3] T. Gottschall et al., *Phys. Rev. B* **93**, 184431 (2016).
- [4] F. Scheibel et al., *Energy Technol.* **6**, 1397-1428 (2018).

Sustainability through industrial recycling and advanced manufacturing of nanocrystalline ferrite permanent magnet material

A. Bollero,¹ D. Casaleiz,¹ E.M. Palmero,¹ J. de Vicente,¹ A. Seoane² and R. Altimira²

¹Group of Permanent Magnets and Applications, IMDEA Nanoscience, 28049 Madrid, Spain

²Company Ingeniería Magnética Aplicada, IMA S.L.U., 08291 Ripollet, Spain

Ferrite magnets are one of the most widely used permanent magnets in the world, accounting for the highest production of magnetic materials by weight and experiencing a yearly increase strongly driven by energy and transport applications [1]. The possibility of improving their properties and operating performance –while avoiding critical raw materials (e.g. rare earths)– has led to on-going actions sustained on solid scientific-technological pillars and focused on the creation of future industrial pilot plants in Europe [2].

This work shows the use of improved Sr-ferrite ($\text{SrFe}_{12}\text{O}_{19}$) as precursor powder obtained from a recycling process [3] to produce new bonded material for conventional (extrusion) and emerging (3D-printing) technologies. The recycling process (free of any chemicals) was applied to the residues generated in the manufacture of commercial ferrite magnets and allowed achieving a nanocrystalline powder with a 3.5-fold increase in coercivity and a 25% increase in remanence, by comparison with the brand-new commercial powder [Fig. 1(a)]. This improved ferrite has been embedded in a polymeric matrix by solution-casting [4], resulting in a composite with tuneable magnetic properties based on the permanent magnet content. By comparison with the industrial approach (mechanical mixing), the method here presented combines the possibility of choosing the polymer according to the final application with an improved homogeneity, while guaranteeing scalability. We will discuss successful extrusion of meters-long ferrite filament and the possibility of 3D-printing ferrite objects [Figs. 1(b)-(c)] [4].

These results show the possibility of combining nanoscience and novel technological approaches to achieve sustainability, reduce the environmental impact and provide a feasible scalable route in the production of improved rare earth-free permanent magnets.

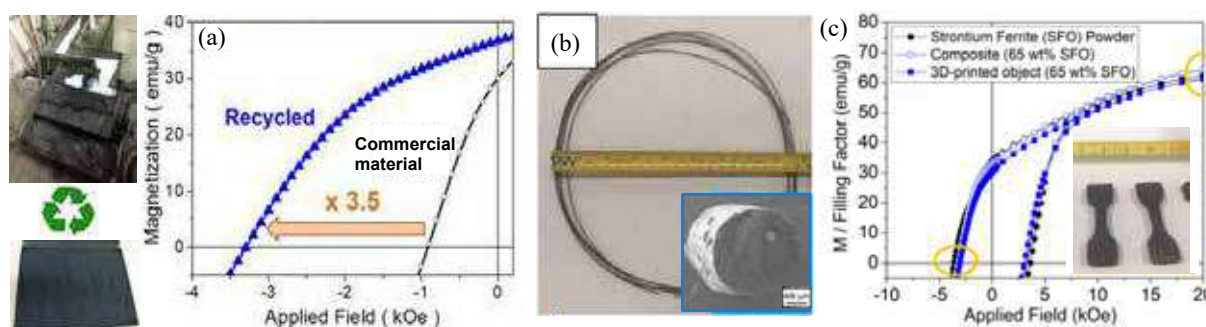


Figure 1: (a) 2nd quadrant hysteresis loop: comparison recycled ferrite vs commercial powder used for magnets fabrication; (b) magnetic filament prepared from recycled ferrite/polymer composite; and (c) preservation of the magnetic properties after processing: recycled Sr-ferrite, magnetic composite and 3D-printed objects (inset).

[1] Bollero, A. and Palmero, E. M., *Recent advances in hard-ferrite magnets*, in J.J. Croat and J. Ormerod (eds.) *Modern Permanent Magnets*, pp. 65-112, Elsevier (2022)

[2] EU H2020 *PASSENGER* project (Ref. 101003914): <https://cordis.europa.eu/project/id/101003914>

[3] Bollero, A. *et al.*, *ACS Sustainable Chem. Eng.* **5** (4), 3243 (2017)

[4] Palmero E.M. *et al.*, *Sci. Technol. Adv. Mater.* **19**, 465 (2018); *Submitted* (2022).

High Pressure Reactive Milling of Nd₂Fe₁₄B-based alloys

I. Dirba, A. Aravindhan, M. Muneeb, O. Gutfleisch

Functional Materials, Institute of Materials Science, Technical University of Darmstadt, Alarich-Weiss-Straße 16, 64287 Darmstadt, Germany

Enhancing coercivity of Nd-Fe-B permanent magnets towards the theoretical limit given by the anisotropy field would enable more cost- and energy-efficient raw materials utilization by reducing heavy rare-earth elements such as Dy or Tb. Coercivity can be increased by reducing the grain size close to the critical single domain criteria. However, practically handling fine powders on industrial scale is difficult due to oxidation. In this light, the hydrogenation disproportionation desorption recombination (HDDR) process [1] offers advantage since sub-micron grains can be realized in large tens of micrometers particles. In this work, we investigate the possibility to further reduce the grain size and thus increase coercivity by using the high-pressure reactive milling (HPRM) technique [2,3].

Nd-Fe-B alloys prepared by induction melting and subsequent homogenization are subjected to first hydrogen decrepitation and milling in a planetary ball mill under 150 bar hydrogen in a high-pressure milling vial with *in operando* pressure and temperature monitoring. This results then in the disproportionation of Nd₂Fe₁₄B phase according to reaction (1), which is reversible and recombination back into the Nd₂Fe₁₄B phase is achieved after a subsequent vacuum heat treatment in another recipient. Figure 1 shows that nearly one order of magnitude grain size reduction from 376 ± 125 nm for d-HDDR processed (a) to 52 ± 12 nm in the case of HPRM (b) is achieved. The influence of processing parameters on the resultant magnetic properties and microstructures will be presented.

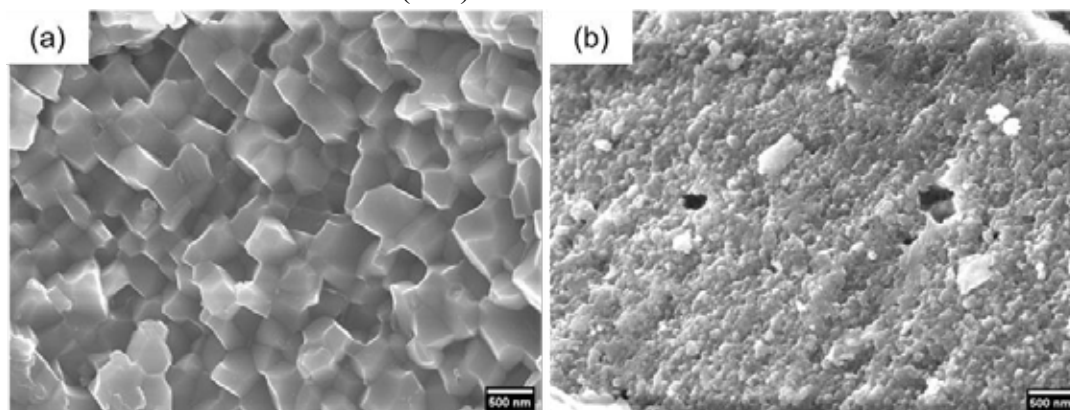
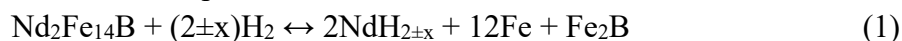


Figure 1: Microstructure of fully recombined Nd-Fe-B powders: after conventional HDDR (a) and after HPRM + desorption (b).

References

- [1] O. Gutfleisch, G. Drazic, C. Mishima, Y. Honkura, IEEE Trans. Mag. **38**(5), 2958–2960 (2002).
- [2] O. Gutfleisch, A. Bollero, M. Kubis, K.H. Müller, L. Schultz, J. Metastable Nanocryst. Mater., **8**, 405–410 (2000).
- [3] K. Güth, J. Lyubina, B. Gebel, L. Schultz, O. Gutfleisch, J. Magn. Magn. Mater. **324** (2012) 2731–2735.

Evolution of magnetic properties of Mn-Fe-P-Si-B alloy: from bulk to microwire

A. Dzubinska¹, M. Ipatov^{2,3}, M. Reiffers⁴, M. Varga¹, T. Ryba⁵, R. Varga^{1,5}, V. Zhukova^{2,3} and A. Zhukov^{2,3,6}

¹CPM-TIP, University of Pavol Jozef Safarik, Tr. SNP 1, 040 11 Kosice, Slovakia

²Department of Polymers and Advanced Materials: Physics, Chemistry and Technology, Faculty of Chemistry, University of Basque Country (UPV/EHU), 200 18 San Sebastian, Spain

³Departamento de Física Aplicada, Escuela de Ingeniería de Gipuzkoa, University of Basque Country (UPV/EHU), 200 18 San Sebastian, Spain

⁴Fac. of Hum. and Nat. Sciences, University of Presov, Ul. 17. novembra 1, 080 01 Presov, Slovakia

⁵RVmagnetics, Nemcovej 30, Kosice, 040 01, Slovakia

⁶IKERBASQUE, Basque Foundation for Science, 480 11 Bilbao, Spain

Functional intermetallic materials include a host of possibilities for their application in actual practice. The first and often essential step is their preparation and subsequent study of their physical and chemical properties. During the last decades, theoretical and experimental interest has focused on the characterization of bulk Mn-Fe-P-Si-B based system as a suitable candidate for magnetocaloric applications [1]. The relationship between size reduction and magnetoelastic coupling plays a key role. In the field of downsizing, some novel devices have been proposed as micro-refrigerators [2], thermal switches [3], microfluidic pumps [4], energy harvesting devices [5] and biomedical applications [6].

In this work, we have prepared and studied crystal structure, microcrystallinity and magnetic properties of Mn-Fe-P-Si-B alloy in bulk and microwire form, prepared by Taylor-Ulitovsky method. The X-ray diffraction results show a multi-phase composition of the hexagonal $P-62m$ and secondary cubic $Im-3m$ phase. The scanning electron microscopy with EDX function confirms stoichiometric composition. From the isothermal magnetization data, magnetic entropy changes $-\Delta S_M$ was determined by a formula using Maxwell's thermodynamic relations. Magnetic data indicates structural transition.

The authors expect continued experimental research of Mn-Fe-P-Si-B material to open the new possibility of being more environmentally friendly and unlocked technical practice, which recommends studied material for possible future applications.

This research work was supported by VEGA 1/0404/21 and VVGS-2022-2117.

- [1] F. Zhang, Ch. Taake, B. Huang et al., *Acta Materialia* **224**, 117532 (2022).
- [2] D. J. Silva, B. D. Bordalo, A. M. Pereira et al., *Applied Energy* **93**, 570-574 (2012).
- [3] K. Klinar, M. M. Rojo, Z. Kutnjak et al., *J. Refrig.* **33** (3), 449-464 (2010).
- [4] S. Pal, A. Datta, S. Sen et al, *J. Magn. Mater.* **323** (21), 2701-2709 (2011).
- [5] D. N. Ba, L. Beccerra, M. Marangolo et al., *Phys. Rev. Appl.* **15** (6) 064045 (2021).
- [6] X. L. Liu, Y. F. Zhang, H. M. Fan et al., *Theranostics* **10** (8), 3739-3815 (2020).

Modifying magnetic interactions and hysteresis by introducing Mn in $\text{La}(\text{Fe},\text{Si})_{13}$

Benedikt Eggert¹, Johanna Lill¹, Cynthia Pillich¹, Alexandra Terwey¹, Iliya Radulov², Fabrice Wilhelm³, Andrei Rogalev³, Mauro Rovezzi³, Konstantin Skokov², Katharina Ollefs¹, Oliver Gutfleisch², Markus E. Gruner¹ and Heiko Wende¹

¹*Faculty of Physics and Center for Nanointegration Duisburg-Essen (CENIDE), University of Duisburg-Essen, Lotharstr. 1, 47057 Duisburg, Germany*

²*Institute of Materials Science, Technical University of Darmstadt, Darmstadt 64287, Germany*

³*European Synchrotron Radiation Facility, Grenoble F-38043, France*

Materials with first-order magnetostructural phase transition exhibit a large magnetocaloric effect and may lead to an environmentally friendly and energy-efficient alternative to conventional vapor compression refrigeration [1]. Here, materials such as FeRh, NiMn-based Heusler alloys or $\text{La}(\text{Fe},\text{Si})_{13}$ exhibit a sizeable magnetocaloric effect, characterized by a large adiabatic temperature change ΔT_{ad} and isothermal entropy change ΔS_{iso} at the phase transition temperature T_{tr} . In order to replace gas compression refrigeration, it is necessary to tune the phase transition close to room temperature and try to minimize the thermal hysteresis. For $\text{La}(\text{Fe},\text{Si})_{13}$, it was shown that it is possible to tailor the phase transition towards room temperature by interstitial H-doping [1], while it is necessary to further dope the system with Mn to avoid phase segregation [2]. In the following, we discuss variations of the electronic and geometric structure in $\text{La}(\text{Fe},\text{Si})_{13}$ with increasing Mn content by means of X-ray absorption Mössbauer spectroscopy. From XMCD and

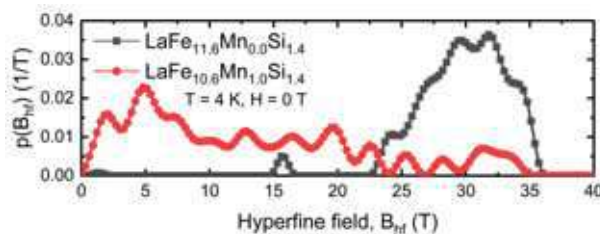


Figure 1: Hyperfine field distribution of the undoped and Mn-doped $\text{La}(\text{Fe},\text{Si})_{13}$ compound. Measurements performed at $T = 4.3\text{ K}$

Mössbauer measurements, we can derive a reduction of the Fe magnetic moment with increasing Mn concentration. For higher Mn-content, Mössbauer measurements indicate a reduction and a broadening of the hyperfine field distribution (see Figure. 1), while in-field measurements indicate a non-collinear spin structure. This is in agreement with DFT calculations [3] that predict antiferromagnetic coupling between Fe and Mn.

By means of Extended X-ray Absorption Fine Structure spectroscopy, we focussed on variations in the short-range ordering. By comparing the fine structure oscillation of La, Fe, and Mn it is evident that increased structural disorder occurs in the first-backscattering shell of La, while similar changes are not so pronounced at Fe or Mn.

We acknowledge the financial support through the DFG (CRC/TRR270) and thank the ESRF for allocation of beamtime.

[1] M. Krautz et al. *Journal of Alloys and Compounds* 598, 27-32 (2014)

[2] O. L. Baumfeld et al. *Journal of Applied Physics* 115, 203905 (2014)

[3] Z. Gersci *Europhysics Letters* 110 47006 (2015)

Induction-heated magnetic nanoparticles for catalytic hydrogen production

C. Frandsen¹

¹ DTU Physics, Technical University of Denmark, DK-2800 Kgs. Lyngby, Denmark

As of today, most of the world's hydrogen is produced from natural gas through steam methane reforming (SMR), a highly endothermic process, in which hydrogen and carbon monoxide are produced in chemical reactors by converting methane and steam at temperatures of up to 950 °C [1]. Conventionally, this process is heated by gas burners on the outside of the reactor tube, causing ~1% of the world's CO₂ emission [1]. Induction-heating by magnetic hysteresis of nanoparticles placed inside chemical reactors, as illustrated in Figure 1, is an interesting alternative approach for heating of high-temperature endothermic catalytic reactions such as SMR [1-4]. Magnetic nanoparticles have the potential to heat locally "from the inside" of the reactor, hence supplying heat where it is needed while avoiding large temperature gradients across the catalyst bed [1-4]. At the same time, the induction heating may be supplied by electricity from renewable sources and may allow for fast reactor startup times potentially exploiting periods of surplus electricity [1-4]. This talk addresses induction heating by magnetic nanoparticles in connection to catalytic hydrogen production. Our recent work shows how CoNi nanoparticles on an alumina support can act both as catalyst and as magnetic susceptor to drive SMR at high methane to hydrogen conversion rate at high temperatures [1-4]. Based on magnetic measurements of CoNi nanoparticles with well-defined compositions and particle sizes, it is shown how Co:Ni

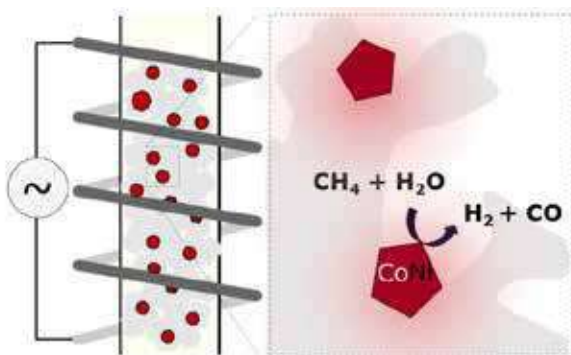


Figure 1: Induction-heated catalytic CoNi nanoparticles driving the SMR process for hydrogen production.

composition can be tuned for optimal performance at given operating temperatures and induction field amplitudes [1]. Moreover, it is shown how Co:Ni composition can be chosen such that Curie temperature prevents overheating [1]. The talk further discusses the applicability of induction heating to drive catalytic reactions [1-4] and compares induction heating with conventional heating [1-4] and resistive heating [5,6] in the case of SMR and more generally.

- [1] M. R. Almind *et al.*, *ACS Applied Nano Materials* **4**, 11537 (2021).
- [2] M. G. Vinum *et al.*, *Angewandte Chemie* **130**, 10729 (2018).
- [3] M. R. Almind *et al.*, *Catalysis Today* **342**, 13 (2020).
- [4] P. M. Mortensen *et al.*, *Industrial and Engineering Chemistry Research* **56**, 14006 (2017).
- [5] S. T. Wismann *et al.*, *Science* **364**, 756 (2019).
- [6] S. T. Wismann *et al.*, *Chemical Engineering Journal* **425**, 131509 (2021).

Fabrication and characterization of Sm-based ThMn12-type compounds for applications as permanent magnets

Andrés García-Franco^{1,2}, James Rosero-Romo^{1,2}, Bosco Rodríguez-Crespo^{1,2}, Paula G. Saiz¹, Jorge Lago², Daniel Salazar¹

¹ *BCMaterials, Basque Center for Materials, Applications and Nanostructures, UPV/EHU Science Park, Barrio Sarriena s/n, 48940 Leioa, Spain.*

² *University of the Basque Country, UPV/EHU Science Park, Barrio Sarriena s/n, 48940 Leioa, Spain.*

The growing interest in novel materials for permanent magnet applications stems from the key role these play in the energy efficiency of technological devices ranging from electrical motors and wind turbines to hard disk drives.

Alloys such as NdFeB and SmCo₅ are among the materials currently being used in these applications. However, their high content in critical raw materials (CRM), such as rare earth elements or Co, has led in the last few years to a renovated scientific effort to find alternative, eco-friendly materials that match their performance. Materials with ThMn12-type structure and lower content in rare-earths and other CRM's are considered primary targets. Nevertheless, the main problem is that the NdFe12 compound is not stable and elements such as Mo, Ti or V are needed to stabilize it. [1]

In this work we have studied the stabilizing effect of V and Mo on SmFe₁₁(Mo,V) samples synthesized by arc-melting. Subsequently, melt-spun ribbons were also prepared by melt-spinning at different wheel speeds in order to investigate their extrinsic properties, such as the influence of the grain size and the microstructure on their coercivity. Coercive fields as high as 0.54T have been obtained for these compositions after varying heat treatments.

XRD was used to determine the crystalline phases of the samples under study and SEM/EDX their microstructure and elemental composition. Samples were then thoroughly characterized magnetically via dc magnetometry using a vibrating sample magnetometer whereas AFM was used to study their surface topography.

Our study corroborates that Sm-Fe alloys with the 1:12 structure containing V and Mo are good candidates for permanent magnet applications.

[1] Schönhöbel, A. M., Madugundo, R., Barandiarán, J. M., Hadjipanayis, G. C., Palanisamy, D., Schwarz, T., Gault, B., Raabe, D., Skokov, K., Gutfleisch, O., Fischbacher, J., & Schrefl, T. (2020). Nanocrystalline Sm-based 1:12 magnets. *Acta Materialia*, 200, 652–658.
<https://doi.org/10.1016/j.actamat.2020.08.075>

Magnetoelastic tuning with site-specific substitution in giant magnetocaloric Fe_2P -type system

Sagar Ghorai¹, Johan Cedervall², Rebecca Clulow³, Martin Sahlberg³ and Peter Svedlindh¹

¹Department of Materials Science and Engineering, Uppsala University, Box 35, SE-751 03, Uppsala, Sweden

²Department of Materials and Environmental Chemistry, Stockholm University, SE, 10691, Stockholm, Sweden

³Department of Chemistry - Ångström Laboratory, Uppsala University, Box 538, 751 21, Uppsala, Sweden

Giant magnetocaloric (GMC) materials constitute a requirement for near room temperature magnetic refrigeration. $(Fe, Mn)_2(P, Si)$ is a GMC compound with strong magnetoelastic coupling. However, the associated large temperature hysteresis (ΔT_{hys}), difference of magnetic transition temperature while cooling and heating is the main hindrance towards the application of this material. Metal site substitution with a nonmagnetic element can substantially reduce ΔT_{hys} . However, the $(Fe, Mn)_2(P, Si)$ compound has two equally populated metal sites, the tetragonally coordinated $3f$ and the pyramidally coordinated $3g$ sites. We have observed a clear difference in saturation magnetization and isothermal entropy change (as high as 37%, see Figure.1) with nonmagnetic element substitution in the $3f$ and $3g$ sites. Antiferromagnetic coupling between Mn atoms in the $3g$ and $3f$ sites is argued to be at the origin of the observed differences in magnetic properties.

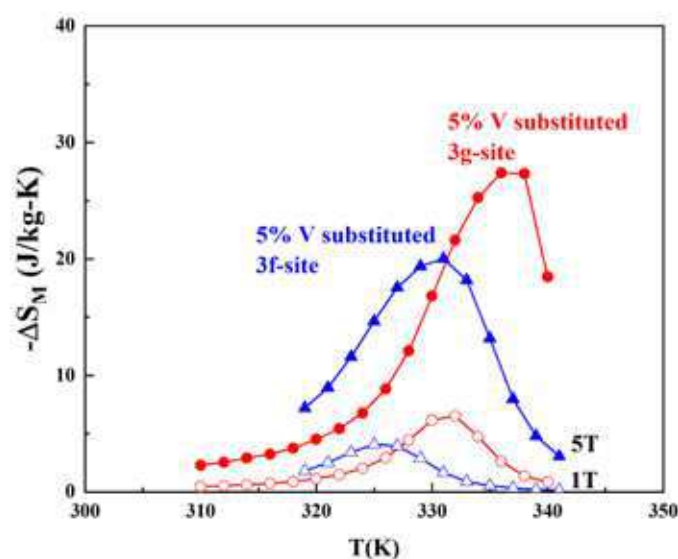


Figure 1: Isothermal entropy change with 5% V substitution in the 3g and 3f sites at $\mu_0 H = 1T$ and $5T$

Magnetocaloric Effect direct measurement through Time-Dependent Magnetometry

R. Almeida¹, C. Amorim², J. S. Amaral², J. P. Araújo¹, J. H. Belo^{*1}

¹ IFIMUP, Departamento de Física e Astronomia, Faculdade de Ciências, Universidade do Porto, Rua do Campo Alegre s/n, 4169-007 Porto, Portugal

² CICECO—Aveiro Institute of Materials, Department of Physics, University of Aveiro, 3810-193 Aveiro, Portugal

The magnetocaloric effect of a given material is typically assessed through indirect estimates of the isothermal magnetic entropy change, ΔS_m . While estimating the adiabatic temperature difference, ΔT_{ad} , is more relevant from the standpoint of refrigeration device engineering, this requires specialized experimental setups, due to the difficulty of assuring adiabaticity [1, 2].

We here present an approach to directly measure ΔT_{ad} through time-dependent magnetometry in a commercial SQUID device. We use Gadolinium as reference material under a 2 T field change and compare our results with results obtained in [3]. For estimating the Gd $\Delta T_{ad}(T)$ curve, we employed a time-dependent protocol for measuring magnetization relaxation in time after applying a 2 T field and subsequently "converted" these into relaxations in temperature through a previously measured $M(T)$ curve, measured at 2 T. Under non-adiabatic experimental conditions, a remarkably similar $\Delta T_{ad}(T)$ curve profile is obtained, however its peak amplitude is underestimated. With a simple compensation methodology, we were able to further approximate the profile of the $\Delta T_{ad}(T)$ curve obtaining the peak amplitude, the maximizing temperature, and the FWHM within relative errors of -4%, -0.7%, and 11%, respectively. Our reported approach makes the measurement of both $\Delta S_m(T)$ and $\Delta T_{ad}(T)$ possible with a single instrument, enabling the accelerated progress towards new, competitive, and industry-ready materials.

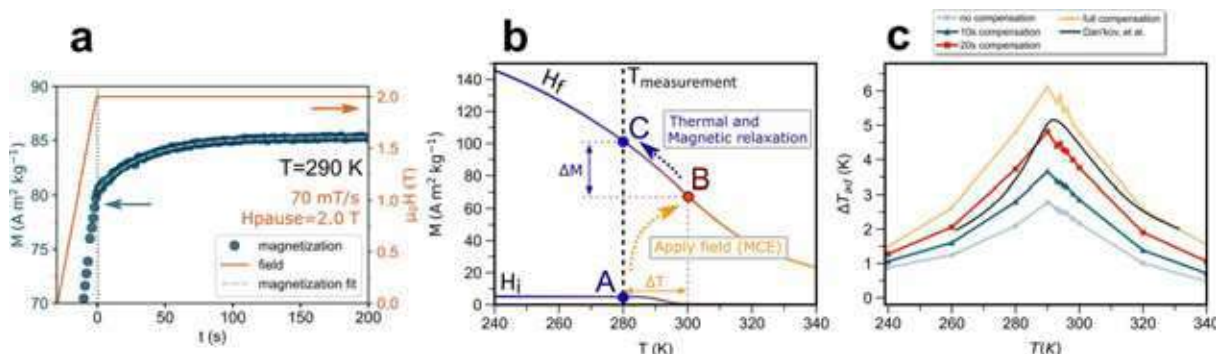


Figure 1: a) Magnetization (left-axis) and field (right-axis) profiles as a function of time under the adopted measurement protocol. b) Schematic representation of the magnetization time-relaxation where Magnetization acts as a “thermometer”. c) Estimation of Gd adiabatic temperature change under a 2T field change as a function of temperature for no-compensation (light blue), 10s (dark-blue), 20s (red) and full compensation (yellow) in comparison with curve presented by Dankov et al in [3].

[1] Y. Koshkidko, J. Cwik, T. Ivanova, S. Nikitin, M. Miller, and K. Rogacki, *Journal of Magnetism and Magnetic Materials*, vol. 433, pp. 234–238, July 2017.

[2] F. Cugini, G. Porcari, C. Viappiani, L. Caron, A. O. dos Santos, L. P. Cardoso, E. C. Passamani, J. R. C. Proveti, S. Gama, E. Bruck, and M. Solzi, *Applied Physics Letters*, vol. 108, p. 012407, Jan. 2016.

[3] S. Y. Dankov, A. M. Tishin, V. K. Pecharsky, and K. A. Gschneidner, *Physical Review B*, vol. 57, pp. 3478–3490, Feb. 1998.

High magnetic anisotropy and rotating magnetocaloric effect in Tb₃Ni single crystal

A. Herrero¹, A. Oleaga¹, and A.F. Gubkin^{2,3}

¹ Departamento de Física Aplicada I, Universidad del País Vasco UPV/EHU, Bilbao, Spain

² M.N. Miheev Institute of Metal Physics, Ekaterinburg, Russia

³ Inst. of Natural Sciences and Mathematics, Ural Federal University, Ekaterinburg, Russia

The magnetic anisotropy of Tb₃Ni and the possibility of exploiting it in order to generate an important rotating magnetocaloric effect (RMCE) have been studied by means of the evaluation of the magnetic properties and magnetic entropy change when a magnetic field is applied along the three different crystallographic axes. Magnetic hysteresis cycles at different temperatures up to 7 T along *a*, *b* and *c* axes have been performed (Fig. 1 left). Our measurements show a clear metamagnetic field induced transition from an AFM state into a FM state when the magnetic field is applied along the *c* axis (easy magnetization axis), whose critical field is highly temperature dependent. This behavior is not found (up to 7T) for the other two directions (hard magnetization plane). Following the discontinuous measuring protocol, the isothermal magnetization curves along the three axes were obtained in the 2-140K temperature range, up to 7 T. The magnetic anisotropy is also observed in these measurements from where we obtain the magnetic entropy change for the three axes. Starting at 2 K a strong inverse magnetocaloric effect (IMCE) followed by a high direct magnetocaloric effect (DMCE) is observed when the field is parallel to *c* axis, while only a small IMCE effect with no practical application is observed when the field is applied along the hard axes. This anisotropy in the MCE effect has been used to evaluate the RMCE produced when the sample is rotated from a hard magnetization axis to an easy one within a fixed magnetic field. The RMCE obtained in this way is one of the largest observed in literature, with $|\Delta S_M^{pk}| = 16.5 \text{ J/kgK}$ and $RC_{FWHM} = 446 \text{ J/kg}$ at 60 K and $|\Delta S_M^{pk}| = 20 \text{ J/kgK}$ (even higher at lower temperatures) and $RC_{FWHM} = 352 \text{ J/kg}$ at 12 K, for $\mu_0 H = 5 \text{ T}$.

These properties make Tb₃Ni a suitable candidate for magnetic refrigeration applications in the gas liquefaction range 4-77 K.

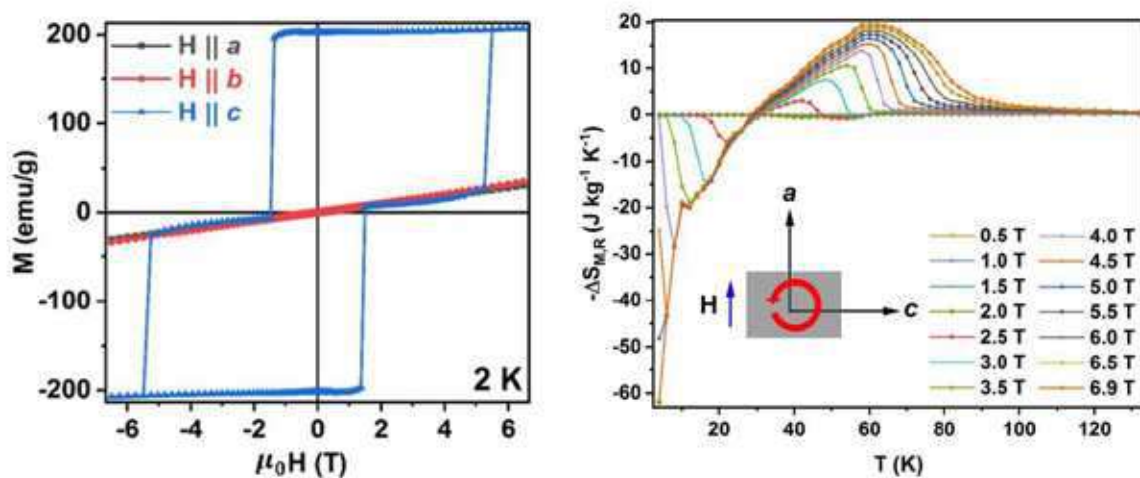


Figure 1: Magnetic hysteresis cycle at 2 K along *a*, *b* and *c* axes (left). RMCE effect (right).

Formation of ThMn₁₂-type phase in (Zr, Nd)_{0.4}Ce_{0.6}Fe₁₀Si₂ alloys and the role of Nd substitution

M. Kołodziej^{1,2}, B. Idzikowski¹, S. Auguste³, J.-M. Greneche⁴, Z. Śniadecki¹

¹ *Institute of Molecular Physics, Polish Academy of Sciences,
M. Smoluchowskiego 17, 60-179 Poznań, Poland*

² *NanoBioMedical Centre of Adam Mickiewicz University,
Wszechnicy Piastowskiej 3, 61-614 Poznań, Poland*

³ *MMM-UMR 6283 CNRS, LUNAM, Faculty of Sciences and Techniques, University of Maine,
Avenue Olivier Messiaen, 72085 Le Mans Cedex 9, France*

⁴ *Institut des Molécules et Matériaux du Mans, IMMM UMR CNRS 6283, Le Mans Université,
Avenue Olivier Messiaen, 72085 Le Mans, Cedex 09, France*

Tetragonal 1:12 structure has been known for over 30 years now [1-3]. There are several compounds from this group which exhibit hard magnetic properties [4]. Their energy product is still lower than that of Nd-based 2:14:1 phase, but the advantage lays on their lower content of rare earth elements (e.g. Nd, Sm). We report on the formation of 1:12 type structure in (Nd, Zr, Ce)Fe₁₀Si₂ alloys, with the emphasis put on the Nd substitution effect [5]. Parent alloy Zr_{0.4}Ce_{0.6}Fe₁₀Si₂ was mainly composed of 1:12 tetragonal structure with addition of bcc-FeSi in as-synthesized state. After replacement of about 50 at.% of Zr atoms with Nd, we observed formation of hexagonal 1:5 structure at expense of 1:12. Trace amount of α -Zr was also observed. To further homogenize our samples, we performed isothermal annealing at 1373 K for 72 h, where various content of the 1:12 structure was observed across the entire range of Zr/Nd substitution. Moreover, formation of bcc-FeSi was also facilitated by the annealing. We further performed ⁵⁷Fe Mössbauer spectrometry, which confirmed much higher homogeneity and much more uniform morphology for the annealed samples.

[1] P. Stefański, *Acta Phys. Pol. A* **85**, 615 (1994)

[2] Y. Harashima et al., *J. Appl. Phys.* **124**, 163902 (2018)

[3] F. Maccari et al., *Acta Mater.* **180**, 15 (2019)

[4] P. Tozman et al., *Scr. Mater.* **194**, 113686 (2021)

[5] Y. Harashima et al., *J. Appl. Phys.* **124**, 163902 (2018)

Acknowledgements

This work was financially supported by the project “Środowiskowe interdyscyplinarne studia doktoranckie w zakresie nanotechnologii” (“Environmental interdisciplinary doctoral studies in nanotechnology”) No. POWR.03.02.00-00-I032/16 under the European Social Fund Operational Programme Knowledge Education Development, Axis III Higher Education for Economy and Development, Action 3.2 PhD Programme.

Rotating magnetocaloric effect in 2D molecular magnets

P. Konieczny¹, R. Pełka¹,
D. Czernia¹

¹ The Henryk Niewodniczański Institute of Nuclear Physics Polish Academy of Sciences,
Radzikowskiego 152, 31-342 Kraków, Poland

Recently a new type of the magnetocaloric effect, the rotating magnetocaloric effect (RMCE), has been introduced. In this effect the applied field is constant and the magnetic material (in a crystal form) is rotated. For samples with significant magnetic anisotropy, the magnetic entropy will depend on the orientation of the magnetic material in respect to the direction of the field. This change of the entropy can be used for cooling cycles.

In our work we have focused on RMCE in low dimensional molecular magnets with weak and significant magnetic anisotropy. In a 2D compound with easy plane anisotropy based on Mn(II) and Nb(IV) ions ($\{[\text{Mn}^{\text{II}}(\text{R-mpm})_2][\text{Nb}^{\text{IV}}(\text{CN})_8]\} \cdot 4\text{H}_2\text{O}$, where mpm = α -methyl-2-pyridinemethanol) [1], the study of conventional magnetocaloric effect (MCE) have shown an anisotropy of magnetic entropy change (ΔS_m) and an inverse magnetocaloric effect (iMCE) in the hard axis orientation. The anisotropy of ΔS_m was employed to study the RMCE. We have also showed that the iMCE can be used to enhance the RMCE. Our measurements proved that magnetic entropy change for RMCE was 51% greater than for the conventional MCE in easy plane orientation in certain conditions. To check the strong anisotropy case, the 2D cyanido-bridged bilayered network $(\text{tetrenH}_5)_{0.8}\{\text{Cu}^{\text{II}}[\text{W}^{\text{V}}(\text{CN})_8]_4\} \cdot 7.2\text{H}_2\text{O}\}_n$ with significant 2D XY magnetic anisotropy and topological phase transition was investigated [2].



Despite the fact that in this case the magnetic properties originate from small magnetic moments of the Cu(II) and W(V) ions ($S = 1/2$ in both), the observed RMCE was one order of magnitude stronger than in weak anisotropy case. The enhancement of RMCE by iMCE over the conventional MCE (in easy plane orientation) reached about 50 %. Moreover, an inverse RMCE was observed.

Figure 1: The idea of rotating magnetocaloric effect.

[1] P. Konieczny, Ł. Michalski, R. Podgajny, S. Chorąży, R. Pełka, D. Czernia, S. Buda, J. Młynarski, B. Sieklucka, T. Wasiutyński, *Inorg. Chem.*, 56 (2017) 2777-2783.

[2] P. Konieczny, R. Pełka, D. Czernia, R. Podgajny, *Inorg. Chem.*, 56 (2017) 11971-980.

The FeCoNiPdCu high-entropy alloy: Excellent magnetic softness arising from a nanocomposite structure

P. Koželj^{1,2}, S. Vrtnik¹, A. Jelen¹, M. Krnel¹, D. Gačnik¹, G. Dražić³, A. Meden⁴, M. Wencka⁵, D. Jezeršek⁶, J. Leskovec⁶, S. Maiti⁷, W. Steurer⁷ and J. Dolinšek^{1,2}

¹ Jožef Stefan Institute, Jamova cesta 39, SI-1000 Ljubljana, Slovenia

² Univ. of Ljubljana, Faculty of Mathematics and Physics, Jadranska 19, SI-1000 Ljubljana, Slovenia

³ National Institute of Chemistry, Hajdrihova ulica 19, SI-1000 Ljubljana, Slovenia

⁴ University of Ljubljana, Faculty of Chemistry and Chemical Technology, Večna pot 113, SI-1000 Ljubljana, Slovenia

⁵ Institute of Mol. Physics, Polish Academy of Sciences, Smoluchowskiego 17, 60-179 Poznań, Poland

⁶ Kolektor Group d.o.o, Vojkova ulica 10, SI-5280 Idrija, Slovenia

⁷ ETH Zurich, Department of Materials, Leopold-Ruzicka-Weg 4, CH-8093 Zürich, Switzerland

Soft magnetic materials are an integral part of various everyday and technological applications – transformers, electric motors, generators, etc. – where they guide or concentrate the magnetic flux. As within the past two decades the alloy design strategy with multiple principal elements in near-equiatom concentrations, called high-entropy alloys (HEAs) [1], has evolved to a contemporary research topic with potential practical applications, it is natural to explore soft magnetism also in these alloys. Though HEAs containing the 3d magnetic elements Fe, Co and Ni are mostly reported as soft magnetic materials [2,3], the majority of them have coercivities as high as 1 – 25 kA/m. To the best of our knowledge, only a handful of HEA materials have ever been reported with a coercivity smaller than 250 A/m, see e.g. Refs [4] and [5].

This contribution will present the magnetic properties of a heat-treated equimolar FeCoNiPdCu HEA [6] as determined by SQUID magnetometry (using also a sample of non-oriented electrical steel as a benchmark). FeCoNiPdCu has a narrow hysteresis loop $M(H)$ with a coercivity of only $H_c \approx 115$ A/m, a reasonable magnetic saturation polarization of 1.3 T and an estimated maximum relative permeability $\mu_r \approx 3600$. These properties are supplemented by a sufficiently high Curie temperature of 962 K and room-temperature electrical resistivity of 33.3 $\mu\Omega\text{cm}$, implying stability of magnetic properties in the application relevant temperature range and a reasonable resilience towards eddy currents losses.

The magnetic softness of our material can be attributed to the two-phase nanocomposite structure that was formed by the attractive and repulsive interactions between the five different atomic species during the annealing at 1100 °C. By HAADF STEM microscopy combined with EDS spectroscopy we have shown that the magnetic elements Fe, Co and Ni formed FeCoNi-rich magnetic domains of dimensions 2–5 nm, which are separated by non-magnetic (or less-magnetic) PdCu-rich spacers of about equal dimensions. The smallness of the FeCoNi-rich domains – meaning that they must be single magnetic domains – and their separation by sufficiently thin PdCu-rich spacers to still be exchange coupled amongst themselves, fulfil the requirements of the mechanism of “exchange averaging of magnetic anisotropy”, explaining the excellent magnetic softness of heat-treated FeCoNiPdCu.

[1] J.W. Yeh, et al. *Adv. Eng. Mater.* **6**, 299 (2004).

[2] M.H. Tsai. *Entropy* **15**, 5338 (2013).

[3] Y. Zhang, T.T. Zuo, Y.Q. Cheng, P.K. Liaw. *Sci. Rep.* **3**, 1455 (2013).

[4] K.X. Zhou, et al. *Intermetallics* **122**, 106801 (2020).

[5] P. Li, A. Wang, C.T. Liu. *J. Alloys Compd.* **694**, 55 (2017).

[6] P. Koželj, et al. *Adv. Eng. Mater.* **21**, 1801055 (2019).

In search for new rare earth free permanent magnets in CoFeTa system

**Sergiu Arapan¹, Pablo Nieves Cordones¹, Andrea Džubinská²,
Marián Reiffers³, and Dominik Legut¹**

¹ IT4Innovations VŠB-TUO, 17. listopadu 2172/15, 708 00 Ostrava-Poruba, Czech Republic

² CPM – TIP, UPJŠ, Tr. SNP 1, 040 11 Košice, Slovak Republic

³ FHNS, University of Prešov, Ul. 17. Novembra 1, 080 01 Prešov, Slovak Republic

The increasing importance of the use of permanent magnets (PM) in technological applications used for information storage and green-energy generation calls for a design of new magnetic materials that are cheaper and contain less critical components like rare earth (RE) elements. The systematic search for novel hard magnetic materials is hardly achievable only via experimental discovery due to the very large combinatorial space spanned by the crystal structures and chemical compositions. Structure predicting techniques based on evolutionary or adaptive genetic algorithms in combination with ab-initio calculations open a promising prospect to discover new materials with given properties [1]. In a recent work, we performed a computational screening of hard magnetic phases in the Fe-Ta binary system [2]. The study revealed the existence of metastable phases with intrinsic magnetic properties, like high saturation magnetization and large magnetocrystalline anisotropy, suitable for PM materials. Interestingly, a predicted low energy Fe₂Ta structure (8 formula units) is experimentally observed in the Co-Ta binary family. The study of the thermodynamic stability of the (Co_{1-x}Fe_x)₂Ta alloys suggests a stable compound for an increased concentration of iron and the experimental study confirms the synthesis of stable magnetic materials in the predicted phase. Though, the new magnetic structure in the CoFeTa system does not exhibit high enough Curie temperature for a practical use as PM, this synergy between computational prediction and experimental validation describes an advance route for design of new magnetic materials.

This research was funded partly by Slovak grant agency APVV-DS-FR-19-0045.

[1] S. Arapan, P. Nieves, and S. Cuesta-López, J. Appl. Phys. **123**, 083904 (2018).

[2] S. Arapan, P. Nieves, H. C. Herper, and D. Legut, Phys. Rev. B **101**, 014426, (2020).

Tuning the magnetic properties of magnetocaloric $\text{La}(\text{Fe},\text{Si})_{13}$ using rare earth doping

J. Lill¹, B. Eggert¹, B. Beckmann², O. N. Miroshkina¹, K. Skokov², J. R. Mardegan³, D. Günzing¹, S. Rauls¹, S. Francoual³, R. Brand¹, K. Ollefs¹, M. E. Gruner¹, O. Gutfleisch², H. Wende¹

¹*Faculty of Physics and CENIDE, University of Duisburg-Essen, Lotharstr. 1-21, Duisburg, Germany*

²*Material Science, Technical University Darmstadt, Alarich-Weiss-Str. 16, Darmstadt, Germany*

³*DESY, Notkestraße 85, Hamburg, Germany*

Magnetocaloric (MC) materials are promising environmental friendly candidates to replace gas-compression refrigerants. There are many MC systems possessing a high MC effect because of their high adiabatic temperature (ΔT_{ad}) or isothermal entropy (ΔS_{iso}) changes [1]. However, for large scale applications, it will be necessary to minimise hysteresis and tune the phase transition temperature towards room temperature (RT). To achieve this, one needs proper knowledge about electronic and magnetic interactions in the different magnetic phases and how to change those precisely. One promising MC material is $\text{La}(\text{Fe},\text{Si})_{13}$ with a phase transition temperature around 200 K [2] that can be shifted towards RT via hydrogenisation. However, stabilization by Mn doping is needed, which increases thermal hysteresis and therefore reduces the reversible magnetocaloric effect [3]. Here, further studies are necessary to find alternatives for Mn doping, e.g. by replacing Mn or by adding further dopants, which minimise thermal hysteresis. We analyse rare earth doping (rare earths being Ce, Pr and Nd) on the La sites for the initial system for this scenario. We first aim to understand the influence of rare earth doping on electronic and magnetic interactions with a special focus on the ferromagnetic state. For all previously studied dopants in the $\text{La}(\text{Fe},\text{Si})_{13}$ system, Fe plays a crucial role in the macroscopic magnetisation. In contrast, our preliminary results indicate that using rare earth doping, drastic changes occur, e.g. in the saturation magnetisation, which seems not to originate only from the Fe atoms. Instead, we find indications that the rare earth elements play a not negligible role for the magnetism. We will discuss possible interactions by presenting vibrating sample magnetometer results to determine macroscopic magnetisation. This will be complemented by ^{57}Fe Mössbauer spectroscopy to resolve the Fe magnetic moment and X-ray magnetic circular dichroism measurements at rare earth $L_{2,3}$ edges to resolve changes of the magnetic moment on the La sites under rare earth doping as well as determine the dopants magnetic moment.

We acknowledge the financial support through the DFG (CRC/TRR270) and thank DESY for allocation of beamtime.

[1] T. Gottschall et al., Adv. Energy. Mater. 9, 1901322 (2019).

[2] F. Scheibel et al., Energy Technol. 6 (8) 1397-1428 (2018).

[3] S. Makarov et al., J. Phys. D: Appl. Phys. 48 305006 (2015).

Effect of Particle Size in Extruding Flexible Permanent Magnet Filaments from Tuned Composites for Additive Manufacturing

Ester M. Palmero, Daniel Casaleiz, Javier de Vicente and Alberto Bollero

Group of Permanent Magnets and Applications, IMDEA Nanociencia, 28049 Madrid, Spain

Additive manufacturing (AM) of composites is attracting much interest in high-tech sectors such as energy, transport, aerospace and medicine, for fabricating complex high-performance objects with tailored properties [1]. For permanent magnets (PMs), the challenge is to develop magnets by AM with no geometrical restrictions, high filling factor (FF), and non-deteriorated PM properties [2] together with finding alternatives (e.g., improved ferrites and the promising MnAlC-based alloys) to rare earth-based magnets [3].

Tuned composites (PM particles/polymer) were synthesized by solution casting, followed by extrusion of filaments for 3D-printing (Fig. 1(a)). Several alternative PM materials were studied (gas-atomized τ -MnAlC, Sr-ferrite and hybrids -Sr-ferrite/NdFeB). Particle size and fine-to-coarse particles ratio (FP/CP) play a key role on the flexibility and powder loading of MnAlC filaments (length > 10 m), reaching FF > 80% and with non-deteriorated PMs properties (Fig. 1(b)) [4]. These results will be compared to the obtained for filaments based on NdFeB ($H_c = 812$ kA/m, FF = 93%), Sr-ferrite ($H_c = 239$ kA/m, FF = 92%) and hybrids ($H_c = 629$ kA/m, FF = 90%). MnAlC-based objects were 3D-printed under controlled temperature, proving that alternative PM materials can be efficiently synthesized and processed to develop novel PMs by AM (Fig. 1(b)) [4].

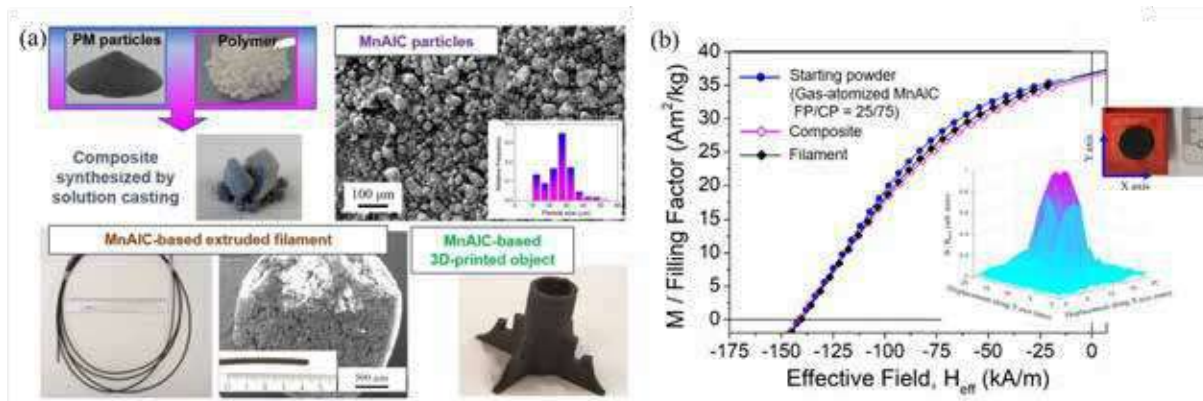


Figure 1: (a) Images of gas-atomized MnAlC particles, polymer, MnAlC/polymer composite, MnAlC-based filament and 3D-printed object; and (b) normalized magnetic response of MnAlC-based samples. Inset shows a 3D-printed MnAlC-based disc and the 3D plot of the magnetic flux density measured at the disc surface.

Acknowledgements. Authors acknowledge collaborations with B. Skårman, H. Vidarsson and P.-O. Larsson (Höganäs, Sweden) by the industrial contract *GAMMA*, and A. Nieto and R. Altimira (IMA, Spain), and support from MICINN by *NEXUS* (PID2020-115215RB-C21). E.M.P. acknowledges support from AEI by the JdC-I program (IJC2020-043011-1/MCIN/AEI/10.13039/501100011033) and EU by NextGenerationEU/PRTR.

[1] L.E. Murr, *J. Mater. Sci. Technol.* **32**, 987 (2016).

[2] J. Jaćimović *et al.*, *Adv. Eng. Mater.* **19**, 1700098 (2017).

[3] A. Bollero *et al.*, *ACS Sustainable Chem. Eng.* **5**, 3243 (2017); J. Rial *et al.*, *Engineering* **6**, 173 (2020).

[4] E.M. Palmero *et al.*, *Sci. Technol. Adv. Mater.* **19**, 465 (2018); *IEEE Trans. Magn.* **55**, 2101004 (2019); *Addit. Manuf.* **33**, 101179 (2020).

Additive manufacturing of magnetocaloric 3D structures: A cost-effective way for printing cellulose-based metallic structures.

Bosco Rodriguez-Crespo¹, Daniel Salazar¹, Volodymyr Chernenko²

¹ BCMaterials, UPV/EHU Scientific Park, Leioa, Spain

² University of Basque Country, Leioa, Spain

Solid-state refrigeration based on magnetocaloric effect is seen as a potential alternative to current less-efficient gas expansion-compression based conventional refrigeration. The heat exchanger, the functional element of this kind of refrigerator, is composed by the magnetocaloric alloy. Additive Manufacturing (AM) is a useful technique to build efficient heat exchangers, and since current AM techniques are expensive and energy consuming a cost-effective way has to be explored. In this work, we developed original inks and implemented printing technique to print 3D metallic structures that would act as the heat exchanger of a magnetic refrigerator, printing at room temperature in a green and a cost-effective way using various metallic powders (including magnetic and magnetocaloric powders), and cellulose as matrix with water as dissolvent. The magnetocaloric ink containing more than 90 wt.% of powder was elaborated by achieving an optimal viscosity whereby high maximum number of layers (250 layers reached) with highest printing resolution (0.5mm wall thickness) was obtained. The elaborated technological route of the treatment of printed structures included: (i) special heat treatments to dry printed structures so the polymer was removed by calcination followed by a sintering to get entirely metallic structure, and (ii) electrodeposition of nickel to protect printed structure from any corrosion. We also demonstrated that any incorrectly printed workpiece can be recycled re-dissolving it in the water so material loss is reduced significantly making the printing more cost-efficient and environmentally friendly.

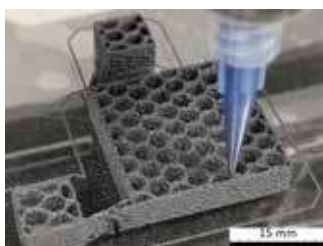


Figure 1: Example of printing a Magnetocaloric structure by Extrusion 3D printer

Novel Processing of Nano-Composite Magnets for Improved Remanence and Coercivity

Lukas Schäfer, Konstantin Skokov, Semih Ener,
Imants Dirba, Oliver Gutfleisch

TU Darmstadt, Functional Materials, Alarich-Weiss-Str. 16, 64287 Darmstadt, Germany

Permanent magnets based on Rare-Earth (RE) – Transition Metal (TM) alloys are widely used for high performance application in electro mobility, renewable energies and automation. Since the demand and usage of such magnets is increasing, the high criticality of RE intensifies the search for RE-lean materials and any improvements in magnetic properties [1]. Our work shows a novel process to obtain nano-composite magnets, which unite the hard magnetic properties of RE-based intermetallic phases and para- or soft magnetic precipitates. The approach relies on the formation of a high-temperature or metastable phase by rapid solidification. By subsequent annealing and/ or hydrogen treatment, the microstructure can be transformed to grains of the hard magnetic phase and inter- and intragranular precipitates. The focus of this work lies on Nd-Fe-B and Sm-Fe-B alloys with specific element modification/ substitution in order to stabilize the high-temperature/ metastable phase and to provoke the formation of precipitates. The experimental result indicate two distinct cases:

I) The formation of paramagnetic precipitates in Nd-Fe-B leads to a magnetic hardening and high coercivity. A specific alloy modification is necessary to stabilize a $\text{Nd}_2(\text{Fe},\text{Co})_{17}\text{B}_x$ metastable phase [2]. After an annealing treatment, the microstructure is comparable to sintered Nd-Fe-B magnets with high coercivity, although several secondary intermetallic phases are observed. **II)** The formation of nanometer size, soft magnetic Fe-based precipitates in Nd-Fe-Co-B and Sm-Fe-B alloys is observed. The microstructures indicate that the size of the precipitates are suitable to realize an exchange-spring coupling between hard- and soft magnetic phases [3], which can improve the remanence above the theoretical limit of the respective single-phase magnets.

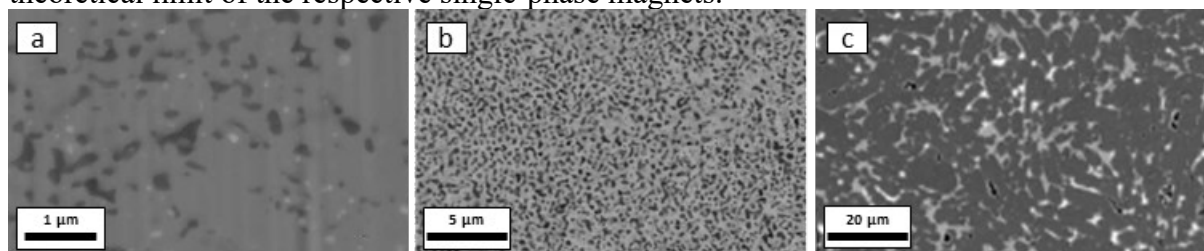


Figure 1: SEM-BSE images of the obtained microstructures with soft magnetic precipitates in a) $\text{Nd}_2\text{Fe}_{7.7}\text{Co}_{6.3}\text{B}$ and b) $\text{SmFe}_{7.7}\text{Co}_{3.3}\text{B}_{0.5}$ and the c) $\text{Nd}_{16}\text{Fe}_{53}\text{Co}_{20}\text{Mo}_2\text{Cu}_2\text{B}_7$ sample with high coercivity and Fe-Mo-B precipitates.

Thus, the realization of nano-composite exchange-spring magnets is possible by the transformation of high temperature/ metastable phases. This effect can be utilized in existing production routes such as sintered or hot compacted magnets but does also offer a possible way for additively manufactured permanent magnets.

This work was supported by the Deutsche Forschungsgemeinschaft (DFG, German Research Foundation), Project ID No. 405553726, TRR 270.

[1] S. Bobba et al, *Critical Raw Materials for Strategic Technologies and Sectors in the EU - a Foresight Study*, **2020**.

[2] S. Ozawa et al, *J. Appl. Phys.* **2006**, 100, 123906.

[3] H. Sepehri-Amin, et al., *Acta Mater.* **2019**, 175, 276.

Nitrogenation study of Nd(Fe,Mo)₁₂ compounds produced by Strip Cast methods

Ryan SEDEK¹, Sorana LUCA¹, and Patricia DE RANGO²

¹ *Univ. Grenoble Alpes, CEA, Liten, DTNM, 38000 Grenoble, France.*

² *Univ. Grenoble Alpes, CNRS, Institut Néel, 38000 Grenoble, France.*

The Rare-Earth-Fe₁₂ compounds, also known as 1-12 phases, are promising candidates for permanent magnet applications with reduced content of RE elements, thanks to their intrinsic magnetic properties. Neodymium-based 1-12 compounds have usually a planar anisotropy and are not suitable for permanent magnets. Insertion of light elements, like B, C or N, turns the planar anisotropy to easy axis and enhances both the magnetocrystalline anisotropy and Curie temperature. Nitrogenation of Nd(Fe,M)₁₂ compounds is not an easy task, as the solid-gas reaction upon nitrogen can lead to the decomposition of the magnetic 1-12 phase and the formation of undesirable α -Fe. The aim of this work is to analyse the nitrogenation reaction of Nd(Fe,Mo)₁₂ compounds produced by strip-casting. This process facilitates the production of single-phased materials with fine microstructure, without the need for lengthy annealing. According to phase diagrams, the composition of the starting alloy was adjusted to both obtain single-phase particles of Nd(Fe,Mo)₁₂ surrounded by an intergranular Nd-rich phase that could help for the development of the coercivity.

To investigate the solid-gas reaction under nitrogen, powders of different grain sizes were obtained from strip-cast materials, by various milling processes and used as precursors. Volumetric measurements allow to emphasize the major impact of the particle size of Nd(Fe,Mo)₁₂ precursors on nitrogenation kinetics for temperatures ranging from 300 °C to 600 °C under nitrogen. Jet-milled powders with fine grain size (7 μ m) make possible to use moderate temperatures and nitrogen gas pressures compared to powders with mean grain size of 150 μ m which need higher temperatures for a complete nitrogenation. Nevertheless, high temperatures and nitrogen pressure lead to a partial decomposition of the material and a decrease of the coercivity. Incomplete nitrogenation of a coarse powder conducts to the formation of a core-shell structure visible on SEM images. This can also be confirmed by magnetic measurements, where two magnetic transitions are observed.

The impact of an annealing applied before nitrogenation was also investigated. Thermomagnetic measurements performed on powders sealed in silica tubes under neutral atmosphere highlight the impact of the initial particle size on the microstructural transformations induced upon heat treatment. For a coarse powder, the annealing allows the complete crystallization of the 1-12 phase and the decrease of the amount of α -Fe. On the other hand, a fine powder shows a higher amount of α -Fe, linked to a partial decomposition of the 1-12 phase.

This solid-gas reaction study allowed to reach higher magnetic properties than a non-optimized compound by tuning nitrogenation parameters.

This work is supported by the Carnot Institute "Energie du futur" as part of the MAG12 project.

Two terminal quantum dot hybrid system as a heat engine

Emil Siuda¹ and Piotr Trocha¹

¹*Faculty of Physics, Institute of Spintronics and Quantum Information, Adam Mickiewicz University, ul. Uniwersytetu Poznańskiego 2, 61-614 Poznań, Poland*

We investigate two-terminal heat engine consisting of a quantum dot (QD) coupled to a magnetic insulator (MI) and metallic conductor (MC). The MI serves as a magnonic reservoir, whereas MC is a reservoir of electrons. Positive temperature gradient set between MI and MC drives a magnonic current between MI and QD which is converted into spin current. The opposite is true when the gradient is reversed. The principle of operation of the system is presented schematically in the figure 1.

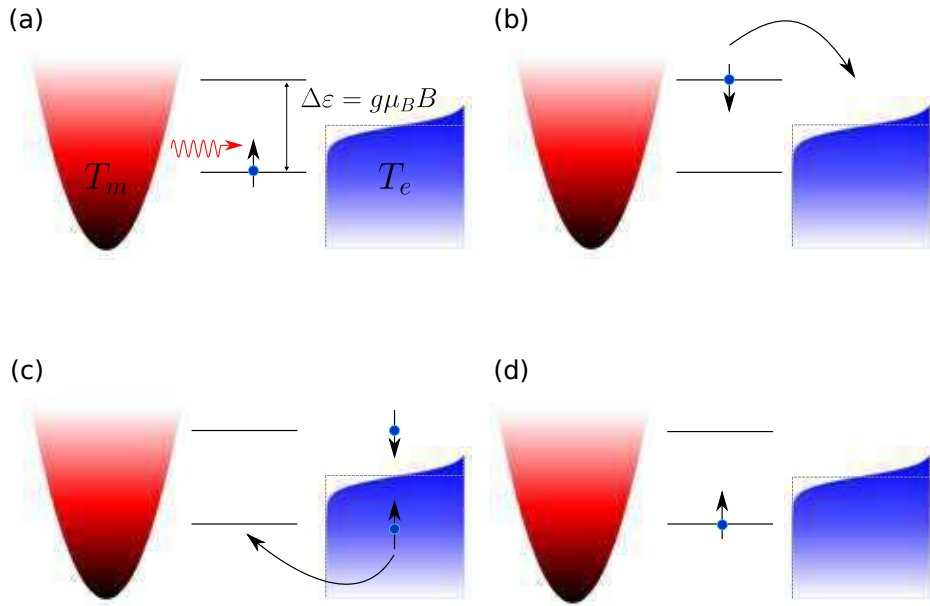


Figure 1: The red parabola symbolizes the magnon reservoir, whereas blue curve stands for density of electrons in the metallic lead. The blue area below the curve denotes states occupied by electrons and the white space above the curve are empty states. We assume $T_m > T_e$. Zeeman split dot's energy level is depicted by two black solid horizontal lines. Magnon, carrying energy equal to the splitting $\Delta\varepsilon$, is depicted as red wavy arrow, whereas blue dot with vertical arrow denotes an electron with a given spin.

We calculate thermopower, efficiency and other thermodynamical parameters of the engine. In the calculations we consider energy-dependant density of states and many-body magnon interactions in the magnonic reservoir.

Anomalous Nernst Effect in Polycrystalline MnBi

Alessandro Sola¹, Elena S. Olivetti¹, and Vittorio Basso¹

¹*Istituto Nazionale di Ricerca Metrologica, Strada delle Cacce 91, 10135 Torino, Italy*

The development of thermoelectric modules for energy harvesting and efficient cooling based on transverse thermoelectric effects requires improved figure of merit and simple fabrication procedures of the chosen material [1]. A large anomalous Nernst effect (ANE) has been recently observed in MnBi single crystals [2]. This is explained by the coexistence in the same compound of ferromagnetism and the heavy metal element.

However, single crystals require special preparation techniques, which can hinder their application in low-cost devices.

We investigate the transverse thermoelectric generation of polycrystalline MnBi samples prepared by powder metallurgy. These are produced from elemental powders annealed under an inert atmosphere in a 1T magnetic field. This technique allows the simple production of the MnBi compound with preferential orientation of the crystals c-axis along the applied magnetic field [3], by a low temperature reaction between liquid Bi and Mn. Thus, these samples develop an easy axis perpendicular to the slab and a remanent magnetization as shown in Figure 1 a).

Thermoelectric measurements are performed with an experimental setup based on the detection of heat currents by means of calibrated Peltier sensors [4]. Results shown in Figure 1 b) reveal two different components of the transverse voltage as a function of the magnetic field at a given heat current, which we interpret as originating from MnBi and unreacted Bi inside the sample. By attributing the thermal conductivity of Bi ($7.87 \text{ Wm}^{-1}\text{K}^{-1}$) to our sample, we can estimate the temperature gradients from which we obtain a Nernst coefficient at remanence of $0.23 \mu\text{V/K}$.

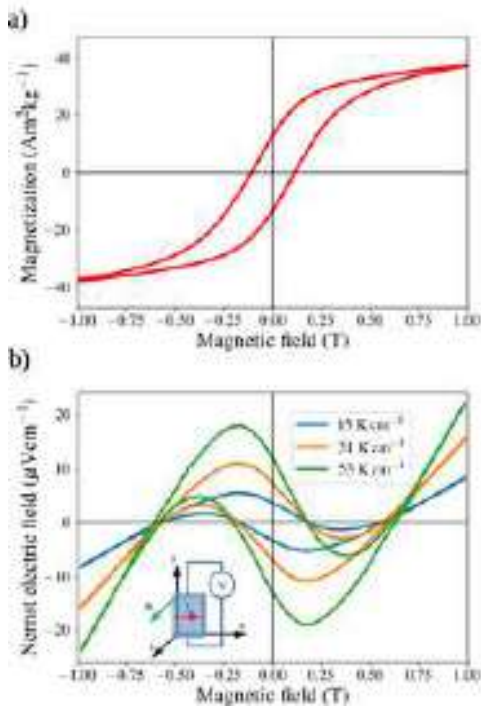


Figure 1: a) Hysteresis loop obtained by vibrating-sample magnetometer with applied magnetic field along the magnetic easy axis. b) Nernst electric field as function of applied magnetic field for three values of heat current j_q that generate in turn the thermal gradients reported in the label. The measurement geometry is shown in the inset.

- [1] K. Uchida et al., *Appl. Phys. Lett.* **118.14**, 140504 (2021).
- [2] B. He et al., *Joule* **5**, 30573067 (2021).
- [3] E. S. Olivetti et al., *Journal of Alloys and Compounds* **643**, S270S274 (2015).
- [4] A. Sola, et al., *Sci. rep.* **7.1**, 1-9 (2017).

Influence of Martensitic Configuration on Hysteretic Properties of Heusler Films Studied by Advanced Imaging in Temperature and Magnetic Field

M. Takhsha¹, A. Chirkova², F. Maccari², F. Casoli¹, S. Ener², K. P. Skokov², R. Cabassi¹, O. Gutfleisch², and F. Albertini¹

¹ IMEM-CNR, Parco Area delle Scienze 37/A, 43124 Parma, Italy

² Functional Materials, TU-Darmstadt, Alarich-Weiss-Str. 16, 64287 Darmstadt, Germany

Magnetic-shape-memory (MSM) Heusler compounds propose a variety of applications in actuating, sensing, energy harvesting, spintronics and multicaloric cooling technologies. Multifunctionality of these materials originates from a reversible martensitic phase transition. However, their full exploitation is prevented by some undesirable characteristics of the martensitic transition: thermal hysteresis and broad transition.

In previous works, we have shown that martensitic twinning configurations can be engineered by varying growth conditions, thickness, substrate/under-layer and post growth treatments. In particular, by changing these parameters it is possible to tune the configuration of twins, i.e. X-type with out-of-plane magnetic easy axis or Y-type with in-plane magnetic easy-axis, which are identified by different orientations of the twinning planes (i.e. at 45° and 90° degrees to the substrate, respectively) [1,2 and references therein].

More recently, we have also shown that in microfabricated structures, size reduction and geometry have a strong impact on twinning configuration [3].

We studied here the role of X-type and Y-type martensitic configurations on the characteristics of the transition. By advanced magnetic force microscopy imaging in a wide temperature (260-350 K) and magnetic field range (up to 14 T), we directly observed the nucleation and the self-accommodation of the martensitic twinning configurations under zero-field, isofield and isothermal conditions.

The experiments were performed on a Ni-Mn-Ga epitaxial thin film grown on (001) MgO. Y-type configuration of twins showed around 33 % higher average transformation rate with respect to X-type twinning configuration in zero-field condition and around twice as large as the average transformation rate of X-type in isothermal condition. The width of the thermal hysteresis of the Y-type was found to be around 22% narrower than of the X-type twinning configuration [4].

[1] M. Takhsha Ghahfarokhi, F. Casoli, S. Fabbri, L. Nasi, F. Celegato, R. Cabassi, G. Trevisi, G. Bertoni, D. Calestani, P. Tiberto, and F. Albertini, *Acta Mater.* **187**, 135 (2020).

[2] M. Takhsha Ghahfarokhi, L. Nasi, F. Casoli, S. Fabbri, G. Trevisi, R. Cabassi, and F. Albertini, *Materials* **13**, 2103 (2020).

[3] M. Takhsha Ghahfarokhi, J. A. Arregi, F. Casoli, M. Horký, R. Cabassi, V. Uhlř, and F. Albertini, *Appl. Mater. Today* **23**, 101058 (2021).

[4] M. Takhsha Ghahfarokhi, A. Chirkova, F. Maccari, F. Casoli, S. Ener, K. P. Skokov, R. Cabassi, O. Gutfleisch, and F. Albertini, *Acta Mater.* **221**, 117356 (2021).

Magnetic properties of high induction metallic ribbons $\text{Fe}_{67}\text{Co}_{20}\text{B}_{13}$ prepared by continuous ultra-rapid annealing method.

P. Zackiewicz¹, L. Hawelek¹, P. Włodarczyk¹, M. Polak¹, A. Kolano-Burian¹

¹ Centre of Functional Materials, Łukasiewicz Research Network - Institute of Non-Ferrous Metals, ul. Sowinskiego 5, 44-100 Gliwice, Poland

Abstract

In the field of new nanocrystalline, magnetically soft materials, one of the key roles plays the possibility of obtaining materials with the highest possible saturation magnetization. New materials are prepared using new technique of continuous ultra-rapid annealing with high heating rate of 150-200 K/s. This process allows to obtain high saturation magnetization and low coercion field.

The high induction metallic glass ribbons obtained via melt spinning technique with the chemical formula $\text{Fe}_{67}\text{Co}_{20}\text{B}_{13}$ were investigated. Thermal stability, crystallization and magnetic properties like complex permeability, magnetic saturation and coercivity were studied. Thermal properties: solidus-liquidus curves, the crystallization temperatures and kinetics of the crystallization process were analysed by applying DSC calorimetry. The B(H) loops were analysed for all the samples prepared by continuous process. The X-ray diffraction was used to analyse the crystalline structure evolution.

Addition of Co slows down the progress of crystallization rate of the Fe-B compound increasing the annealing time and decreasing the heating and cooling rates required for best final properties. Cobalt also improves the glass forming ability and allows to obtain low coercive field and low magnetostriction. Also addition of Co decrease the onset crystallization temperature and increases the Curie temperature which increase the high temperature magnetic properties of amorphous and nanocrystalline alloys. Absence of Cu influence the nucleation process and lack of Nb reduces the grain growth control during the classical annealing process. On the other hand we can avoid this problems using fast heating and cooling of ribbon for a very short time based on the Koster and Meinhardt work[1]. Homogeneous heating and cooling allows good grain refinement and short time of process gives the control for the grain growth.

[1] U.Köster, J. Meinhardt, Materials Science and Engineering A, Vol. 178, Issues 1–2, 1994, 271-278, [https://doi.org/10.1016/0921-5093\(94\)90553-3](https://doi.org/10.1016/0921-5093(94)90553-3).

Impact of F and S doping on (Mn,Fe)₂(P,Si) giant magnetocaloric materials

Fengqi Zhang^{1,*}, Ivan Batashev¹, Qi Shen¹, Ziyang Wu¹, Ronald I. Smith², G.A. de Wijs³, Niels van Dijk¹, Ekkes Brück¹

¹Fundamental Aspects of Materials and Energy (FAME), Faculty of Applied Sciences, Delft University of Technology, Delft, The Netherlands

²The ISIS Facility, STFC Rutherford Appleton Laboratory, Harwell Campus, Didcot, United Kingdom

³Institute for Molecules and Materials, Faculty of Science, Radboud University, Nijmegen, The Netherlands

* Corresponding author: F.Zhang-7@tudelft.nl

The quarternary (Mn,Fe)₂(P,Si)-based materials with a giant magnetocaloric effect (GMCE) at the ferromagnetic transition T_C are promising bulk materials for solid-state magnetic refrigeration [1-3]. In the present study we demonstrate that doping with the light elements fluorine and sulfur can be used to adjust T_C near room temperature and tune the magnetocaloric properties. For F doping the first-order magnetic transition (FOMT) of Mn_{0.60}Fe_{1.30}P_{0.64}Si_{0.36}F_x ($x = 0.00, 0.01, 0.02, 0.03$) is enhanced, which is explained by an enhanced magnetoelastic coupling. The magnetic entropy change $|\Delta S_m|$ at a field change ($\Delta\mu_0 H$) of 2 T markedly improved by 30% from 14.2 Jkg⁻¹K⁻¹ ($x = 0.00$) at 335 K to 20.2 Jkg⁻¹K⁻¹ ($x = 0.03$) at 297 K. For the F doped material the value of $|\Delta S_m|$ for $\Delta\mu_0 H = 1$ T reaches 11.6 Jkg⁻¹K⁻¹ at 294 K, which is consistent with the calorimetric data (12.4 Jkg⁻¹K⁻¹). Neutron diffraction experiments reveal enhanced magnetic moments by F doping in agreement with the prediction of DFT calculation. For S doping in Mn_{0.60}Fe_{1.25}P_{0.66-y}Si_{0.34}S_y ($y = 0.00, 0.01, 0.02, 0.03, 0.04$) three impurity phases have been found from microstructural analysis, which reduce the stability of the FOMT in the main phase and decrease T_C , e.g. the $|\Delta S_m|$ reduces from 7.9(12.6) Jkg⁻¹K⁻¹ (332 K) for the undoped sample to 3.4(6.2) Jkg⁻¹K⁻¹ (313 K) for the maximum doped sample for $\Delta\mu_0 H = 1(2)$ T. Neutron diffraction experiments combined with first-principles theoretical calculation, distinguish the occupation of F/S dopants and the tuning mechanism for light element doping, corresponding to subtle structural changes and a strengthening of the covalent bonding between metal and metalloid atoms. It is found that the light elements F and S can effectively regulate the magnetocaloric properties and provide fundamental understanding of (Mn,Fe)₂(P,Si)-based intermetallic compounds.

References:

- [1] O. Tegus, E. Brück, K.H.J. Buschow, F.R. de Boer, *Nature*. **415**, 150-152 (2002).
- [2] F. Guillou, G. Porcari, H. Yibole, N. van Dijk, E. Brück, *Adv Mater.* **26**, 2671-2675 (2014).
- [3] T. Gottschall, K.P. Skokov, M. Fries, A. Taubel, I. Radulov, F. Scheibel, D. Benke, S. Riegg, O. Gutfleisch, *Adv Energy Mater.* **9**, 1901322 (2019).

Posters

| | | |
|-------------------|--|-----|
| Ivan Batashev | <i>A computer assisted search for the novel magnetocaloric materials</i> | 226 |
| Petro Danylchenko | <i>Experimental Study of Large Rotational Magnetocaloric Effect in $\text{Ni(en)(H}_2\text{O)}_4\cdot 2\text{H}_2\text{O}$</i> | 227 |
| H Hanggai | <i>Optimization in Room Temperature Magnetocaloric Materials $(\text{MnFe})_{1.9}(\text{PSi})$ Fe-Rich Compounds</i> | 228 |
| Miroslav Hennel | <i>Direct magnetocaloric measurements of Heusler Ni_2MnGa microwires</i> | 229 |
| Anika Kiecana | <i>Magnetism, structure and magnetocaloric properties of $\text{Mn}_3\text{Sn}_{1-x}\text{Zn}_x\text{C}$ antiperovskite carbide</i> | 230 |
| Karolina Kowalska | <i>Rear-earth-based magnetocaloric composites for magnetic refrigerators systems</i> | 231 |
| Ivan Petryshynets | <i>Effect of the shear cutting parameters on the magnetic behavior of Fe-Si electrical steel.</i> | 232 |
| Nakai Shinji | <i>Thermal Equilibrium Compositions of Divalent Cation Substituted W-type Ferrites</i> | 233 |
| Sviatoslav Vovk | <i>Influence of the temperature on electro-magnetic properties of hybrid SMC material</i> | 234 |

A computer assisted search for the novel magnetocaloric materials

Ivan Batashev^{1,2}, Gilles A. de Wijs², Niels H. van Dijk¹ and Ekkes Brück¹

¹*TU Delft, Mekelweg 5 2628CD, Delft, The Netherlands*

²*Radboud University, Houtlaan 4 6525XZ, Nijmegen, The Netherlands*

The interest in magnetic cooling devices has led to an intensive search for suitable well-performing magnetocaloric materials. The conventional strategy to material discovery is largely based on trial-and-error experiments typically based on empirical structure-property relationships. This approach requires a significant investment of time and resources, yet the effort spent on investigating a candidate material quite often does not produce the desired results. We demonstrate how a combination of database screening and density functional theory calculations can be utilized to assist and enhance the search for novel magnetocaloric materials.

Two computational databases (Aflowlib[1] and Materials Project[2]) and two experimental databases (COD[3] and ICSD[4]) were used as an initial source of material properties totalling to 800k candidate compositions. We selected several criteria common among various well-known MCE materials to help us identify potentially interesting systems among the ones recorded in the databases. Along with magnetic properties, other factors important for practical applications were taken into consideration including price, availability, and toxicity of candidate materials. Oxygen content, percentage of magnetically active atoms in the composition and the number of unique magnetic sites in the lattice are further used to gauge the potential of the material. After this pre-selection, the remaining candidates are passed on for further investigations with ab-initio calculations.

To predict the magnetocaloric performance we study the magneto-elastic response of each candidate, by modelling the magnetic moment of the material across a range of deformations, both volumetric and uniaxial. This parameter shows a good correlation with magnetic entropy change measured in known magnetocaloric materials. In addition, the strength of magnetism of the candidates is compared by modelling the internal magnetic field. The whole screening process is realized through a set of automated computational tools and additional screening parameters could be easily implemented to further adjust or refine the search process.

The screening resulted in a shortlist of promising compounds ranked by their potential which can serve as a guide for experimental research. The presence of previously discovered materials with the giant magnetocaloric effect in the shortlist validate the criteria used for screening.

- [1] C. E. Calderon, J. J. Plata, C. Toher et al., *Comput. Mater. Sci.* **108**, 108 (2015).
- [2] A. Jain, S. P. Ong, G. Hautier, W. Chen et al., *APL Mater.* **1**, 011002 (2013).
- [3] S. Grazulis, D. Chateigner, R. T. Downs et al., *J. Appl. Crystallogr.* **42**, 726 (2009).
- [4] G. Bergerhoff, R. Hundt, R. Sievers et al., *J. Chem. Inf. Comput. Sci.* **23**, 66 (1983).

Experimental Study of Large Rotational Magnetocaloric Effect in $\text{Ni(en)(H}_2\text{O)}_4\cdot 2\text{H}_2\text{O}$

P. Danylchenko, R. Tarasenko, E. Čižmár, V. Tkáč, A. Feher, A. Orendáčová and M. Orendáč

*Institute of Physics, Faculty of Science, P.J. Šafárik University in Košice, Park Angelinum 9, 041 54
Košice, Slovakia
petro.danylchenko@student.upjs.sk*

The title compound $\text{Ni(en)(H}_2\text{O)}_4\text{SO}_4\cdot 2\text{H}_2\text{O}$ (*en* = ethylenediamine) (NEHS) has been identified as a spin 1 paramagnet with the nonmagnetic ground state introduced by the easy-plane anisotropy $D/k_B = 11.6$ K with $E/D = 0.1$ and negligible exchange interactions $J \approx 0$ [1]. Analysis of the specific heat in zero magnetic field indicated the absence of a phase transition to a magnetically ordered state below 1.8 K as a direct consequence of the dominant influence of the crystal field on the magnetic properties of the studied system. NEHS crystallizes in the monoclinic space group $C 2/c$ with four formula units in a unit cell with the unit cell parameters $a = 9.523$ Å, $b = 12.185$ Å, $c = 11.217$ Å and $\beta = 107.3^\circ$ [31]. The crystal structure consists of $[\text{Ni(en)(H}_2\text{O)}_4]^{2+}$ cations, $[\text{SO}_4]^{2-}$ anions, and two molecules of water. These units are connected by a large number of hydrogen bonds [2]. NEHS single crystals have been prepared in the form of blue prisms from an aqueous solution of nickel sulphate and *en* in stoichiometric amounts.

In this work, we present an experimental study of the rotational magnetocaloric effect (MCE) in NEHS single crystal at temperatures above 2 K, associated with adiabatic crystal rotation between the easy plane and hard axis in magnetic fields up to 7 T. The magnetocaloric properties of studied system are investigated by isothermal magnetization measurement. The experimental observations are completed with *ab initio* calculations of the anisotropy parameters. Besides that, theoretical simulations of the rotational MCE in the $S = 1$ paramagnet were performed and the simulations were compared with experimental data.

A large rotational magnetic entropy change ≈ 12 Jkg⁻¹K⁻¹ and ≈ 16.9 Jkg⁻¹K⁻¹ is achieved in 5 T and 7 T, respectively. The present study shows that, in 7 T, adiabatic rotation of the crystal at the initial temperature of 4.2 K leads to cooling sample down to 0.34 K, which suggests application of this material in cooling processes at low temperatures. Last but not least, theoretical calculations show that $S = 1$ Ni(II)-based systems with easy-plane anisotropy can have better rotational magnetocaloric properties than costly materials containing rare-earth elements in the chemical structure.

This work was supported by the Slovak Research and Development Agency Projects numbers APVV-18-0197, APVV-14-0073, and APVV-SK-BY-RD-19-0008 and VEGA Grant No. 1/0426/19 of the Scientific Grant Agency of the Ministry of Education, Science, Research and Sport of the Slovak Republic.

[1] R. Tarasenko et al., *Acta Physica Polonica A* **113**, 481 (2008).

[2] P.C. Healy et al., *Australian Journal of Chemistry* **37**, 921 (1984).

Optimization in Room Temperature Magnetocaloric Materials (MnFe)_{1.9}(PSi) Fe-Rich Compounds

Wuliji. Hanggai¹, N. H. van Dijk¹, E. Brück¹

¹Fundamental Aspects of Materials and Energy Group, Department of Radiation Science and Technology, Faculty of Applied Sciences, Delft University of Technology, Mekelweg 15, 2629JB, Delft, The Netherlands

Giant magnetocaloric material MnFe-PSi is the most promising candidate for the magnetic heat pump. In giant magnetocaloric materials MnFe-PSi compounds, Fe-rich samples show a higher saturation magnetization (M_s) than Mn-rich samples [1][2]. In this work, change the P-Si ratio on structure, magnetic property and magnetocaloric effects of Fe-rich $\text{Mn}_{0.66}\text{Fe}_{1.24}\text{P}_{1-x}\text{Si}_x$ ($x = 0.34, 0.35, 0.36, 0.37$) compound are studied. According to the XRD results, for the all samples crystallize in the Fe_2P type hexagonal structure, space group is P_{62m} , no other impurity phases were observed from XRD pattern. The transition temperature of the compounds significantly increase with Si content, from 280 K at $x = 0.34$ to 325 K at $x = 0.37$. For an increasing Si content the thermal hysteresis decreases and the maximum isothermal magnetic entropy change ($-\Delta S_m$) increased from of $10 \text{ J kg}^{-1} \text{ K}^{-1}$ to $14 \text{ J kg}^{-1} \text{ K}^{-1}$ for a field change 2 T. The n -value is used to define the type of magnetic phase transition. The magnetic entropy change scales with the magnetic field as $\Delta S_M \propto H^n$ in the vicinity of the phase transition. The index of the magnetic field can be expressed as $n = \frac{d \ln \Delta S_M}{d \ln H}$ [3]. If the maximum n -value is greater than 2, the material behavior corresponds to a first-order phase transition(FOMT), and if it is less than 2, it corresponds to a second-order phase transition(SOMT)[4]. With the Si content increase from 0.34 to 0.37, the maximum of n -value near the phase transition is found to be greater than 2 for all samples, this means during Si content increase from 0.34 to 0.37 phase transition keep the first-order phase transition(FOMT).

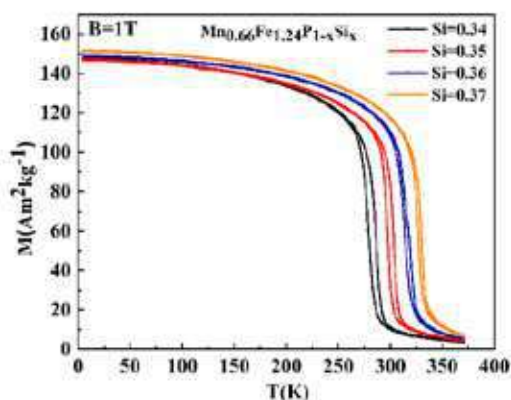


Fig1. Temperature dependence of the magnetization of $\text{Mn}_{0.66}\text{Fe}_{1.24}\text{P}_{1-x}\text{Si}_x$ compounds measured in a magnetic field of 1 T.

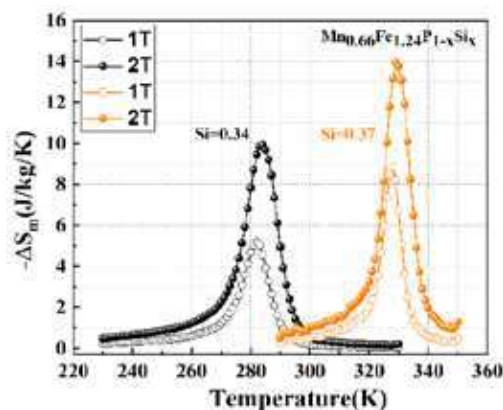


Fig2. Magnetic entropy changes under field changes of 0-2 T (solid symbols)

- [1]. Z.Q. Ou, L. Zhang, N.H. Dung, Journal of Alloys & Compounds, 710,446-451 (2017)
- [2]. J. V. Leita, M. V. D. Haar, A. Lefering, Journal of Magnetism & Magnetic Materials, 49-54 (2013)
- [3]. L. J. Yan, F. Victorino, Nature Communications, 9:2680 (2018)
- [4]. C. Bean & D. Rodbell, Physical Review, 126, 104-115 (1962)

Direct magnetocaloric measurements of Heusler Ni_2MnGa microwires

Miroslav Hennel^{1,2}, Ladislav Galdun¹ and Rastislav Varga¹

¹ Centre of Progressive Materials, TIP-UPJS, Trieda SNP 1, Kosice, Slovakia

² Institute of Physics, Fac. of Science UPJS, Park Angelinum 9, Kosice, Slovakia

Magnetocaloric effect is a non-conventional method that can provide cooling power. Heusler alloys are promising candidates for micro-magnetic cooling applications, thank their desired behaviour. Preparation of Heusler alloys in the form of glass-coated microwires by the Taylor-Ulitovsky technique allows easy and fast production of microwires with many additional advantages such as size scalability of cooling material.

Previous works show standard indirect magnetocaloric measurement of the magnetic entropy change [1, 2].

Therefore, we would like to present *direct magnetocaloric effect measurement using an experimental set-up* based on micro-calorimetry with micro-thermocouple [3]. In this work, experimental set-up and the method will be appropriately explained.

The temperature change of Ni_2MnGa microwire was measured using thermocouple in a wide temperature range from liquid nitrogen temperature to +120 °C in different magnetic fields up to 2720 Oe, see Figure 1. Direct measurement of magnetocaloric effect was evaluated during magnetization and demagnetization of the studied sample.

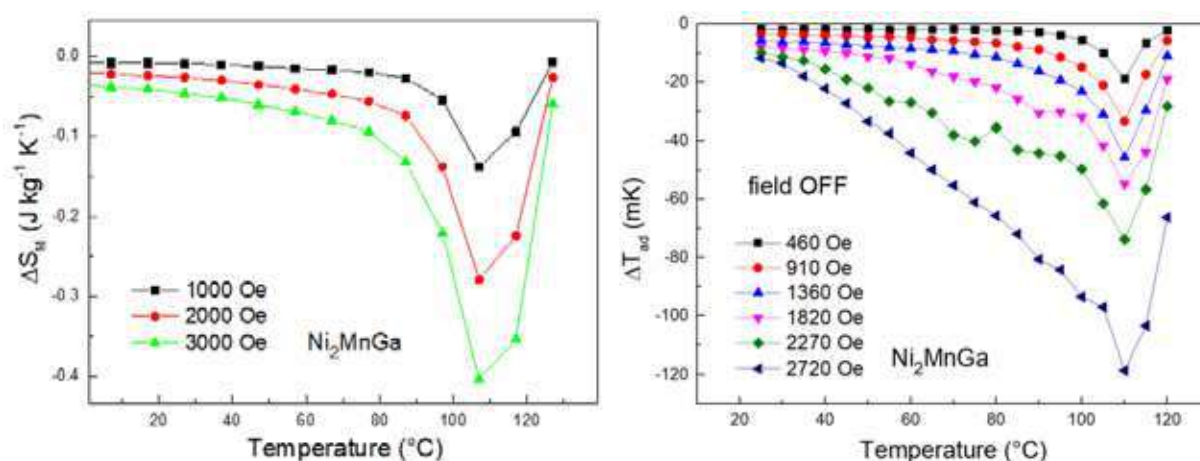


Figure 1 Comparison of indirect magnetic entropy change measurement and direct adiabatic temperature change on Ni_2MnGa microwire

This work was supported by Slovak Grant Agency grant number APVV-16-0079.

[1] M. Hennel, M. Varga, L. Frolova, S. Nalevanko, P. Ibarra-Gaytán, R. Vidyasagar, P. Sarkar, A. Dzubinska, L. Galdun, T. Ryba, Z. Vargova, and R. Varga, *Phys. Status Solidi A*. Accepted Author Manuscript, DOI: 10.1002/pssa.202100657 (2022).

[2] P. J. Ibarra-Gaytán, L. Frolova, L. Galdun, T. Ryba, P. Diko, V. Kavecansky, J. L. Sánchez Llamazares, Z. Vargova and R. Varga, *J. Alloys Compd* **65**, 786 (2019).

[3] J. Kamarád, J. Kaštil, and Z. Arnold, *Review of Scientific Instruments* **83**, 083902 (2012).

Magnetism, structure and magnetocaloric properties of $\text{Mn}_3\text{Sn}_{1-x}\text{Zn}_x\text{C}$ antiperovskite carbides

Anika Kiecana¹, Ward Schaeffers¹, Niels van Dijk¹, Ekkes Brück¹

¹*Fundamental Aspects of Materials and Energy Group, Department of Radiation Science and Technology, Faculty of Applied Sciences, Delft University of Technology, Mekelweg 15, 2629JB, Delft, The Netherlands*

Mn-based antiperovskite carbides Mn_3AX (A= transition metal; X= C, N) display a variety of interesting phenomena such as giant magnetoresistance (GMR), superconductivity, giant negative thermal expansion, piezomagnetic effect, barocaloric effect and magnetocaloric effect (MCE). Recent studies deploying ab-initio methods and Monte Carlo (MC) simulations revealed a great potential of the $\text{Mn}_3(\text{Sn,Zn})\text{C}$ system for an application in magnetic refrigeration [1]. Magnetic cooling, which utilizes magnetocaloric effect (MCE), has attracted broad attention due to many advantages over the traditional compressor-based technology [2], [3]. Since the systematic investigation of MCE in the $\text{Mn}_3\text{Sn}_{1-x}\text{Zn}_x\text{C}$ system was thus far not reported, our main objective was to study magnetism and MCE in these compounds.

The effect of Zn substitution for Sn in the cubic Mn_3SnC antiperovskite carbide has been investigated using magnetization measurements, XRD, DSC, neutron diffraction and DFT calculations. The parent compound – Mn_3SnC , exhibits a sharp Ferrimagnetic (FiM) to Paramagnetic (PM) First Order Magnetic Transition (FOMT) with the Curie temperature (T_C) of 272.8 K and a significant magnetic entropy change ($-\Delta S_m$) of $10 \text{ J kg}^{-1}\text{K}^{-1}$ for a field change 5 T. The compounds of $x (\text{Zn}) < 0.4$ show similar magnetic behaviour. Namely, the FiM-PM transition occurs upon heating, while T_C decreases to 196.6 K. These compounds also show the presence of narrow thermal hysteresis at low magnetic field, indicating FOMT. The occurrence of FOMT is supported by the negative volume change across the transition, as confirmed by the temperature-dependent XRD measurements. The alloys of $x \geq 0.4$ show a drastic change in magnetic behaviour – an abrupt increase in T_C and magnetization can be observed, whereas FiM-PM transition change into FiM-FM-PM. In alloys of $x \geq 0.4$, T_C increases to 402.1 K and magnetization rises from $20.1 \text{ Am}^2\text{kg}^{-1}$ to $76.5 \text{ Am}^2\text{kg}^{-1}$. We report that Zn doping suppresses the exchange interactions between Mn atoms due to enhanced hybridization between Mn 3d and C 2p orbitals, resulting in the initial decrease in T_C . However, the direct exchange between Mn atoms is strongly enhanced for a higher Zn content, leading to an abrupt increase in T_C . Therefore, a non-linear change in T_C results from the lattice shrinkage and electron-type doping

- [1] Y. Benhouria *et al.*, “Carbides-anti-perovskites $\text{Mn}_3(\text{Sn, Zn})\text{C}$: Potential candidates for an application in magnetic refrigeration,” *Phys. E Low-Dimensional Syst. Nanostructures*, vol. 124, no. June, p. 114317, 2020, doi: 10.1016/j.physe.2020.114317.
- [2] A. Smith, C. R. H. Bahl, R. Bjork, K. Engelbrecht, K. K. Nielsen, and N. Pryds, “Materials challenges for high performance magnetocaloric refrigeration devices,” *Adv. Energy Mater.*, vol. 2, no. 11, pp. 1288–1318, 2012, doi: 10.1002/aenm.201200167.
- [3] E. Brück, “Developments in magnetocaloric refrigeration,” *J. Phys. D. Appl. Phys.*, vol. 38, no. 23, 2005, doi: 10.1088/0022-3727/38/23/R01.

Rear-earth-based magnetocaloric composites for magnetic refrigerators systems

K. Kowalska^{1,2}, J. Ćwik², Y. Koshkid'ko² and K. Nenkov³

¹ Faculty of Chemistry, Wrocław University of Science and Technology, Norwida 4/6, 50-373 Wrocław, Poland

² Institute of Low Temperature and Structure Research, PAS, Okólna 2, 50-422 Wrocław, Poland

³ Leibniz IFW Dresden, Institute for Complex Materials, D-01069, Dresden, Germany

The magnetocaloric effect (MCE) is a phenomenon that has attracted considerable attention in the field of solid-state physics. The possibility of implementation of this effect into the magnetic refrigerators systems seems promising. In recent years, significant work has been done while searching for new refrigerants with advanced magnetocaloric properties. The rare-earth metals are elements that exhibit a superior MCE effect. Moreover, they decreased the environmental impact and give a possibility of implementation in various temperature ranges. Here, we investigate a large group of magnetic materials from RNi_2 family. We have investigate pseudo-binary compounds based on TbNi_2 , DyNi_2 , HoNi_2 , and ErNi_2 . The magnetocaloric effect shown by those materials was widely evaluated using two approaches. The first one was based on the magnetization measurements from which we calculated the change of the isothermal magnetic entropy (ΔS_{mag}) using the Maxwell relation. The second one was based on the heat capacity measurements in the case of zero and no-zero magnetic fields, 1T and 2T to name them. Based on that it was possible to choose the most promising and suitable reference composite for further research. The optimal molar ratios of the magnetic composite were estimated using numerical method.[1-3]

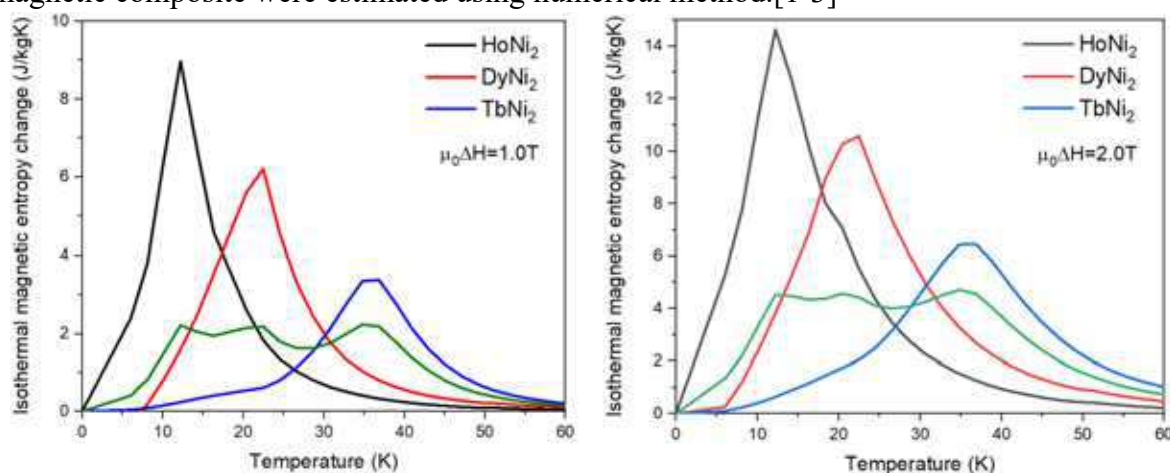


Figure.1.: Temperature dependences of the isothermal magnetic entropy change for $(\text{HoNi}_2)_{0.2}(\text{DyNi}_2)_{0.2}(\text{TbNi}_2)_{0.6}$.

[1] T. Hashimoto, T. Kuzuhara, M. Sahashi, K. Inomata, A. Tomokiyo, and H. Yayama, *J. Appl. Phys.* **62**, 3873 (1987).

[2] G. Diguët, G. Lin, and J. Chen, *Int. J. Refrig.* **36**, 958 (2013).

[3] A. Smaïli and R. Chahine, *Adv. Cryog. Eng.* **42**, 445 (1996).

The work was supported by the National Science Center, Poland through the OPUS Program under Grant No. 2019/33/B/ST5/01853.

Effect of the shear cutting parameters on the magnetic behavior of Fe-Si electrical steel.

I. Petryshynetsa¹, F. Kováča¹, V. Puchý¹, M. Podobová¹, J. Füzér², P. Kollár²

¹ Institute of Materials Research, Division of Metallic Systems, Slovak Academy of Sciences, Watsonova 47, 04001 Košice, Slovakia

² Institute of Physics, Faculty of Science, Pavol Jozef Safarik University, Park Angelinum 9, 041 54 Košice, Slovakia

Non-oriented (NO) electrical steels belong to an important group of soft magnetic materials, that typically use as cores in a variety of electrical rotating equipment. The magnetic quality and practical usability of Fe-Si steel depend on the silicon content, microstructure and texture state, sheet thickness as well as mechanical stresses which are inevitable and originate from different sources, e.g., material processing, machine manufacturing, and cutting processes (punching, blanking).

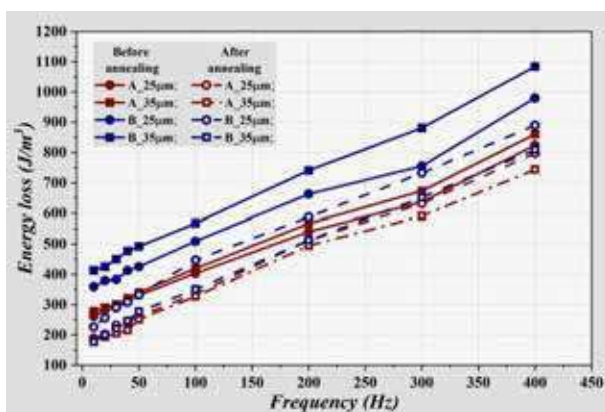


Figure 1: Energy loss behavior versus magnetizing frequency at $B_p = 1.0$ T in two non-oriented electrical sheets of steel punched with different cutting clearance before and after annealing.

In this paper, the effect of residual stresses induced by punching with different shear cutting parameters on the magnetic properties is studied.

As experimental material, two vacuum degassed NO steels A and B were used with the following content of silicon Si = 2.4 wt.% and Si = 1.6 wt.%, respectively. An experimental shear cutting tool was used for punching ring-shaped samples with outer and inner radii of 25mm and 15mm, respectively. The cutting clearances of punching tools were 25µm and 35µm. The evolution of microstructure and texture of

experimental cut edges obtained with different clearances and then heat treatment according to the long-term annealing process was carried out by SEM and EBSD analysis. The analysis of mechanical strains around the cutting edges obtained after punching with different clearances was released by nanoindentation and local misorientation maps (EBSD).

The influence of cutting clearance on the energy loss in experimental samples up to 400 Hz at $B_p=1.0$ T is presented in Figure 1. As one can see, in samples without heat treatment, the minimum loss response is exhibited using the cutting tool with 25µm clearance. In the case of annealed samples, the situation is the opposite. Here, the samples that were cut by punching tools with 35µm cutting clearance are showing the lowest value of energy losses in comparison with samples prepared by tools with narrower clearance. It could be concluded that the final magnetic properties of shear cut segments for the rotors and stators of electrical machines for the individual technological processes are possible to modify by changing the cutting clearance, depending on their application.

This work has been supported by the Slovak Research & Development Agency (APVV-18-0207 and APVV-21-0418)

Thermal Equilibrium Compositions of Divalent Cation Substituted W-type Ferrites

Shinji Nakai¹, Takeshi Waki¹, Yoshikazu Tabata¹ and Hiroyuki Nakamura¹

¹Department of Materials Science and Engineering, Kyoto university, Kyoto 606-8501, Japan

Divalent cation ($M^{2+} = \text{Co, Ni, Zn, Mg, ...}$) substituted W-type ferrites, $AM_2\text{Fe}_{16}\text{O}_{27}$ ($AM_2\text{W}$, $A = \text{Sr, Ba, ...}$), are candidates of magnetic materials because their magnetization is larger than that of M-type ferrites [1]. We found that Fe^{3+} in $\text{Sr}M_2\text{W}$ is partially reduced to Fe^{2+} even when synthesis is initiated from $\text{Sr}M_2\text{Fe}_{16}\text{O}_{27}$, and the actual chemical composition is $\text{Sr}M_{2-\delta}\text{Fe}_{16+\delta}\text{O}_{27}$ (δ represents the content of Fe^{2+}) [2]. We investigate thermal equilibrium compositions of SrCo_2W by growing single crystals at different temperatures.

SrCo_2W single crystals were grown by the $\text{SrO/B}_2\text{O}_3$ flux method by keeping temperature at 1473 and 1573 K, and obtained phases were identified by powder X-ray diffraction (XRD) and scanning electron microscope with energy-dispersive X-ray analysis (SEM-EDX). Compositions of SrCo_2W were determined by wave-dispersive X-ray analysis (WDX).

Single crystals were successfully obtained, but many voids are observed after acid treatment. XRD shows all single crystals contain secondary phases. We found that single crystals grown at higher temperatures contain more Fe^{2+} , which is stable at high temperature. The stable composition of the W-phase shifts during cooling, giving rise to the decomposition of the W-phase.

Table 1: Crystal growing temperatures, Fe, Co contents, and Fe^{2+} content, δ , of W-ferrites, normalized so that the sum of Fe and Co contents is equal to 18

| Growing temperature (K) | Fe content | Co content | δ |
|-------------------------|------------|------------|----------|
| 1473 | 16.39 | 1.61 | 0.39 |
| 1573 | 16.64 | 1.36 | 0.69 |

[1] R. C. Pullar, Prog. Mater. Sci. **57**, 1191 (2012).

[2] S. Nakai, T. Waki, Y. Tabata, M. Kato, H. Ohta, and H. Nakamura, submitted to J. Jpn. Soc. Powder Powder Metallurgy.

Influence of the temperature on electro-magnetic properties of hybrid SMC material

Sviatoslav Vovk ¹, Samuel Dobák ¹, Ján Füzer ¹, Peter Kollár ¹, Radovan Bureš ²,
Mária Fáberová ².

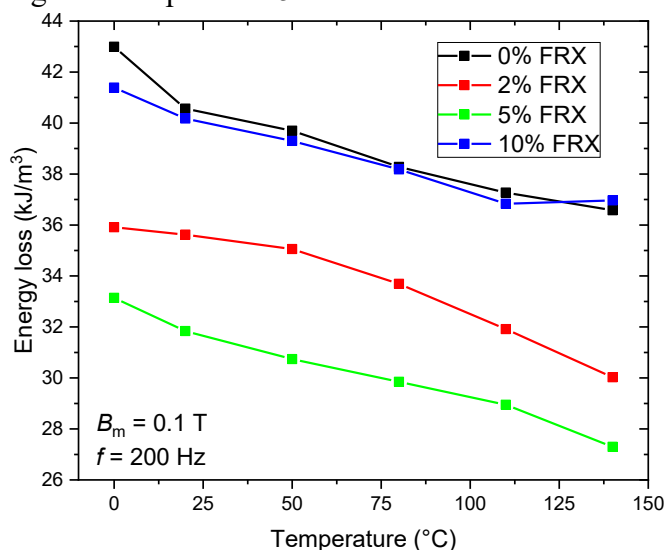
¹ Institute of Physics, Faculty of Science, P.J. Šafárik University in Košice, Park Angelinum 9, 04154 Košice, Slovakia.

² Institute of Materials Research, Slovak Academy of Sciences, Watsonova 47, 04001, Košice, Slovakia.

For the soft magnetic composite sample series based on Fe/SiO₂/ferrite with the percentage of the soft ferrite powder equal to 0%, 2%, 5%, and 10%, were measured influence of the temperature on magnetic permeability and hysteresis loops in AC regime in the temperature spectrum up to 140°C. The results of the study indicate that the addition of a small amount of ferrite to the composition of the sample improves its magnetic properties. On the other hand total magnetization of hybrid SMC rapidly decrease when it reaches Curie temperature of ferrite.

A series of tested samples was produced from Fe powder coated with SiO₂, which was mixed with Ni-Zn/Cu-Zn sintered ferrite at various percentages and pressed under a pressure of 2 GPa. Via impedance analyzer were measured the dependences of magnetic permeability on temperature. The measurements of the influence of the temperature on the AC hysteresis loops were recorded by AC hysteresis-graphs at the frequency up to 300 kHz. The temperature range of the measurements was from room temperature up to 140°C.

Figure 1 shows that lowest energy loss at the entire investigated temperature region belongs the sample with 5% of ferrite.



Permeability vs temperature showing positive trend until the vicinity of the Curie temperature of ferrite above around 120°C and this effect becomes more powerful with higher amount of ferrite in composition of the sample. The influence of ferrite content and temperature on the core loss is analyzed.

Figure 1 : Energy loss vs temperature for the 0%, 2%, 5% and 10% content of ferrite.

This work has been supported by the Slovak Research & Development Agency (APVV-20-0072) and by the Scientific Grant Agency of the Ministry of Education, Science, Research & Sport of the Slovak Republic and the Slovak Academy of Sciences (VEGA 1/0143/20, VEGA 1/0225/20).

Symposium 9. Micromagnetic modelling and magnetization processes

| | | |
|-----------------------------|--|-----|
| Victor H. González | <i>Voltage-control of effective damping in spin Hall nano-oscillators</i> | 238 |
| Adam Papp | <i>Inverse magnonics with SpinTorch</i> | 239 |
| Damien Querlioz | <i>Forecasting the outcome of spintronic experiments with Neural Ordinary Differential Equations</i> | 240 |
| Leoni Breth | <i>Interpretation ambiguity in FORC diagrams</i> | 242 |
| Adriano Di Pietro | <i>Gauged Micromagnetic Model of the Dzyaloshinskii-Moriya Interaction Induced by Symmetry Breaking at the Co/Pt Interface</i> | 243 |
| Amil Ducevic | <i>Micromagnetic simulation of soft magnetic composites utilizing periodic boundary conditions</i> | 244 |
| Yadhu Krishnan Edathumkandy | <i>Comparative study of magnetic properties of Mn^{3+} magnetic clusters in GaN using classical and quantum mechanical approach</i> | 245 |
| Katrijn Everaert | <i>Temperature dependence of the stochastic thermal magnetic field of magnetic nanoparticles</i> | 246 |
| Mouad Fattouhi | <i>Absence of Walker breakdown in the dynamics of chiral Néel domain walls driven by in-plane strain gradients</i> | 247 |
| John Fullerton | <i>Three-dimensional Magnetic Textures in Strongly Coupled Cylindrical Nanowires</i> | 248 |
| Maxwel Gama Monteiro | <i>Asymmetrically Interfaced Double Barrier Magnetic Tunnel Junctions for MRAM Devices</i> | 249 |
| Theodor Griep | <i>Evidence of electron-phonon spin flips as the intrinsic mechanism for ultrafast demagnetization in 3d transition metals</i> | 250 |
| Markus Gusenbauer | <i>Coercivity analysis of twin boundaries in arbitrary field direction by micromagnetic simulations</i> | 251 |
| Andrzej Janutka | <i>Micromagnetic study of response of superferromagnetic and superparamagnetic nanocomposites to high-frequency field</i> | 252 |
| Shun Kanai | <i>Thermal Agitation of Magnetization Dynamics Induced by Electric-field</i> | 253 |
| Grzegorz Kwiatkowski | <i>Optimal protocol for switching of a perpendicular nanomagnet by means of magnetic field and spin-orbit torque.</i> | 254 |
| Ioannis Panagiotopoulos | <i>Micromagnetic simulations of Microwave Assisted Switching in Hard/Soft phase nanowires</i> | 255 |
| Elena Stetco | <i>Micromagnetic Simulations of Spin-Orbit Torque Driven Domain Wall Based Memristor Devices</i> | 256 |
| Takuya Taniguchi | <i>Mode selective excitation of spin-waves utilizing spin-wave conversion</i> | 257 |
| Mateusz Żelent | <i>Mutual and symmetry-breaking magnetostatic interactions in hybrid structure with Néel-type skyrmion</i> | 258 |
| Sławomir Ziętek | <i>Numerical model of harmonic Hall voltage detection for spin orbit torque devices</i> | 259 |
| Kausik Das | <i>Magnetic Dynamical Properties and Ferromagnetic Resonance in $(Ga,Mn)N$ Layers</i> | 261 |

| | | |
|--------------------|---|-----|
| Yuliia Kharlan | <i>Study of the coupling between propagating spin waves in magnetic film</i> | 262 |
| Jakub Mojsiejuk | <i>Numerical model of current induced magnetisation spin-orbit torque switching</i> | 263 |
| Alejandro Rivelles | <i>FORC analysis in arrays of interacting nanodots</i> | 264 |

Invited Oral Presentations

| | | |
|--------------------|--|-----|
| Victor H. González | <i>Voltage-control of effective damping in spin Hall nano-oscillators</i> | 238 |
| Adam Papp | <i>Inverse magnonics with SpinTorch</i> | 239 |
| Damien Querlioz | <i>Forecasting the outcome of spintronic experiments with Neural Ordinary Differential Equations</i> | 240 |

Voltage-control of effective damping in spin Hall nano-oscillators

Victor H. González¹, Roman Khymyn¹, Himanshu Fulara^{1,2}, Johan Åkerman¹
and Afshin Houshang¹

¹*Department of Physics, University of Gothenburg, Gothenburg, Sweden*

²*Department of Physics, Indian Institute of Technology Roorkee, Roorkee, India*

Constriction-based spin Hall nano-oscillators (SHNOs) [1] have attracted interest for their non-linear behavior [2] exhibiting ultra-wide microwave frequency tunability [3], mutual synchronization in chains [4] and 2D arrays [5], and voltage enabled frequency manipulation [6]. The latter provides an efficient path for implementation of neuromorphic and quantum-like computing applications, such as Ising Machines [7]. In this work, we use micromagnetic simulations to explore voltage gate geometries for controlling SHNOs (fig.1a) and obtain strong qualitative and quantitative changes in effective damping as a function of gating voltage (fig.1b), as well as different regimes in the excitation of linear and non-linear modes (fig.1c). We speculate that these effects are due to spin wave localization and reflection at the voltage gate interfaces, and product of a change in magnetic anisotropy as a result of the applied electric field.

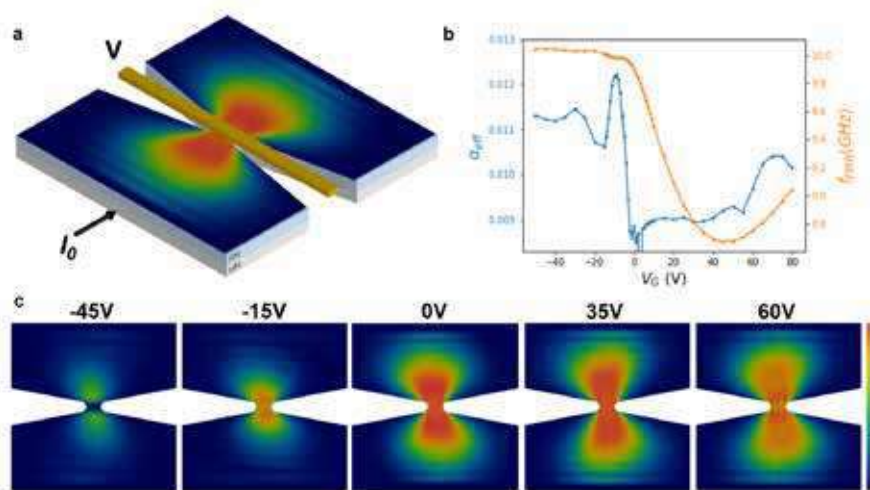


Figure 1: **a.** SHNO and voltage electrode geometries **b.** Effective damping and FMR frequency as a function of voltage. **c.** Space maps of excited modes for different voltages.

- [1] T. Chen, R. K. Dumas, A. Eklund, **Pro. IEEE**, vol. 104, no. 10, pp:1919-1945, (2016)
- [2] M. Dvornik, A. A. Awad and J. Åkerman *Phys. Rev. Applied* **9**, 014017 (2018).
- [3] M. Zahedinejad, H. Mazraati, H. Fulara *et al.*, *Appl. Phys. Lett.* **112**, 132404 (2018).
- [4] A. A. Awad, P. Dürrenfeld, A. Houshang *et al.*, *Nat. Phys.* **13**, 292–299 (2017).
- [5] M. Zahedinejad, A. A. Awad, S. Muralidhar *et al.* *Nat. Nanotech.* **15**, 47-52 (2020).
- [6] H. Fulara, M. Zahedinejad, R. Khymyn *et al.* *Nat. Comm.* **11**, 4006 (2020).
- [7] A. Houshang, M. Zahedinejad, S. Muralidhar *et al.* arXiv:2006.02236 [**cond-mat.mes-hall**] (2020).

Inverse magnonics with SpinTorch

**Adam Papp¹, Martina Kiechle², Markus Becherer², Wolfgang Porod³
and György Csaba¹**

¹ *Pázmány Péter Catholic University, Faculty of Information Technology, Budapest, Hungary*

² *Technical University of Munich, Department of Electrical and Computer Eng., Munich, Germany*

³ *University of Notre Dame, Department of Electrical Engineering, Notre Dame, IN, USA*

Designing spin-wave devices has many challenges due to the complex behavior of spin waves, including anisotropic propagation, nonlinearity at moderate amplitudes, and limited propagation distance due to damping and slow group velocity. Many elementary components were designed and demonstrated in analogy of optical signal processors, including lenses, gratings, and waveguides [1]. However, integration of these blocks into larger functional systems is limited to a few special designs. To best utilize the available space limited by the spin-wave decay length, we turned to machine learning for automatic inverse design of spin-wave devices. We implemented a full micromagnetic simulator, SpinTorch [2], which uses backpropagation through time to achieve a certain functionality. SpinTorch is based on the PyTorch machine-learning framework, which takes care of the gradient calculation automatically, and handles GPU acceleration of the computations. Training is performed in a series of epochs, each of them including a forward path (propagation of waves), and a backward calculation of gradients. After each epoch the design is updated to better match the desired functionality.

We demonstrated the operation of the algorithm by inverse designing spin-wave scatterers that guide spin waves to specific output locations according to the design goal. The scatterer can be based on any physical parameter, e.g.: local modifications of M_s , patterning the propagation medium by removing material in specific regions, or external components like an array of nanomagnets or nanocoils on top of the film. We showed that such a scatterer acts as a neural network, i.e., it can be trained to solve classification problems [3]. A requirement for universal classification is the employment of nonlinearity in the system, which spin waves provide readily: we also demonstrated that SpinTorch can effectively utilize the nonlinear behavior of magnetic dynamics to solve linearly-not-separable problems. Meanwhile, the inverse problem can be a design of a physical component, such as a compact lens (Fig. 1) with a nonintuitive shape and prescribed performance, or a frequency multiplexer.

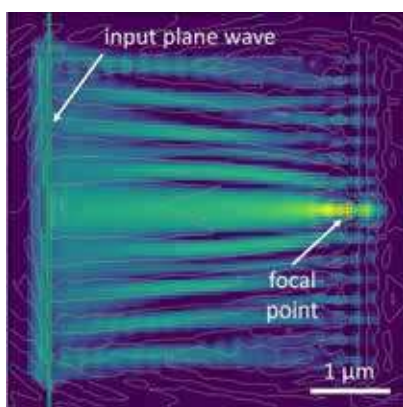


Figure 1: Inverse design of a lens: the figure depicts the resulting intensity pattern in a YIG film as a plane wave is being focused to the center output location.

The SpinTorch code is still under development, but we made the source code available online at [2], with a simple working example provided. With small modifications/extensions the code can easily be used to design devices in many material systems and configurations. We successfully employed SpinTorch with e.g.: anisotropic spin waves, SOT amplification in the design region, and hybrid systems (nanomagnets on top of YIG). We hope that our method can accelerate the research of spin-wave-based computing and signal-processing devices and help us better understand the limitations and advantages of using spin waves as information carrier and processor.

[1] G. Csaba *et al.*, *Physics Letters A*, 381(17), 1471-1476. (2017).

[2] <https://github.com/a-papp/SpinTorch>

[3] A. Papp *et al.*, *Nat. Commun.* 12, 6422 (2021).

Forecasting the outcome of spintronic experiments with Neural Ordinary Differential Equations

**Xing Chen^{1,2}, Flavio Abreu Araujo³, Mathieu Riou⁴,
Jacob Torrejon⁴, Dafiné Ravelosona², Wang Kang¹,
Weisheng Zhao¹, Julie Grollier⁴ and Damien Querlioz²**

¹*Fert Beijing Institute, Beihang University, 100191 Beijing, China.*

²*Université Paris-Saclay, CNRS, Centre de Nanosciences et de Nanotechnologies, Palaiseau, France.*

³*Institute of Condensed Matter and Nanosciences, Université catholique de Louvain, Belgium.*

⁴*Unité Mixte de Physique, CNRS, Thales, Université Paris-Saclay, Palaiseau, France.*

email: damien.querlioz@c2n.upsaclay.fr

Deep learning is having an increasing impact in aiding research, enabling, for example, the discovery of new materials. So far, however, these artificial intelligence techniques have failed to discover the complete differential equation of an experimental physical system. Here we show that a dynamic neural network, trained on a minimal amount of data, can predict the behavior of spintronic devices with high accuracy and extremely efficient simulation time, compared to micromagnetic simulations. To this end, we reframe the formalism of “Neural Ordinary Differential Equations” [1] to the constraints of spintronics: few measured outputs, multiple inputs and internal parameters. We demonstrate with Neural Ordinary Differential Equations a speed-up factor of more than 200 compared to micromagnetic simulations for a complex problem, the simulation of a reservoir computer made of magnetic skyrmions (20 minutes versus three days). In a second achievement, we show that we can predict the noisy response of experimental spintronic nano-oscillators to varying inputs after training the neural ordinary differential equations over five milliseconds of their measured response to a different set of inputs. Neural ordinary differential equations can therefore be a breakthrough tool for the development of spintronic applications as a complement to micromagnetic simulations, which are time-consuming and cannot scale to experiments in the presence of noise or imperfections. Our approach, whose results are reported in [2], can also be generalized to other electronic devices involving dynamics.

[1] Chen, R. T., Rubanova, Y., Bettencourt, J. & Duvenaud, D. K. Advances in Neural Information Processing Systems, 6571–6583 (2018).

[2] Chen, X., Araujo, F. A., Riou, M., Torrejon, J., Ravelosona, D., Kang, W., Zhao, W., Frollier, J., Querlioz, D. (2022). Forecasting the outcome of spintronic experiments with Neural Ordinary Differential Equations. Nature communications, 13(1), 1-12.

Oral Presentations

| | | |
|----------------------------|--|-----|
| Leoni Breth | <i>Interpretation ambiguity in FORC diagrams</i> | 242 |
| Adriano Di Pietro | <i>Gauged Micromagnetic Model of the Dzyaloshinskii-Moriya Interaction Induced by Symmetry Breaking at the Co/Pt Interface</i> | 243 |
| Amil Ducevic | <i>Micromagnetic simulation of soft magnetic composites utilizing periodic boundary conditions</i> | 244 |
| YadhuKrishnan Edathumkandy | <i>Comparative study of magnetic properties of Mn^{3+} magnetic clusters in GaN using classical and quantum mechanical approach</i> | 245 |
| Katrijn Everaert | <i>Temperature dependence of the stochastic thermal magnetic field of magnetic nanoparticles</i> | 246 |
| Mouad Fattouhi | <i>Absence of Walker breakdown in the dynamics of chiral Néel domain walls driven by in-plane strain gradients</i> | 247 |
| John Fullerton | <i>Three-dimensional Magnetic Textures in Strongly Coupled Cylindrical Nanowires</i> | 248 |
| Maxwel Gama Monteiro | <i>Asymmetrically Interfaced Double Barrier Magnetic Tunnel Junctions for MRAM Devices</i> | 249 |
| Theodor Griepe | <i>Evidence of electron-phonon spin flips as the intrinsic mechanism for ultrafast demagnetization in 3d transition metals</i> | 250 |
| Markus Gusenbauer | <i>Coercivity analysis of twin boundaries in arbitrary field direction by micromagnetic simulations</i> | 251 |
| Andrzej Janutka | <i>Micromagnetic study of response of superferromagnetic and superparamagnetic nanocomposites to high-frequency field</i> | 252 |
| Shun Kanai | <i>Thermal Agitation of Magnetization Dynamics Induced by Electric-field</i> | 253 |
| Grzegorz Kwiatkowski | <i>Optimal protocol for switching of a perpendicular nanomagnet by means of magnetic field and spin-orbit torque.</i> | 254 |
| Ioannis Panagiotopoulos | <i>Micromagnetic simulations of Microwave Assisted Switching in Hard/Soft phase nanowires</i> | 255 |
| Elena Stetco | <i>Micromagnetic Simulations of Spin-Orbit Torque Driven Domain Wall Based Memristor Devices</i> | 256 |
| Takuya Taniguchi | <i>Mode selective excitation of spin-waves utilizing spin-wave conversion</i> | 257 |
| Mateusz Zelent | <i>Mutual and symmetry-breaking magnetostatic interactions in hybrid structure with Néel-type skyrmion</i> | 258 |
| Sławomir Ziętek | <i>Numerical model of harmonic Hall voltage detection for spin orbit torque devices</i> | 259 |

Interpretation ambiguity in FORC diagrams

L. Breth¹, T. Schrefl¹, J. Fischbacher¹, C. Czettl², J. Pachthofer², M. Schwarz², S. Kührer² and H. Brückl¹

¹Department for Integrated Sensor Systems, 2700 Wr. Neustadt, Austria

²CERATIZIT Austria GmbH, 6600 Reutte, Austria

First Order Reversal Curve (FORC) diagrams are well known to serve as “magnetic fingerprints” of samples containing various magnetic components that differ regarding e.g. their grain size or crystalline texture [1]. FORCs contain more information about the microscopic reversal processes than major hysteresis loops and hence, their quantitative interpretation based on known features of the microstructure is of interest to a wide range of applications. Here, we present a micromagnetic simulation study of Co cubes with uniaxial anisotropy, for which a series of FORCs was computed using energy minimization [2]. When the cube size is increased, the magnetization reversal changes from single domain switching to reversal by domain wall nucleation and annihilation. Each magnetization jump produces positive or negative peaks in the FORC diagram (see Fig. 1). The FORC diagram features for the domain wall reversal process in the 100 and 150 nm cubes resemble those of interacting patterned microstructures [3]. Our results point to an interpretational ambiguity of the ground truth behind the features in a FORC diagram, which has to be considered if e.g. grain sizes should be inferred from FORC diagrams.

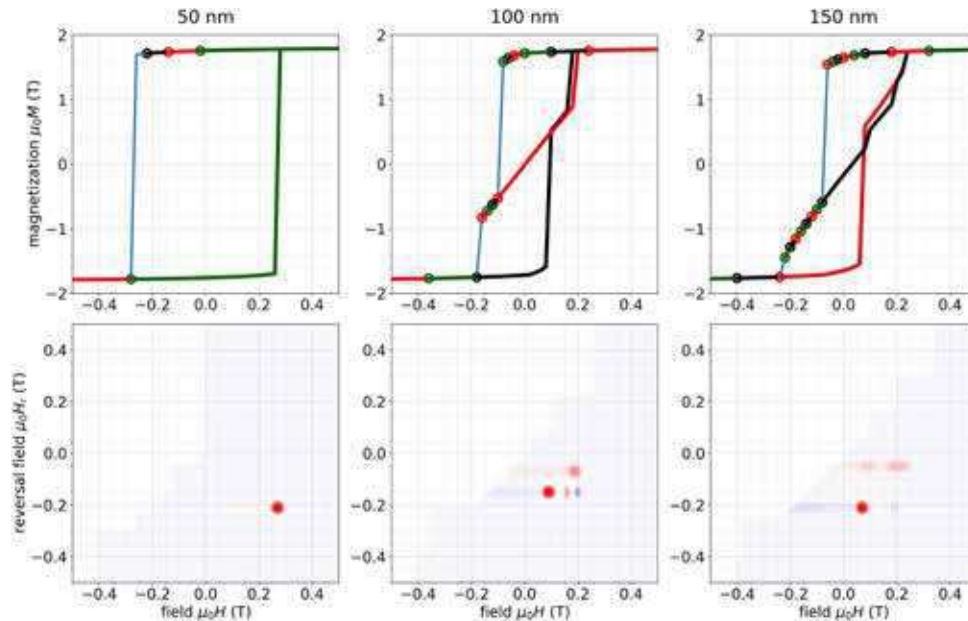


Figure 1: Simulated FORCs (top) and corresponding FORC diagrams (bottom) of hcp Co cubes with varying edge length

- [1] C. Pike, A. P. Roberts, and K. L. Verosub, *J. Appl. Phys.* **85**, 6660 (1999).
- [2] L. Exl *et al.*, *Comp. Phys. Comm.* **235**, 179 (2019).
- [3] F. Groß *et al.*, *Phys. Rev. B* **99**, 064401 (2019).

Gauged Micromagnetic Model of the Dzyaloshinskii-Moriya Interaction Induced by Symmetry Breaking at the Co/Pt Interface

*P. Ansalone¹, A. Di Pietro^{1,2}, E.S. Olivetti¹, A. Magni¹, M. Kuepferling¹, V. Basso¹

¹Istituto Nazionale di Ricerca Metrologica (INRIM), Strada delle Cacce, 91, 10135 Torino, Italy.

²Politecnico di Torino, Corso Duca degli Abruzzi 24, 10129, Torino, Italy.

The Dzyaloshinskii-Moriya-like interaction (DMI) is a source of chirality in magnetism [1]. This interaction is currently at the centre of a growing effort to search for new materials or realise tailored devices supporting novel applications in magnetism and spintronics. We focus both on the interpretation of the DMI in terms of a non-abelian gauge field [2] and on the application of the point groups symmetries to the micromagnetic free energy in thin films of cobalt on heavy metal substrates (*e.g.* platinum) [3]. The model sample, Figure 1, consists of a single-crystalline ultrathin magnetic film of hcp-cobalt with [0001] direction normal to the x - y film plane, with finite thickness and the magnetisation $m(x, y)$ is independent of the z -coordinate.

The cobalt layer viewed along this direction consists of regularly distributed hexagons of Co atoms. The point group of hcp-cobalt is $6/mmm$ ($D6h$), which is the direct product of the $6mm$ ($C6v$) and m (CIh) point groups [4] and does not exhibit DMI interaction because of its centrosymmetry. By breaking the symmetry along e_z , the point group changes from the $6/mmm$ ($D6h$) to the non-centrosymmetric $6mm$ ($C6v$), and the e_z and $-e_z$ directions are no longer equivalent. Experimentally this occurs when the Co film is epitaxially grown onto the Pt(111) single crystal surface, making the Co/Pt interface inversion-asymmetric [5], owing to the presence of an additional layer with a different stacking.

The gauge theory and the symmetry analysis, consistent with the Neumann's principle, applied to the micromagnetic exchange energy, predicts the emergence of the surface DMI in such a system. Moreover, we show a new possible effect of an exchange stiffness tensor [6] obeying the symmetry of the hexagonal lattice and its impact on the DMI.

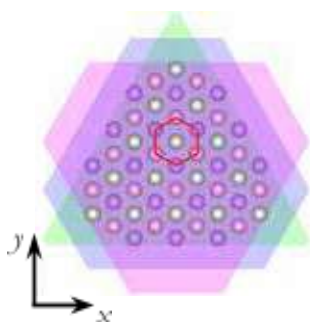


Figure 1. Sketch of the top view of the Pt/Co interface: the green (111) plane (at the bottom) contains the Pt-atoms on which (0001) planes of Co-atoms (pink and purple planes), with the *ABAB* stacking for hcp metals.

[1] M. Kuepferling, *et al.* Measuring interfacial Dzyaloshinskii-Moriya interaction in ultra thin films, ArXiv preprint arXiv:2009.11830 (2020).

[2] P. Ansalone, *et al.*, Gauge theory applied to chiral magnets (AIP Advances, in press).

[3] H. Yang, *et al.*, Anatomy of Dzyaloshinskii-Moriya interaction at Co/Pt interfaces, Physical review letters 115.26 (2015): 267210.

[4] K. Sakoda, Optical properties of photonic crystals, Springer Science & Business Media, 2004.

[5] A. Ullah, *et al.*, Crystal structure and Dzyaloshinski–Moriya micromagnetics, IEEE Transactions on Magnetism 55.7 (2019): 1-5.

[6] A. Hubert, and R. Schäfer, Magnetic domains: the analysis of magnetic microstructures, Springer Science & Business Media, 2008.

* Corresponding author Patrizio Ansalone - p.ansalone@inrim.it

Micromagnetic simulation of soft magnetic composites utilizing periodic boundary conditions

Amil Ducevic¹, Florian Bruckner¹, and Dieter Suess¹

¹Physics of Functional Materials, Faculty of Physics, University of Vienna, Vienna, Austria

Soft magnetic composites consist of ferromagnetic particles, with typical particle sizes between $1 - 100\mu m$, which are separated by an electrical insulating material. The samples can have macroscopic sizes, however the discretization length required is governed by the exchange length, which is in the nm-range. This limits the total simulation size to a few micrometers. Additionally demagnetization effects come into play when a finite sized sample is simulated, however due to the magnetic flux closure of the samples the demagnetization field is zero. Therefore periodic boundary conditions(PBCs)[1] have been implemented into the micromagnetic code to overcome these problems. Assuming PBCs allows one to effectively simulate an infinite sample, and therefore avoids demagnetization effects which are caused by the finite shape. A complete micromagnetic framework including PBCs will be presented with which the spatially- and time-resolved magnetization response to an external field is simulated.

The power-losses of the SMCs can be divided into different contributions, mainly into hysteretic-, eddy current- and residual-losses. The micromagnetic code at hand is capable of calculating the well-known static hysteresis loss and the dynamic hysteresis losses which adds to the total hysteresis loss at high frequencies. The framework will in part be validated by replicating experimental setups which aim to reduce the hysteresis loss. Feng et al.[2] have shown that the application of a transverse field \mathbf{H}_{trans} reduces the power-loss. This was replicated in the simulation and as can be seen in figure 1 the simulated powerloss P_m decreases when a transverse field \mathbf{H}_{trans} is applied at the cost of the relative permeability μ_r decreasing by a lesser degree.

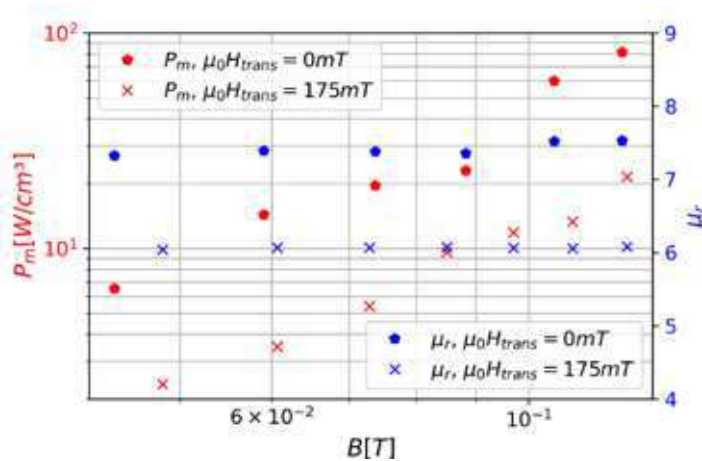


Figure 1: Powerloss P_m and permeability μ_r were calculated from hysteresis simulations utilizing the SMC model with and without transverse field \mathbf{H}_{trans} as was done experimentally in [2].

[1] Bruckner, Florian, et al. "Strayfield calculation for micromagnetic simulations using true periodic boundary conditions." Scientific Reports 11.1 (2021): 1-8.

[2] Feng, S. J., et al. "Reduction of hysteresis loss in soft magnetic composites under transverse magnetic field." Applied Physics Letters 117.12 (2020): 122402.

Comparative study of magnetic properties of Mn^{3+} magnetic clusters in GaN using classical and quantum mechanical approach

Y. K. Edathumkandy¹ and D. Sztenkiel¹

¹*Institute of Physics, Polish Academy of Sciences, PL 02-668 Warszawa, Poland*

Currently, simulations of many-body quantum systems are known to be computationally too demanding to be solved on classical computers. The main problem is that the computation time (number of elementary operations) and memory necessary for performing the calculations usually grow exponentially with the number of particles. An efficient approach to simulate many-body quantum systems is the use of classical approximation. Such approach can reduce the overall computational complexity, but it usually face difficulties in proper reproduction of temperature-dependent properties of the system due to neglect of spin quantization [1]. It is important then to somehow assess the validity of this classical approximation. For practical reasons the quantum simulations of interacting Mn^{3+} ions in GaN, coupled by ferromagnetic super-exchange interaction $J\mathbf{S}_i \cdot \mathbf{S}_j$, are restricted up to small magnetic clusters. Therefore in this work [2], we compare the results of numerical calculations of magnetic clusters (singlet, pairs, triplets and quartets) in (Ga,Mn)N where the Mn spins are treated classically with those where they are treated quantum-mechanically (crystal field model) [3,4]. In the first case, we solve Landau-Lifshitz-Gilbert (LLG) equation, that describe the precessional dynamics of spins represented by classical vectors. On the other hand, in crystal field model, the Mn^{3+} state (d^4 configuration with $S = 2$, $L = 2$) is characterized by the set of orbital and spin quantum numbers $|m_s, m_L\rangle$. The relevant energy level structure of singlet, pair, triplet and quartet of Mn ions are found by the numerical diagonalization of full (25×25) , $(25^2 \times 25^2)$, $(25^3 \times 25^3)$ and $(25^4 \times 25^4)$ Hamiltonian matrix respectively. Particular attention is paid to use numerical parameters that ensure the same single ion magnetic anisotropy in classical and quantum approximation. Finally, a detailed comparative study of magnetization $\mathbf{M}(\mathbf{H}, T)$ as a function of magnetic field \mathbf{H} , temperature T , number of ions in given cluster N and the strength of super-exchange interaction J , obtained from both approaches will be presented.

- [1] R. F. L. Evans *et al.*, *J. Phys: Condens. Matter.* **26**, 103202 (2014).
- [2] Y. K. Edathumkandy and D. Sztenkiel, *arXiv* :2108.01474.
- [3] J. Gosk *et al.*, *Phys.Rev. B.* **71**, 13232 (2005).
- [4] D. Sztenkiel *et al.*, *Nature Comm.* **7**, 094432 (2016).

The work is supported by the National Science Centre, Poland, through projects DEC-2018/31/B/ST3/03438 and by the Interdisciplinary Centre for Mathematical and Computational Modelling at the University of Warsaw through the access to the computing facilities.

Temperature dependence of the stochastic thermal magnetic field of magnetic nanoparticles

Katrijn Everaert^{1,2}, Bartel Van Waeyenberge¹, Frank Wiekhorst², and Jonathan Leliaert¹

¹Ghent University – Department of Solid State Sciences, Krijgslaan 281, 9000 Ghent, Belgium

²Physikalisch-Technische Bundesanstalt – Department of Biosignals, Abbestr. 2-12, 10587 Berlin, Germany

The thermal fluctuations in the magnetic field of a magnetic nanoparticle (MNP) ensemble are often unwanted noise on a measurement signal. However, they can also be used directly in Thermal Noise Magnetometry (TNM)[1] for the characterization of the ensemble. In this work, we compare the effect of temperature variations on the stochastic thermal magnetic field of magnetic nanoparticles induced by the two fluctuation mechanisms: Néel fluctuations and Brownian rotations.

Temperature enters the Power Spectral Density (PSD) S_B of the stochastic thermal magnetic field B a first time via the fluctuation time τ [2]:

$$S_B(f) = A \frac{4\tau}{(2\pi f\tau)^2 + 1} \quad \text{with} \quad \tau = \tau_N = \tau_0 \exp\left(\frac{KV_c}{k_B T}\right), \quad \text{or} \quad \tau = \tau_B = \frac{3\eta V_h}{k_B T} \quad (1)$$

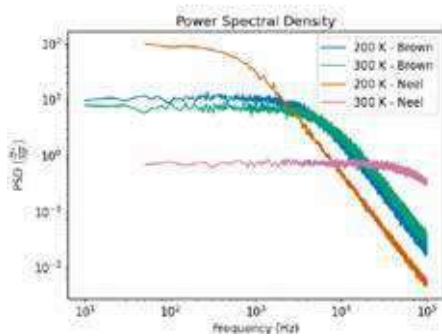


Figure 1: Power Spectral Densities calculated from the simulated time signal for a 20 nm particle subjected to Néel fluctuations and Brownian rotations.

Note the exponential dependence of the Néel fluctuation time τ_N on temperature T , anisotropy constant K and magnetic volume V_c , and the linear dependence of the Brownian rotation time τ_B on temperature T , viscosity η and hydrodynamical volume V_h . The difference in the dependency is clearly visible in the the shapes of the PSDs in Fig. 1.

The temperature can also influence the magnitude of the fluctuations, and thus the amplitude A of the PSD. For Brownian rotation, the magnetic moments are uniformly distributed and their probability density function (PDF) is independent of temperature.

In the case of Néel fluctuations however, temperature defines the available thermal energy to jump the anisotropy barrier KV_c . The distribution of the magnetic moments, and thus the magnitude of the fluctuations, strongly depends on temperature.

Our results shed light on how temperature influences thermal activities for different stochastic processes, which could be of interest in the development of e.g. nanothermometers.

[1] J. Leliaert et al. *Appl. Phys. Lett* **107**, 222401 (2015).

[2] K. Everaert et. al. *IEEE Access* **9**, 111505 (2021).

Absence of Walker breakdown in the dynamics of chiral Néel domain walls driven by in-plane strain gradients

Mouad Fattouhi, Felipe Garcia-Sanchez, Rocio Yanes, Victor Raposo, Eduardo Martinez, Luis Lopez-Diaz

Departamento de Fisica Aplicada, Universidad de Salamanca, 37008, Salamanca, Spain

Magnetic domain wall (DW) motion in perpendicularly magnetized media has been a topic of intensive investigation in the last decade [1]. The conventional manner to drive a DW relies on applying an external magnetic field. Under small fields DW moves rigidly with increasing velocity up to the Walker breakdown limit, where the DW depicts precessional motion and its mobility is significantly reduced [2]. Alternative ways to drive DWs without Joule heating effects nor Walker breakdown need to be explored for novel and efficient DW-based schemes.

Here we investigate the motion of chiral Néel DWs driven by in-plane strain gradients using both micromagnetic simulations and a one-dimensional model [2,3]. The strain gradient creates a force that drives the DW towards region of higher tensile (compressive) strain for materials with positive (negative) magnetostriction. Due to the dependence of DW internal energy on in-plane strain, a damping torque proportional to the local strain arises during motion that opposes the precessional torque due to the driving force, which is proportional to the strain gradient. This prevents the onset of turbulent DW dynamics, and steady DW motion with constant velocity is asymptotically reached for any arbitrarily large strain gradient as shown in Fig.1(a) and (b). In the transient, both the internal DW angle and the velocity change non-monotonically reaching their maximum values asynchronously. Despite complex dynamics, averaged DW velocities in the range of 500 m/s can be obtained using voltage-induced strain in piezoelectric/ferromagnetic devices under realistic conditions.

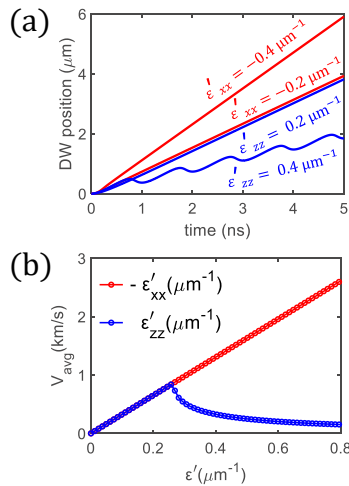


Figure 1: (a) DW position versus time as driven by two different in-plane (blue) and out-of-plane (red) strain gradients. (b) Average DW velocity versus strain slope for the in-plane (blue) and out-of-plane (red) strain gradients. $\epsilon'_{xx} = \frac{\partial \epsilon_{xx}}{\partial x}$ is the strain slope.

- [1] E. Martinez, S. Emori and G. S.D. Beach, *App. Phys. Lett.* **103**, 072406 (2013).
- [2] N. L. Schryer and L. R. Walker, *J. App. Phys.* **45**, 5406 (1974).
- [3] A. Vansteenkiste, J. Leliaert, M. Dvornik, H. Mathias and F. Garcia-Sanchez, and B. Van Waeyenberge, *AIP. adv* **4**, 107133 (2014).

Three-dimensional Magnetic Textures in Strongly Coupled Cylindrical Nanowires

J. Fullerton¹, A. Hierro-Rodriguez², C. Donnelly³, D. Sanz-Hernández⁴, L. Skoric⁵, L. Aballe⁶, D. Raftrey^{7,8}, P. Fischer^{7,8}, D. A. MacLaren¹ and A. Fernández-Pacheco^{1,9}

¹ SUPA, School of Physics and Astronomy, University of Glasgow, Glasgow, UK

² Depto. Fisica, Universidad de Oviedo, Oviedo, Spain

³ Max Planck Institute for Chemical Physics of Solids, Dresden, Germany

⁴ Unité Mixte de Physique, CNRS, Thales, Université Paris-Saclay, Paris, France

⁵ Cavendish Laboratory, University of Cambridge, Cambridge, UK

⁶ ALBA Synchrotron Light Facility, Barcelona, Spain

⁷ Materials Sciences Division, Lawrence Berkeley National Laboratory, Berkeley, USA

⁸ Physics Department, UC Santa Cruz, Santa Cruz, USA

⁹ Institute of Nanoscience & Materials of Aragón, CISC-University of Zaragoza, Zaragoza, Spain

Cylindrical magnetic nanowires show great promise for a multitude of applications. Thanks to recent advances in nanofabrication, such as focused electron beam induced deposition (FEBID), it is now possible to move past single nanowires and fabricate complex three-dimensional (3D) interconnected structures [1, 2]. These structures can possess novel and intriguing spintronic properties that can be controlled by altering the geometry of the system, providing a new route to high density, low power computing and sensing devices [3].

We will outline micromagnetic simulations of a variety of 3D magnetic states that form during the growth of strongly overlapped nanowires. The separation and overlap of the wires was varied in order to determine how the interplay between exchange and magnetostatic energy affects the equilibrium magnetic states, as outlined in figure 1(a). At the two extremes of separation, either the exchange or magnetostatic energy dominate. However, in-between these regimes, simulations reveal the formation of complex 3D spin textures, as shown by figure 1(b). These states consist of a net anti-parallel alignment of wires, as favored by magnetostatic interaction, but with distinct domain structures: either a modulated helical Bloch domain wall or a Landau pattern-like state with a 3D magnetic core, depending on separation.

We will present complementary experimental studies, covering the optimisation of the FEBID process, subsequent electron microscope characterisation and x-ray magnetic dichroism measurements of iron nanowires. These results show how precise control over nanowire coupling can be utilised to finely tune magnetic energies of a system and hence give rise to complex 3D magnetisation.

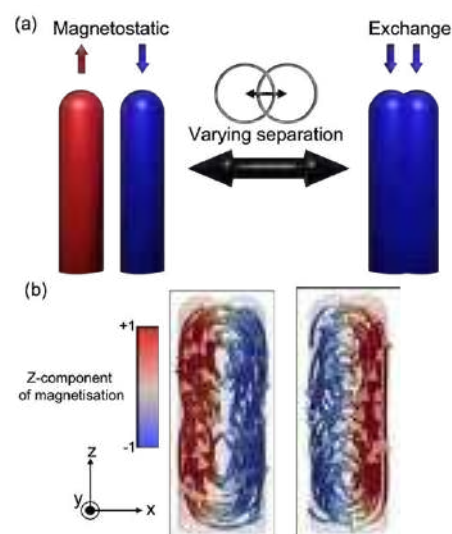


Figure 1: (a) Competing magnetic energies while varying the separation of nanowire pairs. (b) Micromagnetic simulations of nanowire pairs at intermediate overlap values, showing complex spin textures arising from the competition of exchange and magnetostatic energies.

- [1] L. Skoric, et.al., Layer-by-layer growth of complex-shaped three-dimensional nanostructures with focused electron beams, *Nano Lett.*, **20**, 184 (2020).
- [2] D. Sanz-Hernández, et al., Artificial double-helix for geometrical control of magnetic chirality, *ASC Nano.*, **14**, 8084 (2020).
- [3] A. Fernández-Pacheco, et. al., Three-dimensional nanomagnetism, *Nat. Comm.*, **8**, 15756 (2017).

Asymmetrically Interfaced Double Barrier Magnetic Tunnel Junctions for MRAM Devices

M.G.Monteiro^{1,2}, R. Carpenter¹, S. Rao¹, S. Couet¹, G.S. Kar¹

¹IMEC, 3001 Leuven, Belgium

²Department of Electrical Engineering (ESAT), KU Leuven, 3001 Leuven, Belgium

Devices based on Magnetic Tunnel Junctions (MTJs) such as Spin-Transfer Torque Magnetoresistive RAM (STT-MRAM) memories are strong contenders for nonvolatile and low power replacements of current storage technology like Static RAM. However, several challenges remain to actually reach that potential, including trade-offs in between bit stability *vs* switching power and difficulty to achieve high densities.

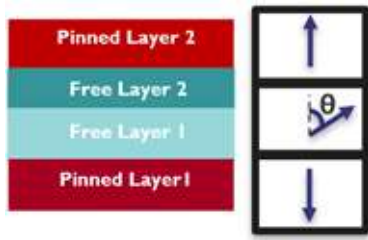


Figure 1: Schematics of DMTJ-based device (left) and magnetic volumes of its Pinned and Free layers (right).

A promising solution proposed to aid efficiency in STT-MRAM designs is a double MTJ (DMTJ), as in Fig. 1. This design was previously explored by Worledge[1] in the case of a Free layer with equal properties on both interfaces to each Pinned layer, as well as the Pinned layers with equal spin polarizations. In this work we instead focus on simulations of the general case hinted at by their model, where not only the polarization of both interfaces are separable, but also the Free layer may have asymmetrical properties across its thickness (i.e Saturation magnetization M_s and Exchange stiffness A_{ex}). In this general model the total antidamping torque acting on the Free layer is resolved across the thickness as the Free layer is no longer reducible to a single interface.

By running simulations of this more general system we obtain results such as Fig. 2 for the switching mechanism of the Free layer in different material compositions. In all simulations the Pinned layers are assumed fixed and the Free layer has equal thicknesses in both interfaces with a fixed total thickness of 1.5(nm) and varying diameters. As we show, the increasingly asymmetrical properties in each interface induce a change of the switching mechanism, essentially from a Bloch domain wall profile to that of a Néel domain wall. This can be shown to reflect in smaller switching times and can be linked to experimental trends, and provides a route for tailoring the dynamics of these devices by playing with the composition and interface properties of the Free layer even across its thickness below the exchange length.

[1]D. C. Worledge, IEEE Magn. Lett. 8, 1-5 (2017).

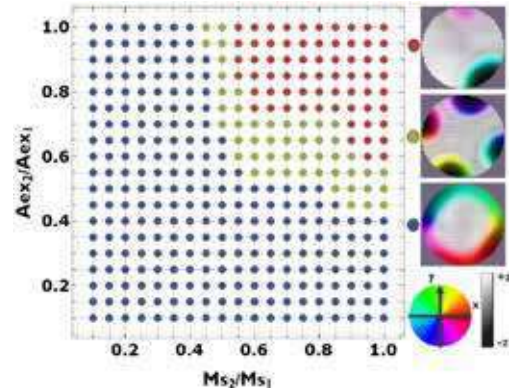


Figure 2: Switching dynamics of asymmetrical DMTJ with mechanisms as a function of composition of Free layer interfaces 1 and 2 (case of 50(nm) diameter).

Evidence of electron-phonon spin flips as the intrinsic mechanism for ultrafast demagnetization in 3d transition metals

Theodor Griede¹, Unai Atxitia¹

¹Freie Universität Berlin, Arnimallee 14, 14195 Berlin, Germany

Complete understanding of the ultrafast magnetization dynamics in 3d ferromagnets has remained elusive since the discovery of a sub-picosecond response of magnetization to femtosecond laser pulses in Nickel. Electron-phonon mediated spin flips as the leading mechanism was proposed by Koopmans et al. in terms of the Microscopic Three Temperature Model (M3TM) [1] by direct comparison of theoretical simulations and experimental data. However, the needed spin-flip probabilities to replicate experimental data was up

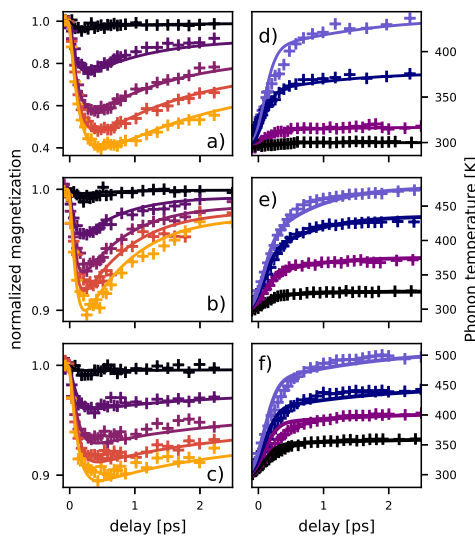


Figure 1: Magnetization (left) and Lattice (right) dynamics of a) Nickel, b) Cobalt and c) Iron retrieved from experiments ('+') [4] [5] [6] and from simulations (solid) for a variety of fluences.

to four times higher than suggested by ab initio calculations [2]. In contradiction to the current understanding, we found evidence that electron-phonon mediated spin flips can very well describe magnetization dynamics in 3d transition metals with spin flip probabilities in the range of predictions by Carva et al. [2]. To do so, we implemented an extended M3TM for arbitrary values of effective spin [3]. Importantly, we have implemented ab initio calculations for the temperature dependent heat capacities of electrons and lattice, as well as electron-phonon coupling [4] [5], leaving only the spin-flip probability as a fit parameter. We have shown that the overestimation of spin-flip probability by Koopmans et al. is based on an overestimation of electronic heat capacity. Furthermore we have introduced an intrinsic energy flow between electrons and spins, important to correctly model the lattice dynamics. Figure 1 shows the comparison of model and experiment. Figures 1 a)-c) show magnetization dynamics of Nickel, Cobalt and Iron, respectively. All fit parameters are kept constant for different fluences and the spin-flip probabilities agree with predictions of Carva et al. [2]. Figure 1 d)-f) show the respective lattice dynamics, using the same system parameters as for the calculation of magnetization dynamics. Despite slightly different sample preparations, the agreement is very good. Our results are evidence that electron-phonon mediated spin flips are the intrinsic mechanism for ultrafast demagnetization of 3d transition metals.

- [1] B. Koopmans, G. Malinowski, F. Dalla Longa, *Nat. Mat.* **9** (2010).
- [2] K. Carva, M. Battiato, D. Legut, *Phys. Rev. B* **87** (2013)
- [2] M. Beens, M. Lalieu, A. Deenen, *Phys. Rev. B* **100** (2019)
- [4] D. Zahn, F. Jakobs, Y. W. Windsor, *Phys. Rev. Res.* **3** (2021)
- [5] D. Zahn, F. Jakobs, Y. H. Seiler, *Phys. Rev. Res.* **4** (2022)
- [6] M. Borchert, C. Schmising, D. Schick, *arXiv:2008.12612v1* (2020)

Coercivity analysis of twin boundaries in arbitrary field direction by micromagnetic simulations

Harald Oezelt¹, Panpan Zhao², Thomas G. Woodcock², Thomas Schrefl¹, and Markus Gusenbauer¹

¹ Department for Integrated Sensor Systems, Danube University Krems, Austria

² Institute for Metallic Materials, Leibniz IFW Dresden, Germany

Processing of raw materials to develop permanent magnets usually results in crystallographic defects, which can have a significant influence on the coercivity H_c of the magnet, as for instance analyzed in MnAl-C [1]. Tuning the processing routes allows promoting or suppressing certain defects, hence quantifying the influence of the defects is necessary.

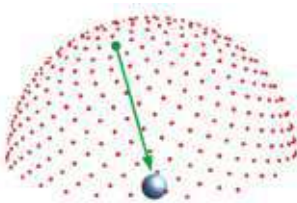


Figure 1: Fibonacci half sphere indicating external field directions pointing towards simulation model.

In this work we demonstrate a simulation procedure, to compute H_c distributions for various single defects over arbitrary applied field directions. In order to exclude demagnetization effects, we model the different defects within a sphere. External field directions are applied evenly distributed around a unit sphere (Fibonacci sphere [2]) pointing to the simulation model in the center (Fig.



Figure 2: Finite element model of a single defect

1). Each point on the unit sphere corresponds to a micromagnetic simulation, solving the Landau-Lifshitz-Gilbert equation on a tetrahedral finite element grid [3]. The model consists of several segregation layers with varying thickness close to the defect to set different magnetic properties according to measured or estimated material concentrations (Fig. 2).

In MnAl-C, twin boundaries have Mn-enriched regions at the defect, Mn-depleted regions a few nm away, and bulk properties far away from the defect [4,5]. Easy axes configurations are set according to the various measured twin boundaries [5]. Corresponding experiments are performed using sophisticated transmission electron microscopy or atom probe tomography. Results show that the coercivity tends to increase with increasing structural and chemical disorder at the defect (Fig. 3).

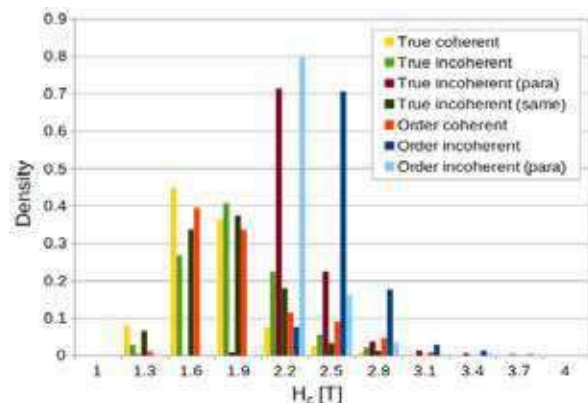


Figure 3: Density of simulated coercivities H_c for different twin configurations.

This work was funded by the Austrian Science Fund (FWF), project no. I 5266-N.

- [1] M. Gusenbauer, A. Kovacs, H. Oezelt, J. Fischbacher, P. Zhao, T. G. Woodcock and T. Schrefl, *J. Appl. Phys.*, **129**(9), 093902 (2021).
- [2] R. Swinbank, R. J. Purser, *Q. J. R. Meteorol. Soc.*, **132**, 1769 (2006).
- [3] D. Suessa, V. Tsiantos, T. Schrefl, J. Fidler, W. Scholz, H. Forster, R. Dittrich and J. Miles, *J. Magn. Magn. Mater.*, **248**, 298 (2002).
- [4] D. Palanisamy, D. Raabe, B. Gault, *Acta Mater.*, **174**, 227 (2019).
- [5] P. Zhao, M. Gusenbauer, H. Oezelt, D. Wolf, T. Gemming, T. Schrefl, K. Nielsch and T. G. Woodcock, *Submitted* (2022).

Micromagnetic study of response of superferromagnetic and superparamagnetic nanocomposites to high-frequency field

A. Janutka¹ and K. Brzuszek¹

¹ Department of Theoretical Physics, Wrocław University of Science and Technology, 50-370, Wrocław, Poland

We investigate the magnetic response of composites of magnetic nanoparticles (MNPs) embedded in dielectric matrices to high-frequency magnetic field with regard to their application as core materials for miniaturized power converters. The major advantage of such nanocomposites is the property of reduced/eliminated conductivity, thus, the suppression of the excess losses. In order to suppress the intra-particle eddy currents, the diameters of the nanoparticles should be below the electronic mean free path. We outline our study of the magnetic response of several superferromagnetic nanocomposites ($\text{Fe}_{65}\text{Co}_{35}\text{-Al}_2\text{O}_3$, $\text{Fe}_{65}\text{Co}_{35}\text{-SiO}_2$, Co-MgF_2) to linearly-polarized or rotating fields of a high frequency, using micromagnetic simulations, with material parameters extracted from data within the random magnetic anisotropy (RMA) model [1]. We have simulated arrays of periodically disposed MNPs (in a matrix that contains a small amount of magnetic ions) and we have verified analytical predictions about the high-frequency permeability. In particular, we have discussed the possibility of breaking the Snoek limit on the permeability at a given frequency of the driving field and the saturation magnetization.

When reducing the volumetric content of the magnetic phase, the superferromagnetic state (maintained due to the magnetic-ion leakage from the nanoparticles to the dielectric matrix) undergoes the transition to a highly-resistive superparamagnetic state. This is related to an unavoidable decrease of the permeability, while, further increase of the resistivity is extremely important at high (microwave) frequency regime. Performing the study of both superferromagnetic and superparamagnetic nanocomposites allows us to directly compare the efficiency of their dynamical responses. The optimization of the power conversion using the superparamagnetic nanocomposite cores is a current problem in technology and it is, contrary to the superferromagnet case, strongly related to temperature [2]. We perform (temperature dependent) micromagnetic simulations of arrays of periodically disposed $\text{Fe}_{65}\text{Co}_{35}$ nanoparticles (the material of extremely high saturation magnetization) of 5nm diameter under linearly-polarized-alternating or rotating fields. Thus, we go beyond the commonly-used macrospin approximation for the magnetic moments of the nanoparticles. We notice considerable enhancement of the high-frequency magnetic susceptibility at elevated temperatures, especially, the response to the rotating field is strengthened by temperature fluctuations. Below the particle concentration of the disappearance of the superferromagnetism, there are different dipolarly-ordered phases identified (the super-spin-glass state and the genuine superparamagnet). We compare their magnetic responses at high-frequencies, finding only quantitative differences.

[1] K. Brzuszek and A. Janutka, *J. Magn. Magn. Mat.* **543**, 168608 (2022).

[2] M. Kin, H. Kura and T. Ogawa, *AIP Advances* **6**, 125013 (2016).

Thermal Agitation of Magnetization Dynamics Induced by Electric-field

S. Kanai¹⁻⁵, Y. Nakatani⁶, F. Matsukura^{1,5,7,8}, and H. Ohno^{1,4,5,7,8}

¹Laboratory for Nanoelectronics and Spintronics, RIEC, Tohoku University, Sendai, Japan

²PRESTO, Japan Science and Technology Agency, Kawaguchi, Japan

³Division for the Establishment of Frontier Science, Tohoku University, Sendai, Japan

⁴Center for Science and Innovation in Spintronics, Tohoku University, Sendai, Japan

⁵Center for Spintronics Research Network, Tohoku University, Sendai, Japan

⁶University of Electro-Communications, Tokyo, Japan

⁷Center for Innovative Integrated Electronic Systems, Tohoku University, Sendai, Japan

⁸WPI-Advanced Institute for Materials Research, Tohoku University, Sendai, Japan

The magnetization dynamics in a free layer of nanoscale magnetic tunnel junctions (MTJs) can be induced by the application of an electric field through the change in magnetic anisotropy [1-4]. Here, we investigate the thermal effect on the magnetization dynamics induced by the electric field through the real-time observation of the precession at room temperature.

The stack structure, buffer layers /CoFeB(0.9 nm)/MgO(1.3 nm)/CoFeB(1.8 nm)/cap layers, is sputtered on a sapphire substrate and processed into an 80-nm-diameter MTJ. The resistance area product and tunnel magnetoresistance (TMR) ratio are $13 \Omega\mu\text{m}^2$ and 84%, respectively. The top and bottom CoFeB layers are the free and reference layers with the perpendicular easy axis, respectively. We apply voltage pulses to induce the magnetization precession in the free layer about the in-plane component of an external magnetic field. The switching probability as a function of the pulse duration shows the clear oscillation, while the oscillation decays within the 5 periods as with our previous works [2-4].

The transmitted voltage measured by a high-speed oscilloscope reflects the magnetization precession due to the change in the junction resistance through the TMR effect. The transmitted voltage shows a clear oscillation. The oscillatory amplitude changes randomly due to the thermal agitation, but does not show significant decay up to 20 ns/ ~ 6 periods (maximum period measured in this work), indicating the precession lasts longer than the decay time of the switching probability. The oscillatory phase randomly changes with time, leading in the rapid decay in the switching probability after averaging over a number of events. We find that the phase randomization is promoted by the oscillatory amplitude dependence of the precessional frequency. This dependence cannot be explained by a conventional macrospin model. On the other hand, the results of micromagnetic simulations, which include the spatial distribution of demagnetizing field, show a similar dependence in the single-domain like free layer. We develop an *adapted* macrospin model for nanoscale magnets by including the dependence phenomenologically. The model successfully describes the experimental results of the switching probability vs. the pulse duration, and has the potential to provide guideline for improving the switching reliability of the electric field-induced magnetization switching.

This work was supported in part by Grants-in-Aid for Scientific Research from JSPS (16H06081, 19KK0130, and 20H02178), JST (JPMJPR21B2), MEXT (26103002), and Cooperative Research Program of RIEC.

[1] Y. Shiota *et al.*, *Nature Mat.* **11**, 39 (2012).

[2] S. Kanai *et al.*, *Appl. Phys. Lett.* **101**, 122403 (2012).

[3] S. Kanai *et al.*, *Appl. Phys. Lett.* **106**, 192406 (2016).

[4] S. Kanai *et al.*, *Jpn. J. Appl. Phys.* **56**, 0802A3 (2017).

Optimal protocol for switching of a perpendicular nanomagnet by means of magnetic field and spin-orbit torque.

Grzegorz J. Kwiatkowski¹, Sergei M. Vlasov², Mohammad H.A. Badarneh¹, Igor S. Lobanov², Dmitry V. Berkov³, Valery M. Uzdin², and Pavel F. Bessarab^{1,2}

¹*Science Institute of the University of Iceland, 107 Reykjavík, Iceland*

²*ITMO University, 197101 St. Petersburg, Russia*

³*General Numerics Research Lab, 07745 Jena, Germany*

By means of optimal control theory it is demonstrated that a proper shaping of a switching pulse allows one to significantly reduce the energy cost of magnetization reversal of a nanomagnet with an easy axis. Spin-orbit torque switching [1] as well as magnetic field switching [2] were considered. For both cases the energy cost is associated with Joule heating and the optimisation goal is to minimize said heating. The time-dependent optimal switching pulses are obtained analytically as solutions to Euler-Lagrange equations in terms of the required reversal time and material properties [1,2]. Special emphasis is put on the way the ratio between field-like and damping-like components of the spin-orbit torque affects the results. A particular sweet-spot balance between said components is found [1] for which not only the energy cost is the lowest but the pulse has a particularly simple form that can be in practice approximated by a simple down-chirped pulse with a constant amplitude. Notion of an optimal switching time is introduced as a tradeoff between energy efficiency and switching speed [1,2]. Similarities and differences between the magnetic field and the spin-orbit torques cases are discussed.

[1] S. M. Vlasov, G. J. Kwiatkowski, I. S. Lobanov, V. M. Uzdin, and P. F. Bessarab, arXiv:2203.01167 [cond-mat.mes-hall] (2022).

[2] G. J. Kwiatkowski, M. H. A. Badarneh, D. V. Berkov, and P. F. Bessarab, *Phys. Rev. Lett.* **126**, 177206 (2021).

Micomagnetic simulations of Microwave Assisted Switching in Hard/Soft phase nanowires

Christos Thanos¹, Ioannis Panagiotopoulos^{1,2}

¹ Department of Materials Science and Engineering University of Ioannina, 45110 Ioannina, Greece

² Institute of Materials Science and Computing, University Research Center of Ioannina (URCI), 45110 Ioannina, Greece

Microwave assisted switching of the magnetization (MAS) has attracted a lot of attention lately due to its application in magnetic recording media to alleviate the conflicting constraints of increased density, high SNR, writability and thermal stability [1]. Using MAS the switching field is lowered by resonantly exciting the precessional motion of the magnetic moment by a radio frequency field, a mechanism which also presents scientific interest as the resonant response is fundamentally different from a thermal one. Here microwave assisted magnetic switching (MAS) is simulated in two phase Co/CoPt nanowires using the mumax3 finite difference micromagnetic simulation program [2]. This is an interesting model system where the processes of nucleation, interfacial domain wall pinning, and propagation can come into play depending on the phase content and interfacial coupling strength between the two phases [3-5]. The coupling strength is varied to cover both smooth (strong coupling) and stepped (weak coupling) hysteresis loops. The reversal time is given for all the conditions (applied dc reversed field, microwave frequency) which led to full reversal. The optimal frequencies are consistent with the ferromagnetic resonances of the system. For the weak coupling cases, these can be sufficiently well predicted by using a simple two-micropin model representing two phases with uniaxial anisotropies H_K , H_S ($H_K > H_S$) coupled by exchange field H_{ex} which gives:

$$\omega_{\pm} = \gamma \left| \left(H + H_{ex} + \frac{H_K + H_S}{2} \right) \pm \sqrt{\left(\frac{H_K - H_S}{2} \right)^2 + H_{ex}^2} \right| \quad (1)$$

$$\omega_{\pm} = \gamma \left| \left(H + \frac{H_K - H_S}{2} \right) \pm \sqrt{\left(\frac{H_K + H_S}{2} - H_{ex} \right)^2 + H_{ex}^2} \right| \quad (2)$$

Where γ is the gyromagnetic ratio and eq.1 refers to the case where the soft is reversed, while eq.2 to the case where the magnetizations of the two phases remain parallelly magnetized. Under optimal conditions the reversal time can be 0.5ns but in most of the cases is close to 2ns. The reversal time is mainly limited by the domain wall propagation in the hard phase.

- [1] Z. Liu et al., IEEE Trans. Magn **54**, 1-5 (2018), doi:10.1109/TMAG.2018.2835155
- [2] A. Vansteenkiste, et al, AIP Advances **4** 107133 (2014), doi:10.1063/1.4899186
- [3] D. Suess et al., J. Magn. Magn. Mater. **321**, 545 (2009), doi:10.1016/j.jmmm.2008.06.041.
- [4] S. Li et al, Appl. Phys. Lett. **94**, 202509 (2009), doi:10.1063/1.3133354
- [5] T. Yamaji and H. Imamura, Appl. Phys. Lett. **109**, 192403 (2016); doi:10.1063/1.4967195

Micromagnetic Simulations of Spin-Orbit Torque Driven Domain Wall Based Memristor Devices

E. M. Stetco^{1,2}, T. Petrisor Jr.¹, O. A. Pop², I. M. Miron³ and M.S. Gabor¹

¹ Centre for Superconductivity, Spintronics and Surface Science, Physics and Chemistry Department, Technical University of Cluj-Napoca, Str. Memorandumului, 400114 Cluj-Napoca, Romania

² Applied Electronics Department, Technical University of Cluj-Napoca, Str. Memorandumului, 400114 Cluj-Napoca, Romania

³ Univ. Grenoble Alpes, CNRS, CEA, Grenoble INP, IRIG-SPINTEC, 38000 Grenoble, France

The memristor is considered the fourth passive fundamental electrical circuit element whose electrical resistance depends on the history of electrical current that had previously passed through it. It recently gained increased scientific interest as it can serve as an artificial synapse in neuromorphic computing architectures due to its analog behavior, intrinsic dynamics, and great scalability [1]. Currently, the memristors are mainly focused on charge-based devices. They include field effect transistors, phase change memory, ion migration resistance change memory devices etc. Besides the more classical charge-based devices, *spin-based memristors* are also proposed because of their improved endurance and energy efficiency. Recently, it was demonstrated that current induced spin-orbit torques (SOTs) can be used to build devices showing analog memristive behavior [2]. Different types of SOT memristors can be considered depending on the action of the SOT on the magnetic texture.

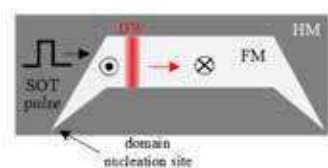


Figure 1: DW - SOT memristor; A up/down DW propagates from the left to the right-hand side for a current pulse in the same direction.

Here, we focus on SOT driven memristors in which the SOTs move a domain wall (DW) within a perpendicular magnetized ferromagnetic (FM) layer (Fig. 1), which can constitute the free electrode of a magnetic tunnel junction. An important challenge for the implementation of DW-SOT memristor, is the domain nucleation and the local control of the DW position. Here, we propose a design of the FM layer with two narrow regions, whose tips become domain nucleation sites, as in Fig.1 [3]. Moreover, DW displacement depends on the relative angle between the

current direction and the DW, which is set by the geometry of the patterned FM layer relative to the current line [3]. Thus, for a certain angle, it is possible to inhibit the motion of one DW type (up-down or down-up), relative to the other (down-up or up-down). Therefore, for a given pulse current direction only one DW type will propagate through the narrow region and enter the rectangular stripe, where the DW will move in the same direction as the current pulse. We validate our proposed design by employing micromagnetic simulations, performed in *MuMax*³ [4] of ideal systems. For more realistic granular systems, we show that one type of DW remains pinned and the other one propagates in the rectangular region of the structure with a certain velocity that depends on the pulse current amplitude and material parameters. We also evidence lateral size effects on the simulated structures ranging from nanometric to micrometric sizes.

[1] Y. Zhang, et al., *Applied Physics Reviews* **7**, 011308 (2020).

[2] S. Emori, et al., *Nature Mater* **12**, 611–616 (2013).

[3] C.K. Safeer, et al., *Nat Nanotech* **11**, 143–146 (2016).

[4] A.V.Steenkiste, et al., *AIP Advances* **4**, 107133 (2014).

Mode selective excitation of spin-waves utilizing spin-wave conversion

T. Taniguchi¹ and C. H. Back¹

¹ Technical University Munich, James-Frank-Strasse 1, Garching, Germany

Magnonic devices are often based on the wave properties of spin waves (SWs), so that one can transport more information in a single device if modes of SWs are freely controllable. SWs in a narrow waveguide have eigenmodes due to standing waves formed in the width direction and the thickness direction [1]. However, excitation of one specific higher order mode of propagating SWs has not been realized, yet. Here, we report that high SW modes can be selectively excited by employing SW conversion.

We numerically investigated SW propagation in a T-shaped structure using MuMax3 [2]. A 5-nanometer-thick Py film is assumed as the device and a magnetic field of 70 mT is applied along the y-direction. By applying an rf field to the cells 1 μm away from the junction, Damon-Eshbach spin waves (DESWs) are excited and travel along the x-direction. The DESWs induce a magnetization precession in the junction, which excites SWs in the magnetostatic backward volume wave configuration (BVSWs).

First, we varied the SW resonant frequency ($f=12, 18$ GHz) using a device having $w_1=500$ nm and $w_2=100$ nm. As shown in Fig. 1a and b, the wavelength of the DESW (λ_{DESW}) depends on f which is well known [2]. In addition, the BVSWs clearly change their wave front. To extract the mode number, we applied a Fourier transformation (FT). The FT results indicate that the 1st mode is dominantly excited at 12 GHz but the 2nd mode is dominant at 18GHz (Fig. 1d and e). We next changed the device to have $w_2=500$ nm and repeated the simulation at 18 GHz (Fig. 1c). The result indicates the 12th mode is dominant at this condition (Fig.1f). To further understand the high-mode-excitation, we varied the frequency and plotted the FT peak height of each mode as a function of the ratio of the width to λ_{DESW} (Fig.1g). The result implies that modes are controllable by optimizing a T-shaped waveguide [4].

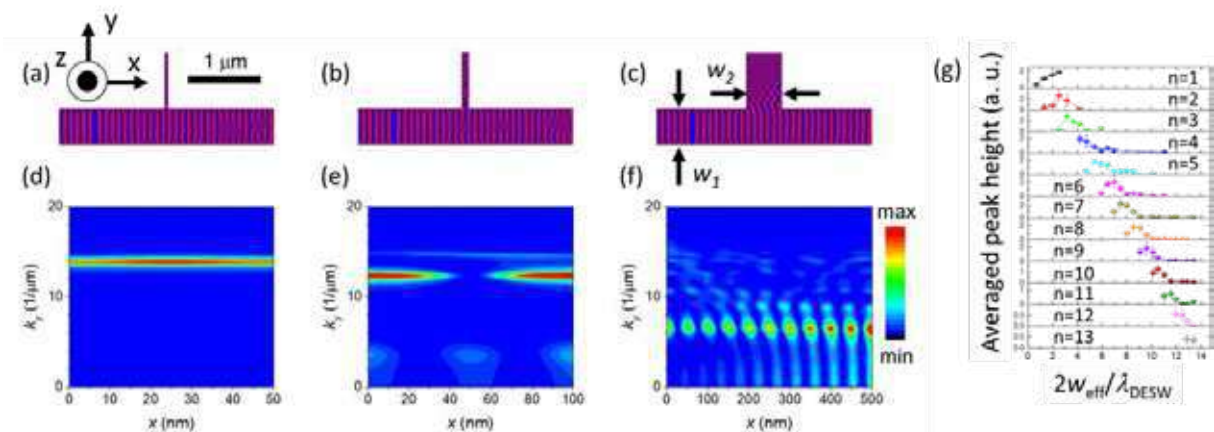


Figure 1: (a)-(c) The spatial dependent z-component of the magnetization and (d)-(f) their corresponding FT of BVSWs. (f, w_2) is (a, d) (12 GHz, 100 nm), (b, e) (18 GHz, 100 nm), and (c, f) (18 GHz, 500 nm). (g) The peak height of FT of each mode obtained from the device with $w_2=500$ nm.

- [1] H. G. Bauer *et al.*, Appl. Phys. Lett. **104**, 102404 (2014). [2] B. A. Kalinikos and A. N. Slavin J. Phys. C **19**, 7013 (1986). [3] A. Vansteenkiste *et al.*, AIP Adv. **4**, 107133 (2014). [4] T. Taniguchi and C. H. Back, Appl., Phys. Lett. **120**, 032402 (2022).

Mutual and symmetry-breaking magnetostatic interactions in hybrid, skyrmionics nanostructures

M. Zelent¹, M. Moalic¹, M. Mruczkiewicz^{2,3}, X. Li⁴, Y. Zhou⁵
and M. Krawczyk¹

¹ *Institute of Spintronics and Quantum Information, Faculty of Physics, Adam Mickiewicz University, Poznan, Poland*

² *Institute of Electrical Engineering, Slovak Academy of Sciences, Bratislava, Slovakia*

³ *Centre For Advanced Materials Application CEMEA, Slovak Academy of Sciences, Bratislava, Slovakia*

⁴ *College of Engineering Physics, Shenzhen Technology University, Shenzhen, China*

⁵ *School of Science and Engineering, The Chinese University of Hong Kong, Shenzhen, China*

Magnetic skyrmions are stable nanometric-size spin textures with potential for memory, spintronic and magnonic applications due to the unique properties governed by their nontrivial topology [1-2]. We show that egg-shaped like deformed Néel skyrmions can be stabilized by magnetostatic interaction in a hybrid structure composed of a multilayered nanodot hosting a skyrmion and the in-plane magnetized thin stripe made of soft ferromagnetic material (see Fig.1). The skyrmion state generates a nonuniform stray magnetic field, which affects the magnetization in the adjacent layer. The disturbed magnetization order in the adjacent layer induces a reverse counter-stray magnetostatic field, which exerts a significant effect on the skyrmion static configuration, breaking its circular symmetry and enhancing an influence of DMI. We show that such hybrid nanostructures can host skyrmions at smaller values of DMI than an isolated dot.

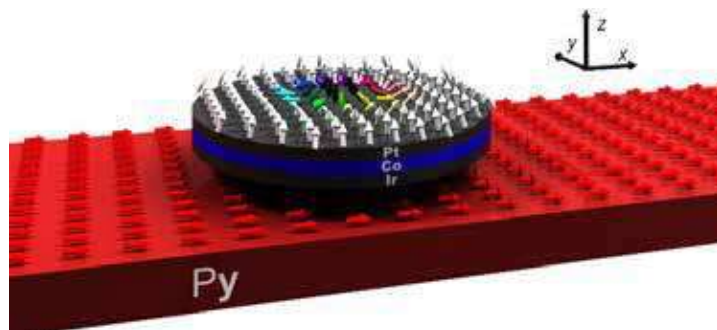


Fig. 1. A visual representation of the system under consideration. The Pt/Co/Ir multilayer dot is located slightly above the Py stripe. In the dot an egg-shape Néel-type skyrmion state is stabilized by the magnetostatic coupling to the in-plane magnetized stripe. The arrows indicate the direction of magnetization.

We explained these effects as a the result of the magnetization texture imprinted by the skyrmion upon the stripe, and its mutual interaction on the skyrmion. We outlined opportunities for further development of hybrid structures towards applications, and demonstrate the proof-of-concept of the skyrmion racetrack memory which exploits properties of mutual interactions in a hybrid structure for skyrmion transport.

Our results demonstrate a promising hybrid structure for applications in magnonics and spintronics.

The research has received funding from National Science Centre of Poland, Grant No. UMO-2018/30/Q/ST3/00416.

[1] Finocchio Giovanni, Panagopoulos Christos. Magnetic Skyrmions and Their Applications. Elsevier; 2021. doi:10.1016/C2019-0-02206-6

[2] Fert A, Reyren N, Cros V. Magnetic skyrmions: advances in physics and potential applications. Nature Reviews Materials. 2017;2(7):17031.

Numerical model of harmonic Hall voltage detection for spin orbit torque devices

J. Mojsiejuk¹, S. Ziętek¹, K. Grochot^{1,2}, S. Łazarski¹, W. Skowroński¹ and T. Stobiecki^{1,2}

¹AGH University of Science and Technology, Institute of Electronics, Al. Mickiewicza 30, 30-059 Kraków, Poland

²AGH University of Science and Technology, Faculty of Physics and Applied Computer Science, Al. Mickiewicza 30, 30-059 Kraków, Poland

Recently, there has been a spiking interest in effects utilising spin-orbit torque (SOT) [1-3] that pave the way to more efficient switching [4] and robust SOT-MRAM [5]. Spin Hall angle (SHA) has thus become one of the key parameters in the SOT study, an indirect measure of the usefulness of a device for spintronics applications. Among the multitude of methods measuring the SHA, the harmonic spin-Hall voltage detection method has gained much popularity due to its simplicity and flexibility. Our model is verified with the experimental data of the heavy metal/ferromagnet structure, where we demonstrate a satisfying agreement of the model with the data for both first (V_ω) and second ($V_{2\omega}$) magnetic field dependent harmonic Hall voltage readouts, see Fig.1, for the in plane longitudinal (H_x) and transversal (H_y) external magnetic field [6]. Therefore, any optimisation of the SHA may help reduce that cost and lead to more efficient spintronic devices. In that spirit, we conduct a study by simulating the structure with different parameter values. Thanks to the efficiency of the numerical model, we are able to perform parameter scans that reveal the dependence of the quadratic region of V_ω and linear region of $V_{2\omega}$ on magnetisation saturation (M_s), anisotropy (K_u) and SOT parameters: field-like and damping-like torques.

Research project partly supported by program „Excellence initiative – research university” for the AGH University of Science and Technology

- [1] C. Song et al., Progress in Materials Science 118, 100761, 2021
- [2] P.Ogrodnik et al., ACS Appl. Materials and Interfaces, 10, 47019, 2021
- [3] W. Skowroński et al., Phys. Rev. Applied 11, 024039, 2019
- [4] E. Grimaldi et al., Nature nanotechnology 15, 111, 2020
- [5] H. Zhou et al., AIP Advances 10, 015317, 2020
- [6] S. Zietek et al., arXiv:2202.00364, 2022

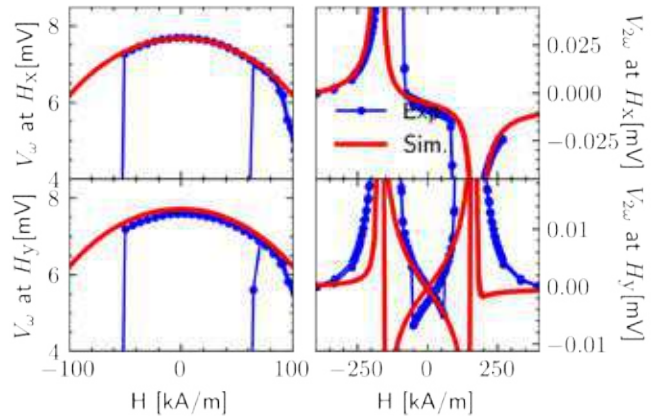


Figure 1: The V_ω and $V_{2\omega}$ for the longitudinal (H_x) and transversal (H_y) arrangements.

Posters

| | | |
|--------------------|---|-----|
| Kausik Das | <i>Magnetic Dynamical Properties and Ferromagnetic Resonance in (Ga,Mn)N Layers</i> | 261 |
| Yuliia Kharlan | <i>Study of the coupling between propagating spin waves in magnetic film</i> | 262 |
| Jakub Mojsiejuk | <i>Numerical model of current induced magnetisation spin-orbit torque switching</i> | 263 |
| Alejandro Rivelles | <i>FORC analysis in arrays of interacting nanodots</i> | 264 |

Magnetic Dynamical Properties and Ferromagnetic Resonance in (Ga,Mn)N Layers

K. Das¹, A. Grochot¹, K. Gas¹, Y. K. Edathumkandy¹, E. Piskorska-Hommel^{2,3}, D. Hommel^{2,3}, H. Przybylinska¹, M. Sawicki¹, D. Sztenkiel¹

¹*Institute of Physics, Polish Academy of Sciences, Warszawa, Poland*

²*Institute of Low Temperature and Structure Research, PAS, Wrocław, Poland*

³*Lukasiewicz Research Network–PORT Polish Center for Technology Development, Wrocław, Poland*

Dilute ferromagnetic semiconductors (DFS), in particular $\text{Ga}_{1-x}\text{Mn}_x\text{N}$, have attained great research attention due to their unique ability to combine properties of semiconductors and magnetic materials [1]. Moreover, GaN being a wide band gap semiconductor has dominated the photonics and high power electronics. So it is important to make an effort to understand the underlying magnetic properties of $\text{Ga}_{1-x}\text{Mn}_x\text{N}$.

Here we investigate both experimentally and theoretically the magnetic properties of GaN doped with Mn. The MBE grown ferromagnetic $\text{Ga}_{1-x}\text{Mn}_x\text{N}$ layers, with x ranging between 3% and 7%, are studied by a superconducting quantum interference device (SQUID) and ferromagnetic resonance (FMR). The uniaxial magnetic anisotropy (MA) of investigated material is inferred from magnetization measurements with magnetic field applied in two (perpendicular) directions with respect to the \mathbf{c} -axis of GaN. Similarly, the angular dependencies of FMR resonance fields enable probing both the uniaxial (trigonal) and triaxial (Jahn-Teller) anisotropies in $\text{Ga}_{1-x}\text{Mn}_x\text{N}$. The FMR experimental data is first analyzed by a traditional analytical approach using a (macrospin) free energy model [2]. However, such an approach does not give satisfactory results in the case of GaN with few percent randomly distributed Mn ions. Therefore, an atomistic spin model, using stochastic Landau-Lifshitz-Gilbert (sLLG) dynamics [3], is being developed. The model takes into account the Zeeman interaction as well as both trigonal and Jahn-Teller anisotropies (cf. Ref. [4]). A large simulation box, with few thousand Mn ions coupled by ferromagnetic interaction $-J\mathbf{S}_1\mathbf{S}_2$, is used. The magnetic moment \mathbf{M} and the microwave power absorbed during a ferromagnetic resonance is calculated after the system has reached a steady state [5]. Preliminary numerical results on small systems suggest the correctness of the applied model. This is the first simulation effort aimed at calculation of both magnetization and FMR in dilute magnetic semiconductor using atomistic approach.

- [1] T. Dietl, H. Ohno, *Rev. Mod. Phys.* **86**, 1 (2000).
- [2] C. Bihler, et al., *Phys. Rev. B*, **75**, 214419 (2007).
- [3] K. D. Usadel, *Phys. Rev. B* **73**, 212405 (2006).
- [4] Y. K. Edathumkandy and D. Sztenkiel, arXiv :2108.01474
- [5] K. Das, et al., *to be published*.

The work is supported by the National Science Centre, Poland, through projects DEC-2018/31/B/ST3/03438 and by the Interdisciplinary Centre for Mathematical and Computational Modelling at the University of Warsaw through the access to the computing facilities.

Study of the coupling between propagating spin waves in magnetic film

J. Kharlan¹, D. Popaduik¹, K. Szulc², E. Tartakovskaya^{1,2} and M. Krawczyk²

¹ Institute of Magnetism of NAS of Ukraine and MES of Ukraine, 36-b Acad. Vernadskogo Ave., Kyiv, Ukraine

² Faculty of Physics, Adam Mickiewicz University, Poznan, Uniwersytetu Poznańskiego 2, Poznan, Poland

Spin-wave (SW) propagation in ferromagnetic films attracts significant attention because of a knowledge of this phenomena physical characteristics is necessary to design modern magnonic devices [1,2]. Here, we present the combined theoretical description supported by micromagnetic simulation results of the hybridization between different propagating SW modes in an in-plane magnetized CoFeB film with thickness 100 nm in dependence on the surface anisotropy. We assume the propagation of SWs perpendicularly to the static magnetization and we consider two cases of boundary conditions, it is a symmetric and asymmetric SW pinning at the film surfaces, which leads to different coordinate dependence of SW profiles along film thickness and interaction between the modes. As it is seen in Fig. 1 the fundamental mode hybridizes with higher-order modes, and the coupling strength depends on the boundary conditions. We estimated the bands' splitting and its dependence on the type of boundary conditions, showing that the asymmetric pinning enhance the coupling between the SW modes. To calculate presented features of the dispersion relation we used and compared two theoretical models of Kalinikos-Slavin [3] and Harmsa-Duine [4].

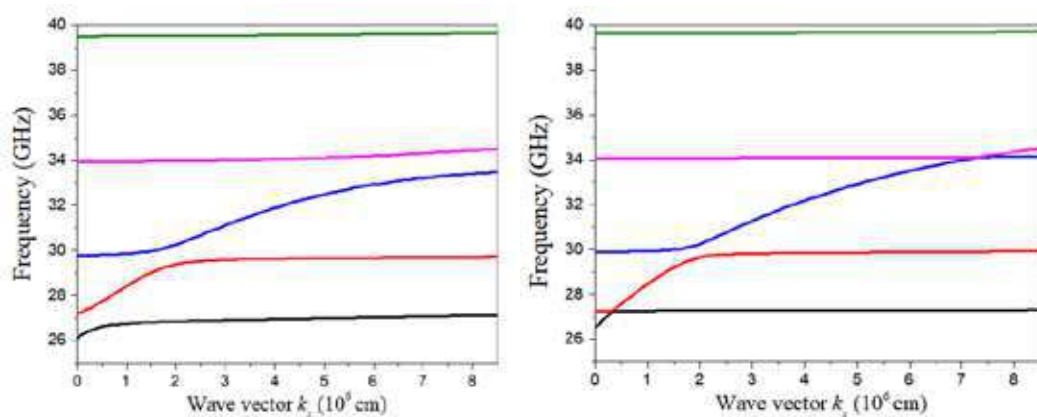


Figure 1: Simulated dispersion relations for 100 nm thick CoFeB film. The left picture corresponds to asymmetrical surface pinning conditions with the surface anisotropy energy density $K_S = 0$ and $200 \mu\text{J}/\text{m}^2$ on the top and bottom face of the layer. The right picture corresponds to symmetrical conditions with $K_S = 200 \mu\text{J}/\text{m}^2$ on both faces of the layer.

The research leading to these results has received funding from the Norwegian Financial Mechanism 2014-2021 project no UMO-2020/37/K/ST3/02450.

[1] M. Vanatka, K. Szulc, O. Wojewoda, C. Dubs, A. Chumak, M. Krawczyk, O. Dobrovolskiy, J. Kłos, and M. Urbanek, *Phys. Rev. Applied* 16, 054033 (2021).

[2] S. Tacchi, et al., *Phys. Rev. B* 100, 104406 (2019).

[3] B. A. Kalinikos and A. N. Slavin, *J. Phys. C: Solid State Phys.* 19 7013 (1986).

[4] J. S. Harmsa, R. A. Duine, ArXiv:2109.10597v2 [cond-mat.mes-hall] 1 Oct 2021.

Numerical model of current induced magnetisation spin-orbit torque switching

J. Mojsiejuk¹, S. Ziętek¹, K. Grochot^{1,2} and W. Skowroński¹

¹AGH University of Science and Technology, Institute of Electronics, Al. Mickiewicza 30, 30-059 Kraków, Poland

²AGH University of Science and Technology, Faculty of Physics and Applied Computer Science, Al. Mickiewicza 30, 30-059 Kraków, Poland

Recent trends in spintronics show an increased interest in the spin-orbit-torque (SOT) induced switching, which promises higher energy efficiency over the classical spin-transfer-torque (STT) switching regime [1,2]. We present a numerical model for current pulse-induced magnetisation switching in multilayer spintronic devices, which is a development of our previous work [3].

We verify the switching model in the trilayer structure FM/HM/FM. Depending on the magnetic anisotropy (MA) of each FM and the coupling energy via HM, different possibilities can be obtained [4].

Specifically, Co/Pt/Co with a mixed in-plane and perpendicular [5] MA, and both perpendicular MA of Co can be used for the field-free or

multistate switching experiment. Here, we demonstrate the dependence of the critical current on the magnitude of external field H_{ext} , and the anisotropy polar angle θ_K or interlayer-exchange coupling (IEC) constant J (Fig.1). The model can also deliver additional information about the dynamics such as the trajectory of magnetisation or the pulse response of resistance, which can be compared with time-resolved magneto-optical Kerr microscopy.

Research project partly supported by program „Excellence initiative – research university” for the AGH University of Science and Technology.

- [1] B. Dieny et al., Nature Electronics, 3, 446–459, 2020
- [2] K. Grochot et al., Physical Review Applied 15.1, 014017, 2021
- [3] S. Zietek et al., arXiv:2202.00364, 2022
- [4] P. Ogrodnik et al., ACS Appl. Mater. Interfaces, 13, 39, 47019–47032, 2021
- [5] S. Lazarski et al., Phys. Rev. Applied 12, 014006, 2019

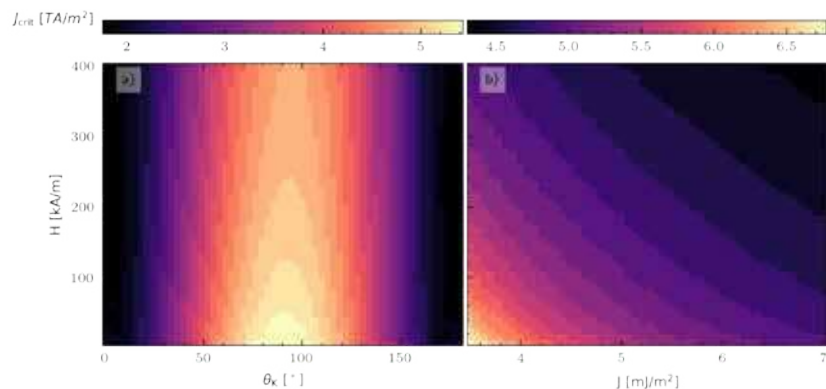


Figure 1: Magnitude of critical current (J_{crit}) in function of the in-plane external field (H_{ext}), and anisotropy polar angle θ_K (a) or IEC coupling constant J (b).

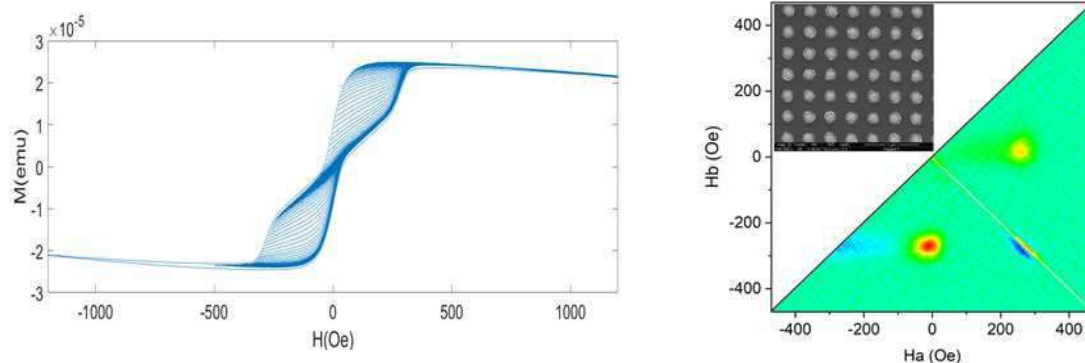
FORC analysis in arrays of interacting nanodots

A. Rivelles, M. Abuín, M. Maicas, J.L. Prieto and M.M. Sanz.

ISOM, Universidad Politécnica de Madrid, Madrid, Spain

FORC (*first-order reversal curves*) diagrams provide a lot of information about magnetic processes in a magnetic material by analyzing a large amount of minor hysteresis loops¹. Interpretation of these diagrams is not easy, specially in complex systems with strongly interacting elements. Therefore, in many situations FORC diagrams are only used as magnetic signatures more than as a characterization technique. Nanotechnology offers the possibility to synthesize ordered arrays of nanoelements where geometry, spacing and composition determine the interaction between elements. FORC diagrams can reveal quantitative information about magnetic coupling and the magnetization process in such structures. In this work we analyze the interaction between Py and Co circular magnetic nanodots with different geometries. Following a similar approach to previous works on nanostrips², we have fabricated arrays of Py and Co circular magnetic nanodots and analyzed FORC diagrams obtained with an AGFM for different geometries (Fig.1). Using magnetron sputtering and EBL lithography we have fabricated arrays of circular dots with a diameter of 200nm covering a total area of 3x3mm and varied the spacing between them starting from a complete non-interacting array and gradually reducing the distances between centres down to a configuration where they are nearly in contact and therefore subject to a strong magnetostatic interaction.

The FORC plot of the non-interacting dots presents very characteristic features with two main peaks that are directly related to the vortex nucleation fields and with an additional double peak related to the asymmetries in the vortex annihilation fields. When reducing the distance between dots these peaks approach each other and a new central peak arises while the previous peaks become weaker. This behaviour corresponds to a gradual transition from the isolated dots towards the FORC distribution of a uniform thin film, which presents just a central peak at the coercivity of the material where the strong crystal anisotropy gives rise to other characteristic features. Micromagnetic simulations with Mumax3 confirm experimental results. With this work we show that FORC analysis on arrays of nanodots can help understanding the statistical behaviour of vortex domain walls, which are key for many spintronic applications.



1. Mayergoyz, I. Mathematical models of hysteresis. *IEEE Transactions on Magnetics* **22**, 603–608 (1986).
2. Groß, F., Ilse, S. E., Schütz, G., Gräfe, J. & Goering, E. Interpreting first-order reversal curves beyond the Preisach model: An experimental permalloy microarray investigation. *Physical Review B* **99**, (2019).

Invited Oral Presentations

| | | |
|----------------------|--|-----|
| Riccardo Battistelli | <i>Revealing 3D magnetic textures in $[Pt/Co/Cu]_{x_{16}}$ multilayers by coherent X-ray imaging with 5 nm resolution</i> | 267 |
| Akira Kikitsu | <i>Application of High Sensitive AC Field Modulation GMR Sensor to Magnetic Field Microscope</i> | 268 |
| Thomas Prokscha | <i>Characterization of magnetic properties of thin films and near-surface regions by low-energy muon spin spectroscopy</i> | 269 |

Revealing 3D magnetic textures in [Pt/Co/Cu]₁₅ multilayers by coherent X-ray imaging with 5 nm resolution

R. Battistelli¹, S. Zayko², K. Bagschik³, C. M. Günter⁴, J. Fuchs⁵, K. Gerlinger⁵, L. Kern⁵, D. Metternich¹, M. Schneider⁵, D. Engel⁵, S. Eisebitt^{4,5}, B. Pfau⁵, F. Büttner¹

¹Helmholtz Zentrum Berlin, Hahn-Meitner-Platz 1, 14109 Berlin, Germany

²Georg-August-Universität Göttingen, Wilhelmsplatz 1, 37073 Göttingen, Germany

³Deutsches Elektronen-Synchrotron, Notkestraße 85, 22607 Hamburg, Germany

⁴Technische Universität Berlin, Straße des 17. Juni 135, 10623 Berlin, Germany

⁵Max Born Institute, Max-Born-Straße 2A, 12489 Berlin, Germany

In the fields of magnetism and spintronics, magnetic multilayers continue to thrive as pivotal structures to functionalize magnetic interactions, including the interfacial Dzyaloshinskii-Moriya interaction (DMI), and to engineer complex non-trivial spin textures [1-3]. However, previous research has focused almost exclusively on 2D structures. The challenge in studying 3D textures is in obtaining the necessary spatial resolution and sensitivity to resolve them. Here we show that this challenge can be met by reference-aided coherent diffractive x-ray imaging combined with a modulated reference beam which amplifies the magnetic signal at large scattering angles [4,5]. Based on this amplified wide-angle scattering, we achieve 5 nm spatial resolution for spin textures in Pt/Co/Cu magnetic multilayers (Fig. 1c). Surprisingly, while conventional low-resolution images only show the well-known stripe domain state characteristic of such multilayers, our high-resolution images additionally reveal several small, mostly circular features of much weaker contrast (Fig. 1a,b). Since the features are larger than our spatial resolution, their weaker contrast identifies them as textures that penetrate only some of the magnetic layers. Interestingly, while these features are clearly magnetic in nature, and interact with the domain walls, they do not annihilate at the largest fields available in our system (220 mT).

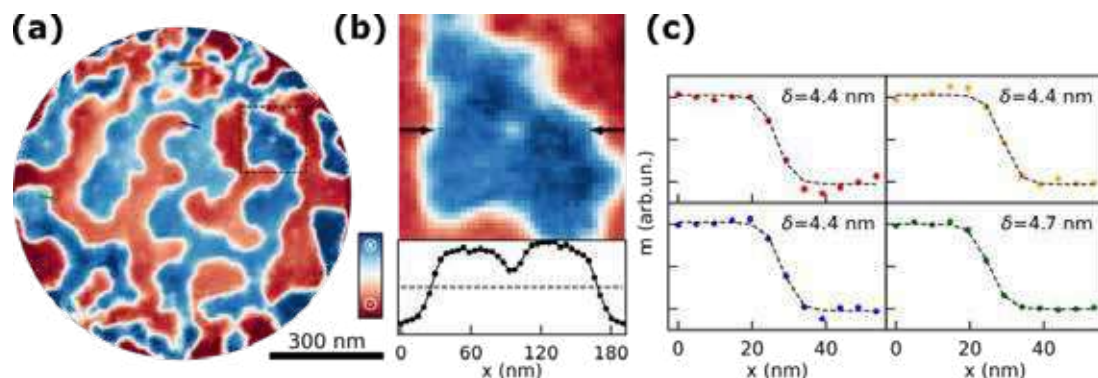


Figure 1: High resolution imaging of pinning-induced 3D textures in Pt/Co/Cu. (a) ~5 nm resolution image. (b) Zoom-in on the dashed square in (a). (c) Domain wall profiles from (a), supporting the resolution claim (lines are fits to the function $m(x) = \tanh(x/\delta)$).

- [1] F. Büttner et al., Nat. Phys. **11**, 225-228 (2015)
- [2] F. Büttner et al., Nat. Nano **12**, 1040-1044 (2017)
- [3] F. Büttner et al., Nat. Mater. **20**, 30-37 (2021).
- [4] O. Kfir et al., Sci. Adv. **3**, eaao4641 (2017)
- [5] S. Zayko et al., Nat. Commun. **12**, 6337 (2021)

Application of High Sensitive AC Field Modulation GMR Sensor to Magnetic Field Microscope

A. Kikitsu¹, Y. Higashi¹, Y. Kurosaki¹, S. Shirotori¹, T. Nagatsuka², K. Suzuki²
and Y. Terui²

¹ Toshiba Corp., 1 Komukai Toshiba-cho Saiwai-ku, Kawasaki, Japan

² Toshiba Nanoanalysis Corp., 8 Shinsugita-cho Isogo-ku, Yokohama, Japan

A novel high-sensitive Giant Magneto-resistance (GMR) sensor has been developed [1]. A small magnetic field is transferred to a higher frequency region by the AC field modulation and can be detected with high SNR [1]. A promising application of this sensor system is a magnetic field microscope, which detects defective leakage current in a semiconductor chips [2]. In this study, the sensor was applied to the magnetic field microscope and magnetic field from a printed Cu wire was observed. Spatial resolution as well as the sensitivity is discussed.

Schematic diagram of the magnetic field microscope is shown in Fig.1 [3]. Sensor unit was a bridge of four units of GMR element and NiFe yokes. AC modulation field (10 kHz) was applied from a Cu line under the GMR. Noise level of the GMR unit was $13 \text{ pT}/\sqrt{\text{Hz}}$ at 100 Hz. Objective sample was a printed Cu wire flowing an AC current (100 Hz). The sensor unit was scanned at 100 ms per pixel. The output signal of the sensor unit was demodulated by a lock-in amplifier with a 10 kHz reference. A 100 Hz component of the output signal was demodulated by secondary lock-in amplifier. Two sensor configurations were investigated: sensor was faced-down (1 mm spacing) over the Cu wire (150 μm width), and sensor was put upright position (0.1 mm spacing) over the three Cu wires (50 μm line and space).

Figure 2 shows the magnetic images for two configurations. In both cases, magnetic field distribution was clearly observed. Sensing limit was examined by reducing the sample AC current. It was found that the sensing limit was determined by an ambient magnetic field noise of about 4 nT, which was far larger than the noise level of the sensor unit.

Magnetic field profile of the image was compared with simulated ones for the case of the face-down configuration. It was found that the detection window was estimated to be about 3 mm, which was a little smaller than the sensor unit. For the case of the upright configuration, small dip in the magnetic field image was observed. The dip corresponded to a magnetic field by the reverse current on the center wire. Magnetic field distribution much smaller than the sensor size (4 mm long along the field sensing direction) was observed. Sensitivity distribution seems to have a peak within the detecting window.

This work was supported by the Cabinet Office (CAO), Cross-ministerial Strategic Innovation Promotion Program (SIP), “Intelligent Processing Infrastructure of Cyber and Physical Systems” (funding agency: NEDO).

[1] S. Shirotori et al., *IEEE Trans. Magn.*, **57**, 4000305 (2021), A. Kikitsu, *JEMS2020*, 2876.

[2] K. Kimura et al., *Electro Packaging Technol.*, **28**, 16 (2012).

[3] A. Kikitsu et al., *2022 Joint InterMag MMM conference*, IOF-07 (2022).

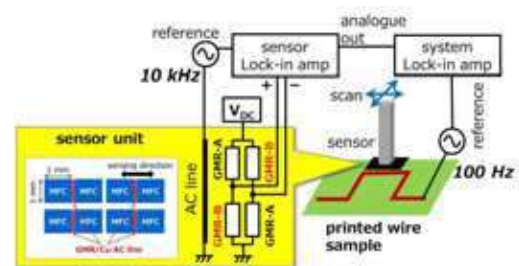


Figure 1: Schematic diagram of the magnetic field microscope system

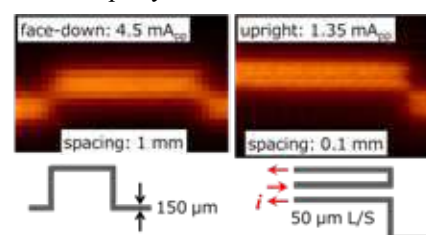


Figure 2: Magnetic field images for two sensor configurations

Characterization of magnetic properties of thin films and near-surface regions by low-energy muon spin spectroscopy

Thomas Prokscha¹, Zaher Salman¹ and Andreas Suter¹

¹ Paul Scherrer Institute, Forschungsstrasse 111, 5232 Villigen PSI, Switzerland

Muon spin spectroscopy (μ SR) is a powerful local probe technique to address topical questions in a large variety of materials, covering fundamental and technologically relevant aspects of structural, magnetic, and electronic phenomena in magnetic systems, superconductors, semiconductors, and insulators. Intense polarized muon beams with MeV energies are generated at high power proton accelerators (0.1-1MW) with proton energies between 500 MeV and 3 GeV. The implantation depth of muons with MeV energies is hundreds of micrometers in condensed matter. Therefore, μ SR is usually applied to study physical properties in the bulk of a material. With the availability of low-energy positive muons at PSI with tunable energies between 1 and 30 keV, it became possible to extend the μ SR technique to investigations of thin film systems at tunable mean depths of a few nanometers up to about 200 nm (Low-energy muon spin spectroscopy, LE- μ SR). In this talk we introduce the low-energy muon beam facility LEM at PSI, and we show the strength of this still young technique with selected applications in thin film and near-surface studies.

In LaNiO_3 superlattices, it was found that the collective phase behavior of correlated-electron systems can be controlled by the thickness/dimensionality of the LaNiO_3 layers [1]. LE- μ SR was essential to prove the occurrence of a magnetic phase transition to an antiferromagnetic state while the system also exhibits a metal-insulator transition. Such a magnetic transition is not present in the nickelates if the system stays metallic.

Muons are often used to study the magnetic homogeneity of a system on a nanometer scale. Evidence for the development of a homogeneous ferromagnetic phase in epitaxial quaternary $(\text{Ga,Mn})(\text{Bi,As})$ layers has been reported [2]. It shows that the incorporation of a small amount of Bi, which enhances the spin-orbit coupling strength and thereby the magneto-transport effects, does not deteriorate the magnetic properties. This finding is important for the application of dilute magnetic semiconductors as a new type of non-volatile memory elements, which relies on a nanometer scale magnetic homogeneity.

Due to the unique sensitivity of LE- μ SR, the magnetic transition temperature of thin films can easily be determined, particularly for systems with antiferromagnetic order. As an example, we show the effect of chemical doping and epitaxy on the magnetoelectric properties of multiferroic thin films of SrMnO_3 . The dependence of the magnetic order temperature of $\text{Sr}_{1-x}\text{Ba}_x\text{MnO}_3$ thin films on epitaxial strain and Ba content revealed, that the unit cell volume is the key parameter to determine the Néel temperature in $\text{Sr}_{1-x}\text{Ba}_x\text{MnO}_3$ thin films showing G-type antiferromagnetic order [3].

Sr_2RuO_4 with strong electronic correlations has been intensively investigated due to its unusual properties. By using LE- μ SR, weak dipolar magnetic fields have been detected at the surface of Sr_2RuO_4 appearing between 50 K and 75 K, well above its superconducting order temperature of 1.45 K. This unconventional magnetism is ascribed to orbital loop currents forming at the reconstructed Sr_2RuO_4 surface, which unveils an electronic ordering mechanism that can have an impact on electron pairing with broken time reversal symmetry.

[1] A.V. Boris et al., *Science* **332**, 937 (2011).

[2] K. Levchenko et al., *Scientific Reports* **9**, 3394 (2019).

[3] L. Maurel et al., *APL Materials* **7**, 04117 (2019).

[4] R. Fittipaldi et al., *Nature Communication* **12**, 5792 (2021).

Oral Presentations

| | | |
|--------------------------------|---|-----|
| Kevin Dalla Francesca | <i>Local magnetic probe microscope integrating magnetoresistive sensors</i> | 271 |
| Matjaž Gomilšek | <i>Many-Body Quantum Effects of Muons</i> | 272 |
| Claudio Gonzalez-Fuentes | <i>Magneto-optical detection of spin-orbit torque vector via first order Kerr effects</i> | 273 |
| Alicia Estela Herguedas-Alonso | <i>A fast method to recover 3D magnetization of 2D structures and multilayers.</i> | 274 |
| Muhammad Waqas Khaliq | <i>High Frequency Sample Excitation at the ALBA-PEEM</i> | 275 |
| Luca Nessi | <i>Ultra-thin free standing graphene membranes for enhanced performances in spin detection</i> | 276 |
| Jack O'Brien | <i>Hardware, methodology and applications of backscatter Mossbauer spectroscopy with simultaneous X-ray and gamma detection</i> | 277 |
| Rastislav Varga | <i>Phase detection using GMI in Ni_2FeGa glass-coated microwires.</i> | 278 |
| Thomas Veile | <i>Magnetometry of nanocrystalline materials in controlled gas atmospheres at high temperatures</i> | 279 |

Local magnetic probe microscope integrating magnetoresistive sensors

**K. Dalla Francesca¹, W. Benmessaoud^{1,2}, J. Moulin¹, N. Sergeeva-Chollet²,
C. Fermon¹, M. Pannetier-Lecoeur¹ and A. Solignac¹**

¹*SPEC, CEA, CNRS, Université Paris Saclay, CEA Saclay 91191 Gif sur Yvette Cedex, France*

²*CEA LIST, Université Paris-Saclay, 91120, Palaiseau, France*

The project consists in developing an ultra-sensitive and quantitative magnetic microscopy, allowing to image at room temperature the magnetic fields emitted by a magnetic sample with a lateral resolution of the order of a hundred nanometers and a sensitivity of the order of a nanotesla [1]. The microscope combines a giant magnetoresistive (GMR) magnetic sensor and a scanning probe microscope. The GMR sensor is integrated inside a flexible micro-arm and allows to measure the magnetic stray fields while the cantilever deflection gives the information on the surface topography.

The GMR sensor, based on spin electronics, is basically composed of two thin ferromagnetic layers separated by a non-magnetic and conductive layer. One ferromagnetic layer is free and its magnetization follows the magnetic signal direction. The second ferromagnetic layer has a magnetization which remains fixed. The resistance of the whole varies according to the relative angle between the magnetizations of the two layers.

The aim of the project is the fabrication and use of flexible micro-arms incorporating a micrometric magnetoresistive sensor. The measurement obtained by the GMR sensor is quantitative and does not require recalibration or regular remagnetization of the probe. The imaging of currents in electronic circuits or the study of the structure of rocks, alloys and magnetic powders are all potential applications for this system. In the continuity of the research work carried out in the laboratory [2], we will show recent developments concerning the fabrication of the sensors, through the design of the AFM tip and the fabrication process. The work to approach the GMR to the surface and the characterization of the magnetoresistance properties of GMR tips and their topographic and magnetic resolutions will be discussed.

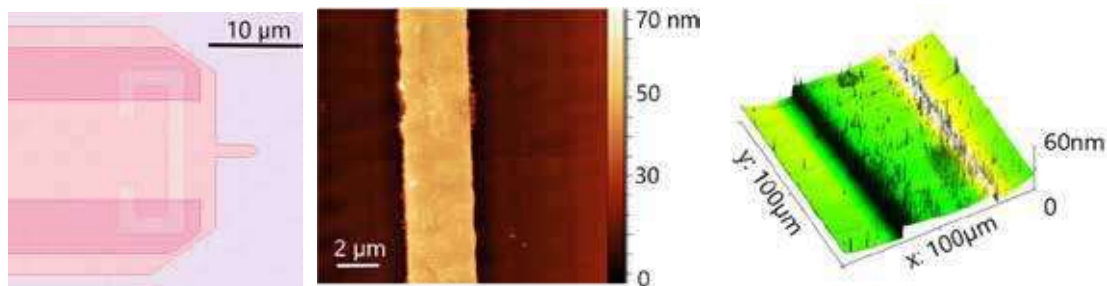


Figure 1: From left to right, schematic view of the GMR nanosensor on the micro-arms and its design, AFM image of a NiFe stripe obtained with this tip and then we have a 3D view superimposing the topography and magnetic stray fields of this magnetic stripe.

[1] S. J. Bending, *Advances in physics*, 1999, vol. 48, issue n° 4, p. 449-535

[2] J. Moulin, PhD 2019.

Many-Body Quantum Effects of Muons

M. Gomilšek^{1,2,3}, F. L. Pratt⁴, S. P. Cottrell⁴, S. J. Clark³ and T. Lancaster³

¹ Jožef Stefan Institute, Jamova c. 39, 1000 Ljubljana, Slovenia

² University of Ljubljana, Jadranska u. 19, 1000 Ljubljana, Slovenia

³ Durham University, South Road, Durham DH1 3LE, United Kingdom

⁴ ISIS Muon Group, Science and Technology Facilities Council (STFC), Didcot OX11 0QX, UK

Once considered exotic, implanted muons are nowadays routinely used as exquisite and unique probes of magnetic materials at the atomic scale. Here, muon spin relaxation (μ SR) has been indispensable in establishing some highly visible recent results in the field of quantum magnetism [1]. However, for unambiguous interpretation of experimental data, a thorough understanding of quantum zero-point motion (ZPM) of muons inside materials is essential. Namely, while ZPM of light nuclei like hydrogen is known to strongly affect the structure and dynamics of many materials [2], quantum effects of muons in solids can be even stronger due to the low mass of muons ($\sim 1/9$ the mass of a proton), which can qualitatively change the measured μ SR signal.

There has been much interest in using *ab initio* computation of muon stopping sites in materials to aid in the interpretation of μ SR measurements. However, most computational techniques employed have either neglected ZPM of muons in solids, or applied uncontrolled approximations to it, with little clarity around their applicability in practice. To address this, we have developed a unified description of ZPM of light particles in materials [3], clarifying the role many-body quantum entanglement and anharmonicity play in determining its behavior, and identifying several distinct ZPM regimes. We applied these insights to our μ SR quadrupolar level-crossing measurements (Fig. 1) to significantly improve the experimental accuracy of an important constant: the ^{14}N nuclear quadrupolar coupling constant of solid nitrogen, $\alpha\text{-N}_2$, which represents the first improvement in its accuracy in over 45 years.

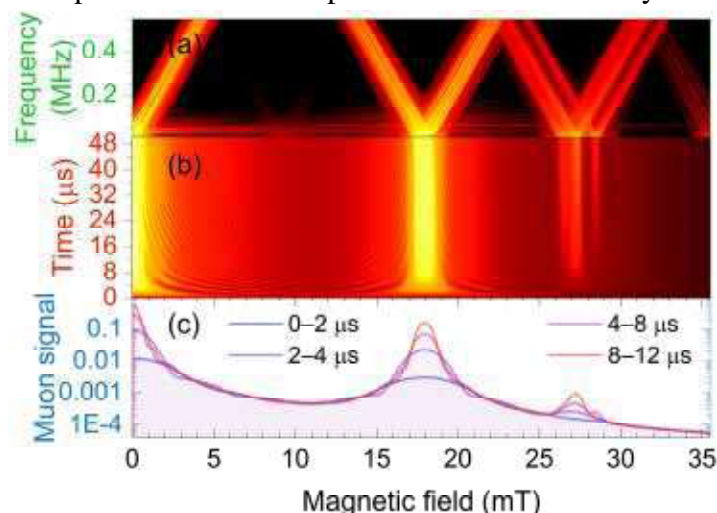


Figure 1: Quadrupolar level crossing resonance spectra from path-integral molecular-dynamics calculations of quantum muon motion in solid nitrogen as a function of (a) frequency, (b) time, or (c) integrated over time.

[1] M. Gomilšek *et al.*, Nat. Phys. **15**, 754 (2019).

[2] T. E. Markland and M. Ceriotti, Nat. Rev. Chem. **2**, 0109 (2018).

[3] M. Gomilšek *et al.*, arXiv:2202.05859.

Magneto-optical detection of spin-orbit torque vector via first order Kerr effects

Claudio Gonzalez-Fuentes¹ and Carlos García¹

¹Universidad Tecnica Federico Santa María, Avenida España 1680, Valparaíso, Chile

When spin polarized currents diffuse into a ferromagnetic (FM) material, they induce spin-orbit torques (SOTs): a powerful mechanism for magnetic order manipulation, with applications in magnetic recording, logic devices and neuro-morphing computing [1].

To the date, detection SOTs have relied almost exclusively on measuring electrical voltages arising from the device under excitation. In this line, techniques such as second harmonic generation, spin transfer torque ferromagnetic resonance (STT-FMR) and spin pumping, have dominated the scenario. In these techniques, signals are often contaminated by unwanted thermoelectric voltages and the sensitivity depends critically on magneto-electric coefficients that can show large variations among even for typical 3d ferromagnetic materials [2].

In this work we present a new and powerful method for the detection of SOTs based on Magneto-Optical Kerr Effect (MOKE). With it, we can quantify both the damping-like and field-like SOT effective fields ($\mathbf{h}_{\text{SO}}^{\text{FL}}$ and $\mathbf{h}_{\text{SO}}^{\text{DL}}$ respectively) of SOTs, employing a simple and low-cost set-up that has been already widely employed in MOKE magnetometry (Fig. 1).

We tested our method in NiFe/Pt, NiFe/Pd, Ta/CoFeB bilayers, obtaining a damping-like SOT efficiency ($\mathbf{h}_{\text{SO}}^{\text{DL}}$) equal to 0.1 ± 0.01 , 0.034 ± 0.004 and -0.15 ± 0.01 respectively. On the other side, we obtained $\mathbf{h}_{\text{SO}}^{\text{FL}}/\mathbf{h}_{\text{SO}}^{\text{DL}}$ ratio equal to 0.24 ± 0.03 and 0.11 ± 0.03 , in the samples with 4 nm thick NiFe and CoFeB, respectively. The results for ξ_{DL} are close to the most accepted values reported in the literature for the studied materials. On the other side, the $\mathbf{h}_{\text{SO}}^{\text{FL}}/\mathbf{h}_{\text{SO}}^{\text{DL}}$ ratios fit well inside the diffusive model of spin accumulation in the ferromagnetic layer [4], with a finite spin dephasing length. This effect has been often disregarded in STT-FMR works.

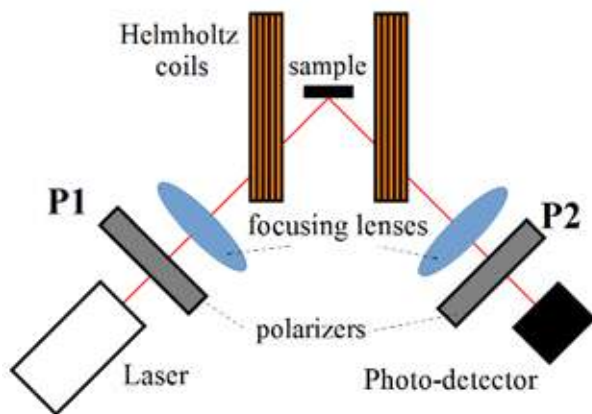


Figure 1: Schematic diagram of the set-up employed for magneto-optical detection of SOTs

[1] A. Hiroata et al., *J. Magn. Magn. Mater.* **509**, 166711 (2017).

[2] M.-H. Nguyen and C.-F. Pai, *APL Materials* **9**, 030902 (2021).

[3] X. Fan et al., *Appl. Phys. Lett.* **109**, 030902 (2016).

[4] S. Zhang, P. M. Levy, and A. Fert, *Phys. Rev. Lett.* **88**, 236601 (2002).

A fast method to recover 3D magnetization of 2D structures and multilayers

A.E. Herguedas-Alonso¹, L. Aballe², J. Fullerton³, M. Vélez^{1,4}, J.I. Martín^{1,4}, A. Sorrentino², E. Pereiro², S. Ferrer², C. Quirós^{1,4} and A. Hierro-Rodriguez^{1,4}

¹ *Departamento de Física, Universidad de Oviedo, 33007, Oviedo, SPAIN*

² *ALBA Synchrotron, 08290, Cerdanyola del Vallès, SPAIN*

³ *SUPA, School of Physics and Astronomy, University of Glasgow, UK*

⁴ *CINN (CSIC – Universidad de Oviedo), 33940, El Entrego, SPAIN*

The advance of Spintronics and 3D Nanomagnetism is highly impacted by the capability of properly resolving the complex magnetic textures present in magnetic systems. In this framework, the use of X-ray Magnetic Circular Dichroism (XMCD) in X-ray transmission microscopes with tomography/laminography capabilities has allowed the community to experimentally access the volume resolved vector magnetization field within arbitrary magnetic systems down to tens of nm resolution [1-3]. However, these experiments are currently very time consuming as a great number of different projections must be recorded in order to accurately reconstruct the magnetization vector field (usually a vector tomography experiment with 240 different projections requires 24 – 28 hours of beamtime).

Here we present a fast method to reduce dramatically the time needed for accurate magnetization vector reconstruction specific for quasi two-dimensional magnetic structures, heterostructures and continuous films. We obtain the 3D configuration of the magnetization of 2D samples by recording 30 projections and exploiting the XMCD effect. The algorithm combines the images to obtain first the electronic charge and, then, the magnetic configuration fitting the Bourguer-Lambert-Beer equation particularized for XMCD [4].

We have validated our method with 40 nm thick Py microstructures (Fig.1). The measurements were performed at the MISTRAL beamline of the ALBA Synchrotron, with a total acquisition time of 4 hours per complete dataset (8 times down than conventional tomography). Work supported by Spanish MCI (PID2019-104604RB/AEI/10.13039/501100011033) and Foundation for the Promotion of Applied Scientific Research and Technology in Asturias (GRUPIN21 AYUD /2021/51185).

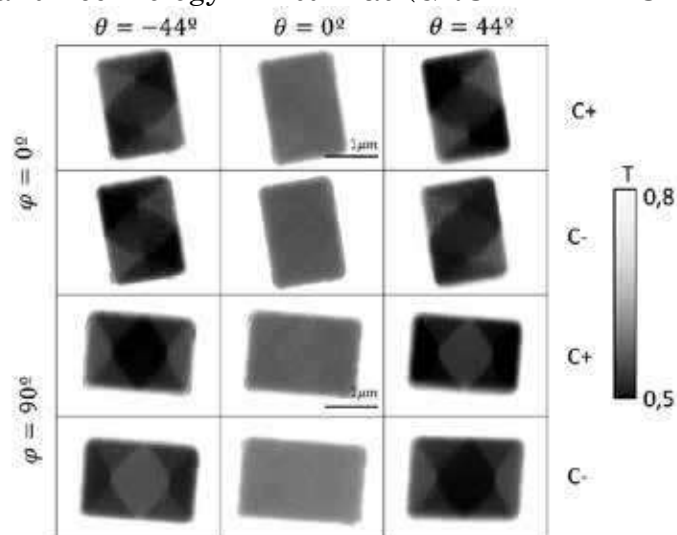


Figure 1: Transmittance images obtained at the MISTRAL beamline of the ALBA Synchrotron with circular right- (C+) and left-handed (C-) polarization at two tilt angles (θ).

[1] C. Donnelly et al, *Nature* **547**, 328–331 (2017)

[2] K. Witte et al, *Nano Lett.* **20**, 1305–1314 (2020)

[3] A. Hierro-Rodriguez et al, *Nature Comms.* **11**, 6382 (2020)

[4] A.E. Herguedas-Alonso et al, in preparation.

High Frequency Sample Excitation at the ALBA-PEEM

M. W. Khaliq^{1,2}, J. M. Álvarez¹, N. González¹, J. Ferrer¹, A. M.-Carboneres¹, J. Prat¹, S. Ruiz-Gómez³, A. Camps¹, M. A. Niño¹, L. Aballe¹, F. Macià², and M. Foerster¹

¹ ALBA Synchrotron Light Facility, Barcelona-08290, Spain

² Department of Condensed Matter Physics, University of Barcelona, Barcelona-08028, Spain

³ Max Planck Institute for Chemical Physics of Solids, Dresden-01069, Germany

We describe a setup that is used for electrical sample excitation in a cathode lens electron microscope with the sample stage at high voltage, as used in many synchrotron light sources. X-ray Photoemission electron microscopes (XPEEM) in combination with the high-brightness, tunable photon energy, and polarization of the ALBA synchrotron provides a variety of laterally resolved operation modes based on X-ray absorption and photoelectron spectroscopy, as well as magnetic imaging possible via the X-ray magnetic circular and linear dichroism effects (XMCD and XMLD) [1]. However, the UHV and high voltage constraints do not allow a modification of the standard electrical feedthroughs which are limited to lower frequencies for sample excitation. Instead a new additional system has been designed which uses dedicated high frequency components until the printed circuit board (PCB) which supports the sample. Sub-miniature push-on (SMP) connectors are used to realize the connection in the ultrahigh vacuum (UHV) chamber, bypassing the standard feedthrough.

The electrical bandwidth was measured up to 4 GHz with -6 dB attenuation at the sample position (Fig. 1a), drastically improving compared to the existing setup. As an application example, in the inset of Fig. 1a, the measurement of a LiNbO₃ (LNO) sample with a surface acoustic wave (SAW) is shown. The characteristics of the sample with transmission peaks at the resonance frequencies of the IDTs are clearly visible that has no comparison with that in the past to excite and measure SAW from 125 to 500 MHz in XPEEM [2]. Examples for new experiments profiting from the extended bandwidth are given [3, 4]. We employ this new setup to excite the SAWs at 3 GHz frequency in LNO and image them in XPEEM, hence, portraying the successful operation of the setup at the available facility.

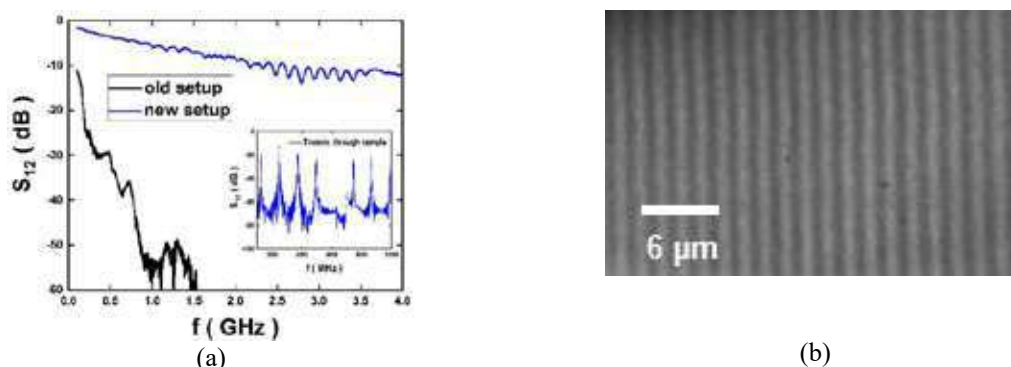


Figure 1: (a) Transmission as a function of frequency through both setups; inset shows the transmission through sample at 125 MHz harmonics (b) XPEEM image of 3 GHz SAWs in LNO

- [1] L. Aballe et al., *J. Synchrotron. Rad.* **22**, 745 (2015)
- [2] B. von Boehn et al., *Angew. Chem. Int. Ed.* **59** 20224 (2020)
- [3] M. Foerster et al., *Nature Comm.* **8**, 407 (2017)
- [4] M. Schöbitz et al., *Phys. Rev. Lett.* **123**, 217201 (2019)

Ultra-thin free standing graphene membranes for enhanced performances in spin detection

L. Nessi^{1,2}, F. Belponer¹, C. Rinaldi^{1,2}, R. Bertacco^{1,2}, M. Cantoni^{1,2}

¹*Department of Physics, Politecnico di Milano, via G. Colombo 81, 20133 Milan, Italy*

²*IFN-CNR, c/o piazza Leonardo da Vinci 32, 20133 Milan, Italy*

Ultrathin free-standing magnetic layers are promising candidates to efficiently detect the spin of the electrons by means of the selective transmission of spin parallel or anti-parallel to the magnetization [1]. The capability to control the direction of this quantization axis joined to the engineering of a device able to guarantee spatial resolution allow to completely reconstruct the spin configuration of an electron beam. This could represent an outstanding tool in spectroscopic experiments, where the spin resolution may be added to the $E - k$ mapping in angle-resolved photoemission spectroscopy (ARPES) [2]. This task was tackled by exploiting a bidimensional matrix of free-standing membranes.

In order to guarantee a sufficiently high transmission of the electrons, the film thickness was chosen not to exceed 10 nm. A suitable heterostructure was designed, consisting in a mechanically robust layer, a buffer layer, the active magnetic layer and finally a capping layer. Graphene was chosen as first layer because of its large mechanical robustness and different thicknesses, from 2 to 8 monolayers, were tested. The buffer layer was selected both for its mechanical properties and to allow the growth of the magnetic layer, guaranteeing sharp and flat interfaces. The desired direction of the magnetization was defined using different magnetic materials (or stacks). Co was chosen for in-plane configuration, while Ta/CoFeB/MgO for the out-of-plane one. Finally, the devices were capped with Au or Ru to protect the underlayer from oxidation. The growth was performed comparing two different techniques: magnetron sputtering and molecular beam epitaxy. A statistical analysis over a large number of samples was performed to obtain the parameters which allow the largest percentage of intact membranes at the end of the whole workflow (up to 94%). A mechanical characterisation was performed by atomic force microscopy (AFM) to infer information about the Young modulus and the film roughness. The magnetic properties were measured on ultrathin membranes by Faraday effect. The key features of sufficiently high coercive field and magnetic remanence were obtained.

The final aim is the characterization of the spin-filtering efficiency and the transmission of the membranes for different orientations of the beam polarization. A preliminary measurement was performed on bare graphene to quantify the transmission, exploiting an *ad hoc* spin-polarized electron beam at low energy (0-30 eV) produced by a GaAs photocathode with negative electron affinity [3]. Spin-resolved measurements through a lock-in detection technique are ongoing to evaluate the spin asymmetry of such devices.

[1] D. Oberli *et al.*, *Phys. Rev. Lett.* **81**, 4228 (1998).

[2] T. Övergaard *et al.*, *arXiv*, 1709.03838v3 (2017).

[3] M. Cantoni and R. Bertacco, *Rev. Sci. Instrum* **75**(7), 2387 (2004).

Hardware, methodology and applications of backscatter Mossbauer spectroscopy with simultaneous X-ray and gamma detection

Jack O'Brien¹, Laura H. Lewis² and Plamen Stamenov¹

¹ School of Physics and AMBER, CRANN, Trinity College, Dublin 2, Ireland

² Snell Engineering Center, Northeastern University, Boston, United States

Mossbauer spectroscopy is one of the standard techniques for the characterization of the magnetic order and chemical local environment, especially of iron-containing magnetic materials. Most data is obtained in transmission mode, and on setups, where the energy discrimination is done early and in hardware. The conversion electron and backscatter Mossbauer techniques are much more sparingly used, primarily on thin films (for the former) and on unprepared sample surfaces, for example on some of the Mars rovers (for the latter).

Here we describe the acquisition hardware, analysis software and parameter extraction methodology for X-ray and γ -ray detection and illustrate the capabilities for the depth resolution of Mossbauer parameters in the range of 10's of micron in samples of polycrystalline YIG and mechanically-polished NiFe meteoritic slab (NWA6259). The damage by excessive surface oxidation or the disruption of the local $L1_0$ order is evidenced, accordingly. It is hoped that this will boost the relative popularity of the methodology.

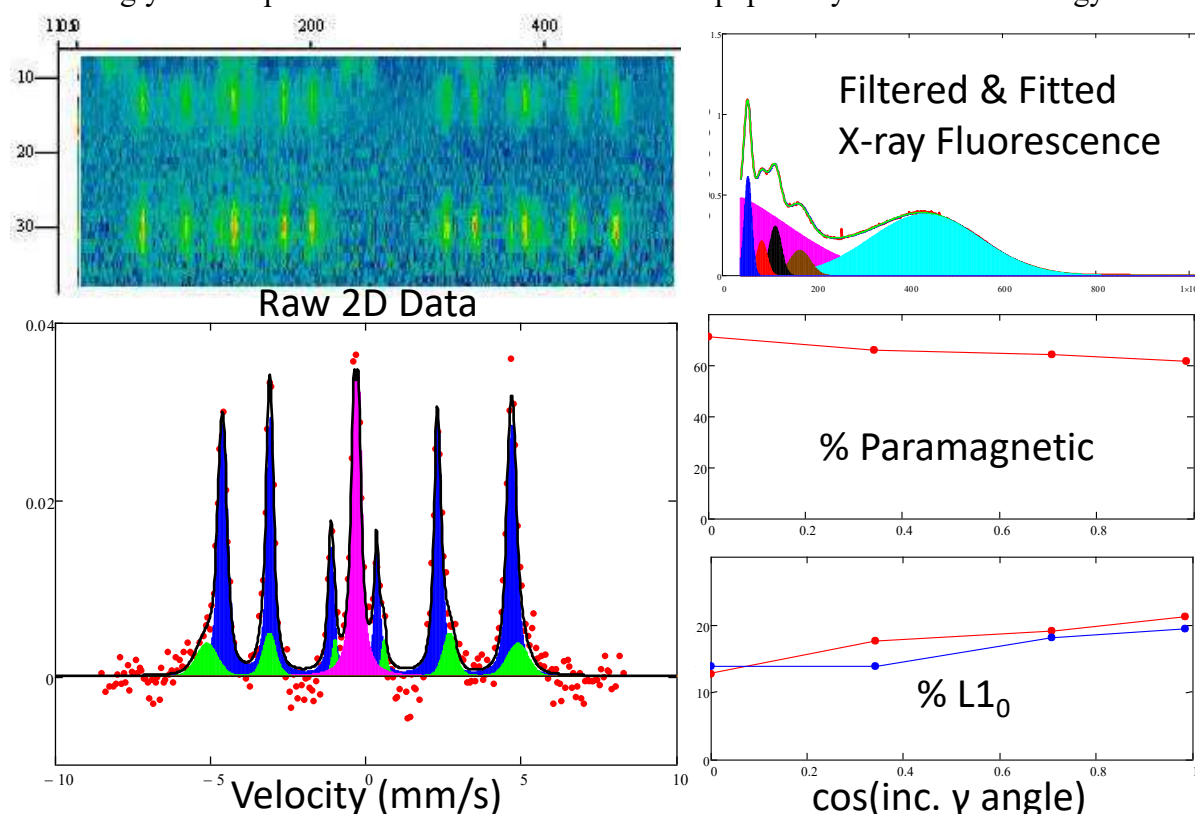


Figure 1. An illustration of the data processing and parameter extraction for simultaneous acquisition of conversion X-ray and γ -ray detection Mossbauer spectroscopy, including raw 2D data, fluorescence analysis and post-processing, fitting of the Mossbauer spectra (X-ray yield illustrated) and the evolution of the extracted parameters as a function of the effective penetration depth (as a function of the angle of γ -ray incidence on the sample surface).

Phase detection using GMI in Ni₂FeGa glass-coated microwires.

P. Sarkar^{1,2}, L. Nulandaya^{1,3}, M. Varga^{1,3}, A. Dzubinska¹, T. Ryba², R. Varga^{1,2}

¹ CMP-TIP, UPJS, Tr. SNP 1, 04001, Kosice, Slovakia

² RVmagnetics, Nemcovej 30, 04001, Kosice, Slovakia

³ Inst. Phys., Fac. Sci., UPJS, Park Angelinum 9, 040 01 Kosice, Slovakia

Heusler alloys are very promising materials for shape memory or magnetocaloric applications. Particularly, Ni-Fe-Ga based alloys offer good mechanical properties accompanied with shape memory effect, sensitivity to magnetocaloric but also baro and elastocaloric effect [1].

Wire shape brings additional functionality comparing to bulk alloys of the same composition. It has been shown [2] that Ni₂FeGa based glass coated microwire shows up to 2% of reversible straining that is accompanied with up to 1200% variation of initial permeability. This is a result of change of easy magnetization axis due to the structural transformation.

Similarly, Giant Magnetoimpedance (GMI) effect in glass-coated microwires is extremely sensitive to the anisotropy orientation [3]. Therefore, we have decided to check the possibility to use GMI effect to detect the phase transition. Ni₂FeGa microwire was used to study having low temperature martensitic phase with the easy axis tilted out of the wire's axis, which is favorable for GMI effect. After transformation (which is shown also by the magnetization increase at 340K – see fig.1) the easy axis changes into direction parallel to the wire's axis, which is accompanied by the 7% decrease of GMI effect. Such decrease can be used to detect the phase transformation and to create SMART actuators that can also sense its straining.

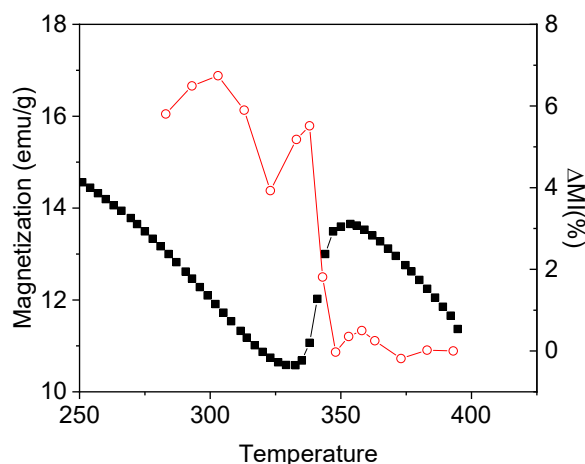


Fig.1: Temperature dependence of magnetization (black squares) and GMI (red circles) of Ni₂FeGa microwires [2].

[1] F. Xiao, M. Jin, J. Liu, X. Jin, *Acta Materialia* 96 (2015), 292.

[2] M. Hennel, M. Varga, L. Frolova et al., *Phys. Stat. Sol. A* (2022), DOI: 10.1002/pssa.202100657

[3] J. Alam, M. Nematov, N. Yudanov et al., *Nanomaterials* 11 (2021), 1208.

Magnetometry of nanocrystalline materials in controlled gas atmospheres at high temperatures

T. Veile¹, M. R. Almind¹, I. Chorkendorff¹, and C. Frandsen¹

¹DTU Physics, Technical University of Denmark, 2800 Kgs. Lyngby, Denmark

Magnetic nanoparticles in rf-fields have shown great potential for delivering heat to their local environments through hysteresis heating. This type of induction heating has recently become of interest for driving catalytic reactions, as the localised heating may improve efficiency, and electrification of the heating may reduce carbon emissions.

One example is steam methane reforming (SMR) for catalytic hydrogen production. It has been demonstrated that this reaction can be driven by induction heating of CoNi particles [1-3]. SMR is a strongly endothermic reaction that requires substantial heat supply and high operational temperature (800-900 °C). Moreover, the chemical environment in reactors are often challenging; SMR reactors having a gaseous mixture of steam, methane, and hydrogen.

In order to develop and optimise magnetic particles for induction heating and other applications at high operation temperature, it is necessary to establish experimental setups that can characterise the magnetic properties of the particles while in the relevant gas environment. In this talk, we present an in-situ holder that is retrofittable to vibrating sample magnetometry (VSM) and AC-calorimetry [4]. This holder makes it possible to measure the magnetic properties of samples in the temperature range of 20-1000 °C while supplying a continuous flow of gas. The exhaust gas can be analysed by e.g. mass spectrometry. This enables the possibility to monitor magnetic properties in reducing, oxidising, and reaction conditions at different temperatures and applied fields (Fig. 1). We show the new design principles, demonstrate examples of its use, and discuss applications within other fields such as in-situ annealing studies of magnetic materials.

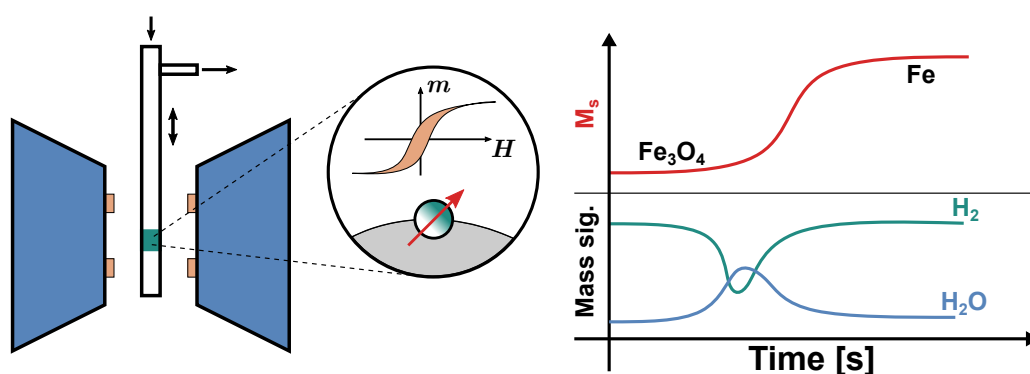


Figure 1: Schematics of magnetometry to monitor the magnetic properties and gas composition while running reactions, such as catalysis, reduction, and oxidation, at high temperatures.

- [1] M. G. Vinum et al. *Angewandte Chemie* **130**, 10729-10733 (2018)
- [2] M. R. Almind et al. *Catalysis Today* **342**, 13-20 (2020)
- [3] M. R. Almind et al. *ACS. Appl. Nano Mater.* **4**, 11537-11544 (2021)
- [4] M. R. Almind et al., T. Veile et al. *In preparation*

Posters

| | | |
|--------------------------|--|-----|
| Wanissa Benmessaoud | <i>Local mapping of the magnetic response of materials.</i> | 281 |
| Tim A. Butcher | <i>Microspectroscopy of Magnetic Nanostructures with Soft X-Ray Ptychography</i> | 282 |
| Katarzyna Gas | <i>In Situ Compensation Methods for Precise Integral Magnetometry of Miniscule Powder Specimens and Thin Layers (2D) on Bulky Substrates</i> | 283 |
| Gabriel Gomez Eslava | <i>Simultaneous measurements of XMCD, bulk magnetization, magnetostriction and temperature change: a HoCo₂ case study</i> | 284 |
| Claudio Gonzalez-Fuentes | <i>Induction magnetometer with micro-emu sensitivity</i> | 285 |
| Sou Jinnouchi | <i>Susceptibility of a Small Diamagnetic Particle Detected from its Parabolic Trejectory Produced by Small Nd magnets in Terrestrial Gravity</i> | 286 |
| Thomas Mueller | <i>DNS - diffuse neutron scattering spectrometer at MLZ</i> | 287 |
| Wojciech Plucinski | <i>Advanced modeling of the Torque Motor magnetic circuit</i> | 288 |
| Hanyin Poh | <i>Quantification of Spin Accumulation Magnetoresistance in Ferromagnetic heterostructure using DC Bias Harmonic Hall Measurement</i> | 289 |

Local mapping of the magnetic response of materials

W. Benmessaoud¹, L. Drigo³, S. Rousse³, C. Fermon¹, M. Pannetier-Lecoeur¹, M. Macouin³, N. Sergeeva-Chollet², A. Solignac¹

¹SPEC, CEA, CNRS, Université Paris-Saclay, CEA Saclay 91191 Gif-sur-Yvette Cedex, France

²CEA LIST, 91191 Gif-sur-Yvette, France

³Géosciences Environnement Toulouse, Université de Toulouse, CNES, CNRS, IRD, UPS, 31400 Toulouse, France

Quantitative characterization at local scale of the magnetic properties of materials is of great interest for applications such as in situ monitoring, non-destructive testing, nanometrology or Earth magnetic field records.

A 3D local probe magnetic microscope has been developed in the laboratory to detect static or dynamic stray fields emitted by various samples. Giant magnetoresistance (GMR) sensors have been combined with a scanning system to achieve this objective. These GMR sensors are based on spin electronics and allow the detection of magnetic fields emitted by the sample surface with a detectivity of the order of $\text{nT}/\sqrt{\text{Hz}}$, a lateral resolution of the order of $10\mu\text{m}$, and over a large frequency range (DC to hundreds of MHz).

When arranged on a pyramidal support, GMR sensors detect the three components of the field [1], allowing the full field vector determination. The 3D mapping is very important for the completeness of the reconstruction and the analysis of the magnetic properties of samples for the study of the rock's magnetic history in paleomagnetism or ferromagnetic materials characterization in non-destructive testing for example.

Here we developed an improved probe containing GMR sensors on a gradiometer setting placed on a 3D support (Figure 1). To improve the lateral resolution, the signal-to-noise ratio, and the stability to disturbances, we implemented in the device a precise height control, temperature and environmental drift suppression, dedicated detection electronics, optimized scans, and a specific acquisition software. Special care has been taken to determine the sensitivity matrix by combining simulation and measurement data for an accurate reconstruction of the field. We report here the performances on natural rocks and calibration samples (Figure 2).

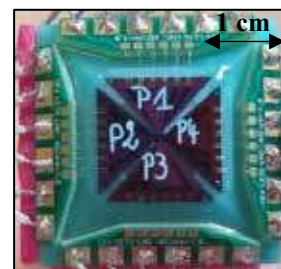


Figure 1: Local 3D probe. P1, P2, P3 and P4 are the 4 chips, each composed by 4 GMR sensors.

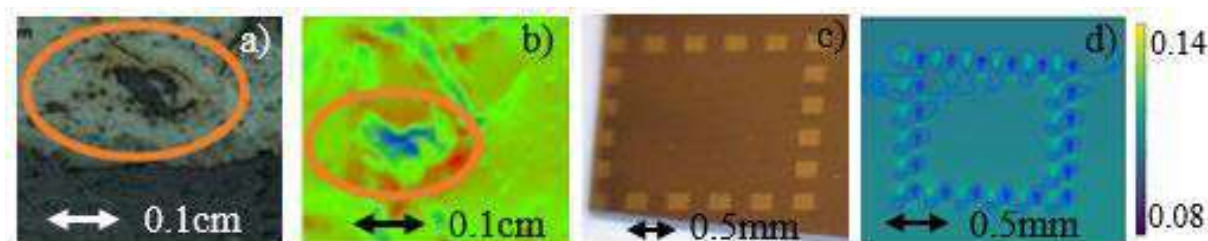


Figure 2: a) Picture of a serpentine thin section containing magnetite veins. b) Voltage mapping of the thin section shown in figure 2.a. c) Picture of a $200 \times 200 \mu\text{m}$ calibration sample. d) Voltage mapping of the calibration samples shown in figure 2.c. (the color bar is in Volt).

[1] F. Hadadeh, et al., IEEE Sensors Journal, **99**, 10.1109 (2019).

Microspectroscopy of Magnetic Nanostructures with Soft X-Ray Ptychography

Tim A. Butcher¹, Simone Finizio¹, Lars Heller¹, Manuel Langer¹,
Mirko Holler¹, Carlos A. F. Vaz¹, Armin Kleibert¹ and Jörg Raabe¹

¹Swiss Light Source, Paul Scherrer Institut, 5232 Villigen PSI, Switzerland

The imaging of magnetic structures in systems such as nanoparticles or thin films is greatly facilitated by spatial resolutions in the order of 10 nm. A way to unlock these resolutions is with the technique of soft x-ray ptychography. This is a lensless imaging approach employing coherent synchrotron light. Ptychography consists of moving the sample through a beam of monochromatic x-rays, all the while collecting diffraction patterns from the overlapping illumination spots (see Fig. 1). Recovery of the complex transmission function is achieved with a reconstruction algorithm. Resolutions of 5 nm have been reported with soft x-ray ptychography [1]. Measurements in the soft x-ray regime benefit from strong x-ray magnetic circular dichroism (XMCD) and x-ray magnetic linear dichroism (XMLD) contrasts. These serve to analyse ferromagnetic [2] and antiferromagnetic materials, respectively. Here, we present the development of a new soft x-ray ptychography endstation at the Swiss Light Source [3].

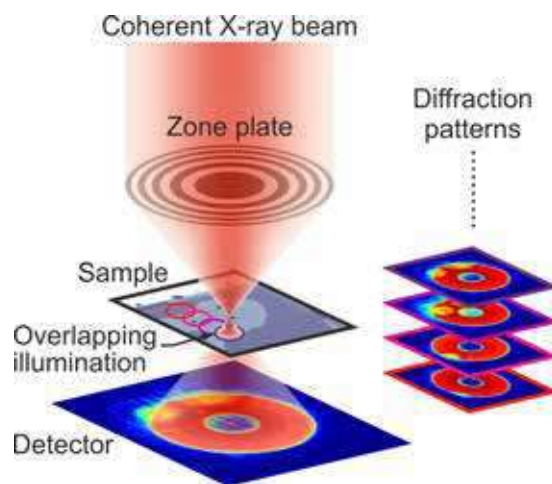


Figure 1: Sketch of an x-ray ptychography scan: A monochromatic beam of x-rays is focused by a Fresnel zone plate and encounters the sample close to its focal plane. The sample is scanned laterally and diffraction patterns are recorded. An image is obtained with a reconstruction algorithm.

- [1] D. Shapiro et al., *Nat. Photonics* **8**, 765 (2014).
- [2] X. Shi et al., *Appl. Phys. Lett.* **108**, 094103 (2016).
- [3] M. Langer, et al., *Microsc. Microanal.* **24**, 54 (2018).

***In Situ* Compensation Methods for Precise Integral Magnetometry of Miniscule Powder Specimens and Thin Layers (2D) on Bulky Substrates**

Katarzyna Gas and Maciej Sawicki

Institute of Physics, Polish Academy of Sciences, Aleja Lotnikow 32/46, PL-02668 Warsaw, Poland

We report on two experimental methods that greatly minimize the experimental artifacts associated with mounting specimens of both solid flat-plate shape [1] or amorphous (miniscule biological, chemical, and powders) [2] for the standard DC volume magnetometry. In this cases the sought weak or a very weak signal is buried in the magnetic response of the substrate or of a carrier (a capsule), therefore can be substantially contaminated by signals brought about by the chosen sample mount and magnetometer's instabilities. We show how *in situ* magnetic compensation (on the sample holder level) reduces the spurious and unwanted signals that are brought about by the bulky crystalline substrates or polycarbonate (or gelatin) capsules, respectively. These two concepts, are based on an elementary approach, in which this large error-bringing necessary signal from the specimen carriers gets reduced dozens of times by substantially restoring the translational symmetry of the whole samples holder, that is otherwise broken by the presence of any of these carriers. As the result the output is much less dependable on the inevitable fluctuations of some environmental variables, which detrimentally reduce the real credibility of the outcome in the standard approach to precision magnetometry. Additionally, a two- to five-fold reduction in the absolute noise level has been observed. Importantly, the solution proposed here can be easily incorporated in any magnetometer, in particular in Quantum Design MPMS and MPMS3 models. Importantly, the method requires neither any modelling of the magnetometer output signal, nor any laborious fitting. The typical examples of the elaborated assemblies are given in Figure 1.

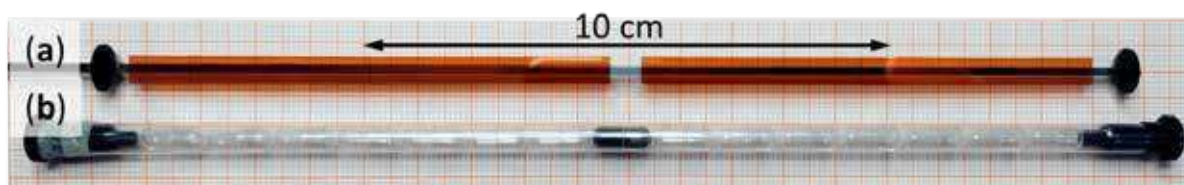


Figure 1: Examples of two assemblies allowing *in situ* compensation of unwanted and disturbing magnetic response of the either (a) semiconductor crystalline bulky substrate (GaP) or (b) a polycarbonate capsule. The investigated crystalline specimen is placed in the opening between the compensating strips of the matching material (a) or in the central capsule, darkened for the reproduction (b).

This work has been supported by the National Science Centre, Poland through grant DEC-2017/27/B/ST3/02470.

[1] K. Gas, M. Sawicki, *In situ compensation method for high-precision and high-sensitivity integral magnetometry*, Meas. Sci. Technol. **30**, 085003 (2019).

[2] K. Gas, M. Sawicki, *In Situ Compensation Method for Precise Integral SQUID Magnetometry of Miniscule Biological, Chemical, and Powder Specimens Requiring the Use of Capsules*, Materials **15**, 495 (2022).

Simultaneous measurements of XMCD, bulk magnetization, magnetostriction and temperature change: a HoCo₂ case study

G. Gomez Eslava^{1,3}, A. Aubert², K. Skokov², A. Karpenkov², O. Gutfleisch², F. Wilhelm³, A. Rogalev³, D. Günzing¹, H. Wende¹ and K. Ollefs¹

1. Faculty of Physics, University of Duisburg – Essen, Germany

2. Functional Materials Group, Technical University of Darmstadt, Germany

3. European Synchrotron Radiation Facility, France

Usually, to study (1) ‘bulk’ properties of a solid by using techniques such as magnetometry, dilatometry, calorimetry etc., and (2) to determine ‘atomistic’ parameters by using for instance X-ray, neutron or electron scattering, different samples with the same composition (or

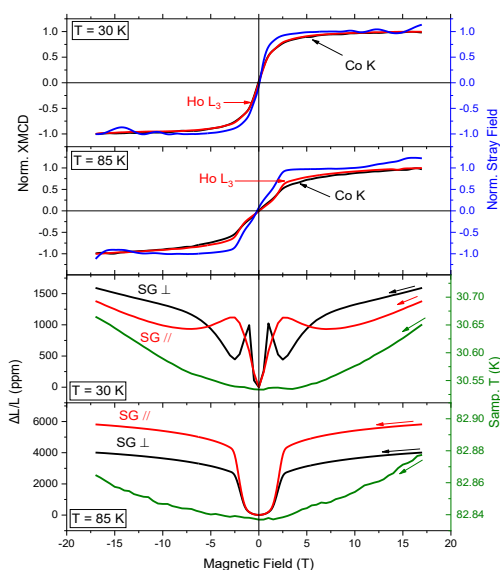


Figure 1: Simultaneous measurements of XMCD and bulk properties of a HoCo₂ sample, at 30 K and 85 K. SG// and SG⊥ stands for longitudinal and transverse strain gauge.

and SG⊥) and sample temperature. All the above measurements were performed simultaneously at 30 K and 85 K, in magnetic fields up to ± 17 T. XMCD signal was obtained at Ho L₃ and Co K-edge energies. At 30 K the XMCD signal at the two above mentioned energies are identical, but the stray field shows a higher slope below saturation. A different field dependence is observed for longitudinal and transverse strain curves. At 85 K the HoCo₂ undergoes a field-induced transition from para- to ferrimagnetic state [2]. At this temperature differences in the XMCD signal at the two edges suggest a misalignment in the rotation of Ho and Co moments. As in the previous case, stray field shows a higher slope than XMCD below saturation. Sample temperature relatively increases much more at 30 K ($[T(17\text{T}) - T(0)]/T(0) \times 100\% = 0.38\%$) than at 85 K (0.048%). With these results we illustrate how this approach can be successfully used for the investigation of materials with strongly correlated degrees of freedom.

This work was supported by the German Federal Ministry of Education and Research, grant No. BMBF-Projekt05K2019, the Collaborative Research Centre CRC/TRR270 and the European Synchrotron Radiation Facility under the long-term proposal HC-4051.

[1] A. Aubert et al., *IEEE Trans. Instrum. Meas.* DOI: 10.1109/TIM.2022.3157001 (2022).

[2] C. M. Bonilla et al., *J. Phys.: Condens. Matter.* **26**, 156001 (2014).

Induction magnetometer with micro-emu sensitivity

Claudio Gonzalez-Fuentes¹ and Ricardo Henriquez¹

¹Universidad Tecnica Federico Santa María, Avenida España 1680, Valparaíso, Chile

Standard experimental tools for probing the magnetic moment of materials research include the superconducting quantum interference device (SQUID) and vibrating sample magnetometer (VSM). A less common alternative is the use of *induction magnetometers* or equivalently *magnetic flux-meters*, which can get magnetization directly by integration of the Faraday's law induction voltage. Despite this alternative is by far more affordable than SQUID and VSM devices as well as intrinsically less restrictive regarding the types of specimens than can be studied, its usage is much less common, probably due its smaller sensibility, in the range of $\sim 10^{-5}$ emu [1].

In this work we present a table-top, own design, very low-cost hysteresis loop (H-loop) tracer based on magnetic-flux quantification, suitable for the study of ferromagnetic thin films. Our device is capable to obtain H-loop curves of ultra-thin films of permalloy (NiFe), in a matter of minutes (Fig. 1). These films have a typical magnetic moment (m) in the range of $\sim 10^{-5}$ emu. In addition, our device is specially suited for the study soft magnetic materials, being capable to detect changes in the coercive field as small as 0.1 Oe. The performance of our device was assessed also by the study of m per area in NiFe ultra-thin films deposited on silicon dioxide substrates (Fig. 2). They revealed a magnetic dead layer on NiFe with a thickness equal 0.95 ± 0.05 nm.

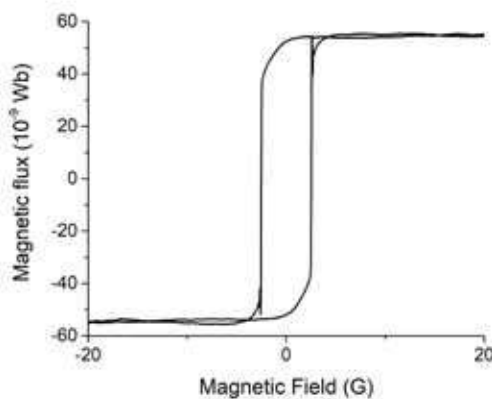


Figure 1: Hysteresis loop curve of a NiFe 6 nm thin film.

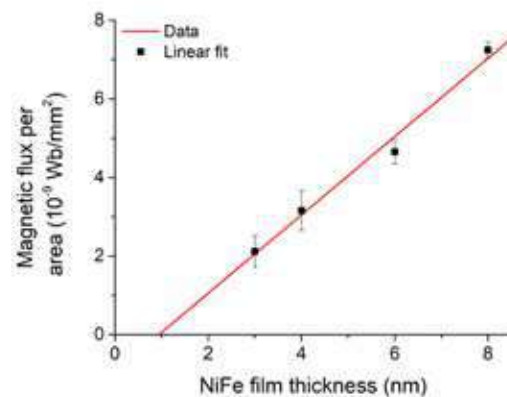


Figure 2: Magnetic flux (\propto magnetic moment) per area in variable thickness NiFe films deposited onto silicon dioxide.

[1] G. Asti, M. Ghidini, and M. Solzi, *J. Mag. Magn. Mater*, **242**, 973 (2002).

Susceptibility of a Small Diamagnetic Particle Detected from its Parabolic Trejectory Produced by Small Nd magnets in Terrestrial Gravity

S. Jinnouchi¹ and C. Uyeda¹

¹ Graduate School of Science, Osaka University, Osaka, Japan

Diamagnetic and paramagnetic materials are not considered to show translation by a low magnetic field produced by parmanent magnets. Diamagnetic magnetization of a single small sample is detected by measuring its parabolic trajectory produced by magnetic field gradient, which was generated by a pair of neodymium magnet in normal normal gravity area [1]. Specifically, susceptibility χ_{DIA} of a single particle is determined from the relationships between horizontal velocity of particle and field intensity observed at different positions of a horizontal coordinate, without measuring mass of particle. The method was based on a previous result that the variance of acceleration detected between two different particles in a common magnetic field is uniquely determined by the variance of their χ_{DIA} . Using a conventional device, χ_{DIA} neasurement generally requires a bulk sample that weight above a level of 1 mg. In the new apparatus, accuracy of measured χ_{DIA} was improved by optimizing the field distribution of the magnetic circuit, thus decreasing the fluctuation of velocity, and χ_{DIA} of a submillimetre sample becomes measureable with an uncertainty below 5×10^{-7} emu/g.

Using this setup, approximate χ_{DIA} of a small particle is swiftly estimated from its position recovered on a collecting plate as shown in Fig.1; here the plate set at bottom of the translating area, and material identification of the particle are possible by collating χ_{DIA} with a list of published data. Unlike most conventional methods of chemical analysis, identification is conducted without consuming the sample. Accordingly the setup will extend as an effective technique of pre-treatment in analyzing a mixture of heterogeneous particles.

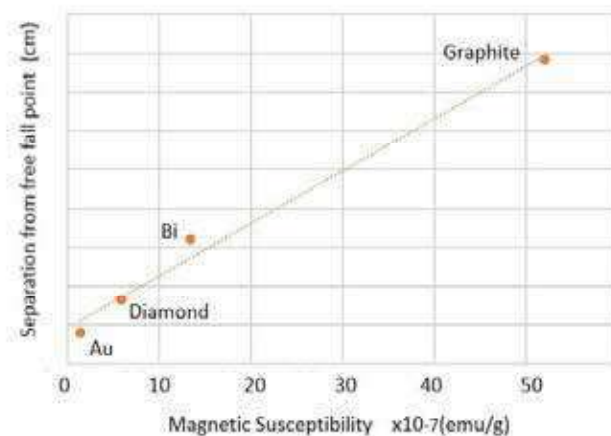


Fig.1 Relationship between horizoantal separation and χ_{DIA} compiled for varios diamagneic materials in the present experiment [2].

[1] K.Hisayoshi et al., Sci Rep. 6, 38431 (2016).

[2] S. Jinnouchi et al, *IEEE Magnetics*.58, 6000204 (2022).

DNS - diffuse neutron scattering spectrometer at MLZ

Y. Su¹, T. Mueller¹

¹ *Forschungszentrum Jülich GmbH, Jülich Centre for Neutron Science (JCNS) at Heinz Maier-Leibnitz Zentrum (MLZ), Lichtenbergstr. 1, 85748 Garching, Germany*

DNS is a versatile polarised neutron scattering instrument, situated at Heinz-Maier-Leibnitz Zentrum (MLZ) in Garching Germany [1] (cf. Fig. 1). It is ideally suited to study both short-range and long-range magnetic correlations in quantum materials, strongly correlated electron systems, unconventional superconductors, and functional magnetic materials. In addition to the diffraction mode, DNS also provides an option with time-of-flight inelastic neutron scattering, which can be used for the measurements of low-energy magnetic excitations. With its compact size, a new-generation Fe/Si based focusing polarising bender and wide-angle polarisation analysers, DNS is optimised as a high intensity polarised instrument with medium resolution.



Figure 1: Picture of the DNS instrument, with the secondary spectrometer to the left and monochromator housing and neutron guide to the right.

With polarization analysis, it allows for the unambiguous separation of nuclear coherent, spin incoherent, and magnetic scattering contributions simultaneously over a large range of scattering vector Q . Polarisation analysis can furthermore significantly increase the signal to noise ratio for the detection of diffuse magnetic scattering. The second non-polarised position sensitive detector array allows access to out-of-plane reflections and drastically improves counting times for inelastic measurements, a sketch is given in Fig. 2.

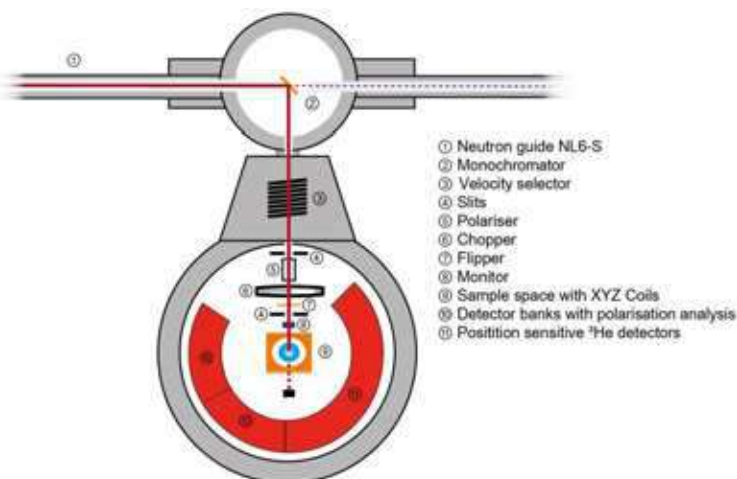


Figure 2: Schematic sketch of the components of the DNS instrument

[1] Y. Su, K. Nemkovskiy, S. Demirdiř, Heinz Maier-Leibnitz Zentrum, *Journal of large-scale research facilities*, **1**, A27, <http://dx.doi.org/10.17815/jlsrf-1-33>

Advanced modeling of the Torque Motor magnetic circuit

Wojciech Pluciński ¹

¹ *Wroclaw University of Science and Technology, Krzywoustego 314-316/19, Wroclaw, Poland*

Torque motors exhibit high sensitivity and reliability. As an element of electrohydraulic servo valve, are used to convert the electrical control signal into a mechanical reaction in form of the generated torque. High accuracy, linear characteristic, low hysteresis and resistance to disturbances resulting from operating environment are especially required for torque motors used for aerospace systems.

Due to the characteristic of the torque motor, the rotation of armature limited to few milliradians [mRad], and high values of the generated torques, the study of such objects required the development of new research methods and tools.

The publication describes the modeling of the Torque Motor magnetic circuit and its characterization. The presented implementation of proposed model is in good agreement with experimental data and creates new possibilities of modelling and testing similar devices.

The test stand built to verify and validate the theoretical model based on the Finite Element Method (FEM) was also discussed.

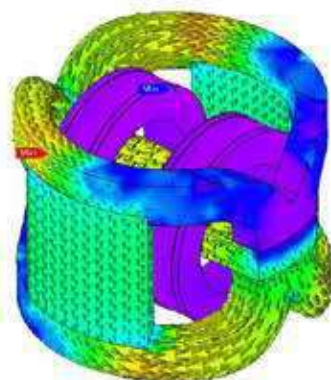


Figure 1: The flux density (B) distribution in the torque motor

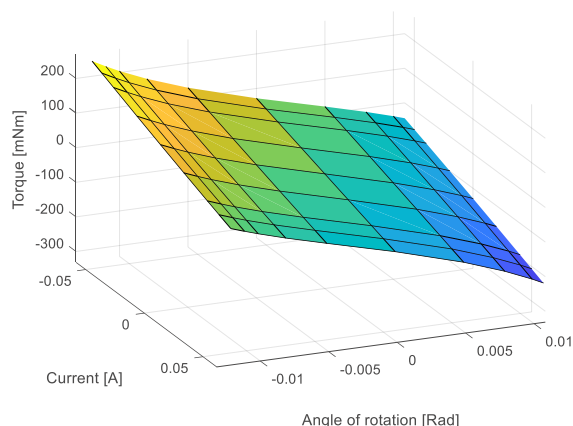


Figure 2: The example of the motor characteristic in form of torque map

Quantification of Spin Accumulation Magnetoresistance in Ferromagnetic heterostructure using DC Bias Harmonic Hall Measurement

H. Y. Poh¹, C. C. I. Ang¹, W. L. Gan¹, G.J. Lim¹, W.S. Lew

¹ School of Physical and Mathematical Sciences, Nanyang Technological University,
21 Nanyang Link, Singapore 637371

Spin accumulation has been a subject of continued pursuit in the understanding of spin-orbit torque switching mechanisms for spintronic device applications. Effective methods for spin accumulation quantification, specifically in the ferromagnetic layer of spin-orbit torque inducing heterostructures has been elusive. Here, we present an all-electrical technique to quantify spin accumulation, by performing a DC-biased harmonic Hall measurement in a typical heavy-metal/ferromagnet Hall-cross structure with in-plane magnetic anisotropy. The inclusion of a DC bias generates a quantifiable amplitude offset in the first harmonics due to spin accumulation. At opposite magnetization states, the first harmonic magnetoresistance is augmented/reduced if the DC-bias-induced accumulated spin polarization aligns parallel/anti-parallel to the magnetization. The cumulative difference in magnetoresistance amplitudes directly provides a quantitative magnitude of the spin accumulation. This technique provides an all-electrical alternative to determine spin accumulation by utilizing the easily accessible harmonic Hall characterization method.

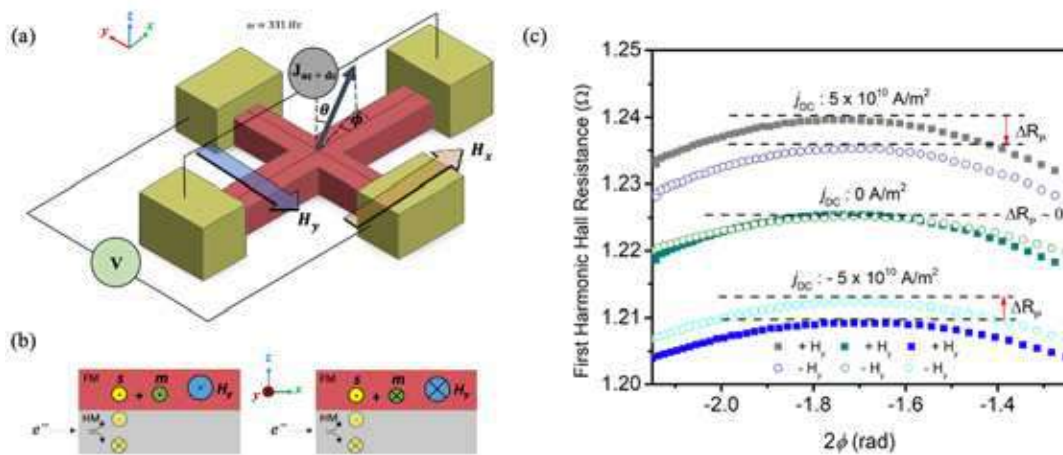


Figure - (a) Schematic of DC bias harmonic Hall setup in the longitudinal configuration. (b) Schematic of the spin accumulation in the FM/HM structure with in-plane anisotropy. Spins are accumulated in the $+\hat{y}$ direction in the FM layer when the injected electron is in the $+\hat{x}$ direction. Local magnetization, \mathbf{m} follows the direction of the external field, H_y . (c) First Harmonic Hall resistance for $+H_y$ (solid square) and $-H_y$ (open circle). Spin accumulation is parallel (antiparallel) to $+H_y$ ($-H_y$), leading to a higher amplitude in the first Harmonic Hall resistance at the current density of $j_{DC} = 5.0 \times 10^{10} \text{ A/m}^2$.

[1] H. Y. Poh, C. C. I. Ang, W. L. Gan, G. J. Lim, and W. S. Lew, Phys. Rev. B **104**, 1 (2021).

Symposium 11. Magnetic materials: alloys, thin-films, interfaces, multilayers and nanomaterials

| | | |
|----------------------------|--|-----|
| Lech Tomasz Baczewski | <i>Chirality and magnetism – new phenomena</i> | 296 |
| Lakhan Bainsla | <i>Ultrathin ferrimagnetic GdFeCo films with very low damping</i> | 297 |
| Tanvi Bhatnagar-Schöffmann | <i>Influence of dusting layers on the magneto-ionic response of Ta/X/CoFeB/Y/MgO/HfO₂ thin film stacks</i> | 298 |
| Marek Cinal | <i>Anatomy of magnetic anisotropy and Gilbert damping in layered systems</i> | 299 |
| Simon Granville | <i>The exceptional magnetic and magnetotransport characteristics of thin film Heusler alloy Co₂MnGa – a room temperature Weyl ferromagnet</i> | 300 |
| Weronika Janus | <i>Strain and ferromagnetic proximity induced spin reorientation transition in antiferromagnetic NiO films</i> | 301 |
| Thomas Kools | <i>Designing compensated Co/Gd ferrimagnets for advanced room temperature spintronic devices</i> | 302 |
| Piotr Kossacki | <i>Semiconductor systems for optical studies of single magnetic ions</i> | 303 |
| Sara Laureti | <i>Disclosing the nature of asymmetric interface magnetism in Co/Pt multilayers</i> | 304 |
| Giacomo Sala | <i>Asynchronous current-induced switching of rare-earth and transition-metal sublattices in ferrimagnetic alloys</i> | 305 |
| Mehran Sedrpooshan | <i>Controlled Self-Assembly and Study of Engineered Magnetic Nanostructures</i> | 306 |
| Jordi Sort | <i>Voltage-driven ON-OFF switching of ferromagnetism in transition metal oxide and nitride films for neuromorphic applications</i> | 307 |
| Andrea Bachmaier | <i>Soft magnetic amorphous Co-Zr alloy by severe plastic deformation</i> | 311 |
| Adam Bonda | <i>Electronic structure and magneto-optical Kerr effect spectra of W/Co/Pt layered systems</i> | 312 |
| Nabil Challab | <i>Flexible magnetic nanostructures: differentiated control of the magnetization</i> | 313 |
| Juliusz Chojenka | <i>Origin of dual magnetoresistance behavior in the nanopatterned titanium/titanium oxide/iron systems</i> | 314 |
| Giuseppe Cuono | <i>Ferromagnetic coupling in doped HgTe: a route for the quantum anomalous Hall effect</i> | 315 |
| Gweha Danny | <i>Size effect on All Optical Switching in GdFeCo</i> | 316 |
| Juan De la Figuera | <i>Towards electric control of magnetism: moving magnetic domains in magnetite / Ru(0001) nanostructures</i> | 317 |
| Samuel Dobák | <i>Competition Between Interparticle Coupling and Demagnetizing Effects in Soft Magnetic Iron Composites</i> | 318 |
| Claudia Fernández-González | <i>Chemically modulated Fe-Ni cylindrical nanowires with asymmetric magnetic response</i> | 319 |
| Martin Friák | <i>A quantum-mechanical study of anomalous magneto-volumetric behavior of ferrimagnetic Ni₃Mn₂₅Sn₈ alloy</i> | 320 |
| Darja Gačnik | <i>Exchange-coupled collective magnetism of a two-phase single-crystalline nanocomposite FeCoCrMnAl high-entropy alloy</i> | 321 |

| | | |
|----------------------------------|---|-----|
| Katarzyna Gas | <i>Quantitative description of magnetic anisotropy in insulating GaN:Mn</i> | 322 |
| Erol Girt | <i>Noncollinear coupling of Co layers across RuCo spacer layers</i> | 323 |
| Georgia Gkouzia | <i>Element specific magnetocrystalline anisotropy of Sm-Co thin films</i> | 324 |
| Daniel Gopman | <i>Influence of heavy sputtering gas on perpendicular magnetic anisotropy and interlayer exchange coupling in Pt/Co/Ir synthetic antiferromagnets</i> | 325 |
| Alejandra Guedeja-Marron | <i>Crystal quality assessment of highly Bi-doped electrodeposited Cu nanowires for spintronics applications</i> | 326 |
| Mariam Hassan | <i>Effect of buffer and capping layers of Co/Ni-based thin film heterostructures: Towards sustainable flexible spintronics</i> | 327 |
| Guillermo Alberto Herrera Huerta | <i>Chemical and Magnetic order of FeRh nanoparticles deposited on BaTiO₃ (001) and SrTiO₃ (001)</i> | 328 |
| Atsufumi Hirohata | <i>Current Induced Crystallisation in Heusler Alloy Films for Memory Potentiation in Neuromorphic Computation</i> | 329 |
| Kristina Ignatova | <i>Magnetic anisotropy and exchange bias in V₂O₃/Ni epitaxial layers</i> | 330 |
| Abdul Khaliq | <i>Spin-glass state and Almeida-Thouless line observation in Ge_{1-x-y}(Sn_xMn_y)Te multiferroics</i> | 331 |
| Akira Kikitsu | <i>Direct On-chip EMI Shielding Layer with Metallic/Magnetic Multilayer for sub-100 MHz frequency range</i> | 332 |
| Anna Kosogor | <i>Impact of the Magnetic Subsystem on the Low-temperature Specific Heat of Metamagnetic Shape Memory Alloy</i> | 333 |
| Michal Krupinski | <i>Control of magnetic properties in ferrimagnetic GdFe and TbFe thin films by He⁺ and Ne⁺ irradiation</i> | 334 |
| Adam Krysztofik | <i>Effect of strain-induced anisotropy on magnetization dynamics in Y₃Fe₅O₁₂ thin films grown on Y₃Al₅O₁₂</i> | 335 |
| Elias Kueny | <i>Spin-structured multilayer THz emitters</i> | 336 |
| Piotr Kuświk | <i>Magnetic patterning by plasma oxidation of Co/Ni bilayers</i> | 337 |
| Ilona Lecerf | <i>Fabrication of rare-earth free permanent magnets for MEMS applications: magnetophoresis assembly of Co nanorods</i> | 338 |
| Jianing Liu | <i>Laser powder bed fusion of (Pr,Nd)-Fe-Cu-B Permanent Magnets</i> | 339 |
| Jike Lyu | <i>Weak ferromagnetism linked to the high-temperature spiral phase of YBaCuFeO₅</i> | 340 |
| Darla Mare | <i>Effect of bending strain on magnetic anisotropy in epitaxial ferrite thin films on mica.</i> | 341 |
| Jorge Marqués-Marchán | <i>Nucleation and current-induced bubble structures motion in PMA multilayers</i> | 342 |
| Giovanni Masciocchi | <i>Control of magnetoelastic coupling in Ni/Fe multilayers using He⁺ ion irradiation</i> | 343 |
| Sergey Nedukh | <i>Influence of antidote form on magnetic resonance response</i> | 344 |
| Volker Neu | <i>Imprinting magnetic micropatterns through geometrical transformation</i> | 345 |
| Felix Nickel | <i>Complex spin structures of ultrathin Fe/Ir films on Re(0001)</i> | 346 |

| | | |
|----------------------------|---|-----|
| Jorge Martín Nuñez | <i>Synthesis and characterization of $\text{Fe}_3\text{O}_4/\text{MgO}/\text{CoFe}_2\text{O}_4$ core/shell/shell magnetic nanoparticles</i> | 347 |
| Gajanan Pradhan | <i>Magnetic properties of FeGa/Kapton for flexible electronics</i> | 348 |
| Sandra Ruiz-Gomez | <i>Magnetic domain wall pinning in cobalt ferrite microstructures</i> | 349 |
| Jose Santiso | <i>Atomic scale structure rearrangements in $\text{Y}_3\text{Fe}_5\text{O}_{12}$ epitaxial films on GGG(111) substrates explored by HR-STEM</i> | 350 |
| Sagar Sen | <i>Ion implantation induced exchange bias in BCC Fe thin film</i> | 351 |
| Sufyan Shehada | <i>Interplay of magnetic states and hyperfine fields of iron dimers on $\text{MgO}(001)$</i> | 352 |
| Natalia Shkodich | <i>Magnetic nanocrystalline CoCrFeNiGa_x ($x = 0.5, 1.0$) high entropy alloys by high energy ball milling</i> | 353 |
| Meg Smith | <i>Optimisation of perpendicular magnetic tunnel junction structures using STEM</i> | 354 |
| Justyn Snarski-Adamski | <i>Effect of transition metal doping on magnetic hardness of CeFe_{12}-based compounds.</i> | 355 |
| Jimena Soler-Morala | <i>Influence of the buffer layer on the nanoscale architecture in NdFeB ultrathin films</i> | 356 |
| Marcin Szpytma | <i>Beating the limitation of the Néel temperature of FeO with antiferromagnetic proximity in FeO/CoO</i> | 357 |
| Dariusz Sztenkiel | <i>Spin orbital reorientation transitions induced by magnetic field</i> | 358 |
| Luding Wang | <i>Picosecond Optospintronic Tunnel Junctions for Non-volatile Photonic Memories</i> | 359 |
| Mirosław Werwiński | <i>Structural phase transition in Fe thin films: DFT study</i> | 360 |
| Oksana Yastrubchak | <i>Ferromagnetism and band structure engineering in the $(\text{Ga,Mn})\text{As}$, $\text{Ga}(\text{Bi,As})$ and $(\text{Ga,Mn})(\text{Bi,As})$ nanolayers</i> | 361 |
| Mathias Zambach | <i>Superparamagnetic particles for micro-inductor applications</i> | 362 |
| Yao Zhang | <i>Voltage-controlled switching of magnetic anisotropy in ambipolar $\text{Mn}_2\text{CoAl}/\text{Pd}$ bilayers</i> | 363 |
| Zhibo Zhao | <i>Energy-efficient magnetoelectrochemical effect of $\text{La}_{0.7}\text{Sr}_{0.3}\text{MnO}_{3-\delta}$ via voltage-driven oxygen motion</i> | 364 |
| Monika Zięba | <i>Electronic structure of ferromagnetic $\text{Sn}_{1-x}\text{Mn}_x\text{Te}$ thin films</i> | 365 |
| Jon Ander Arregi | <i>Optical microscopy of antiferromagnetic and ferromagnetic domains in FeRh thin films</i> | 368 |
| Mohamed Ben Chroud | <i>Magnetron sputtered epitaxial NiAl seed layer on Ge for enhanced VCMA effect.</i> | 369 |
| Mattia Benini | <i>Colossal enhancement of the coercivity in thin Co films interfaced with molecules</i> | 370 |
| Mattia Benini | <i>In-depth modification in Co thin films induced by the interfacing with molecular layers detected by Zero-Field NMR</i> | 371 |
| Mani Teja Bodduluri | <i>Wafer-level Integrated Hard Micromagnets for MEMS Applications</i> | 372 |
| Alonso J. Campos-Hernandez | <i>Study of the magnetic interactions in FeNi nanowires through coercivity angular measurements and FORC analysis</i> | 373 |

| | | |
|--------------------------------|---|-----|
| Oleksandr Chumak | <i>Correlation of magnetoelastic interactions and magnetic damping in thin $\text{Co}_2\text{Fe}_{0.4}\text{Mn}_{0.6}\text{Si}$ and $\text{Co}_2\text{FeGa}_{0.5}\text{Ge}_{0.5}$ magnetic layers</i> | 374 |
| Umit Daglum | <i>Magnetic properties of Mn_3Ga, calculated from first principles and mappend onto an effective spin Hamiltonian for atomistic spin dynamics simulations</i> | 375 |
| Elizabeth Davis-Fowell | <i>Investigation and optimisation of magnetic properties of Ga-doped τ MnAl</i> | 376 |
| Jaydeb Dey | <i>^{55}Mn NMR investigations on Mn_2GaC nanolaminated thin film</i> | 377 |
| Javier Díaz | <i>Analysis of the dysprosium M_5 circularly polarized X ray absorption spectrum to detect magnetically uncoupled rare earth atoms to TM in TM-RE amorphous alloys</i> | 378 |
| Javier Díaz | <i>Vortex chirality observation in trilayer disks of Fe/Al/Co using X ray resonant magnetic scattering</i> | 379 |
| Amar Fakhredine | <i>Huge Dzyaloshinskii-Moriya interactions in Re/Co[n]/Pt thin films</i> | 380 |
| Łukasz Frąckowiak | <i>Experimental Results and Numerical Calculation of Co-Tb Distribution from Magnetron Co-Sputtering Deposition with a Composition Gradient</i> | 381 |
| Martin Friák | <i>An ab initio study of antiphase boundaries in ferromagnetic B_2-phase Fe_2CoAl alloy</i> | 382 |
| Nathan Hale | <i>The 4 × 4 transfer matrix method: a flexible and computationally efficient tool for exploring a system's surface magnon polaritons</i> | 383 |
| Yuan Hong | <i>A High Throughput Study of Hard Magnetic CeCo_5-based Thin Films</i> | 384 |
| Florian Jürries | <i>Stability of MnAl-C magnet alloys in the presence of water</i> | 385 |
| Jiří Kaštil | <i>Exchange spring and exchange bias effects in the bulk Heusler Ni_2MnSn-based alloys</i> | 386 |
| Rafael Morales | <i>Isotropic exchange bias in patterned IrMn/CoFe bilayers</i> | 387 |
| Okan Ozdemir | <i>Magnetic Characterization of Co_2MnAl/ PMN-PT (011) Multiferroic Heterostructures</i> | 388 |
| Tibor Adrian Óvári | <i>Nonlinear Domain Wall Dynamics in Highly Magnetostrictive Amorphous Nanowires Prepared by Rapid Solidification</i> | 389 |
| Parul Rani | <i>Magnetic properties of amorphous $\text{Co}_x\text{Zr}_{100-x}$ films</i> | 390 |
| Pedro A. Sánchez | <i>The impact of finite magnetic anisotropy and hydrodynamics on the response of systems of magnetic colloidal particles</i> | 391 |
| Carlos Henrique Santos Verbeno | <i>Magnetic properties of cobalt ultrathin film structures controlled by buffer-layer roughness</i> | 392 |
| Célia T. Sousa | <i>Multifunctional Fe Au nanostructures synthesized by Laser Ablation in Liquids</i> | 393 |
| Kateryna Sova | <i>Ferromagnetic resonance in Fe_3O_4 nanoparticles in combination with ligands</i> | 394 |
| Dariusz Sztieniel | <i>Crystal field model simulations of magnetic response of pairs, triplets and quartets of Mn^{3+} ions in GaN</i> | 395 |
| Nataliia Tataryn | <i>Valence Band Dispersion in $(\text{Ga,Mn})\text{As}$, $\text{Ga}(\text{Bi,As})$, $(\text{Ga,Mn})(\text{Bi,As})$ epitaxial nanolayers</i> | 396 |
| Michal Varga | <i>Ni_2FeZ ($Z = \text{Ga, In, Tl}$) Heusler alloy nanowires prepared via electrodeposition</i> | 397 |
| Yuliia Veretennikova | <i>Capping layer influence on magnetic characteristics evolution in cobalt nanofilms</i> | 398 |

| | | |
|--------------------|---|-----|
| Zengxin Wei | <i>A strong competition among the anisotropy terms in magnetically coupled Fe/Al/Fe thin film trilayers</i> | 399 |
| Michael Zawodzki | <i>Demonstrating and tailoring exchange bias on novel bulk nanocomposites processed by severe plastic deformation</i> | 400 |
| Nerija Zurauskiene | <i>Tuning of Magnetoresistive Properties of Graphene-Lanthanum Manganite Structures</i> | 401 |

Invited Oral Presentations

| | | |
|----------------------------|--|-----|
| Lech Tomasz Baczewski | <i>Chirality and magnetism – new phenomena</i> | 296 |
| Lakhan Bainsla | <i>Ultrathin ferrimagnetic GdFeCo films with very low damping</i> | 297 |
| Tanvi Bhatnagar-Schöffmann | <i>Influence of dusting layers on the magneto-ionic response of Ta/X/CoFeB/Y/MgO/HfO₂ thin film stacks</i> | 298 |
| Marek Cinal | <i>Anatomy of magnetic anisotropy and Gilbert damping in layered systems</i> | 299 |
| Simon Granville | <i>The exceptional magnetic and magnetotransport characteristics of thin film Heusler alloy Co₂MnGa – a room temperature Weyl ferromagnet</i> | 300 |
| Weronika Janus | <i>Strain and ferromagnetic proximity induced spin reorientation transition in antiferromagnetic NiO films</i> | 301 |
| Thomas Kools | <i>Designing compensated Co/Gd ferrimagnets for advanced room temperature spintronic devices</i> | 302 |
| Piotr Kossacki | <i>Semiconductor systems for optical studies of single magnetic ions</i> | 303 |
| Sara Laureti | <i>Disclosing the nature of asymmetric interface magnetism in Co/Pt multilayers</i> | 304 |
| Giacomo Sala | <i>Asynchronous current-induced switching of rare-earth and transition-metal sublattices in ferrimagnetic alloys</i> | 305 |
| Mehran Sedrpooshan | <i>Controlled Self-Assembly and Study of Engineered Magnetic Nanostructures</i> | 306 |
| Jordi Sort | <i>Voltage-driven ON-OFF switching of ferromagnetism in transition metal oxide and nitride films for neuromorphic applications</i> | 307 |

Chirality and magnetism – new phenomena

L.T. Baczewski¹, O. Ben Dor², S. Yochelis², S.S.P. Parkin^{3,4}, R. Naaman⁵, Y. Paltiel²,

¹ *Institute of Physics Polish Academy of Sciences, Warszawa, Poland.*

² *Department of Applied Physics, Hebrew University, Jerusalem, Israel*

³ *IBM Research Division, Almaden Research Center, USA*

⁴ *Max Planck Institute for Microstructure Physics, Halle, Germany.*

⁵ *Department of Chemical and Biological Physics, Weizmann Institute of Science, Rehovot, Israel.*

Chirality plays a critical role in a wide range of systems, from biology and chemistry to condensed matter physics and high energy physics. For example, in the biochemistry and pharmaceutical industries, enantiomer separation is a major issue, since enantiomers with a specific chirality often have different biochemical properties or pharmacological effects from their counterparts with the opposite chirality. Enantioselectivity is ubiquitous in nature and many of the molecules in plants and living organisms have their properties depending on the type of enantiomer. Chiral recognition and enantiomeric selectivity, both in nature and in artificial systems, are commonly assumed to be related to a spatial effect, with the recognition process typically described by a “lock and key” type model. Accordingly, chromatography-based enantioseparation requires the chiral substrate to be adjusted so as to interact optimally with a specific enantiomer. Indeed, enantioseparation is an extremely important process in the pharmaceutical and chemical industries. The importance of chirality was only realized by scientists in the sixties of last century after a disaster with Thalidomide drug used by pregnant women which caused birth of children with malformations due to mutagenic effect of one of the enantiomers. Since then chromatography and electromigration techniques have long been the methods of choice in this field. However, despite intensive efforts, obtaining enantiomerically pure synthetic materials remains a challenge, as the cost of separation is relatively high and an extensive effort is required. In one of our papers [1] we have demonstrated a new effect of magnetization switching of ferromagnetic thin film without applying a magnetic or electric field but being induced solely by adsorption of chiral molecules. In this case, about 10^{13} electrons per cm^2 are sufficient to induce magnetization reversal. The direction of the magnetization depends on the handedness of the adsorbed chiral molecules. We have shown for the first time that magnetization reorientation of magnetic layer can be realized solely by adsorption of specific enantiomer of chiral molecules on its surface without any presence of magnetic or electric fields. Another important result was to propose a new method of enantio-separation based on the interaction of chiral molecules with a perpendicularly magnetized substrate. It was shown that one enantiomer adsorbs preferentially when the magnetic dipole is pointing up, whereas the other adsorbs faster for the opposite magnetization alignment. Moreover the interaction is not controlled by the magnetic field but by the respective electron spin orientations of the ferromagnetic layer and chiral molecules. This method is versatile as it was tested for different kinds of chiral molecules and allows to avoid costly separation columns which has to be designed individually for a given type of chiral molecules used presently in the pharmaceutical industry.

[1] O. Ben Dor, S. Yochelis, A. Radko, K. Vankayala, E. Capua, A. Capua, S.-H. Yang, L. T. Baczewski, S. S. P. Parkin, R. Naaman, Y. Paltiel, *Nature Commun.* 8, (2017), 14567

[2] K. Banerjee-Ghosh, O. Ben Dor, F. Tassinari, E. Capua, S. Yochelis, A. Capua, See-Hun Yang, S. S. P. Parkin, S. Sarkar, L. Kronik, L. T. Baczewski, R. Naaman, Y. Paltiel, *SCIENCE*, Vol. 360, Issue 6395, (2018), 1331

Ultrathin ferrimagnetic GdFeCo films with very low damping

L. Bainsla,¹ A. Kumar,¹ A. A. Awad,¹ M. Zahedinejad,¹ N. Behera,¹ H. Fulara,¹ R. Khymyn,¹ A. Houshang,¹ and Johan Åkerman¹

¹ Physics Department, University of Gothenburg, 412 96 Gothenburg, Sweden

Ferromagnetic materials dominate as the magnetically active element in spintronic devices but come with drawbacks such as large stray fields and low operational frequencies [1]. Compensated ferrimagnets provide an alternative as they combine the ultrafast magnetization dynamics of antiferromagnets with a ferromagnet-like spin-orbit-torque (SOT) behavior [2]. However, to use ferrimagnets in spintronic devices such as in spin Hall nano-oscillators (SHNOs), it is important to ensure that such films retain their advantageous properties in ultrathin films (thickness less than 10 nm).

In this work, ferrimagnetic $\text{Gd}_x(\text{FeCo})_{1-x}$ thin films were grown using co-sputtering of Gd and $\text{Fe}_{87.5}\text{Co}_{12.5}$ on high resistance (HR) Si (100) substrates, and their magneto-dynamics was studied using ferromagnetic resonance measurements at room temperature. By tuning the stoichiometry of the $\text{Gd}_x(\text{FeCo})_{1-x}$ films, a nearly compensated behavior is for the first time demonstrated in 2 nm thin film (Fig. 1). Values for the effective magnetization and effective Gilbert damping constant (α) of 0.02 Tesla and 0.0078 ± 0.0002 are obtained for a 2 nm

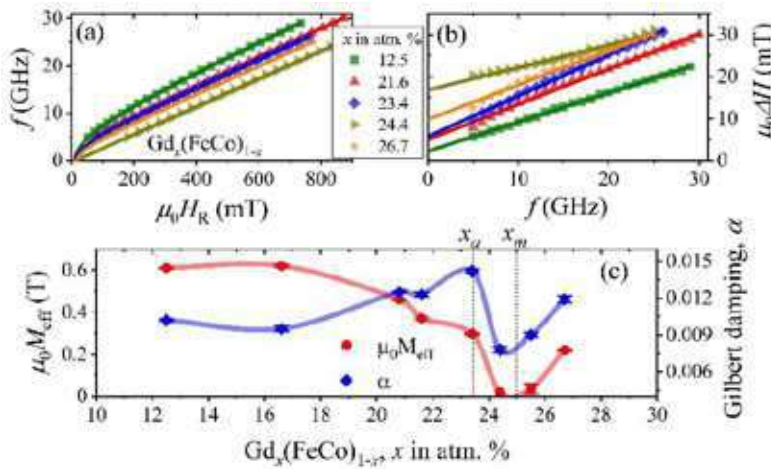


Figure 1: (a) Frequency (f) vs. resonance field and (b) Resonance linewidth vs f , of 2 nm thick $\text{Gd}_x(\text{FeCo})_{1-x}$ films, with x the Gd atomic %. (c) Effective magnetization and effective Gilbert damping constant vs. composition of 2 nm $\text{Gd}_x(\text{FeCo})_{1-x}$ films; solid symbols represent values obtained by fitting the experimental data to the Kittel's equation and equation (10) in reference [5], while solid lines are a guide to the eye.

$\text{Gd}_{24.4}(\text{FeCo})_{75.6}$ film [3], where α is comparable to the lowest value obtained in thick films [4]. The vertical dotted lines in Fig. 1(c) show literature values for the spin angular momentum (x_a) and magnetic momentum (x_m) compensation points in thick films. In search of high-frequency auto-oscillations in SHNOs, constrictions with 50-300 nm widths were also prepared using $\text{Gd}_x(\text{FeCo})_{1-x}$ (2-10nm)/Pt(5nm) based stacks and promising results using Brillouin Light Scattering show SOT controllable ferromagnetic modes in these devices.

- [1] B. Dieny *et al.*, Nat. Elec. **3**, 446 (2020).
- [2] S. K. Kim *et al.*, Nat. Mat. **21**, 24 (2022).
- [3] L. Bainsla *et al.*, Advanced Functional Materials. *in press* (2022).
- [4] D. H. Kim *et al.*, Phys. Rev. L **122**, 127203 (2019).
- [5] L. Bainsla *et al.*, Phys. Rev. B **96**, 094404 (2017).

Influence of dusting layers on the magneto-ionic response of Ta/X/CoFeB/Y/MgO/HfO₂ thin film stacks

**T. Bhatnagar-Schöffmann¹, A. Solignac², D. Ourdani³, R. Pachat¹, M.-A. Syskaki⁵,
Y. Roussigné³, S. Ono⁵, D. Ravelosona^{1,4}, J. Langer⁵, M. Belmeguenai³,
and L. Herrera Diez¹**

¹ *Centre de Nanosciences et de Nanotechnologies, CNRS,
Université Paris-Saclay, 91120 Palaiseau, France*

² *Université Paris-Saclay, CEA, CNRS, SPEC, 91191, Gif-sur-Yvette, France*

³ *Laboratoire des Sciences des Procédés et des Matériaux, CNRS-UPR 3407,
Université Paris 13, Sorbonne Paris Cité, 93430 Villetaneuse, France*

⁴ *Spin-Ion technologies, C2N, 10 Boulevard Thomas Gobert, 91120 Palaiseau, France*

⁵ *Singulus Technologies AG, Hanauer Landstrasse 103, 63796 Kahl am Main, Germany*

⁶ *Central Research Institute of Electric Power Industry, Yokosuka, Kanagawa 240-0196, Japan*

The discovery of perpendicular magnetic anisotropy (PMA) in CoFeB/MgO magnetic tunnel junctions has paved a path in the direction of realizing high density, non-volatile spintronic devices with low power consumption. In this system, PMA is linked to the interfacial hybridization of Co-O and Fe-O, while interfaces with heavy metal elements are of great importance for the observation of Dzyaloshinskii-Moriya interaction (DMI) and spin-orbit torques. This facilitates a broad playground for voltage-driven interface engineering to modulate magnetism.

Here, we present the room temperature magneto-ionic control of magnetic anisotropy, coercivity (H_c) and Dzyaloshinskii-Moriya interaction (DMI) in Ta/X/Co₄₀Fe₄₀B₂₀/Y/MgO/HfO₂, where X and Y are dusting layers of heavy metal elements (Pt,W) sharing different interfaces with CoFeB. We observe a large dependence of the magneto-ionic response on the nature and position of the dusting layers. Dusting layers at the bottom interface (Y) can define a system locked in a PMA state allowing for a reversible magneto-ionic control of H_c , while samples with dusting layers at the top interface (X) can allow for a full and reversible spin-reorientation transition. Samples with both X and Y dusting layers often present a reduced magneto-ionic response.

The intercalation of dusting layers of heavy metal elements in Ta/CoFeB/MgO stacks has the potential not only to fine tune magnetic properties and enhance magneto-ionic effects but also to individually address the contributions from each interface to the magnet-ionic mechanisms. These results are therefore of interest in terms of the understanding of magneto-ionic mechanisms and for the design of multifunctional spintronics devices.

Anatomy of magnetic anisotropy and Gilbert damping in layered systems

M. Cinal

Institute of Physical Chemistry, Polish Academy of Sciences, 01-224 Warsaw, Poland

Magnetocrystalline anisotropy (MCA) energy E_{MCA} , orbital magnetic moment (OM) $\langle L_z \rangle$ along the magnetization (\mathbf{M}) direction ζ and the Gilbert damping constant α are investigated for (001) fcc Co/nonmagnet layered systems. The calculation methods, mutual relations, spatial breakdowns and oscillatory thickness dependences are examined [1]. Tilting of magnetization of ferromagnetic films on vicinal surfaces is also shortly discussed [2].

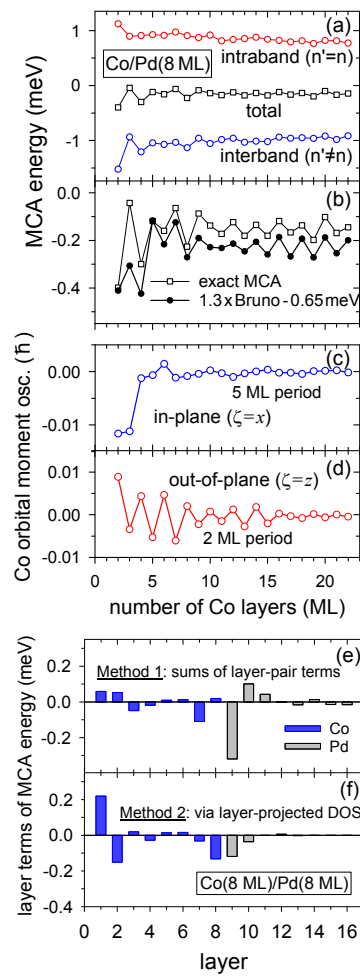


Figure 1: (a,b) MCA energy, (a) its intraband and interband terms, (b) comparison with the Bruno relation, (c,d) oscillatory part of the Co orbital moment, (e,f) MCA layer contributions.

It is shown [1] that the inclusion of the usually neglected *intraband* term in the second-order perturbation theory (PT) expression for E_{MCA} is vital as this term is finite for systems without the inversion symmetry and comparable to the interband term. It is also found that the PT formula is inaccurate and largely overestimates the amplitude of the MCA oscillations for systems with strong spin-orbit coupling, like the Co/Pt bilayer.

The MCA energy $E_{\text{MCA}} = E(\mathbf{M}_{\perp}) - E(\mathbf{M}_{\parallel})$ oscillates versus the Co thickness with the dominating 2 ML period as observed for Co films on a vicinal Cu substrate [3]. The OM of Co is found to oscillate in a distinctly different way for different magnetization directions, with the 2 ML period for the out-of-plane direction (\mathbf{M}_{\perp}) and the 5 ML period oscillations of much smaller amplitude for the in-plane direction (\mathbf{M}_{\parallel}). The quantum-well states responsible for these oscillations are identified. The Bruno relation [4] between the MCA energy and the Co OM anisotropy (OMA) well reproduces the oscillations of E_{MCA} but fails to approximate its mean value [1].

It is shown that layer contributions to the MCA energy are not uniquely determined: two distinct methods lead to different spatial decompositions of E_{MCA} . The layer OM terms are also examined and no clear correlation between the layer MCA and OMA terms, like a local Bruno relation, is found.

Spatial breakdown is also discussed for the damping constant α calculated in the torque-correlation model to investigate the nonlocal origin of the Gilbert damping [5,6].

- [1] M. Cinal, *Phys. Rev. B* **105**, 104403 (2022).
- [2] M. Dąbrowski, M. Cinal, A.K. Schmid, J. Kirschner, and M. Przybylski, *Phys. Rev. B* **99**, 184420 (2019).
- [3] M. Przybylski, M. Dąbrowski, U. Bauer, M. Cinal, and J. Kirschner, *J. Appl. Phys.* **111**, 07C102 (2012).
- [4] P. Bruno, *Phys. Rev. B* **39**, 865 (1989).
- [5] E. Barati, M. Cinal, D. M. Edwards, and A. Umerski, *Phys. Rev. B* **90**, 014420 (2014).
- [6] E. Barati and M. Cinal, *Phys. Rev. B* **91**, 214435 (2015); **95**, 134440 (2017).

The exceptional magnetic and magnetotransport characteristics of thin film Heusler alloy Co_2MnGa – a room temperature Weyl ferromagnet

S. Granville^{1,2}

¹ Robinson Research Institute, Victoria University of Wellington, Wellington, New Zealand

² MacDiarmid Institute for Advanced Materials and Nanotechnology, Wellington, New Zealand

In the first phase of research into thin films of Heusler alloy Co_2MnGa , they were studied as an interesting but unexceptional member of the ferromagnetic Heusler alloys, alongside compositions more promising for high-performance spintronic devices, such as half-metallic $\text{Co}_2(\text{Fe,Mn})\text{Si}$. The prediction 6 years ago of the presence of Weyl states in the electronic structure [1,2], confirmed with measurements on bulk crystals soon after [2], reignited interest in Co_2MnGa . As almost the only known example of a room-temperature Weyl ferromagnet, it has become an ideal candidate for exploring how magnetism and topology mix together to supply enhanced spintronic properties beyond those even of half-metals, with significant potential in a range of thin film structures.

We have produced high quality thin films of Co_2MnGa and studied a range of magnetic and magnetotransport phenomena, finding perpendicular magnetic anisotropy [4] as well as record high anomalous Hall [5], anomalous Nernst [6], and recently, spin Hall [7] effects – showing the influence the Weyl states have on these technologically useful phenomena, even at room temperature. In this presentation I will describe these investigations and outline the potential implications of the exceptional Weyl-boosted magnetotransport properties of Co_2MnGa for thin film devices that rely on spin currents, thermo-spin conversion and spin-orbit torques.

- [1] J. Kübler and C. Felser, *Europhys. Lett.* **114**, 47005 (2016).
- [2] M. Z. Hasan *et al.*, *Phys. Rev. Lett.* **119**, 156401 (2017).
- [3] M. Z. Hasan *et al.*, *Science* **365**, 1278 (2019).
- [4] S. Granville *et al.*, *Appl. Phys. Lett.* **110**, 062408 (2017).
- [5] N. V. Medhekar, S. Granville *et al.*, *npj Quantum Mater.* **6**, 17 (2021).
- [6] S. Granville, H. Yu *et al.*, *IEEE Mag. Lett.*, in press (2022).
- [7] S. Granville, M. Shiraishi *et al.*, *Phys. Rev. B* **103**, L04114 (2021).

Strain and ferromagnetic proximity induced spin reorientation transition in antiferromagnetic NiO films

W. Janus¹, A. Koziol-Rachwał¹, M. Ślęzak¹, M. Zając², P. Drózd¹, M. Szpytma¹, H. Nayyef¹, and T. Ślęzak¹

¹ AGH University of Science and Technology, Faculty of Physics and Applied Computer Science, Krakow, Poland

² National Synchrotron Radiation Centre SOLARIS, Jagiellonian University, Krakow, Poland

Ability to control the spin orientation in antiferromagnets (AFMs) has recently attracted a lot of attention[1]. In this work we use both epitaxial strain and ferromagnetic proximity effects to tailor magnetic anisotropy of the AFM NiO. We used XMLD technique to study magnetic properties of NiO in Fe/NiO/MgO(d_{MgO})/Cr(20 nm)/MgO(001) as a function of the MgO buffer layer thicknesses (d_{MgO}). The so called Ni L_2 ratio (R_{L_2}) was used as a fingerprint of magnetic state of AFM NiO. Figure 1 shows Ni L_2 ratio difference defined as $\Delta R_{L_2} = R_{L_2}(\gamma = 0^\circ) - R_{L_2}(\gamma = 60^\circ)$, where γ is the angle between the sample surface normal and the direction of the x-ray propagation, as a function of d_{MgO} . We noted an increase of ΔR_{L_2} with increasing d_{MgO} , which indicates rotation of NiO spins towards out-of-plane orientation [2]. According to our previous work [3] we interpret this effect as resulting from tensile strain exerted by MgO buffer on NiO layer. To investigate how adjacent Fe layer influences AFM domains distribution in our system, prior to XMLD measurements the sample was magnetized along Fe[001] (NiO[110]) direction. Figure 2 shows R_{L_2} dependencies as a function of azimuthal angle ϕ for different Fe thicknesses (d_{Fe}). Comparison of measured (Fig.2) and simulated (not shown) with Crispy software [4] $R_{L_2}(\phi)$ dependencies indicates multiple domain structure in NiO governed by the spin-flop like coupling at the Fe/NiO interface. In Fig.2 one can note that the $R_{L_2}(\phi)$ azimuthal anisotropy is getting more pronounced with increasing Fe thickness. This can be attributed to Fe-thickness induced repopulation of NiO domains with spin axis closest to NiO[1-10] direction.

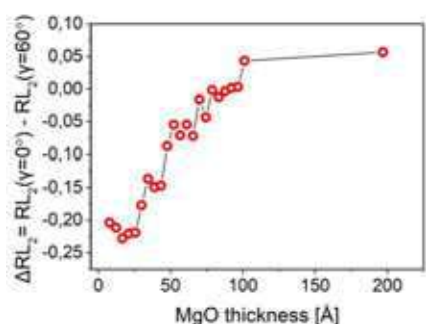


Figure 1. Ni ΔR_{L_2} dependence on MgO thickness in Fe/NiO/MgO/Cr/MgO(001).

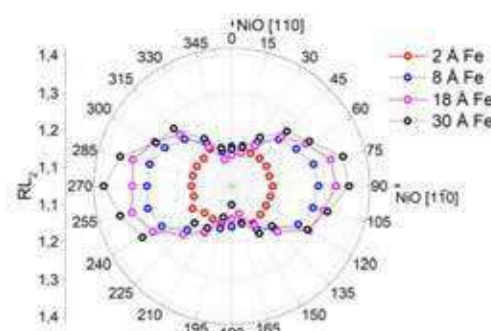


Figure 2. Ni R_{L_2} as a function of azimuthal angle ϕ for Fe(2 Å)/NiO, Fe(8 Å)/NiO, Fe(18 Å)/NiO and Fe(30 Å)/NiO.

- [1] V. Baltz *et al.*, *Rev. Mod. Phys.*, 90, 15005 (2018)
- [2] D. Alders *et al.*, *Phys. Rev. B - Condens. Matter Mater. Phys.*, 57, 11623 (1998)
- [3] A. Koziol-Rachwał *et al.*, *APL Mater.*, 8, 061107 (2020)
- [4] M. Retegan, Crispy: v0.7.3, DOI: 10.5281/zenodo.1008184 (2019)

Designing compensated Co/Gd ferrimagnets for advanced room temperature spintronic devices

Thomas J. Kools¹, Bert Koopmans¹ and Reinoud Lavrijsen¹

¹ Eindhoven University of Technology, Groene Loper 23, Eindhoven, The Netherlands

Flexibility for interface engineering, and access to all-optical switching of the magnetization, make synthetic ferrimagnets (SFIMs) an interesting candidate for advanced spintronic devices like racetrack memory [1,2]. However, the absence of compensation at room temperature (RT) in Co/Gd bilayers has hampered the efficiency with which their magnetic order can be manipulated, as the highest efficiency of spin-orbit torques and current induced domain wall motion (CIDWM) are generally achieved under compensation [3,4]. In order to combine the favourable properties of SFIMs with compensation at RT, Co/Gd/Co/Gd quadlayer structures are investigated.

We present a systematic study of the conditions for magnetization compensation and perpendicular magnetic anisotropy (PMA) in Co/Gd/Co/Gd quadlayers. These conditions were investigated on a sample with the middle Co and Gd films wedged orthogonally with respect to each other, as shown in the inset of Fig. 1. By scanning the polar magneto-optical Kerr effect (MOKE), a magnetostatic phase diagram like in Fig. 1 can be obtained. Three regimes are distinguished: In-plane magnetization (teal), and out-of-plane (OOP) Co (red) and Gd (blue) dominated. The boundaries between these regimes provide valuable insight into the balance between shape anisotropy and PMA, and the conditions for compensation. A simple model based on partial intermixing at Co/Gd interfaces has been developed which explains the experiments well, and provides a tool to qualitatively and to limited extent quantitatively understand these phase diagrams.

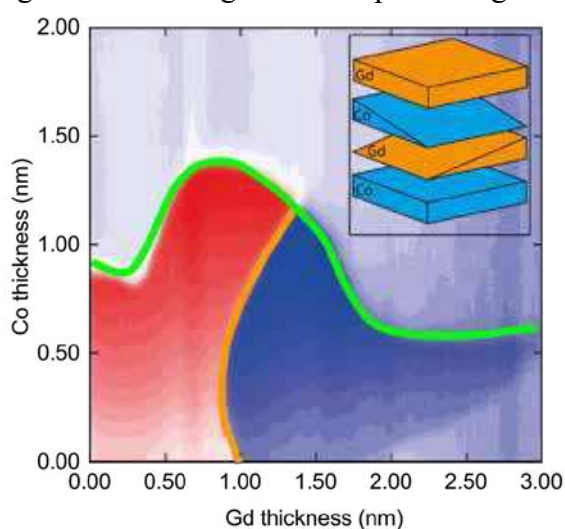


Figure 1: Typical magnetostatic phase diagram of double wedge Co(0.65)/Gd(0-3)/Co(0-2)/Gd(1.5) measured with polar MOKE. Green and orange lines indicate compensation and the transition from out-of-plane to in-plane magnetization respectively

This work provides a simple framework to experimentally characterize, and describe basic magnetostatic properties in these promising heterostructures. The compensated SFIMs investigated in this research, carry the promise of breaking the elusive 1000 m/s barrier for CIDWM, and exhibiting ultrafast exchange-driven dynamics, both relevant properties for future spintronic devices.

- [1]: M. Laliu, R. Lavrijsen and B. Koopmans, Nature communications., Vol. 10.1, p.1 (2019)
- [2]: M. Beens, M. Laliu and B. Koopmans, Physical Review B, Vol. 100(22), p.220409 (2019)
- [3]: R. Bläsing, K. Liu and S. Parkin, Nature communications, Vol. 9(1), p.1 (2018)
- [4]: L. Caretta, M. Schneider and D. Engel, Nature nanotechnology, Vol. 13(12), p.1154. (2018)
- [5]: T. Kools et al., In-Prep (2022)

Semiconductor systems for optical studies of single magnetic ions

P. Kossacki

Institute of Experimental Physics, Faculty of Physics, University of Warsaw, Poland

The magnetic ions embedded in a semiconductor matrix give unique possibility to explore properties of the magnetism down to the limit of an individual impurity. Such studies are particularly effective in semiconductor nanostructures, which combine mature technology of semiconductor epitaxy and processing with good knowledge of the electronic states in quantum dots and wells. The unique advantage of such approach is convenient optical access to the localized spin phenomena, making the semiconductor quantum dots and wells a very attractive playground for spin manipulation. Knowledge gained in simple systems shed new light on limits of more complex applications.

The research of quantum dots with single magnetic impurities was initiated by demonstration of CdTe dots with individual Mn^{2+} ions [1]. For this classical system several basic operations were shown. First of all, the optical orientation of the Mn^{2+} spin was demonstrated [2]. More advanced time-resolved experiments led to the observation of coherent precession of a single Mn^{2+} spin [3,4]. Such optical studies boosted studies on spin relaxation dynamics as well as the coherence time of various magnetic ions in different semiconductor matrixes. Up to now, a number of systems of quantum dots with individual transition metal ions were demonstrated, including: Co [5], Fe [6], Cu, Cr [7], Ni and V. The variety of different systems revealed mechanisms responsible for the spin relaxation and indicated direction of the quest for long spin coherence time.

In my talk I will summarize the most striking results of our recent spectroscopic studies of semiconductor systems with magnetic ions. I will present how magneto-optical measurements of the spin dynamics reveal fundamental properties of the interaction of the magnetic ion with the host semiconductor [8,9]. I will also discuss various effects limiting the spin relaxation and coherence times, such as interaction with carriers, local strain, nuclear spin, and spin-orbit coupling.

- [1] L. Besombes *et al.*, Physical Review Letters **93**, 207403 (2004)
- [2] M. Goryca *et al.*, Physical Review Letters **103**, 087401 (2009)
- [3] M. Goryca *et al.*, Physical Review Letters **113**, 227202 (2014)
- [4] A. Lafuente-Sampietro *et al.* Phys. Rev. **B 92**, 081305(R) (2015)
- [5] J. Kobak, T. Smoleński *et al.*, Nature Communications **5**, 3191 (2014)
- [6] T. Smoleński *et al.*, Nature Communications **7**, 10484 (2016)
- [7] A. Lafuente-Sampietro *et al.* Phys. Rev. **B 93**, 161301(R) (2016)
- [8] A. Bogucki, *et al.*, Phys. Rev. **B 105**, 075412 (2022)
- [9] J. Kasprzak, *et al.*, ACS Photonics **9**, 1033–1041 (2022).

Disclosing the nature of asymmetric interface magnetism in Co/Pt multilayers

S. Laureti¹, P. Alippi¹, F. Offi², G. Barucca⁴, G. Varvaro¹, E. Agostinelli¹, M. Albrecht⁵, B. Rutkowski⁶, A. Ruocco², D. Paoloni², M. Valvidares⁷ and A. Verna^{2,3}

¹Istituto di Struttura della Materia, CNR, nM2-Lab, Monterotondo Scalo (Roma), 00015, Italy

²Dipartimento di Scienze, Università degli Studi Roma Tre, I-00146 Roma, Italy

³ENEA-FSN-Fiss-SNI, Casaccia R.C., 00123 Roma, Italy

⁴Università Politecnica Delle Marche, Dipartimento SIMAU, Ancona, Italy

⁵Institute of Physics, University of Augsburg, D-86159 Augsburg, Germany

⁶Faculty of Metals Engineering and Industrial Computer Science, AGH University of Science and Technology, 30-059 Kraków, Poland

⁷ALBA Synchrotron Light Source, E-08290 Cerdanyola del Vallès, Barcelona, Spain

Nowadays magnetic heterostructures based on ferromagnetic (FM)/heavy metal (HM) interfaces, such as the Co/Pt and Co/Pd multilayers, are considered as key materials for modern spintronics applications since they are able to stabilize peculiar chiral spin configurations that pave the way for the design of innovative devices. All these interesting properties are strongly related to an induced magnetic moment on the heavy metal which results from the so-called magnetic proximity effect (MPE); such an effect has been recently demonstrated to be asymmetric, with an induced magnetic moment on the HM layer that is typically higher at the top FM/HM interface of a HM/FM/HM trilayer.

In this work, advanced microscopy (TEM, STEM) and spectroscopic approaches (XMCD, XRMR) supported by DFT calculations have been applied to clarify the origin of this asymmetry both in Co/Pt trilayers and, for the first time, in multilayered systems Fig. 1. The approach allowed disclosing the compositional features of the interfaces and to intimately correlate the MPE to the different intermixing events occurring during the film growth. By applying a semi-empirical model for predicting the interface roughness in case of two different transition metals as a function of the deposition order (Co on top of Pt or vice versa), it was possible to definitely correlate the Pt induced magnetic moment with the interface profile produced by the interdiffusion processes occurring during the multilayer sputtering deposition [1].

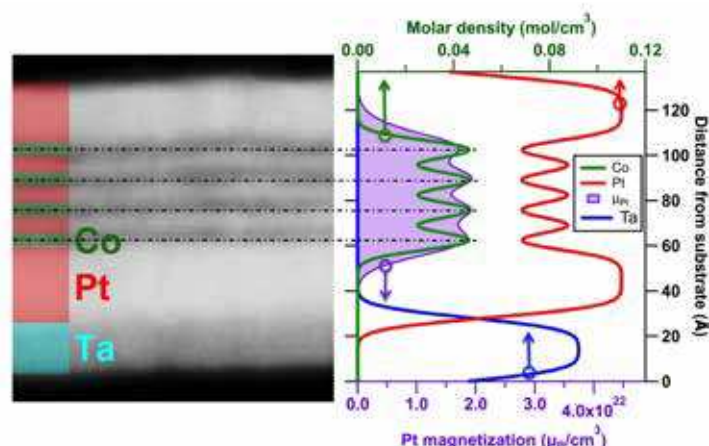


Figure 1: Co/Pt multilayer HAADF image and the corresponding distribution of Pt magnetic moments (violet-shaded area) compared with Pt (red line) and Co (green line) concentration depth profiles.

[1] A. Verna, P. Alippi, F. Offi, G. Barucca, G. Varvaro, E. Agostinelli, M. Albrecht, B. Rutkowski, A. Ruocco, D. Paoloni, M. Valvidares and S. Laureti, *Appl. Mat. Interf.* **14**, 12766 (2022)

Asynchronous current-induced switching of rare-earth and transition-metal sublattices in ferrimagnetic alloys

G. Sala¹

¹ETH Zurich, 8093 Zürich, Switzerland

Rare-earth transition-metal (RE-TM) ferrimagnetic alloys have raised considerable interest because of their ultrafast laser- and current-induced dynamics. Intense laser pulses toggle the RE-TM magnetization in few ps [1,2], and spin-orbit torques drive ferrimagnetic domain walls at record speeds of the order of km/s [3,4]. However, there remain important questions on the current-induced sublattice dynamics and the interaction of the RE and TM magnetic moments with spin-orbit torques. In this talk, I will present complementary studies of the switching of the RE-TM magnetization that address these open points.

First, time-resolved Hall measurements reveal that the overall switching speed is limited by the nucleation of a seed domain and that this process is influenced by stochastic thermal fluctuations [5]. The speed and reproducibility of the dynamics can be enhanced by reducing the duration of the electric pulses to the sub-ns regime. Second, element-resolved X-ray measurements disclose a variety of dynamics characterized by a variable degree of coupling between the RE and TM sublattices [6]. Surprisingly, they can switch asynchronously in time and inhomogeneously in space and form a transient ferromagnetic state as long as 2 ns. Their asynchronous dynamics results from the combination of a weak antiferromagnetic coupling and the unequal action of spin-orbit torques on the two sublattices.

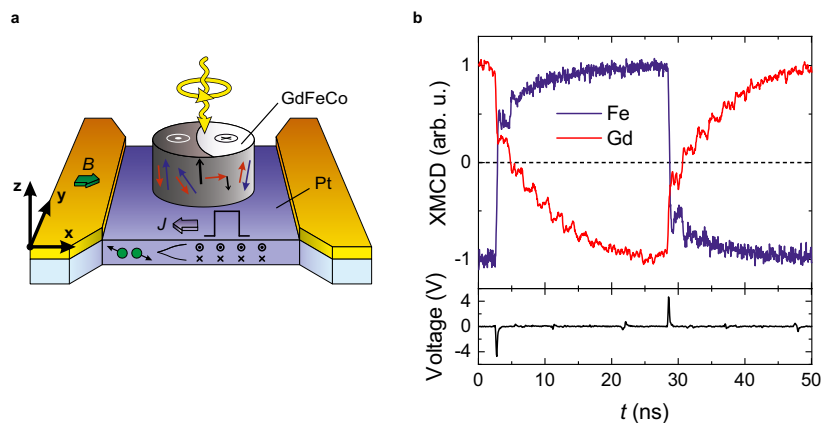


Figure 1: **a**, The magnetization of a GdFeCo dot on a Pt current line is switched by current-induced spin-orbit torques. **b**, Switching of the Fe and Gd magnetizations by 200-ps-long current pulses probed by X-ray magnetic dichroism (XMCD).

- [1] Stanciu, *Phys. Rev. Lett.* **99**, 047601 (2007)
- [2] L. Radu, *Nat.* **472**, 205-208 (2011)
- [3] L. Caretta, *Nat. Nano.* **13**, 1154-1160 (2018)
- [4] K. Cai, *Nat. Elec.* **3**, 37-42 (2020)
- [5] G. Sala, *Nat. Comm.* **12**, 656 (2021)
- [6] G. Sala, *Nat. Mat.* (2022), in press

Controlled Self-Assembly and Study of Engineered Magnetic Nanostructures

Mehran Sedrpooshan^{1,2}, Pau Ternero^{2,3}, Calle Preger^{2,3,4,5}, Adam Burke^{2,3}, Maria E Messing^{1,2,3} and Rasmus Westerström^{1,2}

¹ Synchrotron Radiation Research, Lund University, SE-221 00 Lund, Sweden

² NanoLund, Lund University, SE-221 00 Lund, Sweden

³ Solid State Physics, Lund University, SE-221 00 Lund, Sweden

⁴ Ergonomics and Aerosol Technology, Lund University, SE-221 00 Lund, Sweden

⁵ MAX IV Laboratory, Lund University, SE-221 00 Lund, Sweden

Magnetic nanostructures have unique capabilities in data storage and computing, sensors, permanent magnets, biomedicine, etc. One-dimensional (1D) nanostructures like nanochains (NCs) and nanowires (NWs) are promising candidates for permanent magnets and a variety of devices based on domain wall formation and motion.

Here we present a template-free, bottom-up technique for generating 1D magnetic nanostructures by directed self-assembly of nanoparticles (NPs) with tunable composition. We demonstrate how single-component and segmented NWs, as well as multi-component bundles, can be generated and present a magnetization study using SQUID magnetometry and X-ray microscopy.

The generation of nanostructures starts with the production of magnetic NPs in the gas phase. For this, the spark ablation method is employed to evaporate materials from two metallic electrodes under an inert carrier gas flow¹. The metallic vapor nucleates and condensates to form agglomerates which are then compacted and size selected before being guided onto any substrate of choice. The resulting NPs have a transition-metal ratio almost identical to the seed material, allowing the nanoscale composition to be tuned by the composition of the electrodes. To self-assemble the aerosol nanoparticles, an electric field is used to attract the charged particles to the substrate surface, and a magnetic field is utilized to arrange the incoming NPs into NCs via dipole-dipole interaction (Fig.1 a)². This technique also has the potential to form two and three-dimensional structures by the change of the magnetic field direction.

This approach provides great control over the geometry, composition, and crystallinity of nanostructures by varying the deposition and generation parameters. Apart from single element nanostructures, alloyed and bi-magnetic structures, such as CoFe and Co/Ni segmented NCs (Fig.1 b, c), can be generated, which will be discussed in detail. Furthermore, the generated nanostructures can be transformed into continuous structures like nanowires (Fig.1 d) and are stable enough for post-processing and adding contacts by electron beam lithography (EBL) process (Fig.1 e,f) for transport purposes.

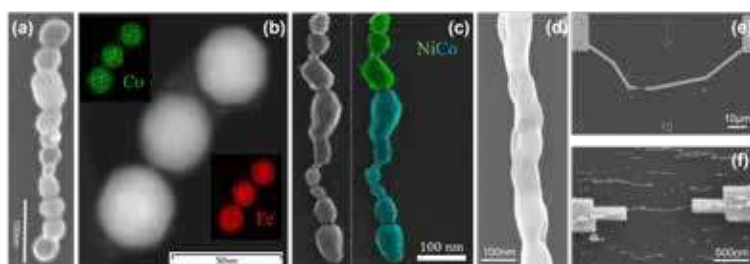


Fig 1. Directed self-assembly of magnetic NPs (a), self-assembly of CoFe alloyed NC (b), and segmented self-assembly of Ni and Co NPs (c). NC shape can be changed by post-annealing (d), or contacted for transport measurements using EBL (e, f).

- Schmidt-Ott, editor, *CRC Press* (2019).
- Preger, C.; Josefsson, M.; Westerström, R.; Messing, M. E. *Nanotechnology* 32, 195603 (2021).

Voltage-driven ON-OFF switching of ferromagnetism in transition metal oxide and nitride films for neuromorphic applications

Zhengwei Tan¹, Julius de Rojas¹, José L. Costa-Krämer², Alberto Quintana³, Enric Menéndez¹ and Jordi Sort^{1,4,*}

¹Departament de Física, Universitat Autònoma de Barcelona, E-08193 Bellaterra, Spain

²IMN-Instituto de Micro y Nanotecnología (CNM-CSIC), 28760 Tres Cantos, Madrid, Spain

³Department of Physics, Georgetown University, Washington, D.C. 20057, United States

⁴Institució Catalana de Recerca i Estudis Avançats (ICREA), E-08010 Barcelona, Spain

*Email: jordi.sort@uab.cat

Voltage-driven ion transport in magnetic materials (i.e., magneto-ionics) usually relies on controlled migration of oxygen ions. Here, I will show that voltage-driven transport of nitrogen ions (i.e., nitrogen magneto-ionics) can be triggered at room temperature in transition metal nitride (CoN, FeN) films via liquid electrolyte gating [1,2]. Nitrogen magneto-ionics can induce reversible ON-OFF transitions of ferromagnetic states at faster rates and lower threshold voltages than oxygen magneto-ionics. This is due to the lower activation energy for ion diffusion and the lower electronegativity of nitrogen compared to oxygen. Remarkably, in contrast to oxygen magneto-ionics, nitrogen transport occurs uniformly creating a plane-wave-like migration front, without assistance of diffusion channels, which is interesting for the implementation of multi-stack memory devices. Furthermore, I will show that nitrogen magneto-ionics can be used to emulate some important neuromorphic functionalities. In particular, by cumulative effects of DC and pulsed voltage actuation (at frequencies in the range 1 – 100 Hz), learning, memory retention, forgetting and self-learning by maturity (with zero energy consumption) can be mimicked by proper adjustment of the CoN film thickness and the pulse frequency. Sub-1s nitrogen magneto-ionics can be achieved by decreasing the CoN film thickness down to 25 nm. The interplay between the high ion speeds in thin CoN films and the pulse frequency results in a trade-off between generation (voltage ON) and partial depletion or recovery (voltage OFF) of ferromagnetism, giving rise to a controllable ion accumulation effect at the interface between the films and the electrolyte [3]. From a hardware viewpoint, this effect can serve as a logical function for the device to decide between self-learning or forgetting emulation, at will, without any additional electric voltage input (i.e., with no power consumption). This constitutes a novel approach to emulate some specific neural functionalities (e.g., learning under deep sleep), not easily achievable using other classes materials currently employed for neuromorphic computing applications.

[1] J. de Rojas, A. Quintana, A. Lopeandía, J. Salguero, B. Muñiz, F. Ibrahim, M. Chshiev, A. Nicolenco, M. O. Liedke, M. Butterling, A. Wagner, V. Sireus, L. Abad, C. J. Jensen, K. Liu, J. Nogués, J. L. Costa-Krämer, E. Menéndez, J. Sort, *Nat. Commun.* **11**, 5871 (2020).

[2] J. de Rojas, J. Salguero, F. Ibrahim, M. Chshiev, A. Quintana, A. Lopeandia, M. O. Liedke, M. Butterling, E. Hirschmann, A. Wagner, L. Abad, J. L. Costa-Krämer, E. Menéndez, J. Sort, *ACS Appl. Mater. Interfaces* **13**, 30826–30834 (2021).

[3] Z. Tan, J. de Rojas, S. Martins, A. Lopeandía, L. Abad, A. Quintana, J. Salguero, M. Cialone, J. Herrero-Martín, J. Meersschaut, A. Vantomme, J. L. Costa-Krämer, J. Sort, E. Menéndez, submitted (2022).

Oral Presentations

| | | |
|----------------------------------|--|-----|
| Andrea Bachmaier | <i>Soft magnetic amorphous Co-Zr alloy by severe plastic deformation</i> | 311 |
| Adam Bonda | <i>Electronic structure and magneto-optical Kerr effect spectra of W/Co/Pt layered systems</i> | 312 |
| Nabil Challab | <i>Flexible magnetic nanostructures: differentiated control of the magnetization</i> | 313 |
| Juliusz Chojenka | <i>Origin of dual magnetoresistance behavior in the nanopatterned titanium/titanium oxide/iron systems</i> | 314 |
| Giuseppe Cuono | <i>Ferromagnetic coupling in doped HgTe: a route for the quantum anomalous Hall effect</i> | 315 |
| Gweha Danny | <i>Size effect on All Optical Switching in GdFeCo</i> | 316 |
| Juan De la Figuera | <i>Towards electric control of magnetism: moving magnetic domains in magnetite / Ru(0001) nanostructures</i> | 317 |
| Samuel Dobák | <i>Competition Between Interparticle Coupling and Demagnetizing Effects in Soft Magnetic Iron Composites</i> | 318 |
| Claudia Fernández-González | <i>Chemically modulated Fe-Ni cylindrical nanowires with asymmetric magnetic response</i> | 319 |
| Martin Friák | <i>A quantum-mechanical study of anomalous magneto-volumetric behavior of ferrimagnetic $\text{Ni}_{31}\text{Mn}_{25}\text{Sn}_8$ alloy</i> | 320 |
| Darja Gačnik | <i>Exchange-coupled collective magnetism of a two-phase single-crystalline nanocomposite FeCoCrMnAl high-entropy alloy</i> | 321 |
| Katarzyna Gas | <i>Quantitative description of magnetic anisotropy in insulating GaN:Mn</i> | 322 |
| Erol Girt | <i>Noncollinear coupling of Co layers across RuCo spacer layers</i> | 323 |
| Georgia Gkouzia | <i>Element specific magnetocrystalline anisotropy of Sm-Co thin films</i> | 324 |
| Daniel Gopman | <i>Influence of heavy sputtering gas on perpendicular magnetic anisotropy and interlayer exchange coupling in Pt/Co/Ir synthetic antiferromagnets</i> | 325 |
| Alejandra Guedeja-Marron | <i>Crystal quality assessment of highly Bi-doped electrodeposited Cu nanowires for spintronics applications</i> | 326 |
| Mariam Hassan | <i>Effect of buffer and capping layers of Co/Ni-based thin film heterostructures: Towards sustainable flexible spintronics</i> | 327 |
| Guillermo Alberto Herrera Huerta | <i>Chemical and Magnetic order of FeRh nanoparticles deposited on BaTiO_3 (001) and SrTiO_3 (001)</i> | 328 |
| Atsufumi Hirohata | <i>Current Induced Crystallisation in Heusler Alloy Films for Memory Potentiation in Neuromorphic Computation</i> | 329 |
| Kristina Ignatova | <i>Magnetic anisotropy and exchange bias in $\text{V}_2\text{O}_3/\text{Ni}$ epitaxial layers</i> | 330 |
| Abdul Khaliq | <i>Spin-glass state and Almeida-Thouless line observation in $\text{Ge}_{1-x-y}(\text{Sn}_x\text{Mn}_y)\text{Te}$ multiferroics</i> | 331 |
| Akira Kikitsu | <i>Direct On-chip EMI Shielding Layer with Metallic/Magnetic Multilayer for sub-100 MHz frequency range</i> | 332 |
| Anna Kosogor | <i>Impact of the Magnetic Subsystem on the Low-temperature Specific Heat of Metamagnetic Shape Memory Alloy</i> | 333 |

| | | |
|------------------------|---|-----|
| Michał Krupinski | <i>Control of magnetic properties in ferrimagnetic GdFe and TbFe thin films by He⁺ and Ne⁺ irradiation</i> | 334 |
| Adam Krysztofik | <i>Effect of strain-induced anisotropy on magnetization dynamics in Y₃Fe₅O₁₂ thin films grown on Y₃Al₅O₁₂</i> | 335 |
| Elias Kueny | <i>Spin-structured multilayer THz emitters</i> | 336 |
| Piotr Kuświk | <i>Magnetic patterning by plasma oxidation of Co/Ni bilayers</i> | 337 |
| Ilona Lecerf | <i>Fabrication of rare-earth free permanent magnets for MEMS applications: magnetophoresis assembly of Co nanorods</i> | 338 |
| Jianing Liu | <i>Laser powder bed fusion of (Pr,Nd)-Fe-Cu-B Permanent Magnets</i> | 339 |
| Jike Lyu | <i>Weak ferromagnetism linked to the high-temperature spiral phase of YBaCuFeO₅</i> | 340 |
| Darla Mare | <i>Effect of bending strain on magnetic anisotropy in epitaxial ferrite thin films on mica.</i> | 341 |
| Jorge Marqués-Marchán | <i>Nucleation and current-induced bubble structures motion in PMA multilayers</i> | 342 |
| Giovanni Masciocchi | <i>Control of magnetoelastic coupling in Ni/Fe multilayers using He⁺ ion irradiation</i> | 343 |
| Sergey Nedukh | <i>Influence of antidote form on magnetic resonance response</i> | 344 |
| Volker Neu | <i>Imprinting magnetic micropatterns through geometrical transformation</i> | 345 |
| Felix Nickel | <i>Complex spin structures of ultrathin Fe/Ir films on Re(0001)</i> | 346 |
| Jorge Martín Nuñez | <i>Synthesis and characterization of Fe₃O₄@MgO@CoFe₂O₄ core/shell/shell magnetic nanoparticles</i> | 347 |
| Gajanan Pradhan | <i>Magnetic properties of FeGa/Kapton for flexible electronics</i> | 348 |
| Sandra Ruiz-Gomez | <i>Magnetic domain wall pinning in cobalt ferrite microstructures</i> | 349 |
| Jose Santiso | <i>Atomic scale structure rearrangements in Y₃Fe₅O₁₂ epitaxial films on GGG(111) substrates explored by HR-STEM</i> | 350 |
| Sagar Sen | <i>Ion implantation induced exchange bias in BCC Fe thin film</i> | 351 |
| Sufyan Shehada | <i>Interplay of magnetic states and hyperfine fields of iron dimers on MgO(001)</i> | 352 |
| Natalia Shkodich | <i>Magnetic nanocrystalline CoCrFeNiGa_x (x = 0.5, 1.0) high entropy alloys by high energy ball milling</i> | 353 |
| Meg Smith | <i>Optimisation of perpendicular magnetic tunnel junction structures using STEM</i> | 354 |
| Justyn Snarski-Adamski | <i>Effect of transition metal doping on magnetic hardness of CeFe₁₂-based compounds.</i> | 355 |
| Jimena Soler-Morala | <i>Influence of the buffer layer on the nanoscale architecture in NdFeB ultrathin films</i> | 356 |
| Marcin Szpytma | <i>Beating the limitation of the Néel temperature of FeO with antiferromagnetic proximity in FeO/CoO</i> | 357 |
| Dariusz Sztenkiel | <i>Spin orbital reorientation transitions induced by magnetic field</i> | 358 |
| Luding Wang | <i>Picosecond Optospintronic Tunnel Junctions for Non-volatile Photonic Memories</i> | 359 |

| | | |
|--------------------|---|-----|
| Mirosław Werwiński | <i>Structural phase transition in Fe thin films: DFT study</i> | 360 |
| Oksana Yastrubchak | <i>Ferromagnetism and band structure engineering in the (Ga,Mn)As, Ga(Bi,As) and (Ga,Mn)(Bi,As) nanolayers</i> | 361 |
| Mathias Zambach | <i>Superparamagnetic particles for micro-inductor applications</i> | 362 |
| Yao Zhang | <i>Voltage-controlled switching of magnetic anisotropy in ambipolar Mn₂CoAl/Pd bilayers</i> | 363 |
| Zhibo Zhao | <i>Energy-efficient magnetoelectrochemical effect of La_{0.7}Sr_{0.3}MnO_{3-δ} via voltage-driven oxygen motion</i> | 364 |
| Monika Zięba | <i>Electronic structure of ferromagnetic Sn_{1-x}Mn_xTe thin films</i> | 365 |

Soft magnetic amorphous Co-Zr alloy by severe plastic deformation

M. Stücker¹, S. Wurster¹, M. Zawodzki¹, M. Alfreider², A. Bachmaier¹

¹ Erich Schmid Institute of Materials Science, Austrian Academy of Sciences, Jahnstrasse 12, 8700 Leoben, Austria

² Department of Materials Physics, Montanuniversität Leoben, Jahnstrasse 12, 8700 Leoben, Austria

Co-based amorphous alloys are reported to exhibit excellent soft magnetic properties [1-3]. Sample processing by severe plastic deformation can be used to induce crystalline-to-amorphous transformations in bulk samples, which retain their shape during deformation [4].

In this study, a CoZr composite with a composition of 75 at% Co and 25 at.% Zr was processed by high pressure torsion using specially designed disks consisting of a pre-defined number of single sector Co and Zr elements. The processed sample finally transformed into a Co-Zr amorphous alloy after being deformed to equivalent strains above 1000.

Microstructural properties, as revealed by transmission electron microscopy and synchrotron X-ray diffraction, are correlated to the magnetic properties, measured with DC-SQUID magnetometry. To optimize magnetic properties and study the alloys phase transformations various annealed states are investigated. A diminishing coercivity with increasing annealing temperature is observed (Fig.1). SQUID-magnetometry reveals soft magnetic properties persisting in a wide temperature range despite the onset of crystallization in the amorphous alloy.

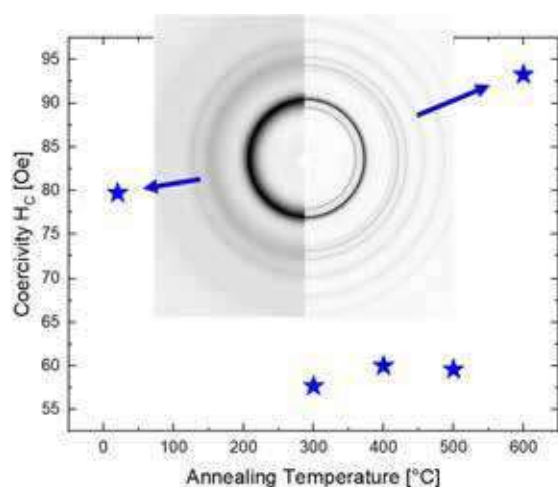


Figure 1: Coercivity as a function of annealing temperature. The inset shows synchrotron X-ray diffraction patterns of the as-deformed and annealed state (600°C, 1h).

This project has received funding from the European Research Council (ERC) under the European Union's Horizon 2020 research and innovation programme (grant agreement No 757333).

- [1] G. Herzer, *Acta Mater.* **61**, 718 (2013).
- [2] H. Fujimori et al., *Jpn. J. Appl. Phys.* **15**, 705 (1976).
- [3] M.G. Nematov et al., *J. Alloys Comp.* **890**, 161740 (2022).
- [4] K. Edalati et al., *Mater. Res. Letters* **10:4**, 163 (2022).

Electronic structure and magneto-optical Kerr effect spectra of W/Co/Pt layered systems

S. Uba¹, A. Bonda¹, L. Uba¹, V. N. Antonov², A. Wawro³, A. Maziewski¹

¹*Faculty of Physics, University of Białystok, K. Ciołkowskiego 1L, PL-15245 Białystok, Poland*

²*G.V. Kurdyumov Institute for Metal Physics of the N.A.S. of Ukraine, 36 Vernadsky Street, UA-03142 Kiev, Ukraine*

³*Institute of Physics Polish Academy of Sciences, Warsaw, Poland*

The W/Co/Pt layered structures are characterized by strong Dzyaloshinskii-Moriya interaction, which is important for fundamental research and application possibility in magnetic information technology [1]. In this work we present the results of experimental and theoretical studies of optical and magneto-optical spectra obtained for this type of structure. The epitaxial W(2.4 nm)/Co(d_{Co})/Pt(5 nm) layered systems were deposited on (0001) sapphire single crystal substrates. The Co layer thickness d_{Co} was changed in the range from 0 to 3 nm. The strong and non-monotonic dependencies of measured Kerr rotation and ellipticity spectra and the off-diagonal components of the optical conductivity tensor on d_{Co} were found in the wide spectral range from 0.8 to 5.5 eV. Density functional theory calculations of the electronic and magnetic structures were performed for the W(n)/Co(m)/Pt(p) model structures with different numbers of atomic layers n, m, p . The calculations show the effect of strong Pt spin polarization [2] due to hybridization of the Co and Pt electronic states at the interface, with the magnitude of the induced spin magnetic moment up to $0.3 \mu_{\text{B}}$ on Pt atom. The calculated spin polarization of the W layer adjacent to the Co one reaches the value of $0.05 \mu_{\text{B}}$ per W atom with the induced magnetic moment oriented antiparallel to Co due to their hybridization. It is found that for all structures studied the calculated magneto-optical conductivity spectra of the interlayer interfaces play a key role in the formation of the magneto-optical response of the systems. The *ab-initio* calculations show that main contributions to the spectra come from the spin polarized Pt and Co layer. It is shown that the calculations for the model of W(n)/Co(m)/Pt(p) layered systems with perfect interfaces reproduce the experimental magneto-optical spectra. The simulations for structure models with imperfect W/Co and Co/Pt interfaces as transition layers of different compositions were also performed. It was found that chemical disorder at the interfaces plays important role in the formation of magneto-optical response of the W(2.4 nm)/Co(d_{Co})/Pt(5 nm) systems in UV spectral range.

[1] S.K. Jena *et al.*, *Nanoscale* **13**, 7685 (2021) and references therein.

[2] L. Uba, S. Uba, V.N. Antonov, A.N. Yaresko, , R. Gontarz, *Phys. Rev. B* **64**, 125105 (2001).

This work was supported by the National Science Centre of Poland, project no. 2020/37/B/ST5/02299.

Flexible magnetic nanostructures: differentiated control of the magnetization

N. Challab¹, D. Faurie¹, M. Haboussi¹, A. O. Adeyeye² and F. Zighem¹

¹ *LSPM-CNRS, UPR3407, Université Sorbonne Paris Nord, France*

² *Durham University, Durham, United Kingdom*

Flexible magnetic systems, obtained by depositing a magnetic material, in a continuous or nano-structured layer (networks of nanodots, nanowires, etc.), of very low thickness (less than 100 nm), on a flexible substrate, such as polyimide, have been the subject of growing interest in recent years, due to the many applications that they allow to be imagined in flexible magnetoelectronics. Due to their flexible nature, these devices are subject to large strain, which can modify the magnetic properties of the system in a complex way. The strain distribution is then presented as a lever to modify and control/adapt the magnetic properties of the system. Among the deformation-induced magnetic evolutions highlighted in this work is the shift of the resonance magnetic field, measured by FMR (FerroMagnetic Resonance), of a magnetic layer with antidote array, under mechanical loading. Thus, by accurately calculating the average stresses transmitted to the magnetic nanostructure using finite elements method, it was possible to reproduce the experimental curves of the resonance magnetic field as a function of the applied stress, thanks to a relatively simple analytical model, fed by the "true" average transmitted stresses [2]. It should be noted that in order to calculate the "true" average transmitted strains, it was necessary to define averaging zones based on purely magnetic calculations carried out in the OOMMF software.

Other numerical investigations were carried out in this work thanks to a calculation code developed in COMSOL Multiphysics® by solving in a coupled way the equations governing the micromagnetism and the mechanical equilibrium of the studied objects, [3]. This code allowed us, among other things, to quantify the role of the geometric characteristics of the nanostructures studied in the reversal of their magnetization under strain, [4]. It also allowed us to study the effect of deformation heterogeneity on the appearance of secondary magnetic modes in a magnetic membrane, during the early stage of the evolution of its magnetization under the effect of mechanical loading, as opposed to homogeneous deformation which gives only the main mode. Furthermore, the simulation does not show any effect of deformation heterogeneity in the post-turnover stage and in the steady state, [5].

- [1] D. Makarov et al., **Adv. Mater.**, **34**, 2101758 (2022)
- [2] N. Challab, D. Faurie, M. Haboussi, A.O. Adeyeye, **F. Zighem**, **ACS AMI** **13**, 29906 (2021)
- [3] N. Challab, D. A. Aboumassound, F. Zighem, D. Faurie, M. Haboussi, **J. Phys. D: Appl. Phys.** **52** 355004 (2019)
- [4] N. Challab, F. Zighem, D. Faurie, M. Haboussi, M. Belmeguenai, P. Lupo and A. O. Adeyeye, **PSS (RRL)** **13**, 1800509 (2018)
- [5] N. Challab, D. Faurie, M. Haboussi, F. Zighem, **Phys. Stat. Sol. (RRL)** **15**, 2100149 (2021)

Origin of dual magnetoresistance behavior in the nanopatterned titanium/titanium oxide/iron systems

J. Chojenka¹, A. Zarzycki¹, M. Perzanowski¹, M. Marszalek¹

¹ *Institute of Nuclear Physics Polish Academy of Sciences, Krakow, Poland*

In this study, we investigated magnetoresistance effect (MR) in the nanopatterned metal/semiconductor/metal junction, where the interlayer is anodized titanium oxide. The choice of TiO₂ results from its peculiar electrical properties. For example, the bulk anatase and rutile are the semiconductors for which the oxygen vacancies and titanium interstitials or vacancies behave either as *n*- or *p*-type dopants. Furthermore, the Ti or O vacancies can induce a weak ferromagnetic signal. The creation of nanostructured titanium oxide by synthesis method introduces the morphology modifications, and leads to the change of the magnetoresistance and transport properties of the deposited films and, in consequence, of the whole junction.

The studied junctions, consisted of a ferromagnetic thin iron layer of 50 nm thickness thermally deposited on anodized titanium oxide (ATiO). Fabrication of the ATiO layer was carried out in electrolyte containing ammonium fluoride (NH₄F) at constant voltages of 5 V, 15 V, and 60 V. To protect the iron from oxidation and ensure good electric contact a layer of gold was deposited on top of the junctions. The XRD measurements revealed the polycrystalline structure of junctions with a variety of titanium oxides. The reflectivity spectroscopy studies affirmed the semiconducting nature of the titanium oxide layer with a band gap of 2.3 eV. ZFC-FC measurements indicated the presence of a spin-glass-like disordered state below 50 K, explained by the formation of iron oxide at the titanium oxide-iron interface with short-range magnetic order. The magnetoresistance properties of the junctions (Figure 1) displayed dual character with positive values at room temperature and negative values at 5 K for all samples.

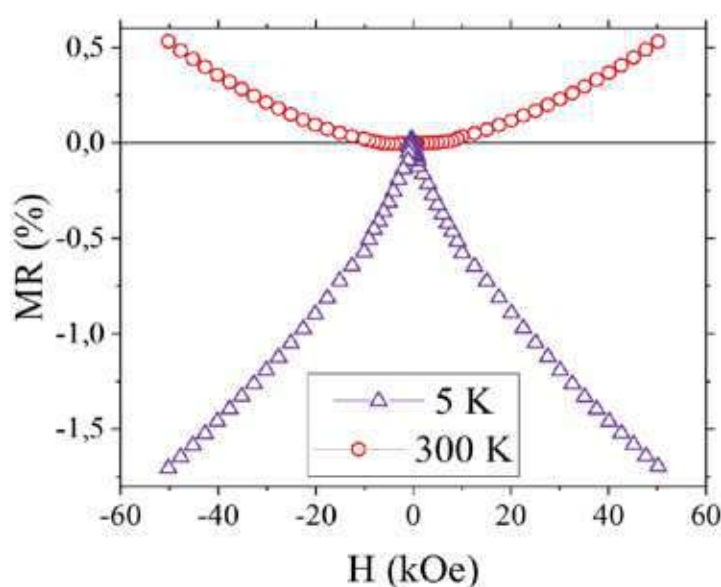


Figure 1. Dual magnetoresistance behavior in TAF system.

Ferromagnetic coupling in doped HgTe: a route for the quantum anomalous Hall effect

Giuseppe Cuono¹, Carmine Autieri^{1,2}, and Tomasz Dietl^{1,3}

¹*International Research Centre Magtop, Institute of Physics, Polish Academy of Science, Aleja Lotników 32/46, PL-02668 Warsaw, Poland*

²*Consiglio Nazionale delle Ricerche CNR-SPIN, UOS Salerno, 84084 Fisciano (Salerno), Italy*

³*WPI-Advanced Institute for Materials Research, Tohoku University, Sendai 980-8577, Japan*

Dilute magnetic semiconductors have played a central role in the demonstrating and describing a strong and intricate influence of the sp-d exchange interactions upon effective mass states in semiconductors, paving the way for the rise of dilute ferromagnetic semiconductors [1] and magnetic topological insulators [2,3]. Recently the exchange splittings of magneto-optical spectra in $\text{Cd}_{1-x}\text{Mn}_x\text{Te}$ and $\text{Hg}_{1-x}\text{Mn}_x\text{Te}$ have been described [4] and it has been demonstrated that superexchange dominates in magnetic topological insulators [5]. Here we investigate the electronic and magnetic properties of the dilute magnetic semiconductors $\text{Cd}_{1-x}\text{Cr}_x\text{Te}$, $\text{Hg}_{1-x}\text{Cr}_x\text{Te}$, $\text{Cd}_{1-x}\text{V}_x\text{Te}$, $\text{Hg}_{1-x}\text{V}_x\text{Te}$ by using a density functional theory approach and we compare to the properties of $\text{Cd}_{1-x}\text{Mn}_x\text{Te}$ and $\text{Hg}_{1-x}\text{Mn}_x\text{Te}$. We obtain the band structures of these systems, we study the distortions produced by the Jahn-Teller effect and the spin splitting. We state that spin-orbit coupling, electronic correlations and Jahn-Teller distortions are necessary to open the gap in these compounds. We find that the crystal field strongly depends on correlations and there is an orbital-selective electronic correlation for Cr and V-doped systems. In the case of doping with Mn we find an inverted crystal field respect to the standard tetrahedron. Then, we study the exchange couplings for all considered cases and we find that the coupling is ferromagnetic in case of doping with Cr and V, differently from the case of doping with Mn, where we find an antiferromagnetic ground state. The ferromagnetic coupling among V and Cr atoms in the insulating phase of topological HgTe can produce the quantum anomalous Hall phase.

[1] T. Dietl and H. Ohno, *Rev. Mod. Phys.* **86**, 187 (2014).

[2] H. Ke, Y. Wang, and Q.-K. Xue, *Annu. Rev. Condens. Matter Phys.* **9**, 329 (2018).

[3] Y. Tokura, K. Yasuda, and A. Tsukazaki, *Nat. Rev. Phys.* **1**, 126 (2019).

[4] C. Autieri, C. Śliwa, R. Islam, G. Cuono and T. Dietl, *Phys. Rev. B* **103**, 115209 (2021).

[5] C. Śliwa, C. Autieri, J. A. Majewski, and T. Dietl, *Phys. Rev. B* **104**, L220404 (2021).

Size effect on All Optical Switching in GdFeCo

Danny Petty Gweha Nyoma¹, M. Verges¹, J. Hohlfield¹, M. Hehn¹, G. Malinowski¹, S. Mangin¹, and F. Montaigne¹

¹ Institut Jean Lamour, Université de Lorraine - CNRS, Nancy, F-54506, France

Achieving control of the magnetization at smaller length scale and faster timescale is the horizon of research in magnetism. Among the different possible factors (magnetic fields, spin-polarized charge currents, spin currents...), ultra-fast laser pulses turned out to be the fastest, with All Optical Switching (AOS) in the picosecond range.

AOS has been intensively studied in ferrimagnetic materials like GdFeCo, but mainly in continuous thin film [1, 2]. In this contribution, we present a systematic study of the reversal for GdFeCo dots whose diameter ranges from 3 μm to 400 nm with 35 fs laser pulses.

Perfect toggle switching is observed for all sizes and the intrinsic reversal threshold is deduced from fluence variations. The size variation of the threshold reveals a non-monotonic behavior which highlights the importance of the specific light absorption in nanostructures.

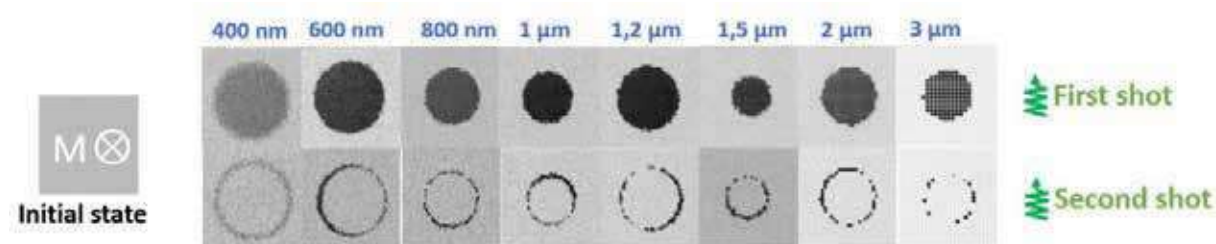


Figure 1 : Magneto-Optical Kerr images of dots for size range from 3 μm to 400 nm in Ta(5 nm)/Cu(5 nm)/Gd₂₄%FeCo(20 nm)/Pt(5 nm) after two consecutive single pulse with linear polarization, 35 fs of pulse duration and 17 mJ/cm² fluence

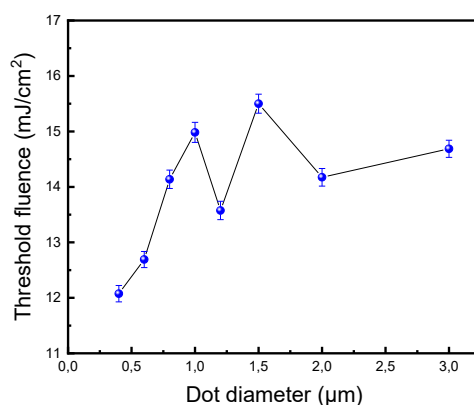


Figure 2 : Variation of the threshold fluence with the dot diameter in GdFeCo alloys.

References

- [1] T.A. Ostler. Et al. Ultrafast heating as a sufficient stimulus for magnetization reversal in ferrimagnet. Nature Communication, **3**(666), 2 2012
- [2] J. Wei Et al. All-optical Helicity-Independent Switching State Diagram in Gd-Fe-Co Alloys. Phys. Rev. Applied **15**, 054065, 5 (2021)

Towards electric control of magnetism: moving magnetic domains in magnetite / Ru(0001) nanostructures

Sandra Ruiz-Gómez¹, Eva M. Trapero², Claudia Fernández-González³, Cecilia Granados-Miralles⁴, Adrián Quesada⁴, Michael Foerster⁵, Lucía Aballe⁵, José E. Prieto² and Juan de la Figuera²

¹ Max-Planck-Institut für Chemische Physik fester Stoffe, 01187 Dresden, Germany

² Instituto de Química Física "Rocasolano", CSIC, Madrid E-28006, Spain

³ Dpto. De Física de Materiales, Universidad Complutense de Madrid, Madrid E-28040, Spain

⁴ Instituto de Cerámica y Vidrio, CSIC, Madrid E-28049, Spain

⁵ Alba Synchrotron Light Facility, 08290, Cerdanyola del Valles E-08290, Spain

Most active layers explored in devices that use electrical control of magnetic domains are polycrystalline. While in many cases this is adequate, in others their properties are dominated by grain boundaries or other defects instead of the properties of the pure material. Such is the case of oxide spinels in general, and magnetite in particular, where the presence of antiphase boundaries promotes magnetic properties in thin films very different from those of the pristine material. In the past few years we have explored the growth of several high quality oxide nanostructures by means of oxygen-assisted high-temperature molecular beam epitaxy on single crystal Ru(0001) substrates, obtaining atomically flat, micrometric-wide and nanometer-high triangular islands of several ferrimagnetic [1-3] and antiferromagnetic oxides [4,5]. Such oxides present magnetic domains in remanence which are orders of magnitude larger than those of typical thin films. In the case of magnetite, closure domains have been observed [6], modified by means of applied magnetic fields [7] and their Verwey transition has been observed by Raman spectroscopy.

Since the use of Ru(0001) single crystals substrates is not useful for devices we have substituted them by Ru thin films grown by magnetron sputtering on sapphire, which can be prepared with quality comparable to bulk crystals [8]. Such films can be lithographically etched by standard solutions developed by the microelectronics industry providing a powerful platform for the study of the modification of high quality magnetic oxides. In the present work, we have followed by x-ray magnetic circular dichroism the *in-situ* modification of the magnetic domains in magnetite nanostructures by the Oersted fields created by pulsing ns currents through the underlying Ru stripes. Our approach can easily be extended to antiferromagnetic materials.

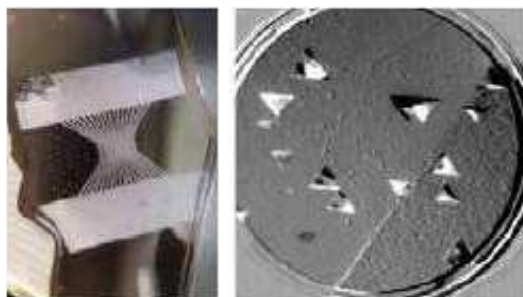


Figure 1: Left: Optical microscopy image of a device composed of Ru stripes with magnetite islands on top. Right: Magnetic domains observed in the magnetite islands.

[1] M. Monti et al., *Phys. Rev. B* **85**, 020404 (2012).

[2] L. Martín-García et al., *Adv. Mater.* **27**, 5955 (2015).

[3] A. Mandziak et al., *Sci. Rep.* **8**, 17980 (2018).

[4] A. Mandziak et al., *Sci. Rep.* **9**, 13584 (2019).

[5] A. Mandziak et al., *Nanoscale* **12**, 21225 (2020).

[6] S. Ruiz-Gomez, et al., *Nanoscale* **10**, 5566 (2018).

[7] A. Mandziak et al., *Ultramicroscopy* **214**, 113010 (2020).

[8] J. E. Prieto et al., *Appl. Surf. Sci.* **582**, 152304 (2022).

Competition Between Interparticle Coupling and Demagnetizing Effects in Soft Magnetic Iron Composites

Samuel Dobák¹, Peter Kollár¹, Ján Füzér¹,
Radovan Bureš², and Mária Fáberová²

¹*Institute of Physics, Faculty of Science, P. J. Šafárik University in Košice, Košice, Slovakia*

²*Institute of Materials Research, Slovak Academy of Sciences, Košice, Slovakia*

Recent technological advances in designing the soft magnetic composite cores of micrometer- or nano-scale Fe-based particles dispersed in manifold dielectric matrices have revolutionized the efforts to develop the lighter, efficient, and generally smarter electric devices [1, 2]. The variability in particles' composition and size with the inherent nature of magnetization process involves a wide range of underlying physical behavior from ferromagnetic or ferrimagnetic multi-domain to single-domain or even superparamagnetic [3].

In this study, we investigate the mechanism of magnetization switching in water-atomized irregular Fe particles encapsulated in organic polymeric resin forming the bulk powder cores with different volume fractions of constituents. The distributed interaction and coercive fields were computed from a set of first-order reversal curves (FORCs), measured by a point-by-point fluxmetric method using a quasi-static hysteresisgraph. An ample grid of a few tens of thousand measurement points allows for precise mapping the magnetization landscape of non-trivial magnetic states that occupy the area enclosed by the major hysteresis loop. Enormous number of acquired data is balanced by a deep insight into the micromagnetic intrinsic processes which are otherwise not accessible.

Analysis discovered a transition in FORC fingerprint related to the interparticle interactions in powder composites which has not yet been observed in the literature. Opposite behavior is demonstrated in Fig. 1 in the contour FORC plots of (a) Somaloy[®] 700 and (b) Fe/10 vol% resin composites. The former is characterized by a significant spot with a pinning field of 250 A/m and a negative interaction field offset whilst the latter captures a wide dipole-dipole interaction ridge. The transition is explained by the mechanism of decoupling with increasing average interparticle distance which brings about the extra-component of magnetostatic demagnetizing field.

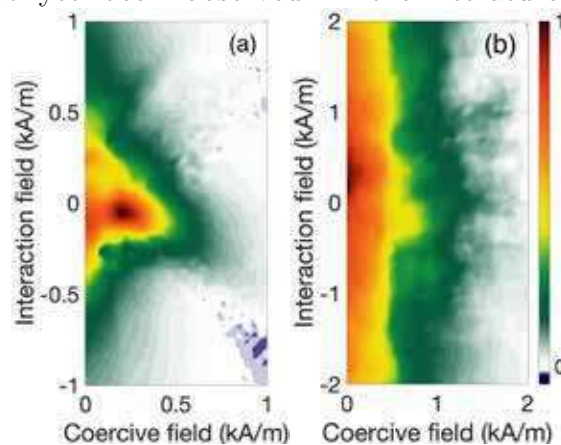


Figure 1: FORC diagrams of (a) Somaloy[®] 700 and (b) Fe/10 vol% resin composite materials.

This work has been supported by the Slovak Res. & Devel. Agency (APVV-20-0072) and by the Scientific Grant Agency of the Ministry of Education, Science, Research & Sport of the Slovak Republic and the Slovak Academy of Sciences (VEGA 1/0143/20, VEGA 1/0225/20).

[1] D. Liu, *et al.*, *Acta Mater.* **146**, 294 (2018).

[2] W. Li, *et al.*, *Acta Mater.* **167**, 267 (2019).

[3] J. M. Silveyra, *et al.*, *Science* **362**, 418 (2018).

Chemically modulated Fe-Ni cylindrical nanowires with asymmetric magnetic response

C. Fernández-González^{1,2}, A. Berja^{2,3}, L. Aballe⁴, L. Álvaro-Gómez¹, C. Martín-Rubio⁵, M. Foerster⁴, M. A. Niño⁴, R. Sanz⁵, A. Mascaraque², L. Pérez^{1,2} and S. Ruiz-Gómez⁶

¹Instituto Madrileño de Estudios Avanzados – IMDEA Nanociencia, 28049, Madrid, Spain

²Dept. Física de Materiales. Universidad Complutense de Madrid, 28040, Madrid, Spain

³Instituto de Cerámica y Vidrio (CSIC), 28049, Madrid, Spain

⁴Alba Synchrotron Light Facility, CELLS, E-08280, Bellaterra, Spain

⁵Instituto Nacional de Técnica Aeroespacial – INTA, 28850, Torrejón de Ardoz, Madrid, Spain

⁶Max Planck Institute for Chemical Physics of Solids, 01187 Dresden, Germany.

The control of the magnetic domain walls (DWs) movement along cylindrical nanowires (NWs) by means of magnetic fields or electric currents is a key aspect in the design of novel spintronic devices [1,2]. In recent studies, we have demonstrated that local changes in composition along the axis of permalloy nanowires can pin the DWs and that the DWs can be moved in a reliable way under the application of magnetic field [3,4]. Expanding this concept, in this work we propose a gradual change in Fe/Ni ratio along the axial direction of the nanowires in order to create an asymmetric energy landscape with the aim to induce asymmetric domain wall motion (ratchet effect).

Nanowires were synthesized using template assisted electrodeposition. Composition was gradually changed along the NWs between Fe₈₀Ni₂₀ and Fe₂₀Ni₈₀ in periods of a few micrometers. Combining laterally resolved X-ray Absorption Spectroscopy (XAS) and X-ray Magnetic Circular Dichroism (XMCD), we correlate the chemical structure of single nanowires with their magnetic configuration. In addition, by applying pulses of magnetic field along the nanowire axis, we study the magnetic state depending on the direction of the applied magnetic field. First Order Reversal Curves (FORC) were also measured in arrays of NWs. Figure 1 shows the FORC diagrams of two arrays of nanowires with (a) homogeneous composition of Fe₂₀Ni₈₀ and (b) chemically modulated ones. While the diagram of homogeneous NWs is highly symmetric with respect to the interaction field (H_u), in the case of modulated NWs, an asymmetry arises (highlighted by a dashed red square), evidencing the emerging of asymmetrical magnetization processes in the array.

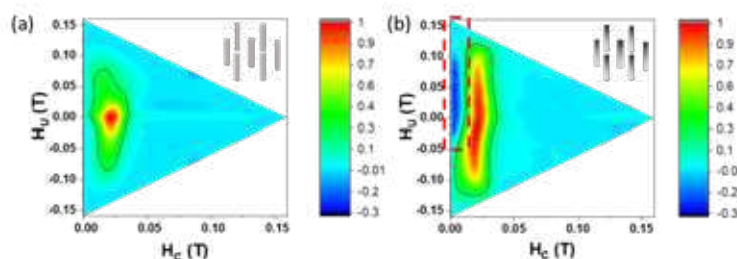


Figure 1: FORC diagrams measured in arrays of (a) Fe₂₀Ni₈₀ NWs and (b) chemically modulated NWs.

[1] Xiao-Ping Ma, et al. *Appl. Phys. Lett.* **117**, 6 (2020).

[2] M. Schöbitz, et al. *Phys. Rev. Lett.* **123**, 21 (2019).

[3] S. Ruiz-Gómez, et al. *Sci. Rep.* **8**, 1 (2018).

[4] S. Ruiz-Gómez, et al. *Nanoscale* **12**, 16695 (2020).

A quantum-mechanical study of anomalous magneto-volumetric behavior of ferrimagnetic $\text{Ni}_{31}\text{Mn}_{25}\text{Sn}_8$ alloy

M. Friák¹, M. Mazalová^{1,2}, I. Miháliková¹, F. Zažímal¹, I. Turek¹, O. Schneeweiss¹, J. Kaštil³, J. Kamarád³, Z. Arnold³, M. Míšek³ and M. Šob^{2,1}

¹ Institute of Physics of Materials, v.v.i., Czech Academy of Sciences, Brno, 616 00 Czech Rep.,

² Department of Chemistry, Faculty of Science, Masaryk University, Brno, 611 37, Czech Rep.,

³ Institute of Physics, v.v.i., Czech Academy of Sciences, Prague 8, 182 21 Czech Rep.

We have performed a quantum-mechanical study of disordered ferrimagnetic $\text{Ni}_{31}\text{Mn}_{25}\text{Sn}_8$ martensite. Employing the supercell approach combined with the special quasi-random structure concept for modeling of disordered states we have determined thermodynamic, magnetic, structural, elastic and vibrational properties of the studied material. Its atomic and magnetic configuration is found to exhibit a pressure-induced increase of the total magnetic moment, i.e. the total magnetic moment increases with decreasing volume. This highly anomalous trend in the total magnetic moment is revealed despite of the fact that the magnitudes of local magnetic moments of atoms decrease with decreasing volume (as is common in magnetic systems). The origin of the identified phenomena may be related to (i) the ferrimagnetic nature of the magnetic state when the parallel and antiparallel magnetic moments nearly compensate each other and (ii) chemical disorder that leads to different local atomic environments [1] and, consequently, also to different local magnetic moments and their different response to hydrostatic pressures (the antiparallel moments are more sensitive to pressures). The studied state is mechanically and dynamically stable (no imaginary-frequency phonons) but, regarding its thermodynamic stability, it is a metastable state [2].

[1] M. Friák, M. Mazalová, I. Turek, A. Zemanová, J. Kaštil, J. Kamarád, M. Míšek, Z. Arnold, O. Schneeweiss, M. Všianská, M. Zelený, A. Kroupa, J. Pavlů, M. Šob, An *ab initio* study of pressure-induced changes of magnetism in austenitic stoichiometric Ni_2MnSn , Materials 14 (2021) 523.

[2] M. Friák, M. Mazalová, I. Turek, O. Schneeweiss, J. Kaštil, J. Kamarád and M. Šob, Pressure-Induced Increase of the Total Magnetic Moment in Ferrimagnetic $\text{Ni}_{1.9375}\text{Mn}_{1.5625}\text{Sn}_{0.5}$ Martensite: A Quantum-Mechanical Study, Materials Transactions (2022) *in press*, doi:10.2320/matertrans.MT-MA2022006.

Exchange-coupled collective magnetism of a two-phase single-crystalline nanocomposite FeCoCrMnAl high-entropy alloy

**D. Gačnik¹, P. Koželj^{1,2}, A. Jelen¹, S. Vrtnik¹, M. Krnel¹,
Z. Jagličić^{3,4}, M. Feuerbacher⁵, J. Dolinšek^{1,2}**

¹ Jožef Stefan Institute, Jamova 39, Ljubljana, Slovenia

² University of Ljubljana, Faculty of Mathematics and Physics, Jadranska 19, Ljubljana, Slovenia

³ Institute of Mathematics, Physics and Mechanics, Jadranska 19, Ljubljana, Slovenia

⁴ University of Ljubljana, Faculty of Civil and Geodetic Engineering, Jamova 2, Ljubljana, Slovenia

⁵ Institut für Mikrostruktur Forschung, Forschungszentrum Jülich, Wilhelm-Johnen-Straße, Jülich, Germany

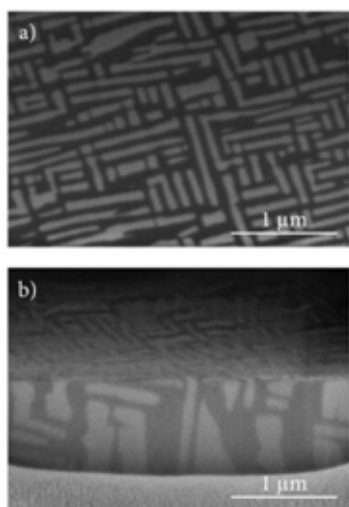


Figure 1: Microstructure images (SEM SE) of 3D nanoplatelet inclusions.

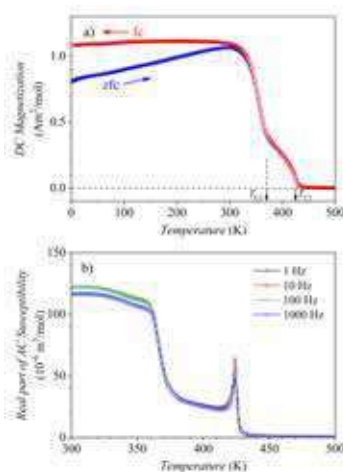


Figure 2: Temperature-dependent DC magnetization and AC susceptibility.

We studied the magnetic state of a FeCoCrMnAl, a two-phase nanocomposite high-entropy alloy (HEA) [1]. Each phase exhibited different chemical composition and crystal structure (bcc and B2), yet their lattice parameters were equal. During the solidification, the specific crystal ordering enabled the lattice planes to pass through the phase boundary continuously, which resulted in a single consistent set of lattice planes - a single crystal. Microstructure analysis of a nanocomposite revealed crystallographically oriented nanoplatelets embedded in a chemically disordered matrix.

The measurements of the sample's magnetism showed that it originates from the interplay between the different types of the matrix' and the inclusions' magnetic states. At 425 K, the matrix transitioned to asperomagnetic (disordered ferromagnetic) state, where the spin ordering was on average parallel, while some of the magnetic domains remained antiparallel. At 370 K, the exchange coupling across the phase boundaries with the asperomagnetic matrix induced ferromagnetic ordering of the nanoplatelets. Below 300 K, the sample exhibited a single, collective magnetic state with strong interaction between the matrix and the inclusions. In this state, the phases no longer behaved separately but rather collectively as a soft ferromagnet.

Our detailed analysis revealed that due to the exchange coupling between the matrix and the nanoplatelets, FeCoCrMnAl nanocomposite exhibits good magnetic softness as well as a large change of the magnetization near the transition temperatures. Even more, the transition temperatures might be regulated with different chemical compositions, morphology, and concentration of each phase. All these properties make the FeCoCrMnAl HEA a promising magnetocaloric material.

[1] M. Feuerbacher, E. Wuertz, A. Kovács, and C. Thomas, *Mater. Res. Lett.* **5**, 128 (2017).

[2] A. Jelen, P. Koželj, D. Gačnik et al., *J. Alloys Compd.* **864**, 158115 (2021).

Quantitative description of magnetic anisotropy in insulating GaN:Mn

Katarzyna Gas¹, Dariusz Sztenkiel¹, Piotr Wiśniewski², Rafal Jakiela¹,
Yadhu Edumkhanty¹, Malgorzata Iwinska³, Tomasz Sochacki³, Hanka Przybylinska¹,
Michał Bockowski³, and Maciej Sawicki¹

¹ *Institute of Physics, Polish Academy of Sciences, Warsaw, Poland*

² *Institute of Low Temperature and Structure Research, Polish Academy of Sciences, Wrocław, Poland*

³ *Institute of High Pressure Physics, Polish Academy of Sciences Warsaw, Poland*

The ferromagnetic form of GaN may have an enormous technological relevance due to the already dominating role of the nitride family in light industry, high-frequency, and high-power electronics. In particular, the existence of sizable piezoelectromagnetic coupling has been evidenced recently in homogeneous (single-phase) (Ga,Mn)N [1], an effect that opens the door for realization of external electric field driven, repeatable magnetization reversal. It is, therefore, very important to understand the physics which governs the behavior and magnetic properties of transition metals in nitrides.

In this paper we report on magnetic properties of the Mn impurity in bulk GaN. Our 1'' in diameter single crystals were crystallized by halide vapor phase epitaxy [2] with Mn concentration ranging from 1×10^{18} to 5×10^{19} cm⁻³. The characterization of magnetic anisotropy in combination with electron paramagnetic resonance revealed predominantly the Mn³⁺ (d⁴) configuration. Such a center is characterized by a very strong single ion magnetic anisotropy. The trigonal-symmetry surrounding and Jahn-Teller effect lead to splitting of the five lowest spin quantum levels (characterized by spin quantum numbers $m_s = 2, -1, 0, 1, 2$). Around $H = 0$ the ground state is composed mostly of $m_s = 0$ and with the increase of magnetic field $m_s = -1$ and $m_s = -2$ become sequentially the lowest states, leading to a well-developed staircase-like magnetization curve at 0.5 K as measured by means of ³He insert to commercial SQUID magnetometer. The unique shape and positions of the magnetization steps observed for the magnetically hard axis configuration (parallel to the wurtzite c-axis of GaN) are accurately described using a single ion crystal field approach relevant to Mn³⁺ state, taking into account the tetrahedral cubic field with trigonal distortion, spin-orbit interaction, static tetragonal Jahn-Teller distortion, and magnetic field [3]. The perfect agreement obtained between the experimental $m(H)$ and theory means that for such strong dilutions there is no need to invoke terms corresponding to Mn-Mn interactions (pair or triplets). Instead we can quantify the contributions brought about Mn³⁺ and Mn²⁺. The latter finding is also of great importance for commercialization of industry-relevant, high quality, insulating substrates.

This work has been supported by the National Science Centre, Poland through OPUS (DEC-2018/31/B/ST3/03438) grant and TEAM TECH program of the Foundation for Polish Science co-financed by the European Union under the European Regional Development Fund (No.POIR.04.04.00-00-5CEB/17-00).

[1] D. Sztenkiel *et al.*, Nature Comm. 7, 13232 (2016).

[2] M. Bockowski *et al.*, Journal of Crystal Growth 499, 1-7 (2018).

[3] D. Sztenkiel *et al.*, New J. Phys. 22, 123016 (2020).

Noncollinear coupling of Co layers across RuCo spacer layers

E. Girtl^{1*}, J. Besler¹, P. Omelchenko¹, Z. Nunn¹, S. Myrtle¹, C. Abert², S. Koraltan²
and D. Seuss²

¹Department of Physics, Simon Fraser University, 8888 University Drive, Burnaby BC, Canada

²Department of Physics, University of Vienna, Universitätsring 1, Vienna

Recently, a class of spacer layers was discovered, which, when inserted between two ferromagnetic layers, can control the angle between the magnetic moments of these ferromagnetic layers between 0° and 180° [1]. These spacer layers consist of a nonmagnetic material (Ru), used to achieve a large antiferromagnetic interlayer exchange coupling between ferromagnetic layers, alloyed with a ferromagnetic material (Fe or Co).

Shown in Fig.1 are the bilinear (J_1) and biquadratic (J_2) coupling constants and zero field coupling angle (θ) between the magnetic moments of the ferromagnetic layers of Co|RuCo(d)|Co as a function of RuCo thickness, d , and Co atomic concentration, x . The noncollinear coupling in Co|RuCo(d)|Co ($0.4 \leq d \leq 1.4$ nm) occurs for x between about 37 and 63. With the introduction of Co into the Ru spacer layer, J_1 experiences a maximum followed by a loss of the oscillatory dependence on d . This maximum coincides with the non-collinear to antiferromagnetic transition. After J_1 reaches its maximum, it smoothly decreases along the same $1/d^2$ curve that describes the dependence of the J_1 maxima of Co|Ru(d)|Co, see Fig.1(a). Initially, J_2 also follows a universal $1/d^2$ dependence for all Ru_{100-x}Co_x spacer layers, which is represented by the broad, grey curve in Fig.1(b). As d increases, J_2 experiences a rapid decrease

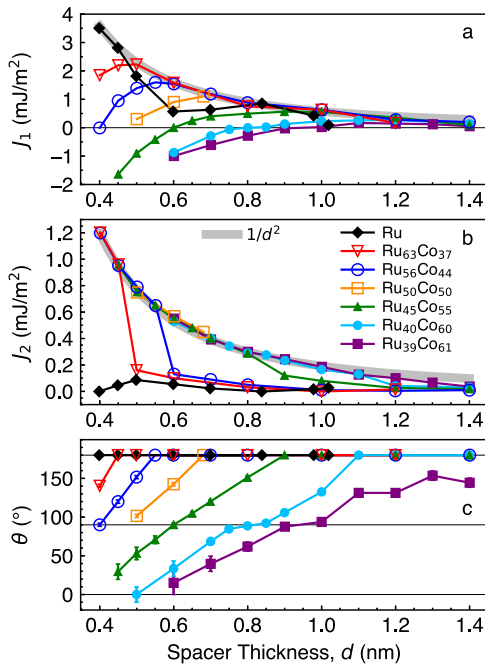


Fig. 1: (a) J_1 , (b) J_2 , and (c) θ of Co(2)|Ru_{100-x}Co_x(d)|Co(2) for $0.4 \leq d \leq 1.4$ nm and $37 \leq x \leq 61$ at 298 K. Co(2)|Ru(d)|Co(2) coupling data and a $1/d^2$ dependence (broad, grey lines in (a) and (b)) are added for comparison.

that coincides with the maximum in J_1 at the non-collinear to antiferromagnetic transition. Fig.1(c) shows that, for all RuCo compositions, θ increases with d , almost linearly for $37 \leq x \leq 55$, until becoming constant when it reaches 180°.

A simple atomistic model reveals that the biquadratic coupling originates from the coupling of ferromagnetic atoms, in all three spatial dimensions, within the spacer layer [2]. These new spacer layers have the potential to be used in most spintronic devices, as the optimal design of these devices almost always requires noncollinear alignment between at least two adjacent ferromagnetic layers.

[1] Z. Nunn, et al., Sci. Adv. 6, 1-7 (2020).

[2] C. Abert, et al., submitted to Phys. Rev. B.

Element specific magnetocrystalline anisotropy of Sm-Co thin films

Georgia Gkouzia¹, Damian Günzing², Teresa Wessels^{2,4}, Alpha T. N' Diaye³, Heiko Wende², Katharina Ollefs² and Lambert Alff¹

¹ *Technical University of Darmstadt, Institute of Materials Science, Alarich-Weiss-Str.2, Darmstadt, Germany*

² *University of Duisburg-Essen, Faculty of Physics and Center for Nanointegration (CENIDE), Lotharstr.1, Duisburg, Germany*

³ *Lawrence Berkeley National Laboratory, 1 Cyclotron Road, Berkeley, United States of America*

⁴ *Ernst Ruska-Centre for Microscopy and Spectroscopy with Electrons and Peter Grünberg Institute, Forschungszentrum Jülich, 52425 Jülich, Germany*

Sm₂(Co,Fe,Cu,Zr)₁₇ pinning controlled magnets have outstanding performance at high temperatures. In this type of magnets, a phase decomposition reaction occurs naturally that yields a complex phase mixture, leading to excellent magnetic properties with the best $(BH)_{\max}$ of 271 kJ/m³ at room temperature [1].

In this work, we start with the controlled composition of a nanostructure in the pure Sm-Co system by thin film model layers [2]. The pure Sm-Co system when grown as thin films has a strong tendency to form a mixture of the SmCo₅ and Sm₂Co₁₇ phases which are difficult to disentangle. Note that we are working here without additional buffer layers (as usually reported in literature [3]) that could potentially alter the magnetic properties. X-ray diffraction (XRD) was carried out for the crystallographic and structural characterization of the films. The thickness of the thin films is about 30 nm as determined by X-ray reflectivity (XRR). The magnetic properties of the films were measured by a superconducting quantum interface device (SQUID) in two directions, out of plane and in plane. X-ray magnetic circular dichroism (XMCD) and X-ray absorption measurements have been performed to have access to element-specific information.

It turns out that extended X-ray absorption fine structure (EXAFS) analysis combined with transmission electron microscopy (TEM) is the best way to quantify the nano-domain phase decomposition in the thin films. For the first time, angle dependent XMCD spectroscopy has been carried out on Sm-Co thin films. From the element specific measurements, we obtain a direct proof of the collinear magnetic order and a strong decrease in the Co orbital moment in plane. In this paper, we investigate how the intertwined nano-structure of SmCo₅ and Sm₂Co₁₇ blocks with coherent interfaces [2] affects the intrinsic magnetic anisotropy.

[1] M. Duerrschnabel *et al.*, Nat. Commun **8**, 54 (2017).

[2] S. Sharma *et al.*, ACS Appl. Mater. Interfaces **13**, 32415 (2021).

[3] J. Sayama *et al.*, J. Magn. Magn. Mater. **301**, 271 (2006).

Influence of heavy sputtering gas on perpendicular magnetic anisotropy and interlayer exchange coupling in Pt/Co/Ir synthetic antiferromagnets

Daniel B. Gopman¹, Marzieh Savadkoochi^{1,2}, Chloe Taylor³ and James Eckert³

¹Materials Science and Engineering Division, NIST, Gaithersburg, Maryland, USA

²Mechanical Engineering Department, University of the District of Columbia, Washington, D.C., USA

³Department of Physics, Harvey Mudd College, Claremont, CA, USA

Pt/Co/Ir-based synthetic antiferromagnets (SAFs) are key building blocks in high performance magnetic memory devices due to their large perpendicular magnetic anisotropy (PMA) and interlayer exchange coupling (IEC) energies, respectively, and tolerance to thermal processing [1-2]. Fortuitously, the IEC field and PMA field both can be enhanced significantly via judicious tuning of the Ir thickness [3]. Further gains in IEC and PMA may be required in emerging memory devices. And while the materials system may appear to be well optimized, additional refinement could be realized through the exploration of alternative processing approaches. In particular, the replacement of Argon with a heavier gas during sputtering (e.g. Krypton) is known to enhance the PMA of Co/Pt multilayers due to reduced bombardment of the growing film from gas species during deposition, reduced intermixing of layers and improved columnar film growth, overall enhancing the PMA [4]. To the best of our knowledge, this remains an unexplored approach for SAFs in general, and particularly not for the Pt/Co/Ir system.

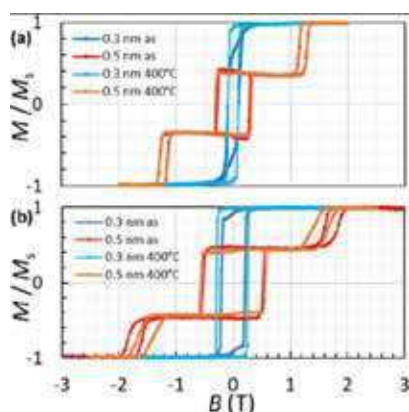


Figure 1: Out-of-plane magnetization versus applied field for Pt/Co/Ir grown in an (a) Ar or (b) Kr working gas environment.

We investigated the role of sputter gas in the properties of a SAF structure grown by DC magnetron sputtering in an ultrahigh vacuum chamber (base pressure $< 10^{-7}$ Pa) on a thermally oxidized Si wafer with the following film stacking structure (thicknesses in parentheses in nm): Ta(5)/Pt(5)/[Co(0.4)/Pt(0.6)]_n/Co(0.4)/Ir(t_{Ir})/[Co(0.4)/Pt(0.6)]_n/Ru(2)/Ta(3). We varied the Ir spacer thickness between 0.3 nm and 0.7 nm to cover the first IEC peak around 0.5 nm. The sample sputtered in an 6 mTorr Kr environment exhibited a peak IEC field of 1.7 T, exceeding its Ar counterpart by over 35% (see Figure 1). This same thickness is also associated with the largest PMA ($\mu_0 H_K = 5.4$ T), which exceeded the Ar-sputtered counterpart by over 30%. A 400°C post-annealing treatment in vacuum ($< 4 \times 10^{-6}$ Pa) only causes a moderate reduction in the IEC field to 1.5 T. These results suggest that using Krypton as the sputtering gas could lead to superior performing SAFs for emerging memory devices.

[1] Y. Huai, H. Gan, Z. Wang, *Appl. Phys. Lett.*, **112**, p.1 (2018)

[2] K. Yakushiji, A. Sugihara, A. Fukushima, *Appl. Phys. Lett.*, **110**, p.1 (2017)

[3] Y. Lau, Z. Chi, T. Taniguchi, *Phys. Rev. Mat.*, **3**, p.1 (2019)

[4] G. Bertero, R. Sinclair, *IEEE Trans. Mag.*, **31**, p.1 (1995)

Crystal quality assessment of highly Bi-doped electrodeposited Cu nanowires for spintronics applications

A. Guedeja-Marrón¹, I. García-Manuz¹, S. Ruiz-Gómez², C. Fernández-González³, L. Pérez³, and M. Varela^{1,4}

¹ Dept. Física de Materiales, Universidad Complutense de Madrid, 28040 Madrid, Spain

² Max Planck Institute for Chemical Physics of Solids, 01187 Dresden, Germany

³ IMDEA Nanociencia, 28049 Madrid, Spain

⁴ Instituto Pluridisciplinar, Universidad Complutense de Madrid, 28040 Madrid, Spain

The spin Hall effect (SHE) is an important spin-charge conversion mechanisms that plays a key role in the development of spintronics devices [1]. To this end, the use of materials that exhibit giant SHE has been proposed [2]. Large spin Hall angle (SHA) has been predicted [3] and reported [4] in CuBi alloys with 0.5% of Bi, making this material a good candidate for integration in spintronics devices. For that, a detailed study of the structure and a fine control of composition and crystal quality is a must for a deeper understanding of the origin of extrinsic SHE in this material.

In a previous work we report the possibility of obtaining Bi-doped Cu nanowires using template assisted electrochemical deposition [5]. This growth method allows the control of crystal quality, cluster formation and microstructure independently. In this work, we present an extensive structural characterization of this material. The atomic resolution scanning transmission electron microscopy (STEM) and TEM structural characterization (Fig 1 a,c) reveals that using low overpotential we have succeeded growing single crystal nanowires (Fig 1 a,c). For low doping levels, Bi does not cluster but instead it appears homogeneously distributed into the Cu matrix, as Fig 1b shows. These results proof that the obtention of single crystal, homogeneously doped wires is indeed possible. This is a much needed step to enable future studies on the correlation between the structure and the spin-transport properties that would pave the way towards understanding the large SHE in these systems.

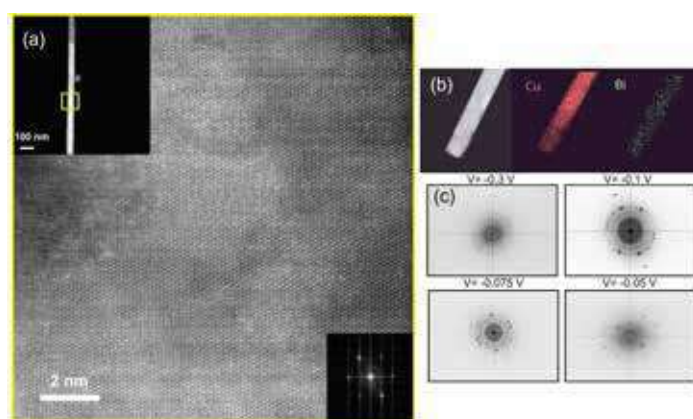


Figure 1: (a) High- angle annular dark field STEM images corresponding to a single-crystal nanowire (NW) with composition Cu₉₅Bi₅ grown at -0.05 V. Bottom left image showing fast Fourier transform in the zone axis [100]. (b) Energy dispersive X-Ray analysis maps measured for Bi and Cu of the simultaneous TEM image. (c) Selected area electron diffraction patterns measured for NWs grown at different overpotential.

- [1] J. Sinova, S. O. Valenzuela et al., *Rev. Mod. Phys.* **87**, 1213 (2015).
- [2] T. Jungwirth, J. Wunderlich, and K. Olejnik, *Nature*. **11**, 5 (2012).
- [3] M. Gradhand, D.V. Fedorov, P. Zahn, I. Mertig, *Phys. Rev. B*. **81**, 245109 (2010).
- [4] Y. Niimi, Y. Kawanishi et al., *Phys. Rev. Lett.* **109**, 15 (2012).
- [5] S. Ruiz-Gomez et al., *J. Magn. Magn. Mater.* **542**, 168645 (2022).

Effect of buffer and capping layers of Co/Ni-based thin film heterostructures: Towards sustainable flexible spintronics

Mariam Hassan^{1,2}, Sara Laureti¹, Christian Rinaldi³, Federico Fagiani³, Gianni Barucca⁴, Francesca Casoli⁵, Alessio Mezzi⁶, Eleonora Bolli⁶, Saulius Kaciulis⁶, Mario Fix², Aladin Ullrich², Gaspare Varvaro¹, Manfred Albrecht²

¹ ISM - CNR, *nM²-Lab, Area della Ricerca Roma 1, Monterotondo Scalo (Roma), 00015, Italy*

² Institute of Physics, University of Augsburg, Universitätsstraße 1 Nord, D-86159 Augsburg, Germany

³ Department of Physics and IFN-CNR, Politecnico di Milano, via G. Colombo 81, 20133 Milano, Italy

⁴ Università Politecnica delle Marche, Dipartimento SIMAU, Via Brecce Bianche, Ancona 60131, Italy

⁵ IMEM - CNR, Parco Area delle Scienze 37/A, Parma 43124, Italy

⁶ ISMN - CNR, Area della Ricerca Roma 1, Monterotondo Scalo (Roma), 00015, Italy

Synthetic antiferromagnets with perpendicular magnetic anisotropy (PMA-SAFs) have gained a growing attention for both conventional and advanced spintronic applications. While the progress of PMA-SAF spintronic devices on rigid substrates has been remarkable, only few examples on flexible heterostructures, all involving the use of X/Pt(Pd) (X = Co, FeCoB) multilayers, are reported in the literature despite their additional functionality, such as light-weight, flexibility, shapeability and wearability [1]. In this contest, Co/Ni system may offer additional advantages with respect to multilayer thin film stacks containing platinum group metals (e.g., low damping, high spin polarization) for the development of advanced spintronic devices. Moreover, decreasing the content of the critical elements (e.g., Pd, Pt), may relieve the demand for strategic raw materials and reduce the environmental impact of related technologies, thus contributing to the transition towards a greener and more sustainable

In this work, Co/Ni-based PMA-SAFs and GMR spin-valve thin film stacks consisting of a [Co/Ni]_N free layer and a [Co/Ni]₆/Ru/[Co/Ni]₆ SAF reference electrode with different combinations of N, buffer and capping layers (i.e., Pt, Pd and Cu/Ta) were deposited on flexible PEN tapes (Fig. 1a). High quality SAFs with a fully compensated AF region and spin-valves with GMR ratio in line with the values reported in the literature for similar systems on rigid substrates have been obtained in all cases. However, due to the different interdiffusion mechanisms occurring at the interfaces between the metallic layers, we could demonstrate that while the critical element allows obtaining the best results when used as buffer layer, Cu is the best choice as capping layer to optimize the properties of the stacks. The results thus indicate that complex Co/Ni-based heterostructures with reduced content of critical elements can be deposited on flexible tapes, allowing the realization of novel flexible and sustainable spintronic devices for applications like wearable electronics, soft robotics, and biomedicine.

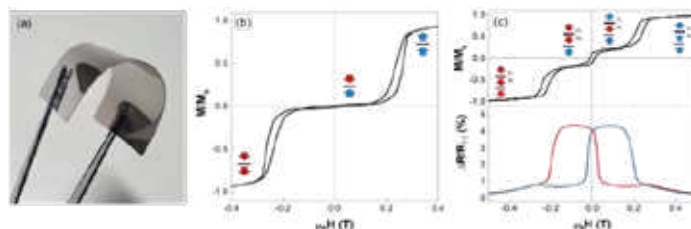


Figure 1. (a) Representative picture of a flexible spin-valve obtained by direct deposition on PEN tapes. (b) Out-of-plane hysteresis loop of a flexible SAF with Pt and Cu as buffer and capping layer, respectively. (c) Out-of-plane hysteresis loop and corresponding magneto-resistance response of a flexible SAF-based spin-valve with Pt and Cu as buffer and capping layer, respectively. All measurements were performed at room temperature.

[1] M. Hassan et al., *Nanoscale Advances*. **3**, 3076 (2021).

Chemical and Magnetic order of FeRh nanoparticles deposited on BaTiO₃ (001) and SrTiO₃ (001).

G. Herrera¹, V. Dupuis¹, S. Gonzalez², I. C. Infante², P. Rojo Romeo², P. Ohresser³, E. Otero³, P. Schoeffmann³, M. Bugnet⁴, B. Vilquin², A. Reyes⁵, A. Vlad³, A. Resta³, A. Coati³, A. Tamion¹, L. Bardotti¹, D. Le Roy¹ and F. Tournus¹

¹ Institut Lumière Matière, UMR 5306, Univ. Lyon 1-CNRS, F-69622 Villeurbanne Cedex.

² Univ Lyon, CNRS INSA Lyon ECL UCBL CPE, INL UMR 5270, 69621 Villeurbanne, France

³ Synchrotron SOLEIL, L'Orme des Merisiers, 91190 Saint Aubin, France

⁴ MATEIS, UMR 5510, Univ Lyon, CNRS, INSA Lyon, UCBL, F-69621 Villeurbanne.

⁵ Faculty of Science, Universidad Autonoma del Estado de México, Toluca, México.

The bimetallic FeRh bulk alloy crystallizes in a chemically ordered B2-phase (CsCl like structure), characterized by a magneto-structural transition close to room temperature (~ 350 K) from anti-ferromagnetic phase to a ferromagnetic one [1]. In nanoscale systems the magnetic order of FeRh is very sensitive to interfaces, size reduction, strain and surface terminations [2,3]. We have investigated the magnetic and structural properties of FeRh nanoparticles deposited on oxide perovskites surfaces, including BaTiO₃ (001) thin films and SrTiO₃ (001) crystals. We showed that randomly deposited particles on BaTiO₃ or SrTiO₃ adopt specific orientations and epitaxy after in-situ UHV annealing, which also ensures chemical ordering from fcc-like A1 phase to the B2 phase (Figure 1). X-ray magnetic circular dichroism has shown that systems does not posses metamagnetic transition regarless the substrate oxidation or annealing process keeping the ferromagnetic state which decrease as function of the temperature (Figure 2) and present a Curie temperature of around 600 K.

Works are in progress in view to show how cluster deposition could offer an alternative to a possible control of FeRh nanomagnet taking advantage of the interfacial coupling with a ferroelectric substrate.

This is part of G. Herrera's PhD supported by VOLCONANO ANR-19-CE09-0023 project.

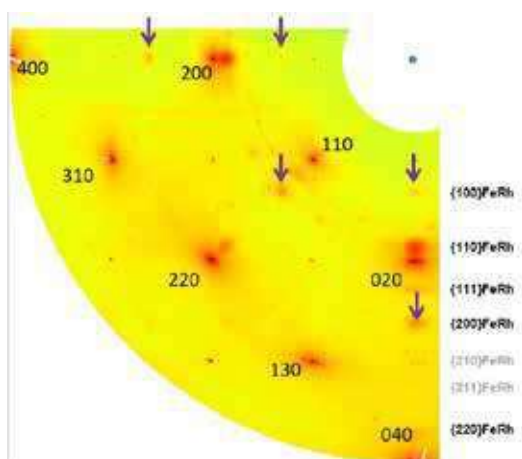


Figure 1: Reciprocal space map of the surface for FeRh particles of 3 nm diameter on SrTiO₃ (hkl planes indicated), after annealing. The unusual epitaxy (cube on cube) is indicated by arrows.

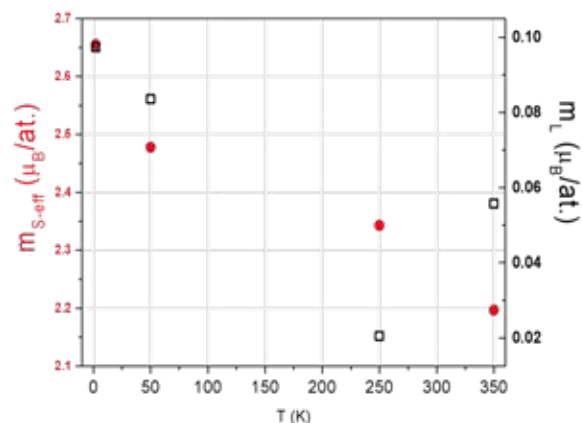


Figure 2: The effective spin ($m_{S\text{-eff}}$) and orbital magnetic moments (m_L) between 2 K and 350 K for FeRh B2 nanoclusters deposited on SrTiO₃.

[1] V. L. Moruzzi et al. *Phys. Rev. B*. **46**: 2864-2873 (1992)

[2] A. Hillion et al, *Phys. Rev. Lett.* **110**: 087207. (2013)

[3] M. Liu et al. *Euro. Phys. Lett.* **116**: 27006. (2016)

Current Induced Crystallisation in Heusler Alloy Films for Memory Potentiation in Neuromorphic Computation

William Frost,¹ Kelvin Elphick,² Marjan Samiepour,² Zhenyu Zhou²
and Atsufumi Hirohata²

¹ Department of Physics, University of York, UK

² Department of Electronic Engineering, University of York, UK

Whilst great efforts have been made in the development and applications of Heusler alloys in spintronic devices, they typically still require high annealing process to achieve the full L_{21} ordering. Recently by growing on the $\{110\}$ planes, 85% of a $\text{Co}_2\text{FeAl}_{0.5}\text{Si}_{0.5}$ (CFAS) thin film has been reported to be crystallised when deposited at a moderate temperature ~ 350 K [1]. This offers significant reduction in the crystallisation energy. In this work, such a film has been implemented in a giant magnetoresistive (GMR) pillar, whereby an applied current is used for crystallisation. This allows for potentiation in neuromorphic-type computing, where the value of the resistance or the MR of the pillar can inform the reader of the history of the device.

A GMR stack consisting of W (10)/CFAS (10)/W (3)/CFAS (5)/Ru (3) (thicknesses in nm) was deposited and patterned into a nanopillar junction with the diameter between 80 and 200 nm using electron-beam lithography and Ar-ion milling. The fabricated devices were measured under an applied current using a conventional four-probe measurement with a sensing current of 50 μA and crystallisation currents between 1 μA and 10 mA with the duration up to 500 μs .

Figure 1(a) shows the resistance change in a (150×100) nm² GMR pillar after the repeated current applications. At low currents of 50 μA , very little change is observed. However, as the current intensity and pulse length increase to 500 μA and 500 μs an asymptotic decrease in the device resistance is observed. This change is irreversible and is therefore easily separated from the change in resistance incurred by simple temperature dependence. The corresponding electron diffraction pattern confirms that the current-induced annealing has contributed to crystallisation of the CFAS layer as shown in Fig. 1(b), indicating a strong $B2$ texturing. This is a significant improvement on the disordered/weakly crystalline as deposited state. Further results and discussion will be presented at the conference.

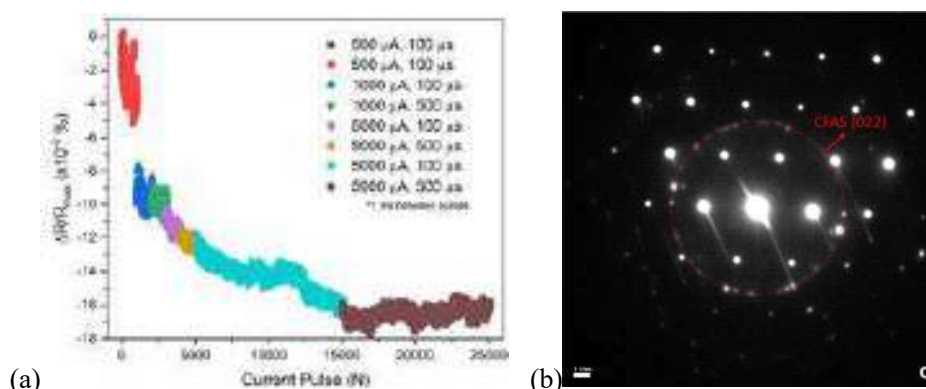


Fig. 1(a) The change in the resistance of a (150×100) nm² nanopillar after a series of current applications and (b) the corresponding TEM electron diffractogram of the CFAS layer after current annealing, showing strong $\{220\}$ reflections [2].

[1] W. Frost *et al.*, *J. Magn. Magn. Mater.* **484**, 100 (2019).

[2] W. Frost *et al.*, *Sci. Rep.* **11**, 17382 (2021).

Magnetic anisotropy and exchange bias in V_2O_3 /Ni epitaxial layers

K. Ignatova, E. B. Thorsteinsson, and U. B. Arnalds

Science Institute, University of Iceland, Dunhaga 3, 107 Reykjavik, Iceland

In this work we present a temperature and angular dependent study of the structural and magnetic properties in highly crystalline V_2O_3 /Ni/Zr hybrid magnetic heterostructure films. Our investigation focuses on the coupling between the ferromagnetic and anti-ferromagnetic layers where the V_2O_3 layer undergoes an antiferromagnetic/paramagnetic phase transition coupled to the structural phase transition of the material at around 150 K [1, 2]. Structural investigations using x-ray diffraction reveal highly crystalline films of a quality which has previously not been reported in the literature. The highly textured (111) layering of the Ni films on the underlying V_2O_3 (0001) oriented layer results in the absence of anisotropy. During the transition we observe a strain related enhancement of the coercivity [3] and the onset of an exchange bias for cooling under an external magnetic field affecting the magnetization of the Ni layer.

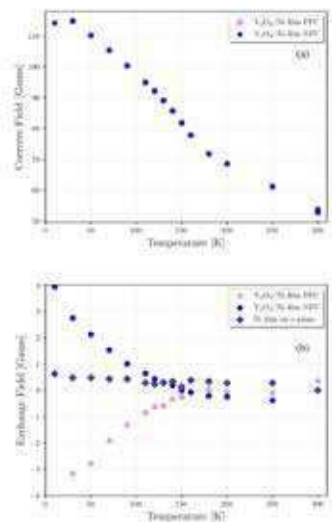


Figure 1: (a) Coercivity and (b) exchange field for the V_2O_3 /Ni/Zr and film extracted from magnetization loops recorded using VSM as a function of increasing temperature after positive field cooling (PFC) under an applied field of 5 T and negative field cooling (NFC) with a field of 5 T.

Figure 1 shows the coercivity and exchange field for the V_2O_3 /Ni/Zr film extracted from magnetization loops recorded using VSM as a function of increasing temperature after field cooling. A corresponding reference sample composed exclusively of Ni/Zr films (without a V_2O_3 layer) showed no indication of an exchange bias and a typical decrease in coercivity with temperature from $H_c = 5.2$ Gauss at 10 K down to $H_c = 1.6$ Gauss at room temperature. The presence of the in-plane exchange bias was verified by carrying out both MOKE and VSM measurements. Heating the films to above the transition temperature the exchange bias in the Ni is removed and can be reversed upon subsequent cooling under an inverted external magnetic field. Using temperature dependent polarized neutron reflectometry we investigate the film structure at the interface, capturing the depth-resolved nuclear and magnetic scattering length density.

- [1] E. B. Thorsteinsson, S. Shayestehaminzadeh, A. S. Ingason, F. Magnus and U. B. Arnalds *Sci. Rep.* **11**, 123 (2021).
- [2] H. Hajihoseini, E. B. Thorsteinsson, V. V. Sigurjonsdottir and U. B. Arnalds *Appl. Phys. Lett.* **16**, 118 (2021).
- [3] V. Polewczyk, S. K. Chaluvadi, P. Orgiani, G. Panaccione, G. Vinai, G. Rossi and P. Torelli *Phys. Rev. Mater.* **5**, 3 (2021).

Spin-glass state and Almeida-Thouless line observation in $\text{Ge}_{1-x-y}(\text{Sn}_x\text{Mn}_y)\text{Te}$ multiferroics

A. Khaliq,^{1,a} S. Lewińska,¹ R. Minikaev,¹ M. Arciszewska,¹ A. Avdonin,¹ B. Brodowska,¹ V.E. Slynko,² E.I. Slynko,² and L. Kilanski,¹

¹*Institute of Physics, Polish Academy of Sciences, Aleja Lotnikow 32/46, PL-02668 Warsaw, Poland*

²*Institute of Materials Science Problems, Ukrainian Academy of Sciences, Chernovtsy, Ukraine*

IV-VI narrow bandgap semiconductors with fundamentally broken spatial symmetry, large spin-orbit interaction and giant Rashba spin splitting are emerging as new class of promising spintronic materials [1-3]. Apart from magnetic features, IV-VI diluted magnetic semiconductors based on GeTe manifest spontaneous ferroelectric polarization which makes them ideal to integrate non-volatile memory and computing features.

In this work, we present structural and magnetic results of Rashba ferroelectric, α -GeTe doped with a series Sn and Mn ions in the range $0.38 \leq x \leq 0.79$ and $0.02 \leq y \leq 0.086$. The $\chi_{AC}(T)$ plots of $\text{Ge}_{1-x-y}(\text{Sn}_x\text{Mn}_y)\text{Te}$ alloys signify a spin-glass type of magnetic ordering for crystals with $x \approx 0.2$, $y = 0.047$ and $x \approx 0.4$, $y = 0.052$ with the freezing temperature values, T_F of 5.1 K and 7.1 K. The zero-field-cooled and field-cooled (zfc-fc) graphs of the spin-glass like crystals demonstrate a shift in freezing temperature, T_F towards lower values at high applied field. The observed shift in freezing temperature, T_F at high applied field designates that the studied alloys follow de Almeida-Thouless (AT) Line, $\delta T_F \propto H^{2/3}$ for our samples. The AT Line shows the switching of a spin glass ordering into a paramagnetic state at elevated temperatures and magnetic field. The magnetization hysteresis, $M(B)$ graphs of the alloy with $x \approx 0.2$, $y = 0.061$ showed anomalous behavior in coercivity and remanence near $T_C \approx 13$ K. Such anomalous behavior in coercivity is attributed to the presence of disorder in spin-glass type of magnetic state.

[1] J. Krempasky et al., Nat Commun. **7**, 13071 (2016).

[2] C. Rinaldi et al., Nano Lett. **18**, 2751-2758 (2018).

[3] S. Picozzi, Front. Phys. **2**, 1-4 (2014).

Direct On-chip EMI Shielding Layer with Metallic/Magnetic Multilayer for sub-100 MHz frequency range

A. Kikitsu¹, Y. Kurosaki¹, S. Shirotori¹, A. Fujita², H. Nishigaki² and S. Matsunaka²

¹ Toshiba Corp., 1 Komukai Toshiba cho Saiwai-ku, Kawasaki, Japan

² Shibaura Mechatronics Corp., 5-14-1 Higashi Kashiwagaya, Ebina, Japan

Electromagnetic interference (EMI) in the range of sub-100 MHz has attracted attention for the applications of smart phones or EVs. Depositing a shielding layer directly on the semiconductor chips is useful for such systems [1]. It was found that a metallic/magnetic multilayer [Cu(100 nm)/NiFeCuMo(100 nm)]₁₀ showed better shielding effect than Cu layer at sub-100 MHz range [2]. Further, by stacking with soft magnetic multilayer units it showed shielding peak at less than 50 MHz [3]. In this paper, experimental results of samples with variety of multilayer stacks are provided and possible mechanism behind them is discussed.

Samples were deposited by magnetron sputtering on glass substrates. Reference film stack was A₁₀/B₅₅/C₁₀, where A, B and C stands for the unit of [Cu(100 nm)/NiFeCuMo(100 nm)], [CrTi(5 nm)/NiFeCuMo(50 nm)], and [CrTi(5 nm)/NiFeCuMo(300 nm)], respectively. Subscript number means the reputation number. Magnetic shielding effect (MSE (dB)) was evaluated by a transmitted power of the electromagnetic wave through the sample [2].

Reputation numbers of each unit were modified in order to investigate the origin of the MSE peak as well as to reduce the total thickness. Figure 1 shows the results. It was found that thinner samples result in a peak shift to higher frequency. Reduction of the thickness of unit B seems critical to maintain high MSE peak.

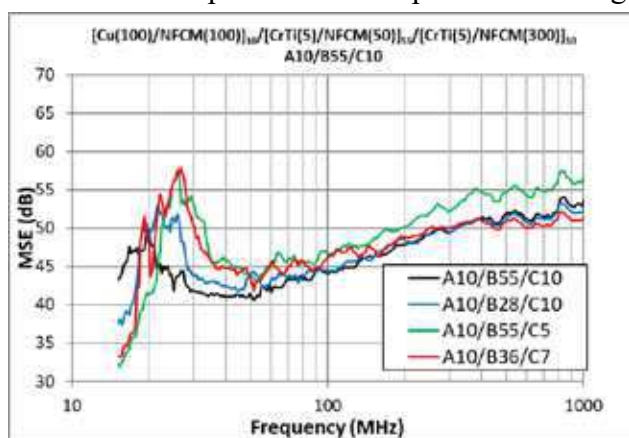


Figure 1: Magnetic shielding effect (MSE) of samples with reduced reputation number of each unit.

around 20 MHz. Expansion of the correlative spin motion to the soft magnetic units seems to be a possible mechanism. Thicker soft magnetic unit generates further motion and results in lower peak frequency due to the reduction of the resonance energy of the domain wall.

Sample A₁₀/B₃₆/C₇ had total thickness thinner than that of sample A₁₀/B₅₅/C₁₀ by 2 μm . Its MSE peak seems to have tail toward 10 MHz range. This stack is promising one for EMI shielding layer at 10 MHz range with further thin thickness.

[1] M. Yamaguchi et al., *IEEE Trans. Magn.*, **46**, 2450 (2010).

[2] A. Kikitsu et al., *J. Magn. Magn. Matr.*, **539**, 168339 (2021).

[3] A. Kikitsu et al., 2022 Joint Interma MMM conference, IOB-10 (2021).

Impact of the Magnetic Subsystem on the Low-temperature Specific Heat of Metamagnetic Shape Memory Alloy

Anna Kosogor¹, Victor A. L'vov¹, Rie Y. Umetsu², Xiao Xu³,
and Ryosuke Kainuma³

¹ Institute of Magnetism NASU and MESU, Kyiv 03142, Ukraine

² Institute for Materials Research, Tohoku University, Sendai 980-8577, Japan

³ Graduate School of Engineering, Tohoku University, Sendai 980-8579, Japan

The metamagnetic Ni-Mn-X (X = In, Sn, Sb) shape memory alloys attract great attention due to their unique properties. The drastic changes in the magnetic characteristics and the relevant phenomena directly connected to applications (e.g., the magnetocaloric effect) are observed in these alloys depending on concentration of X. In particular, the low-temperature state of Ni₅₀Mn_{50-x}In_x alloys is ferromagnetic (FM) austenite if $x > 16$ and antiferromagnetic (AFM) or paramagnetic martensite if $x < 15$ [1,2]. It has been shown experimentally that the low-temperature specific heat measured for FM state of Ni₅₀Mn_{50-x}In_x alloys, is significantly different from that measured for the alloys in AFM state [1]. To explain this difference, the magnetic state of the alloy must be accounted.

The low-temperature specific heat of magnetic solid is a sum of electronic, vibrational and magnetic contributions, which can be expressed as following

$$C(T) = \gamma T + \beta T^3 + C_M(T). \quad (1)$$

Usually the magnetic term is disregarded and in this case the $C(T)/T$ is assumed to be a linear function of T^2 . As so, the coefficients β and γ are determined empirically as the slope and intercept of experimental $C(T)/T$ vs T^2 dependence. Value γ is electronic specific heat coefficient and Debye temperature T_D is estimated from the determined β value.

But the correct estimation of β and γ values is impossible if $C_M(T)$ is disregarded [2]. For FM solid the specific heat of magnetic excitations is equal to $C_M(T) = \kappa_{FM} T^{3/2}$. Fig.1 shows the

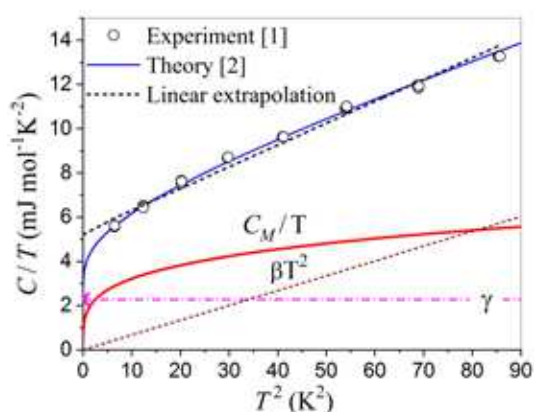


Figure 1: The experimental and theoretical dependences of $C(T)/T$ ratio on T^2 . Magnetic, electronic and lattice contributions to this ratio are shown for comparison

experimental and theoretical dependences of total $C(T)/T$ value vs T^2 obtained for FM state of Ni₅₀Mn_{33.8}In_{16.2} alloy. The magnetic and electronic parts of $C(T)/T$ function are shown for comparison. It is seen that the magnetic part exceeds all others in the temperature range from 2 K to 9 K. Due to this, the value $\gamma = 2.3 \text{ mJ mol}^{-1} \text{ K}^{-2}$, determined by the Eq. (1) fit is strongly different from the value $5.1 \text{ mJ mol}^{-1} \text{ K}^{-2}$, which results from the linear extrapolation of experimental dependence $C(T)/T$ to zero temperature. This difference in γ values is caused by the magnetic part of specific heat.

Therefore, the magnetic contribution to the low-temperature specific heat of FM phase must be taken into account for the correct estimation of electronic contribution to the specific heat.

[1] R. Y. Umetsu, X. Xu, W. Ito, and R. Kainuma, *Metals* **7**, 414 (2017).

[2] A. Kosogor, V. A. L'vov, R. Y. Umetsu, X. Xu, and R. Kainuma, *J. Magn. Magn. Mater.* **541**, 168549 (2022).

Control of magnetic properties in ferrimagnetic GdFe and TbFe thin films by He⁺ and Ne⁺ irradiation

Michał Krupinski¹, Julian Hintermayr², Paweł Sobieszczyk¹
and Manfred Albrecht²

¹ *Institute of Nuclear Physics Polish Academy of Sciences, Radzikowskiego 152, 31342 Krakow, Poland,*

² *Institute of Physics, University of Augsburg, Universitätsstraße 1, 86159 Augsburg, Germany*

Thin films of rare earth (RE)-3d transition metal (TM) systems, especially TbFe and GdFe alloys, are of great interest due to their possible applications in magneto-optical recording, micromechanics, surface acoustic wave filters, and terahertz emitters. Such a wide range of applications results from the unique properties of RE-TM systems, which simultaneously exhibit many interesting magnetic phenomena such as magnetostriction, perpendicular magnetic anisotropy (PMA), and ferrimagnetism that can exhibit a compensation temperature T_{comp} , where the net magnetization is zero. These properties can be further engineered by local modification of the atomic structure, i.e., by ion bombardment [1,2]. Such process can modify the chemical short-range order, which in turn affects the interatomic exchange coupling and macroscopic magnetic properties.

Our study presents the impact of He⁺ and Ne⁺ ion irradiation on the magnetic properties of 20-nm-thick Gd_xFe_{100-x} and Tb_xFe_{100-x} films with PMA. The films were prepared by magnetron co-sputtering and then irradiated using an ion energy of 10 keV for He⁺ and 20 keV for Ne⁺ with doses ranging from 5×10^{13} to 5×10^{15} ions per cm². The magnetic properties were characterized at temperatures down to 40 K by superconducting quantum interference device-vibrating sample magnetometry and Kerr microscopy. To get a better understanding of the observed changes in magnetic properties, numerical simulations of the irradiation process were carried out using the TRIDYN code while the atomistic magnetic simulations were performed using the software Vampire.

We demonstrated that the ion irradiation can be used to engineer magnetization, magnetic anisotropy, and compensation temperature in both alloy systems and to control the spin-flop reorientation transition in GdFe. Compared with the nonirradiated samples, far lower fields are required to induce the spin-flop transition around T_{comp} , which is caused by a decrease in the coupling constant between Gd and Fe moments. We found that fine-tuning of the compensation point in TbFe and GdFe is possible without losing perpendicular magnetic anisotropy by appropriate selection of ion energy and irradiation dose. The atomistic simulations revealed that the observed changes can be attributed to selective oxidation of rare earth atoms. The effect is very strong, and oxidation of 1% of RE atoms in the lattice is enough to explain the changes observed in the experiment, showing how sensitive the system is to small modifications of the atomic composition.

[1] M. Krupinski, J. Hintermayr, P. Sobieszczyk, M. Albrecht, *Phys. Rev. Materials* **5**, 024405 (2021).

[2] L. Frackowiak, P. Kuswik, G. D. Chaves-O'Flynn, M. Urbaniak, M. Matczak, P. P. Michalowski, A. Maziewski, M. Reginka, A. Ehresmann, and F. Stobiecki, *Phys. Rev. Lett.* **124**, 047203 (2020).

Effect of strain-induced anisotropy on magnetization dynamics in $\text{Y}_3\text{Fe}_5\text{O}_{12}$ thin films grown on $\text{Y}_3\text{Al}_5\text{O}_{12}$

A. Krysztofik¹, S. Özoğlu^{2,3}, R. D. McMichael⁴ and E. Coy⁵

¹ Institute of Molecular Physics, Polish Academy of Sciences, 60-179 Poznań, Poland

² Faculty of Physics, Adam Mickiewicz University, 61-614 Poznań, Poland

³ Department of Physics, Hakkari University, 3000 Hakkari, Turkey

⁴ National Institute of Standards and Technology, Gaithersburg, MD 20899 USA

⁵ NanoBioMedical Centre, Adam Mickiewicz University, 61-614 Poznań, Poland

We report on the correlation of structural and magnetic properties of $\text{Y}_3\text{Fe}_5\text{O}_{12}$ (YIG) layers deposited on $\text{Y}_3\text{Al}_5\text{O}_{12}$ substrates using pulsed laser ablation [1]. The recrystallization of YIG on the lattice-mismatched substrate can result in different film properties when compared to the high-temperature deposition. We observe an unexpected formation of interfacial tensile strain and consequently strain-induced anisotropy contributing to the perpendicular magnetic anisotropy. Moreover, the epitaxial strain has a significant impact on FMR linewidth which is significantly increased in comparison to a film on a $\text{Gd}_3\text{Ga}_5\text{O}_{12}$ substrate. Notably, the linewidth dependency on frequency has a negative slope. The unusual linewidth behavior is explained within the proposed anisotropy dispersion model. Good agreement of experimental findings with theoretical predictions suggests that the anisotropy axis is tilted from the film normal and dispersed. We conclude that the strain homogeneity plays a crucial role in the attainment of narrow FMR linewidths reflecting low magnetization damping of the films.

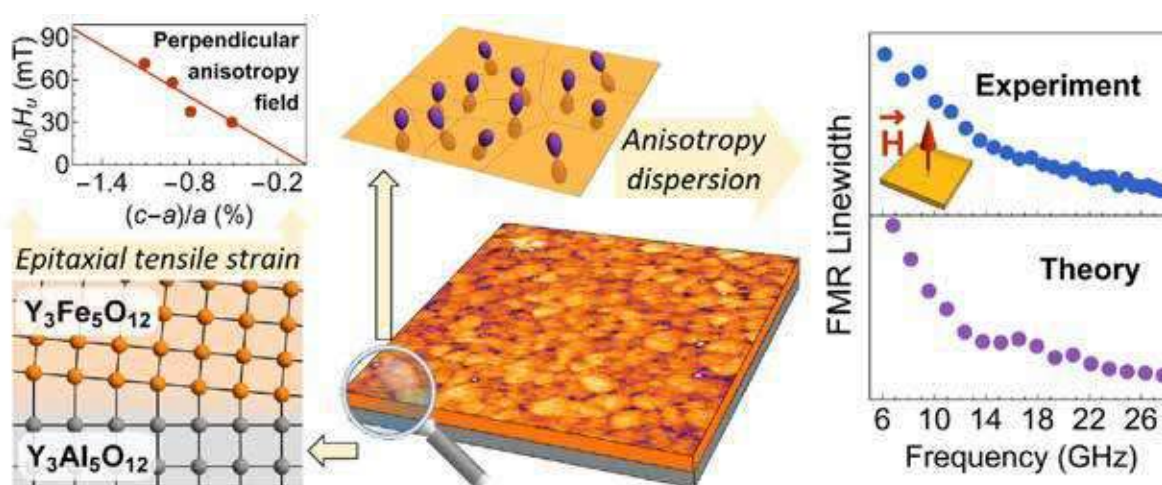


Figure 1: Interrelation between structural and magnetic properties in $\text{Y}_3\text{Fe}_5\text{O}_{12} / \text{Y}_3\text{Al}_5\text{O}_{12}$.

[1] A. Krysztofik, S. Özoğlu, R. D. McMichael, and E. Coy, *Scientific Reports* **11**, 14011 (2021). DOI: [10.1038/s41598-021-93308-3](https://doi.org/10.1038/s41598-021-93308-3)

Spin-structured multilayer THz emitters

Elias Kueny¹, Anne-Laure Calendron², Sven Velten², Lars Bocklage^{2,3}, Franz X. Kärtner^{1,3,4} and Ralf Röhlsberger^{2,3,5,6}

¹Center for Free-Electron Laser Science CFEL, Deutsches Elektronen-Synchrotron DESY, Notkestr. 85, 22607 Hamburg, Germany

²Deutsches Elektronen-Synchrotron DESY, Notkestr. 85, 22607 Hamburg, Germany

³The Hamburg Centre for Ultrafast Imaging, Luruper Chaussee 149, 22761 Hamburg, Germany

⁴Department of Physics, University of Hamburg, Luruper Chaussee 149, 22761 Hamburg, Germany

⁵Friedrich-Schiller Universität Jena, Fröbelstieg 3, 07743 Jena, Germany

⁶Helmholtz-Institut Jena (GSI), Max-Wien-Platz 1, 07743 Jena, Germany

Interest in spintronics THz emitters recently grew since they were shown to be a source of intense and broadband THz radiation [1]. Different approaches exist to improve the versatility of the emitters and control the THz spectrum, waveform [2] and polarization [3].

We manufactured samples using oblique incidence deposition of the ferromagnetic (FM) layers [4], which induces uniaxial magnetic anisotropy with a chosen direction and strength. This allows us to switch the magnetization of the layer using an external magnetic field applied along the easy axis. We take advantage of this to design samples with two independent FM layers to emit versatile THz.

Each FM layer causes THz emission. When they have parallel easy axes but different coercivities (Fig. 1a), we can use the external field to control whether the magnetizations are parallel or antiparallel, and therefore whether the generated THz field add up or cancel each other. This gives the possibility of switching the THz on and off at will in a few hundreds of μ s.

Additionally, two FM layers with orthogonal easy axes generate two perpendicular THz components with a negligible phase difference. By the same principle, switching the magnetization of one layer switches the polarization of the emitted THz by 90° without decreasing the total THz amplitude (Fig. 1b). We simulate the output THz pulse, with a model based on the three-temperature model.

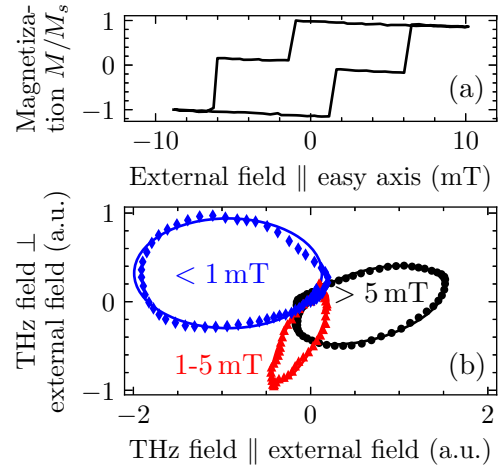


Figure 1: a) Hysteresis loop of a sample with two FM layers. b) Rotation of the THz polarization depending on the external field strength.

[1] T. Seifert, S. Jaiswal, M. Sajadi, G. Jakob, S. Winnerl, M. Wolf, M. Kläui, and T. Kampfrath, *Applied Physics Letters* **110**, 25 (2017).

[2] Y. Liu, Z. Bai, Y. Xu, X. Wu, Y. Sun, H. Li, T. Sun, et al, *Nanotechnology* (2020).

[3] D. Khusyainov, S. Ovcharenko, M. Gaponov, A. Buryakov, A. Klimov, N. Tiercelin, P. Pernod, et al, *Scientific Reports* **11**, 1 (2021).

[4] K. Schlage, L. Bocklage, D. Erb, J. Comfort, H.-C. Wille, and R. Röhlsberger, *Advanced Functional Materials* **26**, 41 (2016).

Magnetic patterning by plasma oxidation of Co/Ni bilayers

Błażej Anastaziak^{1,2}, Rudolf Schäfer³, Ivan Soldatov³, Feliks Stobiecki¹ and Piotr Kuświk¹

¹ Institute of Molecular Physics, Polish Academy of Sciences, Smoluchowskiego 17, Poznań, Poland

² NanoBioMedical Centre, Adam Mickiewicz University, Wszechnicy Piastowskiej 3, Poznań, Poland

³ Leibniz Institute for Solid State and Materials Research (IFW), Helmholtzstraße 20, Dresden, Germany

Local modification of the magnetic properties without significant change in topography is required for many different applications. One of the promising methods to achieve that is plasma oxidation (PO), which enables control of the coercive field and anisotropy of ferromagnetic film [1]. This is particularly important for materials with perpendicular magnetic anisotropy (PMA) along with low damping and high spin polarization. These materials include Co/Ni bilayers, for which we have shown that the PO may enforce PMA and exchange bias coupling. Both effects appear due to the formation of antiferromagnetic oxide as a result of Ni oxidation, wherein for shorter oxidation time, the PMA is also supported by the reduction of the Ni thickness [2]. This shows that PO can serve as a tool to tune the magnetic properties of Co/Ni films, since the coercivity, magnetic anisotropy, and its easy axis can be tailored by a variation of oxidation time and thickness of the Co and the Ni layers.

This opens up a way to apply this method for magnetic patterning. Here, the local modification is achieved by PO through a photoresist mask, with the thickness of the resist been properly tuned. Using this approach, we have fabricated regular square patterns embedded in a matrix, where the magnetic state of matrix and squares can be controlled by the thickness of the Ni layer and the oxidation time. Figure 1 shows an example of such patterning, where matrix and square have PMA with different coercive fields.

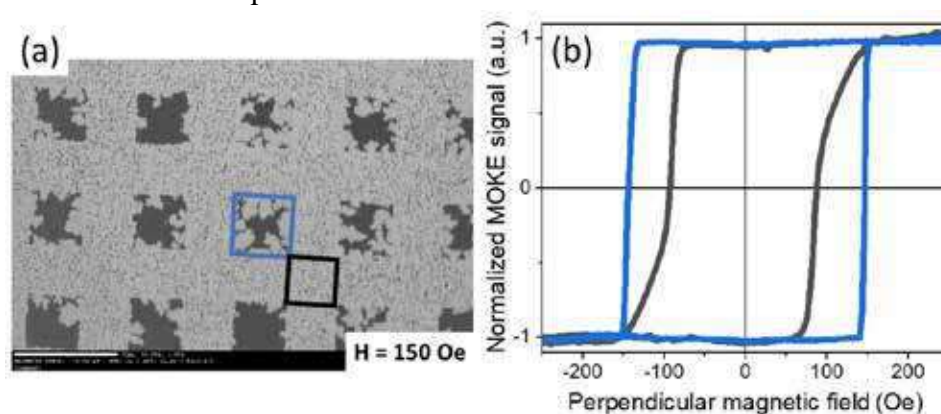


Figure 1 Magnetic patterning by plasma oxidation of Ti4nm/Au60nm/Co1nm/Ni2nm system: (a) domain structure registered at $H=150$ Oe, (b) magneto-optical Kerr effect hysteresis loop measured for two different areas marked on panel (a): matrix - protected from oxidation (black line) and square - modified by Ni oxidation (blue line). Oxidation time was set to 220s.

This work was supported by National Science Centre Poland under OPUS project (UMO-2019/33/B/ST5/02013). B.A. acknowledges support from the project “Środowiskowe interdyscyplinarne studia doktoranckie w zakresie nanotechnologii” POWR.03.02.00-00-I032/16.

[1] B. Dieny and M. Chshiev, *Rev. Mod. Phys.* **89**, 025008 (2017).

[2] B. Anastaziak, H. Głowiński, M. Urbaniak, Ł. Frąckowiak, F. Stobiecki, P. Kuświk, *Phys. Status Solidi RRL*, 2100450 (2021).

Fabrication of rare-earth free permanent magnets for MEMS applications: magnetophoresis assembly of Co nanorods

Ilona Lecerf^{1,2}, Antoine Gonon^{1,3}, Thierry Ondarçuhu³, David Bourrier², Liviu Nicu², Thierry Leïchlé⁴, Nora Dempsey⁵, Thomas Blon¹, Lise-Marie Lacroix¹

¹ Laboratoire de Physique de Chimie des Nano-Objets, Université de Toulouse, France

² LAAS-CNRS, Toulouse, France

³ Institut de Mécanique des Fluides de Toulouse, Université de Toulouse, France

⁴ Georgia Tech-CNRS Joint International Laboratory, Atlanta, GA, USA

⁵ Institut Néel, Université Grenoble Alpes, France

Permanent magnets are needed in many portable devices such as MEMS sensors or actuators for telecommunication, biomedical and automotive applications. Currently, the main obstacle to the development of these micro-devices is the lack of efficient sub-millimeter permanent magnets compatible with microfabrication methods.

A new bottom-up approach, depicted in Figure 1 has been developed at the LPCNO which

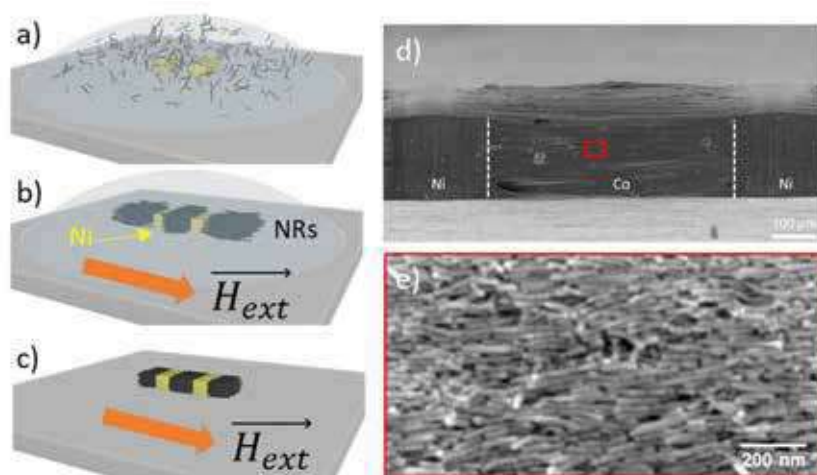


Figure 1: (a,b,c) Schematic views of the successive steps of the fabrication process of magnetic material c) Optical image of the Co NR based-magnet obtained between Ni blocks and d) SEM enlarged view of the aligned Co NRs composing the magnet.

consists in assembling single-crystalline cobalt nanorods (NRs) of 15 nm in diameter and 200 nm in length obtained by a wet-chemistry approach [1]. A concentrated suspension of Co NRs is drop casted on a substrate decorated with electrodeposited Ni blocks. The NRs are oriented thanks to an external magnetic field and attracted towards the high magnetic field

gradient regions generated by the Ni blocks due to magnetophoretic force. Then capillary forces occur during the drying of the solution and allows to form a dense assembly of controlled size and shape exhibiting good magnetic properties ($\mu_0 H_C > 0.5\text{T}$ and $B_r > 0.4\text{T}$) [2]. Due to the submillimeter dimension of the obtained in-plane magnet, large stray fields are induced at a long-range (80mT at a distance of 100 μm) allowing the electromagnetic actuation of a gravimetric MEMS sensor [2].

We are now studying the fabrication of out-of-plane magnet using a similar magnetophoresis approach. Arrays of compact assemblies of nanorods aligned perpendicularly to the substrate were recently obtained, opening promising perspectives for other applications such as electromagnetic energy harvesters [3].

[1] E. Anagnostopoulou *et al.* *Nanoscale* **8**, 4020-4029 (2016)

[2] P. Moritz *et al.*, *ACS Nano* **15**, 5096-5108 (2021)

[3] M. Han *et al.*, *Sensor and actuator A: Physical* **219**, 38-46 (2014)

Laser powder bed fusion of (Pr,Nd)-Fe-Cu-B Permanent Magnets

J. Liu¹, L. Schäfer¹, H. Merschroth², J. Harbig², Y. Yang³, M. Weigold², S. Barcikowski³, O. Gutfleisch¹ and K. Skokov¹

¹ Functional Materials, Department of Material Science, Technical University of Darmstadt, Alarich-Weiss-Str. 16, 64287, Darmstadt, Germany

² Institute of Production Management, Technology and Machine Tools, Department of Mechanical Engineering, Technical University of Darmstadt, Otto-Berndt-Straße 2, 64287, Darmstadt, Germany

³ Faculty of Chemistry, Technical Chemistry I and Center for Nanointegration Duisburg-Essen (CENIDE), University of Duisburg-Essen, Universitätsstr. 7, 45141 Essen, Germany

Additive Manufacturing (AM) of permanent magnets is an upcoming and challenging task in material science and engineering. The binder-free AM technique, Laser Powder Bed Fusion (L-PBF) allows for the fabrication of fully-dense and functionalized components with complex geometry. Obtaining a microstructure necessary for high coercivity is however difficult by L-PBF. The well-known Nd-Fe-B system consists of magnetically decoupled 3-10 μm grains of the hard magnetic $\text{RE}_2\text{Fe}_{14}\text{B}$ (RE = Rare earth element) phase, isolated from each other by a finely distributed RE-rich phase, leading to the highest performance of all magnets around room temperature. L-PBF is normally annihilating this specific microstructure. In order to achieve the desired microstructure and hard magnetic properties after printing, we propose here Pr-Fe-Cu-B based alloy as a useful alloy system [1] and compare this with its Nd-based counterpart. Pr-Fe-Cu-B is known for its high coercivity in bulk state and the formation of, besides others, the uncommon intermetallic $\text{Pr}_6\text{Fe}_{13}\text{Cu}$ grain boundary phase. We show here a novel microstructure stable for additive manufacturing with high coercivity.

Our studies describe the Pr-Fe-Cu-B alloys and their post heat treatment optimization for L-PBF. A wide compositional region in the Pr-Fe-Cu-B system was characterized and qualified regarding the magnetic properties throughout the process chain. In order to achieve an improved flowability and refined microstructure, the grain boundary engineering with nanoparticles (NPs) shows a great potential. The nanoparticle functionalized Pr-Fe-Cu-B powder was validated as precursor for AM. During L-PBF, the hypothesis of heterogeneous nucleation induced by NP inoculums during re-solidification is explored with the goal of suppressing grain coarsening and realizing more uniaxial growth.

We acknowledge the support of the Collaborative Research Centre/Transregio 270 HoMMage.

[1] L. Schäfer, K. Skokov, J. Liu, M. Maccari, T. Braun, S. Riegg, I. Radulov, J. Gassmann, H. Merschroth, J. Harbig, M. Weigold, O. Gutfleisch, Design and Qualification of Pr-Fe-Cu-B Alloys for the Additive Manufacturing of Permanent Magnets, *Advanced Functional Materials*: 2102148.

Weak ferromagnetism linked to the high-temperature spiral phase of YBaCuFeO₅

J. Lyu¹, M. Morin^{1,2}, T. Shang^{1,3}, M. T. Fernández-Díaz⁴ and M. Medarde¹

¹ Laboratory for Multiscale Materials Experiments, Paul Scherrer Institut, 5232 Villigen PSI, Switzerland

² Excelsus Structural Solutions (Swiss) AG, PARK innovAARE, 5234 Villigen, Switzerland

³ Key Laboratory of Polar Materials and Devices (MOE), School of Physics and Electronic Science, East China Normal University, Shanghai 200241, China

⁴ Institut Laue Langevin, 71 avenue des Martyrs, CS 20156, 38042 Grenoble CEDEX 9, France

Frustrated magnets with spiral magnetic phases are currently intensively studied owing to their ability for inducing ferroelectricity. This could potentially be exploited in spintronics and low power memories devices.[1-2] However, the low magnetic order temperatures (typically < 100 K) in most of frustrated magnets greatly restrict their fields of application. An additional disadvantage is that most of them are antiferromagnetic, making the reading and controlling the spiral chirality directly related to the electric polarization quite challenging.

Recently, materials design strategies based in the chemical disorder and lattice control of the magnetic interactions lead to spectacular progress in this direction, allowing to tune the stability range of the spiral phases in Cu/Fe layered perovskites AA'CuFeO₅ far beyond RT.[3-5] However, the influence of magnetic field on the magnetic structures especially spiral phases, imperative for further cross-control of the magnetic and ferroelectric orders, is barely known.

Here, we report a comprehensive description of the evolution of magnetic order in the layered perovskite YBaCuFeO₅ under the application of magnetic fields up to 9 T and at temperatures between 1.5 K and 300 K. Using bulk magnetization measurements and neutron powder diffraction we could reveal the presence of three distinct magnetic phases within this H-T range. More importantly, our investigation uncovers the presence of weak ferromagnetism exclusively that coexists with the spiral modulation, suggesting a significant degree of coupling between the two types of orders. Given that the weak ferromagnetism component can be switched with modest magnetic fields, this result offers new perspectives for the manipulation of the spiral orientation, directly linked to the polarization direction, as well as a possible future use of this material in technological applications. [6]

[1] W. Eerenstein et al., *Nature* **442**, 759 (2006).

[2] T. Kimura et al., *Nature* **426**, 55 (2003).

[3] M. Morin et al., *Phys. Rev. B* **91**, 064408 (2015).

[4] M. Morin et al., *Nat. Commun.* **7**, 1 (2016).

[5] T. Shang et al., *Sci. Adv.* **4**, eaau6386 (2018).

[6] Lyu, J. et al. *Phys. Rev. Res.* **4**, 023008 (2022).

Effect of bending strain on magnetic anisotropy in epitaxial ferrite thin films on mica

Darla Mare¹, Zheng Ma^{1,3}, Vassil Skumryev², Florencio Sánchez¹, Nico Dix¹ and Martí Gich¹

¹ Institut de Ciència de Materials de Barcelona (ICMAB-CSIC), Bellaterra 08193, Barcelona, Spain.

² Institució Catalana de Recerca i Estudis Avançats (ICREA), Barcelona 08010, Spain.

³ Universitat Autònoma de Barcelona, Departament de Física, Bellaterra 08193, Spain.

The stabilization of functional magnetic oxides on flexible substrates is not only appealing for novel flexible electronics, but also allows the detailed study of the influence of bending strain on the magnetic properties of these materials. We are interested in investigating the strain dependence of the magnetic anisotropy in two distinct iron oxides, namely magnetite (Fe_3O_4) and the high anisotropy metastable epsilon iron oxide ($\epsilon\text{-Fe}_2\text{O}_3$) [1]. Both were stabilized by pulsed laser deposition on synthetic fluorophlogopite mica substrates. Magnetite is a well-known cubic spinel ferrite, while $\epsilon\text{-Fe}_2\text{O}_3$ has a low symmetry $\text{Pna}2_1$ orthorhombic structure. We will show the optimization of the growth parameters together with a precise microstructural analysis via X-ray diffraction combining standard omega-2theta, pole figures and reciprocal space mapping. We determined that the spinel phase grows with (LLL) texture and the twinning in magnetite is strongly reduced as only one domain could be identified. On the other hand, epsilon iron oxide shows the formation of three distinct in-plane domains, with out-of-plane (00L) texture. The tight bonding of the epitaxial film to the flexible mica substrate allows a simple approach to test the tunability of the magnetocrystalline anisotropy, by bending the substrate one induces a lattice deformation of the films. Here, we investigate the effect of tensile and compressive bending strain at room temperature and below. We revise the effect of the bending geometry and therefore the film-field orientation by comparing $M(T)$ curves and $M(H)$ hysteresis loops from tensile to compressive strain. The influence on the in-plane and out-of-plane magnetic anisotropy for different measurements is compared for the two iron oxide phases. Interestingly, magnetite thin films show a clear dependence on different bending states displaying changes in the coercive field (figure 1a), remnant/saturation magnetization ratio and Verwey transition. Nevertheless, in contrast other reports [2,3] $\epsilon\text{-Fe}_2\text{O}_3$ thin films only show weak variations of

the magnetic properties with bending strain, and no change can be observed in the hysteresis loops nor on low temperature magnetic transitions (figure 1b). We discuss these discrepancies in connection to the geometry of the measurements as a source of artifacts.

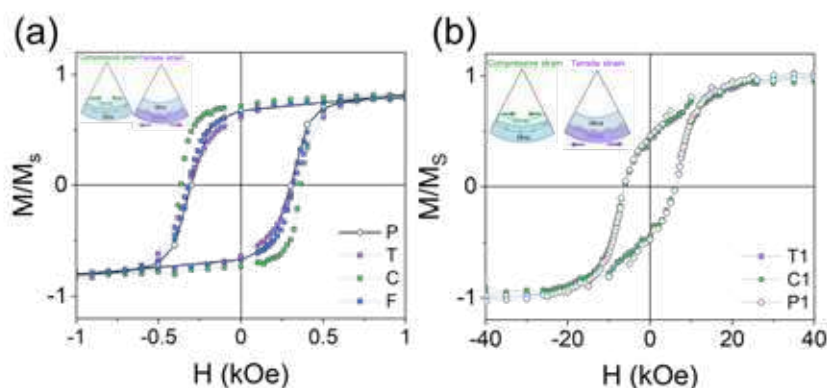


Fig 1: (a) MH loops for the bending states of magnetite thin films.

(b) MH loops for the bending states of epsilon iron oxide thin films.

("P", "T", "C", "F" represents respectively: pristine, tensile, compressive, flattened strain states)

[1] Gich et al., *Journal of App. Physics* (2005), 98, 044307.

[2] P. Wu et al., *ACS Appl. Mater. Interfaces* (2016), 8, 49, 33794–33801.

[3] T. Amrillah et al., *ACS Appl. Mater. Interfaces* (2021), 13, 14, 17006–17012.

Nucleation and current-induced bubble structures motion in PMA multilayers

J. Marqués-Marchán¹, R. Guedas², M.C. Pérez Carmona¹, J.L. Prieto², A. Asenjo¹

¹*Instituto de Ciencia de Materiales de Madrid, CSIC, C/Sor Juana Inés de la Cruz 3, 28049, Spain*

²*Instituto de Sistemas Optoelectrónicos y Microtecnología (ISOM), Universidad Politécnica de Madrid, Avda. Complutense 30, Madrid, E-28040, Spain*

Perpendicular Magnetic Anisotropy (PMA) multilayers have been intensely studied in the past due to their applications in magnetic recording [1]. More recently, this kind of materials has renewed its interest due to the discovery of the DMI (Dzyaloshinskii-Moriya Interaction) that appears in the interfaces of ferromagnetic and heavy metals multilayers [2]. DMI interaction promotes the development of exotic configurations so called “skyrmions” and bubbles of great interest in spintronics [3].

In this work, CoPt nanostructures with different shapes and sizes are fabricated by electron beam lithography. The CoPt multilayers are grown by sputtering over Si/SiO₂ substrates. Apart from the macroscopic characterization of the CoPt thin films, the nanostructures have been studied by AFM (Atomic Force Microscopy) and MFM (Magnetic Force Microscopy). The goal of this work is to control the nucleation, motion and annihilation of the magnetic bubbles by applying external magnetic fields and current. Nanometer size magnetic bubbles are created in these PMA multilayer nanostructures as demonstrated by the MFM imaging experiments. Besides the MFM imaging in remanent state, a Variable Field MFM system has been used to obtain images under in-plane or out of plane magnetic fields [4]. By applying an in-situ out of plane magnetic field in the VF-MFM system, we are able to control the density of bubbles due to their annihilation. The shape and the size of the bubbles is also analyzed as well as the dependence with the geometry of the nanostructures.

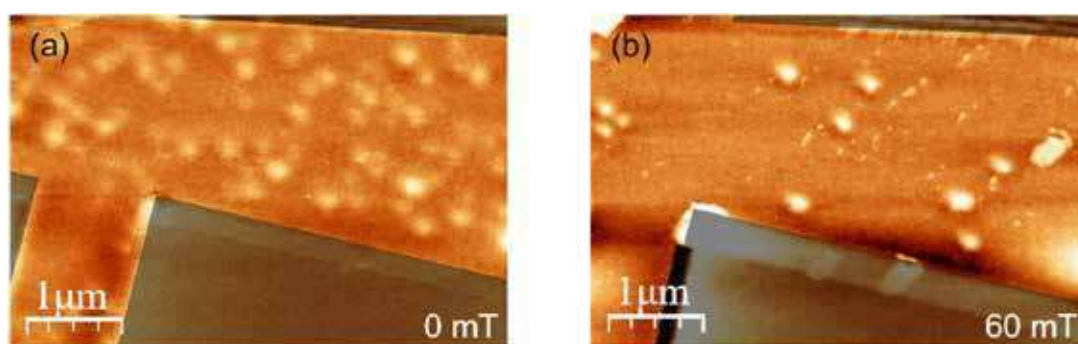


Figure 1. MFM images in remanence of a selected area of a nanostructure (a) after the nucleation of the bubbles and (b) after applying a perpendicular field of 60 mT antiparallel to the bubble magnetic moment.

- [1] A. Kirilyuk et al., *Journal of Magnetism and Magnetic Materials*, 171, 45-63 (1997)
- [2] T. Moriya, *Physical Review*, 120(1), 91-98 (1960)
- [3] J. Sampaio et al., *Nature Nanotechnology*, 8, 839-844 (2013)
- [4] M. Jaafar et al., *Ultramicroscopy*, 109(6), 693-699 (2009)

Control of magnetoelastic coupling in Ni/Fe multilayers using He^+ ion irradiation

G. Masciocchi^{1,2}, J. W. van der Jagt^{3,4}, M.-A. Syskaki^{1,5}, J. Langer⁵,
B. Borie³, G. Jakob¹, A. Kehlberger², D. Ravelosona^{3,6} and M. Kläui¹

¹*Institute of Physics, Johannes Gutenberg University Mainz, Staudingerweg 7, 55099 Mainz, Germany*

²*Sensitec GmbH, Walter-Hallstein-Straße 24, 55130 Mainz, Germany*

³*Spin-Ion Technologies, 10 boulevard Thomas Gobert, 91120 Palaiseau, France*

⁴*Université Paris-Saclay, 3 rue Juliot Curie, 91190 Gif-sur-Yvette, France*

⁵*Singulus Technologies AG, Hanauer Landstrasse 107, 63796 Kahl am Main, Germany*

⁶*C2N, CNRS, Université Paris-Saclay, 10 boulevard Thomas Gobert, 91120 Palaiseau, France*

The magneto-elastic properties of thin films are of great relevance for technological applications as well as of interest for scientific investigations. The requirements for the magnetoelastic coefficient are often demanding. For example, magnetic sensors mostly require strain immunity, while actuators require giant strain effects. One way to obtain the desired value of the saturation magnetostriction (λ_s), is to use the combination of two or more materials with different magnetic and magnetoelastic properties in a multilayer fashion [1]. However, the presence of roughness at the interfaces of sputtered films makes this task even more challenging.

In this study, we investigate the effects of post-growth 20 keV He^+ irradiation on the magneto-elastic properties of a $[\text{Ni}(2\text{ nm})/\text{Fe}(2\text{ nm})] \times 8$ multi-layered stack. The progressive intermixing caused by He^+ irradiation at the interfaces of the multilayer [2], allows us to progressively change the saturation magnetostriction value with increasing He^+ fluences up to $1 \times 10^{16} \text{ cm}^{-2}$, and even to induce a reversal of magnetostriction sign. Additionally, we identify the fluence where the absolute value of the magnetostriction is dramatically reduced, nearly reaching insensitivity to strain of the magnetic stack (Fig. 1).

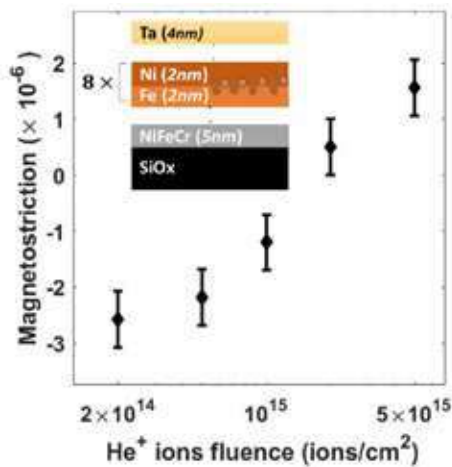


Figure 1: Saturation magnetostriction of a $[\text{Ni}(2\text{ nm})/\text{Fe}(2\text{ nm})] \times 8$ multilayer as a function of He^+ ions fluence during irradiation.

We attribute all the above mentioned effects to the combination of the negative saturation magnetostriction of sputtered Ni, Fe layers and the positive magnetostriction of the $\text{Ni}_x\text{Fe}_{1-x}$ alloy at the intermixed interfaces, whose thickness is gradually increased by irradiation. Importantly, we verify that our treatment causes no structural damages, confirming that post-growth He^+ ion irradiation is an excellent tool to tune the magneto-elastic properties of magnetic samples.

[1] Y. Nagai, M. Senda, and T. Tushima, *J. Appl. Phys.* **63**, 1136–1140 (1988).

[2] J. Fassbender, D. Ravelosona, and Y. Samson, *J. Phys. D* **37**, R179 (2004).

Influence of Antidots Form on Ferromagnetic Resonance Response

S. Nedukh¹, G. Kharchenko¹, S. Tarapov^{1,2}, S. Bunyaev³, Z. Çapku⁴, F. Yıldız⁴

¹*O.Ya. Usikov Institute for Radiophysics and Electronics of NAS of Ukraine, Ac. Proskury str.12, 61085 Kharkiv, Ukraine*

²*V.N. Karazin Kharkiv National University, sq. Svobody, 4, 61022 Kharkiv, Ukraine*

³*IFIMUP-IN/Departamentode Física Universidade do Porto, Rua do Campo Alegre, 687, 4169-007 Porto, Portugal*

⁴*Gebze Technical University, Physics Department, Cumhuriyet, 2254, 41400 Gebze, Turkey*

It is well known that arrays of antidots are a widely used model system for studying the properties of nanostructured magnets [1, 2].

A set of samples of Py magnetic antidots with slots of various sizes arrays was experimentally investigated in microwaves (6-10 GHz) range by FMR. The measurements were carried out in such wide frequency range with using a Rosenberg manufactured coplanar transmission line in 3 orientations between the antidot symmetry axis and the external magnetic field (Fig. 1): 0° , 45° , 90° .

In the case of the antidots with slots or the sample is rotated, the broadening or certain splitting of the FMR resonance peak was observed.

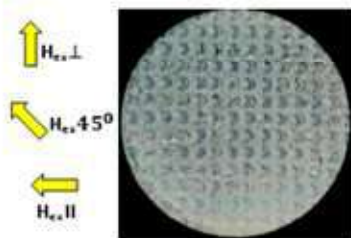


Figure 1: Microscope photo of experimental sample

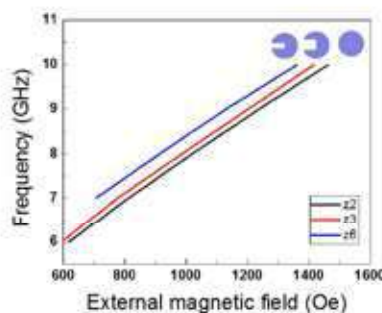


Figure 2: Resonance frequency-field dependence for three samples in the range of 6-10 GHz in perpendicular orientation.

Resonance frequency-field dependences for investigated samples allows us to see that these dependences are almost linear with the same slope angle. There is a field shift between these dependences in accordance with the notation in Fig. 2.

The numerical simulation of the equilibrium distribution of saturation magnetization in the magnetized state as well as the high-frequency response on the external high-frequency excitation for all samples was carried out using the Mumax3 software.

The analysis indicates similar changes in the peak shape for samples with the slot. As a rule, both in the experiment and in the simulation, this leads to peak splitting and broadening.

It is likely, that formation of some local regions in samples with slots, where the perpendicular to the external magnetic field component of saturation magnetization is present, is the main reason for the distortion of the FMR peak shape and the angular dependence of the FMR frequency.

[1] A. S.Silva, A.Hierro-Rodriguez, S. A.Bunyaev, et.al., *AIP Advances* **9**, 3 (2019).

[2] R. V. Verba, D. Navas, A. Hierro-Rodriguez, et.al., *Phys. Rev. Applied* **10** (2018).

Imprinting magnetic micropatterns through geometrical transformation

Volker Neu¹, Ivan Soldatov¹, Rudolf Schäfer¹, Dmitriy, D. Karnaushenko^{1,2}, Alaleh Mirhajivarzaneh¹, Daniil Karnaushenko^{1,2}, and Oliver G. Schmidt^{1,2,3,4}

¹ Leibniz IFW Dresden, 01069 Dresden, Germany

² Center for Materials, Architectures and Integration of Nanomembranes (MAIN), TU Chemnitz, 09126 Chemnitz, Germany

³ Material Systems for Nanoelectronics, TU Chemnitz, 09107 Chemnitz, Germany

⁴ Nanophysics, Faculty of Physics, TU Dresden, 01062 Dresden, Germany

The functionality of a ferroic device is intimately coupled to the configuration of domains, domain boundaries and the possibility for tailoring them [1,2]. We developed a novel approach which allows the creation of new, metastable multidomain patterns with tailored wall configurations through a self-assembled geometrical transformation [3]. The central idea is to bring the 2D layer architecture into an intermediate rolled up 3D tube state with multiple windings in which a simple homogeneous field magnetizes the structure. After unrolling, a multi-domain configuration is achieved (Fig. 1a). To realize the above idea, the magnetic layer is prepared on a so-called polymeric platform (PP), which consists of sacrificial layer, hydrogel as a swelling layer and a stiff polyimide layer. It allows a self-assembled, repeatable geometrical transition in aqueous solution by simple control of the pH-value [4]. Figure 1b displays a [Co/Pt]₅ multilayer sample with perpendicular magnetic anisotropy rolled into a 90 μm diameter tube. After saturation and partial magnetization reversal in a homogeneous field, a regular stripe pattern is imprinted (Fig. 1c). The field history leads to two basic out-of-plane domains per winding after saturation, in which oppositely magnetized domains are additionally imprinted during the partial reversal. The positions of the inner domain transitions (Fig. 1d) encode the angle dependent switching for the given reversal field. The process is linked to the employed magnetic anisotropy with respect to the surface normal, and the geometrical transformation connects the angular with the lateral degrees of freedom. This combination offers unparalleled possibilities for designing new magnetic or other ferroic micropatterns

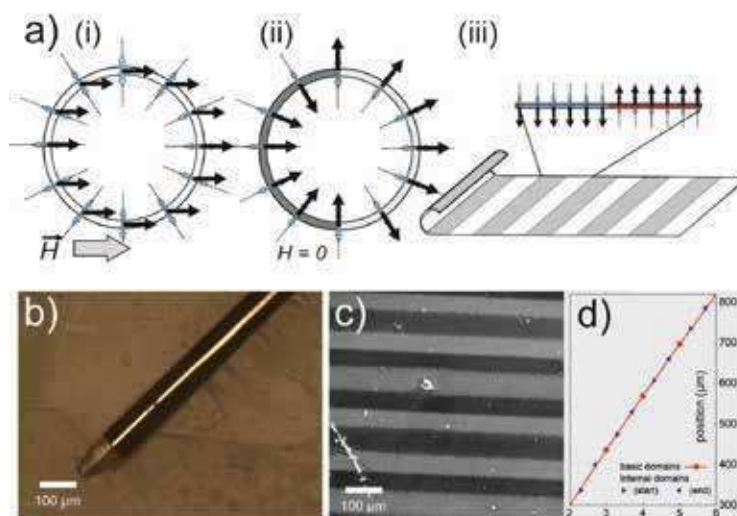


Figure 1: Imprinting magnetic textures. (a) (i) rolled film with perpendicular magnetic anisotropy exposed to a magnetic field, and (ii) after relaxing into the remanent state; (iii) after unwinding, a bipolar magnetic texture is imprinted. (b) [Co/Pt]₅ on PP in rolled state. (c) Magnetic texture after unwinding (Kerr observation). (d) Analysis of domain coordination.

[1] A. Sarella, A. Torti, M. Donolato, M. Pancaldi, P. Vavassori, *Adv. Mater.* **26**, 2384 (2014).

[2] K. Wagner, A. Kákay, K. Schultheiss, A. Henschke, T. Sebastian and H. Schultheiss, *Nat. Nanotechnol.* **11**, 432 (2016).

[3] V. Neu, I. Soldatov, R. Schäfer, D.D. Karnaushenko, A. Mirhajivarzaneh, D. Karnaushenko, O.G. Schmidt, *Nano Letters* **21**, 9889 (2021).

[4] D. Karnaushenko, N. Münzenrieder, D.D. Karnaushenko, B. Koch, A.K. Meyer, S. Baunack, L. Petti, G. Tröster, D. Makarov, and O.G. Schmidt. *Adv. Mater.* **27**, 6797 (2015).

Complex spin structures of ultrathin Fe/Ir films on Re(0001)

Felix Nickel¹, Soumyajyoti Haldar¹, and Stefan Heinze¹

¹*Institute of Theoretical Physics and Astrophysics, University of Kiel, Germany*

Topologically protected states in superconductors such as Majorana bound states are of great interest due to their potential application in quantum computing. Theoretical studies show that noncollinear magnetic structures in the vicinity of an *s*-wave superconductor can form a host for topologically protected states in the band gap of the superconductor [1]. The topological properties in such magnet-superconductor-hybrid (MSH) systems depends critically on the spin structure in the magnetic layers [2]. This makes MSH systems with tunable magnetic properties promising for the manipulation of topologically protected states.

On the route toward the realisation of such systems we study from first-principles the magnetic properties of ultrathin transition-metal films consisting of an Fe monolayer on one to four atomic layers, *n*, of Ir on the Re(0001) surface: Fe/Ir-*n*/Re(0001). This system is very promising, as Re is a superconductor with a critical temperature of $T_c = 1.7$ K and Fe/Ir(111) is known for the formation of complex spin structures [3]. Experimentally Fe/Ir-*n*/Re(0001) has already been investigated using spin-polarized scanning tunneling microscopy [4]. Those experiments revealed an intriguing dependence of the magnetic ground state in the Fe layer on the thickness of the Ir spacer. For $n = 1, 2$ and 4 a Néel state has been proposed as the ground state [4]. Surprisingly, systems with three layers of Ir exhibit a quadratic magnetic unit cell on the hexagonal atomic lattice for one of two possible stackings of the Fe layer. This could make this system a second example of a spontaneous nanoskyrmion lattice similar to that of Fe/Ir(111) [3]. For the other Fe stacking a stripe contrast was observed [4], however, the magnetic structure remained unclear.

In order to investigate the magnetic interactions in Fe/Ir-*n*/Re(0001), we have performed density functional theory calculations using the FLEUR and VASP code for various stacking sequences of the layers and different collinear and non-collinear magnetic configurations including the effect of spin-orbit coupling. We extracted the magnetic interactions by mapping our total energy calculations to an atomistic spin model in order to understand the mechanisms which induce the different magnetic ground states. On the one hand, we aim to reveal the ground states in the system Fe/Ir-3/Re(0001) for both possible stackings of the Fe layer. Up to now only the size of the magnetic unit cells is known. On the other hand, we want to explain the dependence of the magnetic groundstate on the layer thickness of Ir and the stacking sequences of the individual layers.

- [1] W. Chen, *et al. Phys. Rev. B* **92**, (2015).
- [2] E. Mascot *et al. npj Quantum Materials* **6**, (2021).
- [3] S. Heinze, *et al. Nature Phys.* **7**, (2011).
- [4] A. Kubetzka, *et al. Phys. Rev. Materials* **4**, (2020).

Synthesis and characterization of $\text{Fe}_3\text{O}_4@\text{MgO}@\text{CoFe}_2\text{O}_4$ core/shell/shell magnetic nanoparticles

J.M. Nuñez^{1,2,3,4*}, S. Hettler², E. Lima Jr.³, G. F. Goya¹, R.D. Zysler^{3,4}, M.H. Aguirre^{1,2}, E.L. Winkler^{3,4}

¹ *Instituto de Nanociencias y Materiales de Aragón, INMA-CSIC & Dept. Física de la Materia Condensada, Universidad de Zaragoza, C/ Mariano Esquillor s/n, Zaragoza, Spain*

² *Laboratorio de Microscopías Avanzadas, Universidad de Zaragoza, Mariano Esquillor s/n, Zaragoza, Spain*

³ *Instituto de Nanociencia y Nanotecnología (CNEA, CONICET) - Centro Atómico Bariloche Av. Bustillo 9500, S.C. de Bariloche, Argentina*

⁴ *Centro Atómico Bariloche (CNEA, CONICET) - Instituto Balseiro (UNCuyo, CNEA), Av. Bustillo 9500, S.C. de Bariloche, Argentina.*

The Core/shell (CS) architecture make possible to combine in the same nanoparticle (NP) different materials, increasing the degrees of freedom to design and manufacture new systems [1]. Recent studies in CS NPs shown that, by systematically varying the shell composition, is possible to fine-tune the magnetic and electrical transport proprieties of these systems [2-3]. In addition, new properties are observed in CS bimagnetic materials due the exchange interaction at the interface [4], as exchange-bias [5] or exchange-spring [6]. In this frame, the design and fabrication of more complex and higher quality NPs is a key factor to develop new multifunctional nanoparticles for advanced applications [1]. In this work we present that high quality core / shell / shell (CSS) NPs can be grown by adapting the seed-mediated growth method proposed by Sun et al [7].

$\text{Fe}_3\text{O}_4@\text{MgO}@\text{CoFe}_2\text{O}_4$ CSS monodispersed NPs were synthesized by thermal decomposition in a three-step process. Their structure and morphology were characterized by different techniques of transmission electron microscopy (TEM) and powder X ray diffraction. By analyzing TEM images, we obtain a monodisperse size distribution whit mean size of (29 ± 6) nm. CSS structure can be confirmed by observing high angular annular dark field scanning transmission electron microscopy (HAADF STEM) images, that shown a dark annular contrast due to the presence of MgO in the inner shell, and from the elemental mapping performed by electron energy lost spectroscopy (EELS) the stoichiometry is corroborated. The magnetic properties were studied from magnetization measurements as a function of the applied field (MvsH) and temperature (MvsT), in a range of $\pm 2.5\text{T}$ and $5\text{K}-380\text{K}$. In field cooling MvsH curves the presence of a bias field was observed below 125K . The results are analyzed in term of the magnetic coupling between the soft Fe_3O_4 and hard CoFe_2O_4 magnetic phases, and the role of the nonmagnetic MgO separator is discussed.

[1] A. López-Ortega, M. Estrader, G. Salazar-Alvarez, A.G. Roca, J. Nogués, J. Phys. Rep., 553 (2015).

[2] G. Lavorato, E. Lima Jr., M. Vasquez Mansilla, H. Troiani, R. Zysler, E. Winkler, J. Phys.Chem.C, 122 (2018).

[3] F. Fabris, E. Lima, C. Quinteros, L. Neñer, M. Granada, M. Sirena, R. Zysler, H. Troiani, V. Leborán, F. Rivadulla y E. Winkler, Physical Review Applied. 11 (2019).

[4] W.H. Meiklejohn, C.P. Bean, Phys. Rev., 102 (1956).

[5] J. Nogués, J. Sort, V. Langlais, V. Skumryev, S. Suriñach, J. Muñoz, M. Baró, Phys. Rep., 422 (2005).

[6] G. Lavorato, E. Winkler, B. Rivas-Murias, F. Rivadulla. Phys. Rev. B, 94 (2016).

[7] S. Sun y H. Zeng, J. Am. Chem. 124 (2002).

Magnetic properties of FeGa/Kapton for flexible electronics

Gajanan Pradhan^{1,2}, Federica Celegato¹, Gabriele Barrera¹, Elena Sonia Olivetti¹, Marco Coisson¹, Jan Hajducek³, Jon Ander Arregi³, Ladislav Čelko³, Vojtěch Uhlíř³, Paola Rizzi², and Paola Tiberto¹

¹ Istituto Nazionale di Ricerca Metrologica (INRIM), Strada delle Cacce 91, 10135, Torino, Italy

² Chemistry Department and NIS, University of Turin, via Pietro Giuria, 7, 10125, Torino, Italy

³ Central European Institute of Technology (CEITEC), Purkyňova 123, Brno 61200, Czech Republic

Magnetostrictive materials possess the potential to be used in wide variety applications such as sensing, straintronic, spintronic devices etc. due to the coupling between the strain and the magnetization. In this context, FeGa which has a very high magnetostrictive constant, high tensile strength and low coercivity proves to be an efficient material for current research. Fe_{100-x}Ga_x thin films with $x = 20\%$ & 30% has high magnetostriction constant with a value of around $3/2\lambda_{100} \approx 180$ ppm [1]. In our report, we have investigated the structural and magnetic properties of as-deposited and stress-induced states of Fe₇₀Ga₃₀ (28 nm)/Kapton films. The effect of stress brings up a significant change in the magnetic properties of magnetostrictive thin films due to mechanical magneto-elastic coupling [2]. The schematic of the deformation in samples is shown in figure 1(a)-(c). The flat state, the concave state and the convex state corresponds to no strain, compressive strain and tensile strain, respectively. Figure 1(d) shows the in-plane hysteresis loops measure with SQUID-VSM at room temperature for flat (red), concave (green) and convex (blue) configurations. It is observed that the value of remanent magnetization M_r increases with decrease in strain i.e., ϵ (concave state) due to compressive strain and decreases with increase in ϵ , the strain percentage due to tensile strain (convex state). Further, angular 360° plot of M_r/M_s values show uniaxial anisotropy in the system as shown in figure 1 (e). Magnetization reversal via domain wall motion was observed along the easy axis using MOKE microscopy.

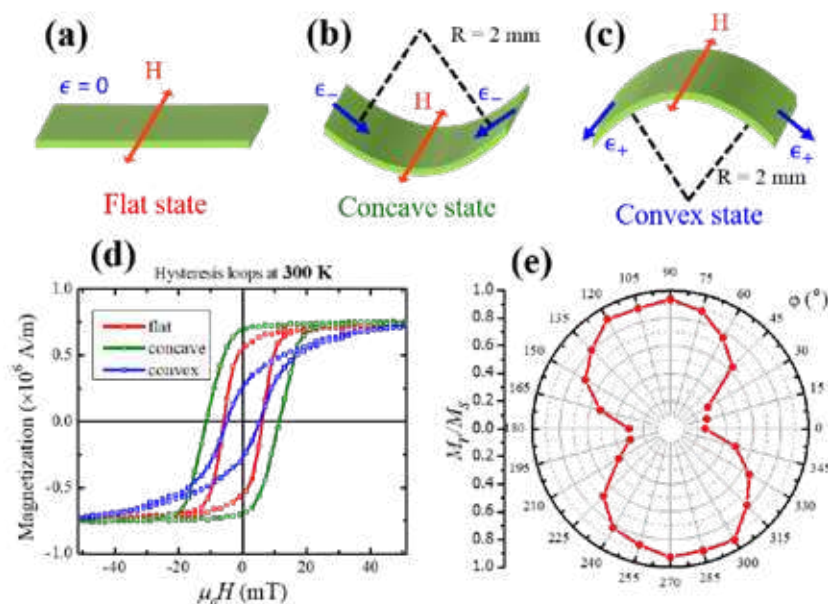


Figure 1: (a) Schematic of FeGa (28 nm)/Kapton for flat (no stress), concave (compressive stress) and convex states (tensile stress) by bending of samples; (b) Magnetic hysteresis curves at room temperature (300 K). (c) M_r/M_s radial plot for the flat state.

- [1] Hattrick-Simpers, Jason R., et al. Applied Physics Letters **93**(10), 102507 (2008)
 [2] G. Dai, et al. Journal of Physics D: Applied Physics **53**(5), 055001 (2019)

Magnetic domain wall pinning in cobalt ferrite microstructures

S. Ruiz-Gómez¹, A. Mandziak², J. E. Prieto³, P. Prieto⁴, C. Munuera⁵, M. Foerster⁶,
A. Quesada⁷, L. Aballe⁶ and J. de la Figuera³

¹ Max Planck Institute for Chemical Physics of Solids, 01069 Dresden, Germany.

² Solaris National Synchrotron Radiation Centre, Krakow 30-392, Poland

³ Instituto de Química Física "Rocasolano," CSIC, Madrid E-28006, Spain

⁴ Dpto. de Física Aplicada, Universidad Autónoma de Madrid, Madrid 28049, Spain

⁵ Instituto de Ciencia de Materiales de Madrid, CSIC, Madrid E-28049, Spain

⁶ Alba Synchrotron Light Facility, Cerdanyola del Valles 08290, Spain

⁷ Instituto de Cerámica y Vidrio, CSIC, Madrid E-28049, Spain

In the last decades, transition metal oxides are growing in importance in spintronic applications. There are many different magnetic oxides, all of them very stable, with a wide range of properties that could allow broadening the range of spintronic applications [1]. Furthermore, the physical properties of these materials can be tuned by reducing the material to the nanoscale, tuning the composition, and/or incorporating it to heterostructures. However, in many cases, growth defects such as antiphase boundaries can strongly affect their magnetic properties, acting as pinning centers for magnetic domain walls. Considering their potential, it is essential to develop growth methods that allow engineering high quality oxide-based epitaxial nanostructures with customizable functionalities [2], as well as to develop the tools to fully characterize them. Extremely high-quality oxide films can be obtained by depositing metals by molecular beam epitaxy on a hot substrate, while the sample is exposed to an oxidizing agent such as molecular oxygen. We have used this method to fabricate ultrathin spinel islands of up to 100 μm^2 area, with nanometer thickness and atomically flat surfaces. By this method many spinel islands (CoFe_2O_4 [3], Fe_3O_4 [4] and NiFe_2O_4 [5]) grow from single crystallographic nuclei and are thus expected to be antiphase boundaries-free. The extremely low defect concentration leads to a robust magnetic order and exceptionally large magnetic domains.

Different microscopy techniques can be used to explore the magnetic configuration of these nanoobjects, but few provide information about the vector configuration of the magnetic moments. In this work we use PhotoEmission Electron Microscopy with X-Ray Magnetic Circular Dichroic contrast (XMCD-PEEM) in order to obtain 3D information of the magnetic configuration of in-situ grown single crystal nanometer-thick islands, by acquiring images at different photon beam incidence angles. A careful analysis of the magnetic configuration was done by combining XMCD-PEEM with atomic force microscopy and Low Energy Electron Microscopy (LEEM) maps to explain the experimental magnetic configuration and unravel the mechanism behind the pinning of the domain wall observed.

We will show how performing correlative microscopy is a very powerful tool for the study of magnetic configurations of nanometer sized objects, and how in the case of ultrathin CoFe_2O_4 ferrites, the most prominent pinning mechanism was found to originate from substrate steps.

[1] S. Gariglio, et al. Rep. Prog. 82, 012501, (2019)

[2] S. Farokhipoor et al. Nature, 515, 379, (2015).

[3] L. Martín-García et al. Adv. Mater. 27, 5955, (2015)

[4] S. Ruiz-Gómez, et al. Nanoscale 10, 5566 (2018).

[5] A. Mandziak et al. Scientific reports 8, 1, (2018)

Atomic scale structure rearrangements in $\text{Y}_3\text{Fe}_5\text{O}_{12}$ epitaxial films on GGG(111) substrates explored by HR-STEM

J. Santiso ^{*,1}, C. García ², C. Romanque ², J.M. Caicedo ¹, N. Bagués ³, N. Bernier ⁴ and F. Sandiumenge ⁵

¹ Catalan Institute of Nanoscience and Nanotechnology (ICN2), CSIC and BIST, Campus UAB 08193 Bellaterra, Spain

² Universidad Técnica Federico Santa María, Av. España 1680, Valparaíso, Chile

³ CEMAS, Ohio State University, Columbus, OH, USA

⁴ CEA-Leti, Université Grenoble Alpes, F-38000 Grenoble, France

⁵ Materials Science Institute of Barcelona (ICMAB-CSIC) Campus UAB 08193 Bellaterra, Spain

$\text{Y}_3\text{Fe}_5\text{O}_{12}$ yttrium iron garnet (YIG) is a prototypical ferrimagnetic insulating material with Curie temperature above room temperature exhibiting very low Gilbert damping [1]. Epitaxial YIG films grown in this work by Pulsed Laser Deposition on matching $\text{Gd}_3\text{Ga}_5\text{O}_{12}$ (111) (GGG) single crystals show excellent crystal quality and damping ($\sim 3 \cdot 10^{-4}$) comparable to the best reported values in literature. [2] However, the XRD characterization reveals a substantial elongation of $\sim 1.2\%$ of the out-of-plane cell parameter along the [111] direction with respect bulk YIG d_{111} interplanar distance, while in-plane cell parameters remain clamped to the substrate, indicating a rhombohedral distortion with an apical angle of about ($90^\circ - 0.62^\circ$). The accurate analysis of HAADF-STEM images along with EDX and EELS chemical composition profiles reveals a deviation from the bulk structure affecting the relative intensities of the atomic columns along linear profiles parallel to the [011] direction extracted from the HAADF images (with [01-1] zone axis), as shown in Fig. 1. In the profiles passing through the octahedral $\text{Fe}^{(a)}$ sites (red line in the Figure) there is a sequence with three atomic columns: the central column should correspond to pure $\text{Fe}^{(a)}$ octahedral sites, while adjacent columns alternate $\text{Y}^{(c)}$ dodecahedral and $\text{Fe}^{(d)}$ tetrahedral sites with equal occupancies. However, the ratio of the intensities (proportional to average $Z^{1.7}$) departs largely from the alleged bulk occupancies not only close to the interface but even far from it. This

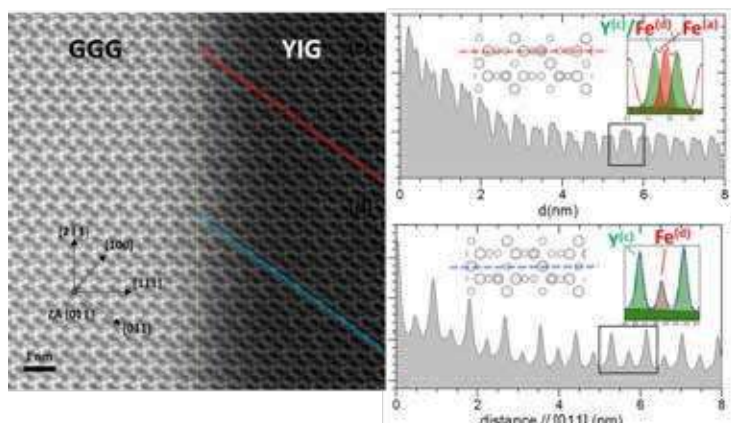


Figure 1: (left) HAADF-STEM image of YIG/GGG with [01-1] zone axis, and (right) intensity profiles parallel to [011] showing either $\text{Y}^{(c)}\text{Fe}^{(d)}/\text{Fe}^{(a)}/\text{Y}^{(c)}\text{Fe}^{(d)}$ or $\text{Y}^{(c)}/\text{Fe}^{(d)}$ sequences.

deviation is discussed in terms of the substitution of Y ions in octahedral sites, and their counterpart Fe substitution in dodecahedral sites (antisite defects) similar to that reported by other authors [3,4]. The observed average cell volume expansion, as well as the slightly enhanced M_{sat} measured for the films, are therefore related to such inherent point defects.

[1] K. Uchida, *et al.*, *Nat. Mater.* **9** (2010) 894–897.

[2] M. C. Onbasli, *et al.*, *APL Mater.*, **2** (2014) 106102.

[3] T. Su, *et al.*, *Phys. Rev. Mater.*, **5** (2021), 94403.

[4] S. Ning, *et al.*, *Nat. Commun.*, **12** (2021) 4298.

Ion implantation induced exchange bias in BCC Fe thin film

Sagar Sen^{1,2}, Ajay Gupta³, V.R. Reddy⁴, Ratnesh Gupta¹

¹ School of Instrumentation, Devi Ahilya Vishwavidyalaya, Khandwa Road Indore-452017, India

² Department of Physics, Maharaja Bhoj Government P.G. College, Dhar-454001, India

³ Centre for Spintronic Devices, Amity University, Noida, India

⁴ UGC DAE CSR Indore Centre, Indore-452017, India

Email sssagarsen@gtmail.com

Exchange bias field is shifting of hysteresis loop along the magnetic field axis when ferromagnetic and antiferromagnetic interfaces coupled and field cooled below the Neel temperature of AFM [1]. The growth of exchange bias in Ferromagnetic films by fluorine ion implantation have been studied by magneto-optical Kerr microscopy and SQUID VSM measurement. The implantation results in the formation of Fe_xF_y embedded in a Fe matrix. Depth profile obtained from secondary ion mass spectrograph of F ion implantations suggested that the implanted Fluorine ion is deposited at the centre of the film, according to the SRIM calculations. From the GIXRD measurements, the pristine film showed a peak corresponding to Fe (110) bcc structure. After ion-implantation, the crystalline size is decreasing as a function of ion fluence. 5×10^{16} ions/cm² and higher ion-fluence induces the exchange bias in the film and it has been increasing with the ion-fluence. Higher ion fluence increased the amount of antiferromagnetic layer which have been increased the exchange bias field value. The saturation magnetic moment of the film has been decreased as a function of ion fluence. The Fe edge absorption spectra suggests that the ratio of the intensity of the L3 and L2 edge peak decreases as a function of F^+ ion fluence. The F K-edge XAS measurement suggests that implantation modified the occupancies of Fe 3d 4s,p level by F 2p hybridization process. The Mössbauer spectrum of pristine film exhibit sharp sextet of α -Fe. As a function of F-ion fluence, the paramagnetic doublets at the center have been evolved and at the ion fluence of 1×10^{17} ions/cm², apart from paramagnetic doublet, a broad hyperfine field distribution has also been observed.

References

[1] J. Nogues and I. K. Schuller, *J. Magn. Magn. Mater.* **192**,203-232(1999).

Interplay of magnetic states and hyperfine fields of iron dimers on MgO(001)

Sufyan Shehada^{1,2,3}, Manuel dos Santos Dias^{4,1}, Muayad Abusaa³, and Samir Lounis^{1,4}

¹*Peter Grünberg Institut and Institute for Advanced Simulation, Forschungszentrum Jülich & JARA, 52425 Jülich, Germany*

²*Department of Physics, RWTH Aachen University, 52056 Aachen, Germany*

³*Department of Physics, Arab American University, Jenin, Palestine*

⁴*Faculty of Physics, University of Duisburg-Essen, 47053 Duisburg, Germany*

Individual nuclear spin states can have very long lifetimes and could be useful as qubits. Progress in this direction was achieved on MgO/Ag(001) via detection of the hyperfine interaction (HFI) of Fe, Ti and Cu adatoms using scanning tunneling microscopy (STM)[1,2]. Previously, we systematically quantified from first-principles the HFI for the whole series of 3d transition adatoms (Sc-Cu) deposited on various ultra-thin insulators (MgO, NaF, NaCl, h-BN and Cu₂N), establishing the trends of the computed HFI with respect to the filling of the magnetic s- and d-orbitals of the adatoms and on the bonding with the substrate[3].

Here we explore the case of dimers by investigating the correlation between the HFI and the magnetic state of free standing Fe dimers, single Fe adatoms and dimers deposited on a bilayer of MgO(001). We find that the magnitude of the HFI can be controlled by switching the magnetic state of the dimers. Furthermore, we demonstrate the ability to substantially modify the HFI by atomic control of the location of the adatoms on the substrate. Our results establish the limits of applicability of the usual hyperfine hamiltonian and we propose an extension based on multiple scattering processes[4].

–Work funded by the Palestinian German Science Bridge (BMBF–01DH16027).

[1] Willke *et al.*, *Science*. **362**, 336 (2018).

[2] Yang *et al.*, *Nat. Nano.* **13**, 1120 (2018).

[3] Shehada *et al.*, *Npj Comput. Mater.* **7**, 87 (2021).

[4] Shehada *et al.*, *arXiv*. **2202.00336** (2022).

Magnetic nanocrystalline CoCrFeNiGa_x ($x = 0.5, 1.0$) high entropy alloys by high energy ball milling

N. F. Shkodich, M. Spasova and M. Farle.

Faculty of Physics and Center of Nanointegration (CENIDE), University of Duisburg-Essen,
47057 Duisburg, Germany

The high energy ball milling (HEBM) in planetary ball mills can yield stable microstructures and nanocrystalline high entropy alloys [1, 2] with better homogeneity compared to other non-equilibrium processes.

We report the successful fabrication of nanocrystalline single *fcc* phase CoCrFeNiGa_x ($x = 0.5, 1.0$) powder particles with good structural and compositional homogeneity by HEBM. The XRD, SEM/EDX (Fig. 1), and TEM/EDX results showed that *fcc* phase with refined microstructure of nanosized grains (~ 10 nm) could be obtained after 190 min of HEBM at 900 rpm.

Based on DSC results the produced HEA powders demonstrated a thermal stability of up to 1273K which is remarkable in regard to the low melting temperature $T_{\text{melt}} = 302.9$ K of Ga.

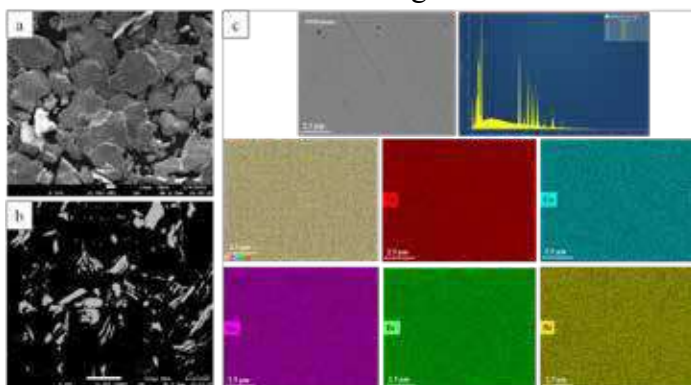


Figure 1: SEM images of CoCrFeNiGa particles produced after 190 min of HEBM at 900/1800 rpm: (a) fracture surface of the particles, (b), (c) - cross-section of particles and EDX mapping.

We used HEBM - produced CoCrFeNiGa_x ($x = 0.5, 1.0$) powders to fabricate *homogeneous* nanocrystalline bulk HEAs by Spark plasma sintering (SPS). SPS at 1073 K of the CoCrFeNiGa_{0.5} powder increased the crystallinity of the *fcc* phase, while for the equiatomic CoCrFeNiGa powder a partial transformation of *fcc* structure into a *bcc* one was observed.

Direct SPS of an elemental powder blend of Co, Cr, Fe, Ni and Ga ingots on the other hand resulted in a less homogeneous compositions.

The obtained nanocrystalline HEA CoCrFeNiGa_x ($x = 0.5, 1.0$) powders showed a paramagnetic behavior at room temperature and a Curie temperature (T_c) is of 130K-150K. After SPS consolidation the equiatomic CoCrFeNiGa bulk material show a ferromagnetic behavior up to $T_c = 735$ -750K. Its saturation magnetization M_s^{FM} (300K) increased by a factor of 10 compared to the one of HEA powder connected to the partial phase transition from a *fcc* to a *bcc* phase. The SPS consolidation at 1073K of CoCrFeNiGa_{0.5} HEA powder, however, did not change its paramagnetic nature at room temperature.

- [1] B.S. Murti, J.W. Yeh, S. Ranganathan, High Entropy Alloys. 2nd ed. London: Elsevier (2019).
- [2] N.F. Shkodich, et al, *J of Alloys and Comp.* **893** 161839, (2021).

This work has been supported by the Deutsche Forschungsgemeinschaft (DFG) within CRC/TRR 270, project S01 (project ID 405553726).

Optimisation of perpendicular magnetic tunnel junction structures using scanning transmission electron microscopy

Meg Smith¹, Charlotte Bull¹, Matthew C. Spink², Paul Nutter¹, Christopher S. Allen^{2,3}, Tom Thomson¹

¹Nano Engineering and Spintronic Technologies (NEST) group, Department of Computer Science, University of Manchester, Oxford Road, Manchester, M13 9PL, UK

²Diamond Light Source Ltd, Diamond House, Harwell Science & Innovation Campus, Didcot, Oxfordshire, OX11 0DE

³Department of Materials, University of Oxford, Oxford, OX1 3PH

Spin-transfer-torque magnetoresistive random access memory (STT-MRAM) and Spin-orbit-torque magnetoresistive random access memory (SOT-MRAM) offer enormous potential as non-volatile data storage technologies due to their scalability, energy efficiency, and fast read/write speed [1]. However, the magnetic recording trilemma, often associated with Hard Disk Drive (HDD) media, remains a problem that must be addressed for the development of ultra-high-density STT/SOT-MRAM [1]. The ability to fabricate high-quality magnetic tunnel junctions (MTJs) in the laboratory is essential if solutions that address the trilemma are to be explored [2]. Whilst MTJs based on MgO tunnel barriers have been commercially produced for many years [3], building successful structures for research remains a significant challenge. Here, we report our work on sputter deposited CoFeB/MgO/CoFeB MTJ stacks, with a CoFeB thickness ≤ 1.5 nm to obtain perpendicular magnetic anisotropy (PMA) and thin continuous layers, essential for good quality MTJs. Scanning transmission electron microscopy (STEM) was used to investigate the structure of fabricated MTJs (Fig.1), showing that all the layers were present but that interfacial roughness led to the MgO layer becoming discontinuous. Optimising the Ta deposition parameters resulted in a smoother seed layer and improved, smoother interfaces. MTJs have been grown at room temperature on Si/SiO₂ (290nm) substrates with the structure (Pt(3nm)/Ta(6nm)/Co₂₀Fe₆₀B₂₀(0.8nm)/MgO(1nm)/Co₂₀Fe₆₀B₂₀(0.7nm)/Ta(6nm)). These MTJs have improved characteristics by optimising the sputter growth conditions of the CoFeB and MgO layers. The thicknesses of the MTJ layers were identified using X-ray reflectivity (XRR), and the magnetic properties were investigated using vibrating sample magnetometry (VSM) (Fig.2). After annealing at 100°C, the MTJs exhibit a strong interfacial PMA, demonstrating the importance of layer quality when growing such structures.

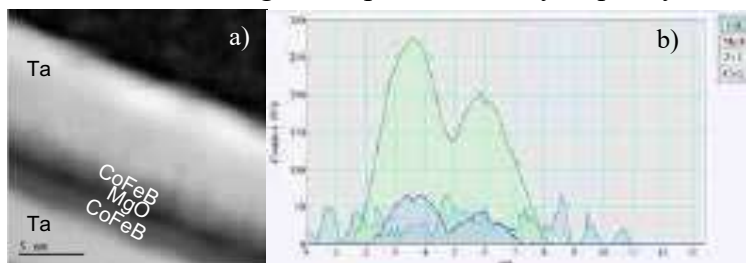


Fig. 1. (a) STEM high-angle annular dark field image showing the individual layers that form the MTJ, showing continuous CoFeB and discontinuous MgO layers (b) Integrated intensity of the electron energy loss spectroscopy core-loss edges taken from a line scan through the MTJ.

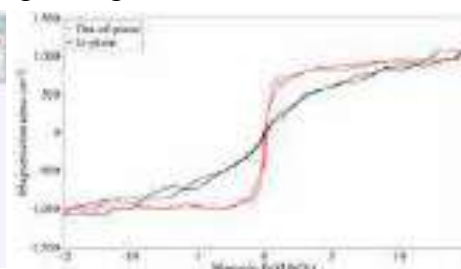


Fig. 2. Magnetic hysteresis loop for an MTJ film annealed to 100°C and measured by VSM, applying a 30kOe field perpendicular (red) and parallel (black) to the sample surface.

[1] D. Apalkov *et al.* Proc. IEEE **104**,1796-1830 (2016).

[2] S. Ikeda *et al.* Appl. Phys. Lett. **93**, 082508 (2008).

[3] Shinya Ota *et al.* Appl. Phys. Express **12** 053001 (2019).

Effect of transition metal doping on magnetic hardness of CeFe₁₂-based compounds

Justyn Snarski-Adamski¹ and Mirosław Werwiński¹

¹*Institute of Molecular Physics, Polish Academy of Sciences,
M. Smoluchowskiego 17, 60-179 Poznań, Poland*

In this work, compositions of CeFe₁₁X (s.g. *Pmmn*, No. 59) and CeFe₁₀X₂ (s.g. *P4/mmm*, No. 123) with all 3d, 4d, and 5d transition metal substitutions are considered. Since many previous studies have focused on the CeFe₁₁Ti compound, this particular case became the starting point of our considerations, and we gave it special attention [1].

First, we determined the optimal symmetry of the simplest CeFe₁₁Ti structure model. Next, we observed that the calculated magnetocrystalline anisotropy energy (MAE) correlates with the magnetic moment, which in turn strongly depends on the choice of the exchange-correlation potential. MAE, magnetic moments, and magnetic hardness were determined for all compositions considered. Moreover, the calculated dependence of MAE on the spin magnetic moment allowed predicting the upper limits of the MAE. We also showed that it does not depend on the choice of the form of the exchange-correlation potential.

The compositions showing very high magnetic hardness include CeFe₁₁W, CeFe₁₀W₂, CeFe₁₁Mn, CeFe₁₀Mn₂, CeFe₁₁Mo, CeFe₁₀Mo₂, and CeFe₁₀Nb₂, which may be unstable, but due to the interesting magnetic properties, they are worth further research in the field of their stabilization, for example by substituting the Ce atom with another rare-earth atom. Further alloying of selected compositions with elements embedded in interstitial positions confirms their positive effect on magnetically hard properties. Calculations carried out for comparison for selected isostructural La compounds lead to similar MAE results as those obtained for Ce compounds, suggesting a secondary effect of 4f electrons. Our preliminary results obtained using the intra-atomic Hubbard repulsion term showed a relatively small difference for CeFe₁₂ compared to the results without the correction. Calculations were performed using the full-potential local-orbital electronic structure code FPLO18 [2], whose unique fully relativistic implementation of the fixed spin moment method allowed the calculation of the MAE dependence of the magnetic moment [3].

References:

- [1] O. Isnard, S. Miraglia, M. Guillot, and D. Fruchart, *J. Alloys Compd.* 275, 637 (1998).
- [2] K. Koepernik, H. Eschrig, *Phys. Rev. B.* 59, 1743 (1999).
- [3] J. Snarski-Adamski and M. Werwiński, *ArXiv.2107.13352 Cond-Mat* (2022)

Acknowledgments: We acknowledge the financial support of the National Science Centre Poland under the decision DEC-2019/35/O/ST5/02980 (PRELUDIUM-BIS 1) and DEC-2018/30/E/ST3/00267 (SONATA-BIS 8).

Influence of the buffer layer on the nanoscale architecture in NdFeB ultrathin films

J. Soler-Morala¹, C. Navío¹, L. Zha^{2,3}, J. Yang^{2,3,4} and A. Bollero¹

¹Group of Permanent Magnets and Applications, IMDEA Nanoscience, 28049, Madrid, Spain

²Beijing Key Laboratory for Magnetoelectric Materials and Devices, Beijing, 100871, China

³State Key Laboratory for Mesoscopic Physics, Peking University, Beijing, 100871, China

⁴Collaborative Innovation Center of Quantum Matter, Beijing, 100871, China

Rare-earth transition metals thin films attract a lot of attention due to their high magnetic anisotropy that makes them excellent candidates for several applications including high density magnetic recording [1], MEMS and actuators [2] and novel spintronic devices [3]. These next-generation permanent magnets require exploring new synthesis paths that move beyond conventional methods and allow a study with a detailed control over composition, interfaces and microstructure [4]. Our study focuses on the understanding of the mechanisms involved in the formation of the Nd₂Fe₁₄B phase in thin films grown by Molecular Beam Epitaxy (MBE). Different buffer layers (Mo and Fe) on MgO (001) have been explored to induce different strains on the NdFeB lattice and influence the magnetic response of the system in a low thickness range of 5-15 nm.

The epitaxial character of the samples has been corroborated by X-Ray Diffraction (XRD) and *in situ* Low Energy Electron Diffraction (LEED) measurements. Magnetic characterization has been carried out by Vibrating Sample Magnetometer (VSM) demonstrating the possibility of inducing a strong magnetic anisotropy in good accordance with the epitaxiality of the films. A thorough stoichiometric and electronic characterization has been carried out by both X-ray and Ultra-Violet Photoelectron Spectroscopy also providing values of the work function of the system which, to authors' knowledge, were not previously reported in the literature. Scanning Electron Microscopy (SEM) shows meaningful differences by changing the underlayer: from arrays of highly oriented nanoislands (Fe underlayer, Fig.1c) to low roughness quasi-continuous films (Mo underlayer, Fig.1d). The understanding and optimization of the nanoscale architecture in these NdFeB thin films is essential when aiming at its integration in novel miniaturized devices (e.g., microdevices for *in vivo* microsurgery applications, as [5]).

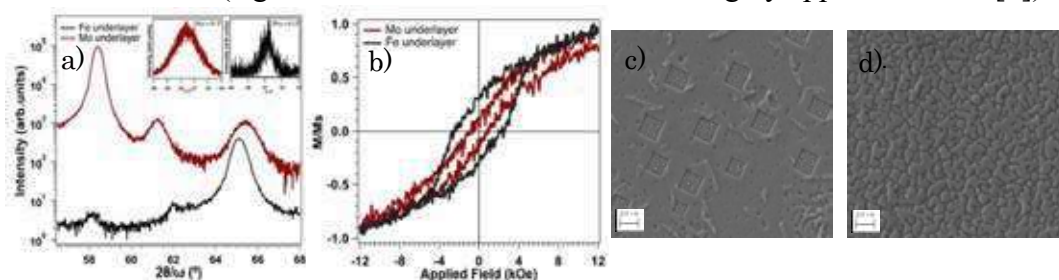


Figure 1: a) XRD pattern of an NdFeB thin film with Fe and Mo underlayer and ω scan of NdFeB (008), b) Out of plane hysteresis loop, c) SEM image of NdFeB with a Fe buffer and d) SEM image of NdFeB with a Mo buffer

[1] X. Liu, T. Okumoto, M. Matsumoto, A. Morisako. *J. Appl. Phys.* **97**, 10K301 (2005).

[2] T.-S. Chin, *J. Magn. Magn. Matter.* **209**, 75-79 (2000).

[3] A. Bollero, V. Neu, V. Baltz *et al.*, *Nanoscale*, **12**, 1155-1163 (2020).

[4] S. Sharma, A. Zintler *et al.*, *ACS Appl. Mater. Interfaces*, **13**, 32415–32423 (2021)

[5] H2020 FET-OPEN project “UWIPOM2”: <https://cordis.europa.eu/project/id/857654>.

Authors acknowledge financial support from EU through the H2020 FET Open UWIPOM2 project (Ref. 857654) and from Comunidad de Madrid through NANOMAGCOST (P2018/NMT-4321). J. S-M. acknowledges financial support from Comunidad de Madrid (PEJD-2019-PRE/IND-17045).

Beating the limitation of the Néel temperature of FeO with antiferromagnetic proximity in FeO/CoO

M. Szpytma¹, A. Koziol-Rachwał¹, N. Spiridis², K. Freindl², J. Korecki², W. Janus¹, H. Nayyef¹, P. Drózd¹, M. Ślęzak¹, M. Zając³ and T. Ślęzak¹

¹ AGH University of Science and Technology, Kraków, Poland

² Jerzy Haber Institute of Catalysis and Surface Chemistry, Polish Academy of Sciences, Kraków, Poland

³ National Synchrotron Radiation Centre SOLARIS, Jagiellonian University, Kraków, Poland

The application of a wide group of antiferromagnets (AFMs) in spintronics is limited due to their low ordering temperature (Néel temperature, T_N). The limitation of low T_N can be overcome with the magnetic proximity effect (MPE) [1, 2]. In our study, we investigated how the MP of CoO influences the magnetic properties of FeO (wüstite) in FeO/CoO bilayers. Magnetic properties of FeO were studied using Conversion Electron Mössbauer Spectroscopy (CEMS). Figure 1 shows CEMS spectra collected for MgO/⁵⁷FeO(1.7 nm)/MgO (Fig. 1(a)) and MgO/⁵⁷FeO(1.7 nm)/CoO(2 nm)/MgO (Figure 1(b)) at 240K, the temperature far above the T_N of bulk FeO (198K). While for wüstite embedded between MgO we noted the spectrum characteristic for the paramagnetic state, for MgO/⁵⁷FeO/CoO/MgO we registered magnetically split spectrum. Systematic measurement of CEMS spectra of MgO/⁵⁷FeO/CoO/MgO recorded as a function of temperature revealed enhancement of the T_N of FeO up to 260K. Our research also shows how the proximity of CoO influences the exchange interaction at Fe/FeO interface in the Fe/FeO/CoO heterostructure. For Fe/FeO/CoO we observed a 500% enhancement in the exchange bias field and a double increase in the blocking temperature compared to the Fe/FeO bilayer. Our results show that the limitation of the low ordering temperature of a seemingly application-useless antiferromagnet can be overcome by antiferromagnetic proximity [3]. This work was supported in part by the National Science Center (NCN), Poland (Grant No. 2020/38/E/ST3/ 00086).

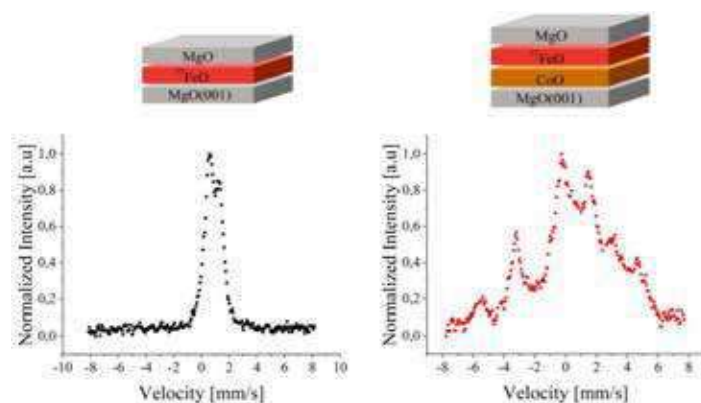


Fig. 1 CEMS spectra collected at 240K on FeO for: a) MgO/⁵⁷FeO(1.7nm)/MgO, b) MgO/⁵⁷FeO(1.7nm)/CoO(2 nm)/MgO [3]

- [1] Q. Li *et al.*, *Sci Rep* **6**, 22355 (2016)
- [2] M. Yang *et al.*, *J. Magn. Magn. Mater.* **460**, 001 (2018)
- [3] A. Koziol-Rachwał *et al.*, *Appl. Phys. Lett.* **420**, 072404 (2022)

Spin orbital reorientation transitions induced by magnetic field

D. Sztenkiel

Institute of Physics, Polish Academy of Sciences, Aleja Lotnikow 32/46, PL-02668, Warsaw, Poland

Here, we report on a new effect similar to the spin reorientation transition (SRT) that takes place at two magnetic fields of B_{SORT1} and B_{SORT2} [1]. Using exact quantum mechanical approach, namely crystal field model (CFM), we simulate the magnetization of small Mn^{3+} clusters in GaN being in the paramagnetic regime. That is, we consider isolated ions, pairs, triplets and quartets coupled by a ferromagnetic superexchange interaction. The magnetization M is computed as a function of the magnetic field \mathbf{B} applied in two (orthogonal) directions with respect to the \mathbf{c} axis of GaN: parallel $\mathbf{B} \parallel \mathbf{c}$ (M_{\parallel}) and perpendicular $\mathbf{B} \perp \mathbf{c}$ (M_{\perp}). The obtained results show, that at low to moderate fields, $|B| < B_{\text{SORT1}}$, a significant magnetic anisotropy with easy axis perpendicular to the \mathbf{c} axis is observed ($|M_{\perp}| > |M_{\parallel}|$). However for $B_{\text{SORT1}} > |B| > B_{\text{SORT2}}$ the magnetic anisotropy seems to reverse its sign, that is $|M_{\perp}| < |M_{\parallel}|$. On increasing B much further the second SRT-like effect appears, resulting in $|M_{\perp}|$ being again larger than $|M_{\parallel}|$ for $|B| > B_{\text{SORT2}}$.

The obtained results suggest that the computed magnetic anisotropy (MA) reverses its sign on increasing magnetic field B across B_{SORT} . A detailed analysis shows however that MA is unchanged for high magnetic fields. We show that the observed effect arises from the interplay of the crystalline environment and the spin-orbit coupling $\lambda \mathbf{SL}$, therefore we name it spin orbital reorientation transition (SORT). The explanation of SORT is given in terms of the spin M_S and orbital momentum M_L contributions to the total magnetization $M = M_S + M_L$.

Importantly, our findings suggest that similar effect should also be present in other materials with not completely quenched (non-zero) orbital angular momentum L , a uniaxial magnetic anisotropy and the positive value of λ . Therefore, we believe that the presented numerical results will constitute the basis for future experimental measurements.

[1] D. Sztenkiel, arXiv:2202.07443

The work is supported by the National Science Centre, Poland, through projects DEC-2018/31/B/ST3/03438 and by the Interdisciplinary Centre for Mathematical and Computational Modelling at the University of Warsaw through the access to the computing facilities.

Picosecond Optospintronic Tunnel Junctions for Non-volatile Photonic Memories^[1]

Luding Wang¹, Weisheng Zhao², Martijn Heck¹ and Bert Koopmans¹

¹Eindhoven Hendrik Casimir Institute, Center for photonic integration, Eindhoven University of Technology, P.O. Box 513, 5600 MB Eindhoven, The Netherlands

²Fert Beijing Institute, Beihang University, 100191 Beijing, China

Perpendicular magnetic tunnel junctions (p-MTJs) are one of the building blocks for spintronic memories, which allow fast nonvolatile data access, offering substantial potential for next-generation nonvolatile memory applications^[2-3]. However, the performance of such devices is fundamentally hindered by spin-polarized-current-based schemes^[2-4], with a nanosecond-spin-precession-time limitation and excessive power dissipation. How to overcome these physical constraints have remained a long-lasting scientific challenge for the modern spintronics community^[3,4].

To address these issues, we report an optospintronic tunnel junction (OTJ) device using the photonic-spintronic combination. By integrating an all-optically-switchable ferrimagnetic Co/Gd bilayer^[5] with a CoFeB/MgO-based p-MTJ, an all-optical “writing” of the OTJ within 10 ps is experimentally demonstrated. It also shows a reliable electrical “read-out” with a relatively high TMR of 34%, as well as promising scaling towards the nanoscale with a low energy consumption.



Figure 1: Artistic illustration of the opto-spintronic tunnel junction device

A brief circuit-level analysis on the technology assessment aligned with other memory technologies, as well as the ultimate limits of this hybrid spintronic-photonic platform are also provided.

Our proof-of-concept demonstration might pave the way towards a new category of nonvolatile integrated photonic memory devices. This development is considered highly promising towards stimulating further innovation of future & emerging technologies, in the field of opto-spintronics.

[1] L. Wang, H. Cheng, and P. Li, *et al.*, *Proc. Natl. Acad. Sci. U.S.A.*, **119**, 24 (2022).

[2] B. Dieny, I. L. Prejbeanu, and K. Garello, *et al.*, *Nat. Electron.*, **3**, 8 (2020).

[3] Z. Guo, J. Yin, and Y. Bai, *et al.*, *Proc. IEEE*, **109**, 8 (2021).

[4] A. V. Kamel, and M. Li, *Nat. Rev. Mater.* **4**, 189 (2019).

[5] M. L. Lalieu, R. Lavrijsen, and B. Koopmans, *Nat. Commun.* **10**, 110 (2019).

Structural phase transition in Fe thin films: DFT study

Justyna Rychły-Gruszecka¹, Justyn Snarski-Adamski¹, Ján Ruzs²,
Mirosław Werwiński¹

¹ *Institute of Molecular Physics, Polish Academy of Sciences, M. Smoluchowskiego 17, 60-179
 Poznań, Poland*

² *Department of Physics and Astronomy, Uppsala University, Box 516, SE-751 20 Uppsala,
 Sweden*

In ultra-thin epitaxial Fe films grown on Cu₃Au (001), a continuous transition from fcc-like ($c/a \sim 1.4$) to bcc-like ($c/a \sim 1.0$) structure was previously observed with increasing Fe coverage [1] with a transition regime between 4 and 12 Fe monolayers. Using the density functional theory code FPLO [2], we calculated the set of Fe slabs with a rectangular-lattice surface with thicknesses between 1 and 12 monolayers. After optimizing the geometry of the considered models, we observed a structural phase transition from $c/a \sim 1.6$ to $c/a \sim 1.0$ with a slab thickness of 9 monolayers. The calculations show that in the investigated range of Fe layer thickness, the decrease in the values of mean magnetic moment and magnetocrystalline anisotropy energy (MAE) is correlated with the increase of layer thickness. By analyzing the course of the dependence of the effective uniaxial anisotropy (K_u) on the tetragonal Fe film thickness, we determined the surface and volume components ($K_s = 0.86 \text{ mJ m}^{-2}$; $K_v = -0.97 \text{ MJ m}^{-3}$) which are in very good agreement with the literature data. Curie temperature calculations performed for a series of layers with increasing thickness reveal that all considered layers have a stable ordered magnetic configuration. The aforementioned structural transition, observed at a thickness of 9 monolayers, is accompanied by a Curie temperature step increase of about 100%. Spike of similar height was previously observed experimentally at a thickness of about 10 monolayers for Fe layers deposited on a Cu (100) substrate [3]. Calculations also indicate that for tetragonal Fe thin films ($c/a \sim 1.6$) the equilibrium lattice parameter a is much lower ($\sim 2.40 \text{ \AA}$) than the lattice parameter of Cu or Au substrates on which Fe layers are customarily deposited ($a > 2.6 \text{ \AA}$). We conclude that the use of substrates with $a \sim 2.4 \text{ \AA}$ would allow the growth of stable Fe thin films with c/a values even higher than the 1.4 observed on Cu₃Au substrate [3]. Such tetragonal Fe thin films can find an application in spintronic devices requiring a magnetic layer with strong perpendicular anisotropy.

We acknowledge the financial support of the National Science Centre Poland under the decisions DEC-2019/35/O/ST5/02980 and DEC-2018/30/E/ST3/00267 (PRELUDIUM BIS 1 and SONATA BIS 8).

- [1] B.R. Cuenya, M. Doi, S. Löbus, R. Courths, W. Keune, *Surf. Sci.* **493**, 338 (2001).
- [2] K. Koepf, H. Eschrig, *Phys. Rev. B* **59**, 1743 (1999).
- [3] J. Thomassen, F. May, B. Feldmann, M. Wuttig, H. Ibach, *Phys. Rev. Lett.* **69**, 3831 (1992).

Ferromagnetism and band structure engineering in the (Ga,Mn)As, Ga(Bi,As) and (Ga,Mn)(Bi,As) nanolayers

O. Yastrubchak¹, N. Tataryn¹, J. Z. Domagała², T. Wosiński², M. Sawicki² and J. Adowski^{2,3}

¹ *V. Lashkaryov Institute of Semiconductor Physics at the National Academy of Science of Ukraine, Prospect Nauky 45, Kyiv-03028, Ukraine
E-mail: plazmonoki@gmail.com*

² *Institute of Physics, PAN, 02-668 Warsaw, Poland*

³ *Department of Physics and Electrical Engineering, Linnaeus University, SE-351 95 Växjö, Sweden*

The GaAs based ferromagnetic semiconductor alloy compounds containing Mn and Bi emerged as potential candidates for novel nanoelectronic and spintronic application. The (Ga,Mn)As, Ga(Bi,As) and (Ga,Mn)(Bi,As) nanolayers are grown using low temperature (230°C) molecular beam epitaxy (MBE). The alloy compositions are determined with high resolution X-ray diffractometry (XRD) followed by the in-situ Reflection High Energy Electron Diffraction (RHEED). The superconducting quantum interference device (SQUID) magnetometry is used for the investigation of the magnetic properties of the heterostructures.

Photoreflectance (PR) measurements are used for the determination of the band gap (E₀) and spin-orbit split-off (ESO) band to conduction band optical transitions. Besides the PR technique, the samples have been investigated by the μ Raman spectroscopy to confirm p-type character of some films by the observation of the Coupled Plasmon-LO Phonon Mode (CPPM). The in-situ UV Angle Resolved Photoemission Spectroscopy (ARPES) is used for the band structure analysis of the epitaxial layers. The low temperature optical-energy-gap measurements supported by complementary characterization, for a series of (Ga,Mn)As, Ga(Bi,As) and (Ga,Mn)(Bi,As) nanolayers, show that the deep modification of the GaAs valence band caused by Mn incorporation occurs for a Mn content much lower than that supporting dilute ferromagnetic phase in the investigated nanofilms.

Superparamagnetic particles for micro-inductor applications

M. Zambach¹, M. Beleggia^{2,3}, Z. Ouyang⁴, M. Knaapila⁵ and C. Frandsen¹

¹ DTU Physics, Technical University of Denmark, Kgs. Lyngby, Denmark

² DTU Nanolab, Technical University of Denmark, Kgs. Lyngby, Denmark

³ Department of Physics, University of Modena and Reggio Emilia, Modena, Italy

⁴ DTU Electrical Engineering, Technical University of Denmark, Kgs. Lyngby, Denmark

⁵ Department of Physics, Norwegian University of Science and Technology, Trondheim, Norway

Magnetic components for power-electronics such as inductors and transformers are difficult to further miniaturize due to losses/heating in magnetic materials [1]. The reason is that miniaturized magnetic components operate at higher frequencies and magnetic losses generally increase strongly with increasing frequency [1]. Commercial high-frequency magnetic materials, e.g. Mn-Zn-ferrites, only offer acceptable losses below 1-2 MHz [2]. Nanocomposites, comprised of nm-size magnetic particles in a solid and non-conducting matrix, have the potential to overcome this limitation by maintaining losses at an acceptable level in the 10-100 MHz range [3].

We have established a framework to guide the design and fabrication of magnetic devices containing magnetic single domain particles embedded in polymer materials [4]. Simulated dynamic susceptibility of dispersed superparamagnetic particles suggest that such systems may be usable as inductor core material for MHz operations [4]. This follows from the combination of large susceptibility and moderate hysteresis losses, as illustrated by the in-phase and out-of-phase AC-susceptibility plots shown in Fig. 1. Based on modelling and preliminary validating experiments, we present here a parameter-space overview of particle characteristics that are most promising for micro-inductor used in power-converters [4]. We focus on a minimal set of parameters; particle material, size, shape, and arrangement of particles to evaluate magnetic susceptibility and losses [4].

Our theoretical and experimental results show that composites of certain superparamagnetic particles, embedded in a polymer matrix, are promising candidates for micro-inductor cores operating in the MHz range. The proposed materials offer high fabrication flexibility and enables tuning of magnetic susceptibility to fit inductor design optimum, allowing improved power-electronic efficiency.

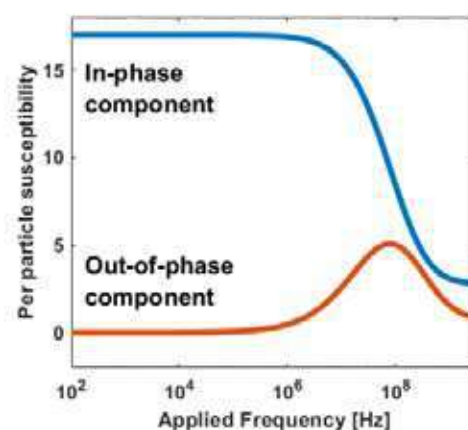


Figure 1: Calculation of dynamic susceptibility for randomly oriented 15±1 nm iron oxide particles.

[1] M. Araghchini *et al.*, IEEE Transactions on Power Electronics, **28**, 4182–4201 (2013).

[2] M. Petrecca *et al.*, Journal of Nanoscience and Nanotechnology, **19**, 4974–4979 (2019).

[3] Michael P. Rowe *et al.*, J. Mater. Chem. C, **3**, 9789–9793 (2015).

[4] M. Zambach *et al.*, in preparation.

Voltage-controlled switching of magnetic anisotropy in ambipolar Mn₂CoAl/Pd bilayers

Yao Zhang^{1,2}, Simon Granville^{1,2}

¹ Robinson Research Institute, Victoria University of Wellington, Wellington, New Zealand.

² MacDiarmid Institute for Advanced Materials and Nanotechnology, Wellington, New Zealand.

An ultrahigh electric field induced by ionic liquid gating (ILG) can be employed to manipulate the ferromagnetism with low Joule heating dissipation showing great potential for spintronics applications [1-2]. In ferromagnetic/heavy metal thin films, however, typical materials used in both layers are electron-carrier dominant which significantly suppresses the ILG effect due to the short electrostatic screening length in metal [3-4]. Here, we employ Mn₂CoAl, a spin gapless semiconductor with hole carriers, as the ferromagnetic layer and investigate the ILG effect in MgO/Mn₂CoAl/Pd ultrathin films with perpendicular magnetic anisotropy [5]. Reversible change of the magnetic anisotropy from out-of-plane to in-plane direction is achieved induced by electrostatic charge accumulation. Moreover, the ambipolar transport behaviour has been observed and explained by a two-carrier model. Finally, we find that the skew-scattering is the mechanism of the anomalous Hall effect and can be strongly enhanced at a positive gate voltage in our system. Our results strongly demonstrate that a significant ILG effect on the magnetism can be easily achieved in the two-carrier dominant ultrathin films.

- [1] A. Goldman, *Annu. Rev. Mater. Res.* **44**, 45 (2014).
- [2] S. Z. Bisri, S. Shimizu, M. Nakano, and Y. Iwasa, *Adv. Mater.* **29**, 1607054 (2017).
- [3] S. Zhao, L. Wang, Z. Zhou, C. Li, G. Dong, L. Zhang, B. Peng, T. Min, Z. Hu, and J. Ma, et al., *Adv. Mater.* **30**, 1801639 (2018).
- [4] L. H. Diez, Y. Liu, D. A. Gilbert, M. Belmeguenai, J. Vogel, S. Pizzini, E. Martinez, A. Lamperti, J. Mohammedi, and A. Laborieux, et al., *Phys. Rev. Appl.* **12**, 034005 (2019).
- [5] Y. Zhang, G. Dubuis, T. Butler, S. Kaltenberg, E. Trewick, and S. Granville, *Phys. Rev. Appl.* **17**, 034006 (2022).

Energy-efficient magnetoelectrochemical effect of $\text{La}_{0.7}\text{Sr}_{0.3}\text{MnO}_{3-\delta}$ via voltage-driven oxygen motion

Zhibo Zhao, Xinglong Ye, Horst Hahn, Robert Kruk

Karlsruhe Institute of Technology, 76344 Eggenstein-Leopoldshafen, Germany

Voltage control of magnetism at solid/liquid interface has been extensively studied for low-power magnetic storage. However, most of solid/liquid magnetic composites are volatily tuned by voltage. In this study, we propose to control the magnetism of $\text{La}_{0.7}\text{Sr}_{0.3}\text{MnO}_{3-\delta}$ (LSMO) through a voltage-driven migration of oxygen ions that mediates the double exchange interaction between Mn ions. Using this approach, we demonstrated a non-volatile and reversible modification of the Curie temperature by ~ 60 K and of the magnetization by 100% upon applying voltage of only $+0.5$ V. X-ray photoemission spectroscopy revealed the valence change of Mn ions, and transmission electron microscopy detected the revolution of the crystal structure due to the incorporation of oxygen ions. Our case suggests a robust magnetoelectrochemical effect in a very multifunctional way, which will contribute to a more sustainable digital world with ultra-low power digital memory, sensor and transduction technologies.

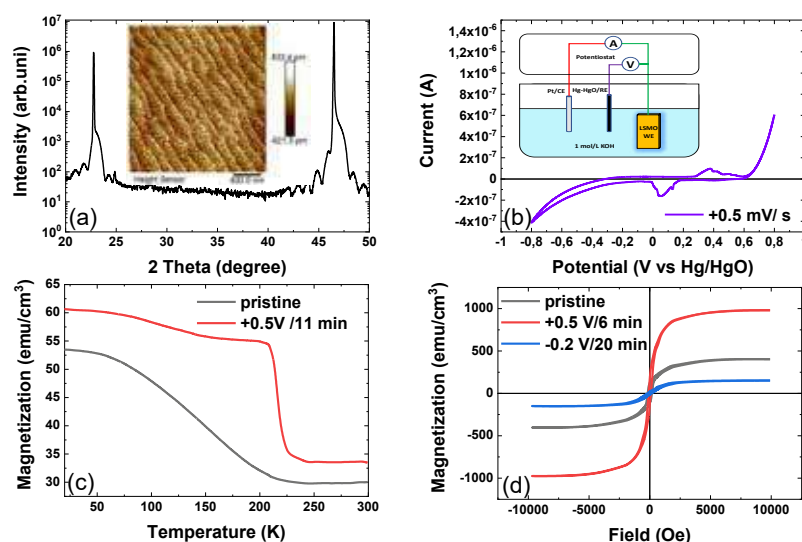
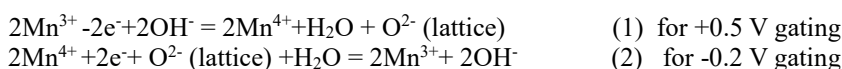


Figure 1. (a) XRD and AFM (inset) of 16 nm high quality LSMO thin film deposited by PLD. (b) Setup of electrochemical control of LSMO thin film at room temperature (inset) and its cyclic voltammetry curve (LSMO sample working electrodes in 1 M KOH with a cycle rate of 0.5 mV/s, Pt as counter electrode and Hg/HgO as reference electrode). Magnetoelectrochemical effect of LSMO/KOH under voltage: Magnetization verse temperature (field-cooling) @150 Oe (c) and magnetization verse field @20 K (d) of LSMO before and after electrochemical gating.

The critical temperature increases 60 K and magnetization is enhanced by 100% after $+0.5$ V electrochemical gating. Followed by -0.2 V gating after $+0.5$ V treatment, the magnetization drops 700%. This robust magnetoelectrochemical effect can be explained with following chemical reaction equations:



The oxygen ion between Mn^{3+} and Mn^{4+} is crucial to double exchange effect for LSMO magnetism. We use electrochemical way to drive oxygen ion reversal motion at LSMO/KOH interface and the magnetism of LSMO can thence be manipulated reversibly.

Electronic structure of ferromagnetic $\text{Sn}_{1-x}\text{Mn}_x\text{Te}$ thin films

M. Zięba¹, B. Turowski², V.V. Volobuev², B.J. Kowalski¹, N. Olszowska³, M. Rosmus³, J. Kołodziej³, A. Kazakov², T. Wojciechowski^{1,2}, M. Aleszkiewicz¹, K. Gas¹, M. Sawicki¹, A. Łusakowski¹, T. Wojtowicz², T. Story^{1,2}

¹ *Institute of Physics, Polish Academy of Sciences, al. Lotników 32/46, 02-668 Warsaw, Poland*

² *International Research Centre MagTop, Institute of Physics, Polish Academy of Sciences*

³ *Solaris National Synchrotron Radiation Centre, ul. Czerwone Maki 98, 30-392 Kraków, Poland*

$\text{Sn}_{1-x}\text{Mn}_x\text{Te}$ is a IV – VI semimagnetic (diluted magnetic) semiconductor with the direct electron band gap located near L – points in the Brillouin zone (BZ). The inverted ordering of the L_{6-} band of light holes and the L_{6+} conduction band, observed in SnTe and also expected in $\text{Sn}_{1-x}\text{Mn}_x\text{Te}$, results in the transition to topological crystalline insulator state. In the electronic structure of this material, the second valence band of heavy holes, located along Σ high symmetry line and characterized by a high density of states, is crucial for the carrier – induced ferromagnetic properties and excellent thermoelectric parameters of $\text{Sn}_{1-x}\text{Mn}_x\text{Te}$. The aim of this study is to use angle – resolved photoemission spectroscopy (ARPES) technique to determine the electron energy dispersion in the valence band and to test the proposed models of the temperature and composition evolution of the $\text{Sn}_{1-x}\text{Mn}_x\text{Te}$ electronic band structure.

Monocrystalline layers of $\text{Sn}_{1-x}\text{Mn}_x\text{Te}$ ($x = 0, 0.015$, and 0.05) with atomically clean surface needed for ARPES experiments were grown by molecular beam epitaxy on (111) BaF_2 substrates. Using an UHV suitcase we transferred the layers from the growth chamber to the Solaris synchrotron facility. Electrical and magnetic measurements of the Hall effect, conductivity and magnetization confirmed the expected p – type metallic conductivity and transition to the ferromagnetic state with a Curie temperature up to $T_C \approx 8$ K (for $x = 0.05$).

We carried out ARPES measurements of the (111) surface of $\text{Sn}_{1-x}\text{Mn}_x\text{Te}$ exploring theoretically indicated regions of the bulk and surface BZ. In photon energy – dependent (18 – 130 eV) ARPES spectra taken along the $\bar{M} - \bar{\Gamma} - \bar{M}$ direction, we observed projections of Dirac cones at the $\bar{\Gamma}$ and \bar{M} points of the surface BZ with different Fermi velocities. Characteristic pockets observed in the bulk $\Gamma - K$ direction can be tentatively assigned to the Σ band. Comparison of Fermi surface maps for different Mn content showed an evolution of the electronic structure, but without a qualitative change in bands ordering. No qualitative changes of the band structure were observed in the whole region studied ($T = 8 - 270$ K). The experimentally observed electron dispersion is analyzed with the help of DFT calculations of electronic structure of $\text{Sn}_{30}\text{Mn}_{2}\text{Te}_{32}$ slabs.

This research was partially supported by the Foundation for Polish Science through the IRA Programme co-financed by EU within SG OP (grant No. MAB/2017/1) and by the National Science Centre (Poland) grants: UMO 2017/27/B/ST3/02470 and UMO-2016/23/B/ST3/03725.

Posters

| | | |
|----------------------------|---|-----|
| Jon Ander Arregi | <i>Optical microscopy of antiferromagnetic and ferromagnetic domains in FeRh thin films</i> | 368 |
| Mohamed Ben Chroud | <i>Magnetron sputtered epitaxial NiAl seed layer on Ge for enhanced VCMA effect.</i> | 369 |
| Mattia Benini | <i>Colossal enhancement of the coercivity in thin Co films interfaced with molecules</i> | 370 |
| Mattia Benini | <i>In-depth modification in Co thin films induced by the interfacing with molecular layers detected by Zero-Field NMR</i> | 371 |
| Mani Teja Bodduluri | <i>Wafer-level Integrated Hard Micromagnets for MEMS Applications</i> | 372 |
| Alonso J. Campos-Hernandez | <i>Study of the magnetic interactions in FeNi nanowires through coercivity angular measurements and FORC analysis</i> | 373 |
| Oleksandr Chumak | <i>Correlation of magnetoelastic interactions and magnetic damping in thin $\text{Co}_2\text{Fe}_{0.4}\text{Mn}_{0.6}\text{Si}$ and $\text{Co}_2\text{FeGa}_{0.5}\text{Ge}_{0.5}$ magnetic layers</i> | 374 |
| Umit Daglum | <i>Magnetic properties of Mn_3Ga, calculated from first principles and mappend onto an effective spin Hamiltonian for atomistic spin dynamics simulations</i> | 375 |
| Elizabeth Davis-Fowell | <i>Investigation and optimisation of magnetic properties of Ga-doped τ MnAl</i> | 376 |
| Jaydeb Dey | <i>^{55}Mn NMR investigations on Mn_2GaC nanolaminated thin film</i> | 377 |
| Javier Díaz | <i>Analysis of the dysprosium M5 circularly polarized X ray absorption spectrum to detect magnetically uncoupled rare earth atoms to TM in TM-RE amorphous alloys</i> | 378 |
| Javier Díaz | <i>Vortex chirality observation in trilayer disks of Fe/Al/Co using X ray resonant magnetic scattering</i> | 379 |
| Amar Fakhredine | <i>Huge Dzyaloshinskii-Moriya interactions in $\text{Re/Co}[n]/\text{Pt}$ thin films</i> | 380 |
| Łukasz Frąckowiak | <i>Experimental Results and Numerical Calculation of Co-Tb Distribution from Magnetron Co-Sputtering Deposition with a Composition Gradient</i> | 381 |
| Martin Friák | <i>An ab initio study of antiphase boundaries in ferromagnetic B_2-phase Fe_2CoAl alloy</i> | 382 |
| Nathan Hale | <i>The 4×4 transfer matrix method: a flexible and computationally efficient tool for exploring a system's surface magnon polaritons</i> | 383 |
| Yuan Hong | <i>A High Throughput Study of Hard Magnetic CeCo_5-based Thin Films</i> | 384 |
| Florian Jürries | <i>Stability of MnAl-C magnet alloys in the presence of water</i> | 385 |
| Jiří Kaštil | <i>Exchange spring and exchange bias effects in the bulk Heusler Ni_2MnSn-based alloys</i> | 386 |
| Rafael Morales | <i>Isotropic exchange bias in patterned IrMn/CoFe bilayers</i> | 387 |
| Okan Ozdemir | <i>Magnetic Characterization of $\text{Co}_2\text{MnAl/PMN-PT}$ (011) Multiferroic Heterostructures</i> | 388 |
| Tibor Adrian Óvári | <i>Nonlinear Domain Wall Dynamics in Highly Magnetostrictive Amorphous Nanowires Prepared by Rapid Solidification</i> | 389 |
| Parul Rani | <i>Magnetic properties of amorphous $\text{Co}_x\text{Zr}_{100-x}$ films</i> | 390 |
| Pedro A. Sánchez | <i>The impact of finite magnetic anisotropy and hydrodynamics on the response of systems of magnetic colloidal particles</i> | 391 |

| | | |
|--------------------------------|--|-----|
| Carlos Henrique Santos Verbeno | <i>Magnetic properties of cobalt ultrathin film structures controlled by buffer-layer roughness</i> | 392 |
| Célia T. Sousa | <i>Multifunctional Fe Au nanostructures synthesized by Laser Ablation in Liquids</i> | 393 |
| Kateryna Sova | <i>Ferromagnetic resonance in Fe_3O_4 nanoparticles in combination with ligands</i> | 394 |
| Dariusz Sztankiel | <i>Crystal field model simulations of magnetic response of pairs, triplets and quartets of Mn^{3+} ions in GaN</i> | 395 |
| Nataliia Tataryn | <i>Valence Band Dispersion in $(\text{Ga,Mn})\text{As}$, $\text{Ga}(\text{Bi,As})$, $(\text{Ga,Mn})(\text{Bi,As})$ epitaxial nanolayers</i> | 396 |
| Michal Varga | <i>Ni_2FeZ ($\text{Z} = \text{Ga, In, Tl}$) Heusler alloy nanowires prepared via electrodeposition</i> | 397 |
| Yuliia Veretennikova | <i>Capping layer influence on magnetic characteristics evolution in cobalt nanofilms</i> | 398 |
| Zengxin Wei | <i>A strong competition among the anisotropy terms in magnetically coupled Fe/Al/Fe thin film trilayers</i> | 399 |
| Michael Zawodski | <i>Demonstrating and tailoring exchange bias on novel bulk nanocomposites processed by severe plastic deformation</i> | 400 |
| Nerija Zurauskiene | <i>Tuning of Magnetoresistive Properties of Graphene-Lanthanum Manganite Structures</i> | 401 |

Optical microscopy of antiferromagnetic and ferromagnetic domains in FeRh thin films

Jon Ander Arregi¹, Tomáš Molnár², and Vojtěch Uhlíř^{1,2}

¹ CEITEC BUT, Brno University of Technology, Purkyňova 123, 612 00 Brno, Czech Republic

² Institute of Physical Engineering, Brno University of Technology, Technická 2, 616 69 Brno, Czech Republic

The equiatomic FeRh alloy attracts a large interest due to its singular first-order phase transition from antiferromagnetic (AF) to ferromagnetic (FM) order near room temperature ($T_M \sim 370$ K). The transition is characterized by hysteretic behavior and phase coexistence at the nanoscale. XMCD/XMLD-PEEM measurements in epitaxial thin films showed that typical AF and FM domain sizes during coexistence are in the ~ 500 nm range and below [1].

Here, we investigate the shape and spatial distribution of AF and FM domains during their coexistence using wide-field optical microscopy. The refractive index variation of FeRh across the phase transition [2] enables visualizing the nucleation of sub-micron FM (AF) domains during heating (cooling) in epitaxial thin films. The typical size of the nucleated regions correlates with the average in-plane crystallographic grain size, which at the same time scales with the film thickness [3]. By imaging the phase transition in FeRh films with different epitaxial texture, we conclude that avalanches of the emerging product phase elongate along preferential crystallographic orientations, revealing that phase domains are pinned at grain boundaries (see Figure 1). We also find that topographic defects in thin films act as nucleation sites for the AF phase during cooling, while the same is not true for the FM phase during heating.

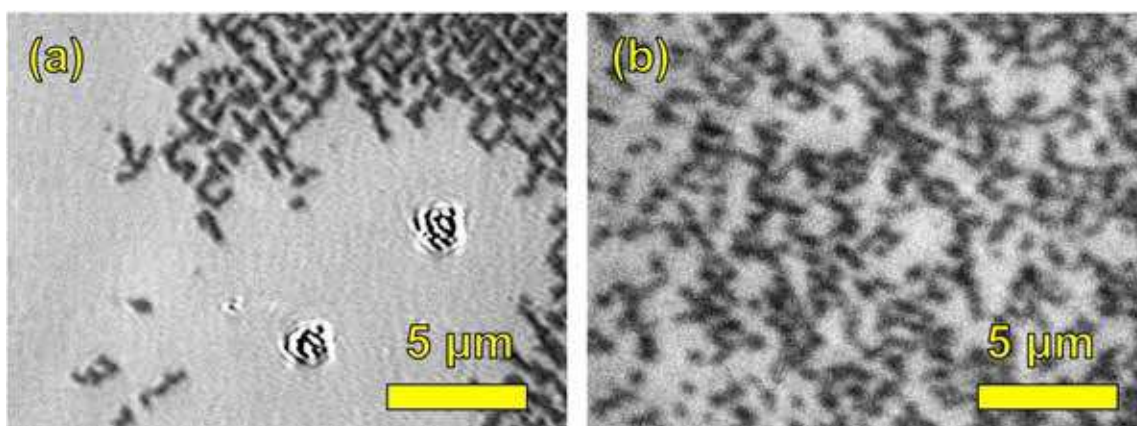


Figure 1: Nucleation of FM domains (dark color) in the AF parent matrix (bright color) as observed via optical reflectivity contrast microscopy for epitaxial (a) FeRh(001) and (b) FeRh(111) textured thin films.

[1] C. Baldasseroni *et al.*, *J. Phys.: Condens. Matter* **27**, 256001 (2015).

[2] V. Saidl *et al.*, *New J. Phys.* **18**, 08301 (2016).

[3] J. A. Arregi, O. Caha, and V. Uhlíř, *Phys. Rev. B* **101**, 174413 (2020).

Magnetron sputtered epitaxial NiAl seed layer on Ge for enhanced VCMA effect

M. Ben Chroud^{1,2}, R. Carpenter¹, S. Mertens¹, J.-P. Soulié¹, S. Couet¹, G. S. Kar¹, K. Temst² and J. Swerts¹

¹ Imec, Kapeldreef 75, 3001 Leuven, Belgium

² Department of Physics and Astronomy, KU Leuven, Celestijnenlaan 200d, 3001 Leuven, Belgium

Voltage-controlled magnetic anisotropy (VCMA) is promising for ultra-low power Magnetic Random-Access Memory (MRAM). Increasing the VCMA coefficient (ζ) is a key focus, with industry compatible MTJs achieving $\zeta \sim 100$ fJ/Vm [1]. However, this is still less than the minimum of 300 fJ/Vm required for embedded MRAM [2]. In epitaxial MTJs, $\zeta > 300$ fJ/Vm has been achieved, however the deposition techniques used are not compatible with industry e.g., molecular beam epitaxy. Sputtered NiAl is known to grow epitaxially (epi) on Si while also having a close lattice match with MgO [3]. In this work, Ge (100) is used as a seed for sputtered NiAl. Ge is selected as it has a smaller lattice mismatch (2%) with NiAl compared to Si (6%). Additionally, the native oxide of Ge can be degassed at much lower temperatures (600 °C), in comparison to those required for Si (1200 °C).

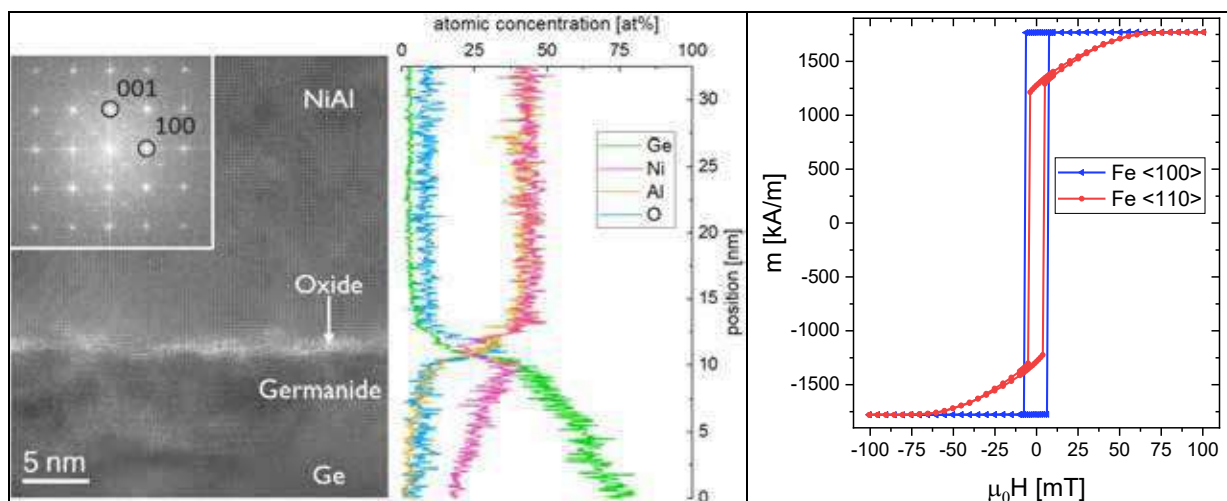


Figure 1: (left) HRTEM image with FFT of the NiAl in the inset. (right) EDS profile with a matching vertical scale.

Figure 2: VSM loops where either Fe<100> or Fe<110> is aligned with the external field.

Ge is deposited using chemical vapor deposition on a thermally degassed Si (100) wafer. NiAl is then sputtered at a wafer temperature of 400 °C. Epi NiAl is obtained only when the degas step is not performed. Thus, the native oxide mediates the growth as shown in figure 1 (left). During growth, Ni diffuses below the oxide while Al is blocked, as seen in figure 1 (right). Next, a simple magnetic stack of Cr/MgO/Fe/cap is deposited on top of NiAl. Magnetic measurement of the easy and medium axis of Fe indicates a uniform crystal orientation, as shown in figure 2, matching the lattice orientation of Ge/Si. In the presentation the growth conditions of the NiAl and its impact on magnetic properties e.g., ζ , will be presented.

[1] R. Carpenter et al., IEEE-IEDM, pp. 17.6.1-17.6.4 (2021)

[2] S. Miwa et al., (2018) J. Phys. D: Appl. Phys. 52, 063001

[3] K. Yakushiji et al., (2019) Appl. Phys. Lett. 115, 202403

Colossal enhancement of the coercivity in thin Co films interfaced with molecules

Mattia Benini^{1,2}, Rajib Kumar Rakshit¹, Manju Singh¹, Gaspare Varvaro³, Alberto Riminucci¹, Ilaria Bergenti¹, Valentin Alek Dediu¹

¹ CNR-ISMN Bologna, Via Piero Gobetti 101, Bologna, Italy

² Department of Physics and Astronomy, University of Bologna, Viale Bert Pichat 6/2, Bologna, Italy

³ ISM-CNR, Area della Ricerca di Roma 1, 00015 Monterotondo Scalo, Rome, Italy

The hybridization at 3d-ferromagnet/molecule interfaces has proved to modify the magnetic anisotropy of the ferromagnetic layer. This was reported for the first time for Co/ZMP interface [1], boosting further research efforts on the topic [2]. The hybridization between molecular orbitals and d-orbitals of the ferromagnetic surface induces modifications of the effective spin-orbit coupling, density of states and other fundamental parameters [3,4]. We report on novel results related to extraordinary modification of the magnetic anisotropy in polycrystalline Co thin films (5 nm) interfaced with a molecular layer (25 nm) of either C₆₀ and Gaq₃.

A drastic, molecule-dependent enhancement of the in plane coercive fields is observed with respect to both Al-capped and bare cobalt samples (see Fig. 1). The effect is present even at room temperature featuring a significant factor of 2 enhancement, and grows enormously when decreasing temperature, showing a qualitatively different trend and reaching a one order of magnitude increase already at 150 K.

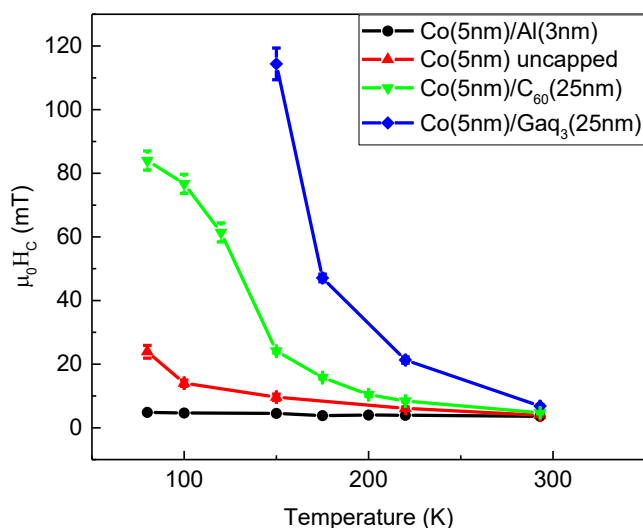


Figure 1 Coercive field as function of temperature for the measured samples.

In addition to this, Co interfaced with both molecules has the in-plane uniaxial anisotropy suppressed and undergoes a hardening of the out-of-plane direction with respect to the reference Co/Al system.

The achievement of this colossal enhancement of the coercivity on polycrystalline samples cannot be quantitatively explained by the current models developed for perfectly crystalline case and based of the hybridization of the d-electrons at the interface, indicating that hybridization effects alone do not account for the complex physics induced by these hybrid magnetic interfaces.

References

- [1] K. V. Raman, A. M. Kamerbeek, Arup Mukherjee *et al.*, Nature, **493**, 509 (2013)
- [2] M. Cinchetti, V. A. Dediu, L. Hueso, Nat. Mater. **16**, 507 (2017)
- [3] K. Bairagi, A. Bellec, V. Repain *et al.*, Phys. Rev. Lett. **114**, 5 (2015)
- [4] T. Moorsom, M. Wheeler, Taukeer Mohd Khan *et al.*, Phys Rev. Lett. B **90**, 6 (2014)

In-depth modification in Co thin films induced by the interfacing with molecular layers detected by Zero-Field NMR

Mattia Benini^{1,2}, Giuseppe Allodi³, Alessandro Surpi¹, Alberto Riminucci¹, Ko-Wei Lin⁴, Samuele Sanna², Valentin Alek Dediu¹, Ilaria Bergenti¹

¹ CNR-ISMN Bologna, Via Piero Gobetti 101, Bologna, Italy

² Department of Physics and Astronomy, University of Bologna, Viale Berti Pichat 6/2, Bologna, Italy

³ Department of Mathematical, Physical and Informatics sciences, University of Parma, Viale Università 12, Parma, Italy

⁴ Department of Materials Science and Engineering, National Chung Hsing University, Taichung 402, Taiwan

The formation of a hybrid molecule/ferromagnet interface, often called *spinterface*, affects the electric and magnetic properties at both sides, inducing a spin polarization in the molecules and modifying the magnetic anisotropy in the ferromagnet [1]. In this work we apply the ^{59}Co Zero Field NMR (FNR) [2] to the investigation of two prototypical interfaces, based on Co thin films covered by Buckminsterfullerene C_{60} or Tris(8-hydroxyquinolato)gallium GaQ_3 .

Polycrystalline Cobalt layers (7 nm thick) were grown on $\text{Al}_2\text{O}_3(0001)$ in UHV and interfaced with molecular layers (25 nm thick). An additional 7 nm Co film interfaced with 8 nm Al was grown and characterized as a reference sample. The FNR characterization was performed by taking the ^{59}Co spin-echo amplitude in the spectral range 193-232 MHz for different values of the applied rf B field power (see Fig. 1). With respect to a reference Co/Al system, interfacing Co with C_{60} and GaQ_3 moves the maximum of the FNR signal to higher power of the applied rf field, regardless of the resonance frequency. This indicates that the whole 7 nm Co layer becomes magnetically harder, the effect being considerably stronger for GaQ_3 than for C_{60} . The analysis of the ^{59}Co FNR spectra shows also that Co/molecule systems undergo a magnetic reconstruction of the environment of the Co atoms near the interface. We tentatively ascribe the detected surface changes to a strong hybridization of the d orbitals of

Co with molecular ones. The in-depth magnetic hardening is instead expected to be promoted by the delocalized electrons, propagating the surface alterations to the bulk of Co. We believe that these results shed conceptually new light on the spinterface-induced effects in such systems.

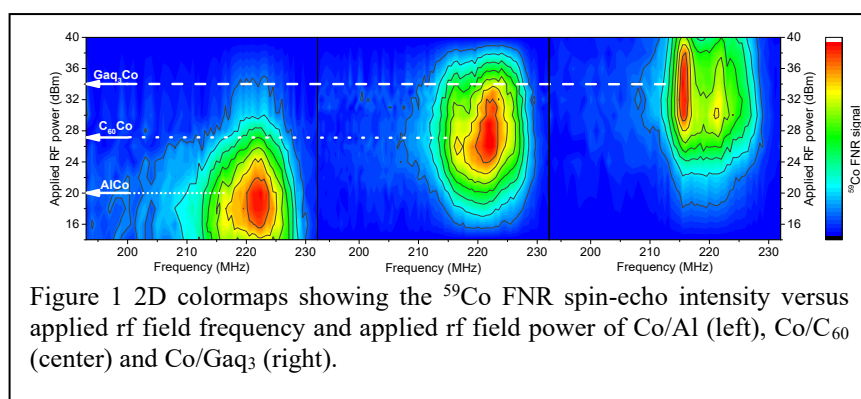


Figure 1 2D colormaps showing the ^{59}Co FNR spin-echo intensity versus applied rf field frequency and applied rf field power of Co/Al (left), Co/ C_{60} (center) and Co/ GaQ_3 (right).

References

- [1] M. Cinchetti, V. A. Dediu, L. Hueso, Nat. Mater. **16**, 507 (2017).
- [2] C. Meny, P. Panissod, Annual Reports on NMR spectroscopy **103** 47 (2021).

Wafer-level Integrated Hard Micromagnets for MEMS Applications

Mani Teja Bodduluri¹, Thomas Lisec¹ and Björn Gjdoka¹

¹ Fraunhofer Institute for Silicon Technology, Fraunhoferstr.1, D-25524 Itzehoe, Germany

Integration of high-performance and voluminous hard magnetic materials into microelectromechanical systems (MEMS) structures have numerous potential applications in areas like energy harvesting, actuation, biomedical and various others [1]. However, miniaturization of bulk hard magnets to hundreds of micrometers employing conventional top-down (micromachining, bonding, etc.) and bottom-up (sputtering, electro-deposition, etc.) approaches is challenging because of issues like high temperature processes, patterning, realization of complex structures, etc [2].

A novel technique, called PowderMEMS, based on the agglomeration of powder materials into rigid structures using atomic layer deposition (ALD) [3], has been used to integrate high-performance and organic-free NdFeB micromagnets on wafer-level into MEMS structures. For this process, NdFeB powder (D50 = 5 μm) is dry filled into etched Si cavities (aspect ratios (t/l) of 0.25 to 5). A low temperature (75 °C) thermal ALD process is used to solidify the NdFeB particles with 75 nm of Al₂O₃. In this way oxidation during the deposition is avoided. The ALD process envelops the particles throughout the structural volume with a homogeneous layer.

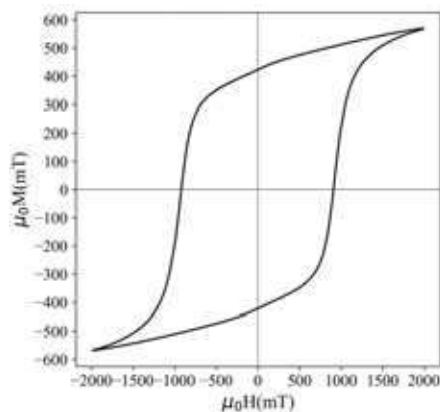


Figure 1: Hysteresis loop of a NdFeB micromagnet (2000×2000×525 μm^3).

In this study, we have investigated the salient factors and process parameters influencing the magnetic properties of the PowderMEMS NdFeB micromagnets. Vibrating sample magnetometer was used to measure the magnetic properties. A remanence and intrinsic coercivity of 422mT and 920mT has been achieved as shown in Figure 1. Experiments were carried out using different geometries and sizes to understand the influence of the filling procedure and particles size on the magnetic properties. Thermal and corrosion stability of the micromagnets were investigated by subjecting them to heat treatments in air and vacuum as well as to pressure

cooker tests. Furthermore, thermal behavior of the micromagnets in relation to their aspect ratio (demagnetization factor) was investigated. NdFeB micromagnets with passivation layer (PECVD layer) showed high corrosion stability and the remanence loss in the high aspect ratio structures is less when compared to thinner structures after annealing the samples at high temperatures.

[1] Niarchos, D. "Magnetic MEMS: key issues and some applications." *Sensors and Actuators A: Physical* **109**, no. 1-2 (2003): 166-173.

[2] Arnold, David P., and Naigang Wang. "Permanent magnets for MEMS." *Journal of microelectromechanical systems* **18**, no. 6 (2009): 1255-1266.

[3] Lisec, Thomas, Ole Behrmann, and Björn Gjdoka. "PowderMEMS—A Generic Microfabrication Technology for Integrated Three-Dimensional Functional Microstructures" *Micromachines* **13**, no. 3 (2022): 398.

Study of the magnetic interactions in FeNi nanowires through coercivity angular measurements and FORC analysis

Alonso J. Campos-Hernandez, Ester M. Palmero and Alberto Bollero

Group of Permanent Magnets and Applications, IMDEA Nanociencia, 28049, Madrid, Spain

Compositional variation in magnetic nanowires (NWs) allows to tailor the magnetic properties under controlled synthesis conditions [1]. In this study arrays of FeNi NWs have been electrodeposited into anodized aluminum oxide (AAO) membranes (Fig. 1a). Chemical composition analysis of the samples showed anomalous co-deposition, where Fe deposits in ratios higher than its electrolyte molar fraction under different trends. These effects were explained within a modified Bocris-Drazic-Despic (BDD) model [2].

Coercivities (H_c) ranging from 0.2 kOe to 1.0 kOe were obtained (Fig. 1b), observing an increase in H_c for a diminished Fe concentration. An angular study of the magnetization reversal mechanisms (dominated by transverse domain wall reversal) indicated the decrease in the magnetostatic interactions between NWs as the source of the rise in H_c . First-order reversal curve (FORC) analysis highlighted a reduced value of the magnetic interactions in the arrays, except for $\text{Fe}_{0.80}\text{Ni}_{0.20}$ NWs which showed a FORC diagram corresponding to magnetically interacting NWs (Fig. 1c). FORC diagrams showed higher intensity at around $H_c = 1$ kOe, with weakening intensity for an increased Fe content due to the higher interactions.

This work shows the possibility of tailoring the magnetic properties of FeNi NWs by tuning the electrochemical parameters and, thus, their composition and crystallographic structure. This approach is of interest in applications such as magnetic recording and sensing devices, and opens the path to explore the possibility of forming ordered phases with outstanding permanent magnet properties (e.g. $L1_0$ -ordered FeNi phase [3]).

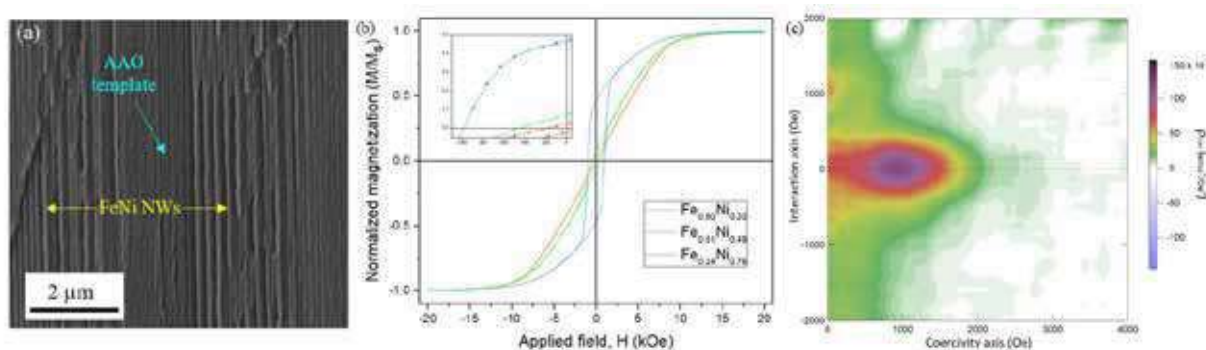


Figure 1: (a) SEM image of an array of FeNi NWs in an AAO membrane; (b) room temperature hysteresis loops measured for arrays of FeNi NWs with different compositions; and (c) FORC diagram for $\text{Fe}_{0.80}\text{Ni}_{0.20}$ NWs.

Acknowledgements: Authors acknowledge financial support from EU M-ERA.NET and MICINN through the projects *COSMAG* (PCI2020-112143) and *NEXUS* (PID2020-11521RB-C21). A.J.C.-H. acknowledges support from “La Caixa” Foundation (ID 100010434) through the Doctoral INPhINIT Incoming program (LCF/BQ/DI20/1178002).

References

- [1] Palmero, E. M. *et al.*, *J. Appl. Phys.* **116**, 033908 (2014)
- [2] Dragos O. *et al.*, *J. Electrochem. Soc.* **163** 3, 83-94 (2015)
- [3] Lewis, L. H. *et al.*, *J. Phys.: Condens. Matter* **26**, 064213 (2014)

Correlation of magnetoelastic interactions and magnetic damping in thin $\text{Co}_2\text{Fe}_{0.4}\text{Mn}_{0.6}\text{Si}$ and $\text{Co}_2\text{FeGa}_{0.5}\text{Ge}_{0.5}$ magnetic layers

Oleksandr M. Chumak¹, Adam Pacewicz², Artem Lynnyk¹, Bartłomiej Salski², Tatsuya Yamamoto³, Takeshi Seki^{3,4}, Jarosław Domagala¹, Hubert Glowinski⁵, Koki Takanashi^{3,4,6}, Lech T. Baczewski¹, Henryk Szymczak¹ and Adam Nabialek¹

¹*Institute of Physics, Polish Academy of Sciences, Al. Lotników 32/46, 02-668 Warsaw, Poland*

²*Warsaw University of Technology, Institute of Radioelectronics and Multimedia Technology, Nowowiejska 15/19, 00-665 Warsaw, Poland*

³*Institute for Materials Research, Tohoku University, 2-1-1 Katahira, Aoba-ku, Sendai 980-8577, Japan*

⁴*Center for Spintronics Research Network, Tohoku University, 2-1-1 Katahira, Aoba-ku, Sendai 980-8577, Japan*

⁵*Institute of Molecular Physics, Polish Academy of Sciences, M. Smoluchowskiego 17, 60-179 Poznań, Poland*

⁶*Center for Science and Innovation in Spintronics, Core Research Cluster, Tohoku University, 2-1-1 Katahira, Aoba-ku, Sendai 980-8577, Japan*

$\text{Co}_2\text{Fe}_{0.4}\text{Mn}_{0.6}\text{Si}$ (CFMS) and $\text{Co}_2\text{FeGa}_{0.5}\text{Ge}_{0.5}$ (CFGG) Heusler alloys belong to the family of the most prospective thin film materials. With low magnetic damping, high level of the spin polarization and impressive tunneling and giant magnetoresistance ratios, they are one of the best options for use in spintronic devices. Up to date numerous studies of the magnetic properties have been carried out for these materials, but the small number of available techniques resulted in the fact that the magnetoelastic properties, as well as their relationship with magnetic anisotropy and magnetic dissipation, remain poorly understood [1]. Here we would like to present the results of the investigation of the epitaxial CFMS and CFGG Heusler alloys layers with a thickness in the range of 15-50 nm [2]. In the function of the magnetic layer thickness the magnetoelastic tensor components and magnetic damping parameters were determined using Strain Modulated [3] Ferromagnetic Resonance (FMR) and Vector Network Analyzer FMR, respectively: magnetoelastic B_{11} constant values vary in the range of -6 to -30×10^6 erg/cm³ and the effective Gilbert damping α_{eff} factor values vary in the range of 1 to 12×10^{-3} . Frequency dependent FMR measurements revealed also the presence of such inhomogeneous non-Gilbert contributions as spin pumping phenomena and two-magnon scattering. The saturation magnetostriction λ_S values were determined to be in the range of 5.4 to 14.4×10^{-6} . On the base of the performed investigations the correlation between α_{eff} and B_{11} depending on magnetic layer thickness was revealed. The most part of the presented results was recently published in [2].

Acknowledgements: This work was supported by the National Science Centre of Poland - project number 2018/31/B/ST7/04006.

[1] O. M. Chumak, A. Nabialek, R. Zuberek, I. Radelytskyi, T. Yamamoto, T. Seki, K. Takanashi, L.T. Baczewski and H. Szymczak, *IEEE Trans. Magn.* **53**, 1 (2017).

[2] O. M. Chumak, A. Pacewicz, A. Lynnyk, B. Salski, T. Yamamoto, T. Seki, J.Z. Domagala, H. Gowiski, K. Takanashi, L.T. Baczewski, H. Szymczak and A. Nabialek, *Sci. Rep.* **11**, 7608 (2021).

[3] K. Nesteruk, R. Zuberek, S. Piechota, M.W. Gutowski and H. Szymczak, *Meas. Sci. Technol.* **25**, 075502 (2014).

Magnetic properties of Mn₃Ga, calculated from first principles and mapped onto an effective spin Hamiltonian for atomistic spin dynamics simulations

Umit Daglum¹, Maria Stamenova¹ and Stefano Sanvito¹

¹ School of Physics and CRANN, Trinity College Dublin, Dublin 2, Ireland

Tetragonal Mn₃Ga is a low moment ferrimagnet, exhibiting a large uniaxial anisotropy, a high spin-polarization and a low Gilbert damping, which makes it a good candidate for a range of spintronic applications. It has been proposed as a material for spintronic oscillators in the THz range [1]. Here we employ first principles calculations to investigate the magnetic properties of the tetragonal (D0₂₂) Mn₃Ga as a functional element in novel magnetic-tunnel junctions (MTJs) with Fe/MgO. Our aim is to map the magnetic properties of Mn₃Ga layers grown epitaxially on Fe/MgO (hence under a lateral tensile strain) onto a classical spin Hamiltonian for atomistic spin dynamics [2] under open-boundary conditions and spin-transfer torques.

It is known that the local density approximation (LDA) is not suitable for describing the experimental properties of tetragonal Mn₃Ga [3]. We show that Hubbard-corrected density functional theory at the level of LDA with U and J parameters (from the rotationally invariant Lichtenstein formulation [4]) for the two inequivalent Mn atoms can reproduce reasonably well the experimental lattice constant and magnetic moments on the two sites [5]. We use this for describing the strained Mn₃Ga in the Fe/MgO MTJ and evaluate the easy axis anisotropy ($K_1 = 0.941$ MJ/m³) and the in-plane effective four-fold secondary easy axis ($K_4 = 0.020$ MJ/m³) applying the magnetic force theorem method. We then use the same level of theory to map the exchange energy contributions of the Mn atoms on to a classical Heisenberg spin Hamiltonian to evaluate a convergent set of Heisenberg-exchange parameters from the frozen magnon approximation. These are to be combined with atomically-resolved spin-transfer torque calculations to extract the remaining set of parameters from first principles which will be used in atomistic spin dynamics calculations of current driven spintronic oscillators.

[1] S. Mizukami, *et al.* (2011) *Phys. Rev. Lett.* **106**, 11720.

[2] R. Evans, *et al.* (2014) *J. Phys. Condens. Matter* **26**, 103202.

[3] S.Saha, *et al.* (2017) *Scientific Reports* **7**, 13221.

[4] A. I. Liechtenstein, V. I. Anisimov and J. Zaanen, (1995) *Phys. Rev. B* **52**, R5467.

[5] K. Rode, *et al.* (2013) *Phys. Rev. B* **87**, 18.

Investigation and optimisation of magnetic properties of Ga-doped τ MnAl

Elizabeth Davis-Fowell¹, Russell Goodall¹, and Daniel Allwood¹

¹Department of Materials Science and Engineering, University of Sheffield, Sir Robert Hadfield Building, Mappin Street, Sheffield City Centre, Sheffield, S1 3JD

τ -MnAl doped with Ga has been previously identified by Mix *et. al.* [1] as a beneficial avenue of investigation towards the optimisation of the metastable τ -MnAl state as a functional permanent magnetic alloy. It does this by leading to an increased thermal stability of the ferromagnetic material by the precipitation of a secondary $L1_0$ phase within the material. Following this discovery, little work has been published both on optimising Ga content within the alloy for a known transformation temperature or looking at the effects of doping below 5at.% Ga.

Fig. 1 shows preliminary results into investigating the effect of low level Ga-doping of τ MnAl on the hysteresis of samples annealed at 700K for 40 minutes to precipitate the $\epsilon \rightarrow \tau$ transformation to bring about ferromagnetic properties. Whilst all samples showed similar coercivities, the addition of Ga lowers the saturation magnetisation and remanence of all observed samples. However, magnetisation of Ga-doped samples was shown to decrease at a slower rate when held at 420°C when compared to undoped MnAl, suggesting that an optimum composition could be found to maintain magnetisation for hot deformation and processing to take place, without degradation of the phase population, allowing for increases in remanence and coercivity with minimal diminishment in saturation magnetisation.

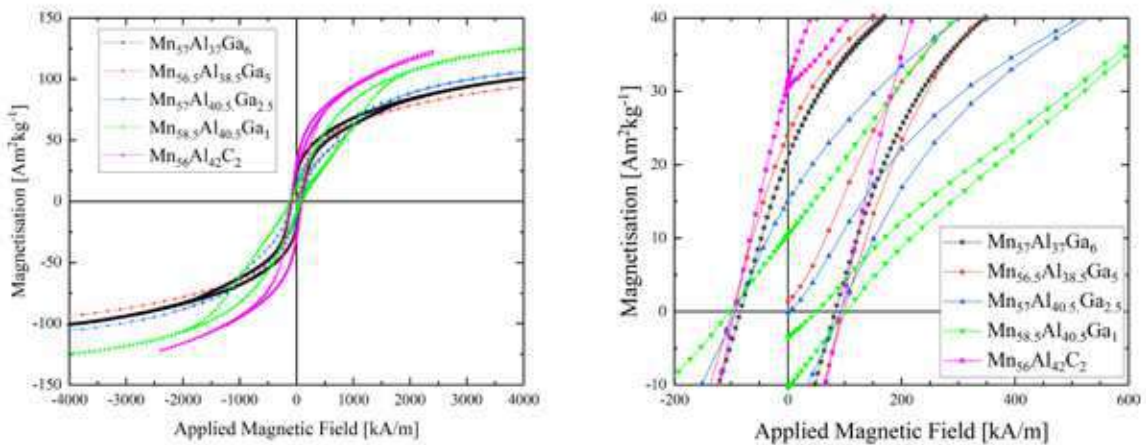


Figure 1: (LHS) MH hysteresis plots of Ga-doped τ -MnAl compared to data for C-doped τ -MnAl. (RHS) Remanence and Coercivity behaviour of Ga-doped τ -MnAl.

[1] T. Mix, F. Bittner, K.-H. Müller, L. Schultz, and T.G. Woodcock, *Acta Materialia* **128** (2017)

⁵⁵Mn NMR investigations on Mn₂GaC nanolaminated thin filmJ. Dey¹, R. Kalvig¹, E. Jędryka¹, M. Wójcik¹, U. Wiedwald², M. Farle², and J. Rosen³¹Institute of Physics, Polish Academy of Sciences, Al. Lotników 32/46, 02-668 Warszawa, Poland²Faculty of Physics and Center for Nanointegration (CENIDE), University of Duisburg-Essen, 47057, Duisburg, Germany³Thin Film Physics, Department of Physics, Chemistry and Biology (IFM), Linköping University, SE-581 83, Linköping, Sweden

The first magnetic material from the MAX phase family was synthesized in 2013. The general formula of the MAX phase family is $M_{n+1}AX_n$ where M denotes early transition elements, A denotes IIIA and IVA group elements, X stands for either carbon or nitrogen, and n (1, 2 or 3) is the number of layers, in both quaternary and ternary phases. In 2014 the Mn-based ternary MAX phase Mn₂GaC has been synthesized as a hetero-epitaxial thin-film [1] with high structural quality and phase purity which makes it an interesting object of investigations aimed at understanding the structural and magnetic properties. Theoretical studies on Mn₂GaC indicate complex magnetic structures where the competing ferromagnetic (FM) and antiferromagnetic (AFM) interactions play a role. The experimental evidence provided by the unpolarized neutron reflectometry suggests a long range AFM order (AFM [0001]₄^A) [2] which is in contrast with the results from macroscopic magnetic measurement, showing the presence of a remanent magnetization [3]. To obtain information about the microscopic magnetic structure, the ⁵⁵Mn Nuclear Magnetic Resonance (NMR) study has been performed at 4.2 K on a 100 nm thin film of MgO (111)/Mn₂GaC in both zero-field (ZF) and at several external magnetic field values applied in the film plane. The results of NMR investigations suggest the presence of a spiral spin structure with Mn spins lying in hexagonal plane and the spiral period extending along the c-axis, incommensurate with the crystal lattice period. The asymmetric distribution of signal intensity observed in the ⁵⁵Mn spectra recorded in presence of the in-plane external field shows that the spiral structure of spins can be easily altered by the magnetic field, revealing a spatial modulation of the spin turning angle along the spiral axis. These observations confirm the extreme sensitivity of the magnetic structure to the competing ferro-antiferro exchange interactions within Mn₂GaC.

1. A.S. Ingason, et al. Materials Research Letters, 2:2, 89-93 (2014)
2. A.S. Ingason, et al. Phys. Rev. B 94, 024416 (2016)
3. M. Dahlgqvist, et al. Phys. Rev. B 93, 014410 (2016)

This work has been supported partially by a grant from National Science Center, Poland (UMO 2019/35/B/ST3/03676).

Analysis of the dysprosium M_5 circularly polarized X ray absorption spectrum to detect magnetically uncoupled rare earth atoms to TM in TM-RE amorphous alloys

J. Díaz^{1,2}, C. Blanco^{1,2}, P. Gargiani³, S. M. Valvidares³ and J.M. Alameda^{1,2}

¹ Departamento de Física, Universidad de Oviedo, 33007 Oviedo, Spain

² CINN (CSIC – Universidad de Oviedo), 33940 El Entrego, Spain

³ ALBA Synchrotron, 08290 Cerdanyola del Vallès, Spain

The magnetism of cobalt and dysprosium sublattices in thin films of disordered $\text{DyCo}_{4.6}$ alloys were analyzed using X ray circularly polarized magnetic dichroism at the Co $L_{2,3}$ and Dy $M_{4,5}$ edges. The detection method used for spectra acquisition was total electron yield. The alloys, 35 nm thick, were ferrimagnetic, with a compensation temperature of 150 K. They have perpendicular magnetic anisotropy. The hysteresis loops of both sublattices measured at RT and 2 K, far away from the compensation temperature of the alloy, were not completely identical, indicating a certain magnetic decoupling between both sublattices. At RT, the dysprosium magnetic moment decreases with increasing field intensity (figure 1a), whereas at 2 K, the dysprosium magnetic moment increases at a reduced rate with increased field compared to cobalt (figure 1b). We also noticed that the dysprosium magnetic moment at RT was below the minimum expected if all dysprosium moments were antiferromagnetically coupled to cobalt, indicating the presence of dysprosium oriented in the direction of the applied field which should be, therefore, magnetically uncoupled or weakly coupled to cobalt.

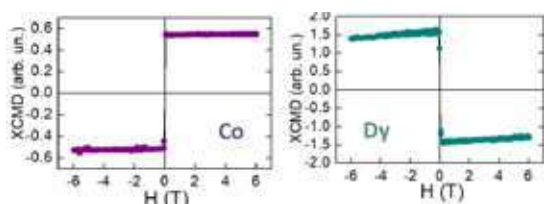


Figure 1. Co and Dy hysteresis loop at RT.

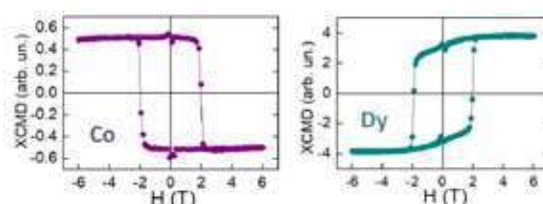


Figure 2. Co and Dy hysteresis loop at 2 K.

To understand these effects, we decomposed the Dy M_5 circularly polarized absorption spectrum in its spectral components related transitions to states with the dysprosium angular moment parallel, antiparallel and perpendicular to the applied field [1]. This was done taking advantage of the atomic-like behavior of the 4f electrons, and the fact that, due to the large orbital moment in dysprosium, the parallel and antiparallel spectral components have very small overlap, and they are easily deconvoluted from the XMCD related spectrum. The intensity of the deconvoluted components in the analyzed dysprosium M_5 spectra at RT and 2 K did not match the expected deduced from the magnetic moment values obtained from the XMCD sum rules. This indicates that the spectra must be formed by dysprosium atoms in different magnetic states, which are attributed to those related to strongly coupled to cobalt, and those uncoupled or weakly coupled to cobalt. A model is proposed that place most of the uncoupled dysprosium atoms at the surface of the alloy, as photoemission spectroscopy measurements done in similar samples proved, indicating rare earth segregation at the surface. This is also coherent with the surface sensitivity of the method used to detect the absorption spectra (TEY). The proposed spectral deconvolution analysis can be extended to other rare earths like Tb and Nd, whose orbital moment in their 4f orbital is not zero.

[1] J. Díaz and C. Blanco. Phys. Rev. B 104, 054439 (2021)

Vortex chirality observation in trilayer disks of Fe/Al/Co using X ray resonant magnetic scattering

J. Díaz^{1,2}, L. M. Álvarez-Prado^{1,2}, M. Vélez^{1,2}, S. M. Valvidares³, I. Montoya⁴, C. Redondo⁴ and R. Morales^{5,6}

¹ *Departamento de Física, Universidad de Oviedo, 33007 Oviedo, Spain*

² *CINN (CSIC – Universidad de Oviedo), 33940 El Entrego, Spain*

³ *ALBA Synchrotron, 08290 Cerdanyola del Vallès, Spain*

⁴ *Dept. of Physical Chemistry, Univ. of the Basque Country UPV/EHU, E-48940 Leioa, Spain*

⁵ *Dept. of Physical Chemistry & BCMaterials, Univ. of the Basque Country UPV/EHU, E-48940 Leioa, Spain*

⁶ *IKERBASQUE, Basque Foundation for Science, E-48011 Bilbao, Spain*

A 2-dimensional square array of trilayer ellipsoidal disks of submicrometer size (800 nm), made of Si/Fe (14 nm)/Al (3 nm)/Co (17 nm) by laser interferometry, has been studied by X ray Resonant Magnetic Scattering (XRMS). Thanks to the chemical and chiral symmetry sensitivity of XRMS [1], the magnetic hysteresis loops of the Cobalt and the Fe layers were distinguished, and chiral asymmetries identified. The hysteresis loops obtained at different Bragg angles were investigated, demonstrating the sensitivity of the experimental technique to accurately determine the chirality of the vortex and their creation and annihilation fields in each of the two layers. The relative intensity of the Bragg peaks at large angles was increased from a pure 2D structure due to the curved shape of the surface of the disks, which was produced during the deposition process. This effect increased the intensity of the magnetic scattering at relatively large angles. The shape of the loops experiences the largest differences at short Bragg angles, stabilizing at large Bragg angles, where they become more like the expected from a magnetic vortex. The reason for this might be the presence of irregular behavior in some of the x ray probed disks whose magnetic scattering would die at large angles due to uncoherent magnetic configurations between their adjacent disks. Chiral asymmetry was clearly observed when the magnetic field was oblique to the disk symmetry axis, at the [11] orientation of the 2D disks lattice. The chiral sense was the same for both layers, contrary to the theoretically expected for two perfectly flat magnetostatically coupled disks. This was probably due to imperfections at their interface with the aluminum spacer, as demonstrated from their X ray resonant magnetic reflectivity curves. Their chiral sense changed with the direction of the magnetic field, indicating that the location of the vortex nucleation remained the same for the two directions of the field, and for the two magnetic layers. The hysteresis loops registered at different Bragg directions were symmetric for cobalt and iron in the chiral symmetric direction ([10] direction). However, they were markedly asymmetric in iron when the field was oriented in the [11] direction. In this case, vortex creation and annihilation fields in Fe were different for the ascending and descending hysteresis loop branches. Vortex annihilation and creation fields were more accurately determined in the loops measured at large Bragg angles by comparing the hysteresis loops taken on the opposite sides, transverse to the incident beam direction.

[1] J. Díaz, P. Gargiani, C. Quirós, C. Redondo, R. Morales, L. M. Álvarez-Prado, J. I. Martín, A. Scholl, S. Ferrer, M. Vélez and S. M. Valvidares. “Chiral asymmetry detected in a 2D array of permalloy square nanomagnets using circularly polarized x-ray resonant magnetic scattering”. *Nanotechnology* 31-2, pp.025702-025702. DOI:10.1088/1361-6528/ab46d7

Huge Dzyaloshinskii-Moriya interactions in Re/Co[n]/Pt thin films

Amar Fakhredine¹, Carmine Autieri², and Andrzej Wawro¹

¹*Institute of Physics, Polish Academy of Sciences, Aleja Lotników 32/46, PL-02688 Warsaw, Poland*

²*International Research Centre MagTop, Institute of Physics, Polish Academy of Sciences, Aleja 32/46, PL-02688 Warsaw, Poland*

In this work, we study the Dzyaloshinskii-Moriya interaction (DMI) in the modeled Re/Co[n]/Pt chiral multilayered system using DFT calculations and report its interfacial and additive character.

DMI is an antisymmetric indirect exchange interaction occurring between two spins \vec{S}_i and \vec{S}_j . It arises also in the systems with broken inversion symmetry e.g. at the interfaces [1], in the presence of spin-orbit coupling. In particular, it is expected in heavy metal/ferromagnet asymmetric layered structures. This interaction is fundamental for the appearance of complex magnetic structures, e.g. skyrmions which are promising for the industry of spintronic applications that offer ultra-small, ultrafast, and low power devices. The control of the DMI strength in multilayered structures allows us to manipulate the different sizes and stability of these magnetic objects [2].

The total DMI strength ($d^{\text{tot}}[\text{meV}]$) in the Re/Co[n]/Pt chiral multilayered system was calculated from the difference in energy between clockwise and anticlockwise configurations of the Co magnetic spin spirals which were further used to determine the micromagnetic DMI [3]. The investigated systems were composed of 5 atomic monolayers (ML) of Pt and 5 MLs of Re sandwiching the Co layer with a tuneable thickness ranging from 1 to 6 MLs. The micromagnetic DMI named as D was found as high as 5.78 mJ/m² for 3 layers of Co which is a considerably large value.

The layer resolved DMI strength at each Co layer shows the highest contributions from the two interfaces of the systems, namely Re/Co and Co/Pt, which add up to produce a huge additive outcome confirming that the DMI is an interfacial effect [4]. This also explains the dependence of the micromagnetic DMI on the number of Co layers since it appears due to the electron hybridization between magnetic moments in the 3d Co atoms and the strong spin-orbit coupling in 5d states of Pt and Re atoms.

This work was supported by the Polish National Science Centre under Project no. 2020/37/B/ST5/02299.

References

- [1] H. Soumyajyoti, S. Meyer, A. Kubetzka, and S. Heinze. Physical Review B 104, no. 18 (2021): L180404.
- [2] Morshed, Md Golam, K. H. Khoo, Y. Quessab, J.W. Xu, R. Laskowski, P. V. Balachandran, A. D. Kent, and A. W. Ghosh. Physical Review B 103, no. 17 (2021): 174414.
- [3] Yang H., Thiaville A., Rohart S., Fert A. & Chshiev M. Physical Review Letters 115, 267210 (2015).
- [4] S. K. Jena, R. Islam, E. Milińska, M. M. Jakubowski, R. Minikayev, S. Lewińska, A. Lynnyk, A. Pietruczik, P. Aleszkiewicz, C. Autieri and A. Wawro. Nanoscale 13, no. 16 (2021): 7685-7693.

Experimental Results and Numerical Calculation of Co-Tb Distribution from Magnetron Co-Sputtering Deposition with a Composition Gradient

Ł. Frąckowiak¹, F. Stobiecki¹, M. Urbaniak¹, M. Matczak², G. D. Chaves-O'Flynn¹,
M. Bilski³ and P. Kuświk¹

¹ Institute of Molecular Physics, Polish Academy of Sciences, Poznań, Poland

² Faculty of Physics, University of Białystok, Białystok, Poland

³ Institute of Applied Mechanics, Poznań University of Technology, Poznań, Poland

The magnetic properties of ferrimagnetic Rare Earth-Transition Metal (RE-TM) thin alloy films strongly depend on their RE concentration (c_{RE}). Therefore precise control of c_{RE} and of the total thickness is crucial for obtaining application quality films.

We present a method for depositing ferrimagnetic Co-Tb alloy films with a Tb concentration (c_{Tb}) gradient. Films are deposited by co-sputtering from two magnetron sputtering sources using the target-substrate configuration shown in FIG.1a. This method is theoretically supported by an mathematical model that considers the directional distribution of atoms emitted from the target (Knudsen's cosine law) to predict the spatial dependence of thickness and concentration across the sample plane [1].

Using this method, we have grown Si/Ti-4nm/Au-30nm/Co_{1-x}Tb_x-30nm/Au-5nm structures. Spatially resolved composition measurements reveal that the proposed technology allows to obtain approximately linear changes c_{Tb} from ~ 7 to 36 at.% along a specific direction of the substrate. From the magnetic properties as a function of c_{Tb} , the compensation point is found at around $c_{Tb} = 22$ at.% (FIG.1b), a lower value than for Co/Tb multilayers [2]. This effect was attributed to the different thickness and to the sperrimagnetic behavior of Co-Tb systems.

This work was financed by the National Science Centre Poland under PRELUDIUM funding Grant No. UMO-2018/31/N/ST5/01810. Ł.F. acknowledge support from the Foundation for Polish Science (FNP)

[1] Ł. Frąckowiak et al., Journal of Magnetism and Magnetic Materials **544**, 168682 (2022)

[2] Ł. Frąckowiak et al., Scientific Reports **8**, 1 (2018)

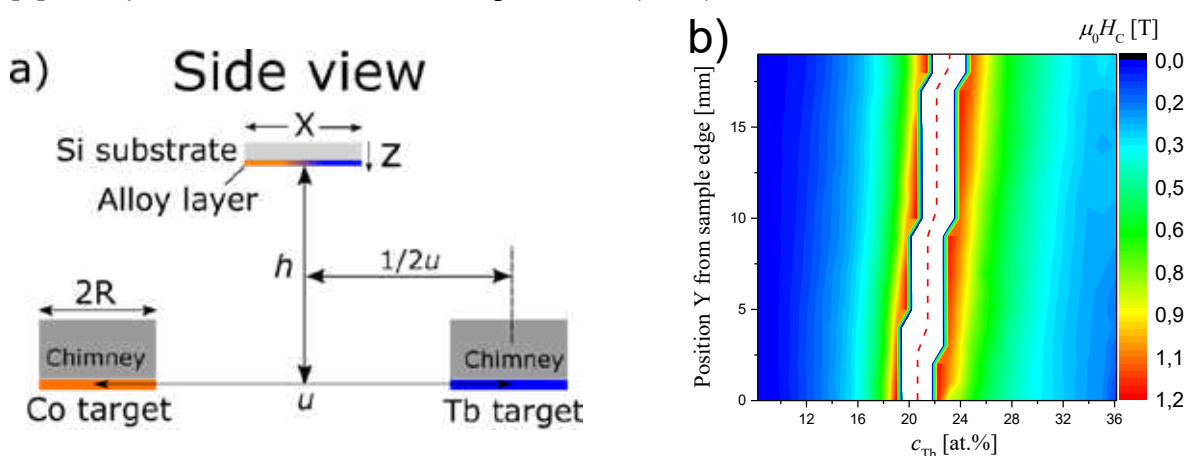


FIG. 1 (a) Schematic view of targets and substrate positions during the co-sputtering deposition of Co-Tb alloy films indicating relevant geometric parameters: R – radius of the target, u – distance between targets, h – distance between target and substrate planes. (b) Map of coercive fields (H_c) dependence on Tb concentration (c_{Tb}) for the Co-Tb film with c_{Tb} gradient (the red dashed line corresponds to the compensation concentration).

An *ab initio* study of antiphase boundaries in ferromagnetic B2-phase Fe₂CoAl alloy

M. Friák¹, J. Gracias², J. Pavlů² and M. Šob^{2,1}

¹ Institute of Physics of Materials, v.v.i., Czech Academy of Sciences, Brno, 616 00 Czech Rep.,

² Department of Chemistry, Faculty of Science, Masaryk University, Brno, 611 37, Czech Rep.,

In this study, we performed a quantum mechanical examination of thermodynamic, structural, elastic, and magnetic properties of single-phase ferromagnetic Fe₂CoAl with a chemically disordered B2-type lattice with and without antiphase boundaries (APBs) with (001) crystallographic orientation. Fe₂CoAl was modeled using two different 54-atom supercells with atoms on the two B2 sublattices distributed according to the special quasi-random structure (SQS) concept. Both computational models exhibited very similar formation energies, B2 structure lattice parameters, magnetic moments (1.266 and 1.274 μ_B /atom) and practically identical single-crystal elastic constants. The averaged APB interface energies were observed to be 199 and 310 mJ/m² for the two models. The studied APBs increased the total magnetic moment by 6 and 8% due to a volumetric increase as well as local changes in the coordination of Fe atoms (their magnetic moments are reduced for increasing number of Al neighbors but increased by the presence of Co), for details see Ref. [1]. Our study is built upon our previous quantum-mechanical calculations of APBs in Fe₃Al [2], Fe₃Al with segregating Cu atoms [3], Fe₇₀Al₃₀ [4], or Fe-Al-Ti superalloys [5].

[1] M. Friák, J. Gracias, J. Pavlů, M. Šob, A quantum-mechanical study of antiphase boundaries in ferromagnetic B2-phase Fe₂CoAl Alloy. *Magnetochemistry* 7 (2021) 137.

[2] M. Friák, M. Černý, M. Všianská, M. Šob, Impact of antiphase boundaries on structural, magnetic and vibrational properties of Fe₃Al, *Materials* 13 (2020) 4884.

[3] M. Friák, M. Černý, M. Šob, The impact of vibrational entropy on the segregation of Cu to antiphase boundaries in Fe₃Al, *Magnetochemistry* 7 (2021) 108.

[4] M. Friák, M. Golian, D. Holec, N. Koutná, M. Šob: An *ab initio* study of magnetism in disordered Fe-Al alloys with thermal antiphase boundaries, *Nanomaterials* 10 (2020) 44.

[5] M. Friák, V. Buršíková, N. Pizúrová, J. Pavlů, Y. Jirásková, V. Homola, I. Miháliková, A. Slávik, D. Holec, M. Všianská, N. Koutná, J. Fikar, D. Janičkovič, M. Šob, J. Neugebauer, Elasticity of phases in Fe-Al-Ti superalloys: Impact of atomic order and anti-phase boundaries, *Crystals* 9 (2019) 299.

The 4×4 transfer matrix method: a flexible and computationally efficient tool for exploring a system's surface magnon polaritons

N. Hale, I. Simonsen, C. Brüne, and M. Kildemo

Department of Physics, NTNU – NO-7491 Trondheim, Norway

The surface magnon polaritons (SMPs) present in thin film antiferromagnet semiconductors (AFSs) can be extremely confined, having most of their energy distributed within the magnetic medium. Berreman's 4×4 transfer matrix method (TMM) is used to study the SMPs supported by AFSs [1]. Specific focus is placed on MnF_2 , which has a uniaxial permeability, the in-plane component of which has a Lorentzian shape [2].

$$\mu_{xx}(\omega) = \mu_{yy}(\omega) = 1 + \frac{2\mu_0\gamma^2 B_a M_s}{\omega_0^2 - (\omega + i\Gamma)^2}, \quad \mu_{zz}(\omega) = 1 \quad (1)$$

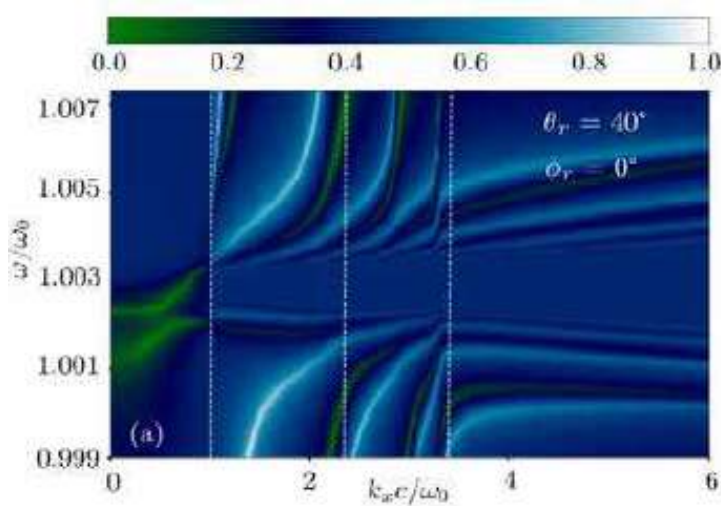


Figure 1: Reflectivity $\log_{10}(\mathcal{R}_{ss})$ (as seen in the colour map) plots of s-polarised light as a function of reduced real component of the in-plane wave vector and reduced angular frequency of an Air/100 μm MnF_2 / 500 μm Si substrate/Air system.

where the gyromagnetic ratio $\gamma/2\pi c = 0.975 \text{ cm}^{-1}/\text{T}$, the anisotropy field $B_a = 0.787 \text{ T}$, the sublattice magnetisation $M_s = 6.0 \times 10^5 \text{ A/m}$, the resonant frequency $\omega_0/2\pi c = 8.94 \text{ cm}^{-1}$, the magnon damping term being $\Gamma/2\pi c = 0.0007 \text{ cm}^{-1}$ and μ_0 being the permeability of free space. Here $\bar{\mu}$'s easy axis is assumed in the z direction. As the TMM is essentially 1D it is consequently much faster than full field methods such as FDTD. The flexibility of this approach means MnF_2 's uniaxial permeability can be rotated according to $\bar{\mu} =$

$\bar{\mathbf{A}}_{\text{rot}}(\phi_r, \theta_r, \psi_r) \bar{\boldsymbol{\mu}}_{ca} \bar{\mathbf{A}}_{\text{rot}}(\phi_r, \theta_r, \psi_r)^{-1}$. where $\bar{\boldsymbol{\mu}}_{ca}$ is the permeability tensor in the crystal's reference frame and $\bar{\mathbf{A}}_{\text{rot}}(\phi_r, \theta_r, \psi_r)$ is the rotation matrix. The angles ϕ_r , θ_r and ψ_r are defined as rotations about the crystal's z axis, the crystal's new y axis and the new z axis respectively. Reflection coefficients can then be modelled, the poles of which correspond to energy channels including surface modes, as seen in Fig. 1. This work offers insights into what to expect from future time-domain THz transmission spectroscopy or THz emission spectroscopy on more realistic SMP supporting systems. This should aid the development for future applications in fields including spintronics and sub-diffractive optics.

[1] D. W. Berreman, J. Opt. Soc. Am. **62**, 502 (1972).

[2] B. Lüthi, D. L. Mills, and R. E. Camley, Phys. Rev. B **28**, 1475 (1983).

A High Throughput Study of Hard Magnetic CeCo₅-based Thin Films

Yuan Hong¹, Thibaut Devillers¹, Stéphane Grenier¹, Leonid V. Pourovskii²,
Konstantin Skokov³, Oliver Gutfleisch³, Masao Yano⁴, Tetsuya Shoji⁴,
Akira Kato⁴, Noritsugu Sakuma⁴, Akihito Kinoshita⁴, Harald Oezelt⁵,
Thomas Schrefl⁵, Nora M. Dempsey¹

¹ Univ. Grenoble Alpes, CNRS, Grenoble INP, Institut NEEL, 38000 Grenoble, France

² Centre de Physique Théorique, Ecole Polytechnique, CNRS, 91128 Palaiseau, France

³ Technische Universität Darmstadt, Materialwissenschaft, D-64287 Darmstadt, Germany

⁴ Advanced Material Engineering Div., Toyota Motor Corporation, 1200 Susono, Shizuoka, Japan

⁵ Depart. Integrated Sensor Systems, Danube University Krems, A-2700 Wiener Neustadt, Austria

Combinatorial studies based on the preparation and characterisation of compositionally graded thin films are being used for the screening and optimization of a range of functional materials, including hard magnetic materials [1]. This high-throughput approach holds much potential to study the effect of element substitution in Rare Earth - Transition Metal hard magnetic phases (2-14-1, 1-5, 1-12), so as to address the RE-balance problem. The large experimental data-sets produced in such studies can feed into data-driven machine learning magnet design. Here we will present a study of compositionally graded Ce-Co and Ce-Co-M films, where the choice of the substituting element (M) is guided by *ab initio* calculations. The films were fabricated with composition gradient by magnetron sputtering of a Co target partially covered by foils of Ce and the substituting element. Sets of such films with different composition gradients have been deposited at room temperature and then annealed. All films underwent high throughput characterization (EDX, XRD, MOKE) to see how phase formation and magnetic properties vary with composition and annealing conditions. Examples of ternary diagrams of coercivity vs composition of Ce-Co-Zn films annealed for 10 minutes at different temperatures are shown in Figure 1. Certain samples were selected for detailed magnetic (VSM-SQUID) and structural (TEM) characterization. Machine learning data analysis was used to establish correlations between structural and magnetic properties. This thin film combinatorial study should help guide the development of high-performance bulk permanent magnets which are free of critical rare earth elements.

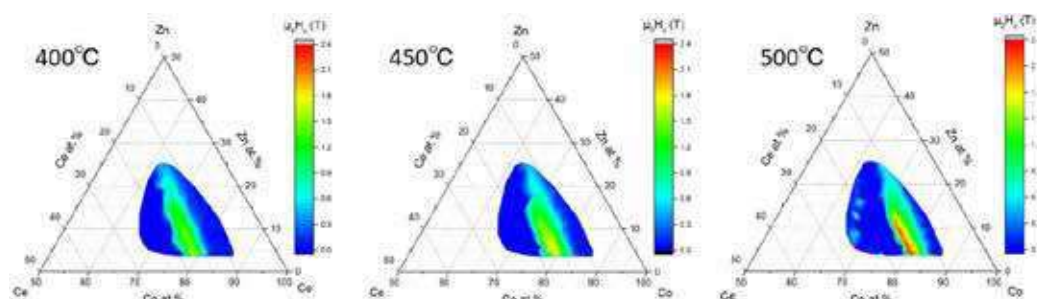


Fig. 1 Ternary diagrams of coercivity (MOKE) vs composition (EDX) of 150nm thick Ce-Co-Zn films annealed for 10 minutes at different temperatures.

[1] Y. Hong et al., *J. Mater. Res. Technol.* In press. doi.org/10.1016/j.jmrt.2022.03.055.

Stability of MnAl-C magnet alloys in the presence of water

F. Jürries^{1,2}, L. Beyer^{1,2}, K. Nielsch^{1,2}, T. G. Woodcock²

¹ Leibniz IFW Dresden, Helmholtzstrasse 20, 01069, Dresden, Germany

² Technische Universität Dresden, 01069, Dresden, Germany

With the increasing demand for permanent magnets, much research aims to find new permanent magnet material with a $(BH)_{\max}$ between that of hard ferrites and of Nd-Fe-B. The phase τ -MnAl is a promising candidate thanks to its excellent intrinsic properties and the low criticality of its raw elements. The best $(BH)_{\max}$ values for bulk MnAl-based magnets are achieved after hot extrusion [1]. Due to the metastable character of the τ -phase, carbon is added to enhance the thermal stability. It was shown that C-addition leads to the formation of Mn_3AlC in extruded MnAl-based magnets, which is believed to improve the coercivity [2]. In addition to this presumably positive effect, Mn_3AlC tends to react in humid environments [3] and therefore the stability of MnAl-C-based materials in the presence of water must be analysed in detail. To our knowledge this work is the first explicitly focusing on the stability of MnAl-C magnets in water, which is an important aspect for possible applications. In this work the stability of carbon-rich MnAl-C alloys in distilled water at 80 °C was analysed alongside that of the magnet composition $(Mn_{53}Al_{45}C_2)_{99.4}Ni_{0.6}$. Structural analysis was done both on a micro- and macro-scale using scanning electron microscopy techniques and X-ray computer tomography. In order to analyse possible hydrolysis reactions a combined method of differential scanning calorimetry, thermogravimetry and mass spectrometry was used. The magnetic properties of the magnet composition were measured with a permeameter. The experiments showed that Mn_3AlC leads to decrepitation of the C-rich alloys; however, structural analysis of the extruded magnet alloy showed no crack formation, and no degradation of the magnetic properties could be seen (Figure 1). This demonstrates the excellent stability of the MnAl-C magnet material in the presence of water despite the presence of Mn_3AlC precipitates.

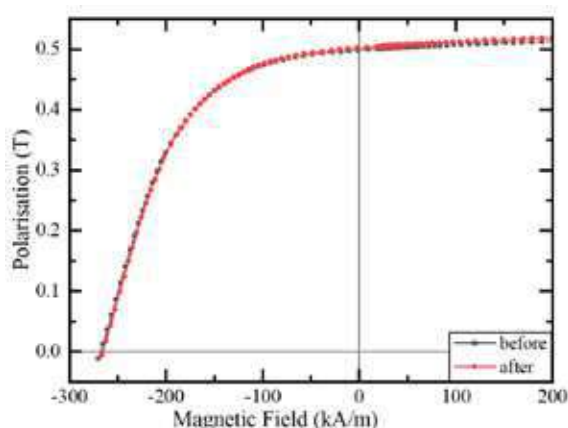


Figure 1: Polarisation vs. Magnetic field curves of $(Mn_{53}Al_{45}C_2)_{99.4}Ni_{0.6}$ before and after 30 days in distilled water at 80 °C. Only the demagnetising branch is shown.

- [1] L. Feng et al., *Acta Mater.*, **199**, pp. 155–168, 2020.
- [2] T. Ohtani et al., *IEEE Transactions on Magnetics*, **13**, pp. 1328-1330, 1977.
- [3] P. Karen et al. , *Collect. Czechoslov. Chem. Community*, **52**, pp. 1216–1222, 1987.

Exchange spring and exchange bias effects in the bulk Heusler Ni_2MnSn -based alloys

J. Kamarád¹, J. Kaštil¹, M. Friák², O. Schneeweiss², I. Turek², Z. Arnold¹

¹*Institute of Physics, Czech Academy of Sciences, 182 21 Prague 8, Czech Republic*

²*Institute of Physics of Materials, Czech Academy of Sciences, 616 62 Brno, Czech Republic*

The structural martensitic transformation from orthorhombic low temperature martensite (M) into cubic high temperature austenite (A) has been detected in the Heusler $\text{Ni}_2\text{Mn}_{1-x}\text{Sn}_{1-x}$ alloys in composition range ($0.3 < x < 0.7$) [1]. We have revealed the extraordinary exchange spring (ESP) and exchange bias (EB) effects at low temperature range in bulk martensite phase of the zero-field-cooled (ZFC) and field-cooled (FC) off-stoichiometric Ni_2MnSn -based alloys, respectively. Antiferromagnetic (AFM) interaction for the nearest neighbor Mn-Mn atoms, ferromagnetic (FM) interaction for Ni-Ni and Ni-Mn pairs and a presence of FM clusters in AFM environment - called as the super-spin glass state (SSG) – were taken into consideration to describe the magnetic behavior of the Heusler alloys [2]. ESP effect is characterized by double hysteresis loop and the spring behavior of magnetization is a consequence of freezing of randomly oriented FM clusters in AFM environment at low temperature (SSG in ZFC alloys), see Fig. 1. EB effect in the FC alloys is seen in Fig. 1 as a shift of hysteresis curve along field axis that is induced by a freezing of the FM clusters oriented into direction of external field. The interfacial exchange interaction between FM clusters and AFM environment that decreases with increasing temperature plays a dominant role in the temperature and field dependence of both the studied effects. Consequently, EB effect continuously decreases and ESP effect gradually transfers into standard hysteresis behavior with increasing temperature. A strength of the interfacial exchange interaction can be tested by a determination of the critical fields of ESP and EB effects. In dependence on composition of the alloys, the critical fields fall into interval from 300 Oe to 1700 Oe at temperature 5 K.

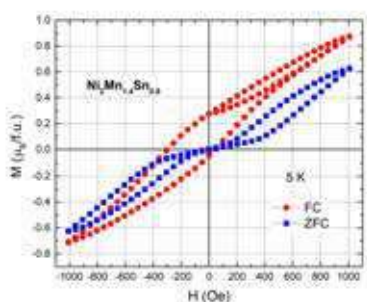


Figure 1: Exchange bias (red) and exchange spring (blue) effects in the Heusler $\text{Ni}_2\text{Mn}_{1.4}\text{Sn}_{0.6}$ alloy.

Based on received and literature data, the combined structural and magnetic phase diagram of the FC Mn-rich Ni_2MnSn -based alloys is proposed that describes temperature induced changes of the magnetic cluster structures. Based on the received results, a dominant role of an inhomogeneity and a variety of structural phases of the off-stoichiometric Ni_2MnSn -based alloys in the exchange spring and exchange bias effects will be discussed in this conference contribution.

[1] P.J. Brown, A.P. Gandy, K. Ishida, R. Kainuma, T. Kanomata, K.-U. Neumann, K. Oikawa, B. Ouladdiaf, K.R.A. Ziebeck, *J. Phys. Condens. Matter* **18**, 2249 (2006).

[2] A.K. Nayak, M. Nicklas, S. Chadov, P. Khuntia, Ch. Shekhar, M. Baenitz, Y. Skourski, V.K. Guduru, A. Puri, U. Zeitler, J.M.D. Coey, C. Felser, *Nature Mater.* **14**, 679 (2015).

Isotropic exchange bias in patterned IrMn/CoFe bilayers

I. Montoya¹, L.E. Fernandez-Outon^{2,3}, C. Redondo¹, W.A.A. Macedo³, R. Morales^{4,5}

¹Physical Chemistry Department, University of the Basque Country UPV/EHU, 48940 Leioa, Spain

²Departamento de Física, Universidade Federal de Minas Gerais, 31270-901, Belo Horizonte, MG, Brazil

³Centro de Desenvolvimento da Tecnologia Nuclear, CDTN, 30123-970 Belo Horizonte, MG, Brazil

⁴Physical Chemistry Dept. & BCMaterials, University of the Basque Country UPV/EHU, 48940 Leioa, Spain

⁵IKERBASQUE, Basque Foundation for Science, 49011 Bilbao, Spain

The exchange bias phenomenon relies on the high anisotropy of pinned antiferromagnetic (AFM) spins to shift the hysteresis loop of ferromagnetic (FM) materials.[1] Strength and direction of the AFM anisotropy can be determined during the material deposition, thermal treatments and cooling protocols.[2] Polycrystalline materials present a broad anisotropy distribution but subsequent treatments can limit the anisotropy dispersion and, consequently, modify the magnetic properties of the material.

This work shows the evolution of a random anisotropy distribution under thermal treatments and the impact on the magnetic behavior of patterned thin films of IrMn/CoFe. As-grown films present isotropic single hysteresis loops. However, magnetization curves of patterned thin films exhibit double hysteresis loops that are also isotropic for in plane magnetic fields. These curves were fitted to a double loop equation to isolate positive and negative exchange bias contributions. Extracted parameters such as magnetization remanence, exchange bias field, and coercive field uncover a general view of the magnetic structure. Additionally, a microscopic model based on AFM/FM grains with random anisotropy orientations accounts for the shape of the hysteresis loops and postulates the underlying physics that explains isotropic loops with both positive and negative exchange bias shifts.

Authors acknowledge financial support from the Brazilian Agencies CNPq (Grant 311677/2018-5), FAPEMIG (Grant PPM-00431-17), LEFO, and the Spanish PID2019-104604RB-C33/AEI/10.13039/501100011033.

[1] R. Morales et al. *ACS Appl. Nano Mater.* **3**, 4037 (2020); doi: 10.1021/acsanm.0c00052

[2] I. Montoya et al. *Appl. Phys. Lett.* **117**, 092401 (2020); doi: 10.1063/5.0021267

Magnetic Characterization of Co₂MnAl/ PMN-PT (011) Multiferroic Heterostructures

Okan Ozdemir^{1,2}, Leyla Colakerol Arslan³

¹Department of Physics, Yıldız Technical University, Esenler, Istanbul 34220, Turkey

²Institute of Nanotechnology, Gebze Technical University, Gebze, Kocaeli 41400, Turkey

³Department of Physics, Gebze Technical University, Gebze, Kocaeli 41400, Turkey

Manipulation of magnetic properties by electric fields is becoming increasingly important for the implementation of spintronics devices in information and communication technologies. In the field of magnetic mediated data storage, sensors, and spintronics devices, voltage control of magnetism is a critical technique for the prevention of warming up and high power consumption. The formation of a hybrid piezoelectric/ferromagnetic device is a method for achieving voltage control of magnetization. In this method, an external voltage applied induced strain transferred from a piezoelectric substrate to a ferromagnetic thin film, allowing the manipulation of magnetic properties. Ferroelectric Pb(Mg_{1/3}Nb_{2/3})O₃-PbTiO₃ (PMN-PT) single crystals have been widely used as piezoelectrically active substrates recently [1,2]. Co₂MnAl (CMA) Heusler alloys are considered of large interest because of their multifunctional nature and the presence of topologically protected surface states [3-5].

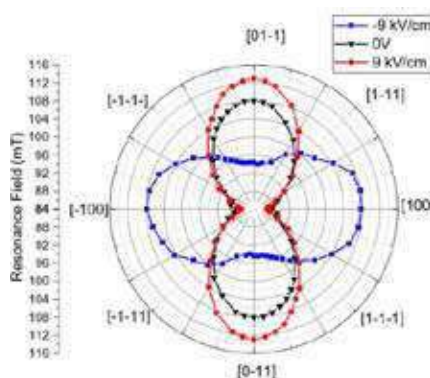


Figure 1: In-plane magnetic anisotropy of the sample obtained from FMR for electric fields of 0 and ± 9 kV/cm.

magnetic anisotropy can be obtained by measuring the angular dependence of resonance field H_r derived from FMR spectra for electric fields of 0 kV/cm and ± 9 kV/cm. The 90° in-plane rotation of the magnetic easy axis controlled by electric field can be attributed to piezoelectric strain generated in the ferroelectric layer. So, E-field controlled magnetization switching in these multiferroic heterostructures is of great interest for new generation spintronic devices. This work was supported by The Scientific and Technological Research Council of Turkey (TUBITAK) under Grant No. 118M193

In this study, CMA ferromagnetic layers on PMN-PT (011) substrate have been grown and characterized. CMA films were prepared at a temperature of 330 °C by magnetron sputtering with different thicknesses. During the deposition process, the film was kept at a fixed azimuthal angle such that an easy axis of magnetization can be aligned to the [001] direction of the substrate azimuthal and perpendicular to the deposition flux direction. In-situ XPS measurements were carried out to determine the atomic concentrations of the elements. The magnetic properties of CMA were investigated by vibrating sample magnetometer (VSM) and Ferromagnetic Resonance (FMR) while an external electric field was applied to the substrate. The voltage induced strain causes large and anisotropic variations in squareness ratio and coercivity at room temperature. As seen in Fig, in-plane

[1] Uchino, K. and Nomura, S., Journal of Applied Physics 51, 1142 (1980).

[2] Choi, S. W., Shrout, R. T. R., Jang, S. J., & Bhalla, A. S., Ferroelectrics, 100:1, 29-38 (1989)

[3] K.K. Meng, J. Miao, X.G. Xu, J.H. Zhao, Y. Jiang, Physics Letters A, 381, 13, 1202-1206 (2017)

[4] Liu, J., Qiao, S., Chen, M., Ning, X., Wang, S., Fu, G., Journal of Alloys and Compounds, 738, 331-335 (2018)

[5] Zhang, B., Wang, H-L., Cao, J., Li, Y.C., Yang, M.Y., Xia, K., Zhao, J.H., Wang, K.Y., Journal of Applied Physics 125, 082503 (2019)

Nonlinear Domain Wall Dynamics in Highly Magnetostrictive Amorphous Nanowires Prepared by Rapid Solidification

Sorin Corodeanu, Costică Hlenschi, Cristian Rotărescu, Horia Chiriac, Nicoleta Lupu and T.-A. Óvári

National Institute of R&D for Technical Physics, 47 Mangeron Boulevard, 700050 Iași, Romania

Amorphous glass-coated nanowires prepared by glass-coated melt spinning are prospective candidates for novel micro- and nanosensing devices, as well as for magnetic domain wall logic-based applications [1].

Here we report on the magnetization reversal and its associated single domain wall displacement in $\text{Fe}_{77.5}\text{Si}_{7.5}\text{B}_{15}$ amorphous glass-coated nanowires with high saturation magnetostriction ($\lambda_s = 25 \times 10^{-6}$). The investigated nanowires were between 90 and 350 nm in diameter, with an average glass coating thickness of 12 μm .

We have measured their hysteresis loops by means of a specifically developed inductive method. All samples exhibit rectangular loops, irrespective of their dimensions, which indicates that magnetization reversal consists in the depinning and propagation of a single magnetic domain wall when the applied field reaches to a certain value called switching field. Using a Sixtus-Tonks-based method, we have measured the velocity of this single domain wall in its displacement from one end of the nanowire to the other. We have also explored the field dependence of the domain wall velocity for applied field values between the switching field and the maximum applied field of 30 kA/m.

Figure 1 shows the dependence of both domain wall velocity and switching field on the diameter of the amorphous nanowires. They display similarly shaped curves, indicating their close interdependence and their shared origin.

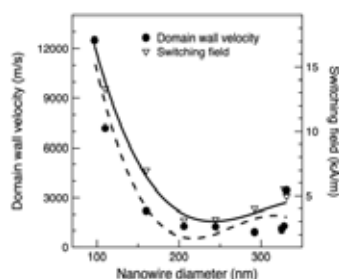


Figure 1: Magnetic domain wall velocity and switching field vs. nanowire diameter.

The thinnest nanowires allow the fastest propagating magnetic domain walls, with the velocity dropping quickly as the diameter increases up to 200 nm. For larger diameters, there is a slight increase in the wall velocity values. The nonlinear behavior is attributed to the magnetoelastic and shape anisotropies, the former resulting from the nonlinear distribution of internal stresses induced during the rapid quenching preparation method.

Summarizing, the magnetic switching field and domain wall velocity can be successfully controlled by means of nanowire dimensions, which is valuable for specific applications based on the domain wall propagation.

This work was supported by the Romanian Executive Unit for Financing Higher Education, Research, Development, and Innovation (UEFISCDI) through project PN-III-P4-ID-PCE-2020-1856 MaDWalls (contract PCE 1/2021).

[1] J. Alam, C. Bran, H. Chiriac, N. Lupu, T.-A. Óvári, L.V. Panina, V. Rodionova, R. Varga, M. Vázquez, and A. Zhukov, *J. Magn. Magn. Mater.* **513**, 167074 (2020).

Magnetic properties of amorphous $\text{Co}_x\text{Zr}_{100-x}$ films

Parul Rani, Vladislav Kurichenko, Björgvin Hjörvarsson and Gabriella Andersson

Department of Physics and Astronomy, Uppsala University, Box 516, SE-751 20 Uppsala, Sweden

We investigated the magnetic properties of amorphous $\text{Co}_x\text{Zr}_{100-x}$ (where $x = 60, 65, 66, 67, 68, 69$, and 70 at. %) thin films in the temperature range $5\text{-}300$ K. The films were deposited on Si (100) substrates by dc magnetron co-sputtering at room temperature. Structural properties of the samples were investigated by “Grating incidence X-ray diffraction” (GIXRD) and “X-ray reflectivity” (XRR), confirming the samples to be x-ray amorphous with uniform thickness (40 nm). Samples with Co content above 65 at. % were found to be ferromagnetic at 5K , while samples containing 61 at. % Co do not exhibit any ferromagnetic signal. The magnetic ordering temperature and saturation magnetization were found to be increased close to linearly with the Co concentration.

Keyword: Amorphous thin films, Dc magnetron Sputtering, Alloys, Magnetic interaction, and Ordering temperature

The impact of finite magnetic anisotropy and hydrodynamics on the response of systems of magnetic colloidal particles

Pedro A. Sánchez^{1,2}, Joan J. Cerdà¹

¹*Physics Department, Universitat de les Illes Balears, Palma, Spain*

²*Faculty of Physics, University of Vienna, Vienna, Austria*

Magnetic micro- and nanoparticles are one of the most important building blocks for the design of advanced magnetoresponsive materials, being particularly ubiquitous in magnetic soft matter systems. The latter include materials of high technological interest such as magnetic fluids, gels and elastomers. This relevance has made magnetic colloidal particles a prominent research topic for already several decades. The theoretical modeling of such systems, however, is still very challenging. Whereas the magnetic properties of single particles can be modeled quite accurately, the behavior of their dispersions in liquid or viscoelastic backgrounds becomes very complex due to the long range nature of the interactions and the broad range of relevant time and length scales involved. Most models of magnetic soft matter systems rely on approximations of the magnetic properties of the particles either in the superparamagnetic limit, which corresponds to small nanoparticles with negligible magnetic anisotropy barriers, or in the rigid ferromagnetic limit, which represents large nanoparticles and microparticles with effective infinite anisotropy barriers. Our goal is to address the more challenging intermediate regime, in which the finite nature of the barrier cannot be neglected, and characterize its impact on diverse relevant systems of magnetic colloidal particles. Our approach is based on an extended, thermally activated Stoner-Wohlfarth scheme to model the Néel relaxation mechanism of the particles [1], combined with molecular dynamics simulations coupled to a hydrodynamic solver.

In this contribution we present preliminary results within the aforementioned framework for two simple systems: first, a small set of nanoparticles dispersed in a viscous fluid under the action of fluctuating external fields; second, a colloidal magnetic polymer, consisting in a chain of polymer crosslinked particles [2], under the combined action of hydrodynamic flows and external fields. These systems can not only serve as an initial step towards the study of more complex ones, but are also relevant for important practical applications, such as magnetic hyperthermia and microfluidics, respectively.

[1] M. A. Chuev, and J. Hesse, *J. Phys.: Condens. Matter* **19**, 506201 (2007).

[2] J. Byrom, P. Han, M. Savory, and S. L. Biswal, *Langmuir* **30**, 9045 (2014).

Magnetic properties of cobalt ultrathin film structures controlled by buffer-layer roughness

Verbeno C.H.¹, Nowak L.¹, Veis M.¹ and Zázvorka J.¹

¹ Institute of Physics, Faculty of Mathematics and Physics, Charles University, 12116, Prague, Czech Republic

Growth optimization of magnetic multilayers containing Co is a topic of interest because of their potential for technological applications, e.g., magnetic tunnel junctions [1]. Since the magnetic properties of thin films are strongly related to the growth parameters [2], the fine tuning of such parameters is necessary to produce multilayered materials with specific properties required in different applications. An efficient approach to tune the coercive field of Co ultrathin films by varying the underlayer thickness is demonstrated in this work. Using a magnetron sputtering system, we prepared thin films of Si/Au_x/Pt_{5nm}/Co_{0.7nm}/Au_{5nm} with various thicknesses of Au underlayer. The surface morphology on which Co layer is deposited (i.e., Si/Au_x/Pt_{5nm} films) was studied by atomic force microscopy measurements. As presented in Fig. 1a, we show the possibility of controlling the interfacial roughness by changing the Au underlayer thickness due to its island-like growth mechanism (Volmer-Weber mode) [3]. The morphology of Au, including the size and density of islands can be modified in the sputtering process. When the nominal Au thickness increases, the islands grow in larger lateral size, resulting in a higher overall roughness of the layer surface. Magnetization measurements indicate a direct influence of underlayer roughness on the coercivity of the films promoting additional magnetic anisotropy (Fig. 1b). With thickness of the Au layer up to 20 nm, we can continuously change the coercive field in the range from ~200 Oe to ~1000 Oe, while remaining a nearly constant saturation magnetization. The use of Cu replacing Au underlayer in the same multilayer structure was also investigated, demonstrating the possibility of coercivity adjustment using different materials. The results are important for applications where the magnetic properties of structures based on Co thin films could be adjusted via buffer-layer roughness engineering, allowing the optimization of these devices.

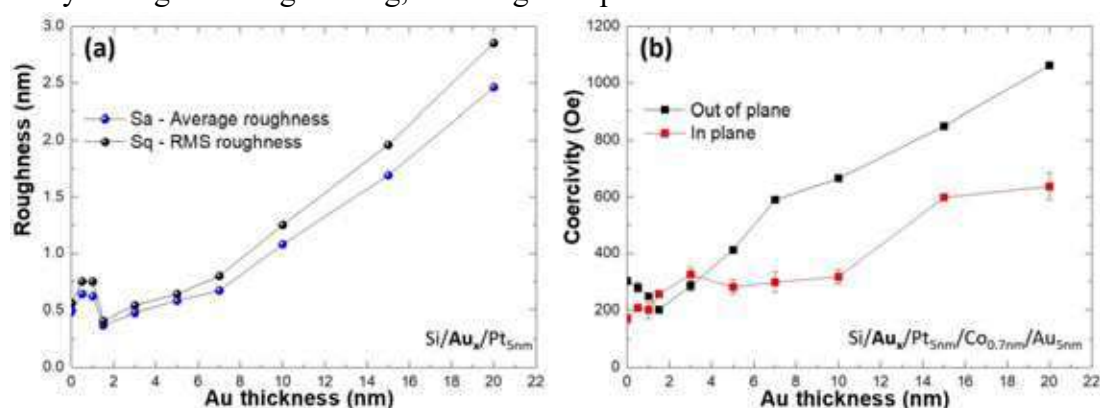


Figure 1: (a) Roughness values as a function of Au thickness obtained by AFM measurements of Si/Au_x/Pt_{5nm} samples. (b) The effect of the Au underlayer thickness on the coercivity of Si/Au_x/Pt_{5nm}/Co_{0.7nm}/Au_{5nm} films.

- [1] Raymenants E., Bultynck O., Wan D. *et al.* Nanoscale domain wall devices with magnetic tunnel junction read and write. *Nat. Electron* **4**, 392–398 (2021).
- [2] Srijani M., Sougata M. and Subhankar B., Effect of the growth conditions on the anisotropy, domain structures and the relaxation in Co thin films. *J. Magn. Magn. Mater* **428**, 50–58 (2017).
- [3] Guimarães A., Principles of Nanomagnetism, first ed., New York-USA, *Springer*, 106–109 (2009).

Multifunctional Fe-Au nanostructures synthesized by Laser Ablation in Liquids

Sara C. Freitas¹, João H. Belo¹, Miguel Canhota¹, Ana S. Silva¹, Helder Crespo¹, João P. Araújo¹ and Célia T. Sousa²

¹ IFIMUP, Departamento de Física e Astronomia, Faculdade de Ciências, Universidade do Porto, rua do Campo Alegre s/n, 4169–007 Porto, Portugal

² Departamento de Física Aplicada, UAM, Campus de Cantoblanco, Madrid, Spain

Pulsed Laser Ablation in Liquids (LAL) is a nanoparticle (NP) production technique that consists of a top-down approach in which a focused laser strikes a target that is immersed in a liquid solution. It can be applied with a wide range of target/liquid combinations and, by laser ablating multi-element target materials, nanoparticles (NP) with complex stoichiometries can be synthesized [1,2]. The primary goal of this work was to produce single element iron NP through the ablation of a bulk target. The second and main objective was to synthesize NP with more complex morphologies composed simultaneously by two materials (iron and gold) by ablating thin-film targets composed of different layers electrodeposited above a glass substrate. The ablations were carried out with a femtosecond (30 fs) pulsed laser operating at a beam wavelength of 800 nm in several liquid solutions including ethanol, acetone, and ultra-pure water. Currently, several efforts are undergoing to improve the control over the NP size distribution but both single and multi-element NP were already synthesized. In fact, NPs under the core-shell regime were successfully produced with this technique. These multifunctional hybrid-design NPs are prime candidates for biomedical applications since its geometry allows to combine different properties simultaneously in the same nanomaterial. The produced iron core-gold shell (Fe@Au CS) NPs, in particular, gather the high magnetization of the iron with the gold tunable plasmonic properties in the NIR region. Hereupon, this magnetoplasmonic nanostructure design can be employed to combine photothermia with magnetic hyperthermia into an efficient bimodal thermotherapy [3]. The Fe-Au-NS have been fully characterized with scanning electron microscopy (SEM), UV-Vis Spectroscopy, Dynamic Light Scattering (DLS) and superconducting quantum interference device (SQUID) techniques.

[1] V. Amendola and M. Meneghetti, PCCP 15(9) (2012).

[2] A. Tymoczko et al., Nanoscale Horizons 4(6) (2019).

[3] X. Liu et al. Theranostics 10(8) (2020).

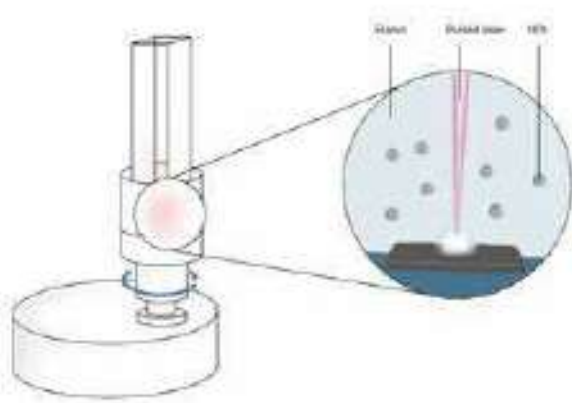


Figure 1: Schematic illustration of the Laser Ablation in Liquids set-up

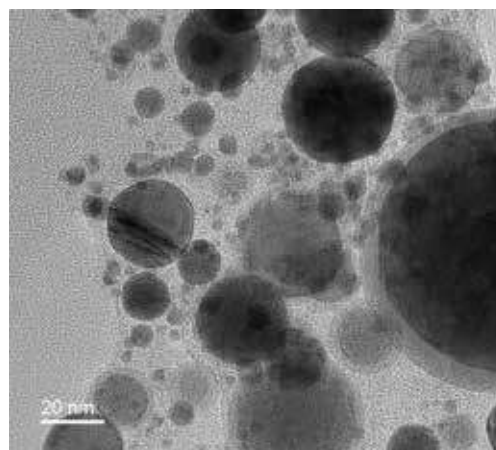


Figure 2: TEM image of the nanoparticles synthesized by Laser Ablation in Liquids enhancing the core-shell regime

Ferromagnetic resonance in Fe₃O₄ nanoparticles in combination with ligands

K. Sova¹, A. Vakula¹, T. Kalmykova¹, E. Bereznyak¹, A. Belous², S. Tarapov¹

¹ O.Ya. Usikov Institute for Radiophysics and Electronics of the National Academy of Sciences of Ukraine, 12 Acad. Proskury St., 61085, Kharkiv, Ukraine

² V.I. Vernadsky Institute of General and Inorganic Chemistry of the National Academy of Sciences of Ukraine, 32/34 Palladina Blvd., 03142, Kyiv, Ukraine

We have experimentally investigated Fe₃O₄ nanoparticles with Fast Green ligand of different concentrations using ferromagnetic resonance method. The obtained results indicate the change of distance between nanoparticles depending on ligand concentration.

Keywords: magnetic nanoparticles, ligands, ferromagnetic resonance.

Magnetic nanoparticles are widely used in medicine [1]. For targeted delivery of drugs they are used in conjunction with medical products. It is possible to evaluate the concentration of a chemotherapeutic drug in a complex using the ferromagnetic resonance (FMR) method. For this purpose, it is convenient to take the Fast Green (FG) ligand as its properties are similar to some medications. Therefore, the aim of the work is experimental study of nanoparticles with FG ligand.

Using the FMR method, we have experimentally investigated Fe₃O₄ nanoparticles with FG of different concentrations in suspended matter. It was found that with addition of the ligand, the FMR curve broadens and shifts to higher fields depending on the ligand concentration (Fig. 1). The FMR frequency in the given samples can be described by [1]:

$$f = (\gamma/2\pi)[H(H+H_a+H_i)]^{1/2}, \quad (1)$$

where γ is the gyromagnetic ratio, H is the external magnetic field, H_a is the total field of the magnetic anisotropy field, H_i is the total field of the magnetic anisotropy field dependent on the distance between the nanoparticles.

This behavior of the peak indicates that an increase in the ligand concentration leads to an increase in the distance between nanoparticles. As a consequence, the dipole-dipole interaction between nanoparticles decreases in accordance with (1). The degree of collinearity of the entire magnetic system also decreases [2]. The efficiency of FMR as a nondestructive method to study of the state of

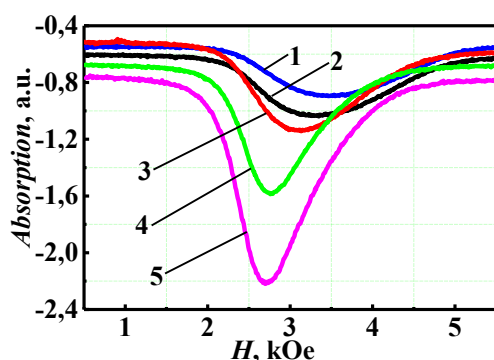


Figure 1: Experimental FMR peak in Fe₃O₄ nanoparticles at $f = 10$ GHz for different concentrations of FG: 0.0307 mg/ml (1), 0.0149 mg/ml (2), 0.004 mg/ml (3) and Fe₃O₄ in H₂O (4), dry Fe₃O₄ (5)

nanoparticles with ligands was shown.

[1] E. Bereznyak, E. Dukhopelnikov, D. Pesina, N. Gladkovskaya, A. Vakula, T. Kalmykova, S. Tarapov, et al., *BioNanoScience* **9**, 406-413 (2019).

[2] A. Vakula, E. Bereznyak, N. Gladkovskaya, E. Dukhopelnikov, A. Herus, S. Tarapov, Spectral Investigation of Magnetite Nanoparticles Interaction with Charged Drugs, MSMW'16, 21-24 June 2016, Kharkiv, Ukraine.

Crystal field model simulations of magnetic response of pairs, triplets and quartets of Mn^{3+} ions in GaN

D. Sztenkiel¹, K. Gas¹, J. Z. Domagala¹, D. Hommel^{2,3} and M. Sawicki¹

¹*Institute of Physics, Polish Academy of Sciences, Aleja Lotnikow 32/46, Warszawa, Poland*

²*Institute of Low Temperature and Structure Research, PAS, Wrocław*

³*Lukasiewicz Research Network–PORT Polish Center for Technology Development, Wrocław, Poland*

In the dilute case, for $x \leq 0.01$, the paramagnetic properties of $\text{Ga}_{1-x}\text{Mn}_x\text{N}$ were successfully described using single ion crystal field model approach. The basis for Mn^{3+} state are characterized by the set of spin and orbital quantum numbers $|m_S, m_L\rangle$. However, there is still a need to investigate the effect of magnetic coupling on magnetic properties of dilute magnetic semiconductors using approach that goes beyond the classical approximation, e.g. Landau-Lifshitz-Gilbert one.

A ferromagnetic coupling between localized Mn spins in GaN was predicted in a series of ab initio and tight binding works and later experimentally verified [1]. Therefore, in order to obtain the magnetization $M(T, H)$ of $\text{Ga}_{1-x}\text{Mn}_x\text{N}$ in the presence of interacting magnetic centers, we extend the previous model of a single substitutional Mn^{3+} ion in GaN, by considering pairs, triplets and quartets of Mn^{3+} ions coupled by a ferromagnetic superexchange interaction $-JS_1S_2$ [2]. Due to the short-ranged nature of spin-spin interactions, only the couplings between the nearest-neighbor Mn ions are taken into account. The relevant eigen-functions and eigen-values are obtained by a numerical diagonalization of the full (25×25) , $(25^2 \times 25^2)$, $(25^3 \times 25^3)$, $(25^4 \times 25^4)$ Hamiltonian matrix, for a single ion, pair, triplet or quartet, respectively. Using this approach we investigate how the magnitude of uniaxial anisotropy field in $\text{Ga}_{1-x}\text{Mn}_x\text{N}$ changes as the number of magnetic Mn ions in a given cluster increases. Our simulations are then exploited in explaining experimental magnetic properties of $\text{Ga}_{1-x}\text{Mn}_x\text{N}$ with $x \approx 0.03$, where the presence of small magnetic clusters gains in significance. As a result the approximate lower and upper limits for the values of exchange couplings between Mn^{3+} ions in GaN, being in nearest neighbors (nns) J_{nn} and next nns J_{nnn} positions, respectively, are established.

[1] A. Bonanni, *et al*, *Phys. Rev. B* **84**, 035206 (2011)

[2] D. Sztenkiel, K. Gas, J. Z. Domagala, D. Hommel and M. Sawicki, *New J. Phys.* **22**, 123016 (2020)

The work is supported by the National Science Centre, Poland, through projects DEC-2018/31/B/ST3/03438 and by the Interdisciplinary Centre for Mathematical and Computational Modelling at the University of Warsaw through the access to the computing facilities.

Valence Band Dispersion in (Ga,Mn)As, Ga(Bi,As), (Ga,Mn)(Bi,As) epitaxial nanolayers

Tataryn N.¹, Yastrubchak O.¹, Gluba L.², Sadowski J.^{3,4}, Gas K.⁴, Sawicki M.⁴

¹*V.E. Lashkaryov Institute of Semiconductor Physics, National Academy of Sciences of Ukraine, pr. Nauky 41, 03028, Kyiv, Ukraine*

²*Institute of Physics, Maria Curie-Skłodowska University in Lublin, Pl. M. Curie-Skłodowskiej 1, 20-031, Lublin, Poland*

³*Department of Physics and Electrical Engineering, Linnaeus University, SE-391 82, Kalmar, Sweden*

⁴*Institute of Physics, Polish Academy of Sciences, Al. Lotników 32/46, PL-02-668, Warsaw, Poland*

Dilute ferromagnetic semiconductors (DFSs) represent a class of alloys which combine semiconductor properties with magnetism in a single material. Their magnetic properties arise from transition metal ions introduced into the semiconductor parent lattice. The unique property of DFS spintronic devices is their capability of generating spin-polarized currents. In addition to the formation of spin current, of interest to spintronics, it is expected that the band structure changes arising from the presence of different doping ions such as Bi in the (Ga,Mn)As matrix, will lead to further developing of novel DFS device concepts.

The GaAs based ferromagnetic semiconductor alloy compounds containing Mn and Bi emerged as potential candidates for novel nanoelectronic and spintronic application. The (Ga,Mn)As, Ga(Bi,As) and (Ga,Mn)(Bi,As) nanolayers are grown using low temperature (230°C) molecular beam epitaxy (MBE). The superconducting quantum interference device (SQUID) magnetometry is used for the investigation of the magnetic properties of the heterostructures.

Photoreflectance (PR) measurements are used for the determination of the band gap (E_0) and spin-orbit split-off (E_{SO}) band to conduction band optical transitions. Besides the PR technique, the samples have been investigated by the μ Raman spectroscopy to confirm p-type character of Mn doped films by the observation of the Coupled Plasmon-LO Phonon Mode (CPPM).

The in-situ UV Angle Resolved Photoemission Spectroscopy (ARPES) is used for the band structure analysis of the epitaxial layers. The low temperature optical-energy-gap measurements supported by complementary characterization, for a series of (Ga,Mn)As, Ga(Bi,As) and (Ga,Mn)(Bi,As) nanolayers, show that the deep modification of the GaAs valence band caused by Mn incorporation occurs for a Mn content much lower than that supporting dilute ferromagnetic phase in the investigated nanofilms.

Fermi energy lies within the valence band and decreases as the Mn concentration increases, in accordance with the p-d Zener model. Our research reveals a shift of the chemical potential with increasing Mn doping and a highly dispersing band, crossing the Fermi level for high Mn concentration. The Bi doping induces modification of the spin-orbit split-off band.

Ni₂FeZ (Z = Ga, In, Tl) Heusler alloy nanowires prepared via electrodeposition

M. Varga^{1,2}, L. Galdun¹, K. Saksl³, R. Varga¹

¹ Center for Progressive Materials, UPJS-TIP, Tr. SNP 1, 04011, Kosice, Slovakia

² Dept. of Condensed Matter Physics, Inst. of Physics, Park Angelinum 9, 04001, Kosice, Slovakia

³ Institute of Materials Research, Slovak Academy of Sciences, Watsonova 47, 04001, Kosice, Slovakia

Heusler alloys with the chemical composition of Ni₂FeGa show a promising application potential regarding their multifunctional behavior, which includes a shape memory, ferromagnetic shape memory and multicaloric behavior [1, 2]. Its fabrication in the form of nanowires shows the preservation of the functional behavior, allowing the Ni-Fe-Ga nanowires to be potentially used as nanodimensional sensors or actuators [3].

The search for a novel composition of a Ni₂FeZ Heusler alloys might enhance the functional capacity of the prepared Heusler alloy nanowires or enlarge the preserved functional behavior. Therefore, we present the characterization of magnetic and structural properties of Ni₂FeZ (Z = Ga, In, Tl) nanowires.

Initially, all of the prepared samples exhibit a cubic structure with a lattice parameter that corresponds to a Heusler structure. Moreover, some of the prepared samples already show a functional behavior regarding their magnetic properties. Ni-Fe-Tl sample with an overall composition of Ni₆₉Fe₂₂Tl₉ shows a wide magnetization hysteresis within the temperature dependence of magnetic moment at 10 kOe (Figure 1a) with a significant change of coercive field (H_C) and saturation field (H_S) at different temperatures (Figure 1b) and a corresponding ΔS_M maximum. These properties suggest a shape memory or magnetocaloric behavior of the novel Ni₂FeZ (Z = Ga, In, Tl) nanowires.

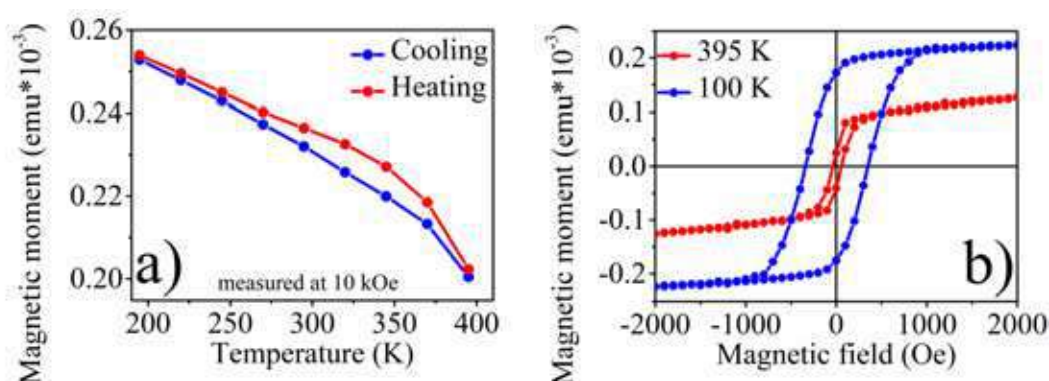


Figure 1: a) – Temperature dependence of magnetic moment for Ni₆₉Fe₂₂Tl₉ nanowires measured at 10 kOe with the temperature step of 25 K and stabilization at each temperature showing a wide hysteresis; b) – Hysteresis loops of the same nanowires showing a significant change of H_C and H_S at different temperatures

[1] M. Hennel, L. Galdun, T. Ryba and R. Varga, *J. Magn. Magn. Mater.* **511**, 166973 (2020).

[2] E. Villa, C.O. Aguilar-Ortiz, A. Nespoli, P. Álvarez-Alonso, J.P. Camarillo-Garcia, D. Salazar, F. Passaretti, H. Flores-Zúñiga, H. Hosoda and V.A. Chernenko, *J. Mater. Res. Technol.* **8**, 4540 (2019).

[3] M. Varga, L. Galdun, B. Kunca, V. Vega, J. García, V.M. Prida, E.D. Barriga-Castro, C. Luna, P. Diko, K. Saksl and R. Varga, *J. Alloys Compd.* **897**, 163211 (2022).

Capping layer influence on magnetic characteristics evolution in cobalt nanofilms

Y. Veretennikova¹, I. Shipkova¹ and S. Roschenko¹

¹ National Technical University Kharkiv Polytechnic Institute, 2, Kyrpychova Str., Kharkiv, Ukraine

Cobalt is very frequently studied in thin film development for applications such as spintronic devices and memory applications [1]. The way in which cobalt films are fabricated and protected from undesired processes has a strong influence on their final composition as well as magnetic properties or inner structure.

In this study we have investigated the kinetics of magnetic moment changes, as well as coercive force and anisotropy of Co films in dependence on the duration of stay in vacuum chamber, ageing in air at room temperature and the annealing temperature in the range from 50 to 150°C. The influence of upper capping layer (copper, silicon monoxide) on the kinetic peculiarities of magnetic properties evolution has been studied too.

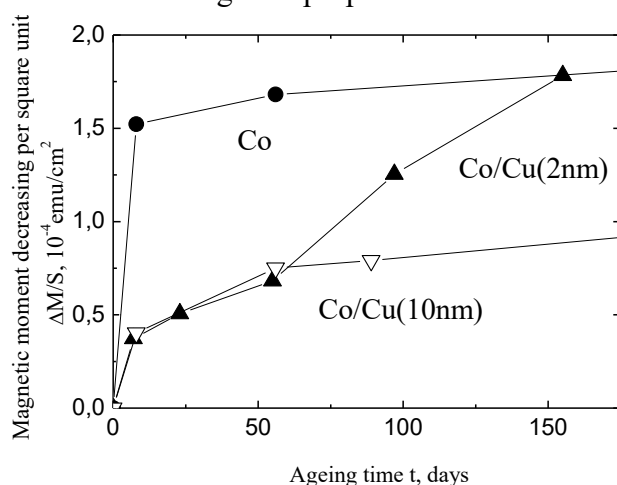


Fig.1 Change of magnetic moment of 2nm-thick Co films

It was revealed that decreasing of magnetic moment M of uncapped films began even in vacuum ($p \sim 10^{-6}$ Torr). At first the fast stage occurred (fig.1). Its rate was equivalent to thickness diminishing $\Delta h/\Delta t \sim 0.05 - 0.1$ nm/min. This stage finished at certain Δh value (0.03 – 1.1 nm) depending on the thickness of deposited film. The slow stage was observed when the sample was removed from vacuum chamber into air. It is possible to reduce the rate of fast stage by deposition of Cu

layer onto Co film. The process of M decreasing may be stopped by SiO layer deposition. At the same time Cu layer did not prevent against M lowering in air.

Behaviour of Co films covered by SiO in various time after Co deposition allows us to conclude that as-prepared films had saturation magnetization values equaled to bulk material one. Decreasing of mean saturation magnetization at calculations is the result of magnetic layer thinning. Probable causes of the effects observed are the oxidation reactions.

We assumed that different coercive force values of Co, Co/Cu and Co(2 nm)/SiO (35, 20 and 5 Oe, respectively) and their changes at ageing and annealing are connected with different extent of surface modification during oxidation. We also discuss a possible influence of similar oxidation processes on magnetic properties of Co/Cu multilayer structures.

[1] M.D. Coey, Magnetism and Magnetic Materials, Cambridge University Press, Cambridge, 2009.

A strong competition among the anisotropy terms in magnetically coupled Fe/Al/Fe thin film trilayers

Zengxin Wei, David Navas, Carlos Prieto and Manuel Vazquez

Instituto de Ciencia de Materiales de Madrid (ICMM-CSIC), Sor Juana Inés de la Cruz 3, 28049 Madrid, Spain

Since the late 1980s, when the antiferromagnetic coupling [1] and the giant magnetoresistance effect in Fe/Cr superlattices [2] were first observed, and until today, when different synthetic antiferromagnets based spintronic [3] and skyrmions [4] devices are being suggested, researchers have intensively worked on engineering the magnetic behaviour of stacks of magnetic and non-magnetic thin layers. In this work, the static and dynamic responses of symmetric systems, consisting of two ferromagnetic Fe thin films separated by a nonmagnetic spacer layer, such as Al, have been analyzed as a function of the Al thickness by performing in-plane angular dependent hysteresis loops and ferromagnetic resonance measurements. Polycrystalline Al (5 nm)/Fe (3 to 20 nm)/Al (5 nm) and Al (5 nm)/Fe (10 nm)/Al (0.4 to 2.0 nm)/Fe (10 nm)/Al (5 nm) multilayers were growth on Si substrates by DC sputtering technique. The reversal behavior, shown in the hysteresis loops (Figure 1), is accompanied by a complex magnetic response which confirms the presence of different competing anisotropy terms. In particular, the coupling between the Fe layers have been studied considering several energy contributions such as the magnetic dipolar, bilinear, and biquadratic exchange interactions, together with an in-plane induced uniaxial and cubic crystal anisotropies. The values of these different terms have been estimated by fitting our experimental results through minimizing the total free energy of the system.

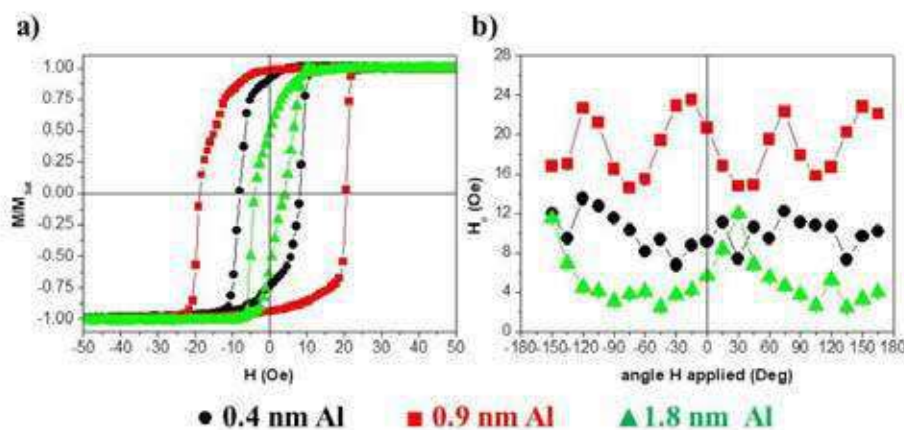


Figure 1: (a) Hysteresis loops of the Al(5 nm)/Fe (10 nm)/Al/Fe (10 nm)/Al(5 nm) trilayers for 0.4 (●), 0.9 (■) and 1.8 nm (▲) Al spacer thicknesses and along a hard magnetization axis (-60°). (b) In-plane angular dependence of the coercivity field for 0.4 (●), 0.9 (■) and 1.8 nm (▲) Al spacer thicknesses.

- [1] P. Grünberg, *et al.*, *Phys. Rev. Lett.* **57**, 2442 (1986).
- [2] M. N. Baibich, *et al.*, *Phys. Rev. Lett.* **61**, 2472 (1988).
- [3] R. A. Duine, *et al.*, *Nature Physics* **14**, 217 (2018).
- [4] W. Legrand, *et al.*, *Nature Materials* **19**, 34 (2020).

Demonstrating and tailoring exchange bias on novel bulk nanocomposites processed by severe plastic deformation

M. Zawodzki¹, L. Weissitsch¹, R. Pippan¹, P. Knoll², H. Krenn², S. Wurster¹ and A. Bachmaier¹

¹*Erich Schmid Institute of Materials Science of the Austrian Academy of Sciences, Jahnstrasse 12, 8700 Leoben, Austria*

²*Institute of Physics, University of Graz, Universitätsplatz 5, 8010 Graz, Austria*

Exchange bias (H_{eb}) has been predominantly investigated in layered nanostructures (mostly bilayers) produced by a variety of deposition methods. Severe plastic deformation (SPD) by high pressure torsion (HPT) opens a new path for demonstrating H_{eb} in bulk nanocomposites. The advantage of HPT compared to other SPD techniques is its large variation of applied strain and therefore the ability to control the microstructure of materials and their magnetic properties.

The focus in this investigation is on rare earth free permanent magnetic materials, which have still antiferromagnetic characteristics at room temperature (RT). The investigated materials consist of different ratios of ferromagnetic (FM) and antiferromagnetic (AFM) components. The goal of this study is to control the microstructure of obtained nanocomposites by applied strain or post thermal treatment and correlated the microstructural conditions to magnetic parameters.

The manufactured bulk nanocomposites were processed from initial powders. Powder compositions based on (Fe)Ni as FM- and NiO as AFM-phase were used. Various compositions were investigated. For powder blends with a high fracture of NiO prior ball milling to HPT processing was performed to enhance phase intermixing. Processed bulk material was analysed by scanning electron microscopy (SEM), X-ray diffraction (XRD) and superconducting quantum interference device (SQUID). SEM measurements showed a refinement of phase size over applied strain. Further wide angle X-ray scattering (WAXS) investigations conducted at Deutsches Elektronen-Synchrotron (DESY) revealed a coherent scattering domain size of a few tenths of nanometres.

Microstructural characterisations were correlated to hysteresis loop measurements. An H_{eb} shift of the hysteresis loops at 8K and RT was detected. Also an influence of applied strain was demonstrated on magnetic parameters like, H_{eb} and magnetic saturation. Additionally, the influence of phase interface morphology on magnetic parameters could be demonstrated.

This project has received funding from the European Research Council (ERC) under the European Union's Horizon 2020 research and innovation programme (grant agreement No:757333).

We acknowledge DESY (Hamburg, Germany), a member of the Helmholtz Association HGF, for the provision of experimental facilities. Parts of this research were carried out at PETRA III and we would like to thank Dr. N. Schell and Dr. E. Maawad for assistance in using P07B-High Energy Materials Science.

Tuning of Magnetoresistive Properties of Graphene-Lanthanum Manganite Structures

Nerija Zurauskiene^{1,2}, Skirmantas Kersulis¹, Voitech Stankevici^{1,2}, Mykola Koliada¹,
Valentina Plausinaitiene^{1,3}

¹ Department of Functional Materials and Electronics, Center for Physical Sciences and Technology, Sauletekio ave. 3, LT-10257, Vilnius, Lithuania,

² Faculty of Electronics, Vilnius Gediminas Technical University, Naugarduko 41, LT-03227, Vilnius, Lithuania

³ Faculty of Chemistry and Geosciences, Vilnius University, Vilnius, Lithuania, Naugarduko 24, LT-03225, Vilnius, Lithuania

The detection of magnetic fields with increased spatial resolution to micro-nanoscales is very important for magnetometry. It is of great interest to have low-dimension sensors with increased sensitivity and extended capabilities. The discovery of magnetoresistive (MR) effects (AMR, TMR, GMR and CMR) in magnetic structures encouraged fundamental research leading to a number of laboratory-scale and commercially available devices. Moreover, nowadays the magnetosensorics becomes very important for wearable electronics and soft robotics. Each application has its specific requirements for sensitivity, temperature and magnetic field ranges of operation, accuracy, sensor's positioning, etc. Therefore, the choice of material with specific properties and design of sensing element becomes very important.

It has been demonstrated that nanostructured manganite films exhibiting negative colossal magnetoresistance (CMR) effect can be successfully used for the development of magnetic field sensors operating in a wide range of magnetic fields (0.1 – 90 T) [1]. The demand of magnetic field sensors with scaled effective volume resulted in the research of magnetoresistive properties of two-dimensional (2D) materials such as graphene, which has a very high mobility of charge carriers. The graphene exhibits Lorentz force induced positive magnetoresistance phenomenon and can achieve large magnetoresistance (MR) values at high magnetic fields [2], however, at low fields the MR is low due to classical quadratic dependence on the field magnitude. On the contrary, the nanostructured manganite films show significant MR at low fields. This property is caused by so-called extrinsic magnetoresistance related to charge carrier transport across grain boundaries of polycrystalline films. Sensors based on nanostructured (polycrystalline) manganite films can measure magnetic field magnitude independently on field direction (B-scalar sensors) [1] which makes easier positioning of the sensors.

Recently, it was shown that hybrid graphene-manganite structure could be used for the development of magnetic field sensors with increased sensitivity in comparison with individual manganite or graphene sensors [3].

In this study, the possibility to tune magnetoresistive properties in a wide range of magnetic fields by changing the main parameters of graphene and manganite films in a hybrid graphene-manganite structure is presented and future perspectives for the application of such structure for the development of magnetic sensors are discussed.

[1] T. Stankevici, L. Medišauskas, V. Stankevici *et al.*, *Rev. Sci. Instrum.* **85**, 044704 (2014).

[2] F. Kisslinger, C. Ott, C. Heide *et al.*, *Nat. Phys.* **11**, 650 (2015).

[3] R. Lukose, N. Zurauskiene, S. Balevicius *et al.*, *Nanotechnology*, **30**, 355503 (2019).

Symposium 12. Magnetorecording media, magnetic memories and magnetic sensors

| | | |
|--------------------------|--|-----|
| Susana Cardoso | <i>Tunnel magnetoresistive sensor architectures for 2D and 3D fields detection</i> | 405 |
| Pavel Ripka | <i>Magnetic Sensors Based on Amorphous and Nano materials</i> | 406 |
| Pedro Brandao Veiga | <i>Engineering of Spin-Transfer-Torque Perpendicular Magnetic Tunnel Junctions at Cryogenic Temperatures with Very Low Switching Voltages</i> | 408 |
| Nuno Caçoilo | <i>Improved dynamical switching properties in Perpendicular Shape Anisotropy Magnetic Tunnel Junctions</i> | 409 |
| Robert Carpenter | <i>z-Field Control Through Stack Design to Enable Field-Free Switching of VCMA-MRAM</i> | 410 |
| Samuel Manceau | <i>Magnetic tunnel junctions with a symmetric response for ultra-sensitive sensors</i> | 411 |
| Dennis Seidler | <i>Single magnetic domain FeCoSiB multilayer-based magnetoelectric composites for biomagnetic field sensing</i> | 412 |
| Balram Singh | <i>Tuning strain-induced anisotropy of soft ferromagnetic structures</i> | 413 |
| Benjamin Spetzler | <i>Exchange-Bias Delta-E Effect Magnetic Field Sensors for Sensor Arrays</i> | 414 |
| Stanislav Vrtník | <i>Nonergodic effects in the spin-glass CoCrFeMnNi high-entropy alloy: Thermoremanent magnetization and Thermal memory cell</i> | 415 |
| Xing-Long Ye | <i>Voltage-driven giant modulation of magnetism in ferromagnetic metals with ultrahigh magnetocrystalline anisotropy</i> | 416 |
| Tomasz Zalewski | <i>Ultrafast photo-induced dynamics of multi states switching of magnetization in garnets</i> | 417 |
| Liza Zaper | <i>Scanning NV Magnetometry for Magnetic Memory Devices</i> | 418 |
| Sebastian Zeilinger | <i>Spin orbit torque enabled magnetic sensor with low offset and tunable sensitivity</i> | 419 |
| Susant Acharya | <i>Ionic Liquid Gating Control of Magnetic Anisotropy in Magnetic Tunneling Junction Stacks for Voltage Tunable Magnetoresistive Sensor</i> | 421 |
| Łukasz Fuśnik | <i>Bias voltage dependence of sensitivity in tunneling magnetoresistance sensors with voltage controlled magnetic anisotropy</i> | 422 |
| Elizaveta Golubeva | <i>Magnetic noise and loss in magnetoelastic magnetic field sensors</i> | 423 |
| Viola Krizakova | <i>Dual-pulse strategies for efficient switching of magnetic tunnel junctions</i> | 424 |
| Wayne Lack | <i>Thermodynamic properties and switching dynamics of perpendicular shape anisotropy MRAM</i> | 425 |
| Peter Leitner | <i>Numerically stable and highly performant implementations of the analytic magnetic field solution of the diametrically magnetized cylinder</i> | 426 |
| Thanh Binh Nguyen | <i>Higher-order Magnetic Anisotropy in Soft-hard Nanocomposite Materials</i> | 427 |
| Thanh Binh Nguyen | <i>HAMR Switching Efficiency in Coreshell L10/Al-FePt Grain</i> | 428 |
| Myriam Pannetier-Lecoeur | <i>Magnetic noise reduction strategies in magnetoresistive sensors for improved detection limits</i> | 429 |

| | | |
|-------------------------|--|-----|
| Joshua M. Salazar-Mejía | <i>Offset free magnetic sensing principle and the role of the spin-orbit torque coefficients</i> | 430 |
| Florian Slanovc | <i>Global Magnetic Topology Optimization</i> | 431 |

Invited Oral Presentations

| | | |
|----------------|--|-----|
| Susana Cardoso | <i>Tunnel magnetoresistive sensor architectures for 2D and 3D fields detection</i> | 405 |
| Pavel Ripka | <i>Magnetic Sensors Based on Amorphous and Nano materials</i> | 406 |

Tunnel magnetoresistive sensor architectures for 2D and 3D fields detection

Susana Cardoso^{1,2}, Pedro Ribeiro^{1,2}, Matko Kandzija^{1,2}, Mustafa Erkovan^{1,2}, Rita Macedo¹, Paulo P.Freitas¹

¹ INESC MN, Rua Alves Redol, 9, 1000-029 Lisboa Portugal

² Instituto Superior Tecnico, Universidade de Lisboa, Portugal

Magnetic field sensors based on magnetic tunnel junctions have been described in a wide range of applications, and offer a versatile choice in the operation parameters such as linear range from $\sim \mu\text{Tesla}$ to $\sim 100 \text{ mTesla}$, power consumption down to few mW, and active sensor dimensions from 20 nm to $\sim 100 \mu\text{m}$, among others. In this work, we describe the mechanisms enabling AlOx- and MgO- based TMR stacks to be viable for monolithic, wafer level, integration as X, Y, Z field sensors.

Discrete chip mounting is a simple solution to create 3D field sensors, but the reduction in the microfabrication costs are counterbalanced with additional costs with corrective electronics for the misalignment during mounting. In contrast, we will show monolithic fabrication of a tunnel magnetoresistance (TMR) sensor capable of measuring magnetic fields in X and Y directions. A discussion on the complexity of magnetic configuration control when a single TMR film stack is used for X and Y detection, when comparing with the use of two different TMR stack depositions will be done [1]. Moreover, the use of AlOx [2] and MgO-based stacks require different thermal annealing strategies for crystallization and reference layer setting. The selection of the MR materials and options regarding the thermal treatment for the reference layer orientation will be discussed in more detail, because the TMR microfabricated elements are often required to be assembled in a Wheatstone bridge architecture, where the reference layers are set at 180° . The integration of out-of-plane (Z) detection has been explored recently [3], and a solution with 10mT linear range is presented, while the paths for the monolithic integration with in-plane TMR structures for X and Y detection are discussed.

- [1] Pedro Ribeiro, et.al., “Bio-inspired ciliary force sensor for robotic platforms”, IEEE Robotics and Automation Letters (RA-L) vol.2 (2), 971-976 (2017)
- [2] S.Knudde, D.C.Leitao, S.Cardoso and P.P.Freitas, “Annealing-free magnetic tunnel junctions for sensing applications” J. Phys. D: Appl. Phys. 50 (16), 165001 (2017)
- [3] Choi, JY., Lee, Dg., Baek, JU. et al. Double MgO-based Perpendicular Magnetic-Tunnel-Junction Spin-valve Structure with a Top Co2Fe6B2 Free Layer using a Single SyAF [Co/Pt]n Layer. Sci Rep 8, 2139 (2018).

Magnetic Sensors Based on Amorphous and Nano materials

Pavel Ripka

Czech Technical University, Technicka 2, 166 57 Praha 6, Czech Republic, ripka@fel.cvut.cz

Amorphous soft magnetic alloys have excellent mechanical properties and they do not require high-temperature annealing. They can be used at high frequencies, which allows reduction of the core size. Orthogonal fluxgate sensor based on zero-magnetostriction amorphous microwire has noise below $1 \text{ pT}/\sqrt{\text{Hz}}$ at 1 Hz, which is a record for room-temperature sensor [1]. However, fluxgates with superior offset stability are still made of amorphous tape. Low saturation flux density of cobalt-based zero-magnetostriction amorphous alloys is here an advantage [2].

Nanocrystalline materials are usually brittle, but they have large saturation flux density and they can be annealed to almost perfectly linear characteristics. Currently they are cheaper than permalloys and they already dominate the production of current transformers. They allow to build smaller transformers, which are tolerant to DC current component and which have very wide frequency characteristics. Fluxgate AC/DC current transformers based on nanocrystalline core can measure DC current component in the power grid, which is caused by geomagnetic storms or inverters used in solar and wind power plants [3].

Rogowski coils serve as extremely linear AC current sensors, which are suitable for the electric power meters with large dynamic range, current fault detectors and plasma current meters. Low-permeability cores made of recycled flakes from nanocrystalline material may serve as cores for Rogowski coils increasing their sensitivity, decreasing size and increasing frequency range [4].

Magnetic ink based on superparamagnetic or ferromagnetic particles can be used for inkjet printing of nonplanar and flexible cores and field concentrators. We have demonstrated fluxgate sensor with 1.5 mT open-loop range based on core printed by home-made ink containing 40 nm $\text{Mn}_{0.62}\text{Zn}_{0.41}\text{Fe}_{1.97}\text{O}_4$ superparamagnetic particles. Compared to classical fluxgates, these sensors have lower sensitivity of only 10 mV/mT, but potentially higher offset stability due to anhysteretic character of the core material [5].

A lot of effort was invested into the development of microfabricated fluxgate sensors. The best parameters were achieved using cores etched from amorphous tape, but these sensors never reached the production stage. Currently the only commercially available integrated fluxgate is DRV425 by Texas Instruments. The device has straight sputtered cores with microfabricated coils. The primary application is DC/AC current sensing, but they are applied also for position detectors and torque meters. Main advantage of this sensor is not low noise, but high temperature stability: offset drift of 2 nT/K and gain drift of 7 ppm/K is much better than of any magnetoresistor.

Sensorial applications of magnetic nanowires and nanowire arrays start to appear. Arrays of nanowires are produced by electrodeposition of permalloy into the pores in alumina or silicon membranes. The main limitation of using such arrays in magnetic sensors is low sensitivity dictated by demagnetization. We have developed simplified model allowing to calculate effective permeability and amplification factor for arrays containing millions of wires [6].

[1] M. Janosek, M. Butta, M. Dressler, *IEEE Tran. Instr. Meas.* **69**, 2552-2560 (2020)

[2] P. Ripka (ed.), *Magnetic sensors and magnetometers*, Artech 2021

[3] V. Grim, P. Ripka, J. Bauer, *JMMM* **500** (2020) 166360

[4] V. Grim, P. Ripka, *Magnetics Lett.* **13** (2022), 8102304

[5] J. Hrakova et al., presented at SMM 2020 and submitted to *JMMM*.

[6] P. Ripka, D. Hrakova, M. Mirzaei, O. Kaman: *AIP Advances* **12**, 035128 (2022)

Oral Presentations

| | | |
|---------------------|---|-----|
| Pedro Brandao Veiga | <i>Engineering of Spin-Transfer-Torque Perpendicular Magnetic Tunnel Junctions at Cryogenic Temperatures with Very Low Switching Voltages</i> | 408 |
| Nuno Caçoilo | <i>Improved dynamical switching properties in Perpendicular Shape Anisotropy Magnetic Tunnel Junctions</i> | 409 |
| Robert Carpenter | <i>z-Field Control Through Stack Design to Enable Field-Free Switching of VCMA-MRAM</i> | 410 |
| Samuel Manceau | <i>Magnetic tunnel junctions with a symmetric response for ultra-sensitive sensors</i> | 411 |
| Dennis Seidler | <i>Single magnetic domain FeCoSiB multilayer-based magnetoelectric composites for biomagnetic field sensing</i> | 412 |
| Balram Singh | <i>Tuning strain-induced anisotropy of soft ferromagnetic structures</i> | 413 |
| Benjamin Spetzler | <i>Exchange-Bias Delta-E Effect Magnetic Field Sensors for Sensor Arrays</i> | 414 |
| Stanislav Vrtnik | <i>Nonergodic effects in the spin-glass CoCrFeMnNi high-entropy alloy: Thermoremanent magnetization and Thermal memory cell</i> | 415 |
| Xing-Long Ye | <i>Voltage-driven giant modulation of magnetism in ferromagnetic metals with ultrahigh magnetocrystalline anisotropy</i> | 416 |
| Tomasz Zalewski | <i>Ultrafast photo-induced dynamics of multi states switching of magnetization in garnets</i> | 417 |
| Liza Zaper | <i>Scanning NV Magnetometry for Magnetic Memory Devices</i> | 418 |
| Sebastian Zeilinger | <i>Spin orbit torque enabled magnetic sensor with low offset and tunable sensitivity</i> | 419 |

Engineering of Spin-Transfer-Torque Perpendicular Magnetic Tunnel Junctions at Cryogenic Temperatures with Very Low Switching Voltages

P. B. Veiga¹, A. M. Hernandez¹, L.B. Prejbeanu¹, I.L.Prejbeanu¹, L. Vila¹, S. Auffret¹, R.C. Sousa¹, B. Dieny¹

¹ Grenoble Alpes Univ., CNRS, CEA, Grenoble INP, IRIG-SPINTEC, Grenoble, France

Quantum computation and cryogenic electronics have gained considerable momentum in this last decade. Currently, a bottleneck for advancing it further is the power consumption of conventional electronic components, which are incompatible with the needs of cryogenic circuitry. Perpendicular Spin-Transfer-Torque Magnetic Random Access Memory (p-STT-MRAM) shows great potential in complying with the requirements of cryo-electronics. Previous work done in cryogenic temperature switching in STT-MRAM have explored its characteristics and their Write Error Rate (WER) for different device diameters [1,2]. While they show promising results, full integration of MRAMs into quantum processors demands a much lower operating voltage (below 100mV) than what is currently required to write an STT-MRAM (around 0.5V). Therefore we focused our research on engineering MTJs with low anisotropy to reduce considerably the critical switching voltage V_C . Our main approach consists in adjusting the storage layer anisotropy so that the memory retention time is maintained at the same levels when operating in low temperatures (i.e. 10K). Compared to MRAMs operating at 300K, this allows reducing the storage layer anisotropy by at least one order of magnitude. Using the coercivity field dependence with temperature as an estimate of the anisotropy, we can predict which devices will have the desired behavior at 10K. Fig.1 shows the coercivity evolution of multiple devices with different storage layer thicknesses exhibiting a range of behavior as they are cooled down. By performing switching measurements on those with the lowest anisotropy, we can obtain a much lower threshold for switching. Device diameter, composition and thickness play an important role in modulating the anisotropy. By tuning these properties we can achieve sub-100mV V_C at cryogenic temperatures of sub 10K.

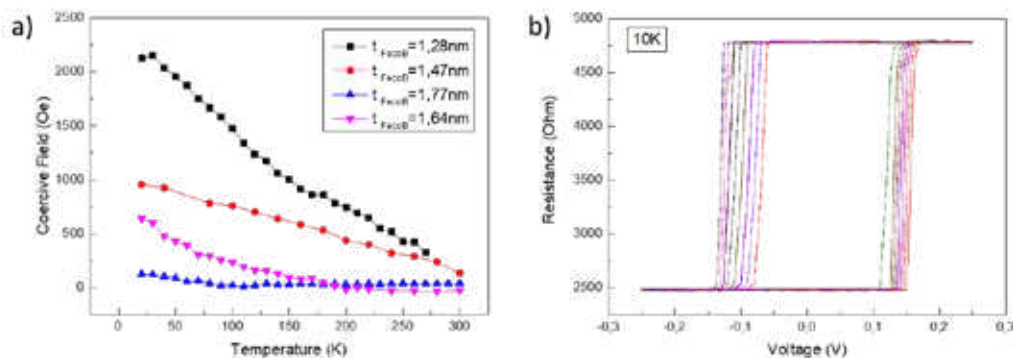


Figure 1: a) Coercivity dependence with temperature of pMTJs with different free layer thicknesses: $t_1 = 1.28$, $t_2 = 1.47$, $t_3 = 1.77$ and $t_4 = 1.64\text{ nm}$. b) Voltage x Resistance measurement of 20 loops for $t_3 = 1.77$ at 10K and 200 Oe offset field, with $TMR = 94\%$ and $V_{C_{AP}} = 0.140 \pm 0.007\text{ V}$ and $V_{C_{AP}} = -0.08 \pm 0.02\text{ V}$.

References

- [1] L. Rehm et al. Appl. Phys. Lett. 115, 182404 (2019).
- [2] L. Lang et al. Appl. Phys. Lett. 116, 022409 (2020).

Improved dynamical switching properties in Perpendicular Shape Anisotropy Magnetic Tunnel Junctions

N. Caçoilo¹, B. M. S. Teixeira¹, B. Dieny¹, R. C. Sousa¹, L. D. Buda-Prejbeanu¹, O. Fruchart¹ and I. L. Prejbeanu¹

¹Univ. Grenoble Alpes, CEA, CNRS, Grenoble INP, SPINTEC, 38000 Grenoble, France

The perpendicular Spin-Transfer-Torque Magnetic Random-Access Memory (p-STT-MRAM) is one of the most promising emerging non-volatile memory technologies. However, these devices are limited by their thermal stability factor at technological nodes smaller than 20 nm [1, 2]. A promising solution to this problem relies on providing a perpendicular shape anisotropy of the storage layer by increasing its thickness. In this case, the magnetostatic energy adds up as a volume contribution to the interfacial anisotropy, resulting in a much larger and easily tunable effective perpendicular anisotropy than in a conventional p-STT-MRAM. This concept allows to extend the downsize scalability of the STT-MRAM at sub-10 nm technological nodes [3, 4]. As the diameter decreases, the aspect-ratio of the storage layer needs to be increased so that the total magnetostatic energy is enough to meet the thermal stability factor requirements. In this work, it is shown that, above a certain thickness threshold, the magnetization reversal follows a non-coherent behavior, detrimental in terms of the switching voltage and switching time [5]. A proposed approach to circumvent this limitation is make use of additional anisotropy sources in the storage layer, which allows for the total thickness of the storage layer to be reduced, while keeping an appropriate thermal stability, leading to an overall lower switching voltage, and switching times (Fig. 1). This approach leads to an improvement in the PSA-MTJ technology, opening the possibility to faster and coherent reversals at sub-10 nm technological nodes.

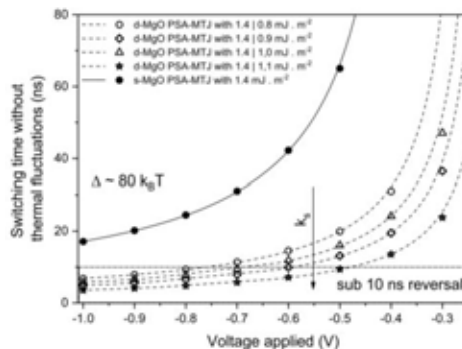


Figure 1: Switching time of the PSA-MTJ for the case of a single interface anisotropy contribution (s-MgO) and for the case of double interface anisotropy (d-MgO) with different surface energies (1.4 mJ/m² fixed in the first interface and variation of 0.8, 0.9, 1.0 and 1.1 mJ/m² in the second interface). In both situations the storage layer is made of a FeCoB alloy.

- [1] C. Yoshida *et al*, Jpn. J. Appl. Phys. 58, SB3B05 (2019).
- [2] H. Sato *et al*, Jpn. J. Appl. Phys. 58, 0802A6 (2017).
- [3] N. Perrissin *et al*, Nanoscale 10, 12187-12195 (2018)
- [4] K. Watanabe *et al*, Nat. Com. 9, 663 (2018)
- [5] N. Caçoilo *et al.*, Phys. Rev. Appl. 16, 024020 (2021)

z-Field Control Through Stack Design to Enable Field-Free Switching of VCMA-MRAM

R. Carpenter¹, W. Kim¹, Y. C. Yu^{1,2}, M. Ben Chroud^{1,3}, G. Potoms¹, S. Couet¹,
G. Sankar Kar¹, J. Swerts¹

¹ Imec, Kapeldreef 75, 3001 Leuven, Belgium

² TSMC, No. 168, Park Ave. II, Hsinchu Science Park, Hsinchu, Taiwan

³ Dep. of Physics and Astronomy, KU Leuven, Celestijnenlaan 200d, 3001 Leuven, Belgium

The Voltage Control of Magnetic Anisotropy (VCMA) is a promising alternative to Spin Transfer Torque (STT) as a writing mechanism for Magnetic Random-Access Memory (MRAM) [1]. The write pulse in VCMA consists of two components: 1) removal of the energy barrier (EB) by applying a voltage over the MgO tunnel barrier and 2) an external in-plane (IP) field in order to induce precession about its axis [2-3]. The efficiency of the VCMA effect is given by the coefficient, ξ (fJ/Vm). The requirements of this are defined by the size of the EB required, typically in excess of 300fJ/Vm for embedded memory [4]. Back End Of Line (BEOL) compatible devices with $\xi \geq 100$ fJ/Vm have been a challenge, until recently [5].

One of the biggest practical challenges for VCMA-MRAM is the control of the out-of-plane (OOP) stray field ($\mu_0 H_{\text{off}}$) seen by the Free-Layer (FL). This is reduced by coupling the Reference and Hard Layers (RL/HL) antiparallel via the RKKY interaction (Figure 1). However, balance of the dipolar fields is non-trivial, especially with respect to the diameter of the device. In this work, $\mu_0 H_{\text{off}}$ is controlled by changing the Co% in, and thickness of, the Co/Pt HL. This is demonstrated by the variation of $\mu_0 H_{\text{off}}$ with respect to pillar diameter (Figure 2). The benefit of $\mu_0 H_{\text{off}} = 0$ mT is shown by the symmetry of the switching probability for the AP \rightarrow P/P \rightarrow AP directions with $\mu_0 H_z = 0$ mT (Figure 3). In the full presentation, a comparison of the control of the field balancing versus the switching probability will be discussed.

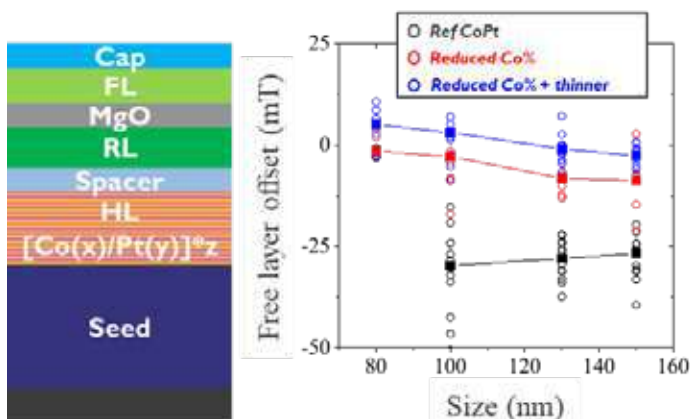


Fig. 1 Simplified schematic of MTJ showing HL variables of H_{off} control

Fig. 2 The change in FL $\mu_0 H_{\text{off}}$ with device size for the changing amount of Co and HL thickness

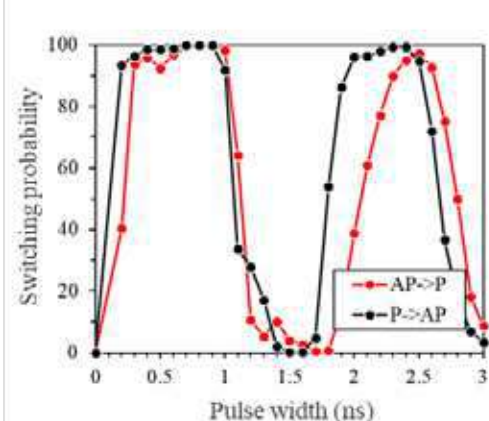


Fig. 3 Switching probability as a function of pulse width in the P to AP and AP to P directions with $\mu_0 H_z = 0$ mT

- [1] K. L. Wang et al., IEEE-IEDM, pp. 36.2.1-36.2.4 (2018)
- [2] Y. Shiota et al., Nat. Mater. 11(1), 39 (2012)
- [3] C. Grezes et al., Appl. Phys. Lett. 108, 012403 (2016)
- [4] Y. C. Wu et al., Phys. Rev. Applied 15, 064015 (2021)
- [5] R. Carpenter et al., IEEE-IEDM, pp. 17.6.1-17.6.4 (2021)

Magnetic Tunnel Junction with Symmetric Response for Sensitive Sensor using Magnetic Modulation

S. Manceau^{1,2}, C. Ducruet³, P. Sabon¹, C. Cavoit, G. Jannet², L. Prejbeanu¹,
M. Kretzschmar² and C. Baraduc²

¹Spintec, 17 rue des Martyrs, Grenoble, France

²LPC2E, 3 avenue de la recherche scientifique, Orléans, France

³Crocus, 4 place Robert Schuman, Grenoble, France

Magnetic Tunnel Junctions (MTJs) are widely used as magnetic sensors thanks to their high sensitivity but their high noise level at low frequency remains a major limitation. To overcome the $1/f$ noise issue, a Symmetric Response MTJ (SR-MTJ) is used to implement a high frequency modulation [1,2]. SR-MTJ are realized by stabilizing the Free-Layer (FL) in a direction parallel to the reference.

The FL stabilization of several SR-MTJs has been studied by using three different techniques: (i) by using shape anisotropy, (ii) by adding an additional external field (H_{ext}) along the reference direction, (iii) by using soft pinning with adding an antiferromagnetic layer and a Ru spacer above the FL [3]. Several batches of micrometer SR-MTJs were processed with different shapes and soft pinning values. The R-H electrical responses were then measured and compared to a theoretical macrospin model.

Our measurements showed that the sensitivity can be improved by reducing the stability of the FL magnetization (fig. 1). However, the macrospin state of the FL is eventually

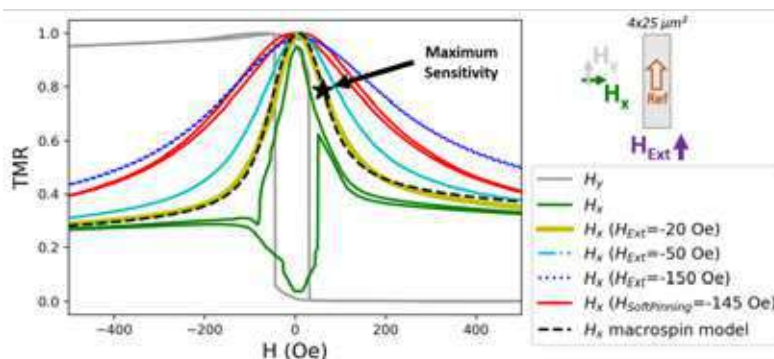


Figure 1: Response of a Magnetic Tunnel Junction in the easy (H_y) and hard (H_x) axis and increase of the stability of the Free-Layer by an external field or a soft pinning.

lost (green curve), which may be accompanied by an increase in noise [4]. Adding an external field higher than 20 Oe on a $4 \times 24 \mu\text{m}^2$ rectangle compensates for the lack of FL stability. On the other hand, a misalignment of the reference of a few degrees affects the symmetry of the response and destabilizes the macrospin

state. A compensation for this misalignment allowed to reduce the external field value required to 5 Oe and reach a better sensitivity of 6.7 %/mT. A Stoner-Wohlfart macrospin model including additional external field and misalignment allows to fit the experimental curves. So far, due to the coexistence of 2 parallel and antiparallel stable configurations, stabilization by shape anisotropy is less promising than other techniques.

- [1] S. Shirotori, A. Kikitsu, and Y. Higashi, *IEEE Transaction on magnetics* **57** (2021).
- [2] A. Bocheux, C. Cavoit, and M. Mouchel, *IEEE (SAS 2016) Proceedings*, 149 (2016).
- [3] R. Ferreira, E. Paz, and P. P. Freitas, *IEEE Transaction on Magnetism* **48**, 3719 (2012).
- [4] J. Moulin, A. Doll, and M. Pannetier-Lecoecur, *Appl. Phys. Lett.* **115**, 122406 (2019).

Single magnetic domain FeCoSiB multilayer-based magnetoelectric composites for biomagnetic field sensing

D. Seidler¹, P. Hayes¹, L. Thormählen¹, D. Meyners¹, E. Quandt¹ and J. McCord¹

¹ Kiel University, Institute for Materials Science, Kaiserstraße 2, 24143 Kiel, Germany

The contactless measurement of biomagnetic signals i.e. magnetocardiography or magnetoencephalography at ambient conditions has gained high interest for medical applications. Magnetoelectric (ME) cantilever-based sensors [1, 2, 3] have shown promising results in that regard. They do not require cryogenic cooling or heating for operation and can be operated in the presence of interfering magnetic fields. To achieve the necessary limit of detection (LOD) a minimization of all noise sources, including dominant magnetic noise, has to be performed. Magnetic noise mainly results from magnetic domain wall activity during sensor operation. We demonstrate a single domain thick magnetic multilayer stack, aiming for minimizing the magnetic noise in ME sensors. The multilayers are prepared via sputter deposition in an applied magnetic field on Si substrate. We utilize a scalable approach based on magneto-statically coupled (Fe₉₀Co₁₀)₇₈Si₁₂B₁₀ layers with the magnetic sensitive layer showing single domain behavior while still achieving high sensitivity.

The simplest approach consists of one phase of exchange-biased FeCoSiB multilayers (EB-ML) and a second single layer phase of FeCoSiB (“free layer”, FL). The phases display nearly zero interlayer coupling through the separating Ta layer. Various multilayer stacks from

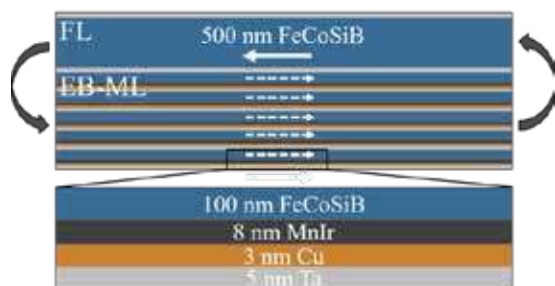


Figure 1: Example multilayer stack consisting of 500 nm total EB layer and 500 nm FL (not to scale).

500 nm to 2000 nm magnetic sensitive layer thickness are compared. An antiparallel (AP) alignment of the FL and fixed EB-ML is achieved by the magneto-static coupling at the edges. This leads to a single domain state in the FL. The magnetic domain state of the FL is evaluated by magneto-optical magnetometry. To verify the AP alignment of the EB-ML and FL, volumetric magnetometry measurements with transverse sensitivity are conducted.

To demonstrate the effectivity, the proposed FeCoSiB multilayers have been integrated into converse magnetoelectric composite sensors [3]. A full sensor characterization of the noise, signal and LOD is performed. With the achieved magnetic domain elimination, we obtain a LOD of 40 pT·Hz^{-0.5} at 10 Hz. We will show and compare strategies to further improve the sensor performance based on varying FL and EB thicknesses.

This work was funded by the German Research Foundation (DFG) through the CRC 1261.

- [1] S. Salzer, V. Röbisch, M. Jovičević Klug, P. Durdaut, J. McCord, D. Meyners, J. Reermann, M. Höft, R. Knöchel, *IEEE Sensors Journal* **18**, 596 (2018)
- [2] M. Jovičević Klug, L. Thormählen, V. Röbisch, S. D. Toxværd, M. Höft, R. Knöchel, E. Quandt, D. Meyners, and J. McCord, *Appl. Phys. Lett.* **114**, (2019)
- [3] P. Hayes, M. Jovičević Klug, S. Toxværd, P. Durdaut, V. Schell, A. Teplyuk, D. Burdin, A. Winkler, R. Weser, Y. Fetisov, M. Höft, R. Knöchel, J. McCord, and E. Quandt, *Sci Rep.* **9**, 16355 (2019)

Tuning strain-induced anisotropy of soft ferromagnetic structures

Balram Singh¹, Jorge. A. Otálora², Tong Kang¹, Ivan Soldatov¹, Dmitriy D. Karnaushenko³, Christian Becker¹, Rudolf Schäfer¹, Daniil Karnaushenko³, Volker Neu¹ and Oliver G. Schmidt³

¹Leibniz IFW Dresden, 01069 Dresden, Germany.

²Departamento de Física, Universidad Católica del Norte, Avenida Angamos 0610, Casilla 1280, Antofagasta, Chile.

³Center for Materials, Architectures, and Integration of Nanomembranes (MAIN), Chemnitz University of Technology, 09126 Chemnitz, Germany.

Geometrical transformations, such as rolling a 2D ferromagnetic film into a 3D cylinder provide means to tune its magnetic properties generating different magnetic ground states [1]. Rolled-up magnetic membranes with azimuthal magnetic anisotropy are very attractive due to expected much higher domain wall velocity (compare to their planar counterparts) [2] and for applications as impedance-based field sensors [1]. However, a clear recipe for acquiring highly mobile azimuthal domains in a soft ferromagnetic tubular geometry is unclear. State of the art studies report the rolling of an extended ferromagnetic film (of hundreds of micro-meters), which after rolling converts into tubular geometry with 2-3 windings [1]. Changes in the magnetic domain configuration in such tubular geometries may arise from modifications of the

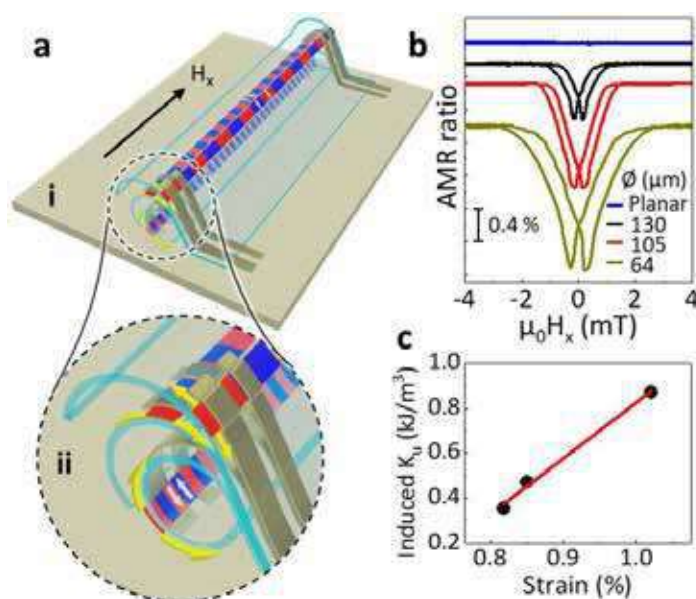


Figure 1: (a) Schematic illustration of self-assembly (ai) roll-down approach for adjusting the size of curvature and strain in a functional magnetic layer on top of the polymeric platform (a ii) magnified view of rolled-down structures, indicating tensile strain (yellow arrows) in the magnetic layer. (b) AMR hysteresis measured for planar and rolled-down stripes of different diameters (\varnothing) (c) Rolling induced azimuthal magnetic anisotropy (K_u) in magnetic stripes extracted from AMR hysteresis.

shape anisotropy in addition to stress-induced anisotropy due to rolling.

In our work, we report on rolling-induced azimuthal anisotropy in $\text{Ni}_{78}\text{Fe}_{22}$ stripes (as shown in figure 1a) purely due to strain, considering that curvature induced changes in shape anisotropy can be neglected due to reduced dimensions of our magnetic stripe in the azimuthal direction. For that, we employed a self-assembly rolling technology based on a polymeric platform, which allows choosing the shape and size of magnetic structure willingly. Magnetic structures patterned on the polymeric platform can be bent controllably and hence the sign and magnitude of strain on the magnetic structure can be adjusted. We quantify the induced azimuthal magnetic

anisotropy (figure 1c) by electrical measurements (figure 1b) capable of providing magnetic properties of magnetic structures hidden under the 3D polymer architecture.

[1] R. Streubel, P. Fischer, F. Kronast, V. P. Kravchuk, D. D. Sheka, Y. Gaididei, O. G. Schmidt, D. Makarov, *J. Phys. D: Appl. Phys.* **2016**, *49*, 363001.

[2] J. Hurst, A. De Riz, M. Staño, J. C. Toussaint, O. Fruchart, D. Gusakova, *Phys. Rev. B* **2021**, *103*, 1.

Exchange-Bias Delta-E Effect Magnetic Field Sensors for Sensor Arrays

**B. Spetzler^{1,2}, P. Wiegand³, C. Bald³, F. Ilgaz², G. Schmidt³, D. Meyners²,
R. Rieger³ and F. Faupel²**

¹ *Department of Electrical Engineering and Information Technology, Technical University Ilmenau, Ilmenau, Germany*

² *Department of Material Science, Kiel University, Kiel, Germany*

³ *Department of Electrical Engineering and Information Technology, Kiel University, Kiel, Germany*

Delta-E effect magnetic field sensors utilize the resonance frequency shift of a magnetoelastic resonator, caused by the change in Young's modulus of the magnetoelastic material in a magnetic field. Such sensors are fully integrable and permit the detection of small-amplitude and low-frequency magnetic fields over a large bandwidth. In recent years, much progress has been made in understanding the complex interplay of magnetic, mechanical, and electrical properties and their influence on device characteristics [1]. Here, we move towards applications and share our recent results on the first delta-E effect sensors based on exchange-biased multilayers [2,3]. The sensors operate without external magnetic bias fields and enable a dual-mode operation scheme to localize the sensor and simultaneously measure magnetic fields, demonstrated with a proof-of-concept application [2]. Additionally, the exchange bias allows us to realize sensor arrays, which could be beneficial for many applications [3]. Signal-and-noise models are developed to simulate the arrays and circumvent several previous limitations. We analyze the prospects and drawbacks of exchange-bias delta-E effect sensors and sensor arrays experimentally and theoretically and discuss the noise performance and limit of detection. Specific requirements for improving the limit of detection with delta-E effect sensor arrays are derived.

This work was funded by the German Research Foundation (DFG) through the Collaborative Research Centre CRC 1261 "Magnetoelectric Sensors – From Composite Materials to Biomagnetic Diagnostics" and the Carl-Zeiss Foundation via the Project MemWerk.

[1] A. D. Matyushov, B. Spetzler, M. Zaeimbashi, J. Zhou, Z. Qian, E. V. Golubeva, C. Tu, Y. Guo, B. F. Chen, D. Wang, A. Will-Cole, H. Chen, M. Rinaldi, J. McCord, F. Faupel, N. X. Sun, *Adv. Mater. Technol.* **6**, 2100294 (2021).

[2] B. Spetzler, C. Bald, P. Durdaut, J. Reermann, C. Kirchhof, A. Teplyuk, D. Meyners, E. Quandt, M. Höft, G. Schmidt, F. Faupel, *Sci Rep* **11**, 5269 (2021).

[3] B. Spetzler, P. Wiegand, P. Durdaut, M. Höft, A. Bahr, R. Rieger, F. Faupel, *Sensors* **21**, 7594 (2021).

Nonergodic effects in the spin-glass CoCrFeMnNi high-entropy alloy: Thermoremanent magnetization and Thermal memory cell

S. Vrtnik¹, P. Koželj^{1,2}, M. Krnel¹, A. Jelen¹, D. Gačnik¹, M. Wencka³, A. Meden⁴, F. Danoix⁵, M. Feuerbacher⁶ and J. Dolinšek^{1,2}

¹ Jožef Stefan Institute, Jamova 39, Ljubljana, Slovenia

² University of Ljubljana, Faculty of Mathematics and Physics, Jadranska 19, Ljubljana, Slovenia

³ Institute of Molecular Physics, Polish Academy of Sciences, Smoluchowskiego 17, Poznań, Poland

⁴ University of Ljubljana, Faculty of Chemistry and Chemical Technology, Ljubljana, Slovenia

⁵ Normandie Université, INSA Rouen, CNRS, Groupe de Physique des Matériaux, Rouen, France

⁶ Institut für Mikrostrukturforschung, Forschungszentrum Jülich, Jülich, Germany

The CoCrFeMnNi high-entropy alloy (HEA) is a magnetically concentrated crystalline system with all lattice sites magnetic, containing randomness (five different types of spins are randomly positioned on the lattice) and frustration (a consequence of mixed ferromagnetic and antiferromagnetic interactions). We have studied experimentally the nature of the magnetic ground state and found out that upon cooling, no long-range magnetic ordering takes place, but the spin system undergoes a kinetic freezing transition to a spin glass phase, where below the spin freezing temperature $T_f \approx 20$ K, ergodicity of the system is broken [1]. The observed broken-ergodicity phenomena include zero field cooled – field cooled magnetization splitting in low magnetic fields, frequency-dependent cusp in the ac susceptibility, ultraslow time-decay of the thermoremanent magnetization (Fig. 1) and the memory effect. All these phenomena are associated with the out-of-equilibrium dynamics of a nonergodic, frustrated system of coupled spins that approach thermal equilibrium, but can never reach it on a finite experimental time scale, so that we are observing only transient effects of partial equilibration within localized spin domains. The observation of the memory effect prompts for the application of the CoCrFeMnNi HEA as a thermal memory cell (Fig. 2), where a byte of digital information can be stored into the material by pure thermal manipulation, in the absence of any external magnetic or electric field [2].

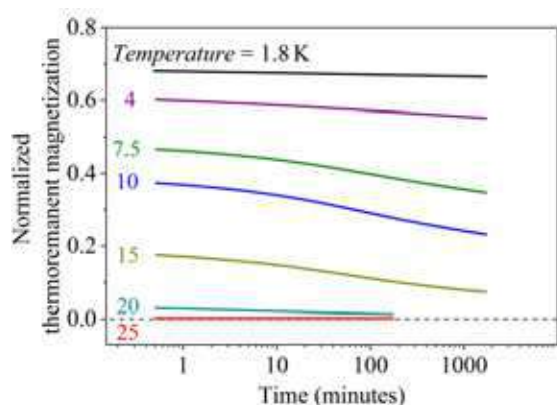


Figure 1: Ultraslow time-decay of the normalized thermoremanent magnetization in the CoCrFeMnNi HEA sample.

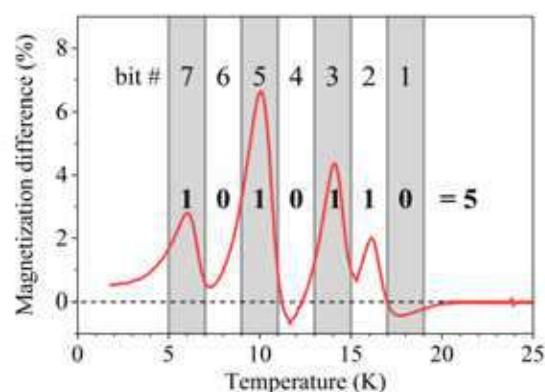


Figure 2: Thermally written ASCII character “5” in a thermal memory cell using the CoCrFeMnNi HEA material.

[1] P. Koželj, S. Vrtnik, M. Krnel, A. Jelen, D. Gačnik, M. Wencka, Z. Jagličić, A. Meden, G. Dražić, F. Danoix, *et al.*, *J. Magn. Magn. Mater.* **523**, 167579 (2021).

[2] J. Dolinšek, M. Feuerbacher, M. Jagodič, Z. Jagličić, M. Heggen, K. Urban, *J. Appl. Phys.* **106**, 043917 (2009).

Voltage-driven giant modulation of magnetism in ferromagnetic metals with ultrahigh magnetocrystalline anisotropy

Xing-Long Ye¹, Oliver Gutfleisch², Horst Hahn¹, Robert Kruk¹ et al.

¹ *Institute of Nanotechnology, Karlsruhe Institute of Technology,
76344 Eggenstein-Leopoldshafen, Germany*

² *Department of Material Science, Technical University Darmstadt, 64287 Darmstadt, Germany*

Controlling magnetism and magnetic properties of materials by small voltages have aroused enormous interests due to its ultralow power consumption. However, in ferromagnetic metals voltage effect is usually restricted to the scale of atomic layers due to strong electric-field screening. Consequently, the modification of magnetic properties is too small for practical applications [1]. Here, we show that the magnetic properties of bulk ferromagnetic metals with ultrahigh magnetocrystalline anisotropy can be hugely and reversibly tuned through electrochemically-controlled insertion/extraction of hydrogen atoms. We manipulated the coercivity of SmCo₅ by more than 1 T by applying voltages of 1 V [2]. Through this effect, a voltage controlled and gated magnetization reversal has been achieved at room temperature. With the same approach, we show in another model material of Sm₂Co₁₇-based magnet, its coercivity can be reversibly adjusted by 1.3 T by applying 1 V. Furthermore, by synchronized analysis of the coercivity change and hydrogen discharging process, we were able to identify the so far overlooked critical role of domain nucleation near grain boundaries in controlling the coercivity [3]. Experimental and density functional theory calculation results show that the change of the coercivity originates from the change of magnetocrystalline anisotropy both in the bulk and at local defects due to hydrogen absorption. Our work may take the voltage-control of magnetism truly beyond the field-effect devices, which can find applications in magnetic recording and in customizing permanent magnets for various requirements.

[1] F. Matsukura, Y. Tokura, H. Ohno, *Nature Nanotech.* **10**, 209-220 (2015).

[2] X.L.Ye, H. Singh, H.B Zhang, H. Geßwein, M.R. Chellali, R. Witte, A. Molinari, K. Skokov, O. Gutfleisch, H. Hahn, R. Kruk. *Nature Comm.* **11**, 4849 (2020).

[3] X.L.Ye, F.K. Yan, L. Schaefer, D. Wang, H. Geßwein, W. Wang, M.R.Chellali, L.Stephenson, K. Skokov, O. Gutfleisch, D. Raabe, H. Hahn, B. Gault, R. Kruk. *Adv. Mater.* **33**, 2006853 (2021).

Ultrafast photo-induced dynamics of multi-states switching of magnetization in garnets

T. Zalewski¹, A. Frej¹ and A. Stupakiewicz¹

¹ Faculty of Physics, University of Białystok, 15-245 Białystok, Poland

The all-optical cold switching mechanism in dielectrics has great application potential, having an unquestionable advantage over all-optical switching of magnetization (AOS) in metallic structures in the form of no heat dissipation. [1] Contrary to the thermal-based switching mechanism in metals, the nonthermal switching in dielectrics is based on a precessional reversal of the magnetization, driven by the photo-induced change of magnetic anisotropy. It was shown that using only a single, linearly polarized laser pulse is enough to reversible switch the magnetization state in dielectric yttrium iron garnet (YIG:Co) film. [2] Such a switching does not require any external magnetic field and can be done at room temperature.

The garnet film has a multi-state of magnetization with four easy magnetization axes along the cube diagonals of $\langle 111 \rangle$ -type. To make the magnetization states distinguishable in the magneto-optical imaging, the 4° miscut from the surface normal to the substrate was added.

Here, using time-resolved single-shot imaging [3], we studied the ultrafast photo-induced dynamics of switching between noncollinear states of magnetization in garnets. We revealed that the switching between four magnetization states for cubic symmetry of garnet occurs not with one but with two different characteristic times. As demonstrated previously [2], [4], the domain magnetization vector along the $[111]$ direction was switched to the $[1-1-1]$ direction during a quarter of its precession period at about 60 ps. However, the magnetization oriented along $[11-1]$ in the other magnetic domain is switched to $[1-11]$ direction during half period of precession at about 120 ps due to the length of the trajectory of magnetization motion. Moreover, the linear polarization of the single 50 fs pump pulse causes the simultaneous motion and rotation of a pair of noncollinear magnetizations in the two domains. The pulse intensity adjustment makes it possible to control the rise time of the first quarter of the precession period and thus the switching time. Our results open a plethora of possibilities to finding novel mechanisms of non-dissipative switching in magnets with unusual magnetization states.

- [1] E. Y. Vedmedenko *et al.*, *J. Phys. D. Appl. Phys.* **53**, 45 (2020)
- [2] A. Stupakiewicz, K. Szerenos, D. Afanasiev, A. Kirilyuk, and A. V. Kimel, *Nature* **542**, 7639 (2017)
- [3] T. Zalewski and A. Stupakiewicz, *Rev. Sci. Instrum.* **92**, 10 (2021)
- [4] A. Stupakiewicz *et al.*, *Nat. Commun.* **10**, 1 (2019)

Scanning NV Magnetometry for Magnetic Memory Devices

P. Rickhaus², U. Celano¹, L. Zaper^{4,2}, F. Braakman⁴, M. Poggio⁴, H. Zhong², F. Ciubotaru¹, L. Stoleriu³, A. Stark², F. Favaro de Oliveira², M. Munsch², P. Favia¹, M. Korytov¹, P. Van Marcke¹, P. Maletinsky^{2,4}, C. Adelman¹, P. van der Heide¹

¹IMEC, Leuven, Belgium

²Qnami AG, Muttens, Switzerland

³Alexandru Ioan Cuza University, Iasi, Romania

⁴University of Basel, Switzerland

Scanning NV magnetometry (SNVM) is an emerging quantum sensing technique which allows to measure minute magnetic fields with nanoscale resolution. In the talk we will discuss the characterization of magnetic nanowires and nanomagnets for qubit. The former are among the essential building-blocks of contemporary spintronic devices [1] since their magnetic properties can be tuned by their geometry, and their fabrication is compatible with standard semiconductor fabrication schemes. While their topography and homogeneity can be well characterized with established techniques, it remains difficult to access their microscopic magnetic properties which are key to improve device performance. For the nanomagnets, a similar challenge appears. The stripes that we discuss are fabricated with FIB lithography and appear entirely homogenous in SEM imaging, however, their magnetic properties hold surprises. This is of relevance since their purpose is to generate a homogenous magnetic field gradient for spin quantum dot devices.

Here, we demonstrate magnetic imaging of these nanostructures by SNVM [2]. The imaging reveals the presence of several magnetic inhomogeneities that are largely undetectable with standard metrology. In this context, we will discuss the potential of SNVM for semiconductor device analysis.

[1] Parkin, S., & Yang, S. H. (2015). Memory on the racetrack. *Nature Nanotechnology*, 10(3), 195–198.

[2] Celano U., et al., (2021) Probing Magnetic Defects in Ultra-Scaled Nanowires with Optically Detected Spin Resonance in Nitrogen-Vacancy Center in Diamond. *Nano Lett.* 2021, 21, 24, 10409–10415.

Spin orbit torque enabled magnetic sensor with low offset and tunable sensitivity

S. Zeilinger^{1,2}, J. Güttinger², A. Satz² and D. Süss¹

¹University of Vienna, Kolingasse 14-16, Vienna, Austria

²Infineon Technologies Austria, Siemensstraße 2, Villach, Austria

In state of the art magnetic field sensors both Hall and xMR based technologies are successfully used. In Hall based sensors each sensor element can be easily tuned individually by the supply current to account for environmental changes like temperature or stress. In xMR based sensors that are measured in a Wheatstone bridge configuration the biasing cannot be used for individual sensor element compensation. In addition, it is not possible to cancel offset as it is done in Hall based sensors by reversing the sign of the sensitivity over the biasing direction.

In this work we show that the Spin Orbit Torque effect can be used to create a sensitive sensor with low offset by controlling the sensitivity with an independent current through a heavy metal layer.

The device consists of a thin heavy metal layer (HM) with a ferromagnetic layer (FM) on top. A current is passed along the x direction through the HM layer and influences the spins in the FM layer through the SOT interaction. In our experiment we applied an external field in x-direction and measured the change of the magnetization in z-direction over the anomalous Hall effect.

The measurements in Fig. 1 show that we can achieve a low offset in the 50 μT range and tune the sensitivity reproducibly by 200-300% which is encouraging for further development of this

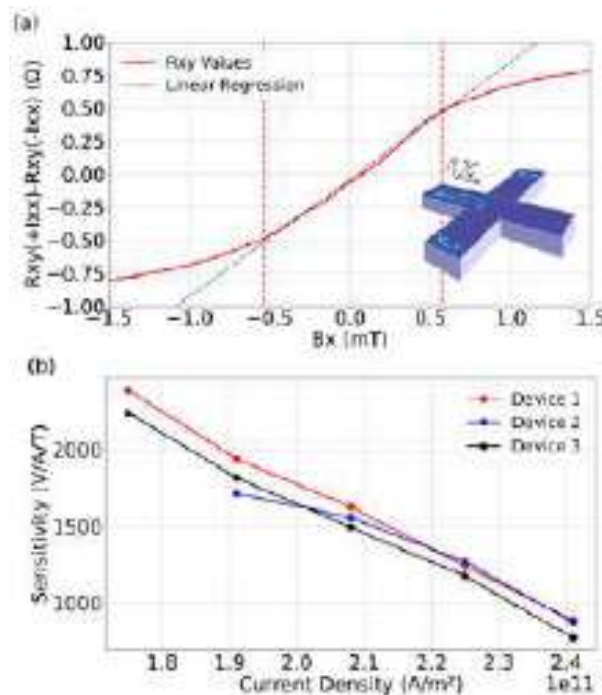


Figure 1: (a) Extraction of the sensitivity from the signal. The Hall resistance R_{xy} describes the magnetization in out-of-plane direction. The current travels along x-direction and creates, via anomalous Hall effect, a voltage V_{xy} in y-direction. (b) The sensitivity over current density for different devices. For Device 2 (blue data) the sensitivity for the lowest current density could not be extracted

sensing principle.

Posters

| | | |
|--------------------------|--|-----|
| Susant Acharya | <i>Ionic Liquid Gating Control of Magnetic Anisotropy in Magnetic Tunneling Junction Stacks for Voltage Tunable Magnetoresistive Sensor</i> | 421 |
| Łukasz Fuśnik | <i>Bias voltage dependence of sensitivity in tunneling magnetoresistance sensors with voltage controlled magnetic anisotropy</i> | 422 |
| Elizaveta Golubeva | <i>Magnetic noise and loss in magnetoelastic magnetic field sensors</i> | 423 |
| Viola Krizakova | <i>Dual-pulse strategies for efficient switching of magnetic tunnel junctions</i> | 424 |
| Wayne Lack | <i>Thermodynamic properties and switching dynamics of perpendicular shape anisotropy MRAM</i> | 425 |
| Peter Leitner | <i>Numerically stable and highly performant implementations of the analytic magnetic field solution of the diametrically magnetized cylinder</i> | 426 |
| Thanh Binh Nguyen | <i>Higher-order Magnetic Anisotropy in Soft-hard Nanocomposite Materials</i> | 427 |
| Thanh Binh Nguyen | <i>HAMR Switching Efficiency in Coreshell L10/Al-FePt Grain</i> | 428 |
| Myriam Pannetier-Lecoeur | <i>Magnetic noise reduction strategies in magnetoresistive sensors for improved detection limits</i> | 429 |
| Joshua M. Salazar-Mejía | <i>Offset free magnetic sensing principle and the role of the spin-orbit torque coefficients</i> | 430 |
| Florian Slanovc | <i>Global Magnetic Topology Optimization</i> | 431 |

Ionic Liquid Gating Control of Magnetic Anisotropy in Magnetic Tunneling Junction Stacks for Voltage Tunable Magnetoresistive Sensor

Susant Acharya*, Atif Islam, Yao Zhang, Simon Granville

¹ Robinson Research Institute, Victoria University of Wellington, Wellington, New Zealand
Susant.acharya@vuw.ac.nz

Magnetoresistive sensors have applications in non-destructive testing (NDT) for the detection of deterioration in pipes, re-enforcing bars in concrete, reliability monitoring, and sensing of faults in high voltage power lines.[1] A limitation of these sensors is their ability to sense on only one axis. This work aims to fabricate the magnetoresistive sensor with the ability to measure small magnetic field signals in three dimensions. The sensing direction in magnetoresistive sensors is linked to the magnetic anisotropy of the reference layer. The key step to obtaining a voltage tunable magnetic sensor is to modulate the magnetic anisotropy of the reference layer comprising the sensor stack through applied voltage. In this work, we will present the reversible tunability of anisotropy in CoFeB based magnetic tunneling junction stacks from out-of-plane to in-plane direction through ionic liquid gating.[2–4] Using magneto-optical Kerr effect (MOKE) microscopy we were able to observe the voltage-induced changes in the spatial magnetic anisotropy distribution. This work paves a way toward realizing voltage tunable magnetoresistive sensors.

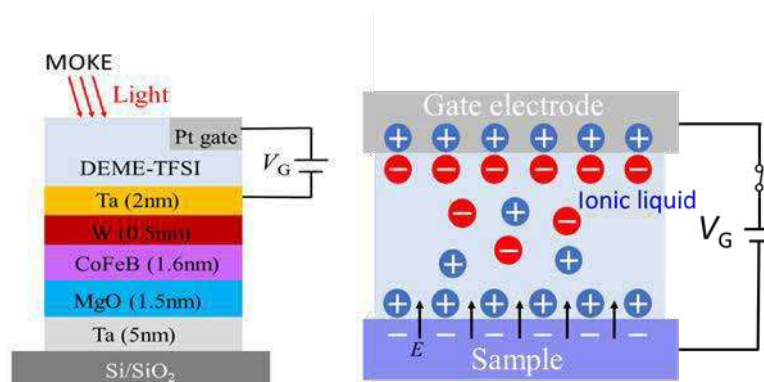


Figure 1: Left: Ionic liquid gating of the thin film stack. right: Phenomenon of Ionic liquid gating [4]

- [1] Khan, M. A.; Sun, J.; Li, B.; Przybysz, A.; Kosel, J. Magnetic sensors-A review and recent technologies. *Eng. Res. Express*, **2021**, 3 (2), 022005.
- [2] Ikeda, S.; Miura, K.; Yamamoto, H.; Mizunuma, K.; Gan, H. D.; Endo, M.; Kanai, S.; Hayakawa, J.; Matsukura, F.; Ohno, H. A perpendicular-anisotropy CoFeB–MgO magnetic tunnel junction. *Nat. Mater.*, **2010**, 9 (9), 721–724.
- [3] Bauer, U.; Yao, L.; Tan, A. J.; Agrawal, P.; Emori, S.; Tuller, H. L.; Van Dijken, S.; Beach, G. S. D. Magneto-ionic control of interfacial magnetism. *Nat. Mater.*, **2015**, 14 (2), 174–181.
- [4] Navarro-Senent, C.; Quintana, A.; Menéndez, E.; Pellicer, E.; Sort, J. Electrolyte-gated magnetoelectric actuation: Phenomenology, materials, mechanisms, and prospective applications. *APL Mater.*, **2019**, 7 (3), 030701.

Bias voltage dependence of sensitivity in tunneling magnetoresistance sensors with voltage controlled magnetic anisotropy

L. Fuśnik¹, P. Wiśniowski¹, B. Szafraniak¹, J. Wrona², S. Cardoso³, P. P. Freitas³

¹AGH University of Science and Technology, Krakow, Poland

²Singulus Technologies AG, Kahl am Main, Germany

³INESC-MN and IN, Lisbon, Portugal

Sensitivity is one of the key properties of tunneling magnetoresistance (TMR) sensors. Typically, it changes significantly with bias voltage magnitude, increases sharply at low bias voltage, reaches a maximum at a certain voltage, and then decreases. However, for TMR sensors based on the voltage controlled magnetic anisotropy (VCMA) effect, the sensitivity is strongly affected not only by the voltage magnitude but also by the polarity [1-3]. In this work, we investigate the dependence of sensitivity ($S=dR/dB \times I$) on bias voltage for TMR sensors with different degrees of VCMA modification by bias voltage determined from measured resistance versus magnetic field (R - B) curves (Fig. 1a).

For sensors with medium and strong VCMA modification (Fig. 1a middle and lower panels), the dependence of sensitivity on bias voltage shows new features not observed for TMR sensors (Fig. 1b). Under positive voltage, the sensitivity increases sharply and does not reach saturation up to 1V (measured range). Under negative bias, it remains approximately constant over a significant range. In contrast, sensors without measurable VCMA effect (Fig. 1a upper panel) show the typical dependence of sensitivity on bias voltage. These characteristics result from the strong influence of VCMA on the magneto-transport properties of the sensors, which will be presented in details.

The increase of sensitivity without saturation for one polarity and its constant value for the opposite indicate a new potential for improving the sensitivity and detection of TMR sensors.

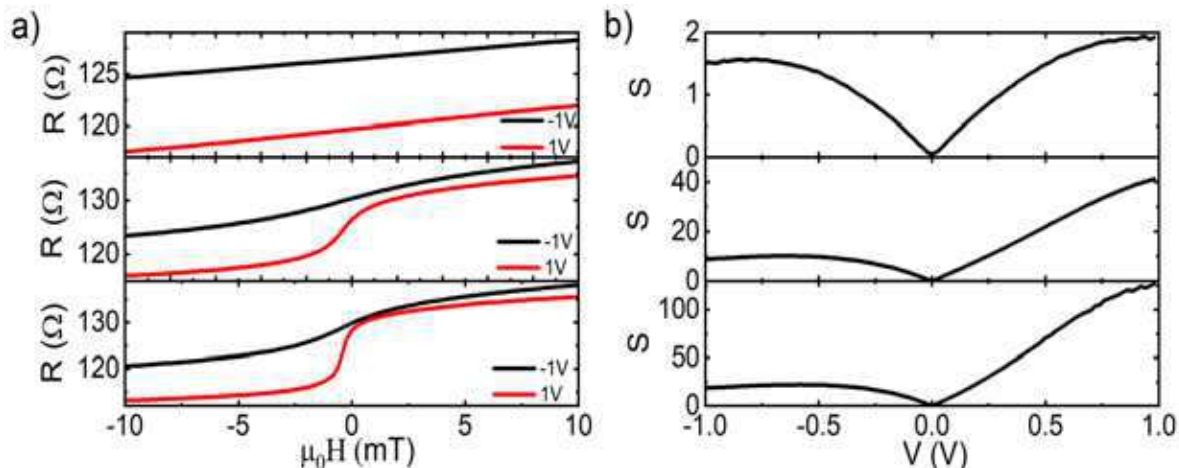


Figure 1: Transfer curves (a) and bias voltage dependence of sensitivity (b) of sensors without, with medium and strong VCMA effect.

This work was funded in part by National Science Centre, Poland, grant number 2021/41/B/ST7/04504.

[1] W. Skowronski, P. Wisniowski et al., Appl. Phys. Lett. 101,192401, (2012)

[2] P. Wisniowski, M. Dabek et al., Appl. Phys. Lett. 105, 082404, (2014)

[3] P. Wisniowski, M. Nawrocki et al., Spintronics XII 110903, (2019)

Magnetic noise and loss in magnetoelastic magnetic field sensors

E. Golubeva¹, B. Spetzler^{1,2}, F. Faupel¹ and J. McCord¹

¹ *Institute for Materials Science, Kiel University, Kiel, Germany*

² *Department of electrical engineering and information technology, Technical University Ilmenau, Ilmenau, Germany*

Reducing magnetic noise is one of the main challenges in developing various magnetic field sensors. Numerous studies on the origin of magnetic noise were performed on magnetoresistance sensors due to their widespread presence in the industry [1]. In the presented work, we expand the previously developed description of the thermal-magnetic noise and eddy current loss to the case of magnetoelastic sensors based on the ΔE effect, which have recently shown their high potential for detecting small-amplitude magnetic fields at low frequencies [2]. The concept of such sensors evolves from the dependency of the stiffness tensor on the applied magnetic field. This effect can be utilized in various configurations, including surface acoustic wave sensors and free-standing resonators. Here we will focus on magnetoelectric composite cantilevers, consisting of piezoelectric and magnetostrictive layers on a poly-Si substrate.

Through thorough experimental analysis and simulations, we have learned that eddy current losses significantly influence the magnetic noise in such systems. At the same time, the intrinsic thermal-magnetic noise becomes relevant for small sample sizes and high operating frequencies. Moreover, we show the connection between magnetic sensitivity, loss, noise, and signal nonlinearity. Besides the general discussion, we present a complete device model covering different levels of the sensor system. It connects physical descriptions of magnetization dynamics and solid mechanics with signal and noise equivalent-circuit models. Such a combination allows us to estimate the fundamental limit of the detectable magnetic field, often quantified by the limit of detection (LOD). The model can also be adapted and applied to other magnetoelectric sensors.

This work was funded by the German Research Foundation (DFG) through the Collaborative Research Centre CRC 1261 "Magnetoelectric Sensors – From Composite Materials to Biomagnetic Diagnostics" and the Carl-Zeiss Foundation via the Project MemWerk.

[1] Weitensfelder, H., Brueckl, H., Satz, A. et al. Comparison of Sensitivity and Low-Frequency Noise Contributions in Giant-Magnetoresistive and Tunneling-Magnetoresistive Spin-Valve Sensors with a Vortex-State Free Layer. *Phys. Rev. Appl.* **10**, 1 (2018).

[2] Spetzler, B., Bald, C., Durdaut, P. et al. Exchange biased delta-E effect enables the detection of low frequency pT magnetic fields with simultaneous localization. *Sci Rep* **11**, 5269 (2021).

Dual-pulse strategies for efficient switching of magnetic tunnel junctions

Viola Krizakova¹, Eva Grimaldi¹, Kevin Garello³, Giacomo Sala¹, Sebastien Couet², Gouri Sankar Kar², and Pietro Gambardella¹

¹Department of Materials, ETH Zurich, 8093 Zürich, Switzerland

²imec, Kapledreef 75, 3001 Leuven, Belgium

³Université Grenoble Alpes, CEA, CNRS, Grenoble INP, SPINTEC, 38054 Grenoble, France

Switching mechanisms relying on the voltage control of magnetic anisotropy (VCMA) and spin-orbit torques (SOTs) are alternatives to spin transfer torque (STT) for applications in which low energy consumption and fast operation are important. Whereas all these mechanisms have been extensively studied separately in magnetic tunnel junctions (MTJs), less attention has been directed to their combined impact on the switching performance. It has been shown that the combined action of SOT and MTJ biasing can enable field-free switching [1], reduce the energy per cycle [2], and minimize the incubation delay and dispersion of switching events [3]. Studying the interplay of both biases is thus not only relevant to understanding the switching dynamics in MTJs but also to improving efficiency.

Here, we investigate dual-pulse strategies for efficient switching of three-terminal MTJs. The used devices are designed for CMOS-compatible SOT-MRAM architectures [4] and allow for field-free operation [5]. We show that simultaneous injection of voltage pulses to the bottom and top input electrodes of a device (see Fig. 1) can reduce the writing energy compared to switching by SOT or STT alone, while simultaneously preserving the ability to switch by sub-nanosecond pulses. Our study further unravels the relative impacts of SOT, STT, VCMA, and self-heating on the switching time [6]. We find that the incubation delay is minimized by self-heating and VCMA, which weaken the free layer anisotropy and thus lower the nucleation energy barrier. The ensuing magnetization reversal can be assisted by STT. We show how the relative impact of these effects depends on the strength, polarity, and duration of the pulses, as well as on the MTJ size; and that specific combinations of biases even result in a decreased switching efficiency compared to SOT. Finally, we provide a compact analytical model relating the effects induced by the MTJ bias to the geometry and material parameters of the device, which allows for their separate tuning and finding the optimal balance between SOT and STT currents [6].

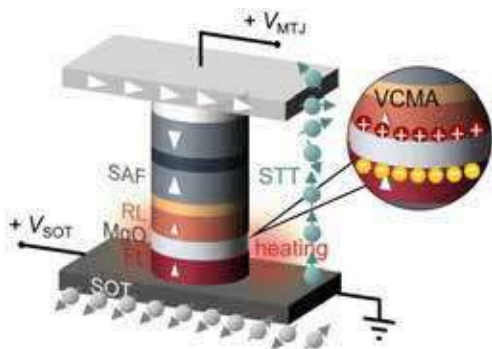


Figure 1: Schematics of the effects induced by voltage bias applied across the MTJ (V_{MTJ}) and on the SOT track (V_{SOT}) in a three-terminal MTJ device. An in-plane magnet providing a stray field on the free layer (FL) is embedded in the hardmask above the pillar, allowing zero-external-field operation.

- [1] M. Wang, W. Cai, D. Zhu, *et al. Nat. Electron.* **1**, 582 (2018)
- [2] Y. C. Wu, K. Garello, W. Kim, *et al. Phys. Rev. Appl.*, **15**(6), 064015 (2021)
- [3] E. Grimaldi, V. Krizakova, G. Sala, *et al. Nat. Nanotech.* **15**, 111-117 (2020)
- [4] K. Garello, F. Yasin, S. Couet *et al. IEEE Symp. VLSI Circ.*, 81–82 (2018)
- [5] K. Garello, F. Yasin, H. Hody, *et al. IEEE Symp. VLSI Technol.*, T194-195 (2019)
- [6] V. Krizakova, E. Grimaldi, K. Garello, *et al. Phys. Rev. Appl.*, **15**(5), 054055 (2021)

Atomistic study of the thermodynamic properties and switching dynamics of perpendicular shape anisotropy MRAM

Wayne Lack¹, Roy W Chantrell¹, Richard F L Evans¹, Sarah Jenkins¹

¹ University of York, UK

MRAM is a non-volatile memory technology that stores a bit as a magnetic state of a ferromagnetic CoFeB free layer, which aligns parallel or anti-parallel with a fixed magnetisation CoFeB layer, where these two layers sandwich a non-magnetic MgO layer, shown in figure 1a. DRAM and SRAM are volatile technologies and draw large amounts of power in high performance computing clusters so scaling MRAM to competing volumes is attracting significant research and development. [1] To achieve practical applications, MRAM must display a high thermal stability, high tunnel magnetoresistance ratio and a low writing current at competing volumes. A recent development to achieve this scalability is to use tower structures with height greater than the diameter, which allows the shape anisotropy and the interfacial anisotropy to favour out-of-plane magnetisation direction. [2] It is vital to understand the switching mechanism at operational temperatures for reliable MRAM. This study uses an atomistic model in VAMPIRE with a CoPt SAF to pin

the fixed CoFeB layer and an enhanced monolayer either side of the MgO. VAMPIRE uses the spin Hamiltonian equation, with thermal fluctuations and dipole fields included with the LLG. [3] We have found in figures 1b, that while the susceptibility of the free layer varies hugely as the volume is increased, if we divide these towers into smaller regions, susceptibility is locally correlated, suggesting non-uniform magnetisation modes. This would suggest taller towers would switch incoherently, which we then demonstrate in figures 1 c, as the taller tower shows nucleated propagation.

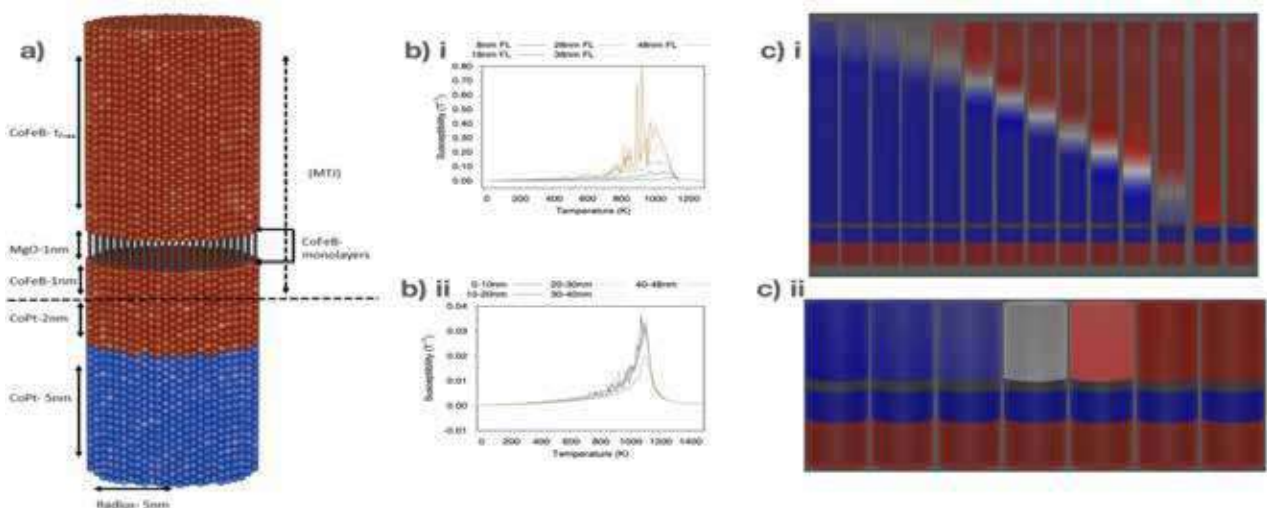


Figure 1. a) shows the dimensions and structure of the PSA MRAM, b) i shows the susceptibility for the whole free layer while ii) shows the susceptibility of local 10nm chunks of the tallest tower. c) i Shows nucleated reversal in the tallest tower and ii shows coherent rotation in the smallest tower

[1] K. Watanabe et al, Nature Communications, 9, article no. 663, 2018

[2] N. Perrissin et al, Nanoscale, issue 25, 2018

[3] R. F. L Evans et al, journal of physics: condensed matter, volume 26, number 10, 2014

Numerically stable and highly performant implementations of the analytic magnetic field solution of the diametrically magnetized cylinder

P. Leitner¹, L. Rauber, F. Slanovc¹, P. Malagó¹ and M. Ortner¹

¹*Silicon Austria Labs, Europastrasse 12, A-9524 Villach, Austria*

A Green's function-based analytical magnetic field solution of the diametrically magnetized cylinder derived from the magnetic surface charge picture is well known in the literature, e.g. [1]. An often employed solution relies on a series expansion based on the Simpsons approximation for the final integration [2]. While any such closed-form solutions – if existing – are in any case preferable to CPU-costly finite element/volume computations, they turn out to be potentially massively unstable when being evaluated at field-points located in a number of numerical instability regions. With this contribution we want to raise the awareness for the numerical instabilities of an otherwise elegantly formulated closed field solution that bears the high risk of erroneous field evaluation when attempted by a naive straight-forward implementation of the published formulas. We discuss the origin of those instabilities and offer a resolution by stable reformulations of the problem in terms of dedicated complete elliptic integrals valid in the prime regions of interest, combined with stable series solutions where such a stabilization is not possible. Our patched solutions are shown to be fully stable throughout the entire \mathbb{R}^3 and additionally have been implemented in an algorithmically highly performant way, surpassing the standard implementations in terms of elliptic integrals of the first and second kind when based on state-of-the-art libraries such as Scipy or Matlab in our benchmarks. Our codes are made available to the general public for use in the Python package Magpylib [3].

- [1] E. Furlani, S. Reznik, W. Janson, *IEEE Transactions on Magnetics* **30**, 2916 (1994).
- [2] A. Caciagli, R.J. Baars, A.P. Philipse, B.W.M. Kuipers, *Journal of Magnetism and Magnetic Materials* **465**, 423 (2017)
- [3] M. Ortner, L. G. Coliado Bandeira, *SoftwareX* **11**, 100466 (2020).

Higher-order Magnetic Anisotropy in Soft-hard Nanocomposite Materials

Nguyen Thanh Binh¹, Sarah Jenkins², Sergiu Ruta¹, Richard Evans¹, Roy Chantrell¹

¹*Department of Physics, University of York, UK*

²*University of Duisburg-Essen, Germany*

Properties of higher-order magnetic anisotropy constants in soft-hard nanocomposite materials still attract much debate [1]. We investigated the magnetic anisotropy in a L1₀/A1 FePt system using the VAMPIRE software package [2]. An elongated, faceted cylindrical core-shell was constructed with a L1₀-FePt core of varied size surrounded by an A1-FePt shell. The system truncated exchange interaction accounts up to the next-next nearest neighbours. A 2-ion Fe-Pt anisotropy component was incorporated to the system Hamiltonian following Mryasov et al. [3]. The angular dependence of the restoring torque was calculated from 0K to 1000K in 5K steps using a constrained Monte-Carlo integrator. Temperature-dependent anisotropy constants were then determined from fitting to the system torque as a function of the constrained angle. We find that the core-shell structure exhibits an unexpected 4th-order anisotropy term of which magnitude depends on the core-size ratio R. The K₂/K₁ ratio, with K₁ and K₂ the 2nd and 4th-order anisotropy constant respectively, displays a non-monotonic pattern with a peak occurring at R ~ 0.55 [Fig.1]. We find that K₂ scales with (M/M_s)⁻² at temperatures below T_C - a remarkable deviation from the Callen-Callen theory [4] which instead predicts a scaling with (M/M_s)¹⁰. A simple analytical model shows the 4th-order term to arise from canting of the core and shell magnetisation. Further, the model demonstrates that the magnitude of the 4th-order term is proportional to K₁²/J, with J the exchange coupling. Given that the 2-ion K₁ term scales approximately with M^{2.1} and J with M², the predicted scaling exponent is 2.2 - in good agreement with simulations. Generally, the 4th-order anisotropy constant is shown to exhibit a strong geometry - dependence, thus suggesting that Callen-Callen power law is valid only for single-ion anisotropies.

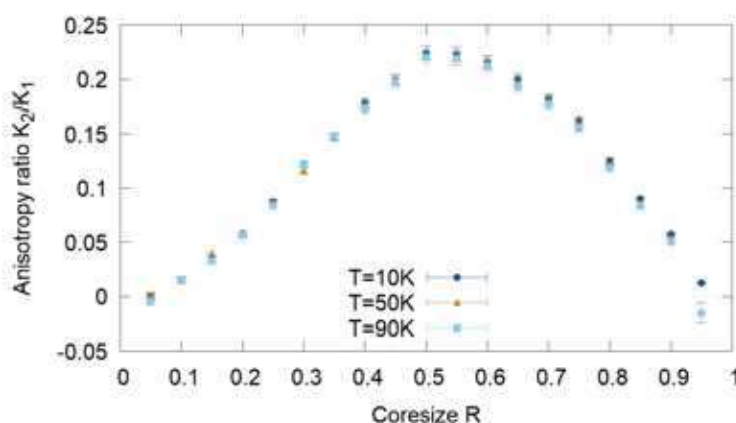


Figure 1: A low temperature scan displays a non-monotonic dependence of K₂/K₁ on core size ratio R with a peak at R ~ 0.55.

- [1] Richter et al., J. Appl. Phys. **109**, 07B713 (2011)
- [2] Evans et al., Journal of Physics: Condensed Matter, **26**, 103202 (2014).
- [3] Mryasov et al., Europhys. Lett., **69** (5), pp. 805–811 (2005)
- [4] Callen et al., J. Phys. Chem. Solids, **16**, 310 (1960)

HAMR Switching Efficiency in Coreshell L1₀/A1-FePt Grain

Nguyen Thanh Binh¹, Sergiu Ruta¹, Sarah Jenkins², Richard Evans¹, Roy Chantrell¹

¹*Department of Physics, University of York, UK*

²*University of Duisburg-Essen, Germany*

Iron Platinum in the L1₀-phase (L1₀-FePt) is being extensively investigated for potential applications in Heat-Assisted Magnetic Recording (HAMR) [1]. However, it is challenging to reduce grain size to below 10nm because of reducing thermal stability and, consequently, thermal writability. In addition, a recent study discovered a size-dependent effect of Pt surface segregation which decreases anisotropy and further destabilises the grain [2]. Therefore, in this research we aim to study computationally the impact of surface disorder on switching efficiency in sub-10nm FePt grain. Our simulations are performed by the VAMPIRE software package [3]. Elongated, faceted cylindrical FePt grains are created with three different configurations in order to investigate the effect of varying size and adding surface disorder. The 2-ion Fe-Pt anisotropy component of FePt, which is the origin of the exceptionally high uniaxial anisotropy of the material, is incorporated into the system Hamiltonian following Mryasov et al.'s [4]. A laser pulse of varied duration and an external cooling field are applied to switch the spins. Simulation data [Fig.1] shows that the switching probabilities of all 3 configurations increase sharply around T_C and finally saturate to less than 100%, which indicates the existence of a non-negligible thermally induced switching error rate. Reducing the grain size and using shorter laser pulses are found to induce higher switching error rate, which are detrimental for HAMR function. These effects, however, could be mitigated by surface engineering – in this case the addition of a disorder A1 shell around the ordered L1₀ core in order to stabilise the magnetisation of the L1₀-phase.

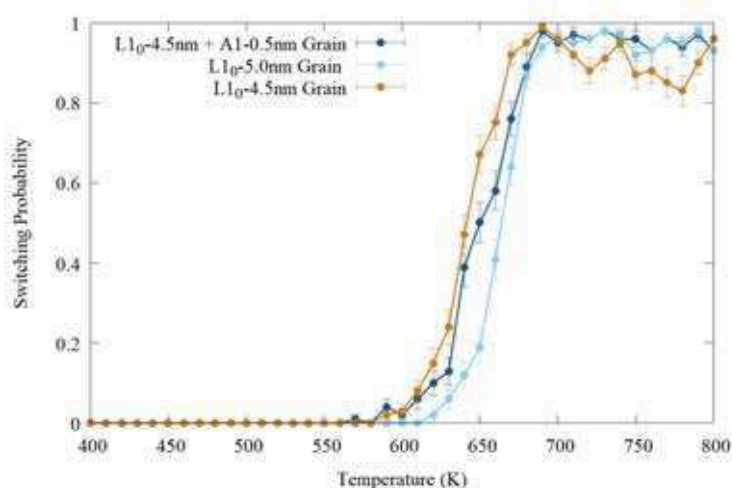


Figure 1: Switching efficiencies for the three simulated configurations of FePt grain with the applied laser pulse of 3.0ns.

[1] D. Weller et al., *Journal of Vacuum Science & Technology B*, **34**, 060801 (2016)

[2] H.S-Amin et al., *Scripta Materialia* **135** (2017) 88–91

[3] Evans et al., *Journal of Physics: Condensed Matter*, **26**, 103202 (2014).

[4] Mryasov et al., *Europhys. Lett.*, **69** (5), pp. 805–811 (2005)

Magnetic noise reduction strategies in magnetoresistive sensors for improved detection limits.

J. Moulin¹, A. Doll¹, E. Paul¹, C. Fermon¹, M. Pannetier-Lecoeur¹, N. Sergeeva-Chollet², A. Solignac¹

¹SPEC - CEA Saclay – CNRS UMR3680, 91191 Gif-sur-Yvette, France

²CEA LIST, 91191 Gif-sur-Yvette, France

Giant magnetoresistances (GMR) and magnetic tunnel junctions (MTJ) are devices based on spintronics. Thanks to their typical level of detection of a few nanoteslas and their large frequency work range, such sensors are widely used for low field measurements, for example [1,2] in automotive, biochips detections or in biological systems. Nevertheless, their detectivity is limited at low frequency by the presence of $1/f$ noise and random telegraphic noise. This noise can have a magnetic origin due to magnetic fluctuations of the free layer. Indeed the sensors are composed by schematically two ferromagnetic layers separated by a non-magnetic spacer. The resistance of the structure depends on the relative orientation of the magnetization of the two layers. One layer (blocked layer) possesses a blocked magnetization independent on the external field while the other (free) layer magnetization rotates with the field. In order to obtain a linear field sensor response, an anisotropy has to be created in the free layer at 90° from the blocked layer. Several linearization strategies exist [3], as apply an external field, shape anisotropy or intrinsic coupling inside the stack. In this work, we have studied the impact of these different strategies on the magnetic noise and on the sensor detectivity. We demonstrate the presence of an optimal pinning field independent on the linearization strategy which allows a magnetic noise stabilization before losing in sensitivity and thus enhancing detectivity by a factor of 10 (Figure 1 and [4]).

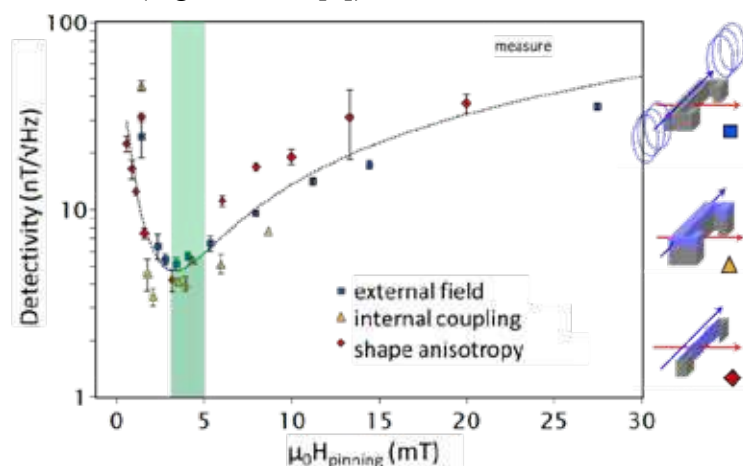


Figure 1: Minimum detectable magnetic signal as a function of the applied pinning field with different techniques (external field, internal coupling, shape anisotropy).

- [1] P. Campiglio, C. Fermon, Large-Volume Applications of Spin Electronics-Based Sensors (2017)
- [2] L. Caruso et al., Neuron, vol. 95, no 6, p. 1283-1291 (2017)
- [3] A. V. Silva et al., Eur. Phys. J. Appl. Phys. 72: 10601, (2015)
- [4] J. Moulin et al., Appl. Phys. Lett. 115, 122406 (2019)

Offset free magnetic sensing principle and the role of the spin-orbit torque coefficients

J. Salazar-Mejía¹, S. Koraltan¹, C. Abert¹, F. Slanovc¹, P. Flauger¹, M. Agrawal², A. Satz³, C. Schmitt⁴, G. Jakob⁴, M. Kläui⁴, H. Brückl⁵ and D. Suess¹

¹University of Vienna, Faculty of Physics, Physics of Functional Materials, Vienna, Austria

²Infineon Technologies AG, Am Campeon 1-15, 85579 Neubiberg, Germany

³Infineon Technologies Austria, Siemensstrasse 2, Villach, Austria

⁴Institute of Physics, Johannes Gutenberg-University Mainz, 55128 Mainz, Germany

⁵Universität für Weiterbildung Krems, Department für Integrierte Sensorsysteme, 2700 Wiener Neustadt Austria

Nowdays magnetic field sensors rely on magnetoresistive effects[1]. Commonly, such sensors are used in a Wheatstone bridge configuration, which in practice leads to a zero field offset due to fabrication tolerances and different temperature drifts.

We propose a robust differential resistivity measurement on a single device with perpendicular anisotropy, which is situated on top of a heavy metal (HM). By applying charge current through the HM, spin-orbit torques (SOT) are induced on the magnetization. For currents under the switching threshold, the magnetization experiences small deviations from its initial out-of-plane state. From $+J$ and $-J$ currents, the induced SOT acts equally in opposite directions. When an external magnetic field is present, the SOT symmetry is broken and a distinct deflection occurs, see Fig. 1a. Consequently, by measuring the magnetization m_z component for both currents a transfer curve with zero-offset can be achieved, as illustrated in Fig. 1b.

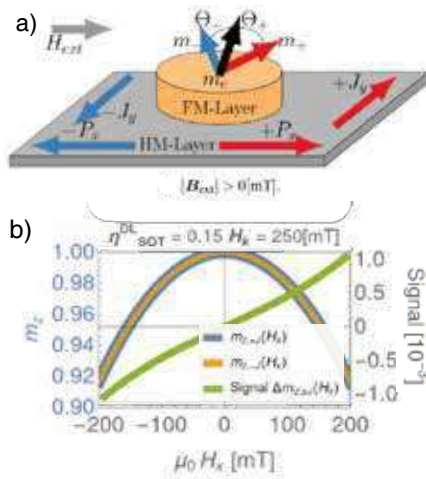


Figure 1: (a): Schematic of the sensor geometry. (b): Analytic solution of the sensor signal

By macrospin simulations, we observe that intrinsic material parameters, such as the field-like and damping-like SOT coefficients play a key role on the magnetization dynamics[2]. Thus, their accurate determination is crucial for correct simulation of the sensor performance. An analytical solution for the magnetization is used to predict the sensing output[3]. To determine the SOT coefficients, a harmonic voltage analysis is performed. Finally, with an adequate set of parameters, micromagnetic simulations are performed using the LLG eqn., in parallel with experimental measurements, to design a sensor with zero-offset for industrial applications.

[1] D. Suess, Bachleitner-Hofmann A., Satz A., et al. *Nature Electronics* **1**, 362 (2018)

[2] C. Abert. *European Phys. Journal B* **92**, 120 (2019).

[3] Z. Daoqian, C. Weishan. *Phys. Rev. A* **13**, 044078 (2020)

Global Magnetic Topology Optimization

Florian Slanovc^{1,2,3}, Michael Ortner¹, Mohssen Moridi¹, Gregor Wautischer², Paul Heistracher², Florian Bruckner², Claas Abert², Dieter Suess²

¹ *Silicon Austria Labs (SAL), Europastraße 12, 9524 Villach, Austria*

² *University of Vienna, Faculty of Physics, Boltzmanngasse 5, 1090 Vienna, Austria*

² *University of Vienna, Vienna Doctoral School in Physics, Boltzmanngasse 5, 1090 Vienna, Austria*

In various applications of magnetic materials like sensor systems and motors, the profile of the magnetic field (in addition to the sensor properties) has a significant influence on the quality of the system. Therefore, it makes sense to use magnets with optimized shapes that generate fields suitable for the specific application.

One possible way to improve the magnetic field in some desired way is magnetic topology optimization, where the shape of the magnets is adjusted by optimization. In general, there exist many different approaches to solving the optimization problem. In the past, several works have presented possible optimization algorithms that allow the magnets to be optimized with respect to a predefined objective function that measures the quality of the obtained field [1]. Since gradient-based optimization algorithms tend to converge to nearby local minima, there is no guarantee that the minimum reached is global. We focus on the search of global optima and present a hybrid topology optimization algorithm based on finite-differences [1] that combines the global cuckoo search optimization algorithm [2] with a very fast and efficient local binary on/off optimization algorithm [3]. We discuss why our approach is predestined for optimization problems in the case of a very high-dimensional domain (number of magnetic cells), only two desirable states (magnetic material or not), available gradient (adjoint method), and the possible presence of multiple local minima.

Our algorithm can find significantly better solutions than pure local or global optimization methods (see Figure 1) and has fast convergence properties due to the possible parallel computation.



Figure 1: Exemplary result for the optimum magnetic shape with a local optimization algorithm (left) and our presented hybrid optimization algorithm (right). The found optimum of the latter variant results in a 75.5% lower value of the given objective function and presents therefore a significantly better optimum with the same depth of local optimization steps.

[1] Claas Abert, Christian Huber, Florian Bruckner, Christoph Vogler, Gregor Wautischer, and Dieter Suess. A fast finite-difference algorithm for topology optimization of permanent magnets. *Journal of Applied Physics*, 122(11):113904, sep 2017.

[2] Xin-She Yang and Suash Deb. Cuckoo search via lévy flights. In 2009 World Congress on Nature & Biologically Inspired Computing (NaBIC). IEEE, 2009.

[3] Yoshifumi Okamoto and Norio Takahashi. A novel topology optimization of nonlinear magnetic circuit using ON/OFF method. *IEEJ Transactions on Fundamentals and Materials*, 125(6):549–553, 2005.

Symposium 13. Domain walls, Skyrmions and spin-orbit related phenomena

| | | |
|-------------------------|--|-----|
| Aisha Aqeel | <i>Magnetic Skyrmions in Electrically Insulating Magnets</i> | 436 |
| Fatima Ibrahim | <i>Unveiling mechanisms of: temperature-dependence of PMA and DMI at MgO-based and 2D materials-based interfaces</i> | 437 |
| Hariom Jani | <i>A potential platform for Antiferromagnetic Skyrmionics</i> | 438 |
| Samir Lounis | <i>Spin-orbit enabled all-electrical read-out of chiral spin-textures and impact of defects</i> | 439 |
| Jan Masell | <i>Antiskyrmions, skyrmions, and mixed-topology skyrmions in crystals with S4 symmetry</i> | 440 |
| Teruo Ono | <i>3D domain wall motion memory with artificial ferromagnet</i> | 441 |
| João Sampaio | <i>Ferrimagnetic skyrmions in GdCo</i> | 442 |
| Saul Velez | <i>Current-induced control of chiral magnetic textures in magnetic insulators</i> | 443 |
| Tobias Weber | <i>Topological magnon band structure of emergent Landau levels in a skyrmion lattice</i> | 444 |
| Amal Aldarawsheh | <i>Emergence of zero-field non-synthetic single and catenated antiferromagnetic skyrmions in thin films</i> | 447 |
| Laura Álvaro Gómez | <i>Current induced domain wall dynamics in chemical modulated nanowires</i> | 448 |
| Maria Azhar | <i>Screw dislocations in chiral magnets</i> | 449 |
| Cristina Balan | <i>Electric field control of chiral magnetic textures in multilayer films with perpendicular magnetic anisotropy</i> | 450 |
| Anne Bernand-Mantel | <i>A micromagnetic theory of skyrmion lifetime in ultrathin ferromagnetic films</i> | 451 |
| Mark De Jong | <i>Facilitating Skyrmion Nucleation in Ir/Co/Pt Multilayers With Ga⁺ Ion Irradiation</i> | 452 |
| Takaaki Dohi | <i>Diffusive motion of antiferromagnetically coupled skyrmions</i> | 453 |
| Claire Donnelly | <i>Domain wall automotion for three-dimensional magnetic interconnectivity</i> | 454 |
| JoseA. Fernandez-Roldan | <i>Current- and Oersted-field-dynamics of a Bloch Point in cylindrical Ni nanowires</i> | 455 |
| Charles-Élie Fillion | <i>Get skyrmions back on track: suppressing skyrmion Hall angle by material engineering or gate voltage</i> | 456 |
| Johanna Fischer | <i>Gate-Controlled Skyrmions in Magnetic Trilayer Tracks</i> | 457 |
| Minori Goto | <i>Stochastic dynamics of skyrmion bubble by alternating magnetic fields</i> | 458 |
| Simon Granville | <i>Magneto-ionic and electrostatic generation of non-volatile and volatile skyrmions in MgO/Mn₂CoAl/Pd thin films using ionic liquid gating</i> | 459 |
| Matthieu Grelier | <i>Non-collinear three-dimensional textures in magnetic multilayers: the emergence of skyrmionic cocoons</i> | 460 |
| Konstantin Gusliyenko | <i>3D topological charge of the Bloch point in a spherical magnetic nanoparticle</i> | 461 |

| | | |
|--------------------|--|-----|
| Mara Gutzeit | <i>Nano-scale collinear multi-Q states driven by higher-order interactions</i> | 462 |
| Javier Hermosa | <i>Domain wall magnetic configuration of soft Py microstructures studied by magnetic X-ray tomography</i> | 463 |
| Mahdi Jaber | <i>Magnetic imaging of domain walls in CoNiB nanotubes for 3D spintronics</i> | 464 |
| Lisa-Marie Kern | <i>Controlled Localization of Magnetic Skyrmion Nucleation</i> | 465 |
| Christopher Klose | <i>Coherent Correlation Imaging: Resolving fluctuating states of matter</i> | 466 |
| Taro Komori | <i>Current induced domain wall motion in $Mn_{4-x}Ni_xN$ benefited from the compensation at room temperature</i> | 467 |
| Pingzhi Li | <i>All-Optical Switchable Racetrack based on Compensated Co/Gd quadlayers</i> | 468 |
| Sougata Mallick | <i>Stabilizing skyrmions in Pt/Co/Tb multilayers with reduced magnetization</i> | 469 |
| Piotr Mazalski | <i>Magnetic domain evolution in W/Co/Pt ultrathin epitaxial layers approaching the superparamagnetic Co thickness regime</i> | 470 |
| Daniel Metternich | <i>Direct observation of bulk-DMI-stabilized Néel-type domain walls in ferrimagnetic rare-earth transition-metal alloys</i> | 471 |
| Santiago Osorio | <i>Creation of single chiral soliton states in monoaxial helimagnets</i> | 472 |
| Van Tuong Pham | <i>Over 1 km/s Current Induced Skyrmion Motion in Synthetic Antiferromagnet without Skyrmion Hall Effect</i> | 473 |
| Klaus Raab | <i>Brownian reservoir computing realized using geometrically confined skyrmions</i> | 474 |
| Malte Römer-Stumm | <i>Statistical analysis of superdiffusion of skyrmion bubbles</i> | 475 |
| Cameron Rudderham | <i>Image-recognition-assisted characterization of metastable topological structures in chiral magnetic thin films</i> | 476 |
| Yanis Sassi | <i>Skyrmion racetrack: confinement by the edge</i> | 477 |
| Daniel Schick | <i>Phase formations in skyrmion ensembles with anisotropic interaction</i> | 478 |
| Krzysztof Sobucki | <i>Bloch hopfion spin-wave spectra in ferromagnetic medium</i> | 479 |
| Samuel Treves | <i>Observation of metastable skyrmion lattice in $NdMn_2Ge_2$ at room temperature</i> | 480 |
| Victor Ukleev | <i>Exchange anisotropy and a new spiral state in the insulating chiral magnet Cu_2OSeO_3</i> | 481 |
| Guru Venkat | <i>Emergent responses in magnetic ring arrays of different lattice arrangements for reservoir computing</i> | 482 |
| Iuliia Vetrova | <i>Investigation of self-nucleated skyrmion states in the ferromagnetic/nonmagnetic multilayer dot</i> | 483 |
| Markus Weißenhofer | <i>The Interplay between Skyrmions and Thermal Magnons</i> | 484 |
| Anuj Dhiman | <i>Magnetic properties of ultrathin Pt/Co/Re and Re/Co/Pt layers</i> | 486 |
| Lucia Fecova | <i>Direct Correlation Between Domain Wall Distortions and Perpendicular Fields in Amorphous Glass-Coated Microwires</i> | 487 |

| | | |
|-----------------------|--|-----|
| Soumyajyoti Haldar | <i>Distorted 3Q state driven by topological-chiral magnetic interaction</i> | 488 |
| Michał Inglot | <i>Edge states at a Rashba spin-orbit domain wall in the magnetized graphene</i> | 489 |
| Jagannath Jena | <i>Stability of antiskyrmions and elliptical Bloch skyrmions in a D2d system</i> | 490 |
| Anastasiia Korniienko | <i>Magnetic configurations in $\text{Fe}_{32}\text{Co}_{68}$ core-shell nanostructures with hexagonal cross-section</i> | 491 |
| Santiago Osorio | <i>Response of the chiral soliton lattice to spin polarized currents</i> | 492 |
| Bibekananda Paikaray | <i>Reconfigurable logic operations via gate controlled skyrmion motion in a nanomagnetic device</i> | 493 |
| Andrea Peralta | <i>Observation of spin textures in $\text{La}_{0.7}\text{Sr}_{0.3}\text{MnO}_3/\text{SrIrO}_3$ bilayers</i> | 494 |
| Dariia Popadiuk | <i>Study of gyrovectors of magnetic hopfions</i> | 495 |
| Subhajit Roy | <i>Modification of domain wall velocity in Ta/CoFeB/MgO due to voltage-induced non-volatile piezoelectric strain</i> | 496 |
| Yanis Sassi | <i>Spin-orbit torque engineering for efficient skyrmion motion</i> | 497 |
| Amir Nasser Zarezad | <i>Topological Hall effect in two-dimensional systems with Skyrmion textures in the presence of electromagnetic impurities.</i> | 498 |

Invited Oral Presentations

| | | |
|----------------|---|-----|
| Aisha Aqeel | <i>Magnetic Skyrmions in Electrically Insulating Magnets</i> | 436 |
| Fatima Ibrahim | <i>Spin-orbit induced phenomena at ferromagnet/oxide and ferromagnet/2D material interfaces from first principles</i> | 437 |
| Hariom Jani | <i>A potential platform for Antiferromagnetic Skyrmionics</i> | 438 |
| Samir Lounis | <i>Spin-orbit enabled all-electrical read-out of chiral spin-textures and impact of defects</i> | 439 |
| Jan Masell | <i>Antiskyrmions, skyrmions, and mixed-topology skyrmions in crystals with S4 symmetry</i> | 440 |
| Teruo Ono | <i>3D domain wall motion memory with artificial ferromagnet</i> | 441 |
| João Sampaio | <i>Ferrimagnetic skyrmions in GdCo</i> | 442 |
| Saul Velez | <i>Current-induced control of chiral magnetic textures in magnetic insulators</i> | 443 |
| Tobias Weber | <i>Topological magnon band structure of emergent Landau levels in a skyrmion lattice</i> | 444 |

Magnetic Skyrmions in Electrically Insulating Magnets

Aisha Aqeel^{1,2}

¹*Technical University of Munich, D-85748 Garching, Germany*

²*Munich Center for Quantum Science and Technology (MCQST), D-80799 München, Germany*

Magnetic skyrmions are promising candidates as information carriers for future memory applications. These are particle-like topological solitons that can be envisaged as nano-sized twists or knots in an otherwise uniform magnetic material. Skyrmions are found in chiral magnets with no inversion symmetry due to finite Dzyaloshinskii-Moriya interaction (DMI). The complex three-dimensional internal structure of magnetic skyrmions and their interaction with each other are imposed by a surrounding magnetic state of the host magnetic material. The detailed understanding of the static and dynamic magnetization of skyrmions in chiral magnets is crucial for their embodiment in practical devices. Here, we investigate the magnetization dynamics of skyrmion [1,2] in a chiral magnetic insulator Cu_2OSeO_3 by broadband microwave spectroscopy. By combining results with the linear spin wave theory, we clearly identify the dynamic modes associated with skyrmions, as well as the hybridization of one mode with a higher order mode mediated by magnetocrystalline anisotropies. Interestingly, our findings suggest that under decreasing fields the hexagonal skyrmion lattice becomes unstable, resulting in the formation of the elongated skyrmions [3]. These findings highlight how the study of dynamic properties may provide valuable insights to static properties, such as microscopic nature of magnetic textures.

[1] A. Chacon, et al., *Nature Physics* **14**, 936-941 (2018).

[2] M. Halder, et al., *Phys. Rev. B* **98**, 144429 (2018).

[3] A. Aqeel, et al., *Phys. Rev. Lett.* **126**, 017202 (2021).

Unveiling mechanisms of: temperature-dependence of PMA and DMI at MgO-based and 2D materials-based interfaces

F. Ibrahim¹, A. Hallal¹, B. Dieny¹, and M. Chshiev^{1,2}

¹ Univ. Grenoble Alpes, CEA, CNRS, SPINTEC, F-38000 Grenoble, FRANCE

² Institut Universitaire de France

Spin-orbit coupling (SOC) at material interfaces leads to the emergence of a wealth of phenomena such as perpendicular magnetic anisotropy (PMA) and Dzyaloshinskii–Moriya interaction (DMI). Magnetic tunnel junctions based on Co(Fe)/oxide and Co/graphene interfaces have attracted much attention due to their low spin-orbit coupling but yet interesting magnetic and spin-orbitronic properties [1,2]. Using first-principles calculations, we investigate both PMA and DMI emerging at such interfaces.

In the first part of the talk, the correlation between temperature dependence of magnetic anisotropy and magnetization in typical Fe/MgO structures is addressed [3]. In an ideal interface, the temperature-dependence of the total and layer-resolved anisotropy follow the Callen and Callen scaling power law and thus intrinsic properties cannot explain deviations from this law. In this respect, we show that such deviations observed experimentally can be attributed to two macroscopic mechanisms: the presence of a magnetic dead layer or the spatial fluctuations of the interfacial PMA. We anticipate that those results will help in understanding the thermal stability of the storage layer magnetization in STT-MRAM applications.

In the second part, we demonstrate a significant PMA and a large DMI at Co/2D materials (graphene or h-BN) interfaces [4]. The PMA at the Co/h-BN interface is preserved as in the case of graphene coverage, thanks to the hybridization of d_z^2 orbitals of Co with p_z ones of 2D materials. By comparing the two interfaces, it is found that the DMI in Co/h-BN increases as a function of Co thickness and beyond three monolayers stabilizes with one order of magnitude larger values compared to those at Co/graphene, where the DMI shows opposite decreasing behavior. The Rashba constant in the case of Co/h-BN is found to be at least twice larger than that of graphene/Co, giving rise to the larger DMI values. The difference between the two interfaces is explained by the presence of two competing dipoles at the graphene/Co interface compared to only one dipole at the Co/h-BN interface. These findings open up further possibilities towards integrating 2D materials in spin–orbitronic devices.

[1] B. Dieny & M. Chshiev, *Rev. Mod. Phys.* **89**, 025008 (2017).

[2] H. X. Yang *et al.*, *Nano Lett.* **16**, 145 (2016).

[3] F. Ibrahim *et al.*, *Phys. Rev. Applied* **17**, 054041 (2022).

[4] A. Hallal *et al.*, *Nano Lett.* **21**, 7138 (2021).

A potential platform for Antiferromagnetic Skyrmionics

H. Jani^{1,2}, JC Lin², J Harrison², J Chen², S Prakash¹, S Hooda¹, F Maccherozzi³, S Finizio⁴, J Schad⁵, CB Eom⁵, T Venkatesan¹, A Ariando¹, PG Radaelli²

¹ National University of Singapore, Singapore

² University of Oxford, UK

³ Diamond Light Source, UK

⁴ Paul Scherrer Institut, Switzerland

⁵ University of Wisconsin-Madison, USA

Swirling magnetic structures such as skyrmions, bimerons and their anti-particles can serve as topologically-protected information carriers in unconventional memory and logic platforms. However, their practical exploitation has been inhibited by sensitivity to stray magnetic fields, strong internal dipolar fields, slow speeds or sideways motion. To address these issues, there has been a surge of interest in antiferromagnetic (AFM) analogues, predicted to be robust, scalable and ultra-fast [1,2]. However, experimental progress in this field has been curtailed by magnetic compensation in AFM systems, which makes it difficult to control AFM textures via standard magnetic techniques.

We overcame this limitation by developing a general field-free approach, employing the Kibble–Zurek transition, to reversibly create a wide multichiral family of topological AFM textures, including exotic (anti)merons and bimerons [3]. In the earth-abundant oxide hematite (α -Fe₂O₃), in both epitaxial and free-standing forms, these nanoscopic topological textures can be nucleated and stabilized at room temperature. Particularly, the presence of widely tunable anisotropy and exchange interactions in this system [3-6] enables unprecedented reversible control over their dimensions and orientation. We further exploit this tunability to locally control AFM states via non-uniform strains and strain gradients in flexible free-standing AFM membranes. We have also found that by introducing new symmetry breaking interactions, it may be possible to realize hitherto undiscovered AFM skyrmions via rational materials design in α -Fe₂O₃ [7]. I will conclude by outlining the path ahead for skyrmionics in natural AFMs by sharing electrical pathways that may be exploited to control members of the topological family [8-10].

- [1] J Barker et al., *Physical Review Letters* **116**, 147203 (2016);
- [2] V Baltz et al., *Review of Modern Physics* **90**, 015005 (2018);
- [3] H Jani et al., *Nature* **590**, 74 (2021);
- [4] FP Chmiel et al., *Nature Materials* **17**, 581 (2018);
- [5] H Jani et al., *Nature Communications* **12**, 1668 (2021);
- [6] ZS Lim*, H Jani* et al., *MRS Bulletin* **46**, 1053 (2021);
- [7] J Harrison, H Jani et al., arXiv:2111.15520 (2021);
- [8] L Baldrati et al., *Physical Review Letters* **123**, 177201 (2019);
- [9] P Zhang et al., *Physical Review Letters* **123**, 247206 (2019);
- [10] Y Cheng et al., *Physical Review Letters* **124**, 027202 (2020);

Spin-orbit enabled all-electrical read-out of chiral spin-textures and impact of defects

Samir Lounis^{1,2}

¹*Peter Grünberg Institute and Institute for Advanced Simulation, Forschungszentrum Jülich, Germany*

²*Faculty of Physics, University of Duisburg Essen & CENIDE, Duisburg, Germany*

Chirality and topology are intimately related fundamental concepts, which are heavily explored to establish spin-textures such as magnetic skyrmions as potential magnetic bits in information technology. This is however hindered by various challenges, among which the highly non-trivial electrical reading of chiral attributes with conventional current-perpendicular-to-plane (CPP) sensing devices and the presence of unavoidable inhomogeneities, which affect the detection, nucleation, motion and velocity of topological bits. In this talk, I will introduce a rich family of magnetoresistances of spin-mixing origin enabling the all-electrical detection of spin-textures, which are categorized in terms of the presence (or not) of non-collinear magnetism, spin-orbit coupling (SOC) and their concomitant intertwining [1]. I will highlight the chiral spin-mixing magnetoresistance (C-XMR), linear in SOC and requiring broken inversion symmetry, which reaches large efficiencies permitting to distinguish and spatially probe the chiral nature of magnetic objects. Besides the traditional AMR quadratic in SOC, we unveil the non-local spin-mixing anisotropic MR (X-AMR) that is non-local and depends on the canting angle between magnetic moments. New MR phenomena [2,3] can be triggered by atomic defects, which simultaneously design the energy-landscape of single skyrmions. I will demonstrate in particular that skyrmion-defect interaction profiles follow a universal shape as function of the defect's electron filling [4]. This finding can be used to design complex energy profiles with targeted device functionalities via atom-by-atom manufacturing of multi-atomic defects [5,6].

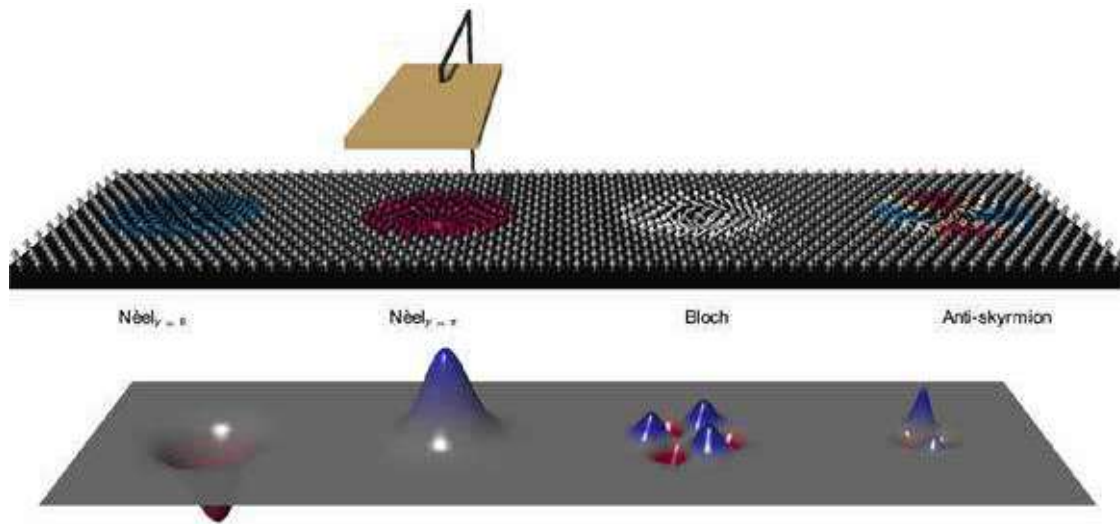


Figure: Chiral spin-mixing magnetoresistance for the detection of chiral nature of skyrmions in a memory racetrack [1].

- [1] I. L. Fernandes, S. Blügel, S. Lounis, Nat. Commun. 13, 1576 (2022)
- [2] I. L. Fernandes, M. Bouhassoune, S. Lounis, Nat. Commun. 11, 1602 (2020)
- [3] M. Bouhassoune, S. Lounis, Nanomaterials 11, 194 (2021)
- [4] I. L. Fernandes, J. Bouaziz, S. Blügel, S. Lounis, Nat. Commun. 9, 4395 (2018)
- [5] I. G. Arjana, I. L. Fernandes, J. Chico, S. Lounis, Sci. Reports 10, 14655 (2020)
- [6] I. L. Fernandes, J. Chico, S. Lounis, Journal of Phys.: Cond. Matt. 32, 425802 (2020)

Antiskyrmions, skyrmions, and mixed-topology skyrmions in crystals with S_4 symmetry

Jan Masell^{1,2}, Kosuke Karube², Licong Peng², Fehmi S. Yasin², Sebastian Schneider², Mamoun Hemmida³, Hans-Albrecht Krug Von Nidda³, István Kézsmárki³, Xiuzhen Yu², Fumitaka Kagawa^{2,4}, Yoshinori Tokura^{2,4,5} and Yasujiro Taguchi²

¹*Institute of Theoretical Solid State Physics, Karlsruhe Institute of Technology (KIT), Karlsruhe, 76049, Germany*

²*RIKEN Center for Emergent Matter Science (CEMS), Wako, 351-0198, Japan*

³*Experimental Physics V, University of Augsburg, Augsburg, 86135, Germany*

⁴*Department of Applied Physics, University of Tokyo, Tokyo, 113-8656, Japan*

⁵*Tokyo College, University of Tokyo, Tokyo, 113-8656, Japan*

Magnetic skyrmions are nowadays found in a variety of different material classes, ranging from single crystals to sputtered films. They often emerge on length scales much larger than the atomic lattice where they appear as vortex-like, rotationally symmetric whirls. Their anti-vortex-like partners, consequently dubbed anti-skyrmions, naturally break this rotational symmetry which leads to a plethora of new effects. However, only a limited number of antiskyrmion-hosting materials are known and, previously, they all belonged to the D_{2d} symmetry class, even though crystals with S_4 symmetry were predicted to also host antiskyrmions.[1]

I will present our recent works on antiskyrmions in crystals with S_4 symmetry. Combining experiments and theory, we studied antiskyrmions, skyrmions, and other textures in the S_4 -symmetric family of schreibersites $(\text{Fe,Ni})_3\text{P}$ with heavy element doping.[2,3,4,5] The competition between the dominant demagnetization energy and small Dzyaloshinskii-Moriya interaction stabilizes both antiskyrmions and skyrmions in the transition region from the stripe phase to the field-aligned ferromagnet and, moreover, renders antiskyrmions square-shaped and skyrmions elliptical.[2] In general, antiskyrmions form in thicker samples and samples with larger uniaxial anisotropy where the bulk DMI can compete with dipolar interactions. Vice versa, skyrmions form in thinner samples where they profit from the strong dipolar interaction.[3] Moreover, I will show how the ellipticity of skyrmions in these systems can be used to estimate the magnitude of the DMI[4] and that, for a broad range of material parameters, antiskyrmions are actually composite mixed-topology skyrmions, i.e., a new type of magnetic texture which is both skyrmion and antiskyrmion.[5]

[1] A. N. Bogdanov and D. A. Yablonskii, *Sov. Phys. JETP* **68**, 101-103 (1989).

[2] K. Karube, L. C. Peng, J. Masell, *et al.*, *Nat. Mater.* **20**, 335-340 (2021).

[3] K. Karube, L. C. Peng, J. Masell, *et al.*, *Adv. Mater.* 202108770 (2022).

[4] S. Schneider, J. Masell, F. S. Yasin, *et al.* (in preparation).

[5] F. S. Yasin, J. Masell, *et al.* (in preparation).

3D domain wall motion memory with artificial ferromagnet

Teruo Ono^{1,2}

¹*Institute for Chemical Research, Kyoto University, Japan*

²*Center for Spintronics Research Network, Institute for Chemical Research, Kyoto University*

Racetrack memory using domain wall (DW) motion in ferromagnetic nanowires is a potential candidate for future memory technologies [1]. However, there are still problems that hamper the commercialization. First, lowering consumption power is crucial for practical application. Second, a precise control of DW position is a problem to be solved. Smaller DW width is preferable for higher density memory. Here, we propose a new type of 3D DW motion memory with an artificial ferromagnet and study its feasibility by micromagnetic simulation.

A schematic illustration of the 3D DW motion memory proposed in this study is shown in Fig. 1. The device consists of an array of cylindrical artificial ferromagnetic wires, which is composed of periodically stacked bilayers of a bit layer with strong magnetic anisotropy (green layers) and a DW layer with no magnetic anisotropy (yellow layers). The data is written by flipping the magnetization of the bottom bit layer using the spin-orbit torque induced by the current in the word line. The written data can be shifted to the arbitrary position in the artificial magnetic wire by the appropriate current injection through the wire. By repeating the writing and shifting, an arbitrary information sequence can be stored in the magnetic wire. The data can be read out with the topmost magnetic tunnel junction while the data is being shifted by the current through the wire. Micromagnetic simulation shows that the precise DW position controllability, narrow DW width down to 3 nm, and low DW motion current down to 2×10^{10} A/m² can be achieved with feasible material parameters [2]. Furthermore, it is found that the high thermal stability and the low DW motion current can be achieved simultaneously [3].

This work was partly supported by JST, CREST (Grant Number JP MJCR21C1), Japan.

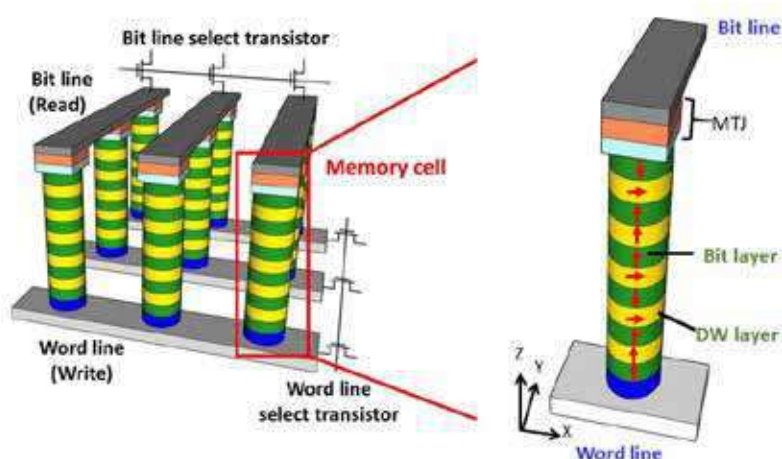


Figure 1. Schematic illustration of 3D DW motion memory.

[1] S. Parkin, M. Hayashi, and L. Thomas, *Science*, 320, 190 (2008).

[2] Y. M. Hung et al., *J. Magn. Soc. Jpn.* 45, 6 (2021).

[3] Y. M. Hung et al., *Appl. Phys. Express* 14, 023001 (2021).

Ferrimagnetic skyrmions in GdCo

Léo Berges¹, Eloi Haltz¹, Sujit Panigrahy¹, Sougata Mallick¹, Raphael Weil¹, Stanislas Rohart¹, Alexandra Mougin¹, and João Sampaio¹

¹ Université Paris-Saclay, CNRS, Laboratoire de Physique des Solides, Orsay, France

Magnetic skyrmions are point-like magnetic textures with a well-defined chirality. They can be stabilized in thin-film nanostructures and efficiently moved by current-induced spin orbit torques, which has led to the proposal of many applications [1]. However, their mobility is predicted to reduce with decreasing radius [2], a problem for the prospect of dense devices. Furthermore, skyrmions show a sideways gyrotropic deflection that is detrimental to some applications [3]. This deflection is inherent to their non-trivial topology and expected to be proportional to the material's angular momentum density (L_S). They are also sensitive to pinning, which slows their velocity, impedes their motion at low drive, interferes with their trajectory, and hinders the study of their dynamics.

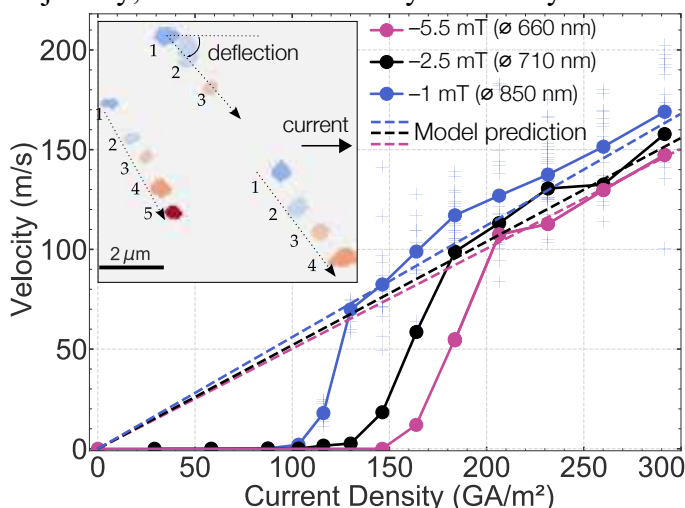


Figure 1: Skyrmion velocity versus current for three skyrmion diameters. Inset: Superposition of magneto-optical images showing 3 propagating skyrmions (10-ns pulses, 210 GA/m²).

We studied the dynamics of skyrmions in thin films of CoGd, a rare earth/transition metal (RETM) ferrimagnetic alloy, with a Pt buffer layer. The effective magnetization and L_S of RETMs can be changed and even reversed with temperature or alloy composition, which we utilized to tune the magnetic anisotropy and thus the skyrmion stability. The skyrmions were driven by current pulses and, above a threshold current density due to pinning, their velocity varied linearly with current, as expected theoretically, up to 170 m/s (Fig. 1). By varying the

skyrmion diameter with an external field, we observed the predicted reduction of mobility for smaller skyrmions, a relation we could reproduce quantitatively with an analytical model with a single fitting parameter. The observed deflection also matched the model's prediction.

To study the effect of L_S on the gyrotropic deflection, we measured a second sample with a composition chosen to produce an effective L_S of opposite sign, and we observed a gyrotropic deflection in the opposite direction to the first sample, as predicted.

The observation of these properties, in particular the linear velocity regime, was only possible due the very low pinning of this amorphous film. The reversal of the gyrotropic deflection with the sign of L_S shows that it can be tuned in RETMs and that deflectionless skyrmion should be attainable. These results confirm, however, that smaller skyrmions have lower mobility, an effect which should occur in all materials.

[1] C. H. Marrows, K. Zeissler, *Appl. Phys. Lett.* **119**, 250502 (2021)

[2] W. Jiang *et al.*, *Nat. Phys.* **13**, 162 (2017); K. Litzius *et al.*, *Nat. Phys.* **13**, 170 (2017); K. Zeissler *et al.*, *Nat. Comm.* **11**, 428 (2020)

[3] J. Sampaio *et al.*, *Nat. Nanotech.* **8**, 839 (2013)

Current-induced control of chiral magnetic textures in magnetic insulators

Saül Vélez

Universidad Autónoma de Madrid, 28049 Madrid, Spain

The use of the spin of the electrons in devices is having a tremendous impact on our electronics and computing technologies. Tell-tale examples are found in the electric switching and reading of magnetic tunnel junctions as well as in the controlled displacement of domains and domain walls in magnetic thin films. Despite the enormous progress that has been made, current devices are restricted to the use of metallic ferromagnets, which typically suffer from high losses and are limited in frequency.

Magnetic insulators (MIs), such as rare earth garnets ($R_3Fe_5O_{12}$; $R=Y, Tm, \dots$), have attracted a lot of interest because of their low Gilbert damping and high-frequency dynamics. Although being electrically insulating, MIs can couple to spin currents, making thus possible to employ these materials as active elements in electronic devices.

In this talk, we show how we can stabilize chiral domain walls and skyrmions in $Tm_3Fe_5O_{12}$ (TmIG) coupled to Pt and manipulate them by proximity electric currents (Fig. 1) [1,2]. We demonstrate the chiral nature of the domain walls and skyrmions via nitrogen-vacancy magnetometry and investigate their dynamics driven by current pulses. We find that the domain walls in TmIG exhibit mobilities comparable to those achieved with metallic ferromagnets and reveal that the dynamics of the skyrmions are governed by the ferrimagnetic order of the crystal and pinning, resulting in a large skyrmion Hall effect characterized by a negative deflection angle and hopping motion. Further, we show that the mobility of the walls and skyrmions can be modified by exchange coupling TmIG to an in-plane magnetized $Y_3Fe_5O_{12}$ (YIG) layer, which distorts the spin texture of the magnetic nanostructures leading to a directional-dependent rectification of their dynamics. This effect, which is equivalent to a magnetic ratchet, is exploited to control the flow of domain walls and skyrmions in devices.

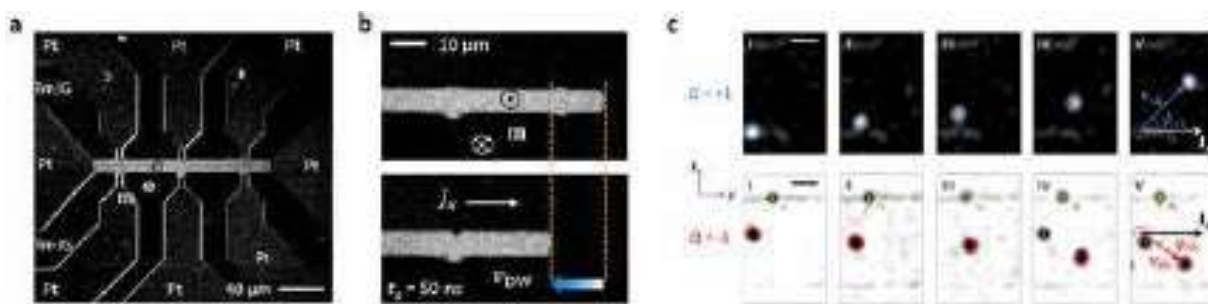


Fig. 1. **a**, Magneto-optical Kerr effect (MOKE) image of a TmIG/Pt device showing current-induced switching of TmIG (bright region). **b**, Demonstration of current-driven wall motion. A current pulse $J_x \sim 10^{12} \text{ A m}^{-2}$ in Pt drives the walls in TmIG at velocities v_{DW} of 300 m/s. **c**, MOKE images showing the displacement of skyrmions in YIG/TmIG/Pt following a sequence of current pulses. The topological charge of the skyrmions (Q), which can be controlled by the orientation of the skyrmion core (bright/dark), results in a transverse deflection of the skyrmions.

[1] S. Vélez et al., *Nat. Comm.* **10**, 4750 (2019).

[2] S. Vélez et al., *Nat. Nanotech.* (in press).

*contact mail: saul.velez@uam.es

Topological magnon band structure of emergent Landau levels in a skyrmion lattice

T. Weber¹, D. Fobes², J. Waizner³, P. Steffens¹, G. S. Tucker⁴, M. Böhm¹, L. Beddich⁵, C. Franz⁵, H. Gabold⁵, R. Bewley⁶, D. Voneshen⁶, M. Skoulatos⁵, R. Georgii⁵, G. Ehlers⁷, A. Bauer⁵, C. Pfleiderer⁵, P. Böni⁵, M. Janoschek⁸, and M. Garst⁹

¹ Institut Laue-Langevin (ILL), CS 20156, 38042 Grenoble Cedex 9, France

² Los Alamos National Laboratory (LANL), Los Alamos, NM, USA

³ University of Cologne, Cologne, Germany

⁴ European Spallation Source ERIC (ESS), P.O. Box 176, SE-221 00, Lund, Sweden

⁵ Technical University of Munich (TUM), Munich, Germany

⁶ ISIS Facility, Rutherford Appleton Laboratory (RAL), Chilton, Didcot OX11 0QX, UK

⁷ Oak Ridge National Laboratory (ORNL), Oak Ridge, TN, USA

⁸ Paul-Scherrer-Institut (PSI), Villigen, Switzerland

⁹ Karlsruhe Institute of Technology (KIT), Karlsruhe, Germany

For temperatures below 30 K and magnetic fields around 0.2 T, the itinerant magnet MnSi features a vortex-like skyrmion order [1] of the manganese electron spins. The study of the structure of magnetic skyrmions has generated much experimental and theoretical interest since its discovery over a decade ago [1]. We present the first comprehensive study of the dynamics of the skyrmion phase, which we recently completed [2].

MnSi's non-centrosymmetric space group has profound consequences for dynamics in all ordered magnetic phases. Namely, it introduces a Dzyaloshinskii-Moriya term, which causes magnon creation and annihilation to take place at two distinct energy levels. This phenomenon is restricted to reduced momentum transfers having a component perpendicular to the skyrmion plane. The dynamical magnetic structure factor becomes asymmetric ("non-reciprocal"). Such an asymmetric behaviour could so far also be observed for the field-polarised [3, 4], the paramagnetic [5], as well as the conical [6,7] phase of MnSi.

For our recently published study [2], we fully mapped out the magnetic dynamics in the skyrmion phase of MnSi. To that end, we employed polarised triple-axis, time-of-flight, and spin-echo experiments. Apart from an in-depth analysis of the non-reciprocal dynamics, we succeeded in observing a splitting of the magnon energies into closely-spaced Landau levels for reduced momentum transfers inside the skyrmion plane. Theoretically, we describe our results using a mean-field linear spin-wave model which is phenomenologically inspired by the band structure theory of electrons. A correction of the theory for instrumental resolution yields an excellent quantitative agreement between experiment and theory.

[1] S. Mühlbauer *et al.*, Science **323** (5916), pp. 915–919 (2009).

[2] T. Weber *et al.*, Science **375** (6584), pp. 1025–1030 (2022).

[3] S. V. Grigoriev *et al.*, Phys. Rev. B **92**, 220415 (2015).

[4] T.J. Sato *et al.*, Phys. Rev. B **94**, 144420 (2016).

[5] B. Roessli *et al.*, Phys. Rev. Lett. **88**, 237204 (2002).

[6] T. Weber *et al.*, Phys. Rev. B **97**, 224403 (2018).

[7] T. Weber *et al.*, Phys. Rev. B **100**, 060404(R) (2019).

Oral Presentations

| | | |
|-------------------------|--|-----|
| Amal Aldarawsheh | <i>Emergence of zero-field non-synthetic single and catenated antiferromagnetic skyrmions in thin films</i> | 447 |
| Laura Álvaro Gómez | <i>Current induced domain wall dynamics in chemical modulated nanowires</i> | 448 |
| Maria Azhar | <i>Screw dislocations in chiral magnets</i> | 449 |
| Cristina Balan | <i>Electric field control of chiral magnetic textures in multilayer films with perpendicular magnetic anisotropy</i> | 450 |
| Anne Bernard-Mantel | <i>A micromagnetic theory of skyrmion lifetime in ultrathin ferromagnetic films</i> | 451 |
| Mark De Jong | <i>Facilitating Skyrmion Nucleation in Ir/Co/Pt Multilayers With Ga⁺ Ion Irradiation</i> | 452 |
| Takaaki Dohi | <i>Diffusive motion of antiferromagnetically coupled skyrmions</i> | 453 |
| Claire Donnelly | <i>Domain wall automotion for three-dimensional magnetic interconnectivity</i> | 454 |
| JoseA. Fernandez-Roldan | <i>Current- and Oersted-field- dynamics of a Bloch Point in cylindrical Ni nanowires</i> | 455 |
| Charles-Élie Fillion | <i>Get skyrmions back on track: suppressing skyrmion Hall angle by material engineering or gate voltage</i> | 456 |
| Johanna Fischer | <i>Gate-Controlled Skyrmions in Magnetic Trilayer Tracks</i> | 457 |
| Minori Goto | <i>Stochastic dynamics of skyrmion bubble by alternating magnetic fields</i> | 458 |
| Simon Granville | <i>Magneto-ionic and electrostatic generation of non-volatile and volatile skyrmions in MgO/Mn₂CoAl/Pd thin films using ionic liquid gating</i> | 459 |
| Matthieu Grelier | <i>Non-collinear three-dimensional textures in magnetic multilayers: the emergence of skyrmionic cocoons</i> | 460 |
| Konstantin Gusliyenko | <i>3D topological charge of the Bloch point in a spherical magnetic nanoparticle</i> | 461 |
| Mara Gutzeit | <i>Nano-scale collinear multi-Q states driven by higher-order interactions</i> | 462 |
| Javier Hermosa | <i>Domain wall magnetic configuration of soft Py microstructures studied by magnetic X-ray tomography</i> | 463 |
| Mahdi Jaber | <i>Magnetic imaging of domain walls in CoNiB nanotubes for 3D spintronics</i> | 464 |
| Lisa-Marie Kern | <i>Controlled Localization of Magnetic Skyrmion Nucleation</i> | 465 |
| Christopher Klose | <i>Coherent Correlation Imaging: Resolving fluctuating states of matter</i> | 466 |
| Taro Komori | <i>Current induced domain wall motion in Mn_{4-x}Ni_xN benefited from the compensation at room temperature</i> | 467 |
| Pingzhi Li | <i>All-Optical Switchable Racetrack based on Compensated Co/Gd quadlayers</i> | 468 |
| Sougata Mallick | <i>Stabilizing skyrmions in Pt/Co/Tb multilayers with reduced magnetization</i> | 469 |
| Piotr Mazalski | <i>Magnetic domain evolution in W/Co/Pt ultrathin epitaxial layers approaching the superparamagnetic Co thickness regime</i> | 470 |

| | | |
|--------------------|---|-----|
| Daniel Metternich | <i>Direct observation of bulk-DMI-stabilized Néel-type domain walls in ferrimagnetic rare-earth transition-metal alloys</i> | 471 |
| Santiago Osorio | <i>Creation of single chiral soliton states in monoaxial helimagnets</i> | 472 |
| Van Tuong Pham | <i>Over 1 km/s Current Induced Skyrmion Motion in Synthetic Antiferromagnet without Skyrmion Hall Effect</i> | 473 |
| Klaus Raab | <i>Brownian reservoir computing realized using geometrically confined skyrmions</i> | 474 |
| Malte Römer-Stumm | <i>Statistical analysis of superdiffusion of skyrmion bubbles</i> | 475 |
| Cameron Rudderham | <i>Image-recognition-assisted characterization of metastable topological structures in chiral magnetic thin films</i> | 476 |
| Yanis Sassi | <i>Skyrmion racetrack: confinement by the edge</i> | 477 |
| Daniel Schick | <i>Phase formations in skyrmion ensembles with anisotropic interaction</i> | 478 |
| Krzysztof Sobucki | <i>Bloch hopfion spin-wave spectra in ferromagnetic medium</i> | 479 |
| Samuel Treves | <i>Observation of metastable skyrmion lattice in NdMn₂Ge₂ at room temperature</i> | 480 |
| Victor Ukleev | <i>Exchange anisotropy and a new spiral state in the insulating chiral magnet Cu₂OSeO₃</i> | 481 |
| Guru Venkat | <i>Emergent responses in magnetic ring arrays of different lattice arrangements for reservoir computing</i> | 482 |
| Iuliia Vetrova | <i>Investigation of self-nucleated skyrmion states in the ferromagnetic/nonmagnetic multilayer dot</i> | 483 |
| Markus Weißenhofer | <i>The Interplay between Skyrmions and Thermal Magnons</i> | 484 |

Emergence of zero-field non-synthetic single and catenated antiferromagnetic skyrmions in thin films

Amal Aldarawsheh^{1,2*}, Imara Lima Fernandes¹, Sascha Brinker¹, Moritz Sallermann^{1,3,4}, MuayadAbusaa⁵, Stefan Blügel¹, and Samir Lounis^{1,2*}

¹ *Peter Grünberg Institute and Institute for Advanced Simulation, Forschungszentrum Jülich and JARA, D-52425 Jülich, Germany*

² *Faculty of Physics, University of Duisburg-Essen and CENIDE, 47053 Duisburg, Germany*

³ *RWTH Aachen University, 52056 Aachen, Germany*

⁴ *Science Institute and Faculty of Physical Sciences, University of Iceland, VR-III, 107 Reykjavík, Iceland*

⁵ *Department of Physics, Arab American University, Jenin, Palestine*

*a.alдарawsheh@fz-juelich.de; s.lounis@fz-juelich.de

Antiferromagnetic (AFM) skyrmions are envisioned as ideal localized topological magnetic bits in future information technologies. In contrast to ferromagnetic (FM) skyrmions, they are immune to the skyrmion Hall effect [1, 2], might offer potential terahertz dynamics [3] while being insensitive to external magnetic fields and dipolar interactions. Although observed in synthetic AFM structures [4] and as complex meronic textures in intrinsic AFM bulk materials [5, 6], their realization in non-synthetic AFM films, of crucial importance in racetrack concepts, has been elusive. In this work [7], we unveil their presence in a row-wise AFM Cr film deposited on PdFe bilayer grown on fcc Ir(111) surface. Using first-principles, we demonstrate the emergence of single and strikingly interpenetrating catenated AFM skyrmions, which can coexist with the rich inhomogeneous exchange field, including that of FM skyrmions, hosted by PdFe. Besides the identification of an ideal platform of materials for intrinsic AFM skyrmions, we anticipate the uncovered knotted solitons to be promising building blocks in AFM spintronics.

[1] Barker and Tretiakov, *Physical Review Letters* **116**, 147203 (2016).

[2] Zhang, Zhou and Ezawa, *Scientific Reports* **6**, 1 (2016).

[3] Gomonay, Baltz, Brataas, Tserkovnyak, *Nature Physics* **14**, 213 (2018).

[4] Legrand et al., *Nature Materials* **19**, 34 (2020).

[5] Gao et al., *Nature* **586**, 37 (2020).

[6] Jani et al., *Nature* **590**, 74 (2021).

[7] Aldarawsheh et al., *ArXiv:2202.12090* (2022).

Current induced domain wall dynamics in chemical modulated nanowires

L. Álvaro Gómez^{1,2,3,4}, S. Ruiz Gómez⁵, C. Fernández González^{2,3}, M. Schöbitz^{1,4}, N. Mille⁶, D. Tiwari^{1,4}, M.W. Khaliq⁷, M. Foerster⁷, L. Aballe⁷, M.A. Niño⁷, R. Belkhou⁶, J.C Toussaint⁴, C. Thirion⁴, A. Masseboeuf¹, D. Gusakova¹, L. Pérez^{2,3}, O. Fruchart¹

¹ Univ. Grenoble Alpes, CNRS, CEA, SPINTEC, 38000, Grenoble, France

² IMDEA Nanociencia, Campus de Cantoblanco, 28049 Madrid, Spain

³ Dpto. de Física de Materiales, Universidad Complutense de Madrid, 28040 Madrid, Spain

⁴ Univ. Grenoble Alpes/CNRS, Institut Néel, 38000 Grenoble, France

⁵ Max Planck Institute for Chemical Physics of Solids, 01187 Dresden, Germany

⁶ SOLEIL Synchrotron, L'Orme des Merisiers, Saint-Aubin, 91192, Gif-sur-Yvette Cedex, France

⁷ ALBA Synchrotron Light Facility, CELLS, 08290, Barcelona, Spain

Cylindrical magnetic nanowires are an excellent system to explore different magnetization phenomena. They can host a unique type of magnetic domain wall (DW) known as the Bloch-Point-Wall (BPW) whose topology allows ultrafast DW motion [1]. Recent experimental studies evidenced for the first time BPW motion under STT with velocities above 600 m/s with stochastic pinning [2].

Here, we propose a more complex system based on Permalloy cylindrical nanowires with effective pinning sites made of local changes in composition ($\text{Fe}_{80}\text{Ni}_{20}$). Moreover, the release of heat during the electric pulse was optimized. We used several types of x-ray magnetic microscopies to access the three-dimensional magnetization textures, all based on XMCD: PEEM in shadow mode, TXM, STXM and ptychography at ALBA and SOLEIL synchrotrons.

Magnetic images revealed curling of magnetization around the wire axis at the chemical modulations and effective pinning of the DWs at their locations. Above a certain current density threshold, we observed deterministic BPW and modulation switching of the circulation driven by the Ørsted field [to be published]. We evidenced different current-induced events: transformation from BPW to TVW and viceversa, DW expulsion out of the modulation, DW coming to the modulation, and DW motion over a distance shorter or longer than the space between modulations (Fig. 1). The direction of motion was 80% of the events along STT. DW velocities obtained exceeds theoretical limits, opening new aspects to clarify. Micromagnetic simulations performed by feeLLGood code show reasonable agreement with the experiments.

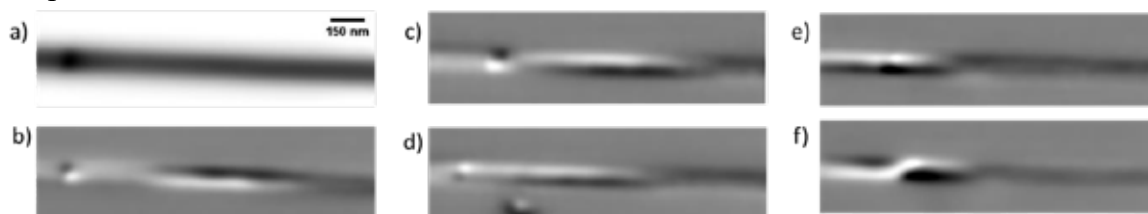


Figure 1: a) Ptychographic XAS reconstructed image at the Fe L3 edge of a 110 nm diameter permalloy nanowire with a $\text{Fe}_{80}\text{Ni}_{20}$ chemical modulation of 20 nm length. b) XMCD image of a). c) d) e) f) XMCD images show DW dynamics under consecutive 1 ns electric pulses of amplitudes (0.46, 1.18, 3.20, 3.20) $\times 10^{12}$ A/m² respectively.

[1] R. Hertel, *J. Phys. Condens. Matter* **28**, 483002 (2016).

[2] M. Schöbitz, et al., *Phys. Rev. Lett.* **123**, 217201 (2019).

Screw dislocations in chiral magnets

Maria Azhar¹, Volodymyr P. Kravchuk^{1,2} and Markus Garst^{1,3}

¹*Institut für Theoretische Festkörperphysik, Karlsruhe Institute of Technology, Karlsruhe, Germany*

²*Bogolyubov Institute for Theoretical Physics of National Academy of Sciences of Ukraine, Kyiv, Ukraine*

³*Institute for Quantum Materials and Technology, Karlsruhe Institute of Technology, Karlsruhe, Germany*

The Dyzalooshinskii-Moriya interaction stabilizes helimagnetic order in cubic chiral magnets for a large range of temperatures and applied magnetic field. In this helimagnetic phase the magnetization varies only along the helix axis, that is aligned with the applied field, giving rise to a one-dimensional periodic magnetic texture. This texture shares many similarities with generic lamellar order like cholesteric liquid crystals, for example, it possesses disclination and dislocation defects [1]. Here, we investigate both analytically and numerically screw dislocations of helimagnetic order. Whereas the far-field of these defects is universal, we find that various core structures can be realized even for the same Burgers vector of the screw dislocation. In particular, we identify screw dislocations with smooth magnetic core structures, that close to the transition to the field-polarized phase continuously connect either to vortices of the XY-order parameter or to skyrmion strings. In addition, close to zero fields we find singular core structure comprising a chain of Bloch points with alternating topological charge [2].

[1] P. Schoenherr et al. *Nature Physics* **14**, 465 (2018).

[2] M. Azhar, V. Kravchuk, and M. Garst, arxiv.org/abs/2109.04338 (accepted in PRL).

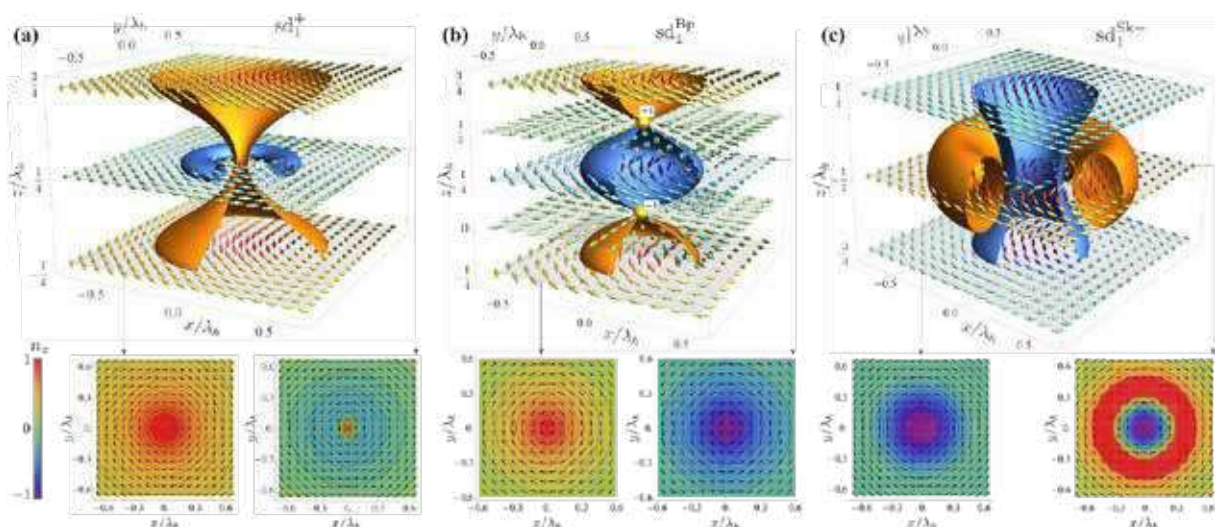


Figure. Core of various screw dislocations with strength $v = 1$ obtained by micromagnetic simulations. Orange and blue isosurfaces are respectively defined by $n_z = 1/2$ and $n_z = -1/2$ except in panel (a) where $n_z = 1/2$ and $n_z = -1/4$.

Electric field control of chiral magnetic textures in multilayer films with perpendicular magnetic anisotropy

C. Balan¹, J. Peña Garcia¹, A. Fassatoui¹, J. Vogel¹, L. Ranno¹ and S. Pizzini¹

¹ *Université Grenoble Alpes, CNRS, Institut Néel, Grenoble, France*

The manipulation of the interfacial magnetic anisotropy *via* an electric field is an active field of research, as it is a promising route toward the realisation of low-power spintronic devices. The largest effects of an electric field on the perpendicular magnetic anisotropy (PMA) have been obtained by triggering the migration of ionic species across a dielectric layer toward or away from a ferromagnet-oxide interface [1]. This magneto-ionic effect leads to a non-volatile modification of the magnetic properties, as opposed to the volatile effect obtained by electron accumulation or depletion.

We will first present the effect of the gate voltage on the magnetic anisotropy of a series of Pt/Co/MOx (M=Al, Tb) trilayers. In these trilayers, both Co interfaces contribute to the PMA and the contribution at the Co/MOx interface strongly depends on its oxidation state. The trilayers are covered with a high-k ZrO₂ or HfO₂ dielectric layer, acting as an oxygen ion conductor, and with micrometer-size Pt electrodes.

The application of a negative/positive voltage triggers the migration of oxygen ions towards/away from the Co/MOx interface, leading to a local modification of the magnetic anisotropy. The PMA can be modified locally, so that under the electrodes the magnetisation easy-axis can be changed from out-of-plane (OOP) to in-plane (IP) in a reversible and non-volatile way. Starting from a OOP saturated state, magnetic textures such as stripe domains or skyrmion bubbles can be stabilised by the gate voltage [2,3] (Figure 1(a,b)).

In a second set of experiments, we studied the effect of the gate voltage on the field-driven dynamics of chiral Néel walls in ferrimagnetic Pt/Co/Tb trilayers. We will show that a negative gate voltage leads to the partial oxidation of the Tb layer, and as a consequence to a variation of the effective magnetisation, the PMA and the interfacial Dzyaloshinskii-Moriya interaction (DMI). The variation of these magnetic parameters is at the origin of a huge variation of the domain wall (DW) velocity. For large magnetic fields, the DW speed varies from 10 m/s in the pristine state to 225 m/s after gating (Figure 1(c)).

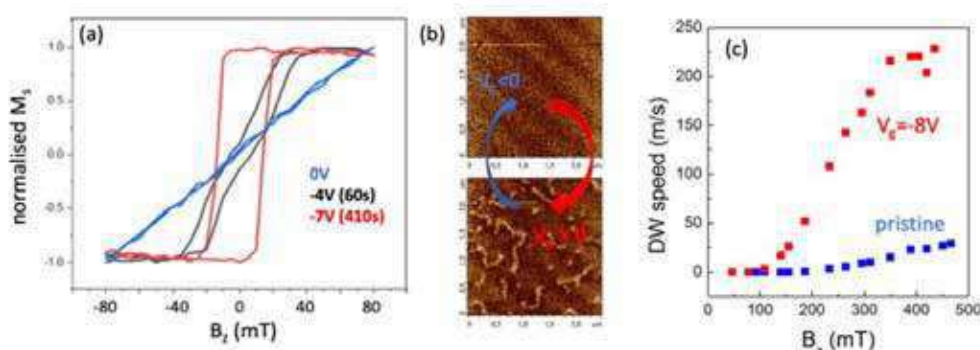


Figure 1: (a) polar Kerr hysteresis loops for Pt/Co/TbOx before and after application of negative gate voltage; (b) MFM images showing the reversible change between OOP saturated state and stripe domains plus skyrmion bubble state with gating (c) DW speeds in Pt/Co/Tb before and after gating. In both cases a ZrO₂ ionic conductor was used as dielectric layer.

[1] C. Bi et al. Phys. Rev. Lett. 113, 267202 (2014).

[2] A. Fassatoui et al. Phys. Rev. Appl. 14, 064041 (2020).

[3] A. Fassatoui *et al.* Small 210242 (2021).

A micromagnetic theory of skyrmion lifetime in ultrathin ferromagnetic films

A. Bernand-Mantel¹, C. Muratov², T. Simon³ and V. Slastikov⁴

¹*Laboratoire de Physique et Chimie des Nano-Objets, UMR 5215, INSA, CNRS, UPS, Université de Toulouse, 135 Avenue de Rangueil, 31077, Toulouse Cedex 4, France*

²*Department of Mathematical Sciences, New Jersey Institute of Technology, Newark, New Jersey, 07102, USA*

³*Institut für Analysis und Numerik, Westfälische Wilhelms-Universität Münster, Einsteinstr. 62, 48149 Münster, Germany*

⁴*School of Mathematics, University of Bristol, Bristol BS8 1TW, United Kingdom*

Magnetic skyrmions are a characteristic example of topological solitons existing at nanoscale. While the fundamental object for applications is an individual skyrmion in a homogeneous ferromagnetic environment, for topological reasons it cannot be created or annihilated by a continuous transformation from the ferromagnetic state. This transition is however enabled by the discrete nature of the condensed matter as observed experimentally. The detailed physical mechanisms of skyrmion annihilation have been investigated at the nanoscale using atomic spin simulations combined with methods of finding the minimum energy path and harmonic transition state theory. However, there are limitations to the atomistic simulations. First, they are computationally expensive, which limits the accessible skyrmion sizes (usually below 5 nm in diameter) and the physical parameter ranges that can be explored. Second, the obtained results depend on the microscopic details that are not necessarily known or controlled in the case of nanocrystalline systems. Under these circumstances, there is clearly a need for a more coarse-grained theory that would provide universal relations between the skyrmion lifetime and the material parameters. Moreover, it is reasonable to expect that under many physically relevant conditions the microscopic details do not play a dominant role for fluctuation-driven skyrmion collapse. We will present a theory of skyrmions [1] and skyrmion lifetime [2] based on the continuum field theory and derive the expressions for both the energy barrier and the attempt frequency as functions of all the material parameters [2]. Starting with the stochastic Landau-Lifshitz-Gilbert partial differential equation, we first derive several integral identities associated with the fundamental continuous symmetry groups of the exchange energy. Then, in the exchange dominated regime, we carry out a finite dimensional reduction of the stochastic skyrmion dynamics and obtain a system of stochastic ordinary differential equations for the skyrmion radius and angle. Finally, in the small thermal noise regime we use the obtained equations to calculate the Arrhenius rate, including the prefactor, by interpreting the skyrmion collapse event as “capture by an absorber” for the skyrmion radius at the atomic scale.

[1] A. Bernand-Mantel, C. Muratov and T. Simon PRB 101, 045416 (2020), ARMA 239 219 (2021)

[2] A. Bernand-Mantel, C. Muratov and V. Slastokikov, <https://arxiv.org/abs/2110.08107>

Facilitating Skyrmion Nucleation in Ir/Co/Pt Multilayers With Ga⁺ Ion Irradiation

Mark C.H. de Jong¹, Bennert H.M. Smit¹, Mariëlle Meijer¹, Juriaan Lucassen¹, Jos van Liempt¹, Henk J.M. Swagten¹, Bert Koopmans¹ & Reinoud Lavrijsen¹

¹ Department of Applied Physics, Eindhoven University of Technology, P.O. Box 513, 5600 MB Eindhoven, The Netherlands

In this contribution we investigate the local tuning of the iDMI and the perpendicular magnetic anisotropy (PMA) using Ga⁺ ion irradiation, as well as its effect on skyrmion nucleation. Ga⁺ ion irradiation affects the coordination of atoms at the interfaces (inset Fig. 1a) by increasing the degree of intermixing between heavy metal (HM) and ferromagnetic (FM) atoms, which is known to decrease both PMA and iDMI [1]. From Fig. 1b, we find that the reduction in PMA and iDMI are correlated, suggesting that both effects depend similarly on the interface quality [2]. This reduces the energy cost of domain walls but does not affect their chirality. Hence, we expect that this will also facilitate the nucleation of more complicated chiral textures, such as skyrmions.

To confirm this, we studied for the first time the current driven nucleation of skyrmions [3] in identical devices with and without Ga⁺ ion irradiation. We find that the ion irradiation indeed affects skyrmion nucleation, as shown in Fig. 2. The critical current density required for nucleation is reduced by almost 30% and the number of skyrmions is doubled by irradiation. Thus, we argue that ion irradiation can be used to facilitate and control the nucleation of skyrmions in novel devices.

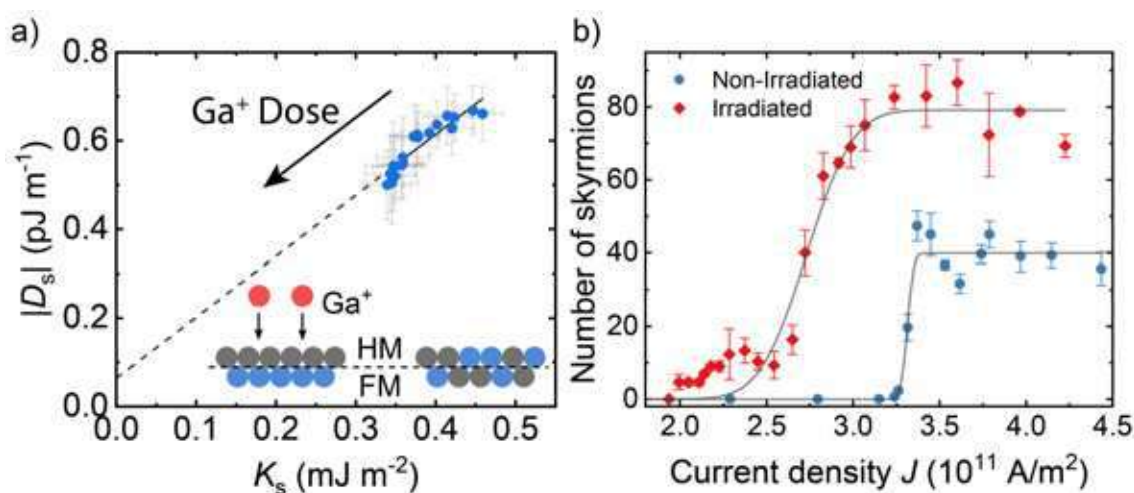


Figure 1. a) iDMI D_s plotted against the interface PMA K_s , both D_s and K_s decrease when the Ga⁺ dose is increased. The inset shows the effect of irradiation on interfaces schematically. b) Number of skyrmions nucleated in our devices after applying 10³, 50 ns long current pulses with current density J . In an irradiated device more skyrmions are nucleated and the required current density is lower.

[1] Zhao, X., Zhang, B., Vernier, N., *et al.*, *Applied Physics Letters* **115**, 122404 (2019)

[2] de Jong, M.C.H., Meijer, M.J., Lucassen, J., *et al.*, *Physical Review B* **105**, 064429 (2022)

[3] Legrand, W., Maccariello, D., Reyren, N., *et al.*, *Nano Letters* **17**, 2703-2712 (2017)

Diffusive motion of antiferromagnetically coupled skyrmions

T. Dohi¹, M. Weißenhofer², N. Kerber^{1,3}, F. Kammerbauer¹, Y. Ge¹, K. Raab¹,
J. Zázvorka⁴, M.-A. Syskaki^{1,5}, A. Shahee¹, M. Ruhwedel⁶, T. Böttcher⁶, P. Pirro⁶,
G. Jakob^{1,3}, U. Nowak², and M. Kläui^{1,3}

¹ *Institut für Physik, Johannes Gutenberg-Universität Mainz, Staudingerweg 7, 55128 Mainz, Germany*

² *Fachbereich Physik, Universität Konstanz, DE-78457 Konstanz, Germany*

³ *Graduate School of Excellence Materials Science in Mainz, Staudingerweg 9, 55128 Mainz, Germany*

⁴ *Institute of Physics, Faculty of Mathematics and Physics, Charles University, Ke Karlovu 5, Prague 12116, Czech Republic*

⁵ *Singulus Technologies AG, 63796 Kahl am Main, Germany*

⁶ *Fachbereich Physik and Landesforschungszentrum OPTIMAS, Technische Universität Kaiserslautern, Gottlieb-Daimler-Straße 46, 67663 Kaiserslautern, Germany*

Magnetic skyrmions, topologically stabilized quasi-particles, are attractive for the intriguing responses governed by their topology [1]. However, some of the topology-dependent features of magnetic skyrmions are recognized as an obstacle to device applications, e.g. the skyrmion Hall effect [2,3], which is a perpendicular motion component to the current flow direction that can lead to the annihilation of skyrmions encoding information. Likewise, theory predicts that the gyrotropic force originating from the finite topology gives rise to a drastic decrease of the diffusion coefficient [4–6]. While being advantageous for deterministic devices, this diffusion suppression is a key obstacle for unconventional devices that are actively making use of stochasticity [7].

Here we demonstrate that an amorphous-like synthetic antiferromagnetic (SyAFM) system [8] with low pinning enables us to observe thermally-activated diffusive motion of antiferromagnetically-coupled skyrmions as shown in Fig. 1. The systematic investigation varying the compensation ratio of magnetic moments in the magnetic sub-lattices with our analysis accounting for pinning effects allows for disentangling the influence of the topology on the diffusive motion. Our analysis reveals an at least 10 times larger diffusion coefficient for highly compensated antiferromagnetically-coupled skyrmions that is a direct consequence of the reduction of the effective topological charge, which enables ultimately energy-efficient unconventional computing leveraging the enhanced stochasticity in antiferromagnetic systems.

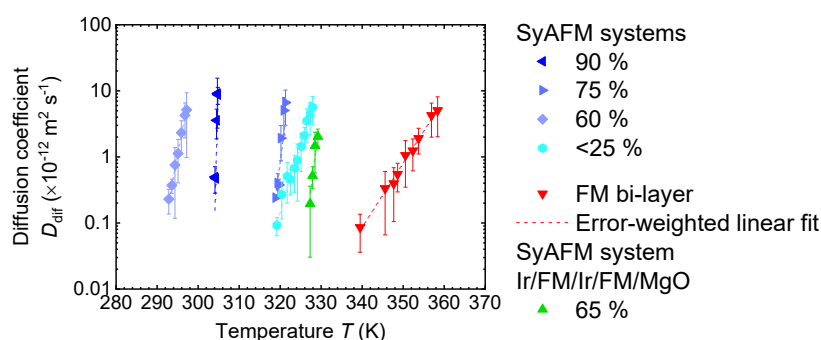


Figure 1: Temperature dependence of the diffusion coefficient for samples with various compensation ratio.

[1] N. Nagaosa and Y. Tokura, *Nat. Nanotechnol.* **8**, 899 (2013). [2] W. Jiang *et al.*, *Nat. Phys.* **13**, 162 (2017). [3] K. Litzius *et al.*, *Nat. Phys.* **13**, 170 (2017). [4] C. Schütte *et al.*, *Phys. Rev. B* **90**, 174434 (2014). [5] J. Barker and O.A. Tretiakov, *Phys. Rev. Lett.* **116**, 147203 (2016). [6] M. Weißenhofer and U. Nowak, *New J. Phys.* **22**, 103059 (2020). [7] J. Zázvorka *et al.*, *Nat. Nanotechnol.* **14**, 658 (2019). [8] T. Dohi *et al.*, *Nat. Commun.* **10**, 5153 (2019).

Domain wall automotion for three-dimensional magnetic interconnectivity

L. Skoric¹, C. Donnelly^{1,2}, A. Hierro-Rodríguez^{3,4}, M. A. Cascales-Sandoval³, S. Ruiz-Gómez^{2,5}, M. Foerster⁵, M. A. Niño Orti⁵, R. Belkhou⁶, C. Abert⁷, D. Suess⁷, and A. Fernández-Pacheco^{1,3,8}

¹Department of Physics, Cavendish Laboratory, University of Cambridge, UK

²Max Planck Institute for Chemical Physics of Solids Dresden, Germany

³SUPA, School of Physics and Astronomy, University of Glasgow, UK

⁴Depto. Física, Universidad de Oviedo, Spain

⁵ALBA Synchrotron, Spain

⁶SOLEIL Synchrotron, France

⁷Faculty of Physics & MMM Research Platform, University of Vienna, Austria

⁸Instituto de Nanociencia y Materiales de Aragón, Spain

The automotion of spin textures, where geometrical gradients are exploited to propagate localized magnetic states without the need of external stimuli, is a promising phenomenon for fast, low-power transmission of magnetic information, as previously demonstrated in planar nanowire systems [1]. Here, we show that automotion is an attractive mechanism in 3D nanowire circuits for the vertical interconnectivity of functional magnetic planes, alternative to the standard current-based spintronic effects normally employed to move spin textures.

To showcase this new approach, we have prototyped 3D spiral nanowires by a combination of 3D-printing Focused Electron Beam Induced Deposition and physical vapor deposition methods [2, 3]. The magnetic devices (**Fig. 1a**) are made of Permalloy and are 3 μm tall, 150 nm wide, presenting curvature gradients of $0.09 \mu\text{m}^{-2}$. Due to the high directionality of the physical deposition process, they have average thickness gradients of $-5.3 \text{ nm}/\mu\text{m}$; this very large thickness gradient results to be the dominating mechanism responsible for 3D domain wall automotion, as micromagnetic simulations indicate (**Fig. 1b**).

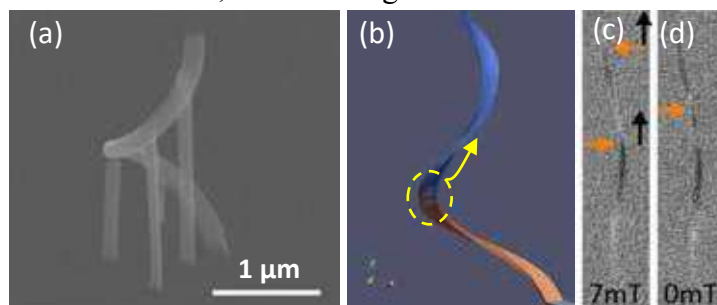


Figure 1: (a) SEM image of a 3D spiral at 45° tilt. (b) Snapshot of a micromagnetic simulation with automotion of a vortex domain wall. (c,d) “Shadow-PEEM” images of a spiral at two field values, showing the automotion of a pair of domain walls.

We have directly imaged the automotion of domain walls in the 3D spirals using “shadow” X-ray photoelectron microscopy [4]. In these experiments, we nucleate a pair of domain walls at different locations within the spirals using external magnetic fields, and directly observe the evolution of the system as the field is reduced until reaching zero value (**Fig. 1c,d**). The

experiments show the successful automotion of the walls along the 3D interconnectors, and its competition with the intrinsic pinning present in the devices at localized regions.

This work thus proposes and successfully demonstrates the automotion of spin textures as a viable effect to create 3D interconnected magnetic devices [5].

[1] K. Richter et al, Phys. Rev. Applied **5**, 024007 (2016).

[2] L. Skoric et al, Nano Lett. **20**, 184 (2020).

[3] D. Sanz-Hernández et al, ACS Nano **11**, 11066 (2017).

[4] Kimling et al, Phys. Rev. B **84**, 174406 (2011).

[5] Skoric et al, arXiv: 2110.04636.

Current- and Oersted-field- dynamics of a Bloch Point in cylindrical Ni nanowires

Jose A. Fernandez-Roldan¹, Cristina Bran², Manuel Vazquez² and Oksana Chubykalo-Fesenko²

¹ Department of physics, University of Oviedo, Oviedo, Spain.

² Instituto de Ciencia de Materiales de Madrid, ICMM-CSIC, Madrid, Spain.

As three-dimensional nanomagnetism evolves, novel non-trivial magnetic textures emerge as appealing information carriers for spintronics based on curved nanosystems and particularly Cylindrical Nanowires (NWs) [1,2]. One of the most fascinating candidates that is likely to reach the high velocities required for fast recording technologies is the Bloch Point (BP) domain wall (DW). Recently, theoretical evidence indicated that BPs in NWs could reach high velocities close to 2 km/s in the magnonic regime [2]. While the observation of the BP DW in cylindrical NWs is no longer recent [2], scarce numerical studies that combine both spin-polarized current and Oersted field have been published in NWs [4], despite first attempts to measure DW velocities are in progress [5].

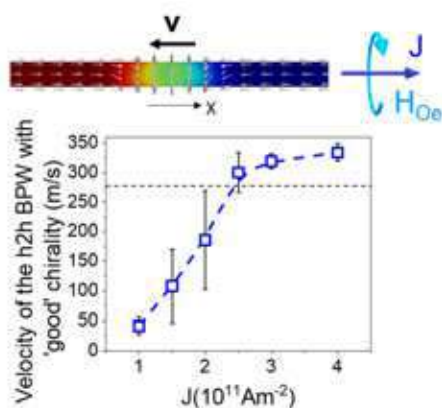


Figure 1: The mean velocity of a head-to-head Bloch Point DW driven by a spin-polarized current in a Ni nanowire as a function of the current density.

In this work we evaluate the dynamics of the BP DW under both current directions in a Ni NW with 100 nm in diameter. We investigate two cases: i) pre-nucleated BP DW, and ii) the BP DW formed from the transformation of a Vortex-Antivortex DW. Here the effects of both spin-polarized current and Oersted field are considered. We discuss in detail the role of the chirality of the BP in relation to the Oersted field, also reported previously in precursors of BPs [4].

Here we show that while the pre-nucleated DW with the same chirality as that of the Oersted field propagates always against the current direction, the BP originated either from the transformation of the BP with the opposite chirality or from the vortex-antivortex DW can either stop the propagation or propagate parallel to the current. Finally, we provide values of the velocities achieved by the BP in the NW as a function of applied current in Fig. 1.

We conclude that BPs with vanishing momentum propagate opposite to the current with velocities that may be suppressed by the Oersted field. Importantly for spintronic applications, both momentum and inertial mass play a major role in the dynamics of BPs that has not been envisaged up to know.

- [1] A. Fernandez-Pacheco et al., Three-dimensional nanomagnetism. *Nat Commun* **8**, 15756 (2017)
- [2] S. Da Col et al., Observation of Bloch-point domain walls in cylindrical magnetic nanowires, *Phys. Rev. B*, **89**, 180405 (2014).
- [3] X.-P. Ma et al., Cherenkov-type three-dimensional breakdown behavior of the Bloch-point domain wall motion in the cylindrical nanowire, *Appl. Phys. Lett.* **117**, 062402 (2020).
- [4] J.A. Fernandez-Roldan et al., Electric current and field control of vortex structures in cylindrical magnetic nanowires, *Phys. Rev. B* **102**, 024421 (2020).
- [5] M. Schöbitz et al., Fast Domain Wall Motion Governed by Topology and Oersted Fields in Cylindrical Magnetic Nanowires. *Phys. Rev. Lett.* **123**, 217201 (2019).

Get skyrmions back on track: suppressing skyrmion Hall angle by material engineering or gate voltage

Ch.-É. Fillion¹, J. Fischer¹, A. Fassatoui², L. Monnier¹, S. Pizzini², L. Ranno², R. Kumar³, S. Auffret¹, I. Joumard¹, O. Boulle¹, L. Buda-Prejbeanu¹, G. Gaudin¹, C. Baraduc¹ and H. Béa¹

¹ Univ. Grenoble Alpes, CEA, CNRS, IRIG-Spintec, Grenoble, France

² Univ. Grenoble Alpes, CNRS, Néel Institute, Grenoble, France

³ now at Antaios, Meylan, France.

In heavy-metal/ferromagnet/metal-oxide trilayers, the inversion asymmetry together with the spin-orbit coupling is at the origin of the interfacial Dzyaloshinskii-Moriya Interaction (iDMI) [1]. In thin films with perpendicular magnetic anisotropy, this additional exchange interaction, together with the dipolar interaction, stabilizes non-collinear chiral magnetic spin textures such as magnetic skyrmions [2]. The control of iDMI amplitude and sign is of great importance, since it gives a control on the domain wall (DW) internal structure and thus on the dynamics of skyrmions [3].

Here, we first report on the experimental observation of gate voltage control of skyrmion chirality in a Ta/FeCoB/TaOx trilayer [4]. This chirality inversion is made possible by tuning the oxidation state of the FeCoB/TaOx interface, via ionic migrations induced by the gate voltage. Besides, using micromagnetic simulations with Co-based parameters, we show that a fine control of the iDMI amplitude and sign allows for a continuous transformation of the nanometer size skyrmion for which chirality is inverted (Fig 1a-d) through a stable Bloch skyrmion at zero iDMI (Fig 1b). Furthermore, we show that a fine-tuning of iDMI coefficient value allows a precise control of the current-induced skyrmion motion direction, notably opening a new way to suppress the skyrmion Hall effect, otherwise detrimental for applications (blue trajectory in Fig. 1e).

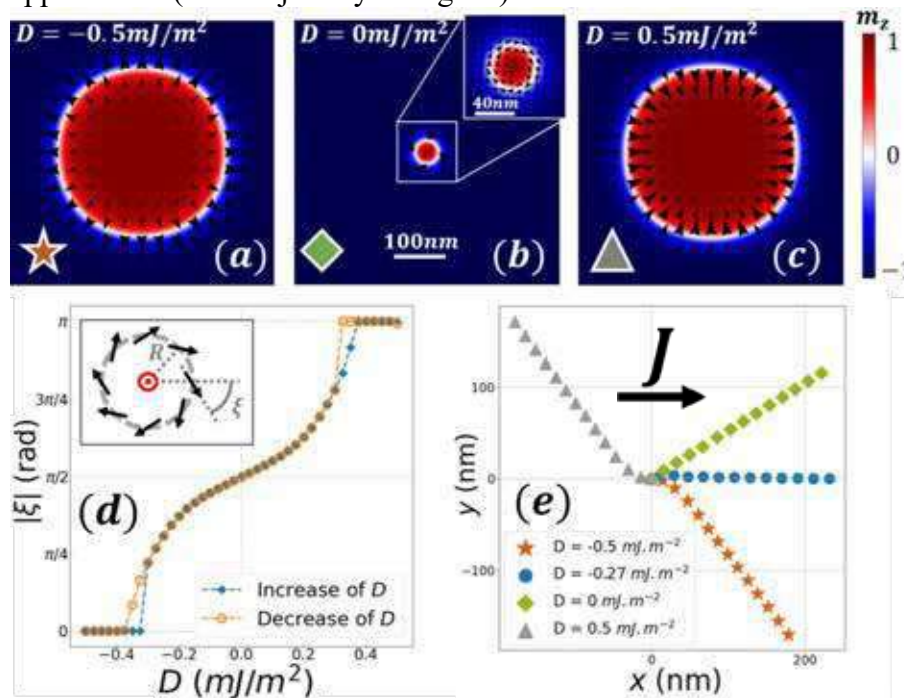


Figure 1 : Micromagnetic simulations with a fine-tuning of the iDMI value: magnetization maps of skyrmions (a-c), extraction of their helicity ξ (d) and skyrmion trajectory under current density J (e).

- [1] I. E. Dzyaloshinskii, *J. Exptl. Theoret. Phys. (U.S.S.R.)*, **46**, 960 (1964)
- [2] A. Fert, N. Reyren and V. Cros, *Nature Review Materials*, **46**, 6 (2017)
- [3] A. Thiaville, S. Rohart, and É. Jué, *EPL (Europhysics Letters)* **100**, 57002 (2012)
- [4] Ch.-É. Fillion, J. Fischer, R. Kumar, *Nature Communications*, submitted

Gate-Controlled Skyrmions in Magnetic Trilayer Tracks

Johanna Fischer¹, Charles-Élie Fillion¹, Raj Kumar¹, Aymen Fassatoui², Stefania Pizzini², Laurent Ranno², Laurent Cagnon², Stéphane Auffret¹, Isabelle Joumard¹, Olivier Boulle¹, Gilles Gaudin¹, Liliana D. Buda-Prejbeanu¹, Claire Baraduc¹, Hélène Bézard¹

¹ SPINTEC, Grenoble, France

² Institut NEEL, Grenoble, France

Structural inversion asymmetry together with spin-orbit coupling can induce interfacial Dzyaloshinskii-Moriya Interaction (iDMI) in heavy-metal/ferromagnet/metal-oxide heterostructures [1]. In such thin film systems with perpendicular magnetic anisotropy the iDMI combined with dipolar interactions can stabilize non-collinear chiral magnetic spin textures such as magnetic skyrmions [2]. The iDMI amplitude and sign determine the internal structure of the DWs and their chirality [3]. Moreover, skyrmions can be moved by a current thanks to spin orbit torques, in a direction depending on their chirality.

In this study we report on a deterministic control of the skyrmion motion related to the gate-voltage control of their chirality in Ta/FeCoB/TaOx trilayers covered by a ZrO₂ ionic conductor (Fig. 1a). Monitored under a polar-magneto-optical Kerr-effect (p-MOKE) microscope we apply a gate voltage through a transparent Indium Tin Oxide (ITO) electrode and demonstrate by real space tracking the reversal of the skyrmion current-induced motion (Fig. 1b).

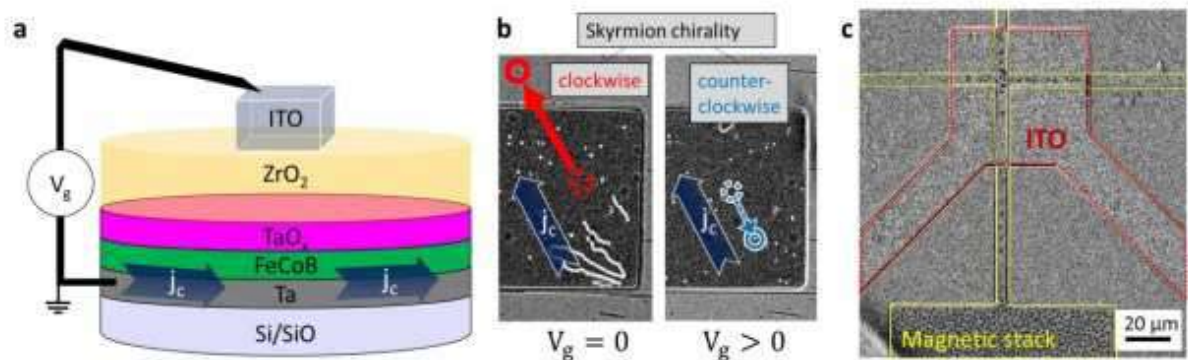


Figure 1a: Ta/FeCoB/TaOx trilayer, covered by ZrO₂ ionic conductor and transparent ITO top electrode. **b** Current-induced and gate-controlled motion of skyrmion bubbles and **c** skyrmion Hall-bar tracks (p-MOKE images).

We have furthermore optimized the fabrication of skyrmion Hall-bar tracks containing magnetic skyrmion bubbles (Fig. 1c), with deposited ITO top electrodes. These skyrmion racetracks of different shapes and sizes allow to assess the effect of gate voltage and lateral confinement on the skyrmion motion. Eventually, the gate would play the role of a pinning potential and control the skyrmion velocity. In a similar Hall-bar geometry with multiple Hallcontacts we envision to demonstrate the electrical tracking of a moving skyrmion in

[1] I. E. Dzyaloshinskii, J. Exptl. Theoret. Phys. 46, 960 (1964)

[2] A. Fert, N. Reyren and V. Cros, Nature Review Materials 46, 6 (2017)

[3] A. Thiaville, S. Rohart, É. Jué et al., EPL (Europhysics Letters) 100, 57002 (2012)

Stochastic dynamics of skyrmion bubble by alternating magnetic fields

Minori Goto^{1, 2}, Hikaru Nomura^{1, 2}, and Yoshishige Suzuki^{1, 2}

¹ Graduate School of Engineering Science, Osaka University, 1-3, Machikaneyamacho, Toyonaka, Osaka 560-8531, Japan

² Center for Spintronics Research Network (CSRN), Graduate School of Engineering Science, Osaka University, 1-3, Machikaneyamacho, Toyonaka, Osaka 560-8531, Japan

Magnetic skyrmion motion has been attracting attention in spintronics because of its rich physical phenomena and possibilities of applications. Furthermore, stochastic dynamics of skyrmion bubbles have a potential for being a Brownian computing [1-2]. To enhance the calculation speed, increase in a skyrmion diffusion coefficient is significant. One of the ways for enhancement of diffusion coefficient is applying alternating magnetic field. While a skyrmion motion under external alternating magnetic field had been investigated [3-5], effect on a diffusion coefficient has never been clarified. We demonstrate the enhancement of diffusion coefficients of skyrmion bubbles by a low frequency alternating magnetic field [6].

The sample composed of Ta(5)|Co-Fe-B(1.3)|Ta(0.24)|MgO(1.5)|SiO₂(2.9) (described in nm) was deposited on a thermally oxidized silicon substrate by a magnetron sputtering. The perpendicular dc magnetic field of 0.3 mT was applied by a permanent magnet, and the perpendicular alternating magnetic field was applied by an air core coil. By observing the Brownian motion of skyrmion bubble by a magneto-optical Kerr effect microscope, we found that both the domain length and diffusion coefficient exponentially increase by the alternating magnetic field (Fig 1). This result suggests that the domain length and diffusion coefficient are correlated. Moreover, we obtained the frequency dependence of them (Fig 2). While the diffusion coefficients vary from 6 to 40 $\mu\text{m}^2/\text{s}$, the domain length decreases by frequency. The reason of decreasing domain length is that the domain wall cannot follow the change in magnetic field for higher frequency. Here, the diffusion coefficient does not correlate to the domain length because the diffusion coefficient increases by the frequency of stretching motion of domain. This research and development work was supported by ULVAC, Inc., MIC, and JSPS Grant-in-Aid for Scientific Research (S) Grant Number JP20H05666.

[1] T. Nozaki *et al.*, Appl. Phys. Lett, **114**, 012402 (2019), [2] Y. Jibiki *et al.*, Appl. Phys. Lett, **117**, 082402 (2020), [3] K. -W. Moon *et al.*, Sci. Rep, **5**, 9166 (2015) [4] T. Schwarze *et al.*, Nat. Mater, **14**, 478 (2015) [5] D. Petit *et al.*, Appl. Phys. Lett, **106**, 022402 (2015) [6] M. Goto *et al.*, J. Magn. Magn. Mater, **536**, 167974 (2021)

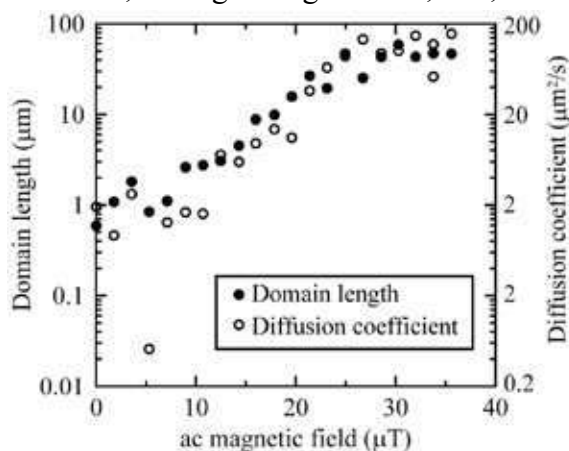


Figure 1 Alternating magnetic field dependence of domain length and diffusion coefficient at the frequency of 46 Hz.

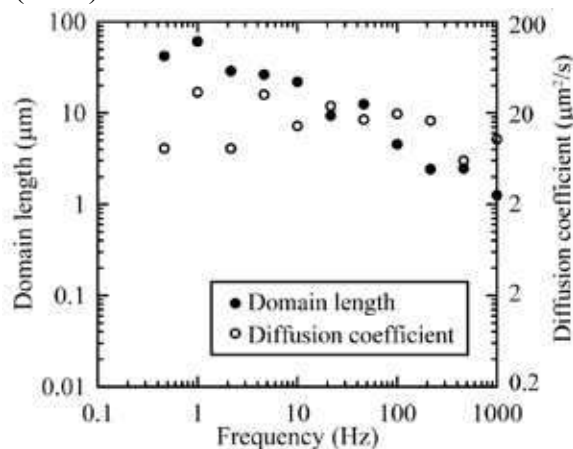


Figure 2 Frequency dependence of domain length and diffusion coefficient at the ac magnetic field of 20 μT .

Magneto-ionic and electrostatic generation of non-volatile and volatile skyrmions in MgO/Mn₂CoAl/Pd thin films using ionic liquid gating

Yao Zhang^{1,2,3}, Guy Dubuis^{1,2}, Colin Doyle⁴, Tane Butler^{1,2} and Simon Granville^{1,2}

¹ Robinson Research Institute, Victoria University of Wellington, Wellington, New Zealand

² MacDiarmid Institute for Advanced Materials and Nanotechnology, Wellington, New Zealand

³ School of Chemical and Physical Sciences, Victoria University of Wellington, Wellington, New Zealand

⁴ Department of Chemical and Materials Engineering, The University of Auckland, Private Bag 92019, Auckland 1042, New Zealand

Magnetic skyrmions are topological spin textures with great potential for spintronics applications [1]. The appearance of skyrmions requires a careful balance between the magnetic anisotropy and the Dzyaloshinskii-Moriya interaction, and being able to tune these values with a voltage is an important tool for material optimisation for skyrmion devices.

In this work we have explored generation of both volatile and non-volatile skyrmions in MgO/Mn₂CoAl/Pd thin films using different ionic liquid gating voltage sequences and magneto-optical Kerr effect (MOKE) microscopy. With a negative gate voltage of -2.5 V, we are able to generate *non-volatile* skyrmions $\sim 1 \mu\text{m}$ diameter in films with perpendicular magnetic anisotropy $K_{\text{eff}} \sim 1 \times 10^4 \text{ Jm}^{-3}$. The same result is achieved in higher K_{eff} films by ‘training’ or repeatedly cycling the gate voltage, achieving a giant voltage tunability of magnetic anisotropy of 109.8 mT V^{-1} . Interestingly, *volatile* skyrmions can also be generated, by first applying a large negative ‘trigger’ voltage, and then skyrmions appear at a *positive* gate voltage. Using X-ray photoelectron spectroscopy, we explain the generation of skyrmions in terms of magneto-ionic and electrostatic effects [2]. Our results show the potential of ionic liquid gating for achieving large anisotropy changes to reversibly or irreversibly generate skyrmions from materials with a range of starting anisotropy values.

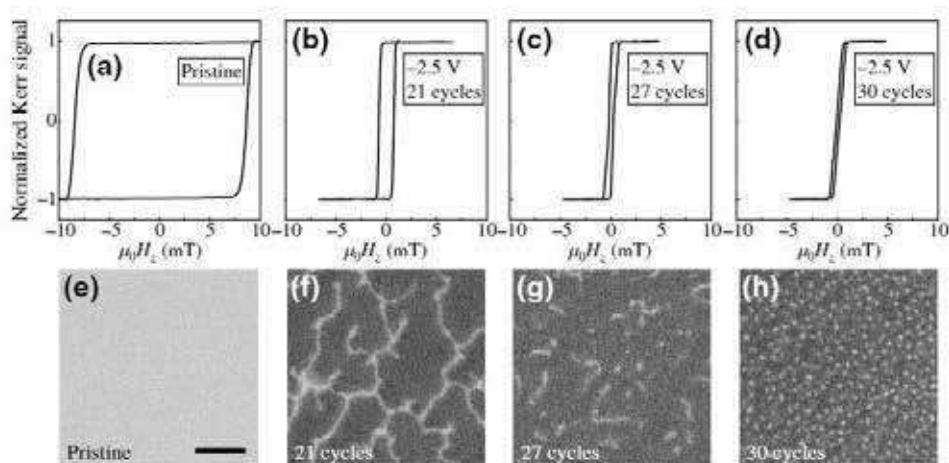


Figure 1: Effect of gate voltage cycling on MOKE loops (a. - d.) and magnetic domains (e. - h.)

[1] X. Zhang, Y. Zhou, K. M. Song, T.-E. Park, J. Xia, M. Ezawa, X. Liu, W. Zhao, G. Zhao, and S. Woo, *J. Phys. Cond. Mat.* **32**, 143001 (2020).

[2] Y. Zhang, G. Dubuis, C. Doyle, T. Butler, and S. Granville, *Phys. Rev. Appl.* **16**, 014030 (2021).

Non-collinear three-dimensional textures in magnetic multilayers: the emergence of skyrmionic cocoons

M. Grelier,¹ Y. Sassi,¹ C. Léveillé,² R. Battistelli,³ S. Collin,¹ A. Vecchiola,¹ F. Godel,¹ K. Bouzehouane,¹ A. Fert,¹ F. Büttner,^{3,4} H. Popescu,² N. Jaouen,² V. Cros,¹ N. Reyren¹

¹ Unité Mixte de Physique, CNRS, Thales, Université Paris-Saclay, 91767, Palaiseau, France.

² Synchrotron SOLEIL, L'Orme des Merisiers, Gif-sur-Yvette, 91192, France.

³ Helmholtz-Zentrum Berlin, 14109 Berlin, Germany

⁴ Institut für Physik, Universität Augsburg, 86159 Augsburg, Germany

In spintronics, magnetic multilayers continue to thrive as pivotal systems to engineer complex non-trivial spin textures thanks to the tunability of their composition and their properties. Two-dimensional magnetic solitons such as chiral domain walls or skyrmions were mostly under focus for the last decade, but recently interest has surged for more complex objects which display some variation of properties over the vertical dimension [1,2] including different skyrmion phases [3], bobbers which could become remarkable assets for the development of logic devices [4], hopfions [5]. In this work, we show how by engineering and exploring three-dimensional (3D) textures in Pt/Co based multilayers, we observe the signature of new textures, called skyrmionic cocoons. At low magnetic field, they resemble tubular skyrmions but upon an increase of the out-of-plane field, they shrink and disappear in the outer layers (Fig 1.b,c), becoming elongated ellipsoids. To observe them, we grew multilayers displaying variable thicknesses of a ferromagnetic material. By carefully tuning the thickness of each magnetic layer, it was possible to observe in a single sample, two distinct types of textures, as shown by the strong difference in the Magnetic Force Microscopy (MFM) contrasts (Fig 1.a). With the support of micromagnetic simulations (Fig 1.b), we identify them as columnar skyrmion tubes (large contrast) and skyrmionic cocoons that are only partially present over the thickness (weak contrast). This claim is furthermore supported by magneto-resistance measurements that are in remarkable agreement with the micromagnetic simulations. Finally, the field dependency of skyrmionic cocoons has also been studied with off-axis holography measurements. The existence of such textures could represent interesting possibilities for potential applications.

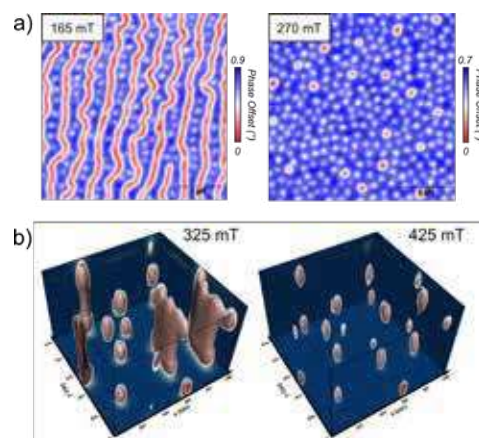


Figure 1. a) Experimental magnetic force microscopy phase maps measured at different out-of-plane magnetic field. b) Corresponding micromagnetic simulations displayed with isosurfaces: red (resp. white) correspond to $m_z = -0.8$ (resp. $m_z = 0$).

Financial supports from FLAG-ERA SographMEM (ANR-15-GRFL-0005), from ANR under the grant ANR-17-CE24-0025 (TOPSKY) and ANR-20-CE42-0012-01(MEDYNA) and as part of the "Investissements d'Avenir" program SPiCY (ANR-10-LABX-0035).

- [1] W. Legrand, et al. *Sci. Adv.* 4, eaat0415 (2018)
- [2] C. Donnelly, et al. *Nature* 547, 328 (2017)
- [3] A.O. Mandru et al. *Nature communications* 11,1 (2020)
- [4] F. Zheng et al. *Nature Nanotech.*, 13, 451 (2018)
- [5] N. Kent, et al. *Nature communications* 12, 1 (2021)

3D topological charge of the Bloch point in a spherical magnetic nanoparticle

Felipe Tejo¹, Rafael Hernández Heredero², Oksana Chubykalo-Fesenko¹, and Konstantin Y. Guslienko^{3,4}

¹ Instituto de Ciencia de Materiales de Madrid, Cantoblanco, 28049 Madrid, Spain

² Depto. Matemática Aplicada, Universidad Politécnica de Madrid, 28031 Madrid, Spain

³ Depto. Polímeros y Materiales Avanzados, Universidad del País Vasco, 20018 San Sebastián, Spain

⁴ IKERBASQUE, the Basque Foundation for Science, 48009 Bilbao, Spain

A hedgehog or Bloch point is a point-like 3D magnetization configuration in a ferromagnet. Regardless of widely spread treatment of a Bloch point as a topological defect, its 3D topological charge has never been calculated. Here, applying the concepts of the emergent magnetic field and Dirac string, we calculate the 3D topological charge (Hopf index) of a spiral Bloch point in a spherical soft magnetic particle. Using an inhomogeneous helicity of the Bloch point magnetization we showed analytically and confirmed by micromagnetic simulations that due to the magnetostatic energy contribution the Hopf index has some finite, non-integer value determined by the magnetization configuration of the Bloch point [1]. Thus, the spiral Bloch points (Figure 1) form a new class of hopfions - 3D topological magnetization configurations, whereas traditional toroidal hopfions (localized topological solitons) considered before have an integer Hopf index [2]. One of the important consequences of this approach, that can be tested experimentally, is a non-zero gyrovector of the Bloch point resulting in its non-trivial dynamics, when the direction of soliton motion is not parallel to a driving force (topological or skyrmion Hall effect).

The Bloch points constitute an essential part of the magnetization configurations of the Bloch point domain walls in nanowires. Therefore, the calculations of the Bloch point 3D topological charge and gyrovector can serve as a benchmark for consideration of the complicated Bloch point domain wall dynamics in magnetic nanowires.

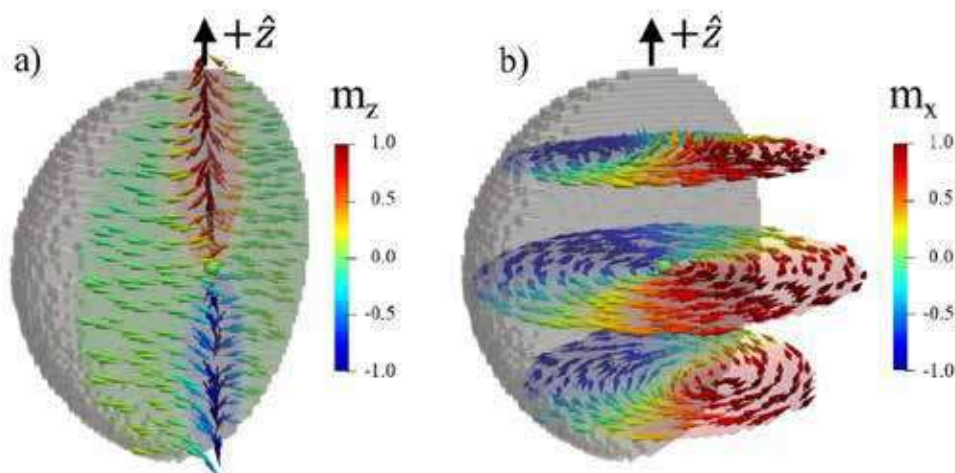


Figure 1: Simulated magnetization configuration of the spiral Bloch point in spherical nanoparticle with the radius of 50 nm [1]. m_x and m_z are the components of the reduced magnetization vector \mathbf{m} .

[1] F. Tejo et al. *Sci. Rep.* **11**, 21714 (2021).

[2] B. Göbel, B., C.A. Akosa, G. Tatara, and I. Mertig, *Phys. Rev. Res.* **2**, 013315 (2020).

Nano-scale collinear multi-Q states driven by higher-order interactions

Mara Gutzeit¹, André Kubetzka², Soumyajyoti Haldar¹, Henning Pralow¹, Roland Wiesendanger², Stefan Heinze¹, and Kirsten von Bergmann²

¹*Institute of Theoretical Physics and Astrophysics, University of Kiel, Leibnizstrasse 15, 24098 Kiel, Germany*

²*Department of Physics, University of Hamburg, 20355 Hamburg, Germany*

Multi-Q states commonly appear as complex, two-dimensional periodic magnetic states that are typically non-collinear and non-coplanar [1]. Recently, they have gained special interest in the field of exchange frustrated systems [1-3] as well as skyrmion lattices and related topological objects [4-5]. Here, using spin-polarized scanning tunneling microscopy we explore Fe/Rh bilayers on the Ir(111) surface which exhibit a variety of competing magnetic phases. Depending on the Fe stacking and number of Rh layers we observe both uniaxial and hexagonal nano-scale spin textures in zero magnetic field (see Figure 1).

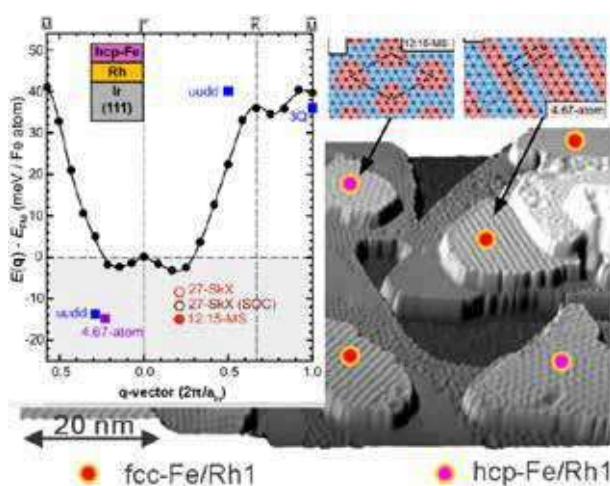


Figure 1: Overview SP-STM image of Fe/Rh/Ir(111) and energy dispersion of flat cycloidal spin spirals for hcp-Fe/Rh/Ir(111) calculated from density functional theory.

First-principles calculations combined with an atomistic spin model elucidate a competition of frustrated Heisenberg exchange and higher-order interactions as the driving mechanism for the formation of different magnetic ground states. In particular, the three-site four spin interaction [6] is found to not only stabilize uniaxial magnetic states like the *uudd* state but also spontaneous hexagonal spin textures. Unexpectedly, in these systems characterized by a weak Dzyaloshinskii-Moriya interaction they do not emerge as non-collinear skyrmion lattices, but can be specified as two-dimensionally modulated collinear multi-Q states, a new class of magnetic order.

[1] S. Hayami and Y. Motome, *J. Phys.:*

Condens. Matter **33**, 443001 (2021).

[2] A.O. Leonov and M. Mostovoy, *Nat. Commun.* **6**, 8275 (2015).

[3] C.D. Batista, S.-Z. Lin, S. Hayami and Y. Kamiya, *Reports on Progress in Physics* **79**, 084504 (2016).

[4] S. Mühlbauer *et al.*, *Science* **323**, 915-919 (2009).

[5] S. Heinze *et al.*, *Nat. Phys.* **7**, 713-718 (2011).

[6] M. Hoffmann and S. Blügel, *Phys. Rev. B* **101**, 024418 (2020).

Domain wall magnetic configuration of soft Py microstructures studied by magnetic X-ray tomography

J. Hermosa¹, A. Hierro-Rodríguez^{1,2}, M. Vélez^{1,2}, A. Sorrentino³, L. Aballe³, E. Pereiro³, J. I. Martín^{1,2}, C. Quirós^{1,2} and S. Ferrer³

¹ Universidad de Oviedo, Oviedo, Spain

² CINN, El Entrego, Spain

³ ALBA synchrotron, Cerdanyola del Vallès, Spain

Domain walls in bulk magnetic materials and thin films have been extensively studied in terms of the basic Bloch and Néel models, that can evolve into more complex configurations depending on sample geometry. The analysis of the magnetic behavior can also be performed in terms of topological singularities such as vortices, antivortices and edge half vortices in 2D magnetic nanostructures (defined by their planar winding number), skyrmions and merons in DMI and perpendicular magnetic anisotropy materials (defined by their planar skyrmion charge) or Bloch points, defined by an integer 3D topological charge.

In the last few years, the development of techniques like magnetic vector tomography [1, 2] or laminography [3] have provided the needed tools for a quantitative characterization of magnetization vector fields in thin films and nanostructures. Then, vector analysis methods can be applied to understand experimental 3D domain walls in terms of an emergent field [1] (or its equivalent: magnetic vorticity [4]) and the topological charges.

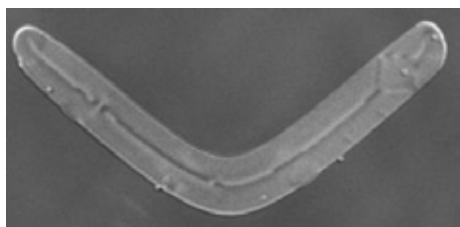


Figure 1: MTXM image of a 140 nm thick Py sample.

In this work we have studied the 3D magnetization vector field of a 140 nm thick permalloy microstructure in an arbitrary remanent state characterized by magnetic transmission soft X-ray microscopy at MISTRAL beamline in ALBA synchrotron. A central asymmetric Bloch wall extends across the sample, dividing the structure into two domains with opposite magnetization direction in a closed-flux configuration. Several Bloch points decorate this central wall, marked by contrast changes in the X-ray transmission microscopy images. Emergent field lines, calculated from the experimental magnetization vector field using vector tomography, are concentrated in high magnetic vorticity tubes (similar to those in [2]) that connect oppositely charged Bloch points and intersect the sample surface at specific magnetic textures. The interaction of emergent field tubes and domain walls will be discussed, as well as topological charge conservation rules.

Work supported by spanish AEI and FICYT.

- [1] A. Hierro-Rodríguez et al., *Nat. Comm.* **11**, 6382 (2020).
- [2] C. Donnelly et al., *Nature* **547**, 328-331 (2017).
- [3] C. Donnelly et al., *Nat. Nanotechnol.* **15**, 356–360 (2020).
- [4] C. Donnelly et al., *Nat. Comm.* **17**, 316-321 (2021).

Magnetic imaging of domain walls in CoNiB nanotubes for 3D spintronics

Mahdi Jaber¹, Martin Christoph Scheuerlein², Dhananjay Tiwari^{1,3}, Jérôme Hurst¹, Jean-Christophe Toussaint³, Wolfgang Ensinger², Olivier Fruchart¹, Daria Gusakova¹, Aurélien Masseboeuf¹

¹ Univ. Grenoble Alpes, CNRS, CEA, SPINTEC, Grenoble, France.

² Technische Universität Darmstadt, Darmstadt, Germany.

³ Univ. Grenoble Alpes, CNRS, Institut Néel, Grenoble, France.

Ferromagnetic conduits have been proposed as the basis for domain-wall (DW) based solid-state low-power-consumption memories. From the fundamental side, 3D nanomagnetism is a fast-rising topic, owing to novel topologies and curvature-induced phenomena [1]. Here we consider nanotubes, which combine curvature effects and the potential for core-shell interfaces, suitable to implement spintronic effects. We focus on the case of azimuthal curling of magnetization [2], caused by curvature-induced magneto-elastic anisotropy. This provides low stray field for applications, and should give rise to non-reciprocal spin wave propagation on the academic side [3]. Here, we present the first experimental evidence of DW inner structure in such nanotubes, using Electron Holography combined with micromagnetic modeling [4], as well as structural and chemical characterisation.

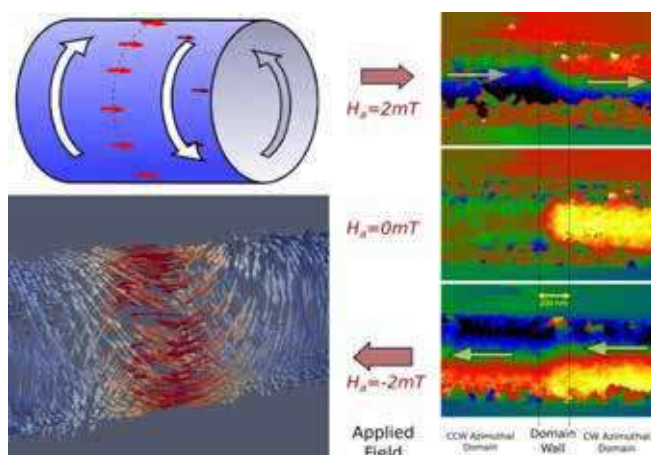


Figure 1: Left: sketch and micromagnetic view of a Néel wall between two domains with opposite azimuthal magnetization. Right: phase images of a domain wall at different applied magnetic fields H_a .

CoNiB nanotubes were fabricated by electroless plating in ion-track-etched polycarbonate templates. Diameters range from 160 to 450 nm, wall thickness from 20 to 65 nm, and several tens of μm in length. Electron holography was used to map and quantify magnetic flux during magnetic reversal associated with DW motion (Fig.1). Azimuthal domains were confirmed in the remanent state, while 30 mT applied field was required to axially magnetize the tube. Smaller fields (2-10 mT) induced DW transformations and motion, as well as the partial rotation of magnetization in the domains, along the

nanotube axis. We experimentally determined the nature and width of domain walls and confirmed our findings with micromagnetic modeling translated into phase images.

[1] Fernández-Pacheco, A. et al., Nat. Comm. 8,15756 (2017)

[2] Michal Stano et al., SciPost Phys. 5, 38 (2018)

[3] Hertel, R., J. Phys. Cond. Matter. 28, 483002 (2016)

[4] <http://feellgood.neel.cnrs.fr>

Controlled Localization of Magnetic Skyrmion Nucleation

L.-M. Kern^{1*}, V. Deinhart^{1,3,4}, K. Gerlinger¹, C. Klose¹, M. Schneider¹,
D. Engel¹, C.M. Günther², K. Höflich^{3,4}, R. Batistelli⁴, D. Metternich⁴,
F. Büttner⁴, B. Pfau¹ and S. Eisebitt^{1,5}

¹Max Born Institute, Berlin, Germany,

²Zentraleinrichtung Elektronenmikroskopie (ZELMI), Technische Universität Berlin, Germany,

³Ferdinand-Braun-Institut gGmbH, Leibniz-Institut für Höchstfrequenztechnik, Berlin, Germany,

⁴Helmholtz Zentrum für Materialien und Energie Berlin, Germany

⁵Institut für Optik und Atomare Physik, Technische Universität Berlin, Germany.

Magnetic skyrmions are quasiparticles with non-trivial topology that attract interest from fundamental and applied research communities due to their emerging topological charge, their high stability and enhanced mobility in suitable materials [1].

Great advances have been reported in generating, annihilating, and shifting skyrmions via spin-orbit torque from spin-polarized currents [2]. Optical nucleation with single laser pulses offers a possibly faster and more energy-efficient alternative to create skyrmions [3]. While the underlying mechanisms of current-induced and laser-induced nucleation are different, both methods produce randomly arranged skyrmions. However, in view of scientific purposes, i.e., for repetitive pump-probe measurement schemes, or applications in future data technology, a controllable and reproducible localization of skyrmion nucleation sites is generally required.

Here, we present that nanopatterning of the magnetic anisotropy landscape with a focused He⁺-ion beam creates well-defined skyrmion nucleation sites. We locally irradiate ferromagnetic multilayers with He⁺-ions in patterns of different shapes and sizes – without changing the topography of the material [4]. By applying a single current pulse or a single laser pulse, we show deterministic skyrmion nucleation on irradiated dot arrays while non-irradiated regions remain in saturation [5]. Moreover, we demonstrate the detachment of the skyrmion from the nucleation site and the subsequent undisturbed motion of the skyrmion by spin-orbit torque in a racetrack. [5]. Finally, we have prepared a He⁺ nanopattern to combine controlled nucleation with a guided motion of the skyrmion. We demonstrate straight motion over tens of micrometers distance back and forth in the magnetic racetrack, fully suppressing the skyrmion Hall effect [5]. Due to this level of control for skyrmion generation and motion, He⁺ nanopatterning provides a promising platform for applied and fundamental research on isolated skyrmions in multilayer materials.

References:

- [1] Fert et al., *Nature Nanotech* **8**, 152–156 (2013).
- [2] Büttner et al., *Nature Nanotech* **12**, 1040–1044 (2017).
- [3] Büttner et al., *Nat. Mater.* **20**, 30–37 (2021).
- [4] Fassbender et al., *J. Phys. D: Appl. Phys.* **37**, R179 (2004).
- [5] Kern et al., *submitted*.

Coherent Correlation Imaging: Resolving fluctuating states of matter

C. Klose¹, F. Büttner^{2,3,4}, W. Hu³, C. Mazzoli³, K. Litzius², R. Battistelli⁴, I. Lemesh², J. M. Bartell², M. Huang², C. M. Günther⁵, M. Schneider¹, A. Barbour³, S. B. Wilkins³, G. S. D. Beach², S. Eisebitt^{1,5} and B. Pfau¹

¹ Max Born Institute, 12489 Berlin, Germany

² Massachusetts Institute of Technology, Cambridge, MA 02139, USA

³ National Synchrotron Light Source II, Upton, NY 11973, USA

⁴ Helmholtz-Zentrum Berlin, 14109 Berlin, Germany

⁵ Technische Universität Berlin, 10623 Berlin, Germany

Fluctuations are ubiquitous in magnetically and charge ordered systems, spanning orders of magnitude in space and time [1,2]. Real-space access to fluctuating states is impeded by a dilemma between spatial and temporal resolution. Averaging over an extended period of time (or repetitions) is key for the majority of high-resolution imaging experiments, especially in weak contrast systems. If, by lack of better knowledge, averaging is indiscriminate, it leads to a loss of temporal resolution and to motion-blurred images.

We present coherent correlation imaging (CCI) – a high-resolution, full-field imaging technique that realizes multi-shot, time-resolved imaging of stochastic processes. The key of CCI is the classification of camera frames that correspond to the same physical state (Fig. 1a) by combining a correlation-based similarity metric with powerful classification algorithm developed for genome research [2].

We apply CCI to study previously inaccessible magnetic fluctuations in a highly degenerate magnetic stripe domain state. Our material is a Co-based chiral ferromagnetic multilayer with magnetic pinning low enough to exhibit stochastically recurring dynamics that resemble thermally-induced Barkhausen jumps near room temperature. CCI reconstructs sharp, high-contrast images of all domain states and, unlike previous approaches, also tracks the time when these states occur. The spatiotemporal imaging reveals an intrinsic transition network between the states and unprecedented details of the magnetic pinning landscape (Fig. 1b).

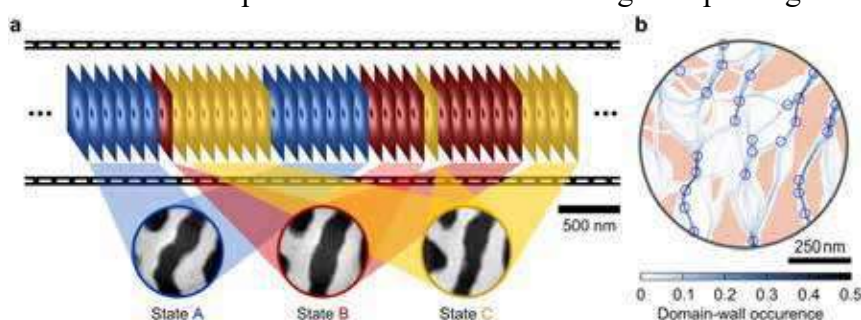


Figure 1: a, Principle of time-resolved coherent correlation imaging. Top: Sequence of camera frames showing Fourier-space coherent scattering patterns. Coherent correlation imaging classifies scattering frames by their underlying domain state, as indicated by the colors. Bottom: Real-space images reconstructed from an informed average of same-state frames. b, Map of attractive (blue dots) and repulsive (red areas) pinning sites. The background shows the position of the domain walls and their relative occurrence observed in the experiment.

[1] O. G. Shpyrko, et. al., Nature 447, 68-71 (2007)

[2] M. H. Seaberg et. al., Phys. Rev. Letters 119, 067403 (2017)

[3] G. Sherlock, et. al., Current Opinion in Immunology 12, 201-205 (2000)

Current induced domain wall motion in $\text{Mn}_{4-x}\text{Ni}_x\text{N}$ benefited from the compensation at room temperature

T. Komori^{1,2}, S. Ghosh^{1,2}, A. Hallal¹, J. P. Garcia³, T. Gushi^{1,2}, T. Hirose², H. Mitarai², H. Okuno⁴, J. Vogel³, M. Chshiev^{1,5}, J.-P. Attané¹, L. Vila¹, T. Suemasu², and S. Pizzini³

¹ Université Grenoble Alpes, CEA, CNRS, Grenoble INP, IRIG-Spintec, 38054 Grenoble, France

² Degree Programs in Pure and Applied Physics, University of Tsukuba, Tsukuba, 305-8573, Japan

³ Université Grenoble Alpes, CEA, CNRS, Institut Néel, 38042 Grenoble, France

⁴ Université Grenoble Alpes, CEA, IRIGMEM, 38000 Grenoble, France

⁵ Institut Universitaire de France, 75231 Paris, France

Current induced domain wall motion (CIDWM) has been one of the most attractive technologies because of the advantage in the application to non-volatile random memory. From the viewpoint of material engineering, compensated ferrimagnets have been the main target of the research. It was reported that ferrimagnets at compensation point showed fast and efficient CIDWM because the precession of magnetizations in DWs were suppressed. This is advantageous for both spin-transfer torque (STT) and spin-orbit torque (SOT) driven CIDWM.

Our group focuses on Mn_4N antiperovskite epitaxial films and their related nitrides as new candidates for CIDWM. We reported Mn_4N have small saturation magnetization (~ 71 kA/m) and high perpendicular magnetic anisotropy (PMA) energy (~ 0.1 MJ/m³) [1]. Both of them are suitable properties for CIDWM. Remarkable is that Mn atoms of Mn_4N can be partially replaced with other elements and we revealed the magnetic compensation of $\text{Mn}_{4-x}\text{Ni}_x\text{N}$ by Ni composition ratio. Figure 1 shows the magnetic structures of $\text{Mn}_{4-x}\text{Ni}_x\text{N}$ experimentally revealed. This is notable to discover the rare-earth free compensated ferrimagnet.

In this work, we propose CIDWM in $\text{Mn}_{4-x}\text{Ni}_x\text{N}$ purely by STTs. Figure 2 shows the DW velocity versus current density of $\text{Mn}_{4-x}\text{Ni}_x\text{N}$ with different Ni composition ratio. As x increased, the velocity became large and got the fastest value of 3,000 m/s (with a current density of $j = 1.26 \times 10^{12}$ A/m²) [3]. We like to mention that these high DW velocities were achieved only by STT without the in-plane magnetic field and comparable to the records by SOT. Note that the change in the direction of CIDWM by Ni composition corresponded with the reversal in the angular momentum below and above the compensation point.

[1] T. Gushi, L. Vila, O. Fruchart, Jpn. J. Appl. Phys. **57**, 120310 (2018).

[2] T. Komori, T. Hirose, T. Gushi, J. Appl. Phys. **127**, 043903 (2020).

[3] S. Ghosh, T. Komori, A. Hallal, Nano Lett. **21**, 2580 (2021).

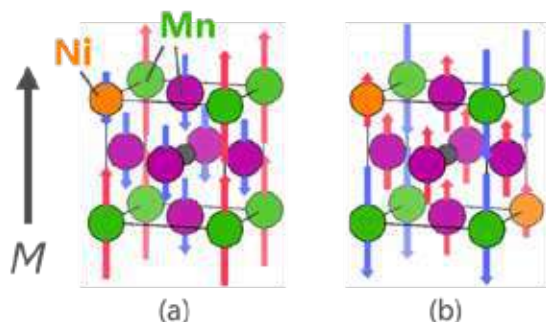


Fig. 1 Schematic images of magnetic structures of $\text{Mn}_{4-x}\text{Ni}_x\text{N}$ (a) below and (b) above the compensation.

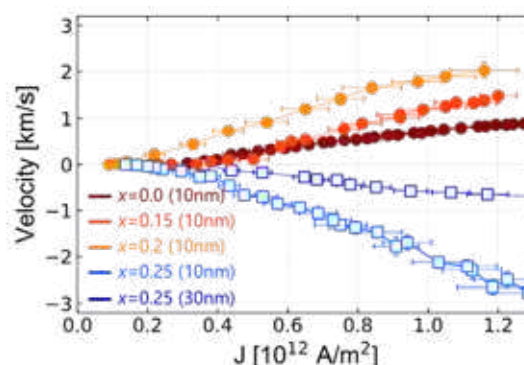


Fig. 2 DW velocity versus current density (J) of $\text{Mn}_{4-x}\text{Ni}_x\text{N}$ with different composition and thickness.

All-Optical Switchable Racetrack based on Compensated Co/Gd quadlayers

Pingzhi Li*, Thomas J. Kools, Reinoud Lavrijsen, Bert Koopmans

Department of Applied Physics, Eindhoven University of Technology, 5600 MB Eindhoven, the Netherlands

*p.li1@tue.nl

Co/Gd based synthetic ferrimagnets have received considerable attention owing to the coexistence of both ultrafast all-optical switching (AOS) [1-2] and current driven domain wall motion (CIDWM) [3-4], allowing for novel, hybrid devices connecting spintronics with integrated photonics. So far, the velocity of CIDWM of Co/Gd is low due to large net magnetic moment.

Here, we experimentally demonstrate a fully layered based synthetic ferrimagnet Co/Gd(x)/Co/Gd quadlayer systems which shows simultaneously fast CIDWM and AOS. We first show the magnetic moment can be compensated at room temperature conditions (see inset of Fig. 1), where single pulse AOS is found to be present in the full range of Gd thickness [5]. The compensation can be seen by the reverse of Kerr contrast and divergence of the coercivity at the compensation thickness. From the wedge of the same batch, we carried out current induced domain wall velocity measurement and plotted the results in Fig. 1 (b). It can be observed that the domain wall velocity spikes at the thickness close angular momentum compensation. As the current density is increased the optimum in the velocity is found to shift towards larger Gd thicknesses, we attribute this to the difference in temperature dependence of the magnetization in Co and Gd leading to a shift in the compensation thickness due to joule heating. We further conducted numerical and theoretical modelling of the domain wall motion considering the Joule heating effect, a reasonable agreement with experiment was found [5].

Our study shows a significant improvement of the room temperature domain wall velocity in synthetic ferrimagnetic systems through stack engineering paving ways for hybrid integration of racetrack memory and AOS (with integrated photonics).

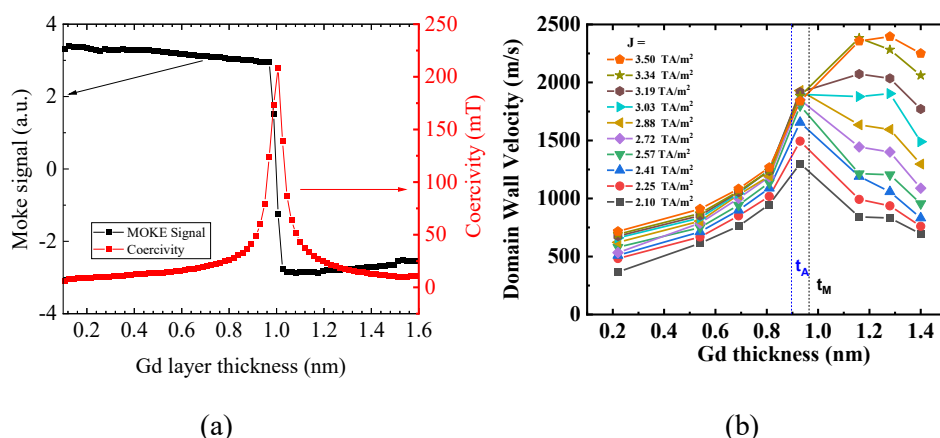


Fig. 1: Coercivity, polar MOKE signal (a) and current-driven domain wall velocity (b) as a function of Gd thickness in a Si/SiO₂(100)/Ta(4)/Pt(4)/Co(0.6)/Gd(x)/Co(0.7)/Gd(1.5)/TaN(4) multilayer system, where the numbers between brackets denote layer thicknesses in nm, and the x indicates the wedged layer given on the x-axis. The dashed vertical line in (b) indicates the Gd thickness where angular momentum compensation is achieved (see(a)).

- [1] Lalieu, M.L.M., *et al. Physical Review B* 96.22 (2017): 220411.
- [2] van Hees, Youri LW, *et al. Nature communications* 11.1 (2020): 1-7.
- [3] Caretta, L. *et al. Nature Nanotechnology* 13.12(2018): 1748-3395
- [4] Blaessing, R. *et al. Nature Communications* 9.1(2018): 2041-1732
- [5] Li *et al. In Progress* (2021).

Stabilizing skyrmions in Pt/Co/Tb multilayers with reduced magnetization

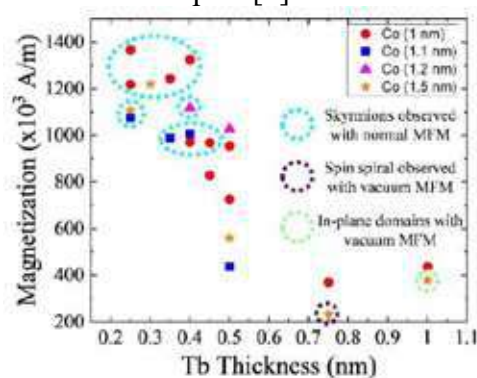
Sougata Mallick¹, Nicolas Reyren¹, Karim Bouzehouane¹, Thibaud Denneulin²,
Rafal Edward Dunin-Borkowski², Vincent Cros¹, Albert Fert¹

¹ Unité Mixte de Physique, CNRS, Thales, Université Paris-Saclay, 91197, Palaiseau, France

² Forschungszentrum Jülich, ER-C for Microscopy and Spectroscopy with Electrons, Jülich, Germany

Being at the same time, a direct signature of the topological nature of magnetic skyrmions and an issue for their implementation in renewed logic and memory devices, the so called skyrmion Hall effect (SkHE) has been the focus of many research in the last few years [1]. In this context, investigation of ferrimagnetic systems in which two sublattices with opposing spin orientations can compensate each other to achieve behaviour similar to that of an antiferromagnet, are of interest thanks to the additional flexibility of tuning the properties by varying temperature and the proportion of the constituting materials, being individually detectable, etc. CoTb alloys are known to form a ferrimagnetic phase at specific atomic concentration range of Co and Tb. However, the anisotropy in such samples is generally too high to promote the stability of any skyrmionic textures. In this study, we focus on multilayers of Pt/Co/Tb by controlling the thickness of Co, Tb, as well as the numbers of repetition to obtain a signature of antiferromagnetic coupling between the Co and Tb moments. Further, the magnetic anisotropy and the chiral exchange (DMI) is controlled in the heterostructure to stabilize the skyrmions. The final aim will be to move the skyrmions with enhanced velocity by virtue of the improved torques and reduced magnetization of the samples [2].

In Fig. 1, we show that, irrespective of the Co thickness, the net magnetization of the samples decreases significantly beyond the Tb thickness of 0.5 nm. From the cross-sectional TEM measurements (data not shown), we obtain strong intermixing between the Pt and Tb layers for multilayers grown with $t_{\text{Tb}} = 0.25$ nm, whereas there is no intermixing between the layers when $t_{\text{Tb}} \geq 0.5$ nm. We have successfully observed skyrmions using conventional MFM in heterostructures in which the Tb thickness is below 0.5 nm (data points marked with cyan circle in Fig. 1). However, due to significant reduction in the magnetization, we do not obtain any signal in conventional MFM when $t_{\text{Tb}} > 0.5$ nm. Nevertheless, we have been able to observe spin spirals (marked with purple circle in Fig. 1), and in-plane domains (marked with green circle in Fig. 1) in samples with $t_{\text{Tb}} \geq 0.5$ nm using MFM in vacuum. The drastic reduction of the multilayer's magnetization with thicker Tb layer indicates the presence of an antiferromagnetic coupling between the Co and Tb magnetic moments.



depending on the Co and Tb thicknesses.

French ANR grant TOPSKY (ANR-17-CE24-0025), DARPA TEE program grant (MIPR#HR0011831554), FLAG-ERA SographMEM (ANR-15-GRFL-0005), are acknowledged for their financial support.

[1] A. Fert *et al*, *Nat. Rev. Mat.* **2**, 17031 (2017)

[2] Z. Zheng *et al*, *Nat. Comm.* **12**, 4555 (2021)

Magnetic domain evolution in W/Co/Pt ultrathin epitaxial layers approaching the superparamagnetic Co thickness regime

P. Mazalski^{1,2}, S. Jarausch³, M. Römer-Stumm³, W. Dobrogowski¹, R. Gieniusz¹, J. McCord³, A. Wawro⁴, A. Maziewski¹

¹ Faculty of Physics, University of Białystok, Białystok, Poland

² Jerzy Haber Institute of Catalysis and Surface Chemistry, Polish Academy of Sciences, Krakow, Poland

³ Nanoscale Magnetic Materials and Magnetic Domains, Institute for Materials Science, Kiel University, Kiel, Germany

⁴ Institute of Physics, Polish Academy of Sciences, Warsaw, Poland

Magnetic structures, like chiral domain walls or skyrmions, are the foundation for future solid-state magnetic information technologies. The magnetic behavior strongly depends on magnetic properties and layer thickness, as well as structural properties. High quality low pinning W(d_W)/Co(d)/Pt(d_{Pt}) layers were deposited on sapphire substrate by molecular beam epitaxy techniques. The studies were focusing on ultrathin Co wedges (with thickness $0 < d < 2.1$ nm), which were patterned for investigations of electric current driven domain wall motion. Experiments were performed by polar magneto-optical Kerr effect (PMOKE) microscopy for imaging the magnetic domain structure (DS), for hysteresis loops registration, as well as Brillouin Light Scattering spectroscopy (BLS). The DS was studied using two registration techniques: (1) long acquisition time PMOKE imaging, applying millisecond light pulses, and (2) short down to microsecond regime laser pulses. Fast Fourier transformation procedures were used to determine the DS's geometrical parameters over the Co thickness from the micrographs.

We investigated Co thicknesses below the spin reorientation region corresponding to preferred out-of-plane magnetization. While decreasing the Co layer thickness we observed: (1) a decrease of the coercivity field H_C , (2) the transformation of the domain geometry from an irregular DS, typical for ultrathin films [1], into a stripe-DS with negligible coercivity, and (3) for further decreasing values of d a transition to the superparamagnetic (SP) state. In the d regime with negligible H_C and while decreasing d , the domain period strongly decreases, and the DS starts to become unstable and to fluctuate. The existence of Dzyaloshinskii-Moriya interaction was deduced from BLS studies. Skyrmion bubbles close to the SP regime were created with the application of perpendicular magnetic fields. The skyrmion bubble fluctuation increased, approaching the SP phase transition. Similar DS instabilities were also observed by Tolley [2] for ultrathin Pt/Co/Os/Pt-type structures. Only by using shorter exposure times (technique 2) the evolution of the DS geometry could be observed in the regime of DS fluctuations. The generation and movement of DS and skyrmion bubbles close to the SP regime were studied for different configurations applied bias field applications and current densities.

This work was supported by the Polish National Science Center and German Research Foundation under the projects 2016/23/G/ST3/04196 and DFG MC 9/19-1 (Polish-German Beethoven project) and also Polish National Science Center 2020/37/B/ST5/02299 and German Research Foundation DFG MC 9/21-1.

[1] J. Ferre, V. Grolier, P. Meyer, A. Maziewski, E. Stefanowicz, S.V. Tarasenko, V.V. Tarasenko, M. Kisielewski, D. Renard, *Phys. Rev. B* **55**, 15092 (1997)

[2] R. Tolley, S.A. Montoya, E.E. Fullerton *Phys. Rev. Mat.* **2**, 044404 (2018)

Direct observation of bulk DMI stabilized Néel type domain walls in ferrimagnetic rare-earth transition metal alloys via X-ray imaging

Daniel Metternich¹, Riccardo Battistelli¹, Chen Luo¹, Florin Radu¹, Sebastian Wintz¹, Kai Litzius², Marcel Möller³, John Gaida³, Klaus Ropers³, Manuel Valvidares⁴, Pierluigi Gargiani⁴, Andrada-O. Mandru⁵, Yaoxuan Feng⁵, Hans J. Hug⁵ and Felix Büttner¹

¹ Helmholtz-Zentrum Berlin für Materialien und Energie, Hahn-Meitner-Platz 1, Berlin, Germany

² Max Planck Institute for Intelligent Systems, Heisenbergstr. 3, 70569 Stuttgart, Germany

³ Georg-August-Universität Göttingen, Friedrich-Hund-Platz 1, 37077 Göttingen, Germany

⁴ ALBA Synchrotron, Carrer de la Llum 2-26, 08290 Cerdanyola del Vallès, Barcelona, Spain

⁵ Empa, Ueberlandstrasse 129, 8600, Dübendorf, Zürich, Switzerland

Since the discovery of bulk DMI within rare-earth transition-metal alloys [1], the possibility to create bulk DMI stabilized skyrmions within these materials is an enticing prospect for potential spintronics applications. Due to their ferrimagnetic nature, such alloys can potentially be operated at the compensation temperature, thus eliminating stray fields and allowing for skyrmion Hall effect free movement. However, so far, no direct observation of the bulk DMI induced chirality in single material layer has been reported.

We present our study on 50-nm-thick DyCo films, which we imaged with scanning transmission X-ray microscopy. Upon reconstructing the spin structure inside the domain walls, we observe strong local variations of the chirality, as well as connected regions of pure Néel type domain walls (compare Fig 1a). Due to the large film thickness, we attribute the

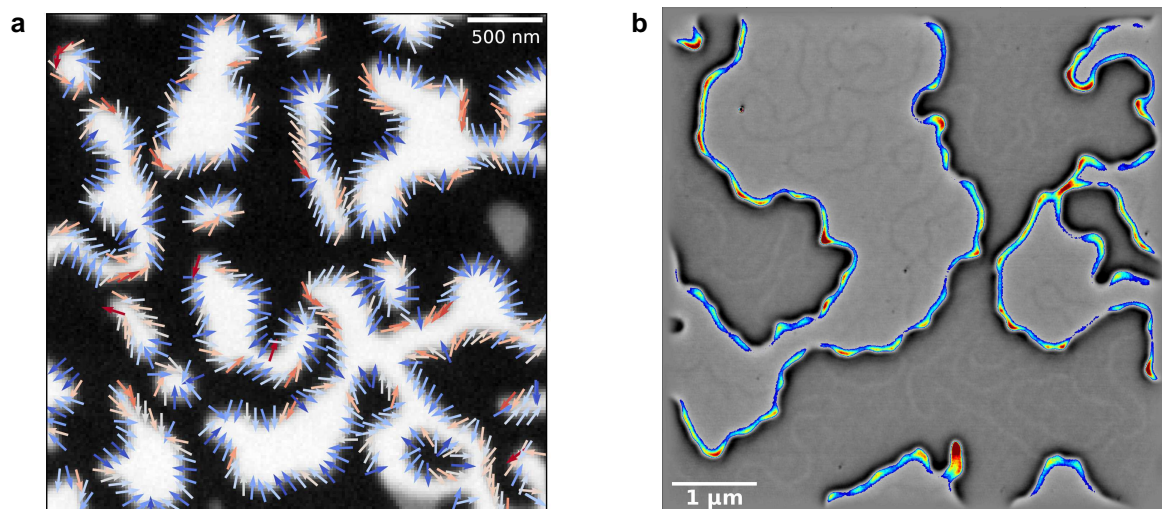


Figure 1: (a) Reconstructed in-plane orientation of the magnetic moments inside the domain walls of the as-grown magnetic state. (b) MFM-image of a demagnetized state of the same sample. The colors indicate the signal strength of the domain walls, revealing strong local variations. Also notice the additional contrast on top of the magnetic domains, potentially indicating areas of varying material composition.

formation of such Néel walls to the presence of significant bulk DMI in our sample and the strong variations to a laterally fluctuating material composition within the magnetic layer. Complementary measurements with Lorentz transmission electron microscopy and magnetic force microscopy (MFM) support our observations of strong domain wall chirality variations, while also revealing a superimposed weaker structure of meandering stray field sources (Fig. 1b) which we interpret as indications of compositional phase separation.

[1] D.-H. Kim et al., *Nat. Mater.* **18**, 685–690 (2019).

Creation of single chiral soliton states in monoaxial helimagnets

Santiago A. Osorio¹, Victor Laliena², Javier Campo³ and Sebastian Bustingorry¹

¹*Instituto de Nanociencia y Nanotecnología, CNEA-CONICET, Centro Atómico Bariloche, (R8402AGP) S. C. de Bariloche, Río Negro, Argentina*

²*Department of Applied Mathematics, University of Zaragoza, C/María de Luna, 3, 50018 Zaragoza, Spain*

³*Aragon Nanoscience and Materials Institute (CSIC-University of Zaragoza) and Condensed Matter Physics Department, University of Zaragoza, C/Pedro Cerbuna 12, 50009 Zaragoza, Spain*

In monoaxial chiral helimagnets the Dzyaloshinskii-Moriya interaction favors inhomogeneous distributions of the magnetization with chiral modulations termed chiral solitons. These localized magnetization textures crystallize at low magnetic field leading to the emergence of a chiral soliton lattice [1]. In a magnetic field perpendicular to the chiral axis the system undergoes a phase transition to the uniform state at a critical field B_c [2].

Above this critical field value, a single chiral soliton comprises the lowest level excitation over the stable uniform state, surviving as a metastable configuration [3].

We study theoretically, using micromagnetic simulations, the metastability of a single chiral soliton and propose a strategy to obtain such a state from the chiral soliton lattice [4]. We show that using spin-polarized currents chiral solitons in the chiral soliton lattice can be pushed against each other and it is possible to destroy the solitons one-by-one in a controlled way. A state with one chiral soliton can be obtained by these means for a suitable choice of the external field and the current density (Fig. 1). An important feature of our proposal is that it exhibits a strong robustness against the magnetization distribution in the initial state, even

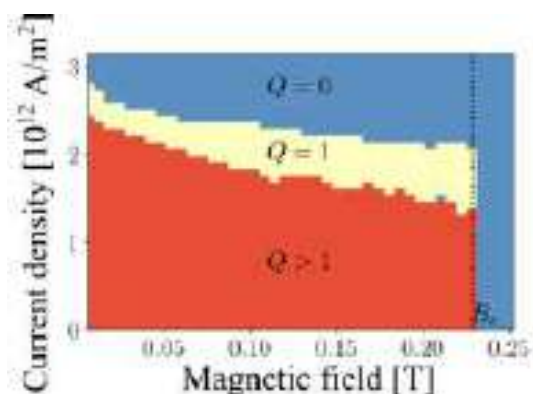


Figure 1: Phase diagram in the “Current density-Magnetic field” space, indicating the final number of chiral solitons Q after applying a pulse of current. In the yellow region a metastable single chiral soliton is obtained ($Q = 1$).

if the initial state is metastable. Our proposal could be relevant in the study of metastable solitons from both the experimental and technological applications.

[1] Y. Togawa, Y. Kousaka, K. Inoue and J. Kishine, *J. Phys. Soc. Jpn.* **85**, 112001 (2016).

[2] V. Laliena *et al*, *Phys. Rev. B* **93**, 134424 (2016).

[3] V. Laliena, S. Bustingorry, and J. Campo, *Sci. Rep.* **10**, 20430 (2020).

[4] S. A. Osorio, V. Laliena, J. Campo and S. Bustingorry, *Appl. Phys. Lett.* **119**, 222405 (2021).

Over 1 km/s Current Induced Skyrmion Motion in Synthetic Antiferromagnet without Skyrmion Hall Effect

Van Tuong Pham¹, Joseba Urrestarazu Larranaga¹, Naveen Sisodia¹, Kaushik Bairagi¹, Stefania Pizzini², Jan Vogel², Gilles Gaudin¹ and Olivier Boulle¹

¹ Université Grenoble Alpes, CEA, CNRS, Grenoble INP, IRIG-SPINTEC, 38054 Grenoble, France

² Université Grenoble Alpes, CNRS, Institut Néel, 38042 Grenoble, France

Skyrmions are topological spin textures which hold great promise as nanoscale bit of information in memory and logic devices [1, 2]. The recent demonstration of room temperature skyrmions [2] as well as their current induced motion in industry compatible sputtered thin films have lifted an important bottleneck toward the realization of skyrmion based devices. [3] However, their development was impeded so far by a too low current induced velocity (about 100 m/s) as well as the skyrmion Hall effect, namely a motion transverse to the current direction due to their topological charge, which can lead to their annihilation in tracks. Antiferromagnetic (AF) skyrmions allow these limitations to be lifted owing to their vanishing magnetization and net zero topological charge, promising fast dynamics without skyrmion Hall effect [5]. In this presentation, we will address the current induced dynamics of AF skyrmion in synthetic antiferromagnets (SAF). Using magnetic force microscopy, we show that skyrmions can be stabilized in Pt/Co/Ru based SAF at room temperature. We show that SAF skyrmions with cancelled net topological charges can be moved by current at velocity over 1 km/s at the current density of $8 \times 10^{11} \text{ J.m}^{-2}$ without skyrmion Hall effect. The dependence of the skyrmion velocity on the applied current is well reproduced by analytical models and micromagnetic simulations using experimental magnetic and transport parameters, including spin-orbit torque efficiency and the magnetic damping. Our results open an important path toward the realization of logic and memory devices based on the fast manipulation of AF skyrmions in tracks.

References

- [1] A. Fert, N. Reyren and V. Cros, *Nat Rev Mater* **2**, 17031 (2017).
- [2] A. Fert, V. Cros, and J. Sampaio, *Nat. Nanotechnol.* **8**, 152 (2013).
- [3] O. Boulle *et al.*, *Nat. Nanotechnol.* **11**, 449 (2016).
- [4] Roméo Juge *et al.*, *Phys. Rev. Appl.* **12**, 044007 (2019).
- [5] Roméo Juge *et al.*, *arXiv:2111.11878 [cond-mat]* (2021).

Brownian reservoir computing realized using geometrically confined skyrmions

Klaus Raab¹, Maarten A. Brems¹, Grischa Beneke¹, Takaaki Dohi¹, Jan Rothörl¹, Johan H. Mentink², Mathias Kläui^{1,3}

¹ *Institut für Physik, Johannes Gutenberg-Universität Mainz, Staudingerweg 7, 55128 Mainz, Germany*

² *Radboud University, Institute for Molecules and Materials, Heyendaalseweg 135, 6525 AJ Nijmegen, The Netherlands*

³ *Graduate School of Excellence Materials Science in Mainz, Staudingerweg 9, 55128 Mainz, Germany*

Reservoir computing (RC) [1,2] has been considered one of the key computational principles beyond von-Neumann computing, for which magnetic systems can provide a suitable platform based on the intrinsic non-linearity, dynamics on a wide range of timescales and easy integration with non-volatile magnetic memory. Magnetic skyrmions, topological particle-like spin textures in magnetic thin films are particularly interesting in this respect, since the magnetic textures in which they are embedded respond strongly non-linearly to external stimuli. However, while several theoretical proposals exist for skyrmion reservoir computing, experimental realizations are missing so far.

We demonstrate experimentally a conceptionally new approach for reservoir computing, that leverages the thermally activated diffusive motion of skyrmions [3] in a confined geometry [4]. By confining the gated and thermal skyrmion motion, we show that already a single skyrmion in a confined geometry suffices to realize all Boolean logic gate operations including the non-linearly separable XOR operation that cannot be realized using a conventional single layer perceptron. An effective potential well created by the confinement allows for a natural reset mechanism, which does not rely on pinning effects, but is instead enabled by the thermal fluctuations of the skyrmions. We demonstrate that the training costs are low and our ultra-low power operation with current densities orders of magnitude smaller than those used in existing spintronic reservoir computing demonstrations is enabled by thermally activated Brownian motion dynamics. Our proposed concept can be easily extended by linking multiple confined geometries and/or by including more skyrmions in the reservoir, suggesting high potential for scalable and low-energy reservoir computing.

[1] Romera, M. *et al.* Vowel recognition with four coupled spin-torque nano-oscillators. *Nature* **563**, 230–234 (2018).

[2] Pinna, D *et al.* Reservoir Computing with Random Skyrmion Textures. *Phys. Rev. Appl.* **14**, 054020 (2020).

[3] Zázvorka, J. *et al.* Thermal skyrmion diffusion used in a reshuffler device. *Nat. Nanotechnol.* **14**, 658–661 (2019).

[4] Song, C. *et al.* Commensurability between Element Symmetry and the Number of Skyrmions Governing Skyrmion Diffusion in Confined Geometries. *Adv. Funct. Mater.* **31**, 2010739 (2021).

Statistical analysis of superdiffusion of skyrmion bubbles

M. Römer-Stumm¹, H. L. Heyen², C. Denker², J. Walowski², Y. Junk²,
P. Mazalski³, I. Sveklo³, U. Guzowska³, R. Gieniusz³, A. Maziewski³, J. McCord¹
and M. Münzenberg²

¹ Institute for Materials Science, Kiel University, Kaiserstr. 2, 24143 Kiel, Germany

² Institute of Physics, University of Greifswald, Felix-Hausdorff-Str. 6, 17489 Greifswald, Germany

³ Faculty of Physics, University of Białystok, 1L Konstantego Ciołkowskiego Str., 15-245 Białystok, Poland

Skyrmions and skyrmion bubbles (SB) have attracted great interest due to their potential applications in spintronic and racetrack memory devices [1]. A common device design comprises a heavy metal - ferromagnet (FM) interface giving rise to the Dzyaloshinskii-Moriya interaction (DMI), which favors a canting of neighboring spins and stabilizes SB [1]. Under application of electric currents, motion of SBs can be observed with the skyrmion Hall angle (SHA) between the direction of current and motion. However, pinning sites may interact with the SBs and cause a change in the skyrmion hall angle. This can impede SB movement, leading to a nonlinear motion.

In this study a statistical evaluation of SB movement in Ta/CoFeB/MgO stacks with varying CoFeB thickness has been carried out by magneto-optical imaging containing several hundreds of SBs. The wedge in the FM leads to a spatial variation of the effective anisotropy ranging from in-plane to out-of-plane in orientation, which allows a simultaneous measurement at different anisotropies on a single sample. Magneto-optical magnetometry and Brillouin Light Scattering experiments were conducted to determine the magnitude of anisotropy and DMI. Current paths were etched and subsequently electrically contacted to perform pump-probe experiments with electric pulses (20 ns to 500 ns in width) with current densities in the range of 10^{12} - 10^{13} A/m². Small out-of-plane magnetic bias fields of a few mT in amplitude were applied during the experiments.

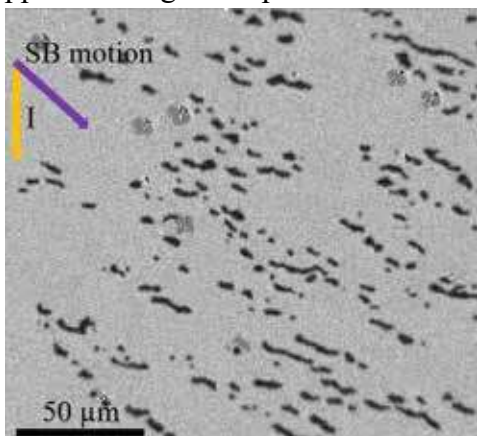


Figure 1: SBs and stripe-like domains after several electrical pulses showing the SHA

We found that the mean square displacement of the SBs vs. number of applied electrical pulses scales with an exponent between one and two, which corresponds to a superdiffusive behavior. The findings indicate a strong influence of pinning potentials on the individual SBs. A large SHA of around 45° (figure 1) is observable when a large number of SBs is analyzed. Furthermore, we correlate the characteristics of the applied pulses and the bias field with properties like the SHA, the rates of nucleation and annihilation, and the velocity of the SB.

This project was funded by the German Research Foundation (DFG) through the Priority Program SPP 2137 (DFG MC9/19-1, DFB MU1780/12-1) and through the Polish-German Research Project Beethoven NCN 2016/23/G/ST3/04196, (DFG MC9/21-1).

[1] A. Fert, V. Cros, and J. Sampaio, *Nature Nanotechnology* **8**, 152-156 (2013)

Image-recognition-assisted characterization of metastable topological structures in chiral magnetic thin films

Cameron D. Rudderham¹, Andrey Zelenskiy¹, Martin L. Plumer^{1,2}, and Theodore L. Monchesky¹

¹*Department of Physics and Atmospheric Science, Dalhousie University, Halifax, Nova Scotia, Canada B3H 3J5*

²*Department of Physics and Physical Oceanography, Memorial University of Newfoundland, St. John's, Newfoundland, Canada A1B 3X7*

We perform micromagnetic simulations wherein randomly magnetized thin-film samples of B20 compounds are allowed to relax in a uniform in-plane external magnetic field. The resulting magnetic textures contain a large number of localized topological states, as shown in Figure 1. Using numerical analysis techniques based on image recognition, we are able to extract detailed statistical information about the shape, size, and locations of these structures, and to explore how the corresponding distributions depend on the usual control parameters - namely the sample film thickness d and the reduced magnetic field strength h . Our approach allows us to quantify the nucleation probabilities of the various different skyrmion species that arise as a result of surface interactions, and to extract descriptions of the ordering of these localized states. The ordering we observe displays a striking similarity to the results of classical circle-packing problems. This work represents a novel approach for exploring the properties of the various metastable magnetic structures supported by chiral magnetic thin films.

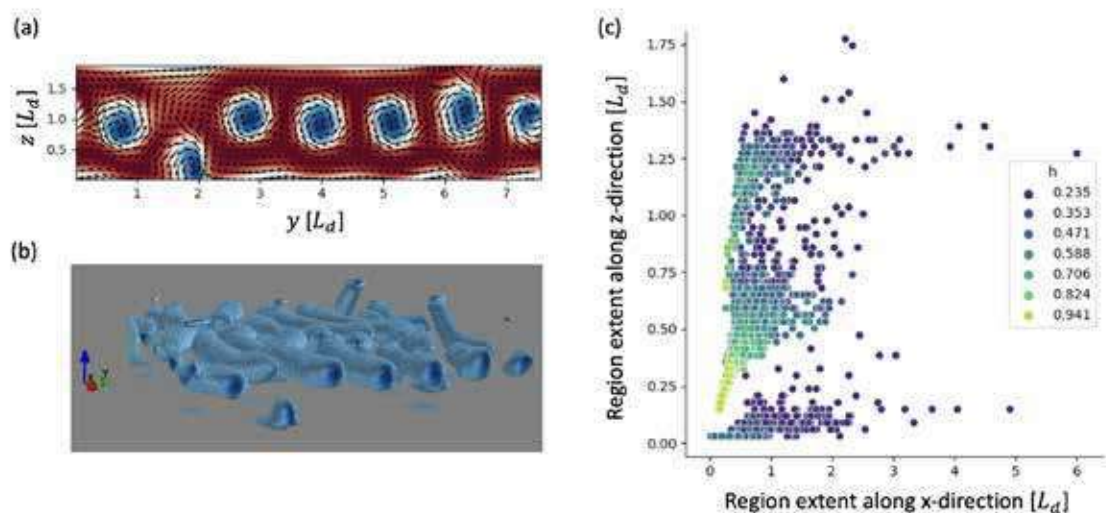


Figure 1: FIG. 1. (a) Representative cross-section of a texture obtained after relaxing a randomly magnetized thin-film ($d = 26.3$ nm) in an in-plane magnetic field ($h = 0.588$). (b) 3D representation of the aforementioned magnetic texture. Only the regions within which the normalized magnetization vectors satisfy $m_x < -0.50$ are rendered. (c) Distribution of sizes for all such regions detected across all simulations (each with different initial magnetizations and/or applied field strengths).

Skyrmion racetrack: confinement by the edge

Yanis Sassi¹, Dédalo Sanz-Hernández¹, Sachin Krishnia¹, Sophie Collin¹,
Karim Bouzehouane¹, Albert Fert¹, Vincent Cros¹, Nicolas Reyren¹

¹ *Unité Mixte de Physique, CNRS, Thales, Université Paris-Saclay, 91197, Palaiseau, France*

Magnetic skyrmions are localized spin textures in thin magnetic multilayers, which behave as particles and are topologically different from the uniform magnetization state. They have been identified as extremely promising for future applications (racetrack memory, neuromorphic computing, etc.), as well as of fundamental interest [1]. Numerous efforts have been made to control and improve their current-induced motion by utilizing spin-orbit torques (SOT) [2]. However, the skyrmion racetrack remain a challenge due to pinning and edge effect.

In this study, we present coherent SOT-induced motion of skyrmions (Fig.1a) at room temperature measured using MOKE microscopy in different geometries. We will discuss the impact of the device's shape regarding the nucleation but also regarding the behavior of the skyrmions, especially at the edges, where we report a cancellation of the skyrmion Hall angle with a straight motion, as predicted [3], and as shown in Fig.1b-f. We will also underline their strong resilience to potential defects along the edges.

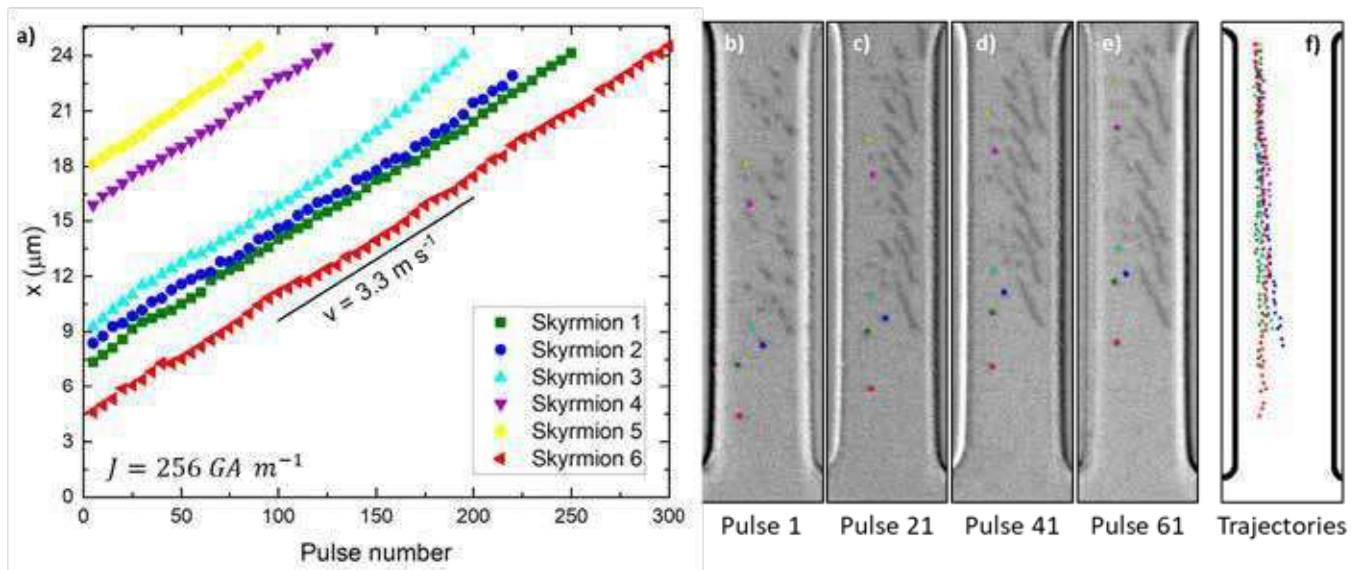


Figure 1: a) Skyrmions position as function of the time underlining a coherent motion. b-e) MOKE images of different skyrmions after respectively 1, 21, 41 and 61 pulses of 20 ns at $J = 256 \text{ GA m}^{-1}$ f) Skyrmions trajectories after 300 pulses.

French ANR grant TOPSKY (ANR-17-CE24-0025), DARPA TEE program grant (MIPR#HR0011831554) and EU grant SKYTOP (H2020 FET Proactive 824123) are acknowledged for their financial support.

- [1] A. Fert, N. Reyren, V. Cros, *Nat. Rev. Mat.* 2 (2017), 17031.
- [2] K. Litzius et al, *Nat. Phys.* 13 (2017), 170 ; S. Woo et al, *Nat. Comm.* 8 (2017), 15573.
- [3] J. Sampaio et al, *Nat. Nanotech* 8 (2013), 839-844

Phase formations in skyrmion ensembles with anisotropic interaction

Daniel Schick¹, Markus Weißenhofer¹, Levente Rózsa¹ and Ulrich Nowak¹

¹*Fachbereich Physik, Universität Konstanz, Universitätsstraße 10, Konstanz, Germany*

Crystals in two dimensions have thoroughly been studied, with one important result being the KTHNY theory [1], which describes their melting and connects them to the concept of topological defects. Skyrmions are magnetic spin structures, characterized by their non-trivial topology, which can be used to study 2-dimensional systems where the size and shape of individual particles is easily controlled via external magnetic fields. We use computer simulations to solve the Thiele equation, taking into account skyrmion-skyrmion interactions. Consequently, we can model skyrmion lattice dynamics at finite temperatures.

Our simulation are based on skyrmions in an Fe monolayer on a Pd(111) surface with a Pt_{0.95}Ir_{0.05} alloy overlayer. In these systems, skyrmions exhibit a lattice-orientation-dependent attractive force [2], which we model using a modified Lennard-Jones potential, and compare to an isotropic Lennard-Jones potential. For the modified lattice-orientation-dependent Lennard-Jones potential, we find long-range orientational order, with lattices having a strongly preferred orientation. This effect diminishes with increasing temperature and density.

One way of externally affecting the system is by applying an in-plane magnetic field. The resulting lattice is shown in Figure 1. The in-plane field changes the diffusive properties of skyrmions [3], but also elongates the skyrmions. Therefore we use a Gay-Berne potential [4] to model the skyrmion-skyrmion interactions in this case.

We acknowledge financial support by the German Research Foundation via SFB 1432 and via Project No. 403502522.

[1] Kosterlitz et. al., *J. Phys. C* **6** (1973) 1181; Kosterlitz J. M., *J. Phys. C* **7** (1974) 1046; Halperin et. al., *Phys. Rev. Lett.* **41** (1978) 121; Young, *Phys. Rev. B* **19** (1979) 1855.

[2] Rózsa, et. al. *Phys. Rev. Lett.* **117**, 157205 (2016).

[3] Kerber et. al. *Phys Rev. Appl.* **15** 044029 (2021).

[4] Cleaver et. al. *Phys. Rev. E* **54**, 1 (1996).

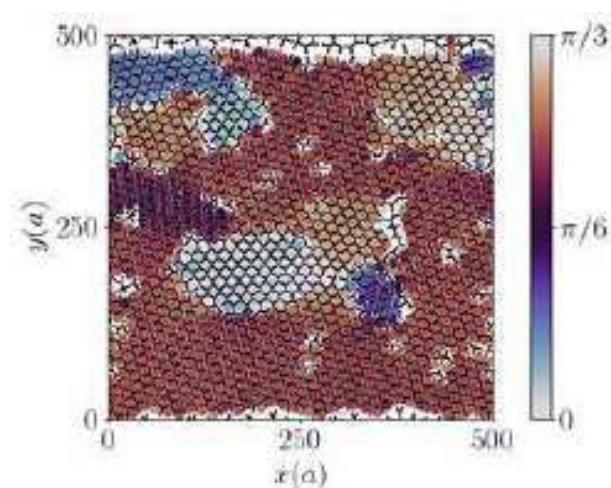


Figure 1: Low density skyrmion lattice with applied in-plane magnetic field at low temperatures. Color-bar indicates lattice orientation, clusters of different local lattice orientations are visible. The lattice constant a is in reference to the underlying spin lattice.

BLOCH HOPFION SPIN-WAVE SPECTRA IN FERROMAGNETIC MEDIUM

Krzysztof Sobucki^{1*}, Maciej Krawczyk¹, Olena Tartakivska^{1,2}, Piotr Graczyk³

¹*Institute of Spintronics and Quantum Information, Faculty of Physics, Adam Mickiewicz University, Poznan, Uniwersytetu Poznańskiego 2, Poznan, Poland*

²*Institute of Magnetism of NAS of Ukraine and MES of Ukraine, 36-b Acad. Vernadskogo Ave., Kyiv, Ukraine*

³*Institute of Molecular Physics, Polish Academy of Science, Smoluchowskiego, Poznań, Poland*

*Correspondent author's email: krzsob@amu.edu.pl

The topologically protected objects are an interesting research topic, especially in magnetism. Among them, the skyrmions are extensively studied and considered for applications in race-track memories and neuromorphic computing [1]. Recently, the interest is moving to three-dimensional systems and 3D solitons. A hopfion is a 3D topologically protected object, which stabilizes due to the Dzyaloshinskii-Moriya interaction and a strong surface anisotropy in ferromagnetic films or disks of thickness comparable to a helical wavelength. The existence of Néel type hopfions has been confirmed experimentally in the multilayered structures [2]; however the Bloch type has been only predicted in theory. The detection of the hopfion is a complex task, which requires advanced and precise experimental techniques. It is already proposed to distinguish different 3D magnetization objects with the measurements of spin-wave dynamics [3]. We perform micromagnetic simulations to study spin-wave spectra of Bloch hopfion in a ferromagnetic nanodisk (200 nm diameter and 70 nm radius) dependent on the magnetization saturation value and the uniaxial magnetocrystalline anisotropy. The finite element method simulations in a frequency domain yielded full spin-wave spectra and identified various modes in a broad frequency range. The finite difference in time domain simulations allowed us to obtain the ferromagnetic resonance intensity spectra for different orientations of the pumping magnetic field direction. We found bountiful spectra of modes, especially at low frequency, with multiple resonances of intensities suitable for broadband ferromagnetic resonance (FMR) measurements. Interestingly, the FMR spectra only weakly depend on the measured component but change with polarization (in-plane or out-of-plane) of the microwave field used for excitation. Our findings can be a valuable clue for hopfion identification using the state-of-the-art measurement technique.

The research leading to these results has received funding from the Norwegian Financial Mechanism 2014-2021 project No. 2020/37/K/ST3/02450 and the National Science Centre of Poland under Grant No 2018/28/C/ST3/00052.

[1] Li S., et al. (2021). Magnetic skyrmions for unconventional computing. *Mater. Horiz.* 8, 854.

[2] Kent N. et al. (2021). Creation and observation of Hopfions in magnetic multilayer systems, *Nat. Commun.* 12, 1562.

[3] Raftrey D., Fisher P. (2021). Field-Driven Dynamics of Magnetic Hopfions. *Phys. Rev. Lett.* 127, 257201.

Observation of metastable skyrmion lattice in NdMn₂Ge₂ at room temperature

Sam Treves^{1,2,3}, Victor Ukleev³, Andreas Apseros^{2,3}, Aki Kitaori⁴, Naoya Kanazawa⁴, Jamie Massey^{2,3}, Simone Finizio³, Yoshinori Tokura⁴, Valerio Scagnoli^{2,3} and Patrick Maletinsky¹

¹*Department of Physics, University of Basel, 4056 Basel, Switzerland*

²*Laboratory for Mesoscopic Systems, Department of Materials, ETH Zurich, 8093 Zurich, Switzerland*

³*Paul Scherrer Institute, 5232 Villigen PSI, Switzerland*

⁴*Department of Applied Physics, University of Tokyo, Tokyo 113-8656, Japan*

Recent discoveries of topological magnetic textures in centrosymmetric, rare-earth based materials have opened new perspectives for technological applications aimed at magnetic storage. Recent transport and Lorentz transmission electron microscopy (LTEM) measurements suggest that NdMn₂Ge₂ is a new room-temperature skyrmion host [1][2]. Here we show varied field and temperature measurements which were undertaken for a 200 nm thick lamella of NdMn₂Ge₂ using scanning transmission x-ray microscopy (STXM) exploiting magnetic sensitivity via the x-ray magnetic circular dichroism (XMCD) effect. Our measurements show that it is possible to stabilise a metastable skyrmion lattice at room temperature and zero field. This lattice was stable from room temperature up until the sample's Curie temperature, and was recoverable when cycling between a negative and positive magnetic field in the out of plane direction. These results suggest NdMn₂Ge₂ to be an ideal candidate material for Skyrmion data and storage applications.

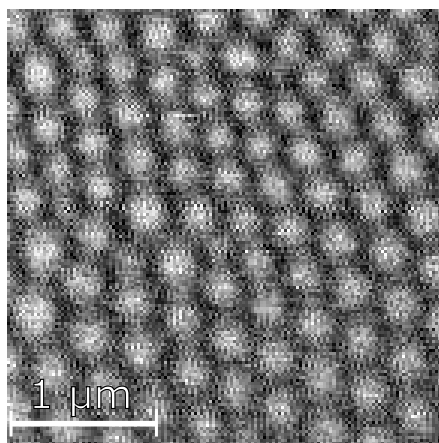


Figure 1: A scanning transmission x-ray microscopy image of a metastable skyrmion lattice, which was stabilised from a random magnetic configuration using a 50 mT out of plane field whilst cooling from 330 K to 300 K.

[1] S. Wang, Q. Zeng, D. Liu, H. Zhang, L. Ma, G. Xu, Y. Liang, Z. Zhang, H. Wu, R. Che, X. Han, and Q. Huang, *ACS Appl. Mater. Interfaces* **12**, 24125 (2020).

[2] Z. Hou, L. Li, C. Liu, X. Gao, Z. Ma, G. Zhou, Y. Peng, M. Yan, X. xiang Zhang, and J. Liu, *Mater. Today Phys.* **17**, 100341 (2021).

Exchange anisotropy and a new spiral state in the insulating chiral magnet Cu_2OSeO_3

Victor Ukleev¹, Priya R. Baral², Oleg Utesov³, Chen Luo⁴, Florin Radu⁴, Pierluigi Gargiani⁵, Manuel Valvidares⁵, Arnaud Magrez² and Jonathan S. White¹

¹ Paul Scherrer Institute, 5232, Villigen PSI, Switzerland

² Institute of Physics, École Polytechnique Fédérale de Lausanne, CH 1015 Lausanne, Switzerland

³ Saint-Petersburg State University, 198504, Saint-Petersburg, Russia

⁴ Helmholtz-Zentrum Berlin for Materials and Energy, 12489, Berlin, Germany

⁵ ALBA Synchrotron Light Source, E-08290, Barcelona, Spain

The ground-state helical magnetic structures of cubic chiral systems are well explained by the Bak-Jensen model that considers the interplay between Heisenberg exchange interaction, antisymmetric Dzyaloshinskii-Moriya interaction (DMI), anisotropic exchange interaction (AEI), and cubic anisotropy [1]. The weak cubic anisotropy determines the spin-wave gap and some additional peculiarities of the helix axis orientation under a magnetic field, while the exchange, DMI and AEI are responsible for the helical spiral and its orientation relative to crystal axes [2]. The latter interaction is often neglected due to its weak impact on experimental observations. However, the cubic and exchange anisotropies are important for defining the propagation direction of the helix, and ultimately the orientation of any field-induced skyrmion lattice (SkL) in these materials. Moreover, their role which has been neglected for decades, has been recently found to be manifested in exotic low-temperature states of Cu_2OSeO_3 : tilted conical spiral and disordered SkL [3]. In the present work we use a simple and reliable method [4] based on resonant x-ray scattering (REXS) in vector magnetic fields to quantify the AEI in chiral cubic Cu_2OSeO_3 ($T_c = 58$ K). We find that in this material, the AEI is very pronounced at low temperatures < 35 K resulting in the conical spiral pitch variation of 10% for particular magnetic field orientations relative to crystal axes (Fig. 1). Moreover, we report on a newly discovered surface conical spiral state that is stabilized in the same low- T range when the magnetic field is applied along $\langle 110 \rangle$ direction.

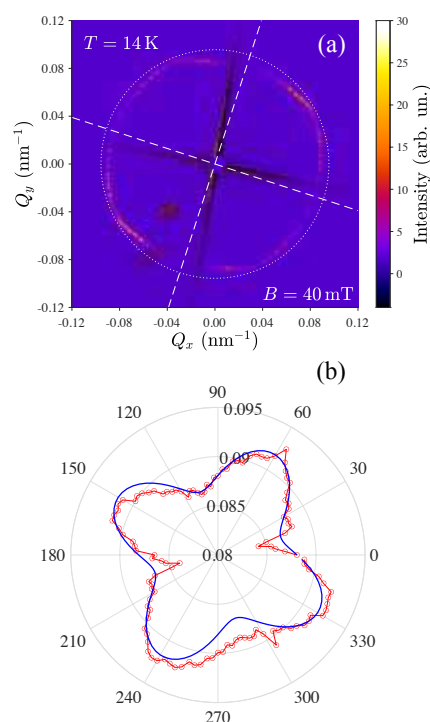


Figure 1 (a) Summed transmission REXS patterns measured from conical states in Cu_2OSeO_3 . Deviations of the scattering signal distribution from a $Q=\text{const}$ ring (dotted line) indicate contributions of the AEI. White dashed lines indicate $\langle 100 \rangle$ axes of the crystal. (b) Measured (symbols) and fitted (line) dependencies of the \mathbf{Q} -vector relative to various crystallographic directions. These measurements were performed at the VEKMAG end-station (Bessy II, Berlin)

[1] P. Bak and M. H. Jensen, Journal of Physics C: Solid State 531 Physics 13, L881 (1980)

[2] S. Maleyev, Physical Review B 73, 174402 (2006)

[3] A. Chacon, et al., Nature Physics 14, 936 (2018)

[4] V. Ukleev, et. al., Physical Review Research 3, 013094 (2021).

Emergent responses in magnetic ring arrays of different lattice arrangements for reservoir computing

G. Venkat¹, I. Vidamour¹, C. Swindells¹, M. Foerster², M. A. Niño², M. C. Rosamond³, T. J. Hayward¹, R. Allenspach⁴, A. Bischof⁴, D. A. Allwood¹

¹Department of Materials Science and Engineering, University of Sheffield, Sheffield, S1 3JD, UK

²ALBA Synchrotron Light Facility, 08290, Cerdanyola del Valles, Spain

³School of Electronic and Electrical Engineering, University of Leeds, Leeds, LS2 9JT, UK

⁴IBM Research-Zurich, 8803 Rüschlikon, Switzerland

Stochastic behaviour has traditionally been a limiting factor in developing nanomagnetic technology. We have recently shown complex probabilistic, emergent behaviour in interconnected nanowire ring arrays [1-2] that is useful for ‘reservoir computing’ (RC), a highly efficient computation scheme for time domain signal processing [3]. We have also simulated RC with such arrays for recognising spoken digits [2] and anticipate a need to derive additional complex behaviour from the arrays for more data and task processing.

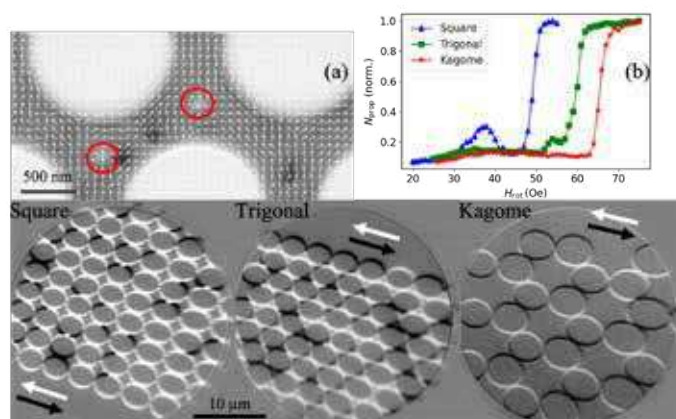


Figure: (a) A spin polarized SEM image of the ground state of a trigonal ring array with circles showing pinned domain sites. (b) The MOKE response of the different lattice arrangements showing the variation of the propagating domain states. Also shown are XPEEM images for the different lattice arrangements.

Here we vary the lattice arrangements of $\text{Ni}_{80}\text{Fe}_{20}$ rings (as square, trigonal and Kagome) to achieve alternative responses. Different lattices show rich ground states (for example pinning sites in the trigonal array in Fig. (a)) and can show diverse dynamics. Magneto-optic Kerr effect (MOKE) measurements with in-plane rotating fields (H_{rot}) were used to characterise the arrays [2] and gave the propagating DW state population N_{prop} (Fig. (b)). The different behaviours are due to interactions at junctions and are seen in X-ray photoemission electron microscopy (XPEEM) images at intermediate fields. The square and trigonal arrays show multiple magnetic states while the Kagome shows vortices. We are now benchmarking computation with these arrays and expect that these varied responses are essential for obtaining additional processing capabilities in reservoir computing.

[1] Negoita et al., *J. Appl. Phys.* 114, 013904 (2013). [2] Dawidek et al., *Adv. Funct. Mater.*, 2008389 (2021). [3] Jensen et al., *ALIFE 2018: The 2018 Conference on Artificial Life* 15, (2018).

Investigation of self-nucleated skyrmion states in the ferromagnetic/nonmagnetic multilayer dot

Iu. V. Vetrova¹, M. Zelent², J. Šoltýs¹, V. A. Gubanov³, A. V. Sadovnikov³, T. Šcepka¹, J. Déder¹, R. Stoklas¹, V. Cambel¹, M. Mruczkiewicz^{1,4}

¹ Institute of Electrical Engineering, Slovak Academy of Sciences, Dubravská cesta 9, SK-841-04 Bratislava, Slovakia

² Faculty of Physics, Adam Mickiewicz University in Poznań, Institute of Spintronics and Quantum Information, ul. Uniwersytetu Poznańskiego 2, Poznań, PL-61-614 Poland

³ Saratov State University, Astrakhanskaya Street 83, Saratov, 410012, Russian Federation

⁴ Centre For Advanced Materials Application CEMEA, Slovak Academy of Sciences, Dubravská cesta 9, 845 11 Bratislava, Slovakia

Magnetic skyrmions are circular domains surrounded by a single chirality domain wall [1]. They can be stabilized at room temperature by the Dzyaloshinskii-Moriya interaction (DMI) induced at the interface of the ferromagnetic/non-magnetic metals [2]. In the case of multilayer structures, there is an interplay between DMI, exchange energy, perpendicular anisotropy and applied magnetic field that leads to stabilization of skyrmions [2]. In addition, it was found that the confinement due to geometry can increase the stability of the skyrmion significantly [3]. Stabilization of skyrmions inside the dot structures could lead to the development of an advanced concept of memory device that combines ultra-high density and fast data transfer rate.

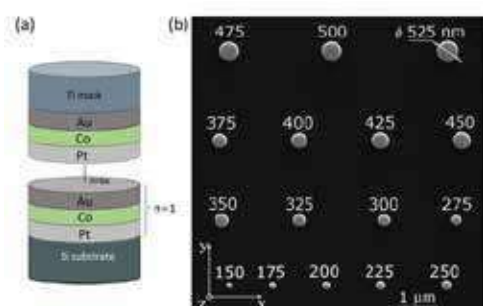


Fig. 1. (a) Schematic representation of a multilayer nanodot based on ultrathin Co layers placed between two different heavy metals (Au, Pt), where n represents the number of tri-layer Au/Co/Pt unit cell repeats is equal to 6; (b) SEM image of an array of multilayer dots patterned by the electron beam lithography and etching method

We have experimentally and numerically demonstrated the formation of skyrmions in nanopatterned dots composed of six repetitions of the interfacially asymmetric Pt/Co/Au multilayer. The skyrmion state can be stabilized at room temperature when the dot has a diameter of about 175 nm. We also examined the stabilization of micromagnetic states such as single domain, horseshoe and worm-like domains in fabricated submicron-sized dots. The evolution of the magnetic state depending on the dot diameter was also investigated.

Acknowledgments: this work was supported by Slovak Grant Agency APVV (Project No. APVV-19-0311), by VEGA (Project No. 2/0168/22), and by the ITMS Project No. 313

[1] T. Srivastava, M. Schott, R. Juge, V. Krizakova, M. Belmeguenai, Y. Roussigné... and A. Stashkevich, *Nano letters*, 18(8), 4871-4877, (2018).

[2] M. Zelent, J. Tobik, M. Krawczyk, K. Y. Guslienko and M. Mruczkiewicz, *physica status solidi (RRL)–Rapid Research Letters*, 11(10), 1700259, (2017).

[3] S. Rohart and A. Thiaville, *Physical Review B*, 88(18), 184422, (2013).

The Interplay between Skyrmions and Thermal Magnons

M. Weißenhofer¹, L. Rózsa¹, and U. Nowak¹

¹*Fachbereich Physik, Universität Konstanz, Universitätsstraße 10, Konstanz, Germany*

As they are small in size and easily movable by electric currents, skyrmions are promising candidates for next generation magnetic logic and memory devices. However, in order to be able to control their dynamics at elevated temperatures, one has to first understand the interplay between skyrmions and thermally occupied magnons.

We investigate the temperature-induced dynamics of skyrmions with various topological charges in a (Pt_{0.95}Ir_{0.05})/Fe bilayer on a Pd(111) surface, both in equilibrium and non-equilibrium. We perform atomistic spin dynamics simulations based on the stochastic Landau-Lifshitz-Gilbert equation and a model hamiltonian parametrized by ab-initio calculations [1]. Our results for the Brownian motion of skyrmions show that existing theory based on Thiele's equation [2] is insufficient to describe the dynamics of skyrmions at finite temperatures (see left panel of Fig. 1). We propose an extended equation of motion that takes into account the coupling of the skyrmion to the magnonic heat bath. This coupling gives rise to an additional dissipative term that dominates for elevated temperatures and Gilbert damping values typical for thin films and multilayers [3]. We further demonstrate that in a temperature gradient the skyrmions move in different directions, depending on their topological charge (see right panel of Fig. 1), and reveal that this is due to the momentum-transfer of the emergent thermal magnon current scattering at the skyrmions.

We acknowledge financial support of the DFG via Project No. 403502522 and the National Research, Development and Innovation Office of Hungary (Project No. K131938).

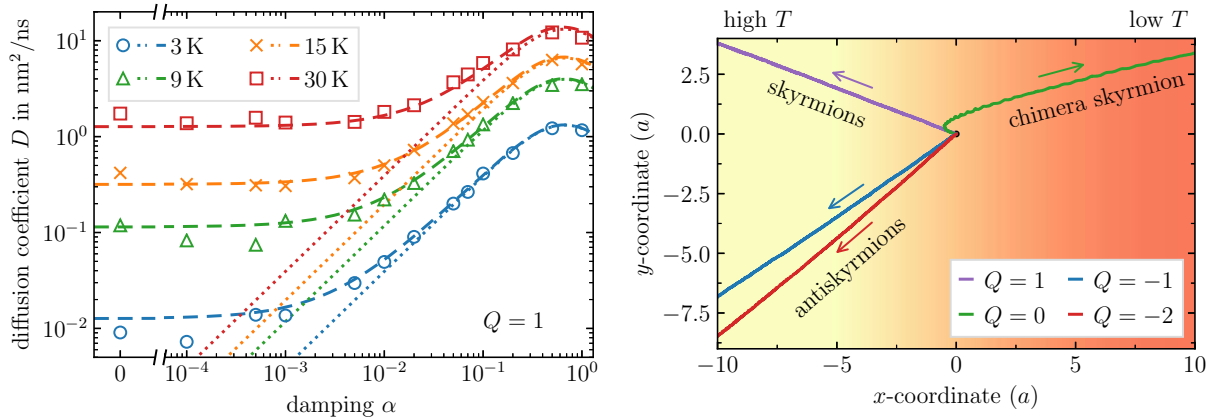


Figure 1: Temperature-induced dynamics of skyrmions in (Pt_{0.95}Ir_{0.05})/Fe/Pd(111). (left) Simulations results (symbols), theory based on Thiele's equation (dotted lines) and our theory including thermal magnons (dashed lines) for the diffusion coefficient. (right) Trajectories of different types of skyrmions with topological charges as labeled in a temperature gradient.

[1] L. Rózsa, A. Deák, E. Simon, R. Yanes, L. Udvardi, L. Szunyogh, and U. Nowak, *Phys. Rev. Lett.* **117**, 157205 (2016).

[2] A. A. Thiele, *Phys. Rev. Lett.* **30**, 230 (1973).

[3] M. Weißenhofer, L. Rózsa, and U. Nowak *Phys. Rev. Lett.* **127**, 047203 (2021).

Posters

| | | |
|-----------------------|--|-----|
| Anuj Dhiman | <i>Magnetic properties of ultrathin Pt/Co/Re and Re/Co/Pt layers</i> | 486 |
| Lucia Fecova | <i>Direct Correlation Between Domain Wall Distortions and Perpendicular Fields in Amorphous Glass-Coated Microwires</i> | 487 |
| Soumyajyoti Haldar | <i>Distorted 3Q state driven by topological-chiral magnetic interaction</i> | 488 |
| Michał Inglot | <i>Edge states at a Rashba spin-orbit domain wall in the magnetized graphene</i> | 489 |
| Jagannath Jena | <i>Stability of antiskyrmions and elliptical Bloch skyrmions in a D2d system</i> | 490 |
| Anastasiia Korniienko | <i>Magnetic configurations in $\text{Fe}_{32}\text{Co}_{68}$ core-shell nanostructures with hexagonal cross-section</i> | 491 |
| Santiago Osorio | <i>Response of the chiral soliton lattice to spin polarized currents</i> | 492 |
| Bibekananda Paikaray | <i>Reconfigurable logic operations via gate controlled skyrmion motion in a nanomagnetic device</i> | 493 |
| Andrea Peralta | <i>Observation of spin textures in $\text{La}_{0.7}\text{Sr}_{0.3}\text{MnO}_3/\text{SrIrO}_3$ bilayers</i> | 494 |
| Dariia Popadiuk | <i>Study of gyrovectors of magnetic hopfions</i> | 495 |
| Subhajit Roy | <i>Modification of domain wall velocity in Ta/CoFeB/MgO due to voltage-induced non-volatile piezoelectric strain</i> | 496 |
| Yanis Sassi | <i>Spin-orbit torque engineering for efficient skyrmion motion</i> | 497 |
| Amir Nasser Zarezad | <i>Topological Hall effect in two-dimensional systems with Skyrmion textures in the presence of electromagnetic impurities.</i> | 498 |

Magnetic properties of ultrathin Pt/Co/Re and Re/Co/Pt layers

A. K. Dhiman¹, R. Gieniusz¹, Z. Kurant¹, I. Sveklo¹, S. K. Jena², A. Wawro², A. Maziewski¹

¹ *Laboratory of Magnetism, Faculty of Physics, University of Białystok, Białystok, Poland*

² *Institute of Physics Polish Academy of Sciences, Warsaw, Poland*

Interfacial Dzyaloshinskii-Moriya interaction (iDMI) is observed in ultrathin magnetic films with asymmetric surroundings [1], [2] due to the broken inversion symmetry at the interfaces. In this work we present the results obtained for ultrathin Co films with Pt and Re covers. Double wedge stacks of Pt/Re(d_{Re})/Co(d_{Co})/Pt and Pt/Co(d_{Co})/Re(d_{Re})/Pt were deposited using molecular beam epitaxy on sapphire substrates. 2D maps (d_{Co} , d_{Re}) of magnetic parameters were obtained employing: (i) polar magneto-optical Kerr effect (PMOKE) magnetometry and (ii) Brillouin Light Scattering (BLS) spectroscopy in Damon-Eshbach mode. Fig.1 shows the remanence image determined as a difference between images registered for sample saturated by magnetic field applied at “up” and “down” directions.

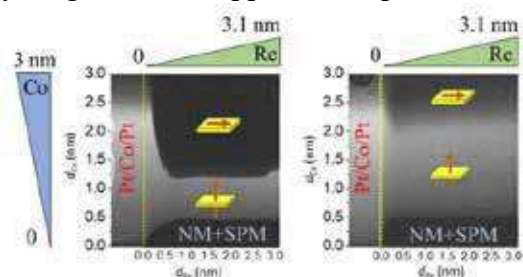


Figure 1: Remanence maps of the samples obtained using PMOKE imaging. The grey regions indicate out of plane magnetization state while the black regions describe the areas of non-magnetic (NM) and superparamagnetic (SPM) phases as well as the in-plane magnetization state for thin and thick Co layer zones, respectively.

qualitative damping behavior. With increase in d_{Re} thickness, the Δf parameter value increases and decreases with changing sign for the bottom and top layer, respectively. While increasing d_{Re} thickness FWHM decreases and increases for the bottom and upper Re layers, respectively.

PMOKE magnetometry enabled determination of effective magnetic anisotropy field (H_1) and spin reorientation transition (SRT) for critical Co layer thickness d_{SRT} . For thick Re in Re(1.14)/Co(d_{Co})/Pt, $d_{\text{SRT}} \sim 1.4$ nm and in Pt/Co(d_{Co})/Re(2.35), $d_{\text{SRT}} \sim 2.1$ nm, while in the reference sample part Pt/Co/Pt, $d_{\text{SRT}} \sim 2.2$ nm. H_1 falls rapidly in the both cases when Re layer is introduced as a bottom and top layer, and even for less than a nm thickness of Re it is found to be saturated. From BLS measurements the difference in Stokes and anti-Stokes frequencies Δf enabled determination of iDMI strength. The full width at half maximum (FWHM) of fitted spectra reveals

This work is supported by the National Science Center in Poland under the projects Beethoven-2 (DEC-2016/23/G/ST3/ 04196), OPUS-19 (2020/37/B/ST5/02299) and IEEE Magnetics Society Educational Seed Funding.

[1] K. Di, V. L. Zhang, H. S. Lim, S. C. Ng, M. H. Kuok, PRL 114, 047201 (2015)

[2] A. Belabbes, G. Bihlmayer, F. Bechstedt, S. Blugel, A. Manchon, PRL 117, 247202 (2016)

Direct Correlation Between Domain Wall Distortions and Perpendicular Fields in Amorphous Glass-Coated Microwires

Lucia Fecova^{1,2}, Rastislav Varga², Kornel Richter²

¹*Institute of Physics, P. J. Safarik University, Park Angelinum 9, 041 54 Kosice, Slovakia*

²*CPM-TIP, P. J. Safarik University, Tr. SNP 1, 040 11, Kosice, Slovakia*

Magnetic microwires are perfect candidates for sensor and actuator applications based on domain wall (DW) propagation [1]. Our previous works [2, 3] showed that microwire's peculiar domain wall dynamics can be effectively tuned by a perpendicular magnetic field [3]. However, induction methods do not allow direct observation of the domain wall behaviour in a perpendicular field.

Here, we employ the setup [4] based on the magneto-optic Kerr effect (MOKE). The method uses an effective one-dimensional magnetic well that warrants a high reproducibility of the domain wall motion.

As seen in Fig. 1a, the domain wall velocity either increases or decreases depending on the perpendicular field direction. In turn, the MOKE measurements show that the domain wall inclination angle decreases for both perpendicular magnetic fields (Fig. 1b). Inclination angle α is 1.13° without perpendicular field (black curve in Fig. 1b), $\alpha = 0.55^\circ$ for $H_p > 0$, and $\alpha = 0.57^\circ$ for $H_p < 0$. A decrease in the inclination angle indicates the domain wall extension. Therefore, the domain wall mobility in Sixtus-Tonks experiments is not directly related to the domain wall width and some other effect(s) must come into play. One possible explanation is the domain wall distortion (Fig. 1b red curve) that remarkably changes the domain wall mobility.

This is also confirmed by our time-resolved visualization of the domain wall that shows enhanced DW pinning in the presence of perpendicular field.

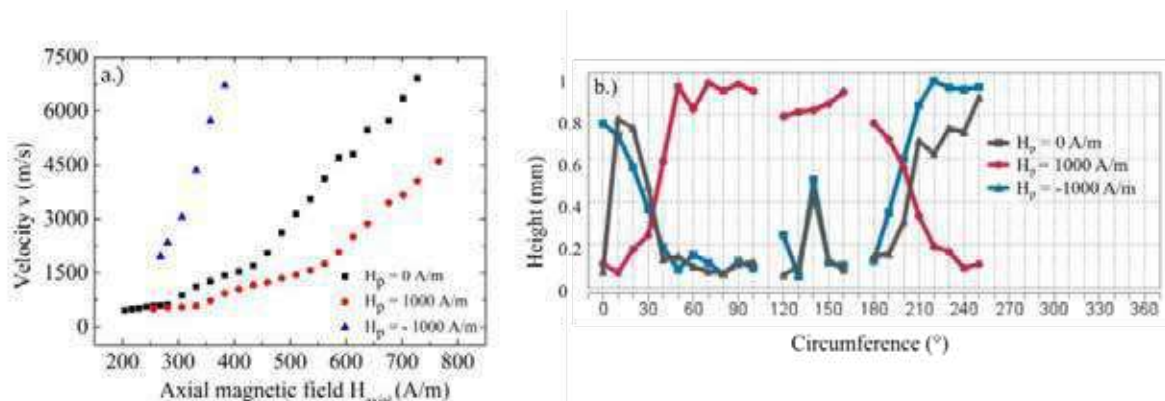


Figure 1 a) Sixtus-Tonks measurements of the DW velocity as a function of the magnetic field. Red and blue curves are plotted for perpendicular fields. b) Circumferential dependence of light intensity profile. The influence of perpendicular field on domain wall distortions is clearly visible at $H_p = 1000$ A/m.

- [1] J. Olivera et al., *Sensors* **19** (21), 4658 (2019).
- [2] L. Fecova, K. Richter, and R. Varga, *AIP Adv.* **11**, 035014 (2021).
- [3] L. Fecova, K. Richter, and R. Varga, *J. Magn. Magn.* **538**, 168274 (2021).
- [4] O. Vahovsky, R. Varga, and K. Richter, *J. Magn. Magn.* **483**, 266 (2019).

Distorted 3Q state driven by topological-chiral magnetic interaction

Soumyajyoti Haldar¹, Sebastian Meyer², André Kubetzka³ and Stefan Heinze¹

¹ *Institute of Theoretical Physics and Astrophysics, University of Kiel, Leibnizstr. 15, 24098 Kiel, Germany*

² *Nanomaterials/CESAM, Université de Liège, B-4000 Sart Tilman, Belgium*

³ *Department of Physics, University of Hamburg, 20355 Hamburg, Germany*

Non-collinear spin structures are of fundamental interest in magnetism since they allow to obtain insight into the underlying microscopic interactions and are promising for spintronic applications [1,2]. Here, we demonstrate that the recently proposed topological-chiral magnetic interactions [3] can play a key role for magnetic ground states in ultrathin films at surfaces [4]. Using density functional theory, we show that significant chiral-chiral interactions occur in hexagonal Mn monolayers due to large topological orbital moments which interact with the emergent magnetic field. Superposition states of spin spirals such as the 2Q [5] state or a distorted 3Q state arise due to the competition with biquadratic and four-spin interactions. Simulations of spin-polarized scanning tunneling microscopy images suggest that the distorted 3Q state could be the magnetic ground state of a Mn monolayer on Re(0001) [6].

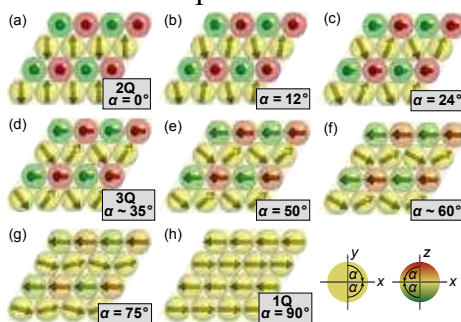


Figure 1: Spin structures for a hexagonal Mn monolayer along the continuous path from (a) the 2Q state via (d) the 3Q to (h) the 1Q state.

- [1] A. Fert *et al.*, Nat. Rev. Mater. **2**, 17031 (2017).
- [2] J. Grollier *et al.*, Nat. Electron. **3**, 360 (2020).
- [3] S. Grytsiuk *et al.*, Nat. Commun. **11**, 511 (2020).
- [4] S. Haldar *et al.*, Phys. Rev. B **104**, L180404 (2021).
- [5] J. Spethmann *et al.* Nat. Commun. **12**, 3488 (2021).
- [6] J. Spethmann *et al.*, Phys. Rev. Lett. **124**, 227203 (2020).

Edge states at a Rashba spin-orbit domain wall in the magnetized graphene

M. Ingot¹, A. Dyrdał², V.K. Dugaev¹ and J. Barnaś^{2,3}

¹*Department of Physics and Medical Engineering, Rzeszów University of Technology, al. Powstańców Warszawy 6, 35-959 Rzeszów, Poland*

²*Faculty of Physics, Adam Mickiewicz University, ul. Uniwersytetu Poznańskiego 2, 61-614 Poznań, Poland*

³*Institute of Molecular Physics, Polish Academy of Sciences, ul. M. Smoluchowskiego 17, 60-179 Poznań, Poland*

The electronic structure of graphene can be modified by external factors such as, e.g., magnetic and electric fields, strength, distortions, and others. Here we demonstrate the occurrence of edge states, which are induced by the domain wall of Rashba type in the electron spectrum of graphene with magnetic overlayer. We use the Dirac Hamiltonian Eq. (1) describing the low energy spectrum with linearity dependence on wave vector \mathbf{k} . Additionally, we include the Zeeman energy originating from the layer with magnetization M . The Hamiltonian of electrons in Dirac point K is

$$\hat{H} = -iv(\tau_x \nabla_x + \tau_y \nabla_y) + \lambda(x)(\tau_x \sigma_y - \tau_y \sigma_x) + \sigma_z M, \quad (1)$$

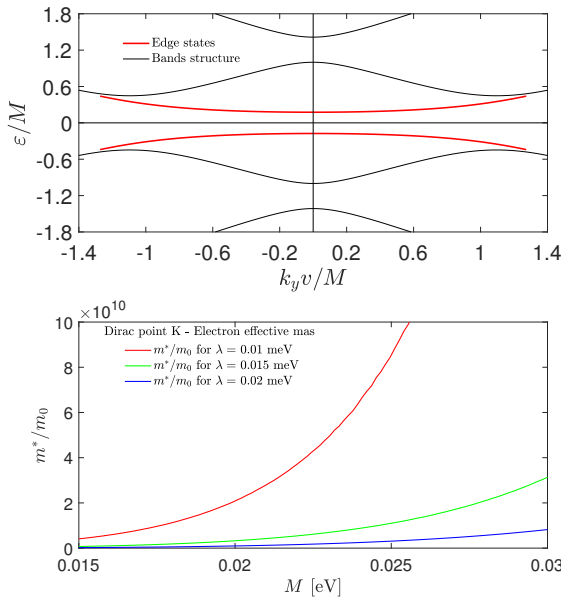


Figure 1: Band structure of magnetized graphene with Rashba SOI (a). The effective mass of electron in the edge state as a function of M for different values of λ_0 (b).

Using the Schrödinger equation we calculated the energy spectrum and wave functions of electrons localized at the domain wall between two regions with opposite signs of Rashba spin-orbit coupling $\lambda(x)$

$$\lambda(x) = \lambda_0 \text{sign } x. \quad (2)$$

The electron energy spectrum is shown in Fig. 1a, where the red lines correspond to the edge states.

Using the kp method we find an effective Hamiltonian describing the edge states and the electron effective mass, which can be giant for small λ_0 . The result of this calculation is presented in Fig. 1b.

This work is supported by the National Science Center in Poland, research project No. DEC-2017/27/B/ST3/02881.

[1] M. Ingot, V.K. Dugaev, A. Dyrdał and J. Barnaś, *Phys. Rev. B* **104**, 214408 (2021).

Stability of antiskyrmions and elliptical Bloch skyrmions in a D_{2d} system

J. Jena¹ and S.S.P. Parkin¹

¹Max Planck Institute of Microstructure Physics, Halle, Germany

Magnetic skyrmions and antiskyrmions are nano-objects with non-trivial topological spin textures[1, 2]. Recently, the presence of both antiskyrmions and elliptical Bloch skyrmions are observed in a non-centrosymmetric D_{2d} Heusler compound $\text{Mn}_{1.4}\text{Pt}_{0.9}\text{Pd}_{0.1}\text{Sn}$ [3]. At low temperatures and a high magnetic moment of the compound, dipole-dipole interactions dominate which help to stabilize elliptical Bloch skyrmions. On the other hand, the decreased net magnetization at higher temperatures reduces the importance of dipole-dipole interactions so that antiskyrmions are favored. The distinct topological phases formation is also verified alternative way by a field heating experiment. First, the elliptical Bloch skyrmions lattice state is stabilized at low temperature by applying the magnetic field. Then, keeping the magnetic field value constant, the temperature of the specimen is raised. A transition to antiskyrmions state is noticed near room temperature via the trivial bubbles state in this field-heated process. Contrary, field-cooled the antiskyrmions state from high temperature, antiskyrmions remain metastable at low temperatures[4]. Our results demonstrate that different spin textures in the D_{2d} system are metastable in response to temperature-field protocols.

- [1] S. Mühlbauer, B. Binz, F. Jonietz, C. Pfleiderer, A. Rosch, A. Neubauer, R. Georgii, P. Böni, *Science* **323**, 915, (2009).
- [2] A. K. Nayak, V. Kumar, T. Ma, P. Werner, E. Pippel, R. Sahoo, F. Damay, U. K. Rößler, C. Felser, S. S. P. Parkin, *Nature* **548**, 561, (2017).
- [3] J. Jena, B. Göbel, T. Ma, V. Kumar, R. Saha, I. Mertig, C. Felser, S. S. P. Parkin, *Nat. Commun.* **11**, 1115, (2020).
- [4] J. Jena, S. S. P. Parkin, Manuscript in preparation (2022).

Magnetic configurations in Fe₃₂Co₆₈ core-shell nanostructures with hexagonal cross-section

Anastasiia Korniienko^{1*}, Alexis Wartelle², Matthias Kronseder³, Michael Foerster⁴, Miguel Ángel Niño⁴, Sandra Ruiz-Gomes⁴, Muhammad Waqas Khaliq^{4,5}, Christian H. Back¹

¹ Department of Physics, Technical University of Munich, D-85748 Garching, Germany

² Univ. Grenoble Alpes, CNRS, Grenoble INP, SIMAP, F-38000 Grenoble, France

³ Institute for Experimental and Applied Physics, University of Regensburg, D-93040 Regensburg, Germany

⁴ Alba Synchrotron Light Facility, CELLS, E-08290 Barcelona, Spain

⁵ Department of Condensed Matter Physics, University of Barcelona, E-08028 Barcelona, Spain

* anastasiia.korniienko@tum.de

Curvilinear geometry of the magnet leads to the appearance of an effective, curvature-driven Dzyaloshinskiy-Moriya interaction and an additional geometry-induced easy-axis anisotropy [1]. Recent studies reveal a curvature-induced asymmetry of the spin waves dispersion relation in cylindrical nanotubes (NTs) [2] and nanotubes with hexagonal cross-section [3]. Considered structures adopted an azimuthal magnetization (i.e. vortex-like state), thus curvature was optimally coupled to the magnetization. It would be of interest to go beyond the sole vortex-like state by designing NTs with distinct easy axes, corresponding to different magnetization components. This would allow to tune the effect of the curvature on the dispersion relation in a single system.

With this in mind we fabricate our core-shell nanostructures consisting of GaAs rod with hexagonal cross-section and thin ferromagnetic Fe₃₂Co₆₈ films as a shell. This FeCo alloy deposited on a certain crystallographic GaAs plane shows an in-plane spin-reorientation transition as a function of thickness [4]. At a chosen thickness of magnetic film, we expect our tube walls to feature biaxial behavior, with easy axes at 28° and at 82° with respect to the tube axis. This would make the NTs promising to study the effect of the curvature for different magnetic configurations.

Here we use the PhotoEmission Electron Microscope of the Circe beamline at the ALBA synchrotron with X-ray Magnetic Circular Dichroic contrast (XMCD-PEEM) to image the magnetic configuration in individual magnetic NTs [5]. The imaging was done at remanence, between applications of magnetic fields and with different angles between x-rays and nanotube's long axis. Dichroic contrast from the structure's top facet surface reveals a large number of domains for some of the NTs. We observed magnetic domains with magnetization tilted by a certain angle with respect to the tube axes, but with opposite windings. Furthermore, we observed a switching between almost longitudinal and azimuthal magnetization for some domains.

[1] D. D. Sheka et al., J. of Phys. A: Math. and Theor. 2015, 48, 125202.

[2] J. A Otálora et al., PRL 117, 227203 (2016).

[3] L. Körber et al., arXiv preprint 2009.02238 (2020).

[4] B. Muermann et al., J. Appl. Phys. 2008, 103, 07B528.

[5] M. Wyss et al., PRB 2017, 96, 024423.

Response of the chiral soliton lattice to spin polarized currents

Santiago A. Osorio¹, Athanasios Athanasopoulos², Victor Laliena³, Javier Campo² and Sebastian Bustingorry¹

¹*Instituto de Nanociencia y Nanotecnología, CNEA-CONICET, Centro Atómico Bariloche, (R8402AGP) S. C. de Bariloche, Río Negro, Argentina*

²*Aragon Nanoscience and Materials Institute (CSIC-University of Zaragoza) and Condensed Matter Physics Department, University of Zaragoza, C/Pedro Cerbuna 12, 50009 Zaragoza, Spain*

³*Department of Applied Mathematics, University of Zaragoza, C/María de Luna, 3, 50018 Zaragoza, Spain*

Spin polarized currents originate a spin transfer torque that enables the manipulation of magnetic textures. In monoaxial chiral helimagnets the Dzyaloshinskii-Moriya interaction favors inhomogeneous distributions of the magnetization with chiral modulations termed chiral solitons. These localized magnetization textures crystallize at low magnetic field leading to the emergence of a chiral soliton lattice (CSL) [1]. These objects present interesting properties, which make them good candidates for spintronic and electronic devices [2,3]. However their potential rely on the stability of this texture under the effect of external perturbations. We theoretically study the effect of a spin-polarized

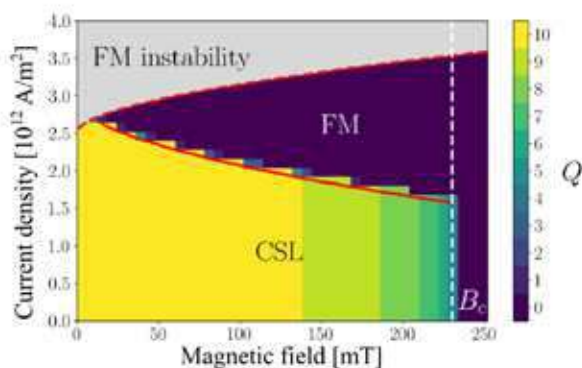


Figure 1: The “Current density-Magnetic field” phase diagram for a monoaxial chiral helimagnet. In the yellow-green region the CSL is stable (the number of chiral solitons is $Q > 1$). In the dark blue region the FM state is stable ($Q = 0$).

current on the magnetic texture corresponding to a chiral soliton lattice in a monoaxial helimagnet under a transverse magnetic field. At sufficiently small current density the chiral soliton lattice reaches a steady motion state with a velocity proportional to the intensity of the applied current, the mobility being independent of soliton density and the magnetic field. This motion is accompanied with a small conical distortion of the chiral soliton lattice. At large current density the spin transfer torque destabilizes the chiral soliton lattice, driving the system to a ferromagnetic state (FM) parallel to the magnetic field (Fig. 1). This phenomenology imposes an upper bound to the maximum velocity at which the chiral

soliton lattice can be moved. The destruction of the chiral soliton lattice under current serves as a possible erasure mechanisms for spintronic applications.

[1] Y. Togawa, Y. Kousaka, K. Inoue and J. Kishine, *J. Phys. Soc. Jpn.* **85**, 112001 (2016).

[2] C. Back *et al*, *J. Phys. D: Appl. Phys.* **53**, 363001 (2020).

[3] N. Nagaosa, *Jpn. J. Appl.* **58**, 120909 (2019).

Reconfigurable logic operations via gate controlled skyrmion motion in a nanomagnetic device

Bibekananda Paikaray¹, Mahathi Kuchibhotla², Arabinda Haldar²
and Chandrasekhar Murapaka¹

¹Department of Materials Science and Metallurgical Engineering, Indian Institute of Technology Hyderabad, Kandi 502284, Telangana, India

²Department of Physics, Indian Institute of Technology Hyderabad, Kandi 502284, Telangana, India

Owing to the topological protection and the ease of efficient manipulation, skyrmions have emerged as potential candidates for carrying information in the future memory and logic devices [1,2]. Magnetic skyrmions are particle like whirling spin texture with topological protection. Skyrmions have attracted much attention recently in the field of spintronics, due to their nanoscale size (~10-100 nm), high speed (~10-100 m/s) and relatively low driving current density (~ 10^6 A/m²) as compared to domain wall [3]. Here, we have proposed a reconfigurable skyrmion-based two-input logic device architecture (see Fig.1(a)). Using micromagnetic simulations, we have demonstrated that the device can perform both OR & AND logic gate functionalities in a reconfigurable manner as shown in Figure 1(b, c). Different logic functionality of the device is selected by flowing current through a metallic gate and the resultant Oersted field controls the trajectory of the skyrmion which in turn determines the logic states. The binary information is denoted by the presence and absence of the skyrmion as “1” and “0”, respectively.

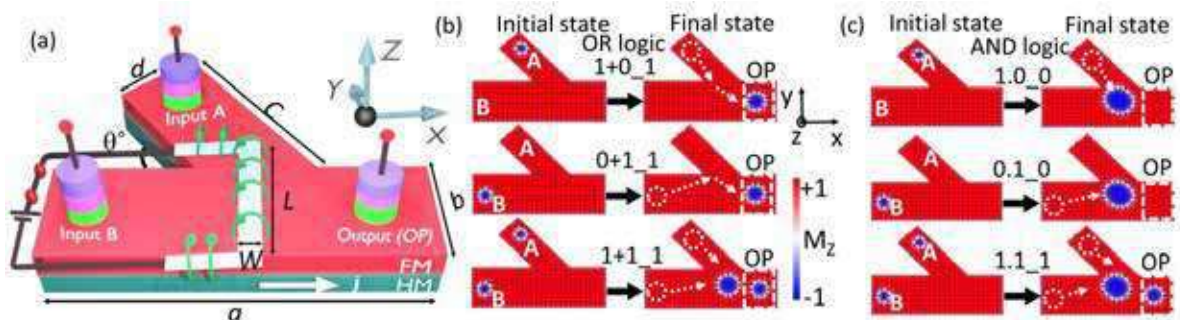


Figure 1: (a) Schematic device structure of the proposed reconfigurable skyrmion based logic gate with two inputs A, B and one output (OP). Initial and final magnetic states of skyrmion motion in FM film for the inputs in logic (b) OR gate and (c) AND gate

The logic functions are implemented on a FM/HM bilayer device structure by virtue of several physical effects such as spin-orbit torque, skyrmion-edge repulsion, skyrmion-skyrmion topological repulsion and skyrmion Hall effect. Skyrmion trajectory have been characterized by estimating skyrmion Hall angle. Skyrmions being a topological entity provides further stability in terms of stray fields or small lithographic variations. Therefore, our results are a step forward toward the practical realizations of an alternative spintronic logic paradigm based on magnetic skyrmions. We believe that our spin orbit torque driven logic design will have potential implication for high speed and low-power skyrmion-based computing architecture.

[1] A. Fert, V. Cros, and J. Sampaio, *Nature Nanotechnology* **8**, 152 (2013).

[2] Luo S., Y. Long. *APL Materials* **9**, 050901 (2021).

[3] Sampaio, S. Rohart, A. Fert, A. *Nature Nanotechnology*, **8**, 839844 (2013).

Observation of spin textures in $\text{La}_{0.7}\text{Sr}_{0.3}\text{MnO}_3$ / SrIrO_3 bilayers

Andrea Peralta¹, Javier Tornos¹, Víctor Zamora¹, Sandra Lopez¹, F. A. Cuellar¹
Sergio Valencia², F. Mompeán^{3,4}, M. García-Hernández^{3,4}, C. León and Jacobo
Santamaría¹

¹ GFMC, Dept. Física de Materiales, Facultad de Física, Universidad Complutense de Madrid, 28040 Madrid, Spain

² Helmholtz Zentrum Berlin für Materialien und Energie, 12489 Berlin, Germany

³ 2D-Foundry Group, Instituto de Ciencia de Materiales de Madrid ICMM-CSIC, 28049 Madrid, Spain

⁴ Laboratorio de Heteroestructuras con Aplicación en Espintrónica, Instituto de Ciencia de Materiales ICMM-CSIC, 28049 Madrid, Spain

Topologically protected spin textures, such as magnetic skyrmions, have attracted considerable interest in recent years, as they can be used as information vectors in low-power information technologies. Spin textures can be stabilized by the interplay between exchange interaction, promoting parallel spin alignment, and Dzyaloshinskii-Moriya interaction, an antisymmetric exchange interaction resulting from the combination of inversion symmetry breaking and strong spin-orbit coupling, which twists spin directions. Although skyrmion or skyrmion bubbles have been observed in non centrosymmetric single magnetic oxide layers [1], interfaces naturally supply the symmetry breaking and favor the observation of spin textures in heterostructures [2,3]. The non-trivial topological charge of the skyrmions gives rise to an antisymmetric contribution to the transverse resistivity, the so called topological Hall effect, THE. Whether THE results from spin chirality or from magnetic inhomogeneity has become an actively debated matter [4,5], boosted by the fact, that, frequently, reports of the THE are not accompanied by real space imaging of the magnetic textures. In this work we report THE in bilayers combining $\text{La}_{0.7}\text{Sr}_{0.3}\text{MnO}_3$ manganite and strong spin orbit SrIrO_3 in a wide temperature range where perpendicular magnetic anisotropy is observed. Real space observations of the magnetic textures by photoemission microscopy using x-ray magnetic circular dichroism contrast evidence a coarsened small grain (100 nm) magnetic structure consistent with the nucleation and clustering of skyrmions or skyrmion bubbles. The temperature dependence of the THE signal is analyzed to extract the expected skyrmion density. Magnetometry and anomalous Hall effect will be discussed to infer the relative importance of magnetic inhomogeneity.

[1] L. Vistoli, et al. Nature Physics 15,1 (2019).

[2] J. Matsuno, et al., Sci Adv. 2, 7(2016).

[3] Y. Li et al., ACS Appl. Mater. Interfaces 11, 23 (2019).

[4] T. C. van Thiel, D. J. Groenendijk, and A. D. Caviglia. Journal of Physics: Materials, 3,025005 (2020).

[5] D. Kan et al. Physical Review B, 98 180408(R) (2018).

Study of gyrovector of magnetic hopfions

D. Popadiuk¹, J. Kharlan¹, O. Tartakovskaya^{1,2}, M. Krawczyk²

¹ *Institute of Magnetism of NAS of Ukraine and MES of Ukraine, 36-b Acad. Vernadskogo Ave., Kyiv, Ukraine*

² *Faculty of Physics, Adam Mickiewicz University, Poznan, Uniwersytetu Poznańskiego 2, Poznan, Poland*

A lot of attention is being paid to hopfions now, three-dimensional, topological localized magnetic structures, which were created and observed recently in magnetic multilayer systems [1]. Such localized structures might be very useful in information technologies. As shown in Ref. [2], the gyrovector of hopfions, in contrast to skyrmions and vortices, is equal to zero. This property of hopfions eliminates the unwanted Hall effect, and makes their current induced motion straightforward. This property is an advantage of hopfions for using them as information carriers in 3D race-track memories. However, this result was obtained for hopfions in infinite magnetic films. We calculated the gyrovector of hopfions in laterally confined magnetic disc and observed, that if the radius of such disc is comparable with the size of hopfion the gyrovector might be nonzero. We obtained the value of the hopfion gyrovector as a function of the radius and thickness of such particles. Our results are important for the analysis of the dynamics of hopfions and their interaction with the elementary magnetic excitations, spin waves.

The research leading to these results has received funding from the Norwegian Financial Mechanism 2014-2021 project no UMO-2020/37/K/ST3/02450.

[1] Kent, N., Reynolds, N., Raftrey, D. et al. Creation and observation of Hopfions in magnetic multilayer systems. Nat. Commun. 12, 1562 (2021). <https://doi.org/10.1038/s41467-021-21846-5>

[2] X. S. Wang, A. Qaiumzadeh, and A. Brataas, Current-driven dynamics of magnetic hopfions, Phys. Rev. Lett. 123, 147203 (2021). <https://doi.org/10.1103/PhysRevLett.123.147203>

Modification of domain wall velocity in Ta/CoFeB/MgO due to voltage-induced non-volatile piezoelectric strain

S. Roy¹, A. Solignac², N. Montblanc³, T. Bhatnagar-Schöffmann¹, R. Pachat¹, A. Harouri¹, R. Juge^{1,3}, T. Maroutian¹, D. Ravelosona^{1,3}, G. Agnus¹ and L. Herrera Diez¹

¹Centre de Nanosciences et de Nanotechnologies, CNRS, Université Paris-Saclay, 91120 Palaiseau, France

²SPEC, CEA Saclay, CNRS, Université Paris-Saclay, 91191 Gif sur Yvette, France

³Spin-Ion technologies, C2N, 10 Boulevard Thomas Gobert, 91120 Palaiseau, France

Magnetic Domain Wall (DW) motion in ferromagnetic materials having perpendicular magnetic anisotropy (PMA) is an interesting topic both from the point of view of fundamental research and spintronics application [1,2]. In particular, strain-induced modification of magnetic properties in a hybrid piezoelectric/ferromagnetic heterostructure has been widely investigated for the past few years [3,4] due to its potential for low power spintronics applications. In this work, we have demonstrated the manipulation of DW motion in $Co_{40}Fe_{40}B_{20}$ (CoFeB) ferromagnetic films by using voltage-tuned anisotropic remnant strain from 011 cut piezoelectric PMN-PT substrate. Using polar magneto-optical Kerr effect (P-MOKE), we investigated the dependence of the DW dynamics and magnetic properties on the non volatile remnant strain from the piezoelectric substrate.

In conclusion, the presence of non volatile piezoelectric strain in hybrid structures gives a one-of-a-kind possibility for electric manipulation of DW dynamics, paving the way for low-power, energy-efficient device applications.

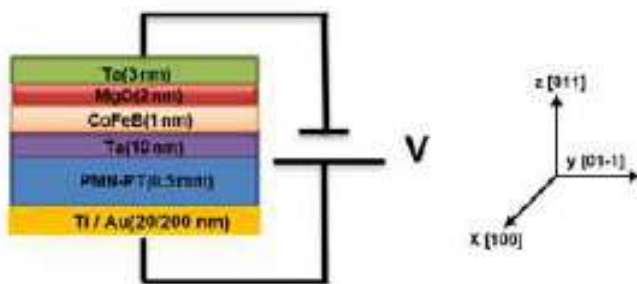


Figure 1: Schematic of the heterostructure

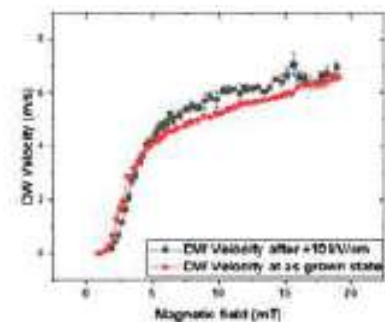


Figure 2: Non Volatile Strain induced DW velocity manipulation

- [1] S. Parkin, M. Hayashi and L. Thomas, *Science* **320**, (2008).
- [2] D. Allwood, G. Xiong, C. Faulkner, D. Atkinson, D. Petit and R. Cowburn, *Science* **309**, (2005).
- [3] Y. Yang, Q. Zhang, D. Wang, Y. Song, L. Wang, L. Lv, Q. Cao and Y. Du, *Applied Physics Letters* **103**, (2013).
- [4] P. Li, A. Chen, D. Li, Y. Zhao, S. Zhang, L. Yang, Y. Liu, M. Zhu, H. Zhang and X. Han, *Advanced Materials* **26**, (2014).

Spin-orbit torque engineering for efficient skyrmion motion

Yanis Sassi¹, Sachin Krishnia¹, Dédalo Sanz-Hernández¹, Sophie Collin¹,
Karim Bouzehouane¹, Albert Fert¹, Vincent Cros¹, Nicolas Reyren¹

¹ *Unité Mixte de Physique, CNRS, Thales, Université Paris-Saclay, 91167, Palaiseau, France*

Magnetic skyrmions are magnetic solitons in thin magnetic multilayers, which behave as particles and are topologically distinct from the uniform magnetization state. They have been identified as extremely promising for future applications (racetrack memory, neuromorphic computing, etc.), as well as of fundamental interest [1]. In fact, most of the research effort focused on material science in the last couple of years aimed at decreasing the skyrmion dimension [2] and enhance their stability. Even though the skyrmion dynamics through spin-orbit torques (SOT) have been investigated extensively [3], only a few studies specifically addressed the optimization of spin-orbit torques in skyrmion multilayers. This is precisely the purpose of this work.

We present SOT-induced motion of ferromagnetic skyrmions at room temperature, measured using MFM and/or MOKE microscopy in various magnetic Co/Pt based multilayer. First, we determine by harmonic measurements the actual amplitude of the damping-like and field-like SOT components in the different systems (Fig.1a). Then we display the evolution of the skyrmion velocity (Fig.1b) and skyrmion Hall angle and discuss the correlation with the torque measurements.

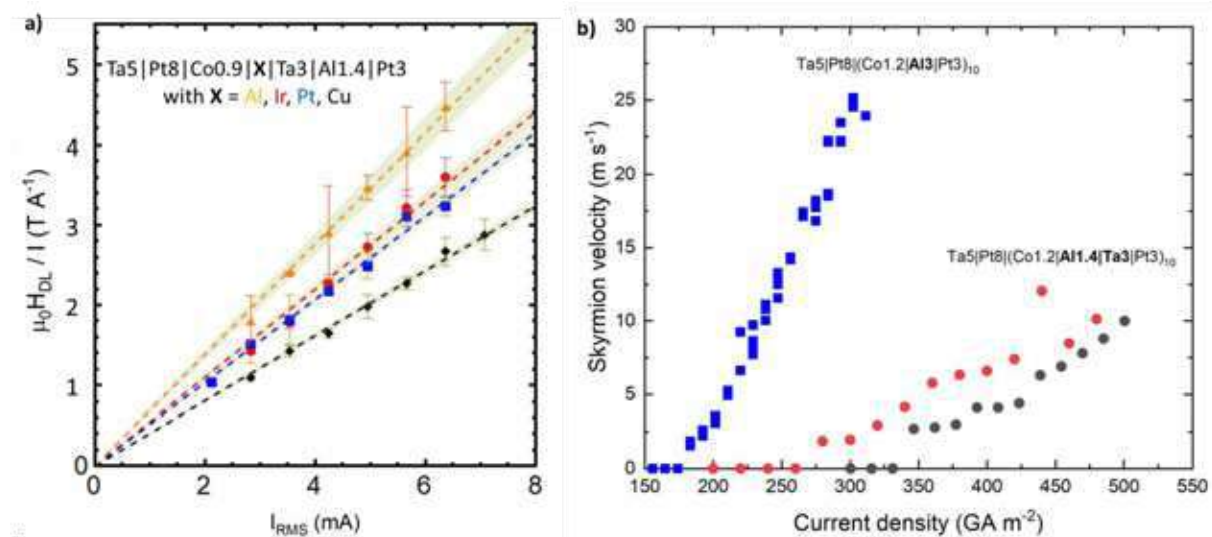


Figure 1: a) H_{DL} measurement for $Ta|Pt|Co|X|Ta|Al|Pt$ with ($X=Al, Ir, Pt \& Cu$) b) Skyrmion velocity as function of the current density for $(Pt|Co|Al|Pt)_{10}$ and $(Pt|Co|Al|Ta|Pt)_{10}$ (for two different track width). The current density is determined for the all thickness of the multilayer.

French ANR grant TOPSKY (ANR-17-CE24-0025), DARPA TEE program grant (MIPR#HR0011831554) and EU grant SKYTOP (H2020 FET Proactive 824123) are acknowledged for their financial support.

- [1] A. Fert, N. Reyren, V. Cros, Nat. Rev. Mat. 2 (2017), 17031.
- [2] C. Moreau-Luchaire et al, Nat. Nanotech, 11 (2016), 444 ; S. Woo et al, Nat. Mater. 15 (2016), 501 ; A. Soumyanarayanan et al, Nat. Mater. 16 (2017)
- [3] K. Litzius et al, Nat. Phys. 13 (2017), 170 ; S. Woo et al, Nat. Comm. 8 (2017), 15573.

Topological Hall effect in two-dimensional systems with skyrmion textures in the presence of electromagnetic impurities.

A.N. Zarezad¹, A. Qaiumzadeh², and A. Dyrda¹

¹*Department of Mesoscopic Physics, ISQI, Faculty of Physics, Adam Mickiewicz University,
ul. Uniwersytetu Poznańskiego 2, 61-614 Poznań, Poland*

²*Department of Physics, Norwegian University of Science and Technology, NO-7491
Trondheim, Norway*

We study the topological Hall effects (THE) in the two-dimensional systems containing the nontrivial skyrmion-like magnetic textures. We use the semi-classical Boltzmann approach to investigate THE derived from the asymmetric carrier scattering on skyrmion-like textures. In our calculation we consider effects of magnetic impurity and spin flip scattering on the spin and charge Hall effect and discuss possible modifications of the THE for different size of the skyrmion in both the weak and strong coupling regime.

- [1] Denisov K.S, *J Phys Condens Matter.* **32**, (2020).
- [2] Denisov K.S, et al., *Journal of Scientific reports* **7**, (2017).
- [3] Denisov K.S, et al., *Physical Review B* **98**, (2018).
- [4] Steven S.-L. Zhang and Olle Heinonen. *Physical Review B* **97**, (2018).

This work has been supported by the Norwegian Financial Mechanism 2014- 2021 under the Polish-Norwegian Research Project NCN GRIEG “2Dtronics” no. 2019/34/H/ST3/00515.

Symposium 14. Spin waves, magnonics, magnetoplasmonics, ultrafast magnetization dynamics, terahertz spintronics and optically driven spin excitations

| | | |
|---------------------------|---|-----|
| Edoardo Albisetti | <i>Three-dimensional nanoscale imaging of propagating spin waves via Time-Resolved X-ray Laminography</i> | 503 |
| Matthieu Bailleul | <i>Higgs and Goldstone spin-wave modes in striped magnetic texture</i> | 504 |
| Giovanni Carlotti | <i>Suppression of the spin waves non-reciprocity due to interfacial Dzyaloshinskii-Moriya interaction by lateral confinement in magnetic nanostructures</i> | 505 |
| Jarosław W. Kłos | <i>The topological interface modes in planar one-dimensional magnonic crystals</i> | 506 |
| Hannah Lange | <i>Polarized phonons carry the missing angular momentum in femtosecond demagnetization</i> | 507 |
| Tom S. Seifert | <i>Terahertz spin and charge currents: Insights into ultrafast spintronics and novel terahertz photonic applications</i> | 508 |
| Qi Wang | <i>Out-of-plane nanomagnonics for exchange spin waves</i> | 509 |
| Sebastian Wintz | <i>Direct imaging of spin-wave dynamics in a low-damping ferrimagnet close to antiferromagnetic compensation</i> | 510 |
| Maarten Beens | <i>Modeling ultrafast demagnetization and spin transport: the interplay of spin-polarized electrons and thermal magnons</i> | 514 |
| Vinayak Shantaram Bhat | <i>Tuning interactions in reconfigurable kagome artificial spin ices for magnonics</i> | 515 |
| Marcin Bialek | <i>Cavity-mediated magnon-magnon coupling at 0.3 THz</i> | 516 |
| David Alexander Breitbach | <i>Spin Hall driven spin-wave sources for magnonic conduits</i> | 517 |
| Charlotte Bull | <i>Effect of Cu doping on the emission of terahertz radiation from CoFeB/Pt_{1-x}Cu_x spintronic thin films</i> | 518 |
| Grzegorz Centała | <i>Magnetoelastic interactions between surface acoustic waves and spin waves in nanopatterned structure</i> | 519 |
| Avinash Kumar Chaurasiya | <i>Observation of Femtosecond Laser Comb Driven Magnetoelastic Modes</i> | 520 |
| Alexander Chekhov | <i>Spintronic detection of terahertz magnetic fields via Zeeman torque</i> | 521 |
| Stéphane Chiroli | <i>Magnonic and phononic modes in Ni₈₀Fe₂₀ array of antidots</i> | 522 |
| Andrii Chumak | <i>Non-reciprocal magnonic directional coupler</i> | 523 |
| Tobias Danneegger | <i>Ultrafast coherent all-optical switching of antiferromagnets</i> | 524 |
| Félix Dusabirane | <i>Electron-Magnon Scattering Dynamics in a 2-Band Stoner Model</i> | 525 |
| Robert Georgii | <i>Non-reciprocal magnons in non-centrosymmetric MnSi</i> | 526 |
| Matthias Golibrzuch | <i>Influencing spin waves with bistable nanomagnet patterns</i> | 527 |
| Paweł Gruszecki | <i>Excitation of leaky modes by obliquely incident spin wave beam onto magnonic Gires-Tournois interferometer and its impact on Goos-Hänchen effect for reflected beams</i> | 528 |

| | | |
|---------------------|--|-----|
| Martin Hennecke | <i>Ultrafast element- and depth-resolved magnetization dynamics probed by transverse magneto-optical Kerr effect spectroscopy in the soft x-ray range</i> | 529 |
| Emmanuelle Jal | <i>Unravelling the Transient Depth Magnetic Profile During Ultrafast Demagnetization of an Iron Thin Film</i> | 530 |
| Konrad J. Kapcia | <i>Role of electronic excitation, relaxation and transport processes for X-ray induced ultrafast demagnetization within magnetic multilayer systems</i> | 531 |
| Jan Klíma | <i>Steering spin waves in corrugated waveguides</i> | 532 |
| Sabri Koraltan | <i>Current driven spin-wave emissions from magnetic vortex cores</i> | 533 |
| Maciej Krawczyk | <i>A new look at spin-wave modes in a ferromagnetic nanorod</i> | 534 |
| Wolfgang Kuch | <i>Ultrafast Optically Induced Ferromagnetic State in an Elemental Antiferromagnet</i> | 535 |
| Mahathi Kuchibhotla | <i>Field orientation dependent magnetization dynamics in sub 100 nm wide magnetic wires</i> | 536 |
| Nikolai Kuznetsov | <i>Optical Control of Spin Waves in YIG/Plasmonic Heterostructures</i> | 537 |
| Kai Leckron | <i>Coulomb Scattering Contribution to Ultrafast Spin Dynamics in a Ferromagnetic Model System: Precession and Relaxation Dynamics</i> | 538 |
| Nikodem Leśniewski | <i>The impact of perpendicular anisotropy, Dzyaloshinskii–Moriya interaction and damping on spin wave dispersion and mode softening in thin magnetic films.</i> | 539 |
| Khrystyna Levchenko | <i>Towards fast exchange magnonics: partially compensated Ga:YIG garnets</i> | 540 |
| Yuefei Liu | <i>Magnon-magnon entanglement's detection and the phonon effects in antiferromagnetic structure</i> | 541 |
| Igor Lyubchanskii | <i>Goos-Hänchen effect at Brillouin light scattering by a magnetostatic wave in the Damon-Eshbach configuration</i> | 542 |
| Avishek Maity | <i>Presence of a sizable out-of-plane interaction in a stripe discommensurated 214-nickelate $\text{Pr}_2/2\text{Sr}/2\text{NiO}_4$ ($\epsilon = 0.4$)</i> | 543 |
| Evgeny Mashkovich | <i>THz-light driven spin-lattice coupling in cobalt difluoride.</i> | 544 |
| Hiroki Matsumoto | <i>Nonreciprocal propagation of surface acoustic waves in a CoFeB/Ru/CoFeB trilayer synthetic antiferromagnet</i> | 545 |
| Ivan Miranda | <i>Spin-lattice couplings and their effects in transition-metal magnetic crystals with ab-initio accuracy</i> | 546 |
| Mathieu Moalic | <i>Dynamic interactions between edge and bulk modes in an antidot lattice with perpendicular magnetic anisotropy</i> | 547 |
| Manuel Müller | <i>Optical detection of magnon-phonon coupling using $\mu\text{FR-MOKE}$ technique</i> | 548 |
| Daniele Narducci | <i>Modelling of magnetoelectric transducers for spin-wave generation</i> | 549 |
| Maryna Pankratova | <i>Heat-conserving three-temperature model for ultrafast magnetisation dynamics simulations</i> | 550 |
| Adrien Petrillo | <i>Using Propagating Spin Wave Spectroscopy to Probe Interfacial Phenomena Modified by an Electric Field</i> | 551 |
| Santa Pile | <i>No standing spin waves found in a rectangular permalloy microstrip under uniform magnetic excitation</i> | 552 |

| | | |
|-----------------------|--|-----|
| Philipp Pirro | <i>Nonlinear magnon-phonon processes in coherently driven microstructures</i> | 553 |
| Eva Prinz | <i>Does the orbital angular momentum of light influence ultrafast demagnetization?</i> | 554 |
| Ilya Razdolski | <i>Inverse magneto-plasmonics for laser-induced spin dynamics</i> | 555 |
| Christian Riedel | <i>Experimental Observation of Spin-Wave Diffraction Phenomena</i> | 556 |
| David Salomoni | <i>Reliable all-optical-switching in Tb/Co multilayers based tunnel junctions</i> | 557 |
| Luis Sánchez-Tejerina | <i>Purely Precessional All-Optical Femtosecond Magnetic Switching</i> | 558 |
| Rostyslav Serha | <i>Paramagnetic resonance in GGG at ultralow temperatures</i> | 559 |
| Titiksha Srivastava | <i>Nonlinear interactions between spin-wave modes probed by parametric excitation in YIG microstructures</i> | 560 |
| Felix Steinbach | <i>Accelerating double pulse all-optical write/erase cycles in metallic ferrimagnets</i> | 561 |
| Tanja Strusch | <i>Lateral spin pumping in an assembly of embedded $\text{Fe}_{60}\text{Al}_{40}$ nanostructures</i> | 562 |
| Silvia Tacchi | <i>Effect of the Dzyaloshinskii-Moriya interaction on the band diagram of one-dimensional magnonic crystals</i> | 563 |
| Vojtěch Uhlíř | <i>Ultrafast metamagnetic phase transition in FeRh driven by non-equilibrium electron dynamics</i> | 564 |
| Steffen Wittrock | <i>Exceptional points controlling oscillation death in coupled spintronic nano-oscillators</i> | 565 |
| Ondřej Wojewoda | <i>Dielectric nanoparticle enhanced Brillouin light scattering spectroscopy of spin waves</i> | 566 |
| Kelvin Yao | <i>All-optical switching on the nanometer scale excited and probed with femtosecond extreme ultraviolet pulses</i> | 567 |
| Rekha Agarwal | <i>Substrate dependence of THz emission from epitaxial-NiO/Pt heterostructures</i> | 569 |
| Nimisha Arora | <i>Spin wave dynamics as a metrological archetype for topologically protected spin structures (TSS)</i> | 570 |
| Adam Bonda | <i>All-optical study of interlayer exchange coupling in Fe/FexSi_{1-x} multilayers</i> | 571 |
| Irina Dolgikh | <i>Laser-induced Spin Dynamics In Ferrimagnetic Iron Garnets in High Magnetic Fields</i> | 572 |
| Abbass Hamadeh | <i>Parametric amplification of spin waves by surface acoustic waves</i> | 573 |
| Artsiom Kazlou | <i>Surface plasmon-assisted control of phase of photo-induced spin precession in Au/YIG:Co structures</i> | 574 |
| Nikolai Kuznetsov | <i>Spin-wave propagation and interference in microscopic YIG waveguides with submicron magnonic crystals</i> | 575 |
| Matthew McMaster | <i>Tunable NiFe Multilayers for High Frequency Applications</i> | 576 |
| Danny Thonig | <i>Spin-mixed states in non-collinear magnets</i> | 577 |

Invited Oral Presentations

| | | |
|-------------------|---|-----|
| Edoardo Albisetti | <i>Three-dimensional nanoscale imaging of propagating spin waves via Time-Resolved X-ray Laminography</i> | 503 |
| Matthieu Bailleul | <i>Higgs and Goldstone spin-wave modes in striped magnetic texture</i> | 504 |
| Giovanni Carlotti | <i>Suppression of the spin waves non-reciprocity due to interfacial Dzyaloshinskii-Moriya interaction by lateral confinement in magnetic nanostructures</i> | 505 |
| Jarosław W. Kłos | <i>The topological interface modes in planar one-dimensional magnonic crystals</i> | 506 |
| Hannah Lange | <i>Polarized phonons carry the missing angular momentum in femtosecond demagnetization</i> | 507 |
| Tom S. Seifert | <i>Terahertz spin and charge currents: Insights into ultrafast spintronics and novel terahertz photonic applications</i> | 508 |
| Qi Wang | <i>Out-of-plane nanomagnonics for exchange spin waves</i> | 509 |
| Sebastian Wintz | <i>Direct imaging of spin-wave dynamics in a low-damping ferrimagnet close to antiferromagnetic compensation</i> | 510 |

Three-dimensional nanoscale imaging of propagating spin waves via Time-Resolved X-ray Laminography

Davide Girardi¹, Simone Finizio², Guglielmo Rubini¹, Sina Mayr², Claire Donnelly³, Federico Maspero¹, Simone Cuccurullo¹, Jörg Raabe², Daniela Petti¹, Edoardo Albisetti¹

¹ *Dipartimento di Fisica, Politecnico di Milano, Via Giuseppe Colombo, 81 Milano 20133, Italy*

² *Paul Scherrer Institut, Forschungsstrasse 111 5232 PSI Villigen, SH, Switzerland*

³ *Max Planck Institute for Chemical Physics of Solids, Nöthnitzer Str. 40, 01187 Dresden, Germany*

Spin waves are one of the most interesting candidates for the development of next generation energy efficient devices for both digital and analog computing and signal processing. While the vast majority of the proposed spin-wave devices are based on planar structures, harnessing the third dimension has recently become one of the most desired capabilities for introducing new functionalities [1]. Nevertheless, the experimental visualization of propagating spin waves in three dimensions has been elusive, due to the harsh requirement of combining nanoscale spatial resolution in 3D, and time resolution across the GHz frequency range.

In this framework, recently, the Time-Resolved Soft X-Ray Laminography (TR-SoXL) technique has been developed at the PolLux beamline of the Swiss Light Source [2]. The TR-SoXL is a synchrotron-based technique that allows to obtain the three-dimensional time-resolved reconstructions of the magnetization dynamics [3] of thin samples, with nanoscale resolution.

Here, first we reconstruct the three-dimensional static magnetization configuration of a NiFe 40 / Ru 0.9 / CoFeB 50 (nm) synthetic antiferromagnet microstructure grown via magnetron sputtering. Then, we study its magnetization dynamics, via TR-SoXL. In particular, we demonstrate the three-dimensional imaging of spin waves which are emitted by nanoscale spin textures, i.e. vortices and domain walls [4] stabilized at 0 field within the microstructure, and study their propagation and in the synthetic antiferromagnet.

This work opens the way to the direct visualization and study of nanoscale propagating spin waves in three-dimensions, within thin films and 3D nanostructures. This in turn allows the design of vertically integrated magnonic devices exploiting the third dimension for novel functionalities.

- [1] G. Gubbiotti, *Three-Dimensional Magnonics*. Jenny Stanford Publishing (2019)
- [2] S. Finizio, C. Donnelly, S. Mayr, A. Hrabec, and J. Raabe, *Nano Lett.*, p. acs.nanolett.1c04662 (2022).
- [3] C. Donnelly *et al.*, *Nat. Nanotechnol.*, **15**, no. 5, pp. 356–360 (2020)
- [4] E. Albisetti *et al.*, *Adv. Mater.*, **32**, no. 9, p. 1906439 (2020)

Higgs and Goldstone spin-wave modes in striped magnetic texture

Matías Grassi¹, Moritz Geilen², Kosseila Ait Oukaci³,
Yves Henry¹, Daniel Lacour³, Daniel Stoeffler¹, Michel Hehn³,
Philipp Pirro² and Matthieu Bailleul¹

¹ Université de Strasbourg, CNRS, Institut de Physique et Chimie des Matériaux de Strasbourg, UMR 7504, F-67000 Strasbourg, France

² Fachbereich Physik and Landesforschungszentrum OPTIMAS, Technische Universität Kaiserslautern, 67663 Kaiserslautern, Germany

³ Institut Jean Lamour, Université de Lorraine, UMR 7198, CNRS, F-54000 Nancy, France

Spontaneous symmetry breaking is ubiquitous in physics. Its spectroscopic signature consists in the softening of a specific mode upon approaching the transition from the high symmetry side and its subsequent splitting into a zero-frequency ‘Goldstone’ mode and a non-zero-frequency ‘Higgs’ mode. Although they determine the whole system dynamics, these features are difficult to address in practice because of their vanishing coupling to most experimental probes and/or their strong interaction with other fluctuations.[1] In this work, we report experimental evidence of this spectroscopic signature in an archetypical system of micromagnetism, namely magnetic weak stripes.[2] We investigate a 180nm thick $\text{Co}_{40}\text{Fe}_{40}\text{B}_{20}$ film featuring a small perpendicular magnetic anisotropy K . Decreasing the in-plane field H down to a critical value of 12mT, we observe by magnetic force microscopy the nucleation a well-ordered weak stripe configuration with a wave-length λ_c of about 300nm. With the help of conventional Brillouin light scattering, we follow the spin-wave dispersions

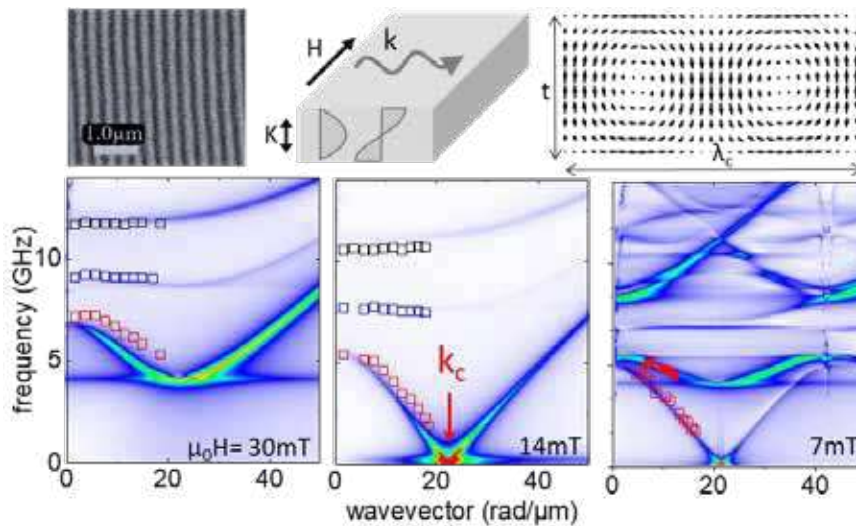


Figure (Bottom): Spin-wave dispersion in a 180nm CoFeB film under decreasing in-plane field H (color plot: simulation, symbols: Brillouin light scattering measurements). (Top): Magnetic force microscope picture of the weak stripe configuration. Spin-wave measurement geometry. Cross-section vector plot of the stripe modulation along one wavelength.

as function of the field.[3] We evidence a downward inflection of the lowest frequency spin-wave mode and a clear softening at the critical field which we associate to stripe nucleation. At smaller fields, we observe a splitting of this mode in two branches. Based on micromagnetic simulations and a simplified Landau theory analysis, we associate these two branches to the Higgs and Goldstone modes of the structure.

- [1] D. Pekker and C.M. Varma, *Annu. Rev. Condens. Matter Phys.* **6**, 269 (2015).
- [2] A. Hubert, R. Schafer, *Magnetic Domains* (Springer, Berlin-Heidelberg, 1998).
- [3] M. Grassi et al., arXiv:2110.00882.

Suppression of the spin waves non-reciprocity due to interfacial Dzyaloshinskii–Moriya interaction by lateral confinement in magnetic nanostructures

S. Tacchi¹, R. Silvani², M. Kuepferling³, A. Fernández Scarioni⁴, S. Sievers⁴, H.W. Schumacher⁴, M.A. Syskaki^{5,6}, G. Jakob⁵, M. Kläui⁵ and G. Carlotti^{2,1}

¹ IOM-CNR, c/o Department of Physics and Geology, University of Perugia, Italy

² Department of Physics and Geology, University of Perugia, Italy

³ Istituto Nazionale di Ricerca Metrologica, Torino, Italy

⁴ Physikalisch-Technische Bundesanstalt, Braunschweig, Germany

⁵ Institute of Physics, Johannes Gutenberg-University Mainz, Mainz, Germany

⁶ Singulus Technologies AG, Kahl, Germany

Even if several studies have been published in the last years about the interfacial Dzyaloshinskii–Moriya interaction (i-DMI) on spin waves (SW) propagation in extended films and multilayers, there is a lack of experimental data concerning the effect of i-DMI on the SW eigenmodes of laterally confined nanostructures. In this study we exploited Brillouin Light Scattering (BLS) to analyze the eigenmodes of arrays of non-interacting circular and elliptical dots, as well as of long stripes, patterned starting from a Pt(3.4 nm)/CoFeB(0.8 nm) bilayer, with lateral dimensions ranging from 100 to 400 nm, i.e. comparable with the wavelength of the thermal spin waves detected in BLS experiments. The aim of the experiments was to determine how the lateral confinement influences the SW non-reciprocity induced by the presence of the sizeable i-DMI supplied by the heavy-metal substrate (Pt) on the thin ferromagnetic film (CoFeB). As illustrated in Fig. 1 for the case of circular dots, our experimental results provide evidence for a strong suppression of the frequency asymmetry Δf between counter-propagating spin waves (corresponding to either Stokes or anti-Stokes peaks in BLS spectra), when the dot diameter is reduced from 400 nm to 100 nm, i.e. when it becomes lower than the light wavelength. Such an evolution reflects the modification of the SW character from propagating to stationary and indicates that the method of quantifying the i-DMI strength from the frequency difference of counter-propagating SW is not applicable in the case of sufficiently small magnetic elements. Micromagnetic simulations based on the MuMax³ software package, are in progress to quantitatively reproduce the above experimental results. Support from the project 17FUN08-TOPS, funded by the EU-EMPIR programme, and project IT-SPIN (PRIN-2020LWPKH7), funded by MUR, is acknowledged.

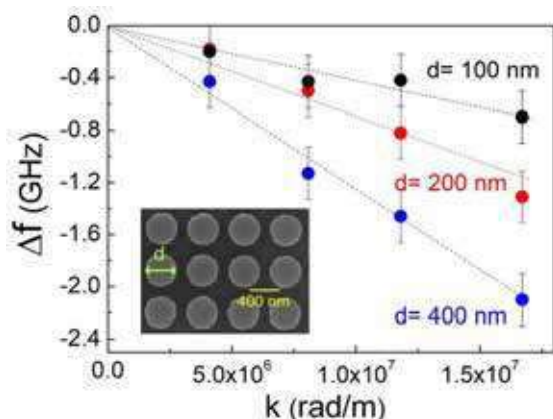


Figure 1: Measured values (dots) of the frequency asymmetry Δf between Stokes and anti-Stokes peaks in Brillouin Light Scattering spectra, measured on patterned arrays of circular magnetic Pt/CoFeB dots of diameter $d=100$ nm, 200 nm and 400 nm for different values of the spin-wave wavevector k . It can be seen that the frequency asymmetry is strongly suppressed for $d=100$ nm, if compared to the case of $d=400$ nm. The dashed lines are guides to the eye. The inset shows a scanning electron microscopy image of the sample with $d=400$ nm.

The topological interface modes in planar one-dimensional magnonic crystals

S. Mieszczak¹, and J. W. Kłos¹

¹ISQI, Faculty of Physics, Adam Mickiewicz University Poznań,
Universytetu Poznańskiego 2, 61-614 Poznań, Poland

Adiabatic change of the wavevector in the momentum space leads to the acquisition of a geometrical phase. These phase calculated on closed loop is topological characteristic. In a 1D system, a loop for the geometrical phase can be realized by swapping the wavenumber across the 1st Brillouin zone. To close the loop, we take advantage of the periodicity of the Bloch function in the reciprocal space. Referred to as the Zak phase, it characterizes each band of a 1D crystal and allows to relate topology of the band structure to the existence of surface/interface modes.

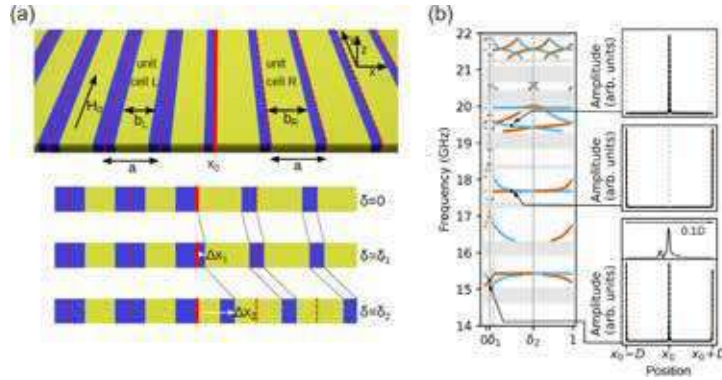


Figure 1: (a) Two semi-infinite magnonic crystals (made of Co and Py stripes: 500 nm wide and 20 nm thick), differing in filling fractions ($ff_L \neq ff_R$), interfaced at the edges of units cells (solid red line). For the magnonic crystal on the left (right) side, we chose a (non-)centrosymmetric unit cell. The parameter $\delta = \Delta x/a = [0, 1)$, describes the selection of the unit cell. (b) The spectrum in dependence on δ (gray areas – bands, blue/orange points – interface modes) for the field $\mu_0 H_0 = 0.2$ T, supplemented by the profiles of selected interface modes.

tween two semi-infinite MCs; (iii) the calculations done for the fictitious model, where the dipolar interactions were switched off, shows a close analogy to the electronic system; (iv) the numerical calculations performed for a realistic, dipolar-exchange system confirm the theoretical predictions regarding the existence of interface spin-wave modes.

The authors acknowledges the support from the National Science Center – Poland (grant No. 2020/37/B/ST3/03936)

The Zak phase and interface modes have been the subject of investigation in 1D continuous systems in the form of layered media or periodically corrugated waveguides, in photonics, plasmonics and phononics. We demonstrated that (i) the same standard formula for the Zak phase as used for electronic states; applies to both exchange and exchange-dipolar spin waves in 1D planar magnonic crystals (MCs); (ii) in MCs with centrosymmetric unit cell the Zak phase can be determined by a symmetry-related criterion, and the values of the Zak phase for successive bands can be used to investigate the existence of interface states on the boundary between two semi-infinite MCs; (iii) the calculations done for the fictitious model, where the dipolar interactions were switched off, shows a close analogy to the electronic system; (iv) the numerical calculations performed for a realistic, dipolar-exchange system confirm the theoretical predictions regarding the existence of interface spin-wave modes.

- [1] J. Rychły and J. W. Kłos, *J. Phys. D: Appl. Phys.* **50**, 164004 (2017).
- [2] S. Mieszczak, and J. W. Kłos, arXiv:2110.14726 [cond-mat.mes-hall].

Polarized phonons carry the missing angular momentum in femtosecond demagnetization

H. Lange¹, M. Evers¹, U. Nowak¹, S. Tauchert^{1,2}, M. Volkov^{1,2}, P. Baum^{1,2}

¹Universität Konstanz, Fachbereich Physik, 78464 Konstanz

²LMU München, Am Coulombwall 1, 85748 Garching

If a thin nickel film is subjected to ultrashort laser pulses, it can lose its magnetic order almost completely within merely femtosecond times. This phenomenon, which can also be observed in many other materials, offers opportunities for rapid information processing or ultrafast spintronics at frequencies approaching those of light. Consequently, ultrafast demagnetization is central to modern material research, but a crucial question has remained elusive: If a material loses its magnetization within only femtoseconds, where is the missing angular momentum on such short time scales?

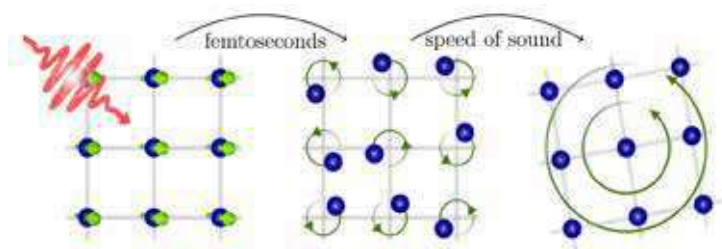


Figure 1: Sequence of events during the demagnetization process: After the laser (red) has impinged on the magnetized material (left panel), circularly polarized phonons with angular momentum are excited on femtosecond time scales (middle panel). The material is demagnetized at this point. Only later, low-frequency shear waves mediate a macroscopic rotation of the specimen as a whole (right panel).

Here we use molecular dynamics simulations to investigate the role of phonons during ultrafast demagnetization in nickel. For this purpose, we transfer angular momentum corresponding to the observed amount of demagnetization into the lattice and calculate the resulting changes in the diffraction pattern. Our results are in line with ultrafast electron diffraction measurements which show an almost instantaneous, long-lasting, non-equilibrium popu-

lation of anisotropic high-frequency phonons that appear as quickly as the magnetic order is lost. The anisotropy plane is perpendicular to the direction of the initial magnetization and the atomic oscillation amplitude is 2 pm. Theory and experiment indicate a rotational lattice motion on atomic dimensions after the excitation with the laser pulse that takes up the missing angular momentum [1] before the onset of a macroscopic Einstein-de Haas rotation [2].

Acknowledgements This research was supported by the German Research Foundation (DFG) via SFB 1432.

[1] S. R. Tauchert et al. *Nature* **602**, 73–77 (2022).

[2] C. Dornes et al. *Nature* **565**, 209–212 (2019).

Terahertz spin and charge currents: Insights into ultrafast spintronics and novel terahertz photonic applications

Tom S. Seifert¹, Oliver Gueckstock¹, Reza Rouzegar¹, Tobias Kampfrath¹

¹ Freie Universität Berlin, Arnimalle 14, 14195 Berlin, Germany

Spintronics aims at implementing the spin degree of freedom into conventional electronics. To be compatible and competitive, spintronic functionalities thus need to keep pace with the ever-increasing speeds of electronic devices that are foreseen to enter the terahertz range eventually [1]. Therefore, one needs to study fundamental spintronic phenomena at terahertz frequencies. Following this approach, one might not only hope to reveal new physics but also to apply these novel insights in terms of innovative terahertz photonic applications.

Here, I will discuss recent experimental efforts to study spin-to-charge current (S2C) conversion [2, 3, 4] effects in ferro-, ferri- and eventually antiferromagnetic systems at terahertz rates using an all-optical approach. The discussed S2C phenomena include the ultrafast analogues of the spin Hall effect [2], the spin Seebeck effect [5,6] as well as the anomalous Hall effect [7] in metallic as well as insulating magnetic systems. The gained knowledge can potentially further enhance the efficiency of a novel ultrafast spintronic application, namely the spintronic terahertz source, the potential of which I will also discuss in detail [8].

[1] Walowski, Jakob, and Markus Münzenberg. "Perspective: Ultrafast magnetism and THz spintronics." *Journal of Applied Physics* 120.14 (2016): 140901.

[2] Seifert, Tom, et al. "Efficient metallic spintronic emitters of ultrabroadband terahertz radiation." *Nature photonics* 10.7 (2016): 483-488.

[3] Gueckstock, Oliver, et al. "Terahertz Spin - to - Charge Conversion by Interfacial Skew Scattering in Metallic Bilayers." *Advanced Materials* 33.9 (2021): 2006281.

[4] Rouzegar, R., et al. "Laser-induced terahertz spin transport in magnetic nanostructures arises from the same force as ultrafast demagnetization." *arXiv preprint arXiv:2103.11710* (2021).

[5] Seifert, Tom S., et al. "Femtosecond formation dynamics of the spin Seebeck effect revealed by terahertz spectroscopy." *Nature communications* 9.1 (2018): 1-11.

[6] Jiménez-Cavero, Pilar, et al. "Tuning laser-induced terahertz spin currents from torque-to conduction-electron-mediated transport." *arXiv preprint arXiv:2110.05462* (2021).

[7] Seifert, Tom S., et al. "Frequency - Independent Terahertz Anomalous Hall Effect in DyCo5, Co32Fe68, and Gd27Fe73 Thin Films from DC to 40 THz." *Advanced Materials* 33.14 (2021): 2007398.

[8] Seifert, Tom S., et al. "Spintronic Sources of Ultrashort Terahertz Pulses." *arXiv preprint arXiv:2112.03070* (2021).

Out-of-plane nanomagnonics for exchange spin waves

Q. Wang^{1,2}, R. Verba³, B. Heinz⁴, M. Schneider⁴, C. Dubs⁵, P. Pirro⁴, and A. V. Chumak¹

¹ Faculty of Physics, University of Vienna, Vienna, Austria

² Research Platform MMM Mathematics-Magnetism-Materials, University of Vienna, Vienna, Austria

³ Institute of Magnetism, Kyiv, Ukraine

⁴ Fachbereich Physik and Landesforschungszentrum OPTIMAS, Technische Universität Kaiserslautern, Kaiserslautern, Germany

⁵ INNOVENT e.V., Technologieentwicklung, Jena, Germany

Magnonics is an emerging field of solid-state physics in which spin waves, the collective excitations of the magnetic order, are used for data transport and processing [1]. One of the spin-wave advantages is their short wavelengths down to a few nanometers that allows for magnonic devices of sizes comparable to CMOS [2]. Here we present a new approach to excite exchange spin waves with a wavelength down to around 200 nm in a 200 nm-wide yttrium iron garnet waveguide with a 2 μm -wide antenna, as shown in Fig. 1(a). The physical concept of the proposed method is based on the nonlinear phenomena that can be observed in the normally-magnetized waveguides for forward volume spin waves [3]. A very large magnetization precession angle of up to $\sim 60^\circ$ can be reached without triggering any spin-wave instabilities due to the geometric confinement and single-mode spin-wave dispersion curve in nanoscale waveguides. By using microfocus Brillouin light scattering (μBLS) spectroscopy, we observed an unprecedented 2.1 GHz up-shift of the FMR frequency due to such a large precession angle – see Fig. 1(b). The analytic calculations and micromagnetic simulations show that such a huge nonlinear frequency shift provides a large wavenumber conversion of up to 30 $\text{rad}/\mu\text{m}$ in k -space for spin waves propagating away from the antenna. This allows for the excitation of spin waves with wavelengths of ~ 200 nm, which are situated in the exchange regime. Consequently, these waves exhibit a large group velocity, which has been experimentally validated by time-resolved μBLS spectroscopy. Further simulations show that wavelengths down to 45 nm can be efficiently excited in out-of-plane magnetized CoFeB waveguides using this mechanism. The proposed method removes the wavelength limitations imposed by the size of conventional rf-antennas and allows for direct integration on-chip.

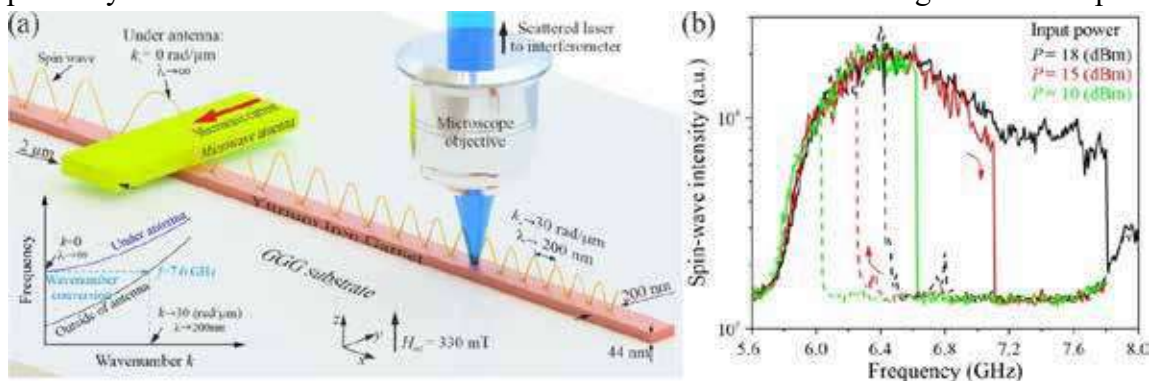


Figure 1: (a) The schematic picture of exchange spin-wave excitation using deep nonlinear dispersion shift. (b) The measured spin-wave spectra for different excitation powers.

[1] Q. Wang et al., *Nat. Electron.* **3**, 765 (2020). [2] S. Wintz et al., *Nat. Nano.* **11**, 948 (2016). [3] Y. Li et al., *Phys. Rev. X* **9**, 041036 (2019).

Direct imaging of spin-wave dynamics in a low-damping ferrimagnet close to antiferromagnetic compensation

S. Mayr^{1,2}, S. Finizio¹, J. Leliaert³, R. Gallardo⁴, M. Weigand⁵, F. Schulz⁶, J. Gräfe⁶, C. Dubs⁷, J. Bailey⁶, J. Reuteler², B. Van Waeyenberge³, H. Stoll^{6,8}, G. Schütz⁶, J. Raabe¹, S. Wintz⁶

¹ Paul Scherrer Institut, Villigen PSI, Switzerland

² ETH Zürich, Zürich, Switzerland

³ Ghent University, Ghent, Belgium

⁴ UT Federico Santa Maria, Valparaíso, Chile

⁵ Helmholtz-Zentrum Berlin, Berlin, Germany

⁶ Max-Planck-Institut für Intelligente Systeme, Stuttgart, Germany

⁷ Innovent e.V. Technologieentwicklung, Jena, Germany

⁸ Institute of Physics, Johannes Gutenberg University Mainz, Mainz, Germany

Spin waves have been studied extensively in the past, both from a fundamental point of view and in prospect of their potential application as information carriers in future spintronic logic and memory devices. For most application scenarios, it will be indispensable to utilize short-wavelength spin waves and materials with low magnetic damping. In that respect, ferrimagnetic yttrium-iron-garnet (YIG) stands out with the highest known magnon life time of all materials. Antiferromagnetic materials on the other hand exhibit ultrafast spin dynamics with frequencies up to the THz range, thereby providing potential benefits for fast spin-wave signal processing. We aim at combining these properties by studying sub-micron spin waves in YIG films that are doped with gallium (Ga) in order to approach antiferromagnetic compensation. Such films were grown by liquid-phase-epitaxy on bulk gadolinium-gallium-garnet (GGG) substrates. We directly imaged GHz spin-wave dynamics in these films by time-resolved scanning transmission x-ray microscopy (TR-STXM). For that purpose, we developed a thinning process to reach soft x-ray transmissivity, employing a combination of mechanical lapping and xenon focused ion beam (FIB) etching from the substrate side (see Fig. 1a) [1]. Spin waves in the Ga-doped YIG were excited using a lithographically patterned microstrip antenna and they exhibited significant propagation lengths (see Fig. 1b,c), confirming the low magnetic damping of the material [2]. We observed an almost isotropic spin-wave dispersion, which suggests that the corresponding waves are already exchange dominated, even for wavelengths above 100 nm. This situation can be explained by the large exchange length of the material, as a result of its low net magnetization. In addition, we observed a strong amplitude nonlinearity in the spin-wave excitation process, leading to a local isotropic emission and exceptionally high spin-wave amplitudes, exceeding precession cone angles of 50°. Our results are in line with complement findings from other groups [3,4].

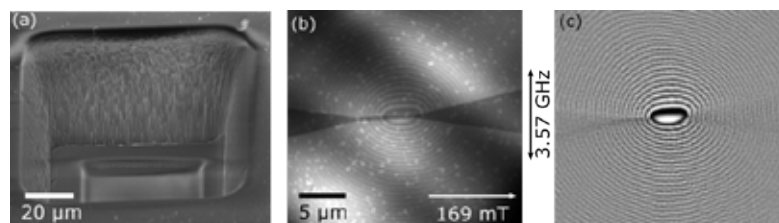


Fig. 1: (a) SEM image of a membrane window etched out of GGG substrate by FIB. (b,c) TR-STXM snapshots displaying spin waves. (b) Absolute absorption image with both topographic and out-of-plane magnetic contrast. (c) Normalized image showing only the temporal magnetic changes with respect to the time average.

[1] S. Mayr, *et al.*, Crystals **11**, 5 (2021).

[2] S. Mayr, *et al.*, (unpublished) (2022).

[3] J. J. Carmiggelt *et al.*, APL **119**, 202403 (2021).

[4] T. Böttcher *et al.*, arXiv 2112.11348 (2021).

Oral Presentations

| | | |
|---------------------------|---|-----|
| Maarten Beens | <i>Modeling ultrafast demagnetization and spin transport: the interplay of spin-polarized electrons and thermal magnons</i> | 514 |
| VinayakShantaram Bhat | <i>Tuning interactions in reconfigurable kagome artificial spin ices for magnonics</i> | 515 |
| Marcin Białek | <i>Cavity-mediated magnon-magnon coupling at 0.3 THz</i> | 516 |
| David Alexander Breitbach | <i>Spin Hall driven spin-wave sources for magnonic conduits</i> | 517 |
| Charlotte Bull | <i>Effect of Cu doping on the emission of terahertz radiation from CoFeB/Pt_{1-x}Cu_x spintronic thin films</i> | 518 |
| Grzegorz Centała | <i>Magnetoelastic interactions between surface acoustic waves and spin waves in nanopatterned structure</i> | 519 |
| Avinash Kumar Chaurasiya | <i>Observation of Femtosecond Laser Comb Driven Magnetoelastic Modes</i> | 520 |
| Alexander Chekhov | <i>Spintronic detection of terahertz magnetic fields via Zeeman torque</i> | 521 |
| Stéphane Chiroli | <i>Magnonic and phononic modes in Ni₈₀Fe₂₀ array of antidots</i> | 522 |
| Andrii Chumak | <i>Non-reciprocal magnonic directional coupler</i> | 523 |
| Tobias Danneegger | <i>Ultrafast coherent all-optical switching of antiferromagnets</i> | 524 |
| Félix Dusabirane | <i>Electron-Magnon Scattering Dynamics in a 2-Band Stoner Model</i> | 525 |
| Robert Georgii | <i>Non-reciprocal magnons in non-centrosymmetric MnSi</i> | 526 |
| Matthias Golibrzuch | <i>Influencing spin waves with bistable nanomagnet patterns</i> | 527 |
| Paweł Gruszecki | <i>Excitation of leaky modes by obliquely incident spin wave beam onto magnonic Gires-Tournois interferometer and its impact on Goos-Hänchen effect for reflected beams</i> | 528 |
| Martin Hennecke | <i>Ultrafast element- and depth-resolved magnetization dynamics probed by transverse magneto-optical Kerr effect spectroscopy in the soft x-ray range</i> | 529 |
| Emmanuelle Jal | <i>Unravelling the Transient Depth Magnetic Profile During Ultrafast Demagnetization of an Iron Thin Film</i> | 530 |
| Konrad J. Kapcia | <i>Role of electronic excitation, relaxation and transport processes for X-ray induced ultrafast demagnetization within magnetic multilayer systems</i> | 531 |
| Jan Klíma | <i>Steering spin waves in corrugated waveguides</i> | 532 |
| Sabri Koraltan | <i>Current driven spin-wave emissions from magnetic vortex cores</i> | 533 |
| Maciej Krawczyk | <i>A new look at spin-wave modes in a ferromagnetic nanorod</i> | 534 |
| Wolfgang Kuch | <i>Ultrafast Optically Induced Ferromagnetic State in an Elemental Antiferromagnet</i> | 535 |
| Mahathi Kuchibhotla | <i>Field orientation dependent magnetization dynamics in sub 100 nm wide magnetic wires</i> | 536 |
| Nikolai Kuznetsov | <i>Optical Control of Spin Waves in YIG/Plasmonic Heterostructures</i> | 537 |
| Kai Leckron | <i>Coulomb Scattering Contribution to Ultrafast Spin Dynamics in a Ferromagnetic Model System: Precession and Relaxation Dynamics</i> | 538 |

| | | |
|-----------------------|--|-----|
| Nikodem Leśniewski | <i>The impact of perpendicular anisotropy, Dzyaloshinskii–Moriya interaction and damping on spin wave dispersion and mode softening in thin magnetic films.</i> | 539 |
| Khrystyna Levchenko | <i>Towards fast exchange magnonics: partially compensated Ga:YIG garnets</i> | 540 |
| Yuefei Liu | <i>Magnon-magnon entanglement's detection and the phonon effects in antiferromagnetic structure</i> | 541 |
| Igor Lyubchanskii | <i>Goos-Hänchen effect at Brillouin light scattering by a magnetostatic wave in the Damon-Eshbach configuration</i> | 542 |
| Avishek Maity | <i>Presence of a sizable out-of-plane interaction in a stripe discommensurated 214-nickelate $\text{Pr}_2/2\text{Sr}_2/2\text{NiO}_4$ ($\epsilon = 0.4$)</i> | 543 |
| Evgeny Mashkovich | <i>THz-light driven spin-lattice coupling in cobalt difluoride.</i> | 544 |
| Hiroki Matsumoto | <i>Nonreciprocal propagation of surface acoustic waves in a CoFeB/Ru/CoFeB trilayer synthetic antiferromagnet</i> | 545 |
| Ivan Miranda | <i>Spin-lattice couplings and their effects in transition-metal magnetic crystals with ab-initio accuracy</i> | 546 |
| Mathieu Moalic | <i>Dynamic interactions between edge and bulk modes in an antidot lattice with perpendicular magnetic anisotropy</i> | 547 |
| Manuel Müller | <i>Optical detection of magnon-phonon coupling using μFR-MOKE technique</i> | 548 |
| Daniele Narducci | <i>Modelling of magnetoelectric transducers for spin-wave generation</i> | 549 |
| Maryna Pankratova | <i>Heat-conserving three-temperature model for ultrafast magnetisation dynamics simulations</i> | 550 |
| Adrien Petrillo | <i>Using Propagating Spin Wave Spectroscopy to Probe Interfacial Phenomena Modified by an Electric Field</i> | 551 |
| Santa Pile | <i>No standing spin waves found in a rectangular permalloy microstrip under uniform magnetic excitation</i> | 552 |
| Philipp Pirro | <i>Nonlinear magnon-phonon processes in coherently driven microstructures</i> | 553 |
| Eva Prinz | <i>Does the orbital angular momentum of light influence ultrafast demagnetization?</i> | 554 |
| Ilya Razdolski | <i>Inverse magneto-plasmonics for laser-induced spin dynamics</i> | 555 |
| Christian Riedel | <i>Experimental Observation of Spin-Wave Diffraction Phenomena</i> | 556 |
| David Salomoni | <i>Reliable all-optical-switching in Tb/Co multilayers based tunnel junctions</i> | 557 |
| Luis Sánchez-Tejerina | <i>Purely Precessional All-Optical Femtosecond Magnetic Switching</i> | 558 |
| Rostyslav Serha | <i>Paramagnetic resonance in GGG at ultralow temperatures</i> | 559 |
| Titiksha Srivastava | <i>Nonlinear interactions between spin-wave modes probed by parametric excitation in YIG microstructures</i> | 560 |
| Felix Steinbach | <i>Accelerating double pulse all-optical write/erase cycles in metallic ferrimagnets</i> | 561 |
| Tanja Strusch | <i>Lateral spin pumping in an assembly of embedded $\text{Fe}_{60}\text{Al}_{40}$ nanostructures</i> | 562 |
| Silvia Tacchi | <i>Effect of the Dzyaloshinskii-Moriya interaction on the band diagram of one-dimensional magnonic crystals</i> | 563 |

| | | |
|------------------|--|-----|
| Vojtěch Uhlíř | <i>Ultrafast metamagnetic phase transition in FeRh driven by non-equilibrium electron dynamics</i> | 564 |
| Steffen Wittrock | <i>Exceptional points controlling oscillation death in coupled spintronic nano-oscillators</i> | 565 |
| Ondřej Wojewoda | <i>Dielectric nanoparticle enhanced Brillouin light scattering spectroscopy of spin waves</i> | 566 |
| Kelvin Yao | <i>All-optical switching on the nanometer scale excited and probed with femtosecond extreme ultraviolet pulses</i> | 567 |

Modeling ultrafast demagnetization and spin transport: the interplay of spin-polarized electrons and thermal magnons

M. Beens¹, R.A. Duine^{1,2} and B. Koopmans¹

¹ Eindhoven University of Technology, 5600 MB Eindhoven, The Netherlands

² Institute for Theoretical Physics, Utrecht University, 3584 CE Utrecht, The Netherlands

Heating magnetic heterostructures with a femtosecond laser pulse generates spin currents on ultrashort time scales [1]. Their unique transient dynamics leads to exciting physics in magnetic multilayers and paves the way towards future spintronic applications. The microscopic origin of laser-induced spin dynamics is still heavily debated. Recent experimental [2] and theoretical [3] studies suggest the important role of electron-magnon scattering, which leads to demagnetization by the generation of thermal magnons, and acts as a source that drives spin transport [2,3,4].

In this work, we model spin transport in rapidly heated magnetic heterostructures, including transport by magnons. We assume that electron-magnon scattering is the driving force of the observed ultrafast spin dynamics and make use of a diffusive description of spin transport that treats itinerant electrons and magnons on an equal footing. We specifically address the relation between the interfacial spin current and the magnetization. In agreement with recent experiments [5,6], we find a direct proportionality between the injected spin current and the temporal derivative of the magnetization, as shown in Fig. 1. Based on an analytical calculation, we discuss that other behavior may arise if the spin current receiving material

displays inefficient spin-flip scattering. Furthermore, we investigate the role of magnon transport, and show in what regime it plays a significant role. Our results imply that magnon transport cannot be neglected a priori. Whether it plays a significant role strongly depends on the material properties. We discuss the underlying physics for various system parameters and situations.

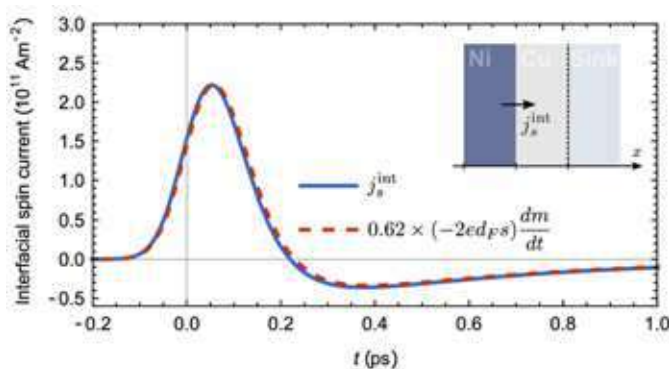


Figure 1: Interfacial spin current (blue) and the (scaled) temporal derivative of the magnetization (dashed red) as a function of time after laser-pulse excitation.

- [1] G. Malinowski, F. Dalla Longa, J.H.H. Rietjens, et al., *Nature Physics* **4**, 855, (2008)
- [2] G.-M. Choi, B.-C. Min, K.-J. Lee, and D.G. Cahill, *Nature Communications* **5**, 4334 (2014)
- [3] E.G. Tveten, A. Brataas, and Y. Tserkovnyak, *Physical Review B* **92**, 180412(R) (2015)
- [4] M. Beens, R.A. Duine, B. Koopmans, *Physical Review B* **102**, 054442 (2020)
- [5] S.M. Rouzegar, L. Brandt, L. Nádovnik, D.A. Reiss, et al., arXiv: 2103.11710 (2021)
- [6] T. Lichtenberg, M. Beens, M.H. Jansen, R.A. Duine, and B. Koopmans, arXiv: 2103.06029 (2021)

Tuning interactions in reconfigurable kagome artificial spin ices for magnonics

Vinayak S. Bhat¹ and Dirk Grundler^{2,3}

¹ *International Research Centre MagTop, Institute of Physics, Polish Academy of Sciences, PL-02668 Warsaw, Poland*

² *Institute of Materials, Laboratory of Nanoscale Magnetic Materials and Magnonics, School of Engineering, Ecole Polytechnique Fédérale de Lausanne, 1015 Lausanne, Switzerland.*

³ *Institute of Electrical and Microengineering, Ecole Polytechnique Fédérale de Lausanne, 1015 Lausanne, Switzerland*

We investigate spin dynamics of a kagome artificial spin ices (KASIs) consisting of Ni₈₁Fe₁₉ nanomagnets arranged on a disconnected kagome lattice [1, 2] using broadband ferromagnetic resonance (FMR) and micromagnetic simulations. Two KASI samples were prepared using ebeam lithography and lift-off techniques [3]. Each KASI covered a writefield area of $120 \times 120 \mu\text{m}^2$, and was repeated on a 35×5 array to increase the signal-to-noise ratio in broadband spectroscopy measurements. The nominal length, width, and thickness of a Ni₈₁Fe₁₉ nanobar were kept at 400 nm, 130 nm, and 25 nm, respectively. The shortest distances between two nanobars in samples named Sample-I and Sample-II were 60 nm and 300 nm, respectively. We observed spin wave spectra that varied characteristically upon the separation between the two nanobars resulting into distinct slope changes in frequency vs. H and depends upon topological defect configuration. We further studied reprogrammable characteristics of spin wave spectra in strongly and weakly dipolarly coupled kagome artificial spin ices. Our work shows disconnected KASIs are promising for reprogrammable spin wave guiding in underlayers.

Acknowledgments: The research was supported by the Swiss National Science Foundation via Grant No. 163016. V. S. Bhat acknowledges support from the foundation for Polish Science through the IRA Programme financed by EU within SG OP Programme.

References:

- [1] E. Mengotti, L. J. Heyderman, A. F. Rodríguez, F. Nolting, R. V. Huergli, and H.-B. Braun, *Nat. Phys.* 7, 68 (2011).
- [2] M. Krawczyk and D. Grundler, *J. Phys.: Condens. Matter* 26, 123202 (2014).
- [3] V. S. Bhat and D. Grundler, *Appl. Phys. Letts.* 119 (9), 092403 (2021).

Cavity-mediated magnon-magnon coupling at 0.3 THz

M. Bialek¹, Anhua Wu², and J.-Ph. Ansermet¹

¹*Institute of Physics, École Polytechnique Fédérale de Lausanne (EPFL), Switzerland*

²*Shanghai Institute of Ceramics Chinese Academy of Sciences, China*

In the regime of strong light-matter coupling, polariton modes are formed that are hybrid light-matter excitations sharing properties of both, a cavity mode and a matter mode. Recently, magnon-polaritons are intensively researched in ferromagnetic materials in the microwave range, but they can be also obtained in the THz range with antiferromagnetic resonance (AFMR) [1]. Here, we report on cavity-mediated magnon-magnon coupling in a system consisting of two parallel-plane crystals forming a Fabry-Perot type cavity. A crystal of yttrium ferrite (YFeO₃) is kept at room temperature, while a crystal of hematite (α -Fe₂O₃) is fixed on a copper mirror placed on a heater. We used a monochromatic continuous-wave spectrometer operating in the range of 0.2-0.35 THz that is based on frequency extenders to a vector network analyzer. Reflection spectra measured as function of hematite temperature T (Fig.1a) show a series of cavity modes that form avoided crossings with AFMR in hematite, frequency of which is rising with T . By measuring temperature-differential (Fig.1b) of these spectra, we reveal only cavity modes coupled to the AFMR in hematite, because AFMR in YFeO₃ does not depend on T . Differential to external magnetic field H (Fig.1c) reveals only cavity modes coupled to the AFMR in YFeO₃, since H is applied in a direction that does not change AFMR in hematite. Differential to gap d between the two crystals (Fig.1d) reveals the cavity modes. Under certain distance between the crystals, at about 0.3 THz where there is AFMR in YFeO₃, we can observe cavity modes that are strongly coupled to AFMR in both crystals.

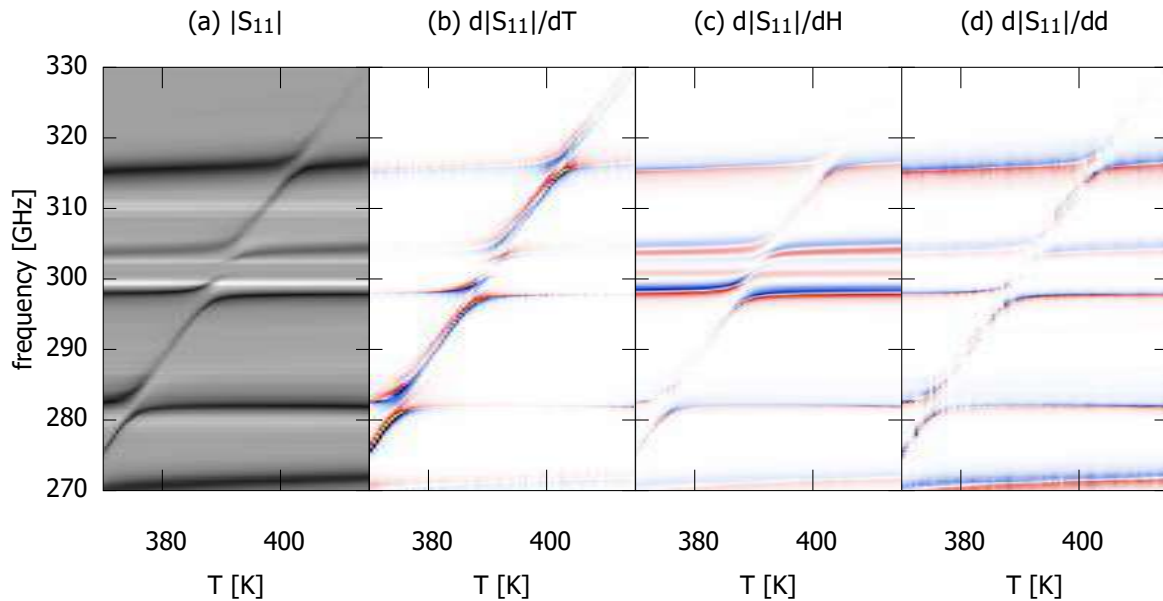


Figure 1: (a) Reflection magnitude, (b) temperature differential, (c) magnetic field differential, (d) differential to gap between the crystals.

[1] M. Bialek et al, Physical Review Applied **15** 044018 (2021).

Spin Hall driven spin-wave sources for magnonic conduits

David A. Breitbach¹, Michael Schneider¹, Laura Scheuer¹, Felix Kohl¹, Rostyslav Serha², Björn Heinz¹, Jan Maskill¹, Thomas Brächer¹, Bert Lägel¹, Carsten Dubs³, Burkard Hillebrands¹, Andrii Chumak² and Philipp Pirro¹

¹*Fachbereich Physik and Landesforschungszentrum OPTIMAS, Technische Universität Kaiserslautern, D-67663 Kaiserslautern, Germany*

²*Faculty of Physics, University of Vienna, A-1090 Vienna, Austria*

³*INNOVENT e.V. Technologieentwicklung, D-07745 Jena, Germany*

Spin currents have been used extensively in the research field of magnon spintronics, as they allow to compensate the damping of magnonic systems [1,2] and the generation of coherent, nonlinear magnetic auto-oscillations [3]. Providing a method of conversion of simple electric DC currents into a magnetic oscillation, spin current driven auto-oscillators represent an attractive source for GHz radiation in the magnetic domain [4,5]. However, their application as a source for propagating spin waves is very limited, given the self-confining nature of the oscillation. Here, we report on the spin-wave emission of an auto-oscillator into a microscopic magnonic waveguide. Our system under study consists of a 2- μm -wide ultralow-damping yttrium iron garnet (YIG) waveguide, transversely magnetized by an in-plane field, into which a spin current is injected locally from a 2- μm -long and 7-nm-thick platinum pad using the spin Hall effect (SHE). Using time- and space-resolved Brillouin-light-scattering spectroscopy, we investigate the spin dynamics at the platinum injector and in the adjacent bare YIG waveguide. Upon increasing the DC current density, we find two thresholds, the first one corresponding to a compensation of the intrinsic damping losses, which leads to an auto-oscillation localized below the spin current injection area, and the second, slightly larger one corresponding to a compensation of radiative losses. For spin current injection exceeding the second threshold, modes of higher radiative losses are excited, which is seen experimentally by the emission of propagating spin-waves, despite the frequency of the localized auto-oscillation being well below the bottom of the spin-wave spectrum.

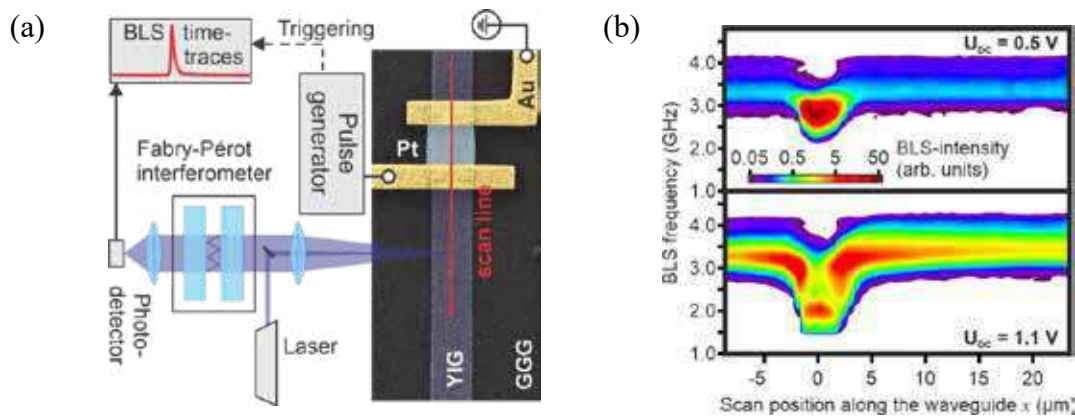


Figure 1: (a) Experimental setup and sample geometry. (b) Spatially resolved BLS-intensity along the waveguide for different current densities (center of injector at $x = 0 \mu\text{m}$).

- [1] Hamadeh, A. *et al.*, Phys. Rev. Lett. **113**, 197203 (2014).
- [2] Evelt, M. *et al.*, Appl. Phys. Lett. **108**, 172406 (2016).
- [3] Lauer, V. *et al.*, IEEE Magn. Lett. **8**, 1-4 (2017).
- [4] Collet, M. *et al.*, Nat. Commun. **7**, 10377 (2016).
- [5] Evelt, M. *et al.*, Phys. Rev. Appl. **10**, 041002 (2018).

Effect of Cu doping on the emission of terahertz radiation from CoFeB/Pt_{1-x}Cu_x spintronic thin films

C. Bull,^{1,2} C.-H. Lin,² R. Ji,² S. Hewett,² T. Thomson,¹ D. Graham,² & P. W. Nutter¹

¹ Nano Engineering and Spintronic Technologies Group, University of Manchester, Manchester, UK

² Photon Science Institute, Dept. of Physics & Astronomy, University of Manchester, Manchester, UK

The ability to generate and control pulses of terahertz (THz) radiation has mediated the advance of non-invasive, investigative technologies for material characterisation, medical diagnosis and weapon detection [1]. Pulses of THz radiation have potential applications in ultrafast control of electron spin states [2] and picosecond magnetisation switching in ferrimagnets and antiferromagnets [3]. Such applications require sources that generate THz pulses with high electric field amplitudes, broad spectral bandwidths and gapless coverage over the full THz spectral region (1-10 THz) [1]. Spintronic emitters, consisting of ferromagnetic (FM)/non-magnetic (NM) thin films, can produce THz pulses with gapless bandwidths of up to 30 THz [4]. In these systems, high THz electric field amplitudes of up to 300 kV/cm [4] can be achieved by combining appropriate FM and NM materials and by choosing a NM material with a large spin-Hall angle, α_H , such as Pt [1].

Recently, it has been shown that doping Pt with Au [5], Cu [6] or N [7] can increase α_H of Pt by up to 75% [5], thus providing a potential to increase the amplitude of the emitted THz pulse through engineering of the Pt layer. A decrease in longitudinal conductivity is observed with doping, therefore the increase in α_H may be attributed to increased electron scattering, due to introducing impurities into the Pt layer [5].

We investigate the effect of Cu doping on the emission of THz radiation from Co₂₀Fe₆₀B₂₀ (2.5 nm)/Pt_{1-x}Cu_x (2 nm) thin films, for $0 \leq x \leq 80$ at %. The films were grown onto fused silica substrates by DC magnetron sputtering (Co₂₀Fe₆₀B₂₀) and co-sputtering (Pt and Cu). Structural properties were characterised using X-ray photon spectroscopy, providing elemental composition, and X-ray diffraction (XRD) (Fig. 1) showing a reduction in crystallinity of the Pt layer with increasing Cu content. Terahertz time-domain spectroscopy (THz-TDS) was used to measure the amplitude of the THz electric field (E_{THz}) (Fig. 2). Initial studies show that Cu doping influences E_{THz} . A full analysis of our results will be presented at the conference.

[1] C. Bull *et al.*, APL Mater. **9**, 090701 (2021). [2] S. Baierl *et al.*, Nat. Photonics **10**, 715 (2016). [3] S. Wienholdt *et al.*, Phys. Rev. Lett. **108**, 247207 (2012). [4] T. Seifert *et al.*, Nat. Photonics **10**, 483 (2016). [5] M. Meinert *et al.*, Phys. Rev. Appl. **14**, 064011 (2020). [6] G. Wong *et al.*, Sci. Rep. **10**, 9631 (2020). [7] Z. Xu *et al.*, Appl. Phys. Lett. **118**, 062406 (2021).

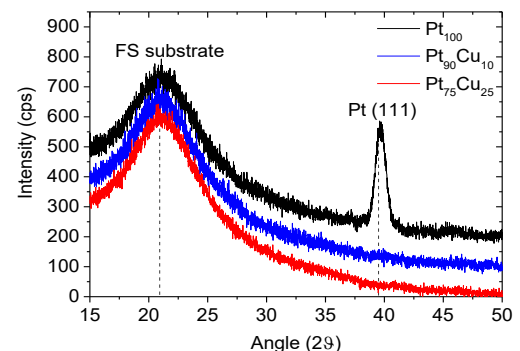


Fig. 1: XRD spectra for Pt_{1-x}Cu_x (4 nm) films with increasing Cu content.

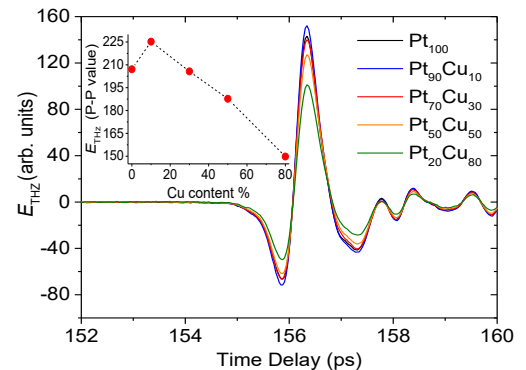


Fig. 2: E_{THz} generated from CoFeB (2.5 nm)/Pt_{1-x}Cu_x (2 nm) emitters, measured by THz-TDS. Inset shows peak-peak E_{THz} with increasing Cu content.

Magnetoelastic interactions between surface acoustic waves and spin waves in nanopatterned structure

G. Centała¹, P. Graczyk², and J. W. Kłos¹

¹ISQI, Faculty of Physics, Adam Mickiewicz University Poznań,
Uniwersytetu Poznańskiego 2, 61-614 Poznań, Poland

²Institute of Molecular Physics, Polish Academy of Sciences,
M. Smoluchowskiego 17, 60-179 Poznań, Poland

In the system where the magnetostrictive layer is deposited on non-magnetic substrate, the spin waves (SWs) can interact with surface acoustic waves (SAWs) in a strongly anisotropic manner [1]. This interaction depends both on the direction of the applied magnetic field and the polarisation of SAW [2]. The matching between the wave vectors of SAW and SW is necessary to avoid the spatial averaging of the dynamic interaction for propagating plane waves and observe the coupling between them [2]. This picture is more complicated for the SWs propagating in the nanostructures.

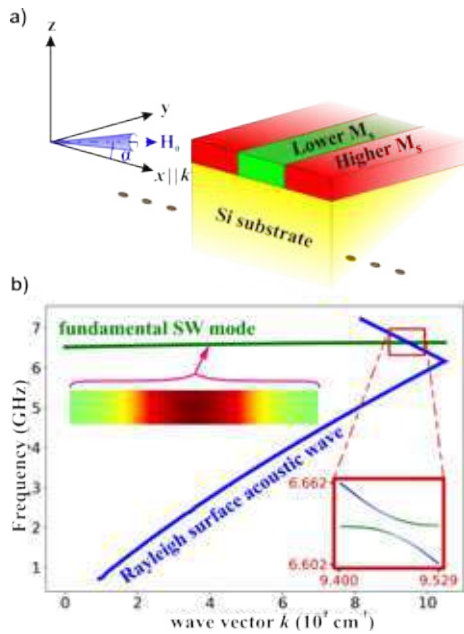


Figure 1: (a) The unit cell of considered system. External magnetic field H_0 is applied at oblique angle to the wave vector k (for SAWs and SWs). (b) The dispersion relation of SAW (Rayleigh wave) and SW with interaction magnified in the red box (for magnetoelastic coupling constants $b_1 = 4.39 \times 10^5 \frac{\text{J}}{\text{m}^3}$, $b_2 = 8.77 \times 10^5 \frac{\text{J}}{\text{m}^3}$). Marked with pink arrow: the profile of the in-plane dynamic magnetization.

We extended our previous work [1] and considered the impact of the patterning on magnetoelastic interactions. Using the finite element method, we calculated the magnetoelastic dispersion relation for an array of thin (30 nm) stripes (of the width 200 nm or 100 nm) differing in saturation magnetization ($M_s = 475$ or $95 \frac{\text{kA}}{\text{m}}$, respectively) but identical in terms of elastic properties ($c_{11}=260 \text{ GPa}$, $c_{12}=176 \text{ GPa}$, $c_{44}=39 \text{ GPa}$, $\rho=11535 \frac{\text{kg}}{\text{m}^3}$).

We investigated the SAWs and SWs propagating in the direction of periodicity, which causes the folding of magnetoelastic dispersion relation into the first Brillouin zone. The magnetic field is applied in-plane at the angle 45° to the k -vector, to make the interaction between Rayleigh SAWs and SWs possible.

Our main findings are: (i) the higher SAW dispersion branches are exhibited only due to the magnetoelastic interactions, (ii) the partial confinement of SWs within the stripes and nonuniform changes of SWs' phase affect their coupling with freely propagating SAWs.

G.C. would like to acknowledge the support from the National Science Center – Poland (grant No. 2020/39/O/ST5/02110)

[1] L. Dreher, *et al. Phys. Rev. B* **86**, 134415 (2012).

[1] N. K. P. Babu, *et al. Nano Lett.* **21**, 946 (2021).

Observation of Femtosecond Laser Comb Driven Magnetoelastic Modes

Avinash Kumar Chaurasiya¹, Ahmad A. Awad¹, Shreyas Muralidhar¹, Roman Khymyn¹, and Johan Åkerman¹

¹Department of Physics, University of Gothenburg, 412 96 Gothenburg, Sweden

Recent advances in magnon spintronics have led to a rapidly increasing research interest into investigating phenomena involving magnons (quanta of spin waves) and phonons (quanta of the elastic crystal lattice waves) from both a fundamental research viewpoint and for potential applications in data communication and information processing [1-2]. Most recently, ultrafast electron diffraction studies of Ni films revealed that ultrafast interactions of spins with high frequency phonons are decisive for the dynamics of rapidly demagnetized magnetic materials [3]. In our work, we use μ -Brillouin light scattering (μ -BLS) microscopy combined with a high repetition rate (1 GHz) femtosecond (fs) laser frequency comb [4] to study the polarization characteristics of both phonons and magnons in NiFe thin films.

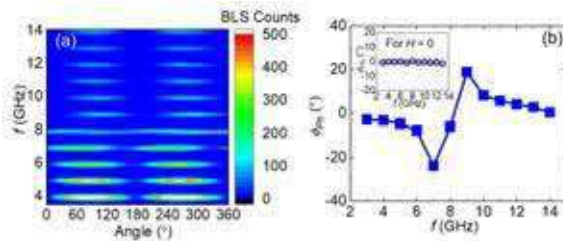


Figure 1: (a) Polarization maps for 20 nm NiFe thin film measured at an applied magnetic field $H = 6$ kOe and pump power (P) = 40 mW. (b) The variation of the extracted angle for phonons as a function of frequency (obtained using Eq. (1)). Solid line is guide to the eye. Inset: The extracted angle (ϕ_{ph}) in the absence of applied magnetic field.

Films of permalloy ($\text{Ni}_{80}\text{Fe}_{20}$) were sputtered onto c -plane sapphire substrates by dc magnetron sputtering under a 3 mTorr Ar atmosphere in an ultrahigh vacuum chamber. In the μ -BLS experiment, the sample is excited with a 1 GHz rep-rate fs-laser of wavelength 816 nm and probed with a continuous wave laser of wavelength 532 nm. The scattered beam from the sample is passed through a polarizer

(which can be rotated from 0° to 360°) and guided to the tandem Fabry-Pérot interferometer for spectral decomposition of the light. Analysis of the polarization angle of the inelastically scattered light without fs-laser excitation reveals that phonons and magnons do not interact as their BLS counts add up incoherently with the expected 90° phase shift between their polarization angles. However, in the presence of fs-laser excitation, a giant rotation ($\approx 45^\circ$) in the phonon polarization angle is observed for frequencies close to ferromagnetic resonance [see Fig. 1(a) and (b)]. We model the observed BLS counts (I) for various frequencies by considering the contribution of both phonons and magnons which is in good qualitative agreement with a \sin^2 dependence of the polarization angle

$$I = A_{ph} \sin^2(x - \phi_{ph}) + A_m \sin^2(x - \phi_m) \quad (1)$$

The respective parameters of the phonons and magnons (A_{ph} and A_m) as well as the polarization angle for phonons (ϕ_{ph}) have been extracted as a function of frequency. Our work underlines the versatility of the frequency comb for the generation of magnon-phonon coupled modes in magnetic thin films.

References:

- [1] A. V. Chumak *et al.*, *Nat. Phys.* **11**, 453 (2015)
- [2] J. Holanda *et al.*, *Nat. Phys.* **14**, 500 (2018)
- [3] S. R. Tauchert *et al.*, *Nature* **602**, 73 (2022)
- [4] A. Aleman *et al.*, *Opt. Express* **28**, 29540 (2020)

Spintronic detection of terahertz magnetic fields via Zeeman torque

A.L. Chekhov^{1,2}, Y. Behovits^{1,2}, B.R. Serrano^{1,2}, U. Martens³, M. Wolf²,
M. Münzenberg³, and T. Kampfrath^{1,2}

¹ Freie Universität Berlin, Arnimallee 14, 14195 Berlin, Germany

² Fritz-Haber-Institut der Max-Planck-Gesellschaft, Faradayweg 4-6, 14195 Berlin, Germany

³ Institut für Physik, Universität Greifswald, Felix-Hausdorff-Straße 6, 17489 Greifswald, Germany

Over the last years, laser-based terahertz (THz) sources have proven to be a powerful tool for performing spectroscopy and investigating dynamics of charge and spin degrees of freedom in various materials in THz range [1,2]. On one hand, recently demonstrated new THz sources like organic crystals and spintronic terahertz emitters (STE) can provide broadband THz pulses [3]. On the other hand, most state-of-the-art THz field detection techniques are based on electro-optical sampling (EOS), which is limited in bandwidth due to phase matching conditions. Therefore, new THz detection techniques are needed to reliably

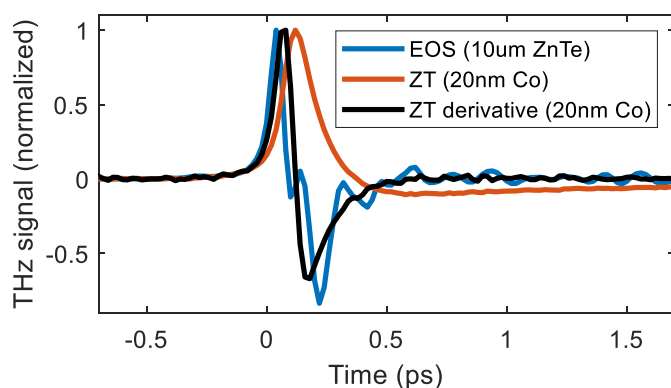


Figure 1: Signals of a THz pulse from an STE through EOS with a 10 μm ZnTe crystal (blue) and Zeeman torque (ZT) probing in a 20 nm Co film (red). The derivative of the ZT signal (black) is the true THz field.

sample the THz transients and perform broadband terahertz spectroscopy.

While EOS is based on coupling the electric field of the THz pulse to the charges in the medium, an alternative sampling method is to utilize Zeeman coupling of the magnetic field of the THz pulse to the spin subsystem [4]. Such coherent interaction leads to magnetization dynamics proportional to the integral of the driving THz field, providing direct access to the THz waveform.

Here, we investigate Zeeman torque (ZT) as a possible THz field detection technique. Using magneto-optical probing through the Faraday effect, we observe coherent magnetization dynamics due to ZT in various materials (metallic ferromagnets and insulating ferrimagnets) and identify optimal structural parameters in terms of bandwidth and signal strength. As a proof of principle, we use our THz ZT detector to sample broadband emission from an STE and compare the extracted field to EOS in various detection crystals (see Fig. 1). The proposed method allows one to not only obtain the true THz field transients, but to also identify the transfer functions of other THz-field detection schemes.

[1] A.L. Chekhov, Y. Behovits, J.J.F. Heitz, C. Denker, D.A. Reiss, M. Wolf, M. Weinelt, P.W. Brouwer, M. Münzenberg, and T. Kampfrath, *Phys. Rev. X* **11**, 041055 (2022)

[2] L. Nádovrník, M. Borchert, L. Brandt, R. Schlitz, K.A. de Mare, K. Výborný, I. Mertig, G. Jakob, M. Kläui, S.T.B. Goennenwein, M. Wolf, G. Woltersdorf, and T. Kampfrath, *Phys. Rev. X* **11**, 021030 (2021)

[3] J.A. Fülöp, S. Tzortzakis, and T. Kampfrath, *Adv. Optical Mater.* **8**, 190068 (2020)

[4] C. Vicario, C. Ruchert, F. Ardana-Lamas, P. M. Derlet, B. Tudu, J. Luning, and C. P. Hauri, *Nat. Photonics* **7**, 720 (2013).

Magnonic and phononic modes in $\text{Ni}_{80}\text{Fe}_{20}$ array of antidots

S. Chiroli¹, D. Faurie¹, N. Challab¹, P. Djemia¹, A. Adeyeye²
and F. Zighem

¹ *LSPM-CNRS UPR3407, Université Sorbonne Paris Nord, Villetaneuse, France*

² *Dept. Phys., Durham University, United Kingdom, & ISML, NUS Singapore*

Phononic and magnonic crystals are artificial periodic nanomaterials in which magnetic and elastic properties follow the spatial periodicity of the lattice. Interest has recently been growing on these crystals because the wide range of application they offer [1,2]. On the one hand, magnonic crystals are media where spin waves can propagate at many sub-Terahertz eigen frequencies that are investigated for next generation of filters and spin wave based logic devices [3]. On the other hand, phononic crystals are nanostructures where acoustic waves propagate at the Gigahertz range which make them good candidates for acoustic micro sensing and signal processing. Some materials are suited for the study of both waves which makes the so called magphonic crystals media with huge potential for the future of logic devices [4,5].

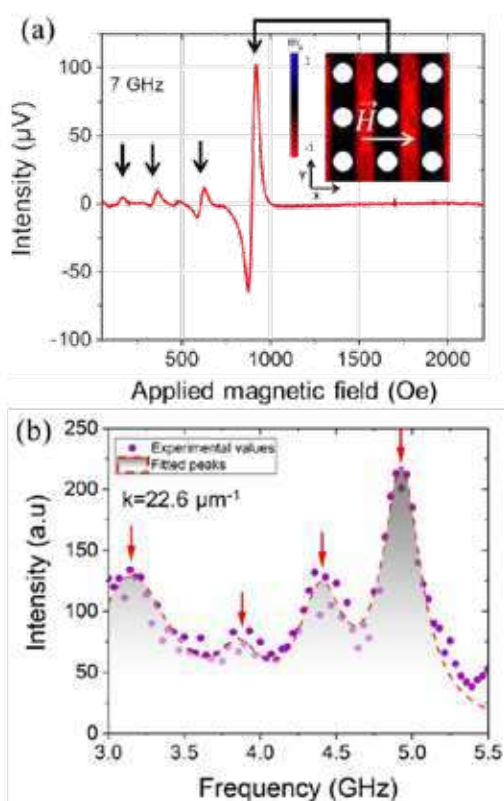


Figure 1: (a) FMR spectrum of the studied antidots sample with OOMMF simulation of the highest intensity mode. (b) BLS spectrum of the phonon modes in the same sample.

$\text{Ni}_{80}\text{Fe}_{20}$ (Py) is an interesting material for the study of magnons and phonons. In our work, we investigated the magnetic and elastic properties of Py of 40 nm thick thin films and periodic structures with 180 nm diameter antidots and a 400 nm periodicity by using BLS and FMR techniques. FMR has been used to study magnetic modes near the first Brillouin zone centre. Many modes have been experimentally highlighted and OOMMF simulations have been performed in order to determine how they are localized on the surface. We extended the study with BLS technique in order to confirm the presence of elastic modes and study their dispersion.

- [1] V. V. Kruglyak, S. O. Demokritov and D. Grundler, J. Phys. D: Appl. Phys. 43, 264001 (2010)
- [2] T. Gorishnyy, C. K. Ullal, M. Maldovan, G. Fytas and E. L. Thomas, Phys. Rev. Letters 94, 115501 (2005)
- [3] S. O. Demokritov and A. N. Slavin, "Eds., Magnonics - From Fundamentals to Applications", Springer, Series: Topics in Applied Physics, 125 (2013)
- [4] V. L. Zhang, F. S. Ma, H. H. Pan, C. S. Lin, H. S. Lim, S. C. Ng, M. H. Kuok, S. Jain and A. O. Adeyeye, Appl. Phys. Lett. 100, 163118 (2012)
- [5] H. Pan, V. L. Zhang, K. Di, M. H. Kuok, H. S. Lim, S. C. Ng, N. Singh, A. O. Adeyeye, Nanoscale Res. Lett. 8, 115 (2013)

Non-reciprocal magnonic directional coupler

Noura Zenbaa^{1,2}, Qi Wang^{1,3}, Kristyna Davidkova⁴, Sebastian Knauer¹, Moritz Ruhwedel⁵, Oleksandr Dobrovolskiy¹, Sabri Koraltan¹, Claas Abert^{1,3}, Carsten Dubs⁶, Michal Urbanek⁴, Philipp Pirro⁵, Dieter Suess^{1,3}, **Andrii V. Chumak¹**

¹University of Vienna, Faculty of Physics, Boltzmanngasse 5, A-1090 Vienna, Austria

²University of Vienna, Vienna Doctoral School in Physics, Vienna, Austria

³Research Platform MMM Mathematics-Magnetism-Materials, University of Vienna, Vienna, Austria

⁴CEITEC BUT, Brno University of Technology, Brno, Czech Republic

⁵Fachbereich Physik and Zentrum OPTIMAS, TU Kaiserslautern, Kaiserslautern, Germany

⁶INNOVENT e.V. Technologieentwicklung, Jena, Germany

Magnon-based computing has been proven as a promising route for the development of alternative signal processing systems. A directional coupler, realised by two dipolar coupled waveguides, provides a universal building block in magnonic circuits and RF applications [1-3]. The energy of the wave excited in one waveguide can be fully transferred to the other after propagating over the coupling length L . The dipolar coupling between the two waveguides leads to the splitting of the first width mode into two branches, corresponding to the symmetric and antisymmetric propagation of the spin wave. This coupling length L is defined as $L = \frac{\pi}{|k_{as}-k_s|} = \frac{\pi}{\Delta k}$, where k_{as} and k_s are the wavenumbers of antisymmetric and symmetric modes, respectively [1]. A magnonic half-adder based on two YIG nano-scale directional couplers has been demonstrated numerically and benchmarked [2].

In this work, we use a structure consisting of YIG(100)/SiO₂(5)/CoFeB(40) to fabricate the waveguides of the directional coupler, to induce non-reciprocity in the spin-wave propagation and, therefore, add new functionalities to the directional coupler. The non-reciprocity due to the symmetry breaking leads to the splitting of Δk in one propagation direction being different compared to the other propagation direction ($+\Delta k \neq -\Delta k$) in the Damon-Eschbach configuration – see the results of numerical simulations and k-resolved Brillouin Light Scattering (BLS) spectroscopy in Fig. 1(a). Therefore, the coupling length L will differ in the two propagation directions. At a special frequency, where $L_{-k} = 2L_{+k}$, the directional coupler can operate as a Y-circulator – see Fig. 1(b).

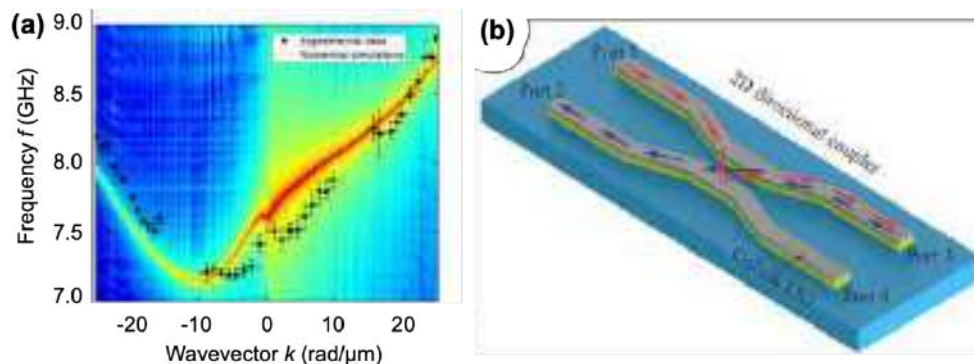


Figure 1: (a) Simulated and measured dispersions of spin waves in YIG(100)/SiO₂(5)/CoFeB(40) plane film.

(b) A proposed structure of the non-reciprocal magnonic directional coupler and its operational as Y-circulator.

[1] A. V. Sadovnikov, et al., Appl. Phys. Lett. **107**, 202405 (2015). [2] Q. Wang et al., Science Advances **4**, 1 (2018). [3] Q. Wang et al., Nature Electronics **3**, 765 (2020).

Ultrafast coherent all-optical switching of antiferromagnets

Tobias Danneegger¹, Marco Berritta², Karel Carva³, Severin Selzer¹, Ulrike Ritzmann⁴, Peter M. Oppeneer², and Ulrich Nowak¹

¹*Fachbereich Physik, Universität Konstanz, DE-78457 Konstanz, Germany*

²*Department of Physics and Astronomy, Uppsala University, Box 516, SE-75120 Uppsala, Sweden*

³*Charles University, Faculty of Mathematics and Physics, Department of Condensed Matter Physics, Ke Karlovu 5, CZ-121 16 Prague, Czech Republic*

⁴*Dahlem Center of Complex Quantum Systems and Department of Physics, Freie Universität Berlin, Arnimallee 14, DE-14195 Berlin, Germany*

The fascinating physics of ultrafast, all-optical switching (AOS), first demonstrated in a ferrimagnet [1] and later also in ferromagnets, holds great potential for the development of fast and efficient magnetic storage devices. While different mechanisms are at play here, they have one commonality: they all require the thermal quenching of the material's magnetic order before remagnetising in a new direction. Even though coherent effects, in particular the optomagnetic moments induced by the inverse Faraday effect (IFE), also play an important role in many cases, the ultrafast heating and ensuing demagnetisation are necessary prerequisites for AOS in ferro- and ferrimagnets.

Here, we consider how AOS can be realised in antiferromagnets, by simulating the effect of an ultrashort, circularly polarised laser pulse on the magnetic state of the easy-plane antiferromagnet CrPt [2]. We use density functional theory to calculate the optomagnetic moments induced by the inverse Faraday effect, leading to the surprising result that the induced magnetic moments are staggered, i.e., aligned opposite to the local magnetisation on each lattice site. We then employ atomistic spin dynamics simulations with an ab initio parameterised model of CrPt to investigate the effect of these induced moments in combination with the ultrafast heating produced by the laser pulse.

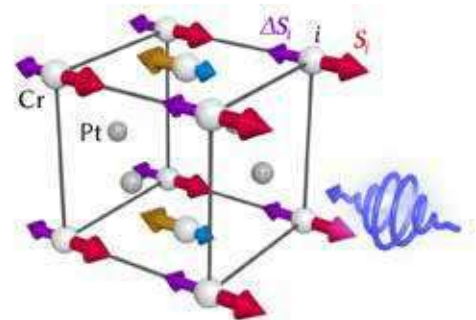


Figure 1: Magnetic structure of CrPt with atomic (yellow/red) and induced (blue/purple) magnetic moments.

We find that the IFE induces a coherent in-plane rotation of the Néel vector. Due to the exchange-enhanced dynamics of antiferromagnets, this rotation takes place very fast, within a few hundred femtoseconds. Our simulations clearly show that this effect is purely coherent, without the material losing its magnetic order, and takes place even in the absence of any laser-induced heating. We also demonstrate how a series of laser pulses with varying intensity can be used to reliably switch between two perpendicular magnetic states.

[1] C. D. Stanciu et al., *Phys. Rev. Lett.* **99**, 047601 (2007).

[2] T. Danneegger et al., *Phys. Rev. B* **104**, L060413 (2021).

Electron-Magnon Scattering Dynamics in a 2-Band Stoner Model

Félix Dusabirane, Kai Leckron and Hans Christian Schneider

Physics Department & Research Center OPTIMAS, University of Kaiserslautern, Germany

Magnons can be viewed as quasiparticle excitations on the ferromagnetic ground state and should therefore also play a role in ultrafast demagnetization of ferromagnets. Recently they have also been investigated for their contributions to transport. Here, we use a microscopic model to study carrier dynamics in ferromagnets due to electron-magnon scattering on ultrafast timescales. We employ a simple model band structure (“Stoner model”) and an idealized excitation as shown in Fig. 1. The electron magnon-interaction is formally obtained as coupling to a Heisenberg spin system [1] in the Hamiltonian. We compute the dynamics of momentum resolved electron and magnon distributions due to electron-magnon and electron-electron scattering, which are treated at the level of Boltzmann scattering integrals. We find that electron-magnon scattering leads to a pronounced non-equilibrium for magnon modes that couple directly to Stoner transitions.

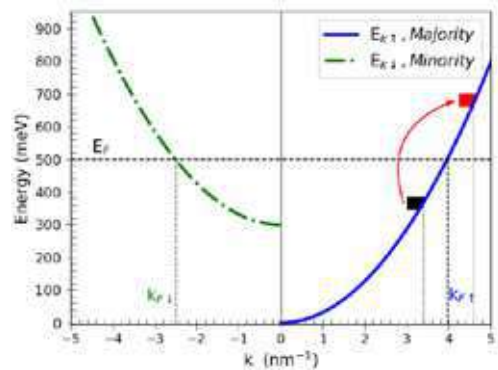


Figure 1: Band dispersion for majority (spin up) and minority (down) electrons with excitation in the majority band.

The coupled equations for the dynamical distributions are for electrons with spin up

$$\frac{\partial n_{k,\uparrow}}{\partial t} = \sum_q M_{e-m}^2 \delta(\epsilon_k^\uparrow - \epsilon_{k+q}^\downarrow + \hbar\omega_q) [n_{k+q,\downarrow}(1 - n_{k,\uparrow})(1 + N_q) - n_{k,\uparrow}(1 - n_{k+q,\downarrow})N_q] \quad (1)$$

and a similar one for spin-down, and for the magnon distribution

$$\frac{\partial N_q}{\partial t} = \sum_k M_{e-m}^2 \delta(\epsilon_k^\uparrow - \epsilon_{k+q}^\downarrow + \hbar\omega_q) [n_{k+q,\downarrow}(1 - n_{k,\uparrow})(1 + N_q) - N_q n_{k,\uparrow}(1 - n_{k+q,\downarrow})]. \quad (2)$$

Figure 2 shows preliminary results for the change of magnon distribution $\delta N = N - N_{eq}$ from its equilibrium value for the weak excitation shown in Fig. 1. The range of energies shown lies in the Stoner continuum, and we have switched off spin-orbit effects. The spin-flip scattering with electrons results in a distinct dynamical redistribution due to magnon creation and annihilation processes. The influence of excitation conditions, the band structure and spin-orbit induced, i.e., Elliott-Yafet-type spin flips will be discussed.

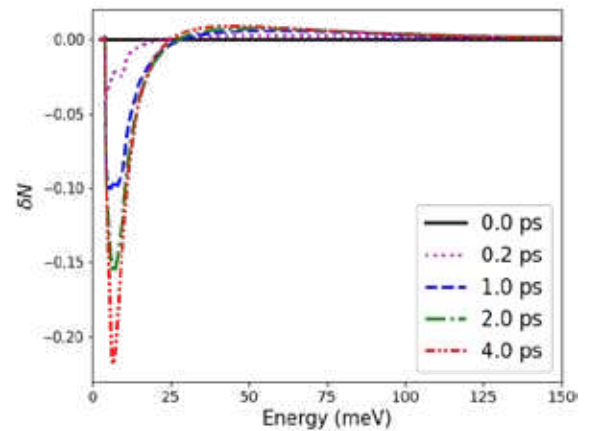


Figure 2: Change in magnon occupation number after excitation shown in Fig.1

[1] R. M. White, R. B. Woolsey, *Phys. Rev.* **50**, 176 (1968).

Non-reciprocal magnons in non-centrosymmetric MnSi

**T. Weber¹, J. Waizner², G. S. Tucker^{3,4}, M. Skoulatos⁵, L. Beddrich⁵, A. Bauer⁶,
R. Georgii⁵, C. Pfleiderer⁶, M. Garst⁷, and P. Böni⁶**

¹ *Institut Laue-Langevin (ILL), 71 Avenue des Martyrs, 38000 Grenoble, France*

² *Institut für Theoretische Physik, Universität zu Köln, Zùlpicher Str. 77a, 50937 Köln, Germany*

³ *Laboratory for Neutron Scattering and Imaging, Paul Scherrer Institut (PSI), CH-5232
Villigen, Switzerland*

⁴ *Laboratory for Quantum Magnetism, École Polytechnique Fédérale de Lausanne, CH-1015
Lausanne, Switzerland*

⁵ *Heinz-Maier-Leibnitz-Zentrum (MLZ), Technische Universität München (TUM), Lichtenbergstr. 1,
85747 Garching, Germany*

⁶ *Physik-Department, Technische Universität München (TUM), James-Franck-Str. 1, 85748
Garching, Germany*

⁷ *Institute of Theoretical Solid State Physics & Institute for Quantum Materials and Technology,
Karlsruhe Institute of Technology, 76131 Karlsruhe, Germany*

Spin waves in chiral magnetic materials are strongly influenced by the Dzyaloshinskii-Moriya interaction, resulting in intriguing phenomena like nonreciprocal magnon propagation and magnetochiral dichroism. We studied the nonreciprocal magnon spectrum of the archetypical chiral magnet MnSi and its evolution as a function of magnetic field in all magnetic phases. Using inelastic neutron scattering, the magnon energies and their spectral weights are determined quantitatively after deconvolution with the instrumental resolution [1,2].

[1] T. Weber, J. Waizner, G. S. Tucker, R. Georgii, M. Kugler, A. Bauer, C. Pfleiderer, M. Garst, and P. Böni, *Phys. Rev. B* **97**, 224403 (2018).

[2] T. Weber, J. Waizner, G. S. Tucker, L. Beddrich, M. Skoulatos, R. Georgii, A. Bauer, C. Pfleiderer, M. Garst, and P. Böni, *AIP Advances* **8**, 101328 (2018).

Influencing spin waves with bistable nanomagnet patterns

M. Golibrzuch^{1,+}, M. Kiechle^{1,+}, A. Papp², C. Calcagno¹, J. Greil¹, S. Mendisch¹, V. Ahrens¹, G. Csaba², and M. Becherer¹

¹Dep. of Electrical and Computer Engineering, Technical University of Munich, Germany

²Fac. of Information Technology and Bionics, Pázmány Péter Catholic University, Hungary

⁺these authors contributed equally to this work

We present a hybrid platform for spin wave (SW) devices consisting of CoPt nanomagnets with perpendicular magnetic anisotropy (PMA) fabricated on top of YIG thin films. Hereby, the CoPt magnets influence the magnetic field landscape of propagating SWs with local dipole fields depending on their shape, arrangement, and magnetization direction. Therefore, we fabricate cubic arrays of square-shaped CoPt multilayer magnets on top of YIG ($t = 100$ nm) using nanoimprint lithography. Due to their PMA, the bistable magnetization state of the nanomagnets can be switched reconfigurably with an external field. The nanomagnets are designed to have coercivities higher than 200 mT to be independent of the bias field needed for the forward volume spin wave (FVSW) configuration in YIG. Isotropic propagation is favorable to make the connection to optical principles, and we investigate the influence of the CoPt nanomagnets by reference to a 2D magnonic crystal. VNA-based, all-electrical SW spectroscopy with two coplanar antennas is used to evaluate the system shown in Fig. 1a. The transmissibility measurement in Fig. 1b shows the expected dispersion in YIG and a second propagation mode originating from the additional dipole field components provided by the magnonic crystal structure. We also exploit SW patterns with different nanomagnet orientations using time-resolved MOKE microscopy. An additional degree of freedom in reconfigurability can be achieved by coercivity engineering of the CoPt nanomagnets by focused ion beam irradiation. The ability of field selective switching opens a path to implement spin wave scattering functions that can perform complex signal processing tasks [1].

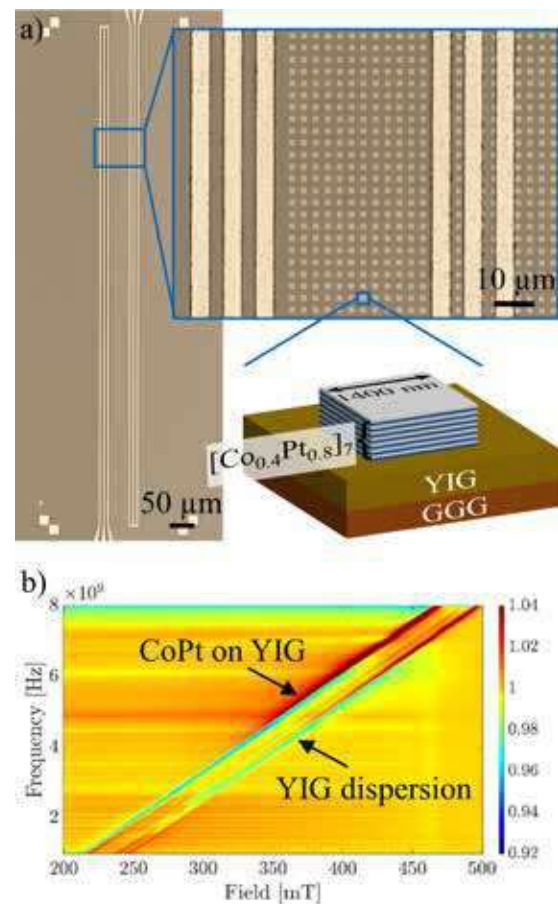


Figure 1: a) Experimental arrangement: CoPt nanomagnets on top of YIG, SW propagation between two coplanar microwave antennas ($s, g = 4 \mu\text{m}$, $\text{dist.} = 40 \mu\text{m}$). b) SW transmission spectra (forward volume) measured in all-electrical configuration with a VNA-based setup.

[1] Papp, A., Porod, W. and Csaba, G., *Nature communications* **12**(1), pp.1-8 (2021).

Excitation of leaky modes by obliquely incident spin wave beam onto magnonic Gires-Tournois interferometer and its impact on Goos-Hänchen effect for reflected beams

Krzysztof Sobucki¹, Wojciech Śmigaj², Piotr Graczyk³, Maciej Krawczyk¹,
and Paweł Gruszecki¹

¹ ISIK, Faculty of Physics, Adam Mickiewicz University, Poznań, 61-614, Poland

² Met Office, FitzRoy Rd, Exeter, EX1 3PB, UK

² Institute of Molecular Physics, Polish Academy of Sciences, Poznań, 60-179, Poland

We use micromagnetic simulations to study the reflection of an obliquely incident spin-wave (SW) beam at a magnonic realization of the Gires-Tournois interferometer (GTI) made of a magnetic stripe placed above the edge of a thin film[1]. We find the conditions for an efficient excitation of modes propagating along stripe by the obliquely incident SW beam. Under these conditions, the reflected beam's amplitude decreases, which we interpret as a magnonic version of Wood's anomaly[2]. Despite being contained within the stripe, the excited mode reemits SWs back to the layer; hence, we classify it as a leaky mode. Consequently, we can observe multiple spatially shifted reflected SW beams (compare Figure 1a and 1b). Furthermore, even the primary reflected beams are shifted relative to each other for different saturation magnetization (M_s) values of the stripe. The values of this shift spans between -175 nm and 225 nm with respect to the case when the leaky modes are not excited. Therefore, the excitation of leaky-states are accompanied by rapid changes of the Goos-Hänchen shift (GHS) [3]. In Figure 1a and 1b, we present the SW intensity distribution in the systems where the leaky-mode is not and is excited, respectively. In Fig. 1b, multiple reflected SW beams are visible, and the primary reflected beam is shifted compared to the beam in Figure 1a by 135 nm. By examining the propagating SWs in thin films with the localized leaky modes, our study contributes to understanding and utilizing SWs, and thus, provides a stepping stone towards utilizing SWs.

We acknowledge the funding from the Polish National Science Centre project No. UMO-2019/33/B/ST5/02013.

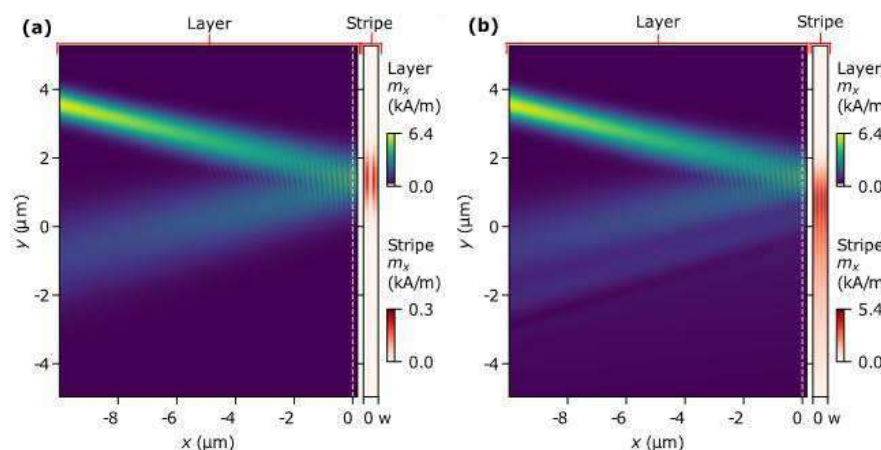


Figure 1. (left panels) The SW intensity distribution in the magnetic film. (right panels) The SW intensity in the stripe of width $w=155$ nm placed above the film. The system with stripe of (a) $M_s = 350$ kA/m and (b) $M_s = 550$ kA/m. The excitation of leaky modes is visible in (b)

[1] Sobucki et al. *Sci. Rep.* 11, 4428 (2021).

[2] Wood, *Lond. Edinb. Dublin philos. Mag. J. sci.* 4, 396 (1902).

[3] Gruszecki et al., *Appl. Phys. Lett.* 105, 242406 (2014).

Ultrafast element- and depth-resolved magnetization dynamics probed by transverse magneto-optical Kerr effect spectroscopy in the soft x-ray range

M. Hennecke¹, D. Schick¹, T. Sidiropoulos¹, F. Willems¹, A. Heilmann¹,
M. Bock¹, L. Ehrentraut¹, D. Engel¹, P. Hessing¹, B. Pfau¹,
M. Schmidbauer², A. Furchner^{3,4}, M. Schnuerer¹, C. von Korff Schmising¹,
and S. Eisebitt^{1,5}

¹Max-Born-Institut, Max-Born-Straße 2A, 12489 Berlin, Germany

²Leibniz-Institut für Kristallzüchtung, Max-Born-Straße 2, 12489 Berlin, Germany

³Helmholtz-Zentrum Berlin, Albert-Einstein-Straße 15, 12489 Berlin, Germany

⁴Leibniz-Institut für Analytische Wissenschaften – ISAS – e.V., Department Berlin,
Schwarzschildstraße 8, 12489 Berlin, Germany

⁵IOAP, Technische Universität Berlin, Straße des 17. Juni 135, 10623 Berlin, Germany

Understanding the light-driven spin dynamics occurring at buried interfaces of complex magnetic heterostructures as used in today's opto-spintronics applications requires a direct experimental access to the depth-resolved magnetic order on sub-picosecond time scales [1].

Here, we report on broadband time- and angle-resolved transverse magneto-optical Kerr effect (TMOKE) spectroscopy probing the Gd $N_{5,4}$ resonance (≈ 150 eV) of a Ta/GdFe/Pt heterostructure via femtosecond soft x-ray pulses provided by a laboratory-scale light source based on high-harmonic generation [2]. Analyzing the time-resolved spectra via magnetic scattering simulations [3,4] allows for a quantitative determination of the transient magnetization depth profiles evolving within the ferrimagnetic GdFe film after strongly layer-dependent infrared (IR) photoexcitation. By disentangling the time scales of femtosecond dynamics dominated by non-equilibrium electron transport (≤ 100 fs) and nanoscale heat diffusion (≥ 1 ps), we are able to rule out significant contributions of femtosecond non-local spin transport phenomena on the demagnetization of Gd. Instead, we can relate the magnetization gradient evolving within GdFe on time scales of ≥ 1 ps to heat injection at the interface with the strongly IR-excited buried Pt seed layer.

Our results demonstrate how the complicated spectral dependence of the TMOKE observable can be utilized to disentangle local and non-local processes on ultrafast time scales, directly correlating experimental observables with functionality in nanoscale device structures, e.g., controlled by charge or spin currents as well as nanoscale heat transfer.

[1] E. Y. Vedmedenko, et al., *J. Phys. D: Appl. Phys.* **53**, 453001 (2020).

[2] M. van Möerbeek-Bock, et al., *Proc. SPIE* **11777**, 11-16 (2021).

[3] M. Elzo, et al., *J. Magn. Magn. Mater.* **324**, 105 (2012).

[4] D. Schick, *Comput. Phys. Commun.* **266**, 108031 (2021).

Unravelling the Transient Depth Magnetic Profile During Ultrafast Demagnetization of an Iron Thin Film

Valentin Chardonnet¹, Marcel Hennes¹, Romain Jarrier¹, Renaud Delaunay¹,
Nicolas Jaouen², Marion Kuhlmann³, Cyril Léveillé², Kelvin Yao⁴, Daniel Schick⁴,
Clemens von Korff Schmising⁴, Georghe S. Chiuzaian¹, Jan Lüning⁵, Boris Vodungbo¹
and Emmanuelle Jal¹

¹ Sorbonne Université, CNRS, Laboratoire de Chimie Physique-Matière et Rayonnement, LCPMR, 75005 Paris, France

² Synchrotron SOLEIL, L'Orme des Merisiers, Saint-Aubin, B.P. 48, 91192 Gif-sur-Yvette, France

³ Deutsches Elektronen-Synchrotron, 22607 Hamburg, Germany

⁴ Max Born Institut für Nichtlineare Optik und Kurzzeitspektroskopie, 12489 Berlin, Germany

⁵ Helmholtz-Zentrum Berlin für Materialien und Energie, 14109 Berlin, Germany

During the last two decades, a variety of models have been developed to explain the ultrafast quenching of magnetization following femtosecond optical excitation [1,2,3]. These models can be classified into two broad categories, relying either on a local or a non-local transfer of angular momentum [3]. To distinguish those local and non-local effects we can measure the magnetization depth profile with femtosecond resolution, thanks to time-resolved x-ray resonant magnetic reflectivity [4, 5]. In this presentation, I will show how, from our experimental results gathered at the free electron laser FLASH, we can unravel the dynamics of the transient inhomogeneous depth magnetic profile of an Fe layer after optical excitation. This inhomogeneous depth magnetic profile shows an accumulation of the demagnetization close to the bottom interface (Fig. 1), and if we compare it to simulation we can directly show that both local and non-local phenomena [6] take place at the same time scale. Additionally, our analysis points towards a contribution from spin currents that could carry the magnetization beyond the magnetic layer [7].

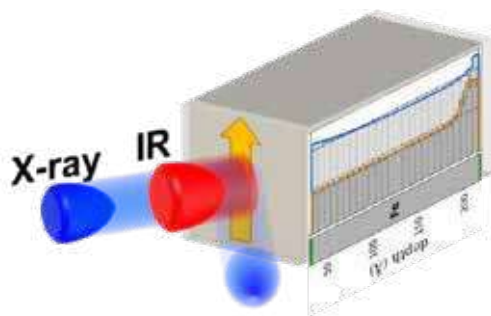


Figure 1: Schematic of x-ray Resonant Magnetic Reflectivity and the depth magnetic profile derived from experimental data without optical excitation (blue) and 300 fs after an optical excitation (orange).

enhanced via magnetostrictive effects.

Furthermore, this technique allows probing simultaneously structural and magnetic dynamics, and our experiment on a polycrystalline Fe sample reveals two distinct dynamics at different time scales for the structure and the magnetization. Until one picosecond, the magnetic signal is quickly evolving while the structural one stays more or less constant. After that, the magnetic signal is slowly coming back to equilibrium while the structural one changes periodically. We observe a maximum dilation of 2Å followed by a coherent damped oscillation of the thickness of the sample. This dynamic is due to stresses that are generated by the rapid increase in temperature and might be

- [1] B. Koopmans et al. *Nat. Mat.* **9**, 259 (2010)
- [2] M. Battiato et al. *Phys. Rev. Lett.* **105**, 027203 (2010)
- [3] G. P. Zhang et al. *Journ. Phys. Cond. Matt.* **30**, 465801 (2018)
- [4] E. Jal et al. *Phys. Rev. B* **95**, 184422 (2017)
- [5] V. Chardonnet et al. *Struct. Dyn.* **8**, 034305 (2021)
- [6] J. Wieczorek et al. *Phys. Rev. B* **97**, 174410 (2015)
- [7] A. Eschenlhor et al. *Nat. Mat.* **12**, 332 (2013)

Role of electronic excitation, relaxation and transport processes for X-ray induced ultrafast demagnetization within magnetic multilayer systems

**K. J. Kapcia^{1,2}, V. Tkachenko^{3,4}, F. Capotondi⁵, A. Lichtenstein^{4,6},
S. Molodtsov⁴, L. Mueller⁷, A. Philippi-Kobs⁷, P. Piekarz³, B. Ziaja^{1,3}**

¹ *Center for Free-Electron Laser Science CFEL, Deutsches Elektronen-Synchrotron DESY,
Notkestr. 85, 22607 Hamburg, Germany*

² *Institute of Spintronics and Quantum Information, Faculty of Physics, Adam Mickiewicz
University in Poznań, Uniwersytetu Poznańskiego 2, 61-614 Poznań, Poland*

³ *Institute of Nuclear Physics, Polish Academy of Sciences, Radzikowskiego 152, 31-342
Kraków, Poland*

⁴ *European XFEL GmbH, Holzkoppel 4, 22869 Schenefeld, Germany*

⁵ *Elettra-Sincrotrone Trieste S.C.p.A, 34149, Trieste, Basovizza, Italy*

⁶ *University of Hamburg, Jungiusstr. 9, 20355 Hamburg, Germany*

⁷ *Deutsches Elektronen-Synchrotron DESY, Notkestr. 85, 22607 Hamburg, Germany*

We investigated the role of electronic excitation, relaxation and transport processes in X-ray induced ultrafast demagnetization of magnetic multilayer systems. In what follows, we report on the results obtained with the newly developed modeling tool, XSPIN, which enables nanoscopic description of electronic processes occurring in X-ray irradiated ferromagnetic materials [1]. With this tool, we have studied the specific response of Co/Pt multilayer system irradiated by an ultrafast XUV pulse at the M-edge of Co (photon energy ~ 60 eV). It was previously studied experimentally at the FERMI free-electron-laser facility, using the magnetic small-angle X-ray scattering technique [2]. The XSPIN simulations show that the magnetic scattering signal from cobalt decreases – on the femtosecond timescales considered – due to electronic excitation, relaxation and transport processes both in the cobalt and in the platinum layers. The signal decrease scales with the increasing fluence of incoming radiation, following the trend observed in the experimental data. Confirmation of the predominant role of electronic processes for X-ray induced demagnetization in the regime below the structural damage threshold, achieved with our theoretical study, is a step towards quantitative control and manipulation of X-ray induced magnetic processes on femtosecond timescales.

[1] K. J. Kapcia, V. Tkachenko, F. Capotondi, A. Lichtenstein, S. Molodtsov, L. Mueller, A. Philippi-Kobs, P. Piekarz, B. Ziaja, arXiv:2202.13845 [cond-mat.mtrl-sci], DOI: <https://doi.org/10.48550/arXiv.2202.13845> (2022).

[2] A. Philippi-Kobs, et al., DOI: <https://doi.org/10.21203/rs.3.rs-955056/v1> (2021).

Steering spin waves in corrugated waveguides

Jan Klíma¹, Václav Roučka¹, Lucie Dočkalová¹, Igor Turčan², Ondřej Wojewoda²,
Ondřej Man², and Michal Urbánek^{1,2}

¹ Institute of Physical Engineering, Brno University of Technology, Brno, Czech Republic

² CEITEC BUT, Brno University of Technology, Brno, Czech Republic

One of the elementary premises of complex magnonic networks is a need for operation in the absence of an external magnetic field. If an external magnetic field is used to stabilize magnetization, even a basic circuit element as spin-wave turn exhibits a large dispersion mismatch for regions before and after the turn. Local control of the effective field would stabilize the magnetization of different parts of the magnonic circuit in the desired direction, thus preventing the dispersion mismatch [1].

We use corrugated magnetic films and waveguides to locally control the effective field. A sinusoidally modulated substrate on which magnetic film is deposited is prepared by focused electron beam induced deposition. The surface curvature in films (Fig. 1 a, b) locally modifies the contributions of dipolar and exchange energies and results in an effective anisotropy term which is perpendicular to the corrugation direction [2]. The direction of the anisotropy axis can be spatially controlled, and arbitrary magnetization landscapes can be created on demand (Fig 1 c). This means that both, frequency and wavevector, can be matched along arbitrary spin wave beam trajectory, which results in minimalization of the losses due to the scattering on the boundaries (Fig 1 d).

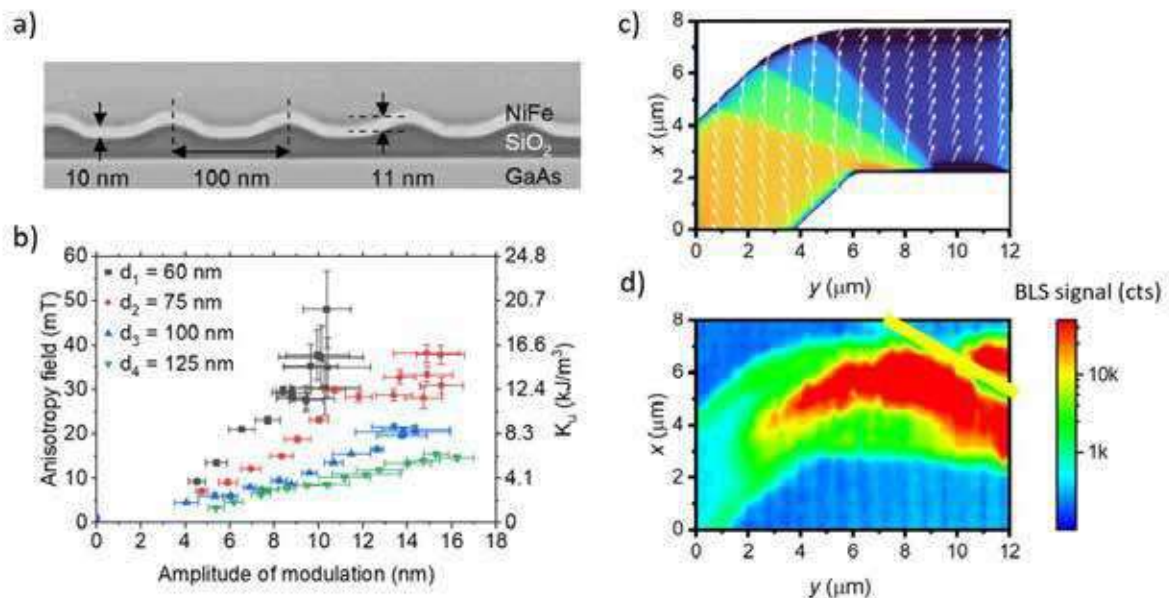


Figure 1: (a) Transmission electron microscopy image of the cross-section of the corrugated magnetic film. (b) Dependence of the anisotropy field on the corrugation period (d_1 - d_4) and amplitude. (c) Magnetization landscape in spin wave turn with magnetic anisotropy controlled by corrugation direction. (d) Brillouin light scattering microscopy image of a spin wave propagating through spin wave turn with matched dispersion.

[1] L. Flajšman et al., Phys. Rev. B 101, 014436 (2020)

[2] I. Turčan et al., Appl. Phys. Lett. 118, 092405 (2021)

Current driven spin-wave emissions from magnetic vortex cores

Sabri Koraltan¹, Sina Mayr², Claas Abert¹, Florian Bruckner¹, Sebastian Wintz³, and Dieter Suess¹

¹ Physics of Functional Materials, University of Vienna, Kolingasse 14-16, 1090, Vienna, Austria

² Paul Scherrer Institut, 5232 Villigen PSI, Switzerland

³ Max Planck Institute for Intelligent Systems, 70569 Stuttgart, Germany

Flash memories or processing units rely today on exploiting electronic charges, where CMOS technologies have improved massively over the past decades. However, the high-power consumptions, and frequency limitations, lead to the search of alternative concepts, such as spintronics [1].

In that respect, magnons, as the quanta of spin-waves, have been proven to be a potential candidate for all-magnon based devices ranging from multiplexers to half-adders, and subsequently enabling magnon-based-computing [2]. Coherent spin-waves are usually excited by means of microwave antennas, where locally focused alternating external Zeeman fields perturb the magnetization. For certain applications, the need of excitation efficient antennas limits the experimental achievable structures which can be investigated. Recently, it was shown that magnetic discs with stable vortex states can be used to propagate spin-waves, when subjected to AC uniform magnetic fields [3]. The vortices are coupled antiferromagnetically (AF) to each other via a thin ruthenium spacing layer.

In this contribution, we report mainly a micromagnetic study, where AF-coupled vortices are subject to in-plane AC currents. We observe the current driven spin-wave emission from the vortex cores. We find fundamental differences in the spin-wave propagation direction, based on the chirality of the system. Furthermore, we demonstrate that the effect that leads to the spin-wave excitation and propagation is the Oersted field generated by the electric current flowing directly through the AF coupled magnetic discs. We compare the effect to that predicted for spin-transfer-torques acting on the vortex core. We find out that in the latter case 100 times

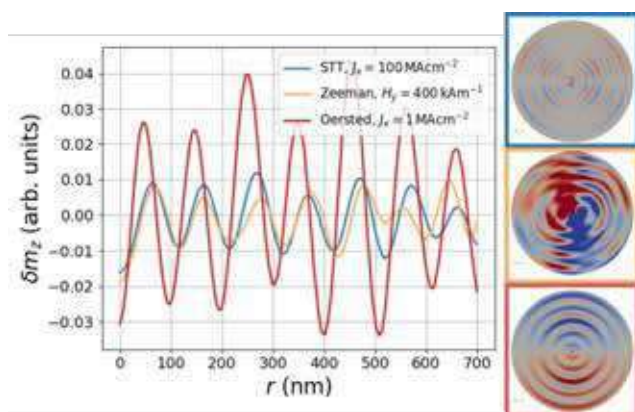


Figure 1: Evolution of the change in magnetization along the radial direction, in which the spin-wave propagates after being excited with STT (blue), Zeeman (yellow) or Oersted fields (red), accompanied

quantified.

higher currents are required in order to excite the spin-waves, with three times lower intensity, as it is shown in Fig. 1. We furthermore apply a uniform Zeeman field along the y-direction, whose amplitude equals the maximum amplitude of Oersted field. We observe that the spin-waves emission is more coherent, and up to three times more efficient if the spin-waves are excited via the current driven Oersted field compared to the so far experimentally used Zeeman fields. Our findings are demonstrated by time-resolved X-ray microscopy (TRXM) images, where the magnetic vortices emit the spin waves when subjected to an AC current, and where the propagating spin-waves are

[1] P. Barla *et al.* J. Comput. Electron. **20**, 805–837 (2021)

[2] A. V. Chumak *et al.*, IEEE Trans. on Magn., doi: 10.1109/TMAG.2022.3149664 (2022).

[3] S. Mayr., *et al.* Nano Letters, **21**, 1584 (2021)

A new look at spin wave modes in a ferromagnetic nanorod

Krzysztof Szulc¹, Elena V. Tartakovskaya^{1,2} and Maciej Krawczyk¹

¹ISQI, Faculty of Physics, Adam Mickiewicz University, Poznań, Poland

²Institute of Magnetism, National Academy of Sciences of Ukraine, Kyiv

The spin-wave excitations in saturated ferromagnetic rods is a topic of research from over 50 years. Starting from the homogeneously-magnetized macroscopic rods, the ferromagnetic resonance and magnetostatic-wave spectra were considered in various configurations [1]. In 2002, R. Arias and D. L. Mills derived the rigorous model and calculated the resonant modes of the infinitely-long circular ferromagnetic nanowire magnetized along the axis [2]. Later on, Rychlý et al. [3] showed an important contribution of the exchange interactions and external magnetic field magnitude on the spin-wave spectra. However, the effects of time-reversal symmetry breaking on the spin-wave modes, inherent to magnetic systems even in this simple geometry, have not yet been elucidated. Here, we propose a fresh look at the spin-wave modes in a ferromagnetic nanorod from the point of view of their circulation sense, their energy distribution inside and outside the rod, and application potential of the frequency split of clockwise and counter-clockwise modes.

We based our study on the analytical calculations and micromagnetic simulations for the nanorods of the circular, square, and rectangular cross-section. We found that all modes in considered nanorods have a rotational character, just as in circular nanowires. Thus, they can be splitted into two groups depending on the sense of the rotation, clockwise and counter-clockwise, with wide frequency difference between the modes of the same order (azimuthal and radial) but opposite rotation. Interestingly, the study of the Poynting vector shows an additional character of the modes—the counter-clockwise modes have a bulk character while the clockwise modes circulate close to the surface of the nanowire (Figs. 1a-b). Moreover, the significant difference is found also in the stray field circulating outside of the rod. Finally, we show how the rotational modes and their peculiar properties can be utilized in multifunctional magnonic devices, which can work as a circulator (Fig. 1c), directional coupler, reflector [4], or logic gate.

The study has received financial support from the NCN Poland (projects nos. UMO-2018/30/Q/ST3/00416, UMO-2020/37/K/ST3/02450 and UMO-2021/41/N/ST3/04478).

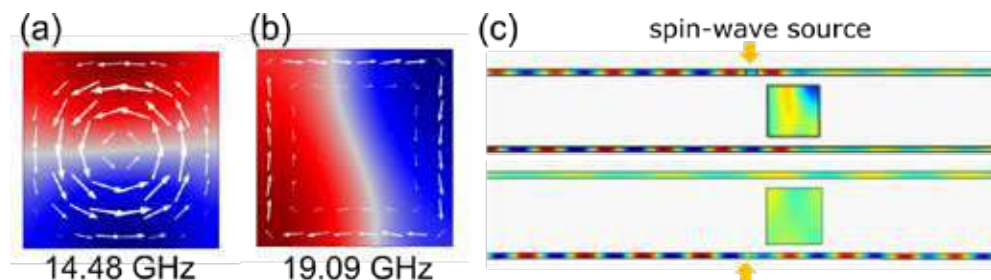


Figure 1: (a) Counter-clockwise and (b) clockwise modes in the square-shaped NiFe nanowire with the width of 50 nm. The color map presents the dynamic, m_x component of the magnetization, the arrows—Poynting vector. (c) The functionality of the circulator in the structure with two 5-nm-thick Co layers and a 100 x 50 nm NiFe resonator (not in scale).

[1] R. I. Joseph and E. Schlömann, J. Appl. Phys. 32, 1001 (1961).

[2] R. Arias and D. L. Mills, Phys. Rev. B 63, 134439 (2001).

[3] J. Rychlý, et al., J. Phys. D: Appl. Phys. 52, 075003 (2019).

[2] P. Roberjot et al., Appl. Phys. Lett. 118, 182406 (2021).

Ultrafast Optically Induced Ferromagnetic State in an Elemental Antiferromagnet

Wolfgang Kuch¹, Evangelos Golias¹, Ivar Kumberg¹, Ismet Gelen¹, Sangeeta Thakur¹, Jendrik G rdes¹, Rahil Hosseinifar¹, Quentin Guillet¹, J. Kay Dewhurst², Sangeeta Sharma³, Christian Sch  bler-Langeheine⁴, and Niko Pontius⁴

¹ Freie Universit t Berlin, Arnimallee 14, 14195 Berlin, Germany

² Max-Planck-Institut f r Mikrostrukturphysik, Weinberg 2, 06120 Halle, Germany

³ Max Born Institute for Nonlinear Optics and Short Pulse Spectroscopy, Max-Born-Str. 2A, 12489 Berlin, Germany

⁴ Helmholtz-Zentrum Berlin f r Materialien und Energie, Albert-Einstein-Str. 15, 12489 Berlin, Germany

Optical excitations might in principle allow for the control of magnetic order at timescales even shorter than the exchange interaction. A mechanism that enables the all-optical manipulation of magnetic order on subexchange timescales is the optically induced intersite spin transfer (OISTR) [1]. Spin-selective electronic transfer is taking place between neighboring atoms driven by the oscillating electric field of light.

Using time-resolved magnetic circular dichroism in soft-x-ray reflectivity, we present evidence for an ultrafast optically induced ferromagnetic alignment of antiferromagnetic Mn in epitaxial [Co/Mn] multilayers on Cu(001) [2]. We observe the transient ferromagnetic signal at the arrival of the pump pulse at the Mn L_3 resonance. The timescale of the effect is comparable to the duration of the excitation of about 60 fs, since the transition is driven by the electric field of the pump pulse in a femtosecond timescale, and occurs before the magnetization in Co is quenched. Time-resolved density functional theory (TDDFT) calculations identify the OISTR effect and the resulting imbalanced population of Mn unoccupied states caused by the Co interface as the underlying mechanism for the emergence of this transient ferromagnetic state (Fig. 1).

Our observation validates the hallmark prediction of an important mechanism for ultrafast optical manipulation of magnetic order and showcases the creation of a transient FM state in a monoelemental antiferromagnet that can play an important role in ultrafast optospintronics.

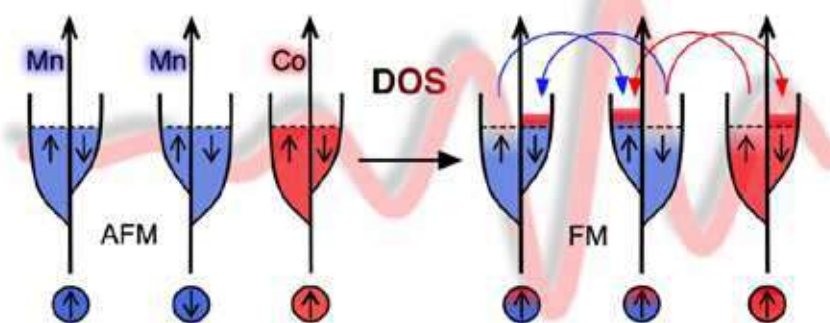


Figure 1: Schematics of the OISTR mechanism leading to the transient ferromagnetic state: The electric field of the light transfers electrons coherently between atoms. Majority states from the first Mn atom are transferred to the minority of the second and vice versa. A charge filling imbalance is introduced from the interface between Mn and Co and a transient ferromagnetic alignment of the Mn magnetic moments emerges.

[1] J. K. Dewhurst et al., *Nano Lett.* **18**, 1842 (2018).

[2] E. Golias et al., *Phys. Rev. Lett.* **126**, 107202 (2021).

Field orientation dependent magnetization dynamics in sub-100-nm-wide magnetic wires

Mahathi Kuchibhotla¹, Abhishek Talapatra², Arabinda Haldar¹ and Adekunle Olusola Adeyeye^{2,3}

¹Department of Physics, Indian Institute of Technology Hyderabad, Kandi 502284, Telangana, India

²Information Storage Materials Laboratory, Department of Electrical and Computer Engineering, National University of Singapore, Singapore 117576

³Department of Physics, Durham University, South Road, Durham, DH1 3LE, United Kingdom

Magnetization dynamics in laterally confined nanostructures have potential applications in magnetic logic, sensors and microwave devices [1]. Here, we have studied the magnetization dynamics in Permalloy (Py) nanowires (width = 90nm) which are fabricated over a large area using deep ultraviolet lithography technique and a field-emission scanning electron microscope (FESEM) image of these nanowires is shown in fig. 1(a). The structures consist of arrays of nanowires with thicknesses $L = 20, 50$ and 70 nm. The reversal processes and dynamic properties are probed using magneto-optical Kerr effect and broadband ferromagnetic resonance (FMR) spectroscopy (fig. 1(b)) techniques, respectively.

Coercive field values strongly depend on the field orientation due to the shape anisotropy of nanowires. The hysteresis loops along the easy and hard axis directions for 20-nm-thick wire are displayed in fig. 1(c). For $L=20$ nm, the magnetization reversal process is dominated by coherent rotation mode and for $L \geq 50$ nm, the magnetization reversal process is dominated by curling mode of reversal. The FMR absorption spectra are sensitive to field orientation as shown in fig. 1(d) for $L=20$ nm. The center mode is also highly sensitive to the film thickness due to the change in demagnetization factors. Nanowires show two well-separated modes near the saturation field; a high-frequency center mode due to the excitations at the center of the nanowire and a low-frequency edge mode due to the inhomogeneous effective field near the edges. In this presentation, we would also discuss the magnetization reversal and dynamic properties in single and trilayer nanodots [2]. Our findings have potential implications for nanoscale magnonic devices.

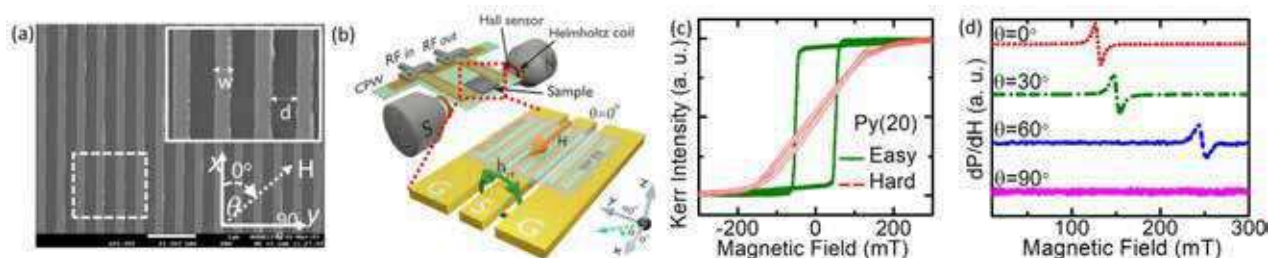


Figure 1 (a) FESEM image of 20-nm-thick nanowire array. (b) Schematic of the FMR experimental setup. (c) Hysteresis loops along easy and hard axis directions and (d) FMR spectra of 20-nm-thick Py measured at different field orientations.

[1] Chumak, A. V. et al. Roadmap on Spin-Wave Computing. IEEE Trans. Magn. 02, 1 (2022).

[2] Kuchibhotla, M. et al. J. Appl. Phys. 130, 083906 (2021).

Optical Control of Spin Waves in YIG/Plasmonic Heterostructures

N. A. Kuznetsov¹, H. Qin¹, L. Flajšman¹ and S. van Dijken¹

¹ NanoSpin, Department of Applied Physics, Aalto University School of Science, Finland.

Optical control of propagating spin waves in yttrium iron garnet (YIG) films enables active reprogramming of the magnonic band structure [1] and redirection of spin-wave transport [2]. For practical devices, real-time manipulation of spin waves should be fast and confined to small areas. Here, we report optical control of propagating spin waves on the microsecond time scale in YIG films with plasmonic nanodisk arrays patterned on top. The YIG films are 300 nm thick and the Au nanodisks are 50 nm thick and have a diameter of 180 nm. By ordering the Au nanodisks in square arrays with different periods, we intentionally utilize the excitation of collective surface lattice resonances (SLRs) to control the absorption of incident laser light. The SLR wavelength tunes with the nanodisk size and array period [3]. The plasmonic arrays are patterned on top of the YIG films between two parallel microwave antennas. Spin-wave transmission between the two antennas is recorded by broadband spin-wave spectroscopy. The wavelength of the laser controlling the spin waves is 915 nm. Figure 1a shows optical transmission spectra for different plasmonic arrays on top of YIG, illustrating the excitation of SLRs (arrows) and a redshift of the SLR resonance with increasing array period. At 915 nm (dashed line), the SLR of the array with a period of 400 nm absorbs most of the incident laser light. Figure 1b shows spin-wave transmission spectra for this plasmonic array demonstrating a drastic reduction of the measurement signal when the laser is turned on. A similar effect is not measured on a bare YIG film. Optical control of spin waves in our YIG/plasmonic heterostructures is explained by thermoplasmonic heating, which causes a local reduction of the magnetization in the YIG film. The timescale of this effect is on the order of microseconds, which is limited by the time resolution of the current experimental setup. Thermoplasmonic simulations predict that optical control of spin waves on the nanosecond timescale is feasible.

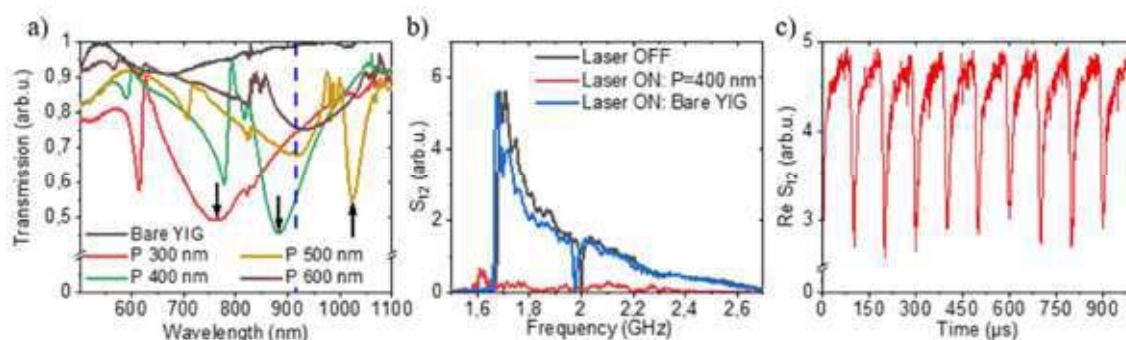


Figure 1. (a) Optical transmission spectra of Au nanodisk arrays on top of YIG. The arrows indicate the positions of the SLRs for arrays with different periods. (b) Spin-wave transmission spectra measured on YIG films without and with a plasmonic array on top. (c) Spin-wave transmission signal at 1.777 GHz during optical pulsing. The period of the plasmonic array on top of the YIG film is 400 nm.

- [1] Vogel, M., Chumak, A., Waller, E. et al. Nat. Phys. 11, 487 (2015).
- [2] Vogel, M., Aßmann, R., Pirro, P. et al. Sci. Rep. 8, 11099 (2018).
- [3] Kravets, V. G., Kabashin, A. V., et al. Chem. Rev. 118, 5912 (2018).

Coulomb Scattering Contribution to Ultrafast Spin Dynamics in a Ferromagnetic Model System: Precession and Relaxation Dynamics

Svenja Vollmar, Kai Leckron and Hans Christian Schneider

Physics Department and Research Center OPTIMAS, University of Kaiserslautern, Germany

A phenomenological description of ultrafast magnetization dynamics, e.g., with the 3-temperature model that couples electrons, spins and phonon systems does not yield microscopic insight into the fundamental processes involved in the transfer of energy and angular momentum between these systems.

We aim at contributing to an understanding of the ultrafast demagnetization by studying microscopic electron dynamics due to electron-electron scattering on ultrashort time scales in ferromagnets. To this end, we employ a ferromagnetic model system with spin-orbit coupled $\mu = \uparrow, \downarrow$ bands (i.e., non-pure spin states) as shown in Fig. 1. [1] After an instantaneous excitation, we (1) compute the Boltzmann-like scattering integrals for the reduced electron spin density matrices $\rho_k^{\mu\mu'}$

$$\frac{\partial}{\partial t} \rho_k^{\mu\mu'} = \frac{i}{\hbar} (\varepsilon_{k\mu} - \varepsilon_{k\mu'}) + \frac{\pi}{\hbar} \sum_{lq} \sum_{\substack{\mu_1\mu_2\mu_3 \\ \mu_4\mu_5\mu_6\mu_7}} (V_{klq}^{\mu\mu_1\mu_2\mu_3})^* (V_{klq}^{\mu_4\mu_5\mu_6\mu_7} - V_{l+q,lk-l}^{\mu_4\mu_5\mu_6\mu_7}) \delta(\Delta E_{klq}^{\mu_4\mu_5\mu_6\mu_7}) \\ \left[\rho_{k+q}^{\mu_3\mu_7} \rho_l^{\mu_2\mu_6} (\delta_{\mu_1\mu_5} - \rho_{l+q}^{\mu_5\mu_1}) (\delta_{\mu'\mu_4} - \rho_k^{\mu_4\mu'}) - \rho_k^{\mu_4\mu'} \rho_{l+q}^{\mu_5\mu_1} (\delta_{\mu_2\mu_6} - \rho_l^{\mu_2\mu_6}) (\delta_{\mu_3\mu_7} - \rho_{k+q}^{\mu_3\mu_7}) \right] \\ + (\mu \leftrightarrow \mu')^*$$

In order to reduce the considerable numerical complexity of such an approach, we propose an extended relaxation-time ansatz that enforces the conservation of energy, density and spin. We

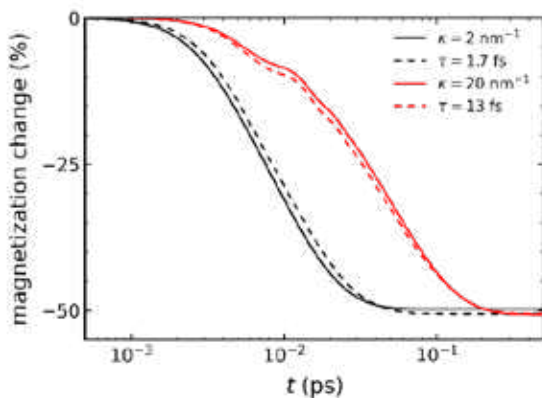


Figure 2: Magnetization dynamics for different screening lengths κ computed with the microscopic Boltzmann-like scattering terms (solid lines) and computed using relaxation times τ that produce similar spin dynamics for the extended relaxation time ansatz (dotted lines).

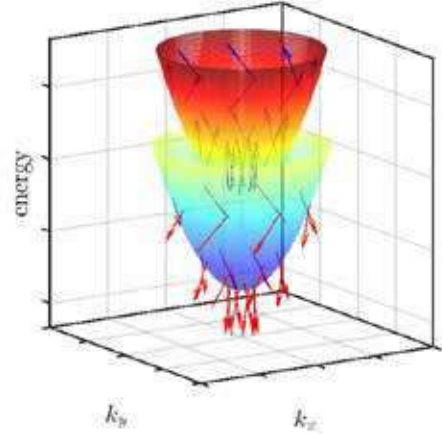


Figure 1: Band structure of the spin-split model system. Local spin expectation values are plotted as arrows for some k -points to indicate the non-pure spin states due to spin-orbit coupling.

compare this novel ansatz to our solution of the full dynamics in Fig. 2. We find a remarkable agreement between these approaches for the demagnetization dynamics shown in the figure. Importantly, the ansatz also captures precessional dynamics induced by spin-orbit coupling combined with spin conserving scattering [1] and is superior to established relaxation-time approximations. We also find a Dyakonov-Perel like behavior of the *spin relaxation time* τ_s on the *momentum scattering time* τ .

[1] K. Leckron, H. C. Schneider, *Phys. Rev. B* **96**, 140408 (2018).

The impact of perpendicular anisotropy, Dzyaloshinskii–Moriya interaction and damping on spin wave dispersion and mode softening in thin magnetic films

Nikodem Leśniewski¹ and Paweł Gruszecki¹

¹ ISIK, Faculty of Physics, Adam Mickiewicz University, Poznań, 61-614, Poland

Basic magnetic parameters determining the internal structure and chirality of domain walls are perpendicular magnetocrystalline anisotropy (PMA), film's thickness, and Dzyaloshinskii–Moriya interaction (DMI)[1]. However, these parameters also significantly influence spin wave (SW) dynamics in uniformly in-plane magnetized thin films. For example, the presence of PMA may induce a minimum in the dispersion relation for a non-zero wave number ($k \neq 0$) in the so-called Damon-Eshbach geometry[2]. DMI, on the other hand, causes the asymmetry of the dispersion relation (breaking of the mirror symmetry with respect to $k=0$) due to the different spatial chirality of the waves propagating in the opposite directions. Furthermore, the thicker film, the more pronounced the dipolar interactions, which also affects SWs. Here, we perform an extensive study of the effects of DMI, PMA, thickness, and damping values on the SW dispersion relation. Using the finite element method, we solve the linearized Landau-Lifshitz-Gilbert equation in the frequency domain for the Damon-Eshbach geometry. In our study, we analyze and compare films of various thicknesses made of two different magnetic materials, i.e., CoFeB and Ga-doped yttrium iron garnet. We show that even for small values of PMA, the minimum for $k \neq 0$ may appear (see the example shown in Figure 1). Furthermore, as the field value decreases, the minimum deepens significantly. This is related to the softening of SWs. Interestingly, for the case shown in Figure 1(b) and the field 60.3 mT, the difference in frequencies for $\alpha=0.03$ is up to 0.4 GHz lower than for $\alpha=0.001$ whereas for 75 mT there is no difference. Finally, we analyze the impact of all the beforementioned parameters on mode profiles of SWs. Our results reveal unique properties of the softened SWs from the bottom of the dispersion relation.

We acknowledge the funding from the Polish National Science Centre project No. UMO-2019/33/B/ST5/02013.

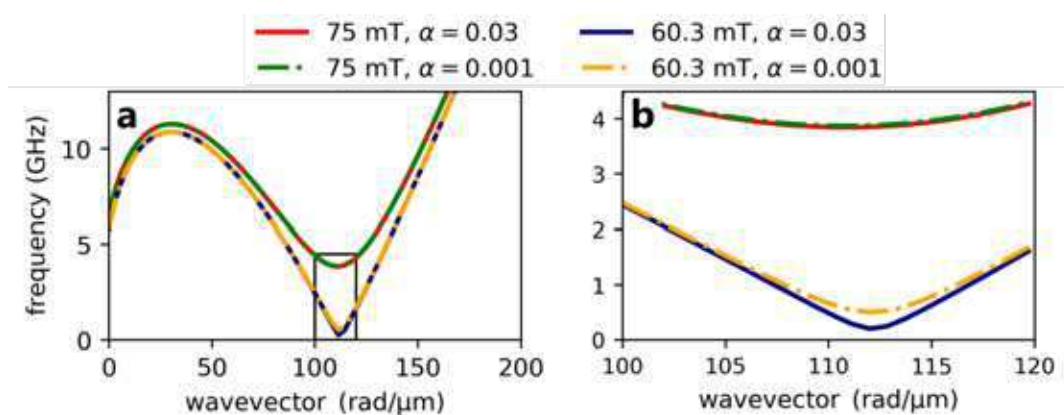


Figure 1. Dispersion relations of SWs in a 15 nm thick uniformly in-plane magnetized CoFeB film with PMA ($K_{\text{PMA}}=690$ kJ/m³) and no DMI for the following combinations of the magnetic field and damping constant: 75 mT and $\alpha=0.03$ (the solid red line); 75 mT and $\alpha=0.001$ (the dash-dotted green line); 60.3 mT and $\alpha=0.03$ (the solid navy blue line); and 60.3 mT and $\alpha=0.001$ (the dash-dotted orange line). (b) shows a zoomed-in section of the dispersion relation from (a) marked by the black rectangle.

[1] Kisielewski et al. *New J. Phys.* 21, 093022 (2019).

[2] Banerjee et al. *Phys. Rev. B* 96, 024421 (2017).

Towards fast exchange magnonics: partially compensated Ga:YIG garnets

Khrystyna O. Levchenko¹, Tobias Böttcher^{2,3}, Moritz Ruhwedel², Qi Wang¹,
Hryhorii L. Chumak⁴, Maksym A. Popov⁴, Igor V. Zavislyak⁴, Carsten Dubs⁵,
Oleksii Surzhenko⁵, Burkard Hillebrands², Andrii V. Chumak¹, and Philipp Pirro²

¹ University of Vienna, Faculty of Physics, Boltzmanngasse 5, A-1090 Vienna, Austria

² Fachbereich Physik and Zentrum OPTIMAS, TU Kaiserslautern, Kaiserslautern, Germany

³ MAINZ Graduate School of Excellence, Staudingerweg 9, 55128 Mainz, Germany

⁴ Faculty of Radiophysics, Electronics, Computer Systems, T. Shevchenko KNU, 01601, Kyiv, Ukraine

⁵ INNOVENT e.V. Technologieentwicklung, Prüssingstrasse 27B, 07745, Jena, Germany

Spin-wave based logic proved to be a CMOS-competitive technology, with an exemplary concept of the magnonic half-adder, demonstrated by Wang et al., [1], surpassing the conventional devices in energy consumption and optimised fabrication methodology. To further facilitate the magnonics technology, the delay time in nanostructures should be improved by utilising fast exchange spin-waves and reaching higher operational frequencies, respectively. Since the exchange contribution to the group velocity v_{gr} is directly proportional to the exchange stiffness λ_{ex} , materials with enhanced stiffness and low saturation magnetisation M_s are promising candidates for the investigation. For this purpose, single-crystalline sub-100 nm thick films of Ga:YIG and 97 nm reference YIG were fabricated via liquid phase epitaxy (LPE) [2]. Ferromagnetic resonance (FMR) measurements of the 59 nm thick Ga:YIG film revealed a small saturation magnetisation ($\mu_0 M_s \sim 20$ mT), a strong out-of-plane uniaxial anisotropy ($\mu_0 H_{u1} \sim 90$ mT) and a good Gilbert damping parameter $\alpha = 6.1 \cdot 10^{-4}$ [3].

The dispersion relation of thermally excited dipole-exchange spin-waves propagating perpendicularly to the applied field in 59-nm Ga:YIG film was probed by Brillouin light scattering (BLS) spectroscopy. The exchange stiffness in the film under investigation $\lambda_{ex} = (13.54 \pm 0.07) \times 10^{-11} \text{ T} \cdot \text{m}^2$ is about three times as large as the one for pure YIG, that results in much higher (~ 3.4 times) group velocities for $k > 30 \text{ rad}/\mu\text{m}$ (Fig. 1). Even the spin waves of the relatively small wave vector $k \approx 4 \text{ rad}/\mu\text{m}$ exhibit an exchange nature and their dispersion relation is significantly more isotropic compared to the waves of the same wavelength in YIG. Thus, Ga:YIG opens access to the operation with the fast isotropic exchange spin-waves of variable wavelengths in future magnonics networks.

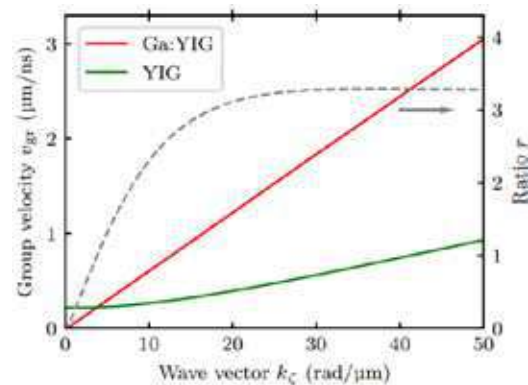


Figure 1: Group velocity [3] calculated from the dispersion relations for 59 nm thick Ga:YIG film (red) and pure YIG (green) at an applied field of 300 mT. The ratio r of the group velocities for Ga:YIG and YIG is plotted by a grey dashed line.

[1] Q. Wang, et al., *Nat. Electron.* **3**, 765–774 (2020).

[2] C. Dubs et al., *Phys. Rev. Materials* **4**, 024416 (2020).

[3] T. Böttcher, et al., *in-print Appl. Phys. Lett.* (accepted 18.02 2022), arXiv:2112.11348.

Magnon-magnon entanglement and its detection in a microwave cavity

Vahid Azimi Mousolou^{1,2}, Yuefei Liu³, Anders Bergman², Anna Delin^{2,3,4}, Olle Eriksson^{3,4}, Manuel Pereiro², Danny Thonig², and Erik Sjöqvist²

¹Department of Applied Mathematics and Computer Science, Faculty of Mathematics and Statistics, University of Isfahan, Isfahan 81746-73441, Iran

²Department of Physics and Astronomy, Uppsala University, Box 516, SE-751 20 Uppsala, Sweden

³Department of Applied Physics, School of Engineering Sciences, KTH Royal Institute of Technology, AlbaNova University Center, SE-10691 Stockholm, Sweden

⁴Swedish e-Science Research Center (SeRC), KTH Royal Institute of Technology, SE-10044 Stockholm, Sweden

⁵School of Science and Technology, Örebro University, SE-701 82, Örebro, Sweden

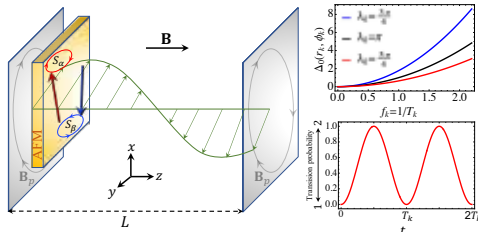


Figure 1: A schematic of magnet-cavity system to measure the entanglement of the magnon modes. The EPR function Δ_0 quantifies the entanglement of magnons in the ground state and it can be inversely deduced by measuring the transition frequency between acoustic magnons and photons (f_k) in the cavity. λ_k is the scaled wavenumber. [1]

and Rosen (EPR) function of the ground state opens up for experimental observation of magnon-magnon continuous variable entanglement and EPR non-locality. Our recent work proposes a practical experimental realization to detect the EPR function of the ground state, in a setting that relies on magnon-photon interaction in a microwave cavity[1]. Moreover, we consider the phonon effect, we analysis the magnon-magnon-phonon steady-state quantum entanglement in antiferromagnetic structure by solving a generalised system based on the Heisenberg-Langevin approach contains bipartite and tripartite coupling terms [2].

[1] Vahid Azimi Mousolou, Yuefei Liu, Anders Bergman, Anna Delin, Olle Eriksson, Manuel Pereiro, Danny Thonig, and Erik Sjöqvist, *Phys. Rev. B* **104**, 224302 (2021).

[2] A manuscript is preparing to publication now.

Quantum magnonics is an emerging research field, with great potential for applications in magnon based hybrid systems and quantum information processing. Quantum correlation, such as entanglement, is a central resource in many quantum information protocols that naturally comes about in any study toward quantum technologies. This applies also to quantum magnonics. First, we investigate antiferromagnets in which sublattices with ferromagnetic interactions can have two different magnon modes, and we show how this may lead to experimentally detectable bipartite continuous variable magnon-magnon entanglement. The entanglement can be fully characterized via a single squeezing parameter, or, equivalently, entanglement parameter. The clear relation between the entanglement parameter and the Einstein, Podolsky,

and Rosen (EPR) function of the ground state opens up for experimental observation

Goos-Hänchen effect at Brillouin light scattering by a magnetostatic wave in the Damon-Eshbach configuration

Yuliya S. Dadoenkova¹, Maciej Krawczyk², and Igor L. Lyubchanskii^{3,4}

¹ *Lab-STICC (UMR 6285), CNRS, ENIB, Brest Cedex 3, 29238, Brest, France*

² *Institute of Spintronics and Quantum Information, Faculty of Physics, Adam Mickiewicz University in Poznań, 61-614, Poznań, Poland*

³ *Donetsk Institute for Physics and Engineering named after O. O. Galkin (Branch in Kharkiv) of the National Academy of Sciences of Ukraine, 03028, Kyiv, Ukraine*

⁴ *V. N. Karazin Kharkiv National University, 61022, Kharkiv, Ukraine*

The Goos-Hänchen effect is characterized by the lateral shift of the reflected electromagnetic wave from the interface of two media in contrast to the laws of the geometric optics. This phenomenon was predicted and observed for the first time by F. Goos and H. Hänchen at the glass-air interface in the forties of the 20-th century [1] and nowadays is known as the Goos-Hänchen effect which is well studied in linear optics [2].

For the three-wave interaction, the Goos-Hänchen effect has been studied for the optical second harmonic generation [3, 4] and for Brillouin light scattering by acoustic phonons [5].

In this communication, we report the results of theoretical investigation of the Goos-Hänchen effect at Brillouin light scattering by magnetostatic waves in the Damon-Eshbach configuration. The lateral shift of an optical beam undergoing Brillouin light scattering by a spin wave propagating along the interface between magnetic and dielectric media (Damon-Eshbach configuration) in the total internal reflection geometry is studied in the framework of phenomenological theory. Linear and quadratic magneto-optic terms in polarization are taken into account. It is shown that the lateral shift depends on the polarization (s- or p-) state of the scattered electromagnetic wave as well as on the frequency of the spin wave [6].

[1] F. Goos and H. Hänchen, *Ann. Phys.* **436**, 333 (1947).

[2] K. Y. Bliokh and A. Aiello, *J. Opt.* **15**, 014001 (2013).

[3] H. Shih and N. Blombergen, *Phys. Rev. A* **3**, 412 (1971).

[4] V. J. Yallapragada, A. V. Gopal, and G. S. Agarwal, *Opt. Express* **21**, 10878 (2013).

[5] Y. S. Dadoenkova, N. N. Dadoenkova, M. Krawczyk, and I. L. Lyubchanskii, *Opt. Letters* **43**, 3965 (2018).

[6] Y. S. Dadoenkova, M. Krawczyk, and I. L. Lyubchanskii, *Opt. Mater. Express* **12**, 717 (2022).

Presence of a sizable *out-of-plane* interaction in a stripe discommensurated 214 -nickelate $\text{Pr}_{3/2}\text{Sr}_{1/2}\text{NiO}_4$ ($\epsilon = 0.4$)

Avishek Maity¹, Rajesh Dutta^{2,3}, and Werner Paulus⁴

¹Heinz Maier-Leibnitz Zentrum (MLZ), Technische Universität München, 85747 Garching, Germany

²Institut für Kristallographie, RWTH Aachen Universität, 52066 Aachen, Germany

³Jülich Centre for Neutron Science (JCNS) at Heinz Maier-Leibnitz Zentrum (MLZ), 85747 Garching, Germany

⁴Institut Charles Gerhardt Montpellier, Université de Montpellier, 34095 Montpellier, France

Here we present our recent inelastic neutron scattering (INS) study on the magnetic excitations of an incommensurate stripe ordered single crystal of $\text{Pr}_{3/2}\text{Sr}_{1/2}\text{NiO}_4$. Magnetic excitations in the stripe-phases of *La*-based 214 -nickelates have been well explored using INS while *Pr*-based 214 -nickelates remains unexplored in this regard. So far in the previous studies the measured magnetic excitations in an incommensurate stripe have been often described in a closest commensurate description of the stripe phase using a linear spin wave (LSW) theory. Whereas in our study, we attempt to consider the underlying incommensurate spin microstructure in the discommensuration spin-stripe (DCSS) model for our LSW calculation. In particular, the magnetic excitations of $\text{Pr}_{3/2}\text{Sr}_{1/2}\text{NiO}_4$ show a symmetrical outward shift of the dispersion from antiferromagnetic (AFM) zone center in the energy range 35 to 45 meV. Our LSW calculation using a 3D model of DCSS unit for $\epsilon = 0.4$, combining a checker board (CB) unit and a $1/3$ -stripe unit, explicitly shows such outward shift of the spin wave dispersion results from the overlap of a separate mode, originating exclusively from the *out-of-plane* interaction ($J_{\perp} \sim 2.2$ meV). This suggests the presence of a significant *out-of-plane* interaction near the half-doped region of $\text{Pr}_{3/2}\text{Sr}_{1/2}\text{NiO}_4$ which has been predominantly neglected in the other hole doped 214 -nickelates proposing them as quasi- or purely 2D AFM in nature. Our LSW calculation taking into account the *out-of-plane* exchange interactions in addition to the *in-plane* interactions shows a very good agreement with the measured magnetic excitations. Our study suggests that a careful consideration of the *out-of-plane* interaction is necessary in the 3D-DCSS model to uncover many interesting features of magnetic excitations in the stripe discommensurated phases of strongly correlated 214 -nickelates.

[1] A. Maity, R. Dutta, and W. Paulus, *Phys. Rev. Lett.* **124**, 147202 (2020).

THz-light driven spin-lattice coupling in cobalt difluoride

E.A. Mashkovich

University of Cologne, Cologne, Germany

Understanding spin-lattice coupling is among the key challenges in modern condensed matter physics [1,2]. The efficiency of angular momentum and energy transfer between spins and lattice imposes fundamental limits on the speed to control spins in spintronics, magnonics and magnetic data storage. At the same time, it has been long believed that a coherent transfer of energy from spins to lattice requires their linear coupling.

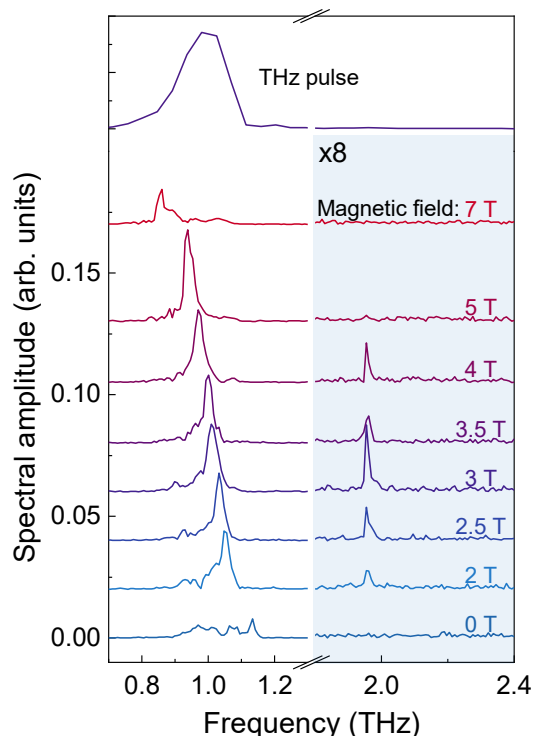


Figure: Fourier spectra of THz induced dynamics at different external magnetic fields. Temperature was set to 5 K. The THz pump frequency was centred at 1 THz with a bandwidth of 20%. THz pulse spectrum measured by electro-optical sampling is shown on the top.

magnon frequency at this resonance is close to earlier mentioned frequency matching condition: the magnon frequency matches half of the phonon frequency. The results demonstrate that spin-lattice coupling can be tuned by an external magnetic field.

Recently we have discovered a new nonlinear mechanism for THz-light driven spin-lattice coupling in CoF_2 [3]. High-intense THz pulse resonantly interacts with a coherent magnonic state (1.14 THz at 5 K) in CoF_2 and excites the Raman-active THz phonon (1.97 THz at 5 K). In our experiments the magnon amplitude scales linear on THz magnetic field strength which is typical for the conventional Zeeman torque excitation mechanism [4]. In contrast, the phonon amplitude scales quadratically with the THz field strength clearly evidencing the nonlinear excitation mechanism [5]. The phonon amplitude reaches maximum near a special temperature at which the magnon frequency matches half of the phonon frequency. Above the Néel temperature, the phonon practically is not excited, thus clearly indicating spin-mediated mechanism of excitation.

Moreover, we have performed unique measurements combining high-intense THz pulses and high static magnetic fields (up to 10 T) in TELBE facility (Dresden, Germany). The phonon excitation shows resonance behaviour while tuning the frequency of the magnon with the help of external magnetic field (see Fig. 1). Interestingly that the

- [1] C. Dornes et al., *Nature* **565**, 209–212 (2019)
- [2] K.S. Burch et al., *Nature* **563**, 47–52 (2018)
- [3] E.A. Mashkovich et. al., *Science* **374**, 1608 (2021)
- [4] T.G.H. Blank et al., *Phys. Rev. Lett.* **127**, 037203 (2021)
- [5] E.A. Mashkovich et al., *Phys. Rev. Lett.* **123**, 157202 (2019)

Nonreciprocal propagation of surface acoustic waves in a CoFeB/Ru/CoFeB trilayer synthetic antiferromagnet

Hiroki Matsumoto, Takuya Kawada, Mio Ishibashi, Masashi Kawaguchi, and Masamitsu Hayashi

The Univ. of Tokyo, Hongo, Bunkyo, Japan

Surface acoustic waves (SAW) excited on a ferroelectric substrate can drive a spin wave in a ferromagnetic (FM) thin film owing to magnetoelastic coupling [1,2]. Recently, nonreciprocal propagation of SAW based on the coupling between SAW and spin wave has been experimentally demonstrated in various systems. Some use a helicity mismatch between SAW and spin wave [3-6] and others take advantage of nonreciprocal dispersion of spin waves [6-9]. In particular, a dipole-coupled FM bilayer with a nonmagnetic spacer is known to have a highly nonreciprocal spin wave dispersion [10, 11], which in turn causes a large amplitude nonreciprocity of SAW with the order of 10 dB/mm (90% power difference for a propagation length of 1 mm) [8,9]. The nonreciprocity of SAW in a synthetic antiferromagnet with an interlayer exchange coupling via RKKY interaction, however, is yet to be reported experimentally. To study this effect, we investigated SAW propagation in CoFeB/Ru/CoFeB tri-layers, in which significant nonreciprocity of spin waves has been found [12,13].

We fabricated CoFeB/Ru/CoFeB tri-layers on a 128°Y-cut LiNbO₃ substrate. By measuring the external magnetic field dependence of the magnetization and planar Hall resistance, we confirmed that magnetizations in the CoFeB layers are antiferromagnetically coupled. Then, we examined SAW-driven spin wave resonance using a vector network analyzer. We found nonreciprocity of 37 dB/mm at 1.4 GHz SAW, which is about 100 times as large as the previous result in FeGaB-based tri-layers without the interlayer exchange coupling. To investigate how the interlayer exchange coupling affects the nonreciprocity, we carried out the same measurement for the devices with different Ru spacer thicknesses. Consequently, we found that the nonreciprocity increases with increasing interlayer exchange coupling strength. The results imply that the interlayer exchange coupling amplifies the nonreciprocity coming from the dipolar coupling.

This work was partly supported by JSPS KAKENHI (Grant Nos.20J20952) from JSPS, and JSR Fellowship, the University of Tokyo.

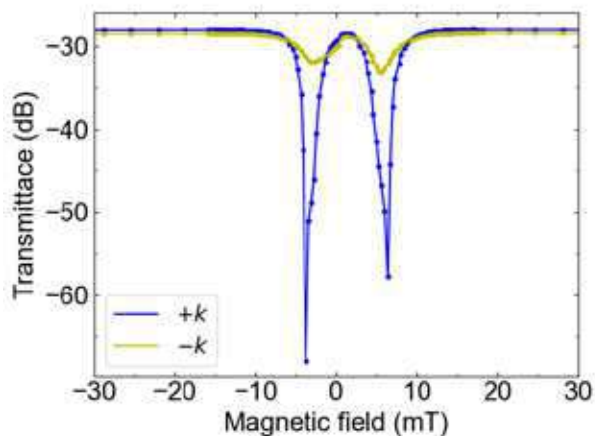


Figure: Magnetic field dependence of the transmittance in the SAW device with a CoFeB/Ru/CoFeB tri-layer.

- [1] M. Weiler *et al.*, *Phys. Rev. Lett.* **106**, 117601 (2011). [2] L. Dreher *et al.*, *Phys. Rev. B* **86**, 134415 (2012). [3] R. Sasaki *et al.*, *Phys. Rev. B* **95**, 020407(R) (2017). [4] S. Tateno and Y. Nozaki, *Phys. Rev. Appl.* **13**, 034704 (2020). [5] A. Hernández-Mínguez *et al.*, *Phys. Rev. Appl.* **13**, 044018 (2020). [6] M. Xu *et al.*, *Sci. Adv.* **6**, eabb1724 (2020). [7] M. Küß *et al.*, *Phys. Rev. Lett.* **125**, 217203 (2020). [8] P.J. Shah *et al.*, *Sci. Adv.* **6**, eabc5648 (2020). [9] M. Küß *et al.*, *Phys. Rev. Appl.* **15**, 034060 (2021). [10] S. Wintz *et al.*, *Nat. Nanotechnol.* **11**, 948 (2016). [11] R.A. Gallardo *et al.*, *Phys. Rev. Appl.* **12**, 034012 (2019). [12] M. Ishibashi *et al.*, *Sci. Adv.* **6**, eaaz6931 (2020). [13] Y. Shiota *et al.*, *Phys. Rev. Lett.* **125**, 017203 (2020).

Spin-lattice couplings and their effects in transition-metal magnetic crystals with *ab-initio* accuracy

Ivan P. Miranda¹, Maryna Pankratova¹, Anders Bergman¹, Olle Eriksson^{1,2}

¹*Department of Physics and Astronomy, Uppsala University, Box 516, SE-75120 Uppsala, Sweden*

²*School of Science and Technology, Örebro University, 702 81 Örebro, Sweden*

In the emergent field of ultrafast magnetization dynamics, understanding the interplay between lattice, spin, and electrons is extremely relevant to the description of several phenomena. For systems with magnetic order, characterized by the existence of a collective motion of spins, both magnetic moments and lattice degrees of freedom are coupled via the electronic medium, which can influence, for instance, both magnon and phonon spectrum and lifetimes. Although a formalism to describe the magnetization dynamics accounting for the spin-lattice coupling (SLC) is known from many years ago [1], there is still a gap in the literature regarding the parameters for real materials, obtained with first-principles accuracy. From a theoretical point of view, this requires computing the magnetic interactions (*e.g.* Heisenberg exchange, Dzyaloshinskii-Moriya) in an inversion symmetry broken situation, making the use of real-space-based *ab-initio* methods a suitable way to calculate such parameters. The combination with state-of-the-art spin-lattice-dynamics simulations [2], then, make it possible to investigate the influence of such SLC parameters in a wide range of materials.

In this talk, the results of spin-lattice calculations and their impact will be shown and discussed. We will consider briefly the well-known ferromagnetic test cases (bcc Fe and fcc Ni), but also - and more interestingly - systems in which the impact of SLC is greater due to significant changes in magnetic moments and/or interactions, such as γ -Fe and Invar (Fe-Ni). For γ -Fe, for instance, our results show that small atomic displacements of less than 0.02 Å in the lower-energy spin-spiral configuration lead to a $\sim 80\%$ change in the noncollinear J_{ij} 's, almost changing the nearest neighbors from AFM to FM.

-
- [1] V. P. Antropov, M. I. Katsnelson, B. N. Harmon, M. van Schilfgaarde, and D. Kusnezov, Phys. Rev. B **54**, 1019 (1996).
 - [2] J. Hellsvik, D. Thonig, K. Modin, D. Iuşan, A. Bergman, O. Eriksson, L. Bergqvist, and A. Delin, Phys. Rev. B **99**, 104302 (2019).

Dynamic interactions between edge and bulk modes in an antidot lattice with perpendicular magnetic anisotropy

M. Moalic¹, M. Zelent¹ and M. Krawczyk¹

¹ Department of Nanostructures, Institute of Spintronic and Quantum Information, Adam Mickiewicz University, Uniwersytetu Poznańskiego 2, Poznań, 61-614, Poland

Patterned arrays in thin films have shown a lot of potential due to their abilities to manipulate magnetic microwave excitation, called spin waves (SWs). These types of periodic nanostructures, also called magnonic crystals, are seen as the magnetic variant of the photonic crystals with the added advantage that SWs can have a wavelength smaller than their optical counterpart, which can lead to the creation of magnonic devices with a very small footprint. In the case of antidot lattices, the inhomogeneous material found around each antidot can bring forward an interesting range of complex, hybridized resonant SW modes. Thin films with out-of-plane magnetization are more interesting than those with in-plane magnetization due to the SWs dispersion relation being isotropic. The out-of-plane magnetization is achieved in ferromagnetic thin films with perpendicular magnetic anisotropy due to a multilayered approach using multiple layers of alternating ferromagnetic metals and heavy metals.

The film we study is made up of 8 repetitions of Co (0.75nm) and Pd (0.9nm) bilayers for a total of 13.2 nm [1]. Periodically throughout this thin-plane film, nanodots were etched out using a 10nm wide focused ion beam creating a pattern of antidots. This process not only removed some material, but also damaged the area around each antidot, creating a 'ring' of low anisotropy in the film. This results in the configuration of the magnetization at the edges of the antidot being almost in-plane. For a circular antidot shape, the ground state of such a system has magnetization in the edge ring in a vortex-like configuration as seen in Fig. 1. Through micromagnetic simulations, we are analysing dynamical coupling between edge localised and bulk modes in the film. We modify many parameters in this system such as lattice constant, antidot shape, antidot size, ring width, external field direction, etc. Different types of modes are identified, such as the ferromagnetic resonant mode of the thin film around 9.5 GHz as well as higher frequency bulk modes resulting from the antidot lattice. A multitude of edge modes have also been identified in the low anisotropy rings at frequencies from 3 to 13 GHz with, for example, the one seen in Fig. 2. We show that the strong dynamical coupling between the rings can be obtained, which demonstrates collective behaviour on the lattice and promises usefulness for magnonic applications.

The authors acknowledge funding from the Polish National Science Centre, project No. UMO-2020/37/B/ST3/03936.

[1] Pan, S., et al. Physical Review B 101.1 (2020): 014403.

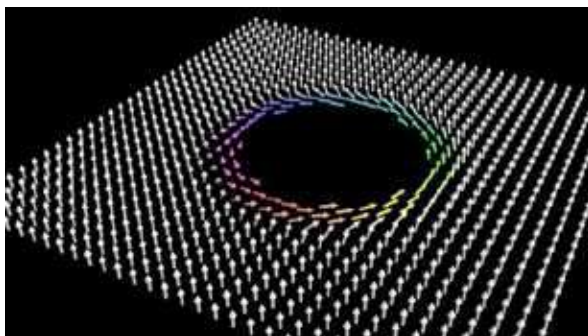


Figure 1. Magnetization for one cell of the antidot lattice

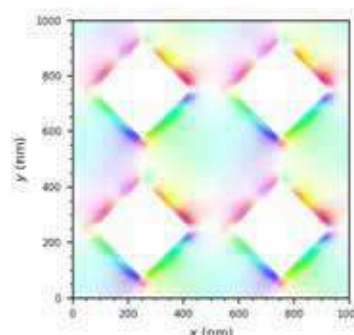


Figure 2. Edge modes for a diamond antidot lattice for a lattice constant of 500 nm.

Optical detection of magnon-phonon coupling using μ FR-MOKE technique

M. Müller^{1,2}, L. Liensberger^{1,2}, T. Luschmann^{1,2,3}, M. Weiler⁴, M. Althammer^{1,2}, R. Gross^{1,2,3} and H. Huebl^{1,2,3}

¹ Walther-Meißner-Institut, Bayerische Akademie der Wissenschaften, Garching, Germany

² Physik-Department, Technische Universität München, Garching, Germany

³ Munich Center for Quantum Science and Technology (MCQST), München, Germany

⁴ Technische Universität Kaiserslautern, Kaiserslautern, Germany

In a recent publication, An et al. [1] experimentally demonstrated the coupling of the Kittel resonances of two ferromagnetic yttrium iron garnet (YIG) thin films via transverse phononic shear waves in a gadolinium gallium garnet (GGG) substrate as well as the transfer of angular momentum via phonons between two YIG layers.

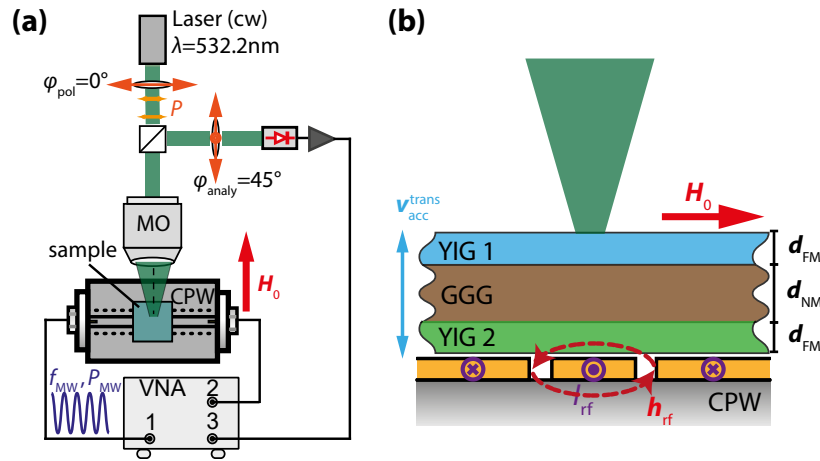


Figure 1: (a) Schematic depiction of the μ FR-MOKE setup. (b) Transverse section of the samples on the CPW. By shifting the focal point of the laser spot from the top YIG 1 to the bottom YIG 2 layer of the sample, the magnon-phonon coupling of the top- and bottom YIG layer can be individually investigated.

We here present an experimental approach to investigate magnon-phonon coupling for the participating YIG layers on an individual basis. In detail, we investigate a YIG/GGG/YIG trilayer sample using microfocused frequency-resolved magneto-optic Kerr effect (μ FR-MOKE) spectroscopy [2] as shown in Fig. 1(a). We will discuss the magnetization dynamics recorded individually for the top and bottom layer with those acquired using broadband ferromagnetic resonance (bbFMR). This data gives insight to the modes at play as well as their coupling. We expect that this technique will allow the investigation of microstructures, which are discussed for frequency conversion applications [3] and are expected to show enhanced coupling rates via their optimized geometry.

[1] K. An *et al.*, *Phys. Rev. B* **101**, 060407(R) (2020).

[2] L. Liensberger *et al.*, *IEEE Magn. Lett.* **10**, 1 (2019).

[3] J. Graf *et al.*, *Phys. Rev. Res.* **3**, 013277 (2021).

Modelling of magnetoelectric transducers for spin-wave generation

**Daniele Narducci^{1,2}, F. Vanderveken^{1,2}, G. Talmelli^{1,2}, M. Heyns^{1,2}, J. De Boeck^{1,3},
C. Adelmann¹ and F. Ciubotaru¹**

¹ imec, Leuven B-3001, Belgium

² KU Leuven, Departement Materiaalkunde, 3001 Leuven, Belgium

³ KU Leuven, Department of Electrical Engineering (ESAT), 3001 Leuven, Belgium

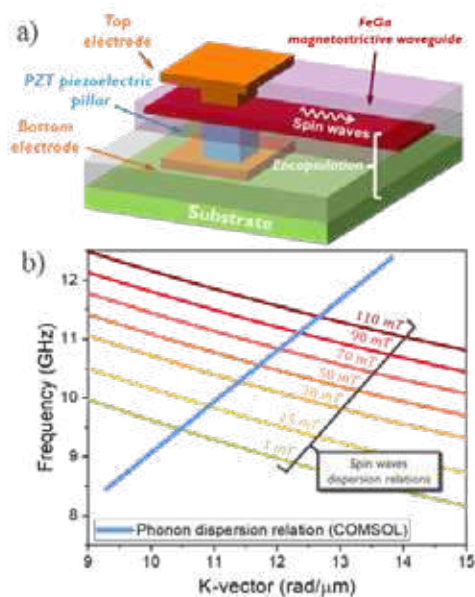


Figure 1. a) Schematic of a simulated device.
b) Dispersion relations for phonons and spin waves in backward volume configuration for different applied magnetic fields.

Spin waves computing relies on the encoding of the information into the phase or the amplitude of the waves. [1] One potential route to generate efficiently spin waves at relevant nano-scale dimensions is based on magnetoelectric (ME) transducers.

[2] A schematic of such a device is shown in Fig. 1(a) and it is consisting of a piezoelectric (PZT) – magnetic (e.g., FeGa) heterostructure. The ME transducers couple magnetic and mechanical degrees of freedom via (inverse) magnetostriction. When the mechanical stress is generated by piezoelectric effects, voltage signals can be used to generate spin waves in a magnetic waveguide.

Here we report on an intensive study by numerical simulations of the mechanical and magnetic behaviour of ME transducers of different geometries from μm to sub-100 nm feature sizes. The mechanical response is studied using COMSOL Multiphysics whereas micromagnetic MuMax code [3] was used to analyse

the magnetic behaviour. The simulated structures include realistic embedding and encapsulation conditions. Both elastic waves (phonons) and spin waves have been studied in terms of dispersion relations and amplitude distributions for various device configurations. The magnetoelastic fields were estimated as well. The intersection between dispersions relations of acoustic and spin waves (Fig. 1(b)) suggests the possibility to generate magnetoelastic waves, where the coupling between the elastic and magnetic domain is maximized.

This work has been funded by the European Union's Horizon 2020 research and innovation program within the FET-OPEN Project CHIRON under Grant Agreement No. 801055. D.N. and F.V. acknowledge financial support from the Research Foundation – Flanders (FWO) through Grant Nos. 1SB9121N and 1S05719N, respectively.

[1] A. Mahmoud, et al. J. Appl. Phys. **128**, 161101 (2020).

[2] S. Manipatruni, D. E. Nikonov, and I. A. Young, Nature Phys., **14**, 338 (2018).

[3] F. Vanderveken et al., Open Research Europe **1**:35 (2021).

Heat-conserving three-temperature model for ultrafast magnetisation dynamics simulations

M. Pankratova¹, I. P. Miranda¹, D. Thonig^{1,2}, M. Pereiro¹, E. Sjöqvist¹,
A. Delin³, O. Eriksson^{1,2}, and A. Bergman¹

¹*Department of Physics and Astronomy, Uppsala University, Box 516, SE-75120 Uppsala, Sweden*

²*School of Science and Technology, Örebro University, SE-701 82, Örebro, Sweden,*

³*Department of Applied Physics, School of Engineering Sciences, KTH Royal Institute of Technology, AlbaNova University Center, SE-10691 Stockholm, Sweden*

Intensive theoretical and experimental studies in the field of ultrafast demagnetization were initialized by the pioneering work of Beurepaire and coauthors [1] who showed demagnetization of nickel on subpicosecond timescales after the application of a femtosecond laser pulse. The dynamics of the system after the absorption of the laser pulse is usually interpreted within the so-called two- or three-temperature models (3TM). These models assume several heat reservoirs, such as spin, electron, and lattice that can exchange energy with each other. The heat transfer between the reservoirs is given by heat transfer coefficients in the 3TM, which are G_{es} for electron-spin, G_{sl} for spin-lattice, and G_{el} for the electron-lattice coefficients. Unfortunately, it is challenging to accurately estimate these coefficients from experiments or first principles. The data for an electron-lattice coefficient of nickel – the popular object of ultrafast demagnetization experiments – can vary one order of magnitude [2].

Therefore, a more accurate description of magnetisation dynamics and thermalisation processes requires a model that reduces the number of approximations used in the phenomenological 3TM. In our work, we propose a so-called heat-conserving three-temperature model (HC3TM). Here, we assume that the spin and lattice subsystems are coupled via damping terms to an electronic heat bath that is considered to be finite and governs the spin and lattice temperatures. Therefore, if the spin and lattice temperatures increase, electronic temperature decreases, as follows from conservation of heat. Spin and lattice temperature dynamics are derived from fluctuations and dissipation of Langevin dynamics. The model has successfully been applied to study magnetisation dynamics of fcc Ni and bcc Fe. In our work, we compare the results of HC3TM with the 3TM and study the importance of introducing temperature-dependent heat capacities. Variable electronic heat capacities were considered in [1,3] but in our work spin and lattice capacities are also temperature-dependent. We show that HC3TM significantly improves the description of magnetisation dynamics in comparison to 3TM, especially during the first picosecond after the application of a laser pulse.

[1] E. Beaurepaire, J.-C. Merle, A. Daunois, and J.-Y. Bigot, Phys. Rev. Letters, **76**, 4250 (1996).

[2] D. Zahn, F. Jakobs, Y. W. Windsor, et al., Phys. Rev. Research, **3**, 023032 (2021).

[3] B. Koopmans, G. Malinowski, F. Dalla Longa, et al., Nature Mater **9**, 259 (2010).

Using Propagating Spin Wave Spectroscopy to Probe Interfacial Phenomena Modified by an Electric Field

Adrien A. D. Petrillo¹, Axel J. M. Deenen¹, Lorenzo Gnoatto¹, Bert Koopmans¹, Reinoud Lavrijsen^{1,3}

¹ Department of Applied Physics, Eindhoven University of Technology, Eindhoven, The Netherlands

Electric field-controlled data storage and logic devices promise an energy consumption up to a hundred times less compared to current state-of-the-art [1]. Although the effect of an electric field on the Magnetic Anisotropy (MA) [2] and interfacial Dzyaloshinskii-Moriya (iDMI) [3] has been reported, no measurement technique is available that can untangle the intricate effect of an electric field simultaneously. In this project, we aim to adapt a technique relying on propagating spin wave spectroscopy [4] to probe all these electric field-induced effects of interfacial magnetic properties, self-consistently.

In this presentation, I will present our latest simulations and experimental results aiming at proving the self-consistency, backed up with conventional techniques. We study the influence of the electric field strength as well as the width of the electric gate (E-gate) (see Fig. 1a) on the transmission of the spin waves through the region where the magnetic properties are locally modulated. Here we localized an electric field at the interface between an insulator (MgO) and the spin-wave guiding ferromagnet (Co), which changes the electronic band-structure and hence is expected to give rise to small changes in the interfacial properties e.g. the MA and the iDMI. As can be seen in Fig. 1b, simulations show a change of amplitude of the transmitted forward volume spin wave once it has travelled through a region where the anisotropy (H_{Anis}) is locally modified by an electric field (H_{Efield}).

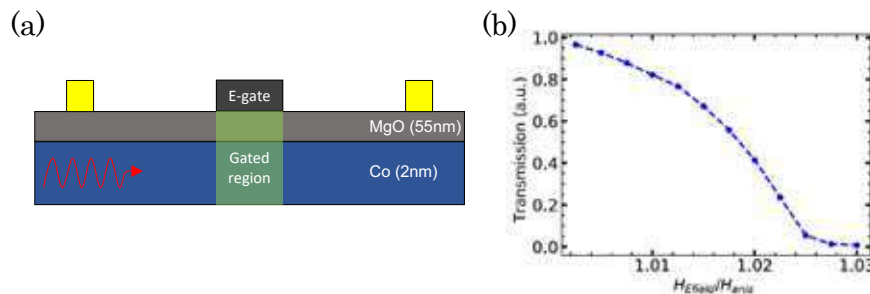


Figure 1: (a) A spin wave (red) is created by the antenna on the left (yellow) and propagates through the gated region (green) before being detected by the antenna on the right. (b) Transmission of a forward volume mode as a function of the relative strength of the anisotropy modified by the electric field in the gated region. Spin wave frequency is 5GHz and Gated region width is 800nm.

Ultimately, as the changes induced by an electric field on MA and iDMI can be small, we hope to provide the scientific community with a technique relying on the propagation of spin waves to probe the smallest change of interfacial magnetic properties, induced by an electric field. Moreover, the wave nature of spin wave and the possibility to control their dispersion relation by locally applying an electric field, could lead to the conception of novel spin-wave based logic devices, contributing to green IT.

- [1] F. Matsukura, Y. Tokura and H. Ohno, *Nat. Nanotechnol.* **10**, 209-220 (2015).
- [2] Z. Huang *et al.*, *Appl. Phys. Lett.* **103**, 222902 (2013).
- [3] T. Strivastava *et al.*, *Phys. Nano. Lett.* **18**, 4871-4877 (2018).
- [4] J. Lucassen *et al.*, *Phys. Rev. B.* **101**, 064432 (2020).

No standing spin waves found in a rectangular permalloy microstrip under uniform magnetic excitation

Santa Pile¹, Sven Stienen², Kilian Lenz², Ryszard Narkowicz², Sebastian Wintz³, Johannes Förster³, Sina Mayr⁴, Martin Buchner¹, Markus Weigand⁵, Verena Ney¹, Jürgen Lindner², Andreas Ney¹

¹Johannes Kepler University Linz, Linz, Austria

²Helmholtz-Zentrum Dresden-Rossendorf, Dresden, Germany

³Max Planck Institute for Intelligent Systems, Stuttgart, Germany

⁴Paul Scherrer Institut, Villigen PSI, Switzerland

⁵Helmholtz-Zentrum Berlin für Materialien und Energie, Berlin, Germany

Magnons or spin waves are to be one of the options to replace the transfer of electronic charges in logic devices [1]. In this work the focus is put on a fundamental understanding

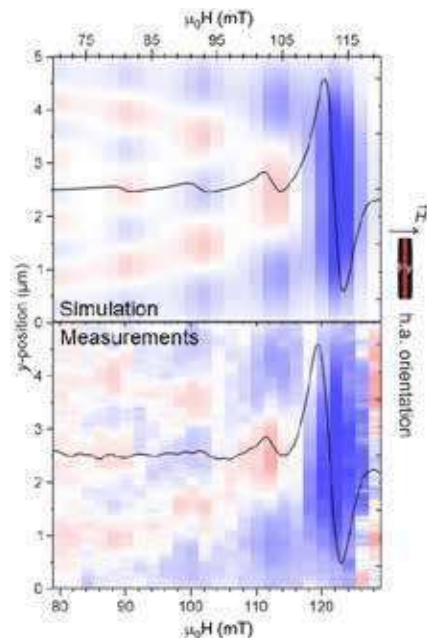


Figure 1: Simulated and measured (black solid lines) FMR spectra and (color plots) overviews of the spin-wave profiles.

of the dynamic magnetic properties of confined rectangular structures, as this is a prerequisite for the development of nanoscale computational devices. Planar microresonators/microantennas [2] made it possible to apply TR-STXM [3] using a phase-locked FMR excitation scheme (STXM-FMR). STXM-FMR enables direct, time-dependent imaging of the spatial distribution of the precessing magnetization across the sample during FMR excitation with elemental selectivity [4]. In the presented work FMR modes in a rectangular $1 \times 5 \times 0.025\text{-}\mu\text{m}^3$ $\text{Ni}_{80}\text{Fe}_{20}$ (Py) microstrip were directly imaged using STXM-FMR and the findings were corroborated by micromagnetic simulations [5]. In Figure 1 simulated and measured FMR spectra (black solid lines) and an overview of the simulated spin-wave profiles (top color plot) and the combined and normalized amplitude/phase data extracted from the STXM-FMR measurements (bottom color plot) of the single strip in h.a. orientation are shown. Analysis of the dynamic behavior showed that although under uniform excitation

in a confined microstructure typically standing spin waves are expected, all imaged spin waves in a single and multiple strips have shown a nonstationary character both, at and off resonance. The latter being additionally detected with FMR. An additional effect of the edge quality on the spin waves was observed in micromagnetic simulations.

[1] A. Barman et al., *Phys.: Condens. Matter* **33**, 413001 (2021).

[2] R. Narkowicz et al., *J. Magn. Reson.* **175**, 275 (2005).

[3] H. Stoll et al., *Front. Phys.* **3**, 26 (2015).

[4] S. Pile et al., *Appl. Phys. Lett.* **116**, 072401 (2020).

[5] S. Pile et al., *ArXiv:2111.07773* (2022).

Nonlinear magnon-phonon processes in coherently driven microstructures

M. Geilen¹, R. Verba², A. Nicoloiu³, D. Narducci⁴, A. Dinescu³, M. Ender¹,
M. Mohseni¹, M. Kewenig¹, A. Hamadeh¹, F. Ciubotaru⁴, F. Vanderveken, M. Weiler¹,
A. Müller³, B. Hillebrands¹, C. Adelmann⁴, and P. Pirro¹

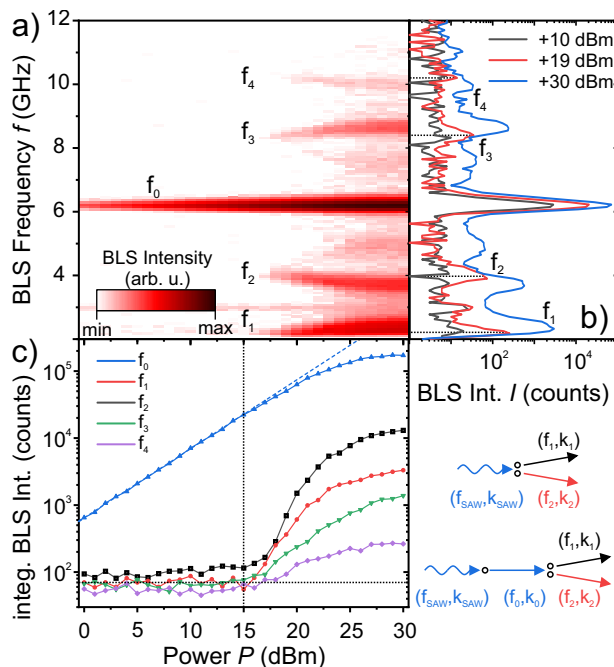
¹ Fachbereich Physik and Landesforschungszentrum OPTIMAS, Technische Universität Kaiserslautern, Germany

² Institute of Magnetism, Kyiv 03142, Ukraine

³ National Institute for Research and Development in Microtechnologies, Bucharest R-07719, Romania

⁴ imec, Leuven B-3001, Belgium 5KU Leuven, Departement Materiaalkunde, 3001 Leuven, Belgium

Magnetoelasticity, the interaction between magnetism and elastic strain, is a promising mechanism for compact and energy-efficient spintronic devices. In particular, the interaction between the fundamental excitations in a magnetic solid, the magnons and the phonons, is of high relevance for future hybrid devices for data processing and computing.



Parametric phonon-to-magnon instability in a CoFeB thin film excited by SAW at frequency f_0 . (a) and (b) BLS spectra (c) intensity of the involved modes as a function of SAW driving power.

simulations of the micromagnetic and elastic domain [2], we demonstrate that the experimentally observed magnon accumulation at the band bottom of the first perpendicular standing spin waves mode can be related to the magnetoelastic interaction.

This work has been supported by the EU Horizon 2020 research and innovation program within the CHIRON project (contract no. 801055).

[1] M. Geilen et al., “Parametric Excitation and Instabilities of Spin Waves driven by Surface Acoustic Waves” arXiv:2201.04033 (2022).

[2] F. Vanderveken, et al. *Finite difference magnetoelastic simulator*, Open Research Europe **1**, 35 (2021).

In this contribution, we present recent results on nonlinear magnon-phonon processes in strongly excited thin film microstructures. First, we present the generation of spin-wave instabilities by coherent surface acoustic waves in a thin metallic ferromagnetic film of CoFeB [1]. Micro-focused Brillouin light scattering spectroscopy (see Figure) and analytical modelling combined with micromagnetic simulations are used to reveal the different instability processes by identifying the involved mechanisms and magnon modes. Depending on the experimental conditions, a four-magnon instability of the magnon mode or a direct first-order parametric phonon-to-magnon instability is observed. The latter is enhanced by three-magnon splitting of the non-resonantly driven magnon.

Second, we investigate the influence of the magnon-phonon interaction on nonlinear redistribution processes in microstructures of Yttrium Iron Garnet (YIG) coherently excited by microwave antennas. Using coupled

Does the orbital angular momentum of light influence ultrafast demagnetization?

Eva Prinz¹, Benjamin Stadtmüller^{1,2}, and Martin Aeschlimann¹

¹ Department of Physics and Research Center OPTIMAS, University of Kaiserslautern, Erwin-Schroedinger-Strasse 46, 67663 Kaiserslautern, Germany

² Institute of Physics, Johannes Gutenberg University Mainz, Staudingerweg 7, 55128 Mainz, Germany

Optical fields can carry an orbital angular momentum (OAM) of $L = l\hbar$ with the OAM quantum number $l \in \mathbb{Z}$ in helical beams with an azimuthal phase dependence. Since its discovery in 1992 [1], a variety of applications for the OAM of light has been brought forward, such as quantum entanglement, micromanipulation, communication, and microscopy [2].

Our research is focused on exploring the potential effects of the OAM of light on laser-induced ultrafast demagnetization. In this field, the question of how the angular momentum is conserved during the demagnetization is not fully answered. While it has been shown that spin angular momentum of light does not influence the ultrafast demagnetization in ferromagnetic thin films such as Ni [3, 4], pumping such a system with photons carrying OAM offers the potential to gain new insights. We investigate the ultrafast demagnetization of ferromagnetic thin films induced by OAM light with time-resolved magneto-optic Kerr-effect measurements.

[1] L. Allen, M.W. Beijersbergen, R.J.C. Spreeuw, and J.P. Woerdman, *Phys. Rev. A* **45**, 8185-8189 (1992).

[2] Y. Shen, X. Wang, Z. Xie, C. Min, X. Fu, Q. Liu, M. Gong, and X. Yuan, *Light: Science & Applications* **8**, 1-29 (2019).

[3] B. Koopmans, M. van Kampen, J.T. Kohlhepp, and W.J.M. de Jonge, *Phys. Rev. Lett.* **85**, 844-847 (2000).

[4] F. Dalla Longa, J.T. Kohlhepp, W.J.M. de Jonge, and B. Koopmans, *Phys. Rev. B* **75**, 224431 (2007)

Inverse magneto-plasmonics for laser-induced spin dynamics

Ilya Razdolski and Andrzej Stupakiewicz

Faculty of Physics, University of Białystok, 15-245 Białystok, Poland

Optical technologies for magnetic recording require nanoscale spatial resolution, thus highlighting the importance of nanophotonics for localizing light-spin interaction. Surface plasmons are known for their ability to confine light in subwavelength volumes and strongly increase the optical energy density which is key for numerous applications.

In this work, we present a novel perspective of plasmonics beyond the conventional enhancement of the electromagnetic fields. We demonstrate our approach in the framework of nanophotonic control of inverse magneto-optical (opto-magnetic) Faraday effect (IFE) and photo-magnetism (PM). Taking the free energy approach and following [1], after the separation of symmetric (γ) and antisymmetric (α) parts of the susceptibility tensor for the effective light-induced magnetic field we get:

$$H_i(0) = \alpha_{ijk} E_j E_k^* + \gamma_{ijkl} E_j E_k^* M_l(0) + c.c. + \dots \quad (1)$$

Here \mathbf{E} is the electric field of light, and $M(0)$ is the static magnetization of the medium. The first and the second terms are responsible for the IFE and PM together with the inverse Cotton-Mouton effect, respectively. We discuss a model surface plasmon-polariton excitation at an interface between a metal and magnetic dielectric. In these systems, Eq. (1) can be rewritten in terms of a total optical intensity $\propto |E|^2$ and a phase shift between the electric field components. We argue that the key role of nanophotonic excitations consists in effectively modifying this phase while simultaneously enhancing and, notably, confining the excitation at the nanoscale. We experimentally and numerically demonstrate its efficiency and flexibility at setting the magnetization into motion via ultrafast plasmonic excitation of the spin system in the dielectric. An exchange precession mode in Yb,Gd-doped BIG [2] and a Kittel mode in Co-doped YIG [3] is excited with about one order enhancement of the specific efficiency, as shown by a quantitative analysis.

Our results emphasize the potential of hybrid magneto-plasmonic structures featuring noble (plasmonic) metals and transparent magnetic dielectrics. We further discuss future development of this novel approach, outlining a promising class of nanophotonic systems demonstrating inverse magneto-plasmonic effects.

[1] A. V. Kimel and A. K. Zvezdin, *Low Temp. Phys.* **41**, 682–688 (2015).

[2] A. L. Chekhov, A. I. Stognij, T. Satoh, T. V. Murzina, I. Razdolski and A. Stupakiewicz, *Nano Lett.* **18**, 2970–2975 (2018).

[3] A. Kazlou, A. L. Chekhov, A. I. Stognij, I. Razdolski, and A. Stupakiewicz, *ACS Photon.* **8**, 2197–2202 (2021).

Experimental Observation of Spin-Wave Diffraction Phenomena

C. Riedel¹, T. Taniguchi¹ and C. H. Back¹

¹Technical University Munich, James-Franck-Str. 1, 85748 Garching, Germany

We present complex spin-wave diffraction patterns in the near-field diffraction limit by using a custom-made time-resolved magneto-optical Kerr effect (TR-MOKE) microscope for visualizing the local and time-resolved dynamic magnetization, i.e. propagating spin-waves. To investigate magnonic interference behaviors, we fabricate a diffraction grating in a 200 nm thick ferrimagnetic YIG film by argon ion-beam etching. A coplanar waveguide (CPW) located parallel to the grating, is used to coherently excite spin-waves.

Our results represent the experimental realization of complex spin-wave interference patterns arising from various diffraction gratings, as preliminary investigated by Mansfeld et al. [1]. We further demonstrate that the interference pattern behind the diffraction grating can be tuned through careful selection of the external magnetic field strength. A reduction in the effective magnetic field between the grating antidots, indicated by the black squares in Fig. 1, can lead to a hybridization of two spin-wave modes and with this to a spin-wave transmission stop-band, as depicted in the central panel of Fig. 1.

This work contributes to the understanding of spin-wave interference behaviors for enhancing the performance of future magnonic devices.

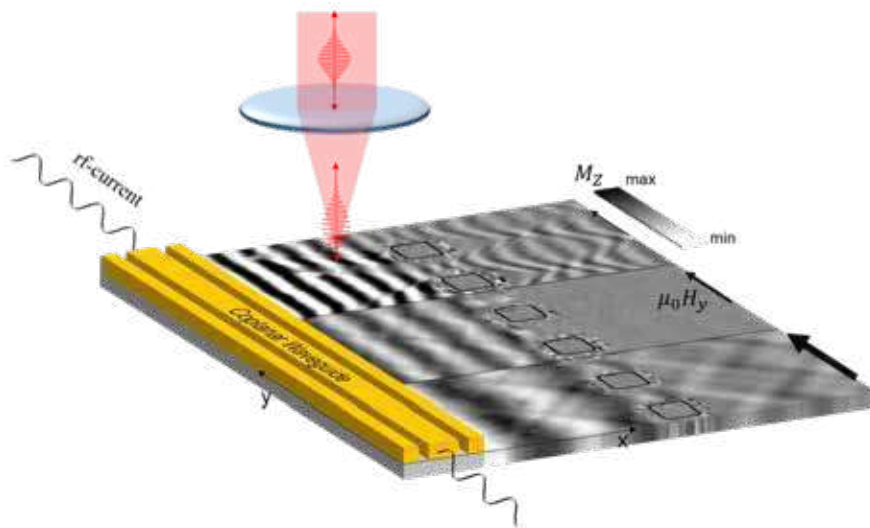


Fig. 1: Simplified overview of a TR-MOKE measurement. Spin-waves propagating through a diffraction grating (indicated by the black squares) are excited by a rf-current in the CPW, which is placed on top of the YIG film. We observe the TR-MOKE signal by focusing femtosecond laser pulses to the sample surface and measuring the Kerr-rotation of the back reflected laser pulses, while scanning the laser across the sample surface. We observe not only complex interference patterns behind the diffraction grating but also a transmission stop-band by varying the external magnetic field strength (indicated by the thickness of the black arrows).

[1] S. Mansfeld *et al.*, Phys. Rev. Lett. **108**, 047204 (2012)

Reliable all-optical-switching in Tb/Co multilayers based tunnel junctions

D. Salomoni¹, Y. Peng², L. Avilés-Félix¹, L. Farcis¹, S. Auffret¹, M. Hehn², G. Malinowski², S. Mangin², B. Dieny¹, L. D. Buda-Prejbeanu¹, R. Sousa¹ and I. L. Prejbeanu¹

¹ Spintec, Université Grenoble Alpes, CNRS, CEA, Grenoble INP, IRIG-SPINTEC, 38000 Grenoble, France

² Institut Jean Lamour, UMR CNRS 7198, Université de Lorraine, Nancy 54011, France

Controlling the magnetization of storage elements through ultrashort laser pulses has advantages for memory applications in terms of speed and energy efficiency. The first complete magnetization reversal driven by ultrashort light pulses was observed in GdFeCo ferrimagnetic alloy [1]. It has since been studied and observed in other material systems. One example was the observed single-shot helicity independent all-optically-switching (AOS) of MTJ stacks based on [Tb/Co] multilayers (ML) [2][3]. A [Tb/Co] multilayer system is particularly interesting due to its large perpendicular magnetic anisotropy allowing for high retention even at small dot sizes.

In this work, by systematic studies of the magnetization response to ultrashort laser pulses, we evidenced a very reliable and robust toggle switching only for specific Tb and Co thickness range (between 0.6 nm and 0.9 nm for Tb and between 1.3 nm and 1.5 nm for Co) – see fig. 1(a) Region 1. This is proven by observing magnetization reversal even after 150.000 pulses, as shown in fig. 1(b). Single shot AOS was achieved using laser pulse durations varying from 50 fs up to 10 ps and fluences from 3.0 mJ/cm² to 6.5 mJ/cm². Close to the boundaries of this specific thickness range (about 0.5nm around), the magnetization reversal starts to become not reproducible and can give rise to a non-saturated magnetization region after multiple pulses – see fig. 1(c) Region 2. Furthermore, single shot AOS was obtained for different stacks including: [Tb/Co]ML as deposited (not annealed) fig. 1(d); [Tb/Co]ML coupled to the FeCoB free layer fig. 1(e). Full MTJ stack with [Tb/Co]ML having as reference layer a synthetic antiferromagnet (SAF), annealed at 250°C fig. 1(f).

These results pave the way towards the development of an ultra-fast and energy-efficient memory that exploits AOS.

- [1] C. Stanciu et al., Phys. Rev. Lett. **99**, 047601 (2007)
- [2] A. Olivier et al., Nanotechnology **31**, 425302 (2020).
- [3] L. Avilés-Félix et al., Scientific Reports **10**, 1 (2020).

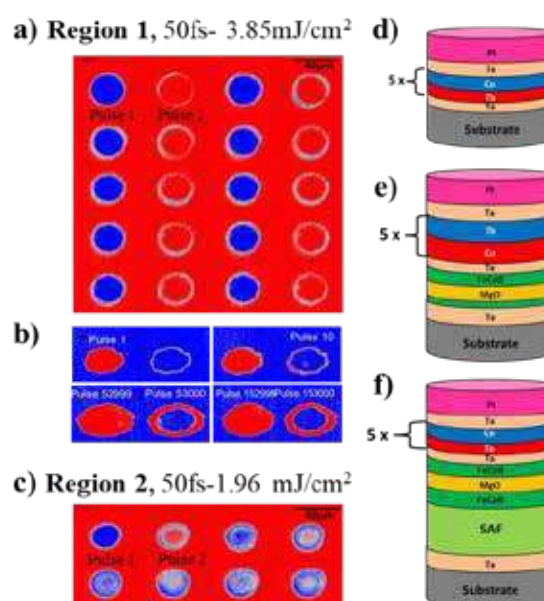


Figure 1: (a-b) Background corrected magneto-optical images showing robust and reliable single shot AOS of half-MTJ stack shown in (e); (c) unsaturated state after few pulses. (d-e-f) Stacks investigated that show single shot AOS.

Purely Precessional All-Optical Femtosecond Magnetic Switching

L. Sánchez-Tejerina¹, R. Yanes², R. Martín-Hernández¹, L. Plaja¹, L. López-Díaz², C. Hernández-García¹

¹ Grupo de Investigación en Aplicaciones del Láser y Fotónica, Departamento de Física Aplicada, Universidad de Salamanca, E-37008, Salamanca, Spain.

² Dpto. Física Aplicada, Universidad de Salamanca, E-37008, Salamanca, Spain

Ultrafast laser sources provide unique tools to control the magnetic properties of materials, both spatially and temporally. Since the pioneering work on ultrafast laser induced demagnetization [1], femtosecond (fs) laser pulses have been widely used in theoretical and experimental studies of femtomagnetism, achieving switching at the picosecond (ps) time scale [2]. Recent technological advances have made possible to harness the polarization structure of ultrashort laser beams, allowing the generation of radially or azimuthally polarized laser pulses. In particular, it has been recently proposed that Tesla-scale fs magnetic fields (B), isolated from the electric field (E), can be obtained through the use of ultrafast azimuthally polarized laser beams [3]. Such configuration offers the opportunity to perform pure magnetic interactions with an intense fs B field.

In this work, we numerically show that it is possible to switch any ferromagnetic material in the fs time scale using an isolated B field, such as that obtained from an azimuthally polarized laser pulse [4]. Up to now, most of the research has been focused on the effect of the E field on magnetization, especially the ability to demagnetize the magnetic ions by driving them to a non-equilibrium state, which may be done in tens of fs. Our micromagnetic simulations demonstrate that the use of intense B fields (up to 10^2 - 10^3 Tesla) obtained from an azimuthally polarized laser pulse, allows to perform ultrafast switching

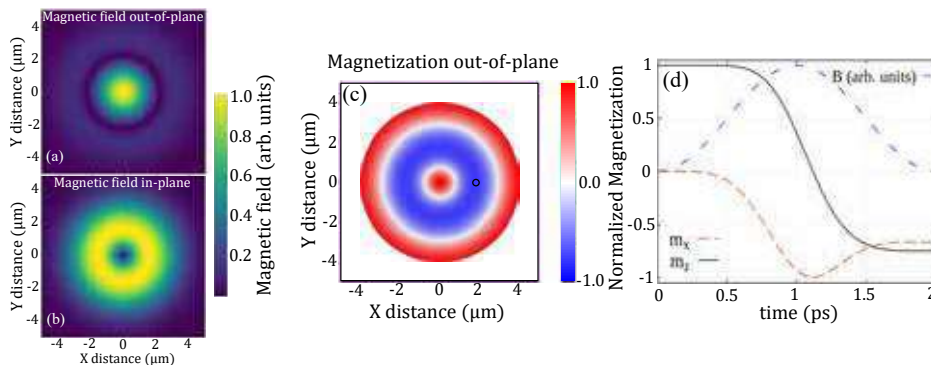


Figure 1: Spatial distribution of (a) the out-of-plane and (b) the in-plane B field carried by an azimuthally polarized laser pulse. (c) Magnetic state after the application of a 720 fs laser pulse of frequency $f=200$ THz. The initial magnetic state is a uniformly magnetized nanodot with a radius of $r=2\mu\text{m}$. (d) Temporal evolution of the magnetization at $r=896$ nm (black circle in (c)), showing purely precessional all-optical magnetic switching in <1 ps.

driven by purely precessional effects (see Fig. 1). In such scenario, the effect of the E field can be avoided and so the possible sample damage. Our work opens a promising scenario to achieve complete switching of a magnetic state at fs time scales through the use of structured laser beams.

References:

- [1] E. Beaurepaire, J.-C. Merle, A. Daunois, and J.-Y. Bigot, Phys. Rev. Lett. 76, 4250 (1996).
- [2] C. Wang, Y. Liu, Nano Convergence 7 (2020).
- [3] M. Blanco, F. Cambroner, M. T. Flores-Arias, E. Conejero Jarque, L. Plaja, and C. Hernández-García ACS Photonics 6 (2019).
- [4] L. Sánchez-Tejerina, R. Yanes, R. Martín-Hernández, L. Plaja, L. López-Díaz, C. Hernández-García, in preparation.

Paramagnetic resonance in GGG at ultralow temperatures

R. O. Serha¹, S. Knauer¹, D. Schmoll¹, K. Davidkova³, Q. Wang¹, B. Budinska¹, O. V. Dobrovolskiy¹, V. E. Demidov², M. Urbanek³, S. O. Demokritov², A. V. Chumak¹

¹University of Vienna, Faculty of Physics, Boltzmanngasse 5, A-1090 Vienna, Austria

²Institute for Applied Physics and Center for Nonlinear Science, University of Muenster, Corrensstrasse 2-4, D-48149 Muenster, Germany

³CEITEC BUT, Brno University of Technology, Purkynova 123, 612 00 Brno, Czech Republic

Magnonics is known to operate with data carried by spin waves and their quanta magnons in magnetically-ordered magnetic media [1]. Nevertheless, magnons also exist in paramagnetic materials and are known as paramagnons [2-3]. Paramagnon properties are governed by the exchange interactions, which does not vanish above Curie/Neel temperature and the dipolar interactions. It is predicted that even long-range paramagnons should be present in paramagnetic media [1,2]. Recently, an incoherent spin transport was demonstrated in gadolinium gallium garnet (GGG) $\text{Gd}_3\text{Ga}_5\text{O}_{12}$ insulators [4].

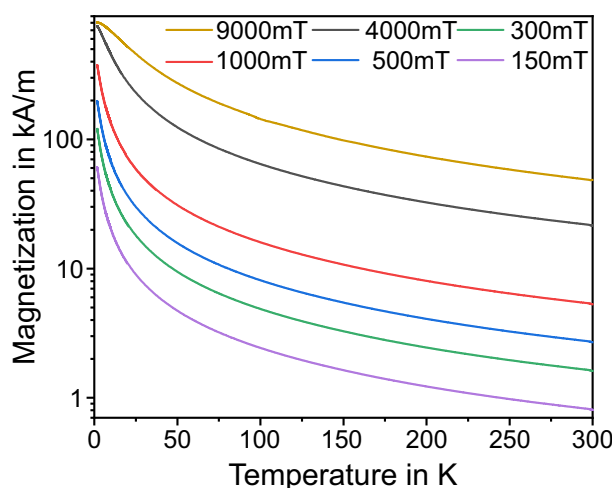


Figure 1: Magnetization of GGG with regard to the temperature for different bias field. Measurements were performed via VSM in a PPMS.

Here we present our results on the investigation of electron paramagnetic resonance (EPR) spectroscopy in GGG 500 μm -thick bulk slabs at temperatures down to 20 mK. GGG is the material of choice, as Gd^{3+} ions have a large spin $S = 7/2$ and its saturation magnetization is about $M_s = 800 \text{ kA/m}$. Millikelvin temperatures allow to reach the saturation of the GGG magnetization, by applying magnetic fields of about hundreds Millitesla. The methodology identical to the ferromagnetic resonance (FMR) spectroscopy is used to define the magnetic parameters of GGG and its damping. The foundational investigations of the GGG magnetization at cryogenic temperatures are performed using vibrating-sample magnetometry (VSM) – see Figure 1. Afterwards, EPR measurements are conducted in a wide range of magnetic fields. These studies form an initial step towards investigations long-distance paramagnon propagation in GGG.

Afterwards, EPR measurements are conducted in a wide range of magnetic fields. These studies form an initial step towards investigations long-distance paramagnon propagation in GGG.

- [1] A. A. Barman, *et al.*, *J. Phys.: Condens. Matter* **33**, 413001 (2021).
- [2] S. K. Sinha, *et al.*, *Phys. Rev. Lett.* **23**, (1969).
- [3] S. O. Demokritov, *et al.*, *JETP Lett.* **43**, 403 (1986).
- [4] K. Oyanagi *et al.*, *Nat. Commun.* **10**, 4740 (2019).

Nonlinear interactions between spin-wave modes probed by parametric excitation in YIG microstructures

T. Srivastava¹, I. Ngouagnia¹, G. de Loubens¹, H. Merbouche², S. O. Demokritov²,
V. E. Demidov², M. d'Aquino³, C. Serpico³, J.-V. Kim⁴, O. Klein⁵, N. Beaulieu⁶,
J. Ben Youssef⁶, M. Muñoz⁷, V. Cros⁸, P. Bortolotti⁸, A. Anane⁸

¹ SPEC, CEA, CNRS, Université Paris-Saclay, France

² Institute for Applied Physics, University of Muenster, Germany

³ Department of Electrical Engineering and ICT, University of Naples Federico II, Italy

⁴ Centre de Nanosciences et de Nanotechnologies, CNRS, Université Paris-Saclay, France

⁵ Spintec, CEA, CNRS, Université Grenoble-Alpes, France

⁶ LabSTICC, CNRS, Université de Bretagne Occidentale, Brest, France

⁷ Instituto de Tecnologías Físicas y de la Información (CSIC), Spain

⁸ Unité Mixte de Physique, CNRS, Thales, Université Paris-Saclay, France

Spin-wave (SW) dynamics exhibits a variety of nonlinear phenomena ranging from parametric instabilities to chaos. In confined structures, SW modes are quantized in wave-vector and energy, which limits the possible nonlinear processes due to conservation laws, but also open opportunities to understand and control them in more detail [1–3].

In this work, we use magnetic resonance force microscopy (MRFM) and micro-focused Brillouin light scattering (BLS) to probe parametric SWs in microdisks patterned from a 50 nm thick YIG film, excited by a pumping field parallel to the in-plane bias magnetic field. As expected and shown in Figure 1, the parametrically excited SWs are quantized [4,5].

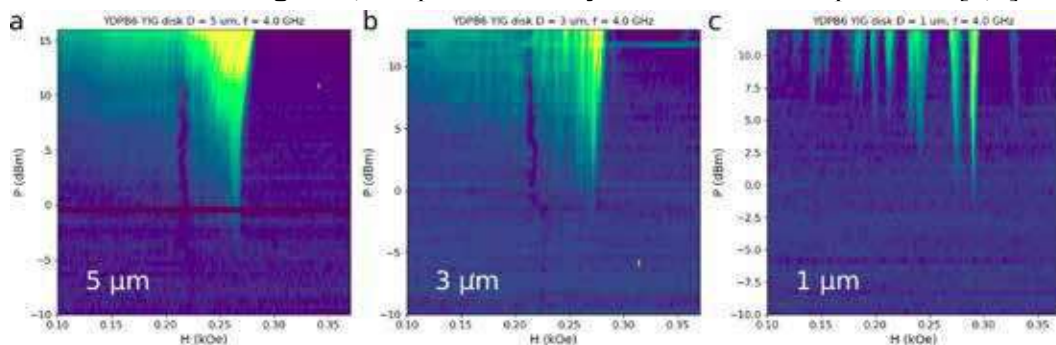


Figure 1: Intensity map of the parametrically excited modes in the field-power coordinates, measured by MRFM on disks with diameter $5 \mu\text{m}$ (a), $3 \mu\text{m}$ (b), and $1 \mu\text{m}$ (c). The parallel pumping field has the frequency $f = 4 \text{ GHz}$.

Next, to study the nonlinear interactions between the SW eigenmodes, we simultaneously excite two of them by parametric pumping. Time-resolved BLS allows to evidence two main scenarios: indirect mode interaction and nonlinear phase locking of the modes. Two-tone MRFM spectroscopy demonstrates that each mode is coupled to all other modes, and shows that nonlinear interactions are complex, with enhanced or suppressed peaks, and the appearance of additional peaks in the spectrum. Micromagnetic simulations provide some insight into these nonlinear processes.

This work has received financial support from the Horizon 2020 Framework Programme of the European Commission under FET-Open grant agreement no. 899646 (k-NET).

- [1] Y. Li et al., Phys. Rev. X **9**, 041036 (2019)
- [2] K. Schultheiss et al., Phys. Rev. Lett. **122**, 097202 (2019)
- [3] M. Mohseni et al., Phys. Rev. Lett. **126**, 097202 (2021)
- [4] H. Ulrichs et al., Phys. Rev. B **84**, 094401 (2011)
- [5] F. Guo et al., Phys. Rev. B **89**, 104422 (2014)

Accelerating double pulse all-optical write/erase cycles in metallic ferrimagnets

F. Steinbach¹, N. Stetzuhn^{1,2}, D. Engel¹, U. Atxitia³, C. von Korff Schmising¹ and Stefan Eisebitt^{1,4}

¹Max-Born-Institute for Nonlinear Optics and Short Pulse Spectroscopy, Max-Born Strasse 2A, 12489 Berlin, Germany

²Department of Physics, Freie Universität Berlin, Arnimallee 14, 14195 Berlin, Germany

³Dahlem Center for Complex Quantum Systems and Fachbereich Physik, Berlin, Arnimallee 14, 14195 Berlin, Germany

⁴Institut für Optik und Atomare Physik, Technische Universität Berlin, Straße des 17. Juni 135, 10623 Berlin, Germany

All-optical switching of magnetic order presents a promising route towards faster and more energy efficient data storage. However, a realization in future devices is ultimately dependent on the maximum repetition rates of optically induced write/erase cycles. Here we present two strategies to minimize the temporal separation of two consecutive femtosecond laser pulses to toggle the out-of-plane direction of the magnetization of ferrimagnetic rare-earth transition metal alloys. First, by systematically changing the heat transfer rates using either amorphous glass, crystalline silicon or polycrystalline diamond substrates, we show that efficient cooling rates of the magnetic system present a prerequisite to accelerate the sequence of double pulse toggle switching. Secondly, we demonstrate that replacing the transition metal iron by cobalt leads to a significantly faster recovery of the magnetization after optical excitation allowing us to approach terahertz frequency of write/erase cycles with a minimum pulse-to-pulse separation of 7 ps [2].

[1] F. Steinbach et al., *J. Appl. Phys.* **130**, 083905 (2021).

[1] F. Steinbach et al., *Appl. Phys. Lett.* submitted (2022).

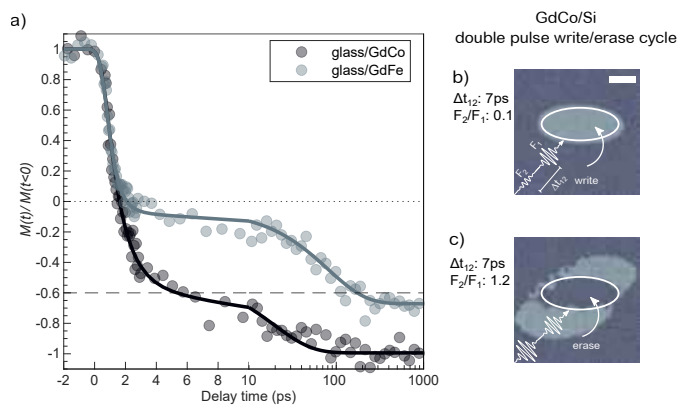


Figure 1: a) Relative change of the magnetization, $M(t)/M(t < 0)$, of glass/GdCo and glass/GdFe measured via time-resolved wide-field Faraday microscopy [1]. Note that the time axis in linear up to 10 ps and logarithmic between 10 ps and 1000 ps. GdCo exhibits a very fast relaxation towards a reversed magnetization reaching $M(7\text{ps})/M(t < 0) = -0.6$, whereas GdFe reaches this value only after ≈ 200 ps. Double pulse switching with an inter-pulse separation of $\Delta t_{12} = 7$ ps and ratio of fluences b) $F_2/F_1 = 0.1$ and c) $F_2/F_1 = 1.2$. For the latter we achieve a write/erase cycle of 7 ps.

Lateral spin pumping in an assembly of embedded Fe₆₀Al₄₀ nanostructures

T. Strusch¹, R. Meckenstock¹, K. Lenz², K. Potzger², R. Bali², J. Lindner², M. Farle¹
and A. Semisalova¹

¹ Faculty of Physics and CENIDE, University of Duisburg-Essen, Duisburg, Germany

² Helmholtz-Zentrum Dresden – Rossendorf, Institute of Ion Beam Physics and Materials Research, Dresden, Germany

The magnetic properties of Fe₆₀Al₄₀ alloys are tailorable from the para- (PM) to the ferromagnetic (FM) state by variation of the structural and chemical order through ion beam irradiation [1], making it a promising material for the fabrication of magnetic landscapes and magnonic crystals [2,3]. Here, we report on ferromagnetic resonance (FMR) detected spin pumping in FM-Fe₆₀Al₄₀/Pd and Py/PM-Fe₆₀Al₄₀ bilayers as well as laterally patterned Fe₆₀Al₄₀ nanostructures and show that Fe₆₀Al₄₀ can be used as spin source and as spin sink. We determine the spin-mixing conductance and the spin-diffusion length [4] to be $g_{FeAl}^{\uparrow\downarrow} = (2.1 \pm 0.2) \times 10^{18} \text{ m}^{-2}$ and a spin diffusion length of $\lambda_{FeAl} = 11.9 \pm 0.2 \text{ nm}$ for PM Fe₆₀Al₄₀ (Figure 1a), and $g_{Pd}^{\uparrow\downarrow} = (3.8 \pm 0.5) \times 10^{18} \text{ m}^{-2}$ and $\lambda_{Pd} = 9.1 \pm 2 \text{ nm}$ for Pd, respectively [5]. Furthermore, we observe spin-wave modes and investigate the lateral spin pumping in patterned Fe₆₀Al₄₀ nanostructures. The pattern consists of 500-nm-wide stripes of FM-Fe₆₀Al₄₀ separated by PM-Fe₆₀Al₄₀ stripes of different width w_p (100-400 nm) produced in a 40 nm thick film using Ne ion irradiation with 20 keV and a fluence of $6 \times 10^{14} \text{ ions/cm}^2$. We find an increase of the damping parameter α with decreasing width of the PM FeAl stripes correlated with the increase of the number of FM/PM interfaces per volume unit (Figure 1b).

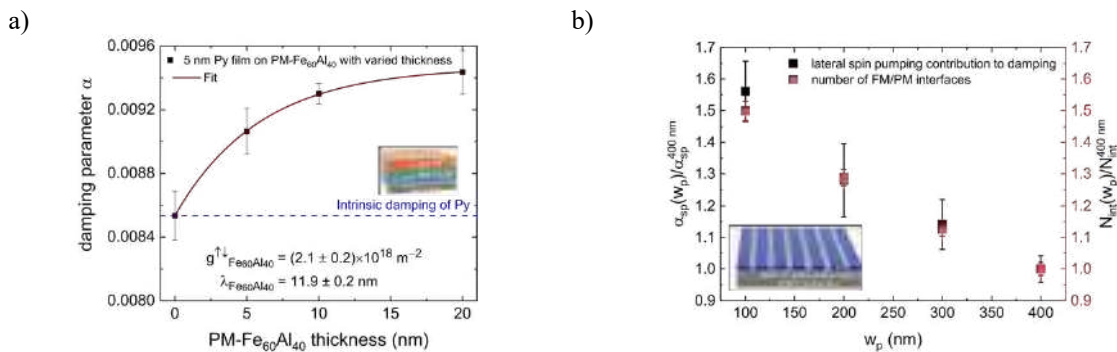


Figure 1: a) Py/PM-Fe₆₀Al₄₀ bilayers: Extracted damping parameter in dependence of the PM-FeAl-layer thickness. The solid red line indicates the fit for extracting the spin mixing conductance and the spin diffusion length. The dashed blue line shows the intrinsic damping contribution of the Py thin film. b) Stripe array: Comparison of spin pumping contribution α_{sp} after subtracting the intrinsic damping of the FM-Fe₆₀Al₄₀ film (black) and number of PM/FM interfaces (red), normalized to the values for $w_p=400 \text{ nm}$.

- [1] R. Bali et al., Nano Lett. 14, 435 (2014)
- [2] D. Holzinger et al., J. Appl. Phys. 114, 013908(5) (2013).
- [3] B. Obry et al., Appl. Phys. Lett. 102, 202403 (2013).
- [4] J. M. Shaw et al., Phys. Rev. B 85, 054412 (2012)
- [5] T. Strusch et al., *submitted*

The work is supported by the DFG funding under Grant No. SE-2853/1-1.

Effect of the Dzyaloshinskii-Moriya interaction on the band diagram of one-dimensional magnonic crystals

S. Tacchi¹, R. A. Gallardo², D. Petti³, A. Cattoni⁴, J. Flores-Farías², E. Albisetti³, G. Carlotti⁵, P. Landeros²

¹ *Istituto Officina dei Materiali del CNR (CNR-IOM), Sede Secondaria di Perugia, c/o Dipartimento di Fisica e Geologia, Università di Perugia, 06123 Perugia, Italy*

² *Departamento de Física, Universidad Técnica Federico Santa María, Avenida España 1680, Valparaíso, Chile*

³ *Dipartimento di Fisica, Politecnico di Milano, Via Giuseppe Colombo, Milano 20133, Italy*

⁴ *Centre de Nanosciences et de Nanotechnologies (C2N), CNRS UMR 9001, Université Paris-Saclay, Palaiseau, 91120, France*

⁵ *Dipartimento di Fisica e Geologia, Università di Perugia, 06123 Perugia, Italy*

Interfacial Dzyaloshinskii-Moriya interaction (*i*-DMI) in extended films and multilayers, has been widely investigated in the last years. In contrast, only few studies [1,2] have been devoted to the influence of *i*-DMI on the spin waves (SWs) band diagram of magnonic crystals (MCs). Recent theoretical investigations of one-dimensional MCs, consisting of a ferromagnetic film in contact with an array of stripes of heavy metal material, showed that periodic *i*-DMI induces the formation of flat bands, due to the appearance of SW modes localized in the sample's regions where *i*-DMI is present [3]. However, no experimental evidence of the formation of the flat bands in MCs has been reported up to now. In this work, we have investigated the effect of periodic *i*-DMI on the SW dispersion relation of one-dimensional MCs consisting of an extended CoFeB film, 1 nm thick, sitting over an array of Pt stripes having a thickness of 7 nm. Two set of samples having a periodicity $p=400$ nm (with a stripe width $w=200$ nm) and $p=200$ nm (with a stripe width in the range between 150 and 170 nm) were analysed. SW dispersion was measured by Brillouin light scattering in the Damon-Eshbach configuration, sweeping the in-plane transferred wave-vector in the direction perpendicular to the external magnetic field applied along the stripe axis. Micromagnetic simulations and theoretical calculations, performed by means of the plane wave method, were used to explain the experimental results. In agreement with theoretical predictions, for all the investigated samples the SW band structure shows low-frequency flat bands, caused by the appearance of SW modes localized in the regions where the Pt stripes are present. The frequency position of the flat bands is found to strongly depend on the stripes period. In addition, for the samples having smaller periodicity, the dispersion curves exhibit a marked qualitative change. In particular, we observe SWs modes, characterized by a strong non-reciprocal intensity, which are present in the SW band diagram only for positive wavevectors. Financial support from the Italian Ministry of University and Research through the PRIN-2020 project entitled "The Italian factory of micromagnetic modeling and spintronics", (cod. 2020LWPKH7) is kindly acknowledged.

[1] F. Ma and Y. Zhou, *RSC Adv.* **4**, 46454 (2014).

[2] M. Mruczkiewicz and M. Krawczyk, *Phys. Rev. B* **94**, 024434 (2016).

[3] R. A. Gallardo, D. Cortés-Ortuño, T. Schneider, A. Roldán-Molina, Fusheng Ma, R. E. Troncoso, K. Lenz, H. Fangohr, J. Lindner, and P. Landeros, *Phys. Rev. Lett.* **122**, 067204 (2019).

Ultrafast metamagnetic phase transition in FeRh driven by non-equilibrium electron dynamics

F. Pressacco^{1,2}, D. Sangalli^{3,4}, V. Uhlíř^{5,6}, D. Kutnyakhov², J. A. Arregi⁵, S. Y. Agustsson⁷, G. Brenner², H. Redlin², M. Heber², D. Vasilyev⁷, J. Demsar⁷, G. Schönhense⁷, M. Gatti^{4,8,9}, A. Marini^{3,4}, W. Wurth^{1,2} and F. Sirotti^{9,10}

¹The Hamburg Centre for Ultrafast Imaging, Hamburg University, Hamburg, Germany

²Deutsches Elektronen-Synchrotron DESY, Hamburg, Germany

³Istituto di Struttura della Materia—Consiglio Nazionale delle Ricerche (CNR-ISM), Monterotondo Stazione, Italy.

⁴European Theoretical Spectroscopy Facility (ETSF)

⁵CEITEC BUT, Brno University of Technology, Brno, Czech Republic

⁶Institute of Physical Engineering, Brno University of Technology, Brno, Czech Republic

⁷Johannes Gutenberg-Universität, Institute of Physics, Mainz, Germany

⁸LSI, CNRS, CEA/DRF/IRAMIS, École Polytechnique, Institut Polytechnique de Paris, Palaiseau, France

⁹Synchrotron SOLEIL, L'Orme des Merisiers, Gif-sur-Yvette, France

¹⁰Physique de la Matière Condensée, CNRS and École Polytechnique, IP Paris, Palaiseau, France

Femtosecond light-induced phase transitions between different macroscopic orders provide the possibility to tune the functional properties of condensed matter on ultrafast timescales. Here, we present a study elucidating the transient subpicosecond processes governing the photoinduced generation of ferromagnetic order in antiferromagnetic FeRh. This metamagnetic phase transition occurs at about 370 K in equilibrium and is accompanied by changes in volume, entropy and resistance. In the AF phase, Fe atoms alone carry magnetic moments which are aligned antiparallel. The transition to the FM phase is the result of a fine interplay between the coupled spin, charge, and lattice degrees of freedom [1], while the exact role of each contribution remained unclear. By combining time-resolved photoelectron spectroscopy and ab-initio electron dynamics calculations we investigate the transient photoemission spectra upon ultrafast laser excitation of FeRh thin films [2]. The FM phase of FeRh, characterized by a minority band near the Fermi energy, is established in less than 500 fs after the laser excitation [3].

[1] F. Pressacco et al., *Sci. Rep.* **6**, (2016).

[2] V. Uhlíř et al., *Appl. Surf. Sci.* **514**, 145923 (2020).

[3] F. Pressacco et al., *Nature Commun.* **12**, 5088 (2021).

Exceptional points controlling oscillation death in coupled spintronic nano-oscillators

S. Wittrock^{1,2}, S. Perna³, R. Lebrun², R. Ferreira⁴, P. Bortolotti², C. Serpico³, V. Cros²

¹Max-Born-Institute, Berlin, Germany

²CNRS-Thales, Palaiseau, France

³Univ. of Naples Federico II, Naples, Italy

⁴INL, Braga, Portugal

Non-hermitian physics was initially considered rather a mathematical-physics concept compared to the dominant paradigm of hermiticity in most physical systems. However, in the past two decades, there has been a growing interest in such systems since PT symmetry was proved a sufficient condition in order to describe meaningful physical quantities. Only recently, the field gained attention due to recent experimental advances particularly in photonics, where the controlled realization of so-called Exceptional points (EPs) could be demonstrated. Exceptional points describe singularities in the parameter space of a >2D system corresponding to the coalescence of two or more eigenvalues and the associated eigenvectors and are a peculiar feature of non-Hermitian physics. EPs are of interest not only from the fundamental viewpoint but also for the design of a new generation of sensors with unprecedented sensitivity.

In magnetic systems that naturally have largely discussed implications for future applications and beyond-CMOS technologies, the emergence of EPs is a very recent phenomenon in theory and as well in experiment. They occur under certain specific conditions in coupled systems and provide novel phenomena, such as topological features in the parameter space and even more complex dynamics that leverages new perspectives in several branches of physics. This includes non-hermiticity in general, non-hermiticity in strongly nonlinear regimes that is anticipated to provide stochastic or chaotic phenomena or complex bifurcations and the potentialities for applications, such as ultra-sensitive sensors or neuromorphic computing schemes. Here, we experimentally show the emergence of EPs in mutually coupled spintronic oscillators [Wittrock et al., arXiv:2108.04804] which are intrinsically strongly nonlinear. We demonstrate the occurrence of complex dynamics, such as oscillation death due to the EP, and discuss topological operations and stochastic features in its vicinity.

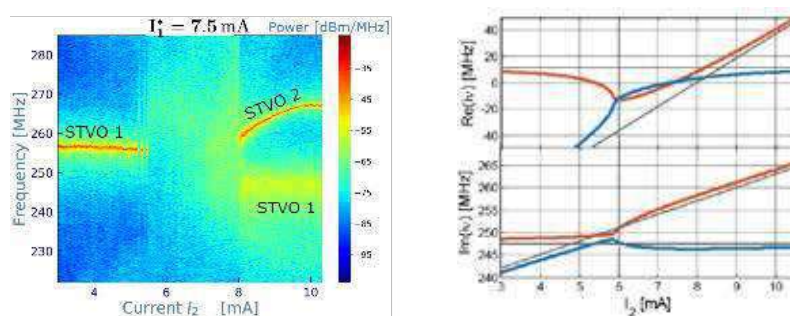


Figure: Death of oscillations in the vicinity of the EP and corresponding complex eigenvalues.

Dielectric nanoparticle enhanced Brillouin light scattering spectroscopy of spin waves

Ondřej Wojewoda¹, Filip Ligmajer¹, Jan Klíma², Jakub Holobrádek¹, Meena Dhankhar¹, Kristýna Davidková², Michal Staňo¹, Michal Kvapil², Tomáš Šíkola^{1,2}, Michal Urbánek^{1,2}

¹ CEITEC BUT, Brno University of Technology, Brno, Czech Republic

² Institute of Physical Engineering, Brno University of Technology, Brno, Czech Republic

Advances in Brillouin light scattering (BLS) spectroscopy allowed us to study and develop first generation of magnon devices and is one of the main reasons why magnonics became one of the most promising candidates for “beyond CMOS” technology. However, further development and especially miniaturization is needed to bring spin-wave devices to real application. Here, BLS is limited with its fundamental limit in probing short wavelength magnons. This limit is given (for the Stokes process) by the momentum conservation condition: $k_i = k_r + k_m$, where k_i (k_r) is wavevector of the incident (reflected) light and k_m is wavevector of the magnon [1]. Thus, in the back-scattering geometry, the maximal wavenumber of spin waves, which can be detected, equals twice the incident light wavenumber. Most BLS experiments utilize light from visible spectra, thus restricting state-of-the-art experiments to the approx. 300 nm wavelengths of spin waves.

To tackle this limitation, we propose a novel way of detecting short-wavelength spin waves beyond the fundamental limitation of the BLS [Fig. 1 (a), (b)]. We employ Mie resonance-based dielectric nano-resonators to localize and amplify the incident electric wave [2]. We were able to increase the maximal detectable wavevector approx. three times [Fig. 3 (c), (d)]. The coherent excitation using the microstrip antenna verified the results obtained by measuring and fitting the thermal spin wave signal.

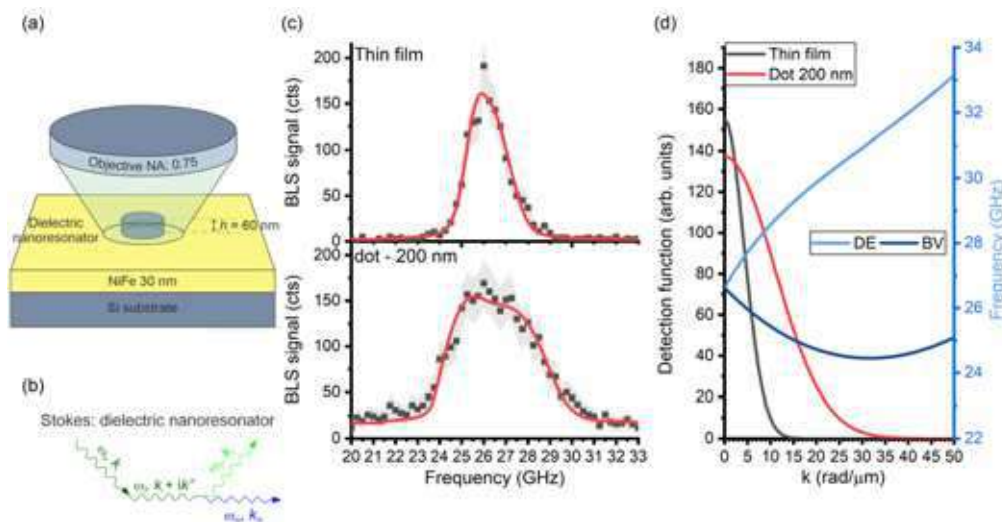


Figure 1: (a) Schematics of the nano-resonator enhanced BLS. (b) Schematics of the Stokes processes during the BLS mediated by the localized resonances. (c) BLS experimental data for bare film (top panel) and dielectric nanoresonator (bottom panel) fitted by the model based on the gaussian detection function of BLS. (d) Left axis: fitted detection function of conventional BLS (black) and nano-resonator enhanced BLS (red). Right axis: calculated dispersion relation of a Permalloy thin film of Damon-Eshbach (DE) and backward volume (BV) modes.

[1] T. Sebastian et al., Front. Phys. 3:35 (2015).

[2] Z. J. Yang et al., Phys. Rep. 701 (2017).

All-optical switching on the nanometer scale excited and probed with femtosecond extreme ultraviolet pulses

Kelvin Yao,¹ Felix Steinbach,¹ Martin Borchert,¹ Daniel Schick,¹ Dieter Engel,¹ Filippo Bencivenga,² Riccardo Mincigrucci,² Laura Foglia,² Emanuele Pedersoli,² Dario De Angelis,² Matteo Pancaldi,² Björn Wehinger,^{2,3} Flavio Capotondi,² Claudio Masciovecchio,² Stefan Eisebitt,¹ and Clemens von Korff Schmising¹

¹Max-Born-Institut, Max-Born-Straße 2A, 12489 Berlin, Germany

²Elettra Sincrotrone Trieste S.C.p.A., Strada Statale 14, km 163.5, 34149 Basovizza (TS)

³ESRF - The European Synchrotron, 71, Avenue des Martyrs, 38043 Grenoble, France

Ultrafast control of magnetization on the nanometer length scale, in particular all-optical switching (AOS), is key to putting ultrafast magnetism on the path towards future technological application in data storage technology. One approach to gain access to ultrafast processes on nanometer scale is to reduce the excitation wavelength to the extreme ultraviolet (XUV) spectral range and induce a spatially periodic excitation via interference of two pulses. This technique has been pioneered at the EIS-Timer beamline of the free-electron laser (FEL) FERMI in Trieste, Italy [1] and has been very recently employed for a first investigations of magnetization dynamics [2].

In this study, we expand XUV transient grating spectroscopy by analyzing the combined ultrafast evolution of the first and second order diffraction. We excite a ferrimagnetic GdFe alloy sample by overlapping two XUV beams and generate a transient magnetic grating (TMG) with a periodicity of 87 nm. The spatial evolution of the magnetization grating is

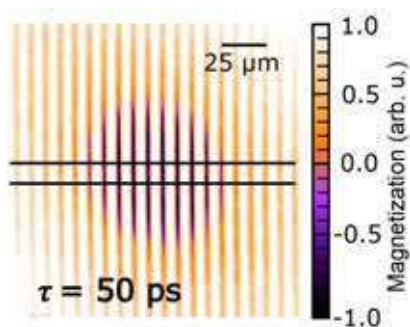


Fig. 1: Real-space image of a magnetization grating with period $1.6\mu\text{m}$, directly imaged with a Faraday microscope. All-optical switching indicated in purple.

probed by diffracting a time-delayed, third XUV pulse tuned to the Gd *N*-edge at 150 eV. Due to the non-linear fluence dependence of AOS, we expect a modified line-space-ratio of the evolving magnetic grating from the initial sinusoidal excitation pattern. This information is directly encoded in the diffraction pattern, such that the simultaneously measured first and second diffraction orders allows us to demonstrate the emergence of AOS. To corroborate these results, we perform supporting all-optical real-space measurements on the same sample using a wide-field magneto-optical microscope in the

visible spectral range, where we directly image how the periodic excitation evolves into a pattern with reversed magnetization, an example shown in Fig. 1. A Fourier analysis yields the corresponding signal in reciprocal-space and serves as a reference to quantify the XUV diffraction experiments.

[1] Bencivenga, F., et al., *Science Advances* 5, no. 7 (2019): 3–10.

[2] Ksenzov, D., et al., *Nano Letters* 21, no. 7 (2021): 2905–11.

Posters

| | | |
|-------------------|--|-----|
| Rekha Agarwal | <i>Substrate dependence of THz emission from epitaxial-NiO/Pt heterostructures</i> | 569 |
| Nimisha Arora | <i>Spin wave dynamics as a metrological archetype for topologically protected spin structures (TSS)</i> | 570 |
| Adam Bonda | <i>All-optical study of interlayer exchange coupling in Fe/Fe_xSi_{1-x} multilayers</i> | 571 |
| Irina Dolgikh | <i>Laser-induced Spin Dynamics In Ferrimagnetic Iron Garnets in High Magnetic Fields</i> | 572 |
| Abbass Hamadeh | <i>Parametric amplification of spin waves by surface acoustic waves</i> | 573 |
| Artsiom Kazlou | <i>Surface plasmon-assisted control of phase of photo-induced spin precession in Au/YIG:Co structures</i> | 574 |
| Nikolai Kuznetsov | <i>Spin-wave propagation and interference in microscopic YIG waveguides with submicron magnonic crystals</i> | 575 |
| Matthew McMaster | <i>Tunable NiFe Multilayers for High Frequency Applications</i> | 576 |
| Danny Thonig | <i>Spin-mixed states in non-collinear magnets</i> | 577 |

Substrate dependence of THz emission from epitaxial-NiO/Pt heterostructures

Rekha Agarwal¹, Sandeep Kumar^{1,2}, Kacho Imtiyaz Ali khan¹, Ekta Yadav^{1,2}, Niru Chowdhury¹, Sunil Kumar^{1,2}, P.K. Muduli¹

¹*Department of Physics, Indian Institute of Technology Delhi, New Delhi - 110016*

²*Femtosecond Spectroscopy and Nonlinear Photonics Laboratory, Indian Institute of Technology Delhi, New Delhi – 110016
Phz188430@iitd.ac.in*

When a femtosecond laser in the visible or near infrared is incident on a ferromagnet/heavy metal (FM/HM) bilayer heterostructure, it produces THz pulses [1,2]. This phenomenon has been studied in several FM/HM systems. Very recently, antiferromagnetic (AFM) materials have been used as a spin source instead of the FM layer for THz emission [3]. In this work, we use high-quality epitaxial-NiO/Pt heterostructure for THz emission. Pulse laser deposition (PLD) technique with KrF excimer laser source of wavelength 248 nm is used to deposit NiO film on two different substrates, Al₂O₃ and MgO at 500 °C. X-ray diffraction technique has been used to determine the crystal structure of NiO film. We observe NiO (111) peak for the films deposited on both the Al₂O₃ and MgO substrates. In both cases, epitaxial films are formed. The ϕ -scan measurement of NiO film on Al₂O₃ substrate shows the formation of two types of crystalline domains that are rotated by 60° with respect to each other, whereas NiO film on MgO substrate shows the formation of a single crystalline domain. The Pt layer was grown by UHV sputtering in a separate chamber after cleaning the NiO surface with substrate RF bias. We found a larger THz amplitude for the NiO/Pt system grown on MgO substrate as compared to the one on the Al₂O₃ substrate. The results show a clear dependence of THz amplitude on crystallinity, which is important for the field of antiferromagnetic spintronics.

References:

- [1] T. Kampfrath *et. al.*, *Nat. Nanotechnol.*, vol. 8, no. 4, pp. 256-260, 2013.
- [2] T. Seifert *et. al.*, *Nat. Photonics*, vol. 10, no.7, pp. 483-488, 2016.
- [3] H. Qiu *et. al.*, *Nat. Phys.*, vol. 17, no. 3, pp. 388-394, 20.

Spin wave dynamics as a metrological archetype for topologically protected spin structures (TSS)

Nimisha Arora, Yogesh Kumar, and Pintu Das

Indian Institute of Technology Delhi, Hauz Khas 11016, New Delhi, India

The global demand for scalable, efficient, and faster electronic devices such as magnetic data storage and processing unit has thrived in the search of materials that have geometrical structures which protect the configuration of electron's spin known as topologically protected spin structures (TSS). These can enable pronounced data storage and device efficiency at lower charge current density. To realize such structures and their response to external stimuli, it is very essential to identify the key parameters which ascertain the formation and stability of TSS.

In this work, we have performed micromagnetic simulations on Co/Pt nanodisk with interfacial Dzyaloshinskii-Moriya interaction (DMI) to investigate the hierarchy of creation and annihilation of distinct TSS. We identify a range of geometrical parameters for which DMI and perpendicular magnetic anisotropy can be tuned to stabilize TSSs viz., radial vortex, target-skyrmion, skyrmionium, and hopfion [1-3] at particular bias field strength. The comprehensive dynamical study of these structures suggests that the behavior of spin-wave (SW) mode with respect to an external bias field carries salient features characteristics to equilibrated TSS. This characteristic SW behavior can be alternatively employed as a meteorological archetype to detect TSS type. Since these structures can be controlled by a magnetic field, spectral fingerprints can be drawn, erase, and redrawn so that proposed devices are reconfigurable and tunable in nature.

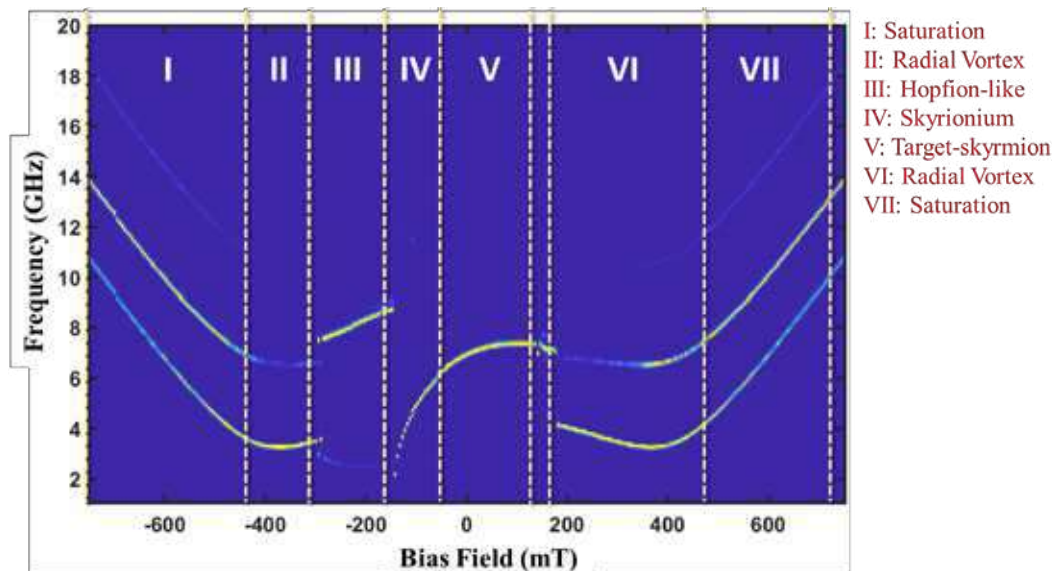


Figure 1: Spin wave mode response to an external bias field.

- [1] Y. Liu et al., Phys. Rev. Lett. **98**, 174437 (2018).
- [2] Y. Liu et al., Phys. Rev. Lett. **124**, 127204 (2020).
- [3] N. Kent et al., Nat. Commun. **12**, 1562 (2021).

All-optical study of interlayer exchange coupling in Fe/Fe_xSi_{1-x} multilayers

A. Bonda¹, L. Uba¹, and S. Uba¹

¹*Faculty of Physics, University of Białystok, K. Ciołkowskiego 1L, PL-15-245 Białystok, Poland*

Laser-induced magnetization precession effects in magnetic layered structures consisting of exchange coupled ferromagnetic layers separated by a nonmagnetic spacer layer are recently widely studied due to their basic and application importance for future spintronics devices. The occurrence of interlayer exchange coupling (IEC) is manifested through complex character of magnetization precession phenomena which can be measured with the use of time-resolved magneto-optical Kerr (TRMOKE) effect, in which the signal measured is superposition of acoustic and optical precession modes characterized by different frequencies and damping. The evaluation of the precession parameters as a function of external magnetic field H and orientation angle θ_H allows for IEC determination on the basis of dispersion relations. In the present work we applied the TRMOKE technique [1] to study the IEC in Fe/Fe_xSi_{1-x} multilayers in which the iron layers are separated by nonmagnetic Fe_xSi_{1-x} alloy spacers of composition $x = 0.50$ and thicknesses $d_s = 0.6, 1.4$ and 2.4 nm. For the interpretation of the experimental results, the dispersion relations derived from the model of macrospin precession with bilinear (BL) and biquadratic (BQ) interlayer exchange coupling, developed on the basis of LLG equations, was used. It is shown that the model predictions are in excellent agreement with the experimental results. Determined coupling parameters J_1 and J_2 , describing the strength of BL and BQ IEC, depend strongly on the thickness of the nonmagnetic spacer layer. For $d_s = 0.6$ nm and 1.4 nm the BL coupling is ferromagnetic and J_1 parameter reaches the value of the order of 1 mJ/m², while for $d_s = 2.4$ nm the BL coupling change into antiferromagnetic with $J_1 \approx -0.2$ mJ/m². The J_2 parameter of BQ coupling is in the range from ~ 0.2 to 1 mJ/m² for all samples. For $d_s = 1.4$ nm and 2.4 nm the effect of mode crossing was observed with the crossing field increasing as θ_H decreases from the in-plane to sample normal direction. It was found that determined Gilbert damping parameters for acoustic and optical modes change strongly between samples and depend on the mode type as well as H and θ_H magnitudes. The obtained results may be important for the study of magnetization precession in structures having simultaneously both bilinear and biquadratic interlayer exchange coupling.

[1] A. Bonda, L. Uba, K. Załęski, S. Uba, *Phys. Rev. B* **99**, 184424 (2019).

This work was supported by the National Science Centre in Poland, Grant No. 2019/03/X/ST3/01500.

Laser-induced Spin Dynamics In Ferrimagnetic Iron Garnets in High Magnetic Fields

I. A. Dolgikh^{1,2}, F. Formisano¹, K. H. Prabhakara¹, M. V. Logunov³, A. K. Zvezdin^{4,5},
P. C. M. Christianen^{1,2} and A. Kimel¹

¹*Institute for Molecules and Materials, Radboud University, 6525 AJ Nijmegen, The Netherlands.*

²*High Field Magnet Laboratory (HFML—EMFL), Radboud University, 6525 ED Nijmegen, The Netherlands.*

³*Kotelnikov Institute of Radio Engineering and Electronics, Russian Academy of Sciences, 125009 Moscow, Russia.*

⁴*Prokhorov General Physics Institute of the Russian Academy of Sciences, 119991 Moscow, Russia.*

⁵*National Research University Higher School of Economics, 101000 Moscow, Russia.*

Time-resolved spectroscopy in high magnetic fields opens up new opportunities for investigations of spin dynamics in yet unexplored and poorly understood non-collinear magnetic phases [1]. In this work we study laser-induced magnetization dynamics in ferrimagnetic iron garnet in magnetic fields up to 30T. The studied sample is a thin film with the thickness of 8 μ m. The material has magnetic anisotropy with “easy axis” along the normal to the sample. The compensation temperature of the ferrimagnet is around 50 K [2]. In order to study laser-induced spin dynamics we excited the medium with a laser pulse at the wavelength of 500 nm and probed the laser-induced magnetic changes with light at the wavelength of 800 nm. After the medium is heated by the pump laser pulse, magnetization dynamics is launched. It is interesting that the dynamics is very sensitive to the sample temperature and the magnetic field. In particular, we find a considerable change of dynamics in upon increase of the field above 4 Tesla and increase of the sample temperature across the compensation point (se Fig. 1). The observed results are explained taking into account HT-phase diagram of the material in the vicinity of the compensation point and spin-flop phase transition, in particular.

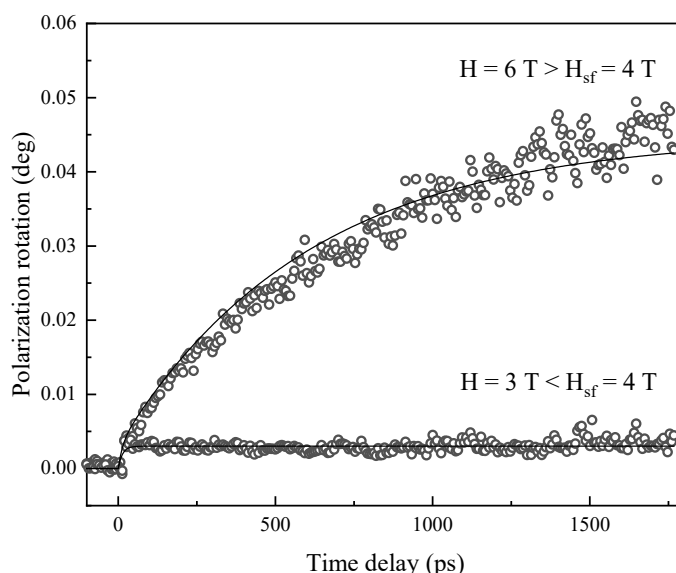


Figure 1: Laser-induced magnetization dynamics through the compensation temperature $T_{com}=50$ K in external magnetic fields below and above the spin flop field (4 T). The trace is measured at the temperature of 40K for the external fields of 3 T and 6T.

[1] J. Becker, et al (2017). *Phys. Rev. Let.* **118**(11), 117203 (2017).

[2] Y. B. Kudasov, M. V. Logunov, et al *Phys. Solid State* **60**(11), 2207-2210 (2018).

Parametric amplification of spin waves by surface acoustic waves

M. Mohseni¹, A. Hamadeh¹, M. Geilen¹, and P. Pirro¹

¹*Fachbereich Physik and Landesforschungszentrum OPTIMAS, Technische Universität Kaiserslautern, Germany*

In recent years, the field of dynamic magneto-elasticity has gained interest in developing compact, energy-efficient and even ultrafast spintronic devices. Several studies presented the excitation and manipulation of spin waves using magneto-elasticity driven by acoustic waves [1]. In this context, we have recently demonstrated experimentally the fully resonant [2] and the parametric excitation and instabilities [3] of spin waves in metallic magnetic thin film structures by short-waved coherent surface acoustic waves. Here, we extend our studies and show that a traveling spin-wave packet can be parametrically amplified using surface acoustic waves. Moreover, we present a design for a magneto-elastic spin-wave frequency converter, where the frequency of the reflection is changed with respect to the input frequency. This effect, which is tunable with the applied field, is enabled by the finite momentum of the surface acoustic waves driving the parametric amplification. Our study paves the way for realizing novel hybrid magnon-phonon device structures for high-frequency applications.

[1] P. G. Gowtham, et. Al., *J. Appl. Phys* **118**, 233910 (2015)

[2] M. Geilen, et. Al., *arXiv:2106.14705* (2022).

[3] M. Geilen, et. Al., *arXiv:2201.04033* (2022).

Surface plasmon-assisted control of phase of photo-induced spin precession in Au/YIG:Co structures

A. Kazlou, T. Kaihara, I. Razdolski and A. Stupakiewicz

Faculty of Physics, University of Białystok, 15-245 Białystok, Poland

Modern magneto-plasmonics is developing very rapidly, as it has the potential to reveal novel mechanisms for the light-matter interaction in magnetic materials. Due to the subwavelength localization of plasmons, all-optical magnetization switching below diffraction limit can be implemented. Before we have demonstrated the possibility of a plasmon-driven control of the spin precession amplitude in metal/dielectric heterostructures [1].

Here, we demonstrate a surface plasmon polariton (SPP)-assisted control of the spin precession phase in 7.5 μm thick Co-doped YIG (YIG:Co) covered with a 50 nm thick Au grating with a 800 nm period (gap width 100 nm). The SPP-driven photomagnetic excitation of magnetization precession was performed using the pump-probe technique with 50 fs temporal resolution. The pump wavelength was continuously tuned from 1160 to 1400 nm, while the wavelength of the probe beam was set to 800 nm. Transient Faraday rotation of the probe beam polarization was employed for monitoring the spin precession in the YIG:Co film. An inversion of the precession phase was found in the vicinity of the SPP resonance.

In our previous work [2] we found a significant phase shift in the photomagnetically induced magnetization precession on a bare garnet film and in an Au/YIG:Co heterostructure. Here, we determine in detail how this phase change occurs. Similar experiments performed at a number of angles of incidence of the pump beam confirmed the phase shift as large as π as well as the tunability of its spectral position together with the SPP resonance.

In bare YIG:Co, the reversal of the spin precession phase can be achieved by varying the pump beam polarization. Our results show that in the vicinity of the SPP resonance in Au/YIG:Co heterostructures, the interference of the SPP and incident electromagnetic fields can drive a similar phase reversal while the polarization of the incident beam remains unperturbed. This novel plasmon-induced mechanism in metal-dielectric heterostructures holds high promise to the further development of non-thermal control of photo-magnetic spin dynamics.

This work has been funded by the National Science Centre Poland (Grant No. DEC-2017/25/B/ST3/01305)

- [1] A. Chekhov, A.I. Stognij, T. Satoh, T.V. Murzina, I. Razdolski, and A. Stupakiewicz, *Nano Lett.* **18**, 5, 2970 (2018).
- [2] A. Kazlou, A.L. Chekhov, A.I. Stognij, I. Razdolski, and A. Stupakiewicz: *ACS Photonics*, **8**, 2197–2202 (2021).

Spin-wave propagation and interference in microscopic YIG waveguides with submicron magnonic crystals

N. A. Kuznetsov¹, H. Qin¹, L. Flajšman¹ and S. van Dijken¹

¹NanoSpin, Department of Applied Physics, Aalto University School of Science, Finland.

Magnonic crystals (MCs) can be utilized to effectively tailor spin-wave transport, which is essential for low-power wave-based data processing [1]. High-quality growth of nm-thick YIG films has enabled substantial downscaling of YIG MCs with a small number of scattering units and enlarged bandgaps [2,3]. Here, we report on spin-wave transport in straight, curved, and Y-shaped YIG waveguides with integrated submicron-scale MCs consisting of three 15-nm-deep and 500-nm-wide air grooves. Using super-Nyquist-sampling magneto-optical Kerr effect microscopy (SNS-MOKE), we demonstrate robust bandgaps with a size of 100-150 MHz in the waveguides (Fig. 1(a-c)). The spin-wave signal is strongly suppressed inside the bandgaps, while it shows limited loss at allowed frequencies compared to bare YIG. The spin waves in the straight waveguide have a decay length of 170 μm (Fig. 1d). In the curved structure, the spin-wave waveguide mode ($m = 1$) efficiently transmits over a 15° bend and reverts to the original wave after the second bend (Fig. 1e). Distinct from the curved structure, the spin-wave modes ($m = 1$) propagating along the two legs of the Y-shaped waveguide interfere with each other at the joint point and convert to the $m = 3$ mode (Fig. 1f). Spin waves with a frequency inside the bandgap show similar transmission characteristics, but with much weaker intensity. The combination of low-loss transmission and wide bandgaps in submicron MCs offers perspectives for spin-wave manipulation in magnonic devices.

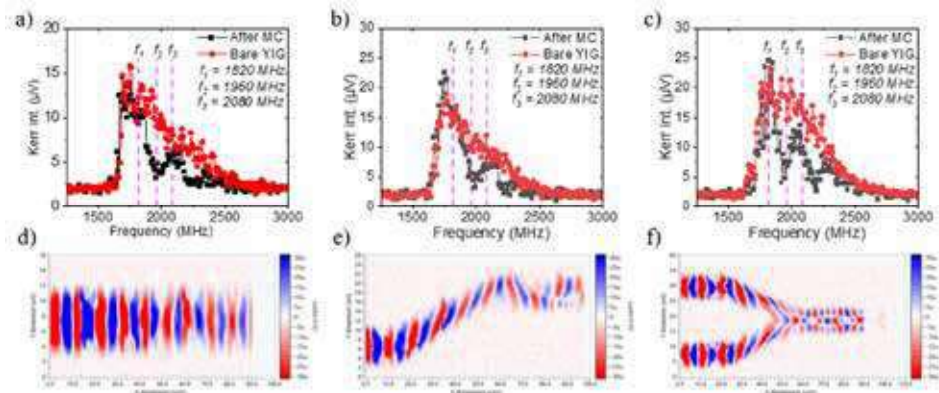


Figure 1. Spin-wave transmission spectra for (a) straight, (b) curved, and (c) Y-shape YIG waveguides with and without MC. (d-f) SNS-MOKE microscopy maps of spin-wave propagation along the straight, curved, and Y-shape YIG waveguides at 1820 MHz.

- [1] A. V. Chumak, V. I. Vasyuchka, A. A. Serga B. Hillebrands, “Magnon spintronics”, Nat. Phys. 11, 453 (2015)
- [2] Qin, H., Both, G.J., Hämäläinen, S.J. *et al.*, “Low-loss YIG-based magnonic crystals with large tunable bandgaps”, Nat. Commun. 9, 5445 (2018).
- [3] Qin, H. and van Dijken, S. “Nanometer-thick YIG-based magnonic crystals: Bandgap dependence on groove depth, lattice constant, and film thickness”, Appl. Phys. Lett. 116, 202403 (2020).

Tunable NiFe Multilayers for High Frequency Applications

Matthew R. McMaster¹, William R. Hendren¹, Jade N. Scott¹ and Robert M. Bowman¹

¹ School of Mathematics and Physics, Queen's University Belfast, University Road, Belfast, UK

Characterisation and control of the electromagnetic properties of synthetic magnetic structures at gigahertz frequencies is advantageous for the simulation and design of components for high frequency applications, such as shielding materials in magnetic recording. In such applications it is desirable to have a high saturation magnetization, low coercivity, high permeability and near zero magnetostriction. A typical material is $\text{Ni}_x\text{Fe}_{100-x}$ alloys where $x \sim 80$ provides near zero magnetostriction but also relatively low magnetization. However, multilayer structures such as $\text{Ni}_{80}\text{Fe}_{20}/\text{Ni}_{20}\text{Fe}_{80}$ may benefit some static properties such as magnetization while retaining low magnetostriction [1]. The purpose of this work is to investigate the dynamic properties of such structures and thus explore the possibility of better performing materials through multilayer design.

We present a systematic study of the ferromagnetic resonance (FMR) of sputter deposited thin film NiFe bilayers of the form $\text{Ni}_x\text{Fe}_{100-x}/\text{Ni}_y\text{Fe}_{100-y}$. Of particular interest are layer combinations involving both fcc and bcc crystal structures, since studies on single films of $\text{Ni}_x\text{Fe}_{100-x}$ have shown dramatically increased damping of the FMR when Ni content is reduced across the transition from fcc to bcc near $x=40$, figure 1. Magnetic and material properties were measured using a vector network analyser FMR set up [2], vibrating sample magnetometry and X-ray diffraction, with the aim of determining the relation between microstructure and the static and dynamic magnetic properties.

A result that was not to be expected from the single layer studies was that the FMR response of certain bilayers was strong even when the bcc NiFe layer was the dominant layer in the structure, figure 2. The possibility of incorporating the best properties of both layers in this way has significance for achieving an optimized material design.

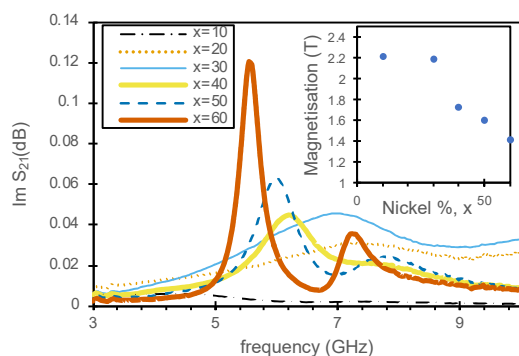


Figure 1: FMR spectra of 100nm $\text{Ni}_x\text{Fe}_{100-x}$ single layer thin films. Note that all measurements were performed at an applied field $H=253\text{Oe}$. Magnetization trend is inset.

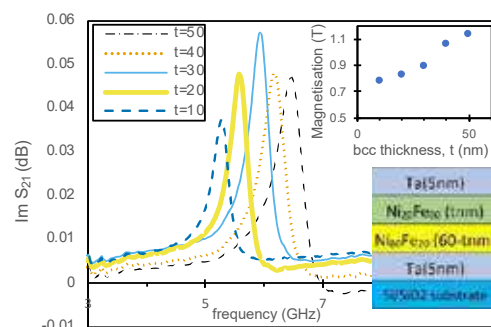


Figure 2: FMR spectra of $\text{Ni}_{80}\text{Fe}_{20}(60\text{-nm})/\text{Ni}_{20}\text{Fe}_{80}(t\text{-nm})$ thin films with varying bcc layer thickness, t . Note that all measurements were performed at an applied field of 253Oe . Magnetization trend and structure schematic is inset.

[1] C.B. Hill. "Manipulation and Magnetostriction of NiFe Films for Advanced Reader Shielding Application", PhD Thesis, Queen's University Belfast (2013).

[2] Y. Ding, T. J. Klemmer, and T. M. Crawford, *J. Appl. Phys.* **96**, 2969 (2004).

Spin-mixed states in non-collinear magnets

Danny Thonig^{1,3}, Sumanta Bhandary², Yaroslav Kvashnin³, Simon Streib³,
Manuel Pereiro³, and Olle Eriksson^{3,1}

¹*School of Science and Technology, Örebro University, SE-701 82 Örebro, Sweden*

²*School of Physics and CRANN Institute, Trinity College Dublin, The University of Dublin,
Dublin 2, Ireland*

³*Department of Physics and Astronomy, University Uppsala, SE-75120 Uppsala, Sweden*

In spintronics, the electron spins are used as information carriers and, thus, the description of spin relaxation in metals and semiconductors is of fundamental relevance. Here, spin relaxation in turn characterizes how rapidly the non-equilibrium spin population decays due to spin mixing. In magnets, this decay is not only depending on the magnetic moment length, as demonstrated for ultrafast demagnetizations processes [1-3], but also on the non-collinearity of the magnetic state. The latter phenomenon is barely understood and, thus, requires a deeper theoretical description of spin relaxation mechanisms.

We quantify the presence of spin-mixed states in non-collinear magnetic 3d transition metals by calculating the Elliot-Yafet spin-mixing parameter b^2 . Here, we are using a self-consistent, relativistic, Slater-Koster parametrized tight-binding electronic structure model implemented in the software *Cahmd* [4] that we have recently extended to treat non-collinear magnetism [5]. We, first, compare our results of the ferromagnetic order in itinerant magnets with density functional theory calculations in *VASP* [6], with literature [1,3], and experiment. We then analyze certain coherent (magnetic soliton) and temperature dependent, disordered non-collinear states, where we find that variations of the electronic states due to the non-collinearity have a drastic impact on the spin mixing. To estimate further the relevance of this effect, we are going to compare the effect of the non-collinearity on b^2 with the role of the spin-orbit coupling; both are expected to have a similar impact on the electronic potential [7].

- [1] D. Steiauf and M. Fähnle, *Phys. Rev. B* **79** 140401 (2009)
- [2] K. Carva, M. Battiato and P. M. Oppeneer *Phys. Rev. Lett.* **107** 207201 (2011); S. Essert and H. C. Schneider *Phys. Rev. B* **84** 224405 (2011)
- [3] B. Koopmans, G. Malinowski, F. Dalla Longa, D. Steiauf, M. Fähnle, T. Roth, M. Cinchetti and M. Aeschlimann *Nat. Mater.* **9** 259 (2010)
- [4] Computer code CAHMD, Classical atomistic hybrid multi-degree dynamics. (Danny Thonig, danny.thonig@oru.se, 2013) (unpublished, available from the author and <https://cahmd.gitlab.io/cahmdweb/>).
- [5] S Streib, V Borisov, M Pereiro, A Bergman, E Sjöqvist, A Delin, O Eriksson, and D Thonig, *Phys. Rev. B* **102** 214407 (2020)
- [6] G. Kresse and J. Hafner, *Phys. Rev. B* **47** 558 (1993); *ibid.* **49** 14251 (1994); G. Kresse and J. Furthmüller, *Comput. Mat. Sci.* **6** 15 (1996).
- [7] L. Nordström and D. J. Singh, *Phys. Rev. Lett.* **76** 4420 (1996)

Symposium 15. Magnetotransport, spin transport, spintronics, spin orbitronics and spin caloritronics, including devices

| | | |
|--------------------|--|-----|
| Anna Dyrdał | <i>Nonlinear magnetotransport in topological insulators and other 2D materials</i> | 582 |
| Marcos Guimarães | <i>Two-Dimensional Materials for Spin-Orbitronics</i> | 583 |
| Kouta Kondou | <i>Large spin orbit torque via magnetic spin Hall effect in the topological antiferromagnet</i> | 584 |
| Akash Kumar | <i>ROBUST MUTUAL SYNCHRONIZATION OF LARGE SPIN HALL NANO-OSCILLATOR CHAINS</i> | 585 |
| Kyung-Jin Lee | <i>Ferromagnet-induced spin-orbit torques</i> | 586 |
| Srijani Mallik | <i>Spin-Charge Interconversion with KTaO₃ two-dimensional electron gas</i> | 587 |
| Carlo Zucchetti | <i>Electric field modulation of spin transport in semiconductors</i> | 588 |
| Khasan Abdukayumov | <i>Spin-charge interconversion in 2D transition metal diselenides</i> | 591 |
| Maria Ameziane | <i>Lithium-ion battery technology for voltage control of perpendicular magnetization</i> | 592 |
| Isabel Arango | <i>Spin-to-charge conversion in highly resistive and sputtered Bi_xSe_{1-x} from all-electrical nanostructured devices</i> | 593 |
| CanOnur Avci | <i>Chiral coupling between magnetic layers with orthogonal magnetization</i> | 594 |
| Sebastian Beckett | <i>Magneto thermal transport in non collinear antiferromagnetic thin films</i> | 595 |
| Federico Bottegoni | <i>Inverse spin-Hall effect in GeSn</i> | 596 |
| Sara Catalano | <i>Spin Hall magnetoresistance effect from a disordered interface</i> | 597 |
| Wonyoung Choi | <i>Influence of intermixing on spin-to-charge conversion in sputtered BiSe</i> | 598 |
| Liza Herrera Diez | <i>Magnetoionic behavior in Ta/Co₂₀Fe₆₀B₂₀/HfO₂ solid state vs ionic liquid</i> | 599 |
| Shilei Ding | <i>Unidirectional orbital magnetoresistance in light metal/ferromagnet bilayers</i> | 600 |
| Federico Fagiani | <i>Tuning the spintronic properties of the ferroelectric Rashba semiconductor GeTe by alloying</i> | 601 |
| Piotr Graczyk | <i>Voltage-induced Stoner instabilities and spin-polarized currents at the MgO/Fe interface resonant states</i> | 602 |
| Krzysztof Grochot | <i>Study of Spin-Orbit Interactions and Multilevel Switching in Co/Pt/Co trilayer</i> | 603 |
| Abbass Hamadeh | <i>Autonomous parametric instability driven spintronic auto-oscillator for multi-mode generation</i> | 604 |
| Sajid Husain | <i>Field-free magnetization switching in sputtering grown epitaxial Tm₃Fe₅O₁₂ magnetic insulator thin films</i> | 605 |
| Sriram Kasilingam | <i>Effect of seed layer thickness on Ta crystalline phase and spin Hall angle</i> | 606 |
| Vaishnavi Kateel | <i>Spin orbit torque switching in coupled free layer designs</i> | 607 |

| | | |
|----------------------------------|--|-----|
| Sachin Krishnia | <i>Large spin-orbit torques on ferromagnetic layer from orbital currents</i> | 608 |
| Viola Krizakova | <i>Tailoring the switching efficiency of magnetic tunnel junctions by the fieldlike spin-orbit torque</i> | 609 |
| Michaela Kuepferling | <i>Spin Hall magnetoresistance and current density distribution in HM/FeCoB (HM=Ta,Pt) bilayers</i> | 610 |
| Miina Leiviskä | <i>Spin transport as a probe of non-linear fluctuations at the spin glass transition in $\text{Pd}_{1-x}\text{Ni}_x$ alloys</i> | 611 |
| Tim Ludwig | <i>Bath-induced spin inertia</i> | 612 |
| Stanisław Łazarski | <i>Spin orbit torque magnetization dynamics and switching in heavy metal/ferromagnet multilayers with mixed anisotropies</i> | 613 |
| Luca Nesi | <i>Spin textures go ferroelectric: perspectives and applications in ferroelectric Rashba semiconductors</i> | 614 |
| Paul Noel | <i>Role of the spin current induced generation of magnons in the current non-linear effects in ferromagnet/normal metal bilayers</i> | 615 |
| Peter Oppeneer | <i>Theory of magnetic spin and orbital Hall and Nernst effects in bulk ferromagnets</i> | 616 |
| Rohit Pachat | <i>Magneto-ionic Reversibility in Annealed W/CoFeB/HfO₂</i> | 617 |
| Van Tuong Pham | <i>Evidence of the interfacial asymmetric spin scattering at ferromagnet/platinum interfaces</i> | 618 |
| Mona Rajabali | <i>Qualitatively different injection locking behavior of distinctly different spin Hall nano-oscillator modes</i> | 619 |
| Philipp Ritzinger | <i>Anisotropic magnetoresistance in systems with non-collinear magnetic order</i> | 620 |
| Sandra Ruiz Gomez | <i>Direct X-ray detection of the spin Hall effect in CuBi</i> | 621 |
| Daniel Scheffler | <i>Anomalous Nernst effect in τ-MnAl thin films</i> | 622 |
| Manuel Suárez-Rodríguez | <i>Gate-tuneable and chirality-dependent charge-to-spin conversion in Tellurium nanowires</i> | 623 |
| Montserrat Xochitl Aguilar Pujol | <i>Detection of Magnon Currents in EuS</i> | 624 |
| Shahin Alam | <i>Spin zero effect in nonmagnetic centrosymmetric dipnictides TaAs₂</i> | 626 |
| Kateryna Boboshko | <i>Bilinear Magnetoresistance and Nonlinear Planar Hall Effect in Topological Insulators with Spin-Orbital Impurities</i> | 627 |
| Adam Cahaya | <i>Electron - Electron Repulsion Effect on Spin Mixing Conductance of Metallic Ferromagnet and Heavy Metal Interface</i> | 628 |
| Louis Farcis | <i>Spin-transfer torque induced dynamics in dual free layer p-MTJ</i> | 629 |
| Rodrigo Guedas García | <i>Reducing the temperature of nanostrips with a coating layer</i> | 630 |
| Ghulam Hussain | <i>Intrinsic spin Hall effect in Nb-based A15 compounds</i> | 631 |
| Fabian Kammerbauer | <i>Current-induced interlayer DMI in synthetic antiferromagnets</i> | 632 |
| Sachin Krishnia | <i>Giant Rashba spin-orbit torque in atomically thin metallic Pt/Co/AlPt multilayers</i> | 633 |

| | | |
|------------------------|--|-----|
| Anna Krzyżewska | <i>Nonlinear Hall effect induced by Berry curvature dipole in a two-dimensional system with k-cubed form of Rashba spin-orbit interaction</i> | 634 |
| Vireshwar Mishra | <i>On the Room Temperature Weak Localization and Anomalous Temperature Dependence of Phase Coherence Length in L_{21} Ordered Heusler Alloy CoFeMnSi Thin Films</i> | 635 |
| Richa Mudgal | <i>Determination of Spin-Orbit Torque in PtSe₂/NiFe Heterostructure</i> | 636 |
| Roselle Ngaloy | <i>Van der Waals Magnet based Spin-Valve Devices at Room Temperature</i> | 637 |
| Sam Parker | <i>A magneto-transport method for measuring the exchange coupling in a synthetic antiferromagnet</i> | 638 |
| Lara Solis | <i>FMR and thermal spin pumping enhanced by perpendicular anisotropy in YIG/Pt bilayers</i> | 639 |
| Izabella Wojciechowska | <i>Topological transport properties of ex-situ van-der-Waals structures</i> | 640 |
| Alexander Wright | <i>Thermal scanning probe lithography as a technique for fabrication of non-local spin valves</i> | 641 |

Invited Oral Presentations

| | | |
|------------------|---|-----|
| Anna Dyrdał | <i>Nonlinear magnetotransport in topological insulators and other 2D materials</i> | 582 |
| Marcos Guimarães | <i>Two-Dimensional Materials for Spin-Orbitronics</i> | 583 |
| Kouta Kondou | <i>Large spin orbit torque via magnetic spin Hall effect in the topological antiferromagnet</i> | 584 |
| Akash Kumar | <i>ROBUST MUTUAL SYNCHRONIZATION OF LARGE SPIN HALL NANO-OSCILLATOR CHAINS</i> | 585 |
| Kyung-Jin Lee | <i>Ferromagnet-induced spin-orbit torques</i> | 586 |
| Srijani Mallik | <i>Spin-Charge Interconversion with KTaO_3 two-dimensional electron gas</i> | 587 |
| Carlo Zucchetti | <i>Electric field modulation of spin transport in semiconductors</i> | 588 |

Nonlinear magnetotransport in topological insulators and other 2D materials

Anna Dyrdał

*Department of Mesoscopic Physics, ISQI, Faculty of Physics, Adam Mickiewicz University in
Poznań, ul. Uniwersytetu Poznańskiego 2, 61-614 Poznań, Poland*

Spin-orbit interaction is responsible for various novel states of matter (chiral spin textures, interfacial and surface spin-polarized states, and others), as well as for the possibility of pure electrical control of the spin degree of freedom. Therefore, the spin-orbit driven phenomena are currently of great interest due to the fundamental aspects of solid-state physics and possible applications in spintronics. The spin Hall effect and current-induced spin polarization (a.k. as Edelstein effect) have become a hallmark of nowadays spintronics, providing efficient mechanisms of the charge-to-spin interconversion. Recently, it was shown that the spin-orbit driven non-equilibrium spin polarization and spin currents are responsible for new interesting magnetotransport phenomena, such as nonlinear magnetoresistance and various nonlinear Hall effects [1-4].

During this talk, I will provide a brief overview of recent studies on nonlinear magnetotransport in selected two-dimensional systems, i.e. in topological insulators and perovskite oxides, where the spin-orbit interaction is strong enough to induce sizable current-induced spin polarization and in consequence a nonlinear transport response such as bilinear magnetoresistance and bilinear planar Hall effect [2, 5-7]. I will also discuss a method that we proposed recently, which allows a quantitative evaluation of the Rashba coupling parameter from the analysis of bilinear response in the angle-dependent magnetotransport experiments [7].

- [1] P. He, S. S.-L. Zhang, D. Zhu, et al., Nat. Phys. 14, 495 (2018)
- [2] A. Dyrdał, J. Barnaś, A. Fert, Phys. Rev. Lett. 124, 046802 (2020)
- [3] I. Sodemann, L. Fu, Phys. Rev. Lett. 115, 216806 (2015)
- [4] Ma Q., S.Y. Xu, H. Shen et al., Nature 565, 337 (2019)
- [5] K. Boboshko, A. Dyrdał, J. Barnaś, JMMM 545, 168698 (2022); K. Boboshko, A. Dyrdał, to be published
- [6] A. N. Zarezad, A. Dyrdał, JMMM 552, 169167 (2022); A. N. Zarezad, A. Dyrdał, to be published
- [7] D. C. Vaz, F. Trier, A. Dyrdał, et al., Phys. Rev. Materials 4, 071001(R) (2020)

This work has been supported partially by the Norwegian Financial Mechanism 2014-2021 under the Polish-Norwegian Research Project NCN GRIEG “2Dtronics” no. 2019/34/H/ST3/00515 and by the NCN in Poland under the project Sonata-14 no. 2018/31/D/ST3/02351.

Two-Dimensional Materials for Spin-Orbitronics

Marcos H. D. Guimarães¹

¹ *Zernike Institute for Advanced Materials, University of Groningen, The Netherlands*

The manipulation of magnetization using materials with large spin-orbit coupling is a promising route for applications in non-volatile magnetic memory devices. In these devices, a charge current flowing through the high spin-orbit coupling material can be used to apply torques on the magnetization of an adjacent ferromagnet. In addition to promising applications, the study of these current-induced spin-orbit torques can unveil many of the material's spintronic properties, such as their spin-dependent band structure.

The large family of layered van der Waals materials has shown many candidates for the efficient generation of spin-orbit torques. The large atomically-flat single crystals with various electronic properties combined with their pristine interfaces are ideal for the fabrication of high-performance spin-orbitronic devices.

In this talk I will present a brief overview of the field and show how the crystal structure and electronic properties of 2D materials can be used to control the magnitude, direction, and symmetries of spin-orbit torques [1, 2, 3]. I will show that a van der Waals insulating antiferromagnet (NiPS₃) in contact with a metallic ferromagnet can be used to generate large interfacial torques [4], with efficiencies comparable to best devices based on heavy-metal/ferromagnet bilayers. Finally, I will present our recent results on two-dimensional semiconductors [5], where we unveil the spin-torque mechanisms in these devices and show the presence of a large uniaxial magnetic anisotropy, which is imprinted on the ferromagnetic layer by the two-dimensional semiconductor crystal structure.

[1] D. MacNeill, G. M. Stiehl, M. H. D. Guimarães, R. A. Buhrman, J. Park, and D. C. Ralph, *Nature Physics* **13**, 300 (2017).

[2] M. H. D. Guimarães, G. M. Stiehl, D. MacNeill, N. D. Reynolds, and D. C. Ralph, *Nano Letters* **18**, 1311 (2018).

[3] A. Roy, M. H. D. Guimarães, and J. Slawinska, *Phys. Rev. Materials* **6**, 045004 (2022).

[4] C. F. Schippers, H. J. M. Swagten, and M. H. D. Guimarães, *Phys. Rev. Materials* **4**, 084007 (2021).

[5] J. Hidding, S. H. Tirion, J. Momand, A. Kaverzin, M. Mostovoy, B. J. van Wees, B. J. Kooi, and M. H. D. Guimarães, *JPhys. Materials* **4**, 04LT01 (2021).

Large spin orbit torque via magnetic spin Hall effect in the topological antiferromagnet

Kouta Kondou

RIKEN, Center for Emergent Matter Science (CEMS), Saitama 351-0198, Japan

Spin-orbit torques (SOT) via spin Hall effect (SHE) and Edelstein effect enable efficient electrical control of the magnetic states of ferromagnet and antiferromagnet in spintronics devices. However, in principle, the conventional SOT has severe limitation that only in-plane spins accumulate near the surface. Such a SOT is not suitable for controlling perpendicular magnetization, which would be more important for realizing low-power-consumption magnetic memory devices.

Recently we have demonstrated magnetic spin Hall effect (MSHE) in the topological Weyl antiferromagnet Mn_3Sn , in which the spin-polarization direction of current-induced spin accumulation changes its sign upon flipping the chiral antiferromagnetic order, i.e., the cluster magnetic octupole [1]. Notably, the antiferromagnetic order can be controlled by a small external magnetic field [2] or a spin-orbit torque [3].

Here, we discuss the magnetic spin Hall effect and our recent experimental results on the large spin orbit torque via the MSHE in the topological antiferromagnet Mn_3Sn , whose direction and size can be tuned by changing the direction of the order parameter [4]. These our findings provide a new route for efficient manipulation of magnetic states and realization of novel functionalities by utilizing topological Weyl antiferromagnets. This is the work in collaboration with M. Kimata, H. Chen, T. Tomita, M. Ikhlas, T. Higo, A. MacDonald, S. Nakatsuji and Y. Otani. This work was partially supported by JST-CREST (No. JPMJCR18T3) and JST-Mirai (JPMJMI20A1) and the Institute for Quantum Matter, an Energy Frontier Research Center funded by DOE, Office of Science, Basic Energy Sciences under Award # DE-SC0019331.”

- [1] M. Kimata et al., *Nature* **565**, 627 (2019).
- [2] S. Nakatsuji, N. Kiyohara, and T. Higo, *Nature* **527**, 212 (2015).
- [3] H. Tsai, T. Higo et al., *Nature* **580**, 608 (2020).
- [4] K. Kondou et al., *Nature Communications* **12** 6491 (2021).

Robust Mutual Synchronization of Large Spin Hall Nano-Oscillator Chains

AKASH KUMAR^{1*}, M. ZAHEDINEZAD¹, H. FULARA^{1,2}, R. KHYMYN¹, A. A. AWAD¹, M. RAJABALI¹, N. BEHERA¹, X. ZHAO¹, A. HOUSHANG¹, JOHAN ÅKERMANN¹

¹ Department of Physics, University of Gothenburg, Gothenburg, 41258 Sweden

² Department of Physics, Indian Institute of Technology Roorkee, Roorkee, 247667 India

*email: akash.kumar@gu.se

Since the advent of spin-torque nano-oscillators (STNOs) {1}, mutual synchronization of two or more STNOs has been of significant interest as it not only improves both the microwave signal power and the signal quality factor (Q-factor) appealing to communication technology but can also be used directly for neuromorphic computing due to the tunable magnetic nature of the interaction between STNOs {2}. Thanks to the spin Hall effect, a new class of spintronic oscillators known as spin Hall nano-oscillators (SHNOs) has emerged. Compared to STNOs, they rely on the current flowing in-plane, which makes their fabrication easier and allow for a large number of SHNOs to synchronize in both chains and arrays {3,4}. In this work, we explore mutual synchronization in nano-constriction (NC) based SHNO chains and demonstrate robust synchronization of SHNOs for longer chains with up to 21 oscillators [Fig. 1(a & b)]. We investigate W(5 nm)/NiFe(3 nm)/Al₂O₃(4 nm) and W(5 nm)/CoFeB(1.4 nm)/MgO(2 nm) {5} SHNOs. We report that the robust mutual synchronization can deliver an enhanced output power and significantly lower linewidth [Fig. 1(c & d)]. A sub-MHz linewidth [Fig. 1(c & d)], as low as 250 KHz for W/NiFe] can be achieved for 21 synchronized oscillators. The high-frequency operation results in a very high-quality factor ($Q=f/\Delta f$) of $>42,000$ for W/NiFe and $>25,000$ for W/CoFeB/MgO, which is the highest reported in chains. A linear decrease in linewidth and increase in output power (up to in-phase synchronization) is observed with the number of oscillators. The low current and low field operation of these oscillators along with wide frequency tunability (2-28 GHz) with both current and magnetic fields, make them ideal candidates for various spintronic applications.

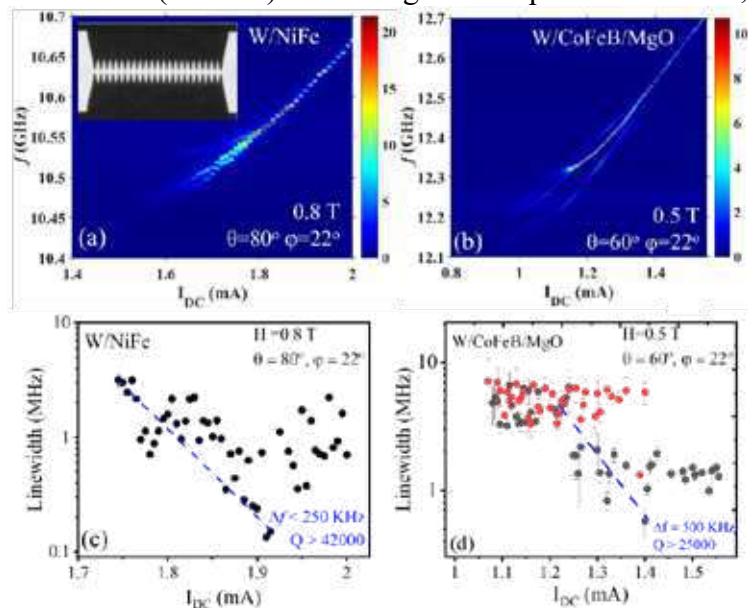


Figure 1(a & b) Power spectral density of mutually synchronized 21 NC SHNOs of W/NiFe and W/CoFeB/MgO, respectively. Inset shows the SEM image of NC SHNOs with 200 nm separation. (c & d) Linewidth (Δf) vs. I_{DC} for synchronized oscillators of W/NiFe and W/CoFeB/MgO, respectively.

- [1]. S. I. Kiselev, *et al.*, Nature 425, 380 (2003).
- [2]. R. Lebrun, *et al.*, Nat. Comm.8, 15825 (2017).
- [3]. A. A. Awad, *et al.*, Nat. Phys. 13, 292–299 (2017)
- [4]. M. Zahedinejad, *et al.*, Nat. Nano. 15, 47–52 (2020).
- [5]. H. Fulara, *et al.*, Sci. Adv. 5, eaax8467 (2019).

Ferromagnet-Induced Spin-Orbit Torques

Kyung-Jin Lee¹

¹ *Department of Physics, Korea Advanced Institute of Science and Technology (KAIST), Daejeon, Korea*

Spin-orbit torque (SOT), which is considered as a write scheme for next-generation MRAMs, arises from the charge-to-spin conversion via spin-orbit coupling (SOC). For efficient SOTs, it is of crucial importance to enhance the charge-to-spin conversion efficiency, which requires a detailed understanding of various SOC effects. In addition to the widely studied spin Hall effect of non-magnet (NM), recent studies found that SOC of ferromagnet (FM) also contributes to the SOT [1]. In this talk, we will discuss about these FM-induced SOTs, which provide additional knobs to enhance the net SOT efficiency. The talk will include:

- (i) The NM/FM interface [2,3] or FM bulk [4,5] generate spin currents polarized normal to the film plane, which allows for field-free SOT switching of perpendicular magnetization at a low current density [6,7].
- (ii) The spin Hall effect is concomitant with more fundamental orbital Hall effect [8]. As the orbital Hall effect is usually much stronger than the spin Hall effect, a direct injection of orbital currents to FMs can enhance the SOT via SOC of FM [9]. We will show an SOT experiment, necessitating the orbital Hall effect to explain the result [10]. If time is allowed, we will also discuss about orbital pumping, the Onsager reciprocity of orbital torque.

- [1] D. Go et al., “Theory of current-induced angular momentum transfer dynamics in spin-orbit coupled systems”, *Phys. Rev. Research* **2**, 033401 (2020).
- [2] S.-h. C. Baek et al., “Spin currents and spin-orbit torques in ferromagnetic trilayers”, *Nat. Mater.* **17**, 509 (2018).
- [3] V. P. Amin, J. Zemen, and M. D. Stiles, “Interface-generated spin currents”, *Phys. Rev. Lett.* **121**, 136805 (2018).
- [4] J. Ryu et al., “Efficient spin-orbit torque in magnetic trilayers using all three polarizations of a spin current”, *Nat. Electron.* **5**, 217 (2022).
- [5] H.-J. Park et al., “Spin swapping effect of band-structure origin in centrosymmetric ferromagnets”, submitted (2022).
- [6] D.-K. Lee and K.-J. Lee, “Spin-orbit torque switching of perpendicular magnetization in ferromagnetic trilayers”, *Sci. Rep.* **10**, 1772 (2020).
- [7] K.-W. Kim and K.-J. Lee, “Generalized spin drift-diffusion formalism in the presence of spin-orbit interaction of ferromagnets”, *Phys. Rev. Lett.* **125**, 207205 (2020).
- [8] H. Kontani et al., “Giant orbital Hall effect in transition metals: Origin of large spin and anomalous Hall effects”, *Phys. Rev. Lett.* **102**, 016601 (2009).
- [9] D. Go and H.-W. Lee, “Orbital torque: Torque generation by orbital current injection”, *Phys. Rev. Research* **2**, 013177 (2020).
- [10] D. Lee et al., “Orbital torque in magnetic bilayers”, *Nat. Commun.* **12**, 6710 (2021).

Spin-Charge Interconversion with KTaO₃ two-dimensional electron gas

Srijani Mallik¹, Sara Varotto¹, Luis M. Vicente-Arche¹, Julien Bréhin¹, Annika Johansson², Börge Göbel², Gerbold Ménard³, Guilhem Saiz³, Raphael Salazar⁴, Paul Noël⁵, Maxen Cosset-Cheneau⁵, Aravind Raji⁶, Alexandre Gloter⁶, Diogo C. Vaz¹, Felix Trier¹, Julien Rault⁴, Lara Benfatto⁷, Nicolas Bergeal³, Laurent Vila⁵, Jean-Philippe Attané⁵, Ingrid Mertig², Manuel Bibes¹

¹Unité Mixte de Physique, CNRS / Thales, Université Paris Saclay, Palaiseau, FRANCE

²Martin Lüther Universität, Halle & Max Planck Institut für Microstrukturphysik, Halle, GERMANY

³Laboratoire de Physique et d'Etude des Matériaux, ESPCI Paris, Université PSL, Paris, France

⁴Synchrotron SOLEIL, L'Orme des Merisiers Saint-Aubin, FRANCE

⁵Spintec, CEA, Université Grenoble Alpes, France

⁶Laboratoire de Physique des Solides, Université Paris-Saclay, CNRS, Orsay, France.

⁷Department of Physics and ISC-CNR, Sapienza University of Rome, Rome, Italy.

The two-dimensional electron gas (2DEG) at the interface between SrTiO₃ (STO) and LaAlO₃ [1], manifests a wide array of functionalities such as high electronic mobility, tunable Rashba spin-orbit coupling (SOC) with efficient spin – charge interconversion [2], and low temperature superconductivity [3]. Among these, the latter two properties pave the path towards the realization of devices for the field of spin-orbitronics [4] and topological quantum computing [5]. We have already demonstrated spin – charge interconversion for STO based 2DEGs and correlated it with the band structure [4]. Similar to STO, KTaO₃ (KTO) is a quantum paraelectric material that in the bulk can be turned into a metal by minute electron doping, leading to high-mobility transport [6]. It is also possible to achieve 2DEG by interfacing KTO with other insulating perovskites (e.g. LaAlO₃, LaVO₃) or metals (e.g. Al, Eu). Due to the presence of Ta (5d element), it is expected that the Rashba SOC in KTO 2DEGs should be larger than that in STO 2DEGs.

In this work, 2DEGs are generated by the simple deposition of Al metal by sputtering on KTO (001) single crystals. The Rashba coefficient is found to be ~5-10 times larger as calculated from the charge to spin conversion experiments as well as by fitting the band structure obtained from angle-resolved photoemission spectroscopy (ARPES) measurement. Further, their spin to charge conversion efficiency is measured and related to the 2DEG electronic structure [7]. Moreover, superconductivity has been observed very recently in KTO (111) and (110) based 2DEGs adding further functionalities to the system. We have used microwave transport to show that KTO (111) 2DEGs exhibit a node-less superconducting order parameter with a gap value significantly larger than expected in a simple BCS weak-coupling limit model [8]. Finally, we will discuss how our finding offers innovative perspectives for device applications related to spin-orbitronics and topological electronics.

[1] A. Ohtomo *et al.* *Nature* **2004**, 427, 423.

[2] A. D. Caviglia *et al.* *Phys. Rev. Lett.* **2010**, 104, 126803.

[3] N. Reyren *et al.* *Science* **2007**, 317, 1196.

[4] D. C. Vaz *et al.* *Nature Materials* **2019**, 18, 1187.

[5] A. Barthelemy *et al.* *Euro. Phys. Lett.* 2021, 133, 17001.

[6] S. H. Wemple *Phys. Rev.* **1965**, 137, A1575.

[7] L. M. Vicente-Arche *et al.* *Adv. Mater.* **2021**, 2102102.

[8] S. Mallik, *et al.* arXiv:2204.09094.

Electric field modulation of spin transport in semiconductors

Carlo Zucchetti¹, Adele Marchionni¹, Monica Bollani², Paolo Grassi², Franco Ciccacci¹, Marco Finazzi¹, and Federico Bottegoni¹

¹*LNESS-Dipartimento di Fisica, Politecnico di Milano, Piazza Leonardo da Vinci 32, 20133 Milan, Italy*

²*Istituto di Fotonica e Nanotecnologie del Consiglio Nazionale delle Ricerche, Piazza Leonardo da Vinci 32, 20133 Milan, Italy*

The finite spin lifetime in solids is often considered a major hindrance for the development of spintronic devices. In this work, we show that this feature can instead be exploited to realize a scheme where spin transport is modulated at room temperature by a modest electric field. To prove this concept we employ a nonlocal spin-injection/detection scheme which enables one to directly image spin transport. We have previously shown that this paradigm allows one to obtain a direct measure of the spin-diffusion length [1]. Here we investigate drift-diffusive spin transport at room temperature with a device-oriented architecture, showing that a finite spin-diffusion length combined with the application of an electric field can be capitalized to manipulate spin accumulation [2]. A field directed antiparallel (parallel) to the spin-diffusion velocity can, in fact, largely increase (decrease) the spin-transport length compared with the zero field case. We find that applying an electric field $E = 24$ V/cm along a $40\text{ }\mu\text{m}$ -long path in germanium results in about one order of magnitude modulation of the spin-polarized electrons entering into the detector. Moreover, in the best case scenario, we directly image a spin-transport length of $\approx 40\mu\text{m}$. Comparable values in semiconductors have been predicted [3] and observed [4] only at cryogenic temperatures.

The investigated scheme could thus modulate spin transport over long distances and is expected to reach fast timescales. Preliminary simulations predict that, for realistic electric field amplitudes, carrier mobility, and spin lifetime, modulation frequencies reaching 10 GHz can be attained. Our platform combines all the following characteristics, which make it extremely promising for the development of next generation spintronic devices: (i) room temperature operation; (ii) a large modulation of spin accumulation; (iii) spin-transport lengths that can be pushed above $40\text{ }\mu\text{m}$; and (iv) application of moderate control electric fields, which is a key point for low power consumption operation. Hence, our work demonstrates that electric fields can be exploited for guiding spins over macroscopic distances and for realizing fast room temperature modulation of spin accumulation.

- [1] C. Zucchetti et al., *Phys. Rev. B* **96**, 014403 (2017).
- [2] C. Zucchetti et al., *APL Materials* **10**, 011102 (2022).
- [3] P. Li, Y. Song, and H. Dery, *Phys. Rev. B* **86**, 085202 (2012).
- [4] F. Bottegoni et al., *Phys. Rev. Lett* **118**, 167402 (2017).

Oral Presentations

| | | |
|----------------------|--|-----|
| Khasan Abdukayumov | <i>Spin-charge interconversion in 2D transition metal diselenides</i> | 591 |
| Maria Ameziane | <i>Lithium-ion battery technology for voltage control of perpendicular magnetization</i> | 592 |
| Isabel Arango | <i>Spin-to-charge conversion in highly resistive and sputtered $\text{Bi}_x\text{Se}_{1-x}$ from all-electrical nanostructured devices</i> | 593 |
| CanOnur Avci | <i>Chiral coupling between magnetic layers with orthogonal magnetization</i> | 594 |
| Sebastian Beckert | <i>Magneto thermal transport in non collinear antiferromagnetic thin films</i> | 595 |
| Federico Bottegoni | <i>Inverse spin-Hall effect in GeSn</i> | 596 |
| Sara Catalano | <i>Spin Hall magnetoresistance effect from a disordered interface</i> | 597 |
| Wonyoung Choi | <i>Influence of intermixing on spin-to-charge conversion in sputtered BiSe</i> | 598 |
| Liza Herrera Diez | <i>Magnetoionic behavior in $\text{Ta}/\text{Co}_{20}\text{Fe}_{60}\text{B}_{20}/\text{HfO}_2$ solid state vs ionic liquid</i> | 599 |
| Shilei Ding | <i>Unidirectional orbital magnetoresistance in light metal/ferromagnet bilayers</i> | 600 |
| Federico Fagiani | <i>Tuning the spintronic properties of the ferroelectric Rashba semiconductor GeTe by alloying</i> | 601 |
| Piotr Graczyk | <i>Voltage-induced Stoner instabilities and spin-polarized currents at the MgO/Fe interface resonant states</i> | 602 |
| Krzysztof Grochot | <i>Study of Spin-Orbit Interactions and Multilevel Switching in Co/Pt/Co trilayer</i> | 603 |
| Abbass Hamadeh | <i>Autonomous parametric instability driven spintronic auto-oscillator for multi-mode generation</i> | 604 |
| Sajid Husain | <i>Field-free magnetization switching in sputtering grown epitaxial $\text{Tm}_3\text{Fe}_5\text{O}_{12}$ magnetic insulator thin films</i> | 605 |
| Sriram Kasilingam | <i>Effect of seed layer thickness on Ta crystalline phase and spin Hall angle</i> | 606 |
| Vaishnavi Kateel | <i>Spin orbit torque switching in coupled free layer designs</i> | 607 |
| Sachin Krishnia | <i>Large spin-orbit torques on ferromagnetic layer from orbital currents</i> | 608 |
| Viola Krizakova | <i>Tailoring the switching efficiency of magnetic tunnel junctions by the fieldlike spin-orbit torque</i> | 609 |
| Michaela Kuepferling | <i>Spin Hall magnetoresistance and current density distribution in HM/FeCoB (HM=Ta,Pt) bilayers</i> | 610 |
| Miina Leiviskä | <i>Spin transport as a probe of non-linear fluctuations at the spin glass transition in $\text{Pd}_{1-x}\text{Ni}_x$ alloys</i> | 611 |
| Tim Ludwig | <i>Bath-induced spin inertia</i> | 612 |
| Stanisław Łazarski | <i>Spin orbit torque magnetization dynamics and switching in heavy metal/ferromagnet multilayers with mixed anisotropies</i> | 613 |
| Luca Nessi | <i>Spin textures go ferroelectric: perspectives and applications in ferroelectric Rashba semiconductors</i> | 614 |

| | | |
|----------------------------------|--|-----|
| Paul Noel | <i>Role of the spin current induced generation of magnons in the current non-linear effects in ferromagnet/normal metal bilayers</i> | 615 |
| Peter Oppeneer | <i>Theory of magnetic spin and orbital Hall and Nernst effects in bulk ferromagnets</i> | 616 |
| Rohit Pachat | <i>Magneto-ionic Reversibility in Annealed W/CoFeB/HfO₂</i> | 617 |
| Van Tuong Pham | <i>Evidence of the interfacial asymmetric spin scattering at ferromagnet/platinum interfaces</i> | 618 |
| Mona Rajabali | <i>Qualitatively different injection locking behavior of distinctly different spin Hall nano-oscillator modes</i> | 619 |
| Philipp Ritzinger | <i>Anisotropic magnetoresistance in systems with non-collinear magnetic order</i> | 620 |
| Sandra Ruiz Gomez | <i>Direct X-ray detection of the spin Hall effect in CuBi</i> | 621 |
| Daniel Scheffler | <i>Anomalous Nernst effect in τ-MnAl thin films</i> | 622 |
| Manuel Suárez-Rodríguez | <i>Gate-tuneable and chirality-dependent charge-to-spin conversion in Tellurium nanowires</i> | 623 |
| Montserrat Xochitl Aguilar Pujol | <i>Detection of Magnon Currents in EuS</i> | 624 |

Spin-charge interconversion in 2D transition metal diselenides

K. Abdulkayumov¹, Céline Vergnaud¹, Alain Marty¹, Frédéric Bonell¹, Hervé Boukari², Hanako Okuno³, Vincent Maurel⁴, Serge Gambarelli⁴, Sukhdeep Dhillon⁵, Martin Micica⁵, and Matthieu Jamet¹

¹ Univ. Grenoble Alpes, CEA, CNRS, Spintec, Grenoble, 38000, France

² Univ. Grenoble Alpes, CEA, CNRS, Néel Institute, Grenoble, 38000, France

³ Univ. Grenoble Alpes, CEA, MEM, Grenoble, 38000, France

⁴ Univ. Grenoble Alpes, CEA, CNRS, SyMMES, Grenoble, 38000, France

⁵ LP ENS Paris, Paris, 75005, France

Transition Metal Diselenides (TMD), a subgroup of Transition metal dichalcogenides, possess a vast variety of physical properties, namely, semiconducting WSe₂ and semimetallic PtSe₂. Moreover, These TMDs show large spin-orbit coupling and various symmetries, hence, offering different physical mechanisms to generate spin-orbit torques (SOT) into an adjacent ferromagnetic layer by charge-to-spin conversion, making them an ideal platform to study and develop fully van der Waals SOT magnetic random access memories (MRAM) in the ultra-compact form.

The existing literature is on flakes of tens of micrometers of TMDs [1]. This work is focused on MBE grown in the van der Waals regime, highly crystalline, and large area (1 cm²) TMDs (WSe₂, PtSe₂). WSe₂ shows out-of-plane spin texture due to spin-valley coupling at K and K' points and, on the other hand, PtSe₂ exhibits in-plane spin texture due to Rashba coupling. The goal of this work is to study spin-charge interconversion by spin Hall or Rashba Edelstein effects (and their inverse). For this, spin pumping-ferromagnetic resonance (SP-FMR), sketched in Fig. 1d [2], and THz time domain spectroscopy (TDS) are employed. SP-

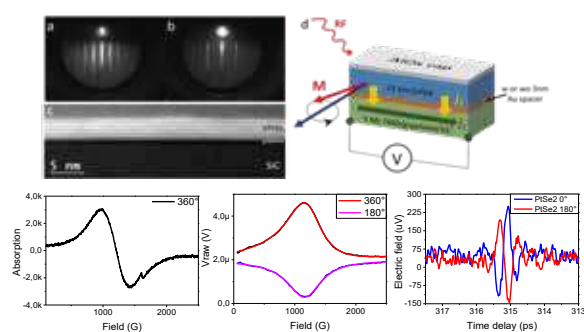


Figure 1 a and b RHEED images of 5 ML PtSe₂ c) cross-section STEM d) sketch of the SP-FMR technique. e) and f) FMR spectra of Co in the stack Au/Co/Au/ W_{0.9}V_{0.1}Se₂ and electro motive force, respectively, and g) THz emission due to ISHE in PtSe₂

FMR results show efficient spin-charge conversion in W_{0.9}V_{0.1}Se₂ (V-alloying to p-dope WSe₂) and no conversion in PtSe₂. On the other hand, THz-TDS shows THz emission originating from Inverse spin Hall effect in PtSe₂, whereas no emission was observed in WSe₂. These discrepancies can be explained by the differences in the techniques used. We will discuss our first conclusions in terms of spin-orbit coupling, symmetries, and the band structures of the TMDs studied. The direct effects will be studied using second Harmonic Hall measurements by magnetotransport.

Support by the French ANR through the project MAGICVALLEY (ANR-18-CE24-0007) is gratefully acknowledged.

References

- [1] Hiddin, J. & Guimaraes, M., . Front. Mater. 7:594771 (2021)
- [2] Ando, K., et al., J. Appl. Phys. **109**, 103913 (2011)

Lithium-ion battery technology for voltage control of perpendicular magnetization

Maria Ameziane¹, Rhodri Mansell¹, Ville Havu¹, Patrick Rinke¹
and Sebastiaan van Dijken¹

¹ Department of Applied Physics, Aalto University School of Science, P.O. Box 15100, FI-00076 Aalto, Finland

Voltage control of magnetism provides a promising path toward the development of low-power spintronic devices. Magneto-ionics exploiting voltage-driven ion migration as a control mechanism has attracted interest because it can generate large magnetoelectric effects at low voltages. Here, we demonstrate the use of all-solid-state lithium-ion battery technology for reversible voltage-controlled switching between perpendicular and in-plane magnetization states in a Co/Pt bilayer.

The magneto-ionic battery structure consists of a 2 nm Ta/5 nm Pt/20 nm LiCoO₂/70 nm LiPON/3 nm Co/5 nm Pt crossbar junction (Fig. 1a). Here, LiPON functions as a solid-state electrolyte for Li⁺ ion conduction and LiCoO₂ (LCO) acts as a Li⁺ storage layer. Using magneto-optical Kerr effect (MOKE) microscopy, we show that the magnetization of the Co film switches between in-plane and perpendicular directions when voltages of +2.5 V and -2 V are applied, respectively (Fig. 1c,d). The magneto-ionic switching effect is reliably reproduced over multiple cycles and switching takes place in less than 0.5 s at room temperature (Fig. 1b). Our structure can be cycled for >500 times without degradation.

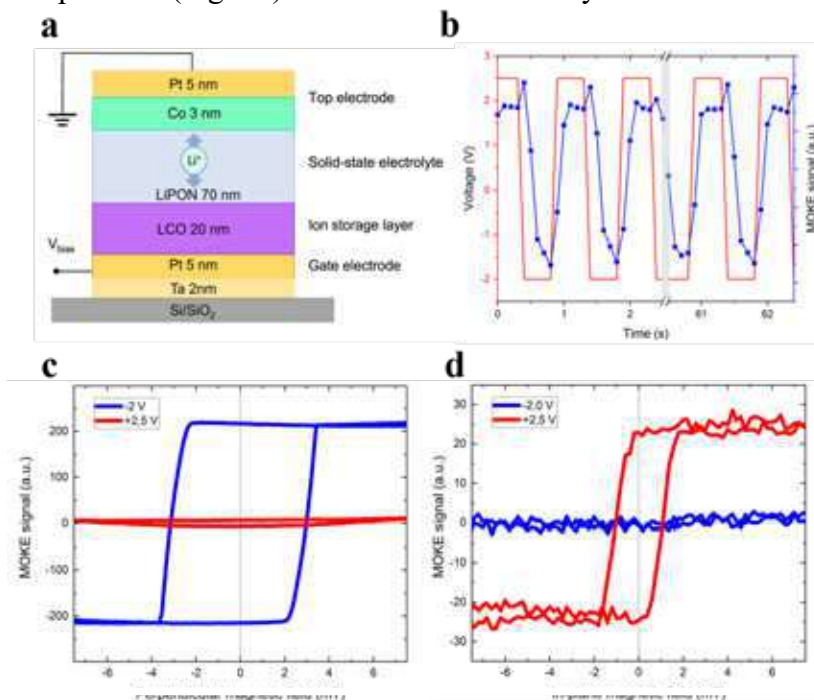


Figure 1: (a) Schematic of the magneto-ionic battery structure.

(b) Time-resolved modulation of the longitudinal MOKE signal at room temperature recorded while toggling the voltage between -2.0 V and +2.5 V in 0.5 s intervals. (c) Polar and (d) longitudinal MOKE hysteresis loops recorded at -2.0 and +2.5 V.

The magnetoelectric coupling efficiency is estimated to be 7,700 fJ/Vm at room temperature, which is the strongest magnetoelectric effect reported to date. We attribute the effect to changes in the hybridization of electron orbitals at the Co/Pt interface upon voltage-controlled insertion and de-insertion of Li⁺ ions.

Our work sets a new benchmark for lithium-based magneto-ionics and showcases battery-inspired design principles as a promising avenue for the development of low-power spintronic devices.

Spin-to-charge conversion in highly resistive and sputtered $\text{Bi}_x\text{Se}_{1-x}$ from all-electrical nanostructured devices

Isabel C. Arango¹, Won Young Choi¹, Inge Groen¹, Diogo Vaz¹, Van Tuong Pham²,
Luis Hueso^{1,3} and Fèlix Casanova^{1,3}

¹ CIC nanoGUNE BRTA, 20018, Donostia-San Sebastian, Basque Country, Spain

² University Grenoble Alpes, CEA, CNRS, Spintec, F-38000 Grenoble, France

³ IKERBASQUE, Basque Foundation for Science, 48009, Bilbao, Basque Country, Spain

Materials with a strong spin-orbit coupling present some effects relevant for the development of spintronics devices, such as the spin Hall effect (SHE) and its inverse (ISHE) which result in conversion between charge currents and spin currents. The efficiency of spin-to-charge current conversion is given by the spin Hall angle θ_{SH} [1]. Large θ_{SH} has been reported in topological insulators such as bismuth selenide (Bi_2Se_3) due to the spin-momentum locking occurring at the topologically protected surface states [2]. Recently, large conversion efficiencies have been reported in sputtered amorphous $\text{Bi}_x\text{Se}_{1-x}$ [3]. Amorphous $\text{Bi}_x\text{Se}_{1-x}$ is thus a promising material that can be used in the recently proposed magneto-electric spin-orbit (MESO) logic device by Intel [4], in which not only large θ_{SH} is needed, but also a high resistivity [5]. However, electrical spin injection in nanostructured devices have not been used in any of the previous works, which is required for a MESO device with integration with standard CMOS electronics. We were able to fabricate sputtered amorphous $\text{Bi}_x\text{Se}_{1-x}$ nanostructures and integrate them in lateral spin valve (LSV) devices by multiple e-beam lithography steps. This is a challenging process that requires a comprehensive understanding of the interface between the topological insulator and the metals used in the LSVs, which is an extremely critical factor to design an all-electrical spintronic device. By using the configuration shown in Fig. 1a [1], we successfully measure the spin Hall signal ($2\Delta R_{\text{SHE}}$), which allows us to quantify θ_{SH} in sputtered $\text{Bi}_x\text{Se}_{1-x}$ (Fig. 1b).

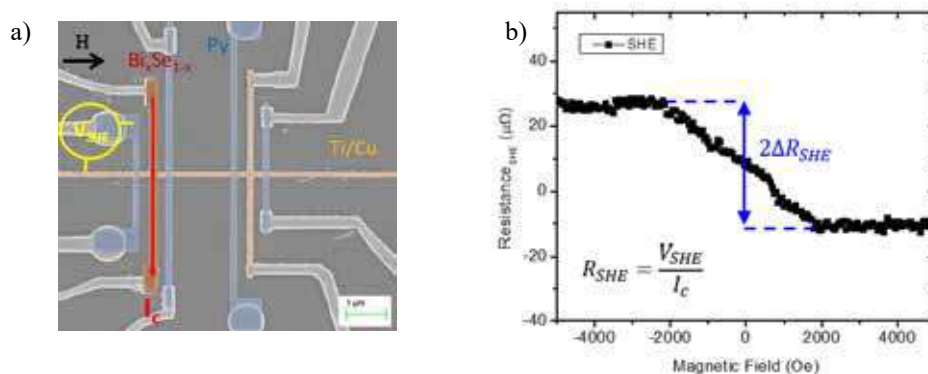


Figure 1: a) SEM image of two Py/Cu-based lateral spin valves: on the left with a middle wire for spin absorption of $\text{Bi}_x\text{Se}_{1-x}$ (30 nm) and on the right as a reference. b) SHE resistance as a function of the external magnetic field measured at 10 K using the configuration in panel a, demonstrating spin-to-charge conversion in a $\text{Bi}_x\text{Se}_{1-x}$ nanostructure.

- [1] E. Sagasta et al., *Phys. Rev. B*. **94**, 060412 (2016).
- [2] Y. Wang et al., *Phys. Rev. Lett.* **114**, 257202 (2015).
- [3] M. DC et al., *Appl. Phys. Lett.* **114**, 102401 (2019); M. DC et al., *Nat. Mater.* **17**, 800 (2018).
- [4] S. Manipatruni et al., *Nature*. **565**, 35 (2019).
- [5] V. T. Pham et al., *Nat. Electron.* **3**, 309 (2020).

Chiral coupling between magnetic layers with orthogonal magnetization

Can Onur Avci^{1,2}, Charles-Henri Labert², Giacomo Sala², and Pietro Gambardella²

¹ *Institute of Materials Science of Barcelona (ICMAB-CSIC), Carrer dels Til·lers s/n, 08193 Bellaterra, Spain*

² *ETH Zürich, Department of Materials, Hönggerberggring 64, 8093 Zürich, Switzerland*

The ability to engineer the coupling between magnetic layers is central to reveal emergent magnetic and electronic interactions at interfaces as well as to improve the functionality of magnetic sensors, nonvolatile memories, and logic gates. Recently, increasing attention has been devoted to the exchange coupling mediated by the Dzyaloshinskii-Moriya interaction (DMI) that favors the orthogonal alignment of neighboring spins in materials with spatial inversion asymmetry. The DMI was originally investigated in bulk systems such as α -Fe₂O₃ and the B20 compounds. However, recent works has shown that a strong DMI emerges at ferromagnet/nonmagnet (FM/NM) interfaces with broken inversion symmetry and strong spin-orbit coupling stabilizing chiral spin textures such as Néel domain walls and skyrmions [1]. More recently, Monte Carlo calculations and experiments have shown that the DMI can also couple two FM layers through a spacer layer where the DMI promotes nontrivial three-dimensional spin textures with both intralayer and interlayer chirality [2]. The interlayer coupling mediated by the DMI thus offers novel opportunities to tune the magnetic texture and functionality of magnetic multilayers.

In this work [3], we report on the occurrence of strong interlayer DMI between an in-plane magnetized Co layer and a perpendicularly magnetized TbFe layer through a Pt spacer. The DMI causes a chiral coupling that favors one-handed orthogonal magnetic configurations of Co and TbFe, which we reveal through Hall effect and magnetoresistance measurements (Fig. 1). The DMI coupling mediated by Pt causes effective magnetic fields on either layer of up to 10–15 mT, which decrease monotonically with increasing Pt thickness. Ru, Ta, and Ti spacers mediate a significantly smaller coupling compared to Pt, highlighting the essential role of Pt in inducing the interlayer DMI. These results are relevant to understand and maximize the interlayer coupling induced by the DMI as well as to design spintronic devices with chiral spin textures.

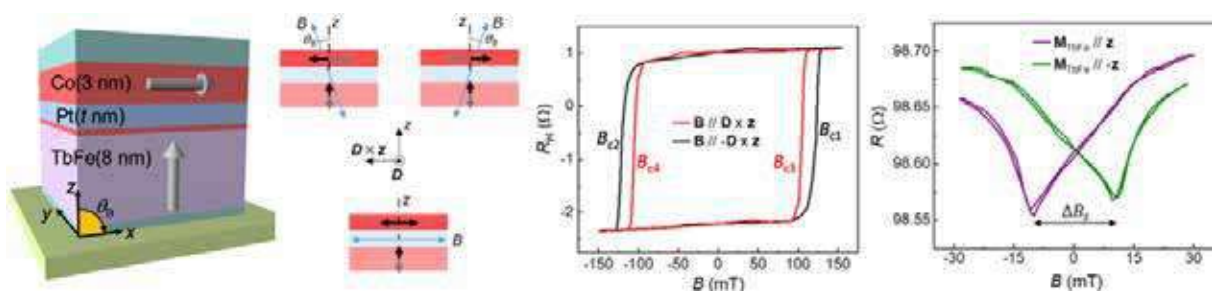


Figure 1 – Left: Sketch of the multilayer structure and coordinate system used in the study. Right: Representative measurements showing interlayer DMI-induced shift of coercivity for the perpendicular TbFe and in-plane Co layer.

[1] Hellman et al., *Rev. Mod. Phys.* **89**, 025006 (2017)

[2] Fernández-Pacheco et al., *Nat. Mater.* **18**, 679 (2019); Han et al., *Nat. Mater.* **18**, 703 (2019)

[3] Avci et al., *Phys. Rev. Lett.* **127**, 167202 (2021)

Magneto-thermal transport in non-collinear antiferromagnetic thin films

S. Beckert,¹ J. Godinho,^{2,4} F. Johnson,³ J. Kimák,⁴ E. Schmoranzarová,⁴ Z. Šobáň,² K. Olejník,² J. Zemen⁵, J. Wunderlich,⁶ P. Němec,⁴ D. Kriegner,^{1,2} L. F. Cohen,³ A. Thomas,^{1,7} S. T. B. Goennenwein,⁸ H. Reichlová^{1,2}

¹IFMP Technische Universität Dresden, 01062 Dresden, Germany

²Institute of Physics of the Czech Academy of Sciences, Cukrovarnicka 10, Prague, Czech Republic

³Department of Physics, Blackett Laboratory, Imperial College London, London SW7 2AZ, UK

⁴Faculty of Mathematics and Physics, Charles University, Ke Karlovu 3, Prague, Czech Republic

⁵Faculty of Electrical Engineering, Czech Technical University in Prague, Technická 2, CR

⁶Institute of Experimental and Applied Physics, University of Regensburg, Regensburg, Germany

⁷IFW Dresden, Helmholtzstrasse 20, 01069 Dresden, Germany

⁸Department of Physics, University of Konstanz, 78457 Konstanz, Germany

Understanding the interplay between topological properties and transport phenomena in non-collinear antiferromagnets is important for exploiting their unconventional characteristics in spintronics. In particular, non-collinear antiferromagnets can exhibit phenomena previously known to be exclusive to ferromagnets, such as the anomalous Hall Effect (AHE) or the anomalous Nernst effect (ANE).

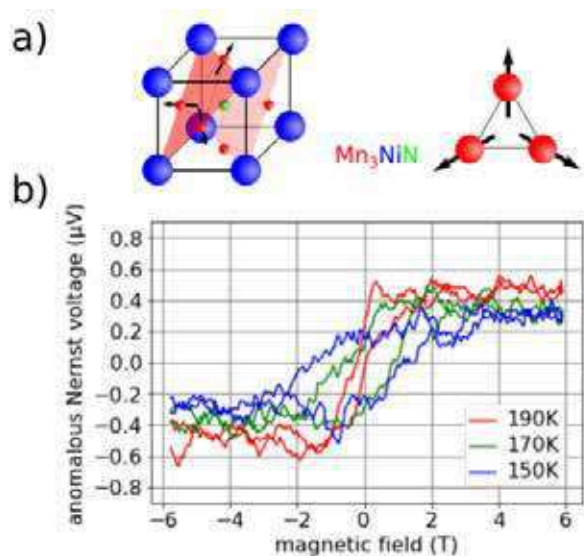


Figure 1: a) Crystal and spin structure of Mn₃NiN.

b) Anomalous Nernst voltage in dependency of the magnetic field for different temperatures.

We experimentally study the magneto-thermal transport in unconventional antiferromagnetic thin magnetic films with complex band structure, namely Mn₃NiN [1]. In previously studied Mn₃Sn films, all spins are arranged in the sample plane. Therefore, AHE and ANE cannot be measured in a standard Hall bar geometry and a comparison of AHE and ANE is also not straightforward [2]. (001)-oriented Mn₃NiN thin films have their spins arranged in the (111) plane and, therefore, in principle, a component of the Hall vector in both out-of plane and in-plane directions [3]. This makes Mn₃NiN an ideal candidate for a systematic study of magneto-thermal transport phenomena and their anisotropy. We will present measurements of ANE, AHE,

magnetoresistance and Seebeck effect in a single device. Based on careful thermal gradient calibration, we can compare the measured amplitudes of the magneto-thermal transport coefficients and discuss them in context of the Mott relation [4].

[1] D. Boldrin et al. ACS Appl. Mater. Interfaces 2018, **10**, 22, 18863–18868 (2018)

[2] H. Reichlová et al. Nat. Commun. **10**, 5459 (2019)

[3] D. Boldrin et al., Phys. Rev. Materials **3**, 094409 (2019)

[4] Y. Pu et al., Phys. Rev. Lett. **101**, 117208 (2008)

Inverse spin-Hall effect in GeSn

A. Marchionni,¹ C. Zucchetti,¹ F. Ciccacci,¹ M. Finazzi,¹ H. S. Funk,² D. Schwarz,²
M. Oehme,² J. Schulze,² and F. Bottegoni¹

¹ *Dipartimento di Fisica, Politecnico di Milano, Piazza Leonardo da Vinci 32, 20133 Milano, Italy*

² *Institute of Semiconductor Engineering (IHT), University of Stuttgart, Pfaffenwaldring 47, 70569 Stuttgart, Germany*

Spintronics aims at the generation, manipulation and transport of spin in solid state systems. Semiconductors with long spin lifetime and optical properties in the near-infrared range represent ideal platforms for the development of spin-based devices [1].

In this context, GeSn is a promising candidate for the integration of spintronics, photonics, and electronics. We investigate the photoinduced inverse spin-Hall effect in a GeSn alloy with 5% Sn concentration. We generate a spin-polarized electron population at the Γ point of the GeSn conduction band by means of optical orientation [2], and we detect the inverse spin-Hall effect signal coming from the spin-to-charge conversion in GeSn. We study the dependence of the inverse spin-Hall signal on the kinetic energy of the spin-polarized carriers by varying the energy of the impinging photons in the 0.5–1.5 eV range.

We rationalize the experimental data within a diffusion model which explicitly accounts for momentum, energy, and spin relaxation of the spin-polarized hot electrons [3]. At high photon energies, when the spin relaxation is mainly driven by phonon scattering, we extract a spin-Hall angle in GeSn which is more than ten times larger than the one of pure Ge. Moreover, the spin–charge interconversion for electrons lying at the Δ valleys of GeSn results to be ≈ 4.3 times larger than the one for electrons at L valleys [4].

[1] I. Zutic', A. Matos-Abiague, B. Scharf, H. Dery, and K. Belashchenko, *Mater. Today* **22**, 85–107 (2019).

[2] F. Bottegoni, C. Zucchetti, G. Isella, M. Bollani, M. Finazzi, and F. Ciccacci, *Riv. Nuovo Cimento* **43**, 45–96 (2020).

[3] C. Zucchetti, F. Bottegoni, G. Isella, M. Finazzi, F. Rortais, C. Vergnaud, J. Widiez, M. Jamet, and F. Ciccacci, *Phys. Rev. B* **97**, 125203 (2018).

[4] A. Marchionni, C. Zucchetti, F. Ciccacci, M. Finazzi, H. S. Funk, D. Schwarz, M. Oehme, J. Schulze, and F. Bottegoni, *Appl. Phys. Lett.* **118**, 212402 (2021).

Spin Hall magnetoresistance effect from a disordered interface

Sara Catalano¹, Juan M. Gomez-Perez¹, M. Xochitl Aguilar-Pujol¹, Andrey Chuvilin^{1,2}, Marco Gobbi^{1,2,3}, Luis E. Hueso^{1,2}, and Fèlix Casanova^{1,2}

¹CIC nanoGUNE, 20018 Donostia-San Sebastián, Basque Country, Spain

²IKERBASQUE, Basque Foundation for Science, 48009 Bilbao, Basque Country, Spain

³Centro de Física de Materiales CFM-MPC (CSIC-UPV/EHU), 20018 Donostia-San Sebastian, Basque Country, Spain

The spin Hall magnetoresistance (SMR) arises in heavy metal (HM)/magnetic compound interfaces, from the interaction between the magnetization and the spin currents generated in the HM layer by spin Hall effect. The SMR allows the magnetization of thin films and surfaces to be probed with an all-electrical set-up and, therefore, could represent a valuable tool to characterize the magnetization of van der Waals magnetic materials.

For this purpose, we have studied the SMR response of heterostructures combining a platinum (Pt) thin film with the van der Waals antiferromagnet MnPSe₃. The bilayers are fabricated by sputtering of the heavy metal on top of exfoliated flakes of the van der Waals compound. We observe a robust SMR effect in the system, which we measure both below and above the Néel temperature of MnPSe₃. By taking advantage of transmission electron microscopy (TEM), we characterize the Pt/MnPSe₃ bilayers, revealing the presence of a nanometers-thick platinum-chalcogen amorphous layer at the interface, whose formation we ascribe to the sputtering deposition process. From our analysis of the transport and TEM data, we conclude that the SMR signal arises from a disordered magnetic system formed at the Pt/MnPSe₃ interface because of the sputtering induced damage. Our results show that damaged interfaces can yield an important contribution to SMR, questioning a widespread assumption on the role of disorder in such measurements [1]. Fig.1 presents an outline of our experiment.

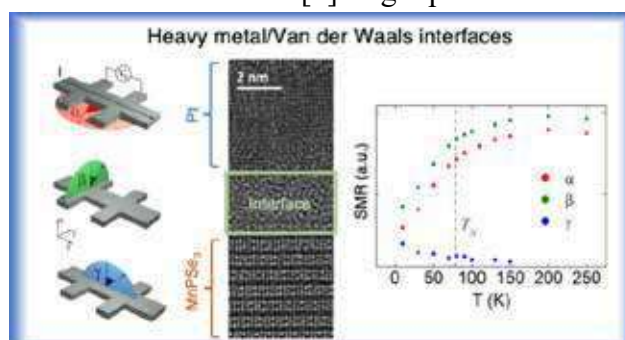


Fig.1: From the left to the right: sketch of the measurements set-up; TEM image of the Pt/MnPSe₃ interface; temperature dependence of the SMR signal.

[1] S. Catalano, J. M. Gomez-Perez, M. X. Aguilar-Pujol, A. Chuvilin, M. Gobbi, L. E. Hueso, and F. Casanova, *ACS Applied Materials & Interfaces* **14**, 6, 8598-8604 (2022)

Influence of intermixing on spin-to-charge conversion in sputtered BiSe

Won Young Choi¹, Isabel C. Arango¹, Van Tuong Pham², Diogo C. Vaz¹, Haozhe Yang¹, Inge Groen¹, Chia-Ching Lin³, Emily Walker³, Kaan Oguz³, Punyashloka Debashis³, John Plombon³, Hai Li³, Dmitri E. Nikonov³, Scott Clendenning³, Luis E. Hueso^{1,4}, Ian A. Young³ and Fèlix Casanova^{1,4}

¹CIC nanoGUNE BRTA, Donostia-San Sebastián, Basque Country, Spain.

²SPINTEC, CEA-INAC/CNRS/Université Grenoble Alpes, Grenoble, France.

³Components Research, Intel Corp., Hillsboro, OR, USA.

⁴IKERBASQUE, Basque Foundation for Science, Bilbao, Basque Country, Spain.

One of the major obstacles to realizing spintronic devices such as MESO logic devices is the small signal magnitude, so it is important to find materials with high spin-to-charge conversion efficiency [1,2]. However, although intermixing at the junction of two materials is a widely occurring phenomenon, its influence on material characterization is easily neglected or underestimated. In this study, we fabricated cross junctions (Fig. 1a) and local spin injection devices (Fig. 1b) consisting of CoFe and BiSe_{1-x}/non-magnetic metal (NM) wires with varying thickness of BiSe. The 3D finite element method simulation based on spin diffusion model is performed to estimate the resistivity and the spin-to-charge conversion efficiency (i.e., spin Hall angle), which are 600 $\mu\Omega\cdot\text{cm}$ and 0.45, respectively. We demonstrate that the resistivity and the spin Hall angle of BiSe can be overestimated by tens of times in the sputtered BiSe/NM structure due to the intermixing induced compositional change and the properties of a polycrystal. It emphasizes that the influence of intermixing on material characterization is by no means small.

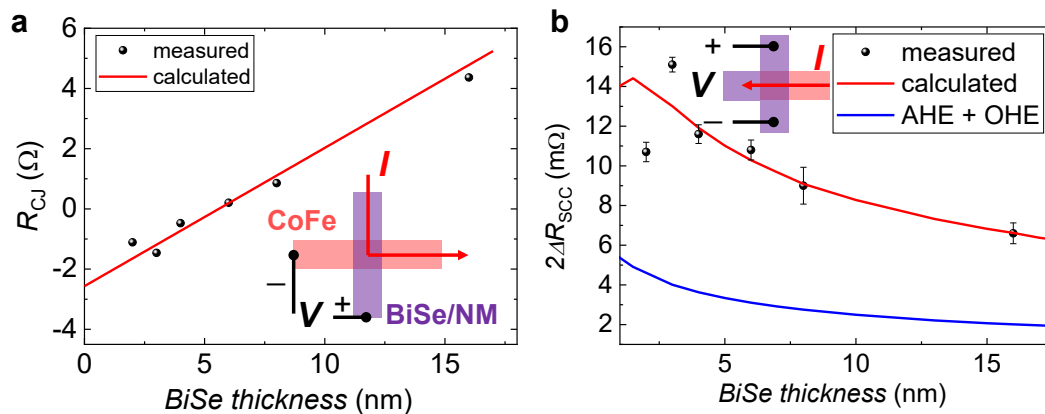


Figure 1: Cross-junction resistance (a) and spin-to-charge conversion signals (b) according to BiSe thickness.

[1] Manipatruni, S. et al. *Nature* **565**, 35–42 (2019).

[2] Pham, V. T. et al. *Nat. Electron.* **3**, 309–315 (2020).

Magnetoionic behavior in Ta/Co₂₀Fe₆₀B₂₀/HfO₂: solid-state vs. ionic liquid

M. Massouras¹, R. Pachat¹, M.-A. Syskaki², T. Bhatnagar-Schöffmann^{1,3},
A. Harouri¹, A. Durnez¹, S. Ono⁴, S. Spiga⁵, J. Langer², D. Ravelosona¹,
D. Querlioz¹ and L. Herrera-Diez¹

¹ Centre de Nanosciences et de Nanotechnologies, CNRS/Université Paris-Saclay, 91120 Palaiseau, France

² Singulus Technology AG, Hanauer Landstrasse 103, 63796 Kahl am Main, Germany

³ SPEC, CEA Saclay, CNRS/Université Paris-Saclay, 91191, France

⁴ Central Research Institute of Electric Power Industry, Yokosuka, Kanagawa 240-0196, Japan

⁵ CNR Institute for Microelectronics and Microsystem, 20864 Agrate Brianza (MB), Italy

Voltage control of magnetic anisotropy is a promising path for low-consumption spintronic devices. Anisotropy modifications rely either on charge accumulation in volatile manner and/or magnetoionic dynamics in a nonvolatile way. It has been shown that magneto-ionics in heavy-metal/ferromagnet/oxide structures depend on both the oxidation state of the elements that constitute the ferromagnetic layer and the ionic mobility in the oxide layer.

Device geometries for magneto-ionics include solid-state [1] and ionic-liquid gating [2], the former is more compatible with applications while the latter offers a playground for understanding the physicochemical mechanisms involved. However, it is yet to be determined how the gating method affects the observed magnetoionic response. In this work, we investigate the changes in anisotropy in Ta/Co₂₀Fe₆₀B₂₀/HfO₂ by: (i) ionic liquid gating with [EMI]⁺[TFSI]⁻ and (ii) solid state devices with a top 20 nm-thick layer of HfO₂ deposited by atomic layer deposition (ALD) as shown in the figure. In this study, samples from the same wafer are used for the two gating methods. Gate voltages drive a reversible spin reorientation transition between perpendicular and in-plane magnetic anisotropies using lower electric fields in the solid-state device compared to the device using ionic liquid. We also show that the solid-state device exhibits a symmetrical behavior in the observed transitions in terms of strength of the electric field. Using ionic liquid, the electric fields required for the in-plane to perpendicular magnetic anisotropies switching are twice as large as the reverse transition. These differences could be attributed to a discrepancy in charge distribution at the surface of the magnetic stacks due to the difference in size and positioning of the ions constituting the ionic liquid and/or the assumptions made to calculate the electric field values. Our results can therefore contribute to the understanding of the intrinsic magnetoionic mechanisms by clarifying the effects of the device geometry on the modulations of the magnetic properties.

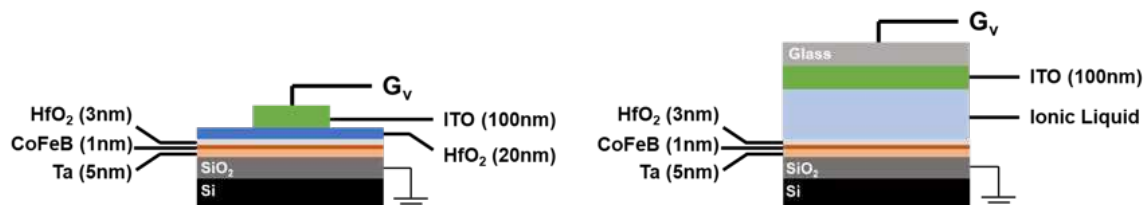


Figure: Schematics of the solid-state (left) and ionic-liquid devices (right).

[1] Fassatoui et al., Phys. Rev. Appl. **14**, 064041 (2020).

[2] Pachat et al., Phys. Rev. Appl. **15**, 064055 (2021).

Unidirectional orbital magnetoresistance in light metal/ferromagnet bilayers

Shilei Ding, Paul Noël, Gunasheel Kawthilyaa Krishnaswamy, Pietro Gambardella

Department of Materials, ETH Zürich, 8093 Zürich, Switzerland

Recent work shows that the orbital angular momentum and orbital torque in light metal/ferromagnetic metal (FM) bilayers allow for the realization of spin-orbitronic devices. Independent of the magnitude of spin-orbit coupling (SOC), inversion symmetry breaking is sufficient for the emergence of a non-equilibrium orbital angular momentum accumulation upon application of an electric field to such heterostructures, as exemplified by the orbital Hall and orbital Rashba Edelstein effect [1]. In general, the interplay of orbital angular momentum with the magnetic moments of a FM is fundamentally different from that of the spin angular momentum and the local magnetization. In the presence of SOC in the FM, the orbital to spin conversion plays a crucial role for the orbital torque [2], and indeed, the effective diffusion length of orbital current is quite long in contrast to the spin current [3]. However, up to now, it is unknown if an orbital current can induce a unidirectional magnetoresistance (UMR) similar to a spin current, where the UMR follows the cross product of current density \mathbf{j} and \mathbf{m} , leading to the odd behavior under \mathbf{j} or \mathbf{m} reversal, and the magnitude is proportional to the applied current density [4].

In this work, we report the UMR in naturally oxidized Cu (denoted by Cu* hereafter)/Co bilayers free from any heavy elements with large SOC. We provide evidence for the orbital-UMR, which shares the same symmetry as spin-UMR, and show that the orbital torque efficiency and orbital-UMR vary simultaneously by changing the thickness of FM layers and temperature, reflecting a similar origin. As the field-dependent orbital-UMR is saturated at a small field and there is no high field suppression of the orbital-UMR, we conclude that electron-magnon scattering does not play a role in the orbital-UMR. The orbital-UMR in Cu*/Co is mainly attributed to the alteration of the resistance through the orbital angular momentum transport and orbital to spin conversion. Our findings reveal a new UMR effect based on the orbital torque scenario and further highlight the potential application of light metal to the novel two-terminal spin-orbitronic devices triggered by the orbital Rashba-Edelstein effect.

- [1] D. Go and H.-W. Lee, *Phys. Rev. Res.* **2**, 13177 (2020).
- [2] D. Lee, D. Go, H.-J. Park, W. Jeong, H.-W. Ko, D. Yun, D. Jo, S. Lee, G. Go, J. H. Oh, K.-J. Kim, B.-G. Park, B.-C. Min, H. C. Koo, H.-W. Lee, O. Lee, and K.-J. Lee, *Nat. Commun.* **12**, 6710 (2021).
- [3] S. Ding, Z. Liang, D. Go, C. Yun, M. Xue, Z. Liu, S. Becker, W. Yang, H. Du, C. Wang, Y. Yang, G. Jakob, M. Kläui, Y. Mokrousov, and J. Yang, *Phys. Rev. Lett.* **128**, 67201 (2022).
- [4] C. O. Avci, K. Garello, A. Ghosh, M. Gabureac, S. F. Alvarado, and P. Gambardella, *Nat. Phys.* **11**, 570 (2015).

Tuning the spintronic properties of the ferroelectric Rashba semiconductor GeTe by alloying

F. Fagiani¹, L. Nesi¹, M. Cantoni¹, F. Belponer¹, S. Cecchi², G. Vinai³, F. Mazzola³, D. Mondal³, J. Fujii³, I. Vobornik³, R. Calarco⁴, F. Delodovici⁵, S. Picozzi⁵, R. Bertacco¹, C. Rinaldi¹

¹ Dipartimento di Fisica, Politecnico di Milano, Milan, Italy

² Paul-Drude-Institut für Festkörperelektronik, Berlin, Germany

³ Istituto Officina dei Materiali (CNR-IOM), Laboratorio TASC, Trieste, Italy

⁴ Istituto per la Microelettronica e Microsistemi (CNR-IMM), Rome, Italy

⁵ Consiglio Nazionale delle Ricerche, CNR-SPIN, Chieti, Italy

Monochalcogenides such as germanium telluride (GeTe) [1] and tin telluride (SnTe) [2] are key members of the class of ferroelectric Rashba semiconductors (FERSC), materials in which the ferroelectric polarization directly controls the spin-orbit coupling. In particular, the Rashba spin texture can be reversed with the ferroelectric polarization, so that an unprecedented non-volatile electric control of spin transport in semiconductors can be envisaged [3]. Noteworthy, we provided a pioneering demonstration that the ferroelectric polarization in GeTe epitaxial thin films can be switched by gating, and used to control and reverse the spin-to-charge current conversion in the semiconductor [4], with an efficiency comparable to that of the reference heavy metal platinum. Anyhow, finding a route to control doping, ferroelectric properties and spin-to-charge conversion is fundamental, especially ahead of applications.

Here, we explore the exciting combination of the two chalcogenides GeTe and SnTe in the bulk ternary compound $\text{Sn}_x\text{Ge}_{(1-x)}\text{Te}$, where the isovalent substitution of Sn by Ge is intended to stabilize ferroelectricity up to room temperature [6], while the presence of Sn may provide additional topological bands that could be beneficial for spin-to-charge conversion [2]. Moreover, it will be displayed the growth of epitaxial $\text{Sn}_x\text{Ge}_{(1-x)}\text{Te}$ (111) thin films by molecular beam epitaxy, with x ranging from 0.3 to 0.5. With the endorsement of *ab-initio* calculations, we will give insights in the anatomy of the Rashba band structure, investigated by spin and angular photoemission spectroscopy. Finally, we will show the compositional tuning of ferroelectric properties (polarization, Curie temperature and switching field) analyzed by electro-resistive measurements.

The robustness of both Rashba effect and ferroelectricity on a relatively wide range of compositions puts the groundwork for the compositional tuning of spin-to-charge current conversion in ferroelectric Rashba semiconductors.

[1] D. Di Sante *et al.*, *Adv. Mater.*, **25**, 509 (2013).

[2] E. Plekhanov *et al.*, *Phys. Rev. B*, **90**, 161108R (2014).

[3] C. Rinaldi *et al.*, *Nano Lett.*, **18**, 2751 (2018).

[4] S. Varotto *et al.*, *Nat. Electron.*, **4**, 740 (2021).

[5] H. Wang *et al.*, *npj Comput. Mater.*, **6**, 7 (2020).

[6] A. I. Lebedev *et al.*, *Ferroelectr.*, **289**, 189 (2004).

Voltage-induced Stoner instabilities and spin-polarized currents at the MgO/Fe interface resonant states

P. Graczyk^{1*}, M. Pugaczowa-Michalska¹, and M. Krawczyk²

¹*Institute of Molecular Physics, Polish Academy of Sciences, Poznań, Poland*

²*Institute of Spintronic and Quantum Information, Faculty of Physics, Adam Mickiewicz University, Poznań, Poland*

*E-mail: graczyk@ifmpan.poznan.pl

Particulars of the electronic structure become prominent at nanomaterial interfaces, where more and more subtle effects are being recognized. We show by numeric simulations that spin-dependent screening at dielectric-ferromagnetic metal interface contributes to the spin-polarized current generation in the system subjected to the ac voltage [1]. Then, we show that spin current driven by spin-dependent screening may be used to modulate spin-wave amplitude in bilayer ferromagnetic system [2]. Finally, we combine *ab initio* calculations of electronic density of states at MgO/Fe interface with continuous model for charge transport. We show that the voltage-driven electron charge accumulation at MgO/Fe interface leads to the Stoner instability because of the electronic interface resonant states. This instability manifests itself in the spin-current anomalies which are present because of the contribution of the dynamic spin-dependent potential to the spin-polarized current. We show that the effect can be measured e.g. by the spin-Hall effect.

This work was conducted under grant no. 2018/28/C/ST3/00052 from National Science Centre in Poland.

[1] P. Graczyk and M. Krawczyk, *Phys. Rev. B*, vol. 100, no. 19, p. 195415, 2019

[2] P. Graczyk and M. Krawczyk, *Sci. Rep.*, vol. 11, 15692, 2021

Fig. 1: (a) resonant states in the electronic DOS at MgO/Fe interface; (b) investigated system; (c) spin-current anomalies induced by Stoner instabilities at resonant states.

Study of Spin-Orbit Interactions and Multilevel Switching in Co/Pt/Co trilayer

K. Grochot^{1,2}, P. Ogrodnik^{1,3}, Ł. Karwacki^{4,5}, P. Mazalski^{6,7}, J. Kanak¹, J. Checiński¹, W. Skowroński¹, S. Zietek¹ and T. Stobiecki^{1,2}

¹*Institute of Electronics, AGH University of Science and Technology, Cracow, Poland.*

²*Faculty of Physics and Applied Computer Science, AGH University of Science and Technology, Cracow, Poland*

³*Faculty of Physics, Warsaw University of Technology, Warsaw, Poland*

⁴*Institute for Theoretical Physics, Utrecht University, Utrecht, Netherlands*

⁵*Institute of Molecular Physics, Polish Academy of Sciences, Poznan, Poland*

⁶*Jerzy Haber Institute of Catalysis and Surface Chemistry of the Polish Academy of Sciences, Cracow, Poland*

⁷*Faculty of Physics, University of Białystok, Białystok, Poland*

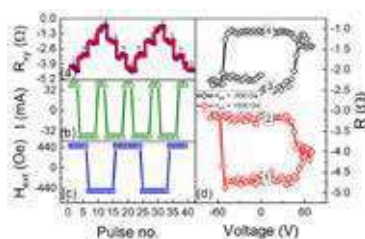


Figure 1: Multi-level current switching in Co/Pt(1.55)/Co (a) driven by combination of current (b) and magnetic field (c) between four stable resistance states (d).

The magnetization dynamics of Co layers, magnetostatic features, and spin-orbit interactions within the multilayer system Ti(2)/Co(1)/Pt(0-4)/Co(1)/MgO(2)/Ti(2) (thicknesses in nanometers) patterned into micrometer-sized Hall-bar devices have been studied. Here, the Pt is used as a source of the spin current, and as a non-magnetic spacer whose variable thickness enables the magnitude of the ferromagnetic interlayer exchange coupling (IEC) to be effectively tuned [1,2]. From anomalous Hall effect (AHE), anisotropic magnetoresistance (AMR) and spin Hall magnetoresistance (SMR) measurements, we found that the increase in Pt thickness (t_{Pt}) leads to the reorientation of Co-magnetizations from the in-plane to the perpendicular direction at $t_{\text{Pt}} \approx 1.3$ nm. Further increase in Pt thickness, above 3 nm, reduces ferromagnetic coupling and, consequently,

two weakly coupled Co layers become magnetized orthogonally to each other. Spin-orbit torque (SOT) ferromagnetic resonance measurements were modeled using Landau-Lifshitz-Gilbert-Slonczewski equation, whereas SMR and AMR were analyzed based on spin diffusion model [2]. Next, the effective SOT field (field-like (H_{FL}) and damping-like (H_{DL})) and the effective spin Hall angle were analyzed as a function of Pt thickness. Finally, we show that the asymmetry of both interfaces Co/Pt and Pt/Co, the IEC and the domain structure, enable multi-level current (Fig.1) and field-free magnetization switching, potentially important in SOT memory applications.

This work was supported by NCS Poland, Grants No.: 2016/23/B/ST3/01430 and 2016/23/G/ST3/04196. KG acknowledges support for conference participation by the EU Project POWR.03.02.00-00-I004/16.

[1] S. Łazarski et al., Phys. Rev. Appl. 12, 014006 (2019)

[2] P. Ogrodnik et al., ACS Appl. Mater. Interfaces 13, 47019 (2021)

Autonomous parametric instability driven spintronic auto-oscillator for multi-mode generation

A. Hamadeh¹, G. de Loubens², R. Moukhader³, M. Mohseni¹, V. Lomakin⁴, S. Mangin⁵, G. Finocchio³, P. Pirro¹ and O. Klein⁶

¹*Fachbereich Physik and Landesforschungszentrum OPTIMAS, Technische Universität Kaiserslautern, 67663 Kaiserslautern, Germany*

²*SPEC, CEA, CNRS, Université Paris-Saclay, 91191 Gif-sur-Yvette, France*

³*Dept. Mathematical and Computer Sciences, Physical Sciences and Earth Sciences, University of Messina, 98166 Messina, Italy*

⁴*center for Magnetic Recording Research, University of California San Diego, La Jolla, California 92093-0401, USA*

⁵*Institut Jean Lamour, Université de Lorraine, UMR 7198 CNRS, 54506 Vandoeuvre-lès-Nancy, France*

⁶*Univ. Grenoble Alpes, CEA, CNRS, Grenoble INP, INAC-Spintec, 38054 Grenoble, France*

Current induced microwave frequency generation in spin transfer torque oscillator (STO) based nano-pillars is a promising candidate for various applications, such as ultra-tunable microwave generation and detection. Generally, only one mode is believed to auto-oscillate in STO at the same time, coinciding with the universal oscillator model [1,2]. In our study, we find experimentally that when STO's are magnetized mainly out of plane, but with a small symmetry break, e.g., a small angle between the applied field and the normal to the layers direction, two oscillating modes (see figure) with different frequency and spatial distribution can be excited simultaneously. Our experimental finding combined with micromagnetic simulations reveal that this multi-mode generation can be explained by a parametric instability process which couples several modes of the oscillator which consequently oscillate together. Our simulations elucidate the physical origin of the multi-modal excitation regime, and, thereby, open opportunities for an effective manipulation of the generation of microwave frequencies.

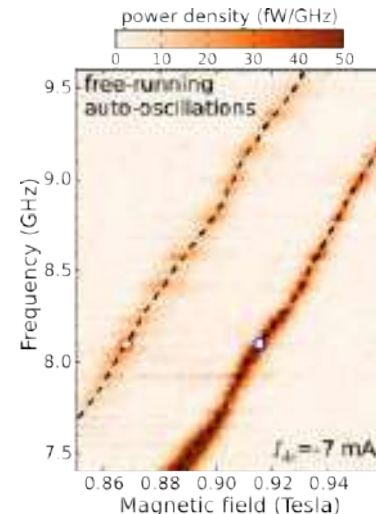


Figure 1: Frequency evolution of the free running oscillations induced by spin transfer at $I_{dc} = 7$ mA as a function of the magnetic field.

- [1] Slavin, Andrei and Tiberkevich, Vasil, *IEEE Transactions on Magnetics* **45**, 875 (2009).
- [2] A. Hamadeh, G. De Loubens, V. Naletov, J. Grollier, C. Ulysse, V. Cros, and O. Klein, *Physical Review B*. **85**, 140408 (2012).

Field-free magnetization switching in sputtering grown epitaxial $\text{Tm}_3\text{Fe}_5\text{O}_{12}$ magnetic insulator thin films

Sajid Husain¹, Nicholas Figueiredo Prestes¹, Sachin Krishnia¹, Sophie Collin¹, Eric Jacquet¹, Thibaud Denneulin², R. E. Dunin-Borkowski², André Thiaville³, Vincent Cros¹, Nicolas Reyren¹, Albert Fert¹, Henri Jaffrès¹, and Jean-Marie George¹

¹Unité Mixte de Physique CNRS, Thales, Université Paris-Saclay, 91767 Palaiseau, France.

²Ernst Ruska-Centre for Microscopy and Spectroscopy with Electrons, Forschungszentrum Jülich, 52425 Jülich, Germany.

³Laboratoire de Physique des Solides, Université Paris-Saclay, CNRS, 91405, Orsay, France.

The spin orbit torques (SOTs) have been extensively studied metallic ferromagnets(FMs) [1]. However, the charge current shunting through metallic FMs leads to inefficient performance of the devices. Thus, to replace the metallic magnetic electrode, ferrimagnetic (FIM) insulators have recently entered the field of spin-orbitronics [2]. In this work, we have deposited high quality epitaxial thin films of Thulium Iron Garnet $\text{Tm}_3\text{Fe}_5\text{O}_{12}$ (TmIG) insulating ferrimagnet using sputtering technique. X-ray diffraction pattern (Figure 1(a)) reveals the epitaxial quality of the TmIG(15nm). Inset(left) shows the rocking curve measured along the (444) peak demonstrates the minimal mosaicity in TmIG film. Inset (right) STEM images of TmIG/GGG. We measured the anomalous Hall effect in TmIG(10nm)/Pt(6nm) bilayers as shown in Figure 1(b). Since the ferromagnetic layer is insulating two mechanisms could be involved, the spin Hall effect (SHE) induced spin Hall magnetoresistance (SMR) [3] and the spin dependent scattering at the interface [4]. The spin orbit torques (SOTs) have been measured by the harmonic Hall voltage technique and the damping-like SOT is found to be relatively larger than the field-like torque (see Figure 1(c)). The striking observation in these bilayers is the magnetization switching in absence of external magnetic field (Figures 1(d)). It was recently proposed that a remanent symmetry breaking introduced by the SOT pulse in presence of chiral exchange interaction (DMI) could allow magnetization switching at zero-external magnetic field [5]. We also measured interfacial DMI ($3.29\mu\text{J}/\text{m}^2$) using Brillouin light scattering in TmIG/Pt. The finding of free field magnetization switching by SOTs in TmIG is an important milestone for future application in spin-orbitronics.

DARPA TEE program grant

(MIPR#HR0011831554) is acknowledged

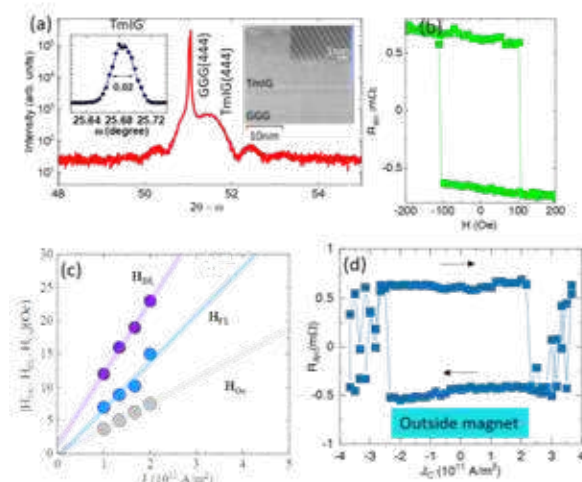


Figure 1: (a) XRD pattern of TmIG(15) grown. Inset (left) rocking curve of TmIG around (444) and (right) the STEM image. (b) AHE loop recorded on TmIG/Pt. (c) Damping-like H_{DL} and field-like H_{FL} field as a function of current density. (d) Magnetization switching loop.

- [1] A. Manchon, J. Železný, I. M. Miron, et al, Rev. Mod. Phys. **91**, 035004 (2019).
- [2] C. O. Avci, A. Quindeau, C. F. Pai, et al, Nat. Mater. **16**, 309 (2017).
- [3] Y. T. Chen, S. Takahashi, H. Nakayama, et al, Phys. Rev. B. **87**, 144411 (2013).
- [4] T. H. Dang, Q. Barbedienne, et al, Phys. Rev. B **102**, 144405 (2020).
- [5] Z. Zheng, Y. Zhang, V. Lopez-Dominguez, et al, Nat. Commun. **12**, 4522 (2021).

Effect of seed layer thickness on Ta crystalline phase and spin Hall angle

K.Sriram¹, Jay Pala¹, Bibekananda Paikaray¹, Arabinda Haldar² and Chandrasekhar Murapaka¹

¹ Department of materials Science and Metallurgical Engineering, Indian Institute of Technology Hyderabad, Kandi, Telangana, India. 502284

² Department of Physics, Indian Institute of Technology Hyderabad, Kandi, Telangana, India. 502284

Spin-orbit coupling (SOC) plays vital role in spin to charge interconversion for heavy metal (HM)-ferromagnet (FM) bilayer structure [1]. Spin pumping is an efficient method to generate pure spin current by precessional motion of magnetization which transfers angular momentum to HM through interface. The efficiency of spin current transport across the interface is quantified by spin-mixing conductance whereas the efficiency of spin to charge conversion is quantified by spin Hall angle (θ_{SH}) [2]. The need of low longitudinal resistivity with high θ_{SH} is challenging and the effect of seed layer on HMs phase is largely overlooked. Here, we report the effect of seed permalloy (Py: $\text{Ni}_{80}\text{Fe}_{20}$) layer thickness on Tantalum (Ta) crystalline phase and its θ_{SH} . We have observed a structural phase transition in Ta as the thickness of the seed layer increases that affects the θ_{SH} of the Ta. Ta exhibits mixed phase ($\alpha+\beta$) on seed Py layer above $t_{Py} > 12$ nm due to strain at the crystalline Py and Ta. However, Ta is grown in α -phase on $t_{Py} < 8$ nm where there is no prominent crystalline nature is observed in Py layer. This Ta phase transition is mainly attributed to the strain at the Py/Ta interface as shown in fig 1 (a). Ferromagnetic resonance (FMR) based spin pumping shows that effective damping is enhanced for all samples. We have quantified the inverse spin Hall effect voltage (ISHE) and θ_{SH} of ($\alpha+\beta$)-Ta which is higher than α -Ta as shown in fig 1 (b). The estimated θ_{SH} for ($\alpha+\beta$)-Ta is 0.15 ± 0.009 . Our systematic study provides an insight about Ta phase transition via seed layer thickness and gives an alternative route for tuning θ_{SH} [3].

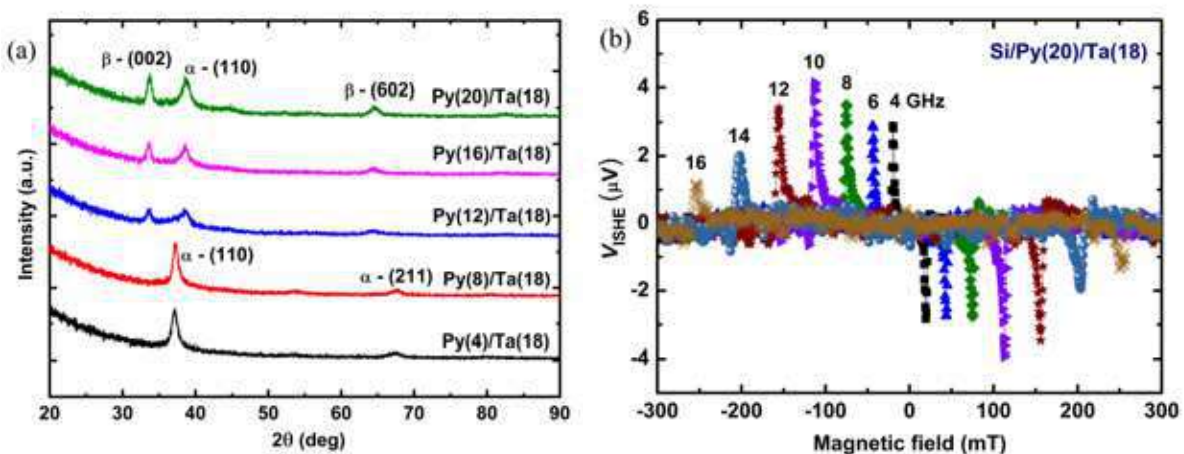


Fig 1. (a) Ta (18) Phase transition from α to ($\alpha+\beta$) phase as a function of Py thickness. (b) Inverse spin Hall voltage drop for Py(20)/ ($\alpha+\beta$)-Ta(18).

- [1] A. Manchon, J. Železný, I. M. Miron, T. Jungwirth, J. Sinova, A. Thiaville, K. Garello, and P. Gambardella, *Rev. Mod. Phys.* 91, 035004 (2019).
- [2] Y. Tserkovnyak, A. Brataas, G. E. W. Bauer, and B. I. Halperin, *Rev. Mod. Phys.* 77, 1375 (2005).
- [3] K. Sriram, J. Pala, B. Paikaray, A. Haldar, and C. Murapaka, *Nanoscale* 13, 19985 (2021).

Spin-orbit torque switching in coupled free layer designs

V. Kateel^{1,2}, S. Jeong¹, G. Talmelli¹, G. Jayakumar¹, B. Sorée^{1,2}, J.D. Boeck^{1,2}, S. Rao¹, S. Couet¹ and G.S. Kar¹

¹IMEC, Kapeldreef 75, Leuven, Belgium

²Department of Electrical Engineering, KU Leuven, Kasteelpark Arenberg 10, Leuven, Belgium

Spin-orbit torque magnetic random-access memories (SOT-MRAM) are considered as a promising candidate for high-speed cache applications owing to its non-volatility, decoupled read/write paths, fast operating speeds, large endurance, and CMOS compatibility [1-2]. For high density memory applications perpendicularly magnetized SOT-MRAM are used, as shown in Fig. 1a, whose material properties can be tuned to ensure high tunnel magnetoresistance ratio (TMR) and thermal stability. While this has been demonstrated at wafer-scale using a single CoFeB/MgO layer interface [1], the device performance degrades with scaling. To address this challenge, the layer contributing to the perpendicular magnetic anisotropy (PMA) and TMR within the free layer (FL) needs to be separated. This can be achieved through the use of coupled FLs that incorporates ferromagnetic or anti-ferromagnetic coupling [2]. While initial assessments have been promising for SOT-driven switching of coupled FLs [2], the influence of the coupling on the switching dynamics has not been well understood.

Table 1: MTJ Properties of coupled FLs at 60 nm CD

| Properties | HFL | SAF-HFL-I | SAF-HFL-II |
|------------|---------|-----------|------------|
| TMR | 88 % | 91 % | 105 % |
| Coercivity | 80.2 mT | 300.7 mT | 255 mT |

In this work, we investigate SOT-driven switching dynamics in scaled magnetic tunnel junctions (MTJs) with three different coupled FL designs. At 60 nm CD (critical dimension), the quality of the fabricated MTJs is confirmed in all three coupled FL as shown in Tab. 1. Interestingly, both coercivity (Tab. 1) and SOT-driven switching efficiency (Fig. 1b) are improved in SAF-based HFL (synthetic anti-ferromagnetic based hybrid free layer) compared to the standard HFL. This suggests that nature of coupling and coupling strength will indeed influence the switching properties of coupled FLs. In this talk, we will explore this impact by engineering the coupling within the FLs. These findings should provide further insight for development of efficient SOT-MRAM devices with coupled FLs.

[1] K. Garello, et al., *2018 IEEE Symposium on VLSI Circuits*, 81-82 (2018).

[2] S. Couet et al., *2021 Symposium on VLSI Technology*, 1-2 (2021).

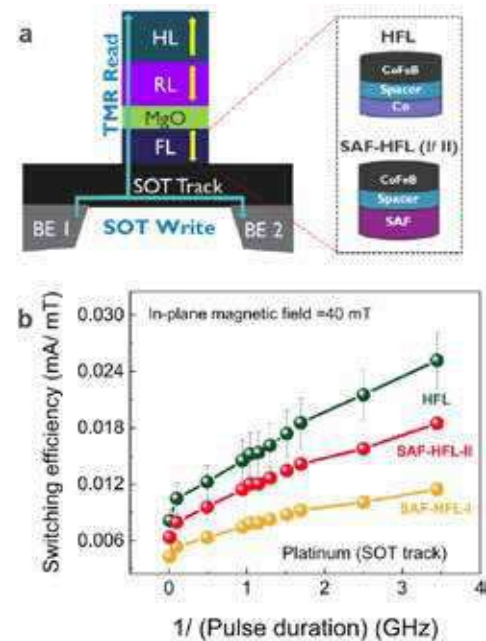


Figure 1: a. SOT-MRAM with coupled FLs, b. Switching efficiency vs inverse of pulse duration at in-plane field of 40 mT for 60 nm CD

Large spin-orbit torques on ferromagnetic layer from orbital currents

S. Krishnia¹, B. Bony¹, S. Collin¹, J. M. George¹, V. Cros¹ and H. Jaffrès¹

¹Unité Mixte de Physique, CNRS, Thales, Université Paris-Saclay, 91767, Palaiseau, France.

In the last decade, charge to spin conversion and resultant torques on magnetization have been extensively studied to achieve efficient electrical functionalities of spintronics devices. The charge-spin conversion, so far, is known to be governed by the mechanism based on spin-orbit interaction such as the spin Hall effect and the Rashba effect¹. Recently, a substantial increase of torques has been observed with Cu/CuOx or Cu/Al₂O₃ thus using light element interfaces. The observation of torques in the absence of spin-orbit interaction can be explained in the framework of orbital currents generation at Cu/CuOx interface².

To demonstrate the contribution from the orbital Hall effect on the torques, we quantify the current-induced torques in Co/Cu, Co/Pt, and Co/Cu/Pt heterostructures by using the second harmonic Hall measurement technique. In Fig. 1 (a), we show the amplitude of $R_{2\omega}$ measured for various external magnetic fields (H_{ex}) for Co/Cu and Co/Pt samples. From the slope of the linear fit, we extract $H_{DL} = 7.01$ Oe for Co(2)/Pt(4) and $H_{DL} = 1.63$ Oe for Co/Cu* sample for 1 mA current in the device. The observation of significant DL torque in the Co/Cu* sample without any heavy metal layer is striking. This clearly indicates that an orbital current is being generated at Cu/Cu* interface. To validate the generation of orbital current at Cu* interface, we investigate in complement the SOTs as a function of Pt layer thickness in Co(2)/Pt(t_{Pt})/Cu* series of samples. Figure 1(b) shows the damping-like torque in Co(2)/Pt(t_{Pt})/Cu* (red), Co(2)/Pt(t_{Pt})/Cu(3)/AlOx(1) (blue) and Co(2)/Pt(t_{Pt}) (black) as a function of Pt thickness. In conclusion, we have observed a two-fold increase in damping-like torques efficiency in Co(2)/Pt(4)/Cu/CuOx(3) sample if compared with a Co(2)/Pt(4) reference sample. The enhancement further validates the hypothesis of additional charge to spin-current generation mediated via orbital Hall and Rashba effects⁵.

Acknowledgment: Financial support from the Agence Nationale de la Recherche, France, No. ANR-20-CE30-0022 (ORION) and the DARPA TEE programme through grant MIPR no. HR0011831554 are acknowledged.

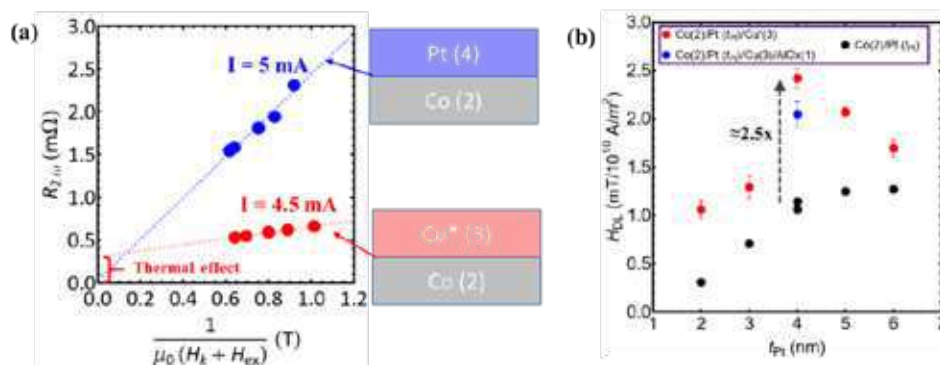


Figure 1. (a) $R_{2\omega}$ for various external magnetic fields in Co(2)/Cu(3)* (red) and in Co(2)/Pt(4) (blue) samples. (b) Comparison of H_{DL} in various capping layers as a function of Pt thickness.

References: [1] Manchon, A. *et al.*, *Rev. Mod. Phys.* **91**, (2019). [2] Ding, S. *et al.*, *Phys. Rev. Lett.* **125**, 177201 (2020). [3] S. Krishnia *et al.*, unpublished

Tailoring the switching efficiency of magnetic tunnel junctions by the fieldlike spin-orbit torque

Viola Krizakova¹, Marco Hoffmann¹, Vaishnavi Kateel², Siddharth Rao², Sebastien Couet², Gouri Sankar Kar², Kevin Garello³, and Pietro Gambardella¹

¹Department of Materials, ETH Zurich, 8093 Zürich, Switzerland

²imec, Kapledreef 75, 3001 Leuven, Belgium

³Université Grenoble Alpes, CEA, CNRS, Grenoble INP, SPINTEC, 38054 Grenoble, France

Spin-orbit torques (SOTs) offer an efficient, scalable, and precise way to control the magnetization in magnetic tunnel junctions (MTJs), skyrmions, or domain walls [1]. Driven by the interest of memory and computing applications, SOT switching has improved in terms of reliability, operation speed, energy efficiency, and removing the need for the external field. These advances were achieved by material engineering, new device geometries, as well as designs combining SOTs with spin transfer torque and voltage gating [2-4]. Nevertheless, most work on SOTs concentrates on the dampinglike torque (DLT), responsible for the reversal [5], and less on the fieldlike torque (FLT). By promoting the magnetization precession, FLT affects the switching threshold and could enable unipolar or field-free switching [6,7]; however, it also impairs reliability. Thus, materials with dominant DLT, like W and Pt, have so far enjoyed greater popularity than strong-FLT materials, such as Ta or Hf.

We present results that elucidate the impact of the FLT on the switching dynamics, reliability, and threshold conditions in (W or Ta)/CoFeB/MgO. To account for the geometrical confinement, we use samples patterned into nanoscale MTJ devices [2,8]. Since the FLT has a similar impact on the magnetization as a transverse magnetic field, it can be probed by studying the switching in different current-field configurations [Fig. 1a,b]. We find the same signatures of FLT influence in MTJ based on W and Ta. We show that the FLT-to-DLT ratio can be estimated from the threshold current dependence on the transverse field [Fig. 1c], providing an alternative means to measure SOTs at the device level. Time-resolved measurements of individual switching events reveal that the FLT directly affects the switching energy barrier – accelerating or decelerating the reversal onset [Fig. 1d]. Using micromagnetic simulations, we further extrapolate the results to materials with different FLT strengths. Finally, we propose device geometries based on MTJs that leverage the FLT for either high-density memory applications or synaptic weight generation.

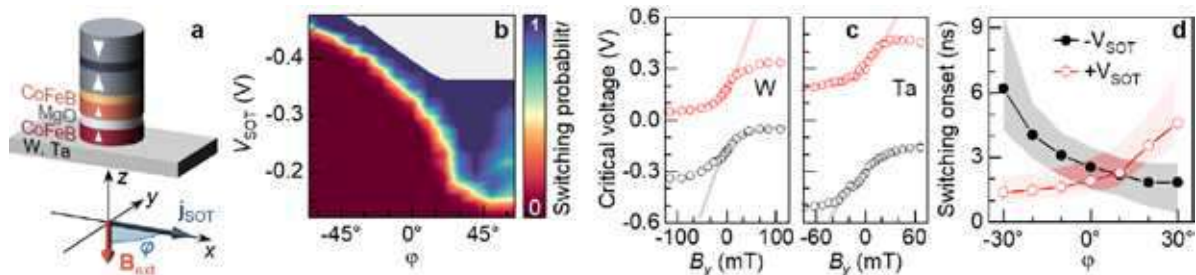


Figure 1: (a) Experimental configuration and (b) probability of switching as a function of the external field direction (ϕ) and SOT pulse amplitude (V_{SOT}). (c) B_y -dependence of the switching threshold for a W- and Ta-based sample. (d) Switching onset vs ϕ obtained from individual switching events.

[1] A. Manchon, J. Železný, I. M. Miron, *et al. Rev. Mod. Phys.*, **91**(3), 035004 (2019) | [2] E. Grimaldi, V. Krizakova, G. Sala, *et al. Nat. Nanotech.* **15**, 111-117 (2020) | [3] V. Krizakova, E. Grimaldi, K. Garello, *et al. Phys. Rev. Appl.*, **15**(5), 054055 (2021) | [4] Y. C. Wu, K. Garello, W. Kim, *et al. Phys. Rev. Appl.*, **15**(6), 064015 (2021) | [5] T. Taniguchi, S. Mitani, and M. Hayashi. *Phys. Rev. B*, **92**(2), 024428 (2015) | [6] W. Legrand, R. Ramaswamy, R. Mishra, and H. Yang. *Phys. Rev. Appl.*, **3**(6), 064012 (2015) | [7] J. M. Lee, J. H. Kwon, R. Ramaswamy, *et al. Commun. Phys.*, **1**(1), 2 (2018) | [8] K. Garello, F. Yasin, S. Couet *et al. IEEE Symp. VLSI Circ.*, 81–82 (2018)

Spin Hall magnetoresistance and current density distribution in HM/FeCoB (HM=Ta,Pt) bilayers

¹M.Kuepferling, ¹A.Magni, ¹A.Sola, ¹V.Basso, ²W. Skowroński, ²K.Grochot, ²S. Łazarski, ³M.V.Khanjani, ³J.Langer, ³B.Ocker,

¹INRIM, Strada delle Cacce 91, 10135 Torino, Italy

²AGH University of Science and Technology, al. Mickiewicza 30, 30-059 Krakow, Poland

³Singulus Technologies AG, Hanauer Landstrasse 103, 63796 Kahl am Main, Germany

The spin-orbit-torque (SOT) efficiency [1-3] is the key physical parameter for spintronic devices, such as magnetic memories, microwave generators or magnetic sensors. The principle of operation of such devices is the alteration of the magnetization state by a spin current. The SOT efficiency therefore determines the efficiency of the device and has to be characterized accurately.

We investigate bilayers composed by a heavy metal (HM) layer (Pt or Ta) of various thicknesses (wedge $d_{\text{HM}}=5\text{-}15\text{nm}$), and a ferromagnetic (FM) layer, $\text{Fe}_{60}\text{Co}_{20}\text{B}_{20}$ ($d_{\text{FM}}=2\text{nm}$), prepared at Singulus Technologies AG. In such bilayers the spin Hall effect (SHE) is the main source for SOT, and a spin current is injected from the HM into the FM layer where it acts on the magnetization state via a torque. Among the several methods to measure the SOT efficiency, the measurement of the spin Hall magnetoresistance (SMR) [4] is one of the most straightforward, if electric current is basically confined in the HM layer. This is the case for FM insulators or ultra-thin films with perpendicular magnetic anisotropy (PMA), but more generally, additional effects in the FM such as the anisotropic or unidirectional magnetoresistance (AMR or UMR) or the anomalous Nernst effect (ANE) [5] have to be considered. Since all these effects depend crucially on the electrical conductivity of the layers, a correct analysis of the current density distribution in the bilayer has to be performed [6].

We therefore study the electrical conductivity and current density distribution in a multilayer system based on a Fuchs-Sondheimer approach [7,8] and analyse in particular the thickness dependence. We then combine the results with our thermodynamical approach [9] in order to analyse magnetoresistance (MR) measurements and evaluate effects on the drift-diffusion model [2] applied to obtain the SOT efficiency. The MR was measured at INRIM following [5,10], additionally a measurement protocol for the elimination of the thermal drift and hysteresis effects was applied and UMR was taken into account [11]. The SOT efficiency was measured for comparison by harmonic Hall voltage measurements at AGH. The results show that for a more accurate analysis of SOT a model taking into account the correct current density distribution in the bilayer is important.

[1] A. Manchon et al., *Rev. Mod. Phys.* **91**, (2019), DOI: 10.1103/RevModPhys.91.035004

[2] P. M. Haney et al., *Phys. Rev. B* **87**, (2013), DOI: 10.1103/PhysRevB.87.174411

[3] Chi Feng Pai et al. *Phys. Rev. B* **92**, (2015), DOI: 10.1103/PhysRevB.92.064426

[4] K. Fritz et al. *Phys. Rev. B* **98**, (2018), DOI: 10.1103/PhysRevB.98.094433

[5] Yan-Ting Liu et al. *Phys. Rev. Appl.* **13**, (2020), DOI: 10.1103/PhysRevApplied.13.044032

[6] M-H. Nguyen et al., *Phys. Rev. Lett.* **116**, (2016), DOI: 10.1103/PhysRevLett.116.126601

[7] K. Fuchs, *Math. Proc.* **34**, **100** (1938), DOI: 10.1017/S0305004100019952

[8] E.H. Sondheimer, *Advances in Physics* **1**, 1 (1952), DOI: 10.1080/00018735200101151

[9] V. Basso et al., *J.Phys.D: Appl.Phys.* **51**, (2018), DOI:10.1088/1361-6463/aabc4c

[10] A. Magni et al., *IEEE Trans. Mag.* **58**, (2021), DOI: 10.1109/tmag.2021.3084866

[11] C.O. Avci et al., *Phys. Rev. Lett.* **121**, (2018), DOI: 10.1103/PhysRevLett.121.087207

Spin transport as a probe of non-linear fluctuations at the spin glass transition in $\text{Pd}_{1-x}\text{Ni}_x$ alloys

M. Leiviskä ¹, R. L. Seeger ¹, L. Nagi Reddy ¹, I. Joumard ¹, E. Gautier ¹, P. Warin ¹, L. Vojáček ¹, F. Ibrahim ¹, M. Chshiev ¹, S. Gambarelli ², and V. Baltz ¹

¹Univ. Grenoble Alpes, CNRS, CEA, Grenoble INP, IRIG-SPINTEC, F-38000 Grenoble

²Univ. Grenoble Alpes, CEA, IRIG-SYMMES, F-38000 Grenoble

Linear and non-linear fluctuations of spins correlated by sd-exchange and spin-orbit interactions give rise to various interesting effects at magnetic phase transitions. Recent studies on these effects have both advanced the basic understanding of spin transport phenomena and facilitated the emergence of relevant applications. Here, we focused on one of these effects, namely the anomalous behaviour of inverse spin Hall effect (ISHE), which is commonly used for spin-to-charge conversion in devices. We have investigated the overlooked and incompletely understood connection between ISHE and non-linear spin fluctuations near magnetic phase transitions [1,2].

The strong spin fluctuations at magnetic phase transitions manifest in anomalous behavior of the linear (χ_0) and non-linear (e.g. χ_1 , χ_2) magnetic susceptibilities. Both susceptibilities can be inspected via ferromagnetic (FM) resonance driven spin pumping - ISHE experiments, where a bilayer comprising of an FM spin injector and a spin sink is placed inside a microwave cavity. The precessing FM pumps pure spin current into the spin sink, where it is converted into charge current via ISHE. The loss of angular momentum through the spin pumping adds a non-local contribution to the damping of the FM dynamics. This damping is related to the linear spin fluctuations (χ_0) [3] of the spin sink, and thus exhibits anomalous behavior at its critical temperature [4]. Probing non-linear fluctuations requires a higher order effect such as the interconversion of spin and charge currents: ISHE is related to χ_2 [1] meaning that it can serve as a probe of non-linear magnetic fluctuations [2].

Here we investigated the non-linear fluctuations in $\text{Pd}_{1-x}\text{Ni}_x$, with x ranging from 0.06 to 0.18. We identified two magnetic phase transitions: a weak ferromagnetic transition and a reentrant spin glass transition at lower temperatures. We observed anomalous behavior of ISHE at the spin glass transition temperature, and the peak-and-trough shape of the anomaly resembles that expected for χ_2 . This observation suggests that non-linear spin fluctuations alter the spin to charge current conversion efficiency at the spin glass transition, thereby allowing its detection through ISHE.

[1] B. Gu, T. Ziman, and S. Maekawa *Phys. Rev. B* **86**, 241303(R), (2012).

[2] Y. Niimi, D. Wei, and Y. Otani, *J. Phys. Soc. Jpn.* **86**, 011004, (2017).

[3] Y. Ohnuma, H. Adachi, E. Saitoh, and S. Maekawa *Phys. Rev. B* **89**, 174417, (2014).

[4] L. Frangou, S. Oyarzún, S. Auffret, L. Vila, S. Gambarelli, and V. Baltz *Phys. Rev. Lett.* **116**, 077203, (2016).

Bath-induced spin inertia

Mario A. Gaspar Quarenta¹, Tim Ludwig¹, Huaiyang Yuan¹,
and Rembert A. Duine^{1,2}

¹*Institute for Theoretical Physics, Utrecht University,
Princetonplein 5, 3584 CC Utrecht, The Netherlands*

²*Department of Applied Physics, Eindhoven University of Technology,
P.O. Box 513, 5600 MB Eindhoven, The Netherlands*

In spintronics, magnetization dynamics is often described by the Landau-Lifshitz-Gilbert equation, where Gilbert damping is included phenomenologically to account for dissipation.

In microscopic models, dissipation can be described by coupling the magnetization to a bath that can absorb energy and angular momentum. Gilbert damping is then obtained if one assumes the bath to be Ohmic; that is, if one assumes the bath spectral density to be linear in frequency. Real baths, however, can be Ohmic only at low frequencies and, as we will argue, the baths' high-frequency modes induce magnetization inertia.

Explicitly, we show for a macrospin coupled linearly to a bath of harmonic oscillators (Caldeira-Leggett model) that the low-frequency bath modes (if Ohmic) lead to Gilbert damping while the high-frequency bath modes universally lead to macrospin inertia.

We expect our results to give new insights into recent experiments on magnetization nutation. But our results might prove to be relevant in general, as they indicate that a Gilbert-damping term should always be accompanied by a term accounting for bath-induced spin inertia.

Spin-orbit torque magnetization dynamics and switching in heavy-metal/ferromagnet multilayers with mixed anisotropies

S. Łazarski¹, W. Skowroński¹, K. Grochot^{1,2}, J. Kanak¹, S. Ziętek¹, T. Stobiecki^{1,2},
L. Karwacki³ and F. Stobiecki³

¹ AGH University of Science and Technology, Institute of Electronics, Al. Mickiewicza 30,
30-059 Kraków, Poland

² AGH University of Science and Technology, Faculty of Physics and Applied Computer Science,
Al. Mickiewicza 30, 30-059 Kraków, Poland

³ Institute of Molecular Physics, Polish Academy of Sciences, ul. Smoluchowskiego 17, 60-179
Poznań, Poland

The design of new energy-efficient spin-based storage and processing technologies are of great interest for potential applications [1]. Recently, a number of heavy metals (HM) which exhibits strong spin orbit coupling such as W [2], Ta [3] or Pt [4,5] have been studied. Spin orbit torque (SOT)-induced switching does not require high current densities through a tunnel barrier of a magnetic tunnel junction [1] and enables the magnetization reorientation of a ferromagnet (FM) in the sub-ns regime [6]; however, magnetic field-free switching require breaking of a time-reversal symmetry or unconventional SOT component.

In this work, we present studies carried out in FM/HM/FM structures, in which the HM is used as both a source of the spin current and as a tunable coupler between the two FM layers. The explored systems are characterized by mixed magnetic anisotropy of the two FM, i.e., in-plane and perpendicular magnetization easy axes. This configuration combined with SOT effect under certain conditions allows for switching without an external magnetic field called the field-free switching (FFS). In addition, the interlayer exchange coupling (IEC) energy by which the two FM layers are coupled, changes with a varying HM thickness, resulting in a tilted magnetization of perpendicular magnetic anisotropy FM layer. Finally, the magnetization dynamics study using spin-torque ferromagnetic resonance enabled us to determine the IEC and magnetic properties of each FM separately. The described approach was verified experimentally in a few systems. In Co/Pt/Co structure characterized by ferromagnetic coupling between Co layers, FFS is observed together with gradual magnetization change with in-plane current. In the CoFeB/Ta/CoFeB case, IEC has two regimes - ferromagnetic and antiferromagnetic - where in the former, the FFS is measured. Finally, in all studied FM/HM/FM systems, where we include CoFeB/W/CoFeB structure, analyzing the dynamics of the magnetization enables precise determination of magnetic parameters of each FM.

Work supported by National Science Centre, Poland grants: UMO-2015/17/D/ST3/00500 and UMO-2016/23/B/ST3/01430. Research project partly supported by program „Excellence initiative – research university” for the AGH University of Science and Technology.

- [1] B. Dieny et al. Nat. Electron. 3, 446–459 (2020)
- [2] W. Skowroński et al. Phys. Rev. Appl. 11, 024039 (2019)
- [3] S. Łazarski et al. Phys. Rev. B 103, 134421 (2021)
- [4] S. Łazarski et al. Phys. Rev. Appl. 12, 014006 (2019)
- [5] P. Ogrodnik et al ACS Appl. Mater. Interfaces 13, 47019 (2021)
- [6] E. Grimaldi et al. Nat. Nanotechnol. 15, 111 (2020)

Spin textures go ferroelectric: perspectives and applications in ferroelectric Rashba semiconductors

L. Nessi^{1,2}, S. Varotto¹, S. Cecchi³, J. Sławińska⁴, P. Noël⁵, F. Fagiani¹, M. Cantoni^{1,2}, M. Costa⁶, R. Calarco³, M. Buongiorno Nardelli⁷, M. Bibes⁸, S. Picozzi⁹, J.-P. Attané⁵, L. Vila⁵, R. Bertacco^{1,2}, C. Rinaldi^{1,2}

¹*Department of Physics, Politecnico di Milano, via G. Colombo 81, 20133 Milan, Italy*

²*IFN-CNR, c/o piazza Leonardo da Vinci 32, 20133 Milan, Italy*

³*Paul-Drude-Institut für Festkörperelektronik, Hausvogteiplatz 5-7, D-10117 Berlin, Germany*

⁴*Zernike Institute for Advanced Materials, 9747AG Groningen, Netherlands*

⁵*Université Grenoble Alpes, CEA, CNRS, 38000 Grenoble, France*

⁶*Department of Physics, Fluminense Federal University, Rio de Janeiro, Brazil*

⁷*Department of Physics, University of North Texas, Denton, TX 76203, USA*

⁸*Unité Mixte de Physique, CNRS, Thales, Université Paris-Saclay, 91767 Palaiseau, France*

⁹*CNR-SPIN c/o Università G. D'Annunzio, 66100 Chieti, Italy*

Ferroelectric Rashba semiconductors (FERSC) gained a growing attention since their discovery in 2013 [1]. This class of ferroic compounds is characterized by a one-to-one relation between the ferroelectric polarization direction and the chirality of the Rashba spin texture. This makes FERSC a promising platform for the non-volatile control of spins in semiconductors as well as a rich playground for novel magnetoresistive effects.

Germanium telluride, which displays a robust ferroelectricity far above room temperature (~ 720 K), was the most experimentally investigated compound. The non-volatile control of the Rashba bands was demonstrated in GeTe by spin and angle-resolved photoemission spectroscopy [2] and bilinear magnetoresistance was also detected [3], as signature of a complex spin texture. Beyond bare GeTe, multiferroic Rashba semiconductors were achieved through addition of magnetic impurities (such as Mn), enabling either the magnetic or the electric control of the Rashba spin texture [4]. In ferroelectric monochalcogenides, giant spin Hall effect (SHE) was predicted in the two-dimensional limit [5].

This talk reviews the main findings about FERSC, with particular emphasis to the recently achieved ferroelectric switching of spin-to-charge conversion by SHE in GeTe at room temperature [6]. The non-volatile control of the generation of charge currents from spin currents is remarkable, and opens the way to development of ferroelectric-based logic-in-memory devices holding potential for ultra-low power consumption electronic devices beyond-CMOS. Alloying is shown as viable route to control of ferroelectric properties, conductivity and SHE, as well as a possible route to match the conditions for Rashba states and non-trivial topological features in compounds such as SnGeTe.

[1] D. Di Sante *et al.*, *Adv. Mater.* **25**, 509 (2013).

[2] C. Rinaldi *et al.*, *Nano Lett.* **18**, 2751 (2018).

[3] Y. Li *et al.*, *Nat. Commun.* **12**, 540 (2021).

[4] J. Krempasky *et al.*, *Nat. Commun.* **7**, 13071 (2016).

[5] J. Sławińska *et al.*, *2D Mater.* **6**, 025012 (2019).

[6] S. Varotto *et al.*, *Nat. Electron.* **4**, 740 (2021).

Role of the spin current induced generation of magnons in the current non-linear effects in ferromagnet/normal metal bilayers

P. Noël¹, R. Schlitz¹, E. Karadza¹, F. Binda¹, C.-H. Lambert¹, and P. Gambardella¹

¹ Department of Materials, ETH Zurich, CH-8093 Zurich, Switzerland

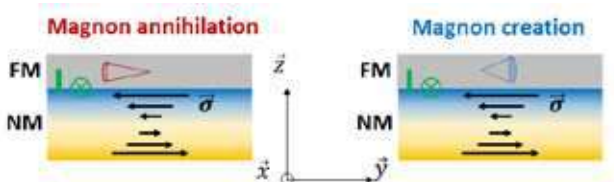


Figure 1: Creation annihilation of magnons due to spin accumulation in the non-magnetic layer.

During the last decade novel magnetotransport phenomena originating from the coupling of charge, heat and spin currents were discovered in a ferromagnet/normal metal bilayer (FM/NM) where the latter has large spin orbit coupling. These effects comprise magnetoresistive phenomena linear with

the charge current such as the spin Hall magnetoresistance (SMR), and current nonlinear effects including the unidirectional spin Hall magnetoresistance (USMR) [1], spin orbit torques [2] and the spin Seebeck effect.

These effects can be detected using harmonic Hall and longitudinal magnetoresistance measurements, and can be disentangled by their particular angular and field dependencies. The so-called harmonic Hall technique has been widely used to evaluate the efficiency of the antidamping like torque and the field like torque in bilayers [3,4].

The interpretation of the second harmonic signals in local measurements usually neglects the role of magnons, even though in a FM/NM bilayer the creation/annihilation of magnons with spin currents (figure 1) can affect the transport, for example the electron-magnon scattering. Indeed, the creation-annihilation of magnons was evidenced to play a key role in the spin-flip USMR [5].

In this presentation I will demonstrate that spin-current driven magnon generation and suppression does not only affect the USMR but can also affect the shape and amplitude of the transverse second harmonic signals. These additional magnon-related effects, if unaccounted for, can be the source of systematic errors in the estimation of the spin orbit torques in ferromagnetic metal/non-magnetic metal bilayers like CoFeB/Pt [6].

[1] Avci, C. O. et al. Unidirectional spin Hall magnetoresistance in ferromagnet/normal metal bilayers. *Nature Phys* 11, 570–575 (2015).

[2] Garello, K. et al. Symmetry and magnitude of spin–orbit torques in ferromagnetic heterostructures. *Nature Nanotech* 8, 587–593 (2013).

[3] Avci, C. O. et al. Interplay of spin-orbit torque and thermoelectric effects in ferromagnet/normal-metal bilayers. *Phys. Rev. B* 90, 224427 (2014).

[4] Hayashi, M., Kim, J., Yamanouchi, M. & Ohno, H. Quantitative characterization of the spin-orbit torque using harmonic Hall voltage measurements. *Phys. Rev. B* 89, 144425 (2014).

[5] Avci, C. O., Mendil, J., Beach, G. S. D. & Gambardella, P. Origins of the Unidirectional Spin Hall Magnetoresistance in Metallic Bilayers. *Phys. Rev. Lett.* 121, 087207 (2018).

[6] Noël, P. et al. (in preparation)

Theory of magnetic spin and orbital Hall and Nernst effects in bulk ferromagnets

Leandro Salemi³ and Peter M. Oppeneer¹

¹ Department of Physics and Astronomy, Uppsala University, P.O. Box 516, S-75120 Uppsala, Sweden

Understanding the generation of spin currents at the microscopic scale is a fundamental issue in the field of spintronics. The spin Hall effect (SHE) is one of the most promising phenomena in this field that has captivated the scientific community since the early 2000s.

Recently, an anomalous charge-to-spin conversion phenomenon, which occurs in ferromagnetic materials, has been introduced [1]. This magnetic spin Hall effect (MSHE) is time-reversal odd, in contrast to the SHE, which is a time-reversal even effect. In this work, we use relativistic *ab initio* calculations to investigate the MSHE for the bulk ferromagnets Fe, Co, and Ni [2]. In contrast to the SHE, for which the electric field, spin current, and induced spin polarization are mutually orthogonal, the MSHE leads to a spin polarization *parallel* to the applied electric field. The magnitudes of the MSHE of Fe and Co are comparable to those of the SHE, but the MSHE is strongly dependent on the electron lifetime and the MSHE and SHE can moreover have opposite signs, see Table 1. For Ni the MSHE is smaller than the SHE. In general, our calculations emphasize that the MSHE cannot be ignored in considerations of the spin-orbit torques in magnetic materials. We analyze how both the MSHE and SHE contribute to a total Hall angle for a charge current in a ferromagnet.

We extend our analysis of the MSHE to its orbital counterpart, that is, the as-yet unobserved magnetic orbital Hall effect (MOHE). We find that the MOHE is in general smaller than the orbital Hall effect (OHE), see Table 1. We compute furthermore the thermal analogs, i.e., the spin and orbital Nernst effects, and their magnetic counterparts. We find that the magnetic spin and orbital Nernst effects of ferromagnetic Ni are substantially larger than those of Fe and Co.

Table 1: Comparison of *ab initio* calculated values for the SHE OHE conductivity tensors as well as the magnetic components MSHE and MOHE, for ferromagnetic bcc Fe, hcp Co, and fcc Ni, in units of $(\hbar/e)(\Omega\text{cm})^{-1}$. The magnetization is along the local z axis.

| | SHE | | | OHE | | | MSHE | | MOHE | |
|----|---------------------|---------------------|---------------------|---------------------|---------------------|---------------------|---------------------|---------------------|---------------------|---------------------|
| | $\sigma_{yz}^{S_z}$ | $\sigma_{xz}^{S_y}$ | $\sigma_{xy}^{S_z}$ | $\sigma_{yz}^{L_z}$ | $\sigma_{xz}^{L_y}$ | $\sigma_{xy}^{L_z}$ | $\sigma_{yz}^{S_z}$ | $\sigma_{xz}^{S_x}$ | $\sigma_{yz}^{L_z}$ | $\sigma_{xz}^{L_x}$ |
| Fe | 441 | 456 | 92 | 4697 | 4698 | 4707 | -593 | 739 | 1343 | 848 |
| Co | 839 | 8 | -44 | 5103 | 4718 | 4737 | 614 | 1074 | -358 | 1356 |
| Ni | 1606 | 1543 | 824 | 3306 | 3297 | 3149 | 394 | -290 | -66 | 1033 |

[1] M. Kimata et al., *Nature* **565**, 627 (2019).

[2] L. Salemi, M. Berritta, and P. M. Oppeneer, *Phys. Rev. Materials* **5**, 074407 (2021).

This work has been funded by the European Union's Horizon2020 Research and Innovation Programme under FET-OPEN Grant agreement No. 863155 (s-Nebula).

Magneto-ionic Reversibility in Annealed W/CoFeB/HfO₂

R. Pachat¹, D. Ourdani², M.-A. Syskaki³, A. Lamperti⁴, S. Roy¹, A. di Pietro⁵, R. Juge⁶, J. W. van der Jagt⁶, G. Agnus¹, G. Durin⁵, Y. Roussigné², S. Ono⁷, J. Langer³, D. Ravelosona^{1,6}, M. Belmeguenai², L. Herrera Diez¹

¹C2N, CNRS, Université Paris-Saclay, 91120 Palaiseau, France

²LSPM, Université Sorbonne Paris Nord, 93430 Villetaneuse, France

³Singulus Technology AG, Hanauer Landstrasse 103, 63796 Kahl am Main, Germany

⁴IMM-CNR, Unit of Agrate Brianza, Via C. Olivetti 2, 20864 Agrate Brianza (MB), Italy

⁵Istituto Nazionale di Ricerca Metrologica, Strada delle Cacce 91, 10135 Torino, Italy

⁶Spin-Ion Technologies, 10 Boulevard Thomas Gobert, 91120 Palaiseau, France

⁷Central Research Institute of Electric Power Industry, Yokosuka, Kanagawa 240-0196, Japan

Magneto-ionics (MI) is of great interest in spintronics primarily due to nonvolatile modulation of magnetic properties. However, the potential application of MI is restricted by the lack of full reversibility and the switching speed. Several works have focused on with different types of ions, oxides, and degrees of oxidation [1-3] to address these limitations, but the influence of annealing temperature on MI reversibility is still lacking in the literature. Thermal annealing is a common technique used to crystallize CoFeB to enhance perpendicular magnetic anisotropy (PMA), Dzyaloshinskii-Moriya interaction (DMI), and tunnel magnetoresistance [4-6]. Therefore, its impact on MI reversibility is of deep concern.

In this work, we study the influence of annealing on MI reversibility in W/CoFeB/HfO₂ where CoFeB is amorphous in the as-grown state. We observe that as-grown samples show in-plane magnetic anisotropy (IPA) and show no change with gate voltage, whereas samples annealed at 350°C and 390°C display PMA and transition to IPA with negative gate voltage. In addition, we show that 390°C annealing allows for higher DMI (0.6 mJ/m²) and anisotropy, but is irreversible, whereas the 350°C annealing shows negligible DMI (0.06 mJ/m²), lower anisotropy, and semi-reversibility of 60%.

This disparity in the degree of MI reversibility with different annealing profiles could be attributed to the degree of crystallization in CoFeB. As different annealing profiles change the size and distribution of CoFeB grains, it affects the ionic mobility inside the stack and therefore the reversibility. Our results show that annealing and phase of CoFeB have a strong impact on tuning between magnetic properties and reversibility, and are of extreme importance for the design of MI based spintronics devices.

[1] Tan, et al., *Nat. Mater.* **18**, 35 (2019).

[2] Fassatoui, et al., *Phys. Rev. Appl.* **14**, 064041 (2020).

[3] Pachat, et al., *Phys. Rev. Appl.* **15**, 064055 (2021).

[4] Cho, et al., *IEEE Trans. on Magnetics* **54**, 15000104 (2018).

[5] Nagata, et al., *Appl. Phys. Lett.* **109**, 132404 (2016).

[6] Wang, et al., *Phys. Rev. B.* **81**, 144406 (2010).

Evidence of the interfacial asymmetric spin scattering at ferromagnet-Pt interfaces

Van Tuong Pham*, Maxen Cosset-Cheneau, Ariel Brenac, Olivier Boule, Alain Marty, Jean-Philippe Attané, Laurent Vila

*Université Grenoble Alpes, CEA, CNRS,
Grenoble INP, IRIG-SPINTEC, 38054 Grenoble, France*

* *Current affiliation: Neel Institute, 38042 Grenoble, France
Email: phamvantuong9999@gmail.com*

Spin Hall effect/ferromagnetic bilayers are the basic element of a new generation of spintronics devices [1,2]. Although these bilayers have been the focus point of a large fundamental effort from the spintronics community, values of essential parameters such as the Spin Hall angle remains widely scattered, which indicates that our understanding of the involved phenomena might be partial. Here, we report electrical measurements of the interconversion between charge and spin currents in various ferromagnetic/platinum nanodevices, due the spin Hall effect in Pt [3,4,5]. The measured spin signals and the extracted effective spin Hall angles of Pt evolve drastically with the ferromagnetic materials (CoFe, Co, and NiFe). Using FEM simulations, we show that assuming transparent interfaces cannot provide a coherent understanding of these results. By carefully measuring the interface resistances values, we show that they are significantly high (10-30 f Ω .m²) and play a very important role, but that it does not lead to a better understanding of our data, even when taking into account the spin memory loss or the spin reflexion (the spin conduction mismatch) at the interface. We then show that a well-known but usually overlooked parameter, the asymmetric spin scattering at the interface, has also to be included to avoid overestimating the spin Hall angles, and to obtain a coherent picture. These results also provide a technological guideline for signal enhancing in readout process [6] in MESO logic [7] and memory applications [8].

- [1] L. Liu *et al.*, *Science* **336**, 555 (2012).
- [2] L. M. Miron *et al.*, *Nat. Mat.* **9**, 230-234 (2010).
- [3] V. T. Pham *et al.*, *Nano Lett.* **16**, 6755–6760 (2016)
- [4] V. T. Pham *et al.*, *Appl. Phys. Lett.* **114**, 222401 (2019)
- [5] V. T. Pham *et al.*, *Phys. Rev. B* **103**, L201403 (2021).
- [6] V. T. Pham *et al.*, *Nature Electron.* **3**, 309–315 (2020).
- [7] S. Manipatruni *et al.*, *Nature* **565**, 35–42 (2019).
- [8] E. Grimaldi *et al.*, *Nature Nanotech.* **15**, 111–117 (2020).

Qualitatively different injection locking behavior of distinctly different spin Hall nano-oscillator modes

Mona Rajabali¹, Ahmad A. Awad¹, Roman Khymyn¹, Mykola Dvornik², Akash Kumar¹, Mohammad Zahedinejad², Johan Åkerman^{1,2}, and Afshin Houshang¹

¹ University of Gothenburg, 412 96 Gothenburg, Sweden

² NanOsc AB, Electrum 229, 164 40 Kista, Stockholm, Sweden

Spin Hall nano-oscillators (SHNOs) can sustain different auto-oscillating modes [1,2], among which the self-localized spin wave (SW) bullet can exhibit a finite power threshold to injection locking [3]. Here, we study the injection locking of two distinctly different SW modes (interior and bullet modes) in a single 120 nm wide Pt (5nm) / NiFe (5 nm) SHNO, observed individually by varying the externally applied field conditions.

We find that the two modes show a dramatically different locking behavior. While the interior mode locks strongly to the injected signal, with a greatly improved linewidth, the spin wave bullet shows a very modest improvement of its linewidth during locking. We used a theoretical model [4] taking into account the power of the two different modes, and find that a single expression can fit the two different behaviors very well provided the thermal noise affecting each mode is taken into account. The apparent finite power threshold of the spin wave bullet mode is hence a consequence of its much smaller mode volume resulting in a much higher noise figure.

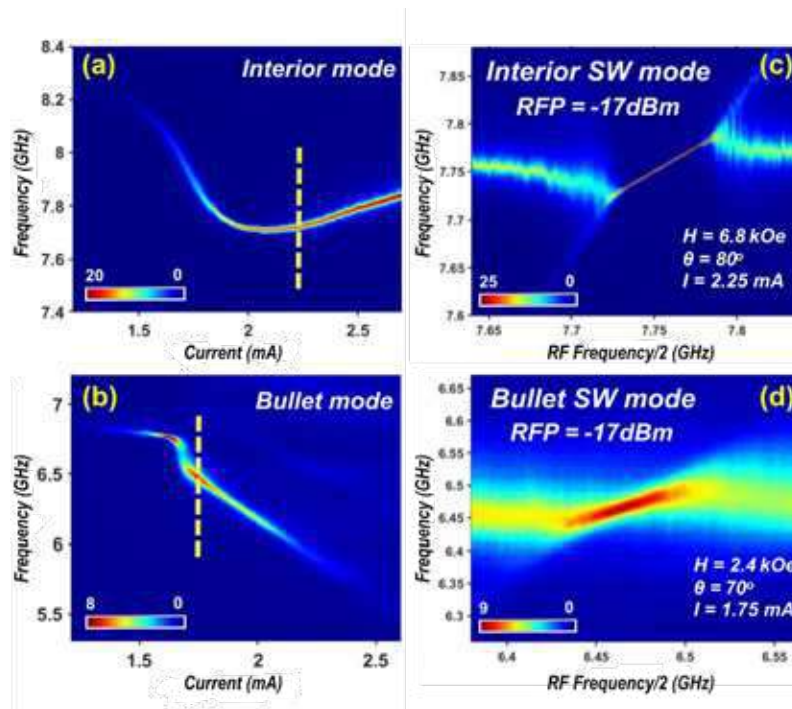


Figure 1: Power spectral density of (a,b) auto-oscillation and (c,d) injection locked SHNO of interior and bullet modes, respectively. As can be seen in (c,d) the linewidth of the injection locked state is dramatically different between the two modes.

- [1] Dvornik M., A. Awad A., Åkerman J., *Phys. Rev. Appl.* **9**, 014017 (2018).
- [2] Fulara, H., et al., *Sci. Adv.* **5**, eaax8467 (2019).
- [3] V. E. Demidov, et al., *Nat. Commun.*, **5**, 1-6 (2014).
- [4] Stratonovich, Rouslan L., *CRC Press* **Vol. 2** (1967).

Anisotropic magnetoresistance in systems with non-collinear magnetic order

Philipp Ritzinger¹ and Karel Výborný¹

¹*Institute of Physics of the Czech Academy of Sciences, Na Slovance 1999/2, 182 21 Prague 8, Czech Republic*

Since its discovery in 1857 by William Thomson [1], the anisotropic magnetoresistance (AMR) has been in focus of many theoretical studies seeking to understand the microscopic mechanisms of this effect. They range from rather simple s-d models [2] to quite complex ab initio calculations [3]. Most attention has been paid to ferromagnets and recently, the scope of research on AMR is extended to include also antiferromagnets (AFMs). The interest in AFMs is mainly motivated by the fact that magnetic order can be manipulated without having a net magnetic moment and thus AFMs are excellent candidates for future spintronic devices [4].

AMR can be due to anisotropic scattering (extrinsic) or an anisotropic Fermi surface (intrinsic) [5]. Here we focus on the latter, much less investigated intrinsic mechanism [3,6], which is achieved by considering non-collinear magnetic order inspired by real materials such as CrSe, δ -FeMn, Mn₃Ge or RbFe(MoO₄)₂. We explore various types of lattices on toy model level amongst which are trigonal, tetrahedral or Kagome lattice. Magnetic moments can be arranged in many different ways on such lattices and seemingly small changes alter the Fermi surface symmetry, spin texture and transport properties. We have investigated systematically the influence of magnetic ordering on these properties which allows to predict general features of spin texture and transport by only considering the symmetry of the underlying system.

As an example of these effects we have shown that AFM systems without spin-orbit coupling on Kagome lattices can develop anisotropy in the electric conductivity under applied in-plane magnetic field. This does not occur in ferromagnets without spin-orbit coupling.

- [1] W. Thomson, *Philos. Trans. R. Soc. London* (1857).
- [2] S. Kokado and M. Tsunoda *J. Phys. Soc. Japan* **84**, 094710 (2015).
- [3] F. L. Zeng, Z.Y. Ren, Y. Li, J.Y. Zeng, M.W. Jia, J. Miao, A. Hoffmann, W. Zhang, Y.Z. Wu, and Z. Yuan, *Phys. Rev. B* **125**, 097201 (2020).
- [4] T. Jungwirth and X. Marti and P. Wadley and J. Wunderlich, *Nature Nanotechnology* **11**, 231-241 (2016).
- [5] K. Výborný, J. Kučera, J. Sinova, A. W. Rushforth, B. L. Gallagher and T. Jungwirth, *Phys. Rev. B* **80**, 165204 (2009).
- [6] L. Nadvornik, M. Borchert, L. Brandt, R. Schlitz, K. A. de Mare, K. Výborný, I. Mertig, G. Jakob, M. Kläui, S. T.B. Goennenwein, M. Wolf, G. Woltersdorf, and T. Kampfrath, *Phys. Rev. X* **11**, 021030 (2021).

Direct X-ray detection of the spin Hall effect in CuBi

S. Ruiz-Gómez¹, R. Guerrero², M. W. Khaliq³, C. Fernández-González^{2,4}, J. Prat³, S. Finizio⁵, P. Perna², J. Camarero^{2,6}, L. Pérez^{2,4}, L. Aballe³, M. Foerster³

¹ Max Planck Institute for Chemical Physics of Solids, 01069 Dresden, Germany.

² Instituto Madrileño de Estudios Avanzados, IMDEA Nanociencia, 28049 Madrid, Spain

³ ALBA Synchrotron Light Facility, CELLS, E-08290 Bellaterra, Spain

⁴ Departamento de Física de Materiales, Universidad Complutense de Madrid, 28040 Madrid, Spain

⁵ Swiss Light Source, Paul Scherrer Institut, CH-5232 Villigen PSI, Switzerland

⁶ universidad Autónoma de Madrid (UAM), Campus de Cantoblanco. Madrid 28049, Spain

The spin Hall effect, and its inverse, are important spin-charge conversion mechanisms widely investigated due to their fundamental importance in the development of spintronics devices. Its measurement has been mostly related to electrical detection schemes involving an interface with another magnetic material and thus, a combination of the properties of both materials as well as the interface are measured. The large scattering of reported results from these methods for the same material and temperature call out for a more direct and interface-free approach. Optical detection schemes have been successfully used for the determination of SHE in semiconductors. This approach is, however, challenging for metallic systems, due to their considerably shorter spin diffusion lengths. Only recently, optical measurements for Pt and W have been reported [1].

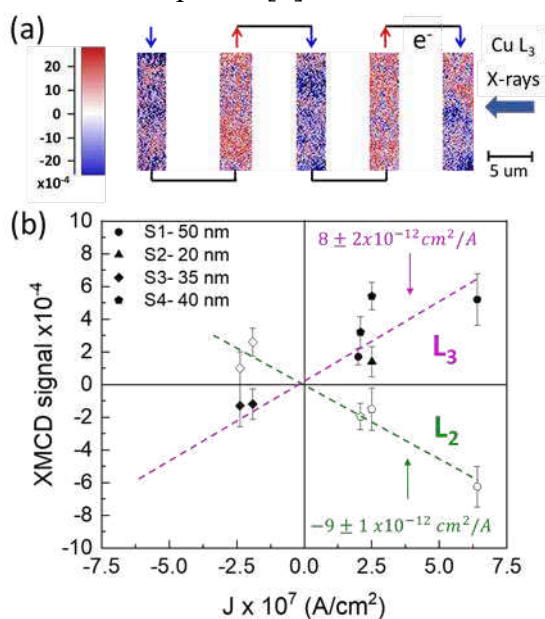


Figure 1: (a) Visualization of the spin accumulation in a Cu₉₅Bi₅ electrode. (b) XMCD signal as function of current density.

Considering that x-ray magnetic circular dichroism (XMCD) has become a reference tool for precision measurement of small or diluted magnetic signals, we propose the use of XMCD-PEEM microscopy for direct, interface-free determination of SHE in metals. In particular, we report the observation of spin separation due to SHE in a single layer of Bi-doped Cu (Cu₉₅Bi₅), a material in which giant SHE has been already reported [2,3]. We have performed interface free x-ray spectroscopy measurements at the Cu L_{3,2} absorption edges while applying electrical current to the sample. The sign of spin accumulation depends on the direction of the current (Figure 1.a) and the amplitude of the X-ray magnetic circular dichroism (XMCD) signal scales with the current density and has different sign when measuring at the L₂ or L₃ absorption edges, as expected for SHE (Figure 1.b). We have measured an induced magnetic moment of $(2.7 \pm 0.5) \times 10^{-12} \mu_B \text{ A}^{-1} \text{ cm}^2$ per Cu atom averaged

over the probing depth, which is of the same order as for Pt measured by magneto-optics. Our results constitute the proof of concept for the direct, interface free and element-selective measurement of the SHE in a single material by means of X-ray spectro-microscopy, and highlight the potential of CuBi for spin-charge conversion applications [4].

- [1] C. Stamm et al. Phys. Rev. Lett. 119, 087203 (2017).
- [2] Y. Niimi et al. Phys. Rev. Lett. 109, 156602 (2012).
- [3] S. Ruiz-Gómez et al. APL Materials 6, 101107 (2018)
- [4] S. Ruiz Gómez et al. arXiv:2107.02620 (2021).

Anomalous Nernst effect in τ -MnAl thin films

Daniel Scheffler¹, Helena Reichlova¹, Torsten Mix², Thomas G. Woodcock²,
Sebastian T.B. Goennenwein³ and Andy Thomas^{1,2}

¹*Institute for Solid State and Materials Physics, Faculty of Physics, Technische Universität Dresden, 01062 Dresden, Germany*

²*Leibniz Institute for Solid State and Materials Research Dresden (IFW Dresden), 01069 Dresden, Germany*

³*Department of Physics, University of Konstanz, 78457 Konstanz, Germany*

τ -MnAl is a ferromagnetic compound with high uniaxial magnetocrystalline anisotropy, making it interesting for permanent magnet applications. The magnetic properties of τ -MnAl have mostly been studied in polycrystalline bulk samples. In single crystalline films, the anomalous Hall effect [1] and the tunnel magnetoresistance effect [2] have been investigated, the magneto-thermal transport properties of τ -MnAl films are unknown. Given the unique anisotropy, this material could allow for a robust spontaneous (present in zero magnetic field) anomalous Nernst effect generated by a thermal gradient applied in the film plane.

We have successfully grown single crystalline τ -MnAl thin films via co-sputtering. X-ray diffraction and DC magnetometry confirm a good structural quality and strong perpendicular magnetic anisotropy. We observe a robust anomalous Hall effect with a coercivity of 1 T in magneto-transport measurements as shown in Fig.1. In the same device, a defined thermal gradient can also be applied in the sample plane, resulting in a clear anomalous Nernst effect response as also evident from Fig 1.

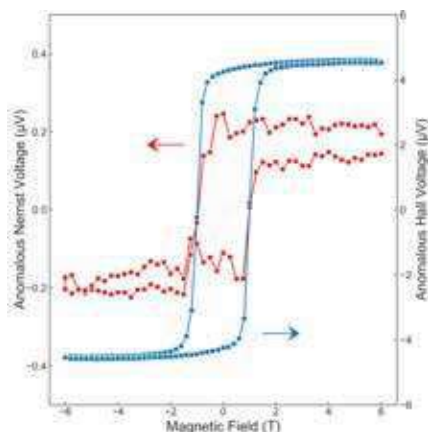


Figure 1: Anomalous Nernst and anomalous Hall voltage in τ -MnAl film at a temperature of 200 K

We will present results from our systematic magneto-transport and magneto-thermopower experiments, which in particular allow to quantify the anomalous Nernst effect coefficient. Our results show that τ -MnAl in thin film form is an interesting material for spin-caloritronic research and devices.

[1] L. J. Zhu et al, *Nat. Commun.* **7**, 10817 (2016).

[2] H. Saruyama et al, *Jpn. J. Appl. Phys.* **52**, 063003 (2013).

Gate-tuneable and chirality-dependent charge-to-spin conversion in Tellurium nanowires

M. Suárez-Rodríguez¹, F. Calavalle¹, B. Martín-García¹, A. Johansson^{2,3}, D. C. Vaz¹, H. Yang¹, I. V. Maznichenko², S. Ostanin², A. Mateo-Alonso^{4,5}, A. Chuvilin^{1,4}, I. Mertig², M. Gobbi^{1,4}, F. Casanova^{1,4}, L. E. Hueso^{1,4}

¹CIC nanoGUNE BRTA, 20018 Donostia-San Sebastian, Basque Country, Spain

²Institute of Physics, Martin Luther University Halle-Wittenberg, 06099 Halle, Germany

³Max Planck Institute of Microstructure Physics, Weinberg 2, 06120 Halle, Germany

⁴IKERBASQUE, Basque Foundation for Science, 48013 Bilbao, Basque Country, Spain

⁵POLYMAT, University of the Basque Country UPV/EHU, 20018 Donostia-San Sebastian, Basque Country, Spain

Chiral materials are an ideal playground for exploring the relation between symmetry, relativistic effects, and electronic transport [1]. Indeed, it has been observed that chiral organic molecules act as efficient spin filters, but their poor electronic conductivity limits their potential for applications. Conversely, chiral inorganic crystals, such as elemental Tellurium (Te), present excellent electrical conductivity and strong spin-orbit coupling. Here, we report a chirality-dependent and gate-tuneable Edelstein effect in naturally hole-doped Te nanowires (NWs) [2]. By recording a unidirectional magnetoresistance (UMR) dependent on the relative orientation of the electrical current and the external applied magnetic field, we link the direction of the spin polarization to the handedness of the crystal (Fig. 1). The measured UMR is explained on the basis of a chirality-dependent Edelstein effect arising from the radial spin texture at the H-point of the valence band of Te, which dominates the transport in our hole-doped Te NWs. In addition, an electrostatic gating enables the tuning of the Edelstein effect, leading to a modulation of the UMR amplitude by a factor of 6. The all-electrical generation, control, and detection of spin polarization in chiral Te NWs opens the path to exploit chirality in the design of solid-state spintronic devices.

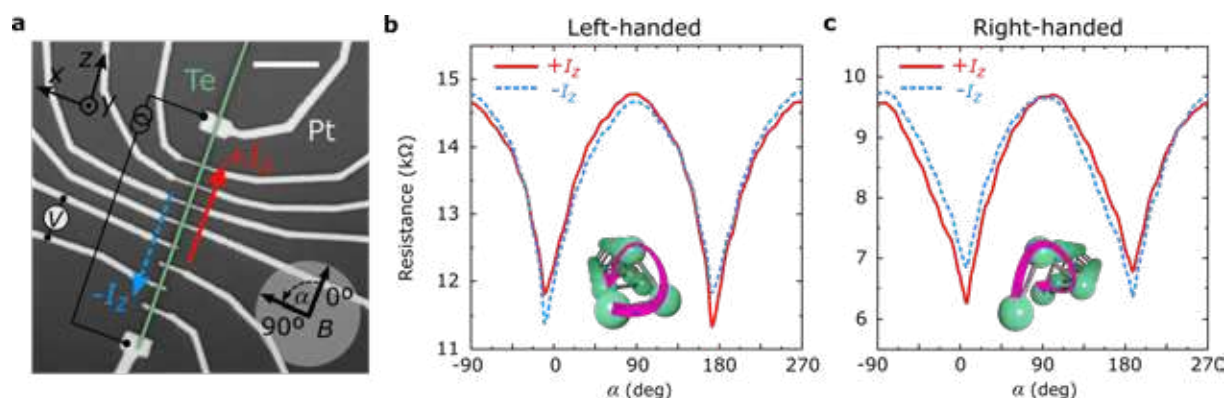


Fig. 1. **a**, Typical Te NW contacted with Pt contacts (the scale bar corresponds to 10 μm). **b,c**, Angular dependences of the magnetoresistance measured at 9 T and 10 K for two Te NWs with opposite handedness. Solid and dashed lines indicate the signal obtained from opposite current directions ($\pm I_z = \pm 1 \mu\text{A}$ in **b** and $\pm I_z = \pm 0.7 \mu\text{A}$ in **c**).

[1] S.-H. Yang et al. *Nat. Rev. Phys.* **3**, 328–343 (2021).

[2] F. Calavalle[†], M. Suárez-Rodríguez[†] et al. *Nat. Mater.* (2022). DOI: 10.1038/s41563-022-01211-7.

Detection of Magnon Currents in EuS

M. Xochitl Aguilar-Pujol¹, Sara Catalano¹, Maxim Ilyn², Carmen González-Orellana², Celia Rogero², Juan M. Gómez-Pérez¹, Marco Gobbi^{1,2,3}, Luis E. Hueso^{1,3} and Fèlix Casanova¹

¹ CIC NanoGUNE BRTA, 20018, Donostia-San Sebastian, Basque Country, Spain

² Centro de Física de Materiales CSIC-UPV/EHU, 20018, Donostia-San Sebastian, Basque Country Spain

³ IKERBASQUE, Basque Foundation for Science, 48009, Bilbao, Basque Country, Spain

Magnons, the quanta of spin wave excitations in magnetic systems, allow for the transport of spin angular momentum through magnetic compounds, including insulators. The ability to control the injection, propagation, and detection of such magnon spin currents represents an asset for the progress of spintronics. So far, magnon transport have been studied mainly through $\text{Y}_3\text{Fe}_5\text{O}_{12}$ (YIG) and a few other ferri- and antiferromagnetic insulators [1], while there exist many materials in which their behavior is little-known. Here, we study for the first time the generation of thermal magnon currents in 15-nm-thick films of the ferromagnetic insulator europium sulfide (EuS), which exhibits a Curie temperature $T_c = 19$ K in thin films [2]. We perform non-local (NL) transport measurements using Pt electrodes, with different separation distances d , as magnon injectors and detectors. We study the NL voltage, generated at the detector due to the inverse spin Hall effect (ISHE), depending on the in-plane angle between the sample magnetization and the polarization direction of the spins induced by ISHE in the Pt, for the temperature range $2 \text{ K} < T < 30 \text{ K}$. The second harmonic component of the NL voltage indicates that thermal magnon currents generated in the injector flow to the detector for distances ranging from $d = 0.8 \text{ }\mu\text{m}$ up to $d = 2 \text{ }\mu\text{m}$ and for temperatures $T < 20 \text{ K}$. By analyzing the length dependence of the second harmonic signal we evaluate the magnon propagation length in the EuS films, which we find to be relatively short, as compared to the YIG case. We discuss our results considering the Gilbert damping and the Curie temperature of the EuS films.

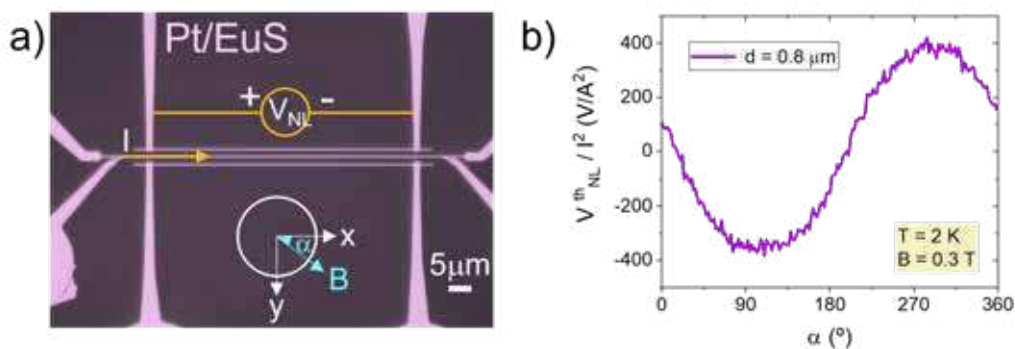


Figure 1: a) Microscope image of a non-local device used in this work ($d = 1.25 \text{ }\mu\text{m}$, $1.5 \text{ }\mu\text{m}$). b) Representative angular-dependent non-local signal detected for thermally excited magnons.

[1] A. Brataas et al., *Physics Reports* **885**, 1 (2020).

[2] J. M. Gómez-Pérez et al., *Nano Letters* **20**, 6815 (2020).

Posters

| | | |
|------------------------|---|-----|
| Shahin Alam | <i>Spin zero effect in nonmagnetic centrosymmetric dipnictides TaAs₂</i> | 626 |
| Kateryna Boboshko | <i>Bilinear Magnetoresistance and Nonlinear Planar Hall Effect in Topological Insulators with Spin-Orbital Impurities</i> | 627 |
| Adam Cahaya | <i>Electron - Electron Repulsion Effect on Spin Mixing Conductance of Metallic Ferromagnet and Heavy Metal Interface</i> | 628 |
| Louis Farcis | <i>Spin-transfer torque induced dynamics in dual free layer p-MTJ</i> | 629 |
| Rodrigo Guedas García | <i>Reducing the temperature of nanostrips with a coating layer</i> | 630 |
| Ghulam Hussain | <i>Intrinsic spin Hall effect in Nb-based A15 compounds</i> | 631 |
| Fabian Kammerbauer | <i>Current-induced interlayer DMI in synthetic antiferromagnets</i> | 632 |
| Sachin Krishnia | <i>Giant Rashba spin-orbit torque in atomically thin metallic Pt[Co]AlPt multilayers</i> | 633 |
| Anna Krzyżewska | <i>Nonlinear Hall effect induced by Berry curvature dipole in a two-dimensional system with k-cubed form of Rashba spin-orbit interaction</i> | 634 |
| Vireshwar Mishra | <i>On the Room Temperature Weak Localization and Anomalous Temperature Dependence of Phase Coherence Length in L₂₁ Ordered Heusler Alloy CoFeMnSi Thin Films</i> | 635 |
| Richa Mudgal | <i>Determination of Spin-Orbit Torque in PtSe₂/NiFe Heterostructure</i> | 636 |
| Roselle Ngalyo | <i>Van der Waals Magnet based Spin-Valve Devices at Room Temperature</i> | 637 |
| Sam Parker | <i>A magneto-transport method for measuring the exchange coupling in a synthetic antiferromagnet</i> | 638 |
| Lara Solis | <i>FMR and thermal spin pumping enhanced by perpendicular anisotropy in YIG/Pt bilayers</i> | 639 |
| Izabella Wojciechowska | <i>Topological transport properties of ex-so-tic van-der-Waals structures</i> | 640 |
| Alexander Wright | <i>Thermal scanning probe lithography as a technique for fabrication of non-local spin valves</i> | 641 |

Spin zero effect in nonmagnetic centrosymmetric dipnictides TaAs₂

Md Shahin Alam¹, P.T. Kumar¹, Krzysztof Dybko^{1,2}, Ashutosh S. Wadge¹,
Przemysław Iwanowski^{1,2}, Andrzej Wiśniewski^{1,2}, Marcin Matusiak^{1,3}

¹*International Research Centre MagTop, Institute of Physics, Polish Academy of Sciences, Aleja Lotnikow 32/46, PL-02668 Warsaw, Poland*

²*Institute of Physics, Polish Academy of Sciences, Aleja Lotnikow 32/46, PL-02668 Warsaw, Poland*

³*Institute of Low Temperature and Structure Research, Polish Academy of Sciences, ul. Okólna 2, 50-422 Wrocław, Poland*

Topological semimetals are a new class of quantum materials that exhibit exotic properties promising for modern device applications [1]. The electrical and thermo-electrical measurements were performed on TaAs₂ single crystal with applied magnetic field along [-210] crystallographic direction. At higher magnetic field, we observed distinct quantum oscillations with more than one periodicity, which could be ascribed to the multiband nature of the system. The fast Fourier transform spectrum of the Nernst oscillations gives two fundamental frequencies $f_{\nu\alpha} \sim 105$ T and $f_{\nu\beta} \sim 221$ T and a second harmonic $2f_{\nu\beta} \sim 442$ T of the later. Analogously we also got two fundamental frequencies $f_{\rho\alpha} \sim 122$ T and $f_{\rho\beta} \sim 210$ T and a second harmonic $2f_{\rho\beta} \sim 420$ T from the FFT spectrum of SdH oscillations. The ratio of amplitudes of the fundamental to the second harmonic of the β frequency for both SdH and Nernst oscillations changes with temperature in an unusual way. Namely, it increases with temperature above $T \sim 15$ K, as opposed to the behavior expected from the Lifshitz-Kosevich thermal damping term $\sim [\sinh(\frac{2\pi^2 k_B m^*}{eB\hbar})]^{-1}$. Around $T \sim 15$ K the second harmonic of the β frequency of Nernst oscillations completely dominates the fundamental one. Such kind of unusual temperature dependencies of quantum oscillations indicate that we observe spin zero effect triggered by the temperature changes [2]. The calculated Landé g-factor shows significant temperature variation, which suggests that this could be a cause of the spin zero effect. Further, a possible reason of the temperature dependent Landé g-factor is the evolution of the spin-orbit coupling, which may influence the topological properties of TaAs₂[3].

[1] A.A. Soluyanov, D. Gresch, Z. Wang, Q. Wu, M. Troyer, X. Dai, and B.A. Bernevig, *Nature* **527**, 495 (2015).

[2] J. Wang, J. Niu, B. Yan, X. Li, R. Bi, Y. Yao, D. Yu, and X. Wu, *Proc. Natl. Acad. Sci.* **115**, 9145 (2020).

[3] W. Zawadzki, P. Pfeffer, R. Bratschitsch, Z. Chen, S. T. Cundiff, B. N. Murdin, and C. R. Pidgeon, *Phys. Rev. B* **78**, 245203 (2008).

Bilinear Magnetoresistance and Nonlinear Planar Hall Effect in Topological Insulators with Spin-Orbital Impurities

Kateryna Boboshko¹, Anna Dyrdał¹

¹*Department of Mesoscopic Physics, ISQI, Faculty of Physics, Adam Mickiewicz University,
ul. Uniwersytetu Poznańskiego 2, 61-614 Poznań, Poland*

Bilinear magnetoresistance (BMR) and nonlinear planar Hall effect (NPHE) in surface states of a 3D topological insulator are discussed theoretically as effects that can emerge in nonmagnetic materials with strong spin-orbit interaction. The phenomena reveal simultaneous linear dependence on charge current density (external electric field) and in-plane magnetic fields. Recent theories have ascribed the appearance of both phenomena as a consequence of the spin-momentum locking inhomogeneities and/or the hexagonal warping of the Dirac cones [1]. We show the new mechanism related to scattering on impurities that inherently contain spin-orbit coupling [2]. Based on Green functions formalism, we derived the expressions for diagonal and transverse conductivities and showed detailed characteristics of BMR and NPHE.

[1] A. Dyrdał, J. Barnaś, and A. Fert, *Phys. Rev. Lett.* **124**, 046802 (2020).

[2] K. Boboshko, A. Dyrdał, and J. Barnaś, *J. Magn. Magn. Mater.* **545**, 168698 (2022).

This work has been supported by the National Science Centre in Poland under the project No. DEC-2018/31/D/ST3/02351.

Electron - Electron Repulsion Effect on Spin Mixing Conductance of Metallic Ferromagnet and Heavy Metal Interface

Adam B. Cahaya¹ and Muhammad Aziz Majidi¹

¹Department of Physics, Faculty of Mathematics and Natural Sciences, Universitas Indonesia, Depok, Indonesia

This document provides instructions for preparing an abstract for “JEMS 2022” and is written in the format according to the guidelines given below.

In a magnetic multilayer, magnetizations can be manipulated by spin transfer torque. Both spin transfer torque and its reciprocal effect, spin pumping, are governed by spin mixing conductance. Theoretically, spin mixing conductance can be related to dynamic magnetic susceptibility due to exchange interaction near the interface [1]. Similar to the enhancement of magnetic susceptibility on heavy metals, the magnitude of spin mixing conductance at the interface of ferromagnet and heavy metal has been experimentally observed to be larger in heavier transition metals [2].

However, another experiment shows decreasing value of spin mixing conductance for metals with larger electron-electron interaction [3]. Here we apply Hubbard model with electron repulsion parameter U to describe the spin mixing conductance of the interface of metallic ferromagnet and heavy metal. By taking into account the effect of U on screening of the exchange interaction at the magnetic interface, we show that the electron-electron interaction suppressed the exchange interaction and spin mixing conductance [4].

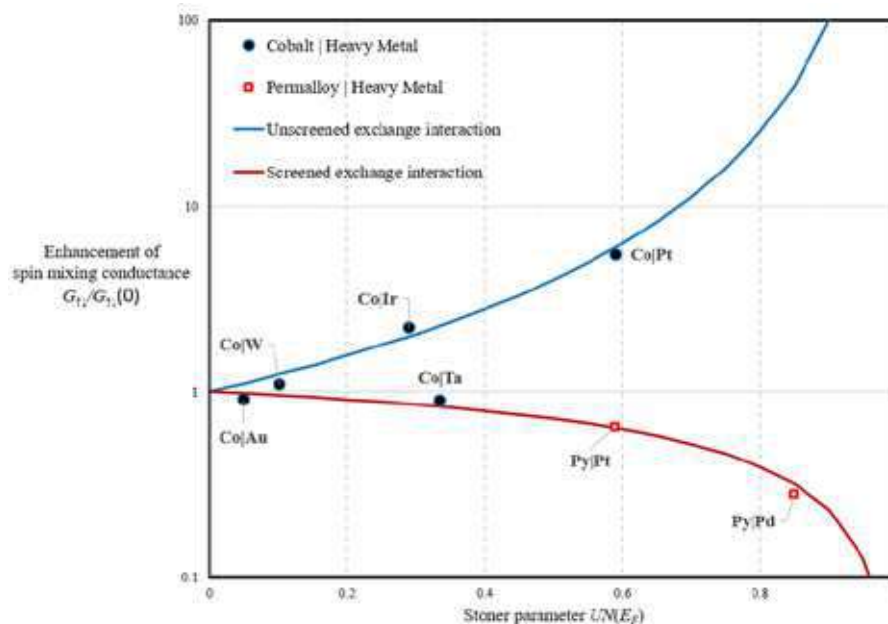


Figure 1. Enhancement of spin mixing conductance of metallic ferromagnets and various heavy metals.

- [1] E Šimánek and B Heinrich, *Phys. Rev. B* **67**, 144418 (2008).
- [2] X. Ma, *et al. Phys. Rev. Lett.* **120**, 157204 (2018).
- [3] M. Caminale, *et al. Phys. Rev. B* **94**, 014414 (2016).
- [4] A. B. Cahaya and M. A. Majidi, *Phys. Rev. B* **103**, 094420 (2021).

Spin-transfer torque induced dynamics in dual free layer p-MTJ

L. Farcis¹, B.-M.S. Teixeira¹, D. Salomoni¹, P. Talatchian¹, S. Auffret¹, B. Dieny¹, I.L. Prejbeanu¹, A. Mizrahi², J. Grollier², R. Sousa¹ and L.D. Buda-Prejbeanu¹

¹ Univ. Grenoble Alpes, CNRS, CEA, Grenoble INP, IRIG, SPINTEC, 38000 Grenoble, France

² Unité Mixte de Physique CNRS/Thales, Université Paris-Saclay, 91177 Palaiseau, France

Magnetic Tunnel Junctions (MTJ) are one of the main spintronic devices, having reached market maturity in magnetic read heads and magnetic random-access memories. Through tunnel magnetoresistive effect (TMR), the electrical read-out of such MTJs probes the magnetization state of the free layer. In this work, we report an MTJ composed of a dual free-layer for the first time and demonstrate its dual magnetization dynamics experimentally. Such dynamics have straightforward applications in brain-inspired computing, stochastic computing, in-memory computing and sensors.

The properties of the complete stack are designed such that the two magnetic layers have similar thermal stability, so that both of their magnetizations can be reversed by spin-transfer torque (STT). Under suitable conditions of applied voltage and magnetic field, the magnetization of both layers switches continuously, creating an oscillation between antiparallel (AP) and parallel (P) resistance states [2,3]. The optimal conditions to achieve this behaviour were identified by simulations using an extended multi-macrospin model accounting for the Joule heating, thermal fluctuations, TMR bias dependency and Callen-Callen laws describing the material parameters temperature dependence. Guided by our simulation results, MTJ pillars based on FeCoB/MgO/FeCoB were designed, nanofabricated and electrically characterized.

The experimental field-voltage phase diagrams show a close correlation with respect to the simulation [Figure 1]. Time-resolved measurements of resistance unveil a wind-mill dynamic state, in which there is a sequential and persistent switching of the two magnetic layers. Magnetic couplings between the layers can be shown to create disturbance in the reversal dynamics. In addition, the large tunability of the mean fluctuation frequency by external magnetic field and applied current opens the path for applications such as sensors, frequency-tunable RF oscillators that can synchronize in networks, promising for cognitive computing.

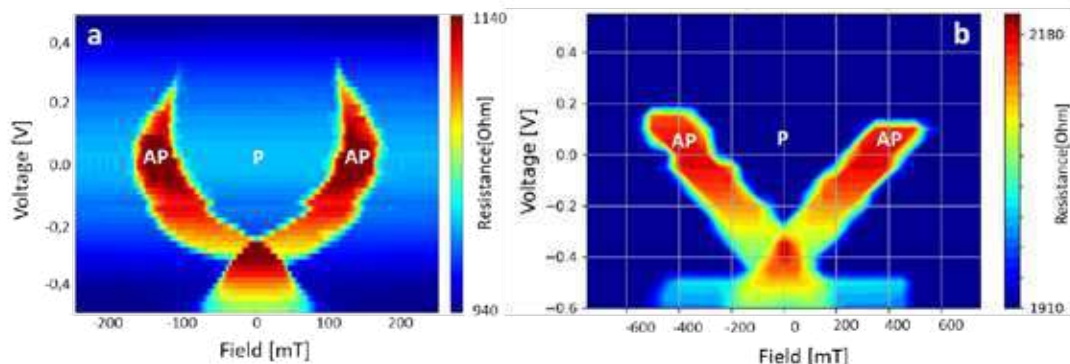


Figure 1 - Comparison between experimental (a) and simulated (b) field-voltage phase diagram

- [1] Camsari, K. Y., Torunbalci, M. M., Borders, W. A., Ohno, H., & Fukami, S. "Double-free-layer magnetic tunnel junctions for probabilistic bits". *Physical Review Applied*, **15**(4), 044049 (2021).
- [2] Matsumoto, R., Lequeux, S., Imamura, H., & Grollier, J. "Chaos and relaxation oscillations in spin-torque windmill spiking oscillators". *Physical Review Applied*, **11**(4), 044093 (2019)
- [3] Gupta, Gaurav, Zhifeng Zhu, and Gengchiao Liang. "Switching based Spin Transfer Torque Oscillator with zero-bias field and large tuning-ratio." *arXiv preprint arXiv*, **1611.05169** (2016).

Reducing the temperature of nanostrips with a coating layer

Rodrigo Guedas¹, Alex Novillo¹ and José L. Prieto¹

¹ Instituto de Sistemas Optoelectrónicos y Microtecnología (ISOM), Universidad Politécnica de Madrid, Avda. Complutense 30, 28040 Madrid, Spain

Since the proposal of the Racetrack Memory [1] there has been an ever-increasing amount of work related to current induced magnetic domain wall movement and magnetic switching driven by Spin Transfer Torque (STT) [2] or Spin Orbit Torques (SOTs) [3]. In order to produce these effects, large current densities of the order of 10^{12} TA/m² are often required, leading to an unavoidable Joule heating, making the interpretation of the results even more complex and/or risking the durability of the device. Recently [4] we have discussed the influence of some parameters on the Joule heating, such as Interface Thermal Resistance (ITR), current density, resistivity, substrate's thermal conductivity and the geometry. Based on simulations, we also showed that, by depositing some layers on top of the stripe (Fig. 1a), the nanostrip could also dissipate heat by the top surface which, in some conditions, could lead to a significant reduction of the maximum temperature of more than 300 K. In fact, in most cases, this strategy can be more effective at keeping the strip temperature under control than performing the measurement in a cryostat at 10 K.

In this work, we have performed an experimental demonstration of how a coating deposited on top of the nanostrip leads to a temperature reduction for the same power delivered to the nanostrip [4]. By measuring the Anisotropic Magnetoresistance (AMR) of the strip for different current densities, we show how the coating bilayer of Ta₂O₃/Au allows to increase the power delivered to the nanostrip before it reaches its Curie temperature (Fig. 1b). A COMSOL simulation, fitted to the experimental results allowed us to extract the Interface Thermal Resistance of the top layer, which is the main parameter limiting the potential of this dissipation strategy.

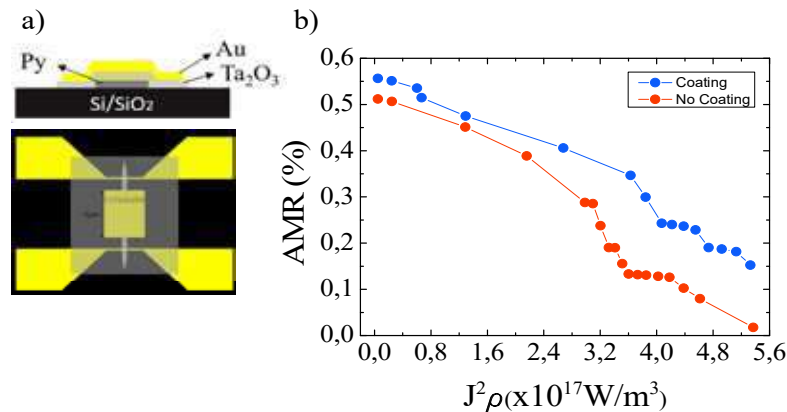


Figure 1. a) Schematics of the nanostrip with the dissipative top layers and b) Graph showing AMR variation vs the power per cubic meter injected by a DC electric current.

- [1] S. S. P. Parkin, M. Hayashi, and L. Thomas, *Science* **320**, 190 (2008).
- [2] M. Hayashi, L. Thomas, C. Rettner, R. Moriya, Y. B. Bazaliy, and S. S. P. Parkin, *Phys. Rev. Lett.* **98**, 037204 (2007).
- [3] I. M. Miron, T. Moore, H. Szambolics, L. D. Buda-Prejbeany, S. Auffret, B. Rodmack, S. Pizzini, J. Vogel, M. Bonfim, A. Schuhl and G. Gaudin, *Nature Mater.* **10**, 419 (2011).
- [4] R. Guedas, V. Raposo, and J.L. Prieto, *J. Appl. Phys.* **130**, 191101 (2021).

Intrinsic spin Hall effect in Nb-based A15 compounds

Ghulam Hussain*, Giuseppe Cuono, Carmine Autieri

International Research Centre MagTop, Institute of Physics, Polish Academy of Sciences, Aleja Lotników 32/46, PL-02668 Warsaw, Poland

**E-mail: ghussain@magtop.ifpan.edu.pl*

The relativistic electronic band structures contain anticrossings points near the Fermi level that gives rise to a large spin Berry curvature (SBC); the intrinsic spin Hall effect (SHE) is directly proportional to SBC. Compounds with highly symmetric crystal structures as the cubic A15 can produce several degeneracies in the band structure that can host anticrossing points when the SOC is switched on [1, 2]. Based on this criterion, we focus on A15 Nb-based compounds as Nb₃Sn, Nb₃Ge and Nb₃Sb. Once fixed the Nb element, we evaluate the evolution of the SHE as a function of the other element. To study and verify the presence of gapped crossings, we calculated the electronic band structures both with and without SOC using the first-principles calculations. The tight-binding model Hamiltonians were constructed, through the projection of Bloch wave functions on the Wannier functions. We then computed the intrinsic spin Hall conductivities from the Kubo formula using the model Hamiltonian. We evaluate the spin Hall conductivity for the Nb₃Sn, Nb₃Ge and Nb₃Sb compounds and analyze the relationship between the SHE and the orbital moments for this material class.

[1] E. Derunova, Y. Sun, C. Felser, S. Parkin, B. Yan, M. Ali, *Science advances*, **5** (2019).

[2] G.-Y. Guo, S. Murakami, T.-W. Chen, N. Nagaosa, *Physical review letters*, **100**, 096401 (2008).

Current-induced interlayer DMI in synthetic antiferromagnets

Fabian Kammerbauer¹, Won-Young Choi², Kyujoon Lee³, Robert Frömter¹, Dong-Soo Han² and Mathias Kläui¹

¹ *Institute of Physics, Johannes Gutenberg University, Staudingerweg 7, 55128 Mainz, Germany*

² *Center for Spintronics, Korea Institute of Science and Technology, Hwarang-ro 14 gil 5, Seoul, Republic of Korea*

³ *Division of display and semiconductor physics, Korea University, Sejong-ro 2511, Sejong, Republic of Korea*

The exchange interaction comes in two flavours – the symmetric and antisymmetric part. The symmetric term (typically Heisenberg Exchange) governs the ferro- and antiferromagnetism while the antisymmetric term, typically called Dzyaloshinskii-Moriya interaction (DMI), promotes topologically non-trivial chiral spin textures that promise new magnetic devices.

Layered synthetic antiferromagnets can display in addition to the typical symmetric interlayer RKKY interaction also an antisymmetric interlayer DMI due to symmetry breaking within the sample plane [1, 2]. This effect favours noncollinear alignment between adjacent layers and thus provides an additional handle to engineer magnetic structures and could enable three-dimensional topological structures.

It has already been reported that electrical currents can be used to tune the strength of the interface DMI, [3]. Here, we report the effect of an electrical current on the antisymmetric interlayer DMI by employing anomalous Hall effect measurements with an additional applied in-plane field. In order to quantify the current dependence of the antisymmetric interlayer exchange interaction, an interlayer DMI field is introduced. Using a model of two superimposed cosine functions accounting for current-dependent and static contributions, we demonstrate that the current-dependent interlayer DMI field increases linearly with current and maximal along the direction of current flow. Additionally, we show that the effect is odd in current. Thus, we demonstrate the possibility to control the interlayer DMI directly by electrical currents, which allows for new switching mechanisms in three-dimensional magnetic textures.

[1] D.-S. Han, et al., Nat. Mater. **18**, 703-708 (2019)

[2] A. Fernández-Pacheco, et al., Nat. Mater. **18**, 679-684 (2019)

[3] G.V. Karnad, et al., Phys. Rev. Lett. **121**, 147203 (2018)

Giant Rashba spin-orbit torque in atomically thin metallic Pt|Co|Al|Pt multilayers

S. Krishnia¹, Y. Sassi¹, F. Ajejas¹, S. Collin¹, A. Fert¹, J. M. George¹, N. Reyren¹, H. Jaffrès¹ and V. Cros¹

¹Unité Mixte de Physique, CNRS, Thales, Université Paris-Saclay, 91177, Palaiseau, France

Spin-orbit interaction in metals and its ability to generate spin-current has been the hallmark of spintronics in the last decade. Beyond its fundamental interest as a source of spin-current, the Graal in spintronics, the manipulation of magnetization via transfer of the spin angular momentum has proven to be energy efficient for spin-based memory (e.g. SOT-MRAM) and also neuromorphic (e.g. spin Hall nano-oscillators) devices. Therein, charge to spin conversion is believed to be governed essentially by two main mechanisms, spin Hall effect (SHE) in the bulk of heavy-metals and Rashba effect at interfaces [1], the latter being often considered negligible in all-metallic interfaces. However, in the case of atomically thin metallic layers, the main facts of the underlying SOT physical mechanisms at play have not been experimentally tackled.

In this study, we examine the impact of light element interface on the nature of the SOT as well as its efficiency in terms of damping-like (H_{DL}) and field-like (H_{FL}) effective fields in ultrathin ferromagnets. Importantly, we observe unexpectedly large H_{FL}/H_{DL} ratio (~ 2.5) upon inserting a 1.4 nm thin Al layer in Pt|Co|Al|Pt as compared to a similar stacking including Cu instead of Al. From our modelling based on generalized drift-diffusion theory, these experimental results strongly evidence the presence of a large interfacial Rashba effect at Co|Al interface producing giant H_{FL} . The occurrence of efficient Rashba states is further validated by reducing the contribution from SHE in the bottom Pt layer that we correlate to a strong increase of the H_{FL}/H_{DL} ratio. We believe that our results are also important from the application point of view as they provide a clear route for reaching ultimate spin-torque efficiency for the associated devices.

Financial support from the Agence Nationale de la Recherche, France, No. ANR-17-CE24-0025 (TOPSKY), the DARPA TEE programme through grant MIPR no. HR0011831554 and the Horizon2020 Framework Programme of the European Commission under FET-Proactive Grant agreement No. 824123 (SKYTOP) and are acknowledged.

[1] Manchon, A. *et al.*, Rev. Mod. Phys. 91, (2019). [2] Krishnia S. *et al.*, submitted (2022)

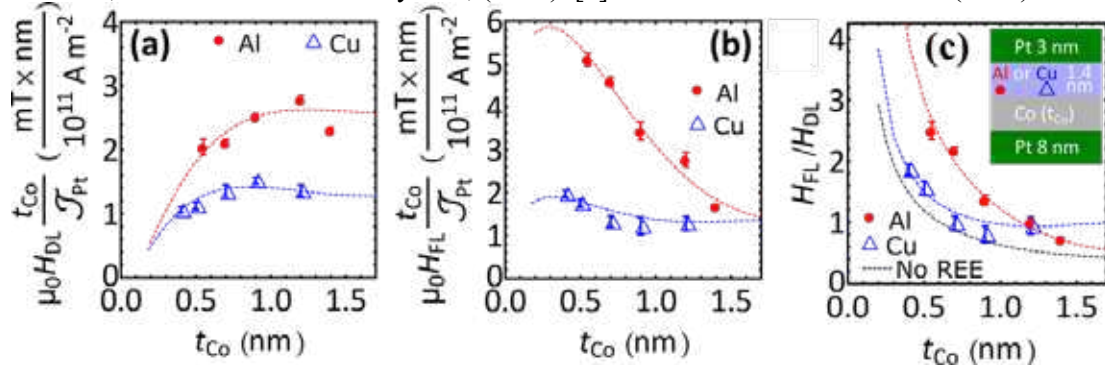


Fig. 1: Co layer thickness (t_{Co}) dependence of (a) DL-SOT field and (b) FL-like SOT field multiplied by Co thickness for 10^{11} A/m^2 current density in Pt in Pt8|Co(t_{Co})|Al1.4|Pt3 (red circles) and Pt8|Co(t_{Co})|Cu1.4|Pt3 (blue triangles) samples (c) $\zeta = H_{FL}/H_{DL}$ as a function of t_{Co} . The dashed lines are fits with the theoretical model.

Nonlinear Hall effect induced by Berry curvature dipole in a two-dimensional system with k -cubed form of Rashba spin-orbit interaction

A. Krzyżewska¹, and A. Dyrdał¹

¹*Department of Mesoscopic Physics, ISQI, Faculty of Physics, Adam Mickiewicz University,
ul. Uniwersytetu Poznańskiego 2, 61-614 Poznań, Poland*

Nonlinear Hall effect (NLHE) is a phenomenon that reveals a second-order response to an external electric field and can be observed even in the systems without the time-reversal symmetry breaking [1,2]. It was found that intrinsic contribution to the NLHE arises from the Berry curvature dipole [1,3].

We have studied theoretically the nonlinear Hall effect within modeled effective Hamiltonian describing high-mobility two-dimensional electron gas, forming at the interfaces of perovskite-oxides (e.g., $\text{LaAlO}_3/\text{SrTiO}_3$). An important feature of this model is the k -cubed form of Rashba spin-orbit interaction [3,4]. What is more, this model is also valid for the two-dimensional hole gas in III-V semiconductors [6,7].

We have found that in two-dimensional electron gas with the k -cubed form of Rashba spin-orbit interaction, an external in-plane magnetic field induces tuneable Berry curvature dipole and therefore, the nonlinear Hall effect.

This work has been supported by the Norwegian Financial Mechanism 2014-2021 under the Polish-Norwegian Research Project NCN GRIEG "2Dtronics" no. 2019/34/H/ST3/00515.

- [1] I. Sodemann, L. Fu, *Phys. Rev. Lett.* **115**, 216806 (2015).
- [2] Q. Ma, S.-Y. Xu, et al., *Nature* **565**, 337 (2019).
- [3] Z. Z. Du, C. M. Wang, *Nat. Commun.* **12**, 1 (2021).
- [4] A. Krzyżewska, A. Dyrdał, et al., *Phys. Status Solidi RRL* **12**, 1800232 (2018).
- [5] A. Krzyżewska, A. Dyrdał, *J. Magn. Magn. Mater.* **497**, 165919 (2020).
- [6] C.-X. Liu, B. Zhou et al., *Phys. Rev. B* **77**, 125345 (2008).
- [7] L. W. van Heeringen, G. A. de Wijs, et al., *Phys. Rev. B* **88**, 205140 (2013).

On the Room Temperature Weak Localization and Anomalous Temperature Dependence of Phase Coherence Length in $L2_1$ Ordered Heusler Alloy CoFeMnSi Thin Films

Vireshwar Mishra, Lalit Pandey, Vineet Barwal, Soumyarup Hait, Nanhe Kumar Gupta, Nikita Sharma, Nakul Kumar, Amar Kumar and Sujeet Chaudhary*

¹Thin Film Laboratory, Department of Physics, Indian Institute of Technology Delhi, New Delhi 110016 (INDIA)

*Corresponding author: sujeetc@iitd.ac.in

Abstract

The spin gapless semiconducting (SGS) compounds have been reported to possess excellent properties in order to be utilized in various spintronics based devices. Here, we report the room temperature weak localization in $L2_1$ ordered CoFeMnSi (CFMS) Heusler alloy thin films grown over Si (100) substrates using pulsed-DC magnetron sputtering technique. We have observed the (111) reflection in the grazing incidence X-ray diffraction curve which confirms its crystallinity of $L2_1$ order. Longitudinal resistivity trend shows similar non-metallic behaviour akin to other reported SGS materials. The temperature-dependent longitudinal conductivity curve fitted with two carrier model revealed that one channel of the system is gapped while the other channel has some band overlap. Further analysis of longitudinal resistivity curve confirmed that weak localization factor dominates over other scattering factors and is larger in higher temperature regime compared to lower temperature regime. Detailed analysis of the magnetoresistance behaviour confirmed the existence of weak localization (sharp negative cusp at low field) even up to room temperature with an *anomalous* increase of phase coherence length with temperature. Further analysis of magnetoresistance behaviour showed that the CFMS system lies in quantum diffusive regime. The anomalous Hall effect study revealed nearly temperature-independent carrier concentration and mobility, which is a characteristic signature of the SGS materials, with room temperature values of $2.77 \pm 0.36 \times 10^{22}$ and $1.13 \pm 0.14 \text{ cm}^2/\text{V.s}$, respectively. The anomalous Hall conductivity values obtained at 5K and 300K are 37.75 S/cm and 56.58 S/cm, respectively.

Spin-Orbit Torque in PtSe₂/NiFe Heterostructure

Richa Mudgal¹, Alka Jakhar², Pankhuri Gupta¹, Himanshu¹, Niru Chowdhury¹,
Samaresh Das², P.K. Muduli¹

¹ Department of Physics, Indian Institute of Technology Delhi, Hauz Khas-110016, New Delhi, India

² The Centre for Applied Research in Electronics, Indian Institute of Technology Delhi, Hauz Khas-110016, New Delhi, India

Transition metal dichalcogenides (TMDs) are potential materials for exerting efficient spin-orbit torque (SOT) on the adjacent ferromagnetic layer due to their high spin-orbit coupling (SOC) and broken inversion symmetry at the interface [1]. An unconventional SOT is recently observed due to low symmetry in TMDs/FM heterostructures [2]. PtSe₂ is one of the TMDs having high SOC [3]. In this work, we measured the spin Hall angle (SHA) of PtSe₂ using spin-torque ferromagnetic resonance (STFMR). PtSe₂ was synthesized by salinization of a sputtered Pt (3 nm) film. The growth of PtSe₂ was confirmed using Raman measurements, which show two peaks at 176 cm⁻¹ (E_g) and 206 cm⁻¹ (A_{1g}). Subsequently, a 6 nm thick NiFe (Py) layer followed by Pt (3 nm) capping layer was deposited on PtSe₂ using magnetron sputtering. For STFMR measurements, RF current of frequency varying from 3 GHz to 7 GHz was applied to the device in the presence of an external magnetic field (H). The mixing voltage (V_{mix}) across the device was measured and the symmetric & anti-symmetric components (V_s , V_A) of V_{mix} , linewidth, and resonance field (H_r) were extracted (Fig.1) from the fitting of STFMR spectra. Effective SHA was calculated using the ratio of V_s and V_A and found to be 0.26 for PtSe₂/Py/Pt which was 53% larger than its reference Py/Pt sample value of 0.17. This change in SHA is due to the presence of PtSe₂, which was further confirmed by making a stack with Pt/Py/Pt structure. STFMR signal of all three stacks has been compared in Fig. 1 (a). No clear signal was observed for Pt/Py/Pt which confirms the presence of SOT due to PtSe₂. Damping parameter was extracted by the fitting of linewidth vs. frequency curve (Fig. 2) and was found to be enhanced by 131% in the case of PtSe₂/Py/Pt compared to its reference Py/Pt. Large enhancement in damping parameter indicates large spin pumping into PtSe₂. These results indicate the suitability of using PtSe₂ as a potential material for spin-orbit torque.

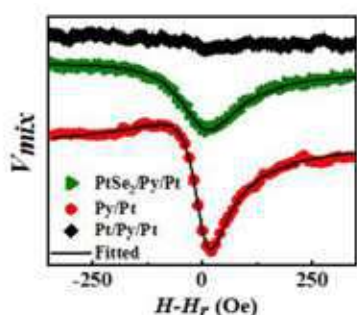


Figure 1. Measured STFMR signal with the magnetic field applied at an angle of 45° with respect to the x-axis at 5 GHz for PtSe₂/Py/Pt, Py/Pt and Pt/Py/Pt. The solid lines represent fits with a symmetric and antisymmetric Lorentzian function.

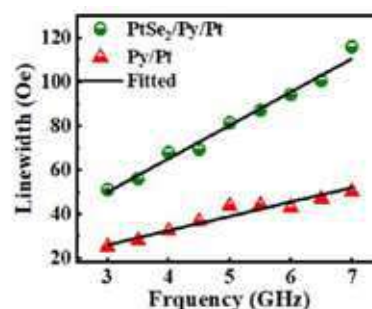


Figure 2. Linewidth Vs. Frequency plot for PtSe₂/Py/Pt and Py/Pt. Solid lines represent fit

References:

- [1] Q. Shao et al., *Nano Letter* **16**, 7514-7520 (2016)
- [2] D. MacNeill et. al., *Nature Physics*, **13**, 300-305 (2017)
- [3] Marcin Karpas and Jaroslav Fabian, *Physical Review B*, **103**, 125409 (2017)

Van der Waals Magnet based Spin-Valve Devices at Room Temperature

Bing Zhao¹, Roselle Ngaloy¹, Anamul Md. Hoque¹, Bogdan Karpiak¹, Dmitrii Khokhriakov¹, Saroj P. Dash¹

¹ Department of Microtechnology and Nanoscience, Chalmers University of Technology, SE-41296, Göteborg, Sweden

The discovery of van der Waals (vdW) magnets opened up a new paradigm for condensed matter physics and spintronic technologies. However, the operations of active spintronic devices with vdW magnets are so far limited to cryogenic temperatures, inhibiting its broader practical applications. Here, for the first time, we demonstrate room temperature spin-valve devices using vdW itinerant ferromagnet Fe₅GeTe₂ in heterostructures with graphene. The tunnel spin polarization of the Fe₅GeTe₂/graphene vdW interface is detected to be significantly large and negative at room temperature [1]. Lateral spin-valve device design enables electrical control of spin signal and realization of basic building blocks for device application such as efficient spin injection, transport, precession, and detection functionalities. Furthermore, measurements with different magnetic orientations provide unique insights into the magnetic anisotropy of Fe₅GeTe₂ and its relation with spin polarization and dynamics in the heterostructure. These findings open opportunities for the applications of vdW magnet-based all-2D spintronic devices and integrated spin circuits at ambient temperatures.

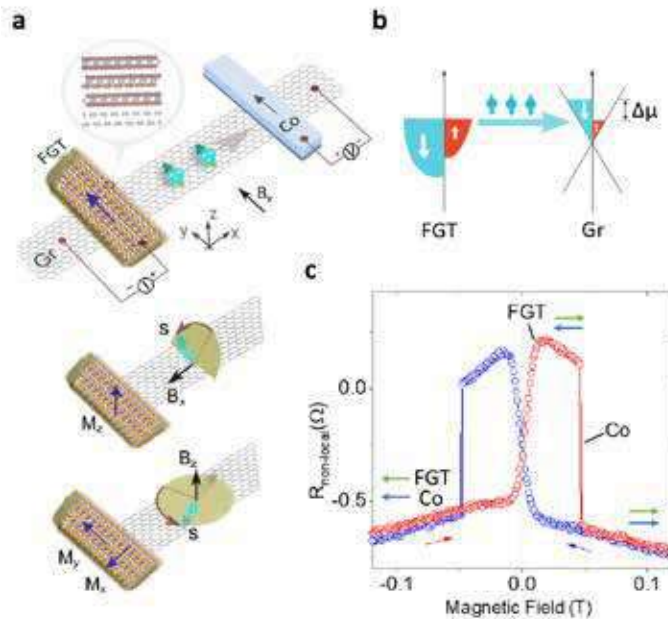


Figure 1: Room temperature spin-valve device with van der Waals magnet Fe₅GeTe₂ and graphene heterostructure. a) Schematic of a spin-valve device with Fe₅GeTe₂ (FGT) on a graphene (Gr) channel. The middle and bottom panels show the schematics for the Hanle spin precession measurements with B_x and B_z fields, respectively. b) Schematic illustration for spin injection from FGT into the graphene channel through the vdW gap, inducing a non-equilibrium spin accumulation Δμ in graphene. c) The measured nonlocal (NL) spin-valve signal $R_{nl}=V_{nl}/I_{dc}$ for parallel and antiparallel alignment of FGT and Co electrodes.

[1] B. Zhao, R. Ngaloy, A.M. Hoque, B. Karpiak, D. Khokhriakov, and S.P. *arXiv:2107.00310*, 2021

A magneto-transport method for measuring the exchange coupling in a synthetic antiferromagnet

S. A. Parker¹, L. X. Barton¹ and A. W. Rushforth¹.

¹School of Physics and Astronomy, *University of Nottingham, University Park, Nottingham, NG7 2RD, United Kingdom*

Synthetic Antiferromagnets (SyAFs) present promise in Spintronics as they retain the favorable qualities of both ferromagnetic and antiferromagnetic materials. SyAFs possess the ease of manipulation through magnetic fields, like the former, and minimize stray fringing fields, as with the latter. SyAFs have a high level of tuneability [1] since their magnetic parameters, such as the magnetocrystalline anisotropy and inter-layer exchange strength, can be controlled in the fabrication process. In this abstract, we present a method for measuring the interlayer exchange coupling (IEC) via magnetotransport measurements. We measure the anisotropic magnetoresistance (AMR) of a polycrystalline SyAF as a function of magnetic field strength. Utilizing the measured AMR magnitudes, we successfully extract the canting angle as a function of the applied magnetic field strength. We use the magnetic free energy [2] to extract the IEC through a relation between the applied magnetic field, the canting angle, and the IEC. We use the extracted canting angles to calculate the magnetization of the device and compare the data to previously obtained SQUID magnetometry data for the same layers. There is a good agreement between the two data sets, indicating that the simple magnetotransport method can be used to provide a measurement of the IEC when other magnetometry techniques are not available, or when the device size is too small to be measured by a magnetometer.

Figure1. (A) Measured AMR at various magnetic field strengths. (B) Magnetisation versus applied magnetic field calculated from magneto-resistance method plotted along with SQUID magnetometry data.

- [1] - Duine, R.A., Lee, K-J., Parkin, S, S,P, and Stiles, M.D., *Nat. Phys.* 14, 217-219, (2018).
 [2] - Rößler, U.K. and Bogdanov, A.N., *J. App. Phys.* 101(9), 09D105 (2007).

FMR and thermal spin pumping enhanced by perpendicular anisotropy in YIG/Pt bilayers

Lara M. Solis^{1,2,3}, Santiago Carreira⁴, Javier Gómez^{5,6}, Javier Briático⁴, Abdelmadjid Anane⁴, Alejandro Butera^{5,6}, Laura Steren^{1,5}, and Myriam H. Aguirre^{3,7,8}

¹*Instituto de Nanociencia y Nanotecnología CNEA-CONICET, Centro Atómico Constituyentes, Villa Maipú, Argentina*

²*Instituto Sábató, Universidad Nacional de San Martín, San Martín, Argentina*

³*Instituto de Nanociencia y Materiales de Aragón, UNIZAR-CSIC, Zaragoza, Spain*

⁴*Unité Mixte de Physique, CNRS, Thales, Université Paris-Saclay, Palaiseau, France*

⁵*Consejo Nacional de Investigaciones Científicas y Técnicas, Argentina*

⁶*Centro Atómico Bariloche CNEA-CONICET, Bariloche, Río Negro, Argentina*

⁷*Departamento de Física de la Materia Condensada, UNIZAR, Zaragoza, Spain*

⁸*Laboratorio de Microscopías Avanzadas, UNIZAR-CSIC, Zaragoza, Spain*

The ferrimagnetic insulator $\text{Y}_3\text{Fe}_5\text{O}_{12}$ (YIG) is recognized as a model system for spintronic and magnonic phenomena including spin pumping, spin Seebeck, proximity effects and spin wave propagation. In those materials, the spin current occurs via spin-waves or magnons. Magnons can be excited and detected electrically via the spin Hall effect (SHE) and the anomalous spin Hall effect (ASHE) and excited thermally via the spin Seebeck effect (SSE). To detect the spin current, a thin non-magnetic layer such as Pt, is deposited on top of the material of interest. This converts the spin current into an observable thermoelectric voltage (VSSE) by way of the Inverse Spin Hall Effect (ISHE). YIG/Pt systems enable the efficient spin-charge conversion and pure detection of spin-current effects, respectively, because their unique spin dynamic and magneto-optical properties [1]. These properties allow clean detection of the pure spin current thanks to spin-orbit effects in YIG/Pt bilayers [2].

Samples with different thicknesses of pure YIG films on $\text{Gd}_3\text{Ga}_5\text{O}_{12}$ (111)(GGG) and substituted (SGGG) substrates were growth by pulsed laser deposition (PLD). We report a perpendicular anisotropy in epitaxial YIG films grown on SGGG. General Phase Analysis (GPA) shows that the films are lattice matched to the substrates with low compressive strain in relation to those grown on GGG substrates. Through ferromagnetic resonance measurements, we find that these YIG films have low Gilbert damping constant. Moreover, the transport behavior of Pt/YIG/SGGG films reveals an enhancement of spin mixing conductance as compared with Pt/YIG/GGG films. In addition, measurements of the Spin Seebeck Effect confirmed what was found in the results of spin pumping.

[1] S. M. Rezende, R. L. Rodríguez-Suárez, R. O. Cunha, A. R. Rodrigues, F. L. A. Machado, G. F. Guerra, and A. Azevedo, *Physical Review B* **89**, 014416 (2014).

[2] C. Du, H. Wang, P. C. Hammel, and F. Yang, *Journal of Applied Physics* **117**, 172603 (2015).

Topological transport properties of *EX-SO-TIC* van-der-Waals structures

I. Wojciechowska¹, A. Woźniak¹, and A. Dyrdał¹

¹*Department of Mesoscopic Physics, ISQI, Faculty of Physics, Adam Mickiewicz University,
ul. Uniwersytetu Poznańskiego 2, 61-614 Poznań, Poland*

Two-dimensional Van-der-Waals materials focus enormous interest due to interesting electronic and magnetic properties controlled by external fields. A special group of van-der-Waals materials is multilayer hybrid structures where due to proximity effects and electric gating, one can turn the time-reversal symmetry on and off on demand and, consequently, swap between an exchange (ex) and spin-orbit (so) coupling. Because of such property these structures are called *ex-so-tic*. [1]

An example of *ex-so-tic* van-der-Waals structure is bilayer graphene (GG) sandwiched by a 2D ferromagnet Cr₂Ge₂Te₆ (CGT) and a monolayer WS₂. The efficient swapping between the presence of exchange and spin-orbit coupling in CGT/GG/WS₂ is possible due to the interplay of gate-dependent layer polarization in bilayer graphene and short-range spin-orbit and exchange proximity effects affecting only the layer of graphene in contact with the sandwiching materials.

We present a theoretical study of electronic and topological properties of CGT/GG/WS₂ based on an effective modeled Hamiltonian derived from symmetry considerations and DFT study [1]. We analyse, among others, a behavior of Berry curvature as a function of characteristic parameters defining the Hamiltonian and discuss possible topological phase transitions. Moreover, we present detailed characteristics of intrinsic anomalous, spin and valley Hall effects [2] that may appear in specific phases.

[1] K. Zollner, M. Gmitra, and J. Fabian, Phys. Rev. Letters 125, 196402 (2020)

[2] A. Dyrdał and J. Barnaś, 2D Materials 4, 034003 (2017)

This work has been supported by the Norwegian Financial Mechanism 2014- 2021 under the Polish-Norwegian Research Project NCN GRIEG “2Dtronics” no. 2019/34/H/ST3/00515.

Thermal scanning probe lithography as a technique for fabrication of non-local spin valves

A. J. Wright¹, M. J. Erickson^{2,3}, D. Bromley¹, O. Barker¹, P. A. Crowell², C. Leighton³ and L. O'Brien¹

¹ Department of Physics, University of Liverpool, Liverpool, L69 7ZE, UK

² School of Physics and Astronomy, University of Minnesota, MN, 55455, USA

³ Department of Chemical Engineering and Materials Science, University of Minnesota, MN, 55455, USA

The non-local spin valve (NLSV) has been widely employed to study spin transport in a variety of materials, owing to its key advantage of complete separation of charge and spin currents [1,2]. In these devices, a non-magnetic metal (NM) channel is contacted by two ferromagnetic (FM) electrodes, a geometry that, to date, has almost exclusively been patterned using electron beam lithography (EBL). Meanwhile, thermal scanning probe lithography (t-SPL) is emerging as an alternative lithographical tool for spintronic devices, with advantages over EBL in cost-effectiveness, resolution and *in situ* imaging. [3]

In this work, we present the first reported use of t-SPL for the fabrication of NLSVs (Fig. 1), using 2-step lithography. Using SEM characterisation, we demonstrate the capability of t-SPL for fabrication of Py/Cu NLSVs with the necessary resolution (50 nm) for clean switching of the FMs, with superior consistency in dimensions between devices when compared with EBL which suffers from proximity effects. Measurements of the non-local resistance, R_{NL} , and the spin-signal, ΔR_{NL} , (Fig. 2), reveal a remarkably strong spin signal in the devices we fabricate, despite use of a very thin (25 nm) NM channel. We attribute this to a sizeable interfacial resistance and elimination of magnetic impurities in the NM channel which can obfuscate spin transport measurements. [4] Our results demonstrate t-SPL to be a viable and advantageous alternative to EBL for fabrication of NLSVs.

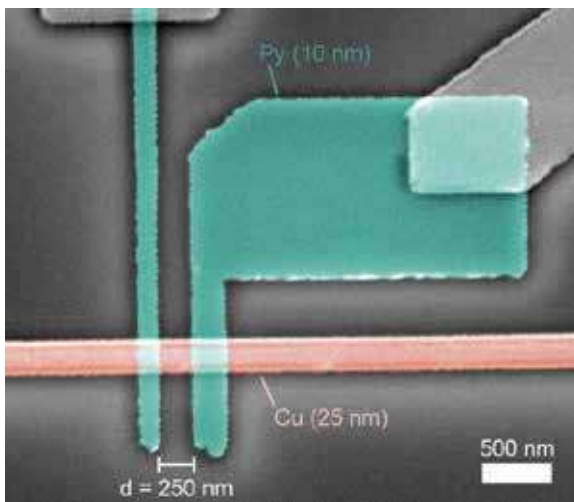


Figure 1: False-colour SEM image of a Py/Cu NLSV fabricated using t-SPL.

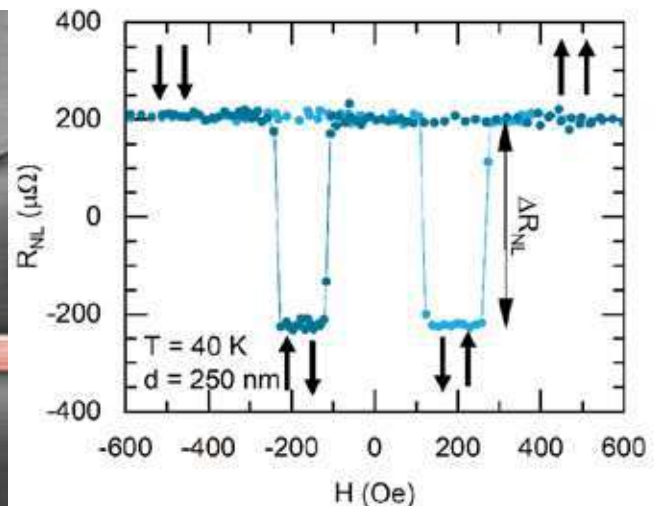


Figure 2: Non-local resistance vs. field of a t-SPL NLSV, demonstrating measurement of ΔR_{NL} .

- [1] F. J. Jedema, M. S. Nijboer, A. T. Filip, and B. J. van Wees, *Phys. Rev. B* **67**, 085319 (2003).
- [2] I. Žutić, J. Fabian, and S. Das Sarma, *Rev. Mod. Phys.* **76**, 323 (2004).
- [3] S. T. Howell, A. Grushina, F. Holzner, and J. Brugger, *Microsystems Nanoeng.* **6**, 21 (2020).
- [4] L. O'Brien, M. J. Erickson, D. Spivak, H. Ambaye, R. J. Goyette, V. Lauter, P. A. Crowell, and C. Leighton, *Nat. Commun.* **5**, 3927 (2014).

Symposium 16. Magnetism and spin transport in topological materials and Weyl semimetals

| | | |
|-----------------------------|---|-----|
| Phil King | <i>Giant valley Zeeman coupling in the NbS₂ surface layer of V_{1/3}NbS₂</i> | 644 |
| Oliver Rader | <i>The ferromagnetic topological insulator MnSb₂Te₄</i> | 645 |
| Cezary Śliwa | <i>Superexchange dominates in magnetic topological insulators</i> | 646 |
| Linda Ye | <i>Quantum oscillation studies of magnetic kagome metals</i> | 647 |
| Wojciech Brzezicki | <i>Berry phase effects in the layered topological metals</i> | 649 |
| Nicholas Figueiredo-Prestes | <i>Spin-Orbit torques and magnetization switching in topological-insulator/2D-ferromagnet heterostructures: MBE-grown CrTe₂/Bi₂Te₃</i> | 650 |
| Jacob Gayles | <i>Hard magnet topological semimetals in XPt₃ compounds with the harmony of Berry curvature</i> | 651 |
| Rajibul Islam | <i>Axion insulating phase in superlattices without inversion symmetry</i> | 652 |
| Yixi Su | <i>Interplay between magnetism and topology in correlated topological materials</i> | 653 |
| Ashutosh Wadge | <i>Surface decorated Weyl semimetal: topological quantum Lifshitz transition</i> | 654 |
| Michael Wissmann | <i>Magnetic Properties of Intrinsic Magnetic Topological Insulators Mn(Bi,Sb)Te</i> | 655 |
| Akinobu Yamaguchi | <i>Study on spin-orbit-torque-induced magnetization modulation using rectifying planar Hall effect</i> | 656 |
| Kacho Imtiyaz Ali Khan | <i>Topological Kagome ferromagnet Fe₃Sn₂ grown on Si-SiO₂ substrates using Pt seed layer.</i> | 658 |
| Aleksandr Kazakov | <i>Magnetotransport in Ferromagnetic Topological Crystalline Insulator Sn_{1-x}Mn_xTe Thin Films</i> | 659 |
| PardeepKumar Tanwar | <i>Chiral zero sound – a new mechanism for heat conduction in Weyl semimetal NbP</i> | 660 |
| Akinobu Yamaguchi | <i>Spin transport properties in multilayer including Pt and NiO layers</i> | 661 |

Invited Oral Presentations

| | | |
|--------------|--|-----|
| Phil King | <i>Giant valley Zeeman coupling in the NbS₂ surface layer of V_{1/3}NbS₂</i> | 644 |
| Oliver Rader | <i>The ferromagnetic topological insulator MnSb₂Te₄</i> | 645 |
| Cezary Śliwa | <i>Superexchange dominates in magnetic topological insulators</i> | 646 |
| Linda Ye | <i>Quantum oscillation studies of magnetic kagome metals</i> | 647 |

Giant valley Zeeman coupling in the NbS₂ surface layer of V_{1/3}NbS₂

**B. Edwards¹, O. Dowinton², A. Hall³, P. Murgatroyd¹, S. Buchberger¹, G. Siemann¹,
E. Abarca Morales¹, T. Antonelli¹, A. Rajan¹, A. Zivanovic¹, G. Balakrishnan³, M.S.
Bahramy² and P. D. C. King¹**

¹ SUPA, School of Physics and Astronomy, University of St Andrews, United Kingdom

² Department of Physics and Astronomy, University of Manchester, United Kingdom

³ Department of Physics, University of Warwick, United Kingdom

One of the most striking properties of the transition-metal dichalcogenides (TMDs) is a locking of their quasiparticle spin to a valley pseudospin. This results from strong spin-orbit coupling and is enabled by global or local inversion symmetry breaking [1,2], providing a route to stabilise novel physical properties such as Ising superconductivity [3,4], and potentially facilitating new computing schemes via 'valleytronics' [1]. Tuning of the resulting spin splittings is thus strongly desired. To date, this has been achieved via externally-applied magnetic fields [5] and by proximity coupling in van der Waals heterostructures [6], but only modest changes of the intrinsic spin-orbit splitting have been realised. Here, we investigate a monolayer-like NbS₂ layer at the surface of the V-intercalated TMD V_{1/3}NbS₂ using spatially- and angle-resolved photoemission spectroscopy (μ -ARPES). Our measurements and corresponding density-functional calculations reveal a giant valley Zeeman interaction exceeding 50 meV, of comparable magnitude to the intrinsic spin-orbit mediated splittings. Our findings thus indicate how magnetism is mediated via the itinerant states in this nominally local-moment system, and reveal new routes to utilise this to gain control over valley spin splittings in transition-metal dichalcogenides and related materials.

[1] Xu *et al.*, *Nature Phys.* **10**, 343 (2014)

[2] Riley *et al.*, *Nature Phys.* **10** (2014) 835

[3] Lu *et al.*, *Science* **350** (2015) 1353

[4] Xi *et al.*, *Nature Phys.* **12** (2016) 139

[5] Srivastava *et al.*, *Nature Phys.* **11** (2015) 141

[6] Zhong *et al.* *Nature Nano.* **15** (2020) 187

The ferromagnetic topological insulator MnSb_2Te_4

Oliver Rader

Helmholtz-Zentrum Berlin für Materialien und Energy, Albert-Einstein-Str. 15, 12489 Berlin, Germany

Magnetically doped topological insulators display the quantum anomalous Hall effect and are considered as materials for lossless interconnects, for a novel edge-state spintronics, for quantum metrology, and for topological qubits. Previous work showed that Mn enables the formation of intrinsic magnetic topological insulators of AB_2C_4 stoichiometry, however, pure MnBi_2Te_4 is an antiferromagnetic topological insulator with 25 K Néel temperature. It is shown that the replacement of Bi by Sb in the present work solved several problems at once [1]: Firstly, the formed MnBi_2Te_4 has the advantage of being slightly p-type in contrast to the strongly n-type MnBi_2Te_4 . Secondly, the system MnBi_2Te_4 was theoretically considered topologically trivial but spin- and angle-resolved photoemission reveal a clear Dirac cone as sign of a topological insulator. Thirdly, and again contrary to predictions and even previous experiments from bulk crystals, the system is ferromagnetic with a high Curie temperature up to 50 K, i. e., the Curie temperature is two times larger than the Néel temperature of the related MnBi_2Te_4 . The ferromagnetism, in turn, enabled the demonstration of the magnetic gap at the Dirac point for the first time using scanning tunneling spectroscopy. This was achieved by the temperature dependence where the gap closes near 50 K and by an in-plane magnetic field of 3 T which reduces the gap [2].

To understand the reason of the unexpected topological insulator property and the equally unexpected ferromagnetism with high T_c required detailed band structure calculations and identified structural disorder caused by a small amount of about 5% of excess Mn as explanation.

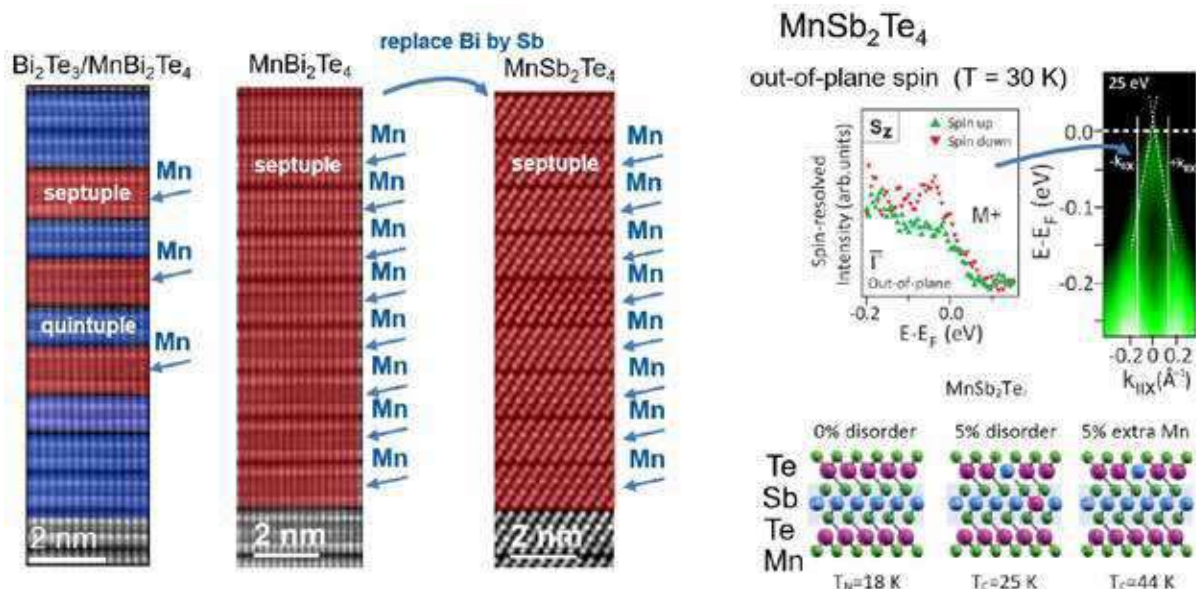


Figure 1: Left: From antiferromagnetic MnBi_2Te_4 to ferromagnetic MnSb_2Te_4 . Top right: Spin polarized Dirac cone demonstrates nontrivial topology. Bottom right: 5% extra Mn are important for the ferromagnetic coupling.

[1] S. Wimmer et al., Adv. Mater. **42**, 2102935 (2021).

[2] P. Küppers et al., arXiv:2202.11540 (2022).

Superexchange dominates in magnetic topological insulators

Cezary Śliwa¹, Carmine Autieri², Jacek A. Majewski³ and Tomasz Dietl²

¹*Institute of Physics, Polish Academy of Sciences, PL-02668 Warsaw, Poland*

²*International Research Centre MagTop, Institute of Physics, Polish Academy of Sciences, Aleja Lotnikow 32/46, PL-02668 Warsaw, Poland*

³*Institute of Theoretical Physics, Faculty of Physics, University of Warsaw, ul. Pasteura 5, PL-02093 Warsaw, Poland*

A consensus has emerged that the enhanced interband spin susceptibility in topological materials leads to a strong and foremost ferromagnetic coupling between transition-metal ions [1,2], the interaction referred to as the Van Vleck mechanism [3]. Here, we call this insight into question and demonstrate theoretically that in the absence of carriers the superexchange is the dominant exchange mechanism in magnetically-doped topological insulators [4]. In particular, we show that the interband susceptibility is conquered by a self-interaction term that does not contribute to the strength of the spin-spin interaction between different magnetic ions. By quantitative computations of the exchange integral magnitudes J_i for neighboring Mn pairs in topological HgTe and nontopological CdTe, we find the remaining interband terms $J_{he,i}$ are rather small and predominantly antiferromagnetic, as shown in Fig. 1. This finding also explains, so far mysterious, results of *ab initio* studies, in particular, a change of the interaction sign when passing from the early to late transition metals in magnetically doped Bi-Sb chalcogenides.

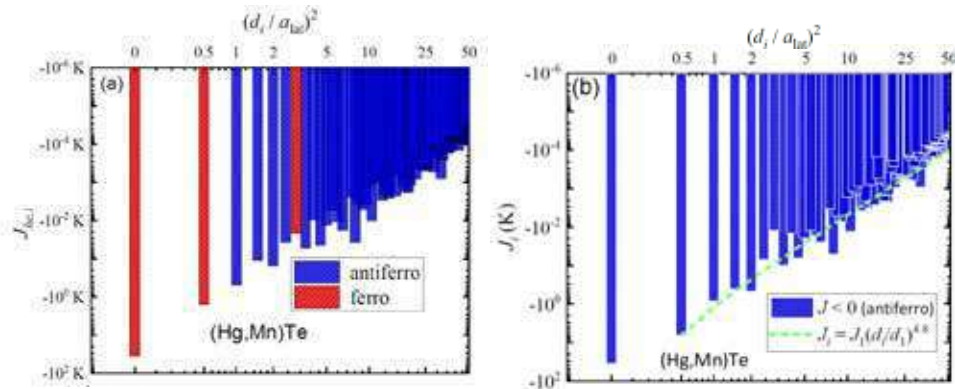


Figure 1: (a) Interband contribution $J_{he,i}$ to the total exchange energy J_i [shown in (b)] as a function of distance d_i between pairs of Mn ions in (Hg,Mn)Te [4-6]. Note a large magnitude of the irrelevant ferromagnetic $J_{he,i}$ term at $d_i = 0$.

- [1] He Ke, Yayu Wang, and Qi-Kun Xue, *Annu. Rev. Cond. Mat. Phys.* **9**, 329 (2018).
- [2] Y. Tokura, K. Yasuda, and A. Tsukazaki, *Nat. Rev. Phys.* **1**, 126 (2019).
- [3] Rui Yu, Wei Zhang, Hai-Jun Zhang, Shou-Cheng Zhang, Xi Dai, and Zhong Fang, *Science* **329**, 61 (2010).
- [4] C. Śliwa, C. Autieri, J. A. Majewski, and T. Dietl, *Phys. Rev. B* **104**, L220404 (2021).
- [5] C. Autieri, C.Śliwa, R.Islam, G.Cuono, and T.Dietl, *Phys. Rev. B* **103**, 115209 (2021).
- [6] C. Śliwa and T. Dietl, *Phys. Rev. B* **98**, 035105 (2018).

Quantum oscillation studies of magnetic kagome metals

Linda Ye¹

¹ *Department of Applied Physics, Stanford University, Stanford, CA 94305, USA*

As a close structural cousin to the honeycomb lattice, the two-dimensional kagome lattice model has long been theoretically known to harbor Dirac dispersions at its Brillouin zone corners; starting from these Dirac states, a rich variety of topological electronic states can be realized, with the interplay between spin-orbit coupling and (broken) time-reversal symmetry playing a key role. In recent years a class of metallic and semimetallic materials hosting kagome lattices of magnetic transition elements have been experimentally identified as host to a wide range of topological electronic features including quasi-two-dimensional massive Dirac fermions and three-dimensional Weyl semimetallic states with elevated ordering temperatures. In this talk we present experimental studies of such states through the lens of magneto-quantum oscillations in transport (Shubnikov-de Haas oscillations) and torque magnetometry (de Haas-van Alphen oscillations) [1-3]. Using the examples of ferromagnetic Fe₃Sn₂ [1], Co₃Sn₂S₂ [2] and antiferromagnetic FeSn [3], we demonstrate that high magnetic field fermiology provides a unique experimental tool for revealing an anisotropic interplay between magnetic moment orientation and the underlying electronic topology in these systems. We anticipate that the findings of our studies can be more broadly applied to improve the manipulation of topological states using magnetic order.

[1] L. Ye, M. K. Chan, R. D. McDonald, D. Graf, M. Kang, J. Liu, T. Suzuki, R. Comin, L. Fu, J. G. Checkelsky, *Nat. Commun.* **10**, 4870 (2019).

[2] L. Ye, J. I. Facio, M. P. Ghimire, M. K. Chan, J.-S. You, D. C. Bell, M. Richter, J. van den Brink, J. G. Checkelsky, *arXiv/2203.04254*

[3] M. Kang, L. Ye *et al.*, *Nat. Mater.* **19**, 163-169 (2019).

Oral Presentations

| | | |
|-----------------------------|---|-----|
| Wojciech Brzezicki | <i>Berry phase effects in the layered topological metals</i> | 649 |
| Nicholas Figueiredo-Prestes | <i>Spin-Orbit torques and magnetization switching in topological-insulator/2D-ferromagnet heterostructures: MBE-grown $\text{CrTe}_2/\text{Bi}_2\text{Te}_3$</i> | 650 |
| Jacob Gayles | <i>Hard magnet topological semimetals in XPt_3 compounds with the harmony of Berry curvature</i> | 651 |
| Rajibul Islam | <i>Axion insulating phase in superlattices without inversion symmetry</i> | 652 |
| Yixi Su | <i>Interplay between magnetism and topology in correlated topological materials</i> | 653 |
| Ashutosh Wadge | <i>Surface decorated Weyl semimetal: topological quantum Lifshitz transition</i> | 654 |
| Michael Wissmann | <i>Magnetic Properties of Intrinsic Magnetic Topological Insulators $\text{Mn}(\text{Bi,Sb})\text{Te}$</i> | 655 |
| Akinobu Yamaguchi | <i>Study on spin-orbit-torque-induced magnetization modulation using rectifying planar Hall effect</i> | 656 |

Berry phase effects in the layered topological metals

W. Brzezicki^{1,2}

¹*International Research Centre MagTop, Institute of Physics PAS, Warsaw, Poland*

²*Institute of Theoretical Physics, Jagiellonian University, Kraków, Poland*

We study the effects related to the Berry phases along Fermi cross-sections in two types of systems: (i) 2D heterostructures of transition metal oxides [1,2] and (ii) multilayers of topological crystalline insulator SnTe [3]. In case (i) we relate the observed sign change of the Hall conductance to the topology of the occupied bands that is affected by the charge pinning of the interface layer, see Fig. 1, whereas in case (ii) we show that mirror symmetry breaking can explain the observed magnetotransport properties of the system via weak antilocalization mechanism.

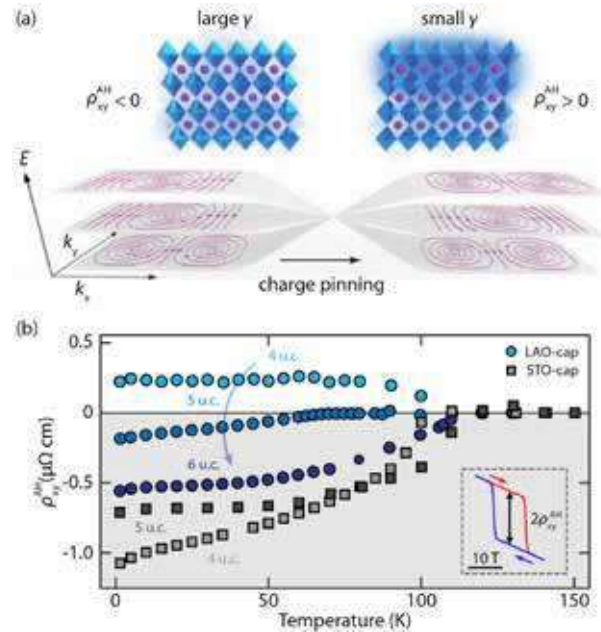


Figure 1: (a) Illustration of the evolution of the momentum-space topological charges. Upon increasing the charge pinning, the system moves through a Weyl point in the synthetic space spanned by k_x , k_y and the charge pinning parameter γ . (b) The measured anomalous Hall resistivity ρ_{xy} for SRO films of varying thickness capped by both STO and LAO as a function of temperature. The inset in (b) shows an example of the magnetic-field dependence of the AHE, from which the amplitude ρ_{xy} is extracted.

- [1] T. C. van Thiel, W. Brzezicki, *et al.*, Phys. Rev. Lett. **127**, 127202 (2021).
- [2] D. J. Groenendijk, C. Autieri, T. C. van Thiel, W. Brzezicki, *et al.*, Phys. Rev. Res. **2**, 023404 (2020).
- [3] A. Kazakov, W. Brzezicki, T. Hyart, *et al.*, Phys. Rev. B **103**, 245307 (2021).

Spin-Orbit torques and magnetization switching in topological-insulator/2D-ferromagnet heterostructures: MBE-grown CrTe₂/Bi₂Te₃

N. Figueredo-Prestes¹, S. Krishnia¹, P. Tsipas², P. Pappas², J. Peiro¹, V. Zatzko¹, N. Reyren¹, H. Jaffrès¹, P. Seneor¹, A. Dimoulas², J.-M. George¹

¹ *Unité Mixte de Physique, CNRS, Thales, Université Paris-Saclay, 91767, Palaiseau, France.*

² *National Center for Scientific Research DEMOKRITOS, Institute of Nanoscience and Nanotechnology, 15341, Athens, Greece.*

One of the main goals of spintronics is the efficient control of magnetization states in nanoscale devices. In the last two decades, several materials and mechanism have been explored to that end. One class of such materials are the so-called topological insulators (TI), materials characterized by topologically non-trivial electronic valence states at their surface [1] and spin-momentum-locked topological surface states (TSS). The use of two-dimensional Van-der-Waals ferromagnets (2D-FM) have been proposed as a possible way to reduce the magnetic coupling at the TI/FM interface and hence preserve the topological nature of the polarized TSS. We investigated the magneto-transport properties of the TI/2D-FM heterostructure CrTe₂/Bi₂Te₃ grown by MBE on a sapphire substrate covered by a WS₂ buffer layer. In this work, we report about magnetoresistance, current induced magnetization switching and evaluation of the SOT by second-harmonic measurements in this heterostructure.

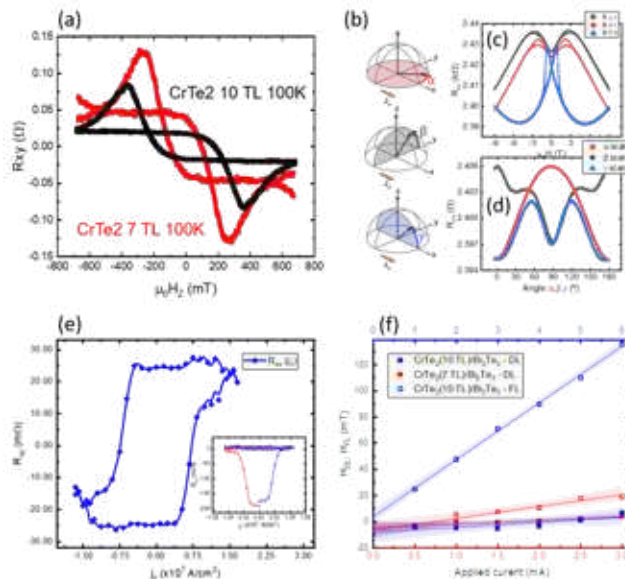


FIGURE 1. (a) AHE curves for CrTe₂ (7 or 10 TL)/Bi₂Te₃ samples. (b) Schematics defining the angle conventions of the magnetoresistance measurements. (c) and (d) longitudinal resistance (R_{xx}) for CrTe₂ (7 ML)/Bi₂Te₃ as a function of the applied field and its angle. (e) Hall resistance a function of the pulsed current intensity at 140 K with an external in-plane field of 120 mT. Inset: the same in absence of field. (f) Extracted DL and FL field amplitudes from 2nd harmonic torque measurements at 15K as a function of the applied current.

First of all, we report the observation of a signal similar topological Hall effect (THE), Fig. 1(a). The THE-like signal could be the signature of the emergence of a skyrmion-rich phase due to enhancement of the DMI at the interface and/or the presence of additional interface-induced contributions to the AHE. The presence of interfacial components to the magnetoresistance curves and the high levels of FL torque, Fig. (b-d) and (f), suggest either the persistence of the topological surface states from the TI film or the occurrence of Rashba states in the 2D-FM/TI interface. Also, the interfacial charge-to-spin conversion leads to current-induced magnetization switching in CrTe₂/Bi₂Te₃, making this heterostructure suitable for further study aiming for spintronic applications.

[1] Mogi, M., Yasuda, K., Fujimura, R. et al., Nat. Comm. **12**, 1404 (2021).

Hard magnet topological semimetals in XPt_3 compounds with the harmony of Berry curvature

Jacob Gayles¹, Bushra Sabir¹, Anastasios Markou², Yan Sun², and Claudia Felser²

¹*University of South Florida Tampa, Florida*

²*Max Planck Institute for Chemical Physics of Solids, Dresden, Germany*

Topological magnetic semimetals, like $\text{Co}_3\text{Sn}_2\text{S}_2$ and Co_2MnGa , display exotic transport properties, such as large intrinsic anomalous (AHE) due to uncompensated Berry curvature. The highly symmetric XPt_3 compounds display anti-crossing gapped nodal lines, a driving mechanism in the intrinsic Berry curvature Hall effects. Uniquely, these compounds contain two sets of gapped nodal lines that harmoniously dominate the Berry curvature in this complex multi-band system. We calculate a maximum AHE of 1965 S/cm in the CrPt_3 by a state-of-the-art first principle electronic structure. We also find the topological structure and the magnetic interactions are significantly disturbed by strain. We have grown high-quality thin films by magnetron sputtering and measured a robust AHE of 1750 S/cm for different sputtering growth conditions. Additionally, the cubic films display a hard magnetic axis along [111] direction. The facile and scalable fabrication of these materials makes them ideal candidates for integration into topological devices

Axion insulating phase in superlattices without inversion symmetry

**Rajibul Islam¹, Sougata Mardanya², Alexander Lau¹, Giuseppe Cuono¹,
Tay-Rong Chang², Carlo M. Canali³, Bahadur Singh⁴, Tomasz Dietl^{1,5} and
Carmine Autieri^{1,6}**

¹*International Research Centre MagTop, Institute of Physics, Polish Academy of Sciences,
Aleja Lotnikow 32/46, PL-02668 Warsaw, Poland*

²*Department of Physics, National Cheng Kung University, Tainan 70101, Taiwan*

³*Department of Physics and Electrical Engineering, Linnaeus University, 392 31 Kalmar,
Sweden*

⁴*Department of Condensed Matter Physics and Materials Science, Tata Institute of
Fundamental Research, Colaba, Mumbai 400005, India.*

⁵*WPI-Advanced Institute for Materials Research, Tohoku University, Sendai 980-8577, Japan*

⁶*Consiglio Nazionale delle Ricerche CNR-SPIN, UOS Salerno, I-84084 Fisciano (Salerno),
Italy*

We have studied the interplay between magnetism and topology in HgTe/MnTe 3D superlattice (SL). Our results show the evaluation of exotic magnetic topological phase in presence of magnetism in the HgTe/MnTe zinc blende 3D SL. The axion insulator phase is observed with anti-ferromagnetic order in both in-plane and out-of-plane magnetization direction, axion states are protected by the combination of a C_2 rotation and time-reversal symmetries $S_2=C_2.T$, the surface protected by S_2 symmetry shows an exotic gapless Dirac cone where as other surface shows Dirac cone. In presence of ferromagnetism, it shows a magnetic Weyl semimetal and magnetic nodal-line semimetal with out of plane and in-plane magnetization direction. We have observed large anomalous Hall conductivity in presence of ferromagnetism in 3D SL. The same crystalline symmetry plays an important role in protected semimetallic phase.

Interplay between magnetism and topology in correlated topological materials

Fengfeng Zhu¹, Xiao Wang¹, Yishui Zhou¹, Thomas Mueller¹, Sabreen Hammouda¹, Adrian Merritt¹, Lichuan Zhang², Yuriy Mokrousov², Stefan Blügel², Thomas Brückel³, Yixi Su¹

¹ Jülich Centre for Neutron Science JCNS at MLZ, Forschungszentrum Jülich, Lichtenbergstr. 1, D-85747 Garching, Germany

² Peter Grünberg Institute (PGI-1), Forschungszentrum Jülich, D-52425 Jülich, Germany

³ Jülich Centre for Neutron Science (JCNS-2) and Peter Grünberg Institute (PGI-4), Forschungszentrum Jülich, D-52425 Jülich, Germany

Recent theoretical predictions and experimental realizations of exotic fermions and topologically protected phases in condensed matter have led to tremendous research interests in topological quantum materials. Especially, correlated topological materials, such as magnetic Dirac and Weyl semimetals, and intrinsic magnetic topological insulators etc., in which both non-trivial topology of single-electron band structures and electronic correlation effects are essential for the underlying physics, have emerged as an exciting platform to explore novel electronic and magnetic phenomena.

In this talk, we will present a couple of the selected examples of our recent neutron scattering studies of novel correlated topological materials. In the Dirac semimetal EuMnBi₂ [1] and magnetic Weyl semimetal Mn₃Sn, an unusual impact of magnetism on the topological fermions has been revealed via extensive single-crystal neutron diffraction studies. Furthermore, via a comprehensive inelastic neutron scattering study and theoretical analysis of the spin-wave excitations, we report the experimental realization of exotic topological magnon insulators in the two-dimensional van der Waals honeycomb ferromagnets CrSiTe₃ and CrGeTe₃ [2]. The emergence of topological magnon properties in these compounds are due to the presence of the sizeable antisymmetric Dzyaloshinskii-Moriya (DM) interactions. The nontrivial nature and intrinsic tunability of the gap opening at the magnon band-crossing Dirac points are confirmed, while the emergence of the corresponding in-gap topological edge states is demonstrated theoretically. The fascinating interplay between magnetism, electronic correlation and band-structure topology can be clearly demonstrated from our neutron scattering studies of these magnetic topological materials.

We would like to also thank the contributions from other co-workers and collaborators: Junda Song, Karin Schmalzl, Wolfgang Schmidt, Martin Meven, Alexandre Ivanov, Jitae Park and Jianhui Xu, Jia Ma, Changjiang Yi, Youguo Shi *et al.*

[1] Fengfeng Zhu, *et al.*, Phys. Rev. Research **2**, 043100 (2020).

[2] Fengfeng Zhu, *et al.*, Sci. Adv. **7**, eabi7532 (2021).

Surface decorated Weyl semimetal: topological quantum Lifshitz transition

A. S. Wadge^{1*}, B. J. Kowalski², C. Autieri¹, P. Iwanowski^{1,2}, A. Hruban², N. Olszowska³, M. Rosmus³, J. Kołodziej³ and A. Wiśniewski^{1,2}

¹International Research Centre MagTop, Institute of Physics, Polish Academy of Sciences, Aleja Lotników 32/46, PL-02668 Warsaw, Poland

²Institute of Physics, Polish Academy of Sciences, Aleja Lotników 32/46, PL-02668 Warsaw, Poland

³National Synchrotron Radiation Centre SOLARIS, Jagiellonian University, Czerwone Maki 98, PL-30392 Cracow, Poland

An idea of proximity induced superconductivity in Weyl semimetals (WSM) is recently developed in order to obtain Majorana zero bias states [1]. Thus it is essential to manipulate and control the surface states in WSM [2]. To detect them, the angle resolved photoemission spectroscopic measurements were taken on cleaved single crystal of NbP, which has two possible terminations P and Nb [3]. These terminations were separately covered with Pb and Nb to observe the corresponding changes. One mono-layer (ML) Pb deposited on P-terminated NbP showed strong Fermi surface modifications whereas 0.8 ML of Nb on another P-terminated NbP crystal showed the change in a constant energy contour. In both systems, the cause of those modifications was due to topological quantum Lifshitz transition (TQLT). In case of Nb-terminated NbP covered with 1.9 ML of Pb, topological characteristics were preserved with manipulated surface states. In conclusion, we showed the capability of direct manipulating and controlling surface states in WSM via surface decoration [4].

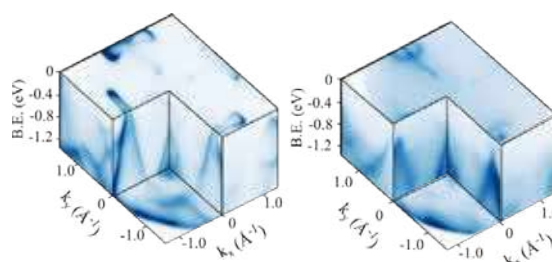


Figure 1: Comparison of 3D intensity plots before and after one ML of Pb decorated on (0 0 1) surface of P-terminated NbP

[1] G. Grabecki, A. Dabrowski, P. Iwanowski, A. Hruban, B. J. Kowalski, N. Olszowska, J. Kołodziej, M. Chojnacki, K. Dybko, A. Łusakowski, T. Wojtowicz, T. Wojciechowski, R. Jakiela, and A. Wiśniewski, *Phys. Rev. B* **101**, 085113 (2020).

[2] H. F. Yang, L. X. Yang, Z. K. Liu, Y. Sun, C. Chen, H. Peng, M. Schmidt, D. Prabhakaran, B. A. Bernevig, C. Felser, B. H. Yan, and Y. L. Chen, *Nat. Commun.* **10**, 3478 (2019).

[3] Y. Sun, S. C. Wu, and B. Yan, *Phys. Rev. B* **92**, 115428 (2015).

[4] A. S. Wadge, B. J. Kowalski, C. Autieri, P. Iwanowski, A. Hruban, N. Olszowska, M. Rosmus, J. Kołodziej and A. Wiśniewski (<https://doi.org/10.48550/arXiv.2202.06061>).

Magnetic Properties of Intrinsic Magnetic Topological Insulators Mn(Bi,Sb)Te

Michael Wissmann^{1,2}, Aoyu Tan^{1,2}, Joseph Dufouleur², Anna Isaeva³ and Romain Giraud^{1,2}

¹ Université Grenoble-Alpes, CNRS, CEA, SPINTEC, F-38000 Grenoble, France

² Leibniz Institute for Solid State and Materials Research IFW Dresden, 01069 Dresden, Germany

³ Department of Physics and Astronomy, University of Amsterdam, 1098 XH Amsterdam, Netherlands

The new family of intrinsically magnetic van-der-Waals layered topological insulators Mn(Bi,Sb)Te, with strong spin-orbit coupling, is of great interest to investigate the interplay between topology and magnetic order in electronic band structures [1]. When introducing magnetism into a 3D topological insulator, the combination of an exchange gap and of a modified crystal symmetry can generate topological quantum states like the quantum anomalous Hall effect (QAH) or the axion insulator [2], which can be modified by tuning the magnetization.

Using magneto-transport measurements, we investigated the magnetic properties of thin nanostructures exfoliated from two representative members of this family, MnBi₂Te₄ and MnBi₄Te₇, which are stacks of 2D ferromagnets with antiferromagnetic interlayer exchange interaction. The latter has an intercalation Bi₂Te₃ layer that weakens the interlayer exchange interaction, and we revealed the formation of a meta-magnetic state [3] with a fully saturated remnant magnetization below 5K, of interest for the QAH in zero magnetic field.

Our more recent studies also consider the MnSb₂Te₄ compound, a ferromagnet with a perpendicular-to-plane anisotropy and a critical Curie-Weiss temperature as high as 35K. MnSb₂Te₄ has been controversially discussed to be a magnetic Weyl semimetal or a candidate to realize the axion insulator [4,5]. We investigated the thickness-dependent properties of exfoliated nanoflakes using magneto-transport, revealing the change in important parameters such as the resistivity, the Curie temperature and the magnetic coercive field. The influence of both the intrinsic electrical doping and disorder in magnetic topological insulators is considered as well.

This work was supported by the European Commission via the TOCHA project H2020-FETPRO ACT-01-2018 under Grant Agreement No. 824140 and by the SPINTEC-IFW laboratory association “SPINMAT”.

[1] Otrokov et al., *Nature* **576**, 416–422 (2019)

[2] Li et al., *Sci. Adv.* **5**, 6 (2019)

[3] Tan et al., *PRL* **124**, 197201 (2020)

[4] Murakami et al., *Phys. Rev. B* **100**, 195103 (2019)

[5] Ereemeev et al., *J. Phys. Chem. Lett.* **12** (17), 4268–4277 (2021)

Study on spin-orbit-torque-induced magnetization modulation using rectifying planar Hall effect

Akinobu Yamaguchi ¹, Nobuko Matsumoto ², Wataru Yoshikawa ², Yasuhisa Fujii ²

¹ University of Hyogo, 3-1-2, Kouto, Kamigori, Hyogo, Japan

² KRI inc., 134 Chudoujiminamimachi, Kyoto, Kyoto, Japan

The control of magnetization modulation or reversal has attracted much attention for not only fundamental researches but also engineering application such as modern data processing and recording [1]. It has been discovered that magnetization dynamics can be excited by spin torque and spin-orbit-torque (SOT), and its application is drawing attention. The SOT-induced magnetization reversal of in-plane free magnetic layers has been experimentally investigated. In these systems, the planar Hall effect (PHE) allows the detection and evaluation for the quantitative SOT. Recent studies of thin film trilayer systems comprised of a normal metal (NM), an antiferromagnetic insulator (AFM), and a ferromagnetic layer (F) revealed spin Hall magnetoresistance, originating from the interplay between NM/F is affected by the magnetization orientation in the F when the NM consisting of heavy element metal such as Pt and Ta induces a spin current via the spin Hall effect originated from the in-plane charge current [2].

In this study, to study the SOT-induced magnetization modulation through the AFM layer, we measure the rectifying PHE voltage of cross-shaped multilayer wires. Using electron-beam lithography and a lift-off process, we fabricated the following system comprising 25-nm-thick $\text{Ni}_{81}\text{Fe}_{19}$ /3-nm-thick NiO /5-nm-thick $\text{Ni}_{81}\text{Fe}_{19}$ /Pt electrode on Si/SiO_2 substrate. An external magnetic field was applied at an angle θ from one axis of the cross, which was fixed parallel along to rf + dc electric current. Figures 1(a) and 1(b) show the rectifying anisotropic magnetoresistance (AMR) and PHE voltage spectra, respectively. The magnetic field angle dependences of these rectifying voltages are in good agreement with the analytical prediction curves of $\sin 2\theta \cos \theta$ and $\cos 2\theta \cos \theta$. [1] Next, we measured dc current dependence of the PHE spectra. As shown in Figs. 1(c) and 1(d), the spectral shape strongly depends on the dc current.

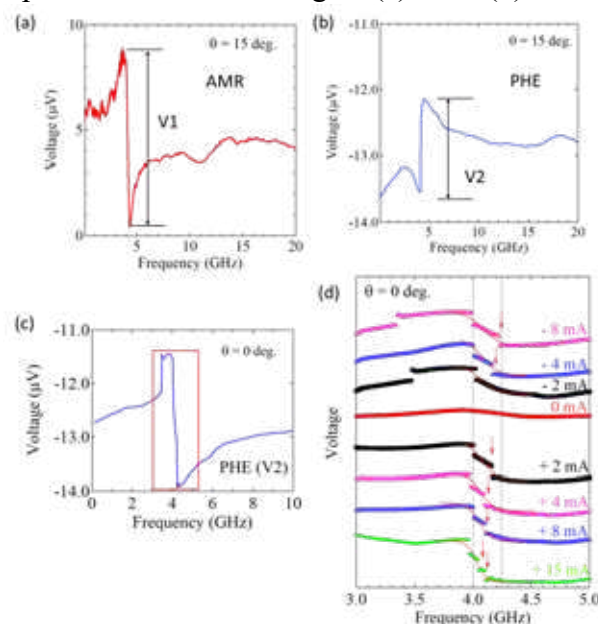


Figure 1: Rectifying (a) AMR and (b) PHE spectra. (c) PHE spectrum at $\theta = 0$ deg in the absence of dc current. (d) dc current dependence of rectifying PHE spectra.

Since the dc current dependence of the resonance frequency is linear, there is almost no effect of Joule heating generation, and it is considered that the modulation effect of the magnetization dynamics by SOT is observed.

These results indicate that the efficient spin current transmission even through NiO layer. This result shed light on the study of spin current in AFM and engineering applications in the future high frequency communication system.

[1] A. Yamaguchi, A. Hirohata, B. Stadler, *Nanomagnetic Materials: Fabrication, Characterization and application*, Elsevier, 2021.

[2] X. Qiu, K. Narayanapillai, Y. Wu, P. Deorani, D. -H. Yang, W. -S. Noh, J. H. Park, K. -J. Lee, H. -W. Lee, and H. Yang, *Nat. Nanotechnol.* **10**, 333 (2015).

Posters

| | | |
|------------------------|--|-----|
| Kacho Imtiyaz Ali Khan | <i>Topological Kagome ferromagnet Fe₃Sn₂ grown on Si-SiO₂ substrates using Pt seed layer.</i> | 658 |
| Aleksandr Kazakov | <i>Magnetotransport in Ferromagnetic Topological Crystalline Insulator Sn_{1-x}MnxTe Thin Films</i> | 659 |
| PardeepKumar Tanwar | <i>Chiral zero sound – a new mechanism for heat conduction in Weyl semimetal NbP</i> | 660 |
| Akinobu Yamaguchi | <i>Spin transport properties in multilayer including Pt and NiO layers</i> | 661 |

Topological Kagome ferromagnet Fe_3Sn_2 grown on Si-SiO₂ substrates using Pt seed layer

Kacho Imtiyaz Ali Khan¹, Ram Singh Yadav¹, Himanshu Bangar¹, Akash Kumar¹, Niru Chowdhury¹, Prasanta Kumar Muduli² and Pranaba Kishor Muduli¹

¹ Indian Institute of Technology Delhi, Hauz Khas, New Delhi, India

² Indian Institute of Technology Madras, Chennai, Tamil Nadu, India

Fe_3Sn_2 , a Kagome ferromagnet, is a potential quantum material with intriguing topological features [1-3]. Despite substantial experimental work on the bulk single crystals thin film growth of Fe_3Sn_2 remains relatively unexplored. Here, we investigate the effect of two different seed layer (Ta and Pt) on the growth of Fe_3Sn_2 thin films. We demonstrate growth of polycrystalline Fe_3Sn_2 thin films on Si/SiO₂ substrates by room temperature sputter deposition, followed by in-situ annealing at 500 °C. In Figure 1(a, b), our structural and magnetic measurements indicate that a pure ferromagnetic phase is formed for Pt/ Fe_3Sn_2 thin film while a mixed phase (consisting of ferromagnetic, Fe_3Sn_2 and antiferromagnetic, FeSn) is formed for Ta/ Fe_3Sn_2 . Fe_3Sn_2 films grown on Pt seed layer exhibit large magneto-transport properties (summarized in Table 1), indicating an intrinsic mechanism of anomalous Hall effect originating from Berry curvature. These results highlight the choice of seed layer is crucial for realizing novel topological spintronic devices on a CMOS compatible substrate.

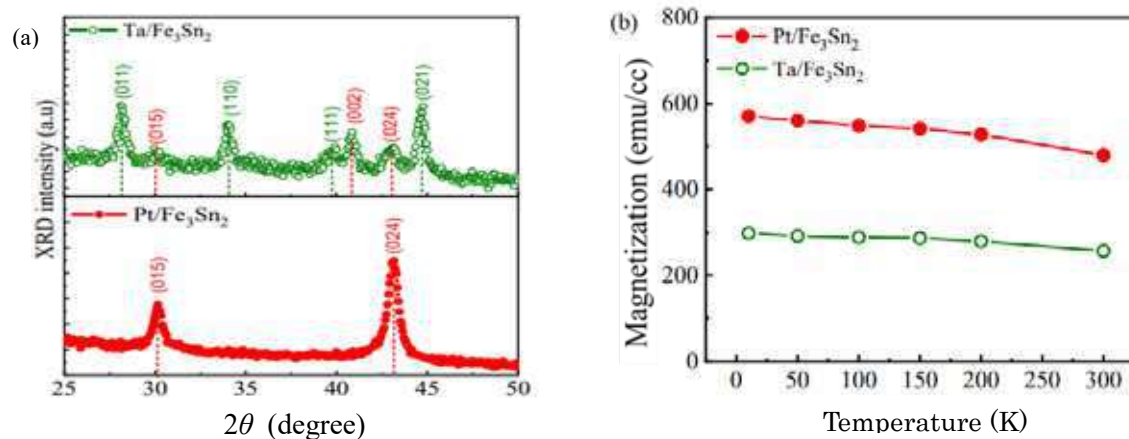


Figure 1: (a) GIXRD pattern for the Fe_3Sn_2 thin films deposited on Ta and Pt seed layers. Both the films are grown at room temperature and annealed at 500 °C for 1 hour. The Magnetization – Temperature curve for both the thin films over the temperature range of 5 - 350 K.

Table 1: Comparison of extracted magneto-transport properties at room temperature from AHE measurement for Pt/ Fe_3Sn_2 and Ta/ Fe_3Sn_2 thin films.

| Sample | Magnetic phase | M_s (emu/cc) | ρ_{xy}^{AHE} ($\mu\Omega \text{ cm}$) | $\sigma_{xy}^{\text{int.}}$ ($\Omega^{-1} \text{ cm}^{-1}$) | R_s ($10^{-10} \Omega^{-1} \text{ cm}^{-1} \text{ G}^{-1}$) |
|------------------------------|----------------|----------------|---|---|---|
| Pt/ Fe_3Sn_2 | FM | 464 | 1.91 ± 0.02 | 23 ± 11 | 2.6 |
| Ta/ Fe_3Sn_2 | AFM+FM | 240 | 1.41 ± 0.01 | 5 ± 0.5 | 3.6 |

Reference

- [1] Kang, M., Fang, S., Ye, L. et al., *Nat. Mater.* **19**, 163 (2020).
- [2] Ghimire, N.J., Mazin, I.I., *Nat. Mater.* **19**, 137 (2020)
- [3] Ye, L., Chan, M.K., McDonald, R.D. et al., *Nat. Commun.* **10**, 4870 (2019).

Magnetotransport in Ferromagnetic Topological Crystalline Insulator $\text{Sn}_{1-x}\text{Mn}_x\text{Te}$ Thin Films

A. Kazakov¹, V.V. Volobuev¹, M. Zięba², B. Turowski¹, W. Zaleszczyk^{1,2},
T. Wojciechowski^{1,2}, K. Gas², M. Sawicki², T. Story^{1,2}, T. Wojtowicz¹

¹International Research Centre MagTop, Institute of Physics, Polish Academy of Sciences,
al. Lotników 32/46, 02-668 Warsaw, Poland

²Institute of Physics, Polish Academy of Sciences, al. Lotników 32/46, 02-668 Warsaw, Poland

$\text{Sn}_{1-x}\text{Mn}_x\text{Te}$ is a IV-VI semimagnetic semiconductor, that is based on the archetypical topological crystalline insulator SnTe on the one hand, and exhibits a ferromagnetic order at low temperature on the other hand. It is known, that anomalous contribution to the Hall effect, the so-called anomalous Hall effect (AHE), is observed in magnetic materials. AHE is a unique experimental tool because it depends on both electronic and magnetic properties of the conductor. In the present work, a systematic study of the AHE in $\text{Sn}_{1-x}\text{Mn}_x\text{Te}$ epilayers was carried out as a function of Mn content x .

High-quality $\text{Sn}_{1-x}\text{Mn}_x\text{Te}$ epilayers were grown on (111)-oriented BaF_2 substrates using molecular beam epitaxy (MBE). The thickness of all epilayers was 1 μm , and Mn content varied from 0 to 10%. An increase in Mn content results in increased longitudinal resistance R (not shown) as well as increased residual scattering, which causes weaker temperature dependence. This is confirmed by determination of the residual resistivity ratio for the measured films, which is weaker for films with higher Mn content. The ferromagnetic phase transition is well seen in the magnetotransport behavior at low temperatures.

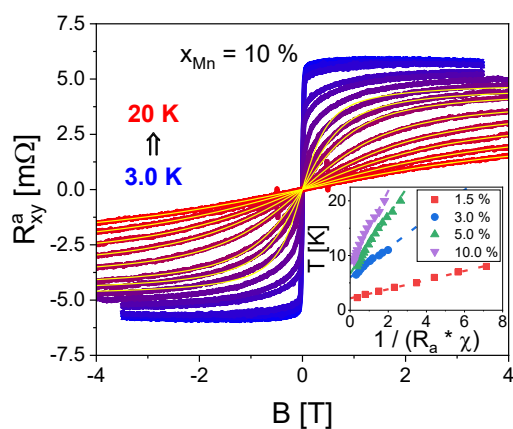


Figure 1: AHE contribution to the Hall resistance R_{xy}^a in $\text{Sn}_{0.9}\text{Mn}_{0.1}\text{Te}$ measured as a function of the magnetic field B for various temperatures (yellow lines are Langevin fits). Inset depicts determination of the Curie temperature from plots of the inverse susceptibility (χ) multiplied by anomalous Hall constant (R_a).

Magnetotransport properties systematically evolve with increasing Mn content, e.g. the negative magnetoresistance becomes more pronounced for higher Mn concentrations. Anomalous Hall effect was observed in all the studied films containing Mn. The high temperature Hall curves were fitted using Langevin function, and the fitting results were used to determine the Curie temperature T_C from the plots of the inverse susceptibility (χ) multiplied by anomalous Hall constant (R_a). Both the Curie temperature and the AHE contribution to the Hall resistance increase with increasing Mn content. Overall, magnetotransport properties agree well with the results of SQUID measurements. AHE coefficients were extracted from the experimental data and their behavior was analyzed.

This research was partially supported by the Foundation for Polish Science through the IRA Programme co-financed by EU within SG OP (Grant No. MAB/2017/1) and by the NCN Grant: UMO 2017/27/B/ST3/02470.

Chiral zero sound – a new mechanism for heat conduction in Weyl semimetal NbP

Pardeep Kumar Tanwar¹, Md Shahin Alam¹, Dariusz Kaczorowski² and Marcin Matusiak^{1,2}

¹*International Research Centre MagTop, Institute of Physics, Polish Academy of Sciences, Aleja Lotnikow 32/46, 02-668 Warsaw, Poland*

²*Institute of Low Temperature and Structure Research, Polish Academy of Sciences, ul. Okolna 2, 50-422 Wroclaw, Poland*

Weyl semimetals, as a topologically non-trivial form of matter, are characterized by linearly dispersed bands in energy and momentum space. In addition, a Weyl semimetal with multiple pairs of Weyl nodes can host the low energy chargeless-topological excitations. These excitations were studied by measuring the thermal and electrical conductivities (κ and σ , respectively) in the Weyl semimetal NbP. The magnetic field (B) and thermal gradient (and electric current) was applied parallel to $[0\ 0\ 1]$ direction. In the low-temperature regime, the electrical conductivity $\sigma(B)$ and thermal conductivity $\kappa(B)$ exhibit quantum oscillations with frequencies: 4.6 (F1), 12 (F2), 30 (F3), 38 (F4) and 58 (2F3) T for the former, and 15 (F2) 30 (F3) for the latter. The frequencies of $\kappa(B)$ match and antiphase with two of several frequencies determined from the Shubnikov – de Haas effect. Both matching frequencies originate from the electron pocket enclosing a pair of Weyl nodes.

At low temperature, the magnitude of $\kappa(B)$ turns out to be two orders larger than the electronic contribution of thermal conductivity, $\kappa_e(B)$ calculated using the Wiedemann – Franz law. A thorough analysis indicates that other contributions like phononic and ambipolar are less pronounced. We ascribed such a huge difference between $\kappa(B)$ and $\kappa_e(B)$ to a recently postulated additional heat channel emerging as a result of the chargeless-topological excitation called chiral zero sound effect.

Spin transport properties in multilayer including Pt and NiO layers

Akinobu Yamaguchi

University of Hyogo, 3-1-2, Kouto, Kamigori, Hyogo, Japan

Manipulation of magnetic properties and its dynamics in magnets have attracted a great deal of attention in various fields such as energy power systems and spintronic devices. When combined with spin-orbit coupling, they give rise to spin-orbit torques (SOTs) which are more powerful tool for magnetization control. Therefore, the SOT, which is mostly based on the spin Hall effect, paves the way to develop the engineering applications. Recently, the planar Hall effect (PHE) also allows the detection of magnetization reversal induced by the SOT. In particular, the PHE can provide a very simple detection method and evaluation for the quantitative SOT. Recent studies of thin film trilayer systems comprised of a normal metal (NM), an antiferromagnetic insulator (AFM), and a ferromagnetic insulator (FI) revealed spin Hall magnetoresistance, originating from the interplay between the spin accumulation at the interface [1]. Here, the spin accumulation induced at the interface between NM/FI is affected by the magnetization orientation in the FI when the NM consisting of a heavy element metal such as Pt and Ta induces a spin current via the spin Hall effect by the in-plane charge current.

Here, to study the SOT-induced magnetization reversal or magnetization modulation, we measured the PHE of cross-shaped multilayer structure as schematically illustrated in Fig. 1(a). Using electron-beam lithography and a lift-off process, we fabricated two following systems comprising (a) 15-nm-thick $\text{Ni}_{81}\text{Fe}_{19}$ /60-nm-thick NiO/4-nm-thick Pt and (b) 15-nm-thick $\text{Ni}_{81}\text{Fe}_{19}$ /60-nm-thick NiO/4-nm-thick Ta on Si/SiO_2 substrates, respectively. The width of cross was 8 μm . An external magnetic field was applied at an angle of θ from one axis of the cross, which was fixed parallel along to ac + dc electric current flow direction. Ac current with 255 Hz and 1.4 μA was fixed, and dc current was varied from -400 μA to +400 μA every 40 μA step. All measurements were performed at room temperature.

Figures 1(b) and 1(c) show a typical PHE voltage as a function of magnetic field at $\theta = 30^\circ$. Here, the dc electric current dependence of PHE voltages are vertically shifted for easy viewing. However, the signs of PHE hysteresis curves are displayed without any change. Comparing these results, it can be seen that the baseline sign inversion occurs in Pt and Ta top-layer of multilayers. This is attributable to that spin Hall angle characteristics. These results indicate that the efficient spin current transmission even through NiO layer. This result sheds light on the study of spin current in AFMs.

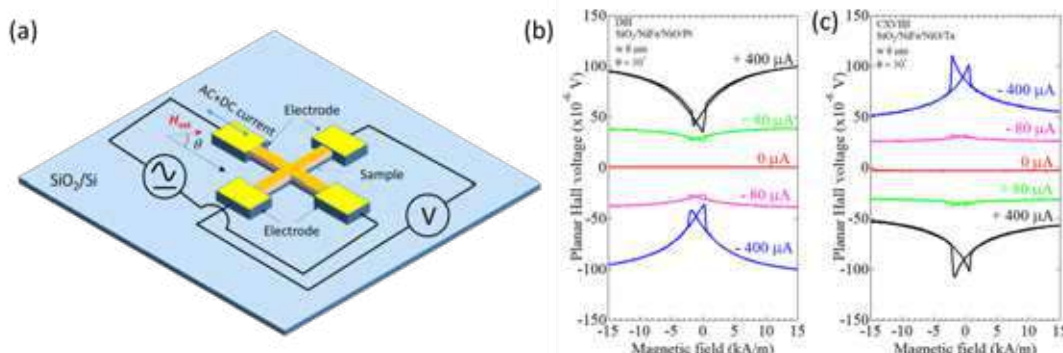


Fig1. (a) Schematic of measurement setup. PHE voltage measured by magnetic field sweeping for (a) $\text{SiO}_2/\text{NiFe}/\text{NiO}/\text{Pt}$ and (b) $\text{SiO}_2/\text{NiFe}/\text{NiO}/\text{Ta}$ at $\theta = 30^\circ$.

[1] D. Hou, Z. Qiu, J. Barker, K. Sato, K. Yamamoto, S. Vélez, J. M. Gomez-Perez, L. E. Hueso, F. Casanova, and E. Saitoh, *Phys. Rev. Lett.* **118**, 147202 (2017).

Symposium 17. Multifunctional and magnetoelastic magnetic materials, complex oxides, multiferroics and composite multiferroics

| | | |
|------------------------|---|-----|
| Gael Bastien | <i>Quasi-bidimensional lattices of magnetic and electric dipolar moments in $\text{EuAl}_{12}\text{O}_{19}$</i> | 665 |
| Gustav Bihlmayer | <i>(Super)conducting filaments in reduced SrTiO_3: local polarization and electronic properties</i> | 666 |
| Gabriel Chaves-O'Flynn | <i>Energy Landscape of Nanodisks with Dzyaloshinskii-Moriya Interaction and Perpendicular Magnetic Anisotropy</i> | 667 |
| Piotr Kuświk | <i>Artificial Magnetic Domains Without Domain Walls in Rare Earth-Transition Metal Films Patterned by Ion Bombardment</i> | 668 |
| Andrzej Szewczyk | <i>Low-temperature magnetic phase transition in $\text{TbAl}_3(\text{BO}_3)_4$ - quantum and classical aspects</i> | 669 |
| Carmine Autieri | <i>Electronic, charge and topological reconstructions at the oxide interfaces</i> | 671 |
| João H. Belo | <i>Mastering negative thermal expansion via tunable induced strain in $\text{La}(\text{Fe,Si})_{13}$-based compounds</i> | 672 |
| Francesca Casoli | <i>Effect of Nanoindentation on Martensitic Phase Transition of Heusler Films Studied by High-Resolution Imaging in Temperature</i> | 673 |
| Erik Cizmar | <i>Magnetic phase transitions in multiferroic perovskite solid solutions based on BiFeO_3</i> | 674 |
| Bogdan Dabrowski | <i>Search For the Single-ion Displacive-type Perovskite Multiferroics</i> | 675 |
| Deepak Dagur | <i>Light-induced Magnetic Modifications in Ni/PMN-PT Multiferroic Heterostructure</i> | 676 |
| Anaïs Guerenneur | <i>Measuring the magnetoelectric coupling of piezoelectric/magnetostrictive nanostructures using the anisotropic magnetoresistance effect</i> | 677 |
| Oleg Heczko | <i>Antiphase Boundaries in Ni-Mn-Ga Single Crystal Exhibiting Magnetic Shape Memory Effects</i> | 678 |
| Jasnamol Palakkal | <i>Interplay between the two magnetic phases of $\text{La}_2\text{NiMnO}_6$ and their impact on the oxygen evolution reaction</i> | 679 |
| Lukas Pfeuffer | <i>Material and microstructure design for a multicaloric cooling cycle which exploits thermal hysteresis</i> | 680 |
| Neenu Prasannan | <i>Evolution of structural and magnetic properties in electron-doped Ruddlesden Popper based bilayer manganite $\text{Ca}_{2-x}\text{Nd}_x\text{Mn}_2\text{O}_7$</i> | 681 |
| Patrick Schöffmann | <i>Contribution of charge and strain coupling in artificial multiferroic $\text{Fe}_3\text{O}_4/\text{PMN-PT}$ heterostructures</i> | 682 |
| Witold Skowronski | <i>Multiferroicity and Magnetization Dynamics in Fe/BTO/LSMO Tunnel Junction</i> | 683 |
| Andrzej Wisniewski | <i>Impact of pressure on magnetic properties of compensated GdCrO_3 ferrimagnet</i> | 684 |
| Hatem Ben Mahmoud | <i>Magneto-mechanical properties of thin films on stretchable substrate measured by in situ MOKE</i> | 686 |
| Nico Dix | <i>Low temperature magnetic transition and spin-lattice coupling in $\varepsilon\text{-Fe}_2\text{O}_3$ epitaxial thin films</i> | 687 |

| | | |
|-----------------------|---|-----|
| Borislava Geogieva | <i>Effect of half substitution with nickel for magnesium on the magnetic properties of Y-type $Ba_{0.5}Sr_{1.5}NiMgFe_{12}O_{22}$ hexaferrite synthesized by citric acid sol-gel auto-combustion</i> | 688 |
| Iwona Lazar | <i>Defect-driven magnetic properties of PZT single crystals</i> | 689 |
| Dominik Legut | <i>MAELAS: MAgneto-ELAStic properties calculation via computational high-throughput approach</i> | 690 |
| Matilde Saura-Múzquiz | <i>Phase transition, hidden order and magnetic structure of complex scheelites</i> | 691 |
| Kilian Schäfer | <i>Improving control of 3D printed shape programmable magneto active artificial muscles by analysis of their magnetization profile</i> | 692 |
| Michał Stekiel | <i>Magnetoelastic excitations in $CeAuAl_3$ measurements and calculations</i> | 693 |